VOLUME 29 / NUMBER 11
JUNE 8, 1991
ACC. NOS. N91-19024 TO N91-20039

STAR
AN ABSTRACT JOURNAL

Scientific and Technical Aerospace Reports

PRODUCED BY THE
SCIENTIFIC AND TECHNICAL
INFORMATION
DIVISION

NASA

NATIONAL AERONAUTICS AND SPACE ADMINISTRATION

***Scientific and Technical Aerospace Reports* (*STAR*)** is an abstract journal that provides comprehensive coverage of worldwide aerospace-related reports. It is a major product of the International Aerospace Database managed by the NASA Scientific and Technical Information (STI) Program. The coverage includes reports on aeronautics, space, and supporting disciplines. *STAR* lists current, publicly available reports entered into the NASA STI Database during the 2-week period preceding publication. An explanation of items that appear in each citation is given on the last page of each volume.

NASA sponsors a companion journal, *International Aerospace Abstracts* (*IAA*), that lists abstracts of the open literature on aerospace subjects available worldwide. *IAA* is available through the American Institute of Aeronautics and Astronautics.

Entries found in *STAR* and *IAA* are available through NASA's online service, RECON, as the International Aerospace Database and through DIALOG as the Aerospace Database.

Information on aerospace and related subjects is gathered by the NASA STI Program through national and international agreements and exchanges and is made available to the NASA community as well as to the public in many forms through various outlets. The section on NASA STI Program Products and Services contains additional information.

US ISSN 0036-8741

Volume 29 Number 11 / June 8, 1991

TABLE OF CONTENTS

AERONAUTICS For related information see also *Astronautics.*

01 AERONAUTICS (GENERAL) **1637**

02 AERODYNAMICS **1639**
Includes aerodynamics of bodies, combinations, wings, rotors, and control surfaces; and internal flow in ducts and turbomachinery. For related information see also *34 Fluid Mechanics and Heat Transfer.*

03 AIR TRANSPORTATION AND SAFETY **1645**
Includes passenger and cargo air transport operations; and aircraft accidents. For related information see also *16 Space Transportation* and *85 Urban Technology and Transportation.*

04 AIRCRAFT COMMUNICATIONS AND NAVIGATION ..... **N.A.**
Includes digital and voice communication with aircraft; air navigation systems (satellite and ground based); and air traffic control. For related information see also *17 Space Communications, Spacecraft Communications, Command and Tracking* and *32 Communications and Radar.*

05 AIRCRAFT DESIGN, TESTING AND PERFORMANCE **1646**
Includes aircraft simulation technology. For related information see also *18 Spacecraft Design, Testing and Performance* and *39 Structural Mechanics.* For land transportation vehicles see *85 Urban Technology and Transportation.*

06 AIRCRAFT INSTRUMENTATION **1650**
Includes cockpit and cabin display devices; and flight instruments. For related information see also *19 Space craft Instrumentation* and *35 Instrumentation and Photography.*

07 AIRCRAFT PROPULSION AND POWER **1650**
Includes prime propulsion systems and systems components, e.g., gas turbine engines and compressors; and onboard auxiliary power plants for aircraft. For related information see also *20 Spacecraft Propulsion and Power, 28 Propellants and Fuels,* and *44 Energy Production and Conversion.*

08 AIRCRAFT STABILITY AND CONTROL **1651**
Includes aircraft handling qualities; piloting; flight controls; and autopilots. For related information see also *05 Aircraft Design, Testing and Performance.*

09 RESEARCH AND SUPPORT FACILITIES (AIR) **1651**
Includes airports, hangars and runways; aircraft repair and overhaul facilities; wind tunnels; shock tubes; and aircraft engine test stands. For related information see also *14 Ground Support Systems and Facilities (Space).*

ASTRONAUTICS For related information see also *Aeronautics.*

12 ASTRONAUTICS (GENERAL) **1653**
For extraterrestrial exploration see *91 Lunar and Planetary Exploration.*

13 ASTRODYNAMICS **1654**
Includes powered and free-flight trajectories; and orbital and launching dynamics.

14 GROUND SUPPORT SYSTEMS AND FACILITIES (SPACE) **1654**
Includes launch complexes, research and production facilities; ground support equipment, e.g., mobile transporters; and simulators. For related information see also *09 Research and Support Facilities (Air).*

15 LAUNCH VEHICLES AND SPACE VEHICLES **1655**
Includes boosters; operating problems of launch/space vehicle systems; and reusable vehicles. For related information see also *20 Spacecraft Propulsion and Power.*

16 SPACE TRANSPORTATION **1655**
Includes passenger and cargo space transportation, e.g., shuttle operations; and space rescue techniques. For related information see also *03 Air Transportation and Safety* and *18 Spacecraft Design, Testing and Performance.* For space suits see *54 Man/System Technology and Life Support.*

17 SPACE COMMUNICATIONS, SPACECRAFT COMMUNICATIONS, COMMAND AND TRACKING . **N.A.**
Includes telemetry; space communications networks; astronavigation and guidance; and radio blackout. For related information see also *04 Aircraft Communications and Navigation* and *32 Communications and Radar.*

N.A.—no abstracts were assigned to this category for this issue.

18 SPACECRAFT DESIGN, TESTING AND PERFORMANCE **1656**
Includes satellites; space platforms; space stations; spacecraft systems and components such as thermal and environmental controls; and attitude controls. For life support systems see *54 Man/System Technology and Life Support.* For related information see also *05 Aircraft Design, Testing and Performance, 39 Structural Mechanics,* and *16 Space Transportation.*

19 SPACECRAFT INSTRUMENTATION ..... **N.A.**
For related information see also *06 Aircraft Instrumentation* and *35 Instrumentation and Photography.*

20 SPACECRAFT PROPULSION AND POWER **1664**
Includes main propulsion systems and components, e.g., rocket engines; and spacecraft auxiliary power sources. For related information see also *07 Aircraft Propulsion and Power, 28 Propellants and Fuels, 44 Energy Production and Conversion,* and *15 Launch Vehicles and Space Vehicles.*

CHEMISTRY AND MATERIALS

23 CHEMISTRY AND MATERIALS (GENERAL) **1674**

24 COMPOSITE MATERIALS **1674**
Includes physical, chemical, and mechanical properties of laminates and other composite materials. For ceramic materials see *27 Nonmetallic Materials.*

25 INORGANIC AND PHYSICAL CHEMISTRY **1681**
Includes chemical analysis, e.g., chromatography; combustion theory; electrochemistry; and photochemistry. For related information see also *77 Thermodynamics and Statistical Physics.*

26 METALLIC MATERIALS **1681**
Includes physical, chemical, and mechanical properties of metals, e.g., corrosion; and metallurgy.

27 NONMETALLIC MATERIALS **1686**
Includes physical, chemical, and mechanical properties of plastics, elastomers, lubricants, polymers, textiles, adhesives, and ceramic materials. For composite materials see *24 Composite Materials.*

28 PROPELLANTS AND FUELS **1690**
Includes rocket propellants, igniters and oxidizers; their storage and handling procedures; and aircraft fuels. For related information see also *07 Aircraft Propulsion and Power, 20 Spacecraft Propulsion and Power,* and *44 Energy Production and Conversion.*

29 MATERIALS PROCESSING **1692**
Includes space-based development of products and processes for commercial application. For biological materials see *55 Space Biology.*

ENGINEERING For related information see also *Physics.*

31 ENGINEERING (GENERAL) **1692**
Includes vacuum technology; control engineering; display engineering; cryogenics; and fire prevention.

32 COMMUNICATIONS AND RADAR **1693**
Includes radar; land and global communications; communications theory; and optical communications. For related information see also *04 Aircraft Communications and Navigation* and *17 Space Communications, Spacecraft Communications, Command and Tracking.* For search and rescue see *03 Air Transportation and Safety,* and *16 Space Transportation.*

33 ELECTRONICS AND ELECTRICAL ENGINEERING **1696**
Includes test equipment and maintainability; components, e.g., tunnel diodes and transistors; microminiaturization; and integrated circuitry. For related information see also *60 Computer Operations and Hardware* and *76 Solid-State Physics.*

34 FLUID MECHANICS AND HEAT TRANSFER **1700**
Includes boundary layers; hydrodynamics; fluidics; mass transfer and ablation cooling. For related information see also *02 Aerodynamics* and *77 Thermodynamics and Statistical Physics.*

35 INSTRUMENTATION AND PHOTOGRAPHY **1706**
Includes remote sensors; measuring instruments and gauges; detectors; cameras and photographic supplies; and holography. For aerial photography see *43 Earth Resources and Remote Sensing.* For related information see also *06 Aircraft Instrumentation* and *19 Spacecraft Instrumentation.*

36 LASERS AND MASERS **1709**
Includes parametric amplifiers. For related information see also *76 Solid-State Physics.*

37 MECHANICAL ENGINEERING **1714**
Includes auxiliary systems (nonpower); machine elements and processes; and mechanical equipment.

38 QUALITY ASSURANCE AND RELIABILITY **1718**
Includes product sampling procedures and techniques; and quality control.

39 STRUCTURAL MECHANICS **1719**
Includes structural element design and weight analysis; fatigue; and thermal stress. For applications see *05 Aircraft Design, Testing and Performance* and *18 Spacecraft Design, Testing and Performance.*

GEOSCIENCES For related information see also *Space Sciences.*

42 GEOSCIENCES (GENERAL) ..... **N.A.**

43 EARTH RESOURCES AND REMOTE SENSING **1725**
Includes remote sensing of earth resources by aircraft and spacecraft; photogrammetry; and aerial photography. For instrumentation see *35 Instrumentation and Photography.*

44 ENERGY PRODUCTION AND CONVERSION **1725**
Includes specific energy conversion systems, e.g., fuel cells; global sources of energy; geophysical conversion; and windpower. For related information see also *07 Aircraft Propulsion and Power, 20 Spacecraft Propulsion and Power,* and *28 Propellants and Fuels.*

45 ENVIRONMENT POLLUTION **1730**
Includes atmospheric, noise, thermal, and water pollution.

46 GEOPHYSICS **1737**
Includes aeronomy; upper and lower atmosphere studies; ionospheric and magnetospheric physics; and geomagnetism. For space radiation see *93 Space Radiation.*

47 METEOROLOGY AND CLIMATOLOGY **1739**
Includes weather forecasting and modification.

48 OCEANOGRAPHY **1739**
Includes biological, dynamic, and physical oceanography; and marine resources. For related information see also *43 Earth Resources and Remote Sensing.*

LIFE SCIENCES

51 LIFE SCIENCES (GENERAL) **1740**

52 AEROSPACE MEDICINE **1765**
Includes physiological factors; biological effects of radiation; and effects of weightlessness on man and animals.

53 BEHAVIORAL SCIENCES **1771**
Includes psychological factors; individual and group behavior; crew training and evaluation; and psychiatric research.

54 MAN/SYSTEM TECHNOLOGY AND LIFE SUPPORT **1771**
Includes human engineering; biotechnology; and space suits and protective clothing. For related information see also *16 Space Transportation.*

55 SPACE BIOLOGY ..... **N.A.**
Includes exobiology; planetary biology; and extraterrestrial life.

MATHEMATICAL AND COMPUTER SCIENCES

59 MATHEMATICAL AND COMPUTER SCIENCES (GENERAL) **1772**

60 COMPUTER OPERATIONS AND HARDWARE **1773**
Includes hardware for computer graphics, firmware, and data processing. For components see *33 Electronics and Electrical Engineering.*

61 COMPUTER PROGRAMMING AND SOFTWARE **1773**
Includes computer programs, routines, algorithms, and specific applications, e.g., CAD/CAM.

62 COMPUTER SYSTEMS **1779**
Includes computer networks and special application computer systems.

63 CYBERNETICS **1780**
Includes feedback and control theory, artificial intelligence, robotics and expert systems. For related information see also *54 Man/System Technology and Life Support.*

64 NUMERICAL ANALYSIS **1782**
Includes iteration, difference equations, and numerical approximation.

65 STATISTICS AND PROBABILITY **1785**
Includes data sampling and smoothing; Monte Carlo method; and stochastic processes.

66 SYSTEMS ANALYSIS ..... **N.A.**
Includes mathematical modeling; network analysis; and operations research.

67 THEORETICAL MATHEMATICS **1786**
Includes topology and number theory.

PHYSICS For related information see also *Engineering.*

70 PHYSICS (GENERAL) **1786**
For precision time and time interval (PTTI) see *35 Instrumentation and Photography;* for geophysics, astrophysics or solar physics see *46 Geophysics, 90 Astrophysics,* or *92 Solar Physics.*

71 ACOUSTICS **1790**
Includes sound generation, transmission, and attenuation. For noise pollution see *45 Environment Pollution.*

72 ATOMIC AND MOLECULAR PHYSICS **1792**
Includes atomic structure, electron properties, and molecular spectra.

73 NUCLEAR AND HIGH-ENERGY PHYSICS **1796**
Includes elementary and nuclear particles; and reactor theory. For space radiation see *93 Space Radiation.*

74 OPTICS **1798**
Includes light phenomena and optical devices. For lasers see *36 Lasers and Masers.*

75 PLASMA PHYSICS **1800**
Includes magnetohydrodynamics and plasma fusion. For ionospheric plasmas see *46 Geophysics.* For space plasmas see *90 Astrophysics.*

76 SOLID-STATE PHYSICS **1806**
Includes superconductivity. For related information see also *33 Electronics and Electrical Engineering* and *36 Lasers and Masers.*

77 THERMODYNAMICS AND STATISTICAL PHYSICS **1812**
Includes quantum mechanics; theoretical physics; and Bose and Fermi statistics. For related information see also *25 Inorganic and Physical Chemistry* and *34 Fluid Mechanics and Heat Transfer.*

SOCIAL SCIENCES

80 SOCIAL SCIENCES (GENERAL) ..... **N.A.**
Includes educational matters.

81 ADMINISTRATION AND MANAGEMENT **1812**
Includes management planning and research.

82 DOCUMENTATION AND INFORMATION SCIENCE **1813**
Includes information management; information storage and retrieval technology; technical writing; graphic arts; and micrography. For computer documentation see *61 Computer Programming and Software.*

83 ECONOMICS AND COST ANALYSIS ..... **N.A.**
Includes cost effectiveness studies.

84 LAW, POLITICAL SCIENCE AND SPACE POLICY **1815**
Includes NASA appropriation hearings; aviation law; space law and policy; international law; international cooperation; and patent policy.

85 URBAN TECHNOLOGY AND TRANSPORTATION **1815**
Includes applications of space technology to urban problems; technology transfer; technology assessment; and surface and mass transportation. For related information see *03 Air Transportation and Safety, 16 Space Transportation,* and *44 Energy Production and Conversion.*

SPACE SCIENCES For related information see also *Geosciences.*

88 SPACE SCIENCES (GENERAL) **1816**

89 ASTRONOMY **1816**
Includes radio, gamma-ray, and infrared astronomy; and astrometry.

90 ASTROPHYSICS **1817**
Includes cosmology; celestial mechanics; space plasmas; and interstellar and interplanetary gases and dust. For related information see also *75 Plasma Physics.*

91 LUNAR AND PLANETARY EXPLORATION **1820**
Includes planetology; and manned and unmanned flights. For spacecraft design or space stations see *18 Spacecraft Design, Testing and Performance.*

92 SOLAR PHYSICS **1823**
Includes solar activity, solar flares, solar radiation and sunspots. For related information see *93 Space Radiation.*

93 SPACE RADIATION **1823**
Includes cosmic radiation; and inner and outer earth's radiation belts. For biological effects of radiation see *52 Aerospace Medicine.* For theory see *73 Nuclear and High-Energy Physics.*

GENERAL

Includes aeronautical, astronautical, and space science related histories, biographies, and pertinent reports too broad for categorization; histories or broad overviews of NASA programs.

99 GENERAL **1824**

SUBJECT INDEX **I-1**

PERSONAL AUTHOR INDEX **I-71**

CORPORATE SOURCE INDEX **I-81**

CONTRACT NUMBER INDEX **I-93**

REPORT/ACCESSION NUMBER INDEX **I-97**

APPENDIX **A-1**

TYPICAL CITATION AND ABSTRACT

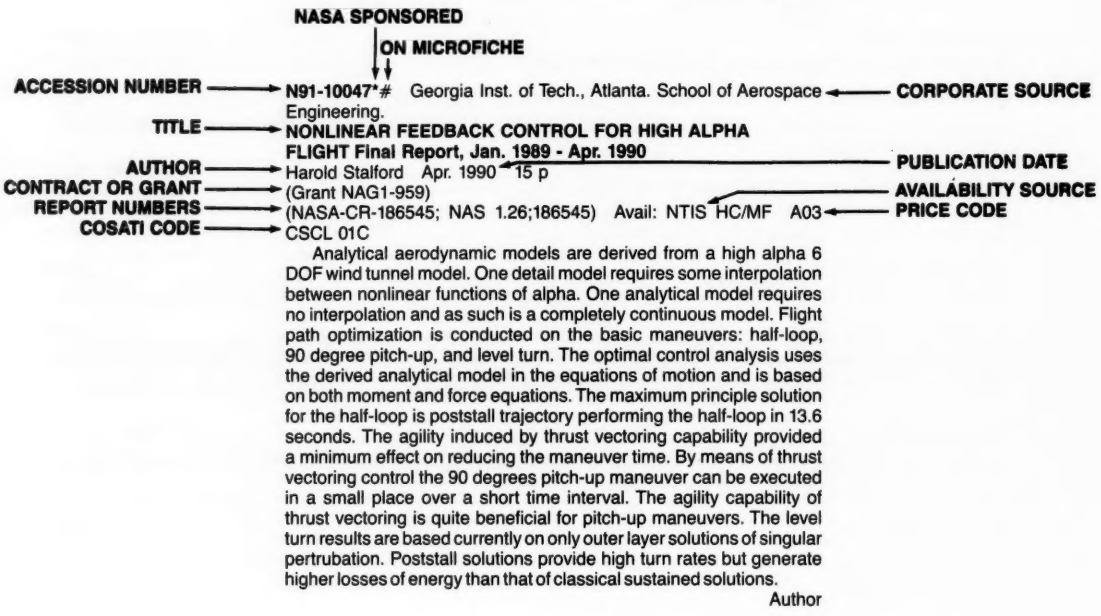
NASA SPONSORED
ON MICROFICHE
ACCESSION NUMBER
N91-10047*# Georgia Inst. of Tech., Atlanta. School of Aerospace Engineering.
CORPORATE SOURCE
TITLE
NONLINEAR FEEDBACK CONTROL FOR HIGH ALPHA FLIGHT Final Report, Jan. 1989 - Apr. 1990
PUBLICATION DATE
AUTHOR
Harold Stalford Apr. 1990 15 p
CONTRACT OR GRANT
(Grant NAG1-959)
AVAILABILITY SOURCE
REPORT NUMBERS
(NASA-CR-186545; NAS 1.26;186545) Avail: NTIS HC/MF A03
PRICE CODE
COSATI CODE
CSCL 01C
Analytical aerodynamic models are derived from a high alpha 6 DOF wind tunnel model. One detail model requires some interpolation between nonlinear functions of alpha. One analytical model requires no interpolation and as such is a completely continuous model. Flight path optimization is conducted on the basic maneuvers: half-loop, 90 degree pitch-up, and level turn. The optimal control analysis uses the derived analytical model in the equations of motion and is based on both moment and force equations. The maximum principle solution for the half-loop is poststall trajectory performing the half-loop in 13.6 seconds. The agility induced by thrust vectoring capability provided a minimum effect on reducing the maneuver time. By means of thrust vectoring control the 90 degrees pitch-up maneuver can be executed in a small place over a short time interval. The agility capability of thrust vectoring is quite beneficial for pitch-up maneuvers. The level turn results are based currently on only outer layer solutions of singular pertrubation. Poststall solutions provide high turn rates but generate higher losses of energy than that of classical sustained solutions.
Author

VOLUME 29 NUMBER 11 / JUNE 8, 1991

Scientific and Technical Aerospace Reports

A Semimonthly Publication of the National Aeronautics and Space Administration

01 AERONAUTICS (GENERAL)

N91-19024*# National Aeronautics and Space Administration. Langley Research Center, Hampton, VA.
JOINT UNIVERSITY PROGRAM FOR AIR TRANSPORTATION RESEARCH, 1989-1990
Frederick R. Morrell, comp. Washington Dec. 1990 183 p Conference held in Athens, OH, 14-15 Jun. 1990; sponsored by NASA and FAA
(NASA-CP-3095; L-16848; NAS 1.55:3095) Avail: NTIS HC/MF A09 CSCL 01A

Research conducted during the academic year 1989-90 under the NASA/FAA sponsored Joint University Program for Air Transportation research is discussed. Completed works, status reports and annotated bibliographies are presented for research topics, which include navigation, guidance and control theory and practice, aircraft performance, human factors, and expert systems concepts applied to airport operations. An overview of the year's activities for each university is also presented. For individual titles, see N91-19025 through N91-19039.

N91-19025*# Massachusetts Inst. of Tech., Cambridge. Flight Transportation Lab.
AUTOMATIC SPEECH RECOGNITION IN AIR TRAFFIC CONTROL: A HUMAN FACTORS PERSPECTIVE **c54**
Joakim Karlsson *In* NASA, Langley Research Center, Joint University Program for Air Transportation Research, 1989-1990 Dec. 1990 p 9-13 (For primary document see N91-19024 11-01)
Avail: NTIS HC/MF A09 CSCL 05H

The introduction of Automatic Speech Recognition (ASR) technology into the Air Traffic Control (ATC) system has the potential to improve overall safety and efficiency. However, because ASR technology is inherently a part of the man-machine interface between the user and the system, the human factors issues involved must be addressed. Here, some of the human factors problems are identified and related methods of investigation are presented. Research at M.I.T.'s Flight Transportation Laboratory is being conducted from a human factors perspective, focusing on intelligent parser design, presentation of feedback, error correction strategy design, and optimal choice of input modalities. Author

N91-19026*# Massachusetts Inst. of Tech., Cambridge. Flight Transportation Lab.
THE TEMPORAL LOGIC OF THE TOWER CHIEF SYSTEM **c04**
Lyman R. Hazelton, Jr. *In* NASA, Langley Research Center, Joint University Program for Air Transportation Research, 1989-1990 Dec. 1990 p 15-28 (For primary document see N91-19024 11-01)
(Grant NGL-22-009-640)
Avail: NTIS HC/MF A09 CSCL 17G

The purpose is to describe the logic used in the reasoning scheme employed in the Tower Chief system, a runway configuration management system. First, a review of classical logic is given. Defensible logics, truth maintenance, default logic, temporally dependent propositions, and resource allocation and planning are discussed. Author

N91-19027*# Massachusetts Inst. of Tech., Cambridge.
BUBBLES: AN AUTOMATED DECISION SUPPORT SYSTEM FOR FINAL APPROACH CONTROLLERS **c04**
Zhizang Chi *In* NASA, Langley Research Center, Joint University Program for Air Transportation Research, 1989-1990 Dec. 1990 p 29-36 (For primary document see N91-19024 11-01)
Avail: NTIS HC/MF A09 CSCL 17G

With the assumptions that an explicit schedule exists for landings (and takeoffs) at each runway, that each aircraft has declared an IAS for final approach and will be obligated to fly it as accurately as possible, and that there is a continuous estimate of average windspeed on approach, the objective was to provide automated cues to assist controllers in the spacing of landing aircraft. The cues have two characteristics. First, they are adaptive to estimation errors in position and speed by the radar tracking process and piloting errors in the execution of turns and commanded speed reductions. Second, the cues are responsive to the desires of the human controller. Several diagrams are used to help explain the system. Author

N91-19028*# Ohio Univ., Athens. Dept. of Electrical and Computer Engineering.
INVESTIGATION OF AIR TRANSPORTATION TECHNOLOGY AT OHIO UNIVERSITY, 1989-1990 **c03**
Robert W. Lilley *In* NASA, Langley Research Center, Joint University Program for Air Transportation Research, 1989-1990 Dec. 1990 p 61-66 (For primary document see N91-19024 11-01)
Avail: NTIS HC/MF A09 CSCL 01A

The activities of the participants in the Joint University Program (JUP) at Ohio University are briefly surveyed. During 1989 to 1990, five topics received emphasis. A spectrum-efficient weather data uplink system was designed, constructed, and flight tested. An integrated Global Positioning System/Inertial Navigation System (GPS/INS) study continued, utilizing the Redundant strapdown Inertial Measurement Unit (IMU) on loan from NASA. The Ridge Regression theory was refined and applied to air navigation scenarios. System Identification theory was applied to GPS data to point the way to better understanding of the effects of Selective Availability on civilian users of this navigation system. An analysis of thought-related (electroencephalographic) signals for application to control of computer systems that could have significance in aiding paraplegics or for hands-off systems control in industrial or air traffic control areas was carried out. Author

N91-19029*# Ohio Univ., Athens.
RIDGE REGRESSION SIGNAL PROCESSING **c04**
Mark R. Kuhl *In* NASA, Langley Research Center, Joint University Program for Air Transportation Research, 1989-1990 Dec. 1990 p 67-75 (For primary document see N91-19024 11-01)
Avail: NTIS HC/MF A09 CSCL 17G

The introduction of the Global Positioning System (GPS) into the National Airspace System (NAS) necessitates the development of Receiver Autonomous Integrity Monitoring (RAIM) techniques. In order to guarantee a certain level of integrity, a thorough understanding of modern estimation techniques applied to navigational problems is required. The extended Kalman filter (EKF)

is derived and analyzed under poor geometry conditions. It was found that the performance of the EKF is difficult to predict, since the EKF is designed for a Gaussian environment. A novel approach is implemented which incorporates ridge regression to explain the behavior of an EKF in the presence of dynamics under poor geometry conditions. The basic principles of ridge regression theory are presented, followed by the derivation of a linearized recursive ridge estimator. Computer simulations are performed to confirm the underlying theory and to provide a comparative analysis of the EKF and the recursive ridge estimator. Author

N91-19030*# Ohio Univ., Athens.
MODELING SELECTIVE AVAILABILITY OF THE NAVSTAR GLOBAL POSITIONING SYSTEM **c04**
Michael Braasch *In* NASA, Langley Research Center, Joint University Program for Air Transportation Research, 1989-1990 Dec. 1990 p 77-89 (For primary document see N91-19024 11-01)
Avail: NTIS HC/MF A09 CSCL 17G

As the development of the NAVSTAR Global Positioning System (GPS) continues, there will increasingly be the need for a software centered signal model. This model must accurately generate the observed pseudorange which would typically be encountered. The observed pseudorange varies from the true geometric (slant) range due to range measurement errors. Errors in range measurement stem from a variety of hardware and environment factors. These errors are classified as either deterministic or random and, where appropriate, their models are summarized. Of particular interest is the model for Selective Availability which is derived from actual GPS data. The procedure for the determination of this model, known as the System Identification Theory, is briefly outlined. The synthesis of these error sources into the final signal model is given along with simulation results. Author

N91-19031*# Ohio Univ., Athens.
ANALYZING THOUGHT-RELATED ELECTROENCEPHALOGRAPHIC DATA USING NONLINEAR TECHNIQUES **c52**
Trent Skidmore *In* NASA, Langley Research Center, Joint University Program for Air Transportation Research, 1989-1990 Dec. 1990 p 91-95 (For primary document see N91-19024 11-01)
Avail: NTIS HC/MF A09 CSCL 06P

A unique method is presented for collecting, studying and interpreting thought-related electroencephalogram (EEG) data. The use of a chaos based nonlinear analysis technique is shown to be promising in providing insight into relating conscious thought to specific EEG data. A discussion of the practical limitations of this technique is also included. Author

N91-19032*# Ohio Univ., Athens.
INTEGRATED INERTIAL/GPS **c04**
Paul Kline and Frank vanGraas *In* NASA, Langley Research Center, Joint University Program for Air Transportation Research, 1989-1990 Dec. 1990 p 97-103 (For primary document see N91-19024 11-01)
Avail: NTIS HC/MF A09 CSCL 17G

The presence of failures in navigation sensors can cause the determination of an erroneous aircraft state estimate, which includes position, attitude, and their derivatives. Aircraft flight control systems rely on sensor inputs to determine the aircraft state. In the case of integrated Inertial/NAVSTAR Global Positioning System (GPS), sensor failures could occur in the on-board inertial sensors or in the GPS measurements. The synergistic use of both GPS and the Inertial Navigation System (INS) allows for highly reliable fault detection and isolation of sensor failures. Integrated Inertial/GPS is a promising technology for the High Speed Civil Transport (HSCT) and the return and landing of a manned space vehicle. Author

N91-19033*# Princeton Univ., NJ. Dept. of Mechanical and Aerospace Engineering.
INVESTIGATION OF AIR TRANSPORTATION TECHNOLOGY AT PRINCETON UNIVERSITY, 1989-1990 **c03**
Robert F. Stengel *In* NASA, Langley Research Center, Joint University Program for Air Transportation Research, 1989-1990 Dec. 1990 p 105-118 (For primary document see N91-19024 11-01)
Avail: NTIS HC/MF A09 CSCL 01A

The Air Transportation Technology Program at Princeton University proceeded along six avenues during the past year: microburst hazards to aircraft; machine-intelligent, fault tolerant flight control; computer aided heuristics for piloted flight; stochastic robustness for flight control systems; neural networks for flight control; and computer aided control system design. These topics are briefly discussed, and an annotated bibliography of publications that appeared between January 1989 and June 1990 is given. Author

N91-19034*# Princeton Univ., NJ.
PROGRESS ON INTELLIGENT GUIDANCE AND CONTROL FOR WIND SHEAR ENCOUNTER **c03**
D. Alexander Stratton *In* NASA, Langley Research Center, Joint University Program for Air Transportation Research, 1989-1990 Dec. 1990 p 119-131 (For primary document see N91-19024 11-01)
Avail: NTIS HC/MF A09 CSCL 01A

Low altitude wind shear poses a serious threat to air safety. Avoiding severe wind shear challenges the ability of flight crews, as it involves assessing risk from uncertain evidence. A computerized intelligent cockpit aid can increase flight crew awareness of wind shear, improving avoidance decisions. The primary functions of a cockpit advisory expert system for wind shear avoidance are discussed. Also introduced are computational techniques being implemented to enable these primary functions. Author

N91-19035*# Princeton Univ., NJ. Dept. of Mechanical and Aerospace Engineering.
FLIGHT SIMULATION FOR WIND SHEAR ENCOUNTER **c09**
Sandeep S. Mulgund *In* NASA, Langley Research Center, Joint University Program for Air Transportation Research, 1989-1990 Dec. 1990 p 133-139 (For primary document see N91-19024 11-01)
Avail: NTIS HC/MF A09 CSCL 14B

A real-time piloted flight simulator is under development in the Laboratory for Control and Automation at Princeton University. This facility will be used to study piloted flight through a simulated wind shear. It will also provide a testbed for real-time flight guidance laws. The hardware configuration and aerodynamic model used are discussed. The microburst model to be incorporated into the simulation is introduced, and some proposed cockpit display concepts are described. Author

N91-19036*# Princeton Univ., NJ. Dept. of Mechanical and Aerospace Engineering.
STOCHASTIC ROBUSTNESS: TOWARDS A COMPREHENSIVE ROBUSTNESS TOOL **c08**
Laurie Ryan Ray *In* NASA, Langley Research Center, Joint University Program for Air Transportation Research, 1989-1990 Dec. 1990 p 141-150 (For primary document see N91-19024 11-01)
Avail: NTIS HC/MF A09 CSCL 01C

Stochastic robustness is a simple technique to determine the robustness of linear, time-invariant systems by Monte Carlo methods. Stochastic stability robustness has been described previously. Those results are extended here to provide insight into control system design for performance. Together, stochastic stability and performance robustness concepts constitute a comprehensive tool that can be used to analyze control system robustness properties. As well, they offer control system design insight that can set the stage for stochastic robustness synthesis. The concept of stochastic stability robustness is reviewed,

stochastic performance robustness is introduced, and stochastic robustness synthesis is described qualitatively. Confidence intervals necessary for comparing control laws statistically are presented. Author

N91-19037*# Princeton Univ., NJ. Dept. of Mechanical and Aerospace Engineering.
NEURAL NETWORKS IN NONLINEAR AIRCRAFT CONTROL **c08**
Dennis J. Linse *In* NASA, Langley Research Center, Joint University Program for Air Transportation Research, 1989-1990 Dec. 1990 p 151-161 (For primary document see N91-19024 11-01)
Avail: NTIS HC/MF A09 CSCL 01C

Recent research indicates that artificial neural networks offer interesting learning or adaptive capabilities. The current research focuses on the potential for application of neural networks in a nonlinear aircraft control law. The current work has been to determine which networks are suitable for such an application and how they will fit into a nonlinear control law. Author

N91-19038*# Princeton Univ., NJ. Dept. of Mechanical and Aerospace Engineering.
STOCHASTIC SATBILITY AND PERFORMANCE ROBUSTNESS OF LINEAR MULTIVARIABLE SYSTEMS **c08**
Laurie E. Ryan and Robert F. Stengel *In* NASA, Langley Research Center, Joint University Program for Air Transportation Research, 1989-1990 Dec. 1990 p 181-186 (For primary document see N91-19024 11-01)
(Contract NGL-31-001-252; DAAL03-89-K-0092)
Avail: NTIS HC/MF A09 CSCL 01C

Stochastic robustness, a simple technique used to estimate the robustness of linear, time invariant systems, is applied to a single-link robot arm control system. Concepts behind stochastic stability robustness are extended to systems with estimators and to stochastic performance robustness. Stochastic performance robustness measures based on classical design specifications are introduced, and the relationship between stochastic robustness measures and control system design parameters are discussed. The application of stochastic performance robustness, and the relationship between performance objectives and design parameters are demonstrated by means of example. The results prove stochastic robustness to be a good overall robustness analysis method that can relate robustness characteristics to control system design parameters. Author

N91-19039*# Princeton Univ., NJ. Dept. of Mechanical and Aerospace Engineering.
SYSTEM IDENTIFICATION FOR NONLINEAR CONTROL USING NEURAL NETWORKS **c08**
Robert F. Stengel and Dennis J. Linse *In* NASA, Langley Research Center, Joint University Program for Air Transportation Research, 1989-1990 Dec. 1990 p 187-192 (For primary document see N91-19024 11-01)
(Contract NGL-31-001-252; DAAL03-89-K-0092)
Avail: NTIS HC/MF A09 CSCL 01C

An approach to incorporating artificial neural networks in nonlinear, adaptive control systems is described. The controller contains three principal elements: a nonlinear inverse dynamic control law whose coefficients depend on a comprehensive model of the plant, a neural network that models system dynamics, and a state estimator whose outputs drive the control law and train the neural network. Attention is focused on the system identification task, which combines an extended Kalman filter with generalized spline function approximation. Continual learning is possible during normal operation, without taking the system off line for specialized training. Nonlinear inverse dynamic control requires smooth derivatives as well as function estimates, imposing stringent goals on the approximating technique. Author

N91-19040# Wichita State Univ., KS. National Inst. for Aviation Research.
DEDICATION OF NATIONAL INSTITUTE FOR AVIATION RESEARCH
William H. Wentz, Jr. Jul. 1990 15 p
(NIAR-90-21) Avail: NTIS HC/MF A03

The research activities performed at the Wichita State University are reviewed. The following subject areas are covered: aerodynamics, propulsion, de-icing, human factors, flight controls, navigation, advanced composites, materials, cryogenics/superconductors, CIM (Computer-Integrated-Manufacturing), aircraft inspection robot, crash sled, and crash computations. Y.S.

N91-19041*# Army Aviation Research and Development Command, Moffett Field, CA. Aeroflightdynamics Directorate.
A FLIGHT-DYNAMIC HELICOPTER MATHEMATICAL MODEL WITH A SINGLE FLAP-LAG-TORSION MAIN ROTOR
Marc D. Takahashi Feb. 1990 114 p
(NASA-TM-102267; A-90037; NAS 1.15:102267; USAAVSCOM-TM-90-A-004) Avail: NTIS HC/MF A06 CSCL 01B

A mathematical model of a helicopter system with a single main rotor that includes rigid, hinge-restrained rotor blades with flap, lag, and torsion degrees of freedom is described. The model allows several hinge sequences and two offsets in the hinges. Quasi-steady Greenberg theory is used to calculate the blade-section aerodynamic forces, and inflow effects are accounted for by using three-state nonlinear dynamic inflow model. The motion of the rigid fuselage is defined by six degrees of freedom, and an optional rotor rpm degree of freedom is available. Empennage surfaces and the tail rotor are modeled, and the effect of main-rotor downwash on these elements is included. Model trim linearization, and time-integration operations are described and can be applied to a subset of the model in the rotating or nonrotating coordinate frame. A preliminary validation of the model is made by comparing its results with those of other analytical and experimental studies. This publication presents the results of research compiled in November 1989. Author

02 AERODYNAMICS

Includes aerodynamics of bodies, combinations, wings, rotors, and control surfaces; and internal flow in ducts and turbomachinery.

For related information see also *34 Fluid Mechanics and Heat Transfer.*

N91-19042*# National Aeronautics and Space Administration. Langley Research Center, Hampton, VA.
EXPERIMENTAL INVESTIGATION OF POROUS-FLOOR EFFECTS ON CAVITY FLOW FIELDS AT SUPERSONIC SPEEDS
Floyd J. Wilcox, Jr. Washington Nov. 1990 105 p
(NASA-TP-3032; L-16711; NAS 1.60:3032) Avail: NTIS HC/MF A06 CSCL 01A

An experimental investigation was conducted to determine the effectiveness of a passive-venting system to modify the flow field characteristics of a rectangular-box cavity at supersonic speeds. The passive-venting system consists of a porous floor with a vent chamber beneath the floor. For certain cavity length-to-height ratios, this configuration allowed high-pressure air at the rear of the cavity to vent to the forward part of the cavity, thereby modifying the cavity flow field. The wind-tunnel model consisted of a flat plate that housed a cavity mounted on a balance such that only the cavity drag was measured. The cavity height remained constant, and the length varied with rectangular-block inserts. Both solid-and porous-floor cavities were tested for comparison at Mach numbers of 1.60, 1.90, 2.16, and 2.86. These results showed that the passive-venting system did modify the cavity flow field. In order to determine the type flow field which existed for the porous-floor configuration, pressures were measured

inside the cavity at the same conditions and for the same configurations as those used in the drag tests. Pressure data were also obtained with stores mounted in the cavity. These results, along with Schlieren photographs and the tabulated data, are presented to document the porous-floor cavity flow field. Author

N91-19043*# Institute for Computer Applications in Science and Engineering, Hampton, VA.
MULTIGRID SOLUTION OF COMPRESSIBLE TURBULENT FLOW ON UNSTRUCTURED MESHES USING A TWO-EQUATION MODEL Final Report
D. J. Mavriplis and L. Martinelli (Princeton Univ., NJ.) Jan. 1991 42 p Previously announced in IAA as A91-21425 Submitted for publication
(Contract NAS1-18605)
(NASA-CR-187513; NAS 1.26:187513; ICASE-91-11) Avail: NTIS HC/MF A03 CSCL 01A

The system of equations consisting of the full Navier-Stokes equations and two turbulence equations was solved for in the steady state using a multigrid strategy on unstructured meshes. The flow equations and turbulence equations are solved in a loosely coupled manner. The flow equations are advanced in time using a multistage Runge-Kutta time stepping scheme with a stability bound local time step, while the turbulence equations are advanced in a point-implicit scheme with a time step which guarantees stability and positively. Low Reynolds number modifications to the original two equation model are incorporated in a manner which results in well behaved equations for arbitrarily small wall distances. A variety of aerodynamic flows are solved for, initializing all quantities with uniform freestream values, and resulting in rapid and uniform convergence rates for the flow and turbulence equations. Author

N91-19044*# National Aeronautics and Space Administration. Lewis Research Center, Cleveland, OH.
IMPROVED VISUALIZATION OF FLOW FIELD MEASUREMENTS
Jeffrey Hilton Miles 1991 36 p Presented at the 29th Aerospace Sciences Meeting, Reno, NV, 7-10 Jan. 1991; sponsored by AIAA Original contains color illustrations
(NASA-TM-103679; E-5896; NAS 1.15:103679; AIAA-91-0273)
Avail: NTIS HC/MF A03; 3 functional color pages CSCL 01A

A capability was developed that makes it possible to apply to measured flow field data the visualization tools developed to display numerical solutions for computational fluid dynamic problems. The measurement monitor surface (MMS) procedure was applied to the analysis of flow field measurements within a low aspect ratio transonic axial flow fan rotor obtained with 2-D laser anemometry. The procedure generates input for the visualization tools developed to display numerical solutions for computational fluid dynamics problems. The relative Mach number contour plots obtained by this method resemble the conventional contour plots obtained by more traditional methods. The results show that the MMS procedure can be used to generate input for the multidimensional processing and analysis tools developed for data from numerical flow field simulations. They show that an experimenter can apply the MMS procedure to his data and then use an interactive graphics program to display scalar quantities like the Mach number by profiles, carpet plots, contour lines, and surfaces using various colors. Also, flow directionality can be shown by display of vector fields and particle traces. Author

N91-19045*# National Aeronautics and Space Administration. Lewis Research Center, Cleveland, OH.
INFLIGHT SOURCE NOISE OF AN ADVANCED FULL-SCALE SINGLE-ROTATION PROPELLER
Richard P. Woodward and Irvin J. Loeffler 1991 20 p Presented at the 29th Aerospace Sciences Meeting, Reno, NV, 7-10 Jan. 1991; sponsored by AIAA
(NASA-TM-103687; E-5906; NAS 1.15:103687; AIAA-91-0594)
Avail: NTIS HC/MF A03 CSCL 01A

Flight tests to define the far field tone source at cruise conditions were completed on the full scale SR-7L advanced turboprop which was installed on the left wing of a Gulfstream II aircraft. This program, designated Propfan Test Assessment (PTA), involved aeroacoustic testing of the propeller over a range of test conditions. These measurements defined source levels for input into long distance propagation models to predict en route noise. Inflight data were taken for 7 test cases. The sideline directivities measured by the Learjet showed expected maximum levels near 105 degrees from the propeller upstream axis. However, azimuthal directivities based on the maximum observed sideline tone levels showed highest levels below the aircraft. An investigation of the effect of propeller tip speed showed that the tone level of reduction associated with reductions in propeller tip speed is more significant in the horizontal plane than below the aircraft. Author

N91-19046*# National Aeronautics and Space Administration. Lewis Research Center, Cleveland, OH.
ICING CHARACTERISTICS OF A NATURAL-LAMINAR-FLOW, A MEDIUM-SPEED, AND A SWEPT, MEDIUM-SPEED AIRFOIL
Colin S. Bidwell 1991 32 p Presented at the 29th Aerospace Sciences Meeting, Reno, NV, 7-10 Jan. 1991; sponsored by AIAA
(NASA-TM-103693; E-5912; NAS 1.15:103693; AIAA-91-0447)
Avail: NTIS HC/MF A03 CSCL 01A

Tests were conducted at the Icing Research Tunnel at the NASA Lewis Research Center to determine the icing characteristics of three modern airfoils, a natural laminar flow, a medium speed and a swept medium speed airfoil. Tests measured the impingement characteristics and drag degradation for angles of attack typifying cruise and climb for cloud conditions typifying the range that might be encountered in flight. The maximum degradation occurred for the cruise angle of attack for the long glaze ice condition for all three airfoils with increases over baseline drag being 486 percent, 510 percent, and 465 percent for the natural laminar flow, the medium speed and the swept medium speed airfoil respectively. For the climb angle of attack, the maximum drag degradation (and extent of impingement) observed were also for the long glaze ice condition, and were 261 percent, 181 percent and 331 percent respectively. The minimum drag degradation (and extent of impingement) occurred for the cruise condition and for the short, rime spray which increases over baseline drag values of 47 percent, 28 percent and 46 percent respectively. Author

N91-19047*# National Aeronautics and Space Administration. Lewis Research Center, Cleveland, OH.
PREDICTION OF ICE SHAPES AND THEIR EFFECT ON AIRFOIL PERFORMANCE
Jaiwon Shin, Brian Berkowitz, Hsun Chen, and Tuncer Cebeci (California State Univ., Long Beach.) 1991 23 p Presented at the 29th Aerospace Sciences Meeting, Reno, NV, 7-10 Jan. 1991; sponsored by AIAA
(NASA-TM-103701; E-5924; NAS 1.15:103701; AIAA-91-0264)
Avail: NTIS HC/MF A03 CSCL 01A

Calculations of ice shapes and the resulting drag increases are presented for experimental data on a NACA 0012 airfoil. They were made with a combination of LEWICE and interactive boundary-layer codes for a wide range of conditions which include air speed and temperature, the droplet size and liquid water content of the cloud, and the angle of attack of the airfoil. In all cases, the calculated results account for the drag increase due to ice accretion and, in general, show good agreement. Author

N91-19048*# CFD Research Corp., Huntsville, AL.
RAPID MIX CONCEPTS FOR LOW EMISSION COMBUSTORS IN GAS TURBINE ENGINES Final Report
Milind V. Talpallikar, Clifford E. Smith, and Ming-Chia Lai (Wayne State Univ., Detroit, MI.) Oct. 1990 70 p LIMITED REPRODUCIBILITY: More than 20% of this document may be affected by color photographs Original contains color illustrations
(Contract NAS3-25834)
(NASA-CR-185292; NAS 1.26:185292) Avail: NTIS HC/MF A04; 13 functional color pages CSCL 01A

NASA LeRC has identified the Rich burn/Quick mix/Lean burn (RQL) combustor as a potential gas turbine combustor concept to reduce NOx emissions in High Speed Civil Transport (HSCT)

aircraft. To demonstrate reduced NOx levels, NASA LeRC soon will test a flametube version of an RQL combustor. The critical technology needed for the RQL combustor is a method of quickly mixing combustion air with rich burn gases. Two concepts were proposed to enhance jet mixing in a circular cross-section: the Asymmetric Jet Penetration (AJP) concept; and the Lobed Mixer (LM) concept. In Phase 1, two preliminary configurations of the AJP concept were compared with a conventional 12-jet radial-inflow slot design. The configurations were screened using an advanced 3-D Computational Fluid Dynamics (CFD) code named REFLEQS. Both non-reacting and reacting analyses were performed. For an objective comparison, the conventional design was optimized by parametric variation of the jet-to-mainstream momentum flux (J) ratio. The optimum J was then employed in the AJP simulations. Results showed that the three-jet AJP configuration was superior in overall mixedness compared to the conventional design. However, in regards to NOx emissions, the AJP configuration was inferior. The higher emission level for AJP was caused by a single hot spot located in the wake of the central jet as it entered the combustor. Ways of maintaining good mixedness while eliminating the hot spot were identified for Phase 2 study. Overall, Phase 1 showed the viability of using CFD analyses to evaluate quick-mix concepts. A high probability exists that advancing mixing concepts will reduce NOx emissions in RQL combustors, and should be explored in Phase 2, by parallel numerical and experimental work. Author

N91-19049*# Hamilton Standard, Windsor Locks, CT.
UNIFIED AEROACOUSTICS ANALYSIS FOR HIGH SPEED TURBOPROP AERODYNAMICS AND NOISE. VOLUME 1: DEVELOPMENT OF THEORY FOR BLADE LOADING, WAKES, AND NOISE Final Report
D. B. Hanson Mar. 1991 135 p
(Contract NAS3-23720)
(NASA-CR-4329; E-6021-Vol-1; NAS 1.26:4329) Avail: NTIS HC/MF A07 CSCL 01A

A unified theory for the aerodynamics and noise of advanced turboprops are presented. Aerodynamic topics include calculation of performance, blade load distribution, and non-uniform wake flow fields. Blade loading can be steady or unsteady due to fixed distortion, counter-rotating wakes, or blade vibration. The aerodynamic theory is based on the pressure potential method and is therefore basically linear. However, nonlinear effects associated with finite axial induction and blade vortex flow are included via approximate methods. Acoustic topics include radiation of noise caused by blade thickness, steady loading (including vortex lift), and unsteady loading. Shielding of the fuselage by its boundary layer and the wing are treated in separate analyses that are compatible but not integrated with the aeroacoustic theory for rotating blades. Author

N91-19050*# Continuum Dynamics, Inc., Princeton, NJ.
FREE WAKE ANALYSIS OF HOVER PERFORMANCE USING A NEW INFLUENCE COEFFICIENT METHOD
Todd R. Quackenbush, Donald B. Bliss, Ching Cho Ong, and Cho Ong Ching Washington, DC NASA Jul. 1990 100 p
(Contract NAS2-12148)
(NASA-CR-4309; A-90091; NAS 1.26:4309) Avail: NTIS HC/MF A05 CSCL 01A

A new approach to the prediction of helicopter rotor performance using a free wake analysis was developed. This new method uses a relaxation process that does not suffer from the convergence problems associated with previous time marching simulations. This wake relaxation procedure was coupled to a vortex-lattice, lifting surface loads analysis to produce a novel, self contained performance prediction code: EHPIC (Evaluation of Helicopter Performance using Influence Coefficients). The major technical features of the EHPIC code are described and a substantial amount of background information on the capabilities and proper operation of the code is supplied. Sample problems were undertaken to demonstrate the robustness and flexibility of the basic approach. Also, a performance correlation study was carried out to establish the breadth of applicability of the code, with very favorable results. Author

N91-19051*# National Aeronautics and Space Administration. Hugh L. Dryden Flight Research Facility, Edwards, CA.
F-18 HIGH ALPHA RESEARCH VEHICLE SURFACE PRESSURES: INITIAL IN-FLIGHT RESULTS AND CORRELATION WITH FLOW VISUALIZATION AND WIND-TUNNEL DATA
David F. Fisher, Daniel W. Banks, and David M. Richwine (PRC Systems Services Co., Edwards, CA.) Aug. 1990 36 p Presented at the AIAA 8th Applied Aerodynamics Conference, Portland, OR, 20-22 Aug. 1990 Previously announced in IAA as A90-45885
(NASA-TM-101724; H-1633; NAS 1.15:101724; AIAA-90-3018)
Avail: NTIS HC/MF A03 CSCL 01A

Pressure distributions measured on the forebody and the leading-edge extensions (LEX's) of the NASA F-18 high alpha research vehicle (HARV) were reported at 10 and 50 degree angles of attack and at Mach 0.20 to 0.60. The results were correlated with HARV flow visualization and 6-percent scale F-18 wind-tunnel-model test results. The general trend in the data from the forebody was for the maximum suction pressure peaks to first appear at an angle of attack (alpha) of approximately 19 degrees and increase in magnitude with angle of attack. The LEX pressure distribution general trend was the inward progression and increase in magnitude of the maximum suction peaks up to vortex core breakdown and then the decrease and general flattening of the pressure distribution beyond that. No significant effect of Mach number was noted for the forebody results. However, a substantial compressibility effect on the LEX's resulted in a significant reduction in vortex-induced suction pressure as Mach number increased. The forebody primary and the LEX secondary vortex separation lines, from surface flow visualization, correlated well with the end of pressure recovery, leeward and windward, respectively, of maximum suction pressure peaks. The flight to wind-tunnel correlations were generally good with some exceptions. Author

N91-19052*# National Aeronautics and Space Administration. Ames Research Center, Moffett Field, CA.
MODAL ANALYSIS OF UH-60A INSTRUMENTED ROTOR BLADES
Karen S. Hamade and Robert M. Kufeld Washington Nov. 1990 45 p
(NASA-TM-4239; A-90252; NAS 1.15:4239) Avail: NTIS HC/MF A03 CSCL 01A

The dynamic characteristics of instrumented and production UH-60A Black Hawk main rotor blades were measured, and the results were validated with NASTRAN finite element models. The blades tested included pressure and strain-gage instrumented blades, which are part of the NASA Airloads Flight Research Phase of the Modern Technology Rotor Program. The dynamic similarity of the blades was required for accurate data collection in this program. Therefore, a nonrotating blade modal analysis was performed on the first 10 free-free modes to measure blade similarities. The results showed small differences between the modal frequencies of instrumented and production blades and a close correlation with the NASTRAN models. This type of modal testing and analysis is recommended as a standard procedure for future instrumented blade flight testing. Author

N91-19053*# National Aeronautics and Space Administration. Lewis Research Center, Cleveland, OH.
ACOUSTIC RADIATION FROM LIFTING AIRFOILS IN COMPRESSIBLE SUBSONIC FLOW
Hafiz M. Atassi, Shankar Subramaniam (Notre Dame Univ., IN.), and James R. Scott 1990 22 p Presented at the 13th Aeroacoustics Conference, Tallahassee, FL, 22-24 Oct. 1990; sponsored by AIAA Previously announced in IAA as A91-12427
(NASA-TM-103650; E-5830; NAS 1.15:103650; AIAA-90-3911)
Avail: NTIS HC/MF A03 CSCL 01A

The far field acoustic radiation from a lifting airfoil in a three-dimensional gust is studied. The acoustic pressure is calculated using the Kirchhoff method, instead of using the classical

acoustic analogy approach due to Lighthill. The pressure on the Kirchhoff surface is calculated using an existing numerical solution of the unsteady flow field. The far field acoustic pressure is calculated in terms of these values using Kirchhoff's formula. The method is validated against existing semi-analytical results for a flat plate. The method is then used to study the problem of an airfoil in a harmonic three-dimensional gust, for a wide range of Mach numbers. The effect of variation of the airfoil thickness and angle of attack on the acoustic far field is studied. The changes in the mechanism of sound generation and propagation due to the presence of steady loading and nonuniform mean flow are also studied. Author

N91-19054*# National Aeronautics and Space Administration. Lewis Research Center, Cleveland, OH.
IMPLEMENTATION OF CONTROL POINT FORM OF ALGEBRAIC GRID-GENERATION TECHNIQUE
Yung K. Choo, David P. Miller, and Charles J. Reno (Cleveland State Univ., OH.) 1991 13 p Presented at the 3rd International Conference on Numerical Grid Generation in Computational Fluid Dynamics and Related Fields, Barcelona, Spain, 3-7 Jun. 1991; sponsored by the UPC, Catalonia Univ., and ESA
(Contract NCC3-153)
(NASA-TM-103748; E-5997; NAS 1.15:103748) Avail: NTIS HC/MF A03 CSCL 01A

The control point form (CPF) provides explicit control of physical grid shape and grid spacing through the movement of the control points. The control point array, called a control net, is a space grid type arrangement of locations in physical space with an index for each direction. As an algebraic method CPF is efficient and works well with interactive computer graphics. A family of menu-driven, interactive grid-generation computer codes (TURBO) is being developed by using CPF. Key features of Turbol (a TURBO member) are discussed and typical results are presented. Turbol runs on any IRIS 4D series workstation. Author

N91-19055*# National Aeronautics and Space Administration. Hugh L. Dryden Flight Research Facility, Edwards, CA.
SUMMARY OF IN-FLIGHT FLOW VISUALIZATION OBTAINED FROM THE NASA HIGH ALPHA RESEARCH VEHICLE
David F. Fisher, John H. DelFrate, and Fanny A. Zuniga Jan. 1991 41 p Presented at the High Angle of Attack Technology Symposium, Hampton, VA, 30 Oct. - 1 Nov. 1990
(NASA-TM-101734; H-1686; NAS 1.15:101734) Avail: NTIS HC/MF A03 CSCL 01A

A summary of the surface and off-surface flow visualization results obtained in flight on the F-18 high alpha research vehicle (HARV) is presented, highlighting the extensive 3-D vortical flow on the aircraft at angles of attack up to 50 degs. The emitted fluid technique, as well as tufts and flow cones, were used to document the surface flow. A smoke generator system injected smoke into the vortex cores generated by the forebody and leading edge extensions (LEXs). Documentation was provided by onboard still and video, by air-to-air, and by postflight photography. The surface flow visualization techniques revealed laminar separation bubbles near the forebody apex, lines of separation on the forebody and LEX, and regions of attached and separated flow on the wings and fins. The off-surface flow visualization techniques showed the path of the vortex cores on the forebody and LEX as well as the LEX vortex core breakdown location. An interaction between the forebody and LEX vortices was noted. The flow over the surfaces of the vertical tail was categorized into regions of attached, unsteady, or separated flow using flow tufts. Author

N91-19056*# Sverdrup Technology, Inc., Brook Park, OH.
ONGOING DEVELOPMENT OF A COMPUTER JOBSTREAM TO PREDICT HELICOPTER MAIN ROTOR PERFORMANCE IN ICING CONDITIONS Final Report
Randall K. Britton Feb. 1991 16 p Proposed for presentation at the 47th Annual Forum and Technology Display, Phoenix, AZ, 6-8 May 1991; sponsored by American Helicopter Society
(Contract NAS3-25266)
(NASA-CR-187076; E-6026; NAS 1.26:187076) Avail: NTIS HC/MF A03 CSCL 01A

Work is currently underway at the NASA Lewis Research Center to develop an analytical method for predicting the performance degradation of a helicopter operating in icing conditions. A brief survey is performed of possibilities available to perform such a calculation along with the reasons for choosing the present approach. A complete description of the proposed jobstream is given as well as a discussion of the present state of the development. Author

N91-19057*# National Aeronautics and Space Administration. Lewis Research Center, Cleveland, OH.
THREE-COMPONENT LASER ANEMOMETER MEASUREMENT SYSTEMS
Louis J. Goldman Washington Jan. 1991 20 p
(NASA-TP-3080; E-5526; NAS 1.60:3080) Avail: NTIS HC/MF A03 CSCL 01A

A brief overview of the different laser anemometer (LA) optical designs available is presented. Then, the LA techniques that can be used to design a three-component measurement system for annular geometries are described. Some of the facility design considerations unique to these LA systems are also addressed. Following this, the facilities and the LA systems that were used to successfully measure the three components of velocity in the blading of annular-flow machines are reviewed. Finally, possible LA system enhancements and future research directions are presented. Author

N91-19058*# National Aeronautics and Space Administration. Ames Research Center, Moffett Field, CA.
PANEL METHODS: AN INTRODUCTION
Larry L. Erickson Washington Dec. 1990 64 p
(NASA-TP-2995; A-89266; NAS 1.60:2995) Avail: NTIS HC/MF A04 CSCL 01A

Panel methods are numerical schemes for solving (the Prandtl-Glauert equation) for linear, inviscid, irrotational flow about aircraft flying at subsonic or supersonic speeds. The tools at the panel-method user's disposal are (1) surface panels of source-doublet-vorticity distributions that can represent nearly arbitrary geometry, and (2) extremely versatile boundary condition capabilities that can frequently be used for creative modeling. Panel-method capabilities and limitations, basic concepts common to all panel-method codes, different choices that were made in the implementation of these concepts into working computer programs, and various modeling techniques involving boundary conditions, jump properties, and trailing wakes are discussed. An approach for extending the method to nonlinear transonic flow is also presented. Three appendices supplement the main test. In appendix 1, additional detail is provided on how the basic concepts are implemented into a specific computer program (PANAIR). In appendix 2, it is shown how to evaluate analytically the fundamental surface integral that arises in the expressions for influence-coefficients, and evaluate its jump property. In appendix 3, a simple example is used to illustrate the so-called finite part of the improper integrals. Author

N91-19059*# Sverdrup Technology, Inc., Brook Park, OH.
SOLAR ROCKET PLUME/MIRROR INTERACTIONS Final Report
Sheng-Tao Yu, Chau-Lyan Chang, and Charles L. Merkle (Pennsylvania State Univ., University Park.) Jan. 1991 26 p Previously announced in IAA as A86-42639
(Contracts NAS3-25266; F04611-84-C-0028)
(NASA-CR-185300; E-5774; NAS 1.26:185300) Avail: NTIS HC/MF A03 CSCL 01A

The extent to which the plume from a solar thermal rocket will impinge on the solar collector is studied by flow field analysis. Such interaction can adversely affect collector performance through fouling, excessive heat loading, or pressure loads that deform the delicate structures. The geometrical shape of the collector is such that only the flow from the nozzle boundary layer can reach it, but the thrust levels of interest lead to very viscous nozzle flows

with thick boundary layers. Reasonable accuracy in solving these flows requires a fully coupled viscous-inviscid procedure. Results show that the fraction of the plume that hits the collector can be well estimated by continuum theory, but that transitional and rarefied phenomena will have some impact on how it is distributed over the surface. Initial results for one representative condition show that approx. 4 percent of the total flow in the jet makes its way to the collector. The pressures on the collector, however, remain quite low because of its distance from the engine. Additional work is needed to document the effect of thrust scaling and wall cooling on impingement. Author

N91-19060*# Analytical Methods, Inc., Redmond, WA.
A NOVEL POTENTIAL/VISCOUS FLOW COUPLING TECHNIQUE FOR COMPUTING HELICOPTER FLOW FIELDS
J. Michael Summa, Daniel J. Strash, and Sungyul Yoo Aug. 1990 39 p Original contains color illustrations
(Contract NAS2-12962)
(NASA-CR-177568; A-90283; NAS 1.26:177568) Avail: NTIS HC/MF A03; 3 functional color pages CSCL 01A

Because of the complexity of helicopter flow field, a zonal method of analysis of computational aerodynamics is required. Here, a new procedure for coupling potential and viscous flow is proposed. An overlapping, velocity coupling technique is to be developed with the unique feature that the potential flow surface singularity strengths are obtained directly from the Navier-Stokes at a smoother inner fluid boundary. The closed-loop iteration method proceeds until the velocity field is converged. This coupling should provide the means of more accurate viscous computations of the near-body and rotor flow fields with resultant improved analysis of such important performance parameters as helicopter fuselage drag and rotor airloads. Author

N91-19061*# National Aeronautics and Space Administration. Langley Research Center, Hampton, VA.
A FINITE REYNOLDS NUMBER APPROACH FOR THE PREDICTION OF BOUNDARY LAYER RECEPTIVITY IN LOCALIZED REGIONS
Meelan Choudhari (High Technology Corp., Hampton, VA.) and Craig L. Street Jan. 1991 46 p
(Contract NAS1-18240)
(NASA-TM-102781; NAS 1.15:102781) Avail: NTIS HC/MF A03 CSCL 01A

Previous theoretical work on the boundary layer receptivity problem has utilized large Reynolds number asymptotic theories, thus being limited to a narrow part of the frequency - Reynolds number domain. An alternative approach is presented for the prediction of localized instability generation which has a general applicability, and also accounts for finite Reynolds number effects. This approach is illustrated for the case of Tollmien-Schlichting wave generation in a Blasius boundary layer due to the interaction of a free stream acoustic wave with a region of short scale variation in the surface boundary condition. The specific types of wall inhomogeneities studied are: regions of short scale variations in wall suction, wall admittance, and wall geometry (roughness). Extensive comparison is made between the results of the finite Reynolds number approach and previous asymptotic predictions, which also suggests an alternative way of using the latter at Reynolds numbers of interest in practice. Author

N91-19062*# National Aeronautics and Space Administration. Ames Research Center, Moffett Field, CA.
AN EXPERIMENTAL STUDY OF THE TURBULENT BOUNDARY LAYER ON A TRANSPORT WING IN SUBSONIC AND TRANSONIC FLOW
Frank W. Spaid, Frederick W. Roos (McDonnell-Douglas Research Labs., Saint Louis, MO.), and Raymond M. Hicks Aug. 1990 78 p Contains MF as supplement
(NASA-TM-102206; A-89194; NAS 1.15:102206) Avail: NTIS HC/MF A05 CSCL 01A

The upper surface boundary layer on a transport wing model was extensively surveyed with miniature yaw probes at a subsonic and a transonic cruise condition. Additional data were obtained at a second transonic test condition, for which a separated region was present at mid-semispan, aft of mid-chord. Significant variation in flow direction with distance from the surface was observed near the trailing edge except at the wing root and tip. The data collected at the transonic cruise condition show boundary layer growth associated with shock wave/boundary layer interaction, followed by recovery of the boundary layer downstream of the shock. Measurements of fluctuating surface pressure and wingtip acceleration were also obtained. The influence of flow field unsteadiness on the boundary layer data is discussed. Comparisons among the data and predictions from a variety of computational methods are presented. The computed predictions are in reasonable agreement with the experimental data in the outboard regions where 3-D effects are moderate and adverse pressure gradients are mild. In the more highly loaded mid-span region near the trailing edge, displacement thickness growth was significantly underpredicted, except when unrealistically severe adverse pressure gradients associated with inviscid calculations were used to perform boundary layer calculations. Author

N91-19063*# National Aeronautics and Space Administration. Lewis Research Center, Cleveland, OH.
DEVELOPMENT OF A LASER-INDUCED HEAT FLUX TECHNIQUE FOR MEASUREMENT OF CONVECTIVE HEAT TRANSFER COEFFICIENTS IN A SUPERSONIC FLOWFIELD
A. Robert Porro, Theo G. Keith, Jr. (Toledo Univ., OH.), Warren R. Hingst, Randall M. Chriss, and Kirk D. Seablom Mar. 1991 60 p
(NASA-TM-103778; E-6049; NAS 1.15:103778) Avail: NTIS HC/MF A04 CSCL 01A

A technique is developed to measure the local convective heat transfer coefficient on a model surface in a supersonic flow field. The technique uses a laser to apply a discrete local heat flux at the model test surface, and an infrared camera system determines the local temperature distribution due to heating. From this temperature distribution and an analysis of the heating process, a local convective heat transfer coefficient is determined. The technique was used to measure the load surface convective heat transfer coefficient distribution on a flat plate at nominal Mach numbers of 2.5, 3.0, 3.5, and 4.0. The flat plate boundary layer initially was laminar and became transitional in the measurement region. The experimental results agreed reasonably well with theoretical predictions of convective heat transfer of flat plate laminar boundary layers. The results indicate that this non-intrusive optical measurement technique has the potential to obtain high quality surface convective heat transfer measurements in high speed flowfields. Author

N91-19064# Sandia National Labs., Albuquerque, NM.
THE DEVELOPMENT OF A RAM AIR DECELERATOR FOR THE RECOVERY OF ARTILLERY SHELLS
V. L. Behr, J. K. Cole, and R. H. Croll 1991 8 p Presented at the 11th AIAA Aerodynamic Decelerator Systems Technology Conference, San Diego, 9-11 Apr. 1991
(Contract DE-AC04-76DP-00789)
(DE91-007732; SAND-90-2220C; CONF-9104171-2) Avail: NTIS HC/MF A02

Sandia National Laboratories is responsible for the design of recovery systems for atomic artillery shells that are periodically tested by artillery firings. It is desirable to have a recovery system that exhibits a high degree of reliability due to the costs associated with each test shell. A Ram Air Decelerator (RAD) has been investigated as a candidate replacement for the current parachute recovery system. Tests have included proof-of-concept tests on a truck towing rig, non-spinning airdrop tests, spin tests in a high altitude chamber and artillery fired projectile tests. Although testing had to be terminated before the program could be completed, significant strides were made in RAD design for this harsh environment. Possible design improvements were identified for future testing should the program be revived. DOE

N91-19065# Sandia National Labs., Albuquerque, NM.
THE DESIGN AND FLIGHT TESTING OF A HIGH-PERFORMANCE LOW-COST PARACHUTE SYSTEM FOR A 1000 lb PAYLOAD
V. L. Behr 1991 8 p Presented at the 11th AIAA Aerodynamic Decelerator Systems Technology Conference, San Diego, 9-11 Apr. 1991
(Contract DE-AC04-76DP-00789)
(DE91-007733; SAND-90-2113C; CONF-9104171-1) Avail: NTIS HC/MF A02

An airdrop system is being developed by Sandia National Laboratories for the U.S. Army which is to be delivered as low as 300 ft above ground level and at speeds as high as Mach 0.95. The development of the system includes both the vehicle and the parachute recovery system. The gross weight of the vehicle when dropped is approximately 950 lbs. The parachute system employs an aerodynamically deployed tailplate, a reefed and staged drogue parachute, and a cluster of three main parachutes. The three main parachutes are T-10 personnel parachutes. The use of these parachutes will help minimize the cost of the parachute system. This system has been both ground and flight tested. This paper stresses the results of the flight test program and the impact those results had on the design of the parachute system. DOE

N91-19066# National Aerospace Lab., Tokyo (Japan).
RESULT OF ONERA STANDARD MODEL TEST IN 2m X 2m TRANSONIC WIND TUNNEL
H. Sawada, K. Suzuki, M. Nakamura, M. Suzuki, Y. Komatsu, and A. Koike Mar. 1990 28 p In JAPANESE
(DE91-750115; NAL-TM-616) Avail: NTIS HC/MF A03

Wind tunnel test under the international correspondence between Japan and France are reported. In the past, when test was made in a 2 x 2 m transonic wind tunnel (TWT) in the National Aerospace Laboratory (NAL), by use of a standard model NAL-M5, reproduced from the drawing, drawn by the ONERA, France, discrepancy existed in a part of pressure distribution from the ONERA data. The heightening in pressure was sluggish by the wing surface impact wave at the same elevation angle. Discrepancy existed in lift coefficient (C sub L)-pitching moment (C sub m) curve. In C sub L-elevation angle of model alpha curve, C sub L alpha was measured to be large with an early appearance of stall phenomenon. To solve those points of problem, test was made by having borrowed models M5 and M2, similar to those of ONERA standard. The discrepancy in data was elucidated to be caused by error in measurement, difference in compared condition and difference between both the models NAL-M5 and ONERA-M5. The C sub L-alpha curve and C sub L-C sub m curve of ONERA-M2 agrees well with those, adjusted in lift interference, of test result by ONERA-M5. Discrepancy exists in C sub L-drag coefficient (C sub D) curve, which necessitates the model M5 data to be adjusted. DOE

N91-19067*# Continuum Dynamics, Inc., Princeton, NJ.
A NEW METHODOLOGY FOR FREE WAKE ANALYSIS USING CURVED VORTEX ELEMENTS Final Report
Donald B. Bliss, Milton E. Teske, and Todd R. Quackenbush Washington Dec. 1987 137 p
(Contract NAS2-11295)
(NASA-CR-3958; NAS 1.26:3958; CDI-84-6) Avail: NTIS HC/MF A07 CSCL 01A

A method using curved vortex elements was developed for helicopter rotor free wake calculations. The Basic Curve Vortex Element (BCVE) is derived from the approximate Biot-Savart integration for a parabolic arc filament. When used in conjunction with a scheme to fit the elements along a vortex filament contour, this method has a significant advantage in overall accuracy and efficiency when compared to the traditional straight-line element approach. A theoretical and numerical analysis shows that free wake flows involving close interactions between filaments should utilize curved vortex elements in order to guarantee a consistent level of accuracy. The curved element method was implemented into a forward flight free wake analysis, featuring an adaptive far wake model that utilizes free wake information to extend the vortex filaments beyond the free wake regions. The curved vortex element free wake, coupled with this far wake model, exhibited rapid convergence, even in regions where the free wake and far wake turns are interlaced. Sample calculations are presented for tip vortex motion at various advance ratios for single and multiple blade rotors. Cross-flow plots reveal that the overall downstream wake flow resembles a trailing vortex pair. A preliminary assessment shows that the rotor downwash field is insensitive to element size, even for relatively large curved elements. Author

N91-19068# Bristol Univ. (England). Dept. of Aerospace Engineering.
THE EFFECT OF BODY SHAPE ON THE DEVELOPMENT OF VORTEX ASYMMETRY IN THE FLOW PAST SLENDER BODIES
A. L. Williams Jun. 1990 28 p
(BU-413; ETN-91-98864) Avail: NTIS HC/MF A03

The vortex sheet model originally described by Legendre and developed by Smith is applied to the study of inviscid separated flow past slender bodies with rounded corner 'square' or 'triangular' cross sections. The effect of the cross sectional shape and orientation on asymmetry is examined. The simplified case of conical flow is considered in detail, whilst preliminary results from a non conical model are also included. The existence of symmetric and asymmetric vortices above a cone of 'square' cross section is confirmed using a laser light sheet to illuminate cross flow planes along the slender body. ESA

N91-19069# Technische Univ., Delft (Netherlands). Dept. of Aerospace Engineering.
THE BEHAVIOUR OF FLUX-DIFFERENCE AND FLUX-VECTOR SPLITTING METHODS IN EXPLICIT SCHEMES FOR HYPERSONIC BLUNT BODY FLOW
A. C. J. Venis Sep. 1990 38 p
(LR-643; ETN-91-98944) Avail: NTIS HC/MF A03

A survey of the behavior of the flux difference and flux vector splitting methods is given. The schemes of Roe, van Leer, and Hanel are examined for a 2-D, inviscid, hypersonic blunt body flow of a perfect gas. It appears that on fine meshes Roe's scheme is not dissipative enough to sufficiently damp errors in the solution. A modified entropy correction with a properly dosed amount of numerical viscosity is needed to avoid the generation of physically unrealistic solutions and to provide convergence on fine meshes. The schemes of van Leer and Hanel perform well on the fine meshes. The Hanel scheme offers a better preservation of total enthalpy. For the present test problem, the use of the critical speed of sound in the scheme of Hanel could not be confirmed to be more approriate that the static speed of sound used in van Leer's original scheme. Difficulties related to the incorrect calculation of thermodynamic quantities existed at high CFL numbers less than one where the integration scheme becomes unstable. All three numerical flux formulations exhibit this behavior. The present results do not withstand the experience as reported by other authors. ESA

N91-19070# Oxford Univ. (England).
PITOT MEASUREMENTS IN THE EXHAUST OF A CLUSTER OF FOUR SMALL SCALE SUPERSONIC NOZZLES
T. M. Cain and T. V. Jones 1990 21 p Sponsored by Ministry of Defence Procurement Executive, London, England
(OUEL-1862/90; ETN-91-98960) Avail: NTIS HC/MF A03

The variation of pitot pressure along the axis of symmetry of four interacting underexpanded jets is measured at two different stagnation to background pressure ratios. Three of the nozzles are then blocked and the variation of Pitot pressure on the axis of a single nozzle plume is obtained. The single plume result is well predicted by a conical flow model, and the quadruple plume results are in reasonble agreement with analytical calculations based on a well known source model. Schlieren photographs of the quadruple plumes that demonstrate that the interaction shock shapes are independent of pressure ratio are presented. ESA

N91-19071# California Inst. of Tech., Pasadena. Graduate Aeronautical Labs.
RESEARCH ON BLUFF-BODY VORTEX WAKES Annual Report
Anatol Roshko and Anthony Leonard 1 Dec. 1990 5 p
(Contract N00014-90-J-1589)
(AD-A229875) Avail: NTIS HC/MF A01 CSCL 20/4

A computational technique, based on two dimensional vortex methods, was developed to study unsteady flows past flat plates with large-scale separation and in the RE range of 10,000. The technique captures the actual scale of the vortex sheets as they emerge from the edges of the plate. This scale defines the flow Reynolds number. The accuracy of the method was verified by comparison with tow-tanks measurements of time-dependent drag during a ramp start, comparison with theoretical results of Pullin on the time-dependent vortex circulation after an impulsive start, and comparison with experiment of the growth of the recirculation bubble before flow asymmetry begins. An experiment has been initiated in our 20 X 20 in. wind tunnel. Behind circular cylinders or the bluff cylinders spanning the tunnel, solid splitter plates or screens (open splitter plates) can be installed. Preliminary measurements show the expected effect of the screen splitter, i.e., reduction of drag but not so much as for a solid splitter. Variations with Reynolds number were observed. GRA

03 AIR TRANSPORTATION AND SAFETY

Includes passenger and cargo air transport operations; and aircraft accidents.

For related information see also *16 Space Transportation* and *85 Urban Technology and Transportation.*

N91-19072 Department of the Navy, Washington, DC.
COLLISION DETECTION SYSTEM Patent
Randall D. Cope, inventor (to Navy) and Mark P. Egan, inventor (to Navy) 21 Aug. 1990 11 p Filed 26 Jun. 1989
(AD-D014645; US-Patent-4,951,056; US-Patent-Appl-SN-374127; US-Patent-Class-342-29) Avail: US Patent and Trademark Office CSCL 17/9

The detection, by Doppler frequencies in reflected wave energy, of an object, such as an obstruction on a landing surface approached along a path at a shallow angle to the surface, using Doppler frequencies returned from a fixed range. The frequencies returned by the surface and the obstruction are distinguished by their relation to a threshold frequency determined by the velocity along the path and the angle. Returns from the surface as the angle of incidence at the fixed range increases from the initial normal angle of incidence are minimized by selection of the carrier frequency, and clutter is rejected by ignoring a return at the fixed range that does not correspond to a subsequent return at a nearer range. GRA

N91-19073*# National Aeronautics and Space Administration. Langley Research Center, Hampton, VA.
ROBUST FAULT DIAGNOSIS OF PHYSICAL SYSTEMS IN OPERATION Ph.D. Thesis - Rutgers - The State Univ.
Kathy Hamilton Abbott Jan. 1991 166 p
(NASA-TM-102767; NAS 1.15:102767) Avail: NTIS HC/MF A08 CSCL 01C

Ideas are presented and demonstrated for improved robustness in diagnostic problem solving of complex physical systems in operation, or operative diagnosis. The first idea is that graceful degradation can be viewed as reasoning at higher levels of abstraction whenever the more detailed levels proved to be incomplete or inadequate. A form of abstraction is defined that applies this view to the problem of diagnosis. In this form of abstraction, named status abstraction, two levels are defined. The lower level of abstraction corresponds to the level of detail at which most current knowledge-based diagnosis systems reason. At the higher level, a graph representation is presented that describes the real-world physical system. An incremental, constructive approach to manipulating this graph representation is demonstrated that supports certain characteristics of operative diagnosis. The suitability of this constructive approach is shown for diagnosing fault propagation behavior over time, and for sometimes diagnosing systems with feedback. A way is shown to represent different semantics in the same type of graph representation to characterize different types of fault propagation behavior. An approach is demonstrated that threats these different behaviors as different fault classes, and the approach moves to other classes when previous classes fail to generate suitable hypotheses. These ideas are implemented in a computer program named Draphys (Diagnostic Reasoning About Physical Systems) and demonstrated for the domain of inflight aircraft subsystems, specifically a propulsion system (containing two turbofan systems and a fuel system) and hydraulic subsystem. Author

N91-19074*# Continuum Dynamics, Inc., Princeton, NJ.
FEASIBILITY OF AN ONBOARD WAKE VORTEX AVOIDANCE SYSTEM Final Report
Alan J. Bilanin, Milton E. Teske, and Howard C. Curtiss, Jr. Apr. 1987 80 p
(Contracts NAS1-17742; DTRS-57-85-C-000123)
(NASA-CR-187521; NAS 1.26:187521; CDI-87-02) Avail: NTIS HC/MF A05 CSCL 01C

It was determined that an onboard vortex wake detection system using existing, proven instrumentation is technically feasible. This system might be incorporated into existing onboard systems such as a wind shear detection system, and might provide the pilot with the location of a vortex wake, as well as an evasive maneuver so that the landing separations may be reduced. It is suggested that this system might be introduced into our nation's commuter aircraft fleet and major air carrier fleet and permit a reduction of current landing separation standards, thereby reducing takeoff and departure delays. Author

N91-19075# MiTech, Inc., Washington, DC.
THE 1990-1991 AVIATION SYSTEM CAPACITY PLAN Report, Jul. 1989 - Jun. 1990
Sep. 1990 312 p
(Contract DTFA01-89-Y-01047)
(AD-A229863) Avail: NTIS HC/MF A14 CSCL 01/3

This is a comprehensive review of the Federal Aviation Administration's program to improve the capacity of the National Air Transportation System. The Plan identifies the causes and extent of capacity and delay problems currently associated with air travel in the U.S., and outlines various planned and ongoing FAA projects that will reduce the severity of the problem in the future. The major areas of discussion are: (1) Airport Development; (2) Airport and Airspace Capacity Improvement; (3) Technological Improvements; and (4) Marketplace Solutions. GRA

N91-19028*# Ohio Univ., Athens. Dept. of Electrical and Computer Engineering.
INVESTIGATION OF AIR TRANSPORTATION TECHNOLOGY AT OHIO UNIVERSITY, 1989-1990
Robert W. Lilley *In* NASA, Langley Research Center, Joint University Program for Air Transportation Research, 1989-1990 Dec. 1990 p 61-66 (For primary document see N91-19024 11-01)
Avail: NTIS HC/MF A09 CSCL 01A

N91-19033*# Princeton Univ., NJ. Dept. of Mechanical and Aerospace Engineering.
INVESTIGATION OF AIR TRANSPORTATION TECHNOLOGY AT PRINCETON UNIVERSITY, 1989-1990
Robert F. Stengel *In* NASA, Langley Research Center, Joint University Program for Air Transportation Research, 1989-1990 Dec. 1990 p 105-118 (For primary document see N91-19024 11-01)
Avail: NTIS HC/MF A09 CSCL 01A

N91-19034*# Princeton Univ., NJ.
PROGRESS ON INTELLIGENT GUIDANCE AND CONTROL FOR WIND SHEAR ENCOUNTER
D. Alexander Stratton *In* NASA, Langley Research Center, Joint University Program for Air Transportation Research, 1989-1990 Dec. 1990 p 119-131 (For primary document see N91-19024 11-01)
Avail: NTIS HC/MF A09 CSCL 01A

04 AIRCRAFT COMMUNICATIONS AND NAVIGATION

Includes digital and voice communication with aircraft; air navigation systems (satellite and ground based); and air traffic control.

For related information see also *17 Space Communications, Spacecraft Communications, Command and Tracking* and *Communications and Radar.*

N91-19026*# Massachusetts Inst. of Tech., Cambridge. Flight Transportation Lab.
THE TEMPORAL LOGIC OF THE TOWER CHIEF SYSTEM
Lyman R. Hazelton, Jr. *In* NASA, Langley Research Center, Joint University Program for Air Transportation Research, 1989-1990 Dec. 1990 p 15-28 (For primary document see N91-19024 11-01)
(Grant NGL-22-009-640)
Avail: NTIS HC/MF A09 CSCL 17G

N91-19027*# Massachusetts Inst. of Tech., Cambridge.
BUBBLES: AN AUTOMATED DECISION SUPPORT SYSTEM FOR FINAL APPROACH CONTROLLERS
Zhizang Chi *In* NASA, Langley Research Center, Joint University Program for Air Transportation Research, 1989-1990 Dec. 1990 p 29-36 (For primary document see N91-19024 11-01)
Avail: NTIS HC/MF A09 CSCL 17G

N91-19029*# Ohio Univ., Athens.
RIDGE REGRESSION SIGNAL PROCESSING
Mark R. Kuhl *In* NASA, Langley Research Center, Joint University Program for Air Transportation Research, 1989-1990 Dec. 1990 p 67-75 (For primary document see N91-19024 11-01)
Avail: NTIS HC/MF A09 CSCL 17G

N91-19030*# Ohio Univ., Athens.
MODELING SELECTIVE AVAILABILITY OF THE NAVSTAR GLOBAL POSITIONING SYSTEM
Michael Braasch *In* NASA, Langley Research Center, Joint University Program for Air Transportation Research, 1989-1990 Dec. 1990 p 77-89 (For primary document see N91-19024 11-01)
Avail: NTIS HC/MF A09 CSCL 17G

N91-19032*# Ohio Univ., Athens.
INTEGRATED INERTIAL/GPS
Paul Kline and Frank vanGraas *In* NASA, Langley Research Center, Joint University Program for Air Transportation Research, 1989-1990 Dec. 1990 p 97-103 (For primary document see N91-19024 11-01)
Avail: NTIS HC/MF A09 CSCL 17G

05 AIRCRAFT DESIGN, TESTING AND PERFORMANCE

Includes aircraft simulation technology.

For related information see also *18 Spacecraft Design, Testing and Performance* and *39 Structural Mechanics.*For land transportation vehicles see *85 Urban Technology and Transportation.*

N91-19076 Department of the Navy, Washington, DC.
WIRE-FREE ARMING SYSTEM FOR AN AIRCRAFT-DELIVERED BOMB Patent
Brent A. Teeter, inventor (to Navy) 26 Jun. 1990 15 p Filed 20 Apr. 1989
(AD-D014611; US-Patent-4,936,187; US-Patent-Appl-SN-341598; US-Patent-Class-89-1.55) Avail: US Patent and Trademark Office CSCL 09/1

A system for wire free arming of a bomb releasably carried by an aircraft bomb rack includes an emitter circuit mounted on the bomb rack, and an electrical power generator circuit, a detector circuit, and an arming circuit mounted on the bomb. The emitter circuit on the bomb rack is activated when the aircraft pilot releases the bomb. The emitter circuit emits a predetermined transmission of electromagnetic energy, such as an infrared pulse train or a pulsed magnetic field, in the direction of the bomb rack and bomb. The electrical power generator circuit on the bomb is activated by release of the bomb for generating electrical power as the released bomb separates from the aircraft bomb rack and produces an output power signal after release of the bomb from the bomb rack. The detector circuit on the bomb is responsive to the output power signal from the generator circuit and to the detection of the emitted transmission from the emitter circuit for producing an arming signal. The arming circuit is responsive to the output power signal from the generator circuit and to the arming signal from the detector circuit for producing arming of the bomb. GRA

N91-19077*# National Aeronautics and Space Administration. Ames Research Center, Moffett Field, CA.
SINGLE-STRAIN-GAGE FORCE/STIFFNESS BUCKLING PREDICTION TECHNIQUES ON A HAT-STIFFENED PANEL
Larry D. Hudson and Randolph C. Thompson (PRC Systems Services Co., Edwards, CA.) Feb. 1991 21 p Presented at the ASME Structures and Materials Conference, Dallas, TX, 25-30 Nov. 1990
(NASA-TM-101733; H-1660; NAS 1.15:101733) Avail: NTIS HC/MF A03 CSCL 01C

Predicting the buckling characteristics of a test panel is necessary to ensure panel integrity during a test program. A single-strain-gage buckling prediction method was developed on a hat-stiffened, monolithic titanium buckling panel. The method is an adaptation of the original force/stiffness method which requires back-to-back gages. The single-gage method was developed because the test panel did not have back-to-back gages. The method was used to predict buckling loads and temperatures under various heating and loading conditions. The results correlated well with a finite element buckling analysis. The single-gage force/stiffness method was a valid real-time and post-test buckling prediction technique. Author

N91-19078*# National Aeronautics and Space Administration. Ames Research Center, Moffett Field, CA.
INTRODUCTION OF THE M-85 HIGH-SPEED ROTORCRAFT CONCEPT
Robert H. Stroub Jan. 1991 32 p
(NASA-TM-102871; A-90307; NAS 1.15:102871) Avail: NTIS HC/MF A03 CSCL 01C

As a result of studying possible requirements for high-speed rotorcraft and studying many high-speed concepts, a new high-speed rotorcraft concept, designated as M-85, was derived. The M-85 is a helicopter that is reconfigured to a fixed-wing aircraft for high-speed cruise. The concept was derived as an approach to enable smooth, stable conversion between fixed-wing and rotary-wing while retaining hover and low-speed flight

characteristics of a low disk loading helicopter. The name, M-85, reflects the high-speed goals of 0.85 Mach number at high altitude. For a high-speed rotorcraft, it is expected that a viable concept must be a cruise-efficient, fixed-wing aircraft so it may be attractive for a multiplicity of missions. It is also expected that a viable high-speed rotorcraft concept must be cruise efficient first and secondly, efficient in hover. What makes the M-85 unique is the large circular hub fairing that is large enough to support the aircraft during conversion between rotary-wind and fixed-wing modes. With the aircraft supported by this hub fairing, the rotor blades can be unloaded during the 100 percent change in rotor rpm. With the blades unloaded, the potential for vibratory loads would be lessened. In cruise, the large circular hub fairing would be part of the lifting system with additional lifting panels deployed for better cruise efficiency. In hover, the circular hub fairing would slightly reduce lift potential and/or decrease hover efficiency of the rotor system. The M-85 concept is described and estimated forward flight performance characteristics are presented in terms of thrust requirements and L/D with airspeed. The forward flight performance characteristics reflect recent completed wind tunnel tests of the wing concept. Also presented is a control system technique that is critical to achieving low oscillatory loads in rotary-wing mode. Hover characteristics, C(sub p) versus C(sub T) from test data, is discussed. Other techniques pertinent to the M-85 concept such as passively controlling inplane vibration during starting and stopping of the rotor system, aircraft control system, and rotor drive technologies are discussed. Author

N91-19079*# National Aeronautics and Space Administration. Hugh L. Dryden Flight Research Facility, Edwards, CA.
A SIMPLE DYNAMIC ENGINE MODEL FOR USE IN A REAL-TIME AIRCRAFT SIMULATION WITH THRUST VECTORING
Steven A. Johnson Oct. 1990 21 p Presented at the AIAA/SAE/ASME/ASEE Joint Propulsion Conference, Orlando, FL, 16-18 Jul. 1990 Previously announced in IAA as A90-42054
(NASA-TM-4240; H-1643; NAS 1.15:4240; AIAA-90-2166) Avail: NTIS HC/MF A03 CSCL 01C

A simple dynamic engine model was developed at the NASA Ames Research Center, Dryden Flight Research Facility, for use in thrust vectoring control law development and real-time aircraft simulation. The simple dynamic engine model of the F404-GE-400 engine (General Electric, Lynn, Massachusetts) operates within the aircraft simulator. It was developed using tabular data generated from a complete nonlinear dynamic engine model supplied by the manufacturer. Engine dynamics were simulated using a throttle rate limiter and low-pass filter. Included is a description of a method to account for axial thrust loss resulting from thrust vectoring. In addition, the development of the simple dynamic engine model and its incorporation into the F-18 high alpha research vehicle (HARV) thrust vectoring simulation. The simple dynamic engine model was evaluated at Mach 0.2, 35,000 ft altitude and at Mach 0.7, 35,000 ft altitude. The simple dynamic engine model is within 3 percent of the steady state response, and within 25 percent of the transient response of the complete nonlinear dynamic engine model. Author

N91-19080*# National Aeronautics and Space Administration. Hugh L. Dryden Flight Research Facility, Edwards, CA.
TECHNIQUES FOR HOT STRUCTURES TESTING
V. Michael DeAngelis and Roger A. Fields Nov. 1990 28 p Presented at the First Thermal Structures Conference, Charlottesville, VA, 13-15 Nov. 1990 Previously announced in IAA as A91-16035
(NASA-TM-101727; H-1664; NAS 1.15:101727) Avail: NTIS HC/MF A03 CSCL 01C

Hot structures testing have been going on since the early 1960's beginning with the Mach 6, X-15 airplane. Early hot structures test programs at NASA-Ames-Dryden focused on operational testing required to support the X-15 flight test program, and early hot structures research projects focused on developing lab test techniques to simulate flight thermal profiles. More recent efforts involved numerous large and small hot structures test programs that served to develop test methods and measurement techniques to provide data that promoted the correlation of test data with results from analytical codes. In Nov. 1988 a workshop was sponsored that focused on the correlation of hot structures test data with analysis. Limited material is drawn from the workshop and a more formal documentation is provided of topics that focus on hot structures test techniques used at NASA-Ames-Dryden. Topics covered include the data acquisition and control of testing, the quartz lamp heater systems, current strain and temperature sensors, and hot structures test techniques used to simulate the flight thermal environment in the lab. Author

N91-19081*# National Aeronautics and Space Administration. Hugh L. Dryden Flight Research Facility, Edwards, CA.
MONITORING TECHNIQUES FOR THE X-29A AIRCRAFT'S HIGH-SPEED ROTATING POWER TAKEOFF SHAFT
David F. Voracek Dec. 1990 25 p Presented at the 2nd International Machinery Monitoring and Diagnostic Conference, Los Angeles, CA, 22-25 Oct. 1990
(NASA-TM-101731; H-1680; NAS 1.15:101731) Avail: NTIS HC/MF A03 CSCL 01C

The experimental X-29A forward swept-wing aircraft has many unique and critical systems that require constant monitoring during ground or flight operation. One such system is the power takeoff shaft, which is the mechanical link between the engine and the aircraft-mounted accessory drive. The X-29A power takeoff shaft opertes in a range between 0 and 16,810 rpm, is longer than most jet engine power takeoff shafts, and is made of graphite epoxy material. Since the X-29A aircraft operates on a single engine, failure of the shaft during flight could lead to loss of the aircraft. The monitoring techniques and test methods used during power takeoff shaft ground and flight operations are discussed. Test data are presented in two case studies where monitoring and testing of the shaft dynamics proved instrumental in discovering and isolating X-29A power takeoff shaft problems. The first study concerns the installation of an unbalanced shaft. The effect of the unbalance on the shaft vibration data and the procedure used to correct the problem are discussed. The second study deals with the shaft exceeding the established vibration limits during flight. This case study found that the vibration of connected rotating machinery unbalances contributed to the excessive vibration level of the shaft. The procedures used to identify the contributions of other rotating machinery unbalances to the power takeoff shaft unbalance are discussed. Author

N91-19082*# National Aeronautics and Space Administration. Ames Research Center, Moffett Field, CA.
STATE ESTIMATION APPLICATIONS IN AIRCRAFT FLIGHT-DATA ANALYSIS: A USER'S MANUAL FOR SMACK
Ralph E. Bach, Jr. Mar. 1991 134 p
(NASA-RP-1252; A-88203; NAS 1.61:1252) Avail: NTIS HC/MF A07 CSCL 01C

The evolution in the use of state estimation is traced for the analysis of aircraft flight data. A unifying mathematical framework for state estimation is reviewed, and several examples are presented that illustrate a general approach for checking instrument accuracy and data consistency, and for estimating variables that are difficult to measure. Recent applications associated with research aircraft flight tests and airline turbulence upsets are described. A computer program for aircraft state estimation is discussed in some detail. This document is intended to serve as a user's manual for the program called SMACK (SMoothing for AirCraft Kinematics). The diversity of the applications described emphasizes the potential advantages in using SMACK for flight-data analysis. Author

N91-19083*# National Aeronautics and Space Administration. Hugh L. Dryden Flight Research Facility, Edwards, CA.
THERMOELASTIC VIBRATION TEST TECHNIQUES
Michael W. Kehoe and H. Todd Snyder (PRC Kentron, Inc., Edwards, CA.) Apr. 1991 21 p Presented at the 9th International Modal Analysis Conference, Florence, Italy, 14-18 Apr. 1991

(NASA-TM-101742; H-1707; NAS 1.15:101742) Avail: NTIS HC/MF A03 CSCL 01C

The structural integrity of proposed high speed aircraft can be seriously affected by the extremely high surface temperatures and large temperature gradients throughout the vehicle's structure. Variations in the structure's elastic characteristics as a result of thermal effects can be observed by changes in vibration frequency, damping, and mode shape. Analysis codes that predict these changes must be correlated and verified with experimental data. The experimental modal test techniques and procedures used to conduct uniform, nonuniform, and transient thermoelastic vibration tests are presented. Experimental setup and elevated temperature instrumentation considerations are also discussed. Modal data for a 12 by 50 inch aluminum plate heated to a temperature of 475 F are presented. These data show the effect of heat on the plate's modal characteristics. The results indicated that frequency decreased, damping increased, and mode shape remained unchanged as the temperature of the plate was increased.

Author

N91-19084# Messerschmitt-Boelkow-Blohm G.m.b.H., Munich (Germany, F.R.).

PROPULSION SYSTEM CONCEPT FOR THE EUROFAR TILT ROTOR AIRCRAFT

Axel Fischer and Josef Unterhitzenberger Sep. 1990 13 p Presented at the 16th European Rotorcraft Forum, Glasgow, Scotland, 18-21 Sep. 1990

(MBB-UD-0573-90-PUB; ETN-91-98823) Avail: NTIS HC/MF A03

A three year preliminary working phase is being carried out in order to define the baseline for the European tilt rotor aircraft Eurofar. This program is commonly conducted by the following European partners: Aerospatiale (France), Augusta (Italy), Casa (Spain), Westland (U.K.) and MBB (Germany). A vital part of the tiltrotor aircraft is the propulsion system. In contrast to the American V22 tiltrotor (completely tiltable propulsion nacelles) the Eurofar team has mainly concentrated on a nacelle concept with stationary engines. A first overview about findings gained up to now is given as well as the current status of design investigations comprising: tilt concepts; propulsion nacelle arrangement; main gearbox design; cross shaft design; engine; and nacelle structure design. ESA

N91-19085# Messerschmitt-Boelkow-Blohm G.m.b.H., Munich (Germany, F.R.). Helicopter Div.

BO 108 DEVELOPMENT STATUS AND PROSPECTS

Helmut Huber and Werner Reinl Sep. 1990 12 p Presented at the 16th European Rotorcraft Forum, Glasgow, Scotland, 18-21 Sep. 1990

(MBB-UD-0574-90-PUB; ETN-91-98824) Avail: NTIS HC/MF A03

In 1983, the MBB helicopter division started design and development of a new light twin, multipurpose helicopter, now designated as the BO 108. After an intensive phase of technology investment, many technology advances were incorporated into the design, in order to meet the demanding requirements of the future market. The aircraft (prototype 1) flew for the first time in October 1988, and has accomplished about 110 flight test hours so far. The design philosophy is illustrated and the technology advances in terms of the various components involved are reviewed. An overview about the current status of bench and inflight testing are reviewed, and the progress achieved in the fields of performance, flying qualities, noise and vibrations, weight, reliability, and safety is assessed. Activities for increasing the aircraft's capabilities are described and a prospective about the future program plans is given. ESA

N91-19086# Messerschmitt-Boelkow-Blohm G.m.b.H., Munich (Germany, F.R.).

DEVELOPMENT OF BEARINGLESS TAIL ROTORS

Valentin Kloeppel, Helmut Huber, and Bernhard Enenkl Sep. 1990 15 p Presented at the 16th European Rotorcraft Forum, Glasgow, Scotland, 18-21 Sep. 1990

(MBB-UD-0575-90-PUB; ETN-91-98825) Avail: NTIS HC/MF A03

Conventional helicopter Tail Rotors (CTR) represent a highly efficient but complex control concept. They provide uniquely low power requirements and outstanding controllability. On the other hand, they often imply problems with respect to maintenance efforts and lifetime. The key for overcoming such problems is the application of new composite materials which, for several reasons, is particularly attractive for tail rotors. This enables a new design solution in the form of the bearingless tail rotor (BTR). An overview of the development and tests of advanced composite tail rotors since the late 1970's and early 1980's is given. After the discussion of general design aspects, the layout structural design and testing of several bearingless prototypes are demonstrated. Emphasis is also on the assessment of relevant technological criteria, such as weight, manufacturing costs, maintenance effort, reliability, and vulnerability. A view is taken of the BTR's potential for further development and its application to future product range. ESA

N91-19087# Messerschmitt-Boelkow-Blohm G.m.b.H., Munich (Germany, F.R.). Henschel Flugzeug-Werke.

DESIGN AND FIRST TESTS OF INDIVIDUAL BLADE CONTROL ACTUATORS

Peter Richter, Hans-Dieter Eisbrecher, and Valentin Kloeppel Sep. 1990 10 p Presented at the 16th European Rotorcraft Forum, Glasg, Scotland, 18-21 Sep. 1990

(MBB-UD-0577-90-PUB; ETN-91-98827) Avail: NTIS HC/MF A02

In order to increase the helicopter's share in future air traffic, its efficiency, reliability and its public acceptance have to be improved. Using modern technologies it is possible to reduce weight, power requirement, noise, pilot's workload and maintenance efforts and to increase comfort and flight envelope. One tool to realize a relevant part of these goals is the Higher Harmonic Control (HHC) but it is only possible to superimpose some selected harmonic functions to the 1/rev input. By means of a new control system using actuators between swashplate and rotor blade, the total range of superimposition from single harmonic control up to individual blade control can be opened. Such a new control system was designed. Tests were carried out on test benches and on a whirl tower before flight tests on a BO 105 started. The results of these tests are shown and an outlook to the planned program continuation is given. ESA

N91-19088# Messerschmitt-Boelkow-Blohm G.m.b.H., Munich (Germany, F.R.).

CRASHWORTHINESS INVESTIGATIONS IN THE PRELIMINARY DESIGN PHASE OF THE NH90

Dieter Nitschke and Johannes Frese Sep. 1990 11 p Presented at the 16th European Rotorcraft Forum, Glasgow, Scotland, 18-21 Sep. 1990

(MBB-UD-0579-90-PUB; ETN-91-98829) Avail: NTIS HC/MF A03

After the introduction of MIL STD 1290, several helicopters like the AH64 Apache and the UH60 Black Hawk were built in accordance with the whole range of requirements of that standard. The primary structure of the first generation of crashworthy helicopters consisted more or less completely of metal. In the meantime, more experience has been gathered which led to a reduction of crash requirements as well as to the application of new structural materials. Therefore, new helicopters like the Tiger (PAH2/HAP/HAC) and the NH90 are designed to a 90 and 85 percent fulfilment of MIL STD 1290 respectively. After some technology programs (ACAP, BK 117 composite airframe), they are the first helicopters whose primary fuselage structure consists nearly completely of composites: like Carbon Fiber reinforced plastic (CFRP) or Aramid Fiber Reinforced Plastic (AFRP). To identify problem areas and to verify the present design concept, simulations with KRASH85 were performed for the NH90. Due to the early state of the program, a simplified two dimensional model was judged to be the best compromise between effort and accuracy of results. After some iterations a quite good representation of the structure was found and parametric studiesGRere performed

under consideration of the main crash features of composites like high specific energy absorption, lack of ductility and higher susceptibility to the loss of structural integrity in areas of energy absorption. The high potential crashworthiness of the NH90 was confirmed and the main crash design parameters were determined. ESA

N91-19089# Messerschmitt-Boelkow-Blohm G.m.b.H., Munich (Germany, F.R.). Helicopter Div.
NEW COMPUTER CODES FOR THE STRUCTURAL ANALYSIS OF COMPOSITE HELICOPTER STRUCTURES
Helmut Rapp Sep. 1990 14 p Presented at the 16th European Rotorcraft Forum, Glasgow, Scotland, 18-21 Sep. 1990
(MBB-UD-0580-90-PUB; ETN-91-98830) Avail: NTIS HC/MF A03

Helicopters of the new generation will show a very high portion of structural components made of fiber composites. To take the best advantage of these materials, modern tools for structural design and analysis are necessary. With methods of structural optimization at panel level already in early design phases the best fiber orientation and laminate thicknesses can be chosen. By means of a helicopter fuselage sidewall and a sandwich panel of the horizontal stabilizer, it is shown that large weight savings can be achieved with optimal laminates. Combination of composite materials with very different Poisson's ratios in bar like components result in additional stresses perpendicular to the load direction, which may have a noticeable influence in the tension and bending stiffness. The basic theory is given and a special testbar shows the large influence these stresses may have. Investigations of a helicopter rotor blade as a typical application of such a nonhomogeneous structural part; however, shows that in this case the influence of the additional stresses is small. In future helicopter projects thickwalled composite parts for rotor components are often used. The stress and stiffness evaluation of such components require finite element analysis. To reduce the necessary effort, a computer code was developed to determine the material properties of a thick laminate and to evaluate the stresses in a single layer of this laminate due to membrane and bending forces. ESA

N91-19090# Messerschmitt-Boelkow-Blohm G.m.b.H., Ottobrunn (Germany, F.R.).
SYSTEM DESIGN FOR THE TIGER HELICOPTER
Rudolf Schranner (Aerospatiale, Marignane, France) and G. Dufour Sep. 1990 7 p Presented at the 16th European Rotorcraft Forum, Glasgow, Scotland, 18-21 Sep. 1990
(MBB-UD-0581-90-PUB; ETN-91-98831) Avail: NTIS HC/MF A02

The first activities in development of the avionic system of the Tiger helicopter (PAH2/HAC, HAP) concentrated on the consolidation of system requirements and the system design. This led to the selection of suppliers for the main avionic subsystems, such as computers, displays, navigation, flight control and electronic countermeasures system. The result is a selection of advanced technologies with rather low volumes and masses of equipment, a main consideration for such weapon systems. Through the introduction of standardization requirements not only large economical benefits but also technologically advanced solutions with considerable benefit for the user in the service phase may be achieved. The actual status of the system architecture of the Tiger as resulting from the subsystem selection is presented. Some of the main features for some important subsystems and equipments such as the computing and display subsystem are given. ESA

N91-19091# Messerschmitt-Boelkow-Blohm G.m.b.H., Munich (Germany, F.R.). Helicopter Div.
MBB'S INVOLVEMENT IN MILITARY HELICOPTER PROGRAMMES
Helmut Huber Nov. 1989 49 p Presented at the 1989 USAEUR Aviation Professional Conference, Willingen, Fed. Republic of Germany, 28-30 Nov. 1989
(MBB-UD-0588-90-PUB; ETN-91-98832) Avail: NTIS HC/MF A03

A briefing of the studies, projects, and programs are reviewed. Previews and diagrammatic explanations of the following programs are given: Escort Helicopter (BSH1); PAH1 Upgrade; BO 108; HAP - PAH2/HAC; NH 90; Advanced Light Helicopter (ALH); lead concept 'HC 2000', second generation escort helicopter; and EUROFAR. The technology basis of the company is broad and is continuously extended. Future helicopter development is exclusively a subject of international cooperation and MBB is fully prepared to play an active role in this respect. ESA

N91-19092# Cranfield Inst. of Tech., Bedford (England). College of Aeronautics.
TF89 DESIGN PROJECT AIRBRAKE AND ARRESTER HOOK DESIGN M.S. Thesis
A. Dodd May 1990 224 p
(ETN-91-98853) Copyright Avail: NTIS HC/MF A10

Details of the field performance calculations and a description of the aspects of Computer Aided Design (CAD) work for the airbrake and arrester hook installation of the TF89 project aircraft are presented. The airbrakes are designed to operate at any speed up to the maximum design speed of the aircraft, with the deployment angle being limited by a sophisticated control system. Finite element methods of analysis are employed as the primary design tool. Two structures are evaluated, one of conventional aluminum alloy and one of carbon composite material. The final design is a composite structure which is evaluated for static stength and fatigue stength. A suitable construction method is also investigated. The estimated weight of the airbrake installation is 64 kg. The arrester hook installation is designed to slow the aircraft to rest without damage to the aircraft structure, even at abnormally high landing weight and cable engagement speed. A dynamic analysis of an arrested landing is used to determine the nose slam characteristics of the aircraft. The installation incorporates a damping system to prevent the hook from bouncing on contact with the runway. The estimated weight of the arrester hook installation is 22 kg. The takeoff and landing distances are calculated to be 533 m and 884 m respectively. The landing distance is satisfactory, but the takeoff distance exceeds the specification distance by 33 m. CAD methods are employed in the airbrake and arrester hook design and CAD generated drawings are included. ESA

N91-19093# Cranfield Inst. of Tech., Bedford (England). Dept. of Aircraft Design.
S87 CLOSE AIR SUPPORT AIRCRAFT FATIGUE ANALYSIS M.S. Thesis
M. E. J. Render Sep. 1988 275 p
(ETN-91-98854) Copyright Avail: NTIS HC/MF A12

The likely operational use of the S87 aircraft during peacetime is assessed and a selection of missions are outlined by means of sortie profile codes. Using the perceived flying regime as a basis, g level exceedances spectra are derived, both vertically and laterally, arising from maneuvers, gusts and ground loads. The critical components from a fatigue viewpoint are taken to be the wing fuselage attachment lugs. The (vertical) exceedance spectrum is converted to occurrence spectra based upon the lug stresses. The occurrence spectrum are presented to a fracture mechanics program and to an S-N curve analysis. The latter method revealed an unacceptably short fatigue life well short of the aircraft's design life of 6000 hours. However, after a design change the (factored) life was satisfactory. The influence of aircraft mass on fatigue damage rates is established. A mass dependent fatigue formula, whereby damage can be readily calculated using aircraft mass(es) and the exceedance counts of discrete fatigue meter g levels, is established. ESA

N91-19094# Technische Univ., Delft (Netherlands). Dept. of Aerospace Engineering.
BULGING OF FATIGUE CRACKS IN A PRESSURIZED AIRCRAFT FUSELAGE
D. Chen Oct. 1990 238 p
(LR-647; ETN-91-98947) Avail: NTIS HC/MF A11

Three new setups were developed for testing of sheet

specimens under biaxial tensile loading, for tensile loading of sheet specimens with a curvature, and for sheet specimens with a large radius of curvature loaded by an internal air pressure and hoop stress. Studies were carried out on the fatigue crack growth behavior of thin aluminum alloy sheets and ARamid Aluminum Laminates (ARALL) under various aircraft fuselage loading conditions, including stress biaxiality, combined bending and extension and crack edge bulge out conditions. Some residual tensile strength tests were also conducted. Theories for the effect of combined bending and extension as well for the effect of bulging were developed. The theories agree well with the present test results from the literature. ESA

06 AIRCRAFT INSTRUMENTATION

Includes cockpit and cabin display devices; and flight instruments.

For related information see also *19 Spacecraft Instrumentation* and *35 Instrumentation and Photography.*

N91-19095*# National Aeronautics and Space Administration. Hugh L. Dryden Flight Research Facility, Edwards, CA.

PRELIMINARY RESULTS FROM AN AIRDATA ENHANCEMENT ALGORITHM WITH APPLICATION TO HIGH-ANGLE-OF-ATTACK FLIGHT

Timothy R. Moes and Stephen A. Whitmore Feb. 1991 41 p Presented at the AIAA 29th Aerospace Sciences Meeting, Reno, NV, 7-10 Jan. 1990 Previously announced in IAA as A91-19405 (NASA-TM-101737; H-1691; NAS 1.15:101737) Avail: NTIS HC/MF A03 CSCL 01D

A technique was developed to improve the fidelity of airdata measurements during dynamic maneuvering. This technique is particularly useful for airdata measured during flight at high angular rates and high angles of attack. To support this research, flight tests using the F-18 high alpha research vehicle (HARV) were conducted at NASA Ames Research Center, Dryden Flight Research Facility. A Kalman filter was used to combine information from research airdata, linear accelerometers, angular rate gyros, and attitude gyros to determine better estimates of airdata quantities such as angle of attack, angle of sideslip, airspeed, and altitude. The state and observation equations used by the Kalman filter are briefly developed and it is shown how the state and measurement covariance matrices were determined from flight data. Flight data are used to show the results of the technique and these results are compared to an independent measurement source. This technique is applicable to both postflight and real-time processing of data. Author

N91-19096# Cranfield Inst. of Tech., Bedford (England). School of Mechanical Engineering.

THE APPLICATION OF AERO GAS TURBINE ENGINE MONITORING SYSTEMS TO MILITARY AIRCRAFT M.S. Thesis

C. A. R. Burgess Aug. 1990 187 p (ETN-91-98852) Copyright Avail: NTIS HC/MF A09

The application of Engine Monitoring Systems (EMS) to military aircraft has not developed as rapidly as in the civil sector. Nevertheless, they offer a very significant reduction in life cycle costs including a marked improvement in flight safety. Both the operational and organizational factors which mould the military environment are considered. The development of EMS in the RAF (Royal Air Force) is described and the practical application and limitations of both new and existing methods are investigated drawing on examples of their performance in operational service. The role of ground based systems and their strengths and weaknesses are examined. Various EMS development programs are studied, in particular the manner in which timescales, funding, contractual arrangements and project organization profoundly influence the final product and the lessons that can be learnt for the future from mistakes or successes in the past. A cost analysis is undertaken to explore the order of possible savings and the role that modern EMS techniques could and do play in these savings. The effect of availability and costs of equipment unreliability is examined and areas which give the most favorable return on investment are highlighted. Assumptions made are validated as far as possible against published quantitative benefits from operational systems. ESA

07 AIRCRAFT PROPULSION AND POWER

Includes prime propulsion systems and systems components, e.g., gas turbine engines and compressors; and onboard auxilliary power plants for aircraft.

For related information see also *20 Spacecraft Propulsion and Power, 28 Propellants and Fuels,* and *44 Energy Production and Conversion.*

N91-19097*# National Aeronautics and Space Administration. Lewis Research Center, Cleveland, OH.

THE SELECTION OF CONVERTIBLE ENGINES WITH CURRENT GAS GENERATOR TECHNOLOGY FOR HIGH SPEED ROTORCRAFT

Joseph D. Eisenberg 1990 27 p Presented at the Vertical Lift Aircraft Design Conference, San Francisco, CA, 17-19 Jan. 1990; cosponsored by American Helicopter Society Previously announced in IAA as A90-46933 (NASA-TM-103774; E-6041; NAS 1.15:103774) Avail: NTIS HC/MF A03 CSCL 21E

NASA-Lewis sponsored two studies to determine the most promising convertible engine concepts for high speed rotorcraft. These studies projected year 2000 convertible technology limited to present gas generator technology. Propulsion systems for utilization on aircraft needing thrust only during cruise and those aircraft needing both power and thrust at cruise were investigated. Mission calculations for the two contractors involved were based upon the fold tilt rotor concept. Analysis and comparison of the General Electric concepts (geared UDF, clutched fan, and Variable Inlet Guide Vane (VIGV) fan), and the Allison Gas Turbine concepts (clutched fan, VIGV fan, variable pitch fan, single rotation tractor propfan, and counter rotation tractor propfan) are presented. Author

N91-19098*# National Aeronautics and Space Administration. Lewis Research Center, Cleveland, OH.

WIND TUNNEL WALL EFFECTS IN A LINEAR OSCILLATING CASCADE

Daniel H. Buffum and Sanford Fleeter (Purdue Univ., West Lafayette, IN.) 1991 14 p Proposed for presentation at the 36th International Gas Turbine and Aeroengine Congress and Exposition, Orlando, FL, 3-6 Jun. 1991; sponsored by ASME (NASA-TM-103690; E-5909; NAS 1.15:103690) Avail: NTIS HC/MF A03 CSCL 21E

Experiments in a linear oscillating cascade reveal that the wind tunnel walls enclosing the airfoils have, in some cases, a detrimental effect on the oscillating cascade aerodynamics. In a subsonic flow field, biconvex airfoils are driven simultaneously in harmonic, torsion-mode oscillations for a range of interblade phase angle values. It is found that the cascade dynamic periodicity - the airfoil to airfoil variation in unsteady surface pressure - is good for some values of interblade phase angle but poor for others. Correlation of the unsteady pressure data with oscillating flat plate cascade predictions is generally good for conditions where the periodicity is good and poor where the periodicity is poor. Calculations based upon linearized unsteady aerodynamic theory indicate that pressure waves reflected from the wind tunnel walls are responsible for the cases where there is poor periodicity and poor correlation with the predictions. Author

N91-19099*# National Aeronautics and Space Administration. Hugh L. Dryden Flight Research Facility, Edwards, CA.

A PROPOSED KALMAN FILTER ALGORITHM FOR ESTIMATION OF UNMEASURED OUTPUT VARIABLES FOR AN F100 TURBOFAN ENGINE

Gurbux S. Alag (PRC Systems Services Co., Edwards, CA.) and

Glenn B. Gilyard Washington Oct. 1990 32 p Presented at the AIAA/SAE/ASME/ASEE Joint Propulsion Conference, Orlando, FL, 16-18 Jul. 1990 Previously announced in IAA as A90-40558 (NASA-TM-4234; H-1639; NAS 1.15:4234) Avail: NTIS HC/MF A03 CSCL 21E

To develop advanced control systems for optimizing aircraft engine performance, unmeasurable output variables must be estimated. The estimation has to be done in an uncertain environment and be adaptable to varying degrees of modeling errors and other variations in engine behavior over its operational life cycle. This paper represented an approach to estimate unmeasured output variables by explicitly modeling the effects of off-nominal engine behavior as biases on the measurable output variables. A state variable model accommodating off-nominal behavior is developed for the engine, and Kalman filter concepts are used to estimate the required variables. Results are presented from nonlinear engine simulation studies as well as the application of the estimation algorithm on actual flight data. The formulation presented has a wide range of application since it is not restricted or tailored to the particular application described. Author

08 AIRCRAFT STABILITY AND CONTROL

Includes aircraft handling qualities; piloting; flight controls; and autopilots.

For related information see also *05 Aircraft Design, Testing and Performance.*

N91-19100 Department of the Navy, Washington, DC.
ALTERNATE APPROACH FOR OBTAINING DYNAMIC RANGE IN MONOPULSE GUIDANCE SYSTEMS Patent
Bobby R. Jarrett, inventor (to Navy) 21 Aug. 1990 5 p Filed 14 Sep. 1976
(AD-D014644; US-Patent-4,950,076; US-Patent-Appl-SN-723262)
Avail: US Patent and Trademark Office CSCL 13/9

A system for improving the dynamic range of guidance systems for missiles and bombs by replacing pseudologarithmic amplifiers in the processing circuits with transimpedance amplifiers having feedback impedance operating in conjunction with lower bandwidth type logarithmic amplifiers in the log of the ratio circuits is described. GRA

N91-19101# Messerschmitt-Boelkow-Blohm G.m.b.H., Munich (Germany, F.R.). Helicopter Div.
I'M ALL 'LIGHT' JACK
Gerhard Kissel and Alan Faulkner Sep. 1990 15 p Presented at the 16th European Rotorcraft Forum, Glasgow, Scotland, 18-21 Sep. 1990
(MBB-UD-0576-90-PUB; ETN-91-98826) Avail: NTIS HC/MF A03

The case for using optical data transmission for helicopter flight control systems FBL (Fly By Light) concluding that the technology is mature for the introduction into future helicopters is presented. Though FBW (Fly By Wire) is able to meet current specification needs, FBL may be a more cost effective solution in the future owing to the increasing EMI (electrical magnetic interference) requirements. The experience gained during the development and experimental flight test program is presented and discussed. Details of the computing technology and hardware installation, the use of 'smart' sensors and 'smart' actuators is given together with the current activities since completion of flight testing. The results of new developments in microcomponents to replace existing accelerometers, rate gyros, and position sensors are shown. ESA

N91-19036*# Princeton Univ., NJ. Dept. of Mechanical and Aerospace Engineering.
STOCHASTIC ROBUSTNESS: TOWARDS A COMPREHENSIVE ROBUSTNESS TOOL
Laurie Ryan Ray *In* NASA, Langley Research Center, Joint University Program for Air Transportation Research, 1989-1990 Dec. 1990 p 141-150 (For primary document see N91-19024 11-01)
Avail: NTIS HC/MF A09 CSCL 01C

N91-19037*# Princeton Univ., NJ. Dept. of Mechanical and Aerospace Engineering.
NEURAL NETWORKS IN NONLINEAR AIRCRAFT CONTROL
Dennis J. Linse *In* NASA, Langley Research Center, Joint University Program for Air Transportation Research, 1989-1990 Dec. 1990 p 151-161 (For primary document see N91-19024 11-01)
Avail: NTIS HC/MF A09 CSCL 01C

N91-19038*# Princeton Univ., NJ. Dept. of Mechanical and Aerospace Engineering.
STOCHASTIC SATBILITY AND PERFORMANCE ROBUSTNESS OF LINEAR MULTIVARIABLE SYSTEMS
Laurie E. Ryan and Robert F. Stengel *In* NASA, Langley Research Center, Joint University Program for Air Transportation Research, 1989-1990 Dec. 1990 p 181-186 (For primary document see N91-19024 11-01)
(Contract NGL-31-001-252; DAAL03-89-K-0092)
Avail: NTIS HC/MF A09 CSCL 01C

N91-19039*# Princeton Univ., NJ. Dept. of Mechanical and Aerospace Engineering.
SYSTEM IDENTIFICATION FOR NONLINEAR CONTROL USING NEURAL NETWORKS
Robert F. Stengel and Dennis J. Linse *In* NASA, Langley Research Center, Joint University Program for Air Transportation Research, 1989-1990 Dec. 1990 p 187-192 (For primary document see N91-19024 11-01)
(Contract NGL-31-001-252; DAAL03-89-K-0092)
Avail: NTIS HC/MF A09 CSCL 01C

N91-19810# Joint Publications Research Service, Arlington, VA.
CONSTRUCTING MATHEMATICAL MODEL OF ADAPTIVE ANTI-FLUTTER SYSTEM Abstract Only
B. O. Kachanov, S. I. Ovcharenko, and A. T. Ponomarev *In its* JPRS Report: Science and Technology. USSR: Physics and Mathematics 31 Oct. 1990 p 12-13 Transl. into ENGLISH from Prikladnaya Mekhanika (Kiev, USSR), v. 26, no. 1, Jan. 1990 p 113-119 (For primary document see N91-19800 11-70)
Avail: NTIS HC/MF A03

09 RESEARCH AND SUPPORT FACILITIES (AIR)

Includes airports, hangars and runways; aircraft repair and overhaul facilities; wind tunnels; shock tubes; and aircraft engine test stands.

For related information see also *14 Ground Support Systems and Facilities (Space).*

N91-19102# Surface Dynamics, Inc., Bloomfield Hills, MI.
SMOOTHNESS CRITERIA FOR RUNWAY REHABILITATION AND OVERLAYS Final Report
Elson B. Spangler, Anthony G. Gerardi, and Donald R. Yager Jul. 1990 174 p
(Contract DTFA01-86-C-00035)
(DOT/FAA/RD-90/23) Avail: NTIS HC/MF A08

Modern aircraft, due to their large size, structural flexibility, and higher take-off and landing speeds, can be excited into a resonant condition by runway profile roughness. Forces generated by the interaction of the aircraft and the runway can produce poor aircraft ride quality, and cause damaging stresses both in the aircraft structure and the runway pavement itself. Wavelength components in the runway profile that cause aircraft resonance often are difficult to identify, isolate, and repair. Advancements in high speed profile measuring systems and the development of a computer simulation of an aircraft responding to the measured runway profile have now provided the ability to identify runway

elevation profile features contributing to poor aircraft ride quality. The research effort evaluates the measuring capability of one high speed profile measuring system, evaluates the methods of analysis developed in the project, and applies the measuring and analysis methods to the rehabilitation of a General Aviation Airport runway. Author

N91-19103# Sandia National Labs., Albuquerque, NM.
DESIGNING FOR EXPLOSIVE SAFETY: THE EXPLOSIVE COMPONENTS FACILITY AT SANDIA NATIONAL LABORATORIES
W. A. Couch Dec. 1990 13 p
(Contract DE-AC04-76DP-00789)
(DE91-006432; SAND-90-2460) Avail: NTIS HC/MF A03

The Explosive Components Facility (ECF) is to be a new major facility in the Sandia National Laboratories (SNL) Weapons Program. The ECF is a self-contained, secure site on SNL property and is surrounded by Kirtland Air Force Base which is located 6-1/2 miles east of downtown Albuquerque, New Mexico. The ECF will be dedicated to research, development, and testing of detonators, neutron generators, batteries, explosives, and other weapon components. It will have capabilities for conducting explosive test fires, gas gun testing, physical analyses, chemical analyses, electrical testing and ancillary explosive storage in magazines. The ECF complex is composed of a building covering an area of approx. 91,000 sq ft, six exterior explosive service magazines and a remote test cell. Approx. 50 percent of the building space will be devoted to highly specialized laboratory and test areas, the other 50 percent of the building is considered nonhazardous. Critical to the laboratory and test areas are the blast-structural design consideration and operational considerations, particularly those concerning personnel access control, safety and environmental protection. This area will be decoupled from the rest of the building to the extent that routine tests will not be heard or felt in the administrative area of the building. While the ECF is designed in accordance with the DOE Explosives Safety Manual to mitigate any off-site blast effects, potential injuries or death to the ECF staff may result from an accidental detonation of explosive material within the facility. Therefore, reducing the risk of exposing operation personnel to hazardous and energetic material is paramount in the design of the ECF. DOE

N91-19104# Oak Ridge National Lab., TN.
FLORIDA RADIOLUMINESCENT TAXIWAY LIGHT DEVELOPMENT PROGRAM
K. W. Haff, J. A. Tompkins, and D. T. Travis Oct. 1990 88 p
(Contract DE-AC05-84OR-21400)
(DE91-005650; ORNL/TM-11633) Avail: NTIS HC/MF A05

In 1980, the U.S. Air Force (USAF) Engineering and Services Center at Tyndall Air Force Base, Florida, requested that the Radioisotope Technology Group of the Chemical Technology Division at Oak Ridge National Laboratory (ORNL) develop large-scale, tritium-powered, radioluminescent (RL) airfield lighting systems. The RL lighting systems possess the advantages of being portable, requiring no electrical power source, having a long shelf life, and being unaffected by environmental extremes. These characteristics make the RL system well-suited for harsh environments where the cost of electrical power production is high and traditional incandescent airfield lighting systems are difficult to maintain. Additionally, the system is well suited for environments where corrosion of wiring and water entry into wiring systems make them difficult to maintain. In 1985, the State of Florida, Department of Transportation (DOT), through contract with the City of St. Petersburg, Florida became a participant in the program to develop RL lighting systems for use in small commercial airports. Radioluminescent lighting is typically a large-surface-area, low-intensity light source that operates 100 percent of the time. The RL light sources gradually decrease in brightness over time, so periodic replacement (every 6 to 8 years) is necessary. RL lighting functions best in low ambient light, which provides the high contrast ratios necessary for successful use of these devices. Previous work with the USAF was primarily devoted to research and development for the large scale light sources necessary for RL airfield lighting. Experiments were conducted on phosphors and phosphor mixtures to develop a brighter blue light for taxiway use. Numerous calculations were made to demonstrate the safety of the system to the Florida Department of Health and to obtain the license. DOE

N91-19105# National Aerospace Lab., Tokyo (Japan).
INVESTIGATION OF ATP BLADES, PART 3
Apr. 1990 46 p In JAPANESE
(DE91-750104; NAL-TM-618) Avail: NTIS HC/MF A03

Impact testare reported of models of ATP blades. Test specimens were made of the following materials: fiber reinforced plastics (FRP) using carbon fiber, glass fiber or polyamide fiber; hybrid FRP that is a laminated sheet using any pair of two out of carbon fiber, glass fiber, polyamide fiber and aluminum sheet. Plate specimens made of these various kinds of FRP or hybrid FRP were put to impact test using small projectiles as impactors, in addition to 1/4 scale models of ATP blade, which were made of hybrid FRP. Results obtained are described in detail under the following items; minimum speed required for penetration, amount of energy absorbed by specimens, models of impact damage, strain produced in responce to impacts, exfoliation of specimens, and others. In the second place, there is given a numerical simulation, using FEM programs, of responses of plate models or 1/4 scale models of ATP blade, both made of composite materials, to impacts exerted on them with small projectiles. In connection with exfoliation of specimens, emphasis is laid on generation of bending waves of higher order modes in those models and on existence of edge waves at both forward and backward edges of the ATP blade models, which are derived from the bending waves. In the third place, responses of a cantilever to impacts exerted on it with a spherical impactor are analyzed, assuring that reaction force associated with impacts can be expressed in terms of the formula due to Hertz. A detailed mathematical discussion is given of this analysis by use of a method based on the variation principle. It is noted that this method is effectively used for analyzing free vibrations of the cantilever which are caused by impacts. DOE

N91-19106# Messerschmitt-Boelkow-Blohm G.m.b.H., Munich (Germany, F.R.). Abt. Forschung und Entwicklung.
AIRPORT APRON RESEARCH AND DEVELOPMENT [FLUGHAFENVORFELD FORSCHUNG UND ENTWICKLUNG]
1990 256 p In GERMAN Presented at Expertengespraech, Bad Toelz, Fed. Republic of Germany, 4-6 Apr. 1990
(MBB-Z-0168-90-PUB; OTN-027673; ISSN-0931-9757; ETN-91-98836) Copyright Avail: NTIS HC/MF A12

Discussions were centered on aircraft ground interface and airport aircraft interface. Subjects covered were safety and control in airports, technical aspects of airport activities, simulation of air traffic, existing difficulties and how to solve them, and infrastructure problems. Scenarios were presented to draw the attention of public authorities to the present and future dramatic changes of apron conditions. For individual titles, see N91-19107 through N91-19110.

N91-19107# Messerschmitt-Boelkow-Blohm G.m.b.H., Munich (Germany, F.R.). Zentralbereich Technik.
AIRPORT SYSTEM TECHNICAL ASPECTS [SYSTEMTECHNISCHE ASPEKTE ZUM FLUGHAFEN]
G. Bauer *In its* Airport Apron Research and Develoment 1990 p 15-26 In GERMAN (For primary document see N91-19106 11-09)
Copyright Avail: NTIS HC/MF A12

The airport system is examined from the passenger point of view. The various activities such as aircraft maintenance, cleaning, energy supply, customs, ground control and safety are examined. Increasing touristic activities and environment problems are also considered. The increasing delays and environmental pollution show that changes and improvements are necessary. ESA

N91-19108# Airbus Industrie, Blagnac (France). Entwicklung.
AIRCRAFTS, REQUIREMENTS FOR GROUND INSTALLATIONS FROM THE AIRCRAFT POINT OF VIEW [FLUGZEUGE, ANFORDERUNGEN VON SEITEN DES FLUGZEUGES AN DIE BODENINSTALLATIONEN]
Schmitt *In* MBB, Airport Apron Research and Development 1990 p 27-64 In GERMAN (For primary document see N91-19106 11-09)
Copyright Avail: NTIS HC/MF A12

The market development, servicing, taxiing, starting runways, noise emission and data communication are examined. The air transport system, passenger kilometer growth rate, trips per inhabitants of selected countries in relation to economic development, frequency limited airports, slot allocation, jet aircraft, fleet status to the year 2006, typical life cycle of a civil aircraft program, fuel price, A320 servicing, towing and taxiing, airport noise, objectives of airbus industry are tabulated or illustrated. ESA

N91-19109# Deutsche Lufthansa A.G., Hamburg (Germany, F.R.). Management Engineering.
AIRCRAFT STANDSTILL, REQUIREMENTS FOR GROUND HANDLING FROM THE POINT OF VIEW OF AIRCRAFT OPERATION [FLUGZEUGHALTER, ANFORDERUNGEN AN DAS HANDLING AM BODEN AUS DER SICHT DES FLUGBETRIEBES]
L. Kilchert *In* MBB, Airport Apron Research and Development 1990 p 65-90 In GERMAN (For primary document see N91-19106 11-09)
Copyright Avail: NTIS HC/MF A12

The taxi system is described. The problems are stated: landing conditions, position determination on the runway, transfer from runway to taxiway, position determination on taxiway, use of hybrid sensors, Global Positioning System (GPS). GPS is to be integrated into the cockpit of Boeing aircrafts. ESA

N91-19110# Deutsche Airbus G.m.b.H., Hamburg (Germany, F.R.).
AIR TRAFFIC SIMULATION WITH A VIEW TO SYSTEM INTERPRETATION [SIMULATION DES LUFTVERKEHRS IM SINNE DER SYSTEMAUSLEGUNG]
J. Schumacher *In* MBB, Airport Apron Research and Development 1990 p 91-120 In GERMAN (For primary document see N91-19106 11-09)
Copyright Avail: NTIS HC/MF A12

The necessity of the simulation of the general air traffic system is underlined. Influences of economy, energy and environment are underlined. The system requirements for worldwide 21st century air transportation are determined. The impact of aircraft design on airports and airspace is stated. Its consequences on airspace utilization, airspace capacity, runway capacity, apron terminal size, payload handling, and ground maneuverability are addressed. ESA

N91-19111# Air Force Inst. of Tech., Wright-Patterson AFB, OH. School of Engineering.
AN EXPERIMENTAL STUDY OF A STING-MOUNTED SINGLE-SLOT CIRCULATION CONTROL WING M.S. Thesis
Michael E. Pelletier Dec. 1990 75 p
(AD-A229867; AFIT/GAE/ENY/90D-18) Avail: NTIS HC/MF A04 CSCL 01/1

This wind tunnel study investigated the feasibility of using a sting and force balance to measure the aerodynamic forces and moments on a circulation control wing. A 20 percent thick, 8.5 percent camber, single blowing slot, rectangular wing was designed, built, and tested in the Air Force Institute of Technology (AFIT) 5-ft wind tunnel. Lift and drag coefficients were referenced to the stability axis. The Reynolds number for all tests was 950,000; angle of attack was varied from -6 to +6 degrees. Trends in the data were similar to two dimensional data, with the exception of high drag coefficients with increased blowing. Results show it is feasible to test three dimensional wings using a sting and force balance if appropriate data corrections are applied. GRA

N91-19035*# Princeton Univ., NJ. Dept. of Mechanical and Aerospace Engineering.
FLIGHT SIMULATION FOR WIND SHEAR ENCOUNTER
Sandeep S. Mulgund *In* NASA, Langley Research Center, Joint University Program for Air Transportation Research, 1989-1990 Dec. 1990 p 133-139 (For primary document see N91-19024 11-01)
Avail: NTIS HC/MF A09 CSCL 14B

12 ASTRONAUTICS (GENERAL)

For extraterrestrial exploration see *91 Lunar and Planetary Exploration.*

N91-19112*# National Aeronautics and Space Administration. Lewis Research Center, Cleveland, OH.
SPACE REACTOR/STIRLING CYCLE SYSTEMS FOR HIGH POWER LUNAR APPLICATION
Paul C. Schmitz (Sverdrup Technology, Inc., Brook Park, OH.) and Lee S. Mason 1991 11 p Presented at the 8th Symposium on Space Nuclear Power Systems, Albuquerque, NM, 6-10 Jan. 1991; cosponsored by New Mexico Univ, Strategic Defense Initiative Organization, DOE, and AF
(NASA-TM-103698; E-5920; NAS 1.15:103698) Avail: NTIS HC/MF A03 CSCL 10B

An analysis is performed to mathematically model a 550 kWe lunar base power supply which uses a SP-100 reactor coupled with Stirling converters. The reactor is placed in an excavation to keep activated coolant in the hole and to allow maintenance of the components outside the hole. Two technology levels are considered. They are 1050 and 1300 K heater head Stirling converts. It is found that for a 1050 K converter the total mass which provided 1000 volts DC at 250 m is 14,366 kg while the 1300 K system mass is 12,104 kg. The radiation area of the 1050 and 1300 K systems are 641 and 356 sq m respectively. Comparisons are made with Brayton and thermionic systems with both near term and advanced technology considered. Author

N91-19113# Bundesministerium fuer Forschung und Technologie, Bonn (Germany, F.R.).
SPACE RESEARCH FOR THE SAKE OF ALL [WELTRAUMFORSCHUNG NUTZEN FUER ALLE]
Rolf D. Guenther, ed. 1990 46 p In GERMAN
(ETN-91-98807) Avail: NTIS HC/MF A03

A review of the present and future developments to be carried out in West Germany in the field of space research is given. Information on the numerous aspects of the space travel technique applications in daily life is given. The consideration of space research, which was looked on over 25 years as an exotic discipline, as a now genuine science and technique is demonstrated. Explanations are given in numerous illustrations and tables. ESA

N91-19114# Technische Univ., Berlin (Germany, F.R.). Inst. fuer Luft- und Raumfahrt.
PROJECT OF A COST ANALYSIS MODEL FOR THE ACQUISITION OF A PERMANENT LUNAR BASE [ENTWURF EINES KOSTENMODELLS FUER DIE AKQUISITION EINER PERMANENTEN MONDBASIS]
Michael Mielke 1 Aug. 1990 51 p In GERMAN; ENGLISH summary
(ILR-Mitt-245(1990); ETN-91-98950) Avail: NTIS HC/MF A04

A mathematical model using Cost Estimation Relationships (CERs) is derived for a comprehensive cost structure that considers development, acquisition and operation of a permanent lunar base, which is likely to be established at the beginning of the next millenium. An illustrative scenario of a lunar base is developed to determine the life cycle cost over a period of sixteen years. The cost of the described scenario will be of the order of a hundred billion dollars. The results of this estimate are complemented by a sensitivity analysis varying important input parameters, in order to obtain a better insight into the cost behavior of this lunar base model. ESA

13 ASTRODYNAMICS

Includes powered and free-flight trajectories; and orbital and launching dynamics.

N91-19115*# National Aeronautics and Space Administration. Lewis Research Center, Cleveland, OH.
AUTOMATIC CONTROL STUDY OF THE ICING RESEARCH TUNNEL REFRIGERATION SYSTEM
Arthur W. Kieffer and Ronald H. Soeder Washington Feb. 1991 27 p
(NASA-TM-4257; E-5588; NAS 1.15:4257) Avail: NTIS HC/MF A03 CSCL 13B

The Icing Research Tunnel (IRT) at the NASA Lewis Research Center is a subsonic, closed-return atmospheric tunnel. The tunnel includes a heat exchanger and a refrigeration plant to achieve the desired air temperature and a spray system to generate the type of icing conditions that would be encountered by aircraft. At the present time, the tunnel air temperature is controlled by manual adjustment of freon refrigerant flow control valves. An upgrade of this facility calls for these control valves to be adjusted by an automatic controller. The digital computer simulation of the IRT refrigeration plant and the automatic controller that was used in the simulation are discussed. Author

14 GROUND SUPPORT SYSTEMS AND FACILITIES (SPACE)

Includes launch complexes, research and production facilities; ground support equipment, e.g., mobile transporters; and simulators.

For related information see also *09 Research and Support Facilities (Air).*

N91-19116# Department of the Navy, Washington, DC.
PNEUMATIC LAUNCHER Patent
David R. Bon, inventor (to Navy) 28 Aug. 1990 5 p Filed 30 Apr. 1984
(AD-D014658; US-Patent-4,951,644; US-Patent-Appl-SN-633361; US-Patent-Class-124-75) Avail: US Patent and Trademark Office CSCL 13/7

A pneumatic launcher is disclosed for instrumented objects which includes a barrel, a breech member having a compressed gas reservoir, a pneumatic piston operated valve for discharging gas from the reservoir into the barrel and is characterized by a fail-safe venting feature and a throttling valve for automatically limiting acceleration of the launched object. GRA

N91-19134*# TRW Defense and Space Systems Group, Redondo Beach, CA.
HIGH VACUUM FACILITY FOR HYDRAZINE THRUSTER TESTING
Patrick F. Neary *In* NASA, Goddard Space Flight Center, 16th Space Simulation Conference Confirming Spaceworthiness Into the Next Millennium Nov. 1990 p 73-74 (For primary document see N91-19126 11-18)
Avail: NTIS HC/MF A20 CSCL 14B

N91-19138*# Boeing Aerospace Co., Seattle, WA.
BOEING INFRARED SENSOR (BIRS) CALIBRATION FACILITY
John D. Hazen and L. V. Scorsone (Pittsburgh-Des Moines Steel Co., PA.) *In* NASA, Goddard Space Flight Center, 16th Space Simulation Conference Confirming Spaceworthiness Into the Next Millennium Nov. 1990 p 133-156 (For primary document see N91-19126 11-18)
Avail: NTIS HC/MF A20 CSCL 14B

N91-19139*# Calspan Field Services, Inc., Arnold AFS, TN.
INFRARED SENSOR TEST METHODOLOGY AND FACILITIES
Jere J. Matty and Ronald Dawbarn *In* NASA, Goddard Space Flight Center, 16th Space Simulation Conference Confirming Spaceworthiness Into the Next Millennium Nov. 1990 p 157-175 (For primary document see N91-19126 11-18)
Avail: NTIS HC/MF A20 CSCL 14B

N91-19140*# Grumman Aerospace Corp., Bethpage, NY. Space Systems Div.
THERMAL CONTROL FOR THE GROUND SIMULATION OF A SPACE IR SENSOR SYSTEM Abstract Only
E. Lee, A. Warren, G. Gasser, and M. Tierney (Itek Corp., Lexington, MA.) *In* NASA, Goddard Space Flight Center, 16th Space Simulation Conference Confirming Spaceworthiness Into the Next Millennium Nov. 1990 p 179 (For primary document see N91-19126 11-18)
Avail: NTIS HC/MF A20 CSCL 14B

N91-19141*# Grumman Aerospace Corp., Bethpage, NY. Space Systems Div.
SPECIAL REQUIREMENTS IN THE DESIGN OF A SENSOR TEST AND INTEGRATION LABORATORY Abstract Only
S. Bellanca, E. Lee, and J. Campbell *In* NASA, Goddard Space Flight Center, 16th Space Simulation Conference Confirming Spaceworthiness Into the Next Millennium Nov. 1990 p 180 (For primary document see N91-19126 11-18)
Avail: NTIS HC/MF A20 CSCL 14B

N91-19142*# Liege Univ. (Belgium). Centre de Recherches IAL SPACE.
IAL SPACE: A TEST LABORATORY FOR THE ISO CRYOGENIC PAYLOAD
A. Cucchiaro, M. Henrist, J. P. Macau, N. Ninane, and R. Blanpain *In* NASA, Goddard Space Flight Center, 16th Space Simulation Conference Confirming Spaceworthiness Into the Next Millennium Nov. 1990 p 181-191 (For primary document see N91-19126 11-18)
Avail: NTIS HC/MF A20 CSCL 14B

N91-19150*# Chicago Bridge and Iron Co., Oak Brook, IL.
SPACE SIMULATION FACILITIES PROVIDING A STABLE THERMAL VACUUM FACILITY
Martin L. Tellalian *In* NASA, Goddard Space Flight Center, 16th Space Simulation Conference Confirming Spaceworthiness Into the Next Millennium Nov. 1990 p 289-313 (For primary document see N91-19126 11-18)
Avail: NTIS HC/MF A20 CSCL 14B

N91-19151*# Liege Univ. (Belgium). Centre de Recherches IAL SPACE.
THE SPACE SIMULATION FACILITIES AT IAL SPACE
M. Henrist, A. Cucchiaro, I. Domken, and J. P. Macau *In* NASA, Goddard Space Flight Center, 16th Space Simulation Conference Confirming Spaceworthiness Into the Next Millennium Nov. 1990 p 314-322 (For primary document see N91-19126 11-18)
Avail: NTIS HC/MF A20 CSCL 14B

N91-19658# Eidgenoessische Technische Hochschule, Zurich (Switzerland). Space Biology Group.
BIOLAB ON COLUMBUS: A FACILITY FOR BASIC SCIENCE AND BIOTECHNOLOGY
Augusto Cogoli *In* ESA, Fourth European Symposium on Life Sciences Research in Space Nov. 1990 p 441-444 (For primary document see N91-19572 11-51)
Copyright Avail: NTIS HC/MF A25; EPD, ESTEC, Noordwijk, Netherlands, HC 80 Dutch guilders

N91-19661# Fokker B.V., Amsterdam (Netherlands).
CELLS IN SPACE: SOUNDING ROCKET FACILITIES FOR CELL BIOLOGY AND BIOTECHNOLOGY IN MICROGRAVITY
Ron Huijser, Louis Aartman, and Harry Willemsen (Centrum voor Constructie en Mechanisatie, Nuenen, Netherlands) *In* ESA, Fourth European Symposium on Life Sciences Research in Space Nov. 1990 p 455-466 Sponsored in part by the Netherlands Agency for Aerospace Programs (For primary document see N91-19572 11-51)

Copyright Avail: NTIS HC/MF A25; EPD, ESTEC, Noordwijk, Netherlands, HC 80 Dutch guilders

N91-19663# Deutsche Agentur fuer Raumfahrtangelegenheiten G.m.b.H., Bonn (Germany, F.R.).
THE SLOW-ROTATING CENTRIFUGE MICROSCOPE (NIZEMI): A NEW RESEARCH TOOL FOR TERRESTRIAL AND SPACE-RELATED GRAVITATIONAL BIOLOGY
Karlheinz Kreuzberg, R. Behrle, O. Joop, and R. Treichel (Dornier System G.m.b.H., Friedrichshafen, Germany, F.R.) *In* ESA, Fourth European Symposium on Life Sciences Research in Space Nov. 1990 p 471-474 (For primary document see N91-19572 11-51)
Copyright Avail: NTIS HC/MF A25; EPD, ESTEC, Noordwijk, Netherlands, HC 80 Dutch guilders

N91-19666# Erno Raumfahrttechnik G.m.b.H. Bremen (Germany, F.R.).
DEVELOPMENT OF A MINIATURE BIOLOGY FACILITY
J. Warrelmann and R. Klintworth *In* ESA, Fourth European Symposium on Life Sciences Research in Space Nov. 1990 p 485-487 (For primary document see N91-19572 11-51)
Copyright Avail: NTIS HC/MF A25; EPD, ESTEC, Noordwijk, Netherlands, HC 80 Dutch guilders

N91-19684# Institute of Biomedical Problems, Moscow (USSR).
PRINCIPLE AND REALIZATION OF THE INSTRUMENT USED FOR THE CIRCE EXPERIMENT ON BOARD THE MIR STATION
V. M. Petrov, J. A. Akatov, S. B. Kozlova, Van Dat Nguyen, J. Kerlau, M. Siegrist, and J. F. Zwilling (Centre National d'Etudes Spatiales, Toulouse, France) *In* ESA, Fourth European Symposium on Life Sciences Research in Space Nov. 1990 p 577-580 (For primary document see N91-19572 11-51)
Copyright Avail: NTIS HC/MF A25; EPD, ESTEC, Noordwijk, Netherlands, HC 80 Dutch guilders

15 LAUNCH VEHICLES AND SPACE VEHICLES

Includes boosters; operating problems of launch/space vehicle systems; and reusable vehicles.

For related information see also *20 Spacecraft Propulsion and Power.*

N91-19117*# Sverdrup Technology, Inc., Brook Park, OH.
LOX/HYDROGEN COAXIAL INJECTOR ATOMIZATION TEST PROGRAM Final Report
M. Zaller Oct. 1990 11 p Presented at the 27th JANNAF Combustion Meeting, Cheyenne, WY, 5-9 Nov. 1990
(Contract NAS3-25266)
(NASA-CR-187037; E-5849; NAS 1.26:187037) Avail: NTIS HC/MF A03 CSCL 22B

Quantitative information about the atomization of injector sprays is needed to improve the accuracy of computational models that predict the performance and stability margin of liquid propellant rocket engines. To obtain this data, a facility for the study of spray atomization is being established at NASA-Lewis to determine the drop size and velocity distributions occurring in vaporizing liquid sprays at supercritical pressures. Hardware configuration and test conditions are selected to make the cold flow simulant testing correspond as closely as possible to conditions in liquid oxygen (LOX)/gaseous H2 rocket engines. Drop size correlations from the literature, developed for liquid/gas coaxial injector geometries, are used to make drop size predictions for LOX/H2 coaxial injectors. The mean drop size predictions for a single element coaxial injector range from 0.1 to 2000 microns, emphasizing the need for additional studies of the atomization process in LOX/H2 engines. Selection of cold flow simulants, measurement techniques, and hardware for LOX/H2 atomization simulations are discussed. Author

16 SPACE TRANSPORTATION

Includes passenger and cargo space transportation, e.g., shuttle operations; and space rescue techniques.

For related information see also *03 Air Transportation and Safety* and *18 Spacecraft Design, Testing and Performance.* For space suits see *54 Man/System Technology and Life Support.*

N91-19118*# National Aeronautics and Space Administration. John F. Kennedy Space Center, Cocoa Beach, FL.
DEBRIS/ICE/TPS ASSESSMENT AND PHOTOGRAPHIC ANALYSIS FOR SHUTTLE MISSION STS-35
Gregory N. Katnik, Scott A. Higginbotham, and James Bradley Davis Feb. 1991 172 p Original contains color illustrations
(NASA-TM-103816; NAS 1.15:103816) Avail: NTIS HC/MF A08; 70 functional color pages CSCL 22A

A debris/ice/Thermal Protection System (TPS) assessment and photographic analysis was conducted for Space Shuttle Mission STS-35. Debris inspections of the flight elements and launch pad were performed before and after the launch. Ice/frost conditions on the External Tank were assessed by the use of computer programs, monographs, and infrared scanner data during cryogenic loading of the vehicle followed by on-pad visual inspection. High speed photography was analyzed after launch to identify ice/debris sources and evaluate potential vehicle damage and/or in-flight anomalies. Documented here are the debris/ice/TPS conditions and photographic analysis of Mission STS-35, and the overall effect of these conditions on the Space Shuttle Program. Author

N91-19119# General Accounting Office, Washington, DC.
SPACE SHUTTLE: NASA SHOULD IMPLEMENT INDEPENDENT OVERSIGHT OF SOFTWARE DEVELOPMENT
Feb. 1991 29 p
(GAO/IMTEC-91-20) Avail: NTIS HC/MF A03

In response to a request from the House Committee on Science, Space, and Technology, the General Accounting Office (GAO) presents information on NASA's efforts to improve shuttle software oversight activities and to establish independent oversight of critical shuttle software processes. GAO identifies NASA's procedures for developing, validating, verifying, and reconfiguring shuttle software. GAO also notes recommendations made by the independent contractor hired by NASA to verify and validate shuttle software; problems hindering NASA's progress in implementing the recommendations; actions taken by NASA to specifically resolve concerns raised by the National Research Council (NRC) and the shuttle program's software steering group formed to recommend changes in the verification and validation processes; and GAO's recommendations. Included as an appendix are NASA's comments on GAO's findings. J.P.S.

N91-19120# Technische Univ., Berlin (Germany, F.R.). Inst. of Aerospace.
A MULTI-VEHICLE SPACE CARRIER FLEET COST MODEL FOR A MULTI-MISSION SCENARIO
H. Hermann Koelle and Bernd Johenning 1 May 1990 105 p
(ILR-Mitt-240(1990); ETN-91-98920) Avail: NTIS HC/MF A06

A computer model to analyze the cost effectiveness of different space transportation fleets in a variety or space markets is described. This model enables the analyst to simulate the acquisition and operation of five different types of space vehicles on 22 routes of a space transportation network serving eight transportation nodes between Earth and Moon. The effects of commonality of subsystems within the transportation fleet can be analyzed in detail. The model is tested within the bounds of two typical scenarios, one driven by the development of a lunar base, the other driven by the acquisition and operation of a 500 GW Space Solar Power System (SSPS) in geostationary orbit. The data resulting from these typical program simulations are presented. ESA

N91-19121# Technische Univ., Berlin (Germany, F.R.). Fachgebiet Raumfahrzeugtechnik.
CYCLING SPACE SHIP TRANSPORTATION DEVICE FOR CONTINUOUS LINK BETWEEN EARTH AND MARS
Jens Lassmann, Matthias Dablies, Klaus Erdmann, Christian Gritzner, Thomas Meier, Thomas Renk, Thomas Schulz, and Oliver Todt 1 Dec. 1990 51 p
(ILR-Mitt-247(1990); ETN-91-98951) Avail: NTIS HC/MF A04

Vehicle concepts that provide reliable, safe, and cost effective space transportation of passengers and cargo are reviewed. One subject of current surveys is a large spacecraft that follows elliptical trajectories around the Sun and periodically meets Earth and Mars without ever being slowed down near one of the two planets. Small passenger and cargo transfer vehicles link the surface of Earth and Mars with the spaceship. This strategy allows large quantitites of cargo and many passengers to travel continuously from Earth to Mars and back. The major advantage of this concept is to accelerate the large spacecraft only once and save tremendous quantities of fuel by using smaller vehicles with less need for velocity to travel between the spaceship and the planet surfaces. ESA

17 SPACE COMM., SPACECRAFT COMM., COMMAND & TRACKING

Includes telemetry; space communications networks; astronavigation and guidance; and radio blackout.

For related information see also *04 Aircraft Communications and Navigation* and *32 Communications and Radar.*

No abstracts in this category.

18 SPACECRAFT DESIGN, TESTING AND PERFORMANCE

Includes satellites; space platforms; space stations; spacecraft systems and components such as thermal and environmental controls; and attitude controls.

For life support systems see *54 Man/System Technology and Life Support.* For related information see also *05 Aircraft Design, Testing and Performance, 39 Structural Mechanics,* and *16 Space Transportation.*

N91-19122*# National Aeronautics and Space Administration. Langley Research Center, Hampton, VA.
THE 5TH ANNUAL NASA SPACECRAFT CONTROL LABORATORY EXPERIMENT (SCOLE) WORKSHOP, PART 2
Lawrence W. Taylor, Jr., comp. Dec. 1990 369 p Workshop held in Lake Arrowhead, CA, 31 Oct. 1988
(NASA-CP-10057-Pt-2; NAS 1.55:10057-Pt-2) Avail: NTIS HC/MF A16 CSCL 22B

A collection of papers from the workshop are presented. The topics addressed include: the modeling, systems identification, and control synthesis for the Spacecraft Control Laboratory Experiment (SCOLE) configuration. Author

N91-19123*# National Aeronautics and Space Administration, Washington, DC.
SPACE STATION: THE NEXT LOGICAL STEP
Andrew J. Stofan 1986 12 p Original contains color illustrations
(NASA-TM-103398; NAS 1.15:103398) Avail: NTIS HC/MF A03; 5 functional color pages CSCL 22B

The following topics with respect to the space station program are discussed: (1) unmanned free-flyers; (2) recent progress; (3) the space shuttle; (4) international participation; (5) science, commerce, and technology; and (6) private sector participation. K.S.

N91-19124# Advisory Group for Aerospace Research and Development, Neuilly-Sur-Seine (France). Flight Mechanics Panel.
SPACE VEHICLE FLIGHT MECHANICS
N. X. Vinh (Michigan Univ., Ann Arbor.) Nov. 1990 16 p Symposium held in Luxembourg, 13-16 Nov. 1989
(AGARD-AR-294; ISBN-92-835-0570-0) Copyright Avail: NTIS HC/MF A03; Non-NATO Nationals requests available only from AGARD/Scientific Publications Executive

In recent years, manned flights into low earth orbits were made both for scientific study and for the placement of unmanned satellites into geosynchronous orbits and also into interplanetary orbits. Efforts of many nations are currently under way to place man into orbit on a semipermanent basis through the use of a space station. At the same time, the aerospace industry worldwide is considering the extension from supersonic flight of advanced fighter aircraft to the hypersonic flight of a future aerospace plane. To meet the challenges of the many technical problems to be solved in this new area, the flight mechanics of vehicles in space and in the upper layer of the atmosphere are identified and the areas of technology relevant to the Flight Mechanics Panel are identified. Author

N91-19125 Old Dominion Univ., Norfolk, VA.
CONTROL AND MECHANISM INTERACTION FOR GROUND-BASED TESTING OF SPACE STRUCTURES Ph.D. Thesis
Li-Farn Yang 1990 279 p
Avail: Univ. Microfilms Order No. DA9025219

In the ground-based validation testing, the adverse effect of terrestrial conditions such as a gravitational force interferes with the dynamic behavior of space structures. A suspension system is developed to assess the structural characteristics in a simulated zero-gravity environment. Using a mechanisms approach, the synthesis of a noncircular disk with a torsional spring at its rotational axis is designed to counteract the gravitational force of test structures during the testing. The multibody dynamics of a flexible steel beam carried on a rigid trolley was investigated. The system is constructed in such a way that the rapid and large angle slewing maneuver is performed by means of hybrid rotational/translational motions. A flexible one-beam structure and a flexible two-beam structure with such noncircular gears is investigated. One optimization technique based on the Generalized Reduced Gradient Method is employed to determine the optimal design of the controllers as well as the noncircular gears for vibrational suppression during the rapid slewing maneuvers. The numerical simulations are implemented to evaluate the effectiveness of the integrated design of control and mechanism for the slewing maneuvers of flexible space structures. Based on the Lyapunov stability criterion, the stability analysis of space structures leads to the design of a Lyapunov-based controller that yields a stable closed-loop system. Such a controller is developed by combining a linear part and a nonlinear part for the rotational/translational maneuver. The simulations of three kinds of nonlinear dynamic systems are performed to verify the usefulness of Lyapunov-based nonlinear feedback control. Two types of beam-like flexible space structure are simulated to implement maneuvering tasks of position control while suppressing the structural vibration simultaneously. Dissert. Abstr.

N91-19126*# National Aeronautics and Space Administration. Goddard Space Flight Center, Greenbelt, MD.
SIXTEENTH SPACE SIMULATION CONFERENCE CONFIRMING SPACEWORTHINESS INTO THE NEXT MILLENNIUM
Joseph L. Stecher, III, ed. Washington Nov. 1990 464 p Symposium held in Albuquerque, NM, 5-8 Nov. 1990; sponsored by NASA, Inst. of Environmental Sciences, AIAA, and the American Society for Testing and Materials
(NASA-CP-3096; Rept-90B00146; NAS 1.55:3096) Avail: NTIS HC/MF A20 CSCL 22B

The conference provided participants with a forum to acquire and exchange information on the state of the art in space

simulation, test technology, thermal simulation and protection, contamination, and techniques of test measurements. For individual titles, see N91-19127 through N91-19161.

N91-19127*# Martin Marietta Aerospace, Denver, CO.
SOLAR THERMAL VACUUM TESTS OF MAGELLAN SPACECRAFT
James C. Neuman *In* NASA, Goddard Space Flight Center, 16th Space Simulation Conference Confirming Spaceworthiness Into the Next Millennium Nov. 1990 p 1-20 (For primary document see N91-19126 11-18)
Avail: NTIS HC/MF A20 CSCL 22B

The Magellen solar/thermal/vacuum test involved a number of unique requirements and approaches. Because of the need to operate in orbit around Venus, the solar intensity requirement ranged up to 2.3 suns or Earth equivalent solar constants. Extensive modification to the solar simulator portion of the test facility were required to achieve this solar intensity. Venus albedo and infrared emission were simulated using temperature controlled movable louver panels to allow the spacecraft to view either a selectable temperature black heat source with closed louvers, or the chamber coldwall behind open louvers. The test conditions included widely varying solar intensities, multiple sun angles, alternate hardware configurations, steady state and transient cases, and cruise and orbital power profiles. Margin testing was also performed, wherein supplemental heaters were mounted to internal thermal blankets to verify spacecraft performance at higher than expected temperatures. The test was successful, uncovering some spacecraft anomalies and verifying the thermal design. The test support equipment experienced some anomalous behavior and a significant failure during the test. Author

N91-19128*# National Aeronautics and Space Administration. Goddard Space Flight Center, Greenbelt, MD.
THE TEST FACILITY REQUIREMENTS FOR THE THERMAL VACUUM THERMAL BALANCE TEST OF THE COSMIC BACKGROUND EXPLORER OBSERVATORY
Laura J. Milam *In its* 16th Space Simulation Conference Confirming Spaceworthiness Into the Next Millennium Nov. 1990 p 21-34 (For primary document see N91-19126 11-18)
Avail: NTIS HC/MF A20 CSCL 22B

The Cosmic Background Explorer Observatory (COBE) underwent a thermal vacuum thermal balance test in the Space Environment Simulator (SES). This was the largest and most complex test ever conducted at this facility. The 4 x 4 m (13 x 13 ft) spacecraft weighed approx. 2223 kg (4900 lbs) for the test. The test set up included simulator panels for the inboard solar array panels, simulator panels for the flight cowlings, Sun and Earth Sensor stimuli, Thermal Radio Frequency Shield heater stimuli and a cryopanel for thermal control in the Attitude Control System Shunt Dissipator area. The fixturing also included a unique 4.3 m (14 ft) diameter Gaseous Helium Cryopanel which provided a 20 K environment for the calibration of one of the spacecraft's instruments, the Differential Microwave Radiometer. This cryogenic panel caused extra contamination concerns and a special method was developed and written into the test procedure to prevent the high buildup of condensibles on the panel which could have led to backstreaming of the thermal vacuum chamber. The test was completed with a high quality simulated space environment provided to the spacecraft. The test requirements, test set up, and special fixturing are described. Author

N91-19129*# Instituto de Pesquisas Espaciais, Sao Jose dos Campos (Brazil).
SCD 02 THERMAL DESIGN Abstract Only
Humberto Pontes Cardoso *In* NASA, Goddard Space Flight Center, 16th Space Simulation Conference Confirming Spaceworthiness Into the Next Millennium Nov. 1990 p 35 (For primary document see N91-19126 11-18)
Avail: NTIS HC/MF A20 CSCL 22B

The Satelite de Coleta de Dados (SCD) 02 (Data Collection Satellite) has the following characteristics: 115 kg weight, octagonal prism shape, 1 m diameter, and 0.67 m height. Its specified orbit is nearly circular, 700 km altitude, is inclined 25 deg with respect to the equator line, and has 100 min period. The electric power is supplied by eight solar panels installed on the lateral sides of the satellite. The equipment is located on the central (both faces) and lower (internal face) panels. The satellite is spin stabilized and its attitude control is such that during its lifetime, the solar aspect angle will vary between 80 and 100 deg with respect to its spin axis. Two critical cases were selected for thermal control design purposes: Hot case (maximum solar constant, solar aspect angle equal to 100 deg, minimum eclipse time and maximum internal heat dissipation); and a passive thermal design concept was achieved and the maximum and minimum equipment operating temperatures were obtained through a 109 node finite difference mathematical model. Author

N91-19130*# Instituto de Pesquisas Espaciais, Sao Jose dos Campos (Brazil).
SCD1 THERMAL DESIGN AND TEST RESULT ANALYSIS
Humberto Pontes Cardoso, Issamu Muraoka, Marcia Barbosa Henri Mantelli, and Rosangela M. G. Leite *In* NASA, Goddard Space Flight Center, 16th Space Simulation Conference Confirming Spaceworthiness Into the Next Millennium Nov. 1990 p 36-51 (For primary document see N91-19126 11-18)
Avail: NTIS HC/MF A20 CSCL 22B

The SCD 01 (Satelite de Coleta de Dados 01) is a spin stabilized low Earth orbit satellite dedicated to the collection and distribution of environmental data. It was completely developed at the Brazilian Institute for Space Research (INPE) and is scheduled to be launched in 1992. The SCD 01 passive thermal control design configuration is presented and the thermal analysis results are compared with the temperatures obtained from a Thermal Balance Test. The correlation between the analytical and experimental results is considered very good. Numerical flight simulations show that the thermal control design can keep all the subsystem temperatures within their specified temperature range. Author

N91-19131*# Spar Aerospace Ltd., Ste-Anne-de-Bellevue (Quebec).
THERMAL BALANCE TESTING OF THE ANIK-E SPACECRAFT Abstract Only
Alex Golob, Cristian Ruel, and Marc Donato *In* NASA, Goddard Space Flight Center, 16th Space Simulation Conference Confirming Spaceworthiness Into the Next Millennium Nov. 1990 p 52 (For primary document see N91-19126 11-18)
Avail: NTIS HC/MF A20 CSCL 22B

Spar Aerospace, Ltd. of Canada has recently completed the first of two infrared thermal balance/thermal vacuum tests on Canada's next generation of telecommunication satellites: Anik-E. Anik-E is a two spacecraft program using a three axis stabilized GE 5000 series bus as the vehicle for its payload. The infrared test setup consists of the mechanical hardware required to support the spacecraft within the thermal vacuum chamber and the infrared rig which supports the spacecraft. Spar developed a software package which calculated the lamp positions to provide the necessary uniform heat flux, based on the required heat inputs on the various isothermal zones of the spacecraft for the different phases of the tests. Infrared heat sensors, radiometers, were installed on the spacecraft surfaces. These were connected to the facility data processing system and continually monitored the flux absorbed by the various spacecraft surfaces. The test set up had distinct advantages. It enabled testing to progress directly from the thermal balance to thermal vacuum. Waveguide runs were installed for the communications portion of the testing prior to pumpdown. This precluded the requirement to return to ambient to reconfigure the setup. Author

N91-19132*# Martin Marietta Aerospace, Denver, CO.
AN OUTGASSING MODEL OF NON-METALLIC MATERIALS FOR THE ASCENT OF A TITAN 4 LAUNCH VEHICLE Abstract Only **c27**
R. D. Barrows and S. L. VanLoon *In* NASA, Goddard Space Flight Center, 16th Space Simulation Conference Confirming

Spaceworthiness Into the Next Millennium Nov. 1990 p 55 (For primary document see N91-19126 11-18)
Avail: NTIS HC/MF A20 CSCL 11C

Outgassing of nonmetallic materials and components inside Titan IV's 2A compartment during ascent may present a problem to the payload community in relation to molecular deposition and degradation of sensitive payload surfaces. The procedure currently being developed to model the amounts, transport, and deposition of outgassed molecular contaminants onto a payload's sensitive surface consists of three phases. The first phase involves the development of a thermogravimetric method that recreates the increasing temperature and decreasing pressure profiles expected in the 2A compartment of the TIV launch vehicle during ascent. The second phase involves the determination of deposition rates of outgassed materials onto a payload surface, and the subsequent evaporation rate as a function of temperature of deposited material. The third phase takes the temperature and pressure profiles from phase one, the deposition and evaporation rates and kinetic coefficients determined in phase two, and incorporates them into the SPACE II computer program to determine which payload surfaces are most susceptible to molecular deposition from TIV's outgassing sources, and the level of permanent deposition expected on those surfaces. Author

N91-19133*# Massachusetts Inst. of Tech., Lexington. Lincoln Lab.
THE PERFORMANCE OF MULTILAYER INSULATION IN A RAPIDLY DEPRESSURIZING ENVIRONMENT c24
Ronald A. Efromson *In* NASA, Goddard Space Flight Center, 16th Space Simulation Conference Confirming Spaceworthiness Into the Next Millennium Nov. 1990 p 56-72 Sponsored in part by Strategic Defense Initiative Organization (For primary document see N91-19126 11-18)
Avail: NTIS HC/MF A20 CSCL 11D

The performance of multilayer insulation in a rapidly depressurizing environment is determined by the variation of heat transfer with internal pressure and the pressure history of the interstitial gas. Measurements of thermal performance were made on three multilayer insulation configurations at room temperature and steady state pressures from 10(exp -6) to 10(exp -1) torr. The heat transfer due to gas conduction alone correlated with the kinetic theory of gases in the molecular flow regime. Pressure histories were measured in a unique apparatus which simulated the depressurization rate of a boost vehicle. The pressure histories on both sides of two of the configurations were measured to bound the actual interstitial pressure. The results of the two types of measurements agreed with earlier work and were combined to make performance predictions using an actual ascent pressure history. Author

N91-19134*# TRW Defense and Space Systems Group, Redondo Beach, CA.
HIGH VACUUM FACILITY FOR HYDRAZINE THRUSTER TESTING c14
Patrick F. Neary *In* NASA, Goddard Space Flight Center, 16th Space Simulation Conference Confirming Spaceworthiness Into the Next Millennium Nov. 1990 p 73-74 (For primary document see N91-19126 11-18)
Avail: NTIS HC/MF A20 CSCL 14B

An ongoing modification is described of a large vacuum chamber to accommodate the ignition of an arcjet hydrazine thruster while maintaining a vacuum level of 1 x 10(exp -5) torr or less. The vacuum facility consists of a 20 ft stainless steel vacuum tank with an internal LN2 shroud, four 35 in. cryopumps and an 8 in. turbopump. To maintain a vacuum level of 1 x 10(exp -5) torr or less, 900 sq ft of liquid helium (LHe) shroud surface was installed to maintain the vacuum level and pumping requirements. A vacuum level of 1 x 10(exp -5) torr or less will allow the hydrazine thrust to exit the thruster nozzle and radiate into a space type environment so that the plume flow field can be analyzed and compared to the analytical model density distribution profile. Some other arcjet thruster characteristics measured are the electromagnetic interference (EMI) and exhaust contamination. This data is used to evaluate if the arcjet thruster with its high specific impulse in comparison to current chemical propulsion thruster can be used for the next generation of communication satellites. Author

N91-19135*# National Aeronautics and Space Administration. Goddard Space Flight Center, Greenbelt, MD.
FLOW FIELDS OF LOW PRESSURE VENT EXHAUSTS c34
John J. Scialdone *In its* 16th Space Simulation Conference Confirming Spaceworthiness Into the Next Millennium Nov. 1990 p 75-83 Previously announced as N89-26902 (For primary document see N91-19126 11-18)
Avail: NTIS HC/MF A20 CSCL 20D

The flow field produced by low pressure gas vents are described based on experimental data obtained from tests in a large vacuum chamber. The gas density, pressure, and flux at any location in the flow field are calculated based on the vent plume description and the knowledge of the flow rate and velocity of the venting gas. The same parameters and the column densities along a specified line of sight traversing the plume are also obtained and shown by a computer generated graphical representation. The fields obtained with a radically scanning Pitot probe within the exhausting gas are described by a power of the cosine function, the mass rate, and the distance from the exit port. The field measurements were made for gas at pressures ranging from 2 to 50 torr venting from pipe fittings with diameters to 3/16 to 1-1/2 inches I.D. (4.76 to 38.1 mm). The N2 mass flow rates ranged from 2E-4 to 3.7E-1 g/s. Author

N91-19136*# TRW Space Technology Labs., Redondo Beach, CA.
MULTIPURPOSE HARDENED SPACECRAFT INSULATION c27
Carlos H. Steimer *In* NASA, Goddard Space Flight Center, 16th Space Simulation Conference Confirming Spaceworthiness Into the Next Millennium Nov. 1990 p 84-110 (For primary document see N91-19126 11-18)
Avail: NTIS HC/MF A20 CSCL 11C

A Multipurpose Hardened Spacecraft Multilayer Insulation (MLI) system was developed and implemented to meet diverse survivability and performance requirements. Within the definition and confines of a MLI assembly (blanket), the design: (1) provides environmental protection from natural and induced nuclear, thermal, and electromagnetic radiation; (2) provides adequate electrostatic discharge protection for a geosynchronous satellite; (3) provides adequate shielding to meet radiated emission needs; and (4) will survive ascent differential pressure loads between enclosed volume and space. The MLI design is described which meets these requirements and design evolution and verification is discussed. The application is for MLI blankets which closeout the area between the laser crosslink subsystem (LCS) equipment and the DSP spacecraft cabin. Ancillary needs were implemented to ease installation at launch facility and to survive ascent acoustic and vibration loads. Directional venting accommodations were also incorporated to avoid contamination of LCS telescope, spacecraft sensors, and second surface mirrors (SSMs). Author

N91-19137*# CBI Na-Con, Oak Brook, IL.
OPTICAL TESTING CRYOGENIC THERMAL VACUUM FACILITY c74
Patrick W. Dohogne and Warren A. Carpenter *In* NASA, Goddard Space Flight Center, 16th Space Simulation Conference Confirming Spaceworthiness Into the Next Millennium Nov. 1990 p 113-132 Sponsored in part by AF (For primary document see N91-19126 11-18)
Avail: NTIS HC/MF A20 CSCL 20F

The construction of a turnkey cryogenic vacuum test facility was recently completed. The facility will be used to measure and record the surface profile of large diameter and 540 kg optics under simulated space conditions. The vacuum test chamber is a vertical stainless steel cylinder with a 3.5 diameter and a 7 m tangent length. The chamber was designed to maximize optical testing quality by minimizing the vibrations between the laser interferometer and the test specimen. This was accomplished by

designing the chamber for a high natural frequency and vibration isolating the chamber. An optical test specimen is mounted on a movable presentation stage. During thermal vacuum testing, the specimen may be positioned to + or - 0.00025 cm accuracy with a fine adjustment mechanism. The chamber is evacuated by a close coupled Roots-type blower and rotary vane pump package and two cryopumps. The chamber is equipped with an optically dense gaseous nitrogen cooled thermal shroud. The thermal shroud is used to cool or warm the optical test specimen at a controlled rate. A control system is provided to automatically evacuate the chamber and cooldown the test specimen to the selected control temperature. Author

N91-19138*# Boeing Aerospace Co., Seattle, WA.
BOEING INFRARED SENSOR (BIRS) CALIBRATION FACILITY **c14**
John D. Hazen and L. V. Scorsone (Pittsburgh-Des Moines Steel Co., PA.) *In* NASA, Goddard Space Flight Center, 16th Space Simulation Conference Confirming Spaceworthiness Into the Next Millennium Nov. 1990 p 133-156 (For primary document see N91-19126 11-18)
Avail: NTIS HC/MF A20 CSCL 14B

The Boeing Infrared Sensor (BIRS) Calibration Facility represents a major capital investment in optical and infrared technology. The facility was designed and built for the calibration and testing of the new generation large aperture long wave infrared (LWIR) sensors, seekers, and related technologies. Capability exists to perform both radiometric and goniometric calibrations of large infrared sensors under simulated environmental operating conditions. The system is presently configured for endoatmospheric calibrations with a uniform background field which can be set to simulate the expected mission background levels. During calibration, the sensor under test is also exposed to expected mission temperatures and pressures within the test chamber. Capability exists to convert the facility for exoatmospheric testing. The configuration of the system is described along with hardware elements and changes made to date are addressed. Author

N91-19139*# Calspan Field Services, Inc., Arnold AFS, TN.
INFRARED SENSOR TEST METHODOLOGY AND FACILITIES **c14**
Jere J. Matty and Ronald Dawbarn *In* NASA, Goddard Space Flight Center, 16th Space Simulation Conference Confirming Spaceworthiness Into the Next Millennium Nov. 1990 p 157-175 (For primary document see N91-19126 11-18)
Avail: NTIS HC/MF A20 CSCL 14B

As the Air Force Systems Command designated Center of Expertise for Space Simulation Testing, AEDC has defined a test methodology for the ground testing of infrared sensor systems. This test methodology and the test facilities envisioned to implement it has been addressed in another report. The progress on the implementation of that test methodology is reported and the status of the test facilities presently existing or under construction to implement it is described. Author

N91-19140*# Grumman Aerospace Corp., Bethpage, NY. Space Systems Div.
THERMAL CONTROL FOR THE GROUND SIMULATION OF A SPACE IR SENSOR SYSTEM Abstract Only **c14**
E. Lee, A. Warren, G. Gasser, and M. Tierney (Itek Corp., Lexington, MA.) *In* NASA, Goddard Space Flight Center, 16th Space Simulation Conference Confirming Spaceworthiness Into the Next Millennium Nov. 1990 p 179 (For primary document see N91-19126 11-18)
Avail: NTIS HC/MF A20 CSCL 14B

Active and passive thermal controls for simulations of a space IR sensor system operating in cryogenic temperatures were designed, built, and tested from a component level to a system level. The test results from component tests and integrated system tests have compared very well with theoretical predictions, and thus verify component and integrated thermal math models. These verified models can be modified for use to predict flight systems thermal performance. Thermal vacuum simulations and demonstrations of a space IR system consisted of a target and background scene generator, telescope mirrors supported by a graphite-epoxy metering structure, and an IR sensor. These components are required to operate at cryogenic temperature levels. Each component has its unique thermal control needs. Descriptions are presented of thermal control systems for the test article from component design level to integrated system level along with discussions of component and integrated demonstration tests, and correlation of test data with thermal finite difference models. Author

N91-19141*# Grumman Aerospace Corp., Bethpage, NY. Space Systems Div.
SPECIAL REQUIREMENTS IN THE DESIGN OF A SENSOR TEST AND INTEGRATION LABORATORY Abstract Only **c14**
S. Bellanca, E. Lee, and J. Campbell *In* NASA, Goddard Space Flight Center, 16th Space Simulation Conference Confirming Spaceworthiness Into the Next Millennium Nov. 1990 p 180 (For primary document see N91-19126 11-18)
Avail: NTIS HC/MF A20 CSCL 14B

Special needs are imposed on the design and operation of a sensor test and integration lab. Cryogenic temperature, vibration isolation for electro-optical equipment, contamination control, thermal control to reduce or minimize thermally induced stresses on mirrors and supporting metering structure, thermal vacuum chamber shroud temperature uniformity, and varying temperature control capability to bring optical equipment from cryogenic temperature to ambient environment, and real time processing are some of the stringent needs that must be addressed before a facility can be accepted to perform sensor test and integration. Most of the sensor tests are performed at cryogenic temperature, and thermal isolation of the test article from the ambient temperature is a strong consideration for the thermal vacuum chamber design. Also, equipment heat and parasitic heat sources must be able to be removed from the chamber without exceeding the chamber shroud temperature gradients. How these needs were met in the design, build, and acceptance test of the Grumman Sensor Test and Integration Lab (STIL) is described. Author

N91-19142*# Liege Univ. (Belgium). Centre de Recherches IAL SPACE.
IAL SPACE: A TEST LABORATORY FOR THE ISO CRYOGENIC PAYLOAD **c14**
A. Cucchiaro, M. Henrist, J. P. Macau, N. Ninane, and R. Blanpain *In* NASA, Goddard Space Flight Center, 16th Space Simulation Conference Confirming Spaceworthiness Into the Next Millennium Nov. 1990 p 181-191 (For primary document see N91-19126 11-18)
Avail: NTIS HC/MF A20 CSCL 14B

The ESA Infrared Space Observatory (ISO) satellite is a 3 axes pointed platform designed to make accurate pointed observations of astronomical objects and sources in the wavelength range between 2.5 and 200 microns. ISO is composed of a service module and a payload module which is a large cylindrical vacuum vessel. The vessel is in fact a cryostat (capacity of 2250 l of liquid He II) which contains the telescope and the four focal scientific instruments. The latter being cooled up to a temperature less than 4 K. The qualification of the payload requires the measurement respectively of: the image quality of the telescope through wave front error (WFE) measurements; and the optical alignment of the scientific instruments with respect to the telescope axis and the telescope focus, and this under cryogenic conditions. Consequently, since 1988, the FOCAL 5 IAL Space facility has been upgraded in order to perform the cryogenic optical tests of the ISO optical subsystems. Author

N91-19143*# National Research Council of Canada, Ottawa (Ontario). Inst. for Aerospace Research.
NON-LINEAR GENERATION OF ACOUSTIC NOISE IN THE IAR SPACECRAFT **c71**
R. Westley, K. Nguyen, and M. S. Westley *In* NASA, Goddard Space Flight Center, 16th Space Simulation Conference Confirming

Spaceworthiness Into the Next Millennium Nov. 1990 p 195-210 (For primary document see N91-19126 11-18)
Avail: NTIS HC/MF A20 CSCL 20A

The requirement to produce high level acoustic noise fields with increasing accuracy in environmental test facilities dictates that a more precise understanding is required of the factors controlling nonlinear noise generation. Details are given of various nonlinear effects found in acoustic performance data taken from the IAR Spacecraft Acoustic Chamber. This type of data has enabled the IAR to test large spacecraft to relatively tight acoustic tolerances over a wide frequency range using manually set controls. An analog random noise automatic control system was available and modified to provide automatic selection of the chamber's spectral sound pressure levels. The automatic control system when used to complete a typical qualification test appeared to equal the accuracy of the manual system and had the added advantage that parallel spectra could be easily achieved during preset tests. Author

N91-19144*# California State Polytechnic Univ., Pomona.
DETAILED MODAL TESTING OF A SOLID ROCKET MOTOR USING A PORTABLE TEST SYSTEM c20
Vladimir Glozman and Ralph D. Brillhart (SDRC, Inc., San Diego, CA.) *In* NASA, Goddard Space Flight Center, 16th Space Simulation Conference Confirming Spaceworthiness Into the Next Millennium Nov. 1990 p 211-226 (For primary document see N91-19126 11-18)
Avail: NTIS HC/MF A20 CSCL 21H

Modern analytical techniques have expended the ability to evaluate solid rocket motors used in launch vehicles. As more detailed models of solid rocket motors were developed, testing methods were required to verify the models. Experimental modal analysis (modal testing) of space structures and launch vehicles has been a requirement for model validation for many years. However, previous testing of solid rocket motors has not typically involved dynamic modal testing of full scale motors for verification of solid propellant or system assembly properties. Innovative approaches to the testing of solid rocket motors were developed and modal testing of a full scale, two segment Titan 34D Solid Rocket Motor (SRM) was performed to validate detailed computer modeling. Special modifications were made to convert an existing facility into a temporary modal test facility which would accommodate the test article. The assembly of conventional data acquisition equipment into a multiple channel count portable system has made modal testing in the field feasible. Special purpose hydraulic exciters were configured to apply the dynamic driving forces required. All instrumentation and data collection equipment were installed at the test site for the duration of the test program and removed upon completion. Conversion of an existing test facility into a temporary modal test facility, and use of a multiple channel count portable test data acquisition system allowed all test objectives to be met and resulted in validation of the computer model in a minimum time. Author

N91-19145*# McDonnell-Douglas Space Systems Co., Huntington Beach, CA.
INNOVATIONS IN DYNAMIC TEST RESTRAINT SYSTEMS
Christopher J. Fuld *In* NASA, Goddard Space Flight Center, 16th Space Simulation Conference Confirming Spaceworthiness Into the Next Millennium Nov. 1990 p 227-245 (For primary document see N91-19126 11-18)
Avail: NTIS HC/MF A20 CSCL 22B

Recent launch system development programs have led to a new generation of large scale dynamic tests. The variety of test scenarios share one common requirement: restrain and capture massive high velocity flight hardware with no structural damage. The Space Systems Lab of McDonnell Douglas developed a remarkably simple and cost effective approach to such testing using ripstitch energy absorbers adapted from the sport of technical rockclimbing. The proven system reliability of the capture system concept has led to a wide variety of applications in test system design and in aerospace hardware design. Author

N91-19146*# Los Alamos National Lab., NM.
ATOMIC OXYGEN EFFECTS ON BORON NITRIDE AND SILICON NITRIDE: A COMPARISON OF GROUND BASED AND SPACE FLIGHT DATA c27
J. B. Cross, E. H. Lan, C. A. Smith, and W. J. Whatley (Sparta, Inc., San Diego, CA.) *In* NASA, Goddard Space Flight Center, 16th Space Simulation Conference Confirming Spaceworthiness Into the Next Millennium Nov. 1990 p 249-258 (For primary document see N91-19126 11-18)
Avail: NTIS HC/MF A20 CSCL 11C

The effects of atomic oxygen on boron nitride (BN) and silicon nitride (Si3N4) were evaluated in a low Earth orbit (LEO) flight experiment and in a ground based simulation facility. In both the inflight and ground based experiments, these materials were coated on thin (approx. 250A) silver films, and the electrical resistance of the silver was measured in situ to detect any penetration of atomic oxygen through the BN and Si3N4 materials. In the presence of atomic oxygen, silver oxidizes to form silver oxide, which has a much higher electrical resistance than pure silver. Permeation of atomic oxygen through BN, as indicated by an increase in the electrical resistance of the silver underneath, was observed in both the inflight and ground based experiments. In contrast, no permeation of atomic oxygen through Si3N4 was observed in either the inflight or ground based experiments. The ground based results show good qualitative correlation with the LEO flight results, indicating that ground based facilities such as the one at Los Alamos National Lab can reproduce space flight data from LEO. Author

N91-19147*# Martin Marietta Aerospace, Denver, CO.
ADVANCES IN ATOMIC OXYGEN SIMULATION c25
Joseph F. Froechtenigt and Lyle E. Bareiss *In* NASA, Goddard Space Flight Center, 16th Space Simulation Conference Confirming Spaceworthiness Into the Next Millennium Nov. 1990 p 259-265 (For primary document see N91-19126 11-18)
Avail: NTIS HC/MF A20 CSCL 07D

Atomic oxygen (AO) present in the atmosphere at orbital altitudes of 200 to 700 km has been shown to degrade various exposed materials on Shuttle flights. The relative velocity of the AO with the spacecraft, together with the AO density, combine to yield an environment consisting of a 5 eV beam energy with a flux of 10(exp 14) to 10(exp 15) oxygen atoms/sq cm/s. An AO ion beam apparatus that produces flux levels and energy similar to that encountered by spacecraft in low Earth orbit (LEO) has been in existence since 1987. Test data was obtained from the interaction of the AO ion beam with materials used in space applications (carbon, silver, kapton) and with several special coatings of interest deposited on various surfaces. The ultimate design goal of the AO beam simulation device is to produce neutral AO at sufficient flux levels to replicate on-orbit conditions. A newly acquired mass spectrometer with energy discrimination has allowed 5 eV neutral oxygen atoms to be separated and detected from the background of thermal oxygen atoms of approx 0.2 eV. Neutralization of the AO ion beam at 5 eV was shown at the Martin Marietta AO facility. Author

N91-19148*# McDonnell-Douglas Space Systems Co., Huntington Beach, CA.
SPACE ENVIRONMENTAL EFFECTS ON SPACECRAFT THERMAL CONTROL COATINGS Abstract Only c27
L. G. Bartosik and H. W. Babel *In* NASA, Goddard Space Flight Center, 16th Space Simulation Conference Confirming Spaceworthiness Into the Next Millennium Nov. 1990 p 266 (For primary document see N91-19126 11-18)
Avail: NTIS HC/MF A20 CSCL 11C

A large portion of the space based applications in the near future are for low Earth orbit (LEO) including the Space Station Freedom (SSF). The lifetime needs for materials on the SSF is 30 years. Materials must be selected which can withstand the deleterious effects of LEO. Environmental effects in the LEO include atomic oxygen, UV, ionizing radiation, and hypervelocity impact. These effects can adversely affect the surface properties of materials. This is particularly critical in the case of thermal control

materials where the efficiency of the thermal control is dependent on the stability of the surface properties. The current baseline thermal coating for the SSF radiators is Ag Teflon. The surface property requirements for the coatings are a solar absorptance of 0.2 and an infrared emittance of 0.8. The effects of atomic oxygen and UV radiation on the baseline coating and several other candidate thermal control materials were studied. The thermal control radiator materials included Ag and Al backed Teflon, H2SO4 anodized Al, sputter deposited SiO2 on Al, and Ag and Al backed polychloro trifluoroethylene. The simulation of several of the LEO environment constituents provided a data base to aid in the selection of the radiator thermal control material to meet the life requirements of the SSF. The effects are illustrated of the environment on thermal control coatings and the importance of this factor in the selection process for long life spacecraft materials. Author

N91-19149*# TRW Defense and Space Systems Group, Redondo Beach, CA.
SPACE SIMULATION TEST FOR THERMAL CONTROL MATERIALS **c27**
W. R. Hardgrove *In* NASA, Goddard Space Flight Center, 16th Space Simulation Conference Confirming Spaceworthiness Into the Next Millennium Nov. 1990 p 267-285 (For primary document see N91-19126 11-18)
Avail: NTIS HC/MF A20 CSCL 11C

Tests were run in TRW's Combined Environment Facility to examine the degradation of thermal control materials in a simulated space environment. Thermal control materials selected for the test were those presently being used on spacecraft or predicted to be used within the next few years. The geosynchronous orbit environment was selected as the most interesting. One of the goals was to match degradation of those materials with available flight data. Another aim was to determine if degradation can adequately be determined with accelerated or short term ground tests. Author

N91-19150*# Chicago Bridge and Iron Co., Oak Brook, IL.
SPACE SIMULATION FACILITIES PROVIDING A STABLE THERMAL VACUUM FACILITY **c14**
Martin L. Tellalian *In* NASA, Goddard Space Flight Center, 16th Space Simulation Conference Confirming Spaceworthiness Into the Next Millennium Nov. 1990 p 289-313 (For primary document see N91-19126 11-18)
Avail: NTIS HC/MF A20 CSCL 14B

CBI has recently constructed the Intermediate Thermal Vacuum Facility. Built as a corporate facility, the installation will first be used on the Boost Surveillance and Tracking System (BSTS) program. It will also be used to develop and test other sensor systems. The horizontal chamber has a horseshoe shaped cross section and is supported on pneumatic isolators for vibration isolation. The chamber structure was designed to meet stability and stiffness requirements. The design process included measurement of the ambient ground vibrations, analysis of various foundation test article support configurations, design and analysis of the chamber shell and modal testing of the chamber shell. A detailed 3-D finite element analysis was made in the design stage to predict the lowest three natural frequencies and mode shapes and to identify local vibrating components. The design process is described and the results are compared of the finite element analysis to the results of the field modal testing and analysis for the 3 lowest natural frequencies and mode shapes. Concepts are also presented for stiffening large steel structures along with methods to improve test article stability in large space simulation facilities. Author

N91-19151*# Liege Univ. (Belgium). Centre de Recherches IAL SPACE.
THE SPACE SIMULATION FACILITIES AT IAL SPACE **c14**
M. Henrist, A. Cucchiaro, I. Domken, and J. P. Macau *In* NASA, Goddard Space Flight Center, 16th Space Simulation Conference Confirming Spaceworthiness Into the Next Millennium Nov. 1990 p 314-322 (For primary document see N91-19126 11-18)
Avail: NTIS HC/MF A20 CSCL 14B

The thermal vacuum facilities of IAL SPACE were tailored for testing of the ESA payloads. They were progressively upgraded for cryogenic payloads including 4 K (liquid helium temperature) experiments. A detailed review of the three vacuum chambers, ranging from 1.5 to 5 m diameter, is presented including the corresponding capabilities in the vacuum, thermal, and optical fields. The various aspects of cleanliness, product assurance, and quality control are also presented. Author

N91-19152*# National Aeronautics and Space Administration. Goddard Space Flight Center, Greenbelt, MD.
CONTAMINATION CONTROL PROGRAM FOR THE COSMIC BACKGROUND EXPLORER: AN OVERVIEW
Richard D. Barney *In its* 16th Space Simulation Conference Confirming Spaceworthiness Into the Next Millennium Nov. 1990 p 323-339 (For primary document see N91-19126 11-18)
Avail: NTIS HC/MF A20 CSCL 22B

Each of the three state of the art instruments flown aboard NASA's Cosmic Background Explorer (COBE) were designed, fabricated, and integrated using unique contamination control procedures to ensure accurate characterization of the diffuse radiation in the universe. The most stringent surface level cleanliness specifications ever attempted by NASA were required by the Diffuse Infrared Background Experiment (DRIBE) which is located inside a liquid helium cooled dewar along with the Far Infrared Absolute Spectrophotometer (FIRAS). The DRIBE instrument required complex stray radiation suppression that defined a cold primary optical baffle system surface cleanliness level of 100A. The cleanliness levels of the cryogenic FIRAS instrument and the Differential Microwave Radiometer (DMR) which were positioned symmetrically around the dewar were less stringent ranging from 300 to 500A. To achieve these instrument cleanliness levels, the entire flight spacecraft was maintained at level 500A throughout each phase of development. The COBE contamination control program is described along with the difficulties experienced in maintaining the cleanliness quality of personnel and flight hardware throughout instrument assembly. Author

N91-19153*# McDonnell-Douglas Space Systems Co., Huntington Beach, CA.
A UNIQUE APPROACH TO SPACE THERMAL SIMULATION **Abstract Only** **c27**
D. Q. Durant *In* NASA, Goddard Space Flight Center, 16th Space Simulation Conference Confirming Spaceworthiness Into the Next Millennium Nov. 1990 p 343 (For primary document see N91-19126 11-18)
Avail: NTIS HC/MF A20 CSCL 11C

The Space Systems Lab of McDonnell Douglas developed several innovative techniques to perform the DELTA Star System thermal vacuum test. Test design constraints included an accelerated test schedule and an ambitious test plan focusing on cyclic absorbed orbital flux simulation. Test design and fabrication was completed in only 4 months, producing a 21 zone computer modeled refectorless lamp array system. Array zone control was based on discreet absorbed flux measurements, provided by adiabatic coupons conceived to eliminate the need for conventional radiometers. Test requirements, methodology, and test thermal model flight data correlation are presented. Author

N91-19154*# Gibbel Corp., Palos Verdes Estates, CA.
THERMAL/VACUUM VS. THERMAL ATMOSPHERIC TESTING OF SPACE FLIGHT ELECTRONIC ASSEMBLIES **c33**
Mark Gibbel *In* NASA, Goddard Space Flight Center, 16th Space Simulation Conference Confirming Spaceworthiness Into the Next Millennium Nov. 1990 p 344-356 (For primary document see N91-19126 11-18)
Avail: NTIS HC/MF A20 CSCL 09A

For space flight hardware, the thermal vacuum environmental test is the best test of a system's flight worthiness. Substituting an atmospheric pressure thermal test for a thermal/vacuum test can effectively reduce piece part temperatures by 20 C or more,

even for low power density designs. Similar reductions in test effectiveness can also result from improper assembly level T/V test boundary conditions. The net result of these changes may reduce the effective test temperatures to the point where there is zero or negative margin over the flight thermal environment.
Author

N91-19155*# European Space Agency. European Space Research and Technology Center, ESTEC, Noordwijk (Netherlands).
PROPOSAL FOR A CONCEPTUALLY NEW COMPACT COLLECTING OPTICS FOR POWERFUL LIGHT SOURCES
c74
G. Saenger *In* NASA, Goddard Space Flight Center, 16th Space Simulation Conference Confirming Spaceworthiness Into the Next Millennium Nov. 1990 p 357-375 (For primary document see N91-19126 11-18)
Avail: NTIS HC/MF A20 CSCL 20F

Testing of a spacecraft under simulated outer space conditions is the best guarantee for a successful mission, and for almost all of the parameters a good match (to within a few percent) may be reached in relevant test facilities (e.g., IR background, earthshine and albedo radiation, residual atmosphere, intensity stability, distribution and spectrum of the solar radiation). The collimation angle of the sun (32 arc min) is, however, a drastic exception, here only + or - 1.5 to 2 deg are achieved which means a relative deviation by nearly one order of magnitude. The main reason for this is the presently used collecting optics having unnecessary large diameters. Here a lens-mirror combination is proposed which allows the reduction of the diameter by nearly a factor of two and to achieve with the present Xenon arc lamps a collimation angle of + or - 0.8 deg. Author

N91-19156*# National Aeronautics and Space Administration. Lewis Research Center, Cleveland, OH.
AEOLIAN REMOVAL OF DUST TYPES FROM PHOTOVOLTAIC SURFACES ON MARS
James R. Gaier and Marla E. Perez-Davis *In* NASA, Goddard Space Flight Center, 16th Space Simulation Conference Confirming Spaceworthiness Into the Next Millennium Nov. 1990 p 379-396 (For primary document see N91-19126 11-18)
Avail: NTIS HC/MF A20 CSCL 22B

Dust elevated in local or global dust storms on the Martian surface could settle on photovoltaic (PV) surfaces and seriously hamper their performance. Using a recently developed technique to apply a uniform dust layer, PV surface materials were subjected to simulated Martian winds in an attempt to determine whether natural aeolian processes on Mars would sweep off the settled dust. Three different types of dust were used. The effects of wind velocity, angle of attack, height above the Martian surface, and surface coating material were investigated. It was found that arrays mounted on an angle of attack approaching 45 deg show the most efficient clearing. Although the angular dependence is not sharp, horizontally mounted arrays required much higher wind velocities to clear off the dust. From this test it appears that the arrays may be erected quite near the ground, but previous studies have suggested that saltation effects can be expected to cause such arrays to be covered by soil if they are set up less than about a meter from the ground. Particle size effect appear to dominate over surface chemistry in these experiments, but additional tests are required to confirm this. Author

N91-19157*# Instituto de Pesquisas Espaciais, Sao Jose dos Campos (Brazil).
EXPERIMENTAL DETERMINATION OF SATELLITE BOLTED JOINTS THERMAL RESISTANCE
Marcia Barbosa Henri Mantelli and Jose Edson Basto *In* NASA, Goddard Space Flight Center, 16th Space Simulation Conference Confirming Spaceworthiness Into the Next Millennium Nov. 1990 p 397-414 (For primary document see N91-19126 11-18)
Avail: NTIS HC/MF A20 CSCL 22B

The thermal resistance was experimentally determined of the bolted joints of the first Brazilian satellite (SCD 01). These joints, used to connect the satellite structural panels, are reproduced in an experimental apparatus, keeping, as much as possible, the actual dimensions and materials. A controlled amount of heat is forced to pass through the joint and the difference of temperature between the panels is measured. The tests are conducted in a vacuum chamber with liquid nitrogen cooled walls, that simulates the space environment. Experimental procedures are used to avoid much heat losses, which are carefully calculated. Important observations about the behavior of the joint thermal resistance with the variation of the mean temperature are made. Author

N91-19158*# Aeritalia S.p.A., Turin (Italy). Space Systems Group.
MAGNETIC CLEANLINESS VERIFICATION APPROACH ON TETHERED SATELLITE
Piero Messidoro, Massimo Braghin, and Maurizio Grande *In* NASA, Goddard Space Flight Center, 16th Space Simulation Conference Confirming Spaceworthiness Into the Next Millennium Nov. 1990 p 415-434 (For primary document see N91-19126 11-18)
Avail: NTIS HC/MF A20 CSCL 22B

Magnetic cleanliness testing was performed on the Tethered Satellite as the last step of an articulated verification campaign aimed at demonstrating the capability of the satellite to support its TEMAG (TEthered MAgnetometer) experiment. Tests at unit level and analytical predictions/correlations using a dedicated mathematical model (GANEW program) are also part of the verification activities. Details of the tests are presented, and the results of the verification are described together with recommendations for later programs. Author

N91-19159*# Rockwell International Corp., Downey, CA.
A FLIGHT EXPERIMENT TO DETERMINE GPS PHOTOCHEMICAL CONTAMINATION ACCUMULATION RATES
A. C. Tribble and J. W. Haffner *In* NASA, Goddard Space Flight Center, 16th Space Simulation Conference Confirming Spaceworthiness Into the Next Millennium Nov. 1990 p 435-446 (For primary document see N91-19126 11-18)
Avail: NTIS HC/MF A20 CSCL 22B

It was recently suggested that photochemically deposited contamination, originating from volatiles outgassed by a spacecraft, may be responsible for the anomalous degradation in power seen on the GPS Block 1 vehicles. In an attempt to confirm, or deny, the photochemical deposition rates predicted, a study was undertaken to design a flight experiment to be incorporated on the GPS vehicles currently in production. The objective was to develop an inexpensive, light weight instrument package that would give information on the contamination levels within a few months of launch. Three types of apparatus were studied, Quartz Crystal Microbalances, (QCM's), modified solar cells, and calorimeters. A calorimeter was selected due primarily to its impact on the production schedule of the GPS vehicles. An analysis of the sensitivity of the final design is compared to the predicted contamination accumulation rates in order to determine how long after launch it will take the experiment to show the effects of photochemical contamination. Author

N91-19160*# National Aeronautics and Space Administration. Lewis Research Center, Cleveland, OH.
SIMULATION OF MARTIAN DUST ACCUMULATION ON SURFACES
Marla E. Perez-Davis, James R. Gaier, Robert Kress, and Justus Grimalda (Massachusetts Inst. of Tech., Boston.) *In* NASA, Goddard Space Flight Center, 16th Space Simulation Conference Confirming Spaceworthiness Into the Next Millennium Nov. 1990 p 447-456 (For primary document see N91-19126 11-18)
Avail: NTIS HC/MF A20 CSCL 22B

Future NASA space missions include the possibility of manned landings and exploration of Mars. Environmental and operational constraints unique to Mars must be considered when selecting and designing the power system to be used on the Mars surface. A technique is described which was developed to simulate the deposition of dust on surfaces. Three kinds of dust materials were

studied: aluminum oxide, basalt, and iron oxide. The apparatus was designed using the Stokes and Stokes-Cunningham law for particle fallout, with additional consideration given to particle size and shape. Characterization of the resulting dust films on silicon dioxide, polytetrafluoroethylene, indium tin oxide, diamondlike carbon, and other surfaces are discussed based on optical transmittance measurements. The results of these experiments will guide future studies which will consider processes to remove the dust from surfaces under Martian environmental conditions.
Author

N91-19161*# Martin Marietta Aerospace, Denver, CO.
TRANSFER ORBIT STAGE MECHANISMS THERMAL VACUUM TEST
Scott T. OLeary *In* NASA, Goddard Space Flight Center, 16th Space Simulation Conference Confirming Spaceworthiness Into the Next Millennium Nov. 1990 p 457-466 (For primary document see N91-19126 11-18)
Avail: NTIS HC/MF A20 CSCL 22B

A systems level mechanisms test was conducted on the Orbital Sciences Corp.'s Transfer Orbit Stage (TOS). The TOS is a unique partially reusable transfer vehicle which will boost a satellite into its operational orbit from the Space Shuttle's cargo bay. The mechanical cradle and tilt assemblies will return to earth with the Space Shuttle while the Solid Rocket Motor (SRM) and avionics package are expended. A mechanisms test was performed on the forward cradle and aft tilting assemblies of the TOS under thermal vacuum conditions. Actuating these assemblies under a 1 g environment and thermal vacuum conditions proved to be a complex task. Pneumatic test fixturing was used to lift the forward cradle, and tilt the SRM, and avionics package. Clinometers, linear voltage displacement transducers, and load cells were used in the thermal vacuum chamber to measure the performance and characteristics of the TOS mechanism assembly. Incorporation of the instrumentation and pneumatic system into the test setup was not routine since pneumatic actuation of flight hardware had not been previously performed in the facility. The methods used are presented along with the problems experienced during the design, setup and test phases.
Author

N91-19162*# Ford Aerospace Corp., Palo Alto, CA. Space Systems/Loral.
SATELLITE SERVICING ECONOMIC STUDY Executive Summary
Dec. 1990 65 p
(Contract NAS8-38142)
(NASA-CR-184112; NAS 1.26:184112) Avail: NTIS HC/MF A04 CSCL 22B

Previous studies have shown that satellite servicing is cost effective; however, all of these studies were of different formats, dollar year, learning rates, availability, etc. Therefore, it was difficult to correlate any useful trends from these studies. The reviewed study was initiated to correlate the economic data into a common data base, using a common set of assumptions. A selected set of existed funded programs was then analyzed to provide an independent analysis of the servicing options and potential economic benefits.
Author

N91-19163*# Ford Aerospace Corp., Palo Alto, CA. Space Systems/Loral.
SATELLITE SERVICING ECONOMIC STUDY Final Report
Dec. 1990 176 p
(Contract NAS8-38142)
(NASA-CR-184113; NAS 1.26:184113) Avail: NTIS HC/MF A09 CSCL 22B

Previous studies have shown that satellite servicing is cost effective; however, all of these studies were of different formats, dollar year, learning rates, availability, etc. Threfore, it was difficult to correlate any useful trends from these studies. The reviewed study was initiated to correlate the economic data into a common data base, using a common set of assumptions. A selected set of existed funded programs was then analyzed to provide an independent analysis of the servicing options and potential economic benefits.
Author

N91-19164*# Alabama Univ., Huntsville. Dept. of Mechanical Engineering.
HYPERVELOCITY IMPACT PHYSICS Final Report
William P. Schonberg, Alan J. Bean, and Kent Darzi Washington NASA Jan. 1991 336 p
(Contract NAS8-36955)
(NASA-CR-4343; NAS 1.26:4343) Avail: NTIS HC/MF A15 CSCL 22B

All large spacecraft are susceptible to impacts by meteoroids and orbiting space debris. These impacts occur at extremely high speed and can damage flight-critical systems, which can in turn lead to a catastrophic failure of the spacecraft. Therefore, the design of a spacecraft for a long-duration mission must take into account the possibility of such impacts and their effects on the spacecraft structure and on all of its exposed subsystems components. The work performed under the contract consisted of applied research on the effects of meteoroid/space debris impacts on candidate materials, design configurations, and support mechanisms of long term space vehicles. Hypervelocity impact mechanics was used to analyze the damage that occurs when a space vehicle is impacted by a micrometeoroid or a space debris particle. An impact analysis of over 500 test specimens was performed to generate by a hypervelocity impact damage database.
Author

N91-19165*# National Aeronautics and Space Administration. Lewis Research Center, Cleveland, OH.
THE EFFECT OF THE LOW EARTH ORBIT ENVIRONMENT ON SPACE SOLAR CELLS
David J. Brinker, John R. Hickey (Eppley Lab., Inc., Newport, RI.), and Donald K. Brasted Nov. 1990 8 p Presented at the 5th International Photovoltaic Science and Engineering Conference, Kyoto, Japan, 26-30 Nov. 1990; sponsored in part by Japan Society of Applied Physics, Inst. of Electrical Engineers of Japan and Foundation for Adv. of Intern. Scienc
(NASA-TM-103735; E-5973; NAS 1.15:103735) Avail: NTIS HC/MF A02 CSCL 22B

The results of a space flight experiment designed to provide reference cell standards for photovoltaic measurements as well as to investigate the solar spectrum and the effect of long-term exposure of solar cells to the space environment are presented. This experiment, the Advanced Photovoltaic Experiment (APEX), was launched into low Earth orbit as part of the Long Duration Exposure Facility in 1984 and retrieved 69 months later. APEX contained over 150 solar cells of a wide variety of materials, designs and coverglasses. Data on cell performance was recorded for the first year-on-orbit.
Author

N91-19166*# National Aeronautics and Space Administration. Langley Research Center, Hampton, VA.
FREE VIBRATION OF HEXAGONAL PANELS SUPPORTED AT DISCRETE POINTS
K. Chauncey Wu Feb. 1991 19 p
(NASA-TM-102688; NAS 1.15:102688) Avail: NTIS HC/MF A03 CSCL 22B

An analytical study to determine the structural dynamic behavior of a hexagonal panel with discrete simple supports is presented. These panels are representative of the facets of a precision reflector surface. The effects of both support point location and panel curvature on the lowest natural frequency of the panel are quantified and discussed.
Author

N91-19167*# Analex Corp., Fairview Park, OH.
COLD-SAT FEASIBILITY STUDY SAFETY ANALYSIS Final Report
Steven T. McHenry and James M. Yost Jan. 1991 178 p
(Contract NAS3-25515)
(NASA-CR-187042; NAS 1.26:187042) Avail: NTIS HC/MF A09 CSCL 22B

The Cryogenic On-orbit Liquid Depot-Storage, Acquisition, and

Transfer (COLD-SAT) satellite presents some unique safety issues. The feasibility study conducted at NASA-Lewis desired a systems safety program that would be involved from the initial design in order to eliminate and/or control the inherent hazards. Because of this, a hazards analysis method was needed that: (1) identified issues that needed to be addressed for a feasibility assessment; and (2) identified all potential hazards that would need to be controlled and/or eliminated during the detailed design phases. The developed analysis method is presented as well as the results generated for the COLD-SAT system. Author

N91-19168*# National Aeronautics and Space Administration. Langley Research Center, Hampton, VA.
COMPARATIVE MORPHOLOGY OF CONFIGURATIONS WITH REDUCED PART COUNT DERIVED FROM THE OCTAHEDRAL-TETRAHEDRAL TRUSS
Haresh Lalvani (George Washington Univ., Hampton, VA.) and Timothy J. Collins Feb. 1991 132 p
(NASA-TM-102768; NAS 1.15:102768) Avail: NTIS HC/MF A07 CSCL 22B

Morphology (the study of structure and form) of the octahedral-tetrahedral (octet) truss is described. Both the geometry and symmetry of the octet truss are considered. Morphological techniques based on symmetry operations are presented which enable the derivation of reduced-part-count truss configurations from the octet truss by removing struts and nodes. These techniques are unique because their Morphological origination and they allow for the systematic generation and analysis of a large variety of structures. Methods for easily determining the part count and redundancy of infinite truss configurations are presented. Nine examples of truss configurations obtained by applying the derivation techniques are considered. These configurations are structurally stable while at the same time exhibiting significant reductions in part count. Some practical and analytical considerations, such as structural performance, regarding the example reduced-part-count truss geometries are briefly discussed. Author

N91-19169# Technische Univ., Delft (Netherlands). Dept. of Aerospace Engineering.
PROJECT HITCH HIKER: A FEASIBILITY STUDY FOR A SMALL TELECOMMUNICATION SATELLITE
M. P. Nieuwenhuizen, Albert-Jan Bunt, Steven P. Verhagen, Dirk deWaart, Marcel J. Belien, Erik P. deHeer, Bryan P. Ho, Mark J. v.Dijk, Edouard P. v.d.Heuvel, and Bas J. Theelen et al Sep. 1990 214 p
(LR-644; ETN-91-98945) Avail: NTIS HC/MF A10

Small satellites for developing countries are a new and interesting area of the communication satellite business. A study for such a satellite to be used for telecommunication is presented. Details of the following are included in the report: management; systems engineering; launcher and orbit dynamics; configuration; payload; the electrical power subsystem; structure; the attitude and orbit control system; thermal control; telemetry and telecommand; propulsion. ESA

N91-19170# Technische Univ., Berlin (Germany, F.R.). Inst. fuer Luft- und Raumfahrt.
ALTERNATIVE STRATEGIES FOR THE MAINTENANCE OF GEOSTATIONARY SPACE POWER PLANTS [ALTERNATIVE STRATEGIEN ZUR INSTANDHALTUNG GEOSTATIONAERER WELTRAUMKRAFWERKE]
Christian Roettger 1 Nov. 1990 84 p In GERMAN; ENGLISH summary
(ILR-Mitt-249(1990); ETN-91-98952) Avail: NTIS HC/MF A05

The feasibility to establish a Space Solar Power System (SSPS) consisting of 111 power plants, with an electrical power output of 5 GW each, is examined. Strategies for maintenance and repair of operating SSPS units are defined. A model simulating the cost effectiveness of the different strategies is developed. The results of this simulation are presented in several figures and tables. The potential margins of error in varying the main parameters are analyzed. A schedule of the SSPS acquisition and operation phase is given. ESA

N91-20008*# Kent Univ., Canterbury (England). Physics Lab.
SPACE DEBRIS: ORBITAL MICROPARTICULATES IMPACTING LDEF EXPERIMENTS FAVOUR A NATURAL EXTRATERRESTRIAL ORIGIN
Tony McDonnell *In* Lunar and Planetary Inst., 22nd Lunar and Planetary Science Conference 1991 p 45-48 (For primary document see N91-19995 11-91)
Avail: NTIS HC/MF A04 CSCL 22B

19 SPACECRAFT INSTRUMENTATION

For related information see also *06 Aircraft Instrumentation* and *35 Instrumentation and Photography.*

No abstracts in this category.

20 SPACECRAFT PROPULSION AND POWER

Includes main propulsion systems and components, e.g., rocket engines; and spacecraft auxilliary power sources.

For related information see also *07 Aircraft Propulsion and Power, 28 Propellants and Fuels, 44 Energy Production and Conversion,* and *15 Launch Vehicles and Space Vehicles.*

N91-19171# Department of the Navy, Washington, DC.
LAUNCHING PROJECTILES WITH HYDROGEN GAS GENERATED FROM TITANIUM-WATER REACTIONS Patent Application
Woodrow W. Lee, inventor (to Navy) 7 Aug. 1990 23 p
(AD-D014653; US-Patent-Appl-SN-564892) Avail: NTIS HC/MF A03 CSCL 19/1

This invention relates to methods of generating gases and more particularly to methods of generating hydrogen gas. Acceleration of projectiles launched from gun, rocket, and missile systems is limited by the sonic velocity of gas products from propellants. Conventional gun propellants (nitrocellulose) generate heavy gases like carbon dioxide, carbon monoxide, nitrogen oxide, and water vapor whose sonic velocity seldom exceeds 500 m/sec at ambient temperature. The maximum speed to projectiles launched from gun barrel by such gases barely reaches 1 km/sec. GRA

N91-19172*# Thiokol Corp., Brigham City, UT. Space Operations.
THE FULL-SCALE PROCESS AND DESIGN CHANGES FOR ELIMINATION OF INSULATION EDGE SEPARATIONS AND VOIDS IN TANG FLAP AREA Final Report
Richard A. Danforth Jan. 1991 31 p
(Contract NAS8-30490)
(NASA-CR-184110; NAS 1.26:184110; TWR-50143-2; Publ-911032) Avail: NTIS HC/MF A03 CSCL 21H

Qualification of the full-scale process and design changes for elimination of redesigned solid rocket motor tang nitrile butadiene rubber insulation edge separations and voids was performed from 24 March to 3 December 1990. The objectives of this test were: to qualify design and process changes on flight hardware using a tie ply between the redesigned solid rocket motor steel case and the nitrile butadiene rubber insulation over the tang capture features; to qualify the use of methyl ethyl ketone in the tang flap region to reduce voids; and to determine if holes in the separator film reduce voids in the tang flap region. The tie ply is intended to aid insulation flow during the insulation cure process, and thus reduce or eliminate edge unbonds. Methyl ethyl ketone is intended to reduce voids in the tang flap area by providing better tacking characteristics. The perforated film was intended to provide possible vertical breathe paths to reduce voids in the tang area.

Tang tie ply testing consisted of 270 deg of the tang circumference using a new layup method and 90 deg of the tang circumference using the current layup methods. Tie ply process success was defined as a reduction of insulation unbonds. Lack of any insulation edge unbonds on the tang area where the new process was used, and the presence of 17 unbonds with the current process, proves the test to be a success. Successful completion of this test has qualified the new processes. Author

N91-19173*# Stuttgart Univ. (Germany, F.R.). Inst. fuer Raumfahrtsysteme.

HIGH POWER ARCJET Progress Report No. 3, Aug. 1990 - Jan. 1991

T. M. Goelz, M. Auweter-Kurtz, H. L. Kurtz, and H. O. Schrade Feb. 1991 24 p Original contains color illustrations

(Grant NAGw-1736)

(NASA-CR-187986; NAS 1.26:187986; IRS-91-P3) Avail: NTIS HC/MF A03; 3 functional color pages CSCL 21H

The activities of the High Power Arcjet Project (HIPARC) from August 1990 to January 1991 are discussed. In this period the HIPARC thruster was ignited for the first time. Power levels up to 140 kW with a mass flow rate of 300 mg/s hydrogen were reached. Specific impulse values of more than 1300 s were shown to be possible. Tests were performed with the baseline thruster version only, which has a 6 mm throat diameter and a conical nozzle with a 20 degree half angle. Measurement data summing up all tests carried out until now is included. All measuring methods are described, including a check on possible error sources. Author

N91-19174*# GenCorp Aerojet, Sacramento, CA. Aerojet Propulsion Div.

ORBITAL TRANSFER VEHICLE OXYGEN TURBOPUMP TECHNOLOGY. VOLUME 1: DESIGN, FABRICATION, AND HYDROSTATIC BEARING TESTING Final Report

P. S. Buckmann, W. R. Hayden, S. A. Lorenc, R. L. Sabiers, and N. R. Shimp Dec. 1990 251 p

(Contract NAS3-23772)

(NASA-CR-185175; NAS 1.26:185175; AEROJET-2459-54-2-Vol-1) Avail: NTIS HC/MF A12 CSCL 21H

The design, fabrication, and initial testing of a rocket engine turbopump (TPA) for the delivery of high pressure liquid oxygen using hot oxygen for the turbine drive fluid are described. This TPA is basic to the dual expander engine which uses both oxygen and hydrogen as working fluids. Separate tasks addressed the key issue of materials for this TPA. All materials selections emphasized compatibility with hot oxygen. The OX TPA design uses a two-stage centrifugal pump driven by a single-stage axial turbine on a common shaft. The design includes ports for three shaft displacement/speed sensors, various temperature measurements, and accelerometers. Author

N91-19175*# National Aeronautics and Space Administration. Lewis Research Center, Cleveland, OH.

ADVANCED CHEMICAL PROPULSION AT NASA LEWIS: METALLIZED AND HIGH ENERGY DENSITY PROPELLANTS

Bryan A. Palaszewski Feb. 1991 7 p Presented at the High Energy Density Materials Contractor's Meeting, Albuquerque, NM, 24-27 Feb. 1991; sponsored in part by AF

(NASA-TM-103771; E-6034; NAS 1.15:103771) Avail: NTIS HC/MF A02 CSCL 21I

Two of the programs at the NASA Lewis Research Center investigating advanced systems for future space missions are the Metallized Propellant Program and the Advanced Concepts Program. Each program includes both experimental and theoretical studies of future propellants and the associated vehicle impacts and significant payload benefits for many types of space transportation. These programs are described. Author

N91-19176*# National Aeronautics and Space Administration. Lewis Research Center, Cleveland, OH.

RADIATION RESISTANCE OF THIN-FILM SOLAR CELLS FOR SPACE PHOTOVOLTAIC POWER

James R. Woodyard (Wayne State Univ., Detroit, MI.) and Geoffrey A. Landis Jan. 1991 35 p Sponsored in part by Wayne State Univ., Detroit, MI

(Contract NAS3-25266; NAG3-833)

(NASA-TM-103715; E-5948; NAS 1.15:103715) Avail: NTIS HC/MF A03 CSCL 10B

Copper indium diselenide, cadmium telluride, and amorphous silicon alloy solar cells have achieved noteworthy performance and are currently being studied for space power applications. Cadmium sulfide cells had been the subject of much effort but are no longer considered for space applications. A review is presented of what is known about the radiation degradation of thin film solar cells in space. Experimental cadmium telluride and amorphous silicon alloy cells are reviewed. Damage mechanisms and radiation induced defect generation and passivation in the amorphous silicon alloy cell are discussed in detail due to the greater amount of experimental data available. Author

N91-19177*# National Aeronautics and Space Administration. Lewis Research Center, Cleveland, OH.

MULTI-DIMENSIONAL MODELING OF A THERMAL ENERGY STORAGE CANISTER M.S. Thesis - Cleveland State Univ., Dec. 1990

Thomas W. Kerslake Jan. 1991 192 p

(NASA-TM-103731; E-5966; NAS 1.15:103731) Avail: NTIS HC/MF A09 CSCL 10C

The Solar Dynamic Power Module being developed for Space Station Freedom uses a eutectic mixture of LiF-CaF2 phase change material (PCM) contained in toroidal canisters for thermal energy storage. Presented are the results from heat transfer analyses of a PCM containment canister. One and two dimensional finite difference computer models are developed to analyze heat transfer in the canister walls, PCM, void, and heat engine working fluid coolant. The modes of heat transfer considered include conduction in canister walls and solid PCM, conduction and pseudo-free convection in liquid PCM, conduction and radiation across PCM vapor filled void regions, and forced convection in the heat engine working fluid. Void shape, location, growth or shrinkage (due to density difference between the solid and liquid PCM phases) are prescribed based on engineering judgment. The PCM phase change process is analyzed using the enthalpy method. The discussion of the results focuses on how canister thermal performance is affected by free convection in the liquid PCM and void heat transfer. Characterizing these effects is important for interpreting the relationship between ground-based canister performance (in 1-g) and expected on-orbit performance (in micro-g). Void regions accentuate canister hot spots and temperature gradients due to their large thermal resistance. Free convection reduces the extent of PCM superheating and lowers canister temperatures during a portion of the PCM thermal charge period. Surprisingly small differences in canister thermal performance result from operation on the ground and operation on-orbit. This lack of a strong gravity dependency is attributed to the large contribution of container walls in overall canister energy redistribution by conduction. Author

N91-19178*# National Aeronautics and Space Administration. Lewis Research Center, Cleveland, OH.

SOLAR ELECTRIC PROPULSION FOR MARS TRANSPORT VEHICLES

J. M. Hickman, H. B. Curtis, S. W. Alexander, J. H. Gilland (Sverdrup Technology, Inc., Brook Park, OH.), K. J. Hack, C. Lawrence, and C. K. Swartz Sep. 1990 17 p

(NASA-TM-103234; E-5654; NAS 1.15:103234) Avail: NTIS HC/MF A03 CSCL 13F

Solar electric propulsion (SEP) is an alternative to chemical and nuclear powered propulsion systems for both piloted and unpiloted Mars transport vehicles. Photovoltaic solar cell and array technologies were evaluated as components of SEP power systems. Of the systems considered, the SEP power system composed of multijunction solar cells in an ENTECH domed fresnel concentrator array had the least array mass and area. Trip times to Mars optimized for minimum propellant mass were calculated. Additionally, a preliminary vehicle concept was designed. Author

N91-19179*# National Aeronautics and Space Administration. Lewis Research Center, Cleveland, OH.
KEY ISSUES IN SPACE NUCLEAR POWER
Henry W. Brandhorst Jan. 1991 8 p Presented at the 8th Symposium on Space Nuclear Power Systems, Albuquerque, NM, 6-10 Jan. 1991; sponsored in part by New Mexico Univ., Strategic Defense Initiative Organization, DOE, AF
(NASA-TM-103656; E-5847; NAS 1.15:103656) Avail: NTIS HC/MF A02 CSCL 10B

The future appears rich in missions that will extend the frontiers of knowledge, human presence in space, and opportunities for profitable commerce. Key to the success of these ventures is the availability of plentiful, cost effective electric power and assured, low cost access to space. While forecasts of space power needs are problematic, an assessment of future needs based on terrestrial experience has been made. These needs fall into three broad categories: survival, self sufficiency, and industrialization. The cost of delivering payloads to orbital locations from LEO to Mars has been determined and future launch cost reductions projected. From these factors, then, projections of the performance necessary for future solar and nuclear space power options has been made. These goals are largely dependent upon orbital location and energy storage needs. Finally the cost of present space power systems has been determined and projections made for future systems. Author

N91-19180*# National Aeronautics and Space Administration. Lewis Research Center, Cleveland, OH.
A 5-kW XENON ION THRUSTER LIFETEST
Michael J. Patterson and Timothy R. Verhey (Sverdrup Technology, Inc., Brook Park, OH.) 1990 53 p Presented at the 21st International Electric Propulsion Conference, Orlando, FL, 18-20 Jul. 1990; sponsored by AIAA, DGLR, and JSASS Previously announced in IAA as A90-52564
(NASA-TM-103191; E-5579; NAS 1.15:103191; AIAA-90-2543)
Avail: NTIS HC/MF A04 CSCL 21H

The results of the first life test of a high power ring-cusp ion thruster are presented. A 30-cm laboratory model thruster was operated steady-state at a nominal beam power of 5 kW on xenon propellant for approximately 900 hours. This test was conducted to identify life-timing erosion modifications, and to demonstrate operation using simplified power processing. The results from this test are described including the conclusions derived from extensive post-test analyses of the thruster. Modifications to the thruster and ground support equipment, which were incorporated to solve problems identified by the lifetest, are also described. Author

N91-19181*# National Aeronautics and Space Administration, Washington, DC.
ENHANCING SPACE TRANSPORTATION: THE NASA PROGRAM TO DEVELOP ELECTRIC PROPULSION
Gary L. Bennett, Marcus A. Watkins, David C. Byers, and John W. Barnett (Jet Propulsion Lab., California Inst. of Tech., Pasadena.) Oct. 1990 29 p
(NASA-TM-4244; NAS 1.15:4244) Avail: NTIS HC/MF A03 CSCL 21C

The NASA Office of Aeronautics, Exploration, and Technology (OAET) supports a research and technology (R and T) program in electric propulsion to provide the basis for increased performance and life of electric thruster systems which can have a major impact on space system performance, including orbital transfer, stationkeeping, and planetary exploration. The program is oriented toward providing high-performance options that will be applicable to a broad range of near-term and far-term missions and vehicles. The program, which is being conducted through the Jet Propulsion Laboratory (JPL) and Lewis Research Center (LeRC) includes research on resistojet, arcjets, ion engines, magnetoplasmadynamic (MPD) thrusters, and electrodeless thrusters. Planning is also under way for nuclear electric propulsion (NEP) as part of the Space Exploration Initiative (SEI). Author

N91-19182*# National Aeronautics and Space Administration. Lewis Research Center, Cleveland, OH.
SPACE PHOTOVOLTAIC RESEARCH AND TECHNOLOGY, 1989
Washington Jan. 1991 515 p Tenth conference held in Cleveland, OH, 7-9 Nov. 1989
(NASA-CP-3107; E-5728; NAS 1.55:3107) Avail: NTIS HC/MF A22 CSCL 10B

Remarkable progress on a wide variety of approaches in space photovoltaics, for both near and far term applications is reported. Papers were presented in a variety of technical areas, including multi-junction cell technology, GaAs and InP cells, system studies, cell and array development, and non-solar direct conversion. Five workshops were held to discuss the following topics: mechanical versus monolithic multi-junction cells; strategy in space flight experiments; non-solar direct conversion; indium phosphide cells; and space cell theory and modeling. For individual titles, see N91-19183 through N91-19221.

N91-19183*# National Aeronautics and Space Administration, Washington, DC.
THE OAST SPACE POWER PROGRAM
Gary L. Bennett *In* NASA, Lewis Research Center, Space Photovoltaic Research and Technology, 1989 Jan. 1991 p 3-17 (For primary document see N91-19182 11-20)
Avail: NTIS HC/MF A22 CSCL 10B

The NASA Office of Aeronautics and Space Technology (OAST) space power program was established to provide the technology base to meet power system requirements for future space missions, including the Space Station, earth orbiting spacecraft, lunar and planetary bases, and solar system exploration. The program spans photovoltaic energy conversion, chemical energy conversion, thermal energy conversion, power management, thermal management, and focused initiatives on high-capacity power, surface power, and space nuclear power. The OAST space power program covers a broad range of important technologies that will enable or enhance future U.S. space missions. The program is well under way and is providing the kind of experimental and analytical information needed for spacecraft designers to make intelligent decisions about future power system options. Author

N91-19184*# Spectrolab, Inc., Sylmar, CA.
PROGRESS TOWARD THE DEVELOPMENT OF DUAL JUNCTION GaAs/Ge SOLAR CELLS **c44**
D. R. Lillington, D. D. Krut, B. T. Cavicchi, E. Ralph, and M. Chung (Air Force Wright Aeronautical Labs., Wright-Patterson AFB, OH.) *In* NASA, Lewis Research Center, Space Photovoltaic Research and Technology, 1989 Jan. 1991 p 29-41 (For primary document see N91-19182 11-20)
(Contract F33615-89-C-2900)
Avail: NTIS HC/MF A22 CSCL 10B

Large area GaAs/Ge cells offer substantial promise for increasing the power output from existing silicon solar array designs and for providing an enabled technology for missions hitherto impossible using silicon. Single junction GaAs/Ge cells offer substantial advantages in both size, weight, and cost compared to GaAs cells but the efficiency is limited to approximately 19.2 to 20 percent AMO. The thermal absorptance of GaAs/Ge cells is also worse than GaAs/GaAs cells (0.88 vs 0.81 typ.) due to the absorption in the Ge substrate. On the other hand dual junction GaAs/Ge cells offer efficiencies up to ultimately 24 percent AMO in sizes up to 8 x 8 cm but there are still technological issues remaining to achieve current matching in the GaAs and Ge cells. This can be achieved through tuned antireflection (AR) coatings, improved quality of the GaAs growth, improved quality Ge wafers and the use of a Back Surface Field (BSF)/Back Surface Reflector (BSR) in the Ge cell. Although the temperature coefficients of efficiency and voltage are higher for dual junction GaAs/Ge cells, it has been shown elsewhere that for typical 28 C cell efficiencies of 22 percent (dual junction) vs 18.5 percent (single junction) there is a positive power tradeoff up to temperatures as high as 120 C. Due to the potential ease of fabrication of GaAs/Ge dual junction

cells there is likely to be only a small cost differential compared to single junction cells. Author

N91-19185*# Applied Solar Energy Corp., City of Industry, CA.
STATUS OF GaAs/Ge SOLAR CELLS **c44**
P. A. Iles, F. Ho, and Y. C. M. Yeh *In* NASA, Lewis Research Center, Space Photovoltaic Research and Technology, 1989 Jan. 1991 p 42-47 (For primary document see N91-19182 11-20)
(Contract F33615-88-C-5415)
Avail: NTIS HC/MF A22 CSCL 10B

With experience at increasing production levels, GaAs/Ge cells are proving their effectiveness for some demanding missions. The experience in producing inactive-Ge structures should benefit parallel work on forming monolithic cascade cells using AlGaAs or GaAs top cell layers grown on Ge or other bottom cell materials. The adjustments needed to ensure that the GaAs/Ge interface is inactive are more likely to preserve the properties of a separately optimized bottom cell. Author

N91-19186*# Research Triangle Inst., Research Triangle Park, NC.
GRADED-BANDGAP AlGaAs SOLAR CELLS FOR AlGaAs/Ge CASCADE CELLS **c44**
M. L. Timmons, R. Venkatasubramanian, T. S. Colpitts, J. S. Hills, J. A. Hutchby, P. A. Iles, and C. L. Chu (Applied Solar Energy Corp., City of Industry, CA.) *In* NASA, Lewis Research Center, Space Photovoltaic Research and Technology, 1989 Jan. 1991 p 48-59 (For primary document see N91-19182 11-20)
(Contract F33615-87-C-2804)
Avail: NTIS HC/MF A22 CSCL 10B

Some p/n graded-bandgap Al(x)Ga(1-x)As solar cells were fabricated and show AMO conversion efficiencies in excess of 15 percent without antireflection (AR) coatings. The emitters of these cells are graded between 0.008 is less than or equal to x is less than or equal to 0.02 during growth of 0.25 to 0.30 micron thick layers. The keys to achieving this performance were careful selection of organometallic sources and scrubbing oxygen and water vapor from the AsH3 source. Source selection and growth were optimized using time-resolved photoluminescence. Preliminary radiation-resistance measurements show AlGaAs cells degraded less than GaAs cells at high 1 MeV electron fluences, and AlGaAs cells grown on GaAs and Ge substrates degrade comparably. Author

N91-19187*# Astropower, Inc., Newark, DE.
AlGaAs TOP SOLAR CELL FOR MECHANICAL ATTACHMENT IN A MULTI-JUNCTION TANDEM CONCENTRATOR SOLAR CELL STACK **c44**
L. C. DiNetta, M. H. Hannon, J. B. McNeely, and A. M. Barnett (Delaware Univ., Newark.) *In* NASA, Lewis Research Center, Space Photovoltaic Research and Technology, 1989 Jan. 1991 p 60-72 (For primary document see N91-19182 11-20)
(Contract NAS3-25570)
Avail: NTIS HC/MF A22 CSCL 10B

The AstroPower self-supporting, transparent AlGaAs top solar cell can be stacked upon any well-developed bottom solar cell for improved system performance. This is an approach to improve the performance and scale of space photovoltaic power systems. Mechanically stacked tandem solar cell concentrator systems based on the AlGaAs top concentrator solar cell can provide near term efficiencies of 36 percent (AMO, 100x). Possible tandem stack efficiencies greater than 38 percent (100x, AMO) are feasible with a careful selection of materials. In a three solar cell stack, system efficiencies exceed 41 percent (100x, AMO). These device results demonstrate a practical solution for a state-of-the-art top solar cell for attachment to an existing, well-developed solar cell. Author

N91-19188*# Varian Associates, Palo Alto, CA.
PROGRESS TOWARD A 30 PERCENT-EFFICIENT, MONOLITHIC, THREE-JUNCTION, TWO-TERMINAL CONCENTRATOR SOLAR CELL FOR SPACE APPLICATIONS **c44**
L. D. Partain, B.-C. Chung, G. F. Virshup, J. C. Schultz, H. F. MacMillan, M. Ladle Ristow, M. S. Kuryla, and K. A. Bertness *In* NASA, Lewis Research Center, Space Photovoltaic Research and Technology, 1989 Jan. 1991 p 73-76 (For primary document see N91-19182 11-20)
(Contract F33615-88-C-2845)
Avail: NTIS HC/MF A22 CSCL 10B

Component efficiencies of 0.2/sq cm cells at approximately 100x AMO light concentration and 80 C temperatures are not at 15.3 percent for a 1.9 eV AlGaAs top cell, 9.9 percent for a 1.4 eV GaAs middle cell under a 1.9 eV AlGaAs filter, and 2.4 percent for a bottom 1.0 eV InGaAs cell under a GaAs substrate. The goal is to continue improvement in these performance levels and to sequentially grow these devices on a single substrate to give 30 percent efficient, monolithic, two-terminal, three-junction space concentrator cells. The broad objective is a 30 percent efficient monolithic two-terminal cell that can operate under 25 to 100x AMO light concentrations and at 75 to 100 C cell temperatures. Detailed modeling predicts that this requires three junctions. Two options are being pursued, and both use a 1.9 eV AlGaAs top junction and a 1.4 eV GaAs middle junction grown by a 1 atm OMVPE on a lattice matched substrate. Option 1 uses a low-doped GaAs substrate with a lattice mismatched 1.0 eV InGaAs cell formed on the back of the substrate. Option 2 uses a Ge substrate to which the AlGaAs and GaAs top junctions are lattice matched, with a bottom 0.7 eV Ge junction formed near the substrate interface with the GaAs growth. The projected efficiency contributions are near 16, 11, and 3 percent, respectively, from the top, middle, and bottom junctions. Author

N91-19189*# National Aeronautics and Space Administration. Lewis Research Center, Cleveland, OH.
TANDEM CONCENTRATOR SOLAR CELLS WITH 30 PERCENT (AMO) POWER CONVERSION EFFICIENCY **c44**
J. E. Avery, L. M. Fraas, V. S. Sundaram, David J. Brinker, J. M. Gee, and Mark J. ONeill (ENTECH Corp., Dallas-Fort Worth Airport, TX.) *In its* Space Photovoltaic Research and Technology, 1989 Jan. 1991 p 77-87 (For primary document see N91-19182 11-20)
Avail: NTIS HC/MF A22 CSCL 10B

Very high efficiency concentrator solar panels are envisioned as economical and reliable electrical power subsystems for space based platforms of the future. GaAs concentrator cells with very high efficiencies and good sub-bandgap transmissions can be fabricated on standard wafers. GaSb booster cell development is progressing very well; performance characteristics are still improving dramatically. Consistent GaAs/GaSb stacked cell AMO efficiencies greater than 30 percent are expected. Author

N91-19190*# Boeing Aerospace Co., Seattle, WA.
PROGRESS IN GaAs/CuInSe2 TANDEM JUNCTION SOLAR CELLS **c44**
N. P. Kim, R. M. Burgess, R. A. Mickelsen, B. J. Stanbery, R. W. McClelland, B. D. King, and R. P. Gale (Kopin Corp., Taunton, MA.) *In* NASA, Lewis Research Center, Space Photovoltaic Research and Technology, 1989 Jan. 1991 p 88-101 (For primary document see N91-19182 11-20)
Avail: NTIS HC/MF A22 CSCL 10B

Much more power is required for spacecraft of the future than current vehicles. To meet this increased demand for power while simultaneously meeting other requirements for launch, deployment, and maneuverability, the development of higher-efficiency, lighter-weight, and more radiation resistant photovoltaic cells is essential. Mechanically stacked tandem junction solar cells based on (AlGaAs)GaAs thin film CLEFT (Cleavage of Lateral Epitaxial Film for Transfer) top cells and CuInSe2(CIS) thin film bottom cells are being developed to meet these power needs. The mechanically stacked tandem configuration is chosen due to its interconnect flexibility allowing more efficient array level performance. It also eliminates cell fabrication processing constraints associated with monolithically integrated multi-junction approaches, thus producing higher cell fabrication yields. The GaAs cell is used as the top cell due to its

demonstrated high efficiency, and good radiation resistance. Furthermore, it offers a future potential for bandgap tuning using AlGaAs as the absorber to maximize cell performance. The CuInSe2 cell is used as the bottom cell due to superb radiation resistance, stability, and optimal bandgap value in combination with an AlGaAs top cell. Since both cells are incorporated as thin films, this approach provides a potential for very high specific power. This high specific power (W/kg), combined with high power density (W/sq m) resulting from the high efficiency of this approach, makes these cells ideally suited for various space applications.
Author

N91-19191*# Midwest Research Inst., Golden, CO.
InP/Ga0.47In0.53As MONOLITHIC, TWO-JUNCTION, THREE-TERMINAL TANDEM SOLAR CELLS **c44**
M. W. Wanlaas, T. A. Gessert, G. S. Horner, K. A. Emery, and T. J. Coutts *In* NASA, Lewis Research Center, Space Photovoltaic Research and Technology, 1989 Jan. 1991 p 102-116 (For primary document see N91-19182 11-20)
Avail: NTIS HC/MF A22 CSCL 10B

The work presented has focussed on increasing the efficiency of InP-based solar cells through the development of a high-performance InP/Ga(0.47)In(0.53)As two-junction, three-terminal monolithic tandem cell. Such a tandem is particularly suited to space applications where a radiation-hard top cell (i.e., InP) is required. Furthermore, the InP/Ga(0.47)In(0.53)As materials system is lattice matched and offers a top cell/bottom cell bandgap differential (0.60 eV at 300 K) suitable for high tandem cell efficiencies under AMO illumination. A three-terminal configuration was chosen since it allows for independent power collection from each subcell in the monolithic stack, thus minimizing the adverse impact of radiation damage on the overall tandem efficiency. Realistic computer modeling calculations predict an efficiency boost of 7 to 11 percent from the Ga(0.47)In(0.53)As bottom cell under AMO illumination (25 C) for concentration ratios in the 1 to 1000 range. Thus, practical AMO efficiencies of 25 to 32 percent appear possible with the InP/Ga(0.47)In(0.53)As tandem cell. Prototype n/p/n InP/Ga(0.47)In(0.53)As monolithic tandem cells were fabricated and tested successfully. Using an aperture to define the illuminated areas, efficiency measurements performed on a non-optimized device under standard global illumination conditions (25 C) with no antireflection coating (ARC) give 12.2 percent for the InP top cell and 3.2 percent for the Ga(0.47)In(0.53)As bottom cell, yielding an overall tandem efficiency of 15.4 percent. With an ARC, the tandem efficiency could reach approximately 22 percent global and approximately 20 percent AMO. Additional details regarding the performance of individual InP and Ga(0.47)In(0.53)As component cells, fabrication and operation of complete tandem cells and methods for improving the tandem cell performance, are also discussed.
Author

N91-19192*# Wright Research Development Center, Wright-Patterson AFB, OH.
PHASE EQUILIBRIUM MODELING FOR HIGH TEMPERATURE METALLIZATION ON GaAs SOLAR CELLS **c44**
M. A. Chung, J. E. Davison, and S. R. Smith (Dayton Univ., OH.) *In* NASA, Lewis Research Center, Space Photovoltaic Research and Technology, 1989 Jan. 1991 p 119-125 (For primary document see N91-19182 11-20)
Avail: NTIS HC/MF A22 CSCL 10B

Recent trends in performance specifications and functional requirements have brought about the need for high temperature metallization technology to be developed for survivable DOD space systems and to enhance solar cell reliability. The temperature constitution phase diagrams of selected binary and ternary systems were reviewed to determine the temperature and type of phase transformation present in the alloy systems. Of paramount interest are the liquid-solid and solid-solid transformations. Data are being utilized to aid in the selection of electrical contact materials to gallium arsenide solar cells. Published data on the phase diagrams for binary systems is readily available. However, information for ternary systems is limited. A computer model is being developed which will enable the phase equilibrium predictions for ternary systems where experimental data is lacking.
Author

N91-19193*# Washington State Univ., Pullman.
GaAs SOLAR CELL PHOTORESPONSE MODELING USING PC-1D V2.1 **c44**
D. A. Huber, L. C. Olsen, G. Dunham, and F. W. Addis *In* NASA, Lewis Research Center, Space Photovoltaic Research and Technology, 1989 Jan. 1991 p 126-135 (For primary document see N91-19182 11-20)
(Grant AF-AFOSR-0182-89)
Avail: NTIS HC/MF A22 CSCL 10B

Photoresponse data of high efficiency GaAs solar cells were analyzed using PC-1D V2.1. The approach required to use PC-1D for photoresponse data analysis, and the physical insights gained from performing the analysis are discussed. In particular, the effect of Al(x)Ga(1-x)As heteroface quality was modeled. Photoresponse or spectral quantum efficiency is an important tool in characterizing material quality and predicting cell performance. The strength of the photoresponse measurement lies in the ability to precisely fit the experimental data with a physical model. PC-1D provides a flexible platform for calculations based on these physical models.
Author

N91-19194*# Varian Associates, Palo Alto, CA.
HIGH-EFFICIENCY, RADIATION-RESISTANT GaAs SPACE CELLS **c44**
K. A. Bertness, M. Ladle Ristow, M. Grounner, M. S. Kuryla, and J. G. Werthen *In* NASA, Lewis Research Center, Space Photovoltaic Research and Technology, 1989 Jan. 1991 p 136-139 (For primary document see N91-19182 11-20)
Avail: NTIS HC/MF A22 CSCL 10B

Although many GaAs solar cells are intended for space applicatons, few measurements of cell degradation after radiation are available, particularly for cells with efficiencies exceeding 20 percent (one-sun, AMO). Often the cell performance is optimized for the highest beginning-of-life (BOL) efficiency, despite the unknown effect of such design on end-of-life (EOL) efficiencies. The results of a study of the radiation effects on p-n GaAs cells are presented. The EOL efficiency of GaAs space cell can be increased by adjusting materials growth parameters, resulting in a demonstration of 16 percent EOL efficiency at one-sun, AMO. Reducing base doping levels to below 3 x 10(exp 17)/cu m and decreasing emitter thickness to 0.3 to 0.5 micron for p-n cells led to significant improvements in radiation hardness as measured by EOL/BOL efficiency ratios for irradiation of 10(exp -15)/sq cm electrons at 1 MeV. BOL efficiency was not affected by changes in emitter thickness but did improve with lower base doping.
Author

N91-19195*# National Aeronautics and Space Administration. Lewis Research Center, Cleveland, OH.
THERMAL ANNEALING OF GaAs CONCENTRATOR SOLAR CELLS **c44**
H. B. Curtis and David J. Brinker *In its* Space Photovoltaic Research and Technology, 1989 Jan. 1991 p 140-153 (For primary document see N91-19182 11-20)
Avail: NTIS HC/MF A22 CSCL 10B

Isochronal and isothermal annealing tests were performed on GaAs concentrator cells which were irradiated with electrons of various energies to fluences up to 1 x 10(exp 16) e/sq cm. The results include: (1) For cells irradiated with electrons from 0.7 to 2.3 MeV, recovery decreases with increasing electron energy. (2) As determined by the un-annealed fractions, isothermal and isochronal annealing produce the same recovery. Also, cells irradiated to 3 x 10(exp 15) or 1 x 10(exp 16) e/sq cm recover to similar un-annealed fractions. (3) Some significant annealing is being seen at 150 C although very long times are required.
Author

N91-19196*# Boeing Co., Seattle, WA.
BURST ANNEALING OF HIGH TEMPERATURE GaAs SOLAR CELLS **c44**

P. R. Brothers and W. E. Horne *In* NASA, Lewis Research Center, Space Photovoltaic Research and Technology, 1989 Jan. 1991 p 154-163 (For primary document see N91-19182 11-20)
Avail: NTIS HC/MF A22 CSCL 10B

One of the major limitations of solar cells in space power systems is their vulnerability to radiation damage. One solution to this problem is to periodically heat the cells to anneal the radiation damage. Annealing was demonstrated with silicon cells. The obstacle to annealing of GaAs cells was their susceptibility to thermal damage at the temperatures required to completely anneal the radiation damage. GaAs cells with high temperature contacts and encapsulation were developed. The cells tested are designed for concentrator use at 30 suns AMO. The circular active area is 2.5 mm in diameter for an area of 0.05 sq cm. Typical one sun AMO efficiency of these cells is over 18 percent. The cells were demonstrated to be resistant to damage after thermal excursions in excess of 600 C. This high temperature tolerance should allow these cells to survive the annealing of radiation damage. A limited set of experiments were devised to investigate the feasibility of annealing these high temperature cells. The effect of repeated cycles of electron and proton irradiation was tested. The damage mechanisms were analyzed. Limitations in annealing recovery suggested improvements in cell design for more complete recovery. These preliminary experiments also indicate the need for further study to isolate damage mechanisms. The primary objective of the experiments was to demonstrate and quantify the annealing behavior of high temperature GaAs cells. Secondary objectives were to measure the radiation degradation and to determine the effect of repeated irradiation and anneal cycles. Author

N91-19197*# Boeing Aerospace Co., Seattle, WA.
AN APPROACH FOR CONFIGURING SPACE PHOTOVOLTAIC TANDEM ARRAYS BASED ON CELL LAYER PERFORMANCE **c44**
C. S. Flora and P. A. Dillard *In* NASA, Lewis Research Center, Space Photovoltaic Research and Technology, 1989 Jan. 1991 p 167-179 (For primary document see N91-19182 11-20)
Avail: NTIS HC/MF A22 CSCL 10B

Meeting solar array performance goals of 300 W/Kg requires use of solar cells with orbital efficiencies greater than 20 percent. Only multijunction cells and cell layers operating in tandem produce this required efficiency. An approach for defining solar array design concepts that use tandem cell layers involve the following: transforming cell layer performance at standard test conditions to on-orbit performance; optimizing circuit configuration with tandem cell layers; evaluating circuit sensitivity to cell current mismatch; developing array electrical design around selected circuit; and predicting array orbital performance including seasonal variations. Author

N91-19198*# National Aeronautics and Space Administration. Lewis Research Center, Cleveland, OH.
REVIEW OF THIN FILM SOLAR CELL TECHNOLOGY AND APPLICATIONS FOR ULTRA-LIGHT SPACECRAFT SOLAR ARRAYS **c44**
Geoffrey A. Landis *In its* Space Photovoltaic Research and Technology, 1989 Jan. 1991 p 180-203 (For primary document see N91-19182 11-20)
Avail: NTIS HC/MF A22 CSCL 10B

Developments in thin-film amorphous and polycrystalline photovoltaic cells are reviewed and discussed with a view to potential applications in space. Two important figures of merit are discussed: efficiency (i.e., what fraction of the incident solar energy is converted to electricity), and specific power (power to weight ratio). Author

N91-19199*# Solarex Corp., Rockville, MD.
PERFORMANCE, SIZE, MASS, AND COST ESTIMATES FOR PROJECTED 1kW EOL Si, InP, AND GaAs ARRAYS **c44**
Luther W. Slifer, Jr. *In* NASA, Lewis Research Center, Space Photovoltaic Research and Technology, 1989 Jan. 1991 p 204-211 (For primary document see N91-19182 11-20)
Avail: NTIS HC/MF A22 CSCL 10B

One method of evaluating the potential of emerging solar cell and array technologies is to compare their projected capabilities in space flight applications to those of established Si solar cells and arrays. Such an application-oriented comparison provides an integrated view of the elemental comparisons of efficiency, radiation resistance, temperature sensitivity, size, mass, and cost in combination. In addition, the assumptions necessary to make the comparisons provide insights helpful toward determining necessary areas of development or evaluation. Finally, as developments and evaluations progress, the results can be used in more precisely defining the overall potential of the new technologies in comparison to existing technologies. The projected capabilities of Si, InP, and GaAs cells and arrays are compared. Author

N91-19200*# National Aeronautics and Space Administration. Lewis Research Center, Cleveland, OH.
DUAL-PURPOSE SELF-DELIVERABLE LUNAR SURFACE PV ELECTRICAL POWER SYSTEM **c44**
Jack H. Arnold, David W. Harris, Eldon R. Cross (Research Triangle Inst., Research Triangle Park, NC.), and Dennis J. Flood *In its* Space Photovoltaic Research and Technology, 1989 Jan. 1991 p 212-222 (For primary document see N91-19182 11-20)
Avail: NTIS HC/MF A22 CSCL 10B

A safe haven and work supported PV power systems on the lunar surface will likely be required by NASA in support of the manned outpost scheduled for the post-2000 lunar/Mars exploration and colonization initiative. Initial system modeling and computer analysis shows that the concept is workable and contains no major high risk technology issues which cannot be resolved in the circa 2000 to 2025 timeframe. A specific selection of the best suited type of electric thruster has not been done; the initial modeling was done using an ion thruster, but Rocketdyne must also evaluate arc and resisto-jets before a final design can be formulated. As a general observation, it appears that such a system can deliver itself to the Moon using many system elements that must be transported as dead payload mass in more conventional delivery modes. It further appears that a larger power system providing a much higher safe haven power level is feasible if this delivery system is implemented, perhaps even sufficient to permit resource prospecting and/or lab experimentation. The concept permits growth and can be expanded to include cargo transport such as habitat and working modules. In short, the combined payload could be manned soon after landing and checkout. NASA has expended substantial resources in the development of electric propulsion concepts and hardware that can be applied to a lunar transport system such as described herein. In short, the paper may represent a viable mission on which previous investments play an invaluable role. A more comprehensive technical paper which embodies second generation analysis and system size will be prepared for near-term presentation. Author

N91-19201*# National Aeronautics and Space Administration. Lewis Research Center, Cleveland, OH.
FEASIBILITY OF SOLAR POWER FOR MARS **c44**
Joseph Appelbaum and Geoffrey A. Landis *In its* Space Photovoltaic Research and Technology, 1989 Jan. 1991 p 223-254 (For primary document see N91-19182 11-20)
Avail: NTIS HC/MF A22 CSCL 10B

NASA, through Project Pathfinder, has put in place an advanced technology program to address future needs of manned space exploration. Included in the missions under study is the establishment of outposts on the surface of Mars. The Surface Power program in Pathfinder is aimed at providing photovoltaic array technology for such an application (as well as for the lunar surface). Another important application is for unmanned precursor missions, such as the photovoltaic-power aircraft, which will scout landing sites and investigate Mars geology for a 1 to 2 year mission without landing on the surface. Effective design and utilization of solar energy depend to a large extent on adequate knowledge of solar radiation characteristics in the region of solar energy system operation. The two major climatic components needed for

photovoltaic system designs are the distributions of solar insolation and ambient temperature. These distributions for the Martian climate are given at the two Viking lander locations but can also be used, to the first approximation, for other latitudes. One of the most important results is that there is a large diffuse component of the insolation, even at high optical depth, so that solar energy system operation is still possible. If the power system is to continue to generate power even on high optical opacity days, it is thus important that the photovoltaic system be designed to collect diffuse irradiance as well as direct. In absence of long term insolation and temperature data for Mars, the data presented can be used until updated data are available. The ambient temperature data are given as measured directly by the temperature sensor; the insolation data are calculated from optical depth measurements of the atmosphere. Author

N91-19202*# Midwest Research Inst., Golden, CO.
RECENT ADVANCES IN THE ITO/InP SOLAR CELL c44
T. A. Gessert, X. Li, M. W. Wanlass, and T. J. Coutts *In* NASA, Lewis Research Center, Space Photovoltaic Research and Technology, 1989 Jan. 1991 p 257-269 (For primary document see N91-19182 11-20)
(Contract NASA Order C-3000-K; DE-AC02-83CH-10093)
Avail: NTIS HC/MF A22 CSCL 10B

It was demonstrated that Indium Tin Oxide (ITO)/InP solar cells can now be made on as-received p(-) bulk substrates which are of nearly equal quality to those which could previously only be made on epitaxially grown p(-) InP base layers. Although this advancement is due in part to both increases in substrate quality and a better understanding of back contact formation, it appears that the passivation/compensation effects resulting from having H2 in the sputtering gas tends to reduce significantly the performance differences previously observed between these two substrates. It is shown that since high efficiency ITO/InP cells can be made from as-received substrates, and since the type conversion process is not highly spatially dependent, large area ITO/InP cells (4 sq cm) with efficiencies approaching 17 percent (Global) can be made. Furthermore, the measured open circuit voltages (V sub OC) and quantum efficiencies (QEs) from these large cells suggest that, when they are processed using optimum grid designs, the efficiencies will be nearly equal to that of the smaller cells thus far produced. It has been shown, through comparative experiments involving ITO/InP and IO/InP cells, that Sn may not be the major cause of type conversion of the InP surface and thus further implies that the ITO may not be an essential element in this type of device. Specifically, very efficient photovoltaic solar cells were made by sputtering (Sn free) In2O3 showing that type conversion and subsequent junction formation will occur even in the absence of the sputtered SN species. The result suggests that sputter damage may indeed be the important mechanism(s) of type conversion. Finally, an initial study of the stability of the ITO/InP cell done over the course of about one year has indicated that the J(sub SC) (short circuit current) and the fill factor (FF) are measurably stable within experimental certainty. Author

N91-19203*# National Aeronautics and Space Administration. Lewis Research Center, Cleveland, OH.
SEMICONDUCTOR STRUCTURAL DAMAGE ATTENDANT TO CONTACT FORMATION IN III-V SOLAR CELLS c44
Navid S. Fatemi (Sverdrup Technology, Inc., Cleveland, OH.) and Victor G. Weizer *In its* Space Photovoltaic Research and Technology, 1989 Jan. 1991 p 270-279 (For primary document see N91-19182 11-20)
Avail: NTIS HC/MF A22 CSCL 10B

In order to keep the resistive losses in solar cells to a minimum, it is often necessary for the ohmic contacts to be heat treated to lower the metal-semiconductor contact resistivity to acceptable values. Sintering of the contacts, however can result in extensive mechanical damage of the semiconductor surface under the metallization. An investigation of the detailed mechanisms involved in the process of contact formation during heat treatment may control the structural damage incurred by the semiconductor surface to acceptable levels, while achieving the desired values of contact resistivity for the ohmic contacts. The reaction kinetics of sintered gold contacts to InP were determined. It was found that the Au-InP interaction involves three consecutive stages marked by distinct color changes observed on the surface of the Au, and that each stage is governed by a different mechanism. A detailed description of these mechanisms and options to control them are presented. Author

N91-19204*# Rensselaer Polytechnic Inst., Troy, NY.
THE EFFECT OF PROCESS CONDITIONS ON THE PERFORMANCE OF EPITAXIAL InP SOLAR CELLS c44
J. M. Borrego and S. K. Ghandi *In* NASA, Lewis Research Center, Space Photovoltaic Research and Technology, 1989 Jan. 1991 p 280-288 (For primary document see N91-19182 11-20)
(Grant NAG3-604)
Avail: NTIS HC/MF A22 CSCL 10B

Indium phosphide solar cells have a higher resistance to electron irradiation than Si or GaAs cells of comparable junction depth. As a result, there is much interest in the use of this material for space applications. Cells of this material were made in bulk InP by a number of techniques, including ion implantation, direct diffusion in sealed ampoules, and by open tube diffusion. However, it is generally considered that the epitaxial approach will be superior to all of these techniques. The epitaxy of InP is considerably more difficult than that of gallium arsenide, for a number of reasons. Perhaps the most important is the fact that the native oxides of Indium are extremely difficult to remove, as compared to that of Gallium. In addition, thermal treatments for the desorption of these oxides often result in the formation of phosphorus vacancies and free indium on the surface. Thus, inadequate sample preparation before epitaxy, poor reactor cleaning procedures, or poor transition procedures between the growth of successive layers, all give rise to trap phenomena and to high interface recombination velocities. Moreover, the lifetime of the grown material is dominated by the occurrence of native defects, so that it is a strong function of growth parameters. These problems are of special interest to the fabrication of solar cells, where long life-time, combined with the absence of traps, is highly desirable. A study of this problem is described using a non-invasive diagnostic technique which was developed. Author

N91-19205*# National Aeronautics and Space Administration. Lewis Research Center, Cleveland, OH.
EFFECTS OF PROTON IRRADIATION ON THE PERFORMANCE OF InP/GaAs SOLAR CELLS c44
Irving Weinberg, C. K. Swartz, David J. Brinker, and D. M. Wilt *In its* Space Photovoltaic Research and Technology, 1989 Jan. 1991 p 289-297 (For primary document see N91-19182 11-20)
Avail: NTIS HC/MF A22 CSCL 10B

InP solar cells are known to be more radiation resistant than either GaAs or Si. In addition, AMO total area efficiencies approaching 19 percent were attained for InP. However, the present high substrate cost presents a barrier to the eventual widespread use of InP cells in space. In addition, if cell thinning becomes desirable, their relative fragility presents a problem. For these reasons, the NASA Lewis Research Center has initiated a program, aimed at producing thin InP cells, by heteroepitaxial deposition of InP on cheaper, more durable substrates. To date, a short term feasibility study as Spire has resulted in cells processed from InP heteroepitaxially deposited on Si substrates with an intervening thin GaAs layer (InP/GaAs/Si) and cells produced from InP deposited on GaAs (InP/GaAs). As a result of this short study efficiencies of over 7 and 9 percent were achieved for InP/GaAs/Si and InP/GaAs respectively. Although these efficiencies are low, they represent a modest and encouraging starting point for a more intensive program. Obviously, when considering economy and mechanical strength, cells processed on silicon substrates are preferred. However, although the InP/GaAs cells are not the final desirable products of this program, their properties serve to highlight several roadblocks to be overcome in producing cells with the

more desirable cost and strength properties. Hence, in the present case, the properties of the InP/GaAs cells before and after irradiation by 10 MeV protons are examined. A similar study of InP/GaAs/Si cells will be reported on at a later date. Author

N91-19206*# National Aeronautics and Space Administration. Lewis Research Center, Cleveland, OH.
KEY FACTORS LIMITING THE OPEN CIRCUIT VOLTAGE OF n(+)pp(+) INDIUM PHOSPHIDE SOLAR CELLS **c44**
Chandra Goradia, William Thesling (Cleveland State Univ., OH.), and Irving Weinberg *In its* Space Photovoltaic Research and Technology, 1989 Jan. 1991 p 298-310 (For primary document see N91-19182 11-20)
Avail: NTIS HC/MF A22 CSCL 10B

Solar cells made from gallium arsenide (GaAs), with a room temperature bandgap of E(sub g) = 1.43 eV have exhibited the best measured open circuit voltage (V sub OC) of 1.05 V at 1 AMO, 25 C. The material InP is in many ways similar to GaAs. A simple calculation comparing InP to GaAs then shows that solar cells made from InP, with E(sub g) = 1.35 at 300 K, should exhibit the best measured (V sub OC) of approximately 950 mV at 1 AMO, 300 K. However, to date, the best measured V(sub OC) for InP solar cells made by any fabrication method is 899 mV at AM1.5, 25 C which would translate to 912 mV at 1 AMO, 25 C. The V(sub OC) of an n(+)pp(+) InP solar cell is governed by several factors. Of these, some factors, such as the thickness and doping of the emitter and base regions, are easily controlled and can be adjusted to desired values dictated by a good performance optimizing model. Such factors were not considered. There are other factors which also govern V(sub OC), and their values are not so easily controlled. The primary ones among these are (1) the indirect or Hall-Shockley-Read lifetimes in the various regions of the cell, (2) the low-doping intrinsic carrier concentration n(sub i) of the InP material, (3) the heavy doping factors in the emitter and BSF regions, and (4) the front surface recombination velocity S(sub F). The influence of these latter factors on the V(sub OC) of the n(+)pp(+) InP solar cell and the results were used to produce a near-optimum design of the n(+)pp(+) InP solar cell. Author

N91-19207*# National Aeronautics and Space Administration. Lewis Research Center, Cleveland, OH.
DETERMINATION OF SERIES RESISTANCE OF INDIUM PHOSPHIDE SOLAR CELLS **c44**
Raj K. Jain and Irving Weinberg *In its* Space Photovoltaic Research and Technology, 1989 Jan. 1991 p 311-315 (For primary document see N91-19182 11-20)
Avail: NTIS HC/MF A22 CSCL 10B

The series resistance of a solar cell is an important parameter, which must be minimized to achieve high cell efficiencies. The cell series resistance is affected by the starting material, its design, and processing. The theoretical approach proposed by Jia, et. al., is used to calculate the series resistance of indium phosphide solar cells. It is observed that the theoretical approach does not predict the series resistance correctly in all cases. The analysis was modified to include the use of effective junction ideality factor. The calculated results were compared with the available experimental results on indium phosphide solar cells processed by different techniques. It is found that the use of process dependent junction ideality factor leads to better estimation of series resistance. An accurate comprehensive series resistance model is warranted to give proper feedback for modifying the cell processing from the design state. Author

N91-19208*# National Aeronautics and Space Administration. Lewis Research Center, Cleveland, OH.
INVESTIGATION OF ANODIC AND CHEMICAL OXIDES GROWN ON p-TYPE InP WITH APPLICATIONS TO SURFACE PASSIVATION FOR n(+)-p SOLAR CELL FABRICATION **c44**
Maria Faur, Mircea Faur, Manju Goradia, Chandra Goradia (Cleveland State Univ., OH.), Phillip Jenkins, Douglas Jayne, and Irving Weinberg *In its* Space Photovoltaic Research and Technology, 1989 Jan. 1991 p 316-331 (For primary document see N91-19182 11-20)
Avail: NTIS HC/MF A22 CSCL 10B

Most of the previously reported InP anodic oxides were grown on a n-type InP with applications to fabrication of MISFET structures and were described as a mixture of In2O3 and P2O5 stoichiometric compounds or nonstoichiometric phases which have properties similar to crystalline compounds In(OH)3, InPO4, and In(PO3)3. Details of the compositional change of the anodic oxides grown under different anodization conditions were previously reported. The use of P-rich oxides grown either by anodic or chemical oxidation are investigated for surface passivation of p-type InP and as a protective cap during junction formation by closed-ampoule sulfur diffusion. The investigation is based on but not limited to correlations between PL intensity and X-ray photoelectron spectroscopy (XPS) chemical composition data. Author

N91-19209*# National Aeronautics and Space Administration. Lewis Research Center, Cleveland, OH.
A COMPARATIVE STUDY OF PERFORMANCE PARAMETERS OF n(+)-p InP SOLAR CELLS MADE BY CLOSED-AMPOULE SULFUR DIFFUSION INTO Cd- AND Zn-DOPED p-TYPE InP SUBSTRATES **c44**
Mircea Faur, Maria Faur, Chandra Goradia, Manju Goradia, Ralph D. Thomas, David J. Brinker, Navid S. Fatemi (Sverdrup Technology, Inc., Cleveland, OH.), and Frank S. Honecy *In its* Space Photovoltaic Research and Technology, 1989 Jan. 1991 p 332-346 (For primary document see N91-19182 11-20)
Avail: NTIS HC/MF A22 CSCL 10B

Preliminary results indicate that Cd-doped substrates are better candidates for achieving high efficiency solar cells fabricated by closed-ampoule sulfur (S) diffusion than Zn-doped substrates. The differences in performance parameters (i.e., 14.3 percent efficiency for Cd-doped vs. 11.83 percent in the case of Zn-doped substrates of comparable doping and etch pit densities) were explained in terms of a large increase in dislocation density as a result of S diffusion in the case of Zn-doped as compared to Cd-doped substrates. The In(x)S(y) and probably Zn(S) precipitates in the case of Zn-doped substrates, produce a dead layer which extends deep below the surface and strongly affects the performance parameters. It should be noted that the cells had an unoptimized single layer antireflective coating of SiO, a grid shadowing of 6.25 percent, and somewhat poor contacts, all contributing to a reduction in efficiency. It is believed that by reducing the external losses and further improvement in cell design, efficiencies approaching 17 percent at 1 AMO, 25 degrees should be possible for cells fabricated on these relatively high defect density Cd-doped substrates. Even higher efficiencies, 18 to 19 percent should be possible by using long-lifetime substrates and further improving front surface passivation. If solar cells fabricated on Cd-doped substrates turn out to have comparable radiation tolerance as those reported in the case of cells fabricated on Zn-doped substrates, then for certain space missions 18 to 19 percent efficient cells made by this method of fabrication would be viable. Author

N91-19210*# Boeing Aerospace Co., Seattle, WA.
RADIOISOTOPE THERMAL PHOTOVOLTAIC APPLICATION OF THE GaSb SOLAR CELL **c44**
M. D. Morgan, W. E. Horne, and A. C. Day *In* NASA, Lewis Research Center, Space Photovoltaic Research and Technology, 1989 Jan. 1991 p 349-358 (For primary document see N91-19182 11-20)
Avail: NTIS HC/MF A22 CSCL 10B

An examination of a RTVP (radioisotopic thermophotovoltaic) conceptual design has shown a high potential for power densities well above those achievable with radioisotopic thermoelectric generator (RTG) systems. An efficiency of 14.4 percent and system specific power of 9.25 watts/kg were predicted for a system with sixteen GPHS (general purpose heat source) sources operating at 1100 C. The models also showed a 500 watt system power by the strontium-90 isotope at 1200 C at an efficiency of 17.0 percent

and a system specific power of 11.8 watts/kg. The key to this level of performance is a high-quality photovoltaic cell with narrow bandgap and a reflective rear contact. Recent work at Boeing on GaSb cells and transparent back GaAs cells indicate that such a cell is well within reach. Author

N91-19211*# Jet Propulsion Lab., California Inst. of Tech., Pasadena.
GaP BETAVOLTAIC CELLS AS A POWER SOURCE c44
F. S. Pool, Paul M. Stella, and B. Anspaugh *In* NASA, Lewis Research Center, Space Photovoltaic Research and Technology, 1989 Jan. 1991 p 359-370 (For primary document see N91-19182 11-20)
Avail: NTIS HC/MF A22 CSCL 10B

Maximum power output for the GaP cells of this study was found to be on the order of 1 microW. This resulted from exposure to 200 and 40 KeV electrons at a flux of 2 x 10(exp 9) electrons/sq cm/s, equivalent to a 54 mCurie source. The efficiencies of the cells ranged from 5 to 9 percent for 200 and 40 KeV electrons respectively. The lower efficiency at higher energy is due to a substantial fraction of energy deposition in the substrate, further than a diffusion length from the depletion region of the cell. Radiation damage was clearly observed in GaP after exposure to 200 KeV electrons at a fluence of 2 x 10(exp 12) electrons/sq cm. No discernable damage was observed after exposure to 40 KeV electrons at the same fluence. Analysis indicates that a GaP betavoltaic system would not be practical if limited to low energy beta sources. The power available would be too low even in the ideal case. By utilizing high activity beta sources, such as Sr-90/Y-90, it may be possible to achieve performance that could be suitable for some space power applications. However, to utilize such a source the problem of radiation damage in the beta cell material must be overcome. Author

N91-19212*# Chronos Research Labs., Inc., San Diego, CA.
LOW COST SPACE POWER GENERATION
Randall B. Olsen *In* NASA, Lewis Research Center, Space Photovoltaic Research and Technology, 1989 Jan. 1991 p 371-381 (For primary document see N91-19182 11-20)
Avail: NTIS HC/MF A22 CSCL 10B

The success of this study has given a method of fabricating durable copolymer films without size limitations. Previously, only compression molded samples were durable enough to generate electrical energy. The strengthened specimens are very long lived materials. The lifetime was enhanced at least a factor of 1,300 in full pyroelectric conversion cycle experiments compared with extruded, non-strengthened film. The new techniques proved so successful that the lifetime of the resultant copolymer samples was not fully characterized. The lifetime of these new materials is so long that accelerated tests were devised to probe their durability. After a total of more than 67 million high voltage electrical cycles at 100 C, the electrical properties of a copolymer sample remained stable. The test was terminated without any detectable degradation to allow for other experiments. One must be cautious in extrapolating to power cycle performance, but 67 million electrical cycles correspond to 2 years of pyroelectric cycling at 1 Hz. In another series of experiments at reduced temperature and electrical stress, a specimen survived over one-third of a billion electrical cycles during nearly three months of continuous testing. The radiation-limited lifetimes of the copolymer were shown to range from several years to millions of years for most earth orbits. Thus, the pyroelectric copolymer has become a strong candidate for serious consideration for future spacecraft power supplies.
Author

N91-19213*# Solarex Corp., Rockville, MD. Aerospace Div.
SPACEFLIGHT PERFORMANCE OF SEVERAL TYPES OF SILICON SOLAR CELLS ON THE LIPS 3 SATELLITE c44
J. Silver and D. Warfield *In* NASA, Lewis Research Center, Space Photovoltaic Research and Technology, 1989 Jan. 1991 p 385-388 (For primary document see N91-19182 11-20)
Avail: NTIS HC/MF A22 CSCL 10B

Results from exposure of several types of Solarex silicon cells to a space environment for nearly two years on the LIPS 3 satellite are presented. Experiments include standard thickness (10 mil) cells with and without back surface fields, and ultrathin (2 mil) cells also with and without back surface fields. A comparison between a widely used coverslide adhesive, DC 93-500 and a potential alternate is also presented. The major findings from the data are that the 2 mil cells without a back surface field show the smallest normalized short circuit current degradation and that the 10 mil back surface field cells show the greatest absolute power output for the radiation exposures and temperatures encountered. The new encapsulant (McGhan Nusil CV-2500) exhibits a degradation comparable to DC 93-500. A comparison is made with each of the cell types in this experiment with expectations based on JPL Radiation Handbook data. Author

N91-19214*# Wayne State Univ., Detroit, MI. Inst. for Manufacturing Research.
ANNEALING CHARACTERISTICS OF IRRADIATED HYDROGENATED AMORPHOUS SILICON SOLAR CELLS c44
J. S. Payson, S. Abdulaziz, Y. Li, and J. R. Woodyard *In* NASA, Lewis Research Center, Space Photovoltaic Research and Technology, 1989 Jan. 1991 p 389-399 (For primary document see N91-19182 11-20)
Avail: NTIS HC/MF A22 CSCL 10B

It was shown that 1 MeV proton irradiation with fluences of 1.25E14 and 1.25E15/sq cm reduces the normalized I(sub SC) of a-Si:H solar cell. Solar cells recently fabricated showed superior radiation tolerance compared with cells fabricated four years ago; the improvement is probably due to the fact that the new cells are thinner and fabricated from improved materials. Room temperature annealing was observed for the first time in both new and old cells. New cells anneal at a faster rate than old cells for the same fluence. From the annealing work it is apparent that there are at least two types of defects and/or annealing mechanisms. One cell had improved I-V characteristics following irradiation as compared to the virgin cell. The work shows that the photothermal deflection spectroscopy (PDS) and annealing measurements may be used to predict the qualitative behavior of a-Si:H solar cells. It was anticipated that the modeling work will quantitatively link thin film measurements with solar cell properties. Quantitative predictions of the operation of a-Si:H solar cells in a space environment will require a knowledge of the defect creation mechanisms, defect structures, role of defects on degradation, and defect passivation and annealing mechanisms. The engineering data and knowledge base for justifying space flight testing of a-Si:H alloy based solar cells is being developed. Author

N91-19215*# Applied Solar Energy Corp., City of Industry, CA.
OPTIMIZATION AND PERFORMANCE OF SPACE STATION FREEDOM SOLAR CELLS c44
S. Khemthong, N. Hansen, and M. Bower *In* NASA, Lewis Research Center, Space Photovoltaic Research and Technology, 1989 Jan. 1991 p 400-409 (For primary document see N91-19182 11-20)
Avail: NTIS HC/MF A22 CSCL 10B

High efficiency, large area and low cost solar cells are the drivers for Space Station solar array designs. The manufacturing throughput, process complexity, yield of the cells, and array manufacturing technique determine the economics of the solar array design. The cell efficiency optimization of large area (8 x 8 m), dielectric wrapthrough contact solar cells are described. The results of the optimization are reported and the solar cell performance of limited production runs is reported. Author

N91-19216*# Jet Propulsion Lab., California Inst. of Tech., Pasadena.
THERMAL CYCLE TESTING OF SPACE STATION FREEDOM SOLAR ARRAY BLANKET COUPONS c44
David A. Scheiman and David A. Schieman (Sverdrup Technology, Inc., Cleveland, OH.) *In* NASA, Lewis Research Center, Space Photovoltaic Research and Technology, 1989 Jan. 1991 p 410-420 (For primary document see N91-19182 11-20)

(Contract NAS3-25266)
Avail: NTIS HC/MF A22 CSCL 10B

Lewis Research Center is presently conducting thermal cycle testing of solar array blanket coupons that represent the baseline design for Space Station Freedom. Four coupons were fabricated as part of the Photovoltaic Array Environment Protection (PAEP) Program, NAS 3-25079, at Lockheed Missile and Space Company. The objective of the testing is to demonstrate the durability or operational lifetime of the solar array welded interconnect design within the durability or operational lifetime of the solar array welded interconnect design within a low earth orbit (LEO) thermal cycling environment. Secondary objectives include the observation and identification of potential failure modes and effects that may occur within the solar array blanket coupons as a result of thermal cycling. The objectives, test articles, test chamber, performance evaluation, test requirements, and test results are presented for the successful completion of 60,000 thermal cycles. Author

N91-19217*# Jet Propulsion Lab., California Inst. of Tech., Pasadena.
THE ADVANCED PHOTOVOLTAIC SOLAR ARRAY (APSA) TECHNOLOGY STATUS AND PERFORMANCE c44
Paul M. Stella and Richard M. Kurland (TRW Space Technology Labs., Redondo Beach, CA.) *In* NASA, Lewis Research Center, Space Photovoltaic Research and Technology, 1989 Jan. 1991 p 421-432 (For primary document see N91-19182 11-20)
Avail: NTIS HC/MF A22 CSCL 10B

In 1985, the Jet Propulsion Laboratory initiated the Advanced Photovoltaic Solar Array (APSA) program. The program objective is to demonstrate a producible array system by the early 1990s with a specific performance of at least 130 W/kG (beginning-of-life) as an intermediate milestone towards the long range goal of 300 W/kG. The APSA performance represents an approximately four-fold improvement over existing rigid array technology and a doubling of the performance of the first generation NASA/OAST SAFE flexible blanket array of the early 1980s. Author

N91-19218*# Sovonics Solar Systems, Troy, MI.
INTEGRAL BYPASS DIODES IN AN AMORPHOUS SILICON ALLOY PHOTOVOLTAIC MODULE c44
J. J. Hanak and H. Flaisher *In* NASA, Lewis Research Center, Space Photovoltaic Research and Technology, 1989 Jan. 1991 p 433-442 (For primary document see N91-19182 11-20)
Avail: NTIS HC/MF A22 CSCL 10B

Thin-film, tandem-junction, amorphous silicon (a-Si) photovoltaic modules were constructed in which a part of the a-Si alloy cell material is used to form bypass protection diodes. This integral design circumvents the need for incorporating external, conventional diodes, thus simplifying the manufacturing process and reducing module weight. Author

N91-19219*# National Aeronautics and Space Administration. Lewis Research Center, Cleveland, OH.
MINI-DOME FRESNEL LENS PHOTOVOLTAIC CONCENTRATOR DEVELOPMENT c44
Mark J. ONeill (ENTECH Corp., Dallas-Fort Worth Airport, TX.) and Michael F. Piszczor, Jr. *In its* Space Photovoltaic Research and Technology, 1989 Jan. 1991 p 443-459 (For primary document see N91-19182 11-20)
Avail: NTIS HC/MF A22 CSCL 10B

Since 1986 work on a new high-performance, light-weight space photovoltaic concentration array has been conducted. An update on the mini-dome lens concentrator array development program is provided. Recent prototype cell and lens test results indicate that near-term array performance goals of 300 w/sq m and 100 w/kg are feasible, and that a longer-term goal of 200 w/kg is reasonable. B.G.

N91-19220*# Aerospace Corp., Los Angeles, CA. Chemistry and Physics Lab.
STRATEGY IN SPACE FLIGHT EXPERIMENTS
Dean Marvin and James Severns (Naval Research Lab., Washington, DC.) *In* NASA, Lewis Research Center, Space Photovoltaic Research and Technology, 1989 Jan. 1991 p 469-473 (For primary document see N91-19182 11-20)
Avail: NTIS HC/MF A22 CSCL 10B

The main topics of the workshop were the evaluation of both the need for flight testing of solar array hardware and the opportunities for such testing. Spacecraft charging effects, array dynamics, cost-effectiveness, and methods of flight planning were also discussed. B.G.

N91-19221*# National Aeronautics and Space Administration. Lewis Research Center, Cleveland, OH.
INDIUM PHOSPHIDE SOLAR CELLS c44
Irving Weinberg *In its* Space Photovoltaic Research and Technology, 1989 Jan. 1991 p 484-486 (For primary document see N91-19182 11-20)
Avail: NTIS HC/MF A22 CSCL 10B

The direction for InP solar cell research; reduction of cell cost; increase of cell efficiency; measurements needed to better understand cell performance; n/p versus p/n; radiation effects; major problems in cell contacting; and whether the present level of InP solar cell research in the USA should be maintained, decreased, or increased were considered. B.G.

N91-19222# Technische Univ., Delft (Netherlands). Faculty of Aerospace Engineering.
SOLID FUEL COMBUSTION CHAMBER Progress Report No. 17, Jan. - Jun. 1990
H. Wittenberg, P. A. O. G. Korting, B. T. C. Zandbergen, ed., T. Wijchers, P. J. M. Elands, J. P. deWilde, and F. Dijkstra Nov. 1990 24 p
(LR-648; PML-1990-C139; SFCC-Publ-61; ETN-91-98936) Avail: NTIS HC/MF A03

The Solid Fuel Combustion Chamber (SFCC) project aims at developing a prediction capability for SFCC performance in order to evaluate the SSFC for propulsions such as solid fuel ramjet, hybrid rocket and turbine, and for the clean combustion of waste materials. An overview of the Jan. - Jun. 1990 experimental and research activities is presented. Management, finances and personnel are discussed. The computer code COPPEF capability to predict both SFCC performance at high supersonic flight conditions and flameout conditions was evaluated and the effect of detailed fuel pyrolysis was investigated. An experimental investigation to improve the performance of metallized HTPB fuels was carried out. The project status and planned program are reviewed. ESA

N91-19144*# California State Polytechnic Univ., Pomona.
DETAILED MODAL TESTING OF A SOLID ROCKET MOTOR USING A PORTABLE TEST SYSTEM
Vladimir Glozman and Ralph D. Brillhart (SDRC, Inc., San Diego, CA.) *In* NASA, Goddard Space Flight Center, 16th Space Simulation Conference Confirming Spaceworthiness Into the Next Millennium Nov. 1990 p 211-226 (For primary document see N91-19126 11-18)
Avail: NTIS HC/MF A20 CSCL 21H

N91-20031*# Indiana Univ.-Purdue Univ., Fort Wayne.
ROCKET NOISE FILTERING SYSTEM USING DIGITAL FILTERS
David Mauritzen *In* NASA, John F. Kennedy Space Center, Research Reports: 1990 NASA/ASEE Summer Faculty Fellowship Program Sep. 1990 p 244-275 (For primary document see N91-20022 11-99)
(Grant NGT-60002)
Avail: NTIS HC/MF A23 CSCL 21H

23 CHEMISTRY AND MATERIALS (GENERAL)

N91-19223*# Eril Research, Inc., Corte Madera, CA.
LDEF EXPERIMENT P0006 LINEAR ENERGY TRANSFER SPECTRUM MEASUREMENT (LETSME) QUICK LOOK REPORT Final Report
19 Dec. 1990 49 p
(Contract NAS8-38188)
(NASA-CR-184115; NAS 1.26:184115) Avail: NTIS HC/MF A03 CSCL 07A

A preliminary analysis of the various passive radiation detector materials included in the P0006 LETSME experiment flown on LDEF (Long Duration Exposure Facility) is presented. It consists of four tasks: (1) readout and analysis of thermoluminescent detectors (TLD); (2) readout and analysis of fission foil/mica detectors; (3) readout and analysis of (6)LiF/CR-39 detectors; and (4) preliminary processing and readout of CR-39 and polycarbonate plastic nuclear track detectors (PNTD). Author

N91-19224*# National Aeronautics and Space Administration. Lewis Research Center, Cleveland, OH.
TRIBOLOGICAL PROPERTIES OF Ag/Ti FILMS ON Al2O3 CERAMIC SUBSTRATES
Christopher DellaCorte, Stephen V. Pepper, and Frank S. Honecy 1991 25 p Presented at the International Conference on Metallurgical Coatings and Thin Films, San Diego, CA, 22-26 Apr. 1991; sponsored by American Vacuum Society
(NASA-TM-103784; E-6060; NAS 1.15:103784) Avail: NTIS HC/MF A03 CSCL 07A

Ag solid lubricant films, with a thin Ti interlayer for enhanced adhesion, were sputter deposited on Al2O3 substrate disks to reduce friction and wear. The dual Ag/Ti films were tested at room temperature in a pin-on-disk tribometer sliding against bare, uncoated Al2O3 pins under a 4.9 N load at a sliding velocity of 1 m/s. The Ag/Ti films reduced the friction coefficient by 50 percent to about 0.41 compared to unlubricated baseline specimens. Pin wear was reduced by a factor of 140 and disk wear was reduced by a factor of 2.5 compared to the baseline. These films retain their good tribological properties including adhesion after heat treatments at 850 C and thus may be able to lubricate over a wide temperature range. This lubrication technique is applicable to space lubrication, advanced heat engines, and advanced transportation systems. Author

24 COMPOSITE MATERIALS

Includes physical, chemical, and mechanical properties of laminates and other composite materials.
For ceramic materials see *27 Nonmetallic Materials*.

N91-19225 Department of the Navy, Washington, DC.
RIGID MULLITEWHISKER FELT AND METHOD OF PREPARATION Patent
Inna G. Talmy, inventor (to Navy) and Deborah A. Haught, inventor (to Navy) 14 Aug. 1990 13 p Filed 5 Aug. 1988
(AD-D014648; US-Patent-4,948,766; US-Patent-Appl-SN-229517; US-Patent-Class-501-128) Avail: US Patent and Trademark Office CSCL 11/4

A process in which (1) AlF3 and SiO2 or AlF3, SiO2, and Al2O3 powders are formed into a green body of a desired shape and size; (2) the green body is heated at 700 to 950 C in an anhydrous SiF4 atmosphere to form barlike topaz crystals; and then (3) heated in an anhydrous SiF4 atmosphere at about 1150 to 1700 C to convert the barlike topaz crystals to needlelike single crystal mullite whiskers which form a porous, rigid felt structure. The felt has the same shape as the green body with about 1.5 or less percent change in linear dimensions. The felt can be used as preforms for ceramic-matrix or metal-matrix composites or by itself as thermal insulation. GRA

N91-19226# Agency of Industrial Science and Technology, Tsukuba (Japan). Industrial Products Research Inst.
A STUDY ON PREDICTION OF LIFE DUE TO CREEP BEHAVIOR IN CF/EPOXY AND CF/PEEK LAMINATES
Kiyoshi Kemmochi, Naoto Koshizaki, Masaki Hojo, Hiroshi Takayanagi, Chohachiro Nagasawa, and Ryuichi Hayashi 1991 8 p
Avail: NTIS HC/MF A02

The prediction of life for quasi-isotropic graphite/epoxy and graphite/PEEK laminates was carried out by utilizing the data obtained from short term creep tests at elevated temperatures. Curve-fit equations and numerical techniques were developed for the efficient life evaluation of the polymer composites. A microcomputer-based test system for automatic creep testing and analysis was developed. The time and temperature dependent response of the composites seems to correlate well with the master curve obtained by using the short term creep data together with a numerical curve fit program. Author

N91-19227# Ecole Nationale Superieure d'Arts et Metiers, Paris (France).
FLEXURE FATIGUE TESTS FOR COMPOSITES
J. P. Trotignon and L. Vincent (Ecole Centrale de Lyon, France) 1991 15 p
Avail: NTIS HC/MF A03

Flexural properties of composites can be established either in three points bending or in four point bending. The methodology is presented described in the French standards and exposed, starting with fatigue results on different composites systems, an interpretation of the long term behavior and an attempt for a predictive approach of the three point bending. These two tests are compared on unidirectional glass fibers epoxy composites. The different results obtained between the two tests are discussed in terms of deflection and volume of composites under stress. Author

N91-19228# Nihon Univ., Narashino (Japan). Dept. of Mechanical Engineering.
FLEXURAL TESTING AND EVALUATION METHODS OF ADVANCED COMPOSITE MATERIALS
Masuji Uemura and Hiroshi Iwai 1991 6 p
Avail: NTIS HC/MF A02

The effects of various factors such as loading mode, specimen size, radius of loading nose, control mode of loading, etc. on the statical and fatigue flexural properties were investigated, using the unidirectional carbon-fiber reinforced plastics (CFRP) as specimens. Those factors were found to have the appreciable effects on the flexural properties obtained by conventional 3- and 4-point flexural tests. The failures took place just beneath the loading points due to stress concentration in experiments, as proved by the numerical finite element method analysis. Finally, the recommendations for improving the flexural tests are proposed. The fatigue flexural tests are discussed. Author

N91-19229*# National Aeronautics and Space Administration. Lewis Research Center, Cleveland, OH.
METCAN UPDATES FOR HIGH TEMPERATURE COMPOSITE BEHAVIOR: SIMULATION/VERIFICATION
H.-J. Lee, P. L. N. Murthy, and Christos C. Chamis 1991 15 p Presented at the 36th International SAMPE Symposium and Exhibition, San Diego, CA, 15-18 Apr. 1991
(NASA-TM-103682; E-5899; NAS 1.15:103682) Avail: NTIS HC/MF A03 CSCL 11D

The continued verification (comparisons with experimental data) of the METCAN (Metal Matrix Composite Analyzer) computer code is updated. Verification includes comparisons at room and high temperatures for two composites, SiC/Ti-15-3 and SiC/Ti-6-4. Specifically, verification of the SiC/Ti-15-3 composite includes comparisons of strength, modulus, and Poisson's ratio as well as stress-strain curves for four laminates at room temperature. High temperature verification includes comparisons of strength and stress-strain curves for two laminates. Verification of SiC/Ti-6-4 is for a transverse room temperature stress-strain curve and

comparisons for transverse strength at three temperatures. Results of the verification indicates that METCAN can be used with confidence to simulate the high temperature nonlinear behavior of metal matrix composites. Author

N91-19230*# National Aeronautics and Space Administration. Lewis Research Center, Cleveland, OH.
COMPUTATIONAL SIMULATION OF HOT COMPOSITES STRUCTURES
Christos C. Chamis, P. L. N. Murthy, and S. N. Singhal (Sverdrup Technology, Inc., Brook Park, OH.) 1991 18 p Presented at the Energy-Sources Technology Conference and Exhibition, Houston, TX, 20-24 Jan. 1991; sponsored by ASME
(NASA-TM-103681; E-5898; NAS 1.15:103681) Avail: NTIS HC/MF A03 CSCL 11D

Three different computer codes developed in-house are described for application to hot composite structures. These codes include capabilities for: (1) laminate behavior (METCAN); (2) thermal/structural analysis of hot structures made from high temperature metal matrix composites (HITCAN); and (3) laminate tailoring (MMLT). Results for select sample cases are described to demonstrate the versatility as well as the application of these codes to specific situations. The sample case results show that METCAN can be used to simulate cyclic life in high temperature metal matrix composites; HITCAN can be used to evaluate the structural performance of curved panels as well as respective sensitivities of various nonlinearities, and MMLT can be used to tailor the fabrication process in order to reduce residual stresses in the matrix upon cool-down. Author

N91-19231*# National Aeronautics and Space Administration. Lewis Research Center, Cleveland, OH.
PROSPECTS FOR USING CARBON-CARBON COMPOSITES FOR EMI SHIELDING
James R. Gaier 1990 6 p Presented at the International Conference on Carbon, Post Symposium on Carbon-Carbon Composites, Tsukuba, Japan, 9 Nov. 1990; sponsored by Carbon Society of Japan
(NASA-TM-103677; E-5893; NAS 1.15:103677) Avail: NTIS HC/MF A02 CSCL 11D

Since pyrolyzed carbon has a higher electrical conductivity than most polymers, carbon-carbon composites would be expected to have higher electromagnetic interference (EMI) shielding ability than polymeric resin composites. A rule of mixtures model of composite conductivity was used to calculate the effect on EMI shielding of substituting a pyrolyzed carbon matrix for a polymeric matrix. It was found that the improvements were small, no more than about 2 percent for the lowest conductivity fibers (ex-rayon) and less than 0.2 percent for the highest conductivity fibers (vapor grown carbon fibers). The structure of the rule of mixtures is such that the matrix conductivity would only be important in those cases where it is much higher than the fiber conductivity, as in metal matrix composites. Author

N91-19232*# National Aeronautics and Space Administration. Lewis Research Center, Cleveland, OH.
AN OVERVIEW OF SELF-CONSISTENT METHODS FOR FIBER-REINFORCED COMPOSITES
Kurt C. Gramoll, Alan D. Freed, and Kevin P. Walker (Engineering Science Software, Inc., Smithfield, RI.) Jan. 1991 29 p
(NASA-TM-103713; E-5946; NAS 1.15:103713) Avail: NTIS HC/MF A03 CSCL 11D

The Walker et al. (1989) self-consistent method to predict both the elastic and the inelastic effective material properties of composites is examined and compared with the results of other self-consistent and elastically based solutions. The elastic part of their method is shown to be identical to other self-consistent methods for non-dilute reinforced composite materials; they are the Hill (1965), Budiansky (1965), and Nemat-Nasser et al. (1982) derivations. A simplified form of the non-dilute self-consistent method is also derived. The predicted, elastic, effective material properties for fiber reinforced material using the Walker method was found to deviate from the elasticity solution for the v sub 31, K sub 12, and mu sub 31 material properties (fiber is in the 3 direction) especially at the larger volume fractions. Also, the prediction for the transverse shear modulus, mu sub 12, exceeds one of the accepted Hashin bounds. Only the longitudinal elastic modulus E sub 33 agrees with the elasticity solution. The differences between the Walker and the elasticity solutions are primarily due to the assumption used in the derivation of the self-consistent method, i.e., the strain fields in the inclusions and the matrix are assumed to remain constant, which is not a correct assumption for a high concentration of inclusions. Author

N91-19233*# National Aeronautics and Space Administration. Lewis Research Center, Cleveland, OH.
LOW-DENSITY, HIGH-STRENGTH INTERMETALLIC MATRIX COMPOSITES BY XD (TRADEMARK) SYNTHESIS
K. S. Kumar, M. S. DiPietro, S. A. Brown (Martin Marietta Corp., Baltimore, MD.), and J. D. Whittenberger Jan. 1991 100 p (Contract NAS3-25787)
(NASA-TM-103724; E-5955; NAS 1.15:103724) Avail: NTIS HC/MF A05 CSCL 11D

A feasibility study was conducted to evaluate the potential of particulate composites based on low-density, L1(sub 2) trialuminide matrices for high-temperature applications. The compounds evaluated included Al22Fe3Ti8 (as a multiphase matrix), Al67Ti25Cr8, and Al66Ti25Mn9. The reinforcement consisted of TiB2 particulates. The TiB2 composites were processed by ingot and powder metallurgy techniques. Microstructural characterization and mechanical testing were performed in the hot-pressed and hot-isostatic-pressed condition. The casting were sectioned and isothermally forged into pancakes. All the materials were tested in compression as a function of temperature, and at high temperatures as a function of strain rate. The test results are discussed. Author

N91-19234*# National Aeronautics and Space Administration. Lewis Research Center, Cleveland, OH.
EFFECT OF FIBER REINFORCEMENTS ON THERMO-OXIDATIVE STABILITY AND MECHANICAL PROPERTIES OF POLYMER MATRIX COMPOSITES
Kenneth J. Bowles Jan. 1991 32 p
(NASA-TM-103648; E-5834; NAS 1.15:103648) Avail: NTIS HC/MF A03 CSCL 11D

A number of studies have investigated the thermo-oxidative behavior of polymer matrix composites. Two significant observations have been made from these research efforts: (1) fiber reinforcement has a significant effect on composite thermal stability; and (2) geometric effects must be considered when evaluating thermal aging data. A compilation of some results from these studies is presented, and this information shows the influence of the reinforcement fibers on the oxidative degradation of various polymer matrix composites. The polyimide PMR-15 was the matrix material that was used in these studies. The control composite material was reinforced with Celion 6000 graphite fiber. T-40R graphite fibers, along with some very stable ceramic fibers were selected as reinforcing fibers because of their high thermal stability. The ceramic fibers were Nicalon (silicon carbide) and Nextel 312 (alumina-silica-boron oxide). The mechanical properties of the two graphite fiber composites were significantly different, probably owing to variations in interfacial bonding between the fibers and the polyimide matrix. The Celion 6000/PMR-15 bond is very tight but the T-40/PMR-15 bond is less tight. Three oxidation mechanisms were observed: (1) the preferential oxidation of the Celion 6000 fiber ends at cut surfaces, leaving a surface of matrix material with holes where the fiber ends were originally situated; (2) preferential oxidation of the composite matrix; and (3) interfacial degradation by oxidation. The latter two mechanisms were also observed on fiber end cut surfaces. The fiber and interface attacks appeared to initiate interfiber cracking along these surfaces.
Author

N91-19235*# National Aeronautics and Space Administration. Lewis Research Center, Cleveland, OH.
CERAMIC COMPOSITES FOR ROCKET ENGINE TURBINES

Thomas P. Herbell and Andrew J. Eckel 1991 9 p Presented at the 1991 Aerospace Atlantic Meeting, Dayton, OH, 23-26 Apr. 1991; sponsored by SAE
(NASA-TM-103743; E-5986; NAS 1.15:103743) Avail: NTIS HC/MF A02 CSCL 11D

The use of ceramic materials in the hot section of the fuel turbopump of advanced reusable rocket engines promises increased performance and payload capability, improved component life and economics, and greater design flexibility. Severe thermal transients present during operation of the Space Shuttle Main Engine (SSME), push metallic components to the limit of their capabilities. Future engine requirements might be even more severe. In phase one of this two-phase program, performance benefits were quantified and continuous fiber reinforced ceramic matrix composite components demonstrated a potential to survive the hostile environment of an advanced rocket engine turbopump. Author

N91-19236*# National Aeronautics and Space Administration. Lewis Research Center, Cleveland, OH.
PROBABILISTIC MICROMECHANICS AND MACROMECHANICS OF POLYMER MATRIX COMPOSITES
G. T. Mase (General Motors Inst., Flint, MI.), P. L. N. Murthy, and Christos C. Chamis 1991 20 p Presented at the 14th Annual Energy-Sources Technology Conference and Exhibition, Houston, TX, 20-24 Jan. 1991; sponsored by ASME
(NASA-TM-103669; E-5876; NAS 1.15:103669) Avail: NTIS HC/MF A03 CSCL 11D

A probabilistic evaluation of an eight ply graphite-epoxy quasi-isotropic laminate was completed using the Integrated Composite Analyzer (ICAN) in conjunction with Monte Carlo simulation and Fast Probability Integration (FPI) techniques. Probabilistic input included fiber and matrix properties, fiber misalignment, fiber volume ratio, void volume ratio, ply thickness and ply layup angle. Cumulative distribution functions (CDFs) for select laminate properties are given. To reduce the number of simulations, a Fast Probability Integration (FPI) technique was used to generate CDFs for the select properties in the absence of fiber misalignment. These CDFs were compared to a second Monte Carlo simulation done without fiber misalignment effects. It was found that FPI requires fewer simulations to obtain the cumulative distribution functions as opposed to Monte Carlo simulation techniques. Furthermore, FPI provides valuable information regarding the sensitivities of composite properties to the constituent properties, fiber volume ratio and void volume ratio. Author

N91-19237*# National Aeronautics and Space Administration. Lewis Research Center, Cleveland, OH.
CONCURRENT MICROMECHANICAL TAILORING AND FABRICATION PROCESS OPTIMIZATION FOR METAL-MATRIX COMPOSITES
M. Morel, D. A. Saravanos (Case Western Reserve Univ., Cleveland, OH.), and Christos C. Chamis 1990 17 p Presented at FEMCAD and Optimization, Los Angeles, CA, 5-6 Nov. 1990; sponsored by Institute for Industrial Technology Transfer
(NASA-TM-103670; E-5877; NAS 1.15:103670) Avail: NTIS HC/MF A03 CSCL 11D

A method is presented to minimize the residual matrix stresses in metal matrix composites. Fabrication parameters such as temperature and consolidation pressure are optimized concurrently with the characteristics (i.e., modulus, coefficient of thermal expansion, strength, and interphase thickness) of a fiber-matrix interphase. By including the interphase properties in the fabrication process, lower residual stresses are achievable. Results for an ultra-high modulus graphite (P100)/copper composite show a reduction of 21 percent for the maximum matrix microstress when optimizing the fabrication process alone. Concurrent optimization of the fabrication process and interphase properties show a 41 percent decrease in the maximum microstress. Therefore, this optimization method demonstrates the capability of reducing residual microstresses by altering the temperature and consolidation pressure histories and tailoring the interphase properties for an improved composite material. In addition, the results indicate that the consolidation pressures are the most important fabrication parameters, and the coefficient of thermal expansion is the most critical interphase property. Author

N91-19238*# Martin Marietta Aerospace, Denver, CO.
COMPOSITE MATERIALS FOR SPACE APPLICATIONS Final Report, 31 Aug. 1987 - 15 Jul. 1990
Suraj P. Rawal, Mohan S. Misra, and Robert G. Wendt Aug. 1990 464 p
(Contract NAS1-18230)
(NASA-CR-187472; NAS 1.26:187472; MCR-90-502) Avail: NTIS HC/MF A20 CSCL 11D

The objectives of the program were to: generate mechanical, thermal, and physical property test data for as-fabricated advanced materials; design and fabricate an accelerated thermal cycling chamber; and determine the effect of thermal cycling on thermomechanical properties and dimensional stability of composites. In the current program, extensive mechanical and thermophysical property tests of various organic matrix, metal matrix, glass matrix, and carbon-carbon composites were conducted, and a reliable database was constructed for spacecraft material selection. Material property results for the majority of the as-fabricated composites were consistent with the predicted values, providing a measure of consolidation integrity attained during fabrication. To determine the effect of thermal cycling on mechanical properties, microcracking, and thermal expansion behavior, approximately 500 composite specimens were exposed to 10,000 cycles between -150 and +150 F. These specimens were placed in a large (18 cu ft work space) thermal cycling chamber that was specially designed and fabricated to simulate one year low earth orbital (LEO) thermal cycling in 20 days. With this rate of thermal cycling, this is the largest thermal cycling unit in the country. Material property measurements of the thermal cycled organic matrix composite laminate specimens exhibited less than 24 percent decrease in strength, whereas, the remaining materials exhibited less than 8 percent decrease in strength. The thermal expansion response of each of the thermal cycled specimens revealed significant reduction in hysteresis and residual strain, and the average CTE values were close to the predicted values. Author

N91-19239# Oak Ridge National Lab., TN.
GELCAST ZIRCONIA-ALUMINA COMPOSITES
O. O. Omatete, A. Bleier, C. G. Westmoreland, and A. C. Young 1991 17 p Presented at the 15th Annual Conference on Composites and Advanced Ceramics, Cocoa Beach, FL, 13-16 Jan. 1991
(Contract DE-AC05-84OR-21400)
(DE91-007835; CONF-910162-2) Avail: NTIS HC/MF A03

Near net-shaped parts of zirconia-alumina composites have been successfully formed by gelcasting, a technique which utilizes in situ polymerization of acrylamide monomers. The high solids loading required for gelcasting (approximately 50 vol percent) was obtained by controlling the pH-dependent stability of the aqueous zirconia-alumina suspensions. A strong correspondence was found among the surface charges on the particles, colloidal stability, and the maximum solids loading. DOE

N91-19240# Oak Ridge National Lab., TN.
THERMAL PROPERTIES OF POLYISOCYANURATE FOAM BOARD INSULATION BLOWN WITH CFC-11 SUBSTITUTES
D. L. McElroy, G. E. Courville, J. E. Christian, R. S. Graves, and R. L. Linkous 1990 27 p Presented at the 3rd International Symposium on Roofing Technology, Montreal, Quebec, 17-19 Apr. 1991
(Contract DE-AC05-84OR-21400)
(DE90-016047; CONF-910446-2) Avail: NTIS HC/MF A03

Participants at government and industry-sponsored workshops decided to fully evaluate several hydrochlorofluorocarbons for their suitability as blowing agents in polyisocyanurate laminate boardstock. Laminated boardstock was chosen because of its superior insulating qualities, commercial significance, high technical dependence on alternate blowing agents and diverse requirements.

The project is under the guidance of a cooperative industry/government steering committee with representation by the Society of the Plastic Industry, the Polyisocyanurate Insulation Manufacturers Association, the National Roofing Contractors Association, the U.S. Environmental Protection Agency, and the U.S. Department of Energy. This study deals with the key question: To what extend are the thermal properties of foams with alternate blowing agents differ from foam with CFC-11? Results are reported that compare foam thermal performance under laboratory conditions, as well as the thermal performance in long-term in situ testing of roof sections. The former involves both full thickness and thin slicing techniques and utilizes an advanced R-Matic apparatus with expanded temperature range capabilities (ASTM C-518) and an Unguarded Thin Heater Apparatus (ASTM C-1114). The long-term in situ testing is carried out on small-scale, conventionally installed roof systems on the Roof Thermal Research Apparatus. All tests are being conducted at the Oak Ridge National Laboratory with technical guidance from the steering committee. DOE

N91-19241*# National Aeronautics and Space Administration. Ames Research Center, Moffett Field, CA.

DEVELOPMENT OF A FATIGUE-LIFE METHODOLOGY FOR COMPOSITE STRUCTURES SUBJECTED TO OUT-OF-PLANE LOAD COMPONENTS

Mark Sumich and Keith T. Kedward (California Univ., Santa Barbara.) Feb. 1991 23 p

(NASA-TM-102885; A-91014; NAS 1.15:102885) Avail: NTIS HC/MF A03 CSCL 11D

The efforts to identify and implement a fatigue life methodology applicable to demonstrate delamination failures for use in certifying composite rotor blades are presented. The RSRA/X-Wing vehicle was a proof-of-concept stopped rotor aircraft configuration which used rotor blades primarily constructed of laminated carbon fiber. Delamination of the main spar during ground testing demonstrated that significant interlaminar stresses were produced. Analysis confirmed the presence of out-of-plane load components. The wear out (residual strength) methodology and the requirements for its implementation are discussed. Author

N91-19242# Argonne National Lab., IL.

THE APPLICATION OF NEUTRON DIFFRACTION TIME-OF-FLIGHT MEASUREMENTS TO THE STUDY OF STRAIN IN COMPOSITES

D. S. Kupperman, S. Majumdar, and J. P. Singh Feb. 1991 26 p Presented at the NATO Advanced Research Workshop on Measurement of Residual Stress and Applied Stress Using Neutron Diffraction, Oxford, England, 18-22 Mar. 1991

(Contract W-31-109-eng-38)

(DE91-008106; CONF-9103130-1) Avail: NTIS HC/MF A03

Neutron diffraction time-of-flight measurements using the Intense Pulsed Neutron Source at Argonne National Laboratory have been employed to study strain (from which stress is calculated) in a variety of metal- and ceramic-matrix composite structures. For example, the effect of fabrication procedures (e.g., thermal cycling) on strain in the constituents of a metal-matrix composite have been studied. In this example, neutron diffraction experiments have been useful to quantify the process induced reduction of strain in the composite fibers. Measurements carried out to 900 C on this material have been used to validate theoretical assumptions in the prediction of fabrication induced residual stress. Neutron diffraction studies of a high-temperature ceramic superconducting composite consisting of yttrium-barium-copper-oxide (YBCO) with various volume fractions of silver have also been carried out. The results of these experiments have provided information of the effect of silver content on stoichiometry, strength of interface bonding between silver and YBCO (indicated by the tensile strains in the silver), and creep mechanisms during fabrication. Ceramic matrix composites with randomly dispersed ceramic whiskers have also been studied. Comparison of measured data with analytical model predictions gave important clues to the micromechanisms involved in the creation of the residual stresses. DOE

N91-19243# Sandia National Labs., Albuquerque, NM.

LOW TEMPERATURE PROPERTIES OF BORON CARBIDES

J. C. J. M. deRooy, D. Reefman, D. vanderPutten, H. B. Brom, T. L. Aselage, and D. Emin 1990 4 p Presented at the 10th International Symposium on Boron, Borides and Related Compounds, Albuquerque, NM, 27-30 Aug. 1990

(Contract DE-AC04-76DP-00789)

(DE91-008172; SAND-91-0460C; CONF-900870-8) Avail: NTIS HC/MF A01

We have investigated boron carbides, B(sub 1-x)C(sub x) with x = 0.1, 0.13 and 0.2, especially below 1 K. The samples were characterized by electron spin resonance (ESR). The integrated intensities are roughly sample independent and correspond to about 10(exp 20) spins per gram. The temperature (T) dependences are Curie-like. The line shapes were Lorentzian and for x = 0.1 and 0.13 are strongly temperature dependent, which is suggestive for a coupling of linewidths and charge carriers. The room temperature linewidths are 0.38 mT, 32.6 mT and 23.5 mT for resp. x = 0.2, 0.13 and 0.1. Also the AC susceptibility (chi) measured down to 100 mK points to a similar small number of spins. There is no sign of a Pauli susceptibility within experimental error. No phase transition (e.g. to a superconducting state) is observed. For x = 0.13 and 0.1 a very small specific heat, C, is seen. The T dependence of C can be described by a T(sup alpha) plus a small cubic term, alpha, about 0.26. The relation between C and chi can be explained with a random exchange model. The C-value for x = 0.2 is below the limit of our experimental accuracy. DOE

N91-19244# Bristol Univ. (England). Dept. of Aerospace Engineering.

UNCERTAINTY REASONING APPLIED TO THE ASSESSMENT OF COMPOSITE MATERIAL FOR STRUCTURAL DESIGN

S. K. Morton and J. P. H. Webber Aug. 1989 38 p Sponsored by Science Research Council, England and Research Council, and British Aerospace Public Ltd. Co., Bristol, England

(BU-405; ETN-91-98857) Avail: NTIS HC/MF A03

The problem of selecting the most suitable fiber reinforced composite material for a given design is discussed. In particular the inherent indeterminacy of the mechanical properties of such materials, and how this affects a reasoned judgement, is focused upon. The artificial intelligence systems programming language FRIL is described: this allows the modeling of uncertain information and supports inference using uncertain rules. The application of FRIL's methodology to the assessment of design materials is illustrated, and the merits of different representations are examined. ESA

N91-19245# Bristol Univ. (England). Dept. of Aerospace Engineering.

AN EXPERT SYSTEM FOR LAMINATED PLATE DESIGN USING COMPOSITE MATERIALS

J. P. H. Webber and S. K. Morton Nov. 1989 39 p Previously announced in IAA as A91-20334

(BU-406; ETN-91-98858) Avail: NTIS HC/MF A03

Fiber reinforced composite materials are introduced as suitable for aircraft design, and the need for computerizing the design process is explained. Following an exposition of the linear theory of composite laminated plates, a prototype expert system for the design of simple load carrying plates or panels is described. The automatic assessment of the relative merits of designs of different materials using uncertainty reasoning techniques is discussed. The semantics and logic calculus and inference of the artificial intelligence systems programming language FRIL are described. ESA

N91-19246# Bristol Univ. (England). Dept. of Aerospace Engineering.

MINIMUM WEIGHT OPTIMIZATION OF COMPOSITE LAMINATED STRUTS

C. M. L. Wu and J. P. H. Webber Jan. 1990 55 p Sponsored by Science Research Council, England

(BU-409; ETN-91-98860) Avail: NTIS HC/MF A04

A formulation for minimum weight optimization for composite laminated struts is given. The minimum weight strut satisfies failure criterion of local buckling, overall buckling and maximum strain or maximum stress. Seven types of strut shapes, six composite materials and aluminum alloy are considered. The formulation requires the evaluation of the buckling coefficient for both ends with one side simply supported and one side free for composite laminated plates of high aspect ratio. The method of evaluation is given. A computer program OPTSTRUT for carrying out the optimization procedure is described. Examples of strut design are carried out using this program and compared with existing designs. It was found that these results compared well with those from past investigators. ESA

N91-19247# Bristol Univ. (England). Dept. of Aerospace Engineering.
A KNOWLEDGE BASED EXPERT SYSTEM FOR LAMINATED COMPOSITE STRUT DESIGN
C. M. L. Wu, J. P. H. Webber, and S. K. Morton Feb. 1990 63 p Sponsored by United Kingdom Science and Engineering Research Council, and British Aerospace Public Ltd.
(BU-410; ETN-91-98861) Avail: NTIS HC/MF A04

A knowledge based expert system for the design and analysis of composite laminated struts is described. This system is part of a composite design expert (CODEX) system that not only performs analysis and design of composite laminated plates and struts, but also incorporates the modeling of uncertainties of information, definition and decision when assessing competing designs. The analysis part of the system is based on a minimum weight optimization that satisfies the failure criteria of local buckling, overall buckling and maximum strain or maximum stress. Available in the system for analysis and assessment are seven types of strut shapes, six composite materials and aluminum alloy. Examples of strut design are carried out and assessed using this system. ESA

N91-19248# Technische Univ., Eindhoven (Netherlands).
CONSTITUTIVE MODELS FOR COMPOSITES BASED ON NUMERICAL MICROMECHANICS Ph.D. Thesis
Wilhelmus Maria Gera Courage 1990 108 p Sponsored in part by Netherlands Organization for Applied Scientific Research
(ISBN-90-9003733-0; ETN-91-98935) Avail: NTIS HC/MF A06

A strategy for the derivation of structural material models is proposed. Micromechanical analyses are made on the representative volume element of a material whose microstructure is modeled in a detailed way. The results are related to an overall material model and effective parameters obtained are evaluated as a function of the structural parameters. The strategy is applied to a composite material reinforced with short fibers. The use and derivation of effective stiffness properties for composite materials is discussed. Numerical tools, including a parameter estimation technique, the use of the regression method, and the finite element method, are discussed. The performance and applicability of the method is discussed. Much attention has to be paid to the detailed analyses in order to obtain accurate results. The derivation of a regression model is not always appropriate because of the large number of structural parameters and the nonlinearities in the model. The numerical strategy can still be used successfully to create a database for the effective parameters as a function of the structural parameters. With such a database, sensitivity analyses or interpolations can be performed to get insight into the relation between the structural and the effective parameters. ESA

N91-19133*# Massachusetts Inst. of Tech., Lexington. Lincoln Lab.
THE PERFORMANCE OF MULTILAYER INSULATION IN A RAPIDLY DEPRESSURIZING ENVIRONMENT
Ronald A. Efromson *In* NASA, Goddard Space Flight Center, 16th Space Simulation Conference Confirming Spaceworthiness Into the Next Millennium Nov. 1990 p 56-72 Sponsored in part by Strategic Defense Initiative Organization (For primary document see N91-19126 11-18)
Avail: NTIS HC/MF A20 CSCL 11D

25 INORGANIC AND PHYSICAL CHEMISTRY

Includes chemical analysis, e.g., chromatography; combustion theory; electrochemistry; and photochemistry.

For related information see also *77 Thermodynamics and Statistical Physics.*.

N91-19249 Department of the Navy, Washington, DC.
MICROBIOLOGICAL ASSAY USING BIOLUMINESCENT ORGANISM Patent
Arthur V. Stiffey, inventor (to Navy) 21 Aug. 1990 5 p Filed 21 Dec. 1987
(AD-D014651; US-Patent-4,950,594; US-Patent-Appl-SN-135969; US-Patent-Class-435-32) Avail: US Patent and Trademark Office CSCL 06/1

A microbiological assay based on bioluminescence employing the bioluminescent dinoflagellate Pyrocystis lunula was discussed. An oil well drilling fluid sample is prepared according to E.P.A. procedures to obtain a suspended particulate phase sample. An aliquot of the sample is added to a growth medium containing Pyrocystis lunula in suspension. The mixture is agitated to subject th Pyrocystis lunula to a shear stress. Light emitted as a result of the shear stress on the Pyrocystis lunula is measure and compared with a control to determine if there is diminution of light produced by the Pyrocystis lunula in the mixture. Diminution of light production is an indication of the presence of a toxic substance in the sample. GRA

N91-19250# Massachusetts Inst. of Tech., Cambridge.
CONTROL OF CATALYTIC HYDROTREATING SELECTIVITY WITH AMMONIA
C. N. Satterfield and Chung M. Lee 1990 13 p
(Contract DE-FG22-89PC-89775)
(DE91-005511; DOE/PC-89775/2) Avail: NTIS HC/MF A03

Research continued on catalytic hydrotreating selectivity with ammonia. In the last quarterly results were presented of the hydrodenitrogenation (HDN) of 8-OH quinoline 8-hydroxyquinoline (8HQ) and showed that three routes are involved beyond those encountered in the HDN of quinoline. A new kinetic model was developed for this reaction, which is adapted from Satterfield and Smith (1986) as applied to quinoline. Some basic assumptions of the model include: (1) the Langmuir-Hinshelwood kinetic model with all sites occupied is applicable; (2) the dehydrogenation rates of 5,6,7,8-tetrahydroquinoline (BzTHQ) and decahydroquinoline (DHQ) to quinoline (Q) and 1,2,3,4-tetrahydroquinoline (PyTHQ) are small enough to be neglected; and (3) the clean hydrocarbon products are not appreciably adsorbed. DOE

N91-19251# Union Carbide Corp., South Charleston, WV. Chemical and Plastics.
DIRECT CONVERSION OF METHANE TO C2'S
B. K. Warren, K. D. Campbell, J. L. Matherne, and G. L. Culp 1 Feb. 1990 197 p
(Contract DE-AC22-87PC-79817)
(DE91-005730; DOE/PC-79817/5) Avail: NTIS HC/MF A09

Exploration of alkaline earth/metal oxide catalysts and other metal/metal oxide catalysts continued. Alkaline earth carbonate/metal oxide catalysts exhibit longer periods of stable performance at higher methane conversions than similar alkaline earth chloride catalysts under comparable conditions. Higher ethylene to ethane ratios results from alkaline earth carbonate on titanium oxide or gallium oxide than from those on alumina. The effect of different levels of ethyl chloride was examined for the carbonate catalysts. Catalyst systems were found which are comparable in selectivity, activity, and C2 yield to the better literature catalysts, but which exhibit higher ethylene to ethane ratios and longer catalyst lifetimes than have been previously reported. Work was continued this quarter on bifunctional catalysts (Pd/SrCl2/alpha-alumina). Layered perovskites were further studied. Sequential methane coupling studies were initiated with the double perovskite, LaCaMnCoO6. The results of the economic evaluation of a hypothetical methane coupling process indicate

that a commercial-scale unit could produce ethylene at a variable cost of $0.0588 per pound. An economic evaluation of the Comparison Case (methane yields synthesis gas yields methanol yields olefins yields fuels) has been completed. Existing technology for the conversion of methane to liquid fuels is not competitive with the current oil based route in the present pricing environment. The impact of methane cost on the required sales cost of gasoline and distillate for the Comparison Case and the Hypothetical Case were reviewed. DOE

N91-19252# Argonne National Lab., IL.
TWO-DIMENSIONAL NON-REACTING JET-GAS MIXING IN AN MHD (MAGNETOHYDRODYNAMIC) SECOND STAGE COMBUSTOR
S. L. Chang, S. A. Lottes, and G. F. Berry 1990 10 p Presented at the 28th Symposium on Engineering Aspects of Magnetohydrodynamics, Chicago, IL, 26-28 Jun. 1990
(Contract W-31-109-eng-38)
(DE91-006015; CONF-9006105-13) Avail: NTIS HC/MF A02

Computer simulation is used to aid in the design of a magnetohydrodynamic (MHD) second stage combustor. A two-dimensional steady state computer model, based on mass and momentum conservation laws for multiple gas species, is used to simulate the hydrodynamics of the combustor in which a jet of oxidizer is injected into a confined cross-stream gas flow. The model predicts jet-gas mixing patterns by computing the velocity and species concentration distributions in the combustor. The effects of parametric variation of jet angle and flow symmetry on the mixing patterns were evaluated. The modeling helps to determine better mixing patterns for the combustor design because improved mixing can increase combustion efficiency and enhance MHD generator performance. A parametric study reveals the following: (1) non-reacting jet-gas mixing strongly depends on jet angle for coflow injection (jet angle less than 90 degrees); (2) counterflow jets have better jet-gas mixing; (3) asymmetry of the inlet gas flow affects the mixing pattern; and (4) exit flow characteristics from two-dimensional simulation can be matched reasonably well with experimental data when experimental jet and simulated slot jet Reynolds numbers are of the same order. DOE

N91-19253# Argonne National Lab., IL.
REMOTE DETECTION OF ORGANICS USING FOURIER TRANSFORM INFRARED SPECTROSCOPY
J. C. Demirgian and S. M. Spurgash 1990 11 p Presented at the 2nd International Symposium on Field Screening Methods for Hazardous Wastes and Toxic Chemicals, Las Vegas, NV, 12-14 Feb. 1990
(Contract W-31-109-eng-38)
(DE91-006045; CONF-9002156-2) Avail: NTIS HC/MF A03

Fourier transform infrared (FTIR) spectroscopy is an ideal technique for remote detection of organic emissions. There is an atmospheric window in the 1200 to 800/cm region, which corresponds to the 'fingerprint' region for organic molecules. Virtually all organic molecules have a unique absorption/emission pattern in the fingerprint region. A remote-passive FTIR relies on ambient emission of infrared energy from organics to obtain spectra. The instrumentation consists of inlet optics, and interferometer, a mercury cadmium telluride (MCT) detector, and an on-board computer. The transportable unit measures 40 cm by 50 cm and has been used to collect data while mounted on a helicopter or ground vehicle. Through the use of this FTIR combined with least squares software, it is possible to analyze qualitatively and quantitatively for organic vapors from either the air or ground. The data presented will include quantitative releases of common organics present in incinerator stacks, hazardous wastes, and illegal laboratories. Data will be presented for pure compounds, mixtures, and target analytes in the presence of interfering compounds. The sensitivity, reproducibility, and the potential of the technique will be discussed. DOE

N91-19254# Lawrence Livermore National Lab., CA.
FINNIGAN ION TRAP MASS SPECTROMETER DETECTION LIMITS AND THERMAL ENERGY ANALYZER INTERFACE STATUS REPORT AND PRESENT CAPABILITIES
A. Alcaraz, B. Andresen, and W. R. Martin 18 Oct. 1990 12 p
(Contract W-7405-eng-48)
(DE91-006220; UCRL-ID-105197) Avail: NTIS HC/MF A03

A new Finnigan ion trap mass spectrometer was purchased and installed at LLNL. Over a period of several months the instrument was tested under a variety of conditions utilizing a capillary gas chromatography interface which allowed separated organic compounds to be carried directly into the ion source of the mass spectrometer. This direct interface allowed maximum analytical sensitivity. A variety of critical tests were performed in order to optimize the sensitivity of the system under a variety of analysis conditions. These tests altered the critical time cycles of the ionization, ion trapping, and detection. Various carrier gas pressures were also employed in order to ascertain the overall sensitivity of the instrument. In addition, a thermal energy analyzer (TEA) was also interfaced to the gas chromatograph in order to simultaneously detect volatile nitrogen containing compounds while mass spectral data is being acquired. This is the first application at this laboratory of simultaneous ultra-trace detections while utilizing two orthogonal analytical techniques. In particular, explosive-related compound and/or residues are of interest to the general community in water, soil and gas sampler. A few examples are highlighted of the analytical power of this new GC-TEA-ITMS technology. DOE

N91-19255# Oak Ridge National Lab., TN.
THEORY OF BULK AND INTERFACE CONSTANT PHASE ELEMENTS IN ELECTRODE-ELECTROLYTE SYSTEMS
S. H. Liu Jan. 1991 36 p Presented at the ICTP Working Party on Electrochemistry (Condensed Matter, Atomic and Molecular Aspects), Trieste, Italy, 17 Aug. - 7 Sep. 1990
(Contract DE-AC05-84OR-21400)
(DE91-007181; CONF-9008186-1) Avail: NTIS HC/MF A03

This paper summarizes the progress gained in the last few years in our understanding of bulk and interface constant-phase-angle (CPA) behavior in electrode-electrolyte systems. It is now fairly well established that the interface constant-phase element originates from the fractal nature of the interface. The complex geometry gives rise to a fractal distribution of parallel current paths, and the competition between these paths results in the fractional power law behavior of the impedance across the interface. On the other hand, the early hope of relating the CPA exponent to the fractal dimension of the interface has been shown to be unattainable. Our understanding of the bulk CPA behavior, which is most prevalent in solid electrolytes, is only tentative. It is illustrated using a simple model that, under nonlinear dynamical laws that govern the flow of ions in the electrolyte, a current in the solid can generate a fractal distribution of vacancies which tend to impede the flow. The current is forced to negotiate a complex path through the solid, and the resulting fluctuation in path length and flow rate could be a source of the CPA behavior. DOE

N91-19256*# National Aeronautics and Space Administration. Lewis Research Center, Cleveland, OH.
REACTIVITY OF PI-COMPLEXES OF Ti, V, AND Nb TOWARDS DITHIOACETIC ACID: SYNTHESIS AND STRUCTURE OF NOVEL METAL SULFUR-CONTAINING COMPLEXES
Stan A. Duraj, Maria T. Andras (Cleveland State Univ., OH.), and Aloysius F. Hepp 1990 6 p Presented at the Fall Meeting of the Materials Research Society, Boston, MA, 26 Nov. - 1 Dec. 1990
(NASA-TM-103666; E-5873; NAS 1.15:103666) Avail: NTIS HC/MF A02 CSCL 07D

In order to use sulfur-containing resources economically and with minimal environmental damage, it is important to understand the desulfurization processes. Hydrodesulfurization, for example, is carried out on the surface of a heterogeneous metal sulfide catalyst. Studies of simple, soluble inorganic systems provide

information regarding the structure and reactivity of sulfur-containing compounds with metal complexes. Further, consistent with recent trends in materials chemistry, many model compounds warrant further study as catalyst precursors. The reactivity of low-valent organometallic sandwich pi-complexes toward dithiocarboxylic acids is described. For example, treatment of bisbenzene vanadium with CH3CSSH affords a divanadium tetrakis(dithioacetate) complex. The crystallographically determined V-V bond distance, 2.800(2), is nearly the same as the V-V bond distance in a V(mu-nu squared-S2)2V' unit in the mineral patonite (VS4)n. The stability of the V2S4 core in the dimer is demonstrated by evidence of V2S4(+) in the mass spectrum (70 eV, solid probe) of the vanadium dimer. Several other systems relevant to HDS catalysis are also discussed. Author

N91-19257# Los Alamos National Lab., NM.
METHANE TO METHANOL CONVERSION BY DIRECT PARTIAL OXIDATION
W. C. Danen, M. J. Ferris, J. L. Lyman, R. C. Oldenborg, C. K. Rofer, and G. E. Streit 1991 10 p Presented at the 201st American Chemical Society National Meeting, Atlanta, 14-19 Apr. 1991
(Contract W-7405-eng-36)
(DE91-007352; LA-UR-91-19; CONF-910402-4) Avail: NTIS HC/MF A02

The objective of this research is to understand the fundamental chemistry necessary to develop a process to effect the partial oxidation of methane to methanol using air or oxygen. The essence of the project is to control the direct, uncatalyzed, partial oxidation of methane to produce useful yields of methanol. It is crucial that complete oxidation to the thermodynamically stable products, carbon dioxide and water, be avoided. The detailed chemistry of the reactive intermediates and of the possible reaction pathways under various conditions must be understood in order to specify the reaction parameters necessary to obtain high yields of methanol. We have developed a comprehensive kinetic working model with predictive capabilities and have demonstrated scientific proof-of-principle by achieving high selectivity for methanol formation for methane-rich CH4/O2 mixtures. The immediate goal is to confirm the kinetic model predictions of high methane conversion with high methanol selectivity for single-pass conditions. DOE

N91-19258# Oak Ridge National Lab., TN.
SCREENING VOLATILE ORGANICS BY DIRECT SAMPLING ION TRAP AND GLOW DISCHARGE MASS SPECTROMETRY
M. B. Wise, G. B. Hurst, C. V. Thompson, M. V. Buchanan, and M. R. Guerin 1991 25 p Presented at the 2nd International Symposium on Field Screening Methods for Hazardous Wastes and Toxic Chemicals, Las Vegas, 12-14 Feb. 1991
(Contract DE-AC05-84OR-21400)
(DE91-007708; CONF-910278-1) Avail: NTIS HC/MF A03

Two different types of direct sampling mass spectrometers are currently being evaluated in the laboratory for use as rapid screening tools for volatile organics in a wide range of environmental matrices. These include a commercially available ITMS ion trap mass spectrometer and a specially designed tandem source glow discharge quadrupole mass spectrometer. Both of these instruments are equipped with versatile sampling interfaces which enable direct monitoring of volatile organics at part-per-billion (ppb) levels in air, water, and soil samples. Direct sampling mass spectrometry does not utilize chromatographic or other separation steps prior to admission of samples into the analyzer. Instead, individual compounds are measured using one or more of the following methods: spectral subtraction, selective chemical ionization, and tandem mass spectroscopy (MS/MS). For air monitoring applications, an active sniffer probe is used to achieve instantaneous response. Water and soil samples are analyzed by means of high speed direct purge into the mass spectrometer. Both instruments provide a range of ionization options for added selectivity and the ITMS can also provide high efficiency collision induced dissociation MS/MS for target compound analysis. Detection limits and response factors have been determined for a large number volatile organics in air, water, and number of different soil types. DOE

N91-19259# Catholic Univ. of America, Washington, DC. Dept. of Chemistry.
STUDIES OF COMBUSTION KINETICS AND MECHANISMS
D. Gutman Jan. 1991 16 p
(Contract DE-FG05-89ER-14015)
(DE91-007829; DOE/ER-14015/2) Avail: NTIS HC/MF A03

The objective of the current research is to gain new quantitative knowledge of the kinetics and mechanisms of elementary reactions of polyatomic free radicals which are important in hydrocarbon combustion processes. A special facility, consisting of a heatable tubular reactor coupled to a photoionization mass spectrometer, is being used to isolate different classes of reactions involving these reactive intermediates for these quantitative investigations. Five studies have been completed at CUA during this period and two others are in progress. Important initial results have also been obtained in new studies currently underway. These investigations are all discussed here in this progress report. The reprint of the published paper and three preprints of completed studies are included as appendices. The investigations completed or in progress include studies of three classes of free radical reactions: R + O reactions (C3H3) + O, C3H5 + O), R + M (neo-C5H11 + M, i-C3H7 + M, C2H5 + M, and and CH3CO + M), and R + O2 (n-C4H5 + O2). Our investigations are the first to isolate these elementary reaction for quantitative study. DOE

N91-19260# Johns Hopkins Univ., Baltimore, MD. Dept. of Chemical Engineering.
ULTRAFINE REFRACTORY PARTICLE FORMATION IN COUNTERFLOW DIFFUSION FLAMES
J. L. Katz and Cheng-Hung Hung Sep. 1990 32 p Presented at the American Institute of Chemical Engineers Fall Annual Meeting, Chicago, 11-16 Nov. 1990
(Contract DE-FG02-88ER-45356)
(DE91-007693; CONF-901155-6) Avail: NTIS HC/MF A03

The effect of process variables (precursor concentration, residence time, temperature, and electric field) on ceramic powder formation was studied using a counterflow diffusion flame burner. GeCl4 and SiCl4 were used as source materials for the formation of GeO2 and SiO2 in H2/Ar-O2/Ar flames. In-situ particle size and number density were determined using dynamic light scattering and 90 degree light scattering. A thermopheric sampling method also was used to collect particles directly onto carbon coated grids, and their size and morphology examined using a transmission electron microscopy. Increasing the precursor concentration caused larger particles to form and enhanced surface growth effects; decreasing residence time favored homogeneous nucleation as the particle formation route; using higher temperatures resulted in larger primary particle size but less aggregation. Using GeCl4 in the presence of a 1250 V/cm electric field, a three fold increase in particle size was obtained. Process variables also can affect particle phase; crystalline particles were usually found when mostly small particles were produced; amorphous particles were found when high precursor concentration, long residence time, and low temperatures were used. These results show how desired particle characteristics (particle size, particle morphology, and particle phase) can be generated through control of flame conditions. DOE

N91-19261# Northwestern Univ., Evanston, IL.
CHEMICAL INTERACTIONS IN MULTIMETAL/ZEOLITE CATALYSTS
W. M. H. Sachtler 1991 8 p
(Contract DE-FG02-87ER-13654)
(DE91-007978; DOE/ER-13654/7) Avail: NTIS HC/MF A02

In this report four subject areas will be focused that appear to reveal a novel type of chemistry with potentially strong impact on heterogeneous catalysis even beyond the field of zeolite supported systems. (1) PtCu/NaY and Pd/Cu/NaY catalysts. Previously we had shown that bimetal particles are formed in

supercages of NaY. With increasing Cu/Pt ratio at given Pt loading of the zeolite the rate of ring opening of methylcyclopentane decreases, but the rate of ring enlargement to benzene and cyclohexane increases. This concept has now been confirmed by studying the nature of the carbonaceous deposit which is formed during use as catalyst. Results show that with increasing Cu content the former peak decreases but the latter peak increases. A second group of results shows that the reduction of Cu(2+) ions in this zeolite is reversible. (2) PdNi/NaY catalysts. The presence of palladium has been found to strongly enhance the reducibility of nickel in NaY. Pretreatment conditions have a pronounced effect on the temperature programmed reduction profiles of monometallic and bimetallic palladium/nickel catalysts. (3) Electron deficiency of Pd(n)-proton adducts. Studies of the rate of isotope exchange between gaseous and zeolite-attached hydrogen shows that the H atoms, in close interaction with a metal particle, are rapidly exchanged at low temperature, where zeolite attached protons would not exchange in the absence of a transition metal. (4) Syngas conversion catalysis. We have tested our Pd/NaY and Pd/HY samples for the conversion of synthesis gas at elevated pressure and temperatures in the range of 200 to 300 C. Methane, methanol, dimethyl ether and higher hydrocarbons (up to C8H16) are the major reaction products. The formation of methane decreases with time on stream; we have indications that this change in selectivity is due to the increasing size of the Pd particles. DOE

N91-19262# Princeton Univ., NJ. Dept. of Mechanical and Aerospace Engineering.
COMPREHENSIVE MECHANISMS FOR COMBUSTION CHEMISTRY: AN EXPERIMENTAL AND NUMERICAL STUDY WITH EMPHASIS ON APPLIED SENSITIVITY ANALYSIS
F. L. Dryer and R. A. Yetter Feb. 1991 25 p
(Contract DE-FG02-86ER-13503)
(DE91-008030; DOE/ER-13503/4) Avail: NTIS HC/MF A03

This program is an integrated effort to determine the reaction mechanisms responsible for the oxidation of small molecule hydrocarbon structures under conditions representative of combustion environments. The experimental aspects of the work are conducted in an atmospheric pressure flow reactor (APFR) as well as in a new variable pressure flow reactor (VPFR) facility which extends the ranges of parameters available in the APFR, particularly the pressure, (1 to 15 atm), the temperature (600 to 1200 K), and the observation time (10 to 20,000 milli-seconds). Analytical techniques used for detecting hydrocarbons and carbon oxides presently include gas chromatography, gas chromatography/mass spectrometry, and non-dispersive infrared analyses. In addition, experiments also utilize Fourier Transform Infrared spectrometry, for continuous on-line sample detection of light hydrocarbons, carbon oxides, and oxygenated species. Modeling aspects emphasize the use of hierarchical mechanistic construction along with path and elemental gradient sensitivity analyses in developing detailed kinetic mechanisms. Issues of particular interest include: the CO/H2/O2 system and its perturbation (to obtain elementary kinetic data) by small amounts of an added hydrocarbon or hydrocarbon oxygenate; the pyrolysis and oxidation mechanisms of simple aldehydes; the pyrolysis and oxidation mechanisms of simple alcohols; and the pyrolysis and oxidation mechanisms of simple olefins. This report discusses the decomposition of trioxane, pyrolysis and oxidation of formaldehyde, and the oxidation of methanol and ethanol. DOE

N91-19263# Lehigh Univ., Bethlehem, PA.
MECHANISMS AND CONTROLLING CHARACTERISTICS OF THE CATALYTIC OXIDATION OF METHANE
K. Klier, G. W. Simmons, R. G. Herman, and A. C. Miller Dec. 1990 11 p
(Contract DE-FG02-86ER-13580)
(DE91-008033; DOE/ER-13580/1) Avail: NTIS HC/MF A03

The objective of the proposed research is to develop new ways to control the catalytic and selective oxidation of methane to oxygenates other than CO2 under mild reaction conditions by using halogen-free surface species that are stable under reaction conditions and that control the size of palladium ensembles available chemisorption of methane and oxygen. This will ensure the absence of Cl-containing products in the product and will result in surface modifiers; e.g., palladium alloy moieties, that are more stable at higher temperatures than are CCl2- and Cl-produced site blocking agents. The model catalysts being utilized are initially single crystals of planar Pd(100), stepped Pd(311), and stepped and kinked Pd(679), which will also provide for the structure sensitivity of the selective oxidation of CH4 to be probed. DOE

N91-19264# Michigan Univ., Ann Arbor.
BASIC RESEARCH MODEL OF NATURAL GAS COMBUSTION IN TURBULENT FLOW Final Report, 1 Jun. 1988 - 30 Jun. 1990
W. J. A. Dahm, G. Tryggvason, and R. Krasny 9 Nov. 1990 94 p
(Contract GRI-5088-260-1692)
(PB91-130260; GRI-90/0262) Avail: NTIS HC/MF A05 CSCL 21B

The model will be a computational tool to aid in the development of low NOx flames for the next generation of natural gas burning applications. Development of the next generation of natural gas burning equipment for industry and utilities will need to rely more than ever before on detailed computational modeling of the complex physical processes at work in turbulent flames in order to meet the stringent requirements for low NOx emission levels being placed on them. The model is based on Lagrangian tracking of dynamical elements in a turbulent reacting flow to approximately solve the time-varying equations of fluid motion and chemical reaction. GRA

N91-19265# Air Force Inst. of Tech., Wright-Patterson AFB, OH. School of Engineering.
FLUORESCENT LIFETIME MEASUREMENTS OF RARE EARTH ELEMENTS IN GALLIUM ARSENIDE M.S. Thesis
Danny J. Topp Dec. 1990 48 p
(AD-A229865; AFIT/GEP/ENP/90D-9) Avail: NTIS HC/MF A03 CSCL 09/1

Lifetime measurements of the excited states of three GaAs semiconductors doped with the rare earth elements Erbium (ER), Praseodymium (Pr), and Thulium (Tm) has been studied using a pulsed nitrogen laser and germanium detector. The measurements were made with an experimental set up with a system response time of 0.34 microseconds. A 330 milliwatt nitrogen laser with a wavelength of 3370 angstroms was used to excite transitions of the rare earth elements. GRA

N91-19147*# Martin Marietta Aerospace, Denver, CO.
ADVANCES IN ATOMIC OXYGEN SIMULATION
Joseph F. Froechtenigt and Lyle E. Bareiss *In* NASA, Goddard Space Flight Center, 16th Space Simulation Conference Confirming Spaceworthiness Into the Next Millennium Nov. 1990 p 259-265 (For primary document see N91-19126 11-18)
Avail: NTIS HC/MF A20 CSCL 07D

N91-20032*# Puerto Rico Univ., Mayaguez. Coll. of Engineering.
LOW LEVEL VAPOR VERIFICATION OF MONOMETHYL HYDRAZINE
Narinder Mehta *In* NASA, John F. Kennedy Space Center, Research Reports: 1990 NASA/ASEE Summer Faculty Fellowship Program Sep. 1990 p 276-307 (For primary document see N91-20022 11-99)
(Grant NGT-60002)
Avail: NTIS HC/MF A23 CSCL 07D

26 METALLIC MATERIALS

Includes physical, chemical, and mechanical properties of metals, e.g., corrosion; and metallurgy.

N91-19266# Materials Research Labs., Ascot Vale (Australia).
MAGNETO-ELASTIC BEHAVIOUR OF STEELS FOR NAVAL

APPLICATIONS
I. M. Robertson 1990 27 p
(MRL-TR-90-27) Copyright Avail: NTIS HC/MF A03

The magneto-elastic behaviors of various steels used in naval construction are compared, with particular emphasis on submarine hull steels. Magnetic field strengths on the order of the Earth's field and stresses up to 200 MPa are examined. All the steels examined have similar qualitative behavior, but the quantitative behavior is quite different. Mild steel is easily magnetized; HSLA80 is more difficult; and HY80 and HY100 are more difficult again. The initial permeability of the steel is a good guide to the degree of magnetization caused by either stress or field cycling. Author

N91-19267# Missouri Univ., Columbia.
LATE TRANSITION METAL (mu)-OXO AND (mu)-IMIDO COMPLEXES Final Report, 15 May 1988 - 14 May 1991
Paul R. Sharp 1990 8 p
(Contract DE-FG02-88ER-13880)
(DE91-005349; DOE/ER-13880/3) Avail: NTIS HC/MF A02

The synthesis and reactions of late-transition-metal oxo and imido complexes was explored. The deprotonation of platinum(II) hydroxo complexes yielded new oxo complexes. Attempted deprotonation of Cp*Rh(III) hydroxo complexes did not give oxo complexes but complex mixtures probably resulting from reduction of the Rh(III) center. The reaction of Na/Hg with (Cp*RhCl2)2 gave the very reactive Rh(II) dimer, (Cp*RhCl)2. Rhodium(I) imido complexes with the bis (dimethyl phosphino) methane ligand were prepared and found to be similar to the previously prepared bis (diphenyl phosphino) methane complexes. Attempts to prepare bis (diphenyl phosphino) methylamine, bis (diphenyl phosphino) phenylamine, PMe(e) and NO(+) analogues were not successful. Attempts to prepare Cp*Rh(III) imido complexes resulted in amido complexes and reduction. Rhodium (III) tris (3,5-dimethyl pyrazoyl) borate analogues are reduction resistant but have not yet yielded imido complexes. The first imido complexes of Au were prepared by treating a Au oxo complex with amines or isocyanates. Dimeric Cp*Rh dioxygen and nitrosobenzene complexes were prepared by insertion into the Rh-Rh bond of (Cp*RhCl)2. The dioxygen complex activates a C-H bond of the Cp* ligand on treatment with PMe(3). Imido and oxo complexes nitrene and oxygen atom transfer product in reactions with CO. A novel electrophilic ring addition was observed with sterically protected aryl imido complexes. DOE

N91-19268# Lawrence Livermore National Lab., CA.
THEORETICAL INVESTIGATION OF PHASE STABILITY IN NON-MAGNETIC Fe-V SUBSTITUTIONAL ALLOYS
M. Sluiter and P. E. A. Turchi 18 Dec. 1990 7 p Presented at the Fall Meeting of the Materials Research Society, Boston, MA, 24 Nov. - 1 Dec. 1990
(Contract W-7405-eng-48)
(DE91-006711; UCRL-JC-104593; CONF-901105-84) Avail: NTIS HC/MF A02

The assessed phase diagram of Fe-V exhibits a continuous high temperature bcc solid solution intersected at lower temperatures by a complex sigma phase centered around equiatomic composition. Slow kinetics of the bcc to sigma transformation make it possible to retain the bcc solid solution at low temperature. It has been observed that this metastable solid solution has a tendency to order with a CsCl type structure (B2) below 970 K. As a first attempt to describe this behavior from an electronic structure approach, this paper will study the phase stability on the bcc lattice using a realistic tight-binding Hamiltonian. Main features are as follows: Element and structure specific Slater-Koster parameters are used and lattice parameter effects are incorporated through scaling. Charge transfer is set to zero by rigidly shifting the onsite energies of one constituent. The Coherent Potential Approximation (CPA) is invoked with four levels corresponding to states with s, p, t(sub 2g) and e(sub g) like symmetry. Effects of off-diagonal disorder (ODD) have not been included, instead, an average alloy Hamiltonian was defined using the Slater-Koster parameters of the components weighted by concentration. At equiatomic composition the effect of this approximation has been evaluated by repeating the electronic structure calculation with inclusion of ODD effects. Effective pair interactions, as defined within the Generalized Perturbation Method (GPM), have been computed and have been used to evaluate the ground states of configurational order on the bcc lattice in the Fe-V system. Furthermore, the theoretically derived energetic properties have been used to determine the phase diagram pertaining to the (metastable) bcc lattice with the Cluster Variation Method (CVM) in the tetrahedron approximation. DOE

N91-19269# Sandia National Labs., Albuquerque, NM.
STRESS CORROSION CRACKING OF Al-Li-Cu-Zr ALLOY 2090 IN AQUEOUS Cl(-) AND MIXED CO3(2-)/Cl(-) ENVIRONMENTS
R. G. Buchheit, F. D. Wall, G. E. Stoner (Virginia Univ., Charlottesville.), and J. P. Moran 1991 19 p Presented at the NACE Corrosion '91 Symposium, Cincinnati, OH, 11-15 Mar. 1991
(Contract DE-AC04-76DP-00789)
(DE91-007064; SAND-90-2548C; CONF-910328-2) Avail: NTIS HC/MF A03

A comparison of the short-transverse SCC behavior of 2090 in pH 5.5 Cl(-) and alkaline CO3(2-)/Cl(-) solutions using a static load smooth bar SCC (Stress Corrosion Cracking) technique was made. In the alkaline CO3(2-)/Cl(-) solutions, E(sub br) for the alpha-Al matrix phase was 0.130 V more positive than the E(sub br) of the subgrain boundary T(sub 1) phase. In this environment, stress corrosion cracking test specimens subjected to potentials in the window defined by the two breakaway potentials failed along an intersubgranular path in less than an hour. In the Cl(-) environment, the E(sub br) values for the two phases were nearly equal and this rapid SCC condition could not be satisfied; accordingly SCC failures were not observed. Rapid SCC failure of 2090 in CO3(2-)/Cl(-) in our static load, constant immersion experiments appear to be related to recently reported pre-exposure embrittlement failures induced by immersing stressed specimens removed into ambient laboratory air after immersion in aerated NaCl solution for 7 days. In those experiments, specimens failed in less than 24 hours after removal from solution. Our polarization experiments have shown that the corrosion behavior of T(sub 1), CO3(2-)/Cl(-) environments, but the alpha-Al phase crack walls, is rapidly passivated. X-ray diffraction of the films which formed in simulated crevices suggests that this passivating film belongs to a class of compounds known as hydrotalcites. DOE

N91-19270# Oak Ridge National Lab., TN.
EFFECTS OF IRRADIATION ON CRACK-ARREST TOUGHNESS OF TWO HIGH-COPPER WELDS
S. K. Iskander, W. R. Corwin, and R. K. Nanstad 1990 44 p Presented at the 15th International Symposium on Effects of Radiation on Materials, Nashville, TN, 17-22 Jun. 1990
(Contract DE-AC05-84OR-21400)
(DE91-007189; CONF-900623-25) Avail: NTIS HC/MF A03

The objective of this study is to determine the effect of neutron irradiation on the shift and shape of the lower-bound curve to crack-arrest data. Two submerged-arc welds with copper contents of 0.23 and 0.31 wt percent were commercially fabricated in 220-mm-thick plate. Crack-arrest specimens fabricated from these welds were irradiated at a nominal temperature of 288 C to an average fluence of 1.9 times 10(exp 19) neutrons/sq cm (greater than 1 MeV). A preliminary evaluation of the results shows that the neutron-irradiation induced crack-arrest toughness temperature shift is about the same as the Charpy V-notch impact temperature shift at the 41-J energy level. The shape of the lower-bound curves, (for the range of test temperatures covered), compared to those of the ASME K(sub Ia)-curve did not seem to have been altered by irradiation. DOE

N91-19271# Pacific Northwest Lab., Richland, WA.
RADIATION-INDUCED CHANGES IN ELECTRICAL CONDUCTIVITY OF A WIDE RANGE OF COPPER ALLOYS
F. A. Garner, K. R. Anderson, and T. Shikama (Tohoku Univ., Sendai, Japan) Jan. 1991 8 p

(Contract DE-AC06-76RL-01830)
(DE91-007200; PNL-SA-19062) Avail: NTIS HC/MF A02

A wide variety of radiation-induced changes in electrical conductivity was observed in a series of irradiation experiments conducted on copper alloys in the Fast Flux Test Facility (FFTF). The behavior of each alloy was found to depend on the alloy composition, starting state, irradiation temperature, and the sometimes complex interaction of three radiation-driven processes. These processes are transmutation, void swelling, and solute redistribution. The objective of this effort is to identify those copper alloys that offer promise as high heat flux materials for fusion application. DOE

N91-19272# Ames Lab., IA.
INTERNAL FRICTION PEAKS DUE TO INTERSTITIALS IN bcc ALLOYS
O. Buck, O. N. Carlson, H. Indrawirawan, L. J. H. Brasche, and D. T. Peterson 1991 35 p Presented at the ASTM Symposium on Mechanics and Mechanisms of Material Damping, Baltimore, MD, 13-15 Mar. 1991
(Contract W-7405-eng-82)
(DE91-007411; IS-M-662; CONF-910374-1) Avail: NTIS HC/MF A03

Richter's and Snoek's original works established the existence of an anelastic relaxation produced by a stress-induced interstitial reorientation in bcc metals. This anelastic relaxation, now referred to as a Snoek peak, has been studied extensively and well characterized in the past for the interstitials carbon, nitrogen, and oxygen. However, the existence of a hydrogen Snoek peak in bcc metals has been a matter of some controversy. We have studied relaxation peaks in V, Nb, and V-Nb alloys recently. The alloys have complete mutual solubility and are of interest since they have an extremely high room temperature solid solubility for hydrogen. They also have, over a certain composition range, not shown any hydride phase precipitation at temperatures as low as 4K. Thus, if a hydrogen Snoek peak does exist, it should be found in such alloys. Indeed there is evidence now of a spectrum of hydrogen relaxation peaks below room temperature. Furthermore, there is a large misfit of V in Nb and Nb in V and, possibly, some chemical interaction such that trapping (or antitrapping) of the interstitials at the substitutional sites, causing solute-interstitial peaks, can be characterized. The present paper provides an overview of our observations regarding: the effect of hydrogen on the oxygen and nitrogen Snoek peaks in pure V and Nb; the oxygen relaxation peaks in V-Nb alloys; the hydrogen relaxation spectrum in V-Nb alloys; and the effect of oxygen on the hydrogen relaxation spectrum in V-Nb alloys. DOE

N91-19273*# National Aeronautics and Space Administration. Lyndon B. Johnson Space Center, Houston, TX.
BEHAVIOR OF SURFACE AND CORNER CRACKS SUBJECTED TO TENSILE AND BENDING LOADS IN Ti-6Al-4V ALLOY
Royce G. Forman and Sambi R. Mettu (Lockheed Engineering and Sciences Co., Houston, TX.) Sep. 1990 64 p
(NASA-TM-102165; S-611; NAS 1.15:102165) Avail: NTIS HC/MF A04 CSCL 11F

The behavior of part-through flaws with regard to failure under monotonic loading and their growth under fatigue loading was studied experimentally and analytically. Comparisons are made of experimental values of toughness obtained using surface and corner cracked specimens with those obtained using standard test specimens, and also experimental growth cycles were compared with numerical predictions using the NASA/FLAGRO computer program. Tests were conducted on various types of surface and corner cracks under tensile and bending loads. Room temperature lab air provided the test environment. The material used in this study was the Ti-6Al-4V alloy in the solution treated and aged (STA) and stress relieved condition. Detailed tabulation of the fracture toughness data and results of life prediction using the NASA/FLAGRO program are presented. Fatigue crack growth rates for the part-through cracked specimens are compared with a base curve fitted from the data obtained using standard specimens. The fatigue loading used in the crack growth testing was constant-amplitude sinusoidal type. Author

N91-19274*# National Aeronautics and Space Administration. Lyndon B. Johnson Space Center, Houston, TX.
AN EVALUATION OF THE FATIGUE CRACK GROWTH AND FRACTURE TOUGHNESS PROPERTIES OF BERYLLIUM-COPPER ALLOY CDA172
Royce G. Forman and Julie A. Henkener (Lockheed Engineering and Sciences Co., Houston, TX.) Sep. 1990 48 p
(NASA-TM-102166; S-612; NAS 1.15:102166) Avail: NTIS HC/MF A03 CSCL 11F

A series of fracture mechanics tests, using the Be-Cu alloy CDA172 in the round rod product form, was conducted in a lab air environment at room temperature. Tensile data is presented in both the L and C directions and K sub Ic data in both the C-R and C-L orientations. Fracture toughness values were derived from M(T) (center cracked), PS(T) (surface cracked) and CC01 (corner cracked) specimens of varying thickness. Fatigue crack growth data were obtained for the C-R orientation at stress ratio of 0.1, 0.4, and 0.7 and for the C-L orientation at stress ratios of 0.1, 0.3, 0.4, and 0.7. Author

N91-19275# Arizona Univ., Tucson. Dept. of Chemistry.
CHEMICAL ACTIVATION OF MOLECULES BY METALS: EXPERIMENTAL STUDIES OF ELECTRON DISTRIBUTIONS AND BONDING
D. L. Lichienberger Oct. 1990 17 p
(Contract DE-FG02-86ER-13501)
(DE91-007695; DOE/ER-13501/2) Avail: NTIS HC/MF A03

Experimental methods of photoelectron spectroscopy and the fundamental relationships between ionization energies and the chemistry of transition metal species were studied. Progress continues on the new gas phase photoelectron spectrometer that combine improved capabilities for HeI/HeII UPS, XPS, and Auger investigations of organometallic molecules. Several measurements were accomplished that were not possible previously. The formal relationship was published between measured molecular ionization energies and thermodynamic bond dissociation energies, and applied the relationships to homonuclear and heteronuclear diatomic molecules, multiple bonds, and metal-ligand bonds. Studies of C-H bond activation have continued with examination of different degrees of Si-H bond addition to metals. The electronic effects of intermolecular interactions have been observed by comparing the ionizations of metal complexes in the gas phase with the ionizations of monolayer solid organometallic films prepared in ultrahigh vacuum. The orientations of the molecules were determined by scanning tunneling microscopy. Especially interesting was the recent application of these techniques to the characterization of the soccer-ball shaped C(sub 60) molecule, buckminsterfullerene. Studies of the following complexes are described: Fe, Os, Nb, Mo, Rh, Re, Al, and Mn. DOE

N91-19276# Sandia National Labs., Albuquerque, NM.
APPLICATION OF NON-CYANIDE GOLD FOR SELECTIVE PLATING OF MICROELECTRONIC CIRCUITS
W. Worobey and D. Rieger 1991 5 p Presented at the Environmentally Conscious Manufacturing/Technology Applications Workshop, Albuquerque, 20 Feb. 1991
(Contract DE-AC04-76DP-00789)
(DE91-007729; SAND-91-0342C; CONF-910279-1) Avail: NTIS HC/MF A01

With the current trends towards miniaturization, high performance, high quality and cost competiveness, the electrodeposition process has become an important manufacturing technology in many new microelectronic applications. Gold electrodeposition plays an increasing role in processes that require this noble metal. Added to these trends is the continuing and increasing emphasis on manufacturing processes which are less damaging to the environment and potentially less hazardous to the operator and personnel in the vicinity of the operation. The present standard gold plating solutions are based on cyanide salts

and are considered acutely hazardous solutions. The trend away from their use is gaining momentum as new non-hazardous gold plating solutions and manufacturing processes making use of them are developed. DOE

N91-19277# Westinghouse Savannah River Co., Aiken, SC.
EFFECTS OF RADIOLYTIC TRITIUM DECAY ON THE THERMODYNAMIC BEHAVIOR OF LaNi(4.25)Al(0.75) TRITIDES
A. Nobile, Jr., R. T. Walters, and W. C. Mosley 31 May 1990 17 p Presented at the International Symposium on Metal-Hydrogen Systems, Banff, Alberta, 2-7 Sep. 1990
(Contract DE-AC09-89SR-18035)
(DE91-007961; WSRC-MS-90-16; CONF-9009141-12) Avail: NTIS HC/MF A03

Intermetallic compounds which react with hydrogen isotopes to form reversible hydrides offer several advantages for storing and processing tritium. Advantages include safe low pressure high density storage, and delivery of high purity He-3-free tritium without the use of pumps. As part of a program to develop metal hydride technology for storing and processing tritium, the effects of tritium aging on the thermodynamic behavior of the tritides are under investigation. During aging of LaNi(4.25)Al(0.75) tritides, the He-3 decay product of tritium produced in the lattice does not leave the lattice but causes changes in the thermodynamics of the gas-solid system. Among the changes noted are (1) decreased tritium desorption pressures, (2) increased slopes of desorption isotherm plateaus, and (3) small quantities of irreversibly-held tritium. Absorption/desorption cycling and brief heating of samples to 350 C while loaded with deuterium partially reverses these effects. While the desorption isotherms of tritium-aged LaNi(4.25)Al(0.75) tritides resemble the desorption isotherms of amorphous hydrogen storage materials, x ray diffraction patterns of tritium-aged samples after desorption of tritium do not exhibit the characteristics of an amorphous material. The diffraction patterns show broadening and anisotropic effects that suggest the presence of lattice strains and orientational effects of He-3 in the LaNi(4.25)Al(0.75) lattice. DOE

N91-19278# Brookhaven National Lab., Upton, NY.
X RAY ABSORPTION SPECTROSCOPY OF OXIDE FILMS ON METALS
H. S. Isaacs and A. J. Davenport 1990 12 p Presented at the 178th Meeting of the Electrochemical Society (ECS), Seattle, 14-19 Oct. 1990
(Contract DE-AC02-76CH-00016)
(DE91-008100; BNL-45672; CONF-901073-14) Avail: NTIS HC/MF A03

The properties of the passivating oxide layer present on metals in aqueous environments determine the corrosion resistance of the metal or its alloys. Corrosion is rapid prior to oxide formation or following its breakdown. In order to improve the corrosion resistance afforded by the oxide the subtleties of the interactions of its chemistry, electrochemistry, structure, and physical properties must be understood. With the availability of broad band high intensity x-rays from synchronous light sources, many of these properties can now be studied in greater detail. A particular advantage in the use of x-ray absorption spectroscopy (XAS) is the ability to carry out surface studies directly in the environment where the oxide is formed and interacts with its environment. DOE

N91-19279# Brookhaven National Lab., Upton, NY.
SPATIAL AND TEMPORAL RELATIONSHIPS BETWEEN LOCALIZED MICROBIAL METABOLIC ACTIVITY AND ELECTROCHEMICAL ACTIVITY OF STEEL
M. J. Franklin, J. B. Guckert (Tennessee Univ., Knoxville.), and D. C. White 1991 14 p Presented at the NACE Corrosion 1991 Symposium, Cincinnati, 11-15 Mar. 1991
(Contracts DE-AC02-76CH-00016; DE-AC05-84OR-21400)
(DE91-008102; BNL-45651; CONF-910328-3) Avail: NTIS HC/MF A03

The relationship between the localized microbial activity and localized electrochemical on corroding steel surfaces was investigated. The scanning vibrating electrode technique provided a sensitive means for defining local anodic and cathodic currents associated with corrosion. Localized bacterial metabolic activity was determined using autoradiography of bacterial incorporated C-14-acetate into insoluble cell material. Microautoradiography of individual bacteria, with the incorporated acetate, was used to determine percentages and morphological types of active bacteria. The results showed a correlation between the location of anodic activity of the steel and the location of incorporated label. Although the results do not necessarily indicate a role for bacterial activity in the initiation of pitting, the results suggest that the actively metabolizing bacteria may exacerbate the propagation of pits by colonizing active anodic sites. DOE

N91-19280# Brookhaven National Lab., Upton, NY.
A STUDY OF CARBON STEEL CORROSION INHIBITION BY PHOSPHATE IONS AND BY AN ORGANIC BUFFER USING A SCANNING VIBRATING ELECTRODE
M. J. Franklin, D. C. White (Tennessee Univ., Knoxville.), and H. S. Isaacs 1990 24 p Presented at the International Congress on Microbially Influenced Corrosion, Knoxville, 7-12 Oct. 1990
(Contracts DE-AC02-76CH-00016; DE-AC05-84OR-21400)
(DE91-008103; BNL-45676; CONF-9010138-1) Avail: NTIS HC/MF A03

The scanning vibrating reference electrode technique (SVET) has been used to map anodic and cathodic currents in solutions over freely corroding type C1020 carbon steel. All solutions contained millimolar concentrations of chloride, and were sterilized. The effect of phosphate and an organic buffer on the corrosion of carbon steel in liquid media were studied because they were added to promote bacterial growth. Phosphate acted as an anodic inhibitor in the media, causing initiated pits to repassivate. However, if initiated pits did not repassivate, for example in stagnant medium or when crevice corrosion initiated adjacent to the sample coating, the corrosion rates increased and the corrosion remained localized. Increased anodic current resulted in a drop in the open circuit potential and a decrease in the polarization resistance. The results show that phosphate can lead to lower average corrosion rates, than uninhibited steel, but as an anodic inhibitor can also lead to rapid penetration at localized sites. DOE

N91-19281# EG and G Mound Applied Technologies, Miamisburg, OH.
HOT ISOSTATIC PRESSING OF HIGH PERFORMANCE GLASS-CERAMIC TO NICKEL- AND IRON-BASED METAL COMPONENTS
D. P. Kramer, W. E. Modderman, and M. D. Kelly 1991 27 p Presented at the 15th Annual Conference on Composites and Advanced Ceramics, Cocoa Beach, 13-16 Jan. 1991
(Contract DE-AC04-88DP-43495)
(DE91-008130; CONF-910162-3) Avail: NTIS HC/MF A03

The fabrication of glass-ceramic to metal components has classically been a two-dimensional process based on the control of time and temperature to yield high quality components. The implementation of hot isostatic pressing (HIP) to the manufacturing of glass-ceramic to metal seals adds a third dimension (i.e., pressure) to the process. HIP processing of a multi-constituent, lithia-alumina-silica glass at high pressures, up to 207 MPa (30,000 psi), was shown to control the crystalline phases that form in the glass-ceramic. In addition, the high pressure processing of components fabricated with the glass-ceramic and several high tensile strength alloys, Inconel 718, Hastelloy C-276, Inconel 625, and Nitronic 40 was found to yield superior pore-free iterfacial seals with improved hermeticity. DOE

N91-19282# Pacific Northwest Lab., Richland, WA.
THE 70 PERCENT TUNGSTEN HEAVY ALLOYS: PROCESSING AND PROPERTIES
W. E. Gurwell Feb. 1991 11 p Presented at the Annual Meeting and Exhibition of the Minerals, Metals and Materials Society, New Orleans, LA, 17-21 Feb. 1991
(Contract DE-AC06-76RL-01830)

(DE91-008259; PNL-SA-19071; CONF-910202-3) Avail: NTIS HC/MF A03

High ductility, 70 percent tungsten heavy alloys were produced by solid state sintering followed by vacuum annealing. Unlike the traditional 90 to 97 percent tungsten alloys that must be liquid-phase resintered, the 70 percent alloy may be mechanically worked and solid state annealed back to the best as-sintered ductilities. Compared to 5 micron tungsten powder, finger, 1 micron tungsten powder yielded higher green strength and sinterability but tended to produce somewhat lower as-sintered ductilities. As-sintered tensile strengths, 80 ksi yield and 140 ksi ultimate, are generally similar to those obtained from liquid phase sintered alloys containing 90 to 95 percent tungsten. Occasional as-sintered defects that markedly reduced elongation were eliminated by mechanical working and annealing. Annealed (1400 C for 3 h) tensile properties of rolled sheet were slightly higher than the best as-sintered properties and more consistent; also there was no dependence on rolling direction or prior tungsten powder size. Cold rolling 50 percent followed by strain aging produced tensile strengths near 210 ksi yield and 223 ksi ultimate with elongation of 4 percent (transverse direction) to 7 percent (longitudinal direction). DOE

N91-19283# Oak Ridge National Lab., TN.
CHARACTERIZATION OF ION-IMPLANTED ALUMINUM AND IRON BY SPECTROSCOPIC ELLIPSOMETRY
J. S. Brodkin, W. Franzen, R. J. Culbertson, and J. M. Williams 1990 6 p Presented at the Fall Meeting of the Materials Research Society, Boston, MA, 24 Nov. - 1 Dec. 1990
(Contract DE-AC05-84OR-21400)
(DE91-008371; CONF-901105-96) Avail: NTIS HC/MF A02

The change in the optical constants of aluminum alloy and iron samples caused by implantation with nitrogen and chromium ions was investigated by spectroscopic ellipsometry. The objective is to develop a method for simple, non-destructive characterization of ion-implanted metals. DOE

N91-19284# Japan Atomic Energy Research Inst., Tokyo.
HIGH TEMPERATURE TENSILE PROPERTIES OF NICKEL-BASE SUPERALLOYS FOR INTERMEDIATE HEAT EXCHANGERS OF HIGH TEMPERATURE GAS-COOLED REACTORS
Yuji Kurata and Hajime Nakajima Sep. 1990 45 p In JAPANESE; ENGLISH summary
(DE91-744958; JAERI-M-90-157) Avail: NTIS HC/MF A03

High temperature tensile properties were investigated in the ranges 600 to 1000 C and 5 x 10(exp -5) to 1.25 x 10 (exp -3)/sec using SSS113M(Ni-23Cr-18W) and KSN(Ni-15Cr-25W) both of which were developed as superalloys for intermediate heat exchangers of high temperature gas-cooled reactors. From the results of the experiments made to study dependence of temperature and of strain rate on high temperature tensile properties, the following conclusions are drawn: (1) Usual stress-strain curves which exhibited significant work hardening after reaching proof stress were obtained below 800 C. However, stress-strain curves which were considered to be caused by dynamic recrystallization began to be observed at the low strain rate above 850 C. Such stress-strain curves with peaks and steady-state deformation were obtained at 1000 C and all strain rates examined. (2) the 0.2 percent proof stress was constant or increased a little up to 800 or 850 C with increasing temperature. It decreased above 850 C with increasing temperature and with decreasing strain rate. Tensile strength decreased in the range 600 to 1000 C with increasing temperature and with decreasing strain rate. (3) Elongation and reduction of area for SSS113M had the minimum between 700 and 800 C, and those for KSN between 800 and 900 C. Ductility of KSN was low above 800 C compared with that of SSS113M. (4) Stress-strain curves at 950 and 1000 C exhibited steady state deformation following single peak or multiple peaks. The relation was formulated among steady-state deformation stress, strain rate and temperature. (5) Fine recrystallized grains were observed in specimens which displayed stress-strain curves with peaks and steady-state deformation. DOE

N91-19285# Technische Univ., Delft (Netherlands). Powder Metallurgy Group.
GAS ENTRAPMENT AND EVOLUTION IN ALUMINIUM ALLOYS PRODUCED BY POWDER METALLURGY Ph.D. Thesis
Jose Luis EstradaHaen 1990 211 p Sponsored by Stichting voor Fundamenteel Onderzoek der Materie; National Polytechnic Inst., Mexico; and Netherlands Program for Innovative Research
(ETN-91-98918) Avail: NTIS HC/MF A10

Part of a comprehensive research program involving different aspects of degassing of powder metallurgy (PM) aluminum alloys is presented. Some fundamentals concerning gas entrapment and evolution such as the relationship between surface composition and chemical reactions are presented. A fundamental semiquantitive description of the degassing process based on thermodynamical and kinetic considerations is given. The consolidation processing of the Al-Si-X PM aluminum alloys is shown to require a degassing step which improves room and elevated temperature properties of the final product. The conventional degassing process was improved by the development of a vacuum degassing process in combination with a flushing procedure using argon or nitrogen; degassing of Al-20Si-X is shown to give products with superior properties. The research concerned rapidly solidified Al-20Si-X aluminum, compressed in vaccum tight containers (cans) with temperatures of the PM compact during evacuation and flushing chosen up to 550 C. ESA

N91-19286# Technische Univ., Eindhoven (Netherlands).
ALKALI METAL CORROSION OF ALUMINA: THERMODYNAMICS, PHASE DIAGRAMS AND TESTING Ph.D. Thesis
Johannes Adrianus Ma vanHoek 1990 149 p
(ETN-91-98933) Avail: NTIS HC/MF A07

Three applications of the use of alumina (Al2O3) in combination with an alkali metal are discussed. Thermodynamical aspects of possible corrosion reactions are given and the compatibility of alumina with the alkali metals at all temperatures are predicted. Phase diagrams, which are essential for understanding the corrosion behavior of alumina are investigated. Study results on phase relations in the CaO-Cs2O-Al2O3 system are described. A method to determine the composition of a hitherto unknown quasiternary compound present in this system is developed and used to find and characterize this compound. Investigations of CaO-K2O-Al2O3 found that the phase relations were not clear at first but the problems in this system were solved by a rigorous thermodynamic evaluation. Together with experimental results, a consistent phase diagram is proposed, a part of which including the K-beta-alumina compound and calcium hexa aluminate is of special interest. A metastabe calcium aluminate with the beta-alumina structure was found and a phase diagram representing metastable equilibria is given. The influence of MgO is examined by investigation of the MgO-Cs2O-Al2O3 and MgO-K2O-Al2O3 systems. To verify the theoretical predictions, the potassium resistance of alumina is examined. ESA

N91-19287# Naval Oceanographic and Atmospheric Research Lab., Bay Saint Louis, MS.
MICROBIOLOGICALLY INFLUENCED CORROSION IN COPPER AND NICKEL SEAWATER PIPING SYSTEMS
Brenda J. Little, Patricia A. Wagner, Joanne M. Jones, and Michael B. McNeil 1990 19 p Presented at the 1st Annual Naval Corrosion Control Workshop, Key West, FL, 29-31 Oct. 1990
(AD-A229874; NOARL-PR-90-055-333) Avail: NTIS HC/MF A03 CSCL 11/6

Sections of CDA 706 piping and Monel 400 tubing were severely pitted after exposure to marine and estuarine waters, respectively. Surfaces of both alloys were uniformly covered with thick surface deposits, ranging in color form blue-green to reddish brown to black. Pits developed under surface deposits containing 0.0001 - 0.00001 sulfate-reducing bacteria (SRB) in association with other bacteria. Pits were irregular in shape, lacking a consistent

morphology. The observed corrosion was attributed to a combination of differential aeration cells, a large cathode::small anode surface area, concentration of chlorides, development of acidity within the pits, and the specific reactions of the base metals with sulfides produced by the SRB. Chlorine and sulfur appear to have reacted selectively with iron and nickel in the alloys. Nickel has been selectivity removed from pitted areas leaving a copper rich spongy pit interior. GRA

N91-20025*# Randolph-Macon Coll., Ashland, VA. Dept. of Chemistry.
ELECTROCHEMICAL IMPEDANCE SPECTROSCOPY OF METAL ALLOYS IN THE SPACE TRANSPORTATION SYSTEM LAUNCH ENVIRONMENT
Luz Calle *In* NASA, John F. Kennedy Space Center, Research Reports: 1990 NASA/ASEE Summer Faculty Fellowship Program Sep. 1990 p 65-114 (For primary document see N91-20022 11-99)
(Grant NGT-60002)
Avail: NTIS HC/MF A23 CSCL 11F

27 NONMETALLIC MATERIALS

Includes physical, chemical, and mechanical properties of plastics, elastomers, lubricants, polymers, textiles, adhesives, and ceramic materials.

For composite materials see *24 Composite Materials.*

N91-19288# Department of the Navy, Washington, DC.
METHOD OF PRODUCING GLASS FIBER WITH CORES OF A DIFFERENT MATERIAL Patent Application
Jack Ayers, inventor (to Navy) 31 Jul. 1990 27 p
(AD-D014664; US-Patent-Appl-SN-560703) Avail: NTIS HC/MF A03 CSCL 11/2

A process is provided for forming a glass fiber having one or more metal filaments in its core. In the process, a metal rod or particles of a metal or semiconducting material optionally mixed with glass powder is introduced into a hollow glass tube closed at one end, and the tube is evacuated while the closed end is heated and a fiber drawn therefrom. The resultant glass fiber contains one or more discrete filaments of the metal or semiconducting material. GRA

N91-19289# Department of the Navy, Washington, DC.
HETEROGENEOUS MAGNETORESISTANT LAYER Patent Application
Alan S. Edelstein, inventor (to Navy) 13 Aug. 1990 20 p
(AD-D014665; US-Patent-Appl-SN-565781) Avail: NTIS HC/MF A03 CSCL 20/3

A magnetoresistant material is comprised of discrete units of magnetostrictive material separated from one another by one or more gaps. In one class of embodiments, magnetostrictive particles are embedded in a phase-separated nonmagnetostrictive matrix. In one embodiment, a magnetoresistant article is made by cosputtering particles of a magnetostrictive material and a quantity of a nonmagnetostrictive material onto an nonmagnetostrictive substrate. The magnetostrictive particles are spaced from one another by distances in the range of 10 to 100 angstroms. In another embodiment, a magnetostrictive substrate. Magnetic field sensors employing such articles are also provided. GRA

N91-19290# Pacific Northwest Lab., Richland, WA.
RADIOLUMINESCENT POLYMER LIGHTS
G. A. Jensen, D. A. Nelson, and P. M. Molton Sep. 1990 5 p Presented at the Technology Transfer Conference: Radioluminescent Lighting Technology, Annapolis, MD, 25-26 Sep. 1990
(Contract DE-AC06-76RL-01830)
(DE91-005521; PNL-SA-18612; CONF-9009201-11) Avail: NTIS HC/MF A01

The preparation of radioluminescent light sources where the tritium is located on the aryl-ring in a polymer was demonstrated with deuterium/tritium substitution. Tests, results, and future applications of radioluminescent polymers are discussed. DOE

N91-19291# Sandia National Labs., Albuquerque, NM.
THE MECHANICAL BEHAVIOR OF MICROCELLULAR FOAMS
M. H. Ozkul, J. E. Mark (Cincinnati Univ., OH.), and J. H. Aubert 1990 7 p Presented at the Fall Meeting of the Materials Research Society, Boston, MA, 24 Nov. - 1 Dec. 1990
(Contract DE-AC04-76DP-00789)
(DE91-006775; SAND-91-0125C; CONF-901105-85) Avail: NTIS HC/MF A02

The mechanical behavior of microcellular open-cell foams prepared by a thermally induced phase separation process are investigated. The foams studied were prepared from isotactic polystyrene, polyacrylonitrile, and poly(4-methyl-1-pentene) (rigid foams), and polyurethane and Lycra (elastomeric foams). Their densities were in the range 0.04 to 0.27 g/cm3. Conventional polystyrene foams were used for comparison. The moduli and collapse stresses of these foams were measured in compression and compared with the current constitutive laws which relate mechanical properties to densities. A reinforcement technique based on the in situ precipitation of silica was used to improve the mechanical properties. DOE

N91-19292*# National Aeronautics and Space Administration. Lewis Research Center, Cleveland, OH.
STRUCTURAL RELIABILITY ANALYSIS OF LAMINATED CMC COMPONENTS
Stephen F. Duffy, Joseph L. Palko (Cleveland State Univ., OH.), and John P. Gyekenyesi 1991 10 p Proposed for presentation at the 36th International Gas Turbine and Aeroengine Congress and Exposition, Orlando, FL, 3-6 Jun. 1991; sponsored by ASME
(NASA-TM-103685; E-5903; NAS 1.15:103685) Avail: NTIS HC/MF A02 CSCL 11C

For laminated ceramic matrix composite (CMC) materials to realize their full potential in aerospace applications, design methods and protocols are a necessity. The time independent failure response of these materials is focussed on and a reliability analysis is presented associated with the initiation of matrix cracking. A public domain computer algorithm is highlighted that was coupled with the laminate analysis of a finite element code and which serves as a design aid to analyze structural components made from laminated CMC materials. Issues relevant to the effect of the size of the component are discussed, and a parameter estimation procedure is presented. The estimation procedure allows three parameters to be calculated from a failure population that has an underlying Weibull distribution. Author

N91-19293*# National Aeronautics and Space Administration. Lewis Research Center, Cleveland, OH.
COMPARISON OF DYNAMIC FATIGUE BEHAVIOR BETWEEN SiC WHISKER-REINFORCED COMPOSITE AND MONOLITHIC SILICON NITRIDES
Sung R. Choi (Cleveland State Univ., OH.) and Jonathan A. Salem Feb. 1991 22 p
(NASA-TM-103707; E-5932; NAS 1.15:103707) Avail: NTIS HC/MF A03 CSCL 11C

The dynamic fatigue behavior of 30 vol percent silicon nitride whisker-reinforced composite and monolithic silicon nitrides were determined as a function of temperature from 1100 to 1300 C in ambient air. The fatigue susceptibility parameter, n, decreased from 88.1 to 20.1 for the composite material, and from 50.8 to 40.4 for the monolithic, with increasing temperature from 1100 to 1300 C. A transition in the dynamic fatigue curve occurred for the composite material at a low stressing rate of 2 MPa/min at 1300 C, resulting in a very low value of n equals 5.8. Fractographic analysis showed that glassy phases in the slow crack growth region were more pronounced in the composite compared to the monolithic material, implying that SiC whisker addition promotes the formation of glass rich phases at the grain boundaries, thereby enhancing fatigue. These results indicate that SiC whisker addition to Si3 N4 matrix

substantially deteriorates fatigue resistance inherent to the matrix base material for this selected material system. Author

N91-19294*# National Aeronautics and Space Administration. Lewis Research Center, Cleveland, OH.
LOW EARTH ORBITAL ATOMIC OXYGEN AND ULTRAVIOLET RADIATION EFFECTS ON POLYMERS
Joyce A. Dever Feb. 1991 15 p
(NASA-TM-103711; E-5943; NAS 1.15:103711) Avail: NTIS HC/MF A03 CSCL 11C

Because atomic oxygen and solar ultraviolet radiation present in the low earth orbital (LEO) environment can alter the chemistry of polymers resulting in degradation, their effects and mechanisms of degradation must be determined in order to determine the long term durability of polymeric surfaces to be exposed on missions such as Space Station Freedom. The effects of atomic oxygen on polymers which contain protective coatings must also be explored, since unique damage mechanisms can occur in areas where the protective coatings has failed. Mechanisms can be determined by utilizing results from previous LEO missions, by performing ground based LEO simulation tests and analysis, and by carrying out focussed space experiments. A survey is presented of the interactions and possible damage mechanisms for environmental atomic oxygen and UV radiation exposure of polymers commonly used in LEO. Author

N91-19295*# National Aeronautics and Space Administration. Lewis Research Center, Cleveland, OH.
THERMAL SHOCK OF FIBER REINFORCED CERAMIC MATRIX COMPOSITES
Andrew J. Eckel, John P. Gyekenyesi (Cleveland State Univ., OH.), Thomas P. Herbell, and Edward R. Generazio 1991 13 p Presented at the 15th Annual Conference on Composites and Advanced Ceramics, Cocoa Beach, FL, 13-16 Jan. 1991; sponsored by American Ceramic Society
(NASA-TM-103777; E-6006; NAS 1.15:103777) Avail: NTIS HC/MF A03 CSCL 11C

Monolithic silicon carbide and silicon nitride and a Nicalon fiber reinforced silicon carbide composite were subjected to severe thermal shock conditions via impingement of a hydrogen-oxygen flame. Surface heating rates of 1000 C/sec to 2500 C/sec were generated. The performance of the monolithic reference materials are compared and contrasted to the significantly greater thermal shock resistance of the composite. Ultrasonic and radiographic NDE techniques were used to evaluate the integrity of the composite subsequent to thermal shock. Tensile tests were performed to determine the residual tensile strength and modulus. Physical property changes are discussed as a function of number and severity of thermal shock cycles. Author

N91-19296*# National Aeronautics and Space Administration. Lewis Research Center, Cleveland, OH.
SYNTHESIS AND STRUCTURES OF METAL CHALCOGENIDE PRECURSORS
Aloysius F. Hepp, Stan A. Duraj, William E. Eckles, and Maria T. Andras (Cleveland State Univ., OH.) 1990 6 p Presented at the Fall Meeting of the Materials Research Society, Boston, MA, 26 Nov. - 1 Dec. 1990 Sponsored in part by Petroleum Research Fund
(Contract NCC3-162)
(NASA-TM-103665; E-5872; NAS 1.15:103665) Avail: NTIS HC/MF A02 CSCL 11C

The reactivity of early transition metal sandwich complexes with sulfur-rich molecules such as dithiocarboxylic acids was studied. Researchers recently initiated work on precursors to CuInSe2 and related chalcopyrite semiconductors. Th every high radiation tolerance and the high absorption coefficient of CuInSe2 makes this material extremely attractive for lightweight space solar cells. Their general approach in early transition metal chemistry, the reaction of low-valent metal complexes or metal powders with sulfur and selenium rich compounds, was extended to the synthesis of chalcopyrite precursors. Here, the researchers describe synthesis, structures, and and routes to single molecule precursors to metal chalcogenides. Author

N91-19297# Sandia National Labs., Albuquerque, NM.
PHENOMENA AFFECTING MORPHOLOGY OF MICROPOROUS POLY(ACRYLONITRILE) PREPARED VIA PHASE SEPARATION FROM SOLUTION
R. R. Legasse, R. J. Weagley, P. K. Leslie, and D. A. Schneider 1990 11 p Presented at the 201st American Chemical Society National Meeting, Atlanta, GA, 14-19 Apr. 1991
(Contract DE-AC04-76DP-00789)
(DE91-004501; SAND-90-2929C; CONF-910402-1) Avail: NTIS HC/MF A03

This paper is concerned with controlling the morphology of microporous polymers prepared via thermal demixing of solutions. Two wt percent solutions of poly(acrylonitrile) in maleic anhydride, a poor solvent, are first cooled to produce separated polymer-rich and solvent-rich phases. Removing the solvent by freeze drying then produces a microporous material having a density of 33 mg/cc, a void fraction of 97 percent and a pore size of about 10 microns. We find that the morphology cannot be explained by existing models, which focus on phase diagrams and kinetics of phase transformations during cooling of the solution. In conflict with those models, we find that two radically different morphologies can be produced even when the polymer concentration and cooling path are held strictly constant. A hypothesis that polymer degradation causes the different morphologies is not supported by GPC, C-13 NMR, and FTIR experiments. Instead, we offer evidence that the different microporous morphologies are caused by different polymer conformations in solutions having the same concentration and temperature. DOE

N91-19298# MSE, Inc., Butte, MT.
CERAMIC FABRICATION R AND D
1990 56 p
(Contract DE-AC07-88ID-12735)
(DE91-006537; DOE/ID-12735/T13) Avail: NTIS HC/MF A04

This project is separated into three tasks. The first task is a design and modeling effort to be carried out by MSE, Inc. The purpose of this task is to develop and analyze designs for various cohesive ceramic fabrication (CCF) components. This quarter, the advanced molybdenum disicilide MHD electrode design was essentially completed. Final refinements will be made after molybdenum disilicide processing results are available and the final layer compositions are established. Work involving whisker incorporation was initiated on the high stress component. It is unlikely that whiskers will become low cost, so particulate reinforcement will be pursued. Modeling work will resume once a suitable aluminum oxide/silicon carbide composition is selected that can be fired to acceptable densities by pressureless sintering. Task 2, subcontracted to Applied Technology Laboratories (ATL), is principally directed at establishing a property data base for monolithic and laminated alumina fabricated using the CCF process. This quarter, ATL demonstrated that the CCF process does not compromise the flexure strength of alumina. Task 3, subcontracted to Ceramics Binder Systems, Inc., focused on CCF silicon carbide particulate reinforced alumina and on the development of processing procedures for nonoxide molybdenum disilicide. Preliminary results indicate that achieving high densities in silicon carbide particulate reinforced aluminum oxide will be difficult. Molybdenum disilicide results are encouraging, and it is clear that the CCF process will work with this nonoxide material. DOE

N91-19299# Argonne National Lab., IL.
EFFECTS OF ATMOSPHERE AND HEATING RATE DURING PROCESSING OF A CERAMIC SUPERCONDUCTOR
U. Balachandran, D. Xu, C. Zhang, S. E. Dorris, R. A. Russell, J. T. Dusek, J. J. Picciolo, R. B. Poeppel, Y. Gao, and K. L. Merkle Jan. 1991 31 p Presented at the High-Temperature Superconductors: Processing and Microstructure Property Relationships, New Orleans, LA, 17-21 Feb. 1991
(Contract W-31-109-eng-38)
(DE91-007761; CONF-910212-1) Avail: NTIS HC/MF A03

Properties of ceramic superconductors depend strongly on the temperature, heating rate, pressure, and atmosphere used during synthesis and fabrication. We have developed a process for synthesizing orthorhombic YBa2Cu3O(x) (123) superconducting powders by calcining the precursor powders under reduced total oxygen pressure. The resultant 123 powders are mixed with organics, and wires and coils are fabricated by extrusion. The wires and coils are fired at a reduced total pressure in flowing O2 to reduce the concentrations of CO2, CO, and H2O and thus prevent decomposition of the 123. Transport critical current density of the superconductor decreases drastically with increasing concentrations of CO2 in the gas mixture. Transmission electron microscopy of materials sintered in O2 atmospheres containing various levels of CO2 clearly shows the extent of grain boundary degradation. DOE

N91-19300# Oak Ridge National Lab., TN.
CERAMIC TECHNOLOGY FOR ADVANCED HEAT ENGINES PROJECT DATABASE Summary Report, Sep. 1989
B. L. P. Keyes Oct. 1990 90 p
(Contract DE-AC05-84OR-21400)
(DE91-007772; ORNL/M-1286) Avail: NTIS HC/MF A05

This is the fourth in a series of semiannual data summary reports on information stored in the Ceramic Technology for Advanced Heat Engines (CTAHE) database. The information in this document covers alumina-based ceramics presently stored in the database and summarizes changes and upgrades to the overall system since creation of the third semiannual data summary report in March 1989. DOE

N91-19301# Argonne National Lab., IL.
ASSESSMENT OF TAMPER-REVEALING CERAMIC SEALS
D. S. Kupperman, S. E. Dorris, S. H. Sheen, R. G. Palm, J. T. Dusek, and A. C. Raptis Sep. 1990 25 p
(Contract W-31-109-eng-38)
(DE91-007793; ANL/ACTV-90/5) Avail: NTIS HC/MF A03

The objective of the program described in this report is the development of a simple and rapidly authenticated tamper-revealing ceramic seal. This seal would resist state-of-the-art tampering, operate under severe conditions, and establish identity and integrity with one interrogation. The seal could be used, for example, on containers of various sizes, valves, or perimeter gates to establish whether tampering or entry has occurred. The feasibility of assembling a ceramic tamperproof seal with seeded defects has been established and a laboratory system for rapid ultrasonic scanning of ceramic components has been assembled. Seeded zirconia samples, two ceramic seals, and one ceramic-and-metal seal have been fabricated. The seeded zirconia samples have been ultrasonically scanned and the uniqueness of their ultrasonic fingerprints due to the presence of seeded defects has been demonstrated. Semper image-processing software has been used to correlate ultrasonic amplitude images. A linear correlation coefficient greater then 0.8 should be achievable for scans of the same seal. Shrink fitting of the connecting and binding parts has also been demonstrated to be feasible and essentially irreversible. Tests have demonstrated that a scheme for coupling ultrasonic waves to the seal can be carried out using commercially available ultrasonic gel pads. Breaking and repair of the stainless steel part of the more flexible ceramic-and-metal seal can be revealed by ultrasonic shear waves reflected from a welded joint. All problems associated with fabrication and authentication have been addressed, and the preliminary conclusion is that the concept presents no major technical difficulties. DOE

N91-19302# Brookhaven National Lab., Upton, NY.
XANES INVESTIGATION OF pH EFFECTS DURING CERIUM-SEALING OF ANODIZED ALUMINUM
A. J. Davenport, H. S. Isaacs, and M. W. Kendig 1990 7 p
Presented at the 178th Meeting of the Electrochemical Society (ECS), Seattle, 14-19 Oct. 1990
(Contracts DE-AC02-76CH-00016; DE-FG05-89ER-45384)
(DE91-008101; BNL-45674; CONF-901073-15) Avail: NTIS HC/MF A02

Cerium ions are under investigation as possible replacements for toxic chromates. The use of cerium ions in sealing anodized films on aluminium and the effect of ph cerium chemistry has been investigated using XANES (X-ray Absorption Near Edge Structure). Cerium ions absorb readily on both aluminum hydroxide and anodized aluminium surfaces. The adsorption is greater at higher pH. At pH 10, 3-valent cerium can be oxidized to the 4-valent state by dissolved oxygen. Sealing of anodized films with cerium ions involves a pore-blocking mechanism similar to that of water sealing. DOE

N91-19303# Sandia National Labs., Albuquerque, NM.
POLYMER CHARACTERIZATION USING THE TIME-RESOLVED PHOSPHORESCENCE OF SINGLET OXYGEN AS A SPECTROSCOPIC PROBE
P. R. Ogilby, M. Kristiansen, M. P. Dillon (New Mexico Univ., Albuquerque.), V. L. Taylor, and R. L. Clough 1990 3 p
Presented at the American Chemical Society (ACS) National Meeting, Atlanta, GA, 14-19 Apr. 1991
(Contract DE-AC04-76DP-00789)
(DE91-001269; SAND-90-2646C; CONF-910473-1) Avail: NTIS HC/MF A01

The lowest excited electronic state of molecular oxygen, singlet oxygen (1 Delta g)O2, can be produced in solid organic polymers by a variety of different methods. Once produced, singlet oxygen will return to the ground triplet state by two pathways, radiative (phosphorescence) and non-radiative decay. Although the quantum efficiency of phosphorescence is small, approximately 10(exp -5), singlet oxygen can be detected by its emission at 1270 nm in both steady-state and time-resolved experiments. The phosphorescence of singlet oxygen can be used to characterize many properties of a solid organic polymer. DOE

N91-19304*# National Aeronautics and Space Administration. Ames Research Center, Moffett Field, CA.
COMPOSITE FLEXIBLE INSULATION FOR THERMAL PROTECTION OF SPACE VEHICLES
Demetrius A. Kourtides, Huy K. Tran, and S. Amanda Chiu (Sterling Software, Palo Alto, CA.) Feb. 1991 19 p Proposed for presentation at the 37th International SAMPE Symposium and Exhibition, Anaheim, CA, 9-12 Mar. 1992
(NASA-TM-103836; A-91062; NAS 1.15:103836) Avail: NTIS HC/MF A03 CSCL 11C

A composite flexible blanket insulation (CFBI) system considered for use as a thermal protection system for space vehicles is described. This flexible composite insulation system consists of an outer layer of silicon carbide fabric, followed by alumina mat insulation, and alternating layers of aluminized polyimide film and aluminoborosilicate scrim fabric. A potential application of this composite insulation would be as a thermal protection system for the aerobrake of the aeroassist space transfer vehicle (ASTV). It would also apply to other space vehicles subject to high convective and radiative heating during atmospheric entry. The thermal performance of this composite insulation as exposed to a simulated atmospheric entry environment in a plasma arc test facility is described. Other thermophysical properties which affect the thermal response of this composite insulation is included. It shows that this composite insulation is effective as a thermal protection system at total heating rates up to 30.6 W/sq cm. Author

N91-19305*# Michigan Univ., Ann Arbor. Radiation Lab.
[TASK REPORTS ON DEVELOPING TECHNIQUES FOR SCATTERING BY 3D COMPOSITE STRUCTURES AND TO GENERATE NEW SOLUTIONS IN DIFFRACTION THEORY USING HIGHER ORDER BOUNDARY CONDITIONS] Semiannual Report, Sep. 1990 - Feb. 1991
John L. Volakis Feb. 1991 48 p
(Grant NAG2-541)
(NASA-CR-188057; NAS 1.26:188057; UMICH-025921-19-T)
Avail: NTIS HC/MF A03 CSCL 11C

There are two tasks described in this report. First, an extension of a two dimensional formulation is presented for a three

dimensional body of revolution. A Fourier series expansion of the vector electric and magnetic fields is employed to reduce the dimensionality of the system, and an exact boundary condition is employed to terminate the mesh. The mesh termination boundary is chosen such that it leads to convolutional boundary operators for low O(n) memory demand. Second, rigorous uniform geometrical theory of diffraction (UTD) diffraction coefficients are presented for a coated convex cylinder simulated with generalized impedance boundary conditions. Ray solutions are obtained which remain valid in the transition region and reduce uniformly those in the deep lit and shadow regions. A uniform asymptotic solution is also presented for observations in the close vicinity of the cylinder. For individual titles, see N91-19306 through N91-19307.

N91-19306*# Michigan Univ., Ann Arbor. Radiation Lab.
A FINITE ELEMENT CONJUGATE GRADIENT FFT METHOD FOR SCATTERING **c32**
Jeffery D. Collins, Dan Ross, J.-M. Jin, A. Chatterjee, and John L. Volakis *In its* Task Reports on Developing Techniques for Scattering by 3D Composite Structures and to Generate New Solutions in Diffraction Theory Using Higher Order Boundary Conditions Feb. 1991 26 p (For primary document see N91-19305 11-27)
Avail: NTIS HC/MF A03 CSCL 11C

Validated results are presented for the new 3D body of revolution finite element boundary integral code. A Fourier series expansion of the vector electric and mangnetic fields is employed to reduce the dimensionality of the system, and the exact boundary condition is employed to terminate the finite element mesh. The mesh termination boundary is chosen such that is leads to convolutional boundary operatores of low O(n) memory demand. Improvements of this code are discussed along with the proposed formulation for a full 3D implementation of the finite element boundary integral method in conjunction with a conjugate gradiant fast Fourier transformation (CGFFT) solution. Author

N91-19307*# Michigan Univ., Ann Arbor. Radiation Lab.
ANALYTICAL SOLUTIONS WITH GENERALIZED IMPEDANCE BOUNDARY CONDITIONS (GIBC) **c32**
H. H. Syed and John L. Volakis *In its* Task Reports on Developing Techniques for Scattering by 3D Composite Structures and to Generate New Solutions in Diffraction Theory Using Higher Order Boundary Conditions Feb. 1991 18 p (For primary document see N91-19305 11-27)
Avail: NTIS HC/MF A03 CSCL 11C

Rigorous uniform geometrical theory of diffraction (UTD) diffraction coefficients are presented for a coated convex cylinder simulated with generalized impedance boundary conditions. In particular, ray solutions are obtained which remain valid in the transition region and reduce uniformly to those in the deep lit and shadow regions. These involve new transition functions in place of the usual Fock-type integrals, characteristics to the impedance cylinder. A uniform asymptotic solution is also presented for observations in the close vicinity of the cylinder. The diffraction coefficients for the convex cylinder are obtained via a generalization of the corresponding ones for the circular cylinder. Author

N91-19308*# National Aeronautics and Space Administration. Lewis Research Center, Cleveland, OH.
CRYSTALLIZATION AND PROPERTIES OF Sr-Ba ALUMINOSILICATE GLASS-CERAMIC MATRICES
Narottam P. Bansal, Mark J. Hyatt, and Charles H. Drummond, III (Ohio State Univ., Columbus.) 1991 24 p Presented at the 15th Annual Conference on Composites and Advanced Ceramics, Cocoa Beach, FL, 13-16 Jan. 1991; sponsored by American Ceramic Society
(NASA-TM-103764; E-6027; NAS 1.15:103764) Avail: NTIS HC/MF A03 CSCL 11C

Powders of roller quenched (Sr,Ba)O-Al2O3-2SiO2 glasses of various compositions were uniaxially pressed into bars and hot isostatically pressed at 1350 C for 4 hours or cold isostatically pressed and sintered at different temperatures between 800 to 1500 C for 10 or 20 hours. Densities, flexural strengths, and linear thermal expansion were measured for three compositions. The glasss transition and crystallization temperatures were determined by Differential Scanning Calorimetry (DSC). The liquidus and crystallization temperature from the melt were measured using high temperature Differential Thermal Analysis (DTA). Crystalline phases formed on heat treatment of the glasses were identified by powder x ray diffraction. In Sr containing glasses, the monoclinic celsian phase always crystallized at temperatures above 1000 C. At lower temperatures, the hexagonal analog formed. The temperature for orthorhombic to hexagonal structure transformation increased monotonically with SrO content, from 327 C for BaO-Al2O3-2SiO2 to 758 C for SrO-Al2O3-2SiO2. These glass powders can be sintered to almost full densities and monoclinic celsian phase at a relatively low temperature of 1100 C. Author

N91-19309# Texas Univ., Austin. Dept. of Chemical Engineering.
SYNTHESIS AND ANALYSIS OF NOVEL POLYMERS WITH POTENTIAL FOR PROVIDING BOTH HIGH PERMSELECTIVITY AND PERMEABILITY IN GAS SEPARATION APPLICATIONS
W. J. Koros and D. R. Paul Jan. 1991 8 p
(Contract DE-FG05-86ER-13507)
(DE91-008283; DOE/ER-13507/6) Avail: NTIS HC/MF A02

The following experimental, analytical and publication objectives were achieved consistent with the project goal to develop advanced materials for gas separation membrane applications. Synthesized and partially completed characterization of a group of additional polysulfone materials beyond those proposed in the renewal proposal to test ideas developed in the course of the work. Characterized on additional polycarbonate material, spirobiindane polycarbonate, in cooperation with General Electric Corp. who provided the material to test ideas developed in the course of the work. Synthesized and characterized are the first two members in the systematic family of polyesters described in the renewal proposal. Also, based on attractive results with the spirobiindane polycarbonate, two members of the polyester family were synthesized based on this monomer to demonstrate the desirable aspects of the simultaneous disruption of packing and suppression of molecular motion caused by the spirobiindane group. DOE

N91-19310# Oak Ridge National Lab., TN.
CONTROL OF TEXTURE AND DEFECT STRUCTURE FOR HOT-FILAMENT-ASSISTED CVD (CHEMICAL VAPOR DEPOSITION) DIAMOND FILMS
R. E. Clausing, L. Heatherly, and E. D. Specht 1990 8 p Presented at the NATO Advanced Study Institute on Diamond and Diamond-Like Films and Coatings, Castelvecchio Pascoli, Italy, 22 Jul. - 2 Aug. 1990
(Contract DE-AC05-84OR-21400)
(DE91-008373; CONF-900731-4) Avail: NTIS HC/MF A02

The morphology of diamond films grown by activated chemical vapor deposition, (CVD), varies greatly depending on the deposition conditions. Small changes in the deposition conditions can cause major changes in the film morphology and crystal perfection. Areas a few millimeters apart in a film may be quite different unless considerable care is taken to ensure uniform deposition conditions. Because the properties of diamond films are strongly dependent upon the crystallite size, orientation, and perfection, it is important to understand the way in which growth conditions affect the film structure in order to design and optimize films for specific applications. In this paper, we describe the development of textures and discuss how the nucleation and growth processes may operate to produce the textures and internal crystallite defect structure of the films described above. We show that the textures develop as the result of growth competition and suggest that the internal defect structure is the direct result of the details of growth on (111) or (100) facets. It is further shown that growth conditions can be controlled to manipulate the film texture and the internal crystallite defect structure. Using these concepts, a film with a (100) texture and only (111) facets was grown. DOE

N91-19311# Messerschmitt-Boelkow-Blohm G.m.b.H., Ottobrunn (Germany, F.R.). Central Lab.
APPLICATION OF FUNCTIONAL GRADIENT MATERIALS IN THE AEROSPACE INDUSTRY
Hannelore Benien, Meinhard Meyer, and Richard Suchentrunk 1990 5 p Presented at the 1st International Symposium on Functionality Gradient Materials, Tokyo, Japan, 8-9 Oct. 1990
(MBB-Z-0320-90-PUB; ETN-91-98837) Avail: NTIS HC/MF A01

Magnetron sputtering in combination with ion beam mixing or reactive sputtering is an advanced technique for the fabrication of functional gradient materials. The first results of recent research and development work in this field is described on two typical samples. The improvement of corrosion protection properties of copper containing aluminum alloys (2024) by a combination of sputter deposition and ion beam mixing is considered. By using this technique a gradient of corrosion inhibiting materials are applied on the surface near the region of the substrate. The increase of wear resistance of fiber reinforced plastics by hard carbon films is also considered. By depositing films with a defined metal content a controlled minimum electrical conductivity can be guaranteed on the surface. Furthermore this will make it possible to coat the surface, for example, by electrodeposition with tightly adherent metallic layers as lightning protection. The mechanism of protection schemes is discussed and the technique of combined deposition processes and characterization of deposited films by surface analysis are described. ESA

N91-19132*# Martin Marietta Aerospace, Denver, CO.
AN OUTGASSING MODEL OF NON-METALLIC MATERIALS FOR THE ASCENT OF A TITAN 4 LAUNCH VEHICLE Abstract Only
R. D. Barrows and S. L. VanLoon *In* NASA, Goddard Space Flight Center, 16th Space Simulation Conference Confirming Spaceworthiness Into the Next Millennium Nov. 1990 p 55 (For primary document see N91-19126 11-18)
Avail: NTIS HC/MF A20 CSCL 11C

N91-19136*# TRW Space Technology Labs., Redondo Beach, CA.
MULTIPURPOSE HARDENED SPACECRAFT INSULATION
Carlos H. Steimer *In* NASA, Goddard Space Flight Center, 16th Space Simulation Conference Confirming Spaceworthiness Into the Next Millennium Nov. 1990 p 84-110 (For primary document see N91-19126 11-18)
Avail: NTIS HC/MF A20 CSCL 11C

N91-19146*# Los Alamos National Lab., NM.
ATOMIC OXYGEN EFFECTS ON BORON NITRIDE AND SILICON NITRIDE: A COMPARISON OF GROUND BASED AND SPACE FLIGHT DATA
J. B. Cross, E. H. Lan, C. A. Smith, and W. J. Whatley (Sparta, Inc., San Diego, CA.) *In* NASA, Goddard Space Flight Center, 16th Space Simulation Conference Confirming Spaceworthiness Into the Next Millennium Nov. 1990 p 249-258 (For primary document see N91-19126 11-18)
Avail: NTIS HC/MF A20 CSCL 11C

N91-19148*# McDonnell-Douglas Space Systems Co., Huntington Beach, CA.
SPACE ENVIRONMENTAL EFFECTS ON SPACECRAFT THERMAL CONTROL COATINGS Abstract Only
L. G. Bartosik and H. W. Babel *In* NASA, Goddard Space Flight Center, 16th Space Simulation Conference Confirming Spaceworthiness Into the Next Millennium Nov. 1990 p 266 (For primary document see N91-19126 11-18)
Avail: NTIS HC/MF A20 CSCL 11C

N91-19149*# TRW Defense and Space Systems Group, Redondo Beach, CA.
SPACE SIMULATION TEST FOR THERMAL CONTROL MATERIALS
W. R. Hardgrove *In* NASA, Goddard Space Flight Center, 16th Space Simulation Conference Confirming Spaceworthiness Into the Next Millennium Nov. 1990 p 267-285 (For primary document see N91-19126 11-18)
Avail: NTIS HC/MF A20 CSCL 11C

N91-19153*# McDonnell-Douglas Space Systems Co., Huntington Beach, CA.
A UNIQUE APPROACH TO SPACE THERMAL SIMULATION Abstract Only
D. Q. Durant *In* NASA, Goddard Space Flight Center, 16th Space Simulation Conference Confirming Spaceworthiness Into the Next Millennium Nov. 1990 p 343 (For primary document see N91-19126 11-18)
Avail: NTIS HC/MF A20 CSCL 11C

N91-20034*# South Carolina Univ., Columbia. Dept. of Physics.
A FLAMMABILITY STUDY OF THIN PLASTIC FILM MATERIALS
S. Ballou Skinner *In* NASA, John F. Kennedy Space Center, Research Reports: 1990 NASA/ASEE Summer Faculty Fellowship Program Sep. 1990 p 339-379 (For primary document see N91-20022 11-99)
(Grant NGT-60002)
Avail: NTIS HC/MF A23 CSCL 11C

28 PROPELLANTS AND FUELS

Includes rocket propellants, igniters, and oxidizers; their storage and handling procedures; and aircraft fuels.

For related information see also *07 Aircraft Propulsion and Power, 20 Spacecraft Propulsion and Power,* and *44 Energy Production and Conversion.*

N91-19312 Department of the Navy, Washington, DC.
EXTRUDABLE PBX MOLDING POWDER Patent
Horace D. Stanton, inventor (to Navy) 28 Aug. 1990 8 p Filed 2 Apr. 1984
(AD-D014667; US-Patent-4,952,255; US-Patent-Appl-SN-596188; US-Patent-Class-149-19.91) Avail: US Patent and Trademark Office CSCL 19/1

This patent discloses an extrudable plastic bonded explosive molding power which contains about 20 percent by weight ethylenevinyl acetate copolymer and 80 percent by weight PETN. GRA

N91-19313# Union Carbide Corp., South Charleston, WV. Chemical and Plastics.
DIRECT CONVERSION OF METHANE TO C2'S AND LIQUID FUELS
B. K. Warren, K. D. Campbell, and J. L. Matherne 14 Feb. 1990 149 p
(Contract DE-AC22-87PC-79817)
(DE91-005729; DOE/PC-79817/6) Avail: NTIS HC/MF A07

Research on promoted metal oxide catalysts has continued with the study of alkaline earth/metal oxide halide catalysts. A barium bromide/alumina catalyst was comparable in methane conversion and selectivity to C2's to barium chloride/alumina catalysts. The effects of varying methane to oxygen feed ratios were explored for one of the best alkaline earth catalysts and one of the best literature catalysts (Li/MgO). A significant decrease in the selectivity to C2's is observed upon addition of ethane to the feed gas (feed gas methane/ethane ratio of 3). This observation demonstrates that a significant amount of ethane should not be recycled during methane oxidation over these types of catalysts under process conditions used. Methane oxidation over barium carbonate alone results in high enough selectivities and methane conversions to suggest an oxidized barium species may be responsible for methane oxidation on barium/metal oxide catalysts. Methane coupling studies have continued using layered perovskite catalysts in the cofeed mode and double perovskite catalysts in the sequential mode. Addition of sodium to the double perovskite LaCaMnCoO6 resulted in a catalyst with improved selectivity over

the one without sodium. A reactor system containing two reactors is under construction. These reactors will be used to study different feed diluents, including steam. One reactor will be used to study the effects of pressure on the reaction. Process economics were explored for a hypothetical methane coupling scheme employing a feed mixture of 7/2/1 nitrogen/methane/oxygen. Economic evaluations of the first two of a series of cases based on extrapolations of Union Carbide methane coupling results have been completed. DOE

N91-19314# Argonne National Lab., IL.
METHANOL REFORMERS FOR FUEL CELL POWERED VEHICLES: SOME DESIGN CONSIDERATIONS
R. Kumar, S. Ahmed, M. Krumpelt, and K. M. Myles 1990 5 p Presented at the Fuel Cell Seminar, Phoenix, AZ, 26-28 Nov. 1990
(Contract W-31-109-eng-38)
(DE91-006465; CONF-901106-3) Avail: NTIS HC/MF A01

Fuel cells are being developed for use in automotive propulsion systems as alternatives for the internal combustion engine in buses, vans, passenger cars. The two most important operational requirements for a stand-alone fuel cell power system for a vehicle are the ability to start up quickly and the ability to supply the necessary power on demand for the dynamically fluctuating load. Methanol is a likely fuel for use in fuel cells for transportation applications. It is a commodity chemical that is manufactured from coal, natural gas, and other feedstocks. For use in a fuel cell, however, the methanol must first be converted (reformed) to a hydrogen-rich gas mixture. The desired features for a methanol reformer include rapid start-up, good dynamic response, high fuel conversion, small size and weight, simple construction and operation, and low cost. The design considerations are presented that are important for developing such a reformer, namely: (1) a small catalyst bed for quick starting, small size, and low weight; (2) multiple catalysts for optimum operation of the dissociation and reforming reactions; (3) reforming by direct heat transfer partial oxidation for rapid response to fluctuating loads; and (4) thermal independence from the rest of the fuel cell system. DOE

N91-19315# Sypher-Mueller International, Inc., Ottawa (Ontario).
ALTERNATIVE FUELS FOR HEAVY DUTY ENGINES: STATUS OF FLEET TRIALS
Nov. 1990 45 p
(Contract DE-GI01-87CE-50182)
(DE91-006799; DOE/CE-50182/T2) Avail: NTIS HC/MF A03

In response to the mandate in Annex 4 issued by the IEA Executive Committee on Alternative Motor Fuels, SYPHER: MUELLER International has gathered and collated an extensive range of data pertaining to the use of alcohol powered heavy-duty vehicles throughout the world. Collection of the data began in 1986. A series of reports has been issued to the committee giving successive updates of the situation, and identifying major trends and significant progress. This is the latest update, containing information current in 1990. The most important events since the last report include: the introduction of several school buses into service as part of the extensive California Safe School Bus Clean Fuel Efficiency Demonstration Program; more Scania high compression ethanol buses entering service in Stockholm; progressive withdrawal of the MAN buses at Seattle Metro Transit. The methanol buses will be re-engined with diesel motors; and resurgence of interest in alternatives to petroleum as a result of the Persian Gulf crisis and rapidly rising oil prices. Performing comparative analysis on the data has not been possible to the extent originally anticipated, due to a number of factors. Many trial programs have been unwilling or unable to provide the range and quantity of data originally suggested. A variety of fuels are in use including methanol, ethanol, and blends incorporating ignition enhancer additives. Some test trials are conducted on closed tracks under carefully controlled conditions. DOE

N91-19316# Technical Research Centre of Finland, Espoo.
HYDROGEN STORAGE IN METAL HYDRIDES
H. Tonteri, O. Krogerus, and S. Taehtinen Apr. 1990 53 p In FINNISH; ENGLISH summary
(DE91-746267; VTT-TUTK-677) Avail: NTIS HC/MF A04

The main problems using hydrogen as an energy source are establishing systems for storing and distribution of hydrogen. Metal hydrides offer advantages in storage applications where safe and large storage capacity is needed, like in cars, submarines, houses etc. Metal hydrides can safely store large volumes of gaseous hydrogen in relatively low pressures. Hydrogen reacts reversibly with these metal alloys. Hydrogen absorption is highly exothermic and also the released heat can be used in some applications. To utilize metal hydrides in the energy technology it is necessary to fully understand the hydriding and dehydriding processes to find the optimum conditions for these processes. The literature review of this report describes different hydrogen storage methods. The thermodynamics and kinetics of metal-hydrogen systems are discussed. Hydrogen absorption in lanthanium nickel based alloys LaNi5, LaNi4.7, Al0.3 and MmNi4.85 Fe0.15 (Mm = Mischmetal) is studied experimentally. When nickel is partly replaced with aluminium in lanthanium nickel the plateau pressure decreases in different temperatures. The particle size of metal hydride powders decreases during the hydriding and dehydriding cycles. DOE

N91-19317*# National Aeronautics and Space Administration. Lewis Research Center, Cleveland, OH.
CONCEPTUAL STUDY OF ON ORBIT PRODUCTION OF CRYOGENIC PROPELLANTS BY WATER ELECTROLYSIS
Matthew E. Moran 1991 24 p Proposed for presentation at the 27th Joint Propulsion Conference, Sacramento, CA, 24-27 Jul. 1991; cosponsored by AIAA, SAE, ASME, and ASEE
(NASA-TM-103730; E-5964; NAS 1.15:103730) Avail: NTIS HC/MF A03 CSCL 21I

The feasibility is assessed of producing cryogenic propellants on orbit by water electrolysis in support of NASA's proposed Space Exploration Initiative (SEI) missions. Using this method, water launched into low earth orbit (LEO) would be split into gaseous hydrogen and oxygen by electrolysis in an orbiting propellant processor spacecraft. The resulting gases would then be liquified and stored in cryogenic tanks. Supplying liquid hydrogen and oxygen fuel to space vehicles by this technique has some possible advantages over conventional methods. The potential benefits are derived from the characteristics of water as a payload, and include reduced ground handling and launch risk, denser packaging, and reduced tankage and piping requirements. A conceptual design of a water processor was generated based on related previous studies, and contemporary or near term technologies required. Extensive development efforts would be required to adapt the various subsystems needed for the propellant processor for use in space. Based on the cumulative results, propellant production by on orbit water electrolysis for support of SEI missions is not recommended. Author

N91-19318# Union Carbide Corp., South Charleston, WV.
DIRECT CONVERSION OF METHANE TO C2'S AND LIQUID FUELS
B. K. Warren and K. D. Campbell 24 Jan. 1990 151 p
(Contract DE-AC22-87PC-79817)
(DE91-007545; DOE/PC-79817/4) Avail: NTIS HC/MF A08

Alkaline earth chloride/metal oxide catalysts were explored as less likely to lose metal components during methane coupling than catalysts containing alkali chlorides. The alkaline earth catalysts exhibit superior C2 yield/ethylene to ethane product ratio catalyst lifetime combinations than literature catalysts, and show high C2 yields after tens of hours of operation. A 26 percent C2 yield is obtained with a CaCl2/Al2O3 catalyst. C2 selectivities of over 60 percent are demonstrated at C2 yields over 20 percent. Analyses of fresh and used catalysts show no significant loss of alkaline earth metals from catalysts made with alkaline earth chlorides, whereas alkali chlorides are rapidly lost from catalysts at temperatures and space velocities suitable for methane coupling. Loss of metal chloride does not correlate with melting point of the chloride. Several other catalysts with different supports (TiO2, Ga2O3, ZrO2) and different chlorides (SrCl2, BaCl2, CaCl2) exhibit

C2 yields of over 15 percent with ethylene to ethane product ratios over 10. A study of the abilities of perovskites to oxidatively couple methane initiated during the third quarter has been completed. Most perovskites show very high reactivities but low C2 selectivities. Complex perovskites, layered perovskites, and double perovskites were also explored as methane coupling catalysts. Rb, Na, Dy, and Gd analogs to K2La2Ti3O10, a layered perovskite identified in the Third Quarterly Report as a good coupling catalyst, do not perform as well as the K2La2Ti3O10 catalyst. Economics of a Comparison Case are complete and will be reported next quarter. The economics are complete for Case 1, direct conversion of methane to ethylene. DOE

29 MATERIALS PROCESSING

Includes space-based development of products and processes for commercial applications.

For biological materials see *55 Space Biology*.

N91-19319*# National Aeronautics and Space Administration, Washington, DC.

MICROGRAVITY STRATEGIC PLAN, 1988

Aug. 1988 25 p

(NASA-TM-103397; NAS 1.15:103397) Avail: NTIS HC/MF A03 CSCL 22A

The NASA agency-wide microgravity strategic plan is presented, and its research, applications, and commercialization for the 1990's is addressed. The plan presents an analysis of the current situation, identifies critical factors, and defines goals, objectives, and strategies, which are intended to: (1) provide a context for decision making; (2) assure realism in long-range planning and direction for hardware development; and (3) establish a framework for developing a national microgravity research plan. Author

N91-19320*# National Aeronautics and Space Administration. Lewis Research Center, Cleveland, OH.

GROWTH KINETICS OF PHYSICAL VAPOR TRANSPORT PROCESSES: CRYSTAL GROWTH OF THE OPTOELECTRONIC MATERIAL MERCUROUS CHLORIDE

N. B. Singh (Westinghouse Research and Development Center, Pittsburgh, PA.) and W. M. Duval Mar. 1991 31 p

(Contract NAS3-25274)

(NASA-TM-103788; E-6065; NAS 1.15:103788) Avail: NTIS HC/MF A03 CSCL 12A

Physical vapor transport processes were studied for the purpose of identifying the magnitude of convective effects on the crystal growth process. The effects of convection on crystal quality were were studied by varying the aspect ratio and those thermal conditions which ultimately affect thermal convection during physical vapor transport. An important outcome of the present study was the observation that the convection growth rate increased up to a certain value and then dropped to a constant value for high aspect ratios. This indicated that a very complex transport had occurred which could not be explained by linear stability theory. Better quality crystals grown at a low Rayleigh number confirmed that improved properties are possible in convectionless environments. Author

N91-19321# Messerschmitt-Boelkow-Blohm G.m.b.H., Bremen (Germany, F.R.).

FREE FLOW ELECTROPHORESIS EXPERIMENT TEPE 3 ON TEXUS 24

Volker Mang, K. Hannig, U. Zimmermann, M. Kowalski, and G. Kloeck (Wuerzburg Univ., Germany, F.R.) 1990 5 p Presented at the 4th European Symposium on Life Science in Space, Trieste, Italy, 25 May - 1 Jun. 1990

(MBB-UO-0130-90-PUB; ETN-91-98834) Avail: NTIS HC/MF A01

Within the German sounding rocket program Texus a free flow Electrophoresis Experiment named TEPE 3 was performed. The objective was to enable direct comparison of the 1 g experiment conditions at the same experiment conditions with the same experiment solutions. The comparison of the cell separations shows relevance of microgravity of the separation method electrophoresis. ESA

N91-19653*# National Aeronautics and Space Administration. Marshall Space Flight Center, Huntsville, AL. Space Science Lab.

A NEW APPROACH TO ELECTROPHORESIS IN SPACE

Robert S. Snyder and Percy H. Rhodes *In* ESA, Fourth European Symposium on Life Sciences Research in Space Nov. 1990 p 411-415 (For primary document see N91-19572 11-51)

Copyright Avail: NTIS HC/MF A25; EPD, ESTEC, Noordwijk, Netherlands, HC 80 Dutch guilders CSCL 12A

N91-19654# Messerschmitt-Boelkow-Blohm G.m.b.H., Bremen (Germany, F.R.).

FREE FLOW ELECTROPHORESIS EXPERIMENT TEPE 3 ON TEXUS 24

Volker Mang, K. Hannig, U. Zimmermann, M. Kowalski, and G. Kloeck (Wuerzburg Univ., Germany, F.R.) *In* ESA, Fourth European Symposium on Life Sciences Research in Space Nov. 1990 p 417-420 (For primary document see N91-19572 11-51)

Copyright Avail: NTIS HC/MF A25; EPD, ESTEC, Noordwijk, Netherlands, HC 80 Dutch guilders

N91-19665*# National Aeronautics and Space Administration. Marshall Space Flight Center, Huntsville, AL.

PROTEIN PURIFICATION IN MULTICOMPARTMENT ELECTROLYZERS FOR CRYSTAL GROWTH OF r-DNA PRODUCTS IN MICROGRAVITY

Pier Giorgio Righetti, Elena Casale, Daniel Carter, Robert S. Snyder, Elisabeth Wenisch, and Michel Faupel (Ciba-Geigy A.G., Basel, Switzerland) *In* ESA, Fourth European Symposium on Life Sciences Research in Space Nov. 1990 p 481-484 Sponsored in part by Italian Space Agency (For primary document see N91-19572 11-51)

Copyright Avail: NTIS HC/MF A25; EPD, ESTEC, Noordwijk, Netherlands, HC 80 Dutch guilders CSCL 12A

31 ENGINEERING (GENERAL)

Includes vacuum technology; control engineering; display engineering; cryogenics; and fire prevention.

N91-19322# Sandia National Labs., Albuquerque, NM.

SANDIA TECHNOLOGY: ENGINEERING AND SCIENCE APPLICATIONS

M. C. Maydew, ed., H. Parrot, ed., B. C. Dale, ed., H. L. Floyd, ed., J. A. Leonard, ed., and L. Parrot, ed. Dec. 1990 119 p

(Contract DE-AC04-76DP-00789)

(DE91-006760; SAND-90-2341) Avail: NTIS HC/MF A06

This report discusses: protecting environment, safety, and health; Sandia's quality initiative; Sandia vigorously pursues technology transfer; scientific and technical education support programs; nuclear weapons development; recognizing battlefield targets with trained artificial neural networks; battlefield robotics: warfare at a distance; a spinning shell sizes up the enemy; thwarting would-be nuclear terrorists; unattended video surveillance system for nuclear facilities; making the skies safer for travelers; onboard instrumentation system to evaluate performance of stockpile bombs; keeping track with lasers; extended-life lithium batteries; a remote digital video link acquires images securely; guiding high-performance missiles with laser gyroscopes; nonvolatile memory chips for space applications; initiating weapon explosives with lasers; next-generation optoelectronics and microelectronics technology developments; chemometrics: new methods for improving chemical analysis; research team focuses ion beam to record-breaking intensities; standardizing the volt to quantum accuracy; new techniques improve robotic software development productivity; a practical laser plasma source for generating soft x-rays; exploring metal grain boundaries; massively parallel

computing; modeling the amount of desiccant needed for moisture control; attacking pollution with sunshine; designing fuel-conversion catalysts with computers; extending a nuclear power plant's useful life; plasma-facing components for the International Thermonuclear Experimental Reactor. DOE

N91-19323*# Lockheed Missiles and Space Co., Palo Alto, CA. Research and Development Div.
INTEGRATED CRYOGENIC EXPERIMENT (ICE) MICROSPHERE INVESTIGATION
I. Spradley and D. Read Sep. 1989 84 p
(Contract NAS2-12897)
(NASA-CR-177538; NAS 1.26:177538; LMSC-F279204) Avail: NTIS HC/MF A05 CSCL 13B

The main objective is to determine the performance of microsphere insulation in a 0-g environment and compare its performance to reference insulations such as multilayer insulation. The Lockheed Helium Extended-Life Dewar (HELD) is used to provide superfluid-helium cold sink for the experiment. The use of HELD allows the low-g dynamic properties of Passive Orbital Disconnect Struts (PODS) to be characterized and provides a flight demonstration of the PODS system. The thermal performance of microspheres in 1 and 0 g was predicted, a flight experiment was designed to determine microsphere thermal performance, and the interface was also designed between the experimental package and the shuttle through HELD and the Hitchhiker-M carrier. A single test cell was designed and fabricated. The cell was filled with uncoated glass microspheres and tested with a liquid-nitrogen cold sink. The data were found to agree with predictions of microsphere performance in 1 g. Author

N91-19324*# National Aeronautics and Space Administration. Lewis Research Center, Cleveland, OH.
DEVELOPMENT OF A VIBRATION ISOLATION PROTOTYPE SYSTEM FOR MICROGRAVITY SPACE EXPERIMENTS
Kirk A. Logsdon, Carlos M. Grodsinsky, and Gerald V. Brown 1990 8 p Presented at the 28th Plenary Meeting of the Committee on Space Research, The Hague, Netherlands, 25 Jun. - 6 Jul. 1990; cosponsored by COSPAR, ESA, and NASDA
(NASA-TM-103664; E-5871; NAS 1.15:103664) Avail: NTIS HC/MF A02 CSCL 13B

The presence of small levels of low-frequency accelerations on the space shuttle orbiters has degraded the microgravity environment for the science community. Growing concern about this microgravity environment has generated interest in systems that can isolate microgravity science experiments from vibrations. This interest has resulted primarily in studies of isolation systems with active methods of compensation. The development of a magnetically suspended, six-degree-of-freedom active vibration isolation prototype system capable of providing the needed compensation to the orbital environment is presented. A design for the magnetic actuators is described, and the control law for the prototype system that gives a nonintrusive inertial isolation response to the system is also described. Relative and inertial sensors are used to provide an inertial reference for isolating the payload. Author

N91-19325*# Sverdrup Technology, Inc., Brook Park, OH.
VIBRATION AND THERMAL VACUUM QUALIFICATION TEST RESULTS FOR A LOW-VOLTAGE TUNGSTEN-HALOGEN LIGHT Final Report
J. Andrew Sexton Feb. 1991 11 p
(Contract NAS3-25266)
(NASA-CR-187050; E-5890; NAS 1.26:187050) Avail: NTIS HC/MF A03 CSCL 13B

The results of a space flight qualification test program for a low-voltage, quartz tungsten-halogen light are presented. The test program was designed to qualify a halogen light for use in the Pool Boiling Experiment, a Get Away Special (GAS) payload that will be flown in the space shuttle payload bay. Vibration and thermal vacuum tests were performed. The test results indicated that the halogen light will survive the launch and ascent loads, and that the convection-free environment associated with the GAS payload system will not detrimentally affect the operation of the halogen light. Author

N91-19326# Department of Transportation, Cambridge, MA. National Transportation Systems Center.
SAFETY OF HIGH SPEED MAGNETIC LEVITATION TRANSPORTATION SYSTEMS. PRELIMINARY SAFETY REVIEW OF THE TRANSRAPID MAGLEV SYSTEM Interim Report, Sep. 1989 - Aug. 1990
R. M. Dorer and W. T. Hathaway Nov. 1990 197 p Sponsored by Federal Railroad Administration
(PB91-129684; DOT-VNTSC-FRA-90-3; DOT/FRA/ORD-90/09) Avail: NTIS HC/MF A09 CSCL 13F

The safety of various magnetically levitated trains under development for possible implementation in the United States is of direct concern to the Federal Railroad Administration. Safety issues are addressed related to a specific maglev technology. The Transrapid maglev system was under development by the German Government over the last 10 to 15 years and was evolved into the current system with the TR-07 vehicle. A technically based safety review was under way over the last year by the U.S. Department of Transportation. The initial results of the review are presented to identify and assess potential maglev safety issues. Author

32 COMMUNICATIONS AND RADAR

Includes radar; land and global communications; communications theory; and optical communications.

For related information see also *04 Aircraft Communications and Navigation* and *17 Space Communications, Spacecraft Communications, Command and Tracking.* For search and rescue see *03 Air Transportation and Safety,* and *16 Space Transportation.*

N91-19327# Beleidscommissie Remote Sensing, Delft (Netherlands).
SLOPE MODULATION OF THE RADAR BACKSCATTER BY SEA WAVES
G. P. deLoor Apr. 1988 33 p
(Contract BCRS-4544/AO-1.2)
(BCRS-88-05; FEL-1987-102; ETN-88-93455) Avail: NTIS HC/MF A03

Measured data of the radar backscatter as a function of incidence angle were investigated to study the influence of the slope modulation by the sea waves on the total modulation observed for the radar backscatter of the sea. Analysis suggests that much if not most of the modulation of the radar backscatter by sea waves can be explained by wave slope modulation. ESA

N91-19328# Department of the Navy, Washington, DC.
HIGH PULSE REPETITION FREQUENCY RADAR EARLY WARNING RECEIVER Patent Application
William P. Huntley, inventor (to Navy) and David J. Swanick, inventor (to Navy) 4 Oct. 1989 8 p
(AD-D014655; US-Patent-Appl-SN-417616) Avail: NTIS HC/MF A02 CSCL 17/9

A ten db coupler receives an RF input signal and transmits an attenuated signal through a wideband/narrow band select switch to an RF amplifier. The signal is next processed through an RF amplitude detector. A comparator then receives the signal and generates a pulse in response to signals exceeding a predetermined threshold. A pulse stretcher then eliminates excessive pulses due to noise or other signal oscillations that exceeded the comparator's threshold. A circuit comprising a retriggerable monostable and an OR gate determine if the pulses received exceed a pulse repetition frequency threshold. A ripple counter then eliminates unwanted signals by resetting if a predetermined number is not reached in a specified time. A unique audio signal is then generated if the desired signal is detected.

the output signal is audible even though the input signal is of a frequency above the normal hearing threshold. Also a visual signal is provided by a light emitting diode. GRA

N91-19329 British Broadcasting Corp., Kingswood (England). Engineering Div.
THE PROVISION OF CIRCUITS TO OUTSIDE BROADCAST LOCATIONS USING SPECTRUM WITHIN THE UHF BROADCASTING BANDS
N. J. Laflin, D. J. Darlington, and R. A. Salmon Jan. 1991 25 p Original contains color illustrations
(BBC-RD-1990/12) Copyright Avail: Issuing Activity; 1 functional color page

It is proposed that the spectrum within the UHF television broadcasting bands is used to provide digital links, carrying control, coordination, and audio monitoring circuits from production centers to outside broadcast locations. Existing methods for establishing these links, known as reverse bearers, either by rented lines or by use of the spectrum currently allocated to services ancillary to broadcasting, are now proving inadequate. The problem is particularly acute in the south east of England where there is a high incidence of major outside broadcast events. The planning aspects of establishing such links in the lower adjacent channels to broadcasting services, and in particular from the Crystal Palace UHF main transmitter station in London, is considered both in terms of providing the desired coverage and compatibility with existing UHF transmissions. Details of a subsequent system field trial which involved the transmission and reception of a 2.048 Mbit/s digitally-modulated data stream radiated a low level 5.6 MHz, below the vision carrier of the BBC-2 national network service is described. The tests demonstrated that such a link can operate reliably and that it will not cause interference to existing television transmissions. Author

N91-19330# Sandia National Labs., Albuquerque, NM.
UNIQUE SIGNAL OVERRIDE PLUG (USOP) ELECTROMAGNETIC TEST REPORT
R. H. Bonn Oct. 1990 34 p
(Contract DE-AC04-76DP-00789)
(DE91-004996; SAND-89-3107) Avail: NTIS HC/MF A03

The MC4039 Unique Signal Override Plug (USOP) provides the unique signal for the B90 when fielded on aircraft that are not equipped with unique signal capability. Since the USOP is field installed, the concern is that it might be susceptible to electromagnetic radiation prior to installation on the weapon. This report documents a characterization of the USOP, evaluates various techniques for attaching electromagnetic shields, and evaluates the susceptibility of a fully assembled passive-USOP. Tests conducted evaluated the electromagnetic susceptibility of the passive, unconnected USOP. During normal operation the USOP is powered directly from the weapon. During the course of this test program two prototypes were developed. The prototype 1 USOP internal circuitry contains one SA3727 chip, five diodes, three resistors, and two capacitors; these are mounted on a circular circuit board and contained inside a metal back shell cover, which serves as an electromagnetic shield. The prototype 2 design incorporated four changes. The manufacturer of the SA3727 chip was changed from Lasarray to LSI Logic, the circuit board ground was tied to the case ground through a straight wire, Cl was changed from 1 microfarad to 0.1 microfarads. and the circuit board was changed, as required. DOE

N91-19331# Lawrence Livermore National Lab., CA.
ELECTROMAGNETIC PENETRATION THROUGH NARROW SLOTS IN CONDUCTING SURFACES AND COUPLING TO STRUCTURES ON THE SHADOW SIDE
E. K. Reed and C. M. Butler (Clemson Univ., SC.) Jul. 1990 295 p
(Contract W-7405-eng-48)
(DE91-007155; UCRL-CR-105773; TR-062188-3273F2) Avail: NTIS HC/MF A13

Electromagnetic field penetration through a curved narrow slot in a planar conducting surface and coupling to a curved, loaded thin wire on the shadow side are determined in the time domain (TD) and the frequency domain (FD) by integral equation methods. Coupled integral equations are derived and solved numerically for the equivalent magnetic current in the slot and the electric current on the wire, from which the field that penetrates the slotted surface is determined. One employs a piecewise linear approximation of the unknown currents and performs equation enforcement by pulse testing. The resulting TD equations are solved by a scheme incorporating a finite-difference approximation for a second partial time derivative which allows one to solve for the unknown currents at a discrete time instant t + 1 in terms of the known excitation and currents calculated at a discrete time instant t and earlier. The FD equations are solved by the method of moments. A hybrid time-domain integral equation - finite-difference time-domain solution technique is described whereby one solves for the field which penetrates a slotted cavity-backed surface. One models the fields in the exterior region and in the slot with integral operators and models the fields inside the cavity with a discretized form of Maxwell's equations. Narrow slots following various contours were chemically etched in thin brass sheets and an apparatus was fabricated to measure shadow-side fields, electric current on a thin wire on the shadow side, and, separately, fields inside a rectangular cavity which backed the slotted brass sheet. The experimentation was conducted at the Lawrence Livermore National Laboratory on a frequency-domain test range employing a monocone source over a large ground plane. One observes very good agreement among the experimental and theoretical results. DOE

N91-19332*# National Aeronautics and Space Administration. Lewis Research Center, Cleveland, OH.
COPLANAR WAVEGUIDE EEsoF MICAD MACROS MAKE CIRCUIT LAYOUT EASY
George E. Ponchak and Nikola Visic (Cleveland State Univ., OH.) Sep. 1990 39 p
(NASA-TM-103272; E-5714; NAS 1.15:103272) Avail: NTIS HC/MF A03 CSCL 09C

A collection of macro files is presented which permit the layout of coplanar waveguide integrated circuits using EEsoF MICAD CAD software. The files must be added to the user's MICAD.ELE file. Author

N91-19333# Los Alamos National Lab., NM.
ASSESSING THE IMPACT OF LARGE-SCALE COMPUTING ON THE SIZE AND COMPLEXITY OF FIRST-PRINCIPLES ELECTROMAGNETIC MODELS
E. K. Miller 1990 24 p Presented at the International Conference on Directions in Electromagnetic Wave Modeling, New York City, 22-24 Oct. 1990
(Contract W-7405-eng-36)
(DE91-007491; LA-UR-91-373; CONF-9010232-2) Avail: NTIS HC/MF A03

There is a growing need to determine the electromagnetic performance of increasingly complex systems at ever higher frequencies. The ideal approach would be some appropriate combination of measurement, analysis, and computation so that system design and assessment can be achieved to a needed degree of accuracy at some acceptable cost. Both measurement and computation benefit from the continuing growth in computer power that, since the early 1950s, has increased by a factor of more than a million in speed and storage. For example, a CRAY2 has an effective throughput (not the clock rate) of about 10(exp 11) floating point operations (FLOPs) per hour compared with the approx. 10(exp 5) provided by the UNIVAC-1. The purpose of this discussion is to illustrate the computational complexity of modeling large (in wavelengths) electromagnetic problems. In particular the point is made that simply relying on faster computers for increasing the size and complexity of problems that can be modeled is less effective than might be anticipated from this raw increase in computer throughput. It is suggested that rather than depending on faster computers alone, various analytical and numerical alternatives need development for reducing the overall FLOP count required to acquire the information desired. One approach is to

decrease the operation count of the basic model computation itself, by reducing the order of the frequency dependence of the various numerical operations or their multiplying coefficients. Another is to decrease the number of model evaluations that are needed, an example being the number of frequency samples required to define a wideband response, by using an auxiliary model of the expected behavior. DOE

N91-19334# Sandia National Labs., Albuquerque, NM.
MEASUREMENT OF ELECTROMAGNETIC FIELDS OVER A SMALL ELECTROLYTIC TANK
T. W. H. Caffey and H. E. Morris Dec. 1990 75 p
(Contract DE-AC04-76DP-00789)
(DE91-007500; SAND-90-0805) Avail: NTIS HC/MF A04

In 1986, Hart proposed a large, hemispherical electrolytic tank and the use of the Surface Electrical Potential method with which to study resistivity changes due to energy-extraction processes in the earth. A second method for the inference of underground resistivity changes, the Controlled Source Audio-MagnetoTelluric method, has been widely used in the field. This method uses measurements of the electromagnetic field from a surface dipole, rather than the surface potential distribution from a buried vertical electrode, as the basis of the technique. If both SEP and CSAMT could be applied to the same model structure in the same electrolytic tank, it would seem that the diagnostic information would be enhanced over the use of each technique separately. Accordingly, the specific objectives were: to determine to what radial extent the bowl could be used as a homogeneous half-space; and to demonstrate acceptable accuracy by measuring the effect of a conducting target immersed in the bowl and comparing the measurements with numerical modeling. Electromagnetic fields over an electrolytic tank have been measured by others, and this report begins with a comparative summary of both prior and present work. The next section presents the formulas for the electromagnetic fields, and explains the choice of a particular method of measuring apparent resistivity. The field theory is also used in the subsequent section to provide error estimates needed for design guidance. The following sections describe the measurements, and the considerations for a larger facility. The appendices include the derivatives of the fields, the electrolyte characteristics, a description of the apparatus, and calibration methods. DOE

N91-19335# General Atomic Co., San Diego, CA.
SOLITON MICROWAVE GENERATOR
J. S. deGrassie Dec. 1990 207 p
(Contract DE-AC03-87SF-17119)
(DE91-008277; GA-C-19942-Rev-1) Avail: NTIS HC/MF A10

The Soliton Microwave Generator (SMG) represents a truly new concept in the field of high power microwave (HPM) generation. A nonlinear, dispersive transmission line is used to convert an input voltage pulse into an HPM burst at the output. The system is all solid state and projects to be efficient and reliable. Single module peak powers in excess of 1 GW appear feasible, while combining modular units leads to a 10 GW system projection. This project for the DOE has allowed the first steps necessary in experimentally demonstrating the SMG. The project has ended successfully. A relatively high power lumped circuit SMG operating in the uhf band was designed, fabricated, and tested. The maximum peak output RF power was 16 MW from this line approx. 90 cm in length and 2 sq cm in cross section with a peak power efficiency of roughly 20 percent. Additionally a low power continuous strip-line approach demonstrated microwave generation well into L band, at approx. 2 GHz. DOE

N91-19336# Messerschmitt-Boelkow-Blohm G.m.b.H., Ottobrunn (Germany, F.R.). Space Communications and Propulsion Systems Div.
C-BAND ANTENNAS FOR REGIONAL COMMUNICATION SYSTEMS
H. Wolf, E. Dudok, N. Nathrath, and E. Sommer 1990 12 p Presented at 1st European Conference on Satellite Communications, Munich, Fed. Republic of Germany, 28-30 Nov. 1989
(MBB-UK-0107-90-PUB; ETN-91-98835) Avail: NTIS HC/MF A03

The advance of C band technology for complex multishaped beam spacecraft antennas allowing operation of the maximum number of channels is described. Relevant results (design and optimization, hardware activities, performance data) of two representative antenna subsystem developments are presented: the engineering model of a C band multibeam antenna subsystem for covering the main areas of Africa, qualification of C band technology and development of variable beam forming network components; and one engineering model and two flight models of a dual polarized contoured beam antenna subsystem with combined transmit and receiver functions for the Chinese communication satellite DFH3. ESA

N91-19337# Technische Univ., Eindhoven (Netherlands).
ELECTROMAGNETIC COMPATIBILITY IN HIGH-VOLTAGE ENGINEERING Ph.D. Thesis
Marinus Albertus vanHouten 1990 138 p
(ISBN-90-9002929-X; ETN-91-98928) Avail: NTIS HC/MF A07

Electro Magnetic Compatibility (EMC) concepts for an efficient and consistant approach to practical interference problems are described. A critical analysis of 'grounding' is given. The design of a 'differentiated/integrated' system to measure fast voltage transients is described. Measurements of steep transient voltages across interruptions in a Gas Insulated Switchear (GIS) installation, due to switching actions, are presented. Available means to reduce the influence of this interference source on the measuring are discussed. General conclusions are that general, linear and basic design methods for the protection of electronics and (large) interconnected electrical systems against interference can be developed which can save production costs and research time. The design methods described concentrate on the reduction of dangerous voltages between critical points which can be achieved by correct layout choice. ESA

N91-19338# Technische Univ., Eindhoven (Netherlands).
A VARIATIONAL APPROACH TO MAGNETO-ELASTIC BUCKLING PROBLEMS Ph.D. Thesis
Peter Henricus vanLieshout 1990 135 p
(ETN-91-98929) Avail: NTIS HC/MF A07

A variational principle that can serve as the basis for a magnetoelastic stability (or buckling) problem is constructed, starting from a specific choice for a magnetoelastic Lagrangian. For evaluation of the principle the first and second variations of the Lagrangian are calculated both inside and outside the solid magnetoelastic body. Thus a general buckling criterion, consisting of an expression for the critical field value together with a set of constraints for the field variables, is constructed. Detailed formulations are given for soft ferromagnetic and superconducting structures. Applications of the principle to one single Ferromagnetic or Superconducting Beam (FSB), a system of two parallel FSBs, and a system of two concentric and coaxial superconducting tori, are solved analytically using Green's identities, integral equations, fundamental solutions and complex analysis. Application to a system of an arbitrary number of parallel superconducting beams is solved using a numerical method involving standard procedures for the eigenvalue problem solution. The advantage of the variational method is that at the moment a reasonable eigenfunctions approximation leads to a very good buckling value approximation. ESA

N91-19339# Technische Univ., Berlin (Germany, F.R.). Fachbereich Mathematik.
EXAMINATIONS OF INVERSE SCATTERING PROBLEM FOR THE SCALAR HELMHOLTZ EQUATION IN THE FIELD OF FIRST ORDER APPROXIMATIONS FOR POTENTIALS WITH COMPACT SUPPORTS AND SAFE REAL WAVE NUMBERS Ph.D. Thesis [UNTERSUCUNGEN ZUM INVERSEN STREUPROBLEM FUER DIE SKALARE HELMHOLTZGLEICHUNG IM RAHMEN VON APPROXIMATIONEN ERSTER ORDNUNG FUER POTENTIALE MIT KOMPAKTEM TRAEGER UND FESTE REELLE WELLENZAHLEN]
Norbert Gorenflo 1990 92 p In GERMAN
(ETN-91-98949) Avail: NTIS HC/MF A05

The concept of fist order approximation includes the Born approximation and the Rytov approximation. The Sommerfeld radiation condition is taken as unique boundary condition. After introducing propagation operators, symmetry considerations were carried out for these operators and their imaging properties were defined. Operator singular value dispersions were given. Exact integral representations of the potential were derived from data. These representations can be considered as a further extension of the approximative inversion formula, as filtered backpropagation. A contribution to the model theory of first order approximation in the scattering theory was presented. ESA

N91-19340# Kansas Univ. Center for Research, Inc., Lawrence. Radar Systems and Remote Sensing Lab.
RADAR BACKSCATTER FROM THE SEA CONTROLLED EXPERIMENTS Final Report
Richard K. Moore Nov. 1990 4 p
(Contract N00014-89-J-3022)
(AD-A229847; CRINC-RSL-TR-4191-13) Avail: NTIS HC/MF A01 CSCL 17/9

This is the final report on ONR Grant N00014-89-J-3022. Since most of the work was in journal articles, conference proceedings, and reports, this report is brief. Work continued, and was largely concluded, on analysis of the TOWARD, SAXON-CLT, and NILDEX data sets. Comparison between optical and radio measurements of ripple spectra at TOWARD showed favorable results. Although the wind direction was usually unfavorable for SAXON-CLT, useful data was obtained on modulation in the crosswind direction. It was also demonstated that a vector slope gauge can work, but for logistic reasons its deployment made its footprint close to the tower. Hence, the data are useful only for proof of concept, not for oceanographic application. A new theory of SAR imaging of the ocean was developed. It incorporates elements of previous theories, but shows an improved way to find out the effects of signal modulations on the observed spectra. It confirms, by a different method, the results from several other theoretical and experimental studies on processor focus adjustment. These show optimum image contrast occurs for along-track wave motion when the processor is set to (phase velocity)/2. The method of analysis used allowed closer examination of the basis for the two-scale (Bragg resonance with slope modulation) model for ocean backscatter. The results cast some doubt on the validity of the Bragg-scatter model for explaining many observed phenomena. GRA

N91-19306*# Michigan Univ., Ann Arbor. Radiation Lab.
A FINITE ELEMENT CONJUGATE GRADIENT FFT METHOD FOR SCATTERING
Jeffery D. Collins, Dan Ross, J.-M. Jin, A. Chatterjee, and John L. Volakis *In its* Task Reports on Developing Techniques for Scattering by 3D Composite Structures and to Generate New Solutions in Diffraction Theory Using Higher Orde: Boundary Conditions Feb. 1991 26 p (For primary document see N91-19305 11-27)
Avail: NTIS HC/MF A03 CSCL 11C

N91-19307*# Michigan Univ., Ann Arbor. Radiation Lab.
ANALYTICAL SOLUTIONS WITH GENERALIZED IMPEDANCE BOUNDARY CONDITIONS (GIBC)
H. H. Syed and John L. Volakis *In its* Task Reports on Developing Techniques for Scattering by 3D Composite Structures and to Generate New Solutions in Diffraction Theory Using Higher Order Boundary Conditions Feb. 1991 18 p (For primary document see N91-19305 11-27)
Avail: NTIS HC/MF A03 CSCL 11C

33 ELECTRONICS AND ELECTRICAL ENGINEERING

Includes test equipment and maintainability; components, e.g., tunnel diodes and transistors; microminiaturization; and integrated circuitry.

For related information see also *60 Computer Operations and Hardware* and *76 Solid-State Physics.*

N91-19341 Department of the Navy, Washington, DC.
PIEZOELECTRIC SANDWICH POLYMER TRANSDUCER Patent
Edward F. Rynne, inventor (to Navy) and Jay C. Brown, inventor (to Navy) 21 Aug. 1990 6 p Filed 9 Mar. 1981
(AD-D014650; US-Patent-4,950,936; US-Patent-Appl-SN-241873)
Avail: US Patent and Trademark Office CSCL 17/8

A sensor, having a sandwich configuration, is able to sense a transduce output parameter in situ without significantly affecting the parameter. The sensor comprises an inner sheet of a polymer having a transducer property. A conductive layer is deposited on parts of at least one of the two surfaces of the inner sheet. A pair of outer sheets of plastic are attached to each side of the inner sheet. Two layers of conductive material may be deposited on the outer, unattached, surfaces of the outer sheets, one layer on each surface. GRA

N91-19342# Naval Ship Research and Development Center, Bethesda, MD. Computation Mathematics-Logistics Dept.
PROPOSED DRAFT MILITARY HANDBOOK PRESENTING REQUIREMENTS FOR AN ELECTRONIC DISPLAY SYSTEM (EDS) FOR INTERACTIVE ELECTRONIC TECHNICAL MANUALS (IETMS) Final Report, Oct. 1989 - May 1990
Eric L. Jorgensen, Joseph J. Fuller, and Samuel C. Rainey (Scientific Management Associates, Inc., Haddonfield, NJ.) Jul. 1990 105 p
(AD-A227471; DTRC-90/025) Avail: NTIS HC/MF A06 CSCL 12/6

The report summarizes recent activities in the Department of Defense and in the U.S. Navy, Army, and Air Force to establish Service use of Interactive Electronic Manuals (IETMs) as replacements for paper Technical Manuals for logistic support of military equipment. the IETM concept is described, and an overview is provided of five IETM acquisition Specifications and Military Handbooks developed by the Tri-Service Interactive Electronic Technical Manual Working Group established in 1989 by the Defense Quality and Standardization Office. GRA

N91-19343*# Michigan Univ., Ann Arbor. Ultrafast Science Lab.
CHARACTERIZATION OF DEVICES, CIRCUITS, AND HIGH-TEMPERATURE SUPERCONDUCTOR TRANSMISSION LINES BY ELECTRO-OPTIC TESTING Final Technical Report, 15 Jan. 1989 - 14 Jan. 1991
John F. Whitaker 14 Jan. 1991 28 p
(Contract NCC3-130)
(NASA-CR-187950; NAS 1.26:187950) Avail: NTIS HC/MF A03 CSCL 09C

The development of a capability for testing transmission lines, devices, and circuits using the optically-based technique of electro-optics sampling was the goal of this project. Electro-optic network analysis of a high-speed device was demonstrated. The project involved research on all of the facets necessary in order to realize this result, including the discovery of the optimum electronic pulse source, development of an adequate test fixture, improvement of the electro-optic probe tip, and identification of a device which responded at high frequency but did not oscillate in

the test fixture. In addition, during the process of investigating patterned high-critical-temperature superconductors, several non-contacting techniques for the determination of the transport properties of high T(sub c) films were developed and implemented. These are a transient, optical pump-probe, time-resolved reflectivity experiment, an impulsive-stimulated Raman scattering experiment, and a terahertz-beam coherent-spectroscopy experiment. The latter technique has enabled us to measure both the complex refractive index of an MgO substrate used for high-T(sub c) films and the complex conductivity of a YBa2Cu3O(7-x) sample. This information was acquired across an extremely wide frequency range: from the microwave to the submillimeter-wave regime. The experiments on the YBCO were conducted without patterning of, or contact to, the thin film. Thus, the need for the more difficult transmission-line experiments was eliminated. Progress in all of these areas was made and is documented in a number of papers. These papers may be found in the section listing the abstracts of the publications that were issued during the course of the research. Author

N91-19344# Sandia National Labs., Albuquerque, NM.
CAPATTERY DOUBLE LAYER CAPACITOR LIFE PERFORMANCE
David A. Evans, Nancy H. Clark, W. E. Baca, John R. Miller, and Thomas B. Barker (Rochester Inst. of Tech., NY.) 1991 5 p Presented at the 11th Capacitor and Resistor Technology Symposium (CARTS), Las Vegas, 4-7 Mar. 1991
(Contract DE-AC04-76DP-00789)
(DE91-006639; SAND-90-2246C; CONF-9103102-4) Avail: NTIS HC/MF A01

Double layer capacitors (DLCs) have received increased use in computer memory backup applications for consumer products during the past ten years. Their extraordinarily high capacitance density along with their maintenance-free operation makes them particularly suited for these products. These same features also make DLCs very attractive in military type applications. Unfortunately, lifetime performance data has not been reported in the literature for any DLC component. Our objective in this study was to investigate the effects that voltage and temperature have on the properties and performance of single and series-connected DLCs as a function of time. Evans model RE110474, 0.47-farad, 11.0-volt Capatteries were evaluated. These components have a tantalum package, use welded construction, and contain a glass-to-metal seal, all incorporated to circumvent the typical DLC failure modes of electrolyte loss and container corrosion. A five-level, two-factor Central Composite Design was used in the study. Single and series-connected Capatteries rated at 85 C, 11.0-volts operation were subjected to test temperatures between 25 and 95 C, and voltages between 0 and 12.9 volts (9 test conditions). Measured responses included capacitance, equivalent series resistance, and discharge time. Data were analyzed using a regression analysis to obtain response functions relating DLC properties to their voltage, temperature, and test time history. These results are described and should aid system and component engineers in using DLCs in critical applications. DOE

N91-19345*# Institute for Computer Applications in Science and Engineering, Hampton, VA.
DIGITAL OPTICAL COMPUTERS AT THE OPTOELECTRONIC COMPUTING SYSTEMS CENTER Final Report
Harry F. Jordan (Colorado Univ., Boulder.) Feb. 1991 20 p Prepared for presentation at the International Congress on Optical Science and Engineering, ECO'4, The Hague, Netherlands, 11-15 Mar. 1991 Submitted for publication
(Contract NAS1-18605; NSF CDR-86-22236)
(NASA-CR-187520; ICASE-91-18; NAS 1.26:187520) Avail: NTIS HC/MF A03 CSCL 09C

The Digital Optical Computing Program within the National Science Foundation Engineering Research Center for Optoelectronic Computing Systems has as its specific goal research on optical computing architectures suitable for use at the highest possible speeds. The program can be targeted toward exploiting the time domain because other programs in the Center are pursuing research on parallel optical systems, exploiting optical interconnection and optical devices and materials. Using a general purpose computing architecture as the focus, we are developing design techniques, tools and architecture for operation at the speed of light limit. Experimental work is being done with the somewhat low speed components currently available but with architectures which will scale up in speed as faster devices are developed. The design algorithms and tools developed for a general purpose, stored program computer are being applied to other systems such as optimally controlled optical communication networks. Author

N91-19346# Edgerton, Germeshausen and Grier, Inc., Idaho Falls, ID.
LABORATORY TESTING OF THE SONNENSCHEIN CHARGER, PART NUMBER DTL 12040
J. E. Hardin and M. E. Martin Sep. 1990 14 p
(Contract DE-AC07-76ID-01570)
(DE91-006543; EGG-EP-9015) Avail: NTIS HC/MF A03

This report describes the results of testing the Sonnenschein DTL 12040 battery charger in the Idaho National Engineering Laboratory (INEL) battery laboratory. The purpose of this testing was to evaluate the suitability of this charger for charging electric vehicle battery packs made up of Sonnenschein sealed lead acid batteries or possibly other similar batteries. This evaluation consists primarily of identifying the charge algorithm used and evaluating the resulting charge behavior. Other characteristics of the charger that could be significant are also noted. DOE

N91-19347# Montana State Univ., Bozeman. Electronics Research Lab.
COMPUTER CONTROLLED MHD POWER CONSOLIDATION AND PULSE GENERATION SYSTEM
R. Johnson, K. Marcotte, and M. Donnelly 1990 53 p
(Contract DE-AC22-87PC-79680)
(DE91-006793; DOE/PC-79680/T4; ERL-290666-3) Avail: NTIS HC/MF A04

The major goal of this research project is to establish the feasibility of a power conversion technology which will permit the direct synthesis of computer programmable pulse power. Feasibility has been established in this project by demonstration of direct synthesis of commercial frequency power by means of computer control. The power input to the conversion system is assumed to be a Faraday connected MHD generator which may be viewed as a multi-terminal dc source and is simulated for the purpose of this demonstration by a set of dc power supplies. This consolidation/inversion (CI), process will be referred to subsequently as Pulse Amplitude Synthesis and Control (PASC). A secondary goal is to deliver a controller subsystem consisting of a computer, software, and computer interface board which can serve as one of the building blocks for a possible phase 2 prototype system. This report period work summarizes the accomplishments and covers the high points of the two year project. DOE

N91-19348*# National Aeronautics and Space Administration. Lewis Research Center, Cleveland, OH.
PULSED RESPONSE OF A TRAVELING-WAVE TUBE
Brian D. May Jan. 1991 15 p
(NASA-TM-103672; E-5884; NAS 1.15:103672) Avail: NTIS HC/MF A03 CSCL 09A

The consequence of frequency-domain multiple access (FDMA) channelization in a satellite communications system is that the ground- and space-based components are often required to operate at reduced output power to prevent the generation of distortions. However, the components of a time-division multiple access (TDMA) satellite system, such as a traveling-wave tube (TWT), can operate at the highest output power because the channelization technique is relatively insensitive to the distortions resulting from saturated operation. A Hughes 30-GHz TWT was tested to determine the suitability of such a device in a TDMA system. Testing was focused on the ability of the TWT to rise up to full power at the leading edge of TDMA bursts, which were simulated by a pulse train. A Wavetek model 8502A peak power meter was used to display and measure the pulsed signal waveform. Measurements of the TWT output signal rise time indicate that

the TWT lengthened the rise time by 10 to 20 nsec. Imposing a modulator turn-on time that precedes the data burst by the TWT rise time is a logical approach to coordinating the traveling-wave tube amplifier and modulator specifications. Author

N91-19349*# National Aeronautics and Space Administration. Lewis Research Center, Cleveland, OH.
USING A MODIFIED HEWLETT PACKARD 8410 NETWORK ANALYZER AS AN AUTOMATED FARFIELD ANTENNA RANGE RECEIVER
John D. Terry and Richard R. Kunath 1990 10 p Presented at the Antenna Measurement Techniques Association Meeting, Philadelphia, PA, 8-11 Oct. 1990
(NASA-TM-103700; E-5922; NAS 1.15:103700) Avail: NTIS HC/MF A02 CSCL 09C

A Hewlett Packard 8410 Network Analyzer was modified to be used as an automated far-field antenna range receiver. By using external mixers, analog to digital signal conversion, and an external computer/controller, the HP8410 is capable of measuring signals as low as -110 dBm. The modified receiver is an integral part of an automated far-field range which features computer controlled test antenna positioning, system measurement parameters, and data acquisition, as well as customized measurement file management. The system described was assembled and made operational, taking advantage of off-the-shelf hardware available at minimal cost. Author

N91-19350*# Analex Corp., Fairview Park, OH.
MEASURED PERFORMANCE OF THE HALF-SCALE ACCURATE ANTENNA REFLECTOR Final Report
Kevin M. Lambert Dec. 1990 29 p
(Contract NAS3-25776)
(NASA-CR-187047; E-5886; NAS 1.26:187047) Avail: NTIS HC/MF A03 CSCL 09A

A corrugated horn was designed and fabricated for use as a feed for the half-scale accurate antenna reflector. This feed allows the reflector to be used in a compact range configuration as part of a microwave reflectance measuring system. The horn design is described, and the measured farfield patterns of the horn are presented. The horn was installed at the focus of the reflector, and the nearfield of the antenna was measured. The results of these measurements are presented and discussed with respect to the compact range application. Author

N91-19351*# National Aeronautics and Space Administration. Lewis Research Center, Cleveland, OH.
ELLIPSOMETRIC STUDY OF InGaAs MODFET MATERIAL
S. A. Alterovitz, R. E. Sieg, H. D. Yao, P. G. Snyder, J. A. Woollam, J. Pamulapati, and P. K. Bhattacharya (Michigan Univ., Ann Arbor.) 1990 6 p Presented at the 1990 Fall Meeting of the Materials Research Society, Boston, MA, 26 Nov. - 1 Dec. 1990
(NASA-TM-103286; E-5705; NAS 1.15:103286) Avail: NTIS HC/MF A02 CSCL 09C

In(x)Ga(1-x)As based MODFET (modulation doped field effect transistor) material was grown by molecular beam epitaxy on semi-insulating InP substrates. Several structures were made, including lattice matched and strained layer InGaAs. All structures also included several layers of In(0.52)Al(0.48)As. Variable angle spectroscopic ellipsometry was used to characterize the structures. The experimental data, together with the calibration function for the constituent materials, were analyzed to yield the thickness of all the layers of the MODFET structure. Results of the ellipsometrically determined thicknesses compare very well with the reflection high energy electron diffraction in situ thickness measurements. Author

N91-19352# Sandia National Labs., Albuquerque, NM.
EXPLORATORY BATTERY TECHNOLOGY DEVELOPMENT AND TESTING REPORT FOR 1989
N. J. Magnani, R. B. Diegle, J. W. Braithwaite, D. M. Bush, J. M. Freese, A. A. Akhil, and S. E. Lott Dec. 1990 123 p
(Contract DE-AC04-76DP-00789)
(DE91-006753; SAND-90-1195) Avail: NTIS HC/MF A06

Sandia National Laboratories, Albuquerque, has been designated as Lead Center for the Exploratory Battery Technology Development and Testing Project, which is sponsored by the U.S. Department of Energy's Office of Energy Storage and Distribution. In this capacity, Sandia is responsible for the engineering development of advanced rechargeable batteries for both mobile and stationary energy storage applications. This report details the technical achievements realized in pursuit of the Lead Center's goals during calendar year 1989. DOE

N91-19353# Beta Power, Inc., Salt Lake City, UT.
SODIUM/METAL CHLORIDE PROGRAM CONCEPTUAL DESIGN STUDY
31 Jul. 1990 135 p
(Contract DE-AC02-89CH-10406)
(DE91-007216; DOE/CH-10406/T2) Avail: NTIS HC/MF A07

The purpose of the Sodium/Metal Chloride Design Study was to investigate and evolve candidate cell designs, using the metal chloride technology, which are responsive to future battery requirements for electric vans. Using the present power and energy requirements for the ETX-2, IDSEP and G-Van Electric Vehicle Programs, the design study was driven by a goal established by DOE/ANL for a 27 percent reduction in battery weight and volume. In addition to battery performance figures of 150 Wh/kg and 200 Wh/liter, the conceptual design had to meet the acceleration power demand throughout discharge, specific to each of the designated vans, even for the case where 10 percent of cells failed early. The power to accelerate the ETX-2 Aerostar, for example, was 65 kW, or 160 W/kg and 230 W/liter. Clearly, the challenges that were established for the metal chloride system were intended to provide a high performance battery system for future van applications, in which a vehicle range of 200 miles and acceleration to 60 MPH in 15 seconds were deemed to be attractive features. This study was perhaps the first DOE sponsored program which has directed the cell design to meet the perceived performance goals of future EVans. The two recommended cell designs are the central cathode multi-tube and the bipolar flat plate concepts. The former allows the use of external fuses in series with each tube to isolate failures and maintain cell operation. Since the fuses have a common termination, the presence of an instantaneous short-circuit creates a high current path through the appropriate fuse, causing it to melt and open-circuit. The action of the fuse is enhanced by the greater numbers of electrolyte tubes associated with the central cathode design. The BFP design, on the other hand, uses smaller capacity cells that are compacted vertically in stacks with intrinsic shorting through failed cells to maintain operation of each string. DOE

N91-19354*# National Aeronautics and Space Administration. Lewis Research Center, Cleveland, OH.
EFFECT OF DISLOCATIONS ON THE OPEN-CIRCUIT VOLTAGE, SHORT-CIRCUIT CURRENT AND EFFICIENCY OF HETEROEPITAXIAL INDIUM PHOSPHIDE SOLAR CELLS
Raj K. Jain and Dennis J. Flood 1990 7 p Presented at the 5th International Photovoltaic Science and Engineering Conference, Kyoto, Japan, 26-30 Nov. 1990; sponsored by the Japan Society of Applied Physics, Inst. of Electrical Engineers of Japan, and the Foundation for the Advancement of In
(NASA-TM-103762; E-6024; NAS 1.15:103762) Avail: NTIS HC/MF A02 CSCL 09C

Excellent radiation resistance of indium phosphide solar cells makes them a promising candidate for space power applications, but the present high cost of starting substrates may inhibit their large scale use. Thin film indium phosphide cells grown on Si or GaAs substrates have exhibited low efficiencies, because of the generation and propagation of large number of dislocations. Dislocation densities were calculated and its influence on the open circuit voltage, short circuit current, and efficiency of heteroepitaxial indium phosphide cells was studied using the PC-1D. Dislocations act as predominant recombination centers and are required to be controlled by proper transition layers and improved growth techniques. It is shown that heteroepitaxial grown cells could achieve efficiencies in excess of 18 percent AMO by controlling

the number of dislocations. The effect of emitter thickness and surface recombination velocity on the cell performance parameters vs. dislocation density is also studied. Author

N91-19355# Jet Propulsion Lab., California Inst. of Tech., Pasadena.
VIABILITY STUDY OF PHOTOVOLTAIC SYSTEMS ADDED TO TERRESTRIAL ELECTRIC VEHICLES
W. E. Rippel Sep. 1990 182 p
(Contract DE-AI01-85CE-89008)
(DE91-007689; JPL-D-7824) Avail: NTIS HC/MF A09

The purpose of the following computer study is to determine the set of necessary conditions under which the addition of photovoltaic (PV) cells to electric vehicles provides a net utility or economic benefit. Economic benefits are given the primary focus and are evaluated in terms of a payback period. DOE

N91-19356# Fermi National Accelerator Lab., Batavia, IL.
MODELING A FERRITE-TUNED RF CAVITY
M. Popovic 1 Nov. 1990 4 p
(Contract DE-AC02-76CH-03000)
(DE91-008235; FNAL-TM-1710) Avail: NTIS HC/MF A01

A Fermilab booster RF cavity has been modeled using computer codes collectively known as MAFIA. Because of the complicated geometry of these cavities, over 87,000 mesh points were used to obtain an accurate simulation. The results of the numerical simulations were then compared with experimentally-measured resonant frequencies. The reasonable agreement found between the calculations and the experimental data indicates that the URMEL-3D part of the MAFIA codes can be used to describe and design RF cavities with a permeability as high as mu = 12.0 and with a geometry as complicated as that exhibited by the Fermilab booster cavities. DOE

N91-19357# Maryland Univ., College Park. Lab. for Plasma Research.
AN ENERGY RECOVERY SYSTEM FOR A QUASI-OPTICAL GYROTRON
A. Singh, V. L. Granatstein, G. Hazel, G. Saraph, J. M. Cooperstein, and T. Hargreaves (Naval Research Lab., Washington, DC.) 1990 4 p Presented at the 15th International Conference on Infrared and Millimeter Waves, Lake Buena Vista, 10-14 Dec. 1990
(Contract DE-FG05-87ER-52147)
(DE91-008317; CONF-901248-1) Avail: NTIS HC/MF A01

Design of a depressed collector system for a quasi-optical gyrotron, which had a severe constraint on the maximum allowable radius of the collector region is outlined. The needs for unwinding of spent beam and for energy sorting could be accommodated by precise control of the magnetic field profile, especially in the collector region. Techniques used for defining and obtaining such profiles; and for dovetailing the profile with the collector geometry are discussed. Results on profiles and electron trajectories are presented, which demonstrate the feasibility of the design. From primary electron trajectories a collector efficiency of up to 68 percent was calculated for a three collector design. DOE

N91-19358# Maryland Univ., College Park. Lab. for Plasma Research.
A PROGRAM OF HIGH POWER MICROWAVE SOURCE RESEARCH AND DEVELOPMENT FROM 8 GHz TO 600 GHz
V. L. Granatstein, T. M. Antonsen, Jr., S. Bidwell, J. Booske, Y. Carmel, W. W. Destler, R. A. Kehs, P. E. Latham, B. Levush, and W. R. Lou et al 1990 12 p Presented at the 8th International Conference on High-Power Particle Beams, Novosibirsk, USSR, 2-5 Jul. 1990
(Contract DE-FG05-87ER-52147)
(DE91-008320; CONF-9007111-15) Avail: NTIS HC/MF A03

Research results are reviewed both on a plasma filled, backward wave oscillator (BWO), and on a free electron laser (FEL) driven by a sheet electron beam. Recently, it was demonstrated that a plasma filled BWO driven by an intense relativistic electron beam can generate hundreds of megawatts of microwave radiation at an unusually high efficiency of 40 percent compared with a typical efficiency of approx. 10 percent in a BWO without a background plasma. Furthermore, the enhanced efficiency can be maintained even for large electron beam currents approaching the vacuum space charge limiting current, and it is anticipated that this might hold even for larger current values. Theoretical studies and numerical simulations indicate that the enhanced efficiency as well as a lower value for the start oscillation current in the linear regime may be due to the finite length of the BWO circuit coupled with modification of the dispersion relation due to the background plasma. In the case of the FEL studies, designs are presented for a 1 MW, CW, tapered FEL amplifier operating at frequencies of 280 and 560 GHz. A short wiggler period (l sub w) approx. 1 cm is combined with a sheet beam of electrons having energy approx. 1 MeV. Depressed collector techniques would allow the main power supply rating to be reduced to approx. 200 kV. Efficient sheet beam transport (greater than 99 percent) was demonstrated through 10 wiggler periods, and transport through 60 wiggler periods is currently under study. Finally, plans for a proof-of-principle tapered FEL amplifier experiment at 94 GHz are presented. DOE

N91-19359# Brookhaven National Lab., Upton, NY.
RADIATION DAMAGE STUDIES ON HYBRID PREAMPLIFIERS
H. W. Kraner, J. A. Kierstead, P. W. Levy, S. Rescia, V. Radeka, and A. Stevens (Argonne National Lab., IL.) Oct. 1990 8 p Presented at the Symposium on Detector Research and Development for the Superconducting Super Collider, Fort Worth, TX, 15-18 Oct. 1990
(Contract DE-AC02-76CH-00016)
(DE91-008411; BNL-45623; CONF-9010212-34) Avail: NTIS HC/MF A02

Low noise hybrid preamplifiers have been irradiated with Co-60 gamma rays and fast neutrons at both room temperature and 120 K to study radiation effects on the noise characteristics. Increase in low frequency parallel noise was observed in preamps powered during irradiation by Co-60 at 1.45 Mrad at room temperature and at 12 Mrad at 120 K and for neutron fluences at 10E13n/sq cm. Annealing and relaxation effects will be discussed. DOE

N91-19360# Brookhaven National Lab., Upton, NY.
MONOLITHIC RADIATION HARD CHARGE SENSITIVE PREAMPLIFIER USING JUNCTION FIELD EFFECT TRANSISTORS
S. Rescia, V. Radeka, P. F. Manfredi, and V. Speziali (Pavia Univ., Italy) Nov. 1990 8 p Presented at the 1990 IEEE Nuclear Science Symposium, Arlington, VA, 23-27 Oct. 1990
(Contract DE-AC02-76CH-00016)
(DE91-008437; BNL-44673; CONF-9010220-26) Avail: NTIS HC/MF A02

A monolithic preamplifier entirely based on epitaxial channel, diffused gate N-JFETs has been designed and thoroughly investigated by means of SPICE simulation and breadboard implementation. Integration of the circuit is now in progress on the base of the technological processes that expected to retain the characteristics of noise and radiation tolerance that these JFETs feature as discrete devices. DOE

N91-19361# Brookhaven National Lab., Upton, NY.
NEUTRON RADIATION DAMAGE STUDIES ON SILICON DETECTORS
Zheng Li, W. Chen, and H. W. Kraner Oct. 1990 9 p Presented at the Symposium on Detector Research and Development for the Superconducting Super Collider, Fort Worth, TX, 15-18 Oct. 1990
(Contract DE-AC02-76CH-00016)
(DE91-008441; BNL-45381; CONF-9010212-35) Avail: NTIS HC/MF A02

Effects of neutron radiation on electrical properties of Si detectors were studied. At high neutron fluence (Phi(sub n) is greater than or equal to 10(exp 12) n/sq cm), C-V characteristics of detectors with high resistivities (rho is greater than or equal to 1 k(Omega)/cm) become frequency dependent. A two-trap level

model describing this frequency dependent effect is proposed. Room temperature anneal of neutron damaged (at LN(sub 2) temperature) detectors shows three anneal stages, while only two anneal stages were observed in elevated temperature anneal.
DOE

N91-19362# Sheffield Univ. (England). Dept. of Control Engineering.
PERFORMANCE MONITORING IN NONLINEAR ADAPTIVE NOISE CANCELLATION
S. A. Billings and F. A. Alturki Nov. 1990 30 p
(RR-409; ETN-91-98843) Avail: NTIS HC/MF A03

Correlation based model validity tests are introduced to monitor the operation of nonlinear adaptive noise cancellation filters and to detect if the filters are operating correctly or incorrectly. The tests are derived for a NARMAX (Nonlinear Auto Regressive Moving Average model with eXogeneous inputs) filter design based on a Sub Optimal Least Squares (SOLS) estimation algorithm. Simulation studies are included to illustrate the performance of the new tests.
ESA

N91-19363# Helsinki Univ. of Technology, Espoo (Finland). Radio Lab.
DEVELOPMENT OF COMPONENTS AND SUBSYSTEMS FOR LOW NOISE RECEIVERS AT MICRO- AND MILLIMETER WAVES Ph.D. Thesis
Juhani K. Peltonen Sep. 1990 66 p
(S-187; ISBN-951-22-0382-0; ISSN-0355-5712; ETN-91-98913)
Avail: NTIS HC/MF A04

The development of low noise receivers at micro- and millimeter wave frequencies mainly intended for radio astronomical studies and remote sensing applications are discussed. The work is divided into three parts: design and construction of cryogenic, low noise MESFET (Metal Semiconductor Field Effect Transistor) and HEMT (High Electron Mobility Transistor) amplifiers, studies on semiconductor local oscillators and phase locking of mm wave Gunn oscillators. The basic theory of low noise transistor amplifiers employing scattering and noise parameters of an active device is reviewed. Stability problems of amplifiers and noise measurement techniques especially applicable to cryogenic systems are discussed. Several low noise amplifiers were constructed for the frequency range of 1 to 22 GHz. As an example, a 4 GHz cryogenic MESFET IF amplifier with 20 K noise temperature was developed. A two stage coaxial HEMT amplifier with T(sub A) = 300 K at room temperature was constructed. Various designs of semiconductor local oscillators needed for mm wave receivers are reviewed. Experimental verification of the theoretical model for the waveguide mounting structure of Gunn diodes is given at frequencies of 35 to 53 GHz. Fundamental frequency local oscillators with an output power of approximately 50 mW and mechanical tuning range of 5 to 10 GHz (center frequency of 45 GHz) were constructed. Description of the phase locking scheme (exploiting bias tuning of Gunn oscillators) of the 72 to 115 GHz receiver is given. The additional factors needed in application of the basic phaselock theory to mm wave oscillators are discussed.
ESA

N91-19154*# Gibbel Corp., Palos Verdes Estates, CA.
THERMAL/VACUUM VS. THERMAL ATMOSPHERIC TESTING OF SPACE FLIGHT ELECTRONIC ASSEMBLIES
Mark Gibbel *In* NASA, Goddard Space Flight Center, 16th Space Simulation Conference Confirming Spaceworthiness Into the Next Millennium Nov. 1990 p 344-356 (For primary document see N91-19126 11-18)
Avail: NTIS HC/MF A20 CSCL 09A

N91-20028*# Savannah State Coll., GA. Dept. of Engineering Technology.
AN EXPANSION PLAN FOR THE 60 Hz POWER DISTRIBUTION SYSTEM AT KSC: LC-39 SUBSTATIONS LOAD ALLOCATION PLAN
Alex Kalu *In* NASA, John F. Kennedy Space Center, Research Reports: 1990 NASA/ASEE Summer Faculty Fellowship Program Sep. 1990 p 169-196 (For primary document see N91-20022 11-99)
(Grant NGT-60002)
Avail: NTIS HC/MF A23 CSCL 10B

34 FLUID MECHANICS AND HEAT TRANSFER

Includes boundary layers; hydrodynamics; fluidics; mass transfer; and ablation cooling.

For related information see also *02 Aerodynamics* and *77 Thermodynamics and Statistical Physics.*

N91-19364 Department of the Navy, Washington, DC.
FLUID MIXING DEVICE HAVING A CONICAL INLET AND A NONCIRCULAR OUTLET Patent
Klaus C. Schadow, inventor (to Navy), Ephraim Gutmark, inventor (to Navy), Kenneth J. Wilson, inventor (to Navy), and Robert A. Smith, inventor (to Navy) 18 Sep. 1990 17 p Filed 12 Apr. 1988
(AD-D014708; US-Patent-4,957,242; US-Patent-Appl-SN-180751; US-Patent-Class-239-590) Avail: US Patent and Trademark Office CSCL 13/7

The patent is directed to a fluid mixing device in which a jet of first fluid is passed through a nozzle having a conical inlet section and a noncircular, elongated, exit section. The jet of first fluid mixes with a second fluid located downstream of the device. In operation, the intersection of the conical and elongated sections produces axial rotation in the first fluid. Intense, 3-D, axial and circumferential vortical structures are created. These structures then interact with the high modes of azimuthal instabilities that are common to the elongated configuration. The jet of first fluid evolves into two secondary jets, generating a double shear layer inside the flow. Highly efficient mixing of the fluids, in both the outside and inside (core) segments of the jet, is achieved within a relatively small mixing space.
GRA

N91-19365 Max-Planck-Inst. fuer Physik und Astrophysik, Garching (Germany, F.R.). Inst. fuer Extraterrestrische Physik.
THERMAL INSTABILITIES IN COOLING FLOWS: THE EVOLUTION OF NEARLY SPHERICAL PERTURBATIONS
W. Brinkmann, S. Massaglia (Politecnico di Torino, Italy), and E. Mueller Feb. 1990 34 p Previously announced in IAA as A91-14712 Submitted for publication Sponsored in part by Max-Planck-Gesellschaft
(MPE-Preprint-176; ETN-91-98600) Copyright Avail: Fachinformationszentrum Karlsruhe, 7514 Leopoldshafen-Eggenstein 2, Fed. Republic of Germany

The temporal evolution of thermally unstable blobs in connection with the problem of mass accretion in cooling flows is studied numerically, in one and two dimensions. The hydrodynamic equations are solved in spherical geometry for an initially homogeneous cooling medium, including thermal conduction. The initial isobaric perturbations are followed in time until self gravity effects, not included in the equations, are thought to become important. In the one dimensional case, it is found that after the linear phase the perturbation evolves on time scales much shorter than the linear ones and depending on the initial matter density, a cool, dense core of size approximately 0.001 - 0.01 times the initial perturbation scale size forms. This grows in size due to continuous accretion from the (hotter) outside gas and may become eventually gravitationally unstable. The one dimensional results are compared with others obtained for a plane-parallel slab geometry. The qualitative difference between a one dimensional and a two dimensional calculation with otherwise very similar physical parameters is shown.
ESA

N91-19366*# Institute for Computer Applications in Science and Engineering, Hampton, VA.
FILTERING ANALYSIS OF A DIRECT NUMERICAL SIMULATION OF THE TURBULENT RAYLEIGH-BENARD PROBLEM Final Interim Report
T. M. Eidson, M. Y. Hussaini, and T. A. Zang Dec. 1990 50 p
(Contract NAS1-18605)
(NASA-CR-187488; NAS 1.26:187488; ICASE-IR-15) Avail: NTIS HC/MF A03 CSCL 20D

A filtering analysis of a turbulent flow was developed which provides details of the path of the kinetic energy of the flow from its creation via thermal production to its dissipation. A low-pass spatial filter is used to split the velocity and the temperature field into a filtered component (composed mainly of scales larger than a specific size, nominally the filter width) and a fluctuation component (scales smaller than a specific size). Variables derived from these fields can fall into one of the above two ranges or be composed of a mixture of scales dominated by scales near the specific size. The filter is used to split the kinetic energy equation into three equations corresponding to the three scale ranges described above. The data from a direct simulation of the Rayleigh-Benard problem for conditions where the flow is turbulent are used to calculate the individual terms in the three kinetic energy equations. This is done for a range of filter widths. These results are used to study the spatial location and the scale range of the thermal energy production, the cascading of kinetic energy, the diffusion of kinetic energy, and the energy dissipation. These results are used to evaluate two subgrid models typically used in large-eddy simulations of turbulence. Subgrid models attempt to model the energy below the filter width that is removed by a low-pass filter. Author

N91-19367*# Texas Univ., Arlington.
CALCULATIONS OF SEPARATED 3-D FLOWS WITH A PRESSURE-STAGGERED NAVIER-STOKES EQUATIONS SOLVER Final Report
S.-W. Kim Mar. 1991 14 p
(Contract NCC3-180)
(NASA-CR-187065; E-5988; NAS 1.26:187065) Avail: NTIS HC/MF A03 CSCL 20D

A Navier-Stokes equations solver based on a pressure correction method with a pressure-staggered mesh and calculations of separated three-dimensional flows are presented. It is shown that the velocity pressure decoupling, which occurs when various pressure correction algorithms are used for pressure-staggered meshes, is caused by the ill-conditioned discrete pressure correction equation. The use of a partial differential equation for the incremental pressure eliminates the velocity pressure decoupling mechanism by itself and yields accurate numerical results. Example flows considered are a three-dimensional lid driven cavity flow and a laminar flow through a 90 degree bend square duct. For the lid driven cavity flow, the present numerical results compare more favorably with the measured data than those obtained using a formally third order accurate quadratic upwind interpolation scheme. For the curved duct flow, the present numerical method yields a grid independent solution with a very small number of grid points. The calculated velocity profiles are in good agreement with the measured data. Author

N91-19368# Pacific Northwest Lab., Richland, WA.
IDENTIFICATION OF FLOW AND VOLUME PARAMETERS IN MULTIZONE SYSTEMS USING A SINGLE GAS TRACER TECHNIQUE
P. J. ONeill and R. R. Crawford Jan. 1991 23 p Presented at the ASHRAE Winter Meeting, New York, NY, 19-23 Jan. 1991
(Contract DE-AC06-76RL-01830)
(DE91-006894; PNL-SA-18944; CONF-910127-4) Avail: NTIS HC/MF A03

This work evaluates a new method, based upon tracer gas techniques, for determining interzonal airflows and effective volumes in a multizone enclosure. The proposed method uses a single tracer gas to disturb the zones. A state-space formulation is used to model the multizone system. The concentration data are used in combination with a recursive least-squares identification algorithm to determine all of the interzonal airflows and effective volumes. A three-zone experimental test facility was constructed to validate the proposed method. The results indicate that the gas technique was able to estimate the interzonal airflows and effective volumes of the experimental facility to within 10 percent in most cases. The tests also showed that for a three-zone system, the best accuracy was obtained using a sampling interval, T, in the range 0.1 less than or equal to T/tau(sub min) less than or equal to 0.2. The fastest time constant of the system, tau(sub min), is based upon the airflows and effective volumes of the continuous-time system representation. DOE

N91-19369*# National Aeronautics and Space Administration. Lewis Research Center, Cleveland, OH.
TWO REFERENCE TIME SCALES FOR STUDYING THE DYNAMIC CAVITATION OF LIQUID FILMS
D. C. Sun and David E. Brewe (Army Aviation Research and Development Command, Cleveland, OH.) 1991 7 p Presented at the 1991 Cavitation Symposium at the Joint ASME/JSME Fluids Engineering Conference, Portland, OR, 23-26 Jun. 1991
(DA Proj. 1L1-61102-AH-45)
(NASA-TM-103673; E-5885; NAS 1.15:103673; AVSCOM-TR-90-C-030) Avail: NTIS HC/MF A02 CSCL 20D

Two formulas, one for characteristic time of filling a void with a vapor of the surrounding liquid, and one of filling the void by diffusion of the dissolved gas in the liquid, are derived. Based on this analysis, it is seen that in an oil film bearing operating under dynamic loads, the content of cavitation region should be oil vapor rather than the air liberated from solution, if the oil is free of entrained air. Author

N91-19370*# National Aeronautics and Space Administration. Lewis Research Center, Cleveland, OH.
TURBULENT BOUNDARY LAYER SEPARATION OVER A REARWARD FACING RAMP AND ITS CONTROL THROUGH MECHANICAL EXCITATION
Daniel J. McKinzie, Jr. 1991 28 p Presented at the 29th Aerospace Sciences Meeting, Reno, NV, 7-10 Jan. 1991; sponsored by AIAA
(NASA-TM-103702; E-5860; NAS 1.15:103702; AIAA-91-0253)
Avail: NTIS HC/MF A03 CSCL 20D

A vane oscillating about a fixed point at the inlet to a two-dimensional 20 degree rearward facing ramp has proven effective in delaying the separation of a turbulent boundary layer. Measurements of the ramp surface static pressure coefficient obtained under the condition of vane oscillation and constant inlet velocity revealed that two different effects occurred with surface distance along the ramp. In the vicinity of the oscillating vane, the pressure coefficients varied as a negative function of the vane's trailing edge rms velocity; the independent variable on which the rms velocity depends are the vane's oscillation frequency and its displacement amplitude. From a point downstream of the vane to the exit of the ramp; however, the pressure coefficient varied as a more complex function of the two independent variables. That is, it was found to vary as a function of the vane's oscillation frequency throughout the entire range of frequencies covered during the test, but over only a limited range of the trailing edge displacement amplitudes covered. More specifically, the value of the pressure coefficient was independent of increases in the vane's displacement amplitude above approximately 35 inner wall units of the boundary layer. Below this specific amplitude it varied as a function of the vane's trailing edge rms velocity. This height is close to the upper limit of the buffer layer. A parametric study was made to determine the variation of the maximum static pressure recovery as a function of the vane's oscillation frequency, for several ramp inlet velocities and a constant displacement amplitude of the vane's trailing edge. The results indicate that the phenomenon producing the optimum delay of separation may be Strouhal number dependent. Corona anemometer measurements obtained in the inner wall regions of the boundary layer for the excited case reveal a large range of unsteadiness in the local velocities. These measurements imply the existence of inflections

in the profiles, which provide a mechanism for resulting inviscid flow instabilities to produce turbulence in the near wall region, thereby delaying separation of the boundary layer. Author

N91-19371*# National Aeronautics and Space Administration. Lewis Research Center, Cleveland, OH.
A SUMMARY OF EXISTING AND PLANNED EXPERIMENT HARDWARE FOR LOW-GRAVITY FLUIDS RESEARCH
Myron E. Hill and Terence F. OMalley 1991 44 p Presented at the 29th Aerospace Sciences Meeting, Reno, NV, 7-10 Jan. 1991; sponsored by AIAA
(NASA-TM-103706; E-5931; NAS 1.15:103706; AIAA-91-0777)
Avail: NTIS HC/MF A03 CSCL 20D

An overview is presented of (1) existing ground-based, low gravity research facilities, with examples of hardware capabilities, and (2) existing and planned space-based research facilities, with examples of current and past flight hardware. Low-gravity, ground-based facilities, such as drop towers and aircraft, provide the experimenter with quick turnaround time, easy access to equipment, gravity levels ranging from 10(exp -2) to 10(exp -6) G, and low-gravity durations ranging from 2 to 30 sec. Currently, the only operational space-based facility is the Space Shuttle. The Shuttle's payload bay and middeck facilities are described. Existing and planned low-gravity fluids research facilities are also described with examples of experiments and hardware capabilities. Author

N91-19372*# National Aeronautics and Space Administration. Lewis Research Center, Cleveland, OH.
THE EFFECT OF SMALL STREAMWISE VELOCITY DISTORTION ON THE BOUNDARY LAYER FLOW OVER A THIN FLAT PLATE WITH APPLICATION TO BOUNDARY LAYER STABILITY THEORY
M. E. Goldstein, S. J. Leib, and S. J. Cowley (Cambridge Univ., England) Dec. 1990 37 p
(NASA-TM-103668; E-5759-1; ICOMP-90-25; NAS 1.15:103668)
Avail: NTIS HC/MF A03 CSCL 20D

Researchers show how an initially linear spanwise disturbance in the free stream velocity field is amplified by leading edge bluntness effects and ultimately leads to a small amplitude but linear spanwise motion far downstream from the edge. This spanwise motion is imposed on the boundary layer flow and ultimately causes an order-one change in its profile shape. The modified profiles are highly unstable and can support Tollmein-Schlichting wave growth well upstream of the theoretical lower branch of the neutral stability curve for a Blasius boundary layer. Author

N91-19373*# National Aeronautics and Space Administration. Lewis Research Center, Cleveland, OH.
CRITICAL-LAYER NONLINEARITY IN THE RESONANCE GROWTH OF THREE-DIMENSIONAL WAVES IN BOUNDARY LAYERS
Reda R. Mankbadi Nov. 1990 58 p
(NASA-TM-103639; E-5000; NAS 1.15:103639) Avail: NTIS HC/MF A04 CSCL 20D

The nonlinear interactions of a triad of initially linear stability waves are addressed. The triad consisted of a single two-dimensional mode at a given frequency and two oblique modes with equal and opposite spanwise wave numbers. The oblique waves were at half the frequency and streamwise wave number of the two-dimensional mode. Attention was focused on the boundary-layer transition at low frequencies and high Reynolds numbers. A five-zoned structure and low-frequency scaling were used to derive the nonlinear-interaction equations. The initial nonlinear development of the waves was analyzed; the results indicated that the two-dimensional wave behaves according to linear theory. Nonlinear interactions caused exponential-of-an-exponential growth of the oblique modes. This resonant amplification of the subharmonic depended on the initial amplitude of the two-dimensional wave and on the initial phase angle between the two-dimensional wave and the oblique waves. The resonant growth of the oblique modes was more pronounced at lower frequencies than at higher frequencies. The results are in good agreement with experimental results and offer explanations of the observed process. Author

N91-19374*# National Aeronautics and Space Administration. Lewis Research Center, Cleveland, OH.
EXPERIMENTAL INVESTIGATION OF A SINGLE FLUSH-MOUNTED HYPERMIXING NOZZLE
David O. Davis, Warren R. Hingst, and A. Robert Porro 1990 13 p Presented at the Second International Aerospace Planes Conference, Orlando, FL, 29-31 Oct. 1990; sponsored by AIAA Previously announced in IAA as A91-14466
(NASA-TM-103726; E-5960; NAS 1.15:103726; AIAA-90-5240)
Avail: NTIS HC/MF A03 CSCL 20D

The results of an experimental wind tunnel investigation of a circular supersonic jet (m sub j = 3.47) injected at a 10 degree angle into a supersonic freestream. The jet penetrates a boundary layer, which has a thickness approximately the same as the jet nozzle exit diameter. Measurements were made for nominal freestream Mach numbers of 1.6, 2.0, 2.5, and 3.0. Three jet total pressures were run at each freestream Mach number, resulting in twelve separate operating conditions. Mean data accumulated by means of static and total pressure probe instrumentation are presented at two axial stations: seven jet nozzle diameters upstream and 15 jet nozzle diameters downstream from where the centerline of the nozzle intersects the wind tunnel wall. For one condition at each freestream Mach number, the jet air was seeded with a hydrocarbon trace gas and the flow was sampled at the downstream measurement plane to quantify the mean mixing of the two streams. Surface oil flow visualization was also used to investigate the flow interaction. All results are for air-to-air mixing. The measurements indicate the presence of two pairs contra-rotating vortices. One pair follows the jet trajectory and tends to split the jet into two streams. A smaller pair, rotating in an opposite sense, develops in the near wall region. Reported results include Mach number and volume fraction distributions in the cross plane, as well as jet penetration and mixing efficiency. Author

N91-19375*# National Aeronautics and Space Administration. Lewis Research Center, Cleveland, OH.
A 2-D OSCILLATING FLOW ANALYSIS IN STIRLING ENGINE HEAT EXCHANGERS
Kyung H. Ahn and Mounir B. Ibrahim (Cleveland State Univ., OH.) 1991 9 p Presented at the 1991 Joint ASME-JSME Fluids Engineering Conference, Portland, OR, 24-26 Jun. 1991
(NASA Order C-99066-G)
(NASA-TM-103781; E-6055; ICOMP-91-04; NAS 1.15:103781)
Avail: NTIS HC/MF A02 CSCL 20D

A two dimensional oscillating flow analysis was conducted, simulating the gas flow inside Stirling heat exchangers. Both laminar and turbulent oscillating pipe flow were investigated numerically for Re(max) = 1920 (Va = 80), 10800 (Va = 272), 19300 (Va = 272), and 60800 (Va = 126). The results are compared with experimental results of previous investigators. Also, predictions of the flow regime on present oscillating flow conditions were checked by comparing velocity amplitudes and phase differences with those from laminar theory and quasi-steady profile. A high Reynolds number k-epsilon turbulence model was used for turbulent oscillating pipe flow. Finally, performance evaluation of the K-epsilon model was made to explore the applicability of quasi-steady turbulent models to unsteady oscillating flow analysis. Author

N91-19376*# Sverdrup Technology, Inc., Brook Park, OH.
COOL-DOWN AND FROZEN START-UP BEHAVIOR OF A GROOVED WATER HEAT PIPE Final Report
Jong Hoon Jang Dec. 1990 8 p Presented at the 1991 International Solar Energy Conference, Reno, NV, 17-22 Mar. 1991; cosponsored by ASME and Japan Society of Mechanical Engineers
(Contract NAS3-25266)

(NASA-CR-187053; E-5923; NAS 1.26:187053) Avail: NTIS HC/MF A02 CSCL 20D

A grooved water heat pipe was tested to study its characteristics during the cool-down and start-up periods. The water heat pipe was cooled down from the ambient temperature to below the freezing temperature of water. During the cool-down, isothermal conditions were maintained at the evaporator and adiabatic sections until the working fluid was frozen. When water was frozen along the entire heat pipe, the heat pipe was rendered inactive. The start-up of the heat pipe from this state was studied under several different operating conditions. The results show the existence of large temperature gradients between the evaporator and the condenser, and the moving of the melting front of the working fluid along the heat pipe. Successful start-up was achieved for some test cases using partial gravity assist. The start-up behavior depended largely on the operating conditions. Author

N91-19377# Syracuse Univ. Research Inst., NY. Dept. of Chemical Engineering.

NUMERICAL AND PHYSICAL MODELLING OF BUBBLY FLOW PHENOMENA

A. S. Sangani Jan. 1991 20 p

(Contract DE-FG02-90ER-14136)

(DE91-007461; DOE/ER-14136/1) Avail: NTIS HC/MF A03

The objective of this study is to develop theoretical tools -- analytical as well as numerical -- for understanding how the flows of bubbly liquids are affected by its microstructure, i.e., the detailed spatial, size, and velocity distribution of bubbles, and how the microstructure, in turn, is affected by the flow. This report describes the progress made to date on the several problems that are being studied. The first problem is concerned with the molecular-dynamics type simulations of monodispersed bubbly liquids under equilibrium and homogeneous conditions and their application to slightly inhomogeneous flows. The Reynolds number is large and the Weber and Froud numbers are small in these simulations. The second problem is concerned with the simulations of flows of bubbly liquids undergoing small amplitude oscillatory motion. Both the cases of bubbles with rigid (due to impurities) and stress-free interfaces are examined. The results are related to the added mass, Basset, and viscous drag coefficients. The third problem is concerned with the acoustic wave propagation in bubbly liquids at frequencies above natural frequency of the bubbles. The second problem is completed as of this writing. Work on the other two problems is currently in progress. A summary of the work to be carried out during the period 1/91 to 6/92 is given in the last section. DOE

N91-19378*# Tennessee Univ., Knoxville. Dept. of Mechanical and Aerospace Engineering.

IN-SPACE EXPERIMENT ON THERMOACOUSTIC CONVECTION HEAT TRANSFER PHENOMENON-EXPERIMENT DEFINITION Final Report

M. Parang and D. S. Crocker Feb. 1991 111 p

(Contract NAS3-25359)

(NASA-CR-187070; NAS 1.26:187070) Avail: NTIS HC/MF A06 CSCL 20D

The definition phase of an in-space experiment in thermoacoustic convection (TAC) heat transfer phenomenon is completed and the results are presented and discussed in some detail. Background information, application and potential importance of TAC in heat transfer processes are discussed with particular focus on application in cryogenic fluid handling and storage in microgravity space environment. Also included are the discussion on TAC space experiment objectives, results of ground support experiments, hardware information, and technical specifications and drawings. The future plans and a schedule for the development of experiment hardware (Phase 1) and flight tests and post-flight analysis (Phase 3/4) are also presented. The specific experimental objectives are rapid heating of a compressible fluid and the measurement of the fluid temperature and pressure and the recording and analysis of the experimental data for the establishment of the importance of TAC heat transfer process. The ground experiments that were completed in support of the experiment definition included fluid temperature measurement by a modified shadowgraph method, surface temperature measurements by thermocouples, and fluid pressure measurements by strain-gage pressure transducers. These experiments verified the feasibility of the TAC in-space experiment, established the relevance and accuracy of the experimental results, and specified the nature of the analysis which will be carried out in the post-flight phase of the report. Author

N91-19379*# Old Dominion Univ., Norfolk, VA. Dept. of Mechanical Engineering and Mechanics.

DEVELOPMENT OF A PERTURBATION GENERATOR FOR VORTEX STABILITY STUDIES Progress Report, period ending 31 Dec. 1990

J. E. Riester and Robert L. Ash Mar. 1991 161 p

(Grant NAG1-530)

(NASA-CR-188051; NAS 1.26:188051) Avail: NTIS HC/MF A08 CSCL 20D

Theory predicts vortex instability when subjected to certain types of disturbances. It was desired to build a device which could introduce controlled velocity perturbations into a trailing line vortex in order to study the effects on stability. A perturbation generator was designed and manufactured which can be attached to the centerbody of an airfoil type vortex generator. Details of design tests and manufacturing of the perturbation generator are presented. The device produced controlled perturbation with frequencies in excess of 250 Hz. Preliminary testing and evaluation of the perturbation generator performance was conducted in a 4 inch cylindrical pipe. Observations of vortex shedding frequencies from a centerbody were measured. Further evaluation with the perturbation generator attached to the vortex generator in a 2 x 3 foot wind tunnel were also conducted. Hot-wire anemometry was used to confirm the perturbation generator's ability to introduce controlled frequency fluctuations. Comparison of the energy levels of the disturbances in the vortex core was made between locations 42 chord lengths and 15 chord lengths downstream. Author

N91-19380# Central Research Inst. of Electric Power Industry, Chiba (Japan).

THE APPLICATION OF SIMULATION MODEL FOR THE FLOW INDUCED BY AIR BUBBLE PLUME IN THERMALLY STRATIFIED RESERVOIRS

S. Matsunashi and Y. Miyanaga 1989 38 p In JAPANESE

(DE91-003064; CRIE-U-88029) Avail: NTIS HC/MF A03

Recently air bubble plume has been suggested as a method of water quality purification. In order to predict the change of water quality in the reservoirs by air bubble plume, the simulation model for the flow induced by air bubble plume is conducted, which is based on the concept of entrainment by the air bubble plume. The model explains the results of experimental data in the laboratory and field. DOE

N91-19381# Lawrence Livermore National Lab., CA.

CONSERVATION OF ENERGY, MOMENTUM, AND ANGULAR MOMENTUM IN LAGRANGIAN STAGGERED-GRID HYDRODYNAMICS

D. E. Burton 16 Nov. 1990 13 p Presented at the 1990 Nuclear Explosives Code Developers' Conference, Monterey, 6-9 Nov. 1990

(Contract W-7405-eng-48)

(DE91-008059; UCRL-JC-105926; CONF-9011149-11) Avail: NTIS HC/MF A03

The conservation properties for general formulations of Lagrangian staggered-grid hydrodynamics (SGH) are investigated in the small timestep limit. Form-preserving definitions and exact conservation laws are found to exist for all physically relevant quantities (mass, linear momentum, total energy, and angular momentum). The analysis is multi-dimensional and applies to arbitrarily connected grids. The momentum equation is found to lead to an exactly conserved energy current between internal and kinetic energy fields. The energy current is not properly calculated by SGH methods in which the work is differenced independently of the differenced momentum equation. This leads to the commonly

observed lack of energy conservation in SHG methods. It is also shown that SGH conserves angular momentum centered at the zone, but not at the node. These angular momentum results apply not only to SGH but to any method using a lumped mass approximation in the acceleration equation. This conservation accounts for the empirical observation in SGH that the motion of the zone centers is free from the spurious vorticity seen in the nodes. Consequently, vorticity can be calculated directly from the zone velocities and need not be separately integrated. This leads to an improved method for removing the spurious vorticity called the Damped Excess Vorticity (DEV) method. DOE

N91-19382# Cornell Univ., Ithaca, NY.
SYSTEMS NEAR THE ONSET AND IN THE WELL-DEVELOPED REGIMES OF TURBULENCE
E. D. Siggia 1991 4 p
(Contract DE-AC02-83ER-13044)
(DE91-008148; DOE/ER-13044/8) Avail: NTIS HC/MF A01

The dynamics of the three dimensional Euler equations as represented by the vorticity and strain have been studied numerically for smooth initial conditions. A variety of adaptive mesh techniques were implemented to follow the solution onto very small scales where characteristic vortex sheet structures appeared. Finite time singularities were not found. For discrete Hamiltonian systems, the geometric implications of the Painleve property (only poles in complex time) were examined. By exploiting the Hamilton-Jacobi equations, a symplectic augmented manifold is defined on which the solutions live for all times. The scaling laws for the heat flux in high Rayleigh number, Ra, Boussinesg convection are derived in the presence of a self generated mean flow. The maximum flow velocity scales as Ra(sup 3/7) and the heat flux as Ra(sup 2/7) in agreement with the Chicago experiments. DOE

N91-19383# Webb Inst. of Naval Architecture, Glen Cove, NY.
LIQUID SLOSHING IN CARGO TANKS. LIQUID SLOSH LOADING IN SLACK SHIP TANKS: FORCES ON INTERNAL STRUCTURE AND PRESSURES Final Report
N. A. Hamlin 1990 124 p Sponsored by Ship Structure Committee, Washington, DC
(Contract DTCG23-82-C-20016)
(PB91-129262; SSC-336) Avail: NTIS HC/MF A06 CSCL 20D

Based on a survey of 12 cases of sloshing damage on 7 tankers and other ships of dry cargo, ore-bulk-oil, bulk, and ore carrier types, 5 structural members were chosen for model testing to measure sloshing forces. Oscillating table tests were then run using partially filled tanks with realistic structure including the instrumented members. Sloshing forces and moment coefficients are reported as well as sloshing pressure coefficients from pressure measurements on the tanks. A linear superposition calculation for sloshing force on one member is shown. Author

N91-19384# Max-Planck-Inst. fuer Stroemungsforschung, Goettingen (Germany, F.R.).
TRAVELING TIME EFFECTS IN A CHANNEL FLOW Thesis
B. Sommerlade Jun. 1990 74 p In GERMAN; ENGLISH summary
(MPIS-10/1990; ISSN-0436-1199; ETN-91-98811) Avail: NTIS HC/MF A04

The influence of the nonlinear traveling time effect and its role in the generation of perturbations of planar channel flow are examined. The traveling time effect is described by an exact solution to the one dimensional equation of motion and continuity boundary value problem. The formalism of a retransformation in Euler coordinates is presented. The water experimental set up is described. The measuring methods enabling the measurement of the velocity and the observation of the layer height are explained. The construction and the mechanism of the equipment which realizes the modulation of the flow velocity by electromagnetic forces and allows the control of the parameter frequency and distortion amplitude are described. ESA

N91-19385# Max-Planck-Inst. fuer Stroemungsforschung, Goettingen (Germany, F.R.).
CALCULATION OF PULSATING LIQUID FREE JETS
Georg Grabitz Jul. 1990 20 p In GERMAN; ENGLISH summary
(MPIS-15/1990; ISSN-0436-1199; ETN-91-98812) Avail: NTIS HC/MF A03

A liquid free jet with strong velocity modulation is treated theoretically. The special shape of the jet is described by a simple analytical model based on kinematic effects. The interaction between different flow particles which start consecutively from the nozzle exit is neglected. This solution shows singular points and triple valued regions. In practice, these are regions where strong interaction of flow particles of different velocities can no longer be neglected. In the theoretical model, these regions are contracted to single points where a velocity jump occurs in the jet, and a secondary flow starts in lateral direction. The variation of the velocity in the jet causes the longitudinal velocity of different flow elements to be different. This is the reason for a bell like shape being formed. ESA

N91-19386# Universitaet der Bundeswehr Muenchen, Neubiberg (Germany, F.R.). Inst. fuer Raumfahrttechnik.
RESPONSE OF A SOLIDLY ROTATING AMPHORA-TYPE LIQUID COLUMN TO AXIAL EXCITATION
Helmut F. Bauer and Werner Eidel 1990 26 p
(LRT-WE-9-FB-06(1990); ETN-91-98813) Avail: NTIS HC/MF A03

The response of a solidly rotating finite liquid column, which under the action of an axial gravity assumes an amphora type equilibrium position, to axial excitation was determined. The column consists of incompressible and frictionless liquid. The response of the free surface elevation was obtained for the elliptic frequency range. ESA

N91-19387# Universitaet der Bundeswehr Muenchen, Neubiberg (Germany, F.R.). Inst. fuer Raumfahrttechnik.
EXPERIMENTAL STUDIES ON A NONLINEAR HYDROELASTIC VIBRATION OF CIRCULAR CYLINDRICAL TANKS
Masakatsu Chiba (Iwate Univ., Morioka, Japan) 1990 101 p
(LRT-WE-9-FB-10(1990); ETN-91-98814) Avail: NTIS HC/MF A06

Experimental studies were carried out on the nonlinear hydroelastic vibrations of a circular cylindrical tank system. A rigid wall tank with a flexible bottom, and a flexible wall tank with a rigid bottom were studied. In both cases, the tank was fully or partially filled with liquid having a free surface. The nonlinearity of the responses of contained liquid and bottom plate or flexible wall was investigated. The influence of the flexible bottom or flexible wall on the natural frequencies of the sloshing response in which liquid motions are predominant, as well as the influence of the contained liquid motions are predominant, as well as the influence of the contained liquid on the natural frequencies of the bulging response in which the motions of a bottom plate or flexible wall is predominant, were also clarified. Polyester foils with thickness 0.25 mm and 0.35 mm were used as a bottom plate and a flexible wall of the test tank, and water was used as a contained liquid. ESA

N91-19388# Universitaet der Bundeswehr Muenchen, Neubiberg (Germany, F.R.). Inst. fuer Raumfahrttechnik.
LIQUID SLOSHING RESPONSE IN A SPINNING CONTAINER DUE TO PITCHING EXCITATION
Helmut F. Bauer 1990 59 p
(LRT-WE-9-FB-11(1990); ETN-91-98815) Avail: NTIS HC/MF A04

In a solidly rotating container in microgravity or for which the axial acceleration is large, the response of the liquid due to pitching excitation exhibits resonances at the natural frequencies belonging to m = 1. These frequencies were determined for a free liquid surface and an interfacial surface of two immiscible liquids. According to twice the speed of rotation one has to distinguish elliptic frequency and a hyperbolic range where the natural

frequencies are greater than twice the spin frequency. The liquids were treated as incompressible and nonviscous. The response of the liquid to harmonic pitch excitation was determined for the free surface or interface displacement and the velocity distribution. ESA

N91-19389# Universitaet der Bundeswehr Muenchen, Neubiberg (Germany, F.R.). Inst. fuer Raumfahrttechnik.
RESPONSE OF A DIFFERENTLY AXIALLY EXCITED VISCOUS LIQUID LAYER IN ZERO-GRAVITY
Helmut F. Bauer 1990 83 p
(LRT-WE-9-FB-12(1990); ETN-91-98816) Avail: NTIS HC/MF A05

A cylindrical liquid layer around a rigid center core consisting of incompressible and viscous liquid is subjected to different axial excitations, such as one sided, counter directional and double sided unequal excitations. The response of the free liquid surface, the velocity and pressure distribution were determined. ESA

N91-19390# Universitaet der Bundeswehr Muenchen, Neubiberg (Germany, F.R.). Inst. fuer Raumfahrttechnik.
RESPONSE OF A VISCOUS LIQUID LAYER TO PITCH- AND ROLL-EXCITATION IN ZERO-GRAVITY ENVIRONMENT
Helmut F. Bauer 1990 113 p
(LRT-WE-9-FB-13(1990); ETN-91-98817) Avail: NTIS HC/MF A06

The response of a viscous liquid layer to pitching and roll excitation was determined. For a simplified analytical treatment, the no slip condition at the top and the bottom of the liquid column was abandoned in the pitching case. The response of the free liquid surface displacement and the velocity distribution were determined as a function of the reduced frequency for various surface tension parameters. Due to viscosity, the resonance amplitudes are finite and disappear for higher modes and shorter liquid layers. The velocity distribution, effective moment of inertia and effective damping were obtained for the liquid layer in roll excitation. ESA

N91-19391# Bristol Univ. (England). Dept. of Aerospace Engineering.
PARALLEL PROCESSING FOR PANEL METHODS
Steven P. Fiddes and Alan G. Chalmers Jul. 1990 11 p
(BU-414; ETN-91-98865) Avail: NTIS HC/MF A03

Panel methods are used extensively in aerodynamic studies of three dimensional inviscid incompressible flows. There are computationally intensive methods with very large data requirements. The sequential solution of these very large problems require supercomputer run times and memory. There is therefore great incentive to consider a cost effective implementation of panel methods on parallel systems. However, panel methods entail the generation and solution of a full non symmetric matrix both of which involve global data dependencies, traditionally regarded as inhibiting factors for parallelization. A novel approach to the efficient parallelization of a panel method on systems of MIMD processors is described. The parallelization of the panel method results in the majority of run time now being spent in solving the system of equations for the source vectors. Future work will therefore investigate more efficient parallel iterative solvers for large dense matrices and the possible use of direct solvers. ESA

N91-19392# Tampere Univ. of Technology (Finland). Lab. of Hydraulics and Automation.
METHODS FOR COMBINING A THEORETICAL AND AN EMPIRICAL APPROACH IN MODELLING PRESSURE AND FLOW CONTROL VALVES FOR CAE-PROGRAMS FOR FLUID POWER CIRCUITS Ph.D. Thesis
Heikki Handroos Helsinki, Finland Finnish Academy of Technology 1990 56 p Sponsored by K.F. and Maria Dunderberg Foundation; Emil Aaltonen Foundation; and Foundation for the Furthering of Technological Research
(Acta-Polytec-Scand-Me-96; ISBN-951-666-315X; ISSN-0001-687X; ETN-91-98914) Avail: NTIS HC/MF A04

An analytical mathematical model for a fluid power valve uses equations based on physical laws. The parameters consist of physical coefficients, dimensions of the internal elements, spring constants, etc. which are not provided by the component manufacturers. The valve has to be dismantled in order to determine their values. The model is only in accordance with a particular type of valve construction and there are a large number of parameters. This is a major common problem in computer aided engineering (CAE) programs for fluid power circuits. Methods for solving this problem by combining a theoretical and an empirical approach are presented. Analytical models for single stage pressure and flow control valves are brought into forms which contain fewer parameters whose values can be determined from measured characteristic curves. The least squares criterion is employed to identify the parameter values describing the steady state of a valve. The steady state characteristic curves that are required data for this identification are quite often provided by the manufacturers. The parameters describing the dynamics of a valve are determined using a simple noncomputational method using dynamic characteristic curves that can be easily measured. The importance of the identification accuracy of the different parameters of the single stage pressure relief valve model is compared using a parameter sensitivity analysis method. A new comparison method called relative mean value criterion is used to compare the influences of variations of the different parameters to a nominal dynamic response. ESA

N91-19393# Technische Univ., Berlin (Germany, F.R.). Fachbereich Physik.
CONTRIBUTIONS TO THE NON EQUILIBRIUM MOLECULAR DYNAMICS (NEMD) COMPUTER SIMULATION FOR TRANSPORT PROCESSES IN SIMPLE FLUIDS Ph.D. Thesis [BEITRAEGE ZUR NICHTGLEICHGEWICHTS MOLEKULARDYNAMIK COMPUTERSIMULATION VON TRANSPORTPROZESSEN IN EINFACHEN FLUIDEN]
Werner Loose 1990 174 p
(ETN-91-98921) Avail: NTIS HC/MF A08

Stationary transport processes far away from thermal equilibrium, which are observed in the simulation variation of the Newton and Fourier linear transport laws, are of particular interest. The results represented concern NEMD methodic questions, as well as the theoretical description of the nonlinear transport phenomena. A detailed comparison is conducted between the predictions of the Boltzmann equation and the simulation results, for determining the viscosity coefficient. An algorithm which generates heat flow in the absence of a temperature gradient is analyzed. The results of the velocity distribution function legitimate the utilization of the efficient algorithm for examining the linear energy transport. The application of continuum theoretical methods is emphasized for describing the phenomena observed in the simulation with some hundreds of particles. ESA

N91-19394# Technische Univ., Delft (Netherlands). Lab. for Aero and Hydrodynamics.
A NUMERICAL METHOD FOR SOLVING STEADY 2D AND AXISYMMETRICAL VISCOELASTIC FLOW PROBLEMS WITH AN APPLICATION TO INERTIA EFFECTS IN CONTRACTION FLOWS
Martin A. Hulsen 1990 65 p
(MEMT-11; ISBN-90-370-0044-4; ETN-91-98937) Copyright Avail: NTIS HC/MF A04

A numerical method for simulating incompressible, isothermal, steady viscoelastic fluid flows in two dimensional and axisymmetrical geometries is given. The basic equation and the constitutive equations are given. A numerical method for solving these equations in rather general geometries is described. The momentum equation and the continuity equation are discretized by the finite element method. The constitutive equations are discretized by a characteristics based method. The characteristics (stream lines for steady flow) are computed by a method based on quadratic interpolation of the stream function. Stability and integration aspects of the discretized constitutive equation are discussed. The equations are solved by a Picard type iteration scheme. The method is capable of solving viscoelastic fluid flows

at high Deborah numbers for many popular fluid models. The method was applied to the flow through a four to one contraction to study the influence of inertia on the vortex growth. The influence of the elongational properties of the fluid and of the inertia forces in particular are studied. It appears that the vortex growth and the divergent flow regime, which are observed in experiments for some fluids, can be found for a choice of the material parameters where both the elongational stresses and the inertia forces are large for the flow rate considered. After studying the type and the vorticity it is concluded that the appearance of a divergent flow regime is a critical phenomenon (i.e., change of type for critical velocity).
ESA

N91-19395# Technische Univ., Delft (Netherlands). Dept. of Aerospace Engineering.
NOTES ON THE UNSTEADY RECTILINEAR MOTION OF A PERFECT GAS. 10: ON THE INFLUENCE OF GRAVITY UPON THE EXPANSION OF AN IDEAL GAS WITH GAMMA = 3
J. A. Steketee Aug. 1990 66 p
(LR-640; ETN-91-98941) Avail: NTIS HC/MF A04

A vertical column of an ideal homentropic gas is at rest in a gravitational field, with constant acceleration of gravity g. At the upper end the column is bounded by a piston, while downwards it extends indefinitely. The gas pressure p at the piston has the value p sub 0, while above the piston there is vacuum extended to infinity. At time t = 0 the piston is suddenly removed, permitting the gas to expand and to move into the vacuum. The motion of the gas for t is greater than 0 is studied. Burgers considered this problem for gamma equals 5/3 and found that the gas starts to move upwards, but after some time, due to the action of the gravity the velocity changes direction and the gas begins to fall back. In this phase of the motion the solution shows some singularities, which indicate that physically a shock wave, moving in downwards direction, makes its appearance. The flow beyond the shock wave can only be analyzed tentatively and the analysis retains a preliminary character. Also a final state of rest is only approximately obtained for large t. Burgers' problem is considered once more for a fictitious gas with gamma = 3. This assumption simplifies the analysis and the singularities found for gamma equals 5/3 are drastically reduced. Also since the answers are simpler it is possible to a large extent to invert the solutions. Distinct from the case with gamma = 5/3 there is no overshoot, followed by a falling back, accompanied by a shock wave. For gamma = 3 the gas begins at t = 0 to move upwards but slows down and reaches a maximum height with speed zero, and density zero. ESA

N91-19135*# National Aeronautics and Space Administration. Goddard Space Flight Center, Greenbelt, MD.
FLOW FIELDS OF LOW PRESSURE VENT EXHAUSTS
John J. Scialdone *In its* 16th Space Simulation Conference Confirming Spaceworthiness Into the Next Millennium Nov. 1990 p 75-83 Previously announced as N89-26902 (For primary document see N91-19126 11-18)
Avail: NTIS HC/MF A20 CSCL 20D

N91-19801# Joint Publications Research Service, Arlington, VA.
LAWS OF HEAT TRANSFER IN THREE-DIMENSIONAL VISCOUS SHOCK LAYER OF STREAM FLOWING PAST BLUNT BODIES AT SOME ANGLES OF ATTACK AND GLIDE Abstract Only
A. I. Borodin and S. V. Peygin *In its* JPRS Report: Science and Technology. USSR: Physics and Mathematics 31 Oct. 1990 p 1 Transl. into ENGLISH from Inzhenerno-Fizicheskiy Zhurnal (Minsk, USSR), v. 58, no. 2, Feb. 1990 p 200-206 (For primary document see N91-19800 11-70)
Avail: NTIS HC/MF A03

N91-20033*# Norwalk State Technical Coll., CT. Dept. of Mathematics/Science.
CORRELATION OF LEAK RATES OF VARIOUS FLUIDS WITH THE LEAK RATE OF AN INERT GAS IN THE SAME CONFIGURATION
Howard Schleier *In* NASA, John F. Kennedy Space Center, Research Reports: 1990 NASA/ASEE Summer Faculty Fellowship Program Sep. 1990 p 308-338 (For primary document see N91-20022 11-99)
(Grant NGT-60002)
Avail: NTIS HC/MF A23 CSCL 20D

N91-20036*# California State Univ., Sacramento. Dept. of Mechanical Engineering.
LOW FLOW VORTEX SHEDDING FLOWMETER FOR HYPERGOLICS/ALL MEDIA
Ngo Thinh *In* NASA, John F. Kennedy Space Center, Research Reports: 1990 NASA/ASEE Summer Faculty Fellowship Program Sep. 1990 p 432-461 (For primary document see N91-20022 11-99)
(Grant NGT-60002)
Avail: NTIS HC/MF A23 CSCL 20D

35 INSTRUMENTATION AND PHOTOGRAPHY

Includes remote sensors; measuring instruments and gages; detectors; cameras and photographic supplies; and holography.

For aerial photography see *43 Earth Resources and Remote Sensing*. For related information see also *06 Aircraft Instrumentation*, and *19 Spacecraft Instrumentation*.

N91-19396 Department of the Navy, Washington, DC.
METHOD FOR MAKING HOLOGRAMS WITH COHERENT RADIATION FROM A STABILIZED LASER DIODE THAT HAS BEEN ACTIVELY COOLED Patent
Gail C. Gilbreath, inventor (to Navy) and Anne E. Clement, inventor (to Navy) 4 Sep. 1990 12 p Filed 13 Jan. 1988
(AD-D014673; US-Patent-4,953,951; US-Patent-Appl-SN-143492; US-Patent-Class-350-320) Avail: US Patent and Trademark Office CSCL 09/3

A technique is presented involving a laser diode stabilized in a single mode employing active cooling at a specific current density to produce a preselected wavelength of coherent radiation. This output is used to expose for a very short time, a very sensitive holographic recording material before the diode can return to an unstable multimode, hence multilength radiation condition which would have a adverse consequences to the hologram making process.
GRA

N91-19397 Department of the Navy, Washington, DC.
AIR/SEA TEMPERATURE PROBE Patent
Jack R. Olson, inventor (to Navy), Herbert V. Hitney, inventor (to Navy), Richard A. Paulus, inventor (to Navy), and Kenneth D. Anderson, inventor (to Navy) 4 Sep. 1990 12 p Filed 27 Apr. 1989
(AD-D014674; US-Patent-4,953,986; US-Patent-Appl-SN-348740; US-Patent-Class-374-136) Avail: US Patent and Trademark Office CSCL 14/1

An air/sea temperature probe is disclosed which can be deployed from a moving ship to detect the temperature profile of the atmosphere and ocean beyond the thermal influence of a ship. The probe includes a temperature transducer which utilizes a bifilar wire that provides a very quick air temperature time constant. The transducer is mounted within a radiation shield having low thermal conductance to minimize thermal and solar radiation contamination and is coupled to a signal processing network. In operation, the probe is deployed from a ship and provides temperature telemetry via an electrical data link coupled between the signal processing network and a receiving transducer located onboard the ship.
GRA

N91-19398*# Georgia Inst. of Tech., Atlanta. School of Electrical Engineering.
DESIGN, PERFORMANCE EVALUATION, AND INVESTIGATION OF THE THEORETICAL CAPABILITIES OF THE NASA MILLIMETER-WAVE IMAGING RADIOMETER (MIR) Final Status Report, 1 Mar. 1990 - 28 Feb. 1991
Albin J. Gasiewski and D. M. Jackson 1991 15 p
(Grant NAG5-1332)
(NASA-CR-187984; NAS 1.26:187984) Avail: NTIS HC/MF A03 CSCL 14B

The development of techniques for passive microwave retrieval of water vapor and precipitation parameters using millimeter- and sub-millimeter wavelength channels is reviewed. Channels of particular interest are in the tropospheric transmission windows at 90, 150, 220, and 340 GHz and centered around the water vapor lines at 183 and 325 GHz. Collectively, these channels have potential application in high-resolution mapping (e.g., from geosynchronous orbit), remote sensing of cloud and precipitation parameters, and retrieval of water vapor profiles. Both theoretical and experimental results to date are discussed. Y.S.

N91-19399# Westinghouse Savannah River Co., Aiken, SC.
EVALUATION OF A PHOTO-ELECTRON REJECTING ALPHA LIQUID SCINTILLATION (PERALS) SPECTROMETER FOR THE MEASUREMENT OF ALPHA-EMITTING RADIONUCLIDES
J. R. Cadieux 1990 20 p Presented at the 7th Symposium on Radiation Measurements and Applications, Ann Arbor, MI, 21-24 May 1990
(Contract DE-AC09-89SR-18035)
(DE91-005652; WSRC-RP-89-1383; CONF-900563-18) Avail: NTIS HC/MF A03

Results from the evaluation of a PERALS spectrometer for alpha particle measurements by liquid scintillation counting in samples from the nuclear fuel cycle are presented. Examples of PERALS spectra of process, waste, and environmental samples containing Th, U, Pu and Am from the Savannah River Site are shown. The advantages, disadvantages, and limitations of the PERALS technique are discussed. DOE

N91-19400# Lawrence Livermore National Lab., CA.
MEASUREMENTS WITH A 35 PSEC GATE TIME MICROCHANNELPLATE CAMERA
P. E. Bell, J. D. Kilkenny, R. Hanks, and O. Landen Jul. 1990 11 p Presented at the 34th SPIE Annual International Technical Symposium on Optical and Optoelectronic Applied Science and Engineering, San Diego, CA, 8-13 Jul. 1990
(Contract W-7405-eng-48)
(DE91-006701; UCRL-JC-104612; CONF-900756-57) Avail: NTIS HC/MF A03

Measurements of the x-ray gate time of 0.2 mm thick microchannel plates with an L/D aspect ratio of 20 as opposed to the more usual L/D=40, demonstrate that gate times of 35 ps can be achieved. Good agreement with time dependent modeling is demonstrated. DOE

N91-19401*# National Aeronautics and Space Administration. Lewis Research Center, Cleveland, OH.
ROTATING PRESSURE MEASUREMENT SYSTEM USING AN ON BOARD CALIBRATION STANDARD
Richard G. Senyitko, Philip Z. Blumenthal (Sverdrup Technology, Inc., Brook Park, OH.), and Robert J. Freedman 1991 15 p Proposed for presentation at the 37th International Instrumentation Symposium, San Diego, CA, 5-9 May 1991; sponsored by Instrument Society of America
(NASA-TM-103676; E-5892; NAS 1.15:103676) Avail: NTIS HC/MF A03 CSCL 14B

A computer-controlled multichannel pressure measurement system was developed to acquire detailed flow field measurements on board the Large Low Speed Centrifugal Compressor Research Facility at the NASA Lewis Research Center. A pneumatic slip ring seal assembly is used to transfer calibration pressures to a reference standard transducer on board the compressor rotor in order to measure very low differential pressures with the high accuracy required. A unique data acquisition system was designed and built to convert the analog signal from the reference transducer to the variable frequency required by the multichannel pressure measurement system and also to provide an output for temperature control of the reference transducer. The system also monitors changes in test cell barometric pressure and rotating seal leakage and provides an on screen warning to the operator if limits are exceeded. The methods used for the selection and testing of the the reference transducer are discussed, and the data acquisition system hardware and software design are described. The calculated and experimental data for the system measurement accuracy are also presented. Author

N91-19402*# National Aeronautics and Space Administration. Lewis Research Center, Cleveland, OH.
CRYOGENIC LIQUID-JET BREAKUP IN TWO-FLUID ATOMIZERS
Robert D. Ingebo 1991 6 p Proposed for presentation at the 5th International Conference on Liquid Atomization and Spray Systems, Gaithersburg, MD, 15-18 Jul. 1991; sponsored by National Inst. of Standards and Technology
(NASA-TM-103734; E-5854; NAS 1.15:103734) Avail: NTIS HC/MF A02 CSCL 20D

A two-fluid atomizer was used to study the breakup of liquid-nitrogen jets in nitrogen, argon, and helium atomizing gas flows. A scattered-light scanner particle sizing instrument previously developed at NASA Lewis Research Center was further developed and used to determine characteristic drop diameters for the cryogenic sprays. In the breakup regime of aerodynamic-stripping, i.e., sonic-velocity conditions, the following correlation of the reciprocal Sauter mean diameter, D(sub 32)exp -1, with the atomizing-gas flowrate, W(g), was obtained: D(sub 32)exp -1 = k(sub c)(W(g)exp 1.33), where k(sub c) is a proportionality constant evaluated for each atomizing gas. Values of k(sub c) = 120, 220, and 1100 were obtained for argon, nitrogen, and helium gasflows, respectively. The reciprocal Sauter mean diameter and gas flowrate have the units of 1/cm and g/sec, respectively. In the regime of capillary-wave breakup, or subsonic conditions, it was found that D(sub 32)exp -1 = k(g)(W(g)exp 0.75), where k = 270, 390, and 880 for argon, nitrogen, and helium gasflows, respectively.
Author

N91-19403*# Sverdrup Technology, Inc., Brook Park, OH.
THE APPARENT STRAIN STABILITY AND REPEATABILITY OF A BCL3 RESISTANCE STRAIN GAGE Final Report
Jih-Fen Lei Feb. 1991 11 p
(Contract NAS3-25266)
(NASA-CR-187056; E-5940; NAS 1.26:187056) Avail: NTIS HC/MF A03 CSCL 14B

Experiments were conducted at NASA-Lewis to study the effect of microstructural instability on the apparent strain stability and reproducibility of a BCL3 resistance strain gage. The resistance drift of the gage at various temperatures in the phase transition temperature range (PTTR) was measured. The effects of the heating and cooling rates with which the gage passed through the PTTR on the apparent strain characteristics of the gage were also studied. BCL3 gage, like other Fe-Cr-Al based gages, exhibited apparent strain instability in the temperature range of 700 to 1100 F due to the reversible microstructural transition the gage materials experienced in this temperature range. The BCL3 gage had a maximum apparent strain drift in the neighborhood of 770 F with an average drift rate of approx. -440 microstrain/hr in 2 hrs. The use of the BCL3 gage as well as other Fe-Cl-Al based gages for static strain measurements within the PTTR should be avoided unless the time durations in the PTTR are small enough to introduce a neglible drift. The microstructure transition that the BCL3 gage underwent occurred in the temperature range of 750 to 1050 F during heating and around 1000 to 800 F during cooling. The heating rate, and, in particular, the cooling rate with which the gage passed through the PTTR affected the shape and the repeatability of the apparent strain curve of the gage. Author

N91-19404*# National Aeronautics and Space Administration. Lewis Research Center, Cleveland, OH.
THREE-DIMENSIONAL COMPUTED TOMOGRAPHY FROM INTERFEROMETRIC MEASUREMENTS WITHIN A NARROW CONE OF VIEWS
Arthur J. Decker and Steven H. Izen (Case Western Reserve Univ., Cleveland, OH.) Mar. 1991 14 p Submitted for publication Original contains color illustrations
(Grant NAG3-832)
(NASA-TM-103257; E-5688; NAS 1.15:103257) Avail: NTIS HC/MF A03; 7 functional color pages CSCL 14B

A theory to determine the properties of a fluid from measurements of its projections was developed and tested. Viewing cones as small as 10 degrees were evaluated, with the only assumption being that the property was space limited. The results of applying the theory to numerical and actual interferograms of a spherical discontinuity of refractive index are presented. The theory was developed to test the practicality and limits of using three-dimensional computer tomography in internal fluid dynamics.
Author

N91-19405# Los Alamos National Lab., NM.
INTERFEROMETRY, STREAK PHOTOGRAPHY, AND STEREO PHOTOGRAPHY OF LASER-DRIVEN MINIATURE FLYING PLATES
D. L. Paisley, N. I. Montoya, D. B. Stahl, and I. A. Garcia 1991 7 p Presented at the 19th International Congress on High Speed Photography and Photonics, Cambridge, England, 16-22 Sep. 1990
(Contract W-7405-eng-36)
(DE91-007493; LA-UR-91-397; CONF-9009248-5) Avail: NTIS HC/MF A02

Optical diagnostics to evaluate the velocity, acceleration profiles, planarity, and integrity of miniature (less than or = 5 microns thick x less than 600 microns diam) plates of aluminum and other metals is reported. By correlating various optical techniques and collected data, a complete understanding of the flying plate can be determined. Velocity interferometer system for any reflector (VISAR), with less than or = 120 ps resolution per data point, is used to record plate acceleration and terminal velocity. Electronic streak and pulsed laser stereo photography can determine planarity and integrity. Flyer-plate performance data are related to the properties of the laser beam that accelerates the plate. Laser parameters, such as energy density, power density, and spatial profile, affect the flying-plate performance parameters, i.e., planarity, acceleration, and velocity. Flying-plate accelerations of greater than or = 10(exp 10) G and terminal velocities of greater than or = 6 mm/microsec were recorded, via a 10-ns-Nd:YAG laser pulse delivered to a tamped, 5 micron aluminum plate.
DOE

N91-19406# Oak Ridge National Lab., TN.
A POCKET-SIZE BROADBAND ELECTRIC FIELD DETECTION AND STORAGE DEVICE
M. R. Moore, R. W. Rochelle, R. S. Thomas, P. D. Ewing, R. A. Hess, and B. S. Hoffheins 1991 8 p Presented at the IEEE Southeastcon 1991, Williamsburg, 7-10 Apr. 1991
(Contract DE-AC05-84OR-21400)
(DE91-007710; CONF-9104161-3) Avail: NTIS HC/MF A02

The radio-frequency (rf) dosimeter developed by the Oak Ridge National Laboratory is a portable, pocket-sized cumulative-dose recording device designed to detect and record the strengths and durations of electric fields present in the work areas of naval vessels. The device measures an integrated dose and records the electric fields that exceed the permissible levels set by the American National Standards Institute. Features of the rf dosimeter include a frequency range of 30 MHz to 10 GHz and a 3D. Data obtained with the rf dosimeter will be used to determine the ambient field-strength profile for shipboard personnel over an extended time. Readings are acquired and averaged over a 6-min period corresponding to the rise time of the core body temperature. These values are stored for up to 6 months, after which the data are transferred to a computer via the dosimeter's serial port. The rf dosimeter should increase knowledge of the levels of electric fields to which individuals are exposed.
DOE

N91-19407# Sandia National Labs., Albuquerque, NM.
THE DEVELOPMENT OF A RUGGED ACCELEROMETER
S. A. Casalnuovo, G. E. Sleefe, and C. E. James (Ktech Corp., Albuquerque, NM.) 1991 19 p Presented at the Environmentally Conscious Manufacturing/Technology Applications Workshop, Albuquerque, 20 Feb. 1991
(Contract DE-AC04-76DP-00789)
(DE91-007731; SAND-91-0348C; CONF-910279-2-Vugraphs)
Avail: NTIS HC/MF A03

Accelerometers, under a variety of names (e.g., vibration, motion, and seismic sensors), serve as sensing elements in a number of systems. The sensing schemes are numerous (mechanical, electric, magnetic, and piezoelectric, for example) and the choice is determined by the application. We describe the development of an optical fiber accelerometer which would have distinct advantages in some applications. The use of optical fibers as the acceleration-sensitive component would be advantageous in three general applications areas. The first involves applications which require sensing in environments which are hostile to electronic devices. Optical fibers can withstand higher temperatures and higher radiation levels than most electronic components and are immune to electromagnetic interference. An example would be the operation of an accelerometer within a nuclear reactor. A second application is one which requires a multiplicity of high-bandwidth sensors. The large bandwidth of optical fibers allows the multiplexing of many sensor signals on to a single input/output fiber. An example of this area would be the vibration testing of a complex vehicle or structure. The third application for the optical accelerometer would be a situation where the presence of the sensor must remain covert. The optical fiber and attached sensor do not emit electromagnetic radiation, thereby making it extremely difficult to detect their presence. An example of this area would be intrusion detection. Naturally, there are specific applications which can benefit from several of these attributes.
DOE

N91-19408# Sandia National Labs., Albuquerque, NM.
SUPERCONDUCTING INSTRUMENTATION FOR CRITICAL He-4 MEASUREMENTS IN SPACE
R. V. Duncan 1991 6 p Presented at the 8th Oregon Conference on LT Physics, Washington, DC, 14-17 Jan. 1991
(Contract DE-AC04-76DP-00789)
(DE91-007894; SAND-91-0038C; CONF-910170-2) Avail: NTIS HC/MF A02

A proposed superconducting transducer capable of measuring and controlling pressure to within 0.5 nanotorr over a 17 torr range is described. Such a device is capable of ultra-accurate measurements of the isobaric thermal expansion coefficient (Beta sub p), the isothermal compressibility, and the isochoric pressure coefficient of pure He-4 within a few nanoKelvin of the superfluid transition temperature (T sub lambda). Such space-born measurements may be used with specific heat measurements (currently planned for the space shuttle) to test predictions from scaling and renormalization group theory with much higher accuracy than is possible in the Earth-boundary laboratory. New superconducting instrumentation for use in viscosity measurements near T(sub lambda) is discussed. A method of simulating microgravity conditions in He-4 near its superfluid transition using a magnetic field gradient is proposed.
DOE

N91-19409# Pacific Northwest Lab., Richland, WA.
A REVIEW OF FIBER OPTIC AND RELATED TECHNOLOGIES FOR ENVIRONMENTAL SENSING APPLICATIONS
J. W. Griffin and K. B. Olsen Jan. 1991 19 p Presented at the Symposium on Ground Water and Vadose Zone Investigations, San Diego, 30 Jan. - 1 Feb. 1991
(Contract DE-AC06-76RL-01830)
(DE91-007736; PNL-SA-19021; CONF-910172-2) Avail: NTIS HC/MF A03

Realization of most fiber optic chemical sensor (FOCS) concepts is the result of numerous recent developments in fiber optic, optoelectronic, and computer technologies. For the most part, these developments have been motivated and funded by the communications industry. This paper provides a review of current technologies and an overview of FOCS concepts currently under development for environmental sensing and monitoring applications. DOE

N91-19410# Rome Univ. (Italy). Dipt. di Fisica.
A CALORIMETER DESIGN FOR HIGH ENERGY PP COLLIDERS
Bruno Borgia (Istituto Nazionale di Fisica Nucleare, Rome, Italy) 13 Dec. 1990 11 p Presented at 2nd International Conference on Advanced Technology and Particle Physics, Como, Italy, 1990
(Nota-Interna-965; ETN-91-98885) Avail: NTIS HC/MF A03

Requirements dictated by the physics most likely to be investigated at the next generation of pp colliders are recalled and the main parameters for a generic hadronic calorimeter are reviewed. The L(*) calorimeter is described. Experiments at LHC or SSC are concluded to be posing a challenge to calorimetry and technical developments will be essential to design a calorimeter with performances to cope with requirements. Silicon calorimeters are an attractive and promising alternative. The L(*) detector includes a designed silicon calorimeter for an experiment at SSC. ESA

N91-19411# Oxford Univ. (England). Dept. of Engineering Science.
APPLICATION OF HIGH SPEED PHOTOGRAPHY TO THE STUDY OF HIGH STRAIN RATE MATERIALS TESTING
D. Ruiz, J. Harding, J. Noble, and G. Hillsdon 1990 12 p Presented at the 19th International Congress on High Speed Photography and Photonics, Cambridge, England, Sep. 1990 Submitted for publication Sponsored by Ministry of Defence Procurement Agency, London, England
(OUEL-1852/90; ETN-91-98955) Avail: NTIS HC/MF A03

The relative merits of the Hadland Imacon image converter camera and the Cordin rotating mirror drum camera are discussed and their use in the gathering of real time, full field displacement data on the DNS high strain rate material test is described. It is concluded that, except where framing rates of more than 200,000/sec are required, the Cordin camera is the superior for these purposes. Possible improvements, such as use of the highest quality lens for the Cordin camera and semi-automatic analysis of the photographic images using digital frame grabbing equipment and a simple computer program, are mentioned. Qualitative observations are made on the behavior of the double notch shear specimen and these are supported by analysis of the high speed photographs. Measurement of the high speed photographs shows that the nominal shear strain varies almost linearly and therefore that the nominal shear strain rate is approximately constant throughout the tests. ESA

N91-19412# Air Force Inst. of Tech., Wright-Patterson AFB, OH. School of Engineering.
DEVELOPMENT OF A PIEZOELECTRIC POLYMER FILM PRESSURE TRANSDUCER FOR LOW FREQUENCY AND DYNAMIC PRESSURE MEASUREMENT M.S. Thesis
Ted H. Halley Dec. 1990 145 p
(AD-A229848; AFIT/GAE/ENY/90D-09) Avail: NTIS HC/MF A07 CSCL 09/1

The purpose of this research was to investigate the characteristics of a small and inexpensive pressure transducer made from piezoelectric film. The pressure transducer was designed to be small and surface mountable so that the pressure distribution could be measured on an aerodynamic body. A charge reset technique was used to overcome the traditional limitations, low frequency measurements and charge decay, of a piezoelectric device. GRA

N91-19413# Naval Research Lab., Washington, DC.
TIME-DEPENDENT MULTIMODE SIMULATION OF GYROTRON OSCILLATORS Memorandum Report
A. W. Fliflet, R. C. Lee, S. H. Gold, W. M. Manheimer, and E. Orr 21 Nov. 1990 35 p Prepared in cooperation with JAYCOR, Vienna, VA and Maryland Univ., College Park
(AD-A229861; NRL-MR-6746) Avail: NTIS HC/MF A03 CSCL 09/1

High power gyrotrons, including both CW and high peak power configurations, are increasingly designed to operate in high mode density regimes. It has been observed that operation is often single-moded even for cavities with dense mode spectra, but the mode density does affect the gyrotron efficiency and the available operating modes. Multimode effects have been studied extensively for the quasi-optical gyrotron but there has been less progress on fully nonlinear formulations for conventional waveguide cavity gyrotrons which involve different transverse modes with irregularly spaced frequencies and unequal coupling impedances. A time-dependent, nonlinear, multimode theory of gyrotrons has been recently developed along with a computer code to carry out the numerical calculations. The code has been used to simulate the operation of a CW-relevant 140 GHz gyrotron experiment carried out at MIT and the 750 kV, 35 GHz intense-beam gyrotron experiment at NRL. The MIT gyrotron involves competition between two transverse modes: the TE03 and TE23 modes. The NRL gyrotron involves competition between TEm2 modes and is an example of a three-mode interaction. GRA

36 LASERS AND MASERS

Includes parametric amplifiers.
For related information see also *76 Solid-State Physics.*

N91-19414# Argonne National Lab., IL.
HIGH POWER, HIGH FREQUENCY LASERTRON RF SOURCES
J. Norem, E. Chojnacki, and R. Konecny 1990 4 p Presented at the EPAC 1990: 2nd European Particle Accelerator Conference ACROPOLIS, Nice, France, 11-16 Jun. 1990
(Contract W-31-109-eng-38)
(DE91-006007; ANL-HEP-CP-90-53; CONF-900603-58) Avail: NTIS HC/MF A01

High power RF sources have historically been limited to frequencies at which intense electron beams could be efficiently modulated. The power, frequency, and efficiency limitations associated with the use of lasertrons for generating modulated beams were explored and these beams were used as high power microwave sources. This effort is an extension of wake field accelerator development, and will proceed as part of the Argonne Wakefield Accelerator construction and use. In the lasertron the electron beam is produced from the photoelectric effect at the photocathode, thus the electron pulse closely resembles the laser pulse in density and spatial extent. One configuration for this device is where a dielectric Cerenkov coupler is used to transfer power from the electron beam to the RF field. Operation at high power and high frequencies, (approximately GW, approximately greater than THz) seems possible using laser optics to compensate electron aberrations due to geometrical optics and space charge. In this paper we show results of simulations that indicate electron pulse lengths of the order of 0.25 ps can be produced if other aberrations are controlled, describe an optical system to compensate aberrations and generate pulse trains from a short pulse laser, discuss design constraints and limitations of RF couplers, and describe constraints on the system as a whole. DOE

N91-19415*# National Aeronautics and Space Administration. Langley Research Center, Hampton, VA.
LASER DOPPLER VELOCIMETRY FOR CONTINUOUS FLOW SOLAR-PUMPED IODINE LASER SYSTEM
Bagher M. Tabibi (Hampton Univ., VA.) and Ja H. Lee Jan. 1991 21 p

(Grant NAG1-1091)
(NASA-TM-104029; NAS 1.15:104029) Avail: NTIS HC/MF A03 CSCL 20E

A laser Doppler velocimetry (LDV) system was employed to measure the flow velocity profile of iodide vapor inside laser tubes of 36 mm ID and 20 mm ID. The LDV, which was operated in the forward scatter mode used a low power (15 mW) He-Ne laser beam. Velocity ranges from 1 m/s was measured to within one percent accuracy. The flow velocity profile across the laser tube was measured and the intensity of turbulence was determined. The flow of iodide inside the laser tube demonstrated a mixture of both turbulence and laminar flow. The flowmeter used for the laser system previously was calibrated with the LDV and found to be in good agreement. Author

N91-19416# Lawrence Livermore National Lab., CA.
SOFT X-RAY LASER GAIN PREDICTION AT HIGH DENSITY FOR THE NITROGEN ISOELECTRONIC SEQUENCE
M. Klapisch, M. Cohen, W. H. Goldstein, and U. Feldman (Naval Research Lab., Washington, DC.) 11 Jan. 1991 10 p Presented at the International Workshop on Radiative Properties of Hot Dense Matter, Sarasota, 22-26 Oct. 1990
(Contracts W-7405-eng-48; DE-AC03-76SF-00098)
(DE91-007616; UCRL-JC-105959; CONF-9010298-2) Avail: NTIS HC/MF A02

In model calculation, population inversions for 2s(sup 2)2p(sup 2)3s-2s(sup 2)2p(sup 2)3p and for 2s(sup 2)2p(sup 2)d3p-2s(sup 2)2p(sup 2)3d are predicted for ions of the N-like isoelectronic sequence (Kr(sup 29+), Zr(sup 33+), Mo(sup 35+), Pd(sup 39+), Sn(sup 43+) and Xe(sup 47+)), at electron densities higher than 10(sup 22) cm(sup (minus)3). Maximum gains of 46 cm(sup (minus)1) for Kr(sup 29+) at 245(angstrom), and 231 cm(sup (minus)1) at 126(angstrom) for Xe(sup 47+) are obtained. The electron temperature T(sub e) is fixed at half the ionization potential for all ions. A detailed analysis shows that the mechanisms responsible for the population inversion enhancement are collisional de-excitation and radiation trapping. DOE

N91-19417# Lawrence Livermore National Lab., CA.
INTENSE MICROWAVE GENERATION USING FREE-ELECTRON LASERS
T. J. Orzechowski Sep. 1990 19 p Presented at the International Workshop on Strong Microwaves in Plasmas, Suzdal, USSR, 18-23 Sep. 1990
(Contract W-7405-eng-48)
(DE91-007262; UCRL-JC-104640; CONF-9009118-2) Avail: NTIS HC/MF A03

In this paper, I will describe a free-electron laser amplifier which operated in the microwave regime. This device, called the Electron Laser Facility (ELF), used an electron beam generated by a Linear Induction Accelerator (LIA). ELF operated as a single pass amplifier at 35 and 140 GHz. Because the device had no cavity, we could study the FEL physics independent of cavity considerations. With a sufficiently large input signal, growth of the signal from noise on the beam did not influence the performance. This device demonstrated significant gain and allowed us to investigate such FEL phenomenon as saturation and synchrotron oscillation of the electrons trapped in the ponderomotive well. We were also able to study the phase shift of the radiation due to the real part of complex gain of the FEL. Because the interaction takes place in a waveguide, the FEL can couple to several spatial modes at a given frequency. The bunched electrons can radiate at harmonics of the fundamental and in this experiment we studied the evolution of the third harmonic. In this paper, I will describe the Electron Laser Facility. I will discuss the FEL performance with regard to gain, saturation, phase evolution, mode coupling and harmonic generation, I will briefly discuss a switching technique which allows the LIA to run at high average power. When driven by such a device, an FEL can produce high average power radiation. We will present the design for such a device which can be used to heat a tokamak plasma. This device is designed to operate at 250 GHz and produce an average power of 2 MW. DOE

N91-19418# Lawrence Livermore National Lab., CA.
SIMULATION OF A STANDING-WAVE FREE-ELECTRON LASER
W. M. Sharp, A. M. Sessler, D. H. Whittum, J. S. Wurtele, D. McDermott, and N. Luhmann (California Univ., Los Angeles.) Sep. 1990 6 p Presented at the Linear Accelerator Conference, Albuquerque, NM, 9-14 Sep. 1990
(Contracts W-7405-eng-48; DE-AC03-76SF-00098)
(DE91-007330; UCRL-JC-103826; CONF-9009123-64) Avail: NTIS HC/MF A02

The standing-wave free-electron laser (FEL) differs from a conventional linear-wiggler microwave FEL in using irises along the wiggler to form a series of standing-wave cavities and in reaccelerating the beam between cavities to maintain the average energy. The device has been proposed for use in a two-beam accelerator (TBA) because microwave power can be extracted more effectively than from a traveling-wave FEL. The standing-wave FEL is modeled in the continuum limit by a set of equations describing the coupling of a one-dimensional beam to a TE(sub 01) rectangular-waveguide mode. Analytic calculations and numerical simulations are used to determine the time variation of the reacceleration field and the prebunching required so that the final microwave energy is the same in all cavities. The microwave energy and phase are found to be insensitive to modest spreads in the beam energy and phase and to errors in the reacceleration field and the beam current, but the output phase appears sensitive to beam-energy errors and to timing jitter. DOE

N91-19419# Los Alamos National Lab., NM.
DEVELOPMENT OF KrF LASERS FOR INERTIAL CONFINEMENT FUSION
J. A. Sullivan and D. B. Harris 1990 9 p Presented at the International Conference on Lasers '90, San Diego, CA, 10-14 Dec. 1990
(Contract W-7405-eng-36)
(DE91-007349; LA-UR-91-7; CONF-901263-2) Avail: NTIS HC/MF A02

Recent reviews of the inertial confinement fusion (ICF) program have resulted in recommendations that promise to focus the research effort on the examination of the feasibility of pellet ignition at 1 MJ of energy on target. If successful, the next major step in the program has been defined to be the construction of an ignition facility. Los Alamos National Laboratory has developed a plan to reach single-pulse multimegajoule ICF facilities using the electron-beam-pumped KrF laser. The Los Alamos plan, its relation to the development of ICF for energy production, and the major features and design issues associated with ICF drivers will be covered in this presentation. DOE

N91-19420# Mississippi State Univ., Mississippi State. Diagnostic Instrumentation and Analysis Lab.
DATA ACQUISITION AND ANALYSIS ON THE TWO-COLOR LASER TRANSMISSOMETER SYSTEM
Hao-Feng Shu and R. D. Benton 1991 5 p
(Contract DE-AC02-80ET-15601)
(DE91-007235; DOE/ET-15601/T53) Avail: NTIS HC/MF A01

The average particle sizes and number densities in a gas stream are measured by the Two-Color Laser Transmissometer (TCLT) in different locations of the magnetohydrodynamic (MHD) power plant. In order to speed up signal collection and analysis, an IBM AT computer is used to control on-line laser intensity signal sampling and data processing. The operating software, written in the C language, performs data acquisition and data analysis by a series of functional modules. A data conversion board is used for the analog-to-digital signal conversion. The system has been tested and implemented in a test at a pilot scale MHD facility. The measured results illustrated the changes in the particle sizes during the test. DOE

N91-19421# Sandia National Labs., Albuquerque, NM.
FOCUSING INFRARED LASER BEAMS ON TARGETS IN SPACE WITHOUT USING ADAPTIVE OPTICS
T. S. McKechnie (Lentec Corp., Albuquerque, NM.) 1991 17 p

Presented at the OE/LASE 1991: 4th Society of Photo-Optical Instrumentation Engineers (SPIE) International Symposium, Los Angeles, 20-25 Jan. 1991
(Contract DE-AC04-76DP-00789)
(DE91-007518; SAND-90-1609C; CONF-910123-2) Avail: NTIS HC/MF A03

A recent prediction that large (5 meter) ground-based telescopes should routinely be able to achieve 0.05 to 0.1 arc second resolution at near infrared wavelengths using direct imaging techniques has been confirmed by experiment. These very high levels of resolution are at odds with conventional theory which predicts only marginal resolution improvement at infrared wavelengths. Conventional theory is based on the assumption that the outer limit of turbulence size, L(sub 0) is large, with estimates ranging from tens of meters to many kilometers. The smaller L(sub 0) value forces modifications to many long-held ideas about imaging with large ground-based telescopes. A much more favorable picture emerges especially at infrared wavelengths. At these wavelengths, it is found that resolution is more likely to be limited by the telescope size and telescope aberrations than by atmospheric turbulence. By building large enough telescopes to diffraction limited standards rather than the currently accepted standards which fall well short of this limit, there is almost no limit to achievable resolution. It is also expected that laser beams at near infrared wavelengths can be focused to diffraction limited accuracy on targets in space without needing adaptive optics or other wavefront compensation techniques. Probing the target and performing wavefront correction to the outgoing beam, though helpful, is not absolutely necessary. Also, the isoplanatic angle of the atmosphere in the near infrared is predicted to be at least several arc minutes (it may possibly be much larger) rather than several arc seconds as previously surmised. Thus, a much wider angular region is available from which to select suitable objects for guiding and tracking. DOE

N91-19422# Brookhaven National Lab., Upton, NY.
PROCEEDINGS OF THE WORKSHOP PROSPECTS FOR A 1 ANGSTROM FREE-ELECTRON LASER
J. C. Gallardo, ed. 1990 224 p Workshop held in Sag Harbor, 22-27 Apr. 1990
(Contract DE-AC02-76CH-00016)
(DE91-007631; BNL-52273; CONF-9004232) Avail: NTIS HC/MF A10

Papers are presented on the following topics: free electron laser theory, scaling relations and simulations; micro-wigglers; photocathode and switched power gun; applications; and summary of working groups. DOE

N91-19423# California Univ., Berkeley. Lawrence Berkeley Lab.
THEORY OF THE ION-CHANNEL LASER Ph.D. Thesis
D. H. Whittum Sep. 1990 305 p
(Contract DE-AC03-76SF-00098)
(DE91-007643; LBL-29720) Avail: NTIS HC/MF A14

A relativistic electron beam propagating through a plasma in the ion-focussed regime exhibits an electromagnetic instability with peak growth rate near a resonant frequency omega approx. 2 gamma(exp 2) omega beta, where gamma is the Lorentz factor and omega beta is the betatron frequency. The physical basis for this instability is that an ensemble of relativistic simple harmonic oscillators, weakly driven by an electromagnetic wave, will lose energy to the wave through axial bunching. This bunching corresponds to the development of an RF component in the beam current, and a coherent centroid oscillation. The theory of a laser capitalizing on this electromagnetic instability is examined. A historical perspective is offered. The basic features of relativistic electron beam propagation in the ion-focussed regime are reviewed. The ion-channel laser (ICL) instability is explored theoretically through an eikonal formalism, analgous to the KMR formalism for the free electron laser (FEL). The dispersion relation is derived, and the dependence of growth rate on three key parameters is explored. Finite temperature effects are assessed. From this work it is found that the typical gain length for amplification is longer than the Rayleigh length and three mechanisms are considered which will tend to guide waveguide. First, the effect is considered of the ion channel as a dielectric waveguide. Next, the use is considered of a conducting waveguide, appropriate for a microwave amplifier. Finally, a form is examined of optical guiding analgous to that found in the FEL. The eikonal formalism is used to model numerically the instability through and beyond saturation. Results are compared with the numerical simulation of the full equations of motion, and with the analytic scalings. The analytical requirement on detuning spread is confirmed. DOE

N91-19424# Sandia National Labs., Albuquerque, NM.
LASER TRACKER 2: SANDIA NATIONAL LABORATORIES' SECOND GENERATION LASER TRACKING SYSTEM
D. L. Patrick 1991 9 p Presented at the SPIE International Symposium on Optical Engineering and Photonics in Aerospace Sensing, Orlando, 1-5 Apr. 1991
(Contract DE-AC04-76DP-00789)
(DE91-007711; SAND-90-3113C; CONF-910450-2) Avail: NTIS HC/MF A02

Sandia National Laboratories obtained its first laser tracker in the late 1960's to replace the method of producing trajectory data by motion picture film analysis. Housed in an 8 in. x 32 in. trailer, the system primarily consisted of a double-gimbaled 12-inch mirror, a laser with one-dimensional optical pedestal, and a magnetic tape drive for recording data. This system was and still is capable of tracking test objects at velocities up to 5000 feet per second at distances as close as 2000 feet back from the intended flight path. In the 1980's when test velocities were expected to increase to as high as 20,000 feet per second a need arose for a second generation laser tracker. Improvements in computer technology and electronic made Laser Tracker 2 possible for fulfilling this mission. This paper will describe LT 2 and its advanced capabilities. Laser Tracker 2 has essentially one moving part. A double-gimbaled mirror directs two laser beams to a cooperative target. The mirror catches the return beams and an optical image for test information. The receivers for the return beams are image dissectors. During the test the dissectors sense a change in target position and generate an error signal to drive the mirror. To produce realtime three-dimensional position data, the tracker uses range, azimuth, and elevation readings. These raw data are shipped through the realtime control microcomputer system to a minicomputer which is also is used to operate the tracker. A second minicomputer is used to produce finished trajectory data. DOE

N91-19425# California Univ., Berkeley. Lawrence Berkeley Lab.
THE EVOLUTION AND LIMITS OF SPECTRAL BANDWIDTH IN FREE ELECTRON LASERS
K. J. Kim Nov. 1990 13 p Presented at the 12th International Free Electron Laser Conference, Paris, France, 17-21 Sep. 1990
(Contract DE-AC03-76SF-00098)
(DE91-007737; LBL-29724; CONF-9009166-17) Avail: NTIS HC/MF A03

We study the bandwidths in free electron lasers (FELs) under different circumstances; for weakly saturated FELs in storage rings, the bandwidth is given by the formula derived in the super mode theory, while it is given by the Fourier transform of the electron pulse length in the strongly saturated FELs in linacs. The limiting bandwidth for the case of a dc beam is given by a Schawlow-Townes formula, but the approach to the limit is very slow. DOE

N91-19426# California Univ., Berkeley. Lawrence Berkeley Lab.
HOLE COUPLING RESONATOR FOR FREE ELECTRON LASERS
Ming Xie and Kwang-Je Kim Nov. 1990 17 p Presented at the 12th International Free Electron Laser Conference, Paris, France, 17-21 Sep., 1990
(Contract DE-AC03-76SF-00098)
(DE91-007745; LBL-29956; CONF-9009166-18) Avail: NTIS HC/MF A03

The performance of two mirror resonators with holes for output

coupling is studied for free electron laser application using a Fox-Li type code. The mode profiles inside and outside the cavity, the diffraction losses at the mirror edges and apertures, the amount of useful power coupled through the hole, etc., are calculated for the dominant mode for different hole and mirror dimensions. It is found that resonators in near concentric geometry can develop a mode degeneracy in certain cases, which should be avoided for the stability of the free electron laser gain output. A resonator configuration for a free electron laser at Lawrence Berkeley Laboratory was found which can provide satisfactory performance over a wavelength range from 25 to 50 microns. The possibility of further increasing the tuning range by an adjustable intracavity aperture is discussed. DOE

N91-19427# Lawrence Livermore National Lab., CA.
PHASE STABILITY OF A STANDING-WAVE FREE-ELECTRON LASER
W. M. Sharp, G. Rangarajan, A. M. Sessler, and J. S. Wurtele (Massachusetts Inst. of Tech., Cambridge.) Jan. 1991 13 p Presented at the OE/LASE 1991: 4th Society of Photo-Optical Instrumentation Engineers International Symposium, Los Angeles, 20-25 Jan. 1991
(Contracts W-7405-eng-48; DE-AC03-76SF-00098)
(DE91-008068; UCRL-JC-105569; CONF-910123-9) Avail: NTIS HC/MF A03

The standing-wave free-electron laser (FEL) differs from a conventional linear-wiggler microwave FEL in using irises along the wiggler to form a series of standing-wave cavities and in reaccelerating the beam between cavities to maintain the average energy. The device has been proposed for use in a two-beam accelerator because microwave power can be extracted more effectively than from a traveling-wave FEL. A simplified numerical simulation indicates that, with appropriate prebunching, the standing-wave FEL can produce an output signal that is effectively the same in all cavities. However, changes in the beam energy of less than 1 percent are found to introduce unacceptably large fluctuations of signal phase along the device. Analytic calculations and single-particle simulations are used here to show that the phase fluctuations result from beam synchrotron motion in the initial signal field, and an approximate analytic expression for the signal phase is derived. Numerical simulations are used to illustrate the dependence of phase fluctuations on the beam prebunching, the beam-current axial profile, and the initial signal amplitude. DOE

N91-19428# Los Alamos National Lab., NM.
EXCIMER LASER SURFACE PROCESSING FOR TRIBOLOGICAL APPLICATIONS IN METALS AND CERAMICS
T. R. Jervis, Juha-Pekka Hivonen, and M. Nastasi 1991 22 p Presented at the Society of Tribologists and Lubrication Engineers Conference, Montreal, Quebec, 29 Apr. - 2 May 1991
(Contract W-7405-eng-36)
(DE91-002324; LA-UR-90-3455; CONF-910478-1) Avail: NTIS HC/MF A03

The use of pulsed excimer lasers, operating at UV wavelengths, for surface modification has many potential applications in the tribology of metals and ceramics. Alterations of surface chemistry and microstructure are possible on standard engineering materials. We have demonstrated improved tribological performance in stainless steel by the formation of a unique oxide and by Ti mixing and in SiC by Ti mixing. Specifically, we have observed reduced friction in dry sliding conditions and a change in the wear process resulting in greatly reduced surface damage. We have also demonstrated the effectiveness of excimer laser mixing in other systems with potential tribological applications. DOE

N91-19429# Lawrence Livermore National Lab., CA.
RECOMBINATION X RAY LASER EXPERIMENTS USING EXPLODING RIBBON Al TARGETS
C. J. Keane, D. C. Eder, B. J. MacGowan, D. L. Matthews, and D. A. Whelan Jan. 1991 8 p Presented at the 2nd International Colloquium on X Ray Lasers, York, England, 17-21 Sep. 1990 Revised
(Contract W-7405-eng-48)
(DE91-007146; UCRL-JC-104407-Rev-1;
CONF-9009266-10-Rev-1) Avail: NTIS HC/MF A02

Results from recent recombination x ray laser experiments carried out on the Nova laser using exploding ribbon Al targets irradiated with 100 ps pulses of 0.53-micron light are described. Data showed, however, that the plasma was insufficiently ionized to produce recombination pumped gain in H-like AL. Some evidence of weak amplification was seen for several transitions in He- and Li-like Al and H-like O. It is clear for the target and irradiation conditions studied that stimulated emission did not dominate over spontaneous emission for the candidate lasing lines. DOE

N91-19430# Lawrence Livermore National Lab., CA.
UPGRADE OF THE LLNL NOVA LASER FOR INERTIAL CONFINEMENT FUSION
J. R. Murray, J. B. Trenholme, J. T. Hunt, D. N. Frank, W. H. Lowdermilk, and E. Storm Jan. 1991 14 p Presented at the OE/LASE 1991: 4th Society of Photo-Optical Instrumentation Engineers (SPIE) International Symposium, Los Angeles, 20-25 Jan. 1991
(Contract W-7405-eng-48)
(DE91-008060; UCRL-JC-104435; CONF-910123-10) Avail: NTIS HC/MF A03

The Lawrence Livermore National Laboratory has proposed to construct an upgrade to the Nova glass laser facility to give an output energy of 1.5 to 2 megajoules at 350 nanometers wavelength in a nominally 3 to 5 nanosecond shaped pulse. The Nova Upgrade will be suitable for driving inertial fusion targets to ignition. This paper reviews the design proposed for the laser. DOE

N91-19431# Sandia National Labs., Albuquerque, NM.
FALCON REACTOR-PUMPED LASER DESCRIPTION AND PROGRAM OVERVIEW
P. S. Pickard 1990 8 p Presented at the Strategic Defense Initiative Organization (SDIO) Laser Propulsion Workshop, Boston, MA, 6-7 Dec. 1990
(Contract DE-AC04-76DP-00789)
(DE91-008185; SAND-91-0259C; CONF-901278-1-Vugraphs)
Avail: NTIS HC/MF A02

The fission activated laser concept (FALCON) reactor-pumped laser program at Sandia National Laboratories is examining the feasibility of high-power systems pumped directly by the energy from a nuclear reactor. In this concept we use the highly energetic fission fragments from neutron induced fission to excite a large volume laser medium. This technology has the potential to scale to extremely large optical power outputs in a primarily self-powered device. A laser system of this type could also be relatively compact and capable of long run times without refueling. DOE

N91-19432# Brookhaven National Lab., Upton, NY.
SUMMARY OF THE WORKING GROUP ON TRANSVERSE EMISSIONS FROM PHOTOCATHODES
J. Fischer, H. Kirk, T. Srinivasan-Rao, T. Tsang, and W. J. Willis (Columbia Univ., New York, NY.) Oct. 1990 6 p Presented at the Prospects for A 1 Angstrom Free-Electron Laser (FEL) Workshop, Sag Harbor, ME, 22-27 Apr. 1990
(Contract DE-AC02-76CH-00016)
(DE91-008414; BNL-45482; CONF-9004232-4) Avail: NTIS HC/MF A02

As the wavelength of the FEL decreases, so does the acceptable emittance of the electron beam entering the wiggler. Eventually, the emittance of the electrons as they leave the cathode begins to play a dominant role. The task facing the working group was to estimate the lowest emittance attainable as they escape the surface. The emittance of these electrons are dictated by many factors including the kinetic energy imparted to them by the photons, the extraction and optical field and the temperature of the electrons and the lattice. Maximum contribution due to each of these effects are estimated in the following section. DOE

N91-19433# Lawrence Livermore National Lab., CA.
NICKEL-LIKE X RAY LASERS

B. J. MacGowan, L. B. DaSilva, D. J. Fields, A. R. Fry, C. J. Keane, D. L. Matthews, S. Maxon, A. L. Osterheld, J. H. Scofield, and G. Shimkaveg 14 Jan. 1991 5 p Presented at the International Conference on Lasers '90, San Diego, CA, 10-14 Dec. 1990
(Contract W-7405-eng-48)
(DE91-008502; UCRL-JC-104161; CONF-901263-7) Avail: NTIS HC/MF A01

Collisionally pumped, 4d-4p, Ni-like x ray lasers have been produced at wavelengths close to, and below the carbon K absorption edge (43.76 Angstrom). The laser medium is a high temperature laser produced plasma of highly stripped ions. To date, ions in the range Z = 62 (Sm) to Z = 79 (Au) have been ionized to the state isoelectronic to Ni-I (Z = 28), and produced evidence of amplification through stimulated emission. The Ni-like Ta amplifier at 44.83 (Angstrom) is being developed as a source for future x ray holography experiments. DOE

N91-19434# Electronics Research Lab., Adelaide (Australia).
INVESTIGATION AT TWO WAVELENGTHS OF A MODULATED He-Xe RARE GAS LASER
Kenneth J. Grant, Shane A. Brunker, and Robert J. Rossiter Jul. 1990 26 p
(AD-A229852; ERL-0508-RN; DODA-AR-006-434) Avail: NTIS HC/MF A03 CSCL 09/3

A He-Xe rare gas laser has previously been reported to emit at several wavelengths in the 2 to 4 micron region in continuous wave and modulated modes. This research note discusses the effect of variation of discharge parameters on the output power and pulse energy of two infrared wavelengths of 3.894 and 3.995 micron. GRA

N91-19802# Joint Publications Research Service, Arlington, VA.
ACOUSTIC STABILIZATION OF LASER BEAM WAVEFRONT IN NONHOMOGENEOUS GASEOUS MEDIUM Abstract Only
D. O. Lapotko and O. G. Martynenko *In its* JPRS Report: Science and Technology. USSR: Physics and Mathematics 31 Oct. 1990 p 1 Transl. into ENGLISH from Inzhenerno-Fizicheskiy Zhurnal (Minsk, USSR), v. 58, no. 2, Feb. 1990 p 235-238 (For primary document see N91-19800 11-70)
Avail: NTIS HC/MF A03

N91-19803# Joint Publications Research Service, Arlington, VA.
PASSIVE MODE LOCKING IN OPTICALLY PUMPED Al2O3:Ti(3+) LASER Abstract Only
M. I. Demchuk, A. A. Demidovich, N. I. Zhavoronkov, V. P. Mikhaylov, A. P. Shkadarevich, A. A. Ishchenko, and A. I. Sopin *In its* JPRS Report: Science and Technology. USSR: Physics and Mathematics 31 Oct. 1990 p 3 Transl. into ENGLISH from Kvantovaya Elektronika (Moscow, USSR), v. 17, no. 2, Feb. 1990 p 133 (For primary document see N91-19800 11-70)
Avail: NTIS HC/MF A03

N91-19804# Joint Publications Research Service, Arlington, VA.
POSSIBILITY OF RAISING EFFICIENCY OF FREE-ELECTRON LASER IN LONGITUDINAL MAGNETIC FIELD Abstract Only
V. A. Bazylev and A. V. Tulupov *In its* JPRS Report: Science and Technology. USSR: Physics and Mathematics 31 Oct. 1990 p 3 Transl. into ENGLISH from Kvantovaya Elektronika (Moscow, USSR), v. 17, no. 2, Feb. 1990 p 156-159 (For primary document see N91-19800 11-70)
Avail: NTIS HC/MF A03

N91-19805# Joint Publications Research Service, Arlington, VA.
QUANTUM FLUCTUATIONS IN LASER WITH INTRACAVITY FREQUENCY DOUBLING Abstract Only
A. I. Zhiliba *In its* JPRS Report: Science and Technology. USSR: Physics and Mathematics 31 Oct. 1990 p 3-4 Transl. into ENGLISH from Optika Atmosfery (Tomsk, USSR), v. 2, no. 10, Oct. 1989 p 1118-1120 (For primary document see N91-19800 11-70)
Avail: NTIS HC/MF A03

N91-19806# Joint Publications Research Service, Arlington, VA.
COPPER VAPOR AS ACTIVE MEDIUM FOR HIGH-POWER OSCILLATOR-AMPLIFIER LASER SYSTEMS Abstract Only
N. A. Lyabin, V. V. Zubov, and A. D. Chursin *In its* JPRS Report: Science and Technology. USSR: Physics and Mathematics 31 Oct. 1990 p 4 Transl. into ENGLISH from Kvantovaya Elektronika (Moscow, USSR), v. 17, no. 1, Jan. 1990 p 28-31 (For primary document see N91-19800 11-70)
Avail: NTIS HC/MF A03

N91-19807# Joint Publications Research Service, Arlington, VA.
CHARACTERISTICS OF EXCIMER LASER WITH NARROW EMISSION LINE Abstract Only
K. A. Valiyev, L. V. Velikov, G. S. Volkov, and D. Yu. Zaroslov *In its* JPRS Report: Science and Technology. USSR: Physics and Mathematics 31 Oct. 1990 p 4-5 Transl. into ENGLISH from Kvantovaya Elektronika (Moscow, USSR), v. 17, no. 1, Jan. 1990 p 43-45 (For primary document see N91-19800 11-70)
Avail: NTIS HC/MF A03

N91-19808# Joint Publications Research Service, Arlington, VA.
INTRACAVITY SECOND-HARMONIC GENERATION BY LASER WITH OPTICAL DELAY LINE AND MODE LOCKING Abstract Only
N. S. Balashov, S. K. Isayev, L. S. Korniyenko, N. V. Kvartsov, L. N. Magdich, V. Yu. Mikhaylov, S. R. Rustamov, and V. V. Firsov *In its* JPRS Report: Science and Technology. USSR: Physics and Mathematics 31 Oct. 1990 p 5 Transl. into ENGLISH from Kvantovaya Elektronika (Moscow, USSR), v. 17, no. 1, Jan. 1990 p 64-66 Original language document was announced in IAA as A90-34616 (For primary document see N91-19800 11-70)
Avail: NTIS HC/MF A03

N91-19811# Joint Publications Research Service, Arlington, VA.
MICROSECOND-PULSE Nd-GLASS LASER WITH MONOPULSE DURATION CONTROL Abstract Only
B. V. Anikeyev and V. V. Krutyakov *In its* JPRS Report: Science and Technology. USSR: Physics and Mathematics 31 Oct. 1990 p 15 Transl. into ENGLISH from Ukrainskiy Fizicheskiy Zhurnal (Kiev, USSR), v. 35, no. 2, Feb. 1990 p 209-213 (For primary document see N91-19800 11-70)
Avail: NTIS HC/MF A03

N91-19812# Joint Publications Research Service, Arlington, VA.
BREAKUP OF FEMTOSECOND PULSES DURING AMPLIFICATION IN Er(3+)-DOPED SINGLE-MODE OPTICAL FIBERS Abstract Only
A. B. Grudinin, Ye. M. Dianov, D. V. Korobkin, A. Yu. Makarenko, A. M. Prokhorov, and I. Yu. Khrushchev *In its* JPRS Report: Science and Technology. USSR: Physics and Mathematics 31 Oct. 1990 p 15-16 Transl. into ENGLISH from Pisma v Zhurnal Eksperimentalnoy i Teoreticheskoy Fiziki (Moscow, USSR), v. 51, no. 3, 10 Feb. 1990 p 121-124 (For primary document see N91-19800 11-70)
Avail: NTIS HC/MF A03

N91-19813# Joint Publications Research Service, Arlington, VA.
He-Ne LASER EMITTING FIVE LINES SIMULTANEOUSLY Abstract Only
Ya. M. Bondarchuk, R. M. Voznyak, and V. Ye. Privalov *In its* JPRS Report: Science and Technology. USSR: Physics and Mathematics 31 Oct. 1990 p 17 Transl. into ENGLISH from Optika i Spektroskopiya (Leningrad, USSR), v. 67, no. 6, Dec. 1989 p 1418-1419 (For primary document see N91-19800 11-70)
Avail: NTIS HC/MF A03

N91-19820# Joint Publications Research Service, Arlington, VA.
COHERENT EFFECTS IN GENERATION OF ULTRASHORT LIGHT PULSES BY SEMICONDUCTOR INJECTION LASER Abstract Only
E. M. Belenov and P. P. Vasilyev *In its* JPRS Report: Science and Technology. USSR: Physics and Mathematics 31 Oct. 1990

p 26 Transl. into ENGLISH from Zhurnal Eksperimentalnoy i Teoreticheskoy Fiziki (Moscow, USSR), v. 96, no. 5, Nov. 1989 p 1629-1637 (For primary document see N91-19800 11-70)
Avail: NTIS HC/MF A03

37 MECHANICAL ENGINEERING

Includes auxiliary systems (nonpower); machine elements and processes; and mechanical equipment.

N91-19435*# Ohio State Univ., Columbus. Dept. of Mechanical Engineering.
VIBRATION TRANSMISSION THROUGH ROLLING ELEMENT BEARINGS IN GEARED ROTOR SYSTEMS Ph.D. Thesis Final Report
Rajendra Singh and Teik Chin Lim Washington, D.C. NASA Nov. 1990 232 p
(Grant NAG3-773)
(NASA-CR-4334; AVSCOM-TR-90-C-019; E-5716; NAS 1.26:4334)
Avail: NTIS HC/MF A11 CSCL 13I

A new mathematical model is proposed to examine the vibration transmission through rolling element bearings in geared rotor systems. Current bearing models, based on either ideal boundary conditions for the shaft or purely translational stiffness element description, cannot explain how the vibratory motion may be transmitted from the rotating shaft to the casing. Experimental results have shown that the casing plate motion is primarily flexural. Here, this issue is clarified qualitatively and quantitatively by developing a comprehensive bearing stiffness matrix of dimension 6 to model precision rolling element bearings using basic principles. The proposed bearing stiffness matrix is partially verified using available analytical and experimental data, and is completely characterized. The study extends the proposed bearing formulation to analyze the overall geared rotor system dynamics including casing and mounts. The bearing stiffness matrix is included in discrete system models using lumped parameter and/or dynamic finite element techniques. Author

N91-19436 Department of the Navy, Washington, DC.
GRADUATED-LOAD SPRING WASHER SYSTEM FOR SCREWS AND THREADED FASTENERS Patent
James D. Rose, inventor (to Navy) and William H. Suder, III, inventor (to Navy) 25 Sep. 1990 7 p Filed 17 Aug. 1988
(AD-D014697; US-Patent-4,958,970; US-Patent-Class-411-12)
Avail: US Patent and Trademark Office CSCL 13/5

A graduated-load spring washer system for screws and threaded fasteners uses a deflection coil spring of slightly less than one coil with special end configurations for anti-marring. A cross-section of the coil spring is substantially trapezoidal, with the outer periphery thickness being the dimension of the trapezoid base and target. When placed under the head of a threaded fastener and flattened upon tightening of the fastener, the device maintains a large tailored preload to prevent loosening even during and after stress relaxation and creep, and eliminates the need for a usual flat washer below the coil to prevent marring. The device also eliminates requirements for use of torque application measuring tools because perload can be determined by sight or tactile sensing. GRA

N91-19437 Department of the Navy, Washington, DC.
SOLID STATE ELECTRONIC EMULATOR OF A MULTIPLE TRACK MOTOR DRIVEN ROTATING MAGNETIC MEMORY Patent
Kris S. Balch, inventor (to Navy) 18 Sep. 1990 29 p Filed 2 Jul. 1985
(AD-D014705; US-Patent-4,958,315; US-Patent-Appl-SN-751350; US-Patent-Class-364-900) Avail: US Patent and Trademark Office CSCL 14/3

A system is disclosed for emulating the memory characteristics of a motor-driven rotating memory having multiple heads per track with odd modular memory lengths. It is intended as a cost effective alternative for replacing magnetic rotating memories. The emulation is accomplished by multiplexing an offset memory address during each bit time. Non-volatile memory arrays translate the memory address to an offset address that is proportional to the odd modular track length of the multiple/single head track. Input/output registers are used for each read/write head that is emulated. An emulation address controller is used to generate all timing and initial addresses. GRA

N91-19438*# Akron Univ., OH.
LIFE AND DYNAMIC CAPACITY MODELING FOR AIRCRAFT TRANSMISSIONS Final Report
Michael Savage Washington NASA Jan. 1991 139 p
(Grant NAG3-55; DA Proj. 1L1-62211-A-47-A)
(NASA-CR-4341; E-5824; NAS 1.26:4341; AVSCOM-TR-90-C-027)
Avail: NTIS HC/MF A07 CSCL 13I

A computer program to simulate the dynamic capacity and life of parallel shaft aircraft transmissions is presented. Five basic configurations can be analyzed: single mesh, compound, parallel, reverted, and single plane reductions. In execution, the program prompts the user for the data file prefix name, takes input from a ASCII file, and writes its output to a second ASCII file with the same prefix name. The input data file includes the transmission configuration, the input shaft torque and speed, and descriptions of the transmission geometry and the component gears and bearings. The program output file describes the transmission, its components, their capabilities, locations, and loads. It also lists the dynamic capability, ninety percent reliability, and mean life of each component and the transmission as a system. Here, the program, its input and output files, and the theory behind the operation of the program are described. Author

N91-19439*# Illinois Univ., Chicago.
LOCAL SYNTHESIS AND TOOTH CONTACT ANALYSIS OF FACE-MILLED SPIRAL BEVEL GEARS Final Report
Faydor L. Litvin and Yi Zhang Washington NASA Jan. 1991 188 p
(Grant NAG3-964; DA Proj. 1L1-62211-A-47-A)
(NASA-CR-4342; E-5865; NAS 1.26:4342; AVSCOM-TR-90-C-028)
Avail: NTIS HC/MF A09 CSCL 13I

Computerized simulation of meshing and bearing contact for spiral bevel gears and hypoid gears is a significant achievement that could substantially improve the technology and the quality of the gears. An approach to the synthesis of face-milled spiral bevel gears and their tooth contact analysis is presented. The proposed approach is based on the following ideas: application of the principle of local synthesis that provides optimal conditions of meshing and contact at the mean contact point, M, and in the neighborhood of M; and application of relations between principle directions and curvatures for surfaces being in line contact or in point contact. The developed local synthesis of gears provides the following: (1) the required gear ratio at M; (2) a localized bearing contact with the desired direction of the tangent to the contact path on gear tooth surface and the desired length of the major axis of contact ellipse at M; (3) a predesigned parabolic function of a controlled level for transmission errors which enables absorption of linear functions of transmission errors caused by misalignment and reduces the level of vibrations. The proposed approach does not require either the tilt of the head-cutter for the process of generation or modified roll for the pinion generation. Improved conditions of meshing and contact of the gears can be achieved without the above mentioned parameters. A computer program for determination of basic machine-tool settings and tooth contact analysis for the designed gears is presented. The approach is illustrated with a numerical example. Author

N91-19440# Argonne National Lab., IL.
OXYGEN-ENRICHED DIESEL ENGINE PERFORMANCE: A COMPARISON OF ANALYTICAL AND EXPERIMENTAL RESULTS
R. R. Sekar, W. W. Marr, R. L. Cole, T. J. Marciniak, D. N. Assanis, and J. E. Schaus 1990 7 p Presented at the 12th Annual Fall Technical Conference of the American Society of Mechanical Engineers (ASME) Internal Combustion Engine Div., Rockford, 7-10

Oct. 1990
(Contract W-31-109-eng-38)
(DE91-006491; CONF-901038-1) Avail: NTIS HC/MF A02

Use of oxygen-enriched combustion air in diesel engines can lead to significant improvements in power density, as well as reductions in particulate emissions, but at the expense of higher NO(x) emissions. Oxygen enrichment would also lead to lower ignition delays and the opportunity to burn lower grade fuels. Analytical and experimental studies are being conducted in parallel to establish the optimal combination of oxygen level and diesel fuel properties. In this paper, cylinder pressure data acquired on a single-cylinder engine are used to generate heat release rates for operation under various oxygen contents. These derived heat release rates are in turn used to improve the combustion correlation -- and thus the prediction capability -- of the simulation code. It is shown that simulated and measured cylinder pressures and other performance parameters are in good agreement. The improved simulation can provide sufficiently accurate predictions of trends and magnitudes to be useful in parametric studies assessing the effects of oxygen enrichment and water injection on diesel engine performance. Measured ignition delays, NO(x) emissions, and particulate emissions are also compared with previously published data. The measured ignition delays are slightly lower than previously reported. Particulate emissions measured in this series of tests are significantly lower than previously reported. DOE

N91-19441*# National Aeronautics and Space Administration. Lewis Research Center, Cleveland, OH.
HIGH TEMPERATURE NASP ENGINE SEAL DEVELOPMENT
Bruce M. Steinetz, Matthew E. Melis, Dirk Orletski, and Mark G. Test (Pratt and Whitney Aircraft, West Palm Beach, FL.) Feb. 1991 21 p Presented at the 9th National Aerospace Plane Technology Symposium, Orlando, FL, 1-2 Nov. 1990
(NASA-TM-103716; E-5949; NAS 1.15:103716) Avail: NTIS HC/MF A03 CSCL 13I

Key to the development of advanced hypersonic engines such as those being considered for the National Aerospace Plane (NASP) is the development and evaluation of high temperature, flexible seals that must seal the many feet of gaps between the articulating and stationary engine panels. Recent seal progress made at NASA-Lewis is reviewed in the areas of seal concept maturation, test rig development, and performance tests. A test fixture was built at NASA capable of subjecting candidate 3 ft long seals to engine simulated temperatures (up to 1500 F), pressures (up to 100 psi), and engine wall distortions (up to 0.15 in only 18 in span). Leakage performance test results at high temperatures are presented for an innovative high temperature, flexible ceramic wafer seal. Also described is a joint Pratt and Whitney/NASA planned test program to evaluate thermal performance of a braided rope seal under engine simulated heat flux rates (up to 400 Btu/sq ft s), and supersonic flow conditions. These conditions are produced by subjecting the seal specimen to hydrogen oxygen rocket exhaust that flows tangent to the specimen. Author

N91-19442*# National Aeronautics and Space Administration. Lewis Research Center, Cleveland, OH.
A TEST FIXTURE FOR MEASURING HIGH-TEMPERATURE HYPERSONIC-ENGINE SEAL PERFORMANCE
Bruce M. Steinetz Dec. 1990 20 p
(NASA-TM-103658; E-5780; NAS 1.15:103658) Avail: NTIS HC/MF A03 CSCL 11A

A test fixture for measuring the performance of several high temperature engine seal concepts was installed at the NASA Lewis Research Center. The test fixture was developed to evaluate seal concepts under development for advanced hypersonic engines such as those being considered for the National Aerospace Plane. The fixture can measure static seal leakage performance from room temperature up to 1500 F and air pressure differentials up to 100 psi. Performance of the seals can be measured while sealing against flat or engine simulated distorted walls, where distortions can be as large as 0.150 in. in only an 18 in. span. The fixture is designed to evaluate seals 3 feet long, a typical engine panel length. The seal channel can be configured to test square, circular, or rectangular seals that are nominally 0.5 in. high. The sensitivity of leakage performance to lateral or axial loading can also be measured using specially designed high temperature lateral and axial bellows preload systems. Leakage data for a candidate ceramic wafer engine seal is provided by way of example to demonstrate the test fixture's capabilities. Author

N91-19443*# National Aeronautics and Space Administration. Lewis Research Center, Cleveland, OH.
HEAT TRANSFER IN ROTATING SERPENTINE PASSAGES WITH TRIPS NORMAL TO THE FLOW
J. H. Wagner, B. V. Johnson, R. A. Graziani (Pratt and Whitney Aircraft, East Hartford, CT.), and F. C. Yeh 1991 15 p Proposed for presentation at the 36th International Gas Turbine and Aeroengine Congress and Exhibition, Orlando, FL, 3-6 Jun. 1991; sponsored by ASME
(Contract NAS3-23691)
(NASA-TM-103758; E-6015; NAS 1.15:103758) Avail: NTIS HC/MF A03 CSCL 13B

Experiments were conducted to determine the effects of buoyancy and Coriolis forces on heat transfer in turbine blade internal coolant passages. The experiments were conducted with a large scale, multipass, heat transfer model with both radially inward and outward flow. Trip strips on the leading and trailing surfaces of the radial coolant passages were used to produce the rough walls. An analysis of the governing flow equations showed that four parameters influence the heat transfer in rotating passages: coolant-to-wall temperature ratio, Rossby number, Reynolds number, and radius-to-passage hydraulic diameter ratio. The first three of these four parameters were varied over ranges which are typical of advanced gas turbine engine operating conditions. Results were correlated and compared to previous results from stationary and rotating similar models with trip strips. The heat transfer coefficients on surfaces, where the heat increased with rotation and buoyancy, varied by as much as a factor of four. Maximum values of the heat transfer coefficients with high rotation were only slightly above the highest levels obtained with the smooth wall model. The heat transfer coefficients on surfaces, where the heat transfer decreased with rotation, varied by as much as a factor of three due to rotation and buoyancy. It was concluded that both Coriolis and buoyancy effects must be considered in turbine blade cooling designs with trip strips and that the effects of rotation were markedly different depending upon the flow direction. Author

N91-19444# Oak Ridge National Lab., TN.
A RIGID BODY MODEL AND DECOUPLED CONTROL ARCHITECTURE FOR TWO MANIPULATORS HOLDING A COMPLEX OBJECT
M. A. Unseren Jan. 1991 42 p
(Contract DE-AC05-84OR-21400)
(DE91-007827; ORNL/TM-11752; CESAR-91/01) Avail: NTIS HC/MF A03

A rigid body dynamical model and control architecture are developed for the closed-chain motion of two manipulators holding an object containing a spherical joint in three-dimensional workspace. The manipulators may have an equal or unequal number of joints. Dynamic and kinematic constraints are determined and combined with the equations of motion of the manipulators to obtain a dynamical model of the entire system in the joint space. The problem of solving the joint space model for the unknown variables is discussed. This includes a new proof that the problem of solving the model for the generalized input forces applied to the joint actuators (i.e., computing the joint torques) is underspecified in nature. The system is transformed to reduce the dimensionality of the model and eliminate the generalized contact forces, which are calculated separately. The problem of solving the reduced order model for the unknown variables is also addressed. A new control architecture consisting of the sum of the outputs of a primary and secondary controller is suggested which, according to the model, decouples the force- and

position-controlled degrees of freedom during motion of the system. The proposed composite controller enables the designer to develop independent, non-interacting control laws for the force- and position-control of the complex closed-chain system. DOE

N91-19445# Oak Ridge National Lab., TN.
DESIGN AND CONTROL OF A FULLY OMNIDIRECTIONAL AND HOLONOMIC WHEELED PLATFORM FOR ROBOTIC VEHICLES
S. M. Killough and F. G. Pin 1991 8 p Presented at the IEEE Robotics and Automation Conference, Sacramento, CA, 7-12 Apr. 1991
(Contract DE-AC05-84OR-21400)
(DE90-017746; CONF-910451-4) Avail: NTIS HC/MF A02

For practical robotics application in outdoors or complex environments (e.g. firefighting, warehouse management, floor cleaning, plant surveillance, emergency handling, etc.), mobile robotic platforms are needed for the transport of the manipulative or perceptive robots to various work sites and to assist robot movements at the work site. An ideal platform would be one with full 3-degree-of-freedom (DOF) movement (x, y translation and rotation) to enable tighter navigation and docking, obstacle avoidance, and improved manipulator reach. Three DOFs would also simplify control of the platform and make it more general, thus providing more opportunities for autonomous control. Such a 3-DOF platform based on an orthogonal wheel assembly has been developed at the Oak Ridge National Laboratory and is being used for robotics and artificial intelligence research. This paper presents the mathematical details of the design and control of this type of platform and discusses the experiences and lessons learned with the first prototype. Improvements on the basic wheel assembly as well as optimum platform configurations that are considered for various applications are also discussed. DOE

N91-19446# Oak Ridge National Lab., TN.
A NEW WHEEL CONTROL SYSTEM FOR THE OMNIDIRECTIONAL HERMIES-3 ROBOT
D. B. Reister 1990 12 p Presented at the IEEE Robotics and Automation Conference, Sacramento, CA, 7-12 Apr. 1991
(Contract DE-AC05-84OR-21400)
(DE90-017764; CONF-910451-6) Avail: NTIS HC/MF A03

We have designed, built, and tested a new wheel control system for the HERMIES-III robot. HERMIES-III is a large mobile robot with omnidirectional steering that is designed for human scale experiments. The wheel control system moves the robot toward a goal and calculates the current position of the robot. The system has seven modes for moving to a goal and allows the goal to be changed (at 20 Hz) during motion by the robot. DOE

N91-19447# Oak Ridge National Lab., TN.
DEMO 89: THE INITIAL EXPERIMENT WITH THE HERMIES-3 ROBOT
D. B. Reister, J. P. Jones, P. L. Butler, M. Beckerman, and F. J. Sweeney 1990 13 p Presented at the IEEE Robotics and Automation Conference, Sacramento, CA, 7-12 Apr. 1991
(Contract DE-AC05-84OR-21400)
(DE90-017765; CONF-910451-5) Avail: NTIS HC/MF A03

HERMIES-III is a large mobile robot designed for human scale experiments. The initial experiment with the robot (DEMO 89) was the cleanup of a simulated chemical spill. To perform the experiment, the robot was required to plan a path through an a priori known world, navigate along the path (avoiding unexpected obstacles) and locate and remove debris from a target area. This paper describes the software system that was developed to perform the experiment. The software system consisted of 19 processes that operated on distributed set of heterogeneous computers. DOE

N91-19448# Sandia National Labs., Albuquerque, NM.
MINIMUM-TIME TRAJECTORY CONTROL OF A TWO-LINK FLEXIBLE ROBOTIC MANIPULATOR
D. A. Schoenwald, J. T. Feddema, G. R. Eisler, and D. J. Segalman 1990 26 p Presented at the IEEE Robotics and Automation Conference, Sacramento, CA, 7-12 Apr. 1991
(Contract DE-AC04-76DP-00789)
(DE91-001261; SAND-90-2472C; CONF-910451-10) Avail: NTIS HC/MF A03

This paper analyzes the experimental and simulation results of a minimum-time trajectory control scheme for a two-link flexible robot. An off-line optimization routine determines a minimum-time, straight line tip trajectory which stays within the torque constraints of the motors and ends in a quiescent state: no vibrational transients. An efficient finite-element model is used in the optimization to approximate the flexible arm dynamics. The control strategy is used to determine the feedback gains for the position, velocity, and strain gage signals from a quadratic cost criterion based on the finite-element model linearized about the straight line tip trajectory. These feedback signals are added to the modeled torque obtained from the optimization routine and used to control the robot arm actuators. The results indicate that this combination of model-based and error-driven control strategies achieves a closer tracking of the desired trajectory and a better handling of modeling errors (such as tip payloads) than either strategy alone. DOE

N91-19449*# National Aeronautics and Space Administration. Goddard Space Flight Center, Greenbelt, MD.
SYSTEM DESCRIPTION DOCUMENT FOR THE ANTHROBOT-2: A DEXTEROUS ROBOT HAND
Michael S. Ali and Charles Engler, Jr. Washington Mar. 1991 17 p
(NASA-TM-104535; Rept-91E01238; NAS 1.15:104535) Avail: NTIS HC/MF A03 CSCL 13I

The Anthrobot-2 is an anatomically correct, fully functioning robot hand. The number of fingers, the proportions of the links, the placement and motion of the thumb, and the shape of the palm follow those of the human hand. Each of the finger and thumb joints are servo-controlled. The Anthrobot-2 also includes a two-degree-of-freedom wrist. The entire package, including wrist, hand, and actuators, will mount on the ends of a variety of industrial manipulators. A patent has been applied for on the design. The Anthrobot-2 will be useful in tasks where dexterous manipulation or telemanipulation are required. Author

N91-19450# Edgerton, Germeshausen and Grier, Inc., Idaho Falls, ID.
LESSONS LEARNED FROM THE DESIGN AND OPERATION OF STEAM GENERATORS FOR HIGH TEMPERATURE GAS-COOLED REACTORS
Nov. 1990 33 p
(Contract DE-AC07-76ID-01570)
(DE91-006139; EGG-NPR-9334) Avail: NTIS HC/MF A03

This report presents a brief description of operating experiences related to steam generators used in high temperature gas-cooled production and test reactor systems. The descriptions were obtained from a review of published reports and papers concerning such experiences. Design philosophies applied to steam generator advanced conceptual designs are also addressed. Highlights of the important lessons learned that may be applicable to the New Production Reactor-Modular High Temperature Gas-Cooled Reactor (NPR-MHTGR) steam generator are presented. DOE

N91-19451# Oak Ridge National Lab., TN.
RESULTS FROM THE THIRD YEAR OF OPERATION OF THE FEDERAL METHANOL FLEET AT ARGONNE NATIONAL LABORATORY
B. H. West, R. N. McGill, S. L. Hillis, and J. W. Hodgson (Tennessee Univ., Knoxville.) Jan. 1991 68 p
(Contract DE-AC05-84OR-21400)
(DE91-007822; ORNL/TM-11736) Avail: NTIS HC/MF A04

Argonne National Laboratory has completed three full years of operation of 19 vehicles in the Federal Methanol Fleet Project; ten of the vehicles are fueled with M85 (85 percent methanol, 15 percent unleaded gasoline). Nearly 675,000 miles were accumulated on the fleet vehicle so far, and comparisons of energy efficiency continue to show nearly equal performance between

the methanol and gasoline vehicles. Emissions tests revealed evidence of degradation of emission control systems for both the methanol and gasoline vehicles. Methanol vehicles continued to require more maintenance than the gasoline vehicles, and maintenance labor intensity (hours per 1000 miles) increased for all the vehicle types being monitored. Metal accumulation rates in lubricating oil of the methanol vehicles continued to be elevated compared to that of the gasoline vehicles. Driver satisfaction in the third year appeared to be about the same as the second year, with the gasoline vehicles generally being rated slightly higher than the methanol vehicles. DOE

N91-19452# Southwest Research Inst., San Antonio, TX.
PERFORMANCE OF UNDERWATER WELDMENTS Final Report
R. J. Dexter, E. B. Norris, W. R. Schick, and P. D. Watson 1990 253 p Sponsored by Ship Structure Committee, Washington, DC (Contract DTCG23-82-C-20017)
(PB91-129254; SSC-335) Avail: NTIS HC/MF A12 CSCL 13H

The wet and wet-backed metal arc welding process can produce welds suitable for structural applications. Welding procedures qualification tests and fracture toughness tests were performed on wet, wet-backed, and dry fillet and groove welds made with (1) A-36 steel and E6013 electrodes, and (2) A-516 steel and nickel alloy electrodes. No hydrogen cracking or brittle fracture behavior was observed. Statistical analysis reveals the effect and interaction of water depth, plate thickness, restraint, material, and location of notch in the weld. A correlation between the toughness and Charpy impact energy was developed. Author

N91-19453# Bristol Univ. (England). Dept. of Aerospace Engineering.
DYNAMIC BEHAVIOR OF PNEUMATIC TYRES
R. J. Hooker Jun. 1990 27 p
(BU-412; ETN-91-98863) Avail: NTIS HC/MF A03

A preliminary account of experimental studies of dynamic behavior of model aircraft tires is given. The program covered longitudinal, lateral and rotational motions for both cross ply and radial ply tires, over ranges of operating conditions. The tires were tested by exciting appropriate resonant sinusoidal vibration. By measurement of frequency, exciting force and response it is possible to determine the dynamic stiffness and damping. ESA

N91-19454# Helsinki Univ. of Technology, Espoo (Finland). Internal Combustion Engine Lab.
A MODELLING OF UNSTEADY AIR FLOW IN THE RESONANCE CHARGING SYSTEM OF HIGH SPEED DIESEL ENGINES Ph.D. Thesis
Raimo Turunen Helsinki, Finland Finnish Academy of Technology 1990 130 p Sponsored by Jenny and Antti Wihuri Foundation, and Helsinki Univ. Foundation for Financial Aid, Finland
(Acta-Polytec-Scand-Me-97; ISBN-951-666-320-6; ISSN-0001-687X; ETN-91-98915) Avail: NTIS HC/MF A07

A model for descibing the unsteady flow in the high speed diesel engine resonance charging system and the formation of the air charge in the cylinder is developed. Attention was paid to parameters like the charging pipe system geometry, the inlet valve discharge coefficient and timing, and the heat transfer in the cylinder during the intake periods. The working of the model is ascertained by experiments with a test engine. The model can be used in the optimizing of the shape of the resonance pipe system. ESA

N91-19455# Technische Univ., Delft (Netherlands).
HEAT TRANSPORT DURING GAS TUNGSTEN ARC WELDING Ph.D. Thesis
Johannes Petrus Zijp 1990 170 p
(ETN-91-98919) Avail: NTIS HC/MF A08

A study to understand the basic heat flow processes during gas tungsten arc welding, which is of importance in assessing the relationship between welding parameters and weld quality, is presented. Calorimetric experiments were performed to determine the influence of welding parameters such as cathode and anode compositions, arc current and length, polarity, and shielding gas flow rate and composition on the heat flow to anode and cathode. The influence of ambient pressure and shielding gas composition was determined in a pressure Vessel in experiments using the thermal cycle of the workpiece to calculate the workpiece heat input. Results are discussed and an adjusted heat flow model is proposed. The electric field strength of the arc is shown to be gradually dependent on axial position so that a strict distinction between the anode and cathode voltage drops and the voltage drop over the arc column region cannot be made. This has consequences in particular for the heat balance of the cathode. ESA

N91-19456# Technische Univ., Delft (Netherlands). Dept. of Aerospace Engineering.
ELEMENTARY CONSIDERATIONS ON THE GAS DYNAMIC DESIGN PARAMETERS OF A MHD FARADAY GENERATOR IN RELATION TO A GAS TURBINE CYCLE
G. Schouten Aug. 1990 23 p
(LR-564; ETN-91-98938) Avail: NTIS HC/MF A03

The selection of design parameters of a Magneto Hydro Dynamic (MHD) Faraday generator is performed referring to the gas turbine power generator. Where the efficiency of an ideal gas turbine conversion cycle with heat recovery is 52 percent, the ideal MHD Faraday generator cycle may achieve an efficiency as high as 72.5 percent. Parameter curves for the gas turbine, presenting the efficiency as a function of pressure ratio and temperature ratio, indicate that high temperature and low pressure ratio yield high efficiency. After selecting a pressure ratio of 10 and a process temperature of 3000 K for the MHD generator, parameter curves are drawn involving the velocity fraction and the pressure gradient combined with the magnetic field strength. For the ideal generator it then follows that it is favorable to extract the energy very gently at low velocity, low current density, low pressure gradient and high magnetic field strength. In a real generator the boundary layer losses oppose these criteria, they would require a short channel implying high velocity, high pressure gradient and high current density. An estimation of the boundary layer losses indicates that in a channel with relative boundary layer thickness of 5 percent of the cross dimensions the efficiency is reduced from 72.5 to 36 percent. ESA

N91-19457# Oxford Univ. (England). Dept. of Engineering Science.
THE SELECTION OF WINDOW FUNCTIONS FOR THE CALCULATION OF TIME DOMAIN AVERAGES ON THE VIBRATION OF THE INDIVIDUAL GEARS IN AN EPICYCLIC GEARBOX
P. D. McFadden 1990 31 p Sponsored by Science Research Council, England
(OUEL-1818/90; ETN-91-98953) Avail: NTIS HC/MF A03

An existing technique which enables the estimation of the time domain averages of the tooth meshing vibration of the individual planet and sun gears in an epicycling gearbox from measured vibration signals is revised. A key feature of the existing technique is the sampling of the vibration signal within a rectangular window in the time domain when one of the planet gears is close to the vibration transducer. The revised technique permits the use of other window functions, and a detailed analysis shows that the errors in the estimate of the time domain average can be expressed in terms of the window function. Several suitable window functions which enable a reduction in the level of the errors are demonstrated by numerical examples and by the analysis of data from a test on a helicopter gearbox with deliberate damage to one of the planet gears. ESA

N91-19458# Oxford Univ. (England). Robotics Research Group.
VISUAL NAVIGATION AROUND CURVED OBSTACLES
A. Blake, M. Brady, R. Cipolla, Z. Xie, and A. Zisserman Sep. 1990 21 p Sponsored by Science Research Council, England

and Commission of the European Communities
(OUEL-1861/90; ETN-91-98959) Avail: NTIS HC/MF A03

Recent progress in theory of visual motion shows how analysis of moving image contours can provide estimates of the shape of curved surfaces. An approach to path planning around smooth obstacles that exploits such visually derived geometry is proposed. A moving robot can scan the silhouette or 'apparent contour' of an obstacle and estimate a minimum length path. This is done by seeking geodesics which can be extrapolated smoothly, around the obstacle and towards the goal. Preliminary implementation of this idea uses a real time visual contour tracker running at 16 Hz, with a camera mounted on an Adept robot arm. The camera first 'dithers' to generate visual motion, a safe path is estimated, and the robot steers the camera around the obstacle with a clearance of a few millimeters. ESA

N91-19459# Oxford Univ. (England). Robotics Research Group.
REAL-TIME SENSOR-BASED APPROACH TO THE IMPROVEMENT OF TRANSITIONS OF ROBOT MANIPULATOR CONTROLS
Youfu Li and R. W. Daniel 1990 16 p
(OUEL-1866/90; ETN-91-98962) Avail: NTIS HC/MF A03

A sensor based control approach, to provide a smooth and fast transition for the robot when it is required to stop or change its control laws upon contacting a target, is proposed. The system is aimed at being capable of providing such a transition even though uncertainties about the target may exist. Proximity sensors are used as external sensors to provide the robot with its environmental information. A closed loop with hierarchical control levels is formed. Dynamic sensing and intelligent robot positioning systems are reviewed. The adopted sensing strategy is given. Different control schemes at high and low levels are presented for the hierarchical robot control proposed. Simulation results are given. ESA

N91-20035*# State Univ. of New York, Farmingdale. Dept. of Mechanical Engineering Technology.
SOME ASPECTS OF ROBOTICS CALIBRATION, DESIGN AND CONTROL
Hazem Tawfik *In* NASA, John F. Kennedy Space Center, Research Reports: 1990 NASA/ASEE Summer Faculty Fellowship Program Sep. 1990 p 380-431 (For primary document see N91-20022 11-99)
(Grant NGT-60002)
Avail: NTIS HC/MF A23 CSCL 13I

38 QUALITY ASSURANCE AND RELIABILITY

Includes product sampling procedures and techniques; and quality control.

N91-19460# Dayton Univ., OH. Analytical and Experimental Systems Group.
RESEARCH ON ADVANCED NDE METHODS FOR AEROSPACE STRUCTURES Final Technical Report, 1 Sep. 1986 - 31 Aug. 1989
Brian G. Frock, Robert J. Andrews, Richard W. Martin, Prasanna Karpur, Mark J. Ruddell, Jeffery A. Fox, Edward L. Klosterman, and Mary L. Papp Sep. 1989 188 p
(Contract F33615-86-C-5016; AF Proj. 2418)
(AD-A226858; UDR-TR-89-81; WRDC-TR-89-4134) Avail: NTIS HC/MF A09 CSCL 14/4

This Final Report describes investigations of the capabilities and limitations of several digital ultrasonic NDE techniques for imaging defects in advance aerospace materials. The goal of these investigations was to determine the feasibility and practicality of transitioning these techniques from the laboratory to field use. Studies of new digital data collection techniques, signal processing, image enhancement, and image restoration techniques revealed that their use can significantly improve the resolution of features in ultrasonic images. The use of narrow software gates to collect data from digitized rf A-scans improved the resolution in C-scan images of closely-spaced planes in advanced composite materials. That technique was used to simultaneously generate C-scan images of (1) material defects throughout the entire thickness of several 32-ply thick, graphite-epoxy composite materials. The depth resolution of ultrasonic B-scan images was improved by generating the images from axially deconvolved A-scans and from axially power-spectrum-equalized A-scans rather than from the rf A-scans. Lateral resolution in C-scan images was significantly improved by collecting data for the images from Wiener-deconvolved A-scan and from the power-spectrum-equalized A-scan rather than from the rf A-scans. GRA

N91-19461*# Virginia Polytechnic Inst. and State Univ., Blacksburg. Dept. of Engineering Science and Mechanics.
MECHANICAL BEHAVIOR OF A CERAMIC MATRIX COMPOSITE MATERIAL M.S. Thesis Final Report
Paul P. Grosskopf and John C. Duke, Jr. Feb. 1991 145 p
(Grant NAG3-172)
(NASA-CR-187072; NAS 1.26:187072) Avail: NTIS HC/MF A07 CSCL 14D

Monolithic ceramic materials have been used in industry for hundreds of years. These materials have proven their usefulness in many applications, yet, their potential for critical structural applications is limited. The existence of an imperfection in a monolithic ceramic on the order of several microns in size may be critical, resulting in catastrophic failure. To overcome this extreme sensitivity to small material imperfections, reinforced ceramic materials were developed. A ceramic matrix which has been reinforced with continuous fibers is not only less sensitive to microscopic flaws, but is also able to sustain significant damage without suffering catastrophic failure. A borosilicate glass reinforced with several layers of plain weave silicon carbide cloth (Nicalon) was studied. The mechanical testing which was performed included both flexural and tensile loading configurations. This testing was done not only to determine the material properties, but also to initiate a controlled amount of damage within each specimen. Several nondestructive testing techniques, including acousto-ultrasonics (AU), were performed on the specimens periodically during testing. The AU signals were monitored through the use of an IBM compatible personal computer with a high speed data acquisition board. Software was written which manipulates the AU signals in both the time and frequency domains, resulting in quantitative measures of the mechanical response of the material. The measured AU parameters are compared to both the mechanical test results and data from other nondestructive methods including ultrasonic C-scans and penetrant enhanced x ray radiography. Author

N91-19462*# National Aeronautics and Space Administration. Lewis Research Center, Cleveland, OH.
ETARA PC VERSION 3.3 USER'S GUIDE: RELIABILITY, AVAILABILITY, MAINTAINABILITY SIMULATION MODEL
David J. Hoffman and Larry A. Viterna Feb. 1991 65 p
(NASA-TM-103751; E-6003; NAS 1.15:103751) Avail: NTIS HC/MF A04 CSCL 14D

A user's manual describing an interactive, menu-driven, personal computer based Monte Carlo reliability, availability, and maintainability simulation program called event time availability reliability (ETARA) is discussed. Given a reliability block diagram representation of a system, ETARA simulates the behavior of the system over a specified period of time using Monte Carlo methods to generate block failure and repair intervals as a function of exponential and/or Weibull distributions. Availability parameters such as equivalent availability, state availability (percentage of time as a particular output state capability), continuous state duration and number of state occurrences can be calculated. Initial spares allotment and spares replenishment on a resupply cycle can be simulated. The number of block failures are tabulated both individually and by block type, as well as total downtime, repair time, and time waiting for spares. Also, maintenance man-hours

per year and system reliability, with or without repair, at or above a particular output capability can be calculated over a cumulative period of time or at specific points in time. Author

N91-19463*# National Aeronautics and Space Administration. Lewis Research Center, Cleveland, OH.
PROPERTY AND MICROSTRUCTURAL NONUNIFORMITY IN THE YTTRIUM-BARIUM-COPPER-OXIDE SUPERCONDUCTOR DETERMINED FROM ELECTRICAL, MAGNETIC, AND ULTRASONIC MEASUREMENTS Ph.D. Thesis - Case Western Reserve Univ.
Don J. Roth Jan. 1991 260 p
(NASA-TM-103732; E-5842; NAS 1.15:103732) Avail: NTIS HC/MF A12 CSCL 14D

The purpose of this dissertation was the following: (1) to characterize the effect of pore fraction on a comprehensive set of electrical and magnetic properties for the yttrium-barium-copper-oxide (YBCO) high temperature ceramic superconductor; and (2) to determine the viability of using a room-temperature, nondestructive characterization method to aid in the prediction of superconducting (cryogenic) properties. The latter involved correlating ultrasonic velocity measurements at room temperature with property-affecting pore fraction and oxygen content variations. The use of ultrasonic velocity for estimating pore fraction in YBCO is presented, and other polycrystalline materials are reviewed, modeled, and statistically analyzed. This provides the basis for using ultrasonic velocity to interrogate microstructure. The effect of pore fraction (0.10-0.25) on superconductor properties of YBCO samples was characterized. Spatial (within-sample) variations in microstructure and superconductor properties were investigated, and the effect of oxygen content on elastic behavior was examined. Experimental methods used included a.c. susceptibility, electrical, and ultrasonic velocity measurements. Superconductor properties measured included transition temperature, magnetic transition width, transport and magnetic critical current density, magnetic shielding, a.c. loss, and sharpness of the voltage-current characteristics. An ultrasonic velocity image constructed from measurements at 1mm increments across a YBCO sample revealed microstructural variations that correlated with variations in magnetic shielding and a.c. loss behavior. Destructive examination using quantitative image analysis revealed pore fraction to be the varying microstructural feature. Author

N91-19464*# National Aeronautics and Space Administration. Lewis Research Center, Cleveland, OH.
NDE STANDARDS FOR HIGH TEMPERATURE MATERIALS
Alex Vary 1991 20 p Presented at the Symposium on Nondestructive Testing Standards 2: New Opportunities for Increased World Trade Through Accepted Standards for NDT and Quality, Gaithersburg, MD, 9-11 Apr. 1991; sponsored by ASTM, NIST, the American Society for Nondestr
(NASA-TM-103761; E-6023; NAS 1.15:103761) Avail: NTIS HC/MF A03 CSCL 14D

High temperature materials include monolithic ceramics for automotive gas turbine engines and also metallic/intermetallic and ceramic matrix composites for a range of aerospace applications. These are materials that can withstand extreme operating temperatures that will prevail in advanced high-efficiency gas turbine engines. High temperature engine components are very likely to consist of complex composite structures with three-dimensionality interwoven and various intermixed ceramic fibers. The thermomechanical properties of components made of these materials are actually created in-place during processing and fabrication stages. The complex nature of these new materials creates strong incentives for exact standards for unambiguous evaluations of defects and microstructural characteristics. NDE techniques and standards that will ultimately be applicable to production and quality control of high temperature materials and structures are still emerging. The needs range from flaw detection to below 100 micron levels in monolithic ceramics to global imaging of fiber architecture and matrix densification anomalies in composites. The needs are different depending on the processing stage, fabrication method, and nature of the finished product. The standards are discussed that must be developed in concert with advances in NDE technology, materials processing research, and fabrication development. High temperature materials and structures that fail to meet stringent specifications and standards are unlikely to compete successfully either technologically or in international markets. Author

N91-19465# Oak Ridge National Lab., TN.
THE CHALLENGE OF STANDARDS FOR EMERGING NDT METHODS
R. W. McClung 1991 8 p Presented at the ASTM Symposium on Nondestructive Testing Standards, Gaithersburg, MD, 8-11 Apr. 1991
(Contract DE-AC05-84OR-21400)
(DE91-007834; CONF-9104111-1) Avail: NTIS HC/MF A02

The preparation of standards for emerging NDT methods may sound paradoxical with the rapid changes normally associated with new and emerging technology. However, consensus documentation of terminology and basic methods of performing tests of NDT equipment can do much to aid in the emergence and acceptance of such technology. Subcommittee E7.10 was established to serve as an 'umbrella' group and home for standards activities on emerging or other technology that has not yet grown sufficiently large to justify an independent subcommittee. Current activities include sections on thermoelectric sorting of metals, optical holography, and infrared methods. In addition, there are task groups on NDT reliability and methods for metal verification, identification, and sorting. DOE

N91-19466# Lawrence Livermore National Lab., CA.
NUCLEAR-SPECTROSCOPY COMPUTERIZED TOMOGRAPHY SCANNERS
G. P. Roberson, H. E. Martz, D. J. Schneberk, and C. M. Logan Feb. 1991 4 p Presented at the American Society for Nondestructive Testing Spring Conference, Oakland, 18-22 Mar. 1991
(Contract W-7405-eng-48)
(DE91-008447; UCRL-JC-105139; CONF-910399-1) Avail: NTIS HC/MF A01

The Lawrence Livermore National Laboratory (LLNL) has been developing industrial computerized tomography (CT) scanners over the last five years for specific programmatic needs. These scanners are used for nondestructive inspection and characterization of materials, components, and assemblies. Nuclear-spectroscopy computed tomography scanners typically use first-generation, single pencil beam scan-geometries. These are well-collimated single-source and single-detector systems where the object of interest is translated and rotated though a pencil-beam of gamma- or x-rays. Although the data acquisition time is much longer when compared to higher-generation CT scanners, these nuclear-spectroscopy-based scanners provide quantitative data and have fewer image artifacts. This artifact-free, quantitative data provides two-dimensional images with pixel values represented by direct absolute measurements of the linear attenuation coefficient that can be used to determine effective-Z, weight-fraction, and absolute-density images. DOE

39 STRUCTURAL MECHANICS

Includes structural element design and weight analysis; fatigue; and thermal stress.

For applications see *05 Aircraft Design, Testing and Performance* and *18 Spacecraft Design, Testing and Performance.*

N91-19467 Pennsylvania Univ., Philadelphia.
THE CORRELATION OF TRANSIENT CRACK GROWTH UNDER SMALL-SCALE-CREEP CONDITIONS Ph.D. Thesis
Ching Shyong Liu 1989 171 p
Avail: Univ. Microfilms Order No. DA9004803

The problem of characterizing growth under small creep and

transition conditions is of great practical significance. A fracture parameter C(sub t), which is related to the creep zone growth rate ahead of crack-tip has been defined by Saxena, Ernst, and Landes (1983) and verified experimentally by Saxena and Landes (1983) and explored numerically by Bassani, Hawk, and Saxena (1987). The correlations between da/dt, the crack velocity, and C(sub t) are extremely encouraging. Transient crack growth due to grain-boundary cavitation, the growth of the creep zone ahead of crack-tip, and da/dt-C(sub t) correlations are analyzed under small scale creep (SSC) conditions. elastic stress intensity factor K(sub I), which is the relevant load measure in SSC, is taken to vary with crack extension for various specimen geometries in the crack growth analyses. The material that deforms both elastically and by power-law creep, the time-dependent continuum stress field around the growing crack-tip under plane strain tensile (Mode-1) conditions evolves in three regions, each dominated by a singular, asymptotic crack-tip solution. A one-dimensional model that incorporates a fracture criterion based on creep controlled growth of grain-boundary cavities is used. The resulting nonlinear integral equation is solved numerically for various initial conditions. The applied far-field loading condition during crack growth in SCC is characterized by the stress intensity factor which is a function of crack extension. The crack-tip starts to extend from a stationary position after an incubation period. Depending on different initial conditions and specimen geometries, different growth histories are observed. Using this model, the creep zone growth-rate ahead of the crack-tip is numerically calculated and the validity of C(sub t) fracture parameter is explored. A modified definition of C(sub t) is proposed. Dissert. Abstr.

N91-19468 Department of the Navy, Washington, DC.
LOAD BEARING CONNECTIVE DAMPER Patent
Eugene C. Fischer, inventor (to Navy) and Roger M. Crane, inventor (to Navy) 4 Sep. 1990 7 p Filed 22 Nov. 1988
(AD-D014676; US-Patent-4,954,377; US-Patent-Appl-SN-274587; US-Patent-Class-428) Avail: US Patent and Trademark Office CSCL 20/11

A load bearing connective damper is disclosed for service in tensile, compression, and torsion as a shock and vibration isolation mounting device. Dampers are constructed using a multidimensionally braided textile shape and a visco-elastic material disposed in the interstrand spaces of the textile shape. GRA

N91-19469# National Aerospace Lab., Tokyo (Japan).
STRENGTH TEST OF CFRP BOX BEAM MODEL
Feb. 1990 25 p In JAPANESE; ENGLISH summary
(NAL-TR-1057; ISSN-0389-4010) Avail: NTIS HC/MF A03

The main goal was to obtain basic design data and technical information on applying advanced composites to primary structures of an aircraft for weight saving. Static and fatigue tests were performed on CFRP spar rib models with corrugated web and four types of CFRP joint assembly models which are typical joints for a tailplane structure. Strength tests of a CFRP Box Beam model with sweptback angle were conducted. The purpose of the tests was to evaluate ultimate strength and strain distributions in critical parts, as well as to investigate behavior of deformation initiation of damages, and sequence of failure. The model and the results of the tests are described. It was concluded that utilization of CFRP as primary structural elements for a tailplane is promising. Author

N91-19470# Sydney Univ. (Australia). Dept. of Aeronautical Engineering.
FINITE ELEMENT ANALYSIS OF GEOMETRICALLY NON-LINEAR PROBLEMS USING A COROTATIONAL LARGE ROTATION FORMULATION
J. D. C. McIvor and G. P. Steven Oct. 1990 27 p
(SU-ATN-9001) Avail: NTIS HC/MF A03

A corotational (CR) formulation that uses an efficient and effective method to calculate the element rigid body rotations is presented. This method is not order dependent and allows relatively large rotations to occur between iterations. This allows larger load steps to be taken which in turn leads to a faster solution. This method combined with a simple faceted element is shown to provide a straightforward but robust and effective treatment of the geometrically nonlinear structural problem. A large number of numerical examples are presented that fully test the capabilities of the new formulation. The code developed was incorporated into existing linear finite element code without having to make major modifications to existing element assembly routines.

Author

N91-19471*# National Aeronautics and Space Administration. Langley Research Center, Hampton, VA.
ACTIVE DAMPING APPLICATION TO THE SHUTTLE RMS
Michael G. Gilbert, Michael A. Scott, and Sean P. Kenny Jan. 1991 19 p Presented at the 4th NASA/DOD CSI Conference, Orlando, FL, 5-7 Nov. 1990
(NASA-TM-102763; NAS 1.15:102763) Avail: NTIS HC/MF A03 CSCL 20K

Control Structure Interaction (CSI) is a relatively new technology developed over the last 10 to 15 years for application to large flexible space vehicles. The central issue is recognition that high performance control systems necessary for good spacecraft performance may adversely interact with the dynamics of the spacecraft structures, a problem increasingly aggravated by the large size and reduced stiffness of modern spacecraft structural designs. The CSI analysis and design methods were developed to avoid interactions while maintaining spacecraft performance without exceeding structural capabilities, but they remain largely unvalidated by hardware experiments or demonstrations, particularly in-space flight demonstrations. One recent proposal for a low cost flight validation of CSI technology is to demonstrate active damping augmentation of the Space Shuttle Remote Manipulator System (RMS). An analytical effort to define the potential for such an active damping augmentation demonstration to improve the structural dynamic response of the RMS following payload maneuvers is described. It is hoped that this study will lead to an actual inflight CSI test with the RMS using existing shuttle hardware to the maximum extent possible. By using the existing hardware, the flight demonstration results may eventually be of direct benefit to actual Space Shuttle RMS operations, especially during the construction of the Space Station Freedom.

Author

N91-19472*# National Aeronautics and Space Administration. Lewis Research Center, Cleveland, OH.
PROBABILISTIC SIMULATION OF UNCERTAINTIES IN THERMAL STRUCTURES
Christos C. Chamis and Michael Shiao (Sverdrup Technology, Inc., Brook Park, OH.) 1990 15 p Presented at the First Thermal Structures Conference, Charlottesville, VA, 13-15 Nov. 1990; sponsored by Virginia Univ.
(NASA-TM-103680; E-5897; NAS 1.15:103680) Avail: NTIS HC/MF A03 CSCL 20K

Development of probabilistic structural analysis methods for hot structures is a major activity at Lewis Research Center. It consists of five program elements: (1) probabilistic loads; (2) probabilistic finite element analysis; (3) probabilistic material behavior; (4) assessment of reliability and risk; and (5) probabilistic structural performance evaluation. Recent progress includes: (1) quantification of the effects of uncertainties for several variables on high pressure fuel turbopump (HPFT) blade temperature, pressure, and torque of the Space Shuttle Main Engine (SSME); (2) the evaluation of the cumulative distribution function for various structural response variables based on assumed uncertainties in primitive structural variables; (3) evaluation of the failure probability; (4) reliability and risk-cost assessment, and (5) an outline of an emerging approach for eventual hot structures certification. Collectively, the results demonstrate that the structural durability/reliability of hot structural components can be effectively evaluated in a formal probabilistic framework. In addition, the approach can be readily extended to computationally simulate certification of hot structures for aerospace environments.

Author

N91-19473*# National Aeronautics and Space Administration. Lewis Research Center, Cleveland, OH.

APPLICATION OF THERMAL LIFE PREDICTION MODEL TO HIGH-TEMPERATURE AEROSPACE ALLOYS B1900+Hf AND HAYNES 188

Gary R. Halford, James F. Saltsman, Michael J. Verrilli, and Vinod K. Arya (Toledo Univ., OH.) Dec. 1990 12 p

(NASA-TM-4226; E-5511; NAS 1.15:4226) Avail: NTIS HC/MF A03 CSCL 20K

The results of the application of a newly proposed thermomechanical fatigue (TMF) life prediction method to a series of laboratory TMF results on two high-temperature aerospace engine alloys are presented. The method, referred to as TMF/TS-SRP, is based on three relatively recent developments: the total strain version of the method of Strainrange Partitioning (TS-SRP), the bithermal testing technique for characterizing TMF behavior, and advanced viscoplastic constitutive models. The high-temperature data reported in a companion publication are used to evaluate the constants in the model and to provide the TMF verification data to check its accuracy. Predicted lives are in agreement with the experimental lives to within a factor of approximately 2. Author

N91-19474*# National Aeronautics and Space Administration. Langley Research Center, Hampton, VA.

MODAL IDENTIFICATION OF A DEPLOYABLE SPACE TRUSS

Axel Schenk (Deutsche Forschungs- und Versuchsanstalt fuer Luft- und Raumfahrt, Goettingen, Germany, F.R.) and Richard S. Pappa Sep. 1990 22 p Presented at the 15th International Seminar on Modal Analysis and Structural Dynamics, Leuven, Belgium, 17-21 Sep. 1990

(NASA-TM-102720; NAS 1.15:102720) Avail: NTIS HC/MF A03 CSCL 20K

Work performed under a collaborative research effort between NASA and the German Aerospace Research Establishment (DLR) is summarized. The objective is to develop and demonstrate advanced technology for system identification of future large space structures. Recent experiences using the eigensystem realization algorithm (ERA) for modal identification of Mini-Mast are reported. Mini-Mast is a 20-meter-long deployable space truss used for structural dynamics and active-vibration control research at the NASA Langley Research Center. Due to nonlinearities and numerous local modes, modal identification of Mini-Mast proved to be surprisingly difficult. Methods available with ERA for obtaining detailed, high-confidence results are illustrated. Author

N91-19475*# National Aeronautics and Space Administration. Lewis Research Center, Cleveland, OH.

CASCADE FLUTTER ANALYSIS WITH TRANSIENT RESPONSE AERODYNAMICS

Milind A. Bakhle, Aparajit J. Mahajan, Theo G. Keith, Jr. (Ohio Aerospace Inst., Brook Park.), and George L. Stefko Feb. 1991 40 p Previously announced in IAA as A91-19448

(Grant NAG3-1137)

(NASA-TM-103746; E-5991; NAS 1.15:103746) Avail: NTIS HC/MF A03 CSCL 20K

Two methods for calculating linear frequency domain aerodynamic coefficients from a time marching Full Potential cascade solver are developed and verified. In the first method, the Influence Coefficient, solutions to elemental problems are superposed to obtain the solutions for a cascade in which all blades are vibrating with a constant interblade phase angle. The elemental problem consists of a single blade in the cascade oscillating while the other blades remain stationary. In the second method, the Pulse Response, the response to the transient motion of a blade is used to calculate influence coefficients. This is done by calculating the Fourier Transforms of the blade motion and the response. Both methods are validated by comparison with the Harmonic Oscillation method and give accurate results. The aerodynamic coefficients obtained from these methods are used for frequency domain flutter calculations involving a typical section blade structural model. An eigenvalue problem is solved for each interblade phase angle mode and the eigenvalues are used to determine aeroelastic stability. Flutter calculations are performed for two examples over a range of subsonic Mach numbers. Author

N91-19476*# National Aeronautics and Space Administration. Lewis Research Center, Cleveland, OH.

ON THE THERMODYNAMICS OF STRESS RATE IN THE EVOLUTION OF BACK STRESS IN VISCOPLASTICITY

Alan D. Freed, J.-L. Chaboche, and K. P. Walker (Engineering Science Software, Inc., Smithfield, RI.) 1991 8 p Prepared for the 3rd International Symposium on Plasticity, Grenoble, France, 12-16 Aug. 1991; sponsored by the Inst. de Mecanique de Grenoble

(NASA-TM-103794; E-6071; NAS 1.15:103794) Avail: NTIS HC/MF A02 CSCL 20K

A thermodynamic foundation using the concept of internal state variables is presented for the kinematic description of a viscoplastic material. Three different evolution equations for the back stress are considered. The first is that of classical, nonlinear, kinematic hardening. The other two include a contribution that is linear in stress rate. Choosing an appropriate change in variables can remove this stress rate dependence. As a result, one of these two models is shown to be equivalent to the classical, kinematic hardening model; while the other is a new model, one which seems to have favorable characteristics for representing ratchetting behavior. All three models are thermodynamically admissible. Author

N91-19477*# National Aeronautics and Space Administration. Lewis Research Center, Cleveland, OH.

THE METHOD OF LINES IN ANALYZING SOLIDS CONTAINING CRACKS

John P. Gyekenyesi Nov. 1990 22 p Presented at the 1st International Symposium on Methods of Lines, Surfaces, and Dimensional Reduction in Computational Mathematics and Mechanics, Athens, Greece, 25-30 Apr. 1991; sponsored by Polytechnic of Central London

(NASA-TM-103626; E-5794; NAS 1.15:103626) Avail: NTIS HC/MF A03 CSCL 20K

A semi-numerical method is reviewed for solving a set of coupled partial differential equations subject to mixed and possibly coupled boundary conditions. The line method of analysis is applied to the Navier-Cauchy equations of elastic and elastoplastic equilibrium to calculate the displacement distributions in various, simple geometry bodies containing cracks. The application of this method to the appropriate field equations leads to coupled sets of simultaneous ordinary differential equations whose solutions are obtained along sets of lines in a discretized region. When decoupling of the equations and their boundary conditions is not possible, the use of a successive approximation procedure permits the analytical solution of the resulting ordinary differential equations. The use of this method is illustrated by reviewing and presenting selected solutions of mixed boundary value problems in three dimensional fracture mechanics. These solutions are of great importance in fracture toughness testing, where accurate stress and displacement distributions are required for the calculation of certain fracture parameters. Computations obtained for typical flawed specimens include that for elastic as well as elastoplastic response. Problems in both Cartesian and cylindrical coordinate systems are included. Results are summarized for a finite geometry rectangular bar with a central through-the-thickness or rectangular surface crack under remote uniaxial tension. In addition, stress and displacement distributions are reviewed for finite circular bars with embedded penny-shaped cracks, and rods with external annular or ring cracks under opening mode tension. The results obtained show that the method of lines presents a systematic approach to the solution of some three-dimensional mechanics problems with arbitrary boundary conditions. The advantage of this method over other numerical solutions is that good results are obtained even from the use of a relatively coarse grid. Author

N91-19478*# McDonnell-Douglas Helicopter Co., Mesa, AZ.
DEVELOPMENT AND APPLICATIONS OF A MULTI-LEVEL STRAIN ENERGY METHOD FOR DETECTING FINITE ELEMENT MODELING ERRORS
Mostafa Hashemi-Kia, Kevin L. Kilroy, and G. Parker Oct. 1990 54 p
(Contract NAS1-17498)
(NASA-CR-187447; NAS 1.26:187447) Avail: NTIS HC/MF A04 CSCL 20K

A computational procedure is described which can be used efficiently in identifying modeling errors which may arise from development of a structural finite element model. The procedure, which is referred to as the multi-level strain energy check, is set up in the form of a set of NASTRAN DMAP alters which provide sufficient information about the modeling errors at G-Set, N-Set, and F-Set levels. This technique was applied to two NASTRAN models, namely, the AH-64A and AH-1G models. Two modeling errors were identified for the AH-1G, which were then corrected. Author

N91-19479*# Sverdrup Technology, Inc., Brook Park, OH.
THE EFFECT OF STEADY AERODYNAMIC LOADING ON THE FLUTTER STABILITY OF TURBOMACHINERY BLADING Final Report
Todd E. Smith and Jaikrishnan R. Kadambi (Case Western Reserve Univ., Cleveland, OH.) Dec. 1990 11 p Proposed for presentation at the 36th International Gas Turbine and Aerospace Congress and Exposition, Orlando, FL, 3-6 Jun. 1991; sponsored by ASME
(Contract NAS3-25266)
(NASA-CR-187055; E-5929; NAS 1.26:187055) Avail: NTIS HC/MF A03 CSCL 20K

An aeroelastic analysis is presented which accounts for the effect of steady aerodynamic loading on the aeroelastic stability of a cascade of compressor blades. The aeroelastic model is a two degree of freedom model having bending and torsional displacements. A linearized unsteady potential flow theory is used to determine the unsteady aerodynamic response coefficients for the aeroelastic analysis. The steady aerodynamic loading was caused by the addition of airfoil thickness and camber and steady flow incidence. The importance of steady loading on the airfoil unsteady pressure distribution is demonstrated. Additionally, the effect of steady loading on the tuned flutter behavior and flutter boundaries indicates that neglecting either airfoil thickness, camber or incidence could result in nonconservative estimates of flutter behavior. Author

N91-19480# Los Alamos National Lab., NM.
TEXTURE AND MICROSTRUCTURE DEVELOPMENT IN Al-2 PERCENT Mg DURING HIGH-TEMPERATURE DEFORMATION
S. R. Chen and U. F. Kocks Dec. 1990 17 p Presented at the Hot Deformation of Aluminum Alloys Metallurgical Society Conference, Detroit, MI, Oct. 1990
(Contract W-7405-eng-36)
(DE91-007355; LA-UR-91-92; CONF-9010317-1) Avail: NTIS HC/MF A03

The high rate sensitivity of the flow stress that is exhibited by alloys under solute drag control, such as Al-Mg at high temperatures, influences texture development because more slip systems contribute to deformation. Al-2 percent Mg was tested in channel-die compression, i.e., idealized rolling, at 290 C and 400 C, at strain rates from 10(exp -1)/s to 10(exp -5)/s. The texture development in rolling predicted by polycrystal plasticity simulation indicates that the brass component increases while the copper component decreases when the rate sensitivity is raised. The experimental results are in good agreement with this prediction. In addition, cube component appears when microstructural change occurs due to dynamic recrystallization. This microstructural change leads to the shift from (011) to (001) fiber texture in free compression at high temperature. DOE

N91-19481# Sandia National Labs., Albuquerque, NM.
LAG-STABILIZED FORCE FEEDBACK DAMPING
B. J. Petterson, R. D. Robinett, and J. C. Werner 1991 9 p Presented at the 1991 American Nuclear Society Meeting, Albuquerque, 24-28 Feb. 1991
(Contract DE-AC04-76DP-00789)
(DE91-007572; SAND-91-0194C; CONF-910252-2) Avail: NTIS HC/MF A02

A lag-stabilized, force feedback controller for damping initial and residual oscillations of a planar, cantilevered flexible arm has been analytically developed and experimentally implemented on a commercial robot. The controller feeds back force sensor measurements that are delayed in time and proportional to the displacement (angular orientation) of the arm in order to damp the oscillation. As a result of the lag (contrary to popular belief), the controlled robot system is stable and provides tunable performance on a Cincinnati Milacron T3-786 robot. DOE

N91-19482*# National Aeronautics and Space Administration. Langley Research Center, Hampton, VA.
NONLINEAR ANALYSIS AND REDESIGN OF THE MIXED-MODE BENDING DELAMINATION TEST
J. R. Reeder and J. H. Crews, Jr. Jan. 1991 43 p
(NASA-TM-102777; NAS 1.15:102777) Avail: NTIS HC/MF A03 CSCL 20K

The Mixed Mode Bending (MMB) test uses a lever to simultaneously apply mode I and mode II loading to a split beam specimen. An iterative analysis that accounts for the geometric nonlinearity of the MMB test was developed. The analysis accurately predicted the measured load displacement response and the strain energy release rate, G, of an MMB test specimen made of APC2 (AS4/PEEK). The errors in G when calculated using linear theory were found to be as large as thirty percent in some cases. Because it would be inconvenient to use a nonlinear analysis to analyze MMB data, the MMB apparatus was redesigned to minimize the nonlinearity. The nonlinear analysis was used as a guide in redesigning the MMB apparatus. With the redesigned apparatus, loads were applied through a roller attached to the level and loaded just above the midplane of the test specimen. The redesigned apparatuus has geometric nonlinearity errors of less than three percent, even for materials substantially tougher than APC2. This apparatus was demonstrated by measuring the mixed mode delamination fracture toughness of APC2. Author

N91-19483# Westinghouse Savannah River Co., Aiken, SC.
AN ON-LINE REAL-TIME SYSTEM FOR FATIGUE CRACK GROWTH MONITORING
G. E. Mertz, K. J. Stoner, R. L. Sindelar, W. L. Daugherty, R. C. Brown, and S. C. Collins 1990 11 p Presented at the International Topical Meeting on the Safety, Status, and Future of Non-Commercial Reactors and Irradiation Facilities, Boise, 4 Oct. 1990
(Contract DE-AC09-89SR-18035)
(DE91-007931; WSRC-MS-90-37; CONF-9010151-8) Avail: NTIS HC/MF A03

An on-line, real-time fatigue monitoring system was successfully used to monitor and ensure the structural integrity of flawed piping during the 1989 L reactor hydraulic test at the Savannah River Site. The monitoring system is comprised of a strain gage data acquisition system and a series of predetermined alarm setpoints. The fatigue monitoring system determined that the vibrational stresses due to simulated accident conditions were relatively benign and that essentially no significant fatigue crack growth had occurred during the test. DOE

N91-19484# Carnegie-Mellon Univ., Pittsburgh, PA. Dept. of Metallurgical Engineering and Materials Science.
THE EFFECT OF ELASTIC STRESS ON OSTWALD RIPENING PHENOMENA
W. C. Johnson 1991 13 p
(Contract DE-FG02-84ER-45166)
(DE91-008034; DOE/ER-45166/3) Avail: NTIS HC/MF A03

The purpose of this research is to understand the influence of elastic misfit strain and applied stress on the development of microstructure in two-phase coherent alloys. This progress report

briefly describes work during the period, proposed work for the next funding year, personnel, publications, and invited seminars.
DOE

N91-19485# Messerschmitt-Boelkow-Blohm G.m.b.H., Ottobrunn (Germany, F.R.). Helicopter Div.
NON-HOMOGENEOUS BARS UNDER TENSION, PURE BENDING, AND TEMPERATURE LOADS
Helmut Rapp Sep. 1990 8 p Presented at the 4th European Conference on Composite Materials, Stuttgart, Fed. Republic of Germany, 25-28 Sep. 1990
(MBB-UD-0572-90-PUB; ETN-91-98822) Avail: NTIS HC/MF A02

Nonhomogeneous bars may show discrepancies in stiffness and thermal expansion between the engineering theory of bending and experiment. The reason for this are additional stresses perpendicular to the bar axis due to different Poisson's ratios of the used materials. These stresses have to be taken into account especially if fiber reinforced materials are used. A theory for evaluating the stiffness of those nonhomogeneous bars is shown. Other methods of calculation, based on the engineering theory of bending and the classical laminate theory are also given. Test results are in good correlation with the theory. ESA

N91-19486# Bristol Univ. (England). Dept. of Aerospace Engineering.
A THEORETICAL SOLUTION FOR THE BUCKLING OF SANDWICH PANELS WITH LAMINATED FACE PLATES USING A COMPUTER ALGEBRA SYSTEM
J. P. H. Webber and I. B. Stewart May 1989 39 p
(BU-407; ETN-91-98859) Avail: NTIS HC/MF A03

The governing equations for both symmetric and asymmetric wrinkling of sandwich panels are derived using operator notation. In each case, differential systems of three equations in three unknowns are obtained and two of the three variables are eliminated by taking combinations of the equations. While the mathematical techniques employed are straightforward, the expressions involved are lengthy and recourse is made to the computer algebra system MACSYMA, without which a solution for the asymmetric case would have been difficult to achieve. Explicit algebraic expressions are given for buckling loads which can be used by structural engineers to calculate allowable design loads for sandwich panels. ESA

N91-19487# Bristol Univ. (England). Dept. of Aerospace Engineering.
COMPUTATIONAL COMPARISON OF EFFICACIES OF AEOLIAN VIBRATION DAMPING DEVICES FOR MULTICONDUCTOR OVERHEAD POWER LINES
A. Simpson, N. J. Salmon, and C. N. Taylor 31 Jan. 1991 9 p Repr. from IEE Proceedings, v. 137, pt. c, no. 3, May 1990 p 225-232
(BU-411; ETN-91-98862) Avail: NTIS HC/MF A02

Aeolian vibration in multiconductor overhead power transmission lines is usually controlled by one of two techniques, namely by a combination of rigid spacing elements and endpoint Stockbridge dampers, or suitably positioned spacer dampers. A comparison study based on theory and computation is presented. It is concluded, consistent with observations over many years, that both philosophies suffice when the conductors are moderately tensioned ACSRs (Aluminum Conductor Steel Reinforced). When the conductors are moderately/highly tensioned AAACs (All Aluminum Alloy Conductors), neither philosophy is totally adequate. If the two philosophies are combined, good vibration control will result in many circumstances. ESA

N91-19488# Bristol Univ. (England). Dept. of Aerospace Engineering.
BOLTED JOINTS IN A LAMINATED COMPOSITE STRUT DESIGN EXPERT SYSTEM
C. M. L. Wu Jul. 1990 54 p Sponsored by United Kingdom Science and Engineering Research Council
(BU-415; ETN-91-98866) Avail: NTIS HC/MF A04

A knowledge based expert system (for the design and analysis of composite laminated struts) is part of a composite design expert (CODEX) system that not only performs analysis and design of composite laminated plates and struts, but also assesses competing designs. The analysis part of the system is based on a minimum weight optimization that satisfies the buckling failure criteria of local and overall buckling, and a stress/strain failure from a choice of maximum strain, maximum stress Tsai-Hill of Tsai-Wu failure criteria. The strut optimization expert system is extended to incorporate bolted joints analysis. Examples of strut design are carried out and assessed using this system. The system is shown to be powerful enough to provide solutions to design analysis and assessment of competing designs using composite materials. ESA

N91-19489# Technische Univ., Delft (Netherlands).
BULGING OF FATIGUE CRACKS IN A PRESSURIZED AIRCRAFT FUSELAGE Ph.D. Thesis
D. Chen 1991 239 p
(ETN-91-98927) Avail: NTIS HC/MF A11

Three new set ups for testing of sheet specimens under biaxial tensile loading, for tensile loading of sheet specimens with a curvature, and for sheet specimens with a large radius of curvature loaded by an internal air pressure and hoop stress are developed. Studies are carried out on the fatigue crack growth behavior of thin aluminum alloy sheets and Aramid Aluminum Laminates (ARALL) under various aircraft fuselage loading conditions, including stress biaxiality, combined bending and extension and crack edge bulge out conditions. Some residual tensile strength tests are also conducted. Theories for the effect of combined bending and extension as well as for the effect of bulging are developed. The theories agree well with the present test results and results from the literature. ESA

N91-19490# Technische Univ., Eindhoven (Netherlands).
CONTINUUM DAMAGE MECHANISMS WITH AN APPLICATION TO FATIGUE Ph.D. Thesis
Michel Hendrik Juliu Paas 1990 123 p
(ISBN-90-9003688-1; ETN-91-98930) Avail: NTIS HC/MF A06

Continuum Damage Mechanics (CDM) is adopted to describe failure mechanisms. Models for brittle failure and fatigue damage are developed. The first describes the behavior of concrete and polystyrene in simple loading situations; the second can be reduced to some widely accepted cumulative damage models. Anisotropic damage is considered by taking the directional nature of damage into account with dyadic vector products. The evolution equation and initial damage are supplied for complete mechanism description. The validity of a developed statistical model is demonstrated for fatigue in rubbers and polystyrene. For practical applications the equilibrium equation and constitutive equations are solved numerically. Simulation techniques consisting of finite element calculations for different realizations of the initial state are applied to analyze stochastic failure processes. In CDM, crack growth is equivalent to the development of a zone of completely damaged elements. Both initiation and propagation of cracks are predicted. ESA

N91-19491# Technische Univ., Delft (Netherlands). Dept. of Aerospace Engineering.
ON THE VECTORIZATION AND PARALLELIZATION OF THE SHOOTING METHOD USING THE CONVEX C-240
E. Deerenberg and E. L. Jansen Jul. 1990 38 p
(LR-639; ETN-91-98940) Avail: NTIS HC/MF A03

The implementation of two programs on a parallel vector computer is discussed. The two special purpose programs, in the field of nonlinear mechanics of cylindrical shell structures, were implemented on a shared memory minisupercomputer with four vector processors. Both programs use the parallel shooting method to solve the governing equations. The theory on which the programs are based and the parallel shooting method are discussed. It is shown that using a minisupercomputer with a small number of vector processors one can accelerate the parallel shooting method

considerably. For some representative test cases the effects of vectorization and parallelization on the central processing time and wall clock time are reported. ESA

N91-19492# Technische Univ., Delft (Netherlands). Dept. of Aerospace Engineering.
CRACK OPENING STRESS MEASUREMENTS OF SURFACE CRACKS IN 7075-T6 Al ALLOY PLATE SPECIMENS THROUGH ELECTRON FRACTOGRAPHY
Ichsan S. Putra and J. Schijve Aug. 1990 58 p
(LR-641; ETN-91-98942) Avail: NTIS HC/MF A04

Crack opening stress measurements were carried out on 9.6 mm thick specimens of 7075-T6 aluminum alloy with semi-elliptical surface cracks. Measurements were made through a fractographic technique based on a load sequence which can produce distinct striation characteristics on the fracture surface. The crack opening stress level (MPa) (Sop) is deduced from the striation pattern. The variation of Sop along the crack periphery and during crack extension was measured. Close to the front surface, Sop is higher due to plane stress condition. At a large crack depth a strong influence of plasticity in the ligament on Sop is higher due to plane stress condition. At a large crack depth a strong influence of plasticity in the ligament of Sop was found, i.e., Sop decreases as the crack extends to breakthrough. The agreement of (da/dN = effective stress intensity range) curves between surface cracks and through cracks data was only found for a limited range of crack depth of the elliptical cracks. ESA

N91-19493# Technische Univ., Delft (Netherlands). Dept. of Aerospace Engineering.
FINITE STRIP ELEMENTS IN THIN PLATE BUCKLING ANALYSIS
Ronald P. Notenboom Sep. 1990 66 p
(LR-642; ETN-91-98943) Avail: NTIS HC/MF A04

An important design limit on thin walled plate structures under compressive loading is the buckling stress. The main goals is to have a tool for thin plate structures under compressive loading and to have a good basis for further development. The subroutines used for calculating the stiffness matrices involved are printed as direct listings of the computer program so that the text of this report can be checked with the computer listings. In order to find the critical buckling stress for a chosen half wave length, two methods were used. First a determinant search is used which gives only the buckling stress. The second method used is the inverse iteration method which gives besides the lowest eigenvalue also the eigenvector (buckling mode). The combination of eigenvalue and eigenvector can be used to calculate the derivative of the eigenvalue with respect to any design variable very efficiently. The first derivative of the eigenvalue with respect to the half wave length is considered only, but derivatives with respect to plate thicknesses could be included without much effort. Further work is done to extend the method to anisotropic material and to include an optimization process. ESA

N91-19494# Technische Univ., Delft (Netherlands). Dept. of Aerospace Engineering.
DESIGN AND TESTING OF A CIRCUMFERENTIAL AND LONGITUDINAL JOINT OF THE A320 FUSELAGE SECTION 13/14 IN GLARE
B. vanWimersmaGreidanus Oct. 1990 64 p
(LR-645; ETN-91-98946) Avail: NTIS HC/MF A04

Recently a feasibility study on the application of aerospace ARALL (Aramid Aluminum Laminates) in the A320 fuselage was performed. This study, limited to fuselage section 13/14, indicates that a weight reduction of 26 percent can be obtained by using GLARE for the fuselage skin and stringers. No reinforcements are needed at the locations of the stringers. Whether reinforcements at the locations of the joints are necesary in the fuselage design in GLARE is investigated by performing static and fatigue tests on two highly loaded joints. The material properties of the skin (GLARE-3 consisting of three layers of 0.2 mm aluminum 2024-T3 and two layers of 0.25 mm crossply glass prepeg) are discussed and compared with those of aluminum 2024-T3. The decisive loading data for the joints is given, and the type of rivets to be applied to the joints is chosen. The strength of the chosen rivets in the GLARE-3 skin material is determined. The choice of the splice plate material and the geometry of the joints are discussed. Conclusions about the joints of the A320 fuselage design in GLARE are drawn. ESA

N91-19495# Oxford Univ. (England). Dept. of Engineering Science.
TIME-FREQUENCY DOMAIN ANALYSIS OF VIBRATION SIGNALS FOR MACHINERY DIAGNOSTICS. 1: INTRODUCTION TO THE WIGNER-VILLE DISTRIBUTION
P. D. McFadden and W. Wang 1990 41 p Sponsored by Science Research Council, England
(OUEL-1859/90; ETN-91-98957) Avail: NTIS HC/MF A03

The definition and some of the properties of the Wigner-Ville distribution for both continuous and discrete signals are reported. A digital computer program implementing the discrete Wigner-Ville distribution is described and its performance is demonstrated by the analysis in the time frequency domain of a series of numerically generated test signals, showing the form of the Wigner-Ville distribution and the interference terms which can be generated due to its nonlinear behavior. The program is then applied to the analysis in the time frequency domain of experimentally measured time domain averages of the vibration of damaged gears in industrial and helicopter gearboxes, in order to detect early signs of impending mechanical failure. It is shown that the damage to the gears can be detected by visual inspection of the changes which occur in the pattern of the Wigner-Ville distribution, but that the damage can be detected more quickly and easily using an existing narrow band enhancement technique. ESA

N91-19496# Air Force Inst. of Tech., Wright-Patterson AFB, OH. School of Engineering.
MODELING AND ANALYSIS OF ORTHOTROPIC PLATE WITH CIRCULAR CUTOUT AND ADHESIVE BONDED PATCH M.S. Thesis
Mark W. Hunter Dec. 1990 106 p
(AD-A229866; AFIT/GAE/ENY/90D-11) Avail: NTIS HC/MF A06 CSCL 11/4

The purpose of this study was to investigate a modeling technique to simply and adequately model an adhesive bonded patch on an orthotropic plate. This report is limited to linear material behavior. This thesis is also the basis for further work into nonlinear material range and three-dimensional stress states. To further advance aerospace battle damage repair techniques for composite repairs, a finite element model of an orthotropic plate with a hole and patch was constructed to investigate the accuracy of such a model. The fundamental problem in this model is the development of a simple and accurate method of modeling the bond between patch and plate. MSC/NASTRAN spring elements were used to this end. The spring elements provided an elastic method of load transfer between the plate and patch. GRA

N91-19809# Joint Publications Research Service, Arlington, VA.
SOLUTION OF ONE-DIMENSIONAL PROBLEM IN NONLINEAR THEORY OF ELASTICITY WITH STRUCTURED SHOCK WAVE Abstract Only
A. A. Burenin and Yu. A. Rossikhin *In its* JPRS Report: Science and Technology. USSR: Physics and Mathematics 31 Oct. 1990 p 12 Transl. into ENGLISH from Prikladnaya Mekhanika (Kiev, USSR), v. 26, no. 1, Jan. 1990 p 103-108 (For primary document see N91-19800 11-70)
Avail: NTIS HC/MF A03

42 GEOSCIENCES (GENERAL)

No abstracts in this category.

43 EARTH RESOURCES AND REMOTE SENSING

Includes remote sensing of earth resources by aircraft and spacecraft; photogrammetry; and aerial photography.

For instrumentation see *35 Instrumentation and Photography.*

N91-19497*# Agricultural Research Service, Beltsville, MD. Remote Sensing Research Lab.

EFFECTS OF SOIL AND CANOPY CHARACTERISTICS ON MICROWAVE BACKSCATTERING OF VEGETATION Final Report

C. S. T. Daughtry and K. J. Ranson (National Aeronautics and Space Administration. Goddard Space Flight Center, Greenbelt, MD.) Feb. 1991 16 p

(Grant NAGw-799)

(NASA-CR-188022; NAS 1.26:188022) Avail: NTIS HC/MF A03 CSCL 02F

A frequency modulated continuous wave C-band (4.8 GHz) scatterometer was mounted on an aerial lift truck and backscatter coefficients of corn were acquired as functions of polarizations, view angles, and row directions. As phytomass and green leaf area index increased, the backscatter also increased. Near anthesis when the canopies were fully developed, the major scattering elements were located in the upper 1 m of the 2.8 m tall canopy and little backscatter was measured below that level. C-band backscatter data could provide information to monitor vegetation at large view zenith angles. Author

N91-19498*# Coherent Technologies, Inc., Boulder, CO.

THEORY OF CW LIDAR AEROSOL BACKSCATTER MEASUREMENTS AND DEVELOPMENT OF A 2.1 MICRONS SOLID-STATE PULSED LASER RADAR FOR AEROSOL BACKSCATTER PROFILING Final Report

Michael J. Kavaya, Sammy W. Henderson, and R. G. Frehlich Washington Mar. 1991 121 p

(Contract NAS8-37580)

(NASA-CR-4347; NAS 1.26:4347) Avail: NTIS HC/MF A06 CSCL 20N

The performance and calibration of a focused, continuous wave, coherent detection CO2 lidar operated for the measurement of atmospheric backscatter coefficient, B(m), was examined. This instrument functions by transmitting infrared (10 micron) light into the atmosphere and collecting the light which is scattered in the rearward direction. Two distinct modes of operation were considered. In volume mode, the scattered light energy from many aerosols is detected simultaneously, whereas in the single particle mode (SPM), the scattered light energy from a single aerosol is detected. The analysis considered possible sources of error for each of these two cases, and also considered the conditions where each technique would have superior performance. The analysis showed that, within reasonable assumptions, the value of B(m) could be accurately measured by either the VM or the SPM method. The understanding of the theory developed during the analysis was also applied to a pulsed CO2 lidar. Preliminary results of field testing of a solid state 2 micron lidar using a CW oscillator is included. Author

N91-19499*# National Aeronautics and Space Administration, Washington, DC.

SOLID EARTH SCIENCE IN THE 1990S. VOLUME 1: PROGRAM PLAN

Feb. 1991 66 p

(NASA-TM-4256-Vol-1; NAS 1.15:4256-Vol-1) Avail: NTIS HC/MF A04 CSCL 08G

This is volume one of a three volume series. A plan for solid earth science research for the next decade is outlined. The following topics are addressed: scientific requirements; status of current research; major new emphasis in the 1990's; interagency and international participation; and the program implementation plan. The following fields are represented: plate motion and deformation; lithospheric structure and evolution; volcanology; land surface (processes of change); earth structure and dynamics; earth rotation and reference frames; and geopotential fields. Other topics of discussion include remote sensing, space missions, and space techniques. K.S.

N91-19500# California Univ., Davis. Inst. of Ecology.

CLIMATIC WATER BUDGETS, EFFECTIVE MOISTURE, AND ELEVATION IN THE SOUTHERN SIERRA NEVADA, CALIFORNIA, 1951-1980

S. M. Kruse Oct. 1990 204 p Sponsored by National Park Service, San Francisco, CA

(PB91-127878; TR-41) Avail: NTIS HC/MF A10 CSCL 08H

This study is presented in eight parts: the need for the study and problems associated with montane climates; a literature review of climate and soils; climatic water budget analysis of 15 stations with measured mean monthly temperature in or directly adjacent to the southern Sierra Nevada; results of analysis; references; and supporting appendices. Long-term climatic analysis for the southern Sierra Nevada establishes a baseline for future ecosystem research, a basis for comparison with the Long-Term Ecological Research (LTER) sites in the United States, and a quantitative method for visualizing effective moisture in a montane area. Author

44 ENERGY PRODUCTION AND CONVERSION

Includes specific energy conversion systems, e.g., fuel cells; global sources of energy; geophysical conversion; and windpower.

For related information see also *07 Aircraft Propulsion and Power, 20 Spacecraft Propulsion and Power,* and *28 Propellants and Fuels.*

N91-19501# Midwest Research Inst., Golden, CO.

RESULTS OF SCOPING TESTS FOR OPEN-CYCLE OTEC (OCEAN THERMAL ENERGY CONVERSION) COMPONENTS OPERATING WITH SEAWATER

F. Zangrando, D. Bharathan, H. J. Green, H. F. Link, B. K. Parsons, J. M. Parsons, A. A. Pesaran, and C. B. Panchal Sep. 1990 318 p

(Contract DE-AC02-83CH-10093)

(DE89-009514; SERI/TP-253-3561) Avail: NTIS HC/MF A14

This report presents comprehensive documentation of the experimental research conducted on open-cycle ocean thermal energy conversion (OC-OTEC) components operating with seawater as a working fluid. The results of this research are presented in the context of previous analysis and fresh-water testing; they provide a basis for understanding and predicting with confidence the performance of all components of an OC-OTEC system except the turbine. Seawater tests have confirmed the results that were obtained in fresh-water tests and predicted by the analytical models of the components. A sound technical basis has been established for the design of larger systems in which net power will be produced for the first time from OC-OTEC technology. Design and operation of a complete OC-OTEC system that produces power will provide sufficient confidence to warrant complete transfer of OC-OTEC technology to the private sector. Each components performance is described in a separate chapter written by the principal investigator responsible for technical aspects of the specific tests. Chapters have been indexed separately for inclusion on the data base. DOE

N91-19502# Midwest Research Inst., Golden, CO. Solar Energy Research Inst.

SOLID STATE PHOTOVOLTAIC RESEARCH BRANCH

Sep. 1990 289 p

(Contract DE-AC02-83CH-10093)

(DE91-002128; SERI/TP-212-3675) Avail: NTIS HC/MF A13

This report summarizes the progress of the Solid State Photovoltaic Research Branch of the Solar Energy Research Institute (SERI) from October 1, 1988, through September 30,

1989. Six technical sections of the report cover these main areas of SERIs in-house research: Semiconductor Crystal Growth, Amorphous Silicon Research, Polycrystalline Thin Films, III-V High-Efficiency Photovoltaic Cells, Solid-State Theory, and Laser Raman and Luminescence Spectroscopy. Sections have been indexed separately for inclusion on the data base. DOE

N91-19503# Department of Energy, Washington, DC. Geothermal Div.
THE NATIONAL ENERGY STRATEGY: THE ROLE OF GEOTHERMAL TECHNOLOGY DEVELOPMENT. PROCEEDINGS
1990 185 p Proceedings held in San Francisco, CA, 18-20 Apr. 1990
(DE91-004623; CONF-9004131) Avail: NTIS HC/MF A09

Each year the Geothermal Division of the U.S. Department of Energy conducts an in-depth review of its entire geothermal R and D program. The conference serves several purposes: a status report on current R and D activities, an assessment of progress and problems, a review of management issues, and a technology transfer opportunity between DOE and the U.S. geothermal industry. Topics in this year's conference included Hydrothermal Energy Conversion Technology, Hydrothermal Reservoir Technology, Hydrothermal Hard Rock Penetration Technology, Hot Dry Rock Technology, Geopressured-Geothermal Technology and Magma Energy Technology. Each individual paper has been cataloged separately. DOE

N91-19504# Doty Scientific, Inc., Columbia, SC.
MICROTUBE STRIP HEAT EXCHANGER
F. D. Doty 27 Dec. 1990 14 p
(Contract DE-FG01-90CE-15440)
(DE91-005741; DOE/CE-15440/T1) Avail: NTIS HC/MF A03

Doty Scientific (DSI) believes their microtube-strip heat exchanger will contribute significantly to the following: (1) the closed Brayton cycles being pursued at MIT, NASA, and elsewhere; (2) reverse Brayton cycle cryocoolers, currently being investigated by NASA for space missions, being applied to MRI superconducting magnets; and (3) high-efficiency cryogenic gas separation schemes for CO2 removal from exhaust stacks. The goal of this current study is to show the potential for substantial progress in high-effectiveness, low-cost, gas-to-gas heat exchangers for diverse applications at temperatures from below 100 K to above 1000 K. To date, the highest effectiveness measured is about 98 percent and relative pressure drops below 0.1 percent with a specific conductance of about 45 W/kgK are reported. During the pre-award period DSI built and tested a 3-module heat exchanger bank using 103-tube microtube strip (MTS) modules. To add to their analytical capabilities, DSI has acquired computational fluid dynamics (CFD) software. This report describes the pre-award work and the status of the ten tasks of the current project, which are: analyze flow distribution and thermal stresses within individual modules; design a heat exchanger bank of ten modules with 400 microtube per module; obtain production quality tubestrip die and AISI 304 tubestrips; obtain production quality microtubing; construct revised MTS heat exchanger; construct dies and fixtures for prototype heat exchanger; construct 100 MTS modules; assemble 8 to 10 prototype MTS heat exchangers; test prototype MTS heat exchanger; and verify test through independent means. DOE

N91-19505# International Fuel Cells Corp., South Windsor, CT.
MOLTEN CARBONATE FUEL CELL TECHNOLOGY IMPROVEMENT
Sep. 1990 32 p
(Contract DE-AC21-87MC-23270)
(DE91-005540; DOE/MC-23270/2923; FCR-11191) Avail: NTIS HC/MF A03

The overall objective is to define a competitive CG/MCFC power plant and the associated technology development requirements and to develop an improved cell configuration for molten carbonate fuel cells which has improved performance, has reduced cell creep and electrolyte management consistent with 40,000 hour projected life, reduces existing cell cost, and is adaptable to a range of power plant applications. The 8 sq ft 20 cell, 25 kW stack assembly and installation in the test facility were completed. Testing of the stack was started and 896 hours of test time were reached. Manifold seal development focused on a seal to reduce electrolyte transport and test rigs were initiated for shunt current and seal leakage evaluation. Development on sheet metal parts was initiated with focus on improved aluminization for separator plate corrosion protection and nickel clad stainless steel for the anode current collector. Development of porous parts was initiated with focus on an alternative binder for the electrodes. Design of a laboratory scale continuous debinding oven was completed. Development of an improved material blend for the matrix was also initiated. DOE

N91-19506# Oak Ridge National Lab., TN.
A SUMMARY OF THE STATUS OF BIOMASS CONVERSION TECHNOLOGIES AND OPPORTUNITIES FOR THEIR USE IN DEVELOPING COUNTRIES
D. B. Waddle, R. D. Perlack, and J. Wimberly 1990 12 p Presented at the 6th International Symposium on Agricultural and Food Processing Wastes (ISAFPW '90) Chicago, IL, 17-18 Dec. 1990
(Contract DE-AC05-84OR-21400)
(DE91-006341; CONF-901269-1) Avail: NTIS HC/MF A03

Biomass plays a significant role in energy use in developing countries: however, these resources are often used very inefficiently. Recent technology developments have made possible improved conversion efficiencies for utility scale technologies. These developments may be of interest in the wake of recent policy changes occurring in several developing countries, with respect to independent power production. Efforts are also being directed at developing biomass conversion technologies that can interface and/or compete with internal combustion engines for small, isolated loads. The technological status is reviewed of biomass conversion technologies appropriate for commercial, industrial, and small utility applications in developing countries. Market opportunities, constraints, and technology developments are also discussed. DOE

N91-19507# Argonne National Lab., IL.
THERMAL-HYDRAULIC MODEL OF A SOLID-OXIDE FUEL CELL
S. Ahmed and R. Kumar 1990 18 p Presented at the American Institute of Chemical Engineers Fall Annual Meeting, Chicago, IL, 11-16 Nov. 1990
(Contract W-31-109-eng-38)
(DE91-006393; CONF-901155-5) Avail: NTIS HC/MF A03

A mathematical model was developed to simulate the electrochemistry and thermal hydraulics in a monolithic solid oxide fuel cell (MSOFC). Dividing a single cell layer into a number of nodes, the model sets up the steady state heat and mass transfer equations for each node in a cell layer. Based on the average thermal and compositional conditions at each node and a specified cell voltage, the model calculates the Nernst potential and the resultant current, heat generation, and heat removal rates at each node. These calculations yield the temperature and the fuel and oxidant compositions and partial pressure matrices for the entire cell. The simulation also provides related performance data for the fuel cell stack, such as energy efficiency, fuel utilization, and power density. The model can be used to simulate operation with different fuel gases, such as hydrogen, coal gas, and methanol reformate. A mathematical model such as this can be used to examine the effects of changing one or more of the various design variables and to evaluate the effectiveness of fabrication improvements in technology development. In the design phase, the model can be used to determine the size of the stack that will be required for a given power rating and to make design decisions regarding structure-specific parameters, such as the thicknesses of the anode, electrolyte, cathode, and interconnect layers and dimensions of the flow channels in the anode and the cathode. The model can also be helpful to the fuel cell system operator. For example, given a particular stack, the most favorable

operating conditions can be determined by determining a priori the effects of altering process variables, such as flow rates and feed conditions. DOE

N91-19508# Argonne National Lab., IL.
DESIGN AND COST OF NEAR-TERM OTEC (OCEAN THERMAL ENERGY CONVERSION) PLANTS FOR THE PRODUCTION OF DESALINATED WATER AND ELECTRIC POWER
T. Rabas, C. B. Panchal, and L. Genens 1990 9 p Presented at the American Society of Mechanical Engineers (ASME) Winter Annual Meeting, Dallas, TX, 25-30 Nov. 1990
(Contract W-31-109-eng-38)
(DE91-006406; CONF-901194-9) Avail: NTIS HC/MF A02

There currently is an increasing need for both potable water and power for many islands in the Pacific and Caribbean. The Ocean Thermal Energy Conversion (OTEC) technology fills these needs and is a viable option because of the unlimited supply of ocean thermal energy for the production of both desalinated water and electricity. The OTEC plant design must be flexible to meet the product-mix demands that can be very different from site to site. Different OTEC plants are described that can supply various mixes of desalinated water and vapor; the extremes being either all water and no power or no water and all power. The economics for these plants are also presented. The same flow rates and pipe sizes for both the warm and cold seawater streams are used for different plant designs. The OTEC plant designs are characterized as near-term because no major technical issues need to be resolved or demonstrated. The plant concepts are based on DOE-sponsored experiments dealing with power systems, advanced heat exchanger designs, corrosion and fouling of heat exchange surfaces, and flash evaporation and moisture removal from the vapor using multiple spouts. In addition, the mature multistage flash evaporator technology is incorporated into the plant designs where appropriate. For the supply and discharge warm and cold uncertainties do exist because the required pipe sizes are larger than the maximum currently deployed; 40 inch high density polyethylene pipe at Keahole Point in Hawaii. DOE

N91-19509# Oregon Inst. of Tech., Klamath Falls. Geo-Heat Center.
DHE (DOWNHOLE HEAT EXCHANGERS)
G. Culver Nov. 1990 101 p
(Contract DE-FG07-90ID-13040)
(DE91-006620; DOE/ID-13040/1) Avail: NTIS HC/MF A06

The use of downhole heat exchangers (DHE) for residential or commercial space and domestic water heating and other applications has several desirable features. Systems are nearly or completely passive -- that is, no or very little geothermal water or steam is produced from the well either reducing or completely eliminating surface environmental concerns and the need for disposal systems or injection wells. Initial cost of pumps and installation are eliminated or reduced along with pumping power costs and maintenance costs associated with pumping often corrosive geothermal fluids. Many residential and small commercial systems do not require circulating pumps because the density difference in the incoming and outgoing sides of the loop are sufficient to overcome circulating friction losses in the entire system. The major disadvantage of DHEs is their dependence on natural heat flow. In areas where geological conditions provide high permeability and a natural hydraulic gradient, DHEs can provide a substantial quantity of heat. A single 500-ft (152 m) well in Klamath Falls, Oregon, supplies over one megawatt thermal and output is apparently limited by the surface area of pipe that can be installed in the well bore. In contrast, DHEs used in conjunction with heat pumps may supply less than 8 KW from a well of similar depth. Here output is limited by conductive heat flow with perhaps a small contribution from convection near the well bore. The highest capacity DHE reported to date, in Turkey, supplies 6 MW thermal from an 820-ft (250 m) well. There were two main goals for this project. The first was to gather, disseminate and exchange internationally information on DHES. The second was to perform experiments that would provide insight into well bore/aquifer interaction and thereby provide more information on which to base DHE designs. DOE

N91-19510# Sandia National Labs., Albuquerque, NM.
THE DESIGN OF FUTURE CENTRAL RECEIVER POWER PLANTS BASED ON LESSONS LEARNED FROM THE SOLAR ONE PILOT PLANT
G. J. Kolb 1991 26 p Presented at the 1991 Solar Power Systems Conference, Yalta, USSR, 22-26 Apr. 1991
(Contract DE-AC04-76DP-00789)
(DE91-005224; SAND-90-3142C; CONF-9104123-1) Avail: NTIS HC/MF A03

The 10-MW(sub e) Solar One Pilot Plant was the world's largest solar central receiver power plant. During its power production years it delivered over 37,000 MWhrs (net) to the utility grid. In this type of electric power generating plant, large sun-tracking mirrors called heliostats reflect and concentrate sunlight onto a receiver mounted on top of a tower. The receiver transforms the solar energy into thermal energy that heats water, turning it into superheated steam that drives a turbine to generate electricity. The Solar One Pilot Plant successfully demonstrated the feasibility of generating electricity with a solar central receiver power plant. During the initial 2 years the plant was tested and 4 years the plant was operated as a power plant, a great deal of data was collected relating to the efficiency and reliability of the plant's various systems. This paper summarizes these statistics and compares them to goals developed by the U.S. Department of Energy. Based on this comparison, improvements in the design and operation of future central receiver plants are recommended. Research at Sandia National Laboratories and the U.S. utility industry suggests that the next generation of central receiver power plants will use a molten salt heat transfer fluid rather than water/steam. Sandia has recently completed the development of the hardware needed in a molten salt power plant. Use of this new technology is expected to solve many of the performance problems encountered at Solar One. Projections for the energy costs from these future central receiver plants are also presented. For reference, these projections are compared to the current energy costs from the SEGS parabolic trough plants now operating in Southern California. DOE

N91-19511# American Public Power Association, Washington, DC.
COMPLEAT (COMMUNITY-ORIENTED MODEL FOR PLANNING LEAST-COST ENERGY ALTERNATIVES AND TECHNOLOGIES): A PLANNING TOOL FOR PUBLICLY OWNED ELECTRIC UTILITIES
Sep. 1990 153 p
(Contract DE-FG01-87CE-27462)
(DE91-006955; DOE/CE-27462/T1) Avail: NTIS HC/MF A08

The community-oriented model for planning least-cost energy alternatives and technologies (COMPLEAT) is an electric utility planning model designed to be principally used by publicly owned electric utilities and agencies serving such utilities. As a model, COMPLEAT is significantly more full-featured and complex than called out in APPA's original plan and proposal to DOE. The additional complexity grew out of a series of discussions early in the development schedule, in which it became clear to APPA staff and advisors that the simplicity characterizing the original plan, while highly desirable in terms of utility applications, was not achievable if practical utility problems were to be addressed. The project teams settled on Energy 20/20, an existing model developed by Dr. George Backus of Policy Assessment Associates, as the best candidate for the kinds of modifications and extensions that would be required. The remainder of the project effort was devoted to designing specific input data files, output files, and user screens and to writing and testing the compute programs that would properly implement the desired features around Energy 20/20 as a core program. This report presents in outline form, the features and user interface of COMPLEAT. DOE

N91-19512# Bristol Univ. (England). Dept. of Aerospace Engineering.
A NON-LINEAR METHOD FOR THE CALCULATION OF THE POWER OUTPUT OF A ROTATING WIND TURBINE
J. Gould and S. P. Fiddes Sep. 1990 27 p
(BU-416; ETN-91-98867) Avail: NTIS HC/MF A03

Errors observed in the prediction of the power output of a wind turbine are addressed. A method for calculating the power output of a horizontal axis wind turbine is presented. An important part of the problem of calculating the power output of a wind turbine is to find the velocity induced at the turbine blades by its wake. An efficient method for the calculation of the velocity at the blades is described. The modeling of the wake is detailed, the calculations of wake influence coefficients are discussed and an analytic method for the far field influence of the wake is given. The resultant velocity induced at the blade and resultant blade section characteristics are calculated using a nonlinear lifting line theory. The advantages of using horseshoe vortices compared with line filament vortices is discussed. The evaluation of the power output is described. ESA

N91-19513# Aeronautical Research Inst. of Sweden, Stockholm. Dept. of Aerodynamics.
SOME CONTROL PROBLEMS WITH BROAD RANGE VARIABLE SPEED FOR HORIZONTAL AXIS WIND TURBINES
Eskil Ulen and Goeran Dalen (Swedish State Power Board, Stockholm.) Oct. 1990 21 p Presented at the IEA Expert Meeting on Control System, 3-4 May 1990
(Contract STEV-506-266-4)
(FFA-TN-1990-37; ETN-91-98906) Avail: NTIS HC/MF A03

Possibilities of using wind energy as a complement in the Swedish energy system is investigated. A short description of the status and development of the energy situation in Sweden, is given. Some control possibilities and problems with fixed pitch variable speed machines are reviewed. Speed regulation is obtained by yawing or stalling. In both cases an efficient control of the electrical torque in the generator is supposed. ESA

N91-19184*# Spectrolab, Inc., Sylmar, CA.
PROGRESS TOWARD THE DEVELOPMENT OF DUAL JUNCTION GaAs/Ge SOLAR CELLS
D. R. Lillington, D. D. Krut, B. T. Cavicchi, E. Ralph, and M. Chung (Air Force Wright Aeronautical Labs., Wright-Patterson AFB, OH.) *In* NASA, Lewis Research Center, Space Photovoltaic Research and Technology, 1989 Jan. 1991 p 29-41 (For primary document see N91-19182 11-20)
(Contract F33615-89-C-2900)
Avail: NTIS HC/MF A22 CSCL 10B

N91-19185*# Applied Solar Energy Corp., City of Industry, CA.
STATUS OF GaAs/Ge SOLAR CELLS
P. A. Iles, F. Ho, and Y. C. M. Yeh *In* NASA, Lewis Research Center, Space Photovoltaic Research and Technology, 1989 Jan. 1991 p 42-47 (For primary document see N91-19182 11-20)
(Contract F33615-88-C-5415)
Avail: NTIS HC/MF A22 CSCL 10B

N91-19186*# Research Triangle Inst., Research Triangle Park, NC.
GRADED-BANDGAP AlGaAs SOLAR CELLS FOR AlGaAs/Ge CASCADE CELLS
M. L. Timmons, R. Venkatasubramanian, T. S. Colpitts, J. S. Hills, J. A. Hutchby, P. A. Iles, and C. L. Chu (Applied Solar Energy Corp., City of Industry, CA.) *In* NASA, Lewis Research Center, Space Photovoltaic Research and Technology, 1989 Jan. 1991 p 48-59 (For primary document see N91-19182 11-20)
(Contract F33615-87-C-2804)
Avail: NTIS HC/MF A22 CSCL 10B

N91-19187*# Astropower, Inc., Newark, DE.
AlGaAs TOP SOLAR CELL FOR MECHANICAL ATTACHMENT IN A MULTI-JUNCTION TANDEM CONCENTRATOR SOLAR CELL STACK
L. C. DiNetta, M. H. Hannon, J. B. McNeely, and A. M. Barnett (Delaware Univ., Newark.) *In* NASA, Lewis Research Center, Space Photovoltaic Research and Technology, 1989 Jan. 1991 p 60-72 (For primary document see N91-19182 11-20)
(Contract NAS3-25570)
Avail: NTIS HC/MF A22 CSCL 10B

N91-19188*# Varian Associates, Palo Alto, CA.
PROGRESS TOWARD A 30 PERCENT-EFFICIENT, MONOLITHIC, THREE-JUNCTION, TWO-TERMINAL CONCENTRATOR SOLAR CELL FOR SPACE APPLICATIONS
L. D. Partain, B.-C. Chung, G. F. Virshup, J. C. Schultz, H. F. MacMillan, M. Ladle Ristow, M. S. Kuryla, and K. A. Bertness *In* NASA, Lewis Research Center, Space Photovoltaic Research and Technology, 1989 Jan. 1991 p 73-76 (For primary document see N91-19182 11-20)
(Contract F33615-88-C-2845)
Avail: NTIS HC/MF A22 CSCL 10B

N91-19189*# National Aeronautics and Space Administration. Lewis Research Center, Cleveland, OH.
TANDEM CONCENTRATOR SOLAR CELLS WITH 30 PERCENT (AMO) POWER CONVERSION EFFICIENCY
J. E. Avery, L. M. Fraas, V. S. Sundaram, David J. Brinker, J. M. Gee, and Mark J. ONeill (ENTECH Corp., Dallas-Fort Worth Airport, TX.) *In its* Space Photovoltaic Research and Technology, 1989 Jan. 1991 p 77-87 (For primary document see N91-19182 11-20)
Avail: NTIS HC/MF A22 CSCL 10B

N91-19190*# Boeing Aerospace Co., Seattle, WA.
PROGRESS IN GaAs/CuInSe2 TANDEM JUNCTION SOLAR CELLS
N. P. Kim, R. M. Burgess, R. A. Mickelsen, B. J. Stanbery, R. W. McClelland, B. D. King, and R. P. Gale (Kopin Corp., Taunton, MA.) *In* NASA, Lewis Research Center, Space Photovoltaic Research and Technology, 1989 Jan. 1991 p 88-101 (For primary document see N91-19182 11-20)
Avail: NTIS HC/MF A22 CSCL 10B

N91-19191*# Midwest Research Inst., Golden, CO.
InP/Ga0.47In0.53As MONOLITHIC, TWO-JUNCTION, THREE-TERMINAL TANDEM SOLAR CELLS
M. W. Wanlaas, T. A. Gessert, G. S. Horner, K. A. Emery, and T. J. Coutts *In* NASA, Lewis Research Center, Space Photovoltaic Research and Technology, 1989 Jan. 1991 p 102-116 (For primary document see N91-19182 11-20)
Avail: NTIS HC/MF A22 CSCL 10B

N91-19192*# Wright Research Development Center, Wright-Patterson AFB, OH.
PHASE EQUILIBRIUM MODELING FOR HIGH TEMPERATURE METALLIZATION ON GaAs SOLAR CELLS
M. A. Chung, J. E. Davison, and S. R. Smith (Dayton Univ., OH.) *In* NASA, Lewis Research Center, Space Photovoltaic Research and Technology, 1989 Jan. 1991 p 119-125 (For primary document see N91-19182 11-20)
Avail: NTIS HC/MF A22 CSCL 10B

N91-19193*# Washington State Univ., Pullman.
GaAs SOLAR CELL PHOTORESPONSE MODELING USING PC-1D V2.1
D. A. Huber, L. C. Olsen, G. Dunham, and F. W. Addis *In* NASA, Lewis Research Center, Space Photovoltaic Research and Technology, 1989 Jan. 1991 p 126-135 (For primary document see N91-19182 11-20)
(Grant AF-AFOSR-0182-89)
Avail: NTIS HC/MF A22 CSCL 10B

N91-19194*# Varian Associates, Palo Alto, CA.
HIGH-EFFICIENCY, RADIATION-RESISTANT GaAs SPACE CELLS
K. A. Bertness, M. Ladle Ristow, M. Grounner, M. S. Kuryla, and J. G. Werthen *In* NASA, Lewis Research Center, Space

Photovoltaic Research and Technology, 1989 Jan. 1991 p 136-139 (For primary document see N91-19182 11-20)
Avail: NTIS HC/MF A22 CSCL 10B

N91-19195*# National Aeronautics and Space Administration. Lewis Research Center, Cleveland, OH.
THERMAL ANNEALING OF GaAs CONCENTRATOR SOLAR CELLS
H. B. Curtis and David J. Brinker *In its* Space Photovoltaic Research and Technology, 1989 Jan. 1991 p 140-153 (For primary document see N91-19182 11-20)
Avail: NTIS HC/MF A22 CSCL 10B

N91-19196*# Boeing Co., Seattle, WA.
BURST ANNEALING OF HIGH TEMPERATURE GaAs SOLAR CELLS
P. R. Brothers and W. E. Horne *In* NASA, Lewis Research Center, Space Photovoltaic Research and Technology, 1989 Jan. 1991 p 154-163 (For primary document see N91-19182 11-20)
Avail: NTIS HC/MF A22 CSCL 10B

N91-19197*# Boeing Aerospace Co., Seattle, WA.
AN APPROACH FOR CONFIGURING SPACE PHOTOVOLTAIC TANDEM ARRAYS BASED ON CELL LAYER PERFORMANCE
C. S. Flora and P. A. Dillard *In* NASA, Lewis Research Center, Space Photovoltaic Research and Technology, 1989 Jan. 1991 p 167-179 (For primary document see N91-19182 11-20)
Avail: NTIS HC/MF A22 CSCL 10B

N91-19198*# National Aeronautics and Space Administration. Lewis Research Center, Cleveland, OH.
REVIEW OF THIN FILM SOLAR CELL TECHNOLOGY AND APPLICATIONS FOR ULTRA-LIGHT SPACECRAFT SOLAR ARRAYS
Geoffrey A. Landis *In its* Space Photovoltaic Research and Technology, 1989 Jan. 1991 p 180-203 (For primary document see N91-19182 11-20)
Avail: NTIS HC/MF A22 CSCL 10B

N91-19199*# Solarex Corp., Rockville, MD.
PERFORMANCE, SIZE, MASS, AND COST ESTIMATES FOR PROJECTED 1kW EOL Si, InP, AND GaAs ARRAYS
Luther W. Slifer, Jr. *In* NASA, Lewis Research Center, Space Photovoltaic Research and Technology, 1989 Jan. 1991 p 204-211 (For primary document see N91-19182 11-20)
Avail: NTIS HC/MF A22 CSCL 10B

N91-19200*# National Aeronautics and Space Administration. Lewis Research Center, Cleveland, OH.
DUAL-PURPOSE SELF-DELIVERABLE LUNAR SURFACE PV ELECTRICAL POWER SYSTEM
Jack H. Arnold, David W. Harris, Eldon R. Cross (Research Triangle Inst., Research Triangle Park, NC.), and Dennis J. Flood *In its* Space Photovoltaic Research and Technology, 1989 Jan. 1991 p 212-222 (For primary document see N91-19182 11-20)
Avail: NTIS HC/MF A22 CSCL 10B

N91-19201*# National Aeronautics and Space Administration. Lewis Research Center, Cleveland, OH.
FEASIBILITY OF SOLAR POWER FOR MARS
Joseph Appelbaum and Geoffrey A. Landis *In its* Space Photovoltaic Research and Technology, 1989 Jan. 1991 p 223-254 (For primary document see N91-19182 11-20)
Avail: NTIS HC/MF A22 CSCL 10B

N91-19202*# Midwest Research Inst., Golden, CO.
RECENT ADVANCES IN THE ITO/InP SOLAR CELL
T. A. Gessert, X. Li, M. W. Wanlass, and T. J. Coutts *In* NASA, Lewis Research Center, Space Photovoltaic Research and Technology, 1989 Jan. 1991 p 257-269 (For primary document see N91-19182 11-20)
(Contract NASA Order C-3000-K; DE-AC02-83CH-10093)
Avail: NTIS HC/MF A22 CSCL 10B

N91-19203*# National Aeronautics and Space Administration. Lewis Research Center, Cleveland, OH.
SEMICONDUCTOR STRUCTURAL DAMAGE ATTENDANT TO CONTACT FORMATION IN III-V SOLAR CELLS
Navid S. Fatemi (Sverdrup Technology, Inc., Cleveland, OH.) and Victor G. Weizer *In its* Space Photovoltaic Research and Technology, 1989 Jan. 1991 p 270-279 (For primary document see N91-19182 11-20)
Avail: NTIS HC/MF A22 CSCL 10B

N91-19204*# Rensselaer Polytechnic Inst., Troy, NY.
THE EFFECT OF PROCESS CONDITIONS ON THE PERFORMANCE OF EPITAXIAL InP SOLAR CELLS
J. M. Borrego and S. K. Ghandi *In* NASA, Lewis Research Center, Space Photovoltaic Research and Technology, 1989 Jan. 1991 p 280-288 (For primary document see N91-19182 11-20)
(Grant NAG3-604)
Avail: NTIS HC/MF A22 CSCL 10B

N91-19205*# National Aeronautics and Space Administration. Lewis Research Center, Cleveland, OH.
EFFECTS OF PROTON IRRADIATION ON THE PERFORMANCE OF InP/GaAs SOLAR CELLS
Irving Weinberg, C. K. Swartz, David J. Brinker, and D. M. Wilt *In its* Space Photovoltaic Research and Technology, 1989 Jan. 1991 p 289-297 (For primary document see N91-19182 11-20)
Avail: NTIS HC/MF A22 CSCL 10B

N91-19206*# National Aeronautics and Space Administration. Lewis Research Center, Cleveland, OH.
KEY FACTORS LIMITING THE OPEN CIRCUIT VOLTAGE OF n(+)pp(+) INDIUM PHOSPHIDE SOLAR CELLS
Chandra Goradia, William Thesling (Cleveland State Univ., OH.), and Irving Weinberg *In its* Space Photovoltaic Research and Technology, 1989 Jan. 1991 p 298-310 (For primary document see N91-19182 11-20)
Avail: NTIS HC/MF A22 CSCL 10B

N91-19207*# National Aeronautics and Space Administration. Lewis Research Center, Cleveland, OH.
DETERMINATION OF SERIES RESISTANCE OF INDIUM PHOSPHIDE SOLAR CELLS
Raj K. Jain and Irving Weinberg *In its* Space Photovoltaic Research and Technology, 1989 Jan. 1991 p 311-315 (For primary document see N91-19182 11-20)
Avail: NTIS HC/MF A22 CSCL 10B

N91-19208*# National Aeronautics and Space Administration. Lewis Research Center, Cleveland, OH.
INVESTIGATION OF ANODIC AND CHEMICAL OXIDES GROWN ON p-TYPE InP WITH APPLICATIONS TO SURFACE PASSIVATION FOR n(+)-p SOLAR CELL FABRICATION
Maria Faur, Mircea Faur, Manju Goradia, Chandra Goradia (Cleveland State Univ., OH.), Phillip Jenkins, Douglas Jayne, and Irving Weinberg *In its* Space Photovoltaic Research and Technology, 1989 Jan. 1991 p 316-331 (For primary document see N91-19182 11-20)
Avail: NTIS HC/MF A22 CSCL 10B

N91-19209*# National Aeronautics and Space Administration. Lewis Research Center, Cleveland, OH.
A COMPARATIVE STUDY OF PERFORMANCE PARAMETERS OF n(+)-p InP SOLAR CELLS MADE BY CLOSED-AMPOULE SULFUR DIFFUSION INTO Cd- AND Zn-DOPED p-TYPE InP SUBSTRATES
Mircea Faur, Maria Faur, Chandra Goradia, Manju Goradia, Ralph D. Thomas, David J. Brinker, Navid S. Fatemi (Sverdrup Technology, Inc., Cleveland, OH.), and Frank S. Honecy *In its* Space Photovoltaic Research and Technology, 1989 Jan. 1991 p 332-346 (For primary document see N91-19182 11-20)
Avail: NTIS HC/MF A22 CSCL 10B

N91-19210*# Boeing Aerospace Co., Seattle, WA.
RADIOISOTOPE THERMAL PHOTOVOLTAIC APPLICATION OF THE GaSb SOLAR CELL
M. D. Morgan, W. E. Horne, and A. C. Day *In* NASA, Lewis Research Center, Space Photovoltaic Research and Technology, 1989 Jan. 1991 p 349-358 (For primary document see N91-19182 11-20)
Avail: NTIS HC/MF A22 CSCL 10B

N91-19211*# Jet Propulsion Lab., California Inst. of Tech., Pasadena.
GaP BETAVOLTAIC CELLS AS A POWER SOURCE
F. S. Pool, Paul M. Stella, and B. Anspaugh *In* NASA, Lewis Research Center, Space Photovoltaic Research and Technology, 1989 Jan. 1991 p 359-370 (For primary document see N91-19182 11-20)
Avail: NTIS HC/MF A22 CSCL 10B

N91-19213*# Solarex Corp., Rockville, MD. Aerospace Div.
SPACEFLIGHT PERFORMANCE OF SEVERAL TYPES OF SILICON SOLAR CELLS ON THE LIPS 3 SATELLITE
J. Silver and D. Warfield *In* NASA, Lewis Research Center, Space Photovoltaic Research and Technology, 1989 Jan. 1991 p 385-388 (For primary document see N91-19182 11-20)
Avail: NTIS HC/MF A22 CSCL 10B

N91-19214*# Wayne State Univ., Detroit, MI. Inst. for Manufacturing Research.
ANNEALING CHARACTERISTICS OF IRRADIATED HYDROGENATED AMORPHOUS SILICON SOLAR CELLS
J. S. Payson, S. Abdulaziz, Y. Li, and J. R. Woodyard *In* NASA, Lewis Research Center, Space Photovoltaic Research and Technology, 1989 Jan. 1991 p 389-399 (For primary document see N91-19182 11-20)
Avail: NTIS HC/MF A22 CSCL 10B

N91-19215*# Applied Solar Energy Corp., City of Industry, CA.
OPTIMIZATION AND PERFORMANCE OF SPACE STATION FREEDOM SOLAR CELLS
S. Khemthong, N. Hansen, and M. Bower *In* NASA, Lewis Research Center, Space Photovoltaic Research and Technology, 1989 Jan. 1991 p 400-409 (For primary document see N91-19182 11-20)
Avail: NTIS HC/MF A22 CSCL 10B

N91-19216*# Jet Propulsion Lab., California Inst. of Tech., Pasadena.
THERMAL CYCLE TESTING OF SPACE STATION FREEDOM SOLAR ARRAY BLANKET COUPONS
David A. Scheiman and David A. Schieman (Sverdrup Technology, Inc., Cleveland, OH.) *In* NASA, Lewis Research Center, Space Photovoltaic Research and Technology, 1989 Jan. 1991 p 410-420 (For primary document see N91-19182 11-20)
(Contract NAS3-25266)
Avail: NTIS HC/MF A22 CSCL 10B

N91-19217*# Jet Propulsion Lab., California Inst. of Tech., Pasadena.
THE ADVANCED PHOTOVOLTAIC SOLAR ARRAY (APSA) TECHNOLOGY STATUS AND PERFORMANCE
Paul M. Stella and Richard M. Kurland (TRW Space Technology Labs., Redondo Beach, CA.) *In* NASA, Lewis Research Center, Space Photovoltaic Research and Technology, 1989 Jan. 1991 p 421-432 (For primary document see N91-19182 11-20)
Avail: NTIS HC/MF A22 CSCL 10B

N91-19218*# Sovonics Solar Systems, Troy, MI.
INTEGRAL BYPASS DIODES IN AN AMORPHOUS SILICON ALLOY PHOTOVOLTAIC MODULE
J. J. Hanak and H. Flaisher *In* NASA, Lewis Research Center, Space Photovoltaic Research and Technology, 1989 Jan. 1991 p 433-442 (For primary document see N91-19182 11-20)
Avail: NTIS HC/MF A22 CSCL 10B

N91-19219*# National Aeronautics and Space Administration. Lewis Research Center, Cleveland, OH.
MINI-DOME FRESNEL LENS PHOTOVOLTAIC CONCENTRATOR DEVELOPMENT
Mark J. ONeill (ENTECH Corp., Dallas-Fort Worth Airport, TX.) and Michael F. Piszczor, Jr. *In its* Space Photovoltaic Research and Technology, 1989 Jan. 1991 p 443-459 (For primary document see N91-19182 11-20)
Avail: NTIS HC/MF A22 CSCL 10B

N91-19221*# National Aeronautics and Space Administration. Lewis Research Center, Cleveland, OH.
INDIUM PHOSPHIDE SOLAR CELLS
Irving Weinberg *In its* Space Photovoltaic Research and Technology, 1989 Jan. 1991 p 484-486 (For primary document see N91-19182 11-20)
Avail: NTIS HC/MF A22 CSCL 10B

45 ENVIRONMENT POLLUTION

Includes atmospheric, noise, thermal, and water pollution.

N91-19514# National Oceanic and Atmospheric Administration, Washington, DC. National Environmental Satellite, Data, and Information Service.
NOAA-9 SOLAR BACKSCATTER ULTRAVIOLET (SBUV/2) INSTRUMENT AND DERIVED OZONE DATA: REVIEW Status Report
Walter G. Planet, ed. Jun. 1990 216 p Review held in Camp Springs, MD, 29 Jan. 1990
(NOAA-TR-NESDIS-53) Avail: NTIS HC/MF A10

The NOAA satellite ozone monitoring program was initiated in December 1984 with the launch of the NOAA-9 operational satellite carrying the first operational Solar Backscatter Ultraviolet (SBUV/2) spectrometer. The instrument and its derived data products have been undergoing extensive characterization and validation studies since the launch. Much has been learned, pro and con. A review of the status of the knowledge of the system was held. The review covered the efforts of the various NOAA, NASA, and contractor scientists who have been engaged in several aspects of the SBUV/2 program. For individual titles, see N91-19515 through N91-19527.

N91-19515# National Oceanic and Atmospheric Administration, Washington, DC.
DATA STATUS AND AVAILABILITY
H. D. Bowman, II *In its* NOAA-9 Solar Backscatter Ultraviolet (SBUV/2) Instrument and Derived Ozone Data: Review Jun. 1990 18 p (For primary document see N91-19514 11-45)
Avail: NTIS HC/MF A10

A list of significant dates related to the NOAA-9 Solar Backscattering Ultraviolet (SBUV/2) instrument data is provided. The SBUV/2 ozone products description; changes in the first reprocessing; ozone products availability; and changes proposed for the second reprocessing are presented in viewgraph format.
B.G.

N91-19516# ST Systems Corp., Lanham, MD.
AN ASSESSMENT OF INSTRUMENT PERFORMANCE FOR THE NOAA-9 SBUV/2
Donald F. Health *In* NOAA, NOAA-9 Solar Backscatter Ultraviolet (SBUV/2) Instrument and Derived Ozone Data: Review Jun. 1990 13 p (For primary document see N91-19514 11-45)
Avail: NTIS HC/MF A10

The requirements for the accuracy of ozone monitoring are given in the National Plan for Stratospheric Monitoring, 1988-1997, FCM-P17-1989. These requirements, 3 percent per decade at the 95 percent confidence level at 40 km or approximately 2 percent per decade in the albedo calibration of the instrument, are more stringent than those contained in the TIROS-N SBUV/2 instrument specification which requires an uncertainty of 1.53 percent at 250

nm and 1.57 percent at 300 nm. This is assumed to be at the 95 percent confidence for an end-to-end spectral bi-directional reflectance instrument calibration for both the instrument pre-flight calibration and its changes throughout its operating lifetime in space. The purpose of the NOAA-9 SBUV/2 summary meeting was to evaluate the overall performance of this instrument. An attempt is made to do this by evaluating the calibration accuracy for all previously flow SBUV type instruments and intercomparing the solar spectral irradiance measurements during the initial period of the instruments observations in space when the effects of instrument degradation is likely to be the smallest. A copy of the OSA symposium presentation was the basis for the report made to the NOAA-9 SBUV/2 summary meeting. Author

N91-19517# National Oceanic and Atmospheric Administration, Washington, DC.
SBUV/2 IN-ORBIT PERFORMANCE
James H. Lienesch *In its* NOAA-9 Solar Backscatter Ultraviolet (SBUV/2) Instrument and Derived Ozone Data: Review Jun. 1990 14 p (For primary document see N91-19514 11-45)
Avail: NTIS HC/MF A10

Spacecraft sun angle as a function of time; a plot of the solar zenith angle of SBUV/2 measurements versus latitude for July 1985, January 1988, and July 1989; SBUV/2 total ozone differences; a plot of the albedo correction factor (ACF) for channel 12; and SBUV/2 total ozone are presented in viewgraph format. Each is briefly discussed. B.G.

N91-19518*# National Aeronautics and Space Administration. Goddard Space Flight Center, Greenbelt, MD.
A STATUS REPORT ON THE ANALYSIS OF THE NOAA-9 SBUV/2 SWEEP MODE SOLAR IRRADIANCE DATA
R. P. Cebula, M. T. DeLand, B. M. Schlesinger (ST Systems Corp., Lanham, MD.), and R. D. Hudson *In* NOAA, NOAA-9 Solar Backscatter Ultraviolet (SBUV/2) Instrument and Derived Ozone Data: Review Jun. 1990 23 p (For primary document see N91-19514 11-45)
Avail: NTIS HC/MF A10 CSCL 13B

Monitoring of the near ultraviolet (UV) solar irradiance is important because the solar UV radiation is the primary energy source in the upper atmosphere. The solar irradiance at wavelengths shortward of roughly 300 nm heats the stratosphere via photodissociation of ozone in the Hartley bands. Shortward of 242 nm the solar UV flux photodissociates O2, which is then available for ozone formation. Upper stratosphere ozone variations coincident with UV solar rotational modulation have been previously reported (Gille et al., 1984). Clearly, short and long term solar irradiance observations are necessary to separate solar-forced ozone variations from anthropogenic changes. The SBUV/2 instrument onboard the NOAA-9 spacecraft has made daily measurements of the solar spectral irradiance at approximately 0.15 nm intervals in the wavelength region 160-405 nm at 1 nm resolution since March 1985. These data are not needed to determine the terrestrial ozone overburden or altitude profile, and hence are not utilized in the NOAA Operational Ozone Product System (OOPS). Therefore, assisted by the ST System Corporation, NASA has developed a scientific software system to process the solar sweep mode data from the NOAA-9 instrument. This software will also be used to process the sweep mode solar irradiance data from the NOAA-11 and later SBUV/2 instruments. An overview of the software system and a brief discussion of analysis findings to date are provided. Several outstanding concerns/problems are also presented. Author

N91-19519# ST Systems Corp., Lanham, MD.
NOAA-9 SBUV/2 OZONE SOUNDING ACCURACY: PRESENTATION SUMMARY
Howard Weiss *In* NOAA, NOAA-9 Solar Backscatter Ultraviolet (SBUV/2) Instrument and Derived Ozone Data: Review Jun. 1990 19 p (For primary document see N91-19514 11-45)
Avail: NTIS HC/MF A10

Three and a half years of radiance measurements by the NOAA-9 SBUV/2 at the wavelengths used for total ozone monitoring were analyzed and presented. It was found that the variability in the radiances is dominated by scene related events. The noise to signal ratio was about 4 percent and decreased in the latter part of the period investigated. Instrumental effects accounted for about 0.5 percent in noise to signal ratio and was fairly constant during this period. There was a fundamental change in the annual signature of the signal possibly due to a solar zenith angle effect. Author

N91-19520*# National Aeronautics and Space Administration. Goddard Space Flight Center, Greenbelt, MD.
A TECHNIQUE FOR DIRECTLY COMPARING RADIANCES FROM TWO SATELLITES
Richard D. McPeters *In* NOAA, NOAA-9 Solar Backscatter Ultraviolet (SBUV/2) Instrument and Derived Ozone Data: Review Jun. 1990 10 p (For primary document see N91-19514 11-45)
Avail: NTIS HC/MF A10 CSCL 13B

Solar Backscattering Ultraviolet-2 (SBUV/2) instrument on NOAA-9 orbit on June 1987, solar zenith angles of the observations; plot of weekly average differences between SBUV (Nimbus-7 and SBUV/2 (NOAA-9); radiance comparisons for March 1986; time dependence of relative change between SBUV and SBUV/2; and explicit wavelength dependence are presented in viewgraph format. Each is briefly discussed. B.G.

N91-19521# National Oceanic and Atmospheric Administration, Washington, DC. Analysis and Information Branch.
SBUV/2 COMPARISONS WITH GROUND-BASED AND SBUV SPACECRAFT DATA
A. J. Miller and R. Nagatani *In its* NOAA-9 Solar Backscatter Ultraviolet (SBUV/2) Instrument and Derived Ozone Data: Review Jun. 1990 21 p (For primary document see N91-19514 11-45)
Avail: NTIS HC/MF A10

The April and December 1985 monthly average results for SBUV/2 minus Dobson; SBUV/2 comparison with SBUV monthly results (Dec 1985); total ozone model; SBUV/2 minus SBUV total ozone (April and December 1985); ascending vs. descending data (July 1985, July 1985 compared to mode 1); SBUV/2 minus Dobson/SBUV2 - all station, averaged trend by group, Lisbon, 5 stations adjusted for aerosols and Umekhr layers; and SBUV/2 vs. SAGE 2 (April 1985) are presented in viewgraph format. Each is discussed briefly. B.G.

N91-19522# National Oceanic and Atmospheric Administration, Washington, DC.
UMKEHR WORK
J. DeLuisi *In its* NOAA-9 Solar Backscatter Ultraviolet (SBUV/2) Instrument and Derived Ozone Data: Review Jun. 1990 10 p (For primary document see N91-19514 11-45)
Avail: NTIS HC/MF A10

The primary focus of the Umkehr work is to produce an Umkehr measurement record of the highest quality for validation of satellite determinations of ozone profile and for determining trends in stratospheric ozone profile as an independent validation of satellite results. To produce Umkehr ozone profiles of the highest quality it is necessary to account for every factor that affects the measurement. To do this, the work involved the following set of tasks: corrections for stratospheric aerosols; qualifying the character of the zenith sky during an observation; turbidity observations for tropospheric aerosol information; algorithm performance evaluation and development of updated versions; and comparisons of Umkehr ozone profiles with other types of ozone profiles. By far the greatest thus far is corrections for stratospheric aerosols because of their tendency to introduce characteristic errors in the upper stratospheric ozone concentrations. The correction effort can be separated into two parts: development of the theory for corrections, and acquisition of stratospheric aerosol information. A schematic diagram of the correction procedure is shown. The accomplishments of the past work, which includes special efforts to acquire stratospheric aerosol information are briefly described. Author

N91-19523*# National Aeronautics and Space Administration. Goddard Space Flight Center, Greenbelt, MD.
INITIAL ESTIMATE OF NOAA-9 SBUV/2 TOTAL OZONE DRIFT: BASED ON COMPARISON WITH RE-CALIBRATED TOMS MEASUREMENTS AND PAIR JUSTIFICATION OF SBUV/2
C. G. Wellemeyer, S. L. Taylor, X. U. Gu (ST Systems Corp., Lanham, MD.), Richard D. McPeters, and R. D. Hudson *In* NOAA, NOAA-9 Solar Backscatter Ultravillet (SBUV/2) Instrument and Derived Ozone Data: Review Jun. 1990 18 p (For primary document see N91-19514 11-45)
Avail: NTIS HC/MF A10 CSCL 13B

Newly recalibrated version 6 Total Ozone Mapping Spectrometer (TOMS) data are used as a reference measurement in a comparison of monthly means of total ozone in 10 degree latitude zones from SBUV/2 and the nadir measurements from TOMS. These comparisons indicate a roughly linear long-term drift in SBUV/2 total ozone relative to TOMS of about 2.5 Dobson units per year at the equator over the first three years of SBUV/2. The pari justification technique is also applied to the SBUV/2 measurements in a manner similar to that used for SBUV and TOMS. The higher solar zenith angles associated with the afternoon orbit of NOAA-9 and the large changes in solar zenith angle associated with its changing equator crossing time degrade the accuracy of the pair justification method relative to its application to SBUV and TOMS, but the results are consistent with the SBUV/2-TOMS comparisons, and show a roughly linear drift in SBUV/2 of 2.5 to 4.5 Dobson units per year in equatorial ozone. Author

N91-19524*# National Aeronautics and Space Administration. Goddard Space Flight Center, Greenbelt, MD.
CALIBRATION OF LONG TERM SATELLITE OZONE DATA SETS USING THE SPACE SHUTTLE
Ernest Hilsenrath *In* NOAA, NOAA-9 Solar Backscatter Ultraviolet (SBUV/2) Instrument and Derived Ozone Data: Review Jun. 1990 19 p (For primary document see N91-19514 11-45)
Avail: NTIS HC/MF A10 CSCL 13B

Trends in atmospheric ozone continue to be an environmental concern. Drifts in satellite observations are the major obstacle in the detection of changes in global ozone over the long term. Careful re-analysis of satellite ozone data along with groundbased observations have more or less corroborated photochemical models which predict ozone depletion. However, there remains the margin of error in the observations that is as large as the trend itself. The National Plan for Stratospheric Monitoring calls for monitoring global ozone for at lease the next ten years employing the NOAA polar orbiting satellites. Ozone observations will be made with the Solar Backscatter Ultraviolet Spectral Radiometer Mod 2 (SBUV/2) which ia a refinement of the SBUV instrument flying on NASA's Nimbus-7 satellite. The first instrument in the operational series began taking data from the NOAA-9 spacecraft in February 1985. A second instrument was launched on NOAA-11 in September 1988. Both continue to operate. Earlier attempts to calibrate satellite data relied on comparisons with ground based observations. However, differences in instrumental techniques severely complicated these efforts. This problem will be over come by regular flights, about once per year, of the Shuttle Solar Backscatter Ultraviolet radiometer (SSBUV). The data from the SSBUV instrument will be compared with nearly coincident data taken by the NOAA satellite instruments. This procedure will permit a direct calibration transfer in space, since the two instruments observe the same qualities thereby bypassing the inversion algorithm which converts the observations to ozone amounts. Author

N91-19525# National Oceanic and Atmospheric Administration, Boulder, CO. Climate Monitoring and Diagnostics Lab.
TOTAL OZONE, OZONESONDE, AND UMKEHR OBSERVATIONS FOR SATELLITE OZONE DATA VALIDATION
W. D. Komhyr, R. D. Grass, G. L. Koenig, R. D. Evans, P. Franchois, and R. K. Leonard (Colorado Univ., Boulder.) *In* NOAA, NOAA-9 Solar Backscatter Ultraviolet (SBUV/2) Instrument and Derived Ozone Data: Review Jun. 1990 20 p (For primary document see N91-19514 11-45)
Avail: NTIS HC/MF A10

The NOAA Air Resources Laboratory, Geophysical Monitoring for Climatic Change (GMCC) Division has been providing total ozone, ozonesonde, and Umkehr data ot the National Environmental Satellite Data and Information Service (NESDIS) for NOAA-9 solar backscattered ultraviolet (SBUV-2) satellite ozone data validation since 1984. The data is described and information is provided on ozone measurement precision and accuracy. Author

N91-19526# National Oceanic and Atmospheric Administration, Boulder, CO.
ANALYSIS OF SBUV/2 MEASUREMENTS OF SOLAR UV IRRADIANCE VARIATIONS
Richard F. Donnelly and Joan Barrett *In* NOAA, NOAA-9 Solar Backscatter Ultraviolet (SBUV/2) Instrument and Derived Ozone Data: Review 6 p(SEE N91-19514 11-45) Jun. 1990 (For primary document see N91-19514 11-45)
Avail: NTIS HC/MF A10

The NOAA-9 and NOAA-11 SBUV2 monitoring measurements in the discrete wavelength mode are discussed for the core-to-wing ratio of the solar Mg II h and k lines near 280 nm. A new ratio, similar to Heath and Schlesinger's (1986) ration for Nimbus-7, has been adopted for NOAA-9 and NOAA-11 to avoid drift problems associated with the low-amplification third intensity range in the photomultiplier cathode circuit. This new ratio provides an excellent ratio of solar signal to instrument noise for NOAA-9 and NOAA-11 because of the SBUV2's superb wavelength repeatability. Recommendations for the SBUV2 instruments that have not yet flown and for future operations of the SBUV2 monitors are presented based on the experience with NOAA-9 and NOAA-11. Author

N91-19527*# National Aeronautics and Space Administration. Goddard Space Flight Center, Greenbelt, MD.
OZONE MEASUREMENTS FROM THE NOAA-9 AND THE NIMBUS-7 SATELLITES: IMPLICATIONS OF SHORT AND LONG TERM VARIABILITIES
S. Chandra, Richard D. McPeters, R. D. Hudson, and Walter G. Planet (National Oceanic and Atmospheric Administration, Washington, DC.) *In* NOAA, NOAA-9 Solar Backscatter Ultraviolet (SBUV/2) Instrument and Derived Ozone Data: Review Jun. 1990 16 p (For primary document see N91-19514 11-45)
Avail: NTIS HC/MF A10 CSCL 13B

An overview is given of the measurements of total ozne and ozone profiles by the SBUV/2 instrument on the NOAA-9 spacecraft relative to similar measurements from the SBUV and TOMS instruments on Nimbus-7. It is shown that during the three year period from March 14, 1985, to February 28, 1988, when these data sets overlap, there have been significant changes in the calibrations of the three instruments which may be attributed to the drift of the NOSS-9 orbit to later equator crossing times (for SBUV/2). These changes in instrument characteristics have affected the absolute values of the trends derived from the three instruments, but their geophysical characteristics and response to short term variations are accurate and correlate well among the three instruments. For example, the total column ozone measured by the three instruments shows excellent agreement with respect to its day to day, seasonal, and latitudinal variabilities. At high latitudes, the day to day fluctuations in total ozone show a strong positive correlation with temperature in the lower stratosphere, as one might expect from the dynamical coupling of the two parameters at these latitudes. Author

N91-19528# Committee on Commerce, Science, and Transportation (U.S. Senate).
GLOBAL CHANGE: WHAT YOU CAN DO
Washington GPO 1990 88 p Hearing before the Committee on Commerce, Science, and Transportation, 101st Congress, 2d Session, 25 Apr. 1990

(S-Hrg-101-1160; GPO-38-022) Avail: Committee on Commerce, Science, and Transportation, Senate, Washington, DC 20510 HC free; also avaliable SOD HC $2.75 as 552-070-09826-7

Hearings before the Senate Committee on Commerce, Science, and Transportation are presented on simple things that a person can do to reduce threats to the global environment. Specific threats addressed include greenhouse warming, ozone depletion, acid rain, and other effects of pollution and global changes in marine ecosystems, agriculture, forestry, and human health. It is noted that even small steps, such as more double-sided photocopying, can save trees; that maintaining a second home wastes resources; and that several books written by one witness describe other things one can do to save the Earth. The Federal Government is urged to set an example and to pass appropriate legislation to encourage conservation and reduce pollution. J.P.S.

N91-19529*# National Aeronautics and Space Administration. Marshall Space Flight Center, Huntsville, AL.

ATMOSPHERIC ENVIRONMENT FOR SPACE SHUTTLE (STS-41) LAUNCH

G. L. Jasper and G. W. Batts (New Technology, Inc., Huntsville, AL.) Nov. 1990 45 p

(NASA-TM-103525; NAS 1.15:103525) Avail: NTIS HC/MF A03 CSCL 13B

A summary of selected atmospheric conditions observed near space shuttle STS-41 launch time on October 6, 1990, at Kennedy Space Center, Florida are presented. Values of ambient pressure, temperature, moisture, ground winds, visual observations (clouds), and winds aloft are included. The sequence of prelaunch Jimsphere-measured vertical wind profiles is given. The final atmospheric tape, which consists of wind and thermodynamic parameters versus altitude, for STS-41 vehicle ascent was constructed. The STS-41 ascent atmospheric data tape was constructed by Marshall Space Flight Center's Earth Science and Applications Division to provide an internally consistent data set for use in postflight performance assessments and represents the best estimate of the launch environment to the 400,000 ft altitude that was traversed by the STS-41 vehicle. Author

N91-19530# Lawrence Livermore National Lab., CA.

ZONAL STATISTICS IN (GENERAL CIRCULATION MODEL) GCM/GCM/DATA INTERCOMPARISONS

S. L. Grotch Nov. 1990 8 p Presented at the 15th Annual Climate Diagnostics Workshop, Asheville, 19 Oct. - 2 Nov. 1990

(Contract W-7405-eng-48)

(DE91-006706; UCRL-JC-105745; CONF-9010277-2) Avail: NTIS HC/MF A02

Comparisons of general circulation model (GCM) results with each other and with climate data are routinely made on a variety of spatial scales. In bridging the gap from larger scale behavior (global, hemispheric) to the regional, zonal statistics are commonly used. Here, statistics are developed using values at all longitudinal gridpoints at a specified latitude and these are displayed as a function of latitude. The zonal average is the most routinely used of these statistics, but there are many other statistics available, few of which are ever examined. These provide a rich array of diagnostic measures for intercomparing models with each other and with observational data. Several of these measures are explored here: (1) histograms or boxplots displaying the detailed distributions, (2) rms or average absolute pointwise differences between model and data sets, and (3) cross correlations and auto correlations. DOE

N91-19531# Sypher-Mueller International, Inc., Ottawa (Ontario).

EXHAUST EMISSIONS FROM HEAVY DUTY VEHICLES

Nov. 1990 46 p

(Contract DE-GI01-87CE-50182)

(DE91-006798; DOE/CE-50182/T1) Avail: NTIS HC/MF A03

Increasing global interest in controlling atmospheric pollution has led legislative authorities in many countries to impose stringent regulations upon motor vehicle emissions. Standards have been in force for many years in most of the developed world, but there is still a great deal of diversity in the approaches taken. A comparison is presented of international emissions regulations including test cycle employed, sampling and measurement techniques, and legislated limits on pollutants. Because of the many variations in these basic criteria, any cross correlation of standards between countries is likely to be impossible in practice. Methanol fueling is now widely recognized as a potential means of reducing pollution from motor vehicles particularly because of its soot-free combustion and low overall emissions levels. An overview is presented of the current work in progress on design, manufacture and testing of heavy duty methanol engines for trucks and buses and also a survey of the application of catalytic converters for exhaust emissions control on these engines. A review of progress in emissions control measures for diesel fueled engines is included for comparison purposes. Prior to methanol being phased in as a diesel fuel substitute, regulatory bodies will have to address its compatibility with existing emissions control standards. In the meantime, researchers and manufacturers must continue developing their engines. The variations in emissions test procedures create a confusing background against which to measure progress in emissions reduction technology. This problem is aggravated by the trend to design modern engines for manufacture and marketing on an international basis. A proposal is presented for Standardized Emissions Research Cycle, which might be used to allow ready comparison between numerous emissions control strategies at present under development. DOE

N91-19532# Atmospheric and Environmental Research, Inc., Cambridge, MA.

NATURAL AND ANTHROPOGENIC CLIMATE CHANGE

W. J. Gutowski, D. A. Portman, M. J. Iacono, and W. C. Wang (State Univ. of New York, Albany.) 30 Sep. 1990 6 p

(Contract DE-FG02-86ER-60422)

(DE91-007363; DOE/ER-60422/6) Avail: NTIS HC/MF A02

This report covers the project progress of grant DE-FG02-86ER-60422 for the period March 1, 1990 to October 1, 1990. The research program includes three tasks: General Circulation Models (GCM) intercomparison and improvement, climate data-model statistics, and China project science coordination. DOE

N91-19533# Oak Ridge National Lab., TN.

THE DILEMMA OF FOSSIL FUEL USE AND GLOBAL CLIMATE CHANGE

R. R. Judkins, W. Fulkerson, and M. K. Sanghvi 1991 15 p Presented at the 201st American Chemical Society (ACS) National Meeting, Atlanta, GA, 14-19 Apr. 1991

(Contract DE-AC05-84OR-21400)

(DE91-007859; CONF-910402-7) Avail: NTIS HC/MF A03

The use of fossil fuels and relationship to climate change is discussed. As the use of fossil fuels has grown, the problems of protecting the environment and human health and safety have also grown, providing a continuing challenge to technological and managerial innovation. Today that challenge is to control atmospheric emissions from combustion, particularly those emissions that cause acidic deposition, urban pollution, and increasing concentrations of greenhouse gases. Technology for reducing acidic deposition is available and needs only to be adopted, and the remedies for urban pollution are being developed and tested. How effective or expensive these will be remains to be determined. The control of emissions of the greenhouse gas, CO2, seems possible only be reducing the total amounts of fossil fuels used worldwide, and by substituting efficient natural gas technologies for coal. Long before physical depletion forces the transition away from fossil fuels, it is at least plausible and even likely that the greenhouse effect will impose a show-stopping constraint. If such a transition were soon to be necessary, the costs would be very high because substitute energy sources are either limited or expensive or undesirable for other reasons. Furthermore, the costs would be unevenly felt and would be more oppressive for developing nations because they would be least able to pay and, on average, their use rates of fossil fuels are

growing much faster than those of many industrialized countries. It is prudent, therefore, to try to manage the use of fossil fuels as if a greenhouse constraint is an important possibility. DOE

N91-19534# Argonne National Lab., IL. Mathematics and Computer Science Div.
ANALYSIS OF WORKLOAD AND LOAD BALANCING ISSUES IN THE NCAR COMMUNITY CLIMATE MODEL
J. G. Michalakes Jan. 1991 23 p
(Contract W-31-109-eng-38)
(DE91-008052; ANL/MCS-TM-144) Avail: NTIS HC/MF A03

Choice of an appropriate strategy for balancing load in climate models running on parallel processors depends on the nature and size of inherent imbalances. Physics routines of the NCAR Community Climate Model were instrumented to produce per-cell load data for each time step, revealing load imbalance resulting from surface type, polar night, weather patterns, and the earth's tormentor. Hourly, daily, and annual cycles in processor performance over the model grid were also uncovered. Data from CCM1 suggested a number of static processor allocation strategies. DOE

N91-19535# Oak Ridge National Lab., TN.
THROUGHFALL AND FOLIAR EXTRACTION
B. B. Hicks, R. R. Draxier, D. L. Albritton, F. C. Fehsenfeld, J. M. Hales, T. P. Meyers, R. L. Vong, M. Dodge, S. E. Schwartz, and R. L. Tanner et al 1990 8 p Presented at the National Acid Precipitation Assessment Program (NAPAP) State-of-Science, Atmospheric Processes Research and Process Model Development Conference, Hilton Head Island, 11-16 Feb. 1990
(Contract DE-AC05-84OR-21400)
(DE91-007184; CONF-9002167-1) Avail: NTIS HC/MF A02

Environmental surfaces, although difficult to simulate either mathematically or physically, have the natural ability to integrate the net result of dry deposition of various airborne compounds. Surface analysis methods can be used to quantify the amount of deposited material residing on such surfaces for constituents that are not irreversibly sorbed. From knowledge of the area of the surface and the duration of the period of deposition, the net dry deposition rate to the surface can be computed. Important problems in quantifying dry deposition to plant canopies include spatial and temporal representativeness of modeled fluxes, and scaling from point measurements (in both space and time) to the landscape. Many micrometeorological approaches are limited to simple terrain and short time intervals and are not applicable to coarse particles. Quantifying dry deposition of coarse aerosols, such as Ca and Mg in soil dust, is necessary to predict the effects of deposition on acidification of surface waters and on forest nutrition. Although surrogate surfaces can be used to measure particle fluxes they do not reproduce foliage. Surface analysis methods address many of these problems. They may be particularly useful for comparison with, and for validation of deposition models. DOE

N91-19536# Carnegie-Mellon Univ., Pittsburgh, PA. Dept. of Mechanical Engineering.
PLASMA ASSISTED NO(x) REDUCTION IN EXISTING COAL COMBUSTORS
S. C. Yao and T. Russell 13 Dec. 1990 8 p
(Contract DE-FG22-88PC-88932)
(DE91-007380; DOE/PC-88932/T3) Avail: NTIS HC/MF A02

Numerical modeling has shown that the reduction of NO by the injection of the NH2 radical is very promising. Conditions which simulate combustion gases at temperatures from 500 K to 6000 K were used to model radical injection near and in the flame. The NH2 reduction scheme functions remarkably well, even at transient local temperatures as high as 4000 K. Complete reduction of the NO to N2 and H2O is achieved nearly instantaneously (10 exp -10 s) in this ideal model. Mixing losses and radical generation must be examined to identify the actual limits of this reduction. NH2 radical production was modeled to occur via high temperature dissociation of ammonia. Production of effective radicals by the combination of the nitrogen radical with hydrogen is less effective than NH3 dissociation. Reduction of NO by the direct injection of the N radical was found to be ineffective in the oxidizing environment of the flue gas. In order to properly evaluate the potential for the NO(x) reduction system, a schematic of the system has been developed for analyzing the sources of the energy required and heat loss during the whole process. Several efficiencies (e.g., the system efficiency and the plasma gun efficiency) were defined. A FORTRAN code was developed for generalized applications, and calculations were performed for the nitrogen plasma and ammonia plasma based on appropriate assumptions. In order to explore the feasibility of using plasma injection to reduce NO(x) emissions, laboratory investigation is in progress. A small scale combustion facility has been designed and constructed. DOE

N91-19537# Colorado Univ., Boulder. Cooperative Inst. for Research in Environmental Sciences.
THERMOHALINE CIRCULATIONS AND GLOBAL CLIMATE CHANGE
H. P. Hanson 1991 6 p
(Contract DE-FG02-90ER-61019)
(DE91-007458; DOE/ER-61019/1) Avail: NTIS HC/MF A02

This report is ultimately concerned with investigating the hypothesis that changes in surface thermal and hydrological forcing of the North Atlantic, changes that might be expected to accompany CO2-induced global warming, could result in ocean-atmosphere interactions' exerting a positive feedback on the climate system. Because the North Atlantic is the source of much of the global ocean's reservoir of deep water, and because this deep water could sequester large amounts of anthropogenically produced CO2, changes in the rate of deep-water production are important to future climates. Since deep-water production is controlled, in part, by the annual cycle of the atmospheric forcing of the North Atlantic, and since this forcing depends strongly on both hydrological and thermal processes as well as the windstress, there is the potential for feedback between the relatively short-term response of the atmosphere to changing radiative forcing and the longer-term processes in the oceans. DOE

N91-19538# Brookhaven National Lab., Upton, NY.
ANALYSIS OF HIGH FREQUENCY SURFACE-INDUCED CONCENTRATION FLUCTUATIONS
Y. Alexander, F. W. Lipfert, K. Lewin, G. Hendrey, and J. Nagy Nov. 1990 7 p Presented at the 7th International Conference on Interactive Information and Processing Systems for Meteorology, Oceanography, and Hydrology, New Orleans, 13-18 Jan. 1991
(Contract DE-AC02-76CH-00016)
(DE91-007561; BNL-44894; CONF-910108-4) Avail: NTIS HC/MF A02

Brookhaven National Laboratory has developed an open-air, controlled fumigation system for investigating the effect of pollutants on plant canopies. The apparatus, the Free Air CO2 Enrichment (FACE) system, allows the average concentration of gaseous pollutants to be maintained at a preset, uniform level over a large region of the plant canopy. During 1989 and 1990 four arrays of the FACE system were in operation in cotton fields at the University of Arizona Maricopa Agricultural Center. Concentration and horizontal wind measurements were taken throughout the growing season at various locations within the regions of monitored CO2 release, and also in control areas. The majority of these measurements were sampled at 1 Hz, though in most cases only averages or 60th second data were recorded. In addition, for the purposes of detailed turbulence studies, data were taken both inside and removed from the areas of controlled fumigation at 1 and 10 Hz; these data, also at various canopy heights and at different times of the growing season, included measurements of the velocity components and to a lesser extent also CO2 concentration. DOE

N91-19539# Oak Ridge National Lab., TN.
SPATIAL AND TEMPORAL VARIATION IN BIOMONITORING DATA
A. J. Stewart and J. M. Loar 1990 44 p Presented at the SIL Monitoring Workshop: Biological Monitoring of Freshwater

Ecosystems: Interpretation and Efficiency To Assess Environmental Quality, West Lafayette, 29 Nov. - 1 Dec. 1990
(Contract DE-AC05-84OR-21400)
(DE91-007843; CONF-9011180-1) Avail: NTIS HC/MF A03

Experiences from biological monitoring programs (BMPs) at three Department of Energy facilities in Oak Ridge, TN are used to evaluate spatial and temporal variability in biomonitoring data. The facilities are sited on streams that are contaminated with radionuclides, mercury, PCBs, hydrocarbons, chlorine, and various metals. The BMPs include measurements of fish, benthic invertebrate, and periphyton communities, toxicity testing of receiving streams, and bioaccumulation studies. Permanent sites provide information about water quality changes over short and long spatial scales; ad hoc sites are used to address issues on smaller spatial scales or at short time intervals. Stream benthic macroinvertebrates seem to be among the most sensitive to poor water quality. Periphyton photosynthesis (chlorophyll-specific) integrates seasonal- and site-related changes in grazing intensity, nutrient regimes, scouring or siltation, and light. Laboratory toxicity tests are used to identify toxicant sources and quantify the degree of water quality degradation, but are most effective only when degradation is already severe. Bioaccumulation studies with fish can be very effective at identifying sources of persistent contaminants. Although spatial and temporal variation in biomonitoring data can be substantial, the degree of variation is nevertheless small enough to allow biomonitoring data to meet reasonable scientific, economic and social objectives. DOE

N91-19540# Southern Methodist Univ., Dallas, TX. Dept. of Statistical Science.
STATISTICAL EXAMINATION OF CLIMATOLOGICAL DATA RELEVANT TO GLOBAL TEMPERATURE VARIATION
H. L. Gray, R. F. Gunst, and W. A. Woodward Jan. 1991 14 p
(Contract DE-FG05-90ER-61015)
(DE91-007881; DOE/ER-61015/1) Avail: NTIS HC/MF A03

The research group at Southern Methodist Univ. began the examination of climatological data. The initial efforts have involved an extensive amount of reading of the relevant literature in order to understand the data which are available and to assess the analyses which have been performed to date. Data from CDIAC, NCAR, the Climate Research Unit at the Univ. of East Anglia, and the Geophysical Institute of the Univ. of Alaska has been acquired and began to be analyzed. The group has had meetings on a weekly basis which have enhanced the interaction among the statisticians, anthropologists and geologists on the team. The initial efforts can be categorized as assessment of the quality of climatological data and times series analysis of data related to climatological variation. The results in these areas along with projected progress within the next six months is discussed. The major accomplishment has been the accessing of the data from the sources listed, the placing of these data on the computer in a readable form, and initiation of not only analyses of these data but also of the critical evaluations of their integrity. DOE

N91-19541# Colorado State Univ., Fort Collins. Dept. of Atmospheric Science.
MONITORING THE RESPONSE OF THE UPPER TROPOSPHERE/LOWER STRATOSPHERE TO A GREENHOUSE GAS SCENARIO
J. M. Davis and S. K. Cox 18 Jan. 1991 14 p
(Contract DE-FG02-90ER-60970)
(DE91-007976; DOE/ER-60970/1) Avail: NTIS HC/MF A03

The primary scientific goal of this project is to develop a methodology which will be able to determine the nature of the link between the increased concentrations in Greenhouse Gases (GGs) and resulting trends in climate change. The method described in the original proposal consists of monitoring the atmospheric infrared emission by the primary GG, CO2, as a means of tracking the increase in its concentration and to detect the predicted temperature response of the stratosphere and troposphere associated with the increases. The data required for this type of study may be gathered with a moderately high resolution interferometer capable of accurate measurements in the appropriate spectral regions. The work accomplished to data has primarily been focused on acquisition, calibration and evaluation of the interferometer system. The funding for this project was received on May 1, 1990. The interferometer was not received until mid October 1990 due to manufacturer's delays primarily relating to the fitting of the instrument with a cryogenically cooled detector. This work is described along with intentions for future improvements and deployments of the system. The proposed analytical work for the next funding year also is described. DOE

N91-19542# Brookhaven National Lab., Upton, NY.
THE NAPAP ASSESSMENT OF DAMAGES TO MATERIALS FROM ACID DEPOSITION
F. W. Lipfert Dec. 1990 11 p Presented at the AWMA International Specialty Conference: Scientific Evaluation of the National Acid Precipitation Assessment Programs, Pittsburgh, 4-6 Dec. 1990
(Contract DE-AC02-76CH-00016)
(DE91-008086; BNL-45645; CONF-901240-1) Avail: NTIS HC/MF A03

Under the terms of PL 96-294, National Acid Precipitation Assessment Program (NAPAP) was charged with assessing the economic effects of acid deposition, including effects on materials. About $500 million has been spent over a 10-year period on the total program. The Integrated Assessment (IA) is the vehicle NAPAP has chosen to present the final findings of this program, as based on the 27 Volume State of Science/Technology (SOS/T) Series. These comments are based on the August 1990 Review Drafts and are intended to review NAPAP's approach and to suggest remedies for some of the weak spots. They are the opinions of the author and are not intended to constitute policy statements of Associated Universities, Inc., or any government agency. This materials damage assessment was prepared by NAPAP Office of Director (OD) staff with only minimal input from Task Group scientists. It is configured as responses to five generic questions, which in essence begin with, Does acidic deposition cause damage, and ending with, How much improvement might be expected if emissions were reduced. While there can be no doubt that the answer to the first question is yes when damage is defined in physical terms, the NAPAP IA does not provide a satisfactory response to the last question, at any of several possible levels. This is indeed unfortunate, since property damage is a problem directly confronted by more people than many of the other categories of acid deposition damage, especially by the residents of the states bearing most of the direct cost of emissions reductions. Specific comments are presented in this report. Also included are detailed charts. DOE

N91-19543# Syracuse Univ., NY.
MECHANISMS CONTROLLING THE PRODUCTION AND TRANSPORT OF METHANE, CARBON DIOXIDE, AND DISSOLVED SOLUTES WITHIN A LARGE BOREAL PEAT BASIN
D. I. Siegel 15 Jan. 1991 11 p
(Contract DE-FG02-90ER-61013)
(DE91-008115; DOE/ER-61013/T1) Avail: NTIS HC/MF A03

Our sponsored DOE research program is to conduct an integrated ecologic and hydrogeochemical study of the Glacial Lake Agassiz peatlands (northern Minnesota) to better understand the carbon dynamics in globally significant peat basins. Specifically, our study will provide local and regional data on (1) rates of carbon accumulation and loss and fluxes of CH4 through peat profiles, (2) the physical and botanical factors controlling the production of CH4 and CO2 in the wetland, and (3) the role hydrogeologic processes in controlling the fluxes of gases and solutes through the peat. We intend to use computer simulation models calibrated to field data to scale-up from local to regional estimates of CO2 and CH4 flux within this large peat basin. Combined, the computer simulations and field data will enable us to determine whether Glacial Lake Agassiz peat basin is currently a source, sink, or steady-state reservoir in the global carbon cycle. DOE

N91-19544# Oak Ridge National Lab., TN.
ENVIRONMENTAL SURVEILLANCE DATA REPORT FOR THE FIRST QUARTER OF 1990
P. Y. Goldberg, B. M. Horwedel, A. E. Osborne-Lee, M. R. Powell, M. M. Stevens, M. F. Tardiff, C. K. Valentine, and D. A. Wolf Feb. 1991 90 p
(Contract DE-AC05-84OR-21400)
(DE91-008552; ORNL/M-1154) Avail: NTIS HC/MF A05

The Environmental Surveillance and Protection Section (ESP) within the Office of Environmental and Health Protection (EHP) at the Oak Ridge National Laboratory (ORNL) is responsible for the development and implementation of an environmental program to (1) ensure compliance with all Federal, state, and U.S. Department of Energy (DOE) reporting requirements to quantitatively demonstrate prevention, control, and abatement of environmental pollution; (2) monitor the adequacy of containment and effluent controls; and (3) assess impacts on the environment of releases from ORNL facilities. Monthly or quarterly summaries are presented in this report for each of the media sampled. The summary tables generally give the number of samples collected during the period and the maximum, minimum, average, and standard error of the average (SE) values of parameters for which determinations were made. This value is based on multiple samples collected throughout the period. It includes the random uncertainty, over time and space, associated with sampling, analysis, and the intrinsic variability of the media. DOE

N91-19545# Alliance Technologies Corp., Chapel Hill, NC.
EVALUATION OF SIGNIFICANT ANTHROPOGENIC SOURCES OF RADIATIVELY IMPORTANT TRACE GASES Final Report, Jan. 1989 - Aug. 1990
S. D. Piccot, A. Chadha, J. DeWaters, T. Lynch, and P. Marsosudiro Nov. 1990 198 p
(Contracts EPA-68-02-4396; EPA-68-02-4274; EPA-68-09-0173)
(PB91-127753; EPA/600/8-90/079) Avail: NTIS HC/MF A09 CSCL 13B

An initial evaluation of significant anthropogenic sources of radiatively important trace gases is reported. Emissions of greenhouse gases from human activities (including fossil fuel combustion, industrial/agricultural activities, and transportation) contribute to the increasing concentrations of radiatively important trace gases (RITGs) in Earth's atmosphere. Trace gases of concern include CO2, N2O, CH4, chlorofluorocarbons, and O3. NOx and nonmethane hydrocarbons, while not themselves radiatively active, can contribute to the buildup of RITGs. The U.S. EPA has conducted several research projects characterizing emissions from specific sources of RITGs, the purpose of which was to rank sources of RITGs according to their potential impacts on radiative forcing and to develop country and source specific emission factors where data were adequate to warrant emission factor development. Country specific emission factors were developed for coal-fired utility boilers, natural gas transmission/distribution systems, municipal solid waste landfills, rice cultivation, and transportation sources. Sources for which country specific emissions data were collected, but for which emission factor development could not be supported at this time, include coal mining operations and miscellaneous/industrial sources of methane. GRA

N91-19546# Computer Sciences Corp., Research Triangle Park, NC.
ESTIMATING LIGHTNING-GENERATED NOx EMISSIONS FOR REGIONAL AIR POLLUTION MODELS
T. E. Pierce, D. H. Coventry, J. H. Novak, and A. R. VanMeter 1990 7 p Presented at the 7th Joint Conference on Applications of Air Pollution Meteorology, New Orleans, LA, 13-18 Jan. 1991 Prepared in cooperation with Research Triangle Inst., Research Triangle Park, NC Sponsored by NOAA, Silver Spring, MD
(Contract EPA-68-01-7365)
(PB91-131664; EPA/600/D-90/177) Avail: NTIS HC/MF A02 CSCL 13B

The specification of natural NOx emissions may be important for regional-scale air pollution modeling. Now that a national lightning detection network is operating, it is possible to make episodic estimates of lightning generated NOx emissions and to resolve these emissions to fine spatial and temporal scales. An approach that was used to estimate NOx emission for the Regional Oxidant Model in the northeastern United States is reported. GRA

N91-19547# Research Triangle Inst., Research Triangle Park, NC. Center for Digital Systems Research.
REGIONAL OXIDANT MODEL MULTI-PROCESSOR (ROMMP)
A. M. Roberts and J. O. Young 1990 26 p Prepared in cooperation with Computer Sciences Corp., Research Triangle Park, NC Sponsored by EPA, Research Triangle Park, NC
(PB91-131680; EPA/600/D-90/173) Avail: NTIS HC/MF A03 CSCL 13B

The EPA Regional Oxidant Model (ROM), a three dimensional model capable of describing photochemical smog on scales of 1000 km, is being used to analyze large scale pollution patterns and the effectiveness of particular emissions control strategies on reducing ozone concentration. The ROM demands considerable computation time to perform its calculations, particularly the chemical calculations. The model currently simulates at much less than one-half of real time on a VAX 11/780 (one day of model time requires over two days of simulation time). A feasibility study ws performed to support the design of a computing solution to accelerate the simulation. The study suggested the construction of a prototype parallel multiprocessor system using off-the-shelf computers, interconnected by Ethernet, as a low-risk method of increasing software performance up to 10-20x over uniprocessor speed. The prototype consists of 22 rtVAX 1000 computers as processing elements (PEs), and a VAXstation 2/GPX host computer. Current work is focused on developing a variation of the tiled ROMMP (Regional Oxidant Model Multi-Processor), in order to distribute the entire computational problem to the PEs. This approach is expected to avoid the host computational bottleneck, and achieve high levels of utilization on all the PEs in the prototype. GRA

N91-19548# National Ocean Service, Anchorage, AK. Ocean Assessments Div.
OUTER CONTINENTAL SHELF ENVIRONMENTAL ASSESSMENT PROGRAM, VOLUME 70 Final Report
Oct. 1990 626 p
(PB91-129288; OCS/MMS-90/0084) Avail: NTIS HC/MF A99 CSCL 13B

The following subject areas are covered: Western Gulf of Alaska tides and circulation; modeling the Alaskan continental shelf waters; residual tidal currents and processing of pressure and current records from the eastern Bering Sea Shelf; northeast Gulf of Alaska program; performance and compatibility analysis of oil weathering and transport-related models for use in the environmental assessment process; and transport processes in the North Aleutian Shelf. Author

N91-19549# Radian Corp., Research Triangle Park, NC.
OVERVIEW OF CLIMATE INFORMATION NEEDS FOR ECOLOGICAL EFFECTS MODELS
R. L. Peer 1990 60 p
(Contract EPA-68-02-4288)
(PB91-125898; EPA/600/3-90/089) Avail: NTIS HC/MF A04 CSCL 13B

Atmospheric scientists engaged in climate change research require a basic understanding of how ecological effects models incorporate climate. An overview is provided of existing ecological models that might be used to model climate change effects on vegetation. Some agricultural models and statistical methods are also discussed. The weather input data requirements, weather simulation methods, and other model characteristics relevant to climate change research are described for a selected number of models. The ecological models are classified as biome, ecosystem, or tree models; the ecosystem models are further subdivided into species dynamics or process models. In general, ecological modelers have had to rely on readily available meteorological data such as temperature and rainfall. Although models are becoming

more sophisticated in their treatment of weather and require more kinds of data (such as wind, solar radiation, or potential evapotranspiration), modelers are still hampered by a lack of data for many applications. Future directions of ecological effects models and the climate variables that will be required by the models are discussed. GRA

N91-19550# Rome Univ. (Italy). Dipt. di Fisica.
NO2 ABSORPTION CROSS-SECTION IN THE 440 TO 460 nm REGION AT 298 AND 220 K
Antonella Amoruso, Giorgio Fiocco, and Massimiliano Volpe 6 Nov. 1990 19 p Sponsored by Italian Space Agency and Piano Nazionale Ricerche
(Nota-Interna-964; ETN-91-98884) Avail: NTIS HC/MF A03

Absolute measurements of the NO absorption cross section in the 440 to 460 nm region at different temperatures are reported. The data cover a range of special interest for remote sensing applications. In order to improve tha accuracy in the determination of the partial pressure of NO2, simultaneous measurements of the concentration of N2O4 were carried out. For this purpose the measurements were carried out both in the 440 to 460 nm wavelength region and at the 334.1 nm Hg emission line. Values of the NO2 and N2O4 cross sections taken from literature were used to obtain the best estimation of the NO partial pressure. Within experimental errors the overall shape of the spectrum does not show a dependence on temperature, but there is a slight increase of a few maxima and a decrease of the other maxima and of the minima when the temperature is lowered. ESA

46 GEOPHYSICS

Includes aeronomy; upper and lower atmosphere studies; ionospheric and magnetospheric physics; and geomagnetism.

For space radiation see *93 Space Radiation.*

N91-19551# Lawrence Livermore National Lab., CA.
CLOUD FORCING: A MODELING PERSPECTIVE
Gerald L. Potter, Robert L. Mobely, Robert S. Drach, Thomas G. Corsetti, Dean N. Williams, Julia M. Slingo, and Jean-Jacques Morcrette (European Centre for Medium-Range Weather Forecasts, Reading, England) Nov. 1990 34 p Presented at the European Centre for Medium-Range Weather Forecasts (ECMWF) Workshop on Clouds, Radiative Transfer and the Hydrological Cycle, Reading, England, 12-15 Nov. 1990
(Contract W-7405-eng-48)
(DE91-007215; UCRL-JC-105536; CONF-9011179-1) Avail: NTIS HC/MF A03

Radiation fields from a perpetual July integration of a T106 version of the ECMWF operational model are used as surrogate observations of the radiation budget at the top of the atmosphere to illustrate various difficulties that modellers might face when trying to reconcile cloud radiation forcings derived from satellite observations with model-generated ones. Differences between the so-called Methods 1 and 2 of Cess and Potter (1987) and a variant Method 3 are addressed. Method 1 is shown to be the least robust of all methods, due to potential uncertainties related to persistent cloudiness, length of the period over which clear-sky conditions are looked for, biases in retrieved clear-sky quantities due to an insufficient sampling of the diurnal cycle. We advocate the use of Method 2 as the only unambiguous one to produce consistent radiative diagnostics for intercomparing model results. Impact of the three methods on the derived sensitivities and cloud feedbacks following an imposed change in sea surface temperature (used as a surrogate climate change) is discussed. DOE

N91-19552# Los Alamos National Lab., NM.
ASSOCIATION OF AN AURORAL SURGE WITH PLASMA SHEET RECOVERY AND THE RETREAT OF THE SUBSTORM NEUTRAL LINE
E. W. Hones, R. Elphinstone, J. S. Murphree, A. B. Galvin, and N. C. Heinemann (Boston Coll., Chestnut Hill, MA.) 1990 24 p Presented at the Chapman Conference on Magnetospheric Substorms, Hakone, Japan, 3-7 Sep. 1990
(Contract W-7405-eng-36)
(DE91-007351; LA-UR-91-16; CONF-9009109-1) Avail: NTIS HC/MF A03

One of the periods being studied is the interval 0000-1200 UT on May 3, 1986, designated Event 9C. A well-defined substorm, starting at 0919 UT, was imaged by both the Dynamics Explorer 1 (DE 1) 1 over the Southern Hemisphere and Viking over the Northern Hemisphere. The images from Viking, at 80-second time resolution, showed a surge-like feature forming at about 0952 UT at the poleward edge of the late evening sector of the oval. The feature remained relatively stationary until about 1000 UT when it seemed to start advancing westward. ISEE 1 and 2 were closely conjugate to the surge as mapped from both the Defense Meteorological Satellite Program (DMSP) and Viking images. We conclude that the plasma sheet recovery was occasioned by the arrival at ISEE 1,2 of a westward traveling wave of plasma sheet thickening, the wave itself being formed by westward progression of the substorm neutral line's tailward retreat. The westward traveling surge was the auroral manifestation of this nonuniform retreat of the neutral line. We suggest that the upward field aligned current measured by DMSP F7 above the surge head was driven by plasma velocity shear in the plasma sheet at the duskward kink in the retreating neutral line. By analogy with this observation we propose that the westward traveling surges and the current wedge field aligned currents that characterize the expanding auroral bulge during substorm expansive phase are manifestations of (and are driven by) velocity shear in the plasma sheet near the ends of the extending substorm neutral line. DOE

N91-19553# Lawrence Livermore National Lab., CA.
THE RELATIONSHIP BETWEEN AEROSOL AND DROP SIZE DISTRIBUTIONS IN THE MARINE ATMOSPHERE
C. Chuang and J. E. Penner Dec. 1990 16 p Presented at the American Geophysical Union Fall Meeting, San Francisco, CA, 3-7 Dec. 1990
(Contract W-7405-eng-48)
(DE91-006514; UCRL-JC-105008; CONF-901259-2) Avail: NTIS HC/MF A03

The characteristics of droplet size distributions near cloud base are initially determined by the aerosol particles that act as cloud condensation nuclei (CCN). Through physical and chemical processes that determine the fraction of aerosol particles that act as CCN, these particles profoundly affect the microphysical structure of clouds and their tendency to form precipitation. This paper provides a parametric study of the condensational growth on aerosol distributions from typical measurements in the marine atmosphere, and answers the following questions with respect to this process. (1) How does the condensationally produced droplet spectrum vary with the initial aerosol size distribution, aerosol number loading, and the updraft velocity. (2) What is the fraction of aerosol particles that act as CCN. This information can be applied to the future study to parameterize the number concentration of cloud droplets in climate models. (3) How do the optical properties of the cloud change as a result of the production of different droplet size distributions. DOE

N91-19554# State Univ. of New York, Stony Brook.
STUDIES OF ATMOSPHERIC MOLECULES BY MULTIPHOTON SPECTROSCOPY
P. M. Johnson Dec. 1990 8 p
(Contract DE-FG02-86ER-13590)
(DE91-006738; DOE/ER-13590/9) Avail: NTIS HC/MF A02

Resonance ionization processes can play an important role in understanding molecules important in combustion processes. They are a reflection of the dynamic as well as the static properties of atomic and molecular species. Due to the sequential or quasisequential nature of photon absorption in resonant multiphoton events, the lifetimes of the intermediate states play an essential role in the overall cross-sections if they are short enough to be competitive with subsequent photon interactions. In molecules, this is particularly important because there are many

dissociative and other radiationless pathways which can contribute to a competitive channel. Under those conditions it should be possible to obtain information about the nature of the dynamics of the intermediate state from the multiphoton ionization process. This will involve looking at not only the ionization cross-section but also other observables such as the kinetic energy of the ejected electrons and possibly the distribution of fragment ions produced in the ionization event. Whether the ionization amplitude is affected or not, the time scales of the dynamic events which alter the ionization path can vary over a large range from the femtoseconds of dissociation to the microseconds of some radiationless transitions in large molecules. When the competing channel has a time scale shorter than the laser pulse length, the kinetics of the ionization are intimately tied into the precise nature of the laser pulse. For time scales longer than the laser pulse, pump-probe ionization schemes in which one laser prepares a state while another does the ionization provide a particularly simple method for investigating the dynamics of the intermediate state. Here the author discusses examples from each of these regimes. CO2 and pyrazine are examined. DOE

N91-19555# Maryland Univ., College Park. Dept. of Meteorology.
ICRCCM (INTERCOMPARISON OF RADIATION CODES USED IN CLIMATE MODELS). PHASE 2: VERIFICATION AND CALIBRATION OF RADIATION CODES IN CLIMATE MODELS
R. G. Ellingson, W. J. Wiscombe, D. Murcray, W. Smith, and R. Strauch 1990 11 p
(Contract DE-FG05-90ER-60971)
(DE91-007323; DOE/ER-60971/1-Phase-2) Avail: NTIS HC/MF A03

Following the finding by the InterComparison of Radiation Codes used in Climate Models (ICRCCM) of large differences among fluxes predicted by sophisticated radiation models that could not be sorted out because of the lack of a set of accurate atmospheric spectral radiation data measured simultaneously with the important radiative properties of the atmosphere, our team of scientists proposed to remedy the situation by carrying out a comprehensive program of measurement and analysis called SPECTRE (Spectral Radiance Experiment). SPECTRE will establish an absolute standard against which to compare models, and will aim to remove the 'hidden variables' (unknown humidities, aerosols, etc.) which radiation modelers have invoked to excuse disagreements with observation. The data to be collected during SPECTRE will form the test bed for the second phase of ICRCCM, namely verification and calibration of radiation codes used to climate models. This should lead to more accurate radiation models for use in parameterizing climate models, which in turn play a key role in the prediction of trace-gas greenhouse effects. Overall, the project is proceeding much as had been anticipated in the original proposal. The most significant accomplishments to date include the completion of the analysis of the original ICRCCM calculations, the completion of the initial sensitivity analysis of the radiation calculations for the effects of uncertainties in the measurement of water vapor and temperature and the acquisition and testing of the inexpensive spectrometers for use in the field experiment. The sensitivity analysis and the spectrometer tests given us much more confidence that the field experiment will yield the quality of data necessary to make significant tests of and improvements to radiative transfer models used in climate studies. DOE

N91-19556# Morgantown Technology Center, WV.
AN EVALUATION OF CO-PLANAR LINEAMENT ANALYSIS AND SOME THOUGHTS ON USING SURFACE GEOLOGICAL DATA TO PREDICT SUB-SURFACE GEOLOGY
A. C. Smith Jun. 1990 48 p
(DE90-009687; DOE/METC-90/4102) Avail: NTIS HC/MF A03

A computerized method of detecting lineaments on the Earth's surface from digital topographic data was evaluated for its usefulness in exploration and development of natural gas from tight sandstones. The method, known as co-planar lineament analysis, was applied to the topography of the Douglas Creek Arch of northwestern Colorado, where significant amounts of natural gas have been produced from the Upper Cretaceous Mancos B sandstone. The locations of the co-planar lineaments detected correspond poorly with the locations of linear trends on contour maps of cumulative production and initial production. Because co-planar lineaments are reflections of surface features that are mostly the results of surface geology, it is not too surprising to see a lack of correlation with natural gas production, which depends upon aspects of sub-surface geology. The conclusion of this study is not that co-planar lineament analysis will never work in the search for tight gas. Rather it is that its application to natural gas exploration and development will not work everywhere. Areas where the technique would be best employed would probably be those where the reservoir is relatively shallow, the surface rocks and reservoir rocks are similar in age and lithology, and where the subsurface geology is relatively simple with no unconformities, thrust faults, or plastic layers such as salt or soft shale between the surface and gas reservoir. In addition, it must be demonstrated that straight stream segments within a given area are indeed caused by joints in the surface rocks and not some other geological phenomenon such as the strike of an easily eroded bed. DOE

N91-19557*# National Aeronautics and Space Administration. Goddard Space Flight Center, Greenbelt, MD.
ON THE JOINT INVERSION OF GEOPHYSICAL DATA FOR MODELS OF THE COUPLED CORE-MANTLE SYSTEM
Coerte V. Voorhies Washington Mar. 1991 28 p
(NASA-TM-104536; Rept-91B00072; NAS 1.15:104536) Avail: NTIS HC/MF A03 CSCL 08G

Joint inversion of magnetic, earth rotation, geoid, and seismic data for a unified model of the coupled core-mantle system is proposed and shown to be possible. A sample objective function is offered and simplified by targeting results from independent inversions and summary travel time residuals instead of original observations. These data are parameterized in terms of a very simple, closed model of the topographically coupled core-mantle system. Minimization of the simplified objective function leads to a nonlinear inverse problem; an iterative method for solution is presented. Parameterization and method are emphasized; numerical results are not presented. Author

N91-19558# Lawrence Livermore National Lab., CA.
LECTURE NOTES ON NONLINEAR INVERSION AND TOMOGRAPHY
W. L. Rodi, comp. (Massachusetts Inst. of Tech., Cambridge.) and J. G. Berryman Nov. 1990 80 p
(Contract W-7405-eng-48)
(DE91-008238; UCRL-LR-105358) Avail: NTIS HC/MF A05

The main topic of these lectures is seismic traveltime tomography in 2-D and 3-D heterogeneous media. The main problem is to infer the (isotropic) P-wave slowness (reciprocal velocity) distribution of a medium, given a set of observed first-arrival traveltimes between sources and receivers of known location within the medium. This problem is typical of borehole-to-borehole seismic tomography in oil field applications. The problem is considered of inverting for wave slowness when the absolute traveltimes are not known, as is expected to be the case in earthquake seismology. DOE

N91-19559# Moscow State Univ. (USSR). Nauchno-Issledovatel'skij Inst. Yadernoj Fiziki.
BAROELECTRIC EFFECT IN THE PRESENT OF GRAVITATIONAL FORCES
A. V. Kalev 1989 10 p In RUSSIAN; ENGLISH summary
(DE91-615469; NIIYaF-MGU-89-23/100) Avail: NTIS HC/MF A02

Based on the microscopic Thomas-Fermi model electrostatic fields in the substance, generated by gravitation effects are investigated. Evaluations according to the Thomas-Fermi method allow one to conclude that baroelectric effect should cause high electrostatic fields in internal presurface planet layers. In particular, for the Earth such a field makes up the order of 10(exp 9) V/cm near the surface. DOE

N91-19560# Coordinating Research Council, Inc., Atlanta, GA.
AEROSOL FORMATION IN ATMOSPHERIC MIXTURES
S. C. Wang, S. E. Paulson, D. Grosjean, R. C. Flagan, and J. H. Sein 1 Aug. 1990 208 p Sponsored by California Inst. of Technology, Pasadena
(PB91-129114) Avail: NTIS HC/MF A10 CSCL 04A

The goal of the study is to obtain an understanding of the mechanisms of formation of organic aerosols in the atmosphere. Specifically, the research program consists of two components: outdoor smog chamber studies of the photooxidation of hydrocarbon/NOx mixtures for key selected alkenes, alkanes, cycloalkanes, and aromatics to assess their aerosol-forming capability and particularly to define the aerosol-forming threshold of atmospheric organics; and outdoor smog chamber studies of the above systems in the presence of SO2 or NH3 to investigate the coupled dynamics of the organic/sulfate/nitrate system that characterizes the atmosphere. Chemical pathways to the formation of ozone and other reactive species were studied extensively for smaller hydrocarbons; long chain (five or more carbons) aliphatic hydrocarbons, both straight chained and cyclic have gone largely unstudied. GRA

47 METEOROLOGY AND CLIMATOLOGY

Includes weather forecasting and modification.

N91-19561# Central Research Inst. of Electric Power Industry, Tokyo (Japan). Energy and Environment Lab.
PROGRESSIVE FEATURE OF STEPPED LEADER ON JAPAN SEA COAST IN WINTER (BASIC DATA TO ESTABLISH SHIELDING THEORY FOR LIGHTNING)
A. Asakawa, K. Miyake, Y. Aihara, T. Shindo, and S. Kanao (Hokuriku Electric Power Co., Japan) Apr. 1990 30 p In JAPANESE; ENGLISH summary
(DE91-742133; CRIE-T-89048) Avail: NTIS HC/MF A03

The developing manner of a stepped leader for a lightning stroke in winter was observed using Automatic Lightning Discharge Progressing Feature Observation System (ALPS) which analyze lightning discharge with time passed, and is described. The lightning stroke in winter was observed during fiscal 1986 to 1988 at microwave relaying towers in Nakanoto substation, The Hokuriku Electric Power Co., Inc. The results are as follows: The progressive velocity of leader streamer in an individual step is 3.01 x 10(exp 6) m/sec for downward leaders, and its value is more than twice as much as upward leaders. The mean progressive velocity of total leader process is given as (0.8 to 1.5) x 10(exp 5) m/sec for upward leaders and 0.8 x 10(exp 5) m/sec for downward leaders. Its values are a little slower than the results measured by the other systems. It is revealed by the picture taken by a high speed streaking camera and the lightning-stroke-current waveform that the increase and decrease of the luminous strength of stepped leader coincides with that of the lightning-stroke-current, and charge density along a leader length is estimated as 1.2 x 10(exp -3) qoulomb/m. DOE

N91-19562# National Oceanic and Atmospheric Administration, Boulder, CO. Wave Propagation Lab.
RADAR-MEASURED HEIGHT PROFILES OF Cn(2) AND TURBULENCE DISSIPATION RATE COMPARED WITH RADIOSONDE DATA DURING OCTOBER 1989 AT DENVER
E. E. Gossard, D. C. Welsh, and R. G. Strauch Aug. 1990 120 p Prepared in cooperation with Colorado Univ., Boulder
(PB91-125500; NOAA-TR-ERL-442-WPL-63) Avail: NTIS HC/MF A06 CSCL 04B

Profiles of radar reflectivity and Doppler spectral width, for the month of October 1989, were recorded with the Stapleton 32 cm wavelength wind profiler. The data were analyzed for hourly intervals centered on radiosonde release times, and each hour was divided into two half-hourly subperiods so that four half-hourly periods of radar data were typically analyzed for each day. The resulting profiles of the turbulence structure parameter for radar refractive index (C sup 2, sub n) extracted from backscattered power and of turbulence dissipation rate (actually C sup 2, sub w) extracted from Doppler spectral width are presented with the temperature, dew point, and refractive index profiles measured by radiosonde and plotted to the same height scale. The presence of elevated temperature inversions and humidity gradients is examined and compared with radar profile measured quantities. A case when clouds were present is considered in some detail, because clouds are a very important source of potential false alarms in any method using radar reflectivity data to extract refractive index or humidity profiles. The experimental precautions needed to achieve the desired accuracy are discussed. GRA

N91-19563# World Meteorological Organization, Geneva (Switzerland).
WORLD WEATHER WATCH: REGIONAL ASSOCIATION 4: HURRICANE OPERATIONAL PLAN, SUPPLEMENT 2
Sep. 1990 30 p
(WMO-524-Suppl-2; ETN-91-98911) NTIS MF A01; hard copy available from World Meteorological Organization Case Postale no. 5, CH-1211 Geneva 20, Switzerland

The purpose of this plan is to enhance the cooperative efforts of members within WMO (World Meteorological Organization) region 4 in the carrying out of their roles of preparing for and issuing forecasts and warnings of all tropical cyclones affecting the area. Responsibilities of members are defined. Tropical cyclone releases issued by the Regional/Specialized Meteorological Center (RSMC) with activity specialization in tropical cyclone analysis, tracking and forecasting, in Miami (RSMC Miami: Hurricane Center) are explained and examples provided. Observational platforms, including land based radar, satellites and aircraft reconnaisance are discussed. Where differences exist between the U.S. National Hurricane Operational Plan (NHOP) and this plan, aircraft radar and upper air observations made by the U.S. Department of Defense will comply with U.S. NHOP. Communication procedures are outlined with special emphasis on headings required to assure proper computer processing and distribution of messages. The lists of hurricane names for the Caribbean Sea, Gulf of Mexico, the North Atlantic Ocean and the eastern North Pacific are included. ESA

N91-20027*# Auburn Univ., AL. Dept. of Aerospace Engineering.
ROCKET-TRIGGERED LIGHTNING STRIKES AND FOREST FIRE IGNITION
James Fenner *In* NASA, John F. Kennedy Space Center, Research Reports: 1990 NASA/ASEE Summer Faculty Fellowship Program Sep. 1990 p 142-168 (For primary document see N91-20022 11-99)
(Grant NGT-60002)
Avail: NTIS HC/MF A23 CSCL 04B

48 OCEANOGRAPHY

Includes biological, dynamic, and physical oceanography; and marine resources.

For related information see also *43 Earth Resources and Remote Sensing.*

N91-19564# Scripps Institution of Oceanography, La Jolla, CA. Inst. of Geophysics and Planetary Physics.
VERY LOW FREQUENCY SEISMO-ACOUSTIC SCATTERING FROM A ROUGH SEAFLOOR
John A. Orcutt 5 Oct. 1990 4 p
(Contract N00014-89-J-1017)
(AD-A227947) Avail: NTIS HC/MF A01 CSCL 20/1

The long range scientific objective is to understand and exploit the interaction between seismic or acoustic waves and the underlying oceanic crusts and sediments. The problem is being studied by using body and interface waves, as well as, seismic and acoustic 'noise' while rigorously considering the effects of an elasticity and vertical and lateral variations in both compressional and shear velocities in the earth. The boundary integral (BI) method

and the asymptotically related Kirchoff-Helmholtz technique are used to model the response of an seafloor and heterogeneous subbottom to incident acoustic energy. The finite difference methods, although less efficient to the BI, can address models of arbitary complexity including elastic heterogenicity and/or attenuation in the subbottom. Ways to inprove the speed and accuracy of the different methods were studied, so that they will be practical for 3D problems. Theoretical results are compared with seafloor scattering data collected during seismic reflection experiments on the East Pacific Rise. Author

N91-19565# Old Dominion Univ., Norfolk, VA.
WAVELETS AND TURBULENCE ON THE SEA SURFACE Final Report
G. T. Csanady 1990 3 p
(Contract N00014-88-K-0101)
(AD-A229862) Avail: NTIS HC/MF A01 CSCL 08/3

This contract's goals were to understand the physical processes determining the small scale structure of the sea surface, identify the roughness elements acting on the air side, explore the character and dynamics of short breaking wavelets on the water side, and quantify their role in the transfer of momentum, heat and mass across the air-sea interface. Analytical model studies were carried out on the dynamics of short, breaking wavelets, their momentum balance, interaction with the wind-induced shear flow at the surface, and the action of shear stress concentrations (spikes) on the upwind face of such wavelets. The conceptual model of the breaking wavelets developed in these studies (roller riding an irrotational wave) was applied to the important problem of air-sea gas transfer, and was shown to account for otherwise puzzling observations of gas transfer. A graduate research assistant supported by this contract applied a matrix inversion technique to explore the hydrodynamic instability of the coupled air-water shear flow at the sea surface. This method allowed the exploration of various physical effects on wavelet generation, and supported the construction of a new conceptual model for the small scale structure of the sea surface. GRA

51 LIFE SCIENCES (GENERAL)

N91-19566*# National Aeronautics and Space Administration. Ames Research Center, Moffett Field, CA.
CENTRIFUGE FACILITY CONCEPTUAL SYSTEM STUDY. VOLUME 1: FACILITY OVERVIEW AND HABITATS
Robert Synnestvedt, ed. Oct. 1990 352 p
(NASA-TM-102860; A-90268-Vol-1; NAS 1.15:102860) Avail: NTIS HC/MF A16 CSCL 06C

The results are presented for a NASA Phase 1 study conducted from mid 1987 through mid 1989 at Ames Research Center. The Centrifuge Facility is the major element of the biological research facility for the implementation of NASA's Life Science Research Program on Space Station Freedom using non-human specimens (such as small primates, rodents, plants, insects, cell tissues). Five systems are described which comprise the Facility: habitats, holding units, centrifuge, glovebox, and service unit. Volume 1 presents a facility overview and describes the habitats - modular units which house living specimens. Author

N91-19567# Joint Publications Research Service, Arlington, VA.
JPRS REPORT: SCIENCE AND TECHNOLOGY. USSR: LIFE SCIENCES
4 Jan. 1991 44 p Transl. into ENGLISH from various Russian articles
(JPRS-ULS-91-001) Avail: NTIS HC/MF A03

Abstracts of Soviet literature in various areas of the life sciences are compiled. The following major subject areas are covered: biochemistry, biotechnology, pharmacology/toxicology, and physiology. There are also a few abstracts presented in the areas of aerospace medicine and radiation effects on rats, mice, and plants. For individual titles, see N91-19568 through N91-19571.

N91-19568# Joint Publications Research Service, Arlington, VA.
REACTIVITY OF EXHAUSTED HUMAN SKELETAL MUSCLE FIBERS FOLLOWING PROLONGED ANTIORTHOSTATIC HYPOKINESIA Abstract Only **c52**
S. L. Kuznetsov and V. V. Stepantsov *In its* JPRS Report: Science and Technology. USSR: Life Sciences 4 Jan. 1991 p 1 Transl. into ENGLISH from Arkhiv Anatomii, Gistologiii i Embriologii (Leningrad, USSR), v. 97, no. 7, Jul. 1989 p 53-59 (For primary document see N91-19567 11-51)
Avail: NTIS HC/MF A03

Ultrastructural and histochemical studies were conducted on skeletal muscle biopsies obtained from eight men subjected to antiorthostatic hypokinesia for 360 days, with and without exercise while in the orthostatic position. The data demonstrated that after 120 days at a 6 degree antiorthostatic incline, there was extensive damage to the contractile and energetic element of the skeletal muscle fibers. Disorganization and destruction was seen to begin with the M-line and then to encompass the entire space between adjacent Z-lines. The Z-lines were unaffected, with the number of affected sarcomeres increasing with time. After 360 days, atrophic changes were particularly severe in the case of type I fibers. Metabolic deterioration was evident in diminished total protein and glycogen levels. Various forms of physical training in the antiorthostatic position were found to diminish the extent and progression of atrophy. The beneficial effects of physical exercise were directly proportional to the intensity of exercise and an early start of the exercise program. The relative stability of the cytoskeleton in the face of myosin and actin breakdown may explain the potential of the myofibrils for recovery. Author

N91-19569# Joint Publications Research Service, Arlington, VA.
GRAVITATION RECEPTOR REACTION IN RESPONSE TO EFFECT OF ACCELERATION Abstract Only **c52**
A. T. Pakunov *In its* JPRS Report: Science and Technology. USSR: Life Sciences 4 Jan. 1991 p 26 Transl. into ENGLISH from Zhurnal Ushnykh, Nosovykh i Gorlovykh Bolezney (Kiev, USSR), no. 2, Mar. - Apr. 1990 p 8-13 (For primary document see N91-19567 11-51)
Avail: NTIS HC/MF A03

A further study of gravitation receptor reaction involved reproduction of gravitational overloading with the use of a centrifuge with radius of rotation of 100 cm and 95 revolutions per minute. The force of centrifugal acceleration was 10.05 g and the duration of effect was 5 minutes. Experiments on 6 guinea pigs and 4 rabbits exposed to this acceleration showed a pronounced increase in gravitation reaction. All experimental animals remained motionless for the first 5 minutes after the end of the effect acceleration. Experiments on 6 guinea pigs and 4 rabbits exposed to this acceleration showed a pronounced increase in gravitation reaction. All experimental animals remained motionless for the first 5 minutes after the end of the effect of acceleration. Marked disturbance of coordination of movement was noted for at least 1 hour. Electron microscopic study of the gravity receptor (utriculus) revealed rather pronounced disturbances in many structures: bulging of some of the pillar cells cytoplasm into the endolymphatic space, surrounding of cynocilia by cytoplasmic matrix, cytoplasm vacuolization, decrease of cell nuclei electron density and pronounced dilation and clarification of calicous nerve terminals. The presence around the cynocilia of a matrix resembling cytoplasm from the pillar cells prevents intense excitation of the receptors. It is possible that, after a 10-minute overload, the advantage of bulging of some of the cytoplasm from the pillar cells involves limitation of mobility of the cynociliae surrouded by the cytoplasmic matrix. Author

N91-19570# Joint Publications Research Service, Arlington, VA.
EFFECTS OF HYPERBARIC OXYGENATION ON CENTRAL HEMODYNAMICS AND OXYGEN CONSUMPTION IN SEVERE PHYSICAL TRAUMA Abstract Only **c52**
A. G. Magomedov *In its* JPRS Report: Science and Technology. USSR: Life Sciences 4 Jan. 1991 p 26 Transl. into ENGLISH from Patologicheskaya Fiziologiya i Eksperimentalnaya Terapiya

(Moscow, USSR), no. 2, Mar. - Apr. 1990 p 26-28 (For primary document see N91-19567 11-51)
Avail: NTIS HC/MF A03

Therapeutic trials were conducted with hyperbaric oxygenation on outbred 12-18 kg dogs subjected to a gunshot wound with skeletal damage. The animals were divided into groups on the basis of treatment and subjected to central hemodynamic and ventilatory monitoring in conjunction with assessment of clinical chemistries. In general, severe trauma complicated by 20-25 percent hypovolemia led to 100 percent mortality of untreated dogs within 1 hr 25 min to 3 hr of the onset of shock. Animals managed in the conventional manner presented with a 29.4 percent survival rate. Finally, animals managed with hyperbaric oxygenation (1-2 atm pressure for 50 min; 4-5 sessions, for 3 days) in combination with conventional medical and surgical management had a survival rate of 76.2 percent. Hyperbaric oxygenation-managed dogs showed a rise in circulating blood volumes, cardiac index and VO2, facilitating correction of all forms of oxygen deficiency. Author

N91-19571# Joint Publications Research Service, Arlington, VA.
EFFECTS OF HIGH TEMPERATURE AND HUMIDITY ON MENTAL STATE AND METABOLISM Abstract Only **c52**
A. S. Shanazarov, V. P. Makhnovskiy, and E. I. Kuzyuta *In its* JPRS Report: Science and Technology. USSR: Life Sciences 4 Jan. 1991 p 27-28 Transl. into ENGLISH from Fiziologiya Cheloveka (Moscow, USSR), v. 15, no. 4, Jul. - Aug. 1989 p 92-96 (For primary document see N91-19567 11-51)
Avail: NTIS HC/MF A03

The effects of a combination of high temperature and humidity on mental state and metabolism were studied in a group of 20 men, 18-20 years old. The studies were conducted in a chamber adjusted to 50 C and a relative humidity of 80 percent, with an average maximum exposure of 20.2 minutes. Neuropsychologic testing revealed that as a result of such exposure, indicators of logical thinking decreased by 54.6-64 percent, and attentiveness indicators, by an average of 32.1 percent. Concomitantly, metabolic studies demonstrated activation of sympathetic mechanisms: urinary epinephrine rose by 68.9 percent and norepinephrine by 151.4 percent. Other data indicated activation of lipid peroxidation by 55.1 percent and elevation of unconjugated bilirubin in the blood by 54.8 percent. These observations demonstrated that a combination of high temperature and humidity exerts an adverse effect on mental faculties. The latter may be related to elevation of unconjugated bilirubin in the blood which transgresses the blood-brain barrier and may lead to uncoupling of oxidative phosphorylation in brain mitochondria. Author

N91-19572# European Space Agency, Paris (France).
FOURTH EUROPEAN SYMPOSIUM ON LIFE SCIENCES RESEARCH IN SPACE
Valerie David, ed. Nov. 1990 599 p In ENGLISH and FRENCH Symposium held in Trieste, Italy, 28 May - 1 Jun. 1990
(ESA-SP-307; ISBN-92-9092-070-X; ETN-91-98803) Copyright Avail: NTIS HC/MF A25; EPD, ESTEC, Noordwijk, Netherlands, HC 80 Dutch guilders

One hundred and twenty-four papers presented at the fourth European Symposium on life sciences and research in space are included in this document. The following subjects are covered: human physiology and space medicine; the biological and medical program of the manned Aragatz mission on the MIR space station; cell and developmental biology; animal physiology; biotechnology and life support systems; plant biology; and the biological effects of radiation. A chairman's report introduces each of these topics. For individual titles, see N91-19573 through N91-19696.

N91-19573# Karolinska Inst., Stockholm (Sweden). Environmental Physiology Lab.
EFFECTS OF SHORT-LASTING WEIGHTLESSNESS ON GAS EXCHANGE DURING LIGHT EXERCISE **c52**
Dad Linnarsson, Pietro E. diPrampero, Juergen P. Stegemann, Carl J. Sundberg, Uwe Hoffmann, and Dieter Essfeld (Deutsche Sporthochschule, Cologne, Germany, F.R.) *In* ESA, Fourth European Symposium on Life Sciences Research in Space Nov. 1990 p 9-11 Sponsored by Swedish Space Board; CNR; BMFT; and ESA (For primary document see N91-19572 11-51)
Copyright Avail: NTIS HC/MF A25; EPD, ESTEC, Noordwijk, Netherlands, HC 80 Dutch guilders

Gas exchange during exercise was studied during short lasting microgravity in parabolic flight. Oxygen uptake at the mouth showed wide fluctuations, with an increase during the 20 to 25 sec period of microgravity and a depression compared to control during the high G phase following immediately after the micro G period. Estimates of the pulmonary and peripheral time courses of oxygen exchanges suggest that peripheral oxygen cost of light exercise does not differ from that of normal G and that the observed oxygen uptake changes at the mouth are caused by G induced changes in the oxygen stores and the blood flow in the lungs.
ESA

N91-19574# Vrije Univ., Brussels (Belgium). Inst. of Interdisciplinary Research.
LUNG VOLUMES, CHEST WALL CONFIGURATION, AND PATTERN OF BREATHING IN MICROGRAVITY **c52**
Manuel Paiva, M. Estenne, and L. A. Engel (Westmead Hospital, Sydney, Australia) *In* ESA, Fourth European Symposium on Life Sciences Research in Space Nov. 1990 p 13-15 (For primary document see N91-19572 11-51)
Copyright Avail: NTIS HC/MF A25; EPD, ESTEC, Noordwijk, Netherlands, HC 80 Dutch guilders

Changes in lung volume and chest wall configuration in five seated subjects was measured during the 5th ESA campaign of parabolic flights. The main results are summarized and an overview of the articles published in the open literature are presented. A consistent relationship between end expiratory lung volume measured by flow integration, the volumetric displacements of the two chest wall compartments (Vsum) and Gz was found in seated subjects, both volumes increasing with increase in Gz and decreasing during periods of microgravity. The volume changes were almost entirely the result of a change in the abdominal compartment. The abdominal contribution to the tidal volume increased substantially under conditions of microgravity and decreased slightly when gravitional forces nearly doubled. Despite the changes in Vsum and configuration, the temporal pattern of breathing appeared to be uninfluenced by the changes in gravity.
ESA

N91-19575# Amsterdam Univ. (Netherlands). Dept. of Physiology.
BLOOD PRESSURE REGULATION IN PARABOLIC FLIGHT **c52**
John M. Karemaker, J. J. Settels (Organization for Health Research, TNO, Amsterdam, Netherlands), H. J. P. Kuykens, and K. H. Wesseling *In* ESA, Fourth European Symposium on Life Sciences Research in Space Nov. 1990 p 17-18 (For primary document see N91-19572 11-51)
(Grant SRON-MG020-1988)
Copyright Avail: NTIS HC/MF A25; EPD, ESTEC, Noordwijk, Netherlands, HC 80 Dutch guilders

The cardiovascular effects of sudden microgravity lasting 25 seconds in parabolic flight in eight test subjects, at rest, sitting upright during three parabolas was measured. The continuous, non invasive finger blood pressure measurements by Finapres (TM) was used. By means of hydrostatic height compensation blood pressure was referred to heart level. Both the responses to the pull up and pull out phase of the aircraft trajectory and to the period of actual microgravity seem to be dominated by the altered hydrostatic conditions at the baroreceptors. In the pull up, blood pressure and heart rate increases were followed, when the phase of microgravity was entered, by a rapid decrease of heart rate, decreasing blood pressure and increased stroke volume. By the end of the microgravity this had changed to a situation where heart rate and cardiac output had returned to control levels, but blood pressure was still decreased. The general outline of the

response is comparable to what is observed when a person is passively tilted from upright to supine. ESA

N91-19576# Institute of Biomedical Problems, Moscow (USSR).
MEDICAL RESULTS OF THE FOURTH PRIME EXPEDITION ON THE ORBITAL STATION MIR **c52**
A. I. Grigoriev, V. V. Poliakov, V. V. Bogomolov, A. D. Egorov, I. D. Pestov, and I. B. Kozlovskaya *In* ESA, Fourth European Symposium on Life Sciences Research in Space Nov. 1990 p 19-22 (For primary document see N91-19572 11-51)
Copyright Avail: NTIS HC/MF A25; EPD, ESTEC, Noordwijk, Netherlands, HC 80 Dutch guilders

The medical objectives of the fourth prime expedition on the orbital station MIR were to monitor the cabin environmental parameters, to control prophylactic measures, and to implement the program of medical investigations. Participation of a trained physician helped to increase the reliability of medical support and to enlarge the scope of medical experiments in flight. The health condition and work capacity of the cosmonauts at different flight stages and after recovery remained satisfactory. Functional changes were adequate to the exposure and reflected both the general pattern of adaptative changes and the specific features of individual crew members. ESA

N91-19577# Hopital Bretonneau, Tours (France). Inst. National de la Sante et de la Recherche Medicale.
ULTRASOUND INVESTIGATION OF THE CARDIOVASCULAR SYSTEM DURING THE 25 DAYS FRENCH-SOVIET SPACEFLIGHT (26 NOVEMBER - 21 DECEMBER 1988) **c52**
Philippe Arbeille, O. Atkov, V. V. Bystrov, J. L. Chretien, Galina Fomina, V. Gratchov, N. Kokova, F. Patat, V. V. Poliakov (Institute of Biomedical Problems, Moscow, USSR), and J. M. Pottier et al *In* ESA, Fourth European Symposium on Life Sciences Research in Space Nov. 1990 p 23-26 Sponsored by CNES (For primary document see N91-19572 11-51)
Copyright Avail: NTIS HC/MF A25; EPD, ESTEC, Noordwijk, Netherlands, HC 80 Dutch guilders

The main hemodynamic parameters of the left heart function and of the peripheral arterial system (cerebral, renal, femoral arteries) were measured six times during the flight (flight day 4, 5, 15, 18, 20, 24) and 5 times post flight (day + 1 +3 +7 +15 +30). The venous return was also explored at the level of the jugular, femoral, and hepatic veins. Most of the hemodynamic changes: the reduction of the cardiac chambers volume, the increase of the heart rate and the acceleration of the venous return, are in favor of a hypovolemia which triggers a decrease of the vascular resistance in the main vascular areas such as the brain or the kidney. The experiment showed that the venous system is strongly disturbed and does not recover during the flight. The results confirm that the vascular disadaptation develops promptly in absence of countermeasure and suggest that the ultrasound methods will be of great interest for the follow up of the vascular deconditioning and the evaluation of the efficiency of the countermeasures already used during long term flights. ESA

N91-19578# Institute of Biomedical Problems, Moscow (USSR).
ULTRASOUND INVESTIGATION OF THE CARDIOVASCULAR SYSTEM DURING THE 25-DAYS SOVIET-FRENCH FLIGHT: CARDIAC ASPECTS **c52**
Galina Fomina, N. Kokova, V. V. Bystrov, V. V. Poliakov, L. Strogonova, V. Gratchev, O. Atkov, J. M. Pottier, Philippe Arbeille, and F. Patat (Hopital Bretonneau, Tours, France) et al *In* ESA, Fourth European Symposium on Life Sciences Research in Space Nov. 1990 p 27-29 (For primary document see N91-19572 11-51)
Copyright Avail: NTIS HC/MF A25; EPD, ESTEC, Noordwijk, Netherlands, HC 80 Dutch guilders

Cardiovascular changes induced by weightlessness were assessed by ultrasound echography and doppler using the As de coeur device. During the flight the left atrium and ventricle volumes were decreased. Despite the reduction of the stroke volume, the cardiac output was slightly elevated due to an increase in heat rate. The cardiac contractility was not affected at any moment. The pulmonary pressure index does not show any significant change. The systemic vascular resistance was decreased. Most of the hemodynamic changes were believed to be due to a hypovolemia. ESA

N91-19579# Amsterdam Univ. (Netherlands).
VESTIBULAR FUNCTION IN ALTERED STATES OF GRAVITY **c52**
Wilhelmus J. Oosterveld, H. A. A. deJong, and Hendrika W. Kortschot *In* ESA, Fourth European Symposium on Life Sciences Research in Space Nov. 1990 p 31-36 (For primary document see N91-19572 11-51)
Copyright Avail: NTIS HC/MF A25; EPD, ESTEC, Noordwijk, Netherlands, HC 80 Dutch guilders

During parabolic flight the caloric test was conducted in human subjects. The horizontal nystagmus disappears in microgravity, after an exponential slow phase velocity decay, that shows a specific time constant. A vertical nystagmus is seen. Both the horizontal and the vertical component are gravity dependent. The vertical component is not directly related to the choice of temperature as well as to the side of the chosen ear. Frequently a reverse directed horizontal nystagmus, a secondary nystagmus, appears in caloric tests, conducted in parabolic flight. The results support Barany's convection theory. It is also clear that the origin of the caloric nystagmus cannot only be explained by Barany's theory. ESA

N91-19580# Mainz Univ. (Germany, F.R.). Dept. of Physiology.
OCULAR ROLL UNDER CHANGING z-AXIS ACCELERATION AND NECK POSITION **c52**
Joachim Wetzig, K. Hofstetter, M. Reiser, and R. vonBaumgarten *In* ESA, Fourth European Symposium on Life Sciences Research in Space Nov. 1990 p 37-42 (For primary document see N91-19572 11-51)
(Grant BMFT-01-QV-223-9)
Copyright Avail: NTIS HC/MF A25; EPD, ESTEC, Noordwijk, Netherlands, HC 80 Dutch guilders

Ocular Counter Rolling (OCR) was measured in four unmedicated subjects under conditions of parabolic flight. A medium size aircraft (Caravelle) performed 30 single parabolae a day, of 20 to 25 seconds duration, spaced two to four minutes apart. This resulted in alternating phases of normal, hyper, hypo and again hyper gravity. Subjects sat yoga fashion upright facing towards the aircraft cockpit. During each pullup, low G phase, and pullout of the parabolae, the left eye was briefly illuminated to record the eyeball rotary position. OCR was enhanced by increase in gravitoinertial force. It decreased, when near weightlessness set in. Upon resumption of hypergravity a complete return to preweightlessness values was observed in two of four subjects, while the other two subjects were incomplete in recovery. Pure neck receptor stimulation did not yield a consistent major OCR reaction. ESA

N91-19581# Provence Univ., Marseille (France). Lab. de Neurobiologie Humaine.
BODY PROPRIOCEPTIVE REFERENCES IN WEIGHTLESSNESS AS STUDIED BY MUSCLE TENDON VIBRATION **c52**
J. P. Roll, K. E. Popov, Victor S. Gurfinkel, M. I. Lipschits, Claudie Andre-Deshays (Centre National de la Recherche Scientifique, Paris, France), J. C. Gilhodes, and Cynthia Quoniam *In* ESA, Fourth European Symposium on Life Sciences Research in Space Nov. 1990 p 43-48 (For primary document see N91-19572 11-51)
(Grants CNES-500193; CNES-500243)
Copyright Avail: NTIS HC/MF A25; EPD, ESTEC, Noordwijk, Netherlands, HC 80 Dutch guilders

The hypothesis that the modifications of both biomechanical and psychological conditions occurring under microgravity involve considerable reorganization of body perception and postural control was investigated. The proprioceptive information originating in various muscles is known to contribute, together with visual, vestibular and sole cutaneous information to postural regulation. The proprioceptive channel was specifically activated by muscle

vibration which is able to elicit both illusory movement sensations and postural responses. Data show that the major functional reorganization of the proprioceptive information processing occurs in microgravity, affecting both perceptual and motor aspects of behavior. It is possible that these proprioceptive adaptations may be partly attributable to the new whole body propulsive foot functions imposed by long term exposure to weightlessness and to the adaptation of motor behavior to the third dimension of space. The results might therefore not so much reflect a major change in the spindle proprioceptive receptor function but rather indicate a more central sensorimotor rearrangement organized by the central nervous system. ESA

N91-19582# Nuevas Tecnologias Espaciales S.A., Llissa d'Amunt (Spain).

DESIGN, IMPLEMENTATION AND EVALUATION OF NEW FULLY AUTOMATED ALGORITHMS FOR THE EXTRACTION OF CARDIAC PARAMETERS FROM 3D, 2D AND M-MODE ECHOCARDIOGRAMS **c54**

Rene Alquezar and X. Lobao *In* ESA, Fourth European Symposium on Life Sciences Research in Space Nov. 1990 p 51-57 (For primary document see N91-19572 11-51)
(Contract ESA-7320/87/NL/PP)
Copyright Avail: NTIS HC/MF A25; EPD, ESTEC, Noordwijk, Netherlands, HC 80 Dutch guilders

A new fully automated algorithm that extracts Left Ventricular (LV) epicardial and endocardial borders on echocardiographic short axis view was developed, and a version for determining the LV endocardium on apical views is derived. Two methods for the accurate measurement of LV volume from a set of apical rotated planes are reviewed: cylindrical and disk integration. New fully automated algorithms for mistral and aortic valve M-mode image analysis were developed to extract cardiac times and valve dynamics. All the algorithms were implemented in a simple architecture based on two transputers; requirements for a real time implementation were extrapolated from it. In vitro and in vivo tests were performed to evaluate the volume calculation procedure and the image analysis algorithms respectively. Telescience application of these tools for crew monitoring in long term missions is under study. ESA

N91-19583# Udine Univ. (Italy). Inst. of Biology.

PEDALLING IN SPACE TO SIMULATE GRAVITY: THE TWIN-BIKE SYSTEM **c52**

Giulioandrea Antonutto, Carlo Capelli, and Pietro E. diPrampero *In* ESA, Fourth European Symposium on Life Sciences Research in Space Nov. 1990 p 59-62 (For primary document see N91-19572 11-51)
Copyright Avail: NTIS HC/MF A25; EPD, ESTEC, Noordwijk, Netherlands, HC 80 Dutch guilders

Microgravity leads to progressive musculoskeletal decay. This results in a significant decrease of the exercise capacity and in orthostatic intolerance, this last manifesting itself upon the return to Earth. Thus, without appropriate countermeasures, long term manned space flights may be seriously jeopardized. A simple mechanical system that may partially obviate the above problems is proposed. The system consists of two mechanically coupled bicycles riding along the inner wall of a cylindrical space module. The bikes' motion induces a force which stimulates gravity on the exercising subjects. The biomechanical and bioenergetical aspects of such a system are discussed. It is concluded that by appropriately selecting the radial dimensions of this last in order to minimize vestibular disturbances, head to feet acceleration gradients and manufacturing costs, it may be possible to combine exercise and simulated gravity, with no need for additional external power. ESA

N91-19584# Technische Univ., Vienna (Austria). Dept. of Sports and Exercise Physiology.

ISOKINETIC FORCE VELOCITY AND ELECTROMYOGRAPHIC CHARACTERISTIC OF KNEE AND ELBOW EXTENSOR AND FLEXOR MUSCLES IN THE 0-g ENVIRONMENT **c52**

Norbert Bachl, R. Baron, Massud Mossaheb, W. Bumba, and R. Albrecht (European Space Agency. European Space Research and Technology Center, ESTEC, Noordwijk, Netherlands) *In* ESA, Fourth European Symposium on Life Sciences Research in Space Nov. 1990 p 63-68 (For primary document see N91-19572 11-51)
Copyright Avail: NTIS HC/MF A25; EPD, ESTEC, Noordwijk, Netherlands, HC 80 Dutch guilders

Electromyographic and force velocity response of knee and elbow extensor and flexor muscles during isokinetic concentric and eccentric work between 1g and 0g environment are compared. A special ergometric dynamometric device which will be flown on the Russian Space Station MIR in the framework of the Austrian Russian space program was constructed. This constant velocity ergometer makes it possible to perform exercise of either the arm or leg muscles while making translatoric movements within a definable angular range, both parallel and diagonal in the sagittal plane. Both acyclic and cyclic concentric and eccentric movements are possible with following characteristics to be adjusted: joint angle, angular velocity, contraction frequency and contraction/decontraction ratio per cycle. Force velocity relationship is measured in real time mode using a strain gauge system with angle positioner. In addition an electromyogram is recorded, integrated and analyzed in relation to the force velocity characteristics. Starting with ground based ergometric and dynamometric tests hard and software development for data acquisition and analysis is described. Some data from ground based experiments are demonstrated to show the differenciated behavior in activation and force velocity characteristics of the working muscles. ESA

N91-19585# Deutsche Forschungsanstalt fuer Luft- und Raumfahrt, Cologne (Germany, F.R.). Inst. for Aerospace Medicine.

MEDEX: A USEFUL TOOL FOR COUNTERACTING ORTHOSTATIC INTOLERANCE RESULTING FROM BODY FLUID LOSS UNDER MICROGRAVITY **c52**

Friedhelm Baisch and Wolfgang Bangert (Panares, Munich, Germany, F.R.) *In* ESA, Fourth European Symposium on Life Sciences Research in Space Nov. 1990 p 69-71 (For primary document see N91-19572 11-51)
Copyright Avail: NTIS HC/MF A25; EPD, ESTEC, Noordwijk, Netherlands, HC 80 Dutch guilders

Dehydration with decreased blood volume due to a microgravity environment is believed to play a decisive role in the etiology of orthostatic intolerance. Increase of body fluid content before landing, especially in the intravascular space, may counteract the symptoms. Long term effects of both a cumulative Lower Body Negative Pressure (LBNP) load and an intravenous infusion of saline during dehydration caused by Head Down Tilted (HDT) bedrest is studied. Intravenous infusion of isotonic saline causes a transient increase in central blood volume and cardiac filling but the long term effect observed during an HDT study is an opposite one with a loss of body fluids. The long term effect of a stressful LBNP stands in contrast to the long term effect of intravenous saline infusion. The cause for the changes in body water content is most likely a change in the relative distribution of plasma protein between the intravascular and interstitial compartments. Different time constants of the mechanisms that regulate water and electrolyte on the one side and lymph formation and flow on the other side lead to the long term effects of these interventions. ESA

N91-19586# Deutsche Sporthochschule, Cologne (Germany, F.R.). Physiologisches Inst.

TIME COURSES OF ENDURANCE PERFORMANCE PARAMETERS FOLLOWING 500 ml BLOOD WITHDRAWAL **c52**

Klaus Baum, Uwe Hoffmann, Dieter Essfeld, and Juergen P. Stegemann *In* ESA, Fourth European Symposium on Life Sciences Research in Space Nov. 1990 p 73-76 (For primary document see N91-19572 11-51)
(Grant BMFT-01-QV-87354)

Copyright Avail: NTIS HC/MF A25; EPD, ESTEC, Noordwijk, Netherlands, HC 80 Dutch guilders

Before and after a 500 ml reduction in blood volume 14 healthy subjects (7 male, 7 female, 20 to 30 years) took part in a series of bicycle ergometer tests in upright body position. Tests were performed 1 week before, 2 hours after volume reduction (no fluid or food intake prior to this test), and 1, 2, 4, 6 and 8 weeks later. Each test consisted of 17 min randomized switchings between 20 W and 80 W for the determination of oxygen uptake kinetics (Pseudo Random Binary Sequence (PRBS) technique) and subsequent step increases (50 W, 4 min per stage) for the determination of maximum oxygen uptake, the heart rate oxygen uptake relationship and blood lactate concentrations. Maximum oxygen uptake was significantly reduced immediately after blood withdrawal, while oxygen uptake kinetics were essentially identical in all tests. ESA

N91-19587# Karolinska Inst., Stockholm (Sweden). Environmental Physiology Lab.

OXYGEN UPTAKE DURING CONCENTRIC AND ECCENTRIC RESISTIVE EXERCISE USING A NEW GRAVITY-INDEPENDENT ERGOMETER **c52**

Hans E. Berg and Per A. Tesch *In* ESA, Fourth European Symposium on Life Sciences Research in Space Nov. 1990 p 77 (For primary document see N91-19572 11-51)

Copyright Avail: NTIS HC/MF A25; EPD, ESTEC, Noordwijk, Netherlands, HC 80 Dutch guilders

An ergometer for strength training of postural muscle groups in microgravity was evaluated. The gravity independent non electrical device examined is designed for heavy resistive exercise of the lower limbs. Oxygen uptake ranged 1.1 to 2.1 l/minutes during exercise, while forces exerted ranged 1365 to 1600 Newtons. Oxygen cost and muscular loading were of the same magnitude as previously reported for heavy resistance exercise using conventional exercise equipment. It is concluded that concentric eccentric heavy resistance training using large postural muscle groups can be performed at a low oxygen cost using the gravity independent ergonometer examined. ESA

N91-19588# Innsbruck Univ. (Austria). Klinik fuer Neurologie.

COORDINATION OF EYE, HEAD AND ARM MOVEMENTS IN WEIGHTLESSNESS **c52**

Meinhard Berger, F. Gerstenbrand, Miklos Marosi, E. Karamat, Armin Muigg, T. Melichar, R. Schauer, I. B. Kozlovskaya, A. Sokolov, and M. Belaeva (Institute of Biomedical Problems, Moscow, USSR) *In* ESA, Fourth European Symposium on Life Sciences Research in Space Nov. 1990 p 79-81 (For primary document see N91-19572 11-51)

Copyright Avail: NTIS HC/MF A25; EPD, ESTEC, Noordwijk, Netherlands, HC 80 Dutch guilders

The experiment MONIMIR will be part of the investigation program of the Austrian Sovjet spaceflight AUSTROMIR in November 1991. In this experiment the coordination and adaptation of the eye, head and arm movement in microgravity will be investigated. The following tests will take place: preprogrammed movements on acoustic and visual targets; tracking movements on visual targets; memory movements; influence of neck reflexes on arm movements; biomechanics of the cervical spine; T-reflex (patellar reflex). The methods and equipment to be used are briefly described. ESA

N91-19589# European Space Agency. European Space Research and Technology Center, ESTEC, Noordwijk (Netherlands).

LIFE SCIENCES IN ESA TRP ACTIVITY **c52**

Nora Bougharouat, J. Kingdon, Peter Schiller, and Francois Brechignac *In its* Fourth European Symposium on Life Sciences Research in Space Nov. 1990 p 83-87 (For primary document see N91-19572 11-51)

Copyright Avail: NTIS HC/MF A25; EPD, ESTEC, Noordwijk, Netherlands, HC 80 Dutch guilders

ESA is supporting a Technological Research Program (TRP) in order to investigate and prepare technologies for future space missions requirements. This TRP program covers nine majors themes. Theme 5 represents microgravity utilization, itself concerned with development in support of six main areas. The poster is concentrating on the three areas representing life sciences activities: space medicine, space biology and applied space biology. Their previous developments, present developments and future developments are briefly presented. ESA

N91-19590# Trondheim Univ. (Norway). Dept. of Biomedical Engineering.

VASCULAR GAS BUBBLES OR DECOMPRESSION SICKNESS: WHAT IS THE PROPER ENDPOINT FOR EVALUATING DECOMPRESSION PROCEDURES **c52**

Alf O. Brubakk *In* ESA, Fourth European Symposium on Life Sciences Research in Space Nov. 1990 p 89-92 (For primary document see N91-19572 11-51)

Copyright Avail: NTIS HC/MF A25; EPD, ESTEC, Noordwijk, Netherlands, HC 80 Dutch guilders

Decompression leads to gas bubble formation in the cardiovascular system to a certain degree in all individuals. The degree of gas bubble formation as well as decompression sickness is not only dependent upon the degree of supersaturation, but on many physiological factors. Changes can occur in several organs, most notably in the central nervous system in the absence of clinical signs of decompression sickness. It is argued that the degree of vascular bubble formation should be used to evaluate decompression procedures. This gas bubble monitoring will lead to reduced health hazards and an increased understanding of the decompression process. ESA

N91-19591# Freie Univ., Berlin (Germany, F.R.). Dept. of Otorhinolaryngology.

MEASUREMENT OF EYE MOVEMENTS IN SPACE-RELATED RESEARCH ENVIRONMENTS **c52**

Andrew H. Clarke, Winfried Teiwes, and H. Scherer *In* ESA, Fourth European Symposium on Life Sciences Research in Space Nov. 1990 p 93-94 (For primary document see N91-19572 11-51)

(Grant BMFT-01-QV-8802)

Copyright Avail: NTIS HC/MF A25; EPD, ESTEC, Noordwijk, Netherlands, HC 80 Dutch guilders

A primary function of the vestibular system is the stabilization of the visual image during head movements; this is facilitated by the elicitation of compensatory eye movements via the Vestibulo Ocular Reflex (VOR). In consequence, evaluation of reflex eye movements has become essential for both the scientific study and clinical diagnosis of the vestibular system. In space oriented research, eye movement evaluation thus enables the investigation of those changes in the vestibular system concomitant with alterations in the gravitoinertial environment. Videooculography represents a flexible, noninvasive instrument for measurement of eye movements in all three orthogonal planes. In particular, the technique should enable comprehensive study of ocular torsion as an indicator of otolith function. The technique is outlined and initial results from a parabolic flight study designed to investigate those components of eye movement elicited by the otolith ocular response are presented. ESA

N91-19592# Technische Univ., Munich (Germany, F.R.). Medizinische Klinik.

PHYSIOLOGY OF BODY WATER AND SALT REGULATION. PART 1: CIRCADIAN RHYTHMS OF ENDOCRINE SYSTEMS AND URINARY ELECTROLYTE EXCRETION IN HUMANS **c52**

Christian Drummer, M. Heer, B. Molz, Matthias Schlossberger, Carsten Stadeager, Lothar Roecker, Peter Norsk, Felice Strollo, Friedhelm Baisch, and Jorgen Warberg (Danish Aerospace Medical Center of Research, Copenhagen.) et al *In* ESA, Fourth European Symposium on Life Sciences Research in Space Nov. 1990 p 95-98 Sponsored by BMFT, and ESA (For primary document see N91-19572 11-51)

Copyright Avail: NTIS HC/MF A25; EPD, ESTEC, Noordwijk, Netherlands, HC 80 Dutch guilders

In a ground based study, the circadian rhythms in urinary

excretion of water and electrolytes and the circadian variations in plasma levels of hormones which participate in body fluid homeostasis, were investigated. Six healthy volunteers spent 9 days in a recumbent body position under strictly controlled conditions. The urinary excretion of water and electrolytes as well as plasma levels of vasopressin, aldosterone, renin, cortisol, epinephrine and cyclic GMP showed striking circadian rhythms. No circadian variability was observed for plasma levels of norepinephrine and atrial natriuretic peptide. ESA

N91-19593# Technische Univ., Munich (Germany, F.R.). Medizinische Klinik.
PHYSIOLOGY OF BODY WATER AND SALT REGULATION. PART 2: VOLUME AND ELECTROLYTE HOMEOSTASIS AFTER AN ACUTE SALINE INFUSION **c52**
Christian Drummer, M. Heer, B. Molz, Matthias Schlossberger, Carsten Stadeager, Lothar Roecker, Peter Norsk, Felice Strollo, Jergen Warberg, and Niels Juel Christensen (Danish Aerospace Medical Center of Research, Copenhagen.) et al *In* ESA, Fourth European Symposium on Life Sciences Research in Space Nov. 1990 p 99-102 Sponsored by BMFT, and ESA (For primary document see N91-19572 11-51)
Copyright Avail: NTIS HC/MF A25; EPD, ESTEC, Noordwijk, Netherlands, HC 80 Dutch guilders

Six healthy male volunteers were investigated under strictly controlled conditions to determine the renal and hormonal responses to an acute isotonic saline infusion. During a nine day study in recumbent body position, the volunteers received an infusion of about two liters within 25 minutes. For comparison, a control experiment without infusion was conducted. The urinary excretion of water, sodium, potassium and chloride increased for about two days following the infusion. Water and sodium balance was not achieved until 40 hours post infusion. The renin aldosterone system and plasma catecholamine concentrations were in parallel reduced for about two days. Only small alterations were observed in plasma vasopressin, cortisol and atrial natriuretic peptide levels. ESA

N91-19594# Deutsche Sporthochschule, Cologne (Germany, F.R.). Physiologisches Inst.
INFLUENCE OF VARIOUS PARAMETERS ON THE V'O2 FREQUENCY RESPONSE OF THE BODY. A THEORETICAL STUDY ON THE BASIS OF A NONLINEAR MODEL **c52**
Dieter Essfeld and Uwe Hoffmann *In* ESA, Fourth European Symposium on Life Sciences Research in Space Nov. 1990 p 103-106 Submitted for publication (For primary document see N91-19572 11-51)
(Grant BMFT-01-QV-87354)
Copyright Avail: NTIS HC/MF A25; EPD, ESTEC, Noordwijk, Netherlands, HC 80 Dutch guilders

During aerobic exercise oxygen uptake kinetics at the pulmonary capillary site is influenced, among others, by: magnitude and kinetics of exercise induced changes in cardiac output and muscle oxygen uptake, basal cardiac output and oxygen uptake, magnitude and distribution of the venous volume. A nonlinear computer model is used to study the influence of these parameters on the oxygen uptake frequency response. The results indicate that the contribution of nonlinear responses is negligible for input periods longer than about 1 min. Variations of the muscle oxygen uptake kinetics showed the greatest effect on gain and phase of the oxygen uptake output signal. ESA

N91-19595# Graz Univ. (Austria). Physiologisches Inst.
IS PHYSIOLOGICAL TREMOR (MICROVIBRATION) INFLUENCED BY MICROGRAVITY **c52**
Eugen Gallasch, N. Burlatschkowa, I. Beljajeva (Institute of Biomedical Problems, Moscow, USSR), M. Moser, and I. Kenner *In* ESA, Fourth European Symposium on Life Sciences Research in Space Nov. 1990 p 107-110 (For primary document see N91-19572 11-51)
Copyright Avail: NTIS HC/MF A25; EPD, ESTEC, Noordwijk, Netherlands, HC 80 Dutch guilders

Many studies have been done to analyze the mechanism of tremors, however there are still many controversies. The use of microgravity conditions may open a wide experimental field in which many questions about the origin of tremors can be reinvestigated. In a joint space flight USSR-Austria (Project AUSTROMIR) a program to take tremor recordings at rest and during different tasks from one cosmonaut by means of two accelerometers is prepared. From these measurements new insight into the complex sensori motor interactions of the musculoskeletal control system during adaptation is expected. ESA

N91-19596# Centre National de la Recherche Scientifique, Tours (France). Lab. de Bio-Informatique.
SIMULATION EXPERT SYSTEM FOR PHYSIOLOGICAL MECHANISMS OF THE SPACE MOTION SICKNESS **c52**
Claude Gaudeau, L. Gouthiere, C. LeToullec, E. Lawton (Societe de Bio-Informatique et Bio-Technologie, Tours, France), and G. Chauvet *In* ESA, Fourth European Symposium on Life Sciences Research in Space Nov. 1990 p 111-116 (For primary document see N91-19572 11-51)
Copyright Avail: NTIS HC/MF A25; EPD, ESTEC, Noordwijk, Netherlands, HC 80 Dutch guilders

Expert systems are elaborated in numerous scientific sectors in the medical field (diagnostics, antibiotic therapy). They enable a better use of knowledge by introducing a new structure of biological information. The conception of an expert system adapted to the knowledge and the modelization of motion sickness should be a powerful and helpful tool adaptable to different uses: modelization and simulation of motion sickness; early detection of motion sickness by using monitoring of electro-splanchnography; biofeedback training before flight and during flight; preventative and therapeuty modality of electro stimulation. Nausea is a serious problem for man trying to adapt himself to life in space. The physiological mechanisms of nausea are still very much discussed. It would be useful to view these mechanisms not purely as a specific answer to the general adaptation of life in space. The stressful factor of zero gravity and its consequences bring about a need to be able to adapt quickly to a new situation. Expert systems for modelization of motion sickness mechanisms try to describe effects of motion sickness and the functioning of nervous centers by the knowledge and the determination of their transfer functions. ESA

N91-19597# Innsbruck Univ. (Austria). Klinik fuer Neurology.
NEUROLOGICAL FINDINGS AFTER 72 HOURS WATER IMMERSION **c52**
F. Gerstenbrand, I. B. Kozlovskaya, Meinhard Berger, Miklos Marosi, N. Burlacskova, A. Sokolov, R. Schauer, and J. Rainer *In* ESA, Fourth European Symposium on Life Sciences Research in Space Nov. 1990 p 117-119 Prepared in cooperation with Inst. of Biomedical Problems, Moscow, USSR (For primary document see N91-19572 11-51)
Copyright Avail: NTIS HC/MF A25; EPD, ESTEC, Noordwijk, Netherlands, HC 80 Dutch guilders

Neurological changes caused by water immersion simulated microgravity were investigated in four male volunteers. All the investigations were performed in the space laboratories for ground based experiments of the Institute for Biomedical Problems, Moscow (USSR). Neurological investigations were carried out before as well as 24, 48 and 72 hours after they were placed in the horizontal water immersion basin. Cerebellar dysfunction, signs of deteriorating function of the peripheral nervous system as well as of the posterior tract and frontal lobe symptoms were observed. Besides those disturbances, compensated cerebral microsymptoms occurred more pronounced in 2 of the 4 volunteers. ESA

N91-19598# Eidgenoessische Technische Hochschule, Zurich (Switzerland). Space Biology Group.
EFFECT OF RUNNING AND HEAD DOWN TILT BEDREST ON LYMPHOCYTE REACTIVITY **c52**
Felix K. Gmuender, Friedheim Baisch, B. Bechler, Augusto Cogoli, Marianne Cogoli, P. W. Joller, H. Maass, J. Mueller, and W. Ziegler (Universitaetsspital, Zurich, Switzerland) *In* ESA, Fourth European Symposium on Life Sciences Research in Space Nov. 1990

p 121-124 Sponsored in cooperation with the Swiss Federal Inst. of Tech. (For primary document see N91-19572 11-51)
(Grant SNSF-3-382-0-86)
Copyright Avail: NTIS HC/MF A25; EPD, ESTEC, Noordwijk, Netherlands, HC 80 Dutch guilders

The mitogenic response of lymphocytes was found to be remarkably reduced during and after spaceflight. To test the hypothesis that these observed changes were induced by stress (including psychological and physical stress, or by body fluid redistribution) lymphocyte activation was measured by concanavalin A after running (42 and 21 km) and in a Head Down Tilt (HDT) bedrest study (10 days). Lymphocyte responsiveness was significantly reduced immediately after both runs. The lymphocyte numbers remained constant. Lymphocyte responsiveness was severely reduced prior to, during, and the day after the HDT, even though the lymphocyte numbers did not change. These results are compared with data obtained during and after spaceflight. It is concluded that the stress of HDT induces changes in immunological responsiveness that are strikingly similar to those arising from the stress of spaceflight. ESA

N91-19599# Milan Univ. (Italy). Cattedra di Semeiotica Medica.
SIMULATED ABSENCE OF GRAVITY IMPAIRS ARTERIAL BARORECEPTOR CONTROL OF HEART RATE IN MAN **c52**
G. Grassi, Antonella Ravogli, G. Parati, P. Coruzzi, A. Novarini, and G. Mancia *In* ESA, Fourth European Symposium on Life Sciences Research in Space Nov. 1990 p 125-127 (For primary document see N91-19572 11-51)
Copyright Avail: NTIS HC/MF A25; EPD, ESTEC, Noordwijk, Netherlands, HC 80 Dutch guilders

The bradycardic effects of carotid baroreceptor stimulation (neck chamber technique) of 7 subjects in control condition and during headout water immersion that increased central blood volume, thus simulating absence of gravity, was studied. Water immersion caused a significant arterial blood pressure and heart rate reduction and increased central venous pressure. During immersion baroreceptor stimulation caused less bradycardia (-19.3 + or -1 b/minutes) in comparison to that obtained in control condition (-30.5 + or -3.0 b/minutes). Thus the baroreflex is impaired under conditions characterized by a central blood volume increase. This phenomenon may be responsible for the alterations in the homeostatic control of circulation often reported during space flights. ESA

N91-19600# Graz Univ. (Austria). Working Group for Volume Regulation and Space Medicine.
A NEW PRINCIPLE FOR DYNAMIC FLUID SHIFT INVESTIGATIONS IN ASTRONAUTS **c52**
H. Hinghofer-Szalkay, Eva Maria Koenig, J. Schmied, and H. Heimel (Labor fuer Messtechnik dr. Hans Stabinger, Graz, Austria) *In* ESA, Fourth European Symposium on Life Sciences Research in Space Nov. 1990 p 129-132 Sponsored by Austrian Ministry for Sciences, and Oesterreichische Akademie der Wissenschaften (For primary document see N91-19572 11-51)
Copyright Avail: NTIS HC/MF A25; EPD, ESTEC, Noordwijk, Netherlands, HC 80 Dutch guilders

A spaceflight experiment which deals with transvascular fluid shifts in astronauts is proposed. The rationale is to compute the amount and the protein content of fluid filtered into interstitial spaces by application of Lower Body Negative Pressure (LBNP) by measuring sound velocity in venous blood and plasma samples drawn from the subject before and during LBNP induced hemoconcentration. Preflight control, and postflight measurements employing an identical protocol should answer the question as to how the permeability within the astronaut leg microvessels is altered by adaptation to spaceflight, and to readaptation to 1 g conditions. A hand held, battery powered equipment which has been newly developed allows for dead space free measurements on blood and plasma samples under ground as well as under micro g conditions. ESA

N91-19601# Deutsche Sporthochschule, Cologne (Germany, F.R.). Physiologisches Inst.
INTRA-INDIVIDUAL VARIABILITY V'O2 FREQUENCY RESPONSES IN PHYSICALLY ACTIVE SUBJECTS **c52**
Uwe Hoffmann, Klaus Baum, Dieter Essfeld, and Juergen P. Stegemann *In* ESA, Fourth European Symposium on Life Sciences Research in Space Nov. 1990 p 133-135 (For primary document see N91-19572 11-51)
(Grant BMFT-01-QV-87354)
Copyright Avail: NTIS HC/MF A25; EPD, ESTEC, Noordwijk, Netherlands, HC 80 Dutch guilders

The reproducibility of individual oxygen consumption frequency responses was studied in 4 highly trained athletes (triathletes) and a group of 4 not specifically endurance trained sports students. Each subject took part in 4 tests at the same daytime, separated by 2 to 5 days. The subjects maintained their everyday physical activities but were requested to avoid extreme physical efforts (competitions) for two days prior to the tests. The results revealed that standard deviations of static and dynamic gains were of the same order. No influence of endurance capacity or forcing frequency could be detected. ESA

N91-19602# Danish Aerospace Medical Center of Research, Copenhagen.
FLUID SHIFTS AND REGULATION OF PLASMA VOLUME IN HUMANS DURING 12 HOURS OF HEAD-OUT WATER IMMERSION **c52**
Lars Bo Johansen, Peter Norsk, Niels Foldager, Carsten Stadeager, Manabu Kamegai, and Flemming Bonde-Petersen *In* ESA, Fourth European Symposium on Life Sciences Research in Space Nov. 1990 p 137-139 Sponsored by Danish Space Board (For primary document see N91-19572 11-51)
Copyright Avail: NTIS HC/MF A25; EPD, ESTEC, Noordwijk, Netherlands, HC 80 Dutch guilders

Seven normal males underwent 12 hours of Water Immersion (WI) and a control group of 9 males rested for 12 hours seated in the empty tank. Plasma Volume (PV), as measured with Evans Blue (EB) and the derived Blood Volume (BV), increased initially during WI and then gradually declined to pre immersion levels at 12 hours. PV, as derived from concomitant changes in Hematocrit (Hct) and Hemoglobin (Hb), increased less compared with the EB measurements and then gradually decreased below pre immersion level at 12 hours. Urinary flow rate and sodium excretion rate increased 3 to 4 fold initially and thereafter gradually declined during WI. It is concluded that BV is increased initially during WI, and then reduced to pre immersion level at 12 hours. Changes in Hct and Hb seem to be inaccurate indicators of PV changes during WI. ESA

N91-19603*# Vanderbilt Univ., Nashville, TN. Dept. of Mechanical Engineering.
SKELETAL ADAPTATION IN ALTERED GRAVITY ENVIRONMENTS **c52**
Tony S. Keller and Alvin M. Strauss *In* ESA, Fourth European Symposium on Life Sciences Research in Space Nov. 1990 p 141-147 Sponsored by NASA (For primary document see N91-19572 11-51)
Copyright Avail: NTIS HC/MF A25; EPD, ESTEC, Noordwijk, Netherlands, HC 80 Dutch guilders

It is generally agreed that the single factor that most limits human survivability in non Earth environments is the phenomenon of bone demineralization and the medical problems induced by the subsequent imbalance in the calcium metabolism. Alterations of skeletal properties occur as a result of disturbances in the normal mechanical loading environment of bone. These alterations or adaptations obey physical laws, but the precise mathematical relationship remains to be determined. Principles governing unloading and overloading of bone are gaining more attention as a consequence of the planning of manned space stations, Moon and Mars bases and spaceflights of long duration. A mathematical framework which allows for the prediction of skeletal adaptation on Earth and in non Earth gravity environments by power law relationships is presented. ESA

N91-19604# Freie Univ., Berlin (Germany, F.R.). Dept. of Physiology.
VERTEBRAL COLUMN LENGTH CHANGES DURING SIMULATED MICROGRAVITY **c52**
K. A. Kirsch, Filippo Castrucci (Rome Univ., Italy), H.-C. Gunga, and Y. Reinach *In* ESA, Fourth European Symposium on Life Sciences Research in Space Nov. 1990 p 149-151 Sponsored in part by ESA (For primary document see N91-19572 11-51)
(Grant BMFT-01-QV-87/2)
Copyright Avail: NTIS HC/MF A25; EPD, ESTEC, Noordwijk, Netherlands, HC 80 Dutch guilders

The human body in space elongates about 5 cm. A reduction in the gravity dependent curvatures of the Vertebral Column (VC) may be the cause. Thus, VC response to simulated microgravity i.e., bed rest and immersion, employing standard anthropometry (N=5) and photogrammetry (N=1) for 2 hours was monitored. The VC elongated during microgravity simulation with nonlinear fluctuating patterns. Growth was greatest in immersion (2.5 cm) and closer to space observation than bed rest in the same conditions, probably due to reduced sympathetic activity in immersion. It is concluded that VC lengthening seems to be microgravity dependent. It may also affect some perivertebral structures, contributing to early flight physiological changes. ESA

N91-19605# Max-Planck-Inst. fuer Verhaltensphysiologie, Seewiesen uber Starnberg (Germany, F.R.).
DETERMINANTS OF SPATIAL ORIENTATION IN WEIGHTLESSNESS **c52**
Horst Mittelstaedt and Stefan Glasauer *In* ESA, Fourth European Symposium on Life Sciences Research in Space Nov. 1990 p 153-155 (For primary document see N91-19572 11-51)
Copyright Avail: NTIS HC/MF A25; EPD, ESTEC, Noordwijk, Netherlands, HC 80 Dutch guilders

The perception of body position with respect to the vertical and the perception of the vertical in the visual field have turned out to be based on different, only partially overlapping sets of afferent, central and efferent subsystems. A relevant test variable, the deviation of the Subjective Horizontal body Position (SHP) from the objective one, appeared to be correlated with the occurrence of the inversion illusion (and possibly also to symptoms of space sickness) in 5 astronauts (Ss) of the Spacelab 1 and D 1 missions. A reliable predictive test demands a larger number of Ss, a quantitative test of the illusion and separate measurement of the two determinants of the SHP, namely the otolithic bias on the one hand, and the bias of an as yet unidentified gravity system in the human trunk on the other. The present state in the pursuit of three objectives is reported. These include: the measurement of the subjective vertical in the three gravity states of parabolic flight; the comparison of the result with measurements of the SHP on the tiltable board, and the measurement of the relative influence of the unidentified truncal gravity system in paraplegic patients with various locations of the lesion in the spinal cord. Present results indicate that the relevant afferent input enters the spinal cord between the 2nd and the 8th thoracic root. Putative sensors for linear acceleration in the sensory fields of the respective spinal ganglia are discussed. ESA

N91-19606# Wien Univ. (Austria). Neurologische Klinik.
VERTICALLY MOVING VISUAL STIMULI AND VERTICAL VECTION: A TOOL AGAINST SPACE MOTION SICKNESS **c52**
Christian Mueller, G. Wiest, and L. Deecke *In* ESA, Fourth European Symposium on Life Sciences Research in Space Nov. 1990 p 157-161 (For primary document see N91-19572 11-51)
Copyright Avail: NTIS HC/MF A25; EPD, ESTEC, Noordwijk, Netherlands, HC 80 Dutch guilders

Vertical vection is a motion illusion that can be elicited by vertical optokinetic stimulation with gaze fixation. Overruling the otolithic and all other sensory canals visual information leads to the perception of lift or pitch vection in a stationary subject. Moving visual cues are used in postural and spatial orientation on Earth. The phenomenon will be examined at the Soviet-Austrian spaceflight in 1991 for the question of an influence on spatial orientation in weightlessness. ESA

N91-19607# Institute of Biomedical Problems, Moscow (USSR).
THE BIOCHEMICAL AND PHYSIOLOGICAL VARIABLES IN MOTION SICKNESS FOLLOWED MODIFIED NEUROENDOCRINE ACTIVITY **c52**
I. A. Nichiporuk, D. V. Grishanin, and A. I. Grigoriev *In* ESA, Fourth European Symposium on Life Sciences Research in Space Nov. 1990 p 163-165 (For primary document see N91-19572 11-51)
Copyright Avail: NTIS HC/MF A25; EPD, ESTEC, Noordwijk, Netherlands, HC 80 Dutch guilders

Twelve healthy male test subjects showed a significant increase of adrenocorticotropin prolactin, growth hormone and cortisol in placebo, reserpine, methyldopa, l-dopa and jumex (MAO type B inhibitor) series after laboratory induced Motion Sickness (MS) with practically unchanged activity of renin-angiotensin-aldosterone system and plasma serotonin levels. Reserpine decreased endurance of vestibular rotating test, l-dopa and jumex induced previously absent spatial illusions and shortened latency of motor, visuo, and audio motor responses in 4 test subjects. Critical interval of discretion of visual stimulus was decreased by reserpine and methyldopa, and increased by l-dopa and jumex in all subjects. The received results suggest an involvement brain serotoninergic and dopaminergic systems in pathogenesis of MS. ESA

N91-19608# Institute of Biomedical Problems, Moscow (USSR).
ASSESSMENT OF BONE TURNOVER IN HUMANS AFTER SPACE FLIGHT AND HYPOKINESIA **c52**
V. S. Oganov, V. E. Novikov, and A. S. Rakhmanov *In* ESA, Fourth European Symposium on Life Sciences Research in Space Nov. 1990 p 167-170 (For primary document see N91-19572 11-51)
Copyright Avail: NTIS HC/MF A25; EPD, ESTEC, Noordwijk, Netherlands, HC 80 Dutch guilders

The results of studying the bone tissue of cosmonauts after flights (4 to 8 months) were compared to the data of investigating healthy individuals during head down tilt (370 days). A decrease in the vertebral spongy mineral density or an increase of this parameter by a similar magnitude versus the individual preflight values in some cosmonauts was revealed through noninvasive methods (computer tomography, gammaphoton absorptiometry). During studies of clinical cases of osteoporosis it was shown that the vertebral mineral density ratios and presence or absence of vertebral compression fractures in different age groups are nonequal. ESA

N91-19609# Deutsche Forschungsanstalt fuer Luft- und Raumfahrt, Cologne (Germany, F.R.). Microgravity User Support Center.
TOOLS FOR THE PREPARATION, PERFORMANCE AND EVALUATION OF LIFE SCIENCES EXPERIMENTS **c54**
Dittmar Padeken, Marianne Schuber, and Dieter Seibt *In* ESA, Fourth European Symposium on Life Sciences Research in Space Nov. 1990 p 171-174 (For primary document see N91-19572 11-51)
Copyright Avail: NTIS HC/MF A25; EPD, ESTEC, Noordwijk, Netherlands, HC 80 Dutch guilders

Life sciences experiments in the field of microgravity research need extensive preparation, performance, and evaluation. Infrastructure for the preparation of experiments covering the disciplines of the human physiology with ESA Anthrorack and gravitational biology and biological processing techniques with the German payload Biolabor is given. A survey of the available multipurpose ground infrastructure for Spacelab missions and for the preparation of Columbus user support was built up. The possible application spectrum for life sciences ground facilities is described. The application field of an information system developed for microgravity research (ARIADNE) is shown. ESA

N91-19610*# National Aeronautics and Space Administration. Lyndon B. Johnson Space Center, Houston, TX.
POSTURAL CHANGES FOLLOWING SENSORY REINTERPRETATION AS AN ANALOG TO SPACEFLIGHT **c52**

William H. Paloski, D. L. Harm, M. F. Reschke, D. D. Doxey, N. C. Skinner, L. J. Michaud, and D. E. Parker (Miami Univ., Oxford, OH.) *In* ESA, Fourth European Symposium on Life Sciences Research in Space Nov. 1990 p 175-178 (For primary document see N91-19572 11-51)
Copyright Avail: NTIS HC/MF A25; EPD, ESTEC, Noordwijk, Netherlands, HC 80 Dutch guilders CSCL 06P

Postural control changes noted in astronauts immediately following spaceflight are thought to be caused by inflight adaptative changes in Central Nervous System (CNS) processing of sensory information from the visual, vestibular, and proprioceptive systems. In order to elicit these adaptative changes in ground based studies, a Tilt Translation Device (TTD) which causes the CNS of exposed subjects to reinterpret tilt generated sensory inputs from the otolith organs as linear translation of the subject was developed. This device was designed to simulate partially the stimulus rearrangement experienced by astronauts during microgravity. Postural stability is assessed in ten subjects before and after 30 minutes of exposure to TTD. The resulting data suggests that exposure to TTD causes decreases in postural stability and shifts in postflight studies of astronauts. It is concluded that the TTD may be an effective weightlessness simulator, and that the postural changes following TTD exposure may provide a useful dependent measure for evaluation of this apparatus. ESA

N91-19611*# National Aeronautics and Space Administration. Lyndon B. Johnson Space Center, Houston, TX.
STANDARDIZATION OF MOTION SICKNESS INDUCED BY LEFT-RIGHT AND UP-DOWN REVERSING PRISMS **c52**

M. F. Reschke, J. M. Vanderploeg, E. A. Brumley, J. J. Kolafa, and S. J. Wood (Krug International, Houston, TX.) *In* ESA, Fourth European Symposium on Life Sciences Research in Space Nov. 1990 p 179-182 (For primary document see N91-19572 11-51)
Copyright Avail: NTIS HC/MF A25; EPD, ESTEC, Noordwijk, Netherlands, HC 80 Dutch guilders CSCL 06P

Reversing prisms are known to produce symptoms of motion sickness, and have been used to provide a chronic stimulus for training subjects on symptom recognition and regulation. However, testing procedures with reversing prisms have not been standardized. A set of procedures were evaluated which could be standardized using prisms for provocation and to compare the results between Right/Left Reversing Prisms (R/L-RP) and Up/Down Reversing Prisms (U/D-RP). Fifteen subjects were tested with both types of prisms using a self paced walking course throughout the laboratory with work stations established at specified intervals. The work stations provided tasks requiring eye-hand-foot coordination and various head movements. Comparisons were also made between these prism tests and two other standardized susceptibility tests, the KC-135 parabolic static chair test and the Staircase Velocity Motion Test (SVMT). Two different types of subjective symptom reports were compared. The R/L-RP were significantly more provocative than the U/D-RP. The incidence of motion sickness symptoms for the R/L-RP was similar to the KC-135 parabolic static chair test. Poor correlations were found between the prism tests and the other standardized susceptibility tests, which might indicate that different mechanisms are involved in provoking motion sickness for these different tests. ESA

N91-19612# Danish Aerospace Medical Center of Research, Copenhagen.
INFLUENCE ON NATRIURESIS OF PROLONGED (12 h) WATER IMMERSION ON CENTRAL HEMODYNAMICS AND ENDOCRINE ELEMENTS IN HUMANS **c52**

Carsten Stadeager, Peter Norsk, Lars Bo Johansen, Jorgen Warberg, Niels Juel Christensen, and Flemming Bonde-Petersen *In* ESA, Fourth European Symposium on Life Sciences Research in Space Nov. 1990 p 183-185 (For primary document see N91-19572 11-51)
(Grant Danish-SB-1112-14/89)
Copyright Avail: NTIS HC/MF A25; EPD, ESTEC, Noordwijk, Netherlands, HC 80 Dutch guilders

Nine healthy males were randomized to 12 hours of thermoneutral Water Immersion (WI) to the neck and a corresponding seated time control period. The WI induced increase in Central Venous Pressure (CVP) was reduced by 38 percent after 12 hours probably due to the increase in renal sodium and water excretion. The decrease in Plasma Renin Activity (PRA) and Plasma Aldosterone (PA) concentration was maintained during the 12 hours of WI and thus not influenced by the gradual decrease in CVP. Plasma Atrial Natriuretic Peptide (ANP) concentration decreased to prestudy levels at the 12th hour of WI following an initial 3 fold increase. In conclusion, natriuresis of prolonged central hypervolemia decreases CVP. Changes in PRA, PA and ANP may mediate the natriuretic response to WI but during prolonged circumstances, changes in CVP, hormonal concentrations and renal sodium excretion are dissociated. ESA

N91-19613# Royal Air Force Inst. of Aviation Medicine, Farnborough (England).
VESTIBULAR TESTS ON UK ASTRONAUT CANDIDATES FOR AN ANGLO/RUSSIAN SPACE FLIGHT (JUNO MISSION) **c52**

J. R. R. Stott and Alan J. Benson *In* ESA, Fourth European Symposium on Life Sciences Research in Space Nov. 1990 p 187-190 (For primary document see N91-19572 11-51)
Copyright Avail: NTIS HC/MF A25; EPD, ESTEC, Noordwijk, Netherlands, HC 80 Dutch guilders

Tests of vestibular function and motion sickness susceptibility were carried out on 16 candidates from whom the one to fly on a Russian space flight would be chosen. Oculomotor responses to angular oscillation, stopping stimuli and caloric stimulation revealed no significant impairment. Motion sickness susceptibility was assessed by two tests: one, intermittent Coriolis stimulation, the other, horizontal linear oscillation at O.2 Hz + or - 4 m/sq sec. Thirteen candidates failed to complete the Coriolis test whereas all but four withstood the oscillatory stimulus. Measures of susceptibility on the two tests had a significant (p less than 0.01) rank order correlation. ESA

N91-19614# Institute for Endocrinological and Metabolic Diseases, Rome (Italy). Unit for Endocrinological and Metabolic Diseases.
HEAD-DOWN TILT TEST AND SPACE-RELATED ENDOCRINE PHYSIOLOGY **c52**

Felice Strollo, G. Strollo, H. More, and G. Riondino *In* ESA, Fourth European Symposium on Life Sciences Research in Space Nov. 1990 p 191-195 (For primary document see N91-19572 11-51)
Copyright Avail: NTIS HC/MF A25; EPD, ESTEC, Noordwijk, Netherlands, HC 80 Dutch guilders

Tilt Test (TT) Aldosterone/Cortisol (Aldo/F) results were compared to those occurring during Supine Position (SP) or during Glucose Challenge Test (GCT) and to check for any other endocrine disturbance during TT. It was found that: Aldo and F were inhibited by both TT and GCT; renin decreased during TT, but AI did not; growth hormone slightly increased and prolactin slightly decreased. Possible explanations are discussed. It is concluded that TT may help better designing of good simulation endocrine protocols in space physiology. ESA

N91-19615# Karolinska Inst., Stockholm (Sweden). Dept. of Baromedicine.
EFFECTS OF TRAINING WITH REDUCED PERFUSION PRESSURE ON PERFORMANCE AND MUSCLE FIBER CHARACTERISTICS **c52**

Carl J. Sundberg, O. Eiken, M. Esbjoernsson, A. Nygren (Karolinska Hospital, Stockholm, Sweden), and L. Kaijser *In* ESA, Fourth European Symposium on Life Sciences Research in Space Nov. 1990 p 197-198 (For primary document see N91-19572 11-51)

Copyright Avail: NTIS HC/MF A25; EPD, ESTEC, Noordwijk, Netherlands, HC 80 Dutch guilders

Endurance training increases Performance Time (PT) during incremental exercise and may increase the Type 1 fiber percentage, capillary supply and oxidative enzyme content in skeletal muscle. Several factors alone or in combination may trigger these responses, e.g., hypoxia, ischemia, substrate deficiency or flux through aerobic metabolism. Leg exercise in microgravity is associated with reduced perfusion pressure, thus creating a relative ischemia compared to upright exercise at 1 G. The effects of training with reduced muscle perfusion (Ischemia) and training with non restricted muscle blood flow on endurance capacity and muscle fiber characteristics are compared. ESA

N91-19616# Karolinska Inst., Stockholm (Sweden). Environmental Physiology Lab.

MUSCLE FUNCTION IMPAIRMENT FOLLOWING LOWER LIMB UNLOADING IN MEN **c52**

Per A. Tesch, Hans E. Berg, T. Haeggmark, H. Ohlsen, and G. A. Dudley (Bionetics Corp., Cocoa Beach, FL.) *In* ESA, Fourth European Symposium on Life Sciences Research in Space Nov. 1990 p 199-200 (For primary document see N91-19572 11-51)

Copyright Avail: NTIS HC/MF A25; EPD, ESTEC, Noordwijk, Netherlands, HC 80 Dutch guilders

Effects of microgravity on skeletal muscle mass and function was simulated in humans. Unilateral lowerlimb unloading was conducted in six healthy men by suspending one lower limb while walking on crutches. Muscle strength (Peak Torque (PT)) was measured during maximal unilateral concentric or eccentric quadriceps actions before and after four weeks of suspension. Thigh muscle Cross Sectional Area (CSA) was assessed by computerized tomography. PT decreased (p less than 0.05) by 22 percent in response to unloading. Four days later PT was still lower (11 percent; p less than 0.05) than before. Muscle CSA decreased (p less than 0.05) by 7 percent and the control limb showed no changes after suspension. It is suggested that this model of unloading could serve to simulate microgravity because reductions in skeletal muscle mass and strength were of similar magnitude to those produced by bedrest or space flight. ESA

N91-19617# Institute of Biomedical Problems, Moscow (USSR).

THE BIOLOGICAL AND MEDICAL PROGRAMME OF THE MANNED ARAGATZ MISSION ON THE MIR SPACE STATION **c52**

A. Kotovskaia and Didier Vassaux (Centre National de la Recherche Scientifique, Paris, France) *In* ESA, Fourth European Symposium on Life Sciences Research in Space Nov. 1990 p 207-214 (For primary document see N91-19572 11-51)

Copyright Avail: NTIS HC/MF A25; EPD, ESTEC, Noordwijk, Netherlands, HC 80 Dutch guilders

The program of biological and medical experiments within the Aragatz program was a logical extension of French-Soviet cooperation in the space biology and medicine fields, and particularly of the studies carried out during the first French-Soviet flight on the Salyut 7 station in 1982, which were continued during the 237 day flight of 1984. This program filled about half the planned crew workload and covered the main topics of space physiology and medicine. The measurements taken on the crew before the flight, during the first half of the mission, and shortly before and after their return to Earth correspond to seven experiments, two of which were performed exclusively on the ground. The overall aim was to make pertinent use of a flight having an original duration of four weeks to gain a deeper understanding of the physiological mechanisms involved in the adaptation to weightlessness and, more generally, to the space environment. ESA

N91-19618# European Space Agency. European Space Research and Technology Center, ESTEC, Noordwijk (Netherlands).

GRAVITY EFFECTS ON CELLS **c52**

Dick A. M. Mesland *In its* Fourth European Symposium on Life Sciences Research in Space Nov. 1990 p 221-225 (For primary document see N91-19572 11-51)

Copyright Avail: NTIS HC/MF A25; EPD, ESTEC, Noordwijk, Netherlands, HC 80 Dutch guilders

Since the first flight of the ESA Biorack on the German Spacelab Mission D1 in 1985 evidence has been obtained that biological cells and small unicellular organisms function differently under conditions of microgravity. However, there is still a lack of scientific proof that these effects are caused by a direct influence on the cells in the weightlessness condition. The question as to how normal gravity may play a role in cellular activity is being addressed and the results show that gravity may provide important signals during certain state transitions in the cell. These would be gravity sensitive windows in the biological process. Also, by amplification mechanisms inside the cell, the cell may assume a state that is typical for normal gravity conditions and would change in microgravity. Experimental tools that would provide the conditions to obtain evidence for direct action of gravity and for the possible existence of gravity sensitive windows are discussed. ESA

N91-19619# Institut National de la Sante et de la Recherche Medicale, Nice (France). Faculty of Medicine.

EXPERIMENT LYMPHOCYTES OF ARAGATZ MISSION: INFLUENCE OF THE SPACE FLIGHT ON HUMAN T LYMPHOCYTE AND MONOCYTE FUNCTIONS **c52**

Laurence Schaffar, Irena V. Konstantinova, S. Manie, I. Serov, J. P. Breittmayer, I. N. Antropova, I. E. Vorotnikova (Institute of Biomedical Problems, Moscow, USSR), and B. Ferrua *In* ESA, Fourth European Symposium on Life Sciences Research in Space Nov. 1990 p 227-228 (For primary document see N91-19572 11-51)

(Grant CNES-89/1263)

Copyright Avail: NTIS HC/MF A25; EPD, ESTEC, Noordwijk, Netherlands, HC 80 Dutch guilders

During the last French-Soviet Aragatz mission the experiment Lymphocytes aimed at analyzing the effects of a long duration space flight on the capacity of human T lymphocytes and monocytes to be activated. Peripheral blood from five cosmonauts sampled 24 hours after recovery of a long duration flight (26 to 166 days) was examined and it was found that T lymphocytes were affected by long duration space flights. The amount of secreted Interleukin 2 (IL2), which represents the major cytokine regulating T cell proliferation, appeared to be significantly enhanced whereas the biological activity of IL2 was decreased. On the other hand, T lymphocytes from 2 cosmonauts out of 5 were not able to normally express IL2 receptor in response to a mitogen. Circulating monocytes were shown to be functional after the space flight and cannot be at the origin of the observed T lymphocyte dysfunctions. ESA

N91-19620# Eidgenoessische Technische Hochschule, Zurich (Switzerland). Space Biology Group.

LYMPHOCYTES ON SOUNDING ROCKETS

Marianne Cogoli, B. Bechler, Augusto Cogoli, N. Arena, S. Barni, P. Pippia, G. Sechi, N. Valora, and R. Monti (Naples Univ., Italy) *In* ESA, Fourth European Symposium on Life Sciences Research in Space Nov. 1990 p 229-234 Sponsored in part by Italian Space Agency (For primary document see N91-19572 11-51)

(Grant SNRF-3-338-0-86)

Copyright Avail: NTIS HC/MF A25; EPD, ESTEC, Noordwijk, Netherlands, HC 80 Dutch guilders

In two experiments performed on sounding rockets the early steps of the binding of Concanavalin A (Con A) to human lymphocytes under microgravity conditions were studied. No significant difference in the binding of Con A to lymphocytes and subsequent patching and capping between the flight samples and 1 g ground control were observed. In a further experiment the effect of gravity on the cytoskeletal structure of lymphocytes was investigated. Preliminary results indicate that the structure of vimentin may be influenced be altered gravity conditions. ESA

N91-19621*# Eidgenoessische Technische Hochschule, Zurich (Switzerland). Space Biology Group.
REDUCED LYMPHOCYTE ACTIVATION IN SPACE: ROLE OF CELL-SUBSTRATUM INTERACTIONS
Felix K. Gmuender, M. Kiess, Gerald Sonnenfeld (Louisville Univ., KY.), J. Lee, and Augusto Cogoli *In* ESA, Fourth European Symposium on Life Sciences Research in Space Nov. 1990 p 235-238 Sponsored in cooperation with the Swiss Federal Inst. of Tech. and ESA (For primary document see N91-19572 11-51)
(Grant NAG9-181)
Copyright Avail: NTIS HC/MF A25; EPD, ESTEC, Noordwijk, Netherlands, HC 80 Dutch guilders CSCL 06C

The effect of substratum adhesiveness on lymphocyte responsiveness was investigated by reducing and blocking cell adhesion with poly-HEMA (poly (2-Hydroxyethyl Methacrylate)) in a simple on ground system. Cells grown on medium thick and thick poly-HEMA films were rounded in shape and displayed no signs of spreading. By contrast, on tissue culture plastic and very thin poly-HEMA films, they showed clear signs of spreading. The mitogenic response of lymphocytes grown on thick poly-HEMA films was reduced by up to 68 percent of the control (tissue culture plastic). Interferon gamma production was virtually nil when the cells were grown on the least adhesive substratum. These results show that activated lymphocytes need to anchor and spread prior to achieving an optimal proliferation response. It is concluded that decreased lymphocyte adhesion could contribute to the depressed in vitro lymphocyte responsiveness found in the microgravity conditions of space flight. ESA

N91-19622# University Coll., London (England). Mammalian Development Unit.
DEVELOPMENTAL BIOLOGY AND MICROGRAVITY
Anne McLaren *In* ESA, Fourth European Symposium on Life Sciences Research in Space Nov. 1990 p 239-242 (For primary document see N91-19572 11-51)
Copyright Avail: NTIS HC/MF A25; EPD, ESTEC, Noordwijk, Netherlands, HC 80 Dutch guilders

Experiments investigating the effects of microgravity on developmental biology, cell biology, insects and vertebrates are reviewed and those planned for the 1991 joint Anglo-Soviet space mission are presented. Microgravity is known to affect the behavior of single cells. It therefore seems unlikely that the multitude of cellular processes and interactions that make up embryonic development will not respond in some way to the absence of a gravity signal. In Drosophila and stick insects, Biorack experiments have suggested that microgravity may cause abnormalities at the time of hatching. The response of vertebrate development to microgravity has not yet been subjected to critical analysis, but axis formation and the establishment of polarity in amphibia and birds are known to respond to gravitational stimuli in ground based experiments. ESA

N91-19623# Hubrecht Lab., Utrecht (Netherlands).
EPIDERMAL GROWTH FACTOR INDUCED SIGNAL TRANSDUCTION IN A431 CELLS IS INFLUENCED BY ALTERED GRAVITY CONDITIONS
Rolf P. deGroot, Philip J. Rijken, Jeroen denHertog, Johannes Boonstra, Arie J. Verkleij (Utrecht State Univ., Netherlands), Siegfried W. deLaat, and Wiebe Kruijer *In* ESA, Fourth European Symposium on Life Sciences Research in Space Nov. 1990 p 243-247 Sponsored by Space Research Organization Netherlands (For primary document see N91-19572 11-51)
Copyright Avail: NTIS HC/MF A25; EPD, ESTEC, Noordwijk, Netherlands, HC 80 Dutch guilders

Epidermal Growth Factor (EGF) activates a well characterized signal transduction cascade in human A431 epidermoid carcinoma cells. It was previously shown that EGF induced cell rounding and protooncogene c-fos expression is influenced by stimulated gravity charges. A study showing that real microgravity conditions significantly decrease EGF induced c-fos expression as well as EGF-receptor clustering is presented. Evidence that the decrease in c-fos expression is caused by a direct effect on the c-fos promoter, and that only a subset of signal transduction pathways leading to c-fos expression is sensitive to gravity changes, is provided. ESA

N91-19624# Hubrecht Lab., Utrecht (Netherlands).
FERTILIZATION OF XENOPUS EGGS IN SPACE
G. A. Ubbels, W. Berendsen (Utrecht State Univ., Netherlands), S. Kerkvliet, and J. Narraway *In* ESA, Fourth European Symposium on Life Sciences Research in Space Nov. 1990 p 249-254 Sponsored by Space Research Organization Netherlands (For primary document see N91-19572 11-51)
Copyright Avail: NTIS HC/MF A25; EPD, ESTEC, Noordwijk, Netherlands, HC 80 Dutch guilders

The role of gravity on developmental biology is studied. Amphibian eggs, favorable because of their small size and because they are easily obtained, are studied. Egg rotation and centrifugation experiments strongly suggest that gravity functions in the determination of the spatial structure of amphibian embryos. Decisive experiments can only be made in space. Eggs of Xenopus laevis, the South African clawed toad, were the first vertebrate eggs which were successfully fertilized on sounding rockets in space. Unfixed, newly fertilized eggs survived reentry, and a reasonable number showed a seemingly normal gastrulation but died between gastrulation and neurulation. Only a few became larvae, but these developed similarly abnormal. Whether this is due to reentry perturbations, a real microgravity effect, or due to other causes, will be tested in the future. ESA

N91-19625# Paris VI Univ., Banyuls-sur-Mer (France). Observatoire Oceanologique.
MICROGRAVITY AND DEVELOPMENT OF AQUATIC ANIMALS
Hans-Juerg Marthy *In* ESA, Fourth European Symposium on Life Sciences Research in Space Nov. 1990 p 255-257 (For primary document see N91-19572 11-51)
Copyright Avail: NTIS HC/MF A25; EPD, ESTEC, Noordwijk, Netherlands, HC 80 Dutch guilders

The usefulness of selected aquatic animals and their eggs, embryos, larvae and/or juveniles for microgravity studies during orbiting and non orbiting space flights is stressed for work in developmental biology research. A recently flown experiment (sounding rocket Maser 4, CIS-2, Kiruna), using sea urchins, to determine possible effects of microgravity on fertilization, is used to illustrate and support this view. ESA

N91-19626# Stuttgart Univ. (Germany, F.R.). Inst. of Zoology.
EFFECT OF HYPER-GRAVITY ON THE SWIMMING BEHAVIOR OF AQUATIC VERTEBRATES
Hinrich Rahmann, Klaus Slenzka, and R. Hilbig *In* ESA, Fourth European Symposium on Life Sciences Research in Space Nov. 1990 p 259-263 (For primary document see N91-19572 11-51)
Copyright Avail: NTIS HC/MF A25; EPD, ESTEC, Noordwijk, Netherlands, HC 80 Dutch guilders

Larvae of developing cichild fish and clawed toads were subjected to hypergravity forces (2 to 4 G) for nine days. Upon returning to 1 G conditions, swimming was measured quantitatively in comparison to a 1 G control group by means of a computer based videographic analysis system (video track). Long term, hyper G fish and toads exhibited typical loop swimming which was performed during a habituation period of 3 to 5 days. In comparison to the control group, they preferred different locations within their mini aquaria and showed significant differences in the duration of their inactive periods, their fast and slow swimming movements and swimming distances. These behavioral studies serve as the basis for further neurobiological investigation and are essential to future D 2 STATEX experiments. ESA

N91-19627# Bertin et Cie., Plaisir (France).
PRELIMINARY STUDY OF A MEMBRANE BIOREACTOR FOR CELL CULTURE IN SPACE
P. Binot, Isabelle Geahel, and R. Mattout *In* ESA, Fourth European Symposium on Life Sciences Research in Space Nov. 1990 p 265-267 Sponsored by CNES (For primary document see

N91-19572 11-51)
Copyright Avail: NTIS HC/MF A25; EPD, ESTEC, Noordwijk, Netherlands, HC 80 Dutch guilders

Cell culture in microgravity may allow a better knowledge of human physiology in space and requires development of bioreactors capable of working continuously under high cell density, without perturbation of, or by, microgravity. Among existing types of bioreactors, hollow fiber reactors appear to be the best suited in spite of the nonhomogeneity of their culture chamber. This nonhomogeneity problem could be alleviated by using flat membranes. A mathematical modeling study of the transfer parameters through a flat feeding membrane working under tangential filtration conditions shows that good transfer homogeneity could be obtained provided there is: a low ratio (filtered medium/circulating medium) (1/10 approximately); a tangential speed lower than used for ultra microfiltration (2 to 15 cm/sec approximately); a transmembrane pressure drop close to usual microfiltration levels (10,000 approximately). Experimentation on a model with miscellaneous types of membranes confirmed the above results and underlined the requirement of using well characterized membranes. Microgravity appears to have little influence on flat membrane bioreactors which are a good prospect for cell physiology experiments in space. ESA

N91-19628# Texas Univ. Health Science Center, Houston.
ALTERED CARTILAGE DIFFERENTIATION IN TIBIAL EPIPHYSEAL PLATES OF COSMOS RATS
P. J. Duke, G. Durnova (Institute of Biomedical Problems, Moscow, USSR), and Dina Montufar-Solis *In* ESA, Fourth European Symposium on Life Sciences Research in Space Nov. 1990 p 269-273 (For primary document see N91-19572 11-51)
Copyright Avail: NTIS HC/MF A25; EPD, ESTEC, Noordwijk, Netherlands, HC 80 Dutch guilders

Growth plates of rats flown aboard the Soviet biosatellites Cosmos 1887 and 2044 were analyzed using light and electron microscopy, and computerized planimetry. Area was significantly less in 1887 animals and collagen fibrils in flight animals were wider than in synchronous controls. The proliferative zone of flight animals was significantly higher and had more cells/column than controls; the hypertrophic/calcification zone was significantly reduced. Reserve zone height was reduced only on 1887. The total number of cells/column was significantly higher in 1887 flight rats only. Results represent both effects of microgravity exposure and initial stages of recovery from that exposure; and confirm previous observations of altered cell proliferation, differentiation and matrix organization in growth plates exposed to microgravity. ESA

N91-19629# Naples Univ. (Italy). Inst. of Human Physiology.
EFFECT OF THE CENTRIFUGE FORCES ON PREGNANT RATS
G. deFranciscis, Riccardo Solimene, C. Donzelli, P. Gambardella, and G. P. Pizzuti *In* ESA, Fourth European Symposium on Life Sciences Research in Space Nov. 1990 p 275-280 (For primary document see N91-19572 11-51)
Copyright Avail: NTIS HC/MF A25; EPD, ESTEC, Noordwijk, Netherlands, HC 80 Dutch guilders

The effects of centrifuge acceleration on rats' embryos at different stages of development was analyzed. Four groups of pregnant rats, respectively in the first, second, fifth and sixth day of pregnancy, were put in the centrifuge in small plexiglass cages and were submitted to transversal acceleration of 3 G for 3 hours with 45 minutes of run and 15 minutes of rest. After this the animals were sacrificed, the first and the second group immediately, the third and the fourth at the eighteenth day of pregnancy. The morphologic analysis showed that the application of the centrifuge acceleration at the first two days of pregnancy inhibits the development of the eggs, whereas at the fifth and the sixth day causes bad deformations. The karyotyping analysis of the foeta is in course. ESA

N91-19630# Centre Hospitalier Univ. Purpan, Toulouse (France). Lab. de Biologie Cellulaire.
HUMAN DERMAL FIBROBLAST SENSITIVITY TO HYPERGRAVITY **c52**
Yolande Gaubin, F. Croute, D. Hartmann (Pasteur, Louis Univ., Lyon, France), B. Pianezzi, and J. P. Soleihavoup *In* ESA, Fourth European Symposium on Life Sciences Research in Space Nov. 1990 p 281-283 (For primary document see N91-19572 11-51)
Copyright Avail: NTIS HC/MF A25; EPD, ESTEC, Noordwijk, Netherlands, HC 80 Dutch guilders

The effects of 10 day chronic hypergravity (2 to 15 G) on cellular functions of human dermal fibroblasts in vitro was investigated. Proliferation or mitogenic response to II sub 1, DNA and protein contents were unaffected by hyper-g culture conditions. Glyceraldehyde-3-P dehydrogenase and pyruvate kinase activities were not disturbed whereas glucose-6-P dehydrogenase was enhanced in a range of 10 to 15 percent. The release of type 1 and 3 collagen, appreciated by a radioimmunoassay, was very similar in control or g-exposed cultures. Nevertheless, indirect immunofluorescence labelling of cell layer type 1 collagen revealed extracellular fibrillar networks in hyper-g exposed cells whereas controls showed a sparse cytoplasmic staining. Elastase activity was increased by about 10 percent. These results suggest that hypergravity could induce changes in the program of extracellular matrix synthesis and the remodeling of its molecules. ESA

N91-19631# Deutsche Forschungsanstalt fuer Luft- und Raumfahrt, Cologne (Germany, F.R.). Inst. for Aerospace Medicine.
CELLULAR FUNCTIONS OF PARAMECIUM UNDER DIFFERENT GRAVITY CONDITIONS
Ruth Hemmersbach-Krause, Donat-P. Haeder, M. Koehler, J. Perdigao (Lisbon Univ., Portugal), and Wolfgang Briegleb *In* ESA, Fourth European Symposium on Life Sciences Research in Space Nov. 1990 p 285-290 (For primary document see N91-19572 11-51)
Copyright Avail: NTIS HC/MF A25; EPD, ESTEC, Noordwijk, Netherlands, HC 80 Dutch guilders

Computer analysis of the negative gravitactic behavior of Paramecium observed in a horizontal microscope was performed. It was found that there exists a strong (negative) correlation between oxygen concentration within the medium and the degree of gravitaxis, and, under some experimental conditions, swimming velocity. Treatment of Paramecium with the metabolic uncoupler CCCP had no influence on the negative gravitaxis. In another set of experiments proliferation of different strains of Paramecium was investigated on the clinostat. All tested strains showed larger fluctuations between cell numbers if two daughter cells were cultivated under 1 G and simulated 0 G than if both cells were cultivated under 1 G. Statistical analysis of these differences revealed a significantly higher proliferation of homozygous P tetraurelia 7s under simulated 0 G. ESA

N91-19632# Institut National de la Sante et de la Recherche Medicale, Toulouse (France).
GROWTH RATE OF BACTERIA WITHOUT AND WITH ANTIBIOTIC AT DIFFERENT LEVELS OF GRAVITY
Lydie Lapchine, N. Moatti, J. P. Moatti, G. Gasset, G. Richoilley, and R. Tixador (Centre Hospitalier Univ. Purpan, Toulouse, France) *In* ESA, Fourth European Symposium on Life Sciences Research in Space Nov. 1990 p 291-293 (For primary document see N91-19572 11-51)
Copyright Avail: NTIS HC/MF A25; EPD, ESTEC, Noordwijk, Netherlands, HC 80 Dutch guilders

Previous cell biology experiments performed in space are reviewed and results concerning the behavior of microorganisms (modifications of the cell growth rate, changes of antibiotic sensitivity, and structural and morphological differences), are found to be different. In order to try to explain these observed results, the cell growth rate of bacteria cultivated at different levels of hypergravity without or with subinhibitory concentrations of antibiotic (Dihydrostreptomycin) was studied. Three levels of hypergravity

(2, 5, 10 G) were investigated at regular intervals (3, 5, 7, 9 hours). No significant differences were noted, for the three levels of hypergravity investigated, compared to the normal gravity of 1 G. ESA

N91-19633# Alicante Univ. (Spain). Dept. de Neuroquimica.
MICROGRAVITY, HYPERGRAVITY, AND AGING: A UNIFYING HYPOTHESIS c52
Jaime Miquel, E. Ramirez, M. C. Holgado, E. deJuan, and R. Marco (Universidad Autonoma de Madrid, Cantoblanco, Spain) *In* ESA, Fourth European Symposium on Life Sciences Research in Space Nov. 1990 p 295-300 Sponsored in part by Ministerio de Educacion y Ciencia (For primary document see N91-19572 11-51)
(Contract CICYT-ESP-88-0351)
Copyright Avail: NTIS HC/MF A25; EPD, ESTEC, Noordwijk, Netherlands, HC 80 Dutch guilders

The data from astronauts and cosmonauts as well as from animal experiments showed that long term exposure to near zero G could exert an influence on physiological processes. Research suggests that at least one of these processes, namely aging, may be quite responsive to abnormal G loads. Data is reviewed and theoretical concepts on the relationship between gravity and aging are presented. They propose a general behavioral-metabolic theory of modulation of aging in abnormal gravity fields, which can be subjected to the experimental test by further clinostat, and space laboratory work, in which both the rate of aging and the metabolic rate are simultaneously determined. ESA

N91-19634*# Bern Univ. (Switzerland). Anatomisches Inst.
INCREASED MITOGENIC RESPONSE IN LYMPHOCYTES FROM CHRONICALLY CENTRIFUGED MICE
Otfried Mueller, E. Hunzinger, Augusto Cogoli, B. Bechler, J. Lee, J. Moore, and J. Duke (Texas Univ. Health Science Center, Houston.) *In* ESA, Fourth European Symposium on Life Sciences Research in Space Nov. 1990 p 301-305 Sponsored by NASA, Swiss Federal Inst. of Tech., and ESA (For primary document see N91-19572 11-51)
(Grant SNSF-3-338-0-86)
Copyright Avail: NTIS HC/MF A25; EPD, ESTEC, Noordwijk, Netherlands, HC 80 Dutch guilders CSCL 06C

The effects upon the mitogenic response of splenic lymphocytes when exposing mice to prolonged hypergravity conditions (3.5 G for 1 year) were studied. Cultures of splenic lymphocytes isolated from both centrifuged and control (1 G) animals were stimulated with Concanavalin A and the response measured using both morphological and biochemical means. Lymphocytes obtained from centrifuged mice exhibited much higher activation rates (as measured by the incorporation of H-3 thymidine) and larger cell aggregates consisting of more lymphoblasts and mitotic figures than those observed in non centrifuged control animals. Isolated splenic lymphocytes thus appear to have been conditioned by hypergravity state. ESA

N91-19635# Deutsche Forschungsanstalt fuer Luft- und Raumfahrt, Cologne (Germany, F.R.). Inst. for Aerospace Medicine.
DOES GRAVITY PLAY A ROLE IN THE MORPHOLOGICAL DEVELOPMENT AND FUNCTION OF THE GRAVITY SENSORY ORGAN OF VERTEBRATES. DLR CONTRIBUTION TO THE D-2 PROJECT GRAVIPERCEPTION AND NEURONAL PLASTICITY, ITS TECHNICAL REALIZATION AND EXPERIMENTAL EXECUTION
Juergen W. Neubert, Wolfgang Briegleb, Albrecht Schatz, B. Bromeis, K. Baeumer, and P. Junk (OHB-System G.m.b.H., Bremen, Germany, F.R.) *In* ESA, Fourth European Symposium on Life Sciences Research in Space Nov. 1990 p 307-312 (For primary document see N91-19572 11-51)
Copyright Avail: NTIS HC/MF A25; EPD, ESTEC, Noordwijk, Netherlands, HC 80 Dutch guilders

Despite many investigations on the effect of gravity on the gravity sensory system of vertebrates, many questions remain unanswered. The D2 mission offers the opportunity to continue the investigation of the effects of gravity on morphogenesis, function, neuronal reaction mechanisms of the vestibular gravity receptors and behavior in aquatic vertebrates taking into account the results of the STATEX D1 experiment. The reactions will be studied on two different aquatic vertebrate species (the South African clawed toad Xenopus laevis Daudin and the cichlid fish Oreochromis mossambicus) with similar developmental profiles during the mission period. Both species allow cultivation within one commonly controlled life support system. Thus, for the first time, the development of two different aquatic vertebrates exposed to identical experimental conditions in space may be compared. ESA

N91-19636# Deutsche Forschungsanstalt fuer Luft- und Raumfahrt, Cologne (Germany, F.R.). Inst. for Aerospace Medicine.
GRAVITY PERCEPTION BY NON-SPECIALIZED STRUCTURES
Albrecht Schatz, R. Reitstetter, A. Linke-Hommes, and Wolfgang Briegleb *In* ESA, Fourth European Symposium on Life Sciences Research in Space Nov. 1990 p 313-314 (For primary document see N91-19572 11-51)
Copyright Avail: NTIS HC/MF A25; EPD, ESTEC, Noordwijk, Netherlands, HC 80 Dutch guilders

Theoretical investigations indicate density variations in the membrane-solution interface which implies gravity interaction with the system. Measurements of single channel currents of gramicidin in planar phosphatidylserine bilayer membranes show a difference of about 20 percent in mean channel current between horizontally and vertically oriented bilayer membranes. These results support the theoretical predictions that the membrane solution interface is a gravity sensitive structure. ESA

N91-19637# Centre d'Etude de l'Energie Nucleaire, Mol (Belgium). Dept. of Radioprotection.
AN ASSAY FOR BONE CELL DIFFERENTIATION IN VITRO AS A TOOL FOR MICROGRAVITY STUDIES IN SPACE
Greet E. R. Schoeters, H. Leppens, F. VanderPlaetse, and J. Maes *In* ESA, Fourth European Symposium on Life Sciences Research in Space Nov. 1990 p 315-319 Sponsored in part by DPWB/SPPS (For primary document see N91-19572 11-51)
Copyright Avail: NTIS HC/MF A25; EPD, ESTEC, Noordwijk, Netherlands, HC 80 Dutch guilders

New bone is produced over the entire lifespan but the exact nature and localization of osteoprogenitor cells in adult tissue is unknown. This information would be essential for understanding and prevention of defects related to bone formation such as may be introduced under microgravity circumstances. The aim is to develop an in vitro assay for differentiation of osteogenic cells which can be performed in an automated experiment container in space and evaluated after return to Earth. It has been shown that bone marrow from adult mice, cultured in vitro as an intact marrow fragment, produces bone. Cell proliferation, collagen synthesis and mineralization rate can be followed with time. This system offers the unique possibility to follow in vitro recruitment and differentiation of osteogenic cells starting from adult marrow cells. ESA

N91-19638# Stuttgart Univ. (Germany, F.R.). Inst. of Zoology.
MORPHOLOGICAL, ELECTRONMICROSCOPICAL AND BIOCHEMICAL ASPECTS OF HYPER-GRAVITY CONDITIONS DURING EARLY ONTOGENETIC DEVELOPMENT OF CICHLID FISH
Klaus Slenzka, R. Anken, A. Baeuerle, J. H. Koertje, U. Paulus, and Hinrich Rahmann *In* ESA, Fourth European Symposium on Life Sciences Research in Space Nov. 1990 p 321-328 (For primary document see N91-19572 11-51)
Copyright Avail: NTIS HC/MF A25; EPD, ESTEC, Noordwijk, Netherlands, HC 80 Dutch guilders

The effect of 2 to 4 G for a period of 9 days on the gross morphology of the brain, on various neuronal enzymes and on the ultrastructure of synaptic terminals was studied based on quantitative behavioral analysis of the effect of hypergravity on the swimming activity of fish and frog larvae. In a study of hyper G animals versus a 1 G control group the total brain volume was

reduced by about 15 percent, creatine kinase activity decreased by 20 percent, there was an increase in cytochrome oxidase, there was no changes in calcium/magnesium ATPase, and there were first indications of ultrastructural changes. ESA

N91-19639# Amsterdam Univ. (Netherlands). Moleculaire Celbiologie.
UNICELLULAR ALGAE IN SPACE. 1: PREPARATORY TESTS
Anna Tomson, Rene Demets, Wies vandenBriel, and Herman vandenEnde *In* ESA, Fourth European Symposium on Life Sciences Research in Space Nov. 1990 p 329-337 Sponsored by Space Research Organization Netherlands (For primary document see N91-19572 11-51)
Copyright Avail: NTIS HC/MF A25; EPD, ESTEC, Noordwijk, Netherlands, HC 80 Dutch guilders

To investigate the mating process of the unicellular green alga Chlamydomonas in a sounding rocket, a new instrument, the flexible tube unit with a miniature illumination device was developed. For gravity independent performance of the tube unit it was necessary to equalize the buoyant density of all liquids used. Special attention was paid to the set up of the 1 G control, because mating algae tend to sink down at 1 G which appeared to affect the rate of the mating process. Further research was aimed at obtaining a proper launch window. Launch simulation tests (vibration, acceleration) were performed. ESA

N91-19640# Amsterdam Univ. (Netherlands). Moleculaire Celbiologie.
UNICELLULAR ALGAE IN SPACE. 2: SOUNDING-ROCKET EXPERIMENT
Rene Demets, Anna Tomson, Wies vandenBriel, and Herman vandenEnde *In* ESA, Fourth European Symposium on Life Sciences Research in Space Nov. 1990 p 339-346 Sponsored by Space Research Organization Netherlands (For primary document see N91-19572 11-51)
Copyright Avail: NTIS HC/MF A25; EPD, ESTEC, Noordwijk, Netherlands, HC 80 Dutch guilders

Complementary gametes of the alga Chlamydomonas were flown in the MASER-3 sounding rocket to test the influence of weightlessness on the sexual interaction of these cells. Clear cut evidence was obtained that the gametes interacted more slowly in the rocket than in the ground. Additional data indicated that the mating capability of the flown cells was reduced from the very start of the period of microgravity. It is proposed that either the cells may have been damaged by launch effects, or the cells reacted instantaneously, i.e., within seconds, to the absence of gravity. These propositions are discussed. ESA

N91-19641# Amsterdam Univ. (Netherlands). Moleculaire Celbiologie.
UNICELLULAR ALGAE IN SPACE. 3: ADDENDUM
Rene Demets, Anna Tomson, Anneke Nederbragt, Jaap deWit, and Herman vandenEnde *In* ESA, Fourth European Symposium on Life Sciences Research in Space Nov. 1990 p 347-348 Sponsored in part by Space Research Organization Netherlands (For primary document see N91-19572 11-51)
Copyright Avail: NTIS HC/MF A25; EPD, ESTEC, Noordwijk, Netherlands, HC 80 Dutch guilders

Evidence was found that the difference between the flight samples and the ground samples in the algae experiment in MASER-3 was not caused by microgravity. This finding indicates that the current set up of cell biological microgravity experiments in sounding rockets is liable to produce erroneous data. It reinforces the idea that an on board 1 G centrifuge is necessary for obtaining unambiguous results. ESA

N91-19642# Institute of Biomedical Problems, Moscow (USSR).
HUMAN AND ANIMAL RESULTS ON VESTIBULAR RESEARCH IN SPACE: VERIS **c52**
I. B. Kozlovskaya, B. M. Babaev, V. A. Barmin, I. N. Beloozerova, L. N. Kornilova, M. G. Sirota, and S. B. Yakushin *In* ESA, Fourth European Symposium on Life Sciences Research in Space Nov. 1990 p 353-357 (For primary document see N91-19572 11-51)
Copyright Avail: NTIS HC/MF A25; EPD, ESTEC, Noordwijk, Netherlands, HC 80 Dutch guilders

The vestibular function in microgravity environment was examined in men and monkeys using as models optokinetic and optomotor reactions in the former and the gaze fixation reaction, based on the eye-head coordination mechanisms, in the latter. Kinematic parameters of eye and head movements as well as neuronal activity of different parts of the vestibular system, i.e. vestibular nuclei, floccular lobe of cerebellum and vestibular fibers were recorded in both cases. The duration of space flights in both cases was 7 to 12 days. The study revealed in space significant changes at the oculomotor and neuronal response pointing to an increase of the dynamic vestibular excitability along with a diminishing of the static vestibular activity. The time course variations of various parameters under study in flight were similar and reflected adaptation of the control system to the new vestibular environment. ESA

N91-19643# Saint-Etienne Univ. (France). Lab. de Biologie du Tissu Osseux.
BONE ADAPTATION TO REAL AND SIMULATED MICROGRAVITY
Laurence Vico, S. Bourrin, J. M. Very, D. Chappard, and C. Alexandre *In* ESA, Fourth European Symposium on Life Sciences Research in Space Nov. 1990 p 359-362 (For primary document see N91-19572 11-51)
Copyright Avail: NTIS HC/MF A25; EPD, ESTEC, Noordwijk, Netherlands, HC 80 Dutch guilders

One, two and three week spaceflight missions of the Soviet Biocosmos series allowed studies of rat bone adaptation to weightlessness. Parallel to the one and two week flights, simulations were done using the Holton tail suspension model. A six week simulation was also designed to investigate long term effects. In both real and simulated microgravity conditions, results obtained from tibial proximal metaphyses at the level of the secondary spongiosa (where remodeling occurs) were compared. At the end of the first inflight week, bone loss with cellular uncoupling may constitute an acute response of bone to the new environmental condition. Later, the trabecular bone volume slowly declined due to continued impairment in bone formation while bone resorption remained normal or slightly reduced. During the first week of suspension, an acute response was observed. During the second week, a recovery phase was observed. Thereafter a slower but sustained bone loss, characterized by cellular uncoupling, took place. After one week, mechanisms of bone loss could be different. In real microgravity bone became older whereas in simulated microgravity it adapted to unloading condition by decreasing mechanical competence. ESA

N91-19644# Milan Univ. (Italy). Ist. di Clinica Medica Generale.
BLOOD PRESSURE MATURATION CURVE IN NORMOTENSIVE RATS DURING GROWTH IN SIMULATED MICROGRAVITATIONAL ENVIRONMENT **c52**
Fabio Magrini, M. Ciulla, R. Meazza, and P. Reggiani *In* ESA, Fourth European Symposium on Life Sciences Research in Space Nov. 1990 p 363-365 Prepared in cooperation with Italian Space Agency, Rome (For primary document see N91-19572 11-51)
Copyright Avail: NTIS HC/MF A25; EPD, ESTEC, Noordwijk, Netherlands, HC 80 Dutch guilders

Systolic blood pressure, heart rate, urinary output and body weight were measured at 10 day intervals from the age of 30 days (weaning) to 150 days in 12 male Sprague-Dawley rats. When compared to the six control rats, the six test rats kept (between the age of 30 and 90 days) in dry water immersion exhibited a downward shift in systolic blood pressure and body weight maturation curve. It is concluded that the physiological rise in systolic blood pressure taking place in rats during growth is partly dependent on gravitational stimulation. ESA

N91-19645# Institute of Biomedical Problems, Moscow (USSR).
ADAPTIVE RESPONSES IN MONKEYS DURING TWO WEEK SPACE FLIGHT
A. N. Truzhennikov, V. I. Korolkov, V. I. Lobachik, and M. A. Dotsenko *In* ESA, Fourth European Symposium on Life Sciences Research in Space Nov. 1990 p 367-370 (For primary document see N91-19572 11-51)
Copyright Avail: NTIS HC/MF A25; EPD, ESTEC, Noordwijk, Netherlands, HC 80 Dutch guilders

Primate studies performed during a two week space flight on board Cosmos biosatellites are discussed. These experiments have made an important contribution to resolving many tasks of space biology and medicine. Using sophisticated equipment and the subtlest methods it was possible to assess some quantitative changes in the functioning of the vestibular system, blood shifting in the body, in the dynamics of parameters of muscular function, and in metabolic changes. This allows not only a control of changes in a living organism during the initial flight stage, but a gain of greater control over adaptation to weightlessness. ESA

N91-19646# Padua Univ. (Italy). CNR Unit for Muscle Biology and Physiopathology.
CONTRACTILE PROTEIN CHANGES INDUCED BY HINDLIMB SUSPENSION IN RAT SKELETAL MUSCLE
M. Campione, G. DeSalvo, S. Ausoni, C. Y. Guezennec, and S. Schiaffino (Centre d'Etudes et de Recherches de Medecine Aerospatiale, Paris, France) *In* ESA, Fourth European Symposium on Life Sciences Research in Space Nov. 1990 p 371-373 (For primary document see N91-19572 11-51)
Copyright Avail: NTIS HC/MF A25; EPD, ESTEC, Noordwijk, Netherlands, HC 80 Dutch guilders

Hindlimb suspension is used as an experimental system to simulate the effect of weightlessness on rat skeletal muscle. Previous studies show that loss of muscle mass and changes in mechanical properties induced by suspension are similar to those observed in space traveled rats. However, the molecular basis and the pathogenesis of these processes are still unclear in this study. Contractile protein changes in the rat soleus muscle were investigated after 21 days of suspension using high resolution polyacrylamide gel electrophoresis and immunoblotting analysis with monoclonal antibodies specific for Myosin Heavy Chain (MHC), troponin T and troponin I isoforms. Unloaded muscles showed a decrease in type 1 and an increase in type 2A and 2X MHC, and a parallel switching from a slow type to a fast type troponin T and troponin I isoform profile. The results indicate that conditions simulating weightlessness induce coordinated changes in the expression of contractile protein genes in rat postural muscles. ESA

N91-19647# Rome Univ. (Italy). Lab. for Experimental Neuropathology.
HINDLIMB SUSPENSION OF RABBIT FOR ONE WEEK: MYOFIBRILLAR DAMAGE IN THE SOLEUS MAY DEPEND ON LONG-LASTING SHORTENING AND PERIODIC CONTRACTION AGAINST NO LOAD
Giuseppe Sancesario, R. Massa, A. P. Anzil (State Univ. of New York, Brooklyn.), and G. Bernardi *In* ESA, Fourth European Symposium on Life Sciences Research in Space Nov. 1990 p 375-380 (For primary document see N91-19572 11-51) (Grant ASI-88-08)
Copyright Avail: NTIS HC/MF A25; EPD, ESTEC, Noordwijk, Netherlands, HC 80 Dutch guilders

The effects of hindlimb suspension on the fine structure of the rabbit tibialis and soleus muscles was studied. The animals were suspended for one week, and the muscles were observed by light and electron microscopy. In suspension, the hindfeet were usually plantar flexed so that the length of the soleus was 35 percent shorter, and that of the tibialis was 30 percent shorter. Morphologically, while the tibialis displayed no significant changes, the soleus fibers of suspended animals showed a multifocal breakdown of the myofibrils, a marked loss in the number and a decrease in the length of the sarcomeres. Such cytoarchitectural remodeling may depend more on the shortening of the soleus against no load, rather than on the inactivity of the suspended hindlimbs. Phasic and tonic contractions without a load can also occur in the soleus of astronauts, and these factors may be detrimental to muscle structural integrity. ESA

N91-19648# Bertin et Cie., Plaisir (France).
PRELIMINARY STUDIES BEFORE DEFINING A PAYLOAD ADAPTED TO THE PRIMATE MODEL
Jean Boquet, Marc Aureille, and Claude Milhaud *In* ESA, Fourth European Symposium on Life Sciences Research in Space Nov. 1990 p 381-385 Previously announced as N91-10107 Prepared in cooperation with Centre d'Etudes et de Recherche de Medecine Aerospatiale, Paris, France (For primary document see N91-19572 11-51)
Copyright Avail: NTIS HC/MF A25; EPD, ESTEC, Noordwijk, Netherlands, HC 80 Dutch guilders

A preliminary study was made before definition of a payload adapted to the primate model to be flown onboard the RRS Lifesat facility. With the prospect of an 8 week mission with a nominal load adapted to two adult rhesus monkeys or four adult cynomolgus monkeys or eight adult squirrel monkeys, the purpose of this study was to determine: the scientific objectives and constraints; the animal maintenance conditions; the functional specifications; the preliminary technical specifications; and the safety specifications. The study confirmed the scientific value of this concept and evidenced its complementarity with research carried out on man or animals onboard manned spacecraft. From a technical standpoint, compatibility with currently proposed Lifesat program characteristics requires reducing the nominal configurations, limiting either the flight duration or the number of flown primates. ESA

N91-19649# Laboratoire de Medecine Aerospatiale, Bretigny-sur-Orge (France). Base d'Essais.
REVIEW OF EEG STUDIES IN NON HUMAN PRIMATES EXPOSED TO MICROGRAVITY
D. Lagarde, Claude Milhaud, G. Anton, G. Chlick, V. Magedov, and V. Rotenberg (Institute of Biomedical Problems, Moscow, USSR) *In* ESA, Fourth European Symposium on Life Sciences Research in Space No. 1990 p 387-391 In FRENCH; ENGLISH summary (For primary document see N91-19572 11-51)
Copyright Avail: NTIS HC/MF A25; EPD, ESTEC, Noordwijk, Netherlands, HC 80 Dutch guilders

A review of published electroencephalographic studies on the Rhesus monkey, a privileged primate model for investigation of human sleep in microgravity, is presented. The main results from observations of Bonny (US Biosatellite 3), Gordyi Vernyi (Soviet Biocosmos 1667) and Erocha Drioma (Soviet Biocosmos 1887) are discussed. ESA

N91-19650# Vrije Univ., Amsterdam (Netherlands). Dept. of Oral Cell Biology.
HYPERGRAVITY AND BONE MINERALIZATION
Jack J. W. A. vanLoon, J. P. Veldhuijzen, and E. H. Burger *In* ESA, Fourth European Symposium on Life Sciences Research in Space Nov. 1990 p 393-396 (For primary document see N91-19572 11-51)
Copyright Avail: NTIS HC/MF A25; EPD, ESTEC, Noordwijk, Netherlands, HC 80 Dutch guilders

Sixteen day old fetal mice long bone rudiments were cultured under hypergravity conditions (1.0, 2.2, 2.5, and 3.1 gravity) to study growth and mineralization of the tissue. Longitudinal growth of the rudiments proceeded normally during the four day culture period. At the same time calcification of the growth plate cartilage and bone determined by the length of the diaphyses and radioactive calcium incorporation was strongly increased, by 87 and 620 percent respectively. This in vitro model allows the study of fetal bone growth, mineralization, and metabolism under increased acceleration conditions. ESA

N91-19651# Milan Univ. (Italy). Ist. di Fisiologia Umana.
GRAVITY DEPENDENCE OF PLEURAL LIQUID TURNOVER
c52
Giuseppe Miserocchi and Daniela Negrini *In* ESA, Fourth

European Symposium on Life Sciences Research in Space Nov. 1990 p 397-399 (For primary document see N91-19572 11-51)
Copyright Avail: NTIS HC/MF A25; EPD, ESTEC, Noordwijk, Netherlands, HC 80 Dutch guilders

The turnover rate of pleural fluid as an experimental model to investigate the interstitial space physiology, in particular its dependence on the gravitational field was studied. Data was gathered in anesthetized animals (rabbits and dogs) breathing spontaneously. Using either cannulas or micropipettes the gravity dependent distribution of the pressure of the pleural liquid and the pressure in the parietal pleural interstitium was measured. The intrapleural gravity dependent pleural liquid flows were also measured by detecting with a gamma camera the interpleural movement of tecnitium labelled albumin. The data allowed a functional model for the filtration absorption interaction to be depicted displaying the following features: pleural liquid is mainly filtered in the less dependent regions of the pleural space; it flows towards the lowermost regions of the cavity where it is drained by the lymphatic action. How exposure to zero g may interfere with the above model, and whether limitations exist, in terms of human adaptation to lack of gravity, considering that lymphatic distribution within the body essentially complies with a physiological gravity dependent absorption, is discussed. ESA

N91-19652# Tuebingen Univ. (Germany, F.R.). Inst. of Pharmaceutical Biology.
REGENERATION AND CHARACTERIZATION OF PROTOPLAST-DERIVED CELL LINES FROM DIGITALIS LANATA EHRH. AND DIGITALIS PURPUREA L. SUSPENSION CULTURES AFTER ELECTROFUSION UNDER MICROGRAVITY CONDITIONS
Thomas Baumann, W. Kreis, Werner Mehrle, R. Hampp, and E. Reinhard *In* ESA, Fourth European Symposium on Life Sciences Research in Space Nov. 1990 p 405-410 (For primary document see N91-19572 11-51)
(Grant BMFT-01-QV-8769)
Copyright Avail: NTIS HC/MF A25; EPD, ESTEC, Noordwijk, Netherlands, HC 80 Dutch guilders

The influence of microgravity on the yield of heterospecific fusion products after electrofusion of Digitalis lanata EHRH. and Digitalis purpurea L. (Scrophulariaceae) protoplasts was investigated. Electrofusions were performed during short time ballistic sounding rocket flights of the TEXUS 21 (1989) and TEXUS 25 (1990) missions in Kiruna, Sweden. Microgravity increased the yield of 1:1 fusion products about eightfold in comparison to terrestrial conditions. A novel feeder system was developed for the cultivation of protoplasts and their regeneration to fast growing cell lines. Two test systems proving the presence of Digitalis specific enzymes were employed for the detection of possible hybrids and the characterization of regenerated cell lines. ESA

N91-19653*# National Aeronautics and Space Administration. Marshall Space Flight Center, Huntsville, AL. Space Science Lab.
A NEW APPROACH TO ELECTROPHORESIS IN SPACE c29
Robert S. Snyder and Percy H. Rhodes *In* ESA, Fourth European Symposium on Life Sciences Research in Space Nov. 1990 p 411-415 (For primary document see N91-19572 11-51)
Copyright Avail: NTIS HC/MF A25; EPD, ESTEC, Noordwijk, Netherlands, HC 80 Dutch guilders CSCL 12A

Previous electrophoresis experiments performed in space are reviewed. There is sufficient data available from the results of these experiments to show that they were designed with incomplete knowledge of the fluid dynamics of the process including electrohydrodynamics. Redesigning laboratory chambers and operating procedures developed on Earth for space without understanding both the advantages and disadvantages of the microgravity environment has yielded poor separations of both cells and proteins. However, electrophoreris is still an important separation tool in the laboratory and thermal convection does limit its performance. Thus, there is a justification for electrophoresis but the emphasis of future space experiments must be directed toward basic research with model experiments to understand the microgravity environment and fluid analysis to test the basic principles of the process. ESA

N91-19654# Messerschmitt-Boelkow-Blohm G.m.b.H., Bremen (Germany, F.R.).
FREE FLOW ELECTROPHORESIS EXPERIMENT TEPE 3 ON TEXUS 24 c29
Volker Mang, K. Hannig, U. Zimmermann, M. Kowalski, and G. Kloeck (Wuerzburg Univ., Germany, F.R.) *In* ESA, Fourth European Symposium on Life Sciences Research in Space Nov. 1990 p 417-420 (For primary document see N91-19572 11-51)
Copyright Avail: NTIS HC/MF A25; EPD, ESTEC, Noordwijk, Netherlands, HC 80 Dutch guilders

Within the German sounding rocket program, TEXUS, a free flow electrophoresis experiment named TEPE 3 was performed. The objective was to enable direct comparison of the 1 g experiment results with the microgravity experiment results in the same experimental conditions with the same experiment solutions. The comparison of the cell separations shows the influence of microgravity in separation method electrophoresis. ESA

N91-19655# European Space Agency. European Space Research and Technology Center, ESTEC, Noordwijk (Netherlands).
TOWARDS BIOREGENERATIVE LIFE SUPPORT SYSTEMS c54
Francois Brechignac *In its* Fourth European Symposium on Life Sciences Research in Space Nov. 1990 p 421-429 (For primary document see N91-19572 11-51)
Copyright Avail: NTIS HC/MF A25; EPD, ESTEC, Noordwijk, Netherlands, HC 80 Dutch guilders

The need for bioregenerative technologies in order to support life in the closed space environments is essential, mainly because the servicing/resupply and associated mass launch capabilities are limited for economical reasons. Therefore, rooting from an analogy with the terrestrial ecosystem, the CELSS (Closed Ecological Life Support Systems) technology aims at regenerating food, oxygen and clean water, out of the various waste, in a controlled manner. As the first step towards the development of bioregenerative technologies, the concept of a small scale artificial pilot CELSS is currently being developed in order to support life of small consumers subject to future microgravity experimentation. In view of reducing the complexity, the pilot model is restricted to only two departments. A symbiotic Chorella is used, which can be tuned, by appropriate culture conditions (low ph), to convert most of the photosynthetically fixed carbon dioxide into maltose, a direct source of carbon and energy for a number of potential consumers. The present status of development of this engineering concept is presented along with the various technologies involved. ESA

N91-19656# Dornier System G.m.b.H., Friedrichshafen (Germany, F.R.).
PLANT PRODUCTION AS PART OF A CONTROLLED ECOLOGICAL LIFE SUPPORT SYSTEM (CELSS) c54
Katja David, Robert Backhaus (Deutsche Forschungsanstalt fuer Luft- und Raumfahrt, Cologne, Germany, F.R.), and Ake Ingemar Skoog *In* ESA, Fourth European Symposium on Life Sciences Research in Space Nov. 1990 p 431-434 (For primary document see N91-19572 11-51)
Copyright Avail: NTIS HC/MF A25; EPD, ESTEC, Noordwijk, Netherlands, HC 80 Dutch guilders

To reduce logistics costs of long distance and long duration manned space missions, resupply has to be reduced by recycling and in orbit production of consumables. An essential biochemical reaction in view of the life support requirements is the photosynthesis performed by algae and higher plants. For system closure it is needed in order to close the carbon loop. In contrast to a natural ecosystem, a controlled ecological life support system (CELSS) is designed to meet only human requirements and has to have a stable performance in every subsystem. Therefore, and because of the miniaturization of the system buffer, capacity and

tolerable variability are extremely reduced. The critical features of plant production in an artificial ecosystem like a CELSS are presented. ESA

N91-19657# Commissariat a l'Energie Atomique, Cadarache (France). Dept. de Physiologie Vegetale et Ecosystemes.
A GROUND BASED MODULE FOR EXPERIMENTATIONS OF CULTIVATIONS AND RECYCLING IN A CLOSED ENVIRONMENT **c54**
Marcel Jean Andre, D. Massimino, J. Massimino, and M.-C. Duchein *In* ESA, Fourth European Symposium on Life Sciences Research in Space Nov. 1990 p 435-440 Sponsored by CNES (For primary document see N91-19572 11-51)
Copyright Avail: NTIS HC/MF A25; EPD, ESTEC, Noordwijk, Netherlands, HC 80 Dutch guilders

Europe has a strong position in many of the scientific disciplines relevant to controlled ecological life support system (CELSS) program but actual experimentations are very rare and do not correspond to its position in other space research. To stimulate and to organize research, a project of a ground based prototype is proposed. Regarding realizations already running in the USSR and the U.S., this project would have the advantages of developing a European concept of a modular and flexible test bed open to collaborations and of using the know how of our countries in technology growth chambers and chemical engineering. Concepts are proposed to progressively link research in food productivity in artificial conditions and engineering of reclamation and recycling. Results of the pre-pilot stage are presented: long term cultivation in closed chamber, water recycling, computer control of carbon dioxide, oxygen, and water fluxes. ESA

N91-19658# Eidgenoessische Technische Hochschule, Zurich (Switzerland). Space Biology Group.
BIOLAB ON COLUMBUS: A FACILITY FOR BASIC SCIENCE AND BIOTECHNOLOGY **c14**
Augusto Cogoli *In* ESA, Fourth European Symposium on Life Sciences Research in Space Nov. 1990 p 441-444 (For primary document see N91-19572 11-51)
Copyright Avail: NTIS HC/MF A25; EPD, ESTEC, Noordwijk, Netherlands, HC 80 Dutch guilders

The status of the planning of multiuser facilities to be installed in the Columbus Attached Laboratory and the Columbus Free Flying Laboratory is presented. An international team of European scientists carried out a phase A study in 1988 to define the scientific objectives of Biolab, the biological multiuser facility for the Columbus Attached Laboratory. Two industrial phase A studies, performed in 1989, demonstrated the feasibility of the concept. Another scientific study for Biolab on the Columbus Free Flying Laboratory was completed in May 1990. ESA

N91-19659# Institute of Crop Science and Plant Breeding, Brunswick (Germany, F.R.).
PHYSIOLOGICAL CRITERIA AND REQUIREMENT OF BIOMASS PRODUCTION UNDER CONTROLLED ECOLOGICAL LIFE SUPPORT SYSTEMS **c54**
Nasir ElBassam, G. Mix, and Katja David (Dornier System G.m.b.H., Friedrichshafen, Germany, F.R.) *In* ESA, Fourth European Symposium on Life Sciences Research in Space Nov. 1990 p 445-448 (For primary document see N91-19572 11-51)
Copyright Avail: NTIS HC/MF A25; EPD, ESTEC, Noordwijk, Netherlands, HC 80 Dutch guilders

Based on the quantitative caloric and nutritional requirements of man under space conditions and on the physiological limits of plant growth and the chemical constituents of higher plant species, a biological life support system has been established in order to create selection parameters of higher plants for controlled ecological life support systems. The determination of the flow of the main macro-elements of plant development is identified in two major items: (1) consumption (inputs) of carbon dioxide, water, mineral nutrients, illumination, energy; and (2) production (outputs) of oxygen, transpiration, edible biomass and nonedible biomass. The quantity of each of these elements consumed or produced per day is given. The necessary area required for plant production to insure an ecological life support system for one person and one day can be summarized as follows: water 3 to 6, oxygen 6 to 10, and biomass 15 to 20 sq m. ESA

N91-19660# Colorado Univ., Boulder. BioServe Space Technologies Center.
TUNING THE EFFICIENCIES OF PLANT LIGHTING SYSTEMS: FROM PRIMARY ENERGY TO EDIBLE BIOMASS: THE LED AS AN ALTERNATIVE LIGHT SOURCE **c54**
Alexander Hoehn and Marvin W. Luttges *In* ESA, Fourth European Symposium on Life Sciences Research in Space Nov. 1990 p 449-454 (For primary document see N91-19572 11-51)
Copyright Avail: NTIS HC/MF A25; EPD, ESTEC, Noordwijk, Netherlands, HC 80 Dutch guilders CSCL 06K

For space based biological life support systems involving higher plants, an efficient light source capable of fully replacing natural sunlight for plant growth may be required. The conversion processes from some form of primary energy through light energy to edible biomass are described. Possibilities and limitations to improve the conversion efficiencies are outlined. The overall conversion efficiency is influenced by the selected hardware (power source, lamps, required filters, light distribution) and by the biological response to the light environment provided. For each conversion process, a corresponding energy conversion efficiency is defined. The possibilities for improvements are outlined. Only the product of all conversion efficiencies is a proper means of comparing different lighting alternatives. Light emitting diodes (LEDs) as an alternative lighting source for plant growth and photophysiological research, are compared to more commonly used plan lighting sources. Limitations and possible benefits are discussed for intermittent light (flash) as a possibility for energy savings. ESA

N91-19661# Fokker B.V., Amsterdam (Netherlands).
CELLS IN SPACE: SOUNDING ROCKET FACILITIES FOR CELL BIOLOGY AND BIOTECHNOLOGY IN MICROGRAVITY **c14**
Ron Huijser, Louis Aartman, and Harry Willemsen (Centrum voor Constructie en Mechanisatie, Nuenen, Netherlands) *In* ESA, Fourth European Symposium on Life Sciences Research in Space Nov. 1990 p 455-466 Sponsored in part by the Netherlands Agency for Aerospace Programs (For primary document see N91-19572 11-51)
Copyright Avail: NTIS HC/MF A25; EPD, ESTEC, Noordwijk, Netherlands, HC 80 Dutch guilders

The cells in space (CIS) multi-user sounding rocket facility has been used twice up to now for the simultaneous execution of four different cell biology experiments in some seven minutes of microgravity: the CIS 1 and CIS 2 modules were launched on MASER 3 and on MASER 4, respectively. At the same time, ground reference experiments were executed in a 1 g set-up. Technical and operational aspects of the existing CIS facility, emphasizing modularity and reconfigurability both in hardware and software are presented. Summarized flight reports are presented and future developments for CIS and beyond are addressed. ESA

N91-19662# Technische Univ., Vienna (Austria). Inst. of Plant Physiology.
PRODUCTIVITY AND PHOTOSYNTHESIS OF SELECTED CROP PLANTS UNDER ORBITAL LIGHT CONDITIONS: AN APPROACH TO SOLAR POWERED CELSS
Heidemarie V. Hurtl, Reinhard A. Sacher, and Karl M. Burian *In* ESA, Fourth European Symposium on Life Sciences Research in Space Nov. 1990 p 467-470 (For primary document see N91-19572 11-51)
Copyright Avail: NTIS HC/MF A25; EPD, ESTEC, Noordwijk, Netherlands, HC 80 Dutch guilders

Controlled ecological life support systems (CELSS) based upon higher plants might use natural sunlight rather than artificial illumination. In the case of a CELSS for a future space station in low Earth obit (LEO), these plants would have to deal with extremely short light/dark cycles. Due to the 90 minutes revolution period of the station, plants would be subjected to 60 minutes sunlight,

followed by 35 minutes darkness in shade. These orbital light/dark cycles (60 minutes/30 minutes) were simulated in a growth chamber, accompanied by control experiments under longday conditions (16 hours light/8 hours dark) in a second chamber. Biometric and gas-exchange measurements showed decreased productivity and carbon uptake in soybean (Glycine max L.), mung bean (Phaseolus mungo L.), and millet (Sorghum bicolor L.) under orbital light conditions. ESA

N91-19663# Deutsche Agentur fuer Raumfahrtangelegenheiten G.m.b.H., Bonn (Germany, F.R.).
THE SLOW-ROTATING CENTRIFUGE MICROSCOPE (NIZEMI): A NEW RESEARCH TOOL FOR TERRESTRIAL AND SPACE-RELATED GRAVITATIONAL BIOLOGY c14
Karlheinz Kreuzberg, R. Behrle, O. Joop, and R. Treichel (Dornier System G.m.b.H., Friedrichshafen, Germany, F.R.) *In* ESA, Fourth European Symposium on Life Sciences Research in Space Nov. 1990 p 471-474 (For primary document see N91-19572 11-51)
Copyright Avail: NTIS HC/MF A25; EPD, ESTEC, Noordwijk, Netherlands, HC 80 Dutch guilders

NIZEMI (German acronym) is a Spacelab facility for optical investigations of small biological or nonbiological transparent specimens under variable accelerations (0.001 to 2 g). A laboratory model (1 to 5 g) was tested by various research groups as a tool for investigations in gravitational biology (gravitaxis, gravitropism, threshold values). A flight model is scheduled for IML 2 mission (Jan. 1993). Basically, NIZEMI consists of a high performance microscope and a macroscope, both mounted on a rotating disc. Standard observation chambers will fit into the Biorack container. Sample temperature will be selectable between 18 and 37 C. The observed television images are displayed on a monitor and recorded continuously on video tape. The scientific program for IML 2 includes research on graviperception in plant cells, flagellates, cilliates, and slime mold. ESA

N91-19664# Celler Pflanzen- und Gewebelabor G.m.b.H., Celle (Germany, F.R.).
PLANT BIOTECHNOLOGY IN SPACE: FACTS AND SPECULATIONS
Ulrich G. Lohmann and Hildegard Jung-Heiliger *In* ESA, Fourth European Symposium on Life Sciences Research in Space Nov. 1990 p 475-479 (For primary document see N91-19572 11-51)
Copyright Avail: NTIS HC/MF A25; EPD, ESTEC, Noordwijk, Netherlands, HC 80 Dutch guilders

Chances and prospects of plant biotechnology in space are discussed from the viewpoint of a small company working with plant tissue cultures. As a fact of current space biotechnology, the possible production of new pharmaceutical metabolites by using cell cultures of medicinal plants is evaluated. The influence of microgravity on phase partition, surface tension, convection or capillarity may also be used for the development of new extraction and separation procedures for natural compounds. Thus, purity grades of plant cell metabolites may be enhanced. The role of innovative small companies in the development of highly specialized bioreactor systems for space biotechnology is illustrated. ESA

N91-19665*# National Aeronautics and Space Administration. Marshall Space Flight Center, Huntsville, AL.
PROTEIN PURIFICATION IN MULTICOMPARTMENT ELECTROLYZERS FOR CRYSTAL GROWTH OF r-DNA PRODUCTS IN MICROGRAVITY c29
Pier Giorgio Righetti, Elena Casale, Daniel Carter, Robert S. Snyder, Elisabeth Wenisch, and Michel Faupel (Ciba-Geigy A.G., Basel, Switzerland) *In* ESA, Fourth European Symposium on Life Sciences Research in Space Nov. 1990 p 481-484 Sponsored in part by Italian Space Agency (For primary document see N91-19572 11-51)
Copyright Avail: NTIS HC/MF A25; EPD, ESTEC, Noordwijk, Netherlands, HC 80 Dutch guilders CSCL 12A

Recombinant-DNA (deoxyribonucleic acid) (r-DNA) proteins, produced in large quantities for human consumption, are now available in sufficient amounts for crystal growth. Crystallographic analysis is the only method now available for defining the atomic arrangements within complex biological molecules and decoding, e.g., the structure of the active site. Growing protein crystals in microgravity has become an important aspect of biology in space, since crystals that are large enough and of sufficient quality to permit complete structure determinations are usually obtained. However even small amounts of impurities in a protein preparation are anathema for the growth of a regular crystal lattice. A multicompartment electrolyzer with isoelectric, immobiline membranes, able to purify large quantities of r-DNA proteins is described. The electrolyzer consists of a stack of flow cells, delimited by membranes of very precise isoelectric point (pI, consisting of polyacrylamide supported by glass fiber filters containing Immobiline buffers and titrants to uniquely define a pI value) and very high buffering power, able to titrate all proteins tangent or crossing such membranes. By properly selecting the pI values of two membranes delimiting a flow chamber, a single protein can be kept isoelectric in a single flow chamber and thus, be purified to homogeneity (by the most stringent criterion, charge homogeneity). ESA

N91-19666# Erno Raumfahrttechnik G.m.b.H. Bremen (Germany, F.R.).
DEVELOPMENT OF A MINIATURE BIOLOGY FACILITY c14
J. Warrelmann and R. Klintworth *In* ESA, Fourth European Symposium on Life Sciences Research in Space Nov. 1990 p 485-487 (For primary document see N91-19572 11-51)
Copyright Avail: NTIS HC/MF A25; EPD, ESTEC, Noordwijk, Netherlands, HC 80 Dutch guilders

The miniature biology facility and its payload components are presented. The miniature biology facility provides a simple life support system for plants under conditions of microgravity and was developed in order to study the scientific problems in the areas of gravitational biology, plant physiology, cell and development biology, and radiology. It is also for the study of technical problems in the areas of controlled life support systems (control instructions, stability of sensors, precision of tests results) and chemical sample fixation before end of mission. ESA

N91-19667# Bonn Univ. (Germany, F.R.). Botanisches Inst.
GRAVIPERCEPTION IN PLANTS
A. Sievers *In* ESA, Fourth European Symposium on Life Sciences Research in Space Nov. 1990 p 491 (For primary document see N91-19572 11-51)
Copyright Avail: NTIS HC/MF A25; EPD, ESTEC, Noordwijk, Netherlands, HC 80 Dutch guilders

Graviperception in plants is discussed and the statocytes, the specialized plant cells which transduce the gravity stimulus into a physiological signal which is transmitted to that part of the organ which responds to gravity via differential flank growth, are described in detail. Statoliths may trigger the transduction mechanisms via actin filaments. Electronical responses and Ca-calmodulin are involved in stimulus transduction. References for further information are given in this one page document. ESA

N91-19668# Ohio State Univ., Columbus. Dept. of Plant Biology.
PLASTIDS AND GRAVITY PERCEPTION
Fred D. Sack *In* ESA, Fourth European Symposium on Life Sciences Research in Space Nov. 1990 p 493-495 (For primary document see N91-19572 11-51)
Copyright Avail: NTIS HC/MF A25; EPD, ESTEC, Noordwijk, Netherlands, HC 80 Dutch guilders

The role of plastids in gravity sensing is discussed and results from experiments are presented. Although it has long been thought that the mass of amyloplasts triggers plant gravity perception, several starch deficient mutants (of Arabidopsis and Nicotiana) have gravitropic roots. Thus, amyloplasts and starch are not essential for gravity perception. But since roots of both mutants show significantly reduced gravitropic sensitivity it is likely that starch contributes to full sensitivity and that amyoplasts play a role in perception in wild type roots. Starch deficiency reduced

gravitropism much more severely in hypocotyls than in roots. The starch deficient plastids may be the likeliest candidates to function in perception in mutant roots. Alternatively, another unknown system of perception might function in addition to amyloplasts. ESA

N91-19669# Bonn Univ. (Germany, F.R.). Botanisches Inst.
GRAVITATIONAL EFFECTS ON SUBCELLULAR STRUCTURES OF PLANT CELLS
Dieter Volkmann and A. Sievers *In* ESA, Fourth European Symposium on Life Sciences Research in Space Nov. 1990 p 497-501 Sponsored by BMFT and the Ministerium fuer Wissenschaft und Forschung (For primary document see N91-19572 11-51)
Copyright Avail: NTIS HC/MF A25; EPD, ESTEC, Noordwijk, Netherlands, HC 80 Dutch guilders

Two sets of experiments performed with cress seedlings under reduced gravitational force (RGF) are described. Dry seeds were activated in orbit and grew for 32 hours under RGF. Electron microscopy of material which was chemically fixed under RGF showed remarkable differences between samples from ground controls and inflight probes. Under RGF the amount of endoplasmic reticulum (ER) membranes and lipid droplets increased up to 400 and 200 percent respectively in gravity perceiving cells, whereas the amount of starch decreased by 30 percent. Lipid droplets showed a strong tendency for confluence. In meristematic (embryonic) cells the amount of protein crystals dropped down by at least 60 percent. The number of secretory vesicles has highly increased especially in fast growing cells of the hypocotyl. Day old seedlings were launched on a sounding rocket and grew for 6 minutes under RGF. Within these 6 minutes sedimentable particles in root statocytes moved up to 3 microns in opposite direction of the originally acting gravity vector. These effects are explained by environmental stress factors including RGF. ESA

N91-19670*# State Univ. of New York, Stony Brook. Dept. of Biochemistry and Cell Biology.
PLANT DEVELOPMENT IN SPACE: OBSERVATIONS ON ROOT FORMATION AND GROWTH
H. G. Levine, R. P. Kann, and Abraham D. Krikorian *In* ESA, Fourth European Symposium on Life Sciences Research in Space Nov. 1990 p 503-508 (For primary document see N91-19572 11-51)
(Contract NAS1-11395; NAGw-1529)
Copyright Avail: NTIS HC/MF A25; EPD, ESTEC, Noordwijk, Netherlands, HC 80 Dutch guilders CSCL 06C

Root growth in space is discussed and observations on root production from plants flown as part of the Chromex project that were defined as to their origin, stage of development and physiological status, are presented. Roots were generated from fully differentiated, aseptically maintained individuals of Haplopappus gracilis (Compositae) under spaceflight conditions. Results are compared for tissue culture generated plantlets and comparably sized seedling clone individuals, both of which had their roots trimmed on Earth before they were loaded into NASA's plant growth unit and subjected to a 5 day shuttle flight (STS-29). Asepsis was maintained throughout the experiment. Overall root production was 40 to 50 percent greater under spaceflight conditions than during ground control tests. However, root formation slowed down towards the end of the flight. This decrease in new roots did not occur in the ground controls that sought to simulate flight except for microgravity. ESA

N91-19671# Academy of Sciences of the Lithuanian SSR, Vilnius. Inst. of Botany.
PLANT GROWTH UNDER MICROGRAVITY CONDITIONS: EXPERIMENTS AND PROBLEMS
A. J. Merkys *In* ESA, Fourth European Symposium on Life Sciences Research in Space Nov. 1990 p 509-515 (For primary document see N91-19572 11-51)
Copyright Avail: NTIS HC/MF A25; EPD, ESTEC, Noordwijk, Netherlands, HC 80 Dutch guilders

The results of the experiments carried out during the years 1974 to 1989 on board the orbital satellites and spacecrafts with the purpose of finding out the peculiarities of growth and development of higher plants under microgravity conditions are summarized. The seed to seed growth and development of plants under microgravity conditions are shown to be feasible. Methodological aspects of the experiments made to determine the role of gravity in the growth and development of plants are discussed. The necessity to improve research techniques is pointed out. ESA

N91-19672# Paris VI Univ. (France).
EFFECT OF GRAVITY ON THE DISTRIBUTION OF ELECTRON DENSE CHROMATIN IN THE NUCLEUS OF ROOT STATOCYTES
G. Perbal and Dominique Driss-Ecole *In* ESA, Fourth European Symposium on Life Sciences Research in Space Nov. 1990 p 517-520 (For primary document see N91-19572 11-51)
(Grant CNES-88/1305)
Copyright Avail: NTIS HC/MF A25; EPD, ESTEC, Noordwijk, Netherlands, HC 80 Dutch guilders

Ultrastructural studies of the root statocyte of lentil seedlings showed that in these cells there was a polarization of the organelles with respect to the g vector. This cellular model permitted the investigation of the effects of gravity on the distribution of Electron Dense Chromatin (EDC) in the nucleus. The clustering of EDC was studied by means of a specific computer program. The texture was similar in microgravity and on the 1 g centrifuge. The distribution of EDC and that of nucleolus was different in both g conditions. It was concluded that the orientation of the nucleus depended upon gravity. ESA

N91-19673# Erlangen-Nuremberg Univ. (Germany, F.R.). Inst. of Botany.
GRAVIORIENTATION IN PHOTOSYNTHETIC FLAGELLATES
Donat-P. Haeder and Kurt Vogel *In* ESA, Fourth European Symposium on Life Sciences Research in Space Nov. 1990 p 521-526 Sponsored by BMFT (For primary document see N91-19572 11-51)
Copyright Avail: NTIS HC/MF A25; EPD, ESTEC, Noordwijk, Netherlands, HC 80 Dutch guilders

A real time image analysis system was used to study motility and graviorientation in the flagellate, Euglena gracilis, before, during and after a sounding rocket (TEXUS) experiment as well as in a slow rotating centrifuge microscope (NIZEMI (German acronym)). Under 1 g conditions, the cells orient negative gravitactically and move randomly under microgravity conditions. The precision of graviorientation increases significantly at higher acceleration forces up to about 3 g in the NIZEMI and most cells were able to swim even against an acceleration vector of 4.5 g. Under microgravity conditions the velocity is about 20 percent higher than at 1 g and the swimming velocity decreases at higher acceleration forces. Gravitaxis was impaired after short exposure to UV radiation which indicates that gravitaxis may be mediated by an active physiological receptor rather than a passive physical effect. ESA

N91-19674# Aarhus Univ. (Denmark). Inst. of Molecular Biology.
PLANT PROTOPLAST DEVELOPMENT ON BIOKOSMOS 9
Ole Rasmussen, Felix K. Gmuender, M. Tairbekov, E. L. Kordyum, V. V. Lozovaya, C. Baggerud, and T.-H. Iversen (Trondheim Univ., Norway) *In* ESA, Fourth European Symposium on Life Sciences Research in Space Nov. 1990 p 527-530 Sponsored by Danish Space Board (For primary document see N91-19572 11-51)
Copyright Avail: NTIS HC/MF A25; EPD, ESTEC, Noordwijk, Netherlands, HC 80 Dutch guilders

The aim is to obtain information on the effects of gravity on basic cell biological processes such as growth, division and differentiation. During a 14 day space flight onboard the Soviet Biokosmos 9 satellite, the growth and development of protoplasts from rapeseed and carrots was studied and growth of protoplasts in the two different culture chambers was compared. The growth of both carrot and rapeseed protoplasts is decreased with 18 and

44 percent, respectively, after 14 days in orbit compared to the ground control. A significant decrease (46 and 29 percent) in production of cellulose was found in rapeseed and carrot, respectively. In general, developmental processes are retarded in flight samples. ESA

N91-19675# Institut fuer Landwirtschaftliche Botanik, Bonn (Germany, F.R.).
ELECTROFUSION AND REGENERATION OF PROTOPLASTS FROM SUNFLOWER (HELIANTHUS ANNUUS L.)
Ursula Biedinger, P. Schmitz, and Heide Schnabl *In* ESA, Fourth European Symposium on Life Sciences Research in Space Nov. 1990 p 531-533 (For primary document see N91-19572 11-51)
Copyright Avail: NTIS HC/MF A25; EPD, ESTEC, Noordwijk, Netherlands, HC 80 Dutch guilders

These investigations contribute to the ground based studies for a D2 mission supported research in order to study membrane damage under gravity and microgravity conditions and to increase the vitality and the yield of somatic hybrids during the electrofusion process of sunflower protoplasts. Ethane, the final product of lipid peroxidation, was used as an indicator of membraneous deterioration. In parallel, a suitable regeneration system for protoplasts was developed resulting in root and shoot formation. ESA

N91-19676# Deutsche Forschungsanstalt fuer Luft- und Raumfahrt, Cologne (Germany, F.R.). Inst. for Aerospace Medicine.
RESPONSES OF PHYSARUM POLYCEPHALUM TO VARYING LIGHT LEVELS DURING FAST CLINOSTAT ROTATION: A SCIENTIFIC PREPARATION OF AN ESA BIORACK EXPERIMENT DURING THE IML-1 MISSION
Ingrid Block, Andreas Wolke, and Wolfgang Briegleb *In* ESA, Fourth European Symposium on Life Sciences Research in Space Nov. 1990 p 535-539 (For primary document see N91-19572 11-51)
Copyright Avail: NTIS HC/MF A25; EPD, ESTEC, Noordwijk, Netherlands, HC 80 Dutch guilders

A scientific preparation of an ESA experiment during the IML 1 (International Microgravity Laboratory) mission is reported. The aim of this investigation was to repeat older experiments on the fast rotating clinostat with the slime mold Physarum polycephalum and to combine them with light sensitivity tests. The need to submerge the organism led to some physiological problems, which were partly overcome. The advantage of submersion for studies of effects of gravity for biological systems is discussed. The study shows that it is important to use the fast clinostat for analyzing results of cell biological experiments performed in space. ESA

N91-19677# Erlangen-Nuremberg Univ. (Germany, F.R.). Inst. of Botany.
SIMULTANEOUS TRACKING OF FLAGELLATES IN REAL TIME BY IMAGE ANALYSIS
Kurt Vogel and Donat-P. Haeder *In* ESA, Fourth European Symposium on Life Sciences Research in Space Nov. 1990 p 541-545 Sponsored by DFG (For primary document see N91-19572 11-51)
Copyright Avail: NTIS HC/MF A25; EPD, ESTEC, Noordwijk, Netherlands, HC 80 Dutch guilders

The hardware and software components which allow up to several hundred organisms to be tracked simultaneously, are described. Real time tracking of many microorganisms simultaneously is achieved by the hardware and software components described. Four video frames are taken at 80 millisecond intervals, digitized at a resolution of 512 by 512 pixels at 256 gray levels each and stored in a dedicated memory. The positions of all organisms are determined in the subsequent frames using the chain code algorithm and the movement vectors (direction and velocity) are calculated and stored in the form of deviation angles from a predefined stimulus direction. Subsequent programs determine circular histograms of movement directions and velocities. Examples of orientation patterns are given for both photo and gravitaxis in the dinoflagellate, Peridinium gatunense. ESA

N91-19678# Deutsche Forschungsanstalt fuer Luft- und Raumfahrt, Cologne (Germany, F.R.). Inst. for Aerospace Medicine.
GRAVITAXIS IN PHYSARUM POLYCEPHALUM
Andreas Wolke, Wolfgang Briegleb, and F. Achenbach (Bonn Univ., Germany, F.R.) *In* ESA, Fourth European Symposium on Life Sciences Research in Space Nov. 1990 p 547-549 (For primary document see N91-19572 11-51)
Copyright Avail: NTIS HC/MF A25; EPD, ESTEC, Noordwijk, Netherlands, HC 80 Dutch guilders

The aim is to develop new test conditions which affect the gravitactic behavior of Physarum. These investigations help to reveal information about the mechanisms of gravi-perception and the regulation of gravitaxis in single cells using Physarum as a model organism. The acellular slime mold Physarum polycephalum is discussed to be an ideal model organism to study gravity perception and the regulation of gravitaxis in single cells. Since a specialized gravity receptor has not yet been found in Physarum it is interesting to observe that the organism performs a clear gravity oriented locomotion. Gravitaxis in Physarum seems to be an actively regulated process, for the sign of the gravitaxis can be altered by varying external conditions. ESA

N91-19679# Commissariat a l'Energie Atomique, Fontenay-aux-Roses (France). Centre d'Etudes Nucleaires.
NEW EXPERIMENTAL APPROACH IN QUALITY FACTOR AND DOSE EQUIVALENT DETERMINATION DURING A LONG TERM MANNED SPACE MISSION **c54**
Van Dat Nguyen, P. Bouisset, N. Parmentier, M. Siegrist, Y. A. Akatov, V. V. Archangelsky, S. Vorojtsov, S. B. Koslova, V. G. Mitrikas, and V. M. Petrov (Institute of Biomedical Problems, Moscow, USSR) et al *In* ESA, Fourth European Symposium on Life Sciences Research in Space Nov. 1990 p 555-558 (For primary document see N91-19572 11-51)
Copyright Avail: NTIS HC/MF A25; EPD, ESTEC, Noordwijk, Netherlands, HC 80 Dutch guilders

Due to high LET (Linear Energy Transfer) particles existing in space environment, the knowledge of the quality factor is one of priority in radiation protection efforts. During the French Soviet space mission Aragatz, the experiment CIRCE (complex beam in space counter integrator) had recorded dose equivalent and quality factor values inside the MIR station. Results obtained with a new experimental approach by using an active dose equivalent meter based on microdosimetric techniques and a low pressure tissue equivalent proportional counter are presented. In terms of lineal energy, the CIRCE device works in the 0.3 to 1200 keV micron range in tissue. The average dose equivalent is equal to 0.6 mSv. per day and the mean value of quality factor is equal to 1.9. Through the SAA the dose equivalent rate rapidly increases until 1.20 mSv./h and the corresponding quality factor decreases to 1.4. ESA

N91-19680# Johann-Wolfgang-Goethe-Univ., Frankfurt am Main (Germany, F.R.). Botanisches Inst.
GENETIC RISK AND PHYSIOLOGICAL STRESS INDUCED BY HEAVY IONS **c52**
A. R. Kranz *In* ESA, Fourth European Symposium on Life Sciences Research in Space Nov. 1990 p 559-563 (For primary document see N91-19572 11-51)
(Grant BMFT-01-QV-85650)
Copyright Avail: NTIS HC/MF A25; EPD, ESTEC, Noordwijk, Netherlands, HC 80 Dutch guilders

For the evaluation of heavy ion radiation to human beings on Earth and in space, complete estimation of the total damage (gene mutation, chromosome aberration, cell lethality) of an individual (high-ionizing high energy particles) ion hit is needed. For this the resting embryo of the Arabidopsis seed was a successful test subject in accelerator and space flight experiments. The high-ionizing high energy particles' effect on the genetic lethality, tumorization and the physiological germination and flowering were

investigated. The observed endpoints of the heavy ion effect correlated with energy and charge of the high-ionizing high energy particles and the target size of cell nucleus. Particular high-ionizing high energy particles cross sections and specific damage endpoints were obtained resembling both the physiological stress and genetic risk. ESA

N91-19681# Centre National de la Recherche Scientifique, Orleans (France). Centre de Biophysique Moleculaire.
EXTRATERRESTRIAL ORGANIC MOLECULES AND THE EMERGENCE OF LIFE ON EARTH
Andre Brack *In* ESA, Fourth European Symposium on Life Sciences Research in Space Nov. 1990 p 565-569 (For primary document see N91-19572 11-51)
Copyright Avail: NTIS HC/MF A25; EPD, ESTEC, Noordwijk, Netherlands, HC 80 Dutch guilders

Terrestrial life can be schematically described as organic molecules organized in liquid water. According to the classical scenario, the organic building blocks required for early life were produced from simple organic molecules formed in the primitive reducing atmosphere. Amino acids, purine and pyrimidine bases, sugars, lipid like materials have been produced in the laboratory under simulating conditions. Geochemists now favor a less reducing atmosphere dominated by carbon dioxide. In such an atmosphere, very few building blocks are formed in the laboratory. Impact of extraterrestrial organic molecules may represent an alternative supply. Contemporary experimental support for such an alternative scenario will be examined at ground level (micrometeorites and meteorites), stratospheric and Earth's orbit level (cosmic dust) and interplanetary level (comets). The analysis of organic molecules in the solar system will help in understanding the emergence of life on Earth. ESA

N91-19682# Johann-Wolfgang-Goethe-Univ., Frankfurt am Main (Germany, F.R.). Botanisches Inst.
DEFECTIVE EMBRYOGENESIS OF ARABIDOPSIS INDUCED BY COSMIC HZE-PARTICLES
U. Bork, A. R. Kranz, S. Sommer, M. W. Immermann, and M. Pickert *In* ESA, Fourth European Symposium on Life Sciences Research in Space Nov. 1990 p 571-572 (For primary document see N91-19572 11-51)
(Grant BMFT-01-QV-85650)
Copyright Avail: NTIS HC/MF A25; EPD, ESTEC, Noordwijk, Netherlands, HC 80 Dutch guilders

Dry seeds containing embryos of the crucifer plant Arabidopsis thaliana (L.) Heynh. were flown in the orbit for 13 days on Biokosmos 8 and for 14 days on the Biokosmos 9 satellite. Among several biological endpoints of radiation damage the summarized damage and the mutation frequencies of embryonic lethal genes were calculated (m sub a, m sub b, and m sub c based on segregating plants, segregating siliques and total sample of embryos). In this way, for the first time a stabilized genetic defect preferentially caused by cosmic HZE particle in an eukaryotic organism is presented. It is expressed by lethal genes of embryogenesis after recombination in the offspring. ESA

N91-19683# Giessen Univ. (Germany, F.R.). Strahlenzentrum.
BIOLOGICAL ACTION OF SINGLE ACCELERATED HEAVY IONS ON INDIVIDUAL YEAST CELLS
Michael Kost, Juergen Kiefer, and Guenter Lenz (Gesellschaft fuer Schwerionenforschung m.b.H., Darmstadt, Germany, F.R.) *In* ESA, Fourth European Symposium on Life Sciences Research in Space Nov. 1990 p 573-575 Sponsored by Gesellschaft fuer Schwerionenforschung and BMFT (For primary document see N91-19572 11-51)
Copyright Avail: NTIS HC/MF A25; EPD, ESTEC, Noordwijk, Netherlands, HC 80 Dutch guilders

Yeast cells were shown to be a suitable test organism for heavy ion irradiation experiments in space or at ground based particle accelerators. Because of the small numbers involved in space the action of single ions on individual cells has to be investigated. This is possible by computer supported image analysis. Cells are embedded in non-nutrient agar and placed on a nuclear track detector. After irradiation, the cells are incubated under growth conditions for the colony forming test. Subsequent track etching reveals the latent particle tracks. Digitized image data of specially marked areas on the track detector allow one to correlate the distance between cell and particle track with the survival probability of the specific biological object. Experiments were performed with neon, argon, xenon and uranium ions with specific energies between 8 and 14 MeV/u. Information on the correlation between particle type and absolute effectiveness, especially with respect to direct hits, can be obtained. Furthermore the influence of the impact parameter as well as the significance of ion type and energy can be studied. It was found that absolute effectiveness increases with ion charge. Penumbra effects become more significant with increasing ion energy. ESA

N91-19684# Institute of Biomedical Problems, Moscow (USSR).
PRINCIPLE AND REALIZATION OF THE INSTRUMENT USED FOR THE CIRCE EXPERIMENT ON BOARD THE MIR STATION c14
V. M. Petrov, J. A. Akatov, S. B. Kozlova, Van Dat Nguyen, J. Kerlau, M. Siegrist, and J. F. Zwilling (Centre National d'Etudes Spatiales, Toulouse, France) *In* ESA, Fourth European Symposium on Life Sciences Research in Space Nov. 1990 p 577-580 (For primary document see N91-19572 11-51)
Copyright Avail: NTIS HC/MF A25; EPD, ESTEC, Noordwijk, Netherlands, HC 80 Dutch guilders

Absorbed dose and dose equivalent measurements on board the MIR station used a microdosimetric system CIRCE made in France. The system includes the tissue equivalent proportional counter and electronic unit based on a microprocessor. Metrological characteristics on the CIRCE device are given. The accuracy of the measurements is 10 percent. The measurement results were recorded on the special memory unit SERCOM. The metrological characteristics of the CIRCE device were investigated with accelerators and neutron and gamma sources. ESA

N91-19685# Johann-Wolfgang-Goethe-Univ., Frankfurt am Main (Germany, F.R.). Botanisches Inst.
ARABIDOPSIS THALIANA (HEYNH.) POLLEN: A NEW TOOL IN HEAVY IONS RADIATION
M. Pickert, A. R. Kranz, and S. Sommer *In* ESA, Fourth European Symposium on Life Sciences Research in Space Nov. 1990 p 581-582 Sponsored by Gesellscheft fuer Schwerionen-forschung (For primary document see N91-19572 11-51)
Copyright Avail: NTIS HC/MF A25; EPD, ESTEC, Noordwijk, Netherlands, HC 80 Dutch guilders

Arabidopsis thaliana pollen was irradiated with three different accelerated heavy ions (U, Pb, Ar). The pollen vitality was measured and the cross section was calculated. A pollination with irradiation pollen on a non-irradiated male sterile mother plant was made and the next two generations investigated and screened. The results of these experiments demonstrate clearly that irradiated pollen can induce highly lethal mutants in the following generations. ESA

N91-19686# Giessen Univ. (Germany, F.R.). Strahlenzentrum.
MUTATION INDUCTION IN DRIED YEAST CELLS AFTER IRRADIATION WITH SELECTED UVC- AND UVB-WAVELENGTHS COMPARED TO SIMULATED SUNLIGHT
Karin Schenk, Karin Pawlowsky, and Juergen Kiefer *In* ESA, Fourth European Symposium on Life Sciences Research in Space Nov. 1990 p 583-585 (For primary document see N91-19572 11-51)
Copyright Avail: NTIS HC/MF A25; EPD, ESTEC, Noordwijk, Netherlands, HC 80 Dutch guilders

Since UV induces a variety of photolesions, the mutagenic action in eukaryotic cells is still an important question. Being simple eukaryotic cell systems, yeast cells are suitable organisms for mutation studies, also under space conditions. Yeast cells of different repair capacities were exposed to natural solar UV light during the European EURECA mission. The involvement of repair processes after irradiation under space conditions was studied.

Because of the long flight duration dried yeast cells had to be used. Laboratory studies consisted of exposure to monochromatic light between 160 nm and 313 nm as well as irradiation with simulated sunlight. Action spectra for survival and mutation induction were determined. Comparison of the whole spectrum irradiation to single wavelength exposure demonstrates the mutagenic potential of simulated sunlight. ESA

N91-19687*# National Aeronautics and Space Administration. John F. Kennedy Space Center, Cocoa Beach, FL.
CENTRAL AND PERIPHERAL CARDIOVASCULAR RESPONSES TO ELECTRICALLY INDUCED AND VOLUNTARY LEG EXERCISE **c52**
B. Saltin, S. Strange, J. Bangsbo, C. K. Kim, M. Duvoisin, A. Hargens, and P. D. Gollnick (Washington State Univ., Pullman.) *In* ESA, Fourth European Symposium on Life Sciences Research in Space Nov. 1990 p 591-595 (For primary document see N91-19572 11-51)
Copyright Avail: NTIS HC/MF A25; EPD, ESTEC, Noordwijk, Netherlands, HC 80 Dutch guilders CSCL 06P

With long missions in space countermeasures have to be used to secure safe operations in space and a safe return to Earth. Exercises of various forms have been used, but the question has arisen whether electrically induced contractions of muscle especially sensitive to weightlessness and crucial for man's performance would aid in maintaining their optimal function. The physiological responses both to short term and prolonged dynamic exercise performed either voluntarily or induced by electrical stimulation were considered. The local and systemic circulatory responses were similar for the voluntary and electrically induced contractions. The metabolic response was slightly more pronounced with electrical stimulation. This could be a reflection of not only slow twitch (type 1) but also fast twitch (type 2) fibers being recruited when the contractions were induced electrically. Intramuscular pressure recordings indicated that the dominant fraction of the muscle group was engaged regardless of mode of activation. Some 70 percent of the short term peak voluntary exercise capacity could be attained with electrical stimulation. Thus, electrically induced contractions of specific muscle groups should indeed be considered as an efficient countermeasure. ESA

N91-19688# Sheffield Univ. (England). Dept. of Medical Physics and Clinical Engineering.
VISUALISATION OF FLUID SHIFTS WITHIN THE BODY DURING A PARABOLIC FLIGHT BY MEASUREMENTS OF ELECTRICAL BIO-IMPEDANCE **c52**
Frank J. McArdle, David Grundy, B. H. Brown, and D. C. Barber *In* ESA, Fourth European Symposium on Life Sciences Research in Space Nov. 1990 p 597-602 (For primary document see N91-19572 11-51)
Copyright Avail: NTIS HC/MF A25; EPD, ESTEC, Noordwijk, Netherlands, HC 80 Dutch guilders

In recent years, a tomographic version of the four electrode method of measuring electrical impedance was developed which can produce low resolution images of resistivity changes within the human body. The use of this technique to demonstrate fluid shifts into and out of the thorax of four subjects during a parabolic flight campaign is investigated. Sequences of images were collected, at one second intervals, during parabolic maneuvers in sitting, standing and supine postures and the resistivity changes in the cardiovascular structures, the lungs and in the spinal region are described. The results illustrate the possibilities of this new non-invasive technique for monitoring subjects during spaceflight. The equipment required can be made small enough to be worn by the subject. ESA

N91-19689# Lyon-1 Univ., Villeurbanne (France). Lab. d'Environ. Physiologie.
VOLUME REGULATING HORMONES, FLUID AND ELECTROLYTE MODIFICATIONS DURING THE ARAGATZ MISSION (MIR STATION) **c52**
Guillemette Gauquelin, G. Geelen, C. Gharib, A. I. Grigoriev, Antonio Guell, R. Kvetnansky, L. Macho, V. Noskov, P. Pasi, and J. Soukanov (Institute of Biomedical Problems, Moscow, USSR) et al *In* ESA, Fourth European Symposium on Life Sciences Research in Space Nov. 1990 p 603-608 Sponsored in part by CNES (For primary document see N91-19572 11-51)
(Grant DRET-89-237)
Copyright Avail: NTIS HC/MF A25; EPD, ESTEC, Noordwijk, Netherlands, HC 80 Dutch guilders

During a 25 day flight on board the MIR station parameters involved in blood volume regulation were studied. Blood samples were taken to determine electrolytes and osmolality. Epinephrine, norepinephrine, dopamine, Anti Diurectic Hormone (ADH), Atrial Natriuretic Factor (ANF), Plasma Renin Activity (PRA), aldosterone, and cortisol, were measured at days 9 and 20 of the spaceflight. Urine was collected at days 5 and 19 to measure the same parameters (except PRA). The modifications of these hormones (generally increased) are discussed and compared to previous flights. Three factors may account for the results, especially the increase in ADH: the well known initial fluid shift in weightlessness and the adaptative mechanisms following this phase, stress, and environmental factors (CO2 and temperature). ESA

N91-19690# Saint-Etienne Univ. (France). Lab. de Biologie du Tissu Osseux.
ARAGATZ MISSION: BONE DENSITOMETRIC RESULTS OBTAINED WITH THE SCOOP MINISCANNER
C. Alexandre, J. F. Pouget, Laurence Vico, and P. Ruegsegger (Eidgenoessische Technische Hochschule, Zurich, Switzerland) *In* ESA, Fourth European Symposium on Life Sciences Research in Space Nov. 1990 p 609-610 (For primary document see N91-19572 11-51)
Copyright Avail: NTIS HC/MF A25; EPD, ESTEC, Noordwijk, Netherlands, HC 80 Dutch guilders

Densiometry equipment which, by measuring the alternation of monoenergetic x rays, makes it possible to appreciate the calcium mass of two peripheral bones, the tibia and radius, is discussed with reference to investigating the occurrence of weightlessness induced osteoporosis. The peripherical calcium mass (tibia and radius) was measured before and after a 28 day space flight at both proximal and distal sites. None of the results obtained were significant although there was a tendency towards an increase in calcium mass in the distal area of the right radius. It is thought that there is a calcium transfer from non-weightbearing towards weightbearing bones in order to balance the body calcium density. Recommendations for future research are given. ESA

N91-19691# Academy of Sciences (USSR), Moscow.
THE REFERENCE SYSTEMS FOR TACTILE PERCEPTION AND FOR THE ORIENTATION WITH RESPECT TO BODY **c52**
Victor S. Gurfinkel, F. Lestienne, Y. S. Levick, K. E. Popov, and L. Lefort (Centre National de la Recherche Scientifique, Paris, France) *In* ESA, Fourth European Symposium on Life Sciences Research in Space Nov. 1990 p 611-615 (For primary document see N91-19572 11-51)
Copyright Avail: NTIS HC/MF A25; EPD, ESTEC, Noordwijk, Netherlands, HC 80 Dutch guilders

The state of spatial orientation systems in microgravity is investigated. The perception of the orientation of complex tactile stimuli (letters and numbers) applied to the different skin areas in different positions of body parts was studied in the conditions of prolonged space flight by means of special tactile matrix. In the tactile perception task in microgravity, the reaction time was the same as on the Earth and the number of mistakes was even less than the preflight testing. The process of drawing ellipses in air by arm motions with long axis oriented parallel or perpendicularly to the longitudinal body axis was studied with the aid of kinesigraph. The orientation of the ellipses relative to the body axis in weightlessness was the same as in preflight tests in standing conditions. It is concluded that a egocentrical reference system ensures the normal performance in many sensorimotor tasks in the absence of gravitational reference. ESA

N91-19692# Centre National de la Recherche Scientifique, Paris (France). Lab. de Physiologie Neurosensorielle.
GAZE CONTROL AND SPATIAL MEMORY IN WEIGHTLESSNESS **c52**
Claudie Andre-Deshays, I. Israel, A. Berthoz, K. E. Popov, and M. I. Lipschits (Academy of Sciences, USSR, Moscow) *In* ESA, Fourth European Symposium on Life Sciences Research in Space Nov. 1990 p 617-621 Sponsored by CNES (For primary document see N91-19572 11-51)
Copyright Avail: NTIS HC/MF A25; EPD, ESTEC, Noordwijk, Netherlands, HC 80 Dutch guilders

Visual information is quite important for spatial orientation, and still more necessary when other sensory inputs may be altered, as in weightlessness. In order to study gaze control, during the long duration flight named Aragatz on board of the MIR Space Station, a series of experiments were performed which explored the different oculomotor subsystems involved in the control of gaze during orientation to a fixed visual target and when tracking a moving target, and the performances of the saccadic system during orientation to remembered target positions, in complete darkness. Two cosmonauts participated in these experiments. The results showed changes in the saccadic system with a decrease of reaction time (an increase in eye peak velocity, an improvement of saccade accuracy), and an increase of the memory guided saccades. ESA

N91-19693# Amsterdam Univ. (Netherlands).
PUPIL SIZE IN PARABOLIC FLIGHT **c52**
Hendrika W. Kortschot, Wilhelmus J. Oosterveld, and H. A. A. deJong *In* ESA, Fourth European Symposium on Life Sciences Research in Space Nov. 1990 p 623-624 Sponsored by Space Research Organization Netherlands (For primary document see N91-19572 11-51)
Copyright Avail: NTIS HC/MF A25; EPD, ESTEC, Noordwijk, Netherlands, HC 80 Dutch guilders

The pupil size was observed in ten human test subjects during parabolic flight. Microgravity induces a pupillary dilation, whereas in periods of high gravity load a constriction of the pupil is seen. The assumption of a vestibulo pupillary reflex mechanism can explain these findings. In animals connections are described between the vestibular nuclei and the centers to regulate the pupil size. It is most likely that in humans such structures also exist. ESA

N91-19694# Centre National de la Recherche Scientifique, Paris (France). Lab. de Physiologie Neurosensorielle.
MENTAL ROTATION OF THREE-DIMENSIONAL SHAPES IN MICROGRAVITY **c52**
Yoani Matsakis, A. Berthoz, M. I. Lipschits, and Victor S. Gurfinkel (Academy of Sciences, USSR, Moscow) *In* ESA, Fourth European Symposium on Life Sciences Research in Space Nov. 1990 p 625-629 (For primary document see N91-19572 11-51)
Copyright Avail: NTIS HC/MF A25; EPD, ESTEC, Noordwijk, Netherlands, HC 80 Dutch guilders

Previous experiments have suggested that gravity could exert a constraint on visual image processing. This hypothesis was investigated using a mental rotation task involving three dimensional objects during a 26 day orbital flight aboard the Soviet MIR Station. The analysis of cosmonauts' response times showed that the average rotation time per degree was shorter in flight than on ground. This decay seemed to be mainly attributable to responses implying roll axis rotations. These results are congruent with the gravity constraint hypothesis in the sense that weightlessness provided a release of this constraint, modifying the dynamic characteristics of the rotation process. As roll rotations do not alter the two dimensional image of objects' projection onto the retina, mental rotation processes could apply differently to two dimensional retinotopic or viewer centered representations and to three dimensional object centered representations. ESA

N91-19695# Deutsche Sporthochschule, Cologne (Germany, F.R.). Inst. fuer Physiologie.
WEIGHTLESSNESS COUNTERMEASURES AND HUMAN PHYSIOLOGY IN SPACE: A POTENTIAL CONFLICT **c52**
Juergen P. Stegemann *In* ESA, Fourth European Symposium on Life Sciences Research in Space Nov. 1990 p 631-635 (For primary document see N91-19572 11-51)
Copyright Avail: NTIS HC/MF A25; EPD, ESTEC, Noordwijk, Netherlands, HC 80 Dutch guilders

Experimental results revealed that the strength of partially athrophic muscles can be regained with relatively small effort. The designing of physical training for long term missions which does not disturb the well being of astronauts is discussed. Derived from some theoretical aspects, it is proposed to reduce their work capacity to 80 percent during about two thirds of the mission time, and then to train them up to their initial work capacity. This might overcome the psychological problems associated with extensive training time. Furthermore, food and oxygen are saved. A device which should allow astronauts to combine scientific work with their fitness program is presented. Potential conflicts between health maintenance and research activities are outlined. ESA

N91-19696# Giessen Univ. (Germany, F.R.). Strahlenzentrum.
POTENTIALS, MESSAGE AND CHALLENGES OF LIFE SCIENCE RESEARCH IN SPACE
Juergen Kiefer *In* ESA, Fourth European Symposium on Life Sciences Research in Space Nov. 1990 p 639-642 (For primary document see N91-19572 11-51)
Copyright Avail: NTIS HC/MF A25; EPD, ESTEC, Noordwijk, Netherlands, HC 80 Dutch guilders

The question of whether life science research in space can contribute to the solution of fundamental biological questions is considered. The possibility of this may seem absurd considering how hostile the space environment is to living things. The lack of atmosphere and low temperatures can be overcome technically by comparatively simple means, but radiation and microgravity remain. The possible influences of microgravity on basic biological processes is considered and several achievements and promises of space biology demonstrated in papers at the conference are discussed. ESA

N91-19697*# National Aeronautics and Space Administration, Washington, DC.
THE 1989-1990 NASA SPACE BIOLOGY ACCOMPLISHMENTS
Thora W. Halstead, ed. Feb. 1991 226 p Prepared in cooperation with George Washington Univ., Washington, DC
(Contract NASw-4324)
(NASA-TM-4258; NAS 1.15:4258) Avail: NTIS HC/MF A11 CSCL 06C

Individual technical summaries of research projects on NASA's Space Biology Program for research conducted during the period May 1989 to April 1990 are presented. This program is concerned with using the unique characteristics of the space environment, particularly microgravity, as a tool to advance the following: (1) knowledge in the biological sciences; (2) understanding of how gravity has shaped and affected life on the Earth; and (3) understanding of how the space environment affects both plants and animals. The summaries for each project include a description of the research, a list of accomplishments, an explanation of the significance of the accomplishments, and a list of publications. DOE

N91-19698# Lawrence Livermore National Lab., CA.
AN INTRODUCTION TO BIOLOGICAL DOSIMETRY
M. L. Mendelsohn Oct. 1990 12 p Presented at the International Symposium on Trends in Biological Dosimetry, Lerici, Italy, 23-27 Oct. 1990
(Contract W-7405-eng-48)
(DE91-007125; UCRL-JC-104810-Rev-1; CONF-9010249-3-Rev-1)
Avail: NTIS HC/MF A03

In the mode of therapeutic medicine and pharmacology, biological dosimetry is the refinement of delivered chemical or physical dose by observation and measurement of the subject for

the purpose of understanding treatment variables, individualizing treatment, minimizing toxicity and maximizing therapeutic effect. In the mode of toxicology and biological research biological dosimetry is a general strategy to pursue cause and effect relationships across subjects, doses and species, to understand and generalize the mechanisms of biological damage, and to predict and prevent ultimate toxic effects. In the mode of epidemiology and human biology, biological dosimetry is the retrospective reconstruction of dose in occupationally, environmentally and medically exposed subjects in order to identify human toxins, to study human toxicology, to improve human risk assessment, to identify unusual human susceptibilities, to provide independent evidence of exposure or risk, and to understand the nature of human disease. DOE

N91-19699*# National Aeronautics and Space Administration. Lyndon B. Johnson Space Center, Houston, TX.

PREDICTIONS OF CELL DAMAGE RATES FOR LIFESAT MISSIONS

Francis A. Cucinotta, William Atwell, Alva C. Hardy, Michael J. Golightly, John W. Wilson, Lawrence W. Townsend, Judy Shinn, John E. Nealy, and Robert Katz (Nebraska Univ., Lincoln.) Nov. 1990 14 p

(NASA-TM-102170; S-616; NAS 1.15:102170) Avail: NTIS HC/MF A03 CSCL 06C

The track model of Katz is used to make predictions of cell damage rates for possible Lifesat experiments. Contributions from trapped protons and electrons and galactic cosmic rays are considered for several orbits. Damage rates for survival and transformation of C3HT10-1/2 cells are predicted for various spacecraft shields. Author

N91-19700*# Lockheed Engineering and Sciences Co., Washington, DC.

USSR SPACE LIFE SCIENCES DIGEST. INDEX TO ISSUES 26-29

Lydia Razran Stone, ed. Washington NASA Mar. 1991 103 p

(Contract NASw-4292)

(NASA-CR-3922(35); NAS 1.26:3922(35)) Avail: NTIS HC/MF A06 CSCL 06C

This bibliography provides an index to issues 26 through 29 of the USSR Space Life Sciences Digest. There are two sections. The first section lists bibliographic citations of abstracts in these issues, grouped by topic area categories. The second section provides a key word index for the same abstracts. The topic categories include exobiology, space medicine and psychology, human performance and man-machine systems, various life/body systems, human behavior and adaptation, biospherics, and others. Author

N91-19701*# Louisville Univ., KY. Dept. of Microbiology and Immunology.

COSMOS: 1989 IMMUNOLOGY STUDIES Semiannual Progress Report No. 3, Oct. 1990 - Mar. 1991

Gerald Sonnenfeld 1991 46 p

(Grant NAG2-614)

(NASA-CR-188046; NAS 1.26:188046) Avail: NTIS HC/MF A03 CSCL 06C

The effects of flight on Cosmos mission 2044 on leukocyte subset distribution and the sensitivity of bone marrow cells to colony stimulating factor-GM were determined. A parallel study with antiorthostatic suspension was also carried out. The study involved repetition and expansion of studies performed on Cosmos 1887. Spleen and bone marrow cells were obtained from flown, vivarium control, synchronous control, and suspended rats. The cells were stained with a series of monoclonal antibodies directed against rat leukocyte cell surface antigens. Control cells were stained with a monoclonal antibody directed against an irrelevant species or were unstained. Cells were then analyzed for fluorescence using a FACSCAN flow cytometer. Bone marrow cells were placed in culture with GM-CSF in McCoy's 5a medium and incubated for 5 days. Cultures were then evaluated for the number of colonies of 50 cells or greater. Author

N91-19702# California Univ., Berkeley. Dept. of Plant Pathology.

CHARACTERIZATION OF A DEFECTIVE INTERFERING RNA THAT CONTAINS A MOSAIC OF A PLANT VIRAL GENOME

T. J. Morris and A. O. Jackson 1990 6 p

(Contract DE-FG03-88ER-13908)

(DE91-007897; DOE/ER-13908/2) Avail: NTIS HC/MF A02

This research addresses the identification of viral sequences important in viral pathogenicity through the molecular characterization of a unique class of symptom modulating RNAs called defective interfering RNAs (DI RNAs). DI RNAs are linear deletion mutants of viral genomes that complete with and interfere with the helper virus thus reducing the severity of the disease. Although DIs are common components of animal virus infections, they are uncommon in plant infections. We have identified DIs in association with turnip crinkle virus (TCV). To evaluate the essential sequences of the DI RNAs, we have completely cloned and sequenced the helper virus genomes and have begun to investigate the origin and evolution DI RNAs which arise de novo when host plants are inoculated with RNA transcripts derived from complete clones of the viral genomes. We have also developed a procedure to permit rapid cloning, sequencing and the evaluation of the biological activity of DI RNAs using PCR amplification methods. To address the mechanism of virus-host interactions leading to symptom attenuations, we have used molecular probes to study the replication and interference effects of DIs in plants and protoplasts. In addition, we are in the process of constructing plasmids to permit the expression of DIs in transgenic tomatoes with the longer term goal of constructing plants with engineered resistance to plant viruses. DOE

N91-19703# California Univ., Berkeley. Dept. of Plant Pathology.

CHARACTERIZATION OF A DEFECTIVE INTERFERING RNA THAT CONTAINS A MOSAIC OF A PLANT VIRAL GENOME

T. J. Morris and A. O. Jackson 1990 6 p

(Contract DE-FG03-88ER-13908)

(DE91-007898; DOE/ER-13908/3) Avail: NTIS HC/MF A02

Our lab was the first to describe and characterize a defective interfering RNA (DI RNAs or DIs) in association with a small RNA plant virus (Hillman et al., 1987). The features of the DIs that we discovered in infections of tomato bushy stunt virus were compatible with the properties of DIs identified in many animal virus infections. Hence our discovery offered a comparably valuable tool for use in plant virus studies for the first time. Since then, we have also discovered the second example of plant viral DI RNAs associated with turnip crinkle virus (TCV), a virus structurally related to TBSV (Li et al., 1989). We had demonstrated that the DIs were collinear deletion mutants of the genome of a cherry strain of tomato bushy stunt virus (TBSV). We had also shown that these low molecular weight RNAs interfered with the helper plant virus and modulated disease expression by preventing the development of a lethal necrotic disease in susceptible host plants. We also suggested that by exploring the mechanisms associated with the symptom attenuation effect, we might be able to devise novel strategies useful for engineering viral disease resistance. Recent results establishing TBSV as the likely etiologic agent of tomato plant decline lends urgency to such application in view of the serious nature of this disease problem in the irrigated desert areas of California (Gerik and Duffus, 1989). To accomplish this, we defined 5 major objectives for the grant period. We have completed three of the proposed research objectives and have made substantial progress on the other two. A reiteration of each of the proposed objectives follows along with a brief statement of the specific accomplishments completed or expected to be completed before the end of the grant period. Additional details of the research are provided in the attached reprints and preprints. DOE

N91-19704# Pacific Northwest Lab., Richland, WA.
BIOLOGICAL EFFECTS OF EXTREMELY LOW-FREQUENCY ELECTROMAGNETIC FIELDS: IN VIVO STUDIES
L. E. Anderson Jan. 1991 57 p Presented at the Scientific Workshop on Health Effects of Electromagnetic Radiation on Workers, Cincinnati, 30-31 Jan. 1991
(Contract DE-AC06-76RL-01830)
(DE91-007899; PNL-SA-19017; CONF-910184-1) Avail: NTIS HC/MF A04

Until the last few decades, the natural background levels of atmospheric electric and magnetic fields were extremely low; however, they have since dramatically increased. The industrialization and the electrification of society have resulted in the exposure of people, animals and plants to a complex milieu of elevated electromagnetic (EM) fields that span all frequency ranges. In the past two decades, research programs throughout the world have greatly expanded in scope and depth to address such issues. Significant progress has been achieved, both in defining the ways living organisms interact with ELF fields and in describing biological effects, both real and potential, from such fields. Much of this effort has been directed toward electric fields of power frequencies. However, frequencies other than 50 and 60 Hz have also been examined, and research has been expanded to include magnetic as well as electric fields. Although it is now clear that ELF EM fields do cause biological effects, the basis for those effects and the underlying mechanisms of interaction remain largely unknown, and the health implications for humans and animals have yet to be fully determined. This paper specifically examines the biological effects of exposure to ELF EM fields observed in in vivo (animal) studies. An attempt is made to evaluate experimental results and, insofar as possible, interpret them with respect to potential health implications. An overview of current concepts and possible mechanisms is given, and possible future directions of research are discussed. DOE

N91-19705# Utah Univ., Salt Lake City. Radiobiology Div.
RESEARCH IN RADIOBIOLOGY: WORK IN PROGRESS IN IMMUNOBIOLOGY OF EXPERIMENTAL HOST-TUMOR RELATIONSHIPS Annual Report
15 Jan. 1991 8 p
(Contract DE-FG02-89ER-60836)
(DE91-007936; DOE/ER-60836/2) Avail: NTIS HC/MF A02

Immunogenic or regressive tumors demonstrate high constitutive or inducible levels of MHC expression, while most virulent, aggressive tumors exhibit a low level of MHC Class 1 expression. Results with UVR-induced tumors suggest that a significant role is played by the T-cell lymphokine, gamma-interferon (gamma-IFN), in the modulation of MHC molecule expression in vivo. Virulent tumors induced by bone-seeking radionuclides may be refractory to gamma-IFN stimulation of MHC molecule expression. In contrast, any regressive tumors might be highly responsive to gamma-IFN, increase MHC expression, and consequently display an immunogenic phenotype. Alternatively, it is also possible that some tumors might be fully responsive to the Class 1 modulatory influences of gamma-IFN, but lack the capacity to stimulate synthesis of this lymphokine by host T cells. We presented experiments designed to: (1) describe the virulence, latency period, and transplantation characteristics of Pu-238, Am-241, and Th-228 tumors arising as osteogenic sarcomas and hepatic carcinomas, (2) determine the relationship between inducible expression of MHC Class 1 molecules by gamma-IFN and in vivo immunogenicity of these radioisotope-induced tumors, and (3) elucidate any molecular mechanisms responsible for a lack of responsiveness to gamma-IFN or a failure to induce host gamma-IFN production exhibited by virulent tumors. Our study has also been designed to determine whether the immunologic status of a prospective host, plays any role in the susceptibility to, the induced malignancies. Our proposal will test these relationships in tumor biology using Pu-238, Am-241, Th-228 induced bone and liver tumors in a syngeneic rodent system. DOE

N91-19706# Utah Univ., Salt Lake City. Dept. of Human Genetics.
ADVANCED SEQUENCING TECHNOLOGY
R. F. Gesteland 15 Jan. 1991 8 p
(Contract DE-FG02-88ER-60700)
(DE91-008031; DOE/ER-60700/3) Avail: NTIS HC/MF A02

The multiplex method of sequencing DNA has made progress on a number of fronts. A new method of organizing the DNA input for large, cosmid size, sequencing projects has been developed. It uses transposons to rapidly and easily make a large number of random insets in a cosmid. The transposon contains primer sequences and identifier senses for multiplexing, going out in both directions from the transposon with the result that multiplexed sequencing from these gives twice the length of read. Fast ways of mapping the random inserts are being developed so that the minimal overlapping set can be identified. Mini-pilot projects have been run including one on genomic sequences in the region of the neurofibromatosis gene in collaboration with Ray White's group. This genomic sequencing played a key role in the identification of this disease gene. A new algorithm for reading gel patterns into DNA sequence using communication theory is being developed and tested. We are continuing work on chemiluminescent detection of sequencing patterns via multiplex probes. The sensitivity looks very good but the problems of reprobing and CCD detection are not fully solved. DOE

N91-19707# California Univ., Davis. Dept. of Bacteriology.
PHYSIOLOGICAL GENETICS OF DENITRIFICATION: A ROUTE TO CONSERVING FIXED NITROGEN
1991 6 p
(Contract DE-FG03-85ER-13356)
(DE91-008157; DOE/ER-13356/T2) Avail: NTIS HC/MF A02

Biological denitrification is the reduction of nitrate or nitrite ions to gaseous species, either nitrous oxide (N2O) or dinitrogen. This is the only significant process by which fixed nitrogen is removed from the environment. Mutant strains of pseudomonas stutzeri; (P. stutzeri) which cannot catalyze the denitrification reaction are being studied. The strain studied, nosA, has a defect in the nosA gene, which doesn't code for N2O reductase. Since the N2O reductase from nosA bacteria contains less than 4% of the copper found in wild-type N2O reductase, nosA 13 is believed to code for an enzyme which inserts copper into N2O reductase. NosA protein is found in the outer membrane of P. stutzeri, and N2O reductase is located in the periplasm. Synthesis of nosA, but not N2O reductase is sensitive to exogenous copper concentrations. NosA protein was isolated and purified, and used to make a polycolonal antisera Western blots shown the sera reacts with nosA protein. Labelling live P. stutzeri with Cu-67, three copper containing proteins were identified. N2O reductase and nosA protein were two of the three; the identity of the third is not known, but it is not believed to be superoxide dizmutage. Two strains of phage specific for wild type nosA protein have been isolated. The antibodies generated are being used with an expression library to clone the nosA gene. So far, about half of the gene has been cloned. In related work, the kinetics of synthesis of proteins specific for aerobic or anaerobic conditions are described. Three proteins which are synthesized in response to anaerobic conditions and two proteins whose synthesis requires aerobic conditions are described. DOE

N91-19708# Messerschmitt-Boelkow-Blohm G.m.b.H., Ottobrunn (Germany, F.R.). Dienstleistungbereich.
EXPERIMENTAL EQUIPMENT FOR SPACE BIOLOGY
J. Schauwer and J. Warrelmann (Erno Raumfahrttechnik G.m.b.H. Bremen, Germany, F.R.) 1990 12 p Presented at the 17th ISTS, Tokyo, Japan, 20-25 May 1990
(MBB-UO-0096-90-PUB; ETN-91-98833) Avail: NTIS HC/MF A03

A facility BLUME (Biological Support Unit for Microgravity Experiments) for biological investigations in space is described. BLUME is an autonomous facility for biological and gravitational biology experiments with controlled life support equipment which will be integrated into a container of the NASA GAS program.

The components of the facility BLUME are mounted within a cylindrical structure with a height of 710 mm a diameter of 480 mm on two mounting plates. On the lower platform a supply unit is fixed consisting of a 28 V AgZn battery as power supply and an experiment control, data acquisition and signal conditioning unit. The second platform carries the life support system. This system consists of an air control loop, a water supply loop, a fixation loop, CO2 and O2 supply and a drying loop. These are illustrated and described. Gas exchange measurements and plant experiments have been performed. Future aspects are considered. ESA

N91-19709# Emory Univ., Atlanta, GA. School of Medicine.
SUBCELLULAR SIGNAL TRANSDUCTION SYSTEMS IN THE CELLULAR TRAUMA OF ISCHEMIA Annual Report, Nov. 1988 - Nov. 1990
Alfred H. Merrill, Jr. 24 Nov. 1990 15 p
(Contract N00014-89-J-1027)
(AD-A229876) Avail: NTIS HC/MF A03 CSCL 06/5

The formation of sphingosine, a potent inhibitor of protein kinase C, has been characterized in cell models of interest to studies of hypoxic and ischemic injury. With J775 macrophages, we find that sphingosine is released in an acidic compartment and is inhibitable by ammonium ion, an agent that is well known to accumulate during ischemia. The increase in sphingosine is correlated with inhibition of protein kinase C; therefore, these findings may provide a link between changes in ammonia in vivo and alteration in cell function. GRA

N91-20026*# Massachusetts Univ., Amherst. Dept. of Plant and Soil Sciences.
CARBON DIOXIDE AND WATER EXCHANGE OF A SOYBEAN STAND GROWN IN THE BIOMASS PRODUCTION CHAMBER
Kenneth A. Corey *In* NASA, John F. Kennedy Space Center, Research Reports: 1990 NASA/ASEE Summer Faculty Fellowship Program Sep. 1990 p 115-141 (For primary document see N91-20022 11-99)
(Grant NGT-60002)
Avail: NTIS HC/MF A23 CSCL 06C

52 AEROSPACE MEDICINE

Includes physiological factors; biological effects of radiation; and effects of weightlessness on man and animals.

N91-19710*# Good Samaritan Hospital and Medical Center, Portland, OR. Clinical Vestibular Lab.
RELATION BETWEEN PERCEPTION OF VERTICAL AXIS ROTATION AND VESTIBULO-OCULAR REFLEX SYMMETRY
Robert J. Peterka and Martha S. Benolken 20 Mar. 1991 21 p
(Grant NAG9-117)
(NASA-CR-187997; NAS 1.26:187997) Avail: NTIS HC/MF A03 CSCL 06P

Subjects seated in a vertical axis rotation chair controlled their rotational velocity by adjusting a potentiometer. Their goal was to null out pseudorandom rotational perturbations in order to remain perceptually stationary. Most subjects showed a slow linear drift of velocity (a constant acceleration) to one side when they were deprived of an earth-fixed visual reference. The amplitude and direction of this drift can be considered a measure of a static bias in the subject's perception of rotation. The presence of a perceptual bias is consistent with a small, constant imbalance of vestibular function which could be of either central or peripheral origin. Deviations from perfect vestibulocular reflex (VOR) symmetry are also assumed to be related to imbalances in either peripheral or central vestibular function. Researchers looked for correlations between perceptual bias and various measures of vestibular reflex symmetry that might suggest a common source for both reflective and perceptual imbalances. No correlations were found. Measurement errors could not account for these results since repeated tests on the same subjects of both perceptual bias and VOR symmetry were well correlated. Author

N91-19711*# National Aeronautics and Space Administration. John F. Kennedy Space Center, Cocoa Beach, FL.
RESPONSES OF WOMEN TO ORTHOSTATIC AND EXERCISE STRESSES Technical Report, 1976 - 1977
G. W. Hoffler, M. M. Jackson, R. L. Johnson, J. T. Baker, and D. Tatro (Bionetics Corp., Cocoa Beach, FL.) Washington Oct. 1990 77 p
(Contracts NAS9-14880; NAS10-11624)
(NASA-TP-3043; NAS 1.60:3043) Avail: NTIS HC/MF A05 CSCL 06P

The results are presented from a special physiological study of women at the Johnson Space Center in 1976 to 1977. Its purpose was to establish a large (98 subjects) database from normal working women. The data sets are medical historical, clinical, anthropometric, and stress response statistics useful for establishing medical criteria for selecting women astronauts. Stressors were lower body negative pressure and static standing (both orthostatic) and treadmill exercise (ergometric). Data shown are original individual values with analyses and subsets, and statistical summaries and correlations relating to human responses to microgravity. Similarities appear between the characteristics of women in this study and those of women astronauts currently flying in Shuttle crews. Author

N91-19712# Brookhaven National Lab., Upton, NY.
MULTIPLE ENERGY COMPUTED TOMOGRAPHY FOR NEURORADIOLOGY WITH MONOCHROMATIC X RAYS FROM THE NATIONAL SYNCHROTRON LIGHT SOURCE
F. A. Dilmanian, R. F. Garrett, W. C. Thomlinson, L. E. Berman, L. D. Chapman, N. F. Gmuer, N. M. Lazarz, H. R. Moulin, T. Oversluizen, and D. N. Slatkin et al 1990 20 p Presented at the 3rd International Conference on Applications of Physics in Medicine and Biology: Medical Diagnostic Imaging, Trieste, Italy, 4-7 Sep. 1990
(Contract DE-AC02-76CH-00016)
(DE91-008108; BNL-45750; CONF-900993-2) Avail: NTIS HC/MF A03

Monochromatic and tunable 33 to 100 keV x rays from the X17 superconducting wiggler of the National Synchrotron Light Source (NSLS) at Brookhaven National Laboratory (BNL) will be used for computed tomography (CT) of the human head and neck. The CT configuration will be one of a fixed horizontal fan-shaped beam and a seated rotating subject. The system, which is under development, will employ a two-crystal monochromator with an energy bandwidth of about 0.1 percent, and high-purity germanium linear array detector with 0.5 mm element width and 200 mm total width. Narrow energy bands not only eliminate beam hardening but are ideal for carrying out the following dial-energy methods: (1) dual-photon absorptiometry CT, that provides separate images of the low-Z and the intermediate-Z elements; and (2) K-edge subtraction CT of iodine and perhaps of heavier contrast elements. As a result, the system should provide approximately 10-fold improvement in image contrast resolution and in quantitative precision over conventional CT. A prototype system for a 45 mm subject diameter will be ready in 1991, which will be used for studies with phantoms and small animals. The human imaging system will have a field of view of 200 mm. The in-plane spatial resolution in both systems will be 0.5 mm FWHM. DOE

N91-19031*# Ohio Univ., Athens.
ANALYZING THOUGHT-RELATED ELECTROENCEPHALOGRAPHIC DATA USING NONLINEAR TECHNIQUES
Trent Skidmore *In* NASA, Langley Research Center, Joint University Program for Air Transportation Research, 1989-1990 Dec. 1990 p 91-95 (For primary document see N91-19024 11-01)
Avail: NTIS HC/MF A09 CSCL 06P

N91-19568# Joint Publications Research Service, Arlington, VA.
REACTIVITY OF EXHAUSTED HUMAN SKELETAL MUSCLE FIBERS FOLLOWING PROLONGED ANTIORTHOSTATIC HYPOKINESIA Abstract Only

S. L. Kuznetsov and V. V. Stepantsov *In its* JPRS Report: Science and Technology. USSR: Life Sciences 4 Jan. 1991 p 1 Transl. into ENGLISH from Arkhiv Anatomii, Gistologiii i Embriologii (Leningrad, USSR), v. 97, no. 7, Jul. 1989 p 53-59 (For primary document see N91-19567 11-51)
Avail: NTIS HC/MF A03

N91-19569# Joint Publications Research Service, Arlington, VA.
GRAVITATION RECEPTOR REACTION IN RESPONSE TO EFFECT OF ACCELERATION Abstract Only
A. T. Pakunov *In its* JPRS Report: Science and Technology. USSR: Life Sciences 4 Jan. 1991 p 26 Transl. into ENGLISH from Zhurnal Ushnykh, Nosovykh i Gorlovykh Bolezney (Kiev, USSR), no. 2, Mar. - Apr. 1990 p 8-13 (For primary document see N91-19567 11-51)
Avail: NTIS HC/MF A03

N91-19570# Joint Publications Research Service, Arlington, VA.
EFFECTS OF HYPERBARIC OXYGENATION ON CENTRAL HEMODYNAMICS AND OXYGEN CONSUMPTION IN SEVERE PHYSICAL TRAUMA Abstract Only
A. G. Magomedov *In its* JPRS Report: Science and Technology. USSR: Life Sciences 4 Jan. 1991 p 26 Transl. into ENGLISH from Patologicheskaya Fiziologiya i Eksperimentalnaya Terapiya (Moscow, USSR), no. 2, Mar. - Apr. 1990 p 26-28 (For primary document see N91-19567 11-51)
Avail: NTIS HC/MF A03

N91-19571# Joint Publications Research Service, Arlington, VA.
EFFECTS OF HIGH TEMPERATURE AND HUMIDITY ON MENTAL STATE AND METABOLISM Abstract Only
A. S. Shanazarov, V. P. Makhnovskiy, and E. I. Kuzyuta *In its* JPRS Report: Science and Technology. USSR: Life Sciences 4 Jan. 1991 p 27-28 Transl. into ENGLISH from Fiziologiya Cheloveka (Moscow, USSR), v. 15, no. 4, Jul. - Aug. 1989 p 92-96 (For primary document see N91-19567 11-51)
Avail: NTIS HC/MF A03

N91-19573# Karolinska Inst., Stockholm (Sweden). Environmental Physiology Lab.
EFFECTS OF SHORT-LASTING WEIGHTLESSNESS ON GAS EXCHANGE DURING LIGHT EXERCISE
Dad Linnarsson, Pietro E. diPrampero, Juergen P. Stegemann, Carl J. Sundberg, Uwe Hoffmann, and Dieter Essfeld (Deutsche Sporthochschule, Cologne, Germany, F.R.) *In* ESA, Fourth European Symposium on Life Sciences Research in Space Nov. 1990 p 9-11 Sponsored by Swedish Space Board; CNR; BMFT; and ESA (For primary document see N91-19572 11-51)
Copyright Avail: NTIS HC/MF A25; EPD, ESTEC, Noordwijk, Netherlands, HC 80 Dutch guilders

N91-19574# Vrije Univ., Brussels (Belgium). Inst. of Interdisciplinary Research.
LUNG VOLUMES, CHEST WALL CONFIGURATION, AND PATTERN OF BREATHING IN MICROGRAVITY
Manuel Paiva, M. Estenne, and L. A. Engel (Westmead Hospital, Sydney, Australia) *In* ESA, Fourth European Symposium on Life Sciences Research in Space Nov. 1990 p 13-15 (For primary document see N91-19572 11-51)
Copyright Avail: NTIS HC/MF A25; EPD, ESTEC, Noordwijk, Netherlands, HC 80 Dutch guilders

N91-19575# Amsterdam Univ. (Netherlands). Dept. of Physiology.
BLOOD PRESSURE REGULATION IN PARABOLIC FLIGHT
John M. Karemaker, J. J. Settels (Organization for Health Research, TNO, Amsterdam, Netherlands), H. J. P. Kuykens, and K. H. Wesseling *In* ESA, Fourth European Symposium on Life Sciences Research in Space Nov. 1990 p 17-18 (For primary document see N91-19572 11-51)
(Grant SRON-MG020-1988)
Copyright Avail: NTIS HC/MF A25; EPD, ESTEC, Noordwijk, Netherlands, HC 80 Dutch guilders

N91-19576# Institute of Biomedical Problems, Moscow (USSR).
MEDICAL RESULTS OF THE FOURTH PRIME EXPEDITION ON THE ORBITAL STATION MIR
A. I. Grigoriev, V. V. Poliakov, V. V. Bogomolov, A. D. Egorov, I. D. Pestov, and I. B. Kozlovskaya *In* ESA, Fourth European Symposium on Life Sciences Research in Space Nov. 1990 p 19-22 (For primary document see N91-19572 11-51)
Copyright Avail: NTIS HC/MF A25; EPD, ESTEC, Noordwijk, Netherlands, HC 80 Dutch guilders

N91-19577# Hopital Bretonneau, Tours (France). Inst. National de la Sante et de la Recherche Medicale.
ULTRASOUND INVESTIGATION OF THE CARDIOVASCULAR SYSTEM DURING THE 25 DAYS FRENCH-SOVIET SPACEFLIGHT (26 NOVEMBER - 21 DECEMBER 1988)
Philippe Arbeille, O. Atkov, V. V. Bystrov, J. L. Chretien, Galina Fomina, V. Gratchov, N. Kokova, F. Patat, V. V. Poliakov (Institute of Biomedical Problems, Moscow, USSR), and J. M. Pottier et al *In* ESA, Fourth European Symposium on Life Sciences Research in Space Nov. 1990 p 23-26 Sponsored by CNES (For primary document see N91-19572 11-51)
Copyright Avail: NTIS HC/MF A25; EPD, ESTEC, Noordwijk, Netherlands, HC 80 Dutch guilders

N91-19578# Institute of Biomedical Problems, Moscow (USSR).
ULTRASOUND INVESTIGATION OF THE CARDIOVASCULAR SYSTEM DURING THE 25-DAYS SOVIET-FRENCH FLIGHT: CARDIAC ASPECTS
Galina Fomina, N. Kokova, V. V. Bystrov, V. V. Poliakov, L. Strogonova, V. Gratchev, O. Atkov, J. M. Pottier, Philippe Arbeille, and F. Patat (Hopital Bretonneau, Tours, France) et al *In* ESA, Fourth European Symposium on Life Sciences Research in Space Nov. 1990 p 27-29 (For primary document see N91-19572 11-51)
Copyright Avail: NTIS HC/MF A25; EPD, ESTEC, Noordwijk, Netherlands, HC 80 Dutch guilders

N91-19579# Amsterdam Univ. (Netherlands).
VESTIBULAR FUNCTION IN ALTERED STATES OF GRAVITY
Wilhelmus J. Oosterveld, H. A. A. deJong, and Hendrika W. Kortschot *In* ESA, Fourth European Symposium on Life Sciences Research in Space Nov. 1990 p 31-36 (For primary document see N91-19572 11-51)
Copyright Avail: NTIS HC/MF A25; EPD, ESTEC, Noordwijk, Netherlands, HC 80 Dutch guilders

N91-19580# Mainz Univ. (Germany, F.R.). Dept. of Physiology.
OCULAR ROLL UNDER CHANGING z-AXIS ACCELERATION AND NECK POSITION
Joachim Wetzig, K. Hofstetter, M. Reiser, and R. vonBaumgarten *In* ESA, Fourth European Symposium on Life Sciences Research in Space Nov. 1990 p 37-42 (For primary document see N91-19572 11-51)
(Grant BMFT-01-QV-223-9)
Copyright Avail: NTIS HC/MF A25; EPD, ESTEC, Noordwijk, Netherlands, HC 80 Dutch guilders

N91-19581# Provence Univ., Marseille (France). Lab. de Neurobiologie Humaine.
BODY PROPRIOCEPTIVE REFERENCES IN WEIGHTLESSNESS AS STUDIED BY MUSCLE TENDON VIBRATION
J. P. Roll, K. E. Popov, Victor S. Gurfinkel, M. I. Lipschits, Claudie Andre-Deshays (Centre National de la Recherche Scientifique, Paris, France), J. C. Gilhodes, and Cynthia Quoniam *In* ESA, Fourth European Symposium on Life Sciences Research in Space Nov. 1990 p 43-48 (For primary document see N91-19572 11-51)
(Grants CNES-500193; CNES-500243)
Copyright Avail: NTIS HC/MF A25; EPD, ESTEC, Noordwijk, Netherlands, HC 80 Dutch guilders

N91-19583# Udine Univ. (Italy). Inst. of Biology.
PEDALLING IN SPACE TO SIMULATE GRAVITY: THE TWIN-BIKE SYSTEM
Giulioandrea Antonutto, Carlo Capelli, and Pietro E. diPrampero *In* ESA, Fourth European Symposium on Life Sciences Research in Space Nov. 1990 p 59-62 (For primary document see N91-19572 11-51)
Copyright Avail: NTIS HC/MF A25; EPD, ESTEC, Noordwijk, Netherlands, HC 80 Dutch guilders

N91-19584# Technische Univ., Vienna (Austria). Dept. of Sports and Exercise Physiology.
ISOKINETIC FORCE VELOCITY AND ELECTROMYOGRAPHIC CHARACTERISTIC OF KNEE AND ELBOW EXTENSOR AND FLEXOR MUSCLES IN THE 0-g ENVIRONMENT
Norbert Bachl, R. Baron, Massud Mossaheb, W. Bumba, and R. Albrecht (European Space Agency. European Space Research and Technology Center, ESTEC, Noordwijk, Netherlands) *In* ESA, Fourth European Symposium on Life Sciences Research in Space Nov. 1990 p 63-68 (For primary document see N91-19572 11-51)
Copyright Avail: NTIS HC/MF A25; EPD, ESTEC, Noordwijk, Netherlands, HC 80 Dutch guilders

N91-19585# Deutsche Forschungsanstalt fuer Luft- und Raumfahrt, Cologne (Germany, F.R.). Inst. for Aerospace Medicine.
MEDEX: A USEFUL TOOL FOR COUNTERACTING ORTHOSTATIC INTOLERANCE RESULTING FROM BODY FLUID LOSS UNDER MICROGRAVITY
Friedhelm Baisch and Wolfgang Bangert (Panares, Munich, Germany, F.R.) *In* ESA, Fourth European Symposium on Life Sciences Research in Space Nov. 1990 p 69-71 (For primary document see N91-19572 11-51)
Copyright Avail: NTIS HC/MF A25; EPD, ESTEC, Noordwijk, Netherlands, HC 80 Dutch guilders

N91-19586# Deutsche Sporthochschule, Cologne (Germany, F.R.). Physiologisches Inst.
TIME COURSES OF ENDURANCE PERFORMANCE PARAMETERS FOLLOWING 500 ml BLOOD WITHDRAWAL
Klaus Baum, Uwe Hoffmann, Dieter Essfeld, and Juergen P. Stegemann *In* ESA, Fourth European Symposium on Life Sciences Research in Space Nov. 1990 p 73-76 (For primary document see N91-19572 11-51)
(Grant BMFT-01-QV-87354)
Copyright Avail: NTIS HC/MF A25; EPD, ESTEC, Noordwijk, Netherlands, HC 80 Dutch guilders

N91-19587# Karolinska Inst., Stockholm (Sweden). Environmental Physiology Lab.
OXYGEN UPTAKE DURING CONCENTRIC AND ECCENTRIC RESISTIVE EXERCISE USING A NEW GRAVITY-INDEPENDENT ERGOMETER
Hans E. Berg and Per A. Tesch *In* ESA, Fourth European Symposium on Life Sciences Research in Space Nov. 1990 p 77 (For primary document see N91-19572 11-51)
Copyright Avail: NTIS HC/MF A25; EPD, ESTEC, Noordwijk, Netherlands, HC 80 Dutch guilders

N91-19588# Innsbruck Univ. (Austria). Klinik fuer Neurologie.
COORDINATION OF EYE, HEAD AND ARM MOVEMENTS IN WEIGHTLESSNESS
Meinhard Berger, F. Gerstenbrand, Miklos Marosi, E. Karamat, Armin Muigg, T. Melichar, R. Schauer, I. B. Kozlovskaya, A. Sokolov, and M. Belaeva (Institute of Biomedical Problems, Moscow, USSR) *In* ESA, Fourth European Sumposium on Life Sciences Research in Space Nov. 1990 p 79-81 (For primary document see N91-19572 11-51)
Copyright Avail: NTIS HC/MF A25; EPD, ESTEC, Noordwijk, Netherlands, HC 80 Dutch guilders

N91-19589# European Space Agency. European Space Research and Technology Center, ESTEC, Noordwijk (Netherlands).
LIFE SCIENCES IN ESA TRP ACTIVITY
Nora Bougharouat, J. Kingdon, Peter Schiller, and Francois Brechignac *In its* Fourth European Symposium on Life Sciences Research in Space Nov. 1990 p 83-87 (For primary document see N91-19572 11-51)
Copyright Avail: NTIS HC/MF A25; EPD, ESTEC, Noordwijk, Netherlands, HC 80 Dutch guilders

N91-19590# Trondheim Univ. (Norway). Dept. of Biomedical Engineering.
VASCULAR GAS BUBBLES OR DECOMPRESSION SICKNESS: WHAT IS THE PROPER ENDPOINT FOR EVALUATING DECOMPRESSION PROCEDURES
Alf O. Brubakk *In* ESA, Fourth European Symposium on Life Sciences Research in Space Nov. 1990 p 89-92 (For primary document see N91-19572 11-51)
Copyright Avail: NTIS HC/MF A25; EPD, ESTEC, Noordwijk, Netherlands, HC 80 Dutch guilders

N91-19591# Freie Univ., Berlin (Germany, F.R.). Dept. of Otorhinolaryngology.
MEASUREMENT OF EYE MOVEMENTS IN SPACE-RELATED RESEARCH ENVIRONMENTS
Andrew H. Clarke, Winfried Teiwes, and H. Scherer *In* ESA, Fourth European Symposium on Life Sciences Research in Space Nov. 1990 p 93-94 (For primary document see N91-19572 11-51)
(Grant BMFT-01-QV-8802)
Copyright Avail: NTIS HC/MF A25; EPD, ESTEC, Noordwijk, Netherlands, HC 80 Dutch guilders

N91-19592# Technische Univ., Munich (Germany, F.R.). Medizinische Klinik.
PHYSIOLOGY OF BODY WATER AND SALT REGULATION. PART 1: CIRCADIAN RHYTHMS OF ENDOCRINE SYSTEMS AND URINARY ELECTROLYTE EXCRETION IN HUMANS
Christian Drummer, M. Heer, B. Molz, Matthias Schlossberger, Carsten Stadeager, Lothar Roecker, Peter Norsk, Felice Strollo, Friedhelm Baisch, and Jorgen Warberg (Danish Aerospace Medical Center of Research, Copenhagen.) et al *In* ESA, Fourth European Symposium on Life Sciences Research in Space Nov. 1990 p 95-98 Sponsored by BMFT, and ESA (For primary document see N91-19572 11-51)
Copyright Avail: NTIS HC/MF A25; EPD, ESTEC, Noordwijk, Netherlands, HC 80 Dutch guilders

N91-19593# Technische Univ., Munich (Germany, F.R.). Medizinische Klinik.
PHYSIOLOGY OF BODY WATER AND SALT REGULATION. PART 2: VOLUME AND ELECTROLYTE HOMEOSTASIS AFTER AN ACUTE SALINE INFUSION
Christian Drummer, M. Heer, B. Molz, Matthias Schlossberger, Carsten Stadeager, Lothar Roecker, Peter Norsk, Felice Strollo, Jergen Warberg, and Niels Juel Christensen (Danish Aerospace Medical Center of Research, Copenhagen.) et al *In* ESA, Fourth European Symposium on Life Sciences Research in Space Nov. 1990 p 99-102 Sponsored by BMFT, and ESA (For primary document see N91-19572 11-51)
Copyright Avail: NTIS HC/MF A25; EPD, ESTEC, Noordwijk, Netherlands, HC 80 Dutch guilders

N91-19594# Deutsche Sporthochschule, Cologne (Germany, F.R.). Physiologisches Inst.
INFLUENCE OF VARIOUS PARAMETERS ON THE V'O2 FREQUENCY RESPONSE OF THE BODY. A THEORETICAL STUDY ON THE BASIS OF A NONLINEAR MODEL
Dieter Essfeld and Uwe Hoffmann *In* ESA, Fourth European Symposium on Life Sciences Research in Space Nov. 1990 p 103-106 Submitted for publication (For primary document see N91-19572 11-51)

(Grant BMFT-01-QV-87354)
Copyright Avail: NTIS HC/MF A25; EPD, ESTEC, Noordwijk, Netherlands, HC 80 Dutch guilders

N91-19595# Graz Univ. (Austria). Physiologisches Inst.
IS PHYSIOLOGICAL TREMOR (MICROVIBRATION) INFLUENCED BY MICROGRAVITY
Eugen Gallasch, N. Burlatschkowa, I. Beljajeva (Institute of Biomedical Problems, Moscow, USSR), M. Moser, and I. Kenner *In* ESA, Fourth European Symposium on Life Sciences Research in Space Nov. 1990 p 107-110 (For primary document see N91-19572 11-51)
Copyright Avail: NTIS HC/MF A25; EPD, ESTEC, Noordwijk, Netherlands, HC 80 Dutch guilders

N91-19596# Centre National de la Recherche Scientifique, Tours (France). Lab. de Bio-Informatique.
SIMULATION EXPERT SYSTEM FOR PHYSIOLOGICAL MECHANISMS OF THE SPACE MOTION SICKNESS
Claude Gaudeau, L. Gouthiere, C. LeToullec, E. Lawton (Societe de Bio-Informatique et Bio-Technologie, Tours, France), and G. Chauvet *In* ESA, Fourth European Symposium on Life Sciences Research in Space Nov. 1990 p 111-116 (For primary document see N91-19572 11-51)
Copyright Avail: NTIS HC/MF A25; EPD, ESTEC, Noordwijk, Netherlands, HC 80 Dutch guilders

N91-19597# Innsbruck Univ. (Austria). Klinik fuer Neurology.
NEUROLOGICAL FINDINGS AFTER 72 HOURS WATER IMMERSION
F. Gerstenbrand, I. B. Kozlovskaya, Meinhard Berger, Miklos Marosi, N. Burlacskova, A. Sokolov, R. Schauer, and J. Rainer *In* ESA, Fourth European Symposium on Life Sciences Research in Space Nov. 1990 p 117-119 Prepared in cooperation with Inst. of Biomedical Problems, Moscow, USSR (For primary document see N91-19572 11-51)
Copyright Avail: NTIS HC/MF A25; EPD, ESTEC, Noordwijk, Netherlands, HC 80 Dutch guilders

N91-19598# Eidgenoessische Technische Hochschule, Zurich (Switzerland). Space Biology Group.
EFFECT OF RUNNING AND HEAD DOWN TILT BEDREST ON LYMPHOCYTE REACTIVITY
Felix K. Gmuender, Friedhelm Baisch, B. Bechler, Augusto Cogoli, Marianne Cogoli, P. W. Joller, H. Maass, J. Mueller, and W. Ziegler (Universitaetsspital, Zurich, Switzerland) *In* ESA, Fourth European Symposium on Life Sciences Research in Space Nov. 1990 p 121-124 Sponsored in cooperation with the Swiss Federal Inst. of Tech. (For primary document see N91-19572 11-51)
(Grant SNSF-3-382-0-86)
Copyright Avail: NTIS HC/MF A25; EPD, ESTEC, Noordwijk, Netherlands, HC 80 Dutch guilders

N91-19599# Milan Univ. (Italy). Cattedra di Semeiotica Medica.
SIMULATED ABSENCE OF GRAVITY IMPAIRS ARTERIAL BARORECEPTOR CONTROL OF HEART RATE IN MAN
G. Grassi, Antonella Ravogli, G. Parati, P. Coruzzi, A. Novarini, and G. Mancia *In* ESA, Fourth European Symposium on Life Sciences Research in Space Nov. 1990 p 125-127 (For primary document see N91-19572 11-51)
Copyright Avail: NTIS HC/MF A25; EPD, ESTEC, Noordwijk, Netherlands, HC 80 Dutch guilders

N91-19600# Graz Univ. (Austria). Working Group for Volume Regulation and Space Medicine.
A NEW PRINCIPLE FOR DYNAMIC FLUID SHIFT INVESTIGATIONS IN ASTRONAUTS
H. Hinghofer-Szalkay, Eva Maria Koenig, J. Schmied, and H. Heimel (Labor fuer Messtechnik dr. Hans Stabinger, Graz, Austria) *In* ESA, Fourth European Symposium on Life Sciences Research in Space Nov. 1990 p 129-132 Sponsored by Austrian Ministry for Sciences, and Oesterreichische Akademie der Wissenschaften (For primary document see N91-19572 11-51)
Copyright Avail: NTIS HC/MF A25; EPD, ESTEC, Noordwijk, Netherlands, HC 80 Dutch guilders

N91-19601# Deutsche Sporthochschule, Cologne (Germany, F.R.). Physiologisches Inst.
INTRA-INDIVIDUAL VARIABILITY V'O2 FREQUENCY RESPONSES IN PHYSICALLY ACTIVE SUBJECTS
Uwe Hoffmann, Klaus Baum, Dieter Essfeld, and Juergen P. Stegemann *In* ESA, Fourth European Symposium on Life Sciences Research in Space Nov. 1990 p 133-135 (For primary document see N91-19572 11-51)
(Grant BMFT-01-QV-87354)
Copyright Avail: NTIS HC/MF A25; EPD, ESTEC, Noordwijk, Netherlands, HC 80 Dutch guilders

N91-19602# Danish Aerospace Medical Center of Research, Copenhagen.
FLUID SHIFTS AND REGULATION OF PLASMA VOLUME IN HUMANS DURING 12 HOURS OF HEAD-OUT WATER IMMERSION
Lars Bo Johansen, Peter Norsk, Niels Foldager, Carsten Stadeager, Manabu Kamegai, and Flemming Bonde-Petersen *In* ESA, Fourth European Symposium on Life Sciences Research in Space Nov. 1990 p 137-139 Sponsored by Danish Space Board (For primary document see N91-19572 11-51)
Copyright Avail: NTIS HC/MF A25; EPD, ESTEC, Noordwijk, Netherlands, HC 80 Dutch guilders

N91-19603*# Vanderbilt Univ., Nashville, TN. Dept. of Mechanical Engineering.
SKELETAL ADAPTATION IN ALTERED GRAVITY ENVIRONMENTS
Tony S. Keller and Alvin M. Strauss *In* ESA, Fourth European Symposium on Life Sciences Research in Space Nov. 1990 p 141-147 Sponsored by NASA (For primary document see N91-19572 11-51)
Copyright Avail: NTIS HC/MF A25; EPD, ESTEC, Noordwijk, Netherlands, HC 80 Dutch guilders

N91-19604# Freie Univ., Berlin (Germany, F.R.). Dept. of Physiology.
VERTEBRAL COLUMN LENGTH CHANGES DURING SIMULATED MICROGRAVITY
K. A. Kirsch, Filippo Castrucci (Rome Univ., Italy), H.-C. Gunga, and Y. Reinach *In* ESA, Fourth European Symposium on Life Sciences Research in Space Nov. 1990 p 149-151 Sponsored in part by ESA (For primary document see N91-19572 11-51)
(Grant BMFT-01-QV-87/2)
Copyright Avail: NTIS HC/MF A25; EPD, ESTEC, Noordwijk, Netherlands, HC 80 Dutch guilders

N91-19605# Max-Planck-Inst. fuer Verhaltensphysiologie, Seewiesen uber Starnberg (Germany, F.R.).
DETERMINANTS OF SPATIAL ORIENTATION IN WEIGHTLESSNESS
Horst Mittelstaedt and Stefan Glasauer *In* ESA, Fourth European Symposium on Life Sciences Research in Space Nov. 1990 p 153-155 (For primary document see N91-19572 11-51)
Copyright Avail: NTIS HC/MF A25; EPD, ESTEC, Noordwijk, Netherlands, HC 80 Dutch guilders

N91-19606# Wien Univ. (Austria). Neurologische Klinik.
VERTICALLY MOVING VISUAL STIMULI AND VERTICAL VECTION: A TOOL AGAINST SPACE MOTION SICKNESS
Christian Mueller, G. Wiest, and L. Deecke *In* ESA, Fourth European Symposium on Life Sciences Research in Space Nov. 1990 p 157-161 (For primary document see N91-19572 11-51)
Copyright Avail: NTIS HC/MF A25; EPD, ESTEC, Noordwijk, Netherlands, HC 80 Dutch guilders

N91-19607# Institute of Biomedical Problems, Moscow (USSR).
THE BIOCHEMICAL AND PHYSIOLOGICAL VARIABLES IN MOTION SICKNESS FOLLOWED MODIFIED NEUROENDOCRINE ACTIVITY
I. A. Nichiporuk, D. V. Grishanin, and A. I. Grigoriev *In* ESA, Fourth European Symposium on Life Sciences Research in Space Nov. 1990 p 163-165 (For primary document see N91-19572 11-51)
Copyright Avail: NTIS HC/MF A25; EPD, ESTEC, Noordwijk, Netherlands, HC 80 Dutch guilders

N91-19608# Institute of Biomedical Problems, Moscow (USSR).
ASSESSMENT OF BONE TURNOVER IN HUMANS AFTER SPACE FLIGHT AND HYPOKINESIA
V. S. Oganov, V. E. Novikov, and A. S. Rakhmanov *In* ESA, Fourth European Symposium on Life Sciences Research in Space Nov. 1990 p 167-170 (For primary document see N91-19572 11-51)
Copyright Avail: NTIS HC/MF A25; EPD, ESTEC, Noordwijk, Netherlands, HC 80 Dutch guilders

N91-19610*# National Aeronautics and Space Administration. Lyndon B. Johnson Space Center, Houston, TX.
POSTURAL CHANGES FOLLOWING SENSORY REINTERPRETATION AS AN ANALOG TO SPACEFLIGHT
William H. Paloski, D. L. Harm, M. F. Reschke, D. D. Doxey, N. C. Skinner, L. J. Michaud, and D. E. Parker (Miami Univ., Oxford, OH.) *In* ESA, Fourth European Symposium on Life Sciences Research in Space Nov. 1990 p 175-178 (For primary document see N91-19572 11-51)
Copyright Avail: NTIS HC/MF A25; EPD, ESTEC, Noordwijk, Netherlands, HC 80 Dutch guilders CSCL 06P

N91-19611*# National Aeronautics and Space Administration. Lyndon B. Johnson Space Center, Houston, TX.
STANDARDIZATION OF MOTION SICKNESS INDUCED BY LEFT-RIGHT AND UP-DOWN REVERSING PRISMS
M. F. Reschke, J. M. Vanderploeg, E. A. Brumley, J. J. Kolafa, and S. J. Wood (Krug International, Houston, TX.) *In* ESA, Fourth European Symposium on Life Sciences Research in Space Nov. 1990 p 179-182 (For primary document see N91-19572 11-51)
Copyright Avail: NTIS HC/MF A25; EPD, ESTEC, Noordwijk, Netherlands, HC 80 Dutch guilders CSCL 06P

N91-19612# Danish Aerospace Medical Center of Research, Copenhagen.
INFLUENCE ON NATRIURESIS OF PROLONGED (12 h) WATER IMMERSION ON CENTRAL HEMODYNAMICS AND ENDOCRINE ELEMENTS IN HUMANS
Carsten Stadeager, Peter Norsk, Lars Bo Johansen, Jorgen Warberg, Niels Juel Christensen, and Flemming Bonde-Petersen *In* ESA, Fourth European Symposium on Life Sciences Research in Space Nov. 1990 p 183-185 (For primary document see N91-19572 11-51)
(Grant Danish-SB-1112-14/89)
Copyright Avail: NTIS HC/MF A25; EPD, ESTEC, Noordwijk, Netherlands, HC 80 Dutch guilders

N91-19613# Royal Air Force Inst. of Aviation Medicine, Farnborough (England).
VESTIBULAR TESTS ON UK ASTRONAUT CANDIDATES FOR AN ANGLO/RUSSIAN SPACE FLIGHT (JUNO MISSION)
J. R. R. Stott and Alan J. Benson *In* ESA, Fourth European Symposium on Life Sciences Research in Space Nov. 1990 p 187-190 (For primary document see N91-19572 11-51)
Copyright Avail: NTIS HC/MF A25; EPD, ESTEC, Noordwijk, Netherlands, HC 80 Dutch guilders

N91-19614# Institute for Endocrinological and Metabolic Diseases, Rome (Italy). Unit for Endocrinological and Metabolic Diseases.
HEAD-DOWN TILT TEST AND SPACE-RELATED ENDOCRINE PHYSIOLOGY
Felice Strollo, G. Strollo, H. More, and G. Riondino *In* ESA, Fourth European Symposium on Life Sciences Research in Space Nov. 1990 p 191-195 (For primary document see N91-19572 11-51)
Copyright Avail: NTIS HC/MF A25; EPD, ESTEC, Noordwijk, Netherlands, HC 80 Dutch guilders

N91-19615# Karolinska Inst., Stockholm (Sweden). Dept. of Baromedicine.
EFFECTS OF TRAINING WITH REDUCED PERFUSION PRESSURE ON PERFORMANCE AND MUSCLE FIBER CHARACTERISTICS
Carl J. Sundberg, O. Eiken, M. Esbjoernsson, A. Nygren (Karolinska Hospital, Stockholm, Sweden), and L. Kaijser *In* ESA, Fourth European Symposium on Life Sciences Research in Space Nov. 1990 p 197-198 (For primary document see N91-19572 11-51)
Copyright Avail: NTIS HC/MF A25; EPD, ESTEC, Noordwijk, Netherlands, HC 80 Dutch guilders

N91-19616# Karolinska Inst., Stockholm (Sweden). Environmental Physiology Lab.
MUSCLE FUNCTION IMPAIRMENT FOLLOWING LOWER LIMB UNLOADING IN MEN
Per A. Tesch, Hans E. Berg, T. Haeggmark, H. Ohlsen, and G. A. Dudley (Bionetics Corp., Cocoa Beach, FL.) *In* ESA, Fourth European Symposium on Life Sciences Research in Space Nov. 1990 p 199-200 (For primary document see N91-19572 11-51)
Copyright Avail: NTIS HC/MF A25; EPD, ESTEC, Noordwijk, Netherlands, HC 80 Dutch guilders

N91-19617# Institute of Biomedical Problems, Moscow (USSR).
THE BIOLOGICAL AND MEDICAL PROGRAMME OF THE MANNED ARAGATZ MISSION ON THE MIR SPACE STATION
A. Kotovskaia and Didier Vassaux (Centre National de la Recherche Scientifique, Paris, France) *In* ESA, Fourth European Symposium on Life Sciences Research in Space Nov. 1990 p 207-214 (For primary document see N91-19572 11-51)
Copyright Avail: NTIS HC/MF A25; EPD, ESTEC, Noordwijk, Netherlands, HC 80 Dutch guilders

N91-19618# European Space Agency. European Space Research and Technology Center, ESTEC, Noordwijk (Netherlands).
GRAVITY EFFECTS ON CELLS
Dick A. M. Mesland *In its* Fourth European Symposium on Life Sciences Research in Space Nov. 1990 p 221-225 (For primary document see N91-19572 11-51)
Copyright Avail: NTIS HC/MF A25; EPD, ESTEC, Noordwijk, Netherlands, HC 80 Dutch guilders

N91-19619# Institut National de la Sante et de la Recherche Medicale, Nice (France). Faculty of Medicine.
EXPERIMENT LYMPHOCYTES OF ARAGATZ MISSION: INFLUENCE OF THE SPACE FLIGHT ON HUMAN T LYMPHOCYTE AND MONOCYTE FUNCTIONS
Laurence Schaffar, Irena V. Konstantinova, S. Manie, I. Serov, J. P. Breittmayer, I. N. Antropova, I. E. Vorotnikova (Institute of Biomedical Problems, Moscow, USSR), and B. Ferrua *In* ESA, Fourth European Symposium on Life Sciences Research in Space Nov. 1990 p 227-228 (For primary document see N91-19572 11-51)
(Grant CNES-89/1263)
Copyright Avail: NTIS HC/MF A25; EPD, ESTEC, Noordwijk, Netherlands, HC 80 Dutch guilders

N91-19630# Centre Hospitalier Univ. Purpan, Toulouse (France). Lab. de Biologie Cellulaire.
HUMAN DERMAL FIBROBLAST SENSITIVITY TO HYPERGRAVITY
Yolande Gaubin, F. Croute, D. Hartmann (Pasteur, Louis Univ., Lyon, France), B. Pianezzi, and J. P. Soleihavoup *In* ESA, Fourth European Symposium on Life Sciences Research in

Space Nov. 1990 p 281-283 (For primary document see N91-19572 11-51)
Copyright Avail: NTIS HC/MF A25; EPD, ESTEC, Noordwijk, Netherlands, HC 80 Dutch guilders

N91-19633# Alicante Univ. (Spain). Dept. de Neuroquimica.
MICROGRAVITY, HYPERGRAVITY, AND AGING: A UNIFYING HYPOTHESIS
Jaime Miquel, E. Ramirez, M. C. Holgado, E. deJuan, and R. Marco (Universidad Autonoma de Madrid, Cantoblanco, Spain) *In* ESA, Fourth European Symposium on Life Sciences Research in Space Nov. 1990 p 295-300 Sponsored in part by Ministerio de Educacion y Ciencia (For primary document see N91-19572 11-51)
(Contract CICYT-ESP-88-0351)
Copyright Avail: NTIS HC/MF A25; EPD, ESTEC, Noordwijk, Netherlands, HC 80 Dutch guilders

N91-19642# Institute of Biomedical Problems, Moscow (USSR).
HUMAN AND ANIMAL RESULTS ON VESTIBULAR RESEARCH IN SPACE: VERIS
I. B. Kozlovskaya, B. M. Babaev, V. A. Barmin, I. N. Beloozerova, L. N. Kornilova, M. G. Sirota, and S. B. Yakushin *In* ESA, Fourth European Symposium on Life Sciences Research in Space Nov. 1990 p 353-357 (For primary document see N91-19572 11-51)
Copyright Avail: NTIS HC/MF A25; EPD, ESTEC, Noordwijk, Netherlands, HC 80 Dutch guilders

N91-19644# Milan Univ. (Italy). Ist. di Clinica Medica Generale.
BLOOD PRESSURE MATURATION CURVE IN NORMOTENSIVE RATS DURING GROWTH IN SIMULATED MICROGRAVITATIONAL ENVIRONMENT
Fabio Magrini, M. Ciulla, R. Meazza, and P. Reggiani *In* ESA, Fourth European Symposium on Life Sciences Research in Space Nov. 1990 p 363-365 Prepared in cooperation with Italian Space Agency, Rome (For primary document see N91-19572 11-51)
Copyright Avail: NTIS HC/MF A25; EPD, ESTEC, Noordwijk, Netherlands, HC 80 Dutch guilders

N91-19651# Milan Univ. (Italy). Ist. di Fisiologia Umana.
GRAVITY DEPENDENCE OF PLEURAL LIQUID TURNOVER
Giuseppe Miserocchi and Daniela Negrini *In* ESA, Fourth European Symposium on Life Sciences Research in Space Nov. 1990 p 397-399 (For primary document see N91-19572 11-51)
Copyright Avail: NTIS HC/MF A25; EPD, ESTEC, Noordwijk, Netherlands, HC 80 Dutch guilders

N91-19680# Johann-Wolfgang-Goethe-Univ., Frankfurt am Main (Germany, F.R.). Botanisches Inst.
GENETIC RISK AND PHYSIOLOGICAL STRESS INDUCED BY HEAVY IONS
A. R. Kranz *In* ESA, Fourth European Symposium on Life Sciences Research in Space Nov. 1990 p 559-563 (For primary document see N91-19572 11-51)
(Grant BMFT-01-QV-85650)
Copyright Avail: NTIS HC/MF A25; EPD, ESTEC, Noordwijk, Netherlands, HC 80 Dutch guilders

N91-19687*# National Aeronautics and Space Administration. John F. Kennedy Space Center, Cocoa Beach, FL.
CENTRAL AND PERIPHERAL CARDIOVASCULAR RESPONSES TO ELECTRICALLY INDUCED AND VOLUNTARY LEG EXERCISE
B. Saltin, S. Strange, J. Bangsbo, C. K. Kim, M. Duvoisin, A. Hargens, and P. D. Gollnick (Washington State Univ., Pullman.) *In* ESA, Fourth European Symposium on Life Sciences Research in Space Nov. 1990 p 591-595 (For primary document see N91-19572 11-51)
Copyright Avail: NTIS HC/MF A25; EPD, ESTEC, Noordwijk, Netherlands, HC 80 Dutch guilders CSCL 06P

N91-19688# Sheffield Univ. (England). Dept. of Medical Physics and Clinical Engineering.
VISUALISATION OF FLUID SHIFTS WITHIN THE BODY DURING A PARABOLIC FLIGHT BY MEASUREMENTS OF ELECTRICAL BIO-IMPEDANCE
Frank J. McArdle, David Grundy, B. H. Brown, and D. C. Barber *In* ESA, Fourth European Symposium on Life Sciences Research in Space Nov. 1990 p 597-602 (For primary document see N91-19572 11-51)
Copyright Avail: NTIS HC/MF A25; EPD, ESTEC, Noordwijk, Netherlands, HC 80 Dutch guilders

N91-19689# Lyon-1 Univ., Villeurbanne (France). Lab. d'Environ. Physiologie.
VOLUME REGULATING HORMONES, FLUID AND ELECTROLYTE MODIFICATIONS DURING THE ARAGATZ MISSION (MIR STATION)
Guillemette Gauquelin, G. Geelen, C. Gharib, A. I. Grigoriev, Antonio Guell, R. Kvetnansky, L. Macho, V. Noskov, P. Pasi, and J. Soukanov (Institute of Biomedical Problems, Moscow, USSR) et al *In* ESA, Fourth European Symposium on Life Sciences Research in Space Nov. 1990 p 603-608 Sponsored in part by CNES (For primary document see N91-19572 11-51)
(Grant DRET-89-237)
Copyright Avail: NTIS HC/MF A25; EPD, ESTEC, Noordwijk, Netherlands, HC 80 Dutch guilders

N91-19691# Academy of Sciences (USSR), Moscow.
THE REFERENCE SYSTEMS FOR TACTILE PERCEPTION AND FOR THE ORIENTATION WITH RESPECT TO BODY
Victor S. Gurfinkel, F. Lestienne, Y. S. Levick, K. E. Popov, and L. Lefort (Centre National de la Recherche Scientifique, Paris, France) *In* ESA, Fourth European Symposium on Life Sciences Research in Space Nov. 1990 p 611-615 (For primary document see N91-19572 11-51)
Copyright Avail: NTIS HC/MF A25; EPD, ESTEC, Noordwijk, Netherlands, HC 80 Dutch guilders

N91-19692# Centre National de la Recherche Scientifique, Paris (France). Lab. de Physiologie Neurosensorielle.
GAZE CONTROL AND SPATIAL MEMORY IN WEIGHTLESSNESS
Claudie Andre-Deshays, I. Israel, A. Berthoz, K. E. Popov, and M. I. Lipschits (Academy of Sciences, USSR, Moscow) *In* ESA, Fourth European Symposium on Life Sciences Research in Space Nov. 1990 p 617-621 Sponsored by CNES (For primary document see N91-19572 11-51)
Copyright Avail: NTIS HC/MF A25; EPD, ESTEC, Noordwijk, Netherlands, HC 80 Dutch guilders

N91-19693# Amsterdam Univ. (Netherlands).
PUPIL SIZE IN PARABOLIC FLIGHT
Hendrika W. Kortschot, Wilhelmus J. Oosterveld, and H. A. A. deJong *In* ESA, Fourth European Symposium on Life Sciences Research in Space Nov. 1990 p 623-624 Sponsored by Space Research Organization Netherlands (For primary document see N91-19572 11-51)
Copyright Avail: NTIS HC/MF A25; EPD, ESTEC, Noordwijk, Netherlands, HC 80 Dutch guilders

N91-19694# Centre National de la Recherche Scientifique, Paris (France). Lab. de Physiologie Neurosensorielle.
MENTAL ROTATION OF THREE-DIMENSIONAL SHAPES IN MICROGRAVITY
Yoani Matsakis, A. Berthoz, M. I. Lipschits, and Victor S. Gurfinkel (Academy of Sciences, USSR, Moscow) *In* ESA, Fourth European Symposium on Life Sciences Research in Space Nov. 1990 p 625-629 (For primary document see N91-19572 11-51)
Copyright Avail: NTIS HC/MF A25; EPD, ESTEC, Noordwijk, Netherlands, HC 80 Dutch guilders

N91-19695# Deutsche Sporthochschule, Cologne (Germany, F.R.). Inst. fuer Physiologie.
WEIGHTLESSNESS COUNTERMEASURES AND HUMAN PHYSIOLOGY IN SPACE: A POTENTIAL CONFLICT
Juergen P. Stegemann *In* ESA, Fourth European Symposium on Life Sciences Research in Space Nov. 1990 p 631-635 (For primary document see N91-19572 11-51)
Copyright Avail: NTIS HC/MF A25; EPD, ESTEC, Noordwijk, Netherlands, HC 80 Dutch guilders

N91-20030*# North Carolina Univ., Greensboro. Dept. of Mathematics and Statistics.
CAROTID-CARDIAC BAROREFLEX INFLUENCE ON FOREARM VASCULAR RESISTANCE DURING LOW LEVEL LBNP
David Ludwig *In* NASA, John F. Kennedy Space Center, Research Reports: 1990 NASA/ASEE Summer Faculty Fellowship Program Sep. 1990 p 222-243 (For primary document see N91-20022 11-99)
(Grant NGT-60002)
Avail: NTIS HC/MF A23 CSCL 06P

53 BEHAVIORAL SCIENCES

Includes psychological factors; individual and group behavior; crew training and evaluation; and psychiatric research.

N91-19713# Army Research Inst. for the Behavioral and Social Sciences, Alexandria, VA.
TEST ANALYSIS PROGRAM EVALUATION: ITEM STATISTICS AS FEEDBACK TO TEST DEVELOPERS Final Report, Feb. 1989 - Mar. 1990
Peter J. Legree Oct. 1990 17 p
(AD-A229851; ARI-RN-91-03) Avail: NTIS HC/MF A03 CSCL 14/2

The test analysis program was evaluated to determine the feasibility of using a personal computer to provide course developers with item statistics. This project was undertaken because of Signal School concern that course tests do not accurately measure student school performance. The evaluation focused on the usefulness of providing item statistics to course test developers and demonstrated that many of the tests contain poorly written items. The evaluation indicates that a computerized test analysis program can be used to identify questionable test items and help ensure Signal School tests are adequate to validate lessons and courses. GRA

54 MAN/SYSTEM TECHNOLOGY AND LIFE SUPPORT

Includes human engineering; biotechnology; and space suits and protective clothing.

For related information see also *16 Space Transportation.*

N91-19714*# Sterling Federal Systems, Inc., Palo Alto, CA.
ARMY-NASA AIRCREW/AIRCRAFT INTEGRATION PROGRAM (A3I) SOFTWARE DETAILED DESIGN DOCUMENT, PHASE 3
Carolyn Banda, Alex Chiu, Gretchen Helms, TehMing Hsieh, Andrew Lui, Jerry Murray, and Renuka Shankar Jun. 1990 303 p
(Contract NAS2-11555)
(NASA-CR-177557; A-90197; NAS 1.26:177557) Avail: NTIS HC/MF A14 CSCL 05H

The capabilities and design approach of the MIDAS (Man-machine Integration Design and Analysis System) computer-aided engineering (CAE) workstation under development by the Army-NASA Aircrew/Aircraft Integration Program is detailed. This workstation uses graphic, symbolic, and numeric prototyping tools and human performance models as part of an integrated design/analysis environment for crewstation human engineering. Developed incrementally, the requirements and design for Phase 3 (Dec. 1987 to Jun. 1989) are described. Software tools/models developed or significantly modified during this phase included: an interactive 3-D graphic cockpit design editor; multiple-perspective graphic views to observe simulation scenarios; symbolic methods to model the mission decomposition, equipment functions, pilot tasking and loading, as well as control the simulation; a 3-D dynamic anthropometric model; an intermachine communications package; and a training assessment component. These components were successfully used during Phase 3 to demonstrate the complex interactions and human engineering findings involved with a proposed cockpit communications design change in a simulated AH-64A Apache helicopter/mission that maps to empirical data from a similar study and AH-1 Cobra flight test. Author

N91-19025*# Massachusetts Inst. of Tech., Cambridge. Flight Transportation Lab.
AUTOMATIC SPEECH RECOGNITION IN AIR TRAFFIC CONTROL: A HUMAN FACTORS PERSPECTIVE
Joakim Karlsson *In* NASA, Langley Research Center, Joint University Program for Air Transportation Research, 1989-1990 Dec. 1990 p 9-13 (For primary document see N91-19024 11-01)
Avail: NTIS HC/MF A09 CSCL 05H

N91-19582# Nuevas Tecnologias Espaciales S.A., Llissa d'Amunt (Spain).
DESIGN, IMPLEMENTATION AND EVALUATION OF NEW FULLY AUTOMATED ALGORITHMS FOR THE EXTRACTION OF CARDIAC PARAMETERS FROM 3D, 2D AND M-MODE ECHOCARDIOGRAMS
Rene Alquezar and X. Lobao *In* ESA, Fourth European Symposium on Life Sciences Research in Space Nov. 1990 p 51-57 (For primary document see N91-19572 11-51)
(Contract ESA-7320/87/NL/PP)
Copyright Avail: NTIS HC/MF A25; EPD, ESTEC, Noordwijk, Netherlands, HC 80 Dutch guilders

N91-19609# Deutsche Forschungsanstalt fuer Luft- und Raumfahrt, Cologne (Germany, F.R.). Microgravity User Support Center.
TOOLS FOR THE PREPARATION, PERFORMANCE AND EVALUATION OF LIFE SCIENCES EXPERIMENTS
Dittmar Padeken, Marianne Schuber, and Dieter Seibt *In* ESA, Fourth European Symposium on Life Sciences Research in Space Nov. 1990 p 171-174 (For primary document see N91-19572 11-51)
Copyright Avail: NTIS HC/MF A25; EPD, ESTEC, Noordwijk, Netherlands, HC 80 Dutch guilders

N91-19655# European Space Agency. European Space Research and Technology Center, ESTEC, Noordwijk (Netherlands).
TOWARDS BIOREGENERATIVE LIFE SUPPORT SYSTEMS
Francois Brechignac *In its* Fourth European Symposium on Life Sciences Research in Space Nov. 1990 p 421-429 (For primary document see N91-19572 11-51)
Copyright Avail: NTIS HC/MF A25; EPD, ESTEC, Noordwijk, Netherlands, HC 80 Dutch guilders

N91-19656# Dornier System G.m.b.H., Friedrichshafen (Germany, F.R.).
PLANT PRODUCTION AS PART OF A CONTROLLED ECOLOGICAL LIFE SUPPORT SYSTEM (CELSS)
Katja David, Robert Backhaus (Deutsche Forschungsanstalt fuer Luft- und Raumfahrt, Cologne, Germany, F.R.), and Ake Ingemar Skoog *In* ESA, Fourth European Symposium on Life Sciences Research in Space Nov. 1990 p 431-434 (For primary document see N91-19572 11-51)
Copyright Avail: NTIS HC/MF A25; EPD, ESTEC, Noordwijk, Netherlands, HC 80 Dutch guilders

N91-19657# Commissariat a l'Energie Atomique, Cadarache (France). Dept. de Physiologie Vegetale et Ecosystemes.
A GROUND BASED MODULE FOR EXPERIMENTATIONS OF CULTIVATIONS AND RECYCLING IN A CLOSED ENVIRONMENT
Marcel Jean Andre, D. Massimino, J. Massimino, and M.-C. Duchein *In* ESA, Fourth European Symposium on Life Sciences Research in Space Nov. 1990 p 435-440 Sponsored by CNES (For primary document see N91-19572 11-51)
Copyright Avail: NTIS HC/MF A25; EPD, ESTEC, Noordwijk, Netherlands, HC 80 Dutch guilders

N91-19659# Institute of Crop Science and Plant Breeding, Brunswick (Germany, F.R.).
PHYSIOLOGICAL CRITERIA AND REQUIREMENT OF BIOMASS PRODUCTION UNDER CONTROLLED ECOLOGICAL LIFE SUPPORT SYSTEMS
Nasir ElBassam, G. Mix, and Katja David (Dornier System G.m.b.H., Friedrichshafen, Germany, F.R.) *In* ESA, Fourth European Symposium on Life Sciences Research in Space Nov. 1990 p 445-448 (For primary document see N91-19572 11-51)
Copyright Avail: NTIS HC/MF A25; EPD, ESTEC, Noordwijk, Netherlands, HC 80 Dutch guilders

N91-19660# Colorado Univ., Boulder. BioServe Space Technologies Center.
TUNING THE EFFICIENCIES OF PLANT LIGHTING SYSTEMS: FROM PRIMARY ENERGY TO EDIBLE BIOMASS: THE LED AS AN ALTERNATIVE LIGHT SOURCE
Alexander Hoehn and Marvin W. Luttges *In* ESA, Fourth European Symposium on Life Sciences Research in Space Nov. 1990 p 449-454 (For primary document see N91-19572 11-51)
Copyright Avail: NTIS HC/MF A25; EPD, ESTEC, Noordwijk, Netherlands, HC 80 Dutch guilders CSCL 06K

N91-19679# Commissariat a l'Energie Atomique, Fontenay-aux-Roses (France). Centre d'Etudes Nucleaires.
NEW EXPERIMENTAL APPROACH IN QUALITY FACTOR AND DOSE EQUIVALENT DETERMINATION DURING A LONG TERM MANNED SPACE MISSION
Van Dat Nguyen, P. Bouisset, N. Parmentier, M. Siegrist, Y. A. Akatov, V. V. Archangelsky, S. Vorojtsov, S. B. Koslova, V. G. Mitrikas, and V. M. Petrov (Institute of Biomedical Problems, Moscow, USSR) et al *In* ESA, Fourth European Symposium on Life Sciences Research in Space Nov. 1990 p 555-558 (For primary document see N91-19572 11-51)
Copyright Avail: NTIS HC/MF A25; EPD, ESTEC, Noordwijk, Netherlands, HC 80 Dutch guilders

55 SPACE BIOLOGY

Includes exobiology; planetary biology; and extraterrestrial life.

No abstracts in this category.

59 MATHEMATICAL AND COMPUTER SCIENCES (GENERAL)

N91-19715*# Institute for Computer Applications in Science and Engineering, Hampton, VA.
COMPLETE EXCHANGE ON THE IPSC-860 Final Report
Shahid H. Bokhari (University of Engineering and Technology, Lahore, Pakistan) Jan. 1991 33 p Presented at the 1991 International Conference on Parallel Processing
(Contract NAS1-18605)
(NASA-CR-187498; NAS 1.26:187498; ICASE-91-4) Avail: NTIS HC/MF A03 CSCL 12A

The implementation of complete exchange on the circuit switched Intel iPSC-860 hypercube is described. This pattern, also known as all-to-all personalized communication, is the densest requirement that can be imposed on a network. On the iPSC-860, care needs to be taken to avoid edge contention, which can have a disastrous impact on communication time. There are basically two classes of algorithms that achieve contention-free complete exchange. The first contains the classical standard exchange algorithm that is generally useful for small message sizes. The second includes a number of optimal or near-optimal algorithms that are best for large messages. Measurement of communication overhead on the iPSC-860 are given and a notation for analyzing communication link usage is developed. It is shown that for the two classes of algorithms, there is substantial variation in performance with synchronization technique and choice of message protocol. Timings of six implementations are given; each of these is useful over a particular range of message size and cube dimension. Since the complete exchange is a superset of communication patterns, these timings represent upper bounds on the time required by an arbitrary communication requirement. These results indicate that the programmer needs to evaluate several possibilities before finalizing an implementation - a careful choice can lead to very significant savings in time. Author

N91-19716*# Institute for Computer Applications in Science and Engineering, Hampton, VA.
MULTIPHASE COMPLETE EXCHANGE ON A CIRCUIT SWITCHED HYPERCUBE Final Report
Shahid H. Bokhari Jan. 1991 25 p Submitted for publication
(Contract NAS1-18605)
(NASA-CR-187499; ICASE-91-5; NAS 1.26:187499) Avail: NTIS HC/MF A03 CSCL 12A

On a distributed memory parallel computer, the complete exchange (all-to-all personalized) communication pattern requires each of n processors to send a different block of data to each of the remaining n - 1 processors. This pattern is at the heart of many important algorithms, most notably the matrix transpose. For a circuit switched hypercube of dimension d(n = 2(sup d)), two algorithms for achieving complete exchange are known. These are (1) the Standard Exchange approach that employs d transmissions of size 2(sup d-1) blocks each and is useful for small block sizes, and (2) the Optimal Circuit Switched algorithm that employs 2(sup d) - 1 transmissions of 1 block each and is best for large block sizes. A unified multiphase algorithm is described that includes these two algorithms as special cases. The complete exchange on a hypercube of dimension d and block size m is achieved by carrying out k partial exchange on subcubes of dimension d(sub i) Sigma(sup k)(sub i=1) d(sub i) = d and effective block size m(sub i) = m2(sup d-di). When k = d and all d(sub i) = 1, this corresponds to algorithm (1) above. For the case of k = 1 and d(sub i) = d, this becomes the circuit switched algorithm (2). Changing the subcube dimensions d, varies the effective block size and permits a compromise between the data permutation and block transmission overhead of (1) and the startup overhead of (2). For a hypercube of dimension d, the number of possible combinations of subcubes is p(d), the number of partitions of the integer d. This is an exponential but very slowly growing function and it is feasible over these partitions to discover the best combination for a given message size. The approach was analyzed for, and implemented on, the Intel iPSC-860 circuit switched hypercube. Measurements show good agreement with predictions and demonstrate that the multiphase approach can substantially improve performance for block sizes in the 0 to 160 byte range. This range, which corresponds to 0 to 40 floating point numbers per processor, is commonly encountered in practical numeric applications. The multiphase technique is applicable to all circuit-switched hypercubes that use the common e-cube routing strategy. Author

60 COMPUTER OPERATIONS AND HARDWARE

Includes hardware for computer graphics, firmware, and data processing.

For components see *33 Electronics and Electrical Engineering.*

N91-19717 Department of the Navy, Washington, DC.
ENHANCED CROSSTIE RANDOM ACCESS MEMORY ELEMENT AND PROCESS FOR THE FABRICATION THEREOF Patent
Leonard J. Schwee, inventor (to Navy) 9 Oct. 1990 6 p Filed 20 Jun. 1983
(AD-D014723; US-Patent-4,962,477; US-Patent-Appl-SN-505617; US-Patent-Class-365-87) Avail: US Patent and Trademark Office CSCL 12/6

This patent discloses an enhanced random access memory element and a process for its fabrication, wherein permalloy thin films are patterned, inter-alia, into a plurality of geminous memory cells to form a matrix or array of juxtaposed sloped columns. Each of the geminous memory cells is configured into a unique pattern comprising twin sub-patterns joined in an opposite fashion, i.e., reversed and inversed, so as to share a common area of permalloy. Consequently, magnetic domain walls (Neel walls) are formed at opposite and adjacent apexes of the unique pattern parallel to the easy axis after a predetermined magnetic field is applied along the hard axis of array of geminous memory cells and then reduced to zero. In this way, the magnetization is properly aligned for use of the array of geminous memory cells as an enhanced nonvolatile random access memory element. Subsequent magnetization of the proper amount at particular ones of the geminous memory cells will cause two crossties and two Bloch lines to form therein so as to couple to each other, crosstie to Bloch line, Bloch line to crosstie. This configuration provides a larger readout signal, a larger signal to noise ratio, and will operate at lower power levels for the same density of information as previous crosstie random access memory elements. GRA

N91-19718*# California Univ., Berkeley. Computer Science Div.
PERFORMANCE MEASUREMENTS OF THE FIRST RAID PROTOTYPE
Ann L. Chervenak 17 May 1990 58 p
(Grant NAG2-591)
(NASA-CR-187958; NAS 1.26:187958; UCB/CSD-90/574) Avail: NTIS HC/MF A04 CSCL 09B

The performance is examined of Redundant Arrays of Inexpensive Disks (RAID) the First, a prototype disk array. A hierarchy of bottlenecks was discovered in the system that limit overall performance. The most serious is the memory system contention on the Sun 4/280 host CPU, which limits array bandwidth to 2.3 MBytes/sec. The array performs more successfully on small random operations, achieving nearly 300 I/Os per second before the Sun 4/280 becomes CPU limited. Other bottlenecks in the system are the VME backplane, bandwidth on the disk controller, and overheads associated with the SCSI protocol. All are examined in detail. The main conclusion is that to achieve the potential bandwidth of arrays, more powerful CPU's alone will not suffice. Just as important are adequate host memory bandwidth and support for high bandwidth on disk controllers. Current disk controllers are more often designed to achieve large numbers of small random operations, rather than high bandwidth. Operating systems also need to change to support high bandwidth from disk arrays. In particular, they should transfer data in larger blocks, and should support asynchronous I/O to improve sequential write performance. Author

N91-19719# Stanford Linear Accelerator Center, CA.
A VALIANT LITTLE TERMINAL: A VLT USER'S MANUAL
Amanda Weinstein Dec. 1990 109 p
(Contract DE-AC03-76SF-00515)
(DE91-007295; SU-SLAC-370-Rev) Avail: NTIS HC/MF A06

A manual for the valiant little terminal is presented. The following subject areas are covered: an introduction to VLT; installation and starting up; the user interface; writing scripts; and troubleshooter. DOE

N91-19720# Westinghouse Savannah River Co., Aiken, SC.
ARCHY (ANALYSIS AND REVERSE ENGINEERING OF CODE USING HIERARCHY AND YOURDON): A TOOL FOR FORTRAN CODE MAINTENANCE AND DEVELOPMENT
J. E. Aull Oct. 1990 12 p Presented at the 1990 Computer Symposium, Pittsburgh, Oct. - Nov. 1990
(Contract DE-AC09-89SR-18035)
(DE91-007241; WSRC-MS-90-150; CONF-9010256-6) Avail: NTIS HC/MF A03

Analysis and Reverse Engineering of Code Using Hierarchy and Yourdon (ARCHY) diagrams is a tool for development and maintenance of FORTRAN programs. When FORTRAN source code is read by ARCHY, it automatically creates a database that includes a data dictionary, which lists each variable, its dimensions, type, category (set, referenced, passed), module calling structure, and common block information. The database exists in an ASCII file that can be directly edited or maintained with the ARCHY database editor. The database is used by ARCHY to product structure charts and Yourdon data flow diagrams in PostScript format. ARCHY also transfers database information such as a variable definitions, module descriptions, and technical references to and from module headers. ARCHY contains several utilities for making programs more readable. It can automatically indent the body of loops and conditionals and resequence statement labels. Various language extensions are translated into FORTRAN-77 to increase code portability. ARCHY frames comment statements and groups FORMAT statements at the end of modules. It can alphabetize modules within a program, end-of-line labels can be added, and it can also change executable statements to upper or lower case. ARCHY runs under the VAX-VMS operating system and inputs from VAX-FORTRAN, IBM-FORTRAN, and CRAY FORTRAN sources files. DOE

61 COMPUTER PROGRAMMING AND SOFTWARE

Includes computer programs, routines, alogorithms, and specific applications, e.g., CAD/CAM.

N91-19721# National Academy of Sciences - National Research Council, Washington, DC. System Security Study Committee.
COMPUTERS AT RISK: SAFE COMPUTING IN THE INFORMATION AGE
1991 318 p
(Contract N00014-89-J-1731)
(LC-90-22329; ISBN-0309-04388-3) Avail: NTIS HC/MF A14

Computer systems need safeguards to prevent intrusions and potential disasters that can cause economic and even human losses from, for example, components of medical and transportation equipment or domestic and international financial systems. Security is constrained by lack of management awareness, lack of public awareness of security risks and options, lack of guidance, government's internecine conflicts, and underfunding. Momentum is building overseas for a new set of criteria and associated system evaluation schemes and standards. U.S. response to these developments will affect the competitiveness of U.S. vendors and the options available to users of commercial computer systems worldwide. This report characterizes the computer security problem and advances recommendations for containing it. It examines technology necessary to achieve system security and trustworthiness, and associated development issues, programming methodology, the design and use of criteria for secure computer system development and evaluation, and problems constraining the market for trustworthy systems. The System Security Study Committee concluded that several steps must be taken to achieve greater computer system security and trustworthiness, and that the best approach to implementing necessary actions is to establish

a new organization, referred to as the Information Security Foundation (ISF). The ISF and roles and limitations of organizations in the computer security arena are discussed. Outlined are topics and tactics for research to enable needed technology development. J.P.S.

N91-19722*# Houston Univ., Clear Lake, TX. Software Engineering Professional Education Center.
RICIS 1988 SYMPOSIUM PROCEEDINGS. PRESENTATION APPENDIX
1988 135 p Symposium held in Clear Lake, TX, 9-10 Nov. 1988
(Contract NCC9-16)
(NASA-CR-188077; NAS 1.26:188077) Avail: NTIS HC/MF A07 CSCL 09B

Additional papers presented at the RICIS (Research Institute for Computing and Information Systems) are presented. The papers are primarily on the study of Software Engineering and Software Tools. For individual titles, see N91-19723 through N91-19730.

N91-19723*# Carnegie-Mellon Univ., Pittsburgh, PA. Software Engineering Inst.
SOFTWARE DEVELOPMENT ENVIRONMENTS: STATUS AND TRENDS
Larry E. Duffel *In* Houston Univ., RICIS 1988 Symposium Proceedings. Presentation appendix 1988 31 p Sponsored in part by DOD (For primary document see N91-19722 11-61)
Avail: NTIS HC/MF A07 CSCL 09B

Currently software engineers are the essential integrating factors tying several components together. The components consist of process, methods, computers, tools, support environments, and software engineers. The engineers today empower the tools versus the tools empowering the engineers. Some of the issues in software engineering are quality, managing the software engineering process, and productivity. A strategy to accomplish this is to promote the evolution of software engineering from an ad hoc, labor intensive activity to a managed, technology supported discipline. This strategy may be implemented by putting the process under management control, adopting appropriate methods, inserting the technology that provides automated support for the process and methods, collecting automated tools into an integrated environment and educating the personnel. E.R.

N91-19724*# Software Productivity Consortium, Reston, VA.
THE NEXT GENERATION
Howard Yudkin *In* Houston Univ., RICIS 1988 Symposium Proceedings. Presentation appendix 1988 20 p (For primary document see N91-19722 11-61)
Avail: NTIS HC/MF A07 CSCL 09B

The next generation of computer systems are studied by examining the processes and methodologies. The present generation is ok for small projects, but not so good for large projects. They are not good for addressing the iterative nature of requirements, resolution, and implementation. They do not address complexity issues of requirements stabilization. They do not explicitly address reuse opportunities, and they do not help with people shortages. Therefore, there is a need to define and automate improved software engineering processes. Some help may be gained by reuse and prototyping, which are two sides of the same coin. Reuse library parts are used to generate good approximations to desired solutions, i.e., prototypes. And rapid prototype composition implies use of preexistent parts, i.e., reusable parts. E.R.

N91-19725*# Concurrent Computer Corp., Westford, MA.
A NEW GENERATION OF REAL-TIME DOS TECHNOLOGY FOR MISSION-ORIENTED SYSTEM INTEGRATION AND OPERATION
E. Douglas Jensen *In* Houston Univ., RICIS 1988 Symposium Proceedings. Presentation appendix 1988 15 p (For primary document see N91-19722 11-61)
Avail: NTIS HC/MF A07 CSCL 09B

Information is given on system integration and operation (SIO) requirements and a new generation of technical approaches for SIO. Real-time, distribution, survivability, and adaptability requirements and technical approaches are covered. An Alpha operating system program management overview is outlined. Author

N91-19726*# National Aeronautics and Space Administration. Lyndon B. Johnson Space Center, Houston, TX.
MISSION OPERATIONS DIRECTORATE: FACILITY AND SUPPORT SYSTEMS DIVISION
Michael J. See *In* Houston Univ., RICIS 1988 Symposium Proceedings. Presentation appendix 1988 7 p (For primary document see N91-19722 11-61)
Avail: NTIS HC/MF A07 CSCL 09B

Information is given in viewgraph form on the responsibilities of the Advanced Projects Section, requirements analysis fundamentals, and the causes of the problem of software products of the current development process that do not meet 'true' user needs upon delivery. Author

N91-19727*# Lockheed Corp., Houston, TX.
TOOL AND DATA INTEROPERABILITY IN THE SSE SYSTEM
Chuck Shotton *In* Houston Univ., RICIS 1988 Symposium Proceedings. Presentation appendix 1988 11 p (For primary document see N91-19722 11-61)
Avail: NTIS HC/MF A07 CSCL 09B

Information is given in viewgraph form on tool and data interoperability in the Software Support Environment (SSE). Information is given on industry problems, SSE system interoperability issues, SSE solutions to tool and data interoperability, and attainment of heterogeneous tool/data interoperability. Author

N91-19728*# Lockheed Missiles and Space Co., Austin, TX. Software Technology Center.
EMPIRICAL STUDIES OF SOFTWARE DESIGN: IMPLICATIONS FOR SSEs
Herb Krasner *In* Houston Univ., RICIS 1988 Symposium Proceedings. Presentation appendix 1988 18 p (For primary document see N91-19722 11-61)
Avail: NTIS HC/MF A07 CSCL 09B

Implications for Software Engineering Environments (SEEs) are presented in viewgraph format for characteristics of projects studied; significant problems and crucial problem areas in software design for large systems; layered behavioral model of software processes; implications of field study results; software project as an ecological system; results of the LIFT study; information model of design exploration; software design strategies; results of the team design study; and a list of publications. B.G.

N91-19729*# National Aeronautics and Space Administration, Washington, DC.
THE ROLE OF SOFTWARE ENGINEERING IN THE SPACE STATION PROGRAM
Dana Hall *In* Houston Univ., RICIS 1988 Symposium Proceedings. Presentation appendix 1988 11 p (For primary document see N91-19722 11-61)
Avail: NTIS HC/MF A07 CSCL 09B

Software engineering applications snapshots within the Space Station Freedom Program; software engineering and Ada training; software reuse; hierarchial command and control; program characteristics; integrated, international environments; software production, integration, and management; and integrated simulation environment are outlined in viewgraph format. B.G.

N91-19730*# Science Applications International Corp., McLean, VA.
LESSONS LEARNED FROM AN Ada CONVERSION PROJECT
Tim Porter *In* Houston Univ., RICIS 1988 Symposium Proceedings. Presentation appendix 1988 13 p (For primary document see N91-19722 11-61)
Avail: NTIS HC/MF A07 CSCL 09B

Background; SAVVAS architecture; software portability; history

of Ada; isolation of non-portable code; simple terminal interface package; constraints of language features; and virtual interfaces are outlined. This presentation is represented by viewgraphs only. B.G.

N91-19731# Advisory Group for Aerospace Research and Development, Neuilly-Sur-Seine (France). Guidance and Control Panel.

COMPUTER AIDED SYSTEM DESIGN AND SIMULATION

George T. Schmidt (Draper, Charles Stark Lab., Inc., Cambridge, MA) Nov. 1990 25 p The 50th symposium was held in Cesme/Izmir, Turkey, 22nd - 25th May 1990

(AGARD-AR-283; ISBN-92-835-0596-6) Copyright Avail: NTIS HC/MF A03; Non-NATO Nationals requests available only from AGARD/Scientific Publications Executive

As guidance and control systems have become more complex, the role of computers in their design and development has become increasingly important. Computer aided design finds application at all stages of development. Topics addressed include: computer aided system design; simulation technology for missile and aircraft applications; hardware-in-the-loop simulation; systems applications; and pilot-in-the-loop simulations. B.G.

N91-19732*# Colorado Univ., Boulder. Computer Systems Design Group.

THE FORCE: A HIGHLY PORTABLE PARALLEL PROGRAMMING LANGUAGE Interim Report

Harry F. Jordan, Muhammad S. Benten, Gita Alaghband, and Ruediger Jakob Feb. 1989 22 p Previously announced in IAA as A90-37513

(Contract NAG1-640; N00014-86-K-0204)

(NASA-CR-187928; NAS 1.26:187928; CSDG-89-2) Avail: NTIS HC/MF A03 CSCL 09B

Here, it is explained why the FORCE parallel programming language is easily portable among six different shared-memory microprocessors, and how a two-level macro preprocessor makes it possible to hide low level machine dependencies and to build machine-independent high level constructs on top of them. These FORCE constructs make it possible to write portable parallel programs largely independent of the number of processes and the specific shared memory multiprocessor executing them. Author

N91-19733*# Jet Propulsion Lab., California Inst. of Tech., Pasadena.

ALGORITHMS FOR A VERY HIGH SPEED UNIVERSAL NOISELESS CODING MODULE

Robert F. Rice and Pen-Shu Yeh (National Aeronautics and Space Administration. Goddard Space Flight Center, Greenbelt, MD.) 15 Feb. 1991 25 p

(NASA-CR-187974; NAS 1.26:187974; JPL-Publ-91-1) Avail: NTIS HC/MF A03 CSCL 09B

The algorithmic definitions and performance characterizations are presented for a high performance adaptive coding module. Operation of at least one of these (single chip) implementations is expected to exceed 500 Mbits/s under laboratory conditions. Operation of a companion decoding module should operate at up to half the coder's rate. The module incorporates a powerful noiseless coder for Standard Form Data Sources (i.e., sources whose symbols can be represented by uncorrelated non-negative integers where the smaller integers are more likely than the larger ones). Performance close to data entropies can be expected over a Dynamic Range of from 1.5 to 12 to 14 bits/sample (depending on the implementation). Author

N91-19734*# Jet Propulsion Lab., California Inst. of Tech., Pasadena.

ON THE OPTIMALITY OF CODE OPTIONS FOR A UNIVERSAL NOISELESS CODER

Pen-Shu Yeh, Robert F. Rice, and Warner Miller (National Aeronautics and Space Administration. Goddard Space Flight Center, Greenbelt, MD.) 15 Feb. 1991 53 p

(NASA-CR-187973; NAS 1.26:187973; JPL-Publ-91-2) Avail: NTIS HC/MF A04 CSCL 09B

A universal noiseless coding structure was developed that provides efficient performance over an extremely broad range of source entropy. This is accomplished by adaptively selecting the best of several easily implemented variable length coding algorithms. Custom VLSI coder and decoder modules capable of processing over 20 million samples per second are currently under development. The first of the code options used in this module development is shown to be equivalent to a class of Huffman code under the Humblet condition, other options are shown to be equivalent to the Huffman codes of a modified Laplacian symbol set, at specified symbol entropy values. Simulation results are obtained on actual aerial imagery, and they confirm the optimality of the scheme. On sources having Gaussian or Poisson distributions, coder performance is also projected through analysis and simulation. Author

N91-19735*# Auburn Univ., AL. Dept. of Computer Science and Engineering.

QUEST/Ada (QUERY UTILITY ENVIRONMENT FOR SOFTWARE TESTING OF Ada: THE DEVELOPMENT OF A PROGRAM ANALYSIS ENVIRONMENT FOR Ada, TASK 1, PHASE 3

David B. Brown Feb. 1991 105 p

(Contract NCC8-14)

(NASA-CR-187983; NAS 1.26:187983) Avail: NTIS HC/MF A06 CSCL 09B

The results of research and development efforts of the first six months of Task 1, Phase 3 of the project are presented. The goals of Phase 3 are: (1) to further refine the rule base and complete the comparative rule base evaluation; (2) to implement and evaluate a concurrency testing prototype; (3) to convert the complete (unit-level and concurrency) testing prototype to a workstation environment; and (4) to provide a prototype development document to facilitate the transfer of research technology to a working environment. These goals were partially met and the results are summarized. Author

N91-19736*# Pennsylvania State Univ., University Park. Dept. of Astronomy and Astrophysics.

C-STATISTIC FITTING ROUTINES: USER'S MANUAL AND REFERENCE GUIDE

John A. Nousek and Vida Farwana 15 Mar. 1991 13 p

(Grant NAG5-1211)

(NASA-CR-187992; NAS 1.26:187992) Avail: NTIS HC/MF A03 CSCL 09B

The computer program is discussed which can read several input files and provide a best set of values for the functions provided by the user, using either C-statistic or the chi(exp 2) statistic method. The program consists of one main routine and several functions and subroutines. Detail descriptions of each function and subroutine is presented. A brief description of the C-statistic and the reason for its application is also presented. Y.S.

N91-19737*# Computer Sciences Corp., Hampton, VA. Applied Technology Div.

TRANSFERABLE OUTPUT ASCII DATA (TOAD) GATEWAY: VERSION 1.0 USER'S GUIDE

Bradford D. Bingel Feb. 1991 18 p

(Contract NAS1-19038)

(NASA-CR-187489; NAS 1.26:187489) Avail: NTIS HC/MF A03 CSCL 09B

The Transferable Output ASCII Data (TOAD) Gateway, release 1.0 is described. This is a software tool for converting tabular data from one format into another via the TOAD format. This initial release of the Gateway allows free data interchange among the following file formats: TOAD; Standard Interface File (SIF); Program to Optimize Simulated Trajectories (POST) input; Comma Separated Value (TSV); and a general free-form file format. As required, additional formats can be accommodated quickly and easily. Author

N91-19738# Pacific Northwest Lab., Richland, WA.
FINDING THE OBJECT PROCEEDINGS ADDENDUM
M. A. Whiting and D. M. Devaney Oct. 1990 11 p Presented at the European Conference on Object Oriented Programing '90, Ottawa, Ontario, 22 Oct. 1990
(Contract DE-AC06-76RL-01830)
(DE91-006724; PNL-SA-18945; CONF-9010307-1) Avail: NTIS HC/MF A03

The purpose of this workshop was to discuss finding the object -- that is, how software engineers imagine, invent, design, or recycle objects and their behaviors for object-oriented software engineering. The workshop organizers felt that this issue is crucial to successful object-oriented software engineering. Unfortunately, when previous workshops have had the opportunity to review and discuss techniques practitioners use to find objects, too often the results were heated debates on what is an object, which becomes all consuming. We believed that, given appropriate control over the question of which kind of object is being discussed (which meant tell us what object you are trying to find, then tell us your method), a workshop to concentrate on techniques for finding objects would be quite appropriate. DOE

N91-19739# Lawrence Livermore National Lab., CA.
DEVELOPMENT OF A NUMERICAL COMPUTER CODE AND CIRCUIT ELEMENT MODELS FOR SIMULATION OF FIRING SYSTEMS
K. H. Carpenter (Kansas State Univ., Manhattan.) 2 Jul. 1990 211 p
(Contract W-7405-eng-48)
(DE91-007162; UCRL-CR-105603) Avail: NTIS HC/MF A10

Numerical simulation of firing systems requires both the appropriate circuit analysis framework and the special element models required by the application. We have modified the SPICE circuit analysis code (version 2G.6), developed originally at the Electronic Research Laboratory of the University of California, Berkeley, to allow it to be used on MSDOS-based, personal computers and to give it two additional circuit elements needed by firing systems - fuses and saturating inductances. An interactive editor and a batch driver have been written to ease the use of the SPICE program by system designers, and the interactive graphical post processor, NUTMEG, supplied by U. C. Berkeley with SPICE version 3B1, has been interfaced to the output from the modified SPICE. Documentation and installation aids have been provided to make the total software system accessible to PC users. Sample problems show that the resulting code is in agreement with the FIRESET code on which the fuse model was based (with some modifications to the dynamics of scaling fuse parameters). In order to allow for more complex simulations of firing systems, studies have been made of additional special circuit elements - switches and ferrite cored inductances. A simple switch model has been investigated which promises to give at least a first approximation to the physical effects of a non ideal switch, and which can be added to the existing SPICE circuits without changing the SPICE code itself. The effect of fast rise time pulses on ferrites has been studied experimentally in order to provide a base for future modeling and incorporation of the dynamic effects of changes in core magnetization into the SPICE code. This report contains detailed accounts of the work on these topics performed during the period it covers, and has appendices listing all source code written documentation produced. DOE

N91-19740# Lawrence Livermore National Lab., CA.
ENERGY SCIENCES SUPERCOMPUTING 1990
A. A. Mirin, ed. and G. V. Kaiper, ed. 1990 62 p
(Contract W-7405-eng-48)
(DE91-007188; UCRL-53916) Avail: NTIS HC/MF A04

This report contains papers on the following topics: meeting the computational challenge; lattice gauge theory: probing the standard model; supercomputing for the superconducting super collider; and overview of ongoing studies in climate model diagnosis and intercomparison; magnetohydrodynamic (MHD) simulation of the fueling of a tokamak fusion reactor through the injection of compact toroids; gyrokinetic particle simulation of tokamak plasmas; analyzing chaos: a visual essay in nonlinear dynamics; supercomputing and research in theoretical chemistry; Monte Carlo simulations of light nuclei; parallel processing; and scientists of the future: learning by doing. DOE

N91-19741*# North Carolina State Univ., Raleigh. Dept. of Computer Science.
SOFTWARE RELIABILITY THROUGH FAULT-AVOIDANCE AND FAULT-TOLERANCE Semiannual Technical Report No. 4, 1 Sep. 1990 - 28 Feb. 1991
Mladen A. Vouk and David F. McAllister Mar. 1991 28 p
(Grant NAG1-983)
(NASA-CR-187998; NAS 1.26:187998) Avail: NTIS HC/MF A03 CSCL 09B

Twenty independently developed but functionally equivalent software versions were used to investigate and compare empirically some properties of N-version programming, Recovery Block, and Consensus Recovery Block, using the majority and consensus voting algorithms. This was also compared with another hybrid fault-tolerant scheme called Acceptance Voting, using dynamic versions of consensus and majority voting. Consensus voting provides adaptation of the voting strategy to varying component reliability, failure correlation, and output space characteristics. Since failure correlation among versions effectively reduces the cardinality of the space in which the voter make decisions, consensus voting is usually preferable to simple majority voting in any fault-tolerant system. When versions have considerably different reliabilities, the version with the best reliability will perform better than any of the fault-tolerant techniques. Author

N91-19742*# National Aeronautics and Space Administration. Hugh L. Dryden Flight Research Facility, Edwards, CA.
REAL-TIME APPLICATION OF ADVANCED THREE-DIMENSIONAL GRAPHIC TECHNIQUES FOR RESEARCH AIRCRAFT SIMULATION
Steven B. Davis Dec. 1990 21 p
(NASA-TM-101730; H-1642; NAS 1.15:101730) Avail: NTIS HC/MF A03 CSCL 09B

Visual aids are valuable assets to engineers for design, demonstration, and evaluation. Discussed here are a variety of advanced three-dimensional graphic techniques used to enhance the displays of test aircraft dynamics. The new software's capabilities are examined and possible future uses are considered. Author

N91-19743# Argonne National Lab., IL.
SOME NEUTRONICS AND THERMAL-HYDRAULICS CODES FOR REACTOR ANALYSIS USING PERSONAL COMPUTERS
W. L. Woodruff 1990 10 p Presented at the International Meeting on Reduced Enrichment for Research and Test Reactors, Newport, 23-27 Sep. 1990
(Contract W-31-109-eng-38)
(DE91-006591; CONF-9009108-2) Avail: NTIS HC/MF A02

Some neutronics and thermal-hydraulics codes formerly available only for main frame computers may now be run on personal computers. Brief descriptions of the codes are provided. Running times for some of the codes are compared for an assortment of personal and main frame computers. With some limitations in detail, personal computer versions of the codes can be used to solve many problems of interest in reactor analyses at very modest costs. DOE

N91-19744# Ames Lab., IA.
A STRUCTURED REPRESENTATION FOR PARALLEL ALGORITHM DESIGN ON MULTICOMPUTERS
Xian-He Sun and L. M. Ni (Michigan State Univ., East Lansing.) 1991 7 p Presented at the 6th Distributed Memory Computing Conference, Portland, 28 Apr. - 2 May 1991
(Contract W-7405-eng-82)
(DE91-006674; IS-M-657; CONF-9104158-1) Avail: NTIS HC/MF A02

Traditionally, parallel algorithms have been designed by brute force methods and fine-tuned on each architecture to achieve

high performance. Rather than studying the design case by case, a systematic approach is proposed. A notation is first developed. Using this notation, most of the frequently used scientific and engineering applications can be presented by simple formulas. The formulas constitute the structured representation of the corresponding applications. The structured representation is simple, adequate and easy to understand. They also contain sufficient information about uneven allocation and communication latency degradations. With the structured representation, applications can be compared, classified and partitioned. Some of the basic building blocks, called computation models, of frequently used applications are identified and studied. Most applications are combinations of some computation models. The structured representation relates general applications to computation models. Studying computation models leads to a guideline for efficient parallel algorithm design for general applications. DOE

N91-19745# Lawrence Livermore National Lab., CA.
TECHNIQUES FOR INTERACTIVE 3-D SCIENTIFIC VISUALIZATION
E. P. Glinert (Rensselaer Polytechnic Inst., Troy, NY.) and M. M. Blattner 24 Sep. 1990 11 p Presented at the CHI 1991, New Orleans, 28 Apr. - 2 May 1991
(Contract W-7405-eng-48)
(DE91-007122; UCRL-JC-105691; CONF-9104168-1) Avail: NTIS HC/MF A03

Interest in interactive 3-D graphics has exploded of late, fueled by (1) the allure of using scientific visualization 'to go where no-one has gone before' and (2) by the development of new input devices which overcome some of the limitations imposed in the past by technology, yet which may be ill-suited to the kinds of interaction required by researchers active in scientific visualization. To resolve this tension, a 'flat 5-D' environment was proposed in which 2-D graphics are augmented by exploiting multiple human sensory modalities using cheap, conventional hardware readily available with personal computers and workstations. How interactions basic to 3-D scientific visualization, like searching a solution space and comparing two such spaces, are effectively carried out in our environment are discussed. Finally, 3DMOVE is described, an experimental microworld was implemented to test out some of the ideas. DOE

N91-19746# Mississippi State Univ., Mississippi State. Diagnostic Instrumentation and Analysis Lab.
STRUCTURED SOFTWARE DESIGN FOR AN ON-LINE LASER-BASED PARTICLE SIZE DISTRIBUTION INSTRUMENT
Teck Hwa Chong, R. D. Benton, and T. Phillip 1990 3 p
(Contract DE-AC02-80ET-15601)
(DE91-007234; DOE/ET-15601/T52) Avail: NTIS HC/MF A01

An on-line, laser-based, nonintrusive particle size distribution (PSD) instrument that characterizes suspended particles has been designed by the Diagnostic Instrumentation and Analysis Laboratory at Mississippi State University. The instrument was designed to operate in ALL-SANFS (Small-Angle, Near-Forward Scattering), Ripple Validated SANFS and Ripple Deconvolution modes that measure particle size from 0.5 to 20 micrometers. With the aid of the PSD instrument, the performance of power plant particulate retention components such as baghouses and electrostatic precipitators can be optimized. The design details of the software to operate the PSD system is presented. A structured approach has been used for the design analysis and design synthesis phases. Speed, accuracy of results, friendly user interface and easy maintenance were primary considerations during the software design and development. The prototype system has been tested successfully. DOE

N91-19747# Lawrence Livermore National Lab., CA.
PHIGS PLUS FOR SCIENTIFIC GRAPHICS
R. A. Crawfis 14 Jan. 1991 7 p Presented at the NCGA 1991 Conference and Exposition, Chicago, 22-25 Apr. 1991
(Contract W-7405-eng-48)
(DE91-007615; UCRL-JC-105797; CONF-9104173-1) Avail: NTIS HC/MF A02

A brief overview is given of the use of computer graphics standards in the scientific community. It particularly details how PHIGS PLUS meets the needs of users at the Lawrence Livermore National Laboratory. Although standards for computer graphics have improved substantially over the past decade, their acceptance in the scientific community has been slow. As the use and diversity of computers has increased, the scientific graphics libraries have not been able to keep pace with the additional capabilities these new machines offer. Therefore, several organizations have or are now working on converting their scientific libraries to reset upon a portable standard. Why the transition has been so slow is addressed and suggestions are offered for future standards work to enhance scientific visualization. DOE

N91-19748# Lawrence Livermore National Lab., CA.
LARGE-SCALE COMPUTING IN THE ENERGY RESEARCH PROGRAMS
Feb. 1991 82 p
(Contract W-7405-eng-48)
(DE91-007907; UCRL-LR-106412) Avail: NTIS HC/MF A05

This report is the Energy Research Supercomputer Users Group (ERSUG) response to the request for an assessment of computational needs and necessary computing environment covering the next five years. Every reasonable effort was made to obtain a response from a broad range of users. It is felt that success was achieved in that objective and that the resulting report reflects the blending of the input from the quite diverse body of researchers. Initial efforts were broken into four subdivisions to be individually coordinated: Basic Energy Sciences and Applied Mathematical Sciences; Magnetic Fusion Energy; High Energy and Nuclear Physics; and Health and Environmental Research which reported back at the summer meeting held at the National Energy Research Supercomputer Center in May 1990. These coordinators were to poll their representative communities. Each of the ERSUG executive committee members was asked to provide their assessments. As the executive committee is configured to represent the community with each member having a definite constituency, this provided a finer grained set of reports. Edited versions of these specific reports are presented in Section 2: Specific Area Assessments. The remaining component of the report consisted of assembling and organizing a large body of discussion occurring at these two meetings and through an electronic mail address. DOE

N91-19749# Oak Ridge National Lab., TN.
A STOCHASTIC PERFORMANCE MODEL FOR THE NEUTRON DIFFUSION NODAL METHOD ON A MULTIUSER PARALLEL SUPERCOMPUTER
B. L. Kirk and Y. Y. Azmy 1990 9 p Prepared for Presentation at the International Topical Meeting on Advances in Mathematics, Computations and Reactor Physics, Pittsburgh, PA, 28 Apr. - 2 May 1991
(Contract DE-AC05-84OR-21400)
(DE90-017015; CONF-910414-3) Avail: NTIS HC/MF A02

In this paper, we discuss the performance of the neutron diffusion nodal method on a Cray Y-MP/8128 in a multiprocessing and multiuser mode. This computer has 8 processors with 128 million words of shared memory and a 6.0 nanosecond clock. Because of the speed and memory capabilities of the Cray Y-MP, the problem size (mesh size) of the test problem presented here is much larger (finer mesh) than those previously studied. Indeed, meshes as fine as the ones presented in this work are not unusual in practical reactor physics calculations. Our main concern here is construct a model for the CPU time in time-sharing mode required for solving a given problem. Performance models are useful tools in the planning and allocation of computational resources that is necessary in conducting large scale calculations. DOE

N91-19750*# Georgia Inst. of Tech., Atlanta. School of Aerospace Engineering.
USE OF SYSTEM IDENTIFICATION TECHNIQUES FOR IMPROVING AIRFRAME FINITE ELEMENT MODELS USING TEST DATA Final Report

Sathya V. Hanagud, Weiyu Zhou, James I. Craig, and Neil J. Weston Mar. 1991 221 p
(Grant NAG1-1007)
(NASA-CR-188041; NAS 1.26:188041) Avail: NTIS HC/MF A10 CSCL 09B

A method for using system identification techniques to improve airframe finite element models was developed and demonstrated. The method uses linear sensitivity matrices to relate changes in selected physical parameters to changes in total system matrices. The values for these physical parameters were determined using constrained optimization with singular value decomposition. The method was confirmed using both simple and complex finite element models for which pseudo-experimental data was synthesized directly from the finite element model. The method was then applied to a real airframe model which incorporated all the complexities and details of a large finite element model and for which extensive test data was available. The method was shown to work, and the differences between the identified model and the measured results were considered satisfactory. Author

N91-19751# Pacific Northwest Lab., Richland, WA.
TECHNOLOGY MODERNIZATION ASSESSMENT FLEXIBLE AUTOMATION
D. W. Bennett, D. R. Boyd, N. H. Hansen, M. A. Hansen, and J. A. Yount Dec. 1990 75 p
(Contract DE-AC06-76RL-01830)
(DE91-005620; PNL-7329) Avail: NTIS HC/MF A04

The objectives of this report are to present technology assessment guidelines to be considered in conjunction with defense regulations before an automation project is developed, to give examples showing how assessment guidelines may be applied to a current project, and to present several potential areas where automation might be applied successfully in the depot system. Depots perform primarily repair and remanufacturing operations, with limited small batch manufacturing runs. While certain activities (such as Management Information Systems and warehousing) are directly applicable to either environment, the majority of applications will require combining existing and emerging technologies in different ways, with the special needs of depot remanufacturing environment. Industry generally enjoys the ability to make revisions to its product lines seasonally, followed by batch runs of thousands or more. Depot batch runs are in the tens, at best the hundreds, of parts with a potential for large variation in product mix; reconfiguration may be required on a week-to-week basis. This need for a higher degree of flexibility suggests a higher level of operator interaction, and, in turn, control systems that go beyond the state of the art for less flexible automation and industry in general. This report investigates the benefits and barriers to automation and concludes that, while significant benefits do exist for automation, depots must be prepared to carefully investigate the technical feasibility of each opportunity and the life-cycle costs associated with implementation. Implementation is suggested in two ways: (1) develop an implementation plan for automation technologies based on results of small demonstration automation projects; (2) use phased implementation for both these and later stage automation projects to allow major technical and administrative risk issues to be addressed. DOE

N91-19752# Academy of Sciences (USSR), Novosibirsk. Inst. Yadernoj Fiziki.
SOFTWARE FOR THE ODRENOK MICROCOMPUTER. PROGRAM PACKAGE FOR GRAPHICS EDITING
M. N. Kondaurov 1989 39 p In RUSSIAN
(DE91-614980; IYaF-89-77) Avail: NTIS HC/MF A03

Programs for graphic editing of printed circuit and electric circuit files are described. Graphic information description format is compatible with the GRAFICA system format. The package is comprised of five programs. Two programs recode information from GRAFICA to the ODRENOK format; another two programs represent the graphic editor itself, and the last program is intended to picture readout to raster printers. DOE

N91-19753# Sheffield Univ. (England). Dept. of Control Engineering.
RATIONAL MODEL IDENTIFICATION USING AN EXTENDED LEAST SQUARES ALGORITHM
S. A. Billings and Q. M. Zhu Nov. 1990 22 p
(Grant SERC-GR/F2417-7)
(RR-388; ETN-91-98839) Avail: NTIS HC/MF A03

A new least squares based parameter estimation algorithm is derived for nonlinear systems which can be represented by a rational model defined as the ratio of two polynomial expansions of past system inputs, outputs and noise. This new algorithm overcomes previous noise problems by removing the bias in both the normal matrix and the correlation vector for the rational model. The algorithm is much simpler than nonlinear least square procedures because it avoids complex minimization routines. Simulation results are included to illustrate the performance of the new algorithm. ESA

N91-19754# Sheffield Univ. (England). Dept. of Control Engineering.
THE QUALITATIVE ANALYSIS OF NONLINEAR PARAMETERISED SYSTEMS. PART 2: A METHOD FOR THE GLOBAL ANALYSIS OF NONLINEAR SYSTEMS
B. R. Haynes (Leeds Univ., England) and S. A. Billings Aug. 1990 34 p Sponsored by Science Research Council, England
(RR-400-Pt-2; ETN-91-98840) Avail: NTIS HC/MF A03

The representation of nonlinear systems, and results from dynamical systems are introduced and a method for the global analysis of nonlinear systems is presented. Several examples are used to illustrate the type of results that can be achieved using the new approach. It is shown that all typical bifurcation phenomena can be detected. A nonlinear feedback system is also analyzed in order to show how the new approach provides both qualitative information and a global perspective over a defined region of the systems parameter space. The method proves to be a powerful tool when used to prove the nonlinear characteristic of a system. ESA

N91-19755# Oxford Univ. (England). Dept. of Engineering Science.
DYNAMIC APPLICATIONS OF ABAQUS
Yiren Xia 1990 62 p Presented at United Kingdom ABAQUS Training Course, Manchester, England, 26 Sep. 1990
(OUEL-1853/90; ETN-91-98956) Avail: NTIS HC/MF A04

Applications of the finite element code ABAQUS in dynamic analyses are presented. Some contact with the code is assumed. Focus is on how to write input files under various cases and how to make less mistakes in both writing input files and in analyzing the results. For stress wave analysis, wave propagation modeling and element design for a lap joint under impact are considered. The response of layered beams and elastoplastic rate dependent modeling are considered. ESA

N91-20023*# California State Univ., Fresno. Dept. of Computer Science.
FORMAL SPECIFICATION OF HUMAN-COMPUTER INTERFACES
Brent Auernheimer *In* NASA, John F. Kennedy Space Center, Research Reports: 1990 NASA/ASEE Summer Faculty Fellowship Program Sep. 1990 p 1-28 (For primary document see N91-20022 11-99)
(Grant NGT-60002)
Avail: NTIS HC/MF A23 CSCL 09B

N91-20029*# Memphis State Univ., TN. Dept. of Mechanical Engineering.
STUDY OF THE AVAILABLE FINITE ELEMENT SOFTWARE PACKAGES AT KSC
Chu-Ho Lu *In* NASA, John F. Kennedy Space Center, Research Reports: 1990 NASA/ASEE Summer Faculty Fellowship Program Sep. 1990 p 197-221 (For primary document see N91-20022 11-99)

(Grant NGT-60002)
Avail: NTIS HC/MF A23 CSCL 09B

62 COMPUTER SYSTEMS

Includes computer networks and special application computer systems.

N91-19756*# Boeing Military Airplane Development, Seattle, WA.
FORMAL PROOF OF THE AVM-1 MICROPROCESSOR USING THE CONCEPT OF GENERIC INTERPRETERS Final Report
P. Windley, K. Levitt, and G. C. Cohen Mar. 1991 211 p Prepared in cooperation with California Univ., Davis
(Contract NAS1-18586)
(NASA-CR-187491; NAS 1.26:187491) Avail: NTIS HC/MF A10 CSCL 09B

A microprocessor designated AVM-1 was designed to demonstrate the use of generic interpreters in verifying hierarchically decomposed microprocessor specifications. This report is intended to document the high-order language (HOL) code verifying AVM-1. The organization of the proof is discussed and some technical details concerning the execution of the proof scripts in HOL are presented. The proof scripts used to verify AVM-1 are also presented. Author

N91-19757# Oak Ridge National Lab., TN.
THE PVM (PARALLEL VIRTUAL MACHINE) SYSTEM: SUPERCOMPUTER LEVEL CONCURRENT COMPUTATION ON A NETWORK OF IBM RS/6000 POWER STATIONS
V. S. Sunderam (Emory Univ., Atlanta, GA.) and G. A. Geist 1991 26 p Presented at the IBM Large Scale Analysis and Modeling Conference, Park City, UT, 24-26 Apr. 1991
(Contract DE-AC05-84OR-21400)
(DE91-007844; CONF-9104166-2) Avail: NTIS HC/MF A03

The PVM (Parallel Virtual Machine) system enables supercomputer level concurrent computations to be performed on interconnected networks of heterogeneous computer systems. Specifically, a network of 13 IBM RS/6000 powerstations has been successfully used to execute production quality runs of superconductor modeling codes at more than 250 Mflops. This work demonstrates the effectiveness of cooperative concurrent processing for high performance applications, and shows that supercomputer level computations may be attained at a fraction of the cost on distributed computing platforms. This paper describes the PVM programming environment and user facilities, as they apply to hardware platforms comprising a network of IBM RS/6000 powerstations. The salient design features of PVM will be discussed; including heterogeneity, scalability, multilanguage support, provisions for fault tolerance, the use of multiprocessors and scalar machines, an interactive graphical front end, and support for profiling, tracing, and visual analysis. The PVM system has been used extensively, and a range of production quality concurrent applications have been successfully executed using PVM on a variety of networked platforms. The paper will mention representative examples, and discuss two in detail. The first is a material sciences problem that was originally developed on a Cray 2. This application code calculates the electronic structure of metallic alloys from first principles and is based on the KKR-CPA algorithm. The second is a molecular dynamics simulation for calculating materials properties. Performance results for both applicants on networks of RS/6000 powerstations will be presented, and accompanied by discussions of the other advantages of PVM and its potential as a complement or alternative to conventional supercomputers. DOE

N91-19758# Lawrence Livermore National Lab., CA.
CONVERGENCE OF LINEAR PROGRAMMING USING A HOPFIELD NET
Shin-yee Lu and J. G. Berryman Nov. 1990 7 p Presented at the Neural Networks Academic/Industrial/NASA/defense Technical Interchange and Tutorials Conference, Alburn, 11-13 Feb. 1991
(Contract W-7405-eng-48)
(DE91-007870; UCRL-JC-105255; CONF-910281-1) Avail: NTIS HC/MF A02

Hopfield nets are interconnected networks of simple analog Processors. Such networks have been applied to a variety of optimization problems including linear programming problems. The energy function used in a Hopfield net is revised such that the network can be implemented on a digital computer to solve linearing programming problems. It is also proved that the revised discrete Hopfield net coverages, and the conditions are given of convergence. The approach is tested on two large and sparse linear programming problems. In both cases the optimal solutions can not be reached, but solutions with 1 percent error can be attained in less than 3 minutes of CPU time on a SUN SPARC station. The optimal solutions can be obtained by the simplex method, but required five times more CPU time. DOE

N91-19759# Pennsylvania State Univ., University Park. Dept. of Nuclear Engineering.
PARALLEL PROCESSING FOR A 1-D TIME-DEPENDENT SOLUTION TO IMPURITY RATE EQUATIONS FOR FUSION PLASMA SIMULATIONS
R. Veerasingam 1990 8 p Prepared for Presentation at the International Topical Meeting on Advances in Mathematics, Computations and Reactor Physics, Pittsburgh, PA, 28 Apr. - 2 May 1991
(Contract DE-FG02-87ER-53252)
(DE90-015857; DOE/ER-53252/22; CONF-910414-1) Avail: NTIS HC/MF A02

In fusion plasmas impurities such as carbon, oxygen or nickel can contaminate the plasma and cause degradation of the performance of a fusion device through radiation. However, impurities can also be used as diagnostics to obtain information about a plasma through spectroscopic experiments which can then be used in plasma modeling and simulations. In the past, serial algorithms have been described for either the time dependent or steady state problem. In this paper, we describe a parallel procedure adopted to solve the time-dependent problem. It can be shown that for the steady state problem a parallel procedure would not be a useful application of parallelization because a few seconds of the Central Processing Unit time on a CRAY-XMP or IBM 3090/600S would suffice to obtain the solution, while this is not the case for the time-dependent problem. In order to study the effects of low Z and high Z impurities on the final state of a plasma, time-dependent solutions are necessary. For purposes of diagnostics and comparisons with experiments, a fast turn around time of the simulations would be advantageous. We have implemented a parallel algorithm on and IBM 3090/600S and tested its performance for a typical set of fusion plasma parameters. DOE

N91-19760# Argonne National Lab., IL.
SUMMER INSTITUTE IN PARALLEL PROGRAMMING
E. Lusk Jan. 1991 12 p Presented at the Summer Institute in Parallel Programming, Argonne, 4-14 Sep. 1990
(Contract W-31-109-eng-38)
(DE91-007922; ANL/MCS-TM-147; CONF-9009344-Summ)
Avail: NTIS HC/MF A03

On September 4 to 14, 1990, Argonne National Laboratory hosted a Summer Institute in Parallel Programming. The institute was organized by the Mathematics and Computer Science Division and was supported in part by the National Science Foundation and by the U.S. Department of Energy. The objective of the institute was to familiarize graduate students and postdoctoral researchers with new methods and tools for parallel programming and to provide hands-on experience with a diverse array of advanced-computer architectures. This report summarizes the activities that took place during the ten-day institute. DOE

N91-19761# Sheffield Univ. (England). Dept. of Control Engineering.
SIMPLE OBJECT RECOGNITION BY NEURAL NETWORKS: APPLICATION OF THE HOUGH TRANSFORM
S. P. Banks and R. F. Harrison Oct. 1990 17 p
(RR-410; ETN-91-98844) Avail: NTIS HC/MF A03

A neural like parallel system is described for the real time implementation of the Hough transform. It is applied to simple object recognition in computer vision. The novelty in the method is the homing in facility in the system which cuts out many unnecessary parameters in the transform. ESA

N91-19762# Essex Univ., Colchester (England). Dept. of Electronic Systems Engineering.
EFFICIENT CONNECTING NETWORKS USING DIRECTED LINKS
S. J. Kinder May 1990 56 p
(ETN-91-98855) Copyright Avail: NTIS HC/MF A04

The pathset construction of forward, return and disjoint paths in the 2-D ADC (Alternately Directed Cycle) product graph is analyzed, and joint generating functions for path length distribution are derived. Expressions for the diamater and mean length of the path loop and alternate paths are presented. The performance of 2-D ADC product graphs as delay networks and switching networks is investigated. While the ADC product graph exhibits improved delay performance in comparison with equivalent ring topologies, its blocking performance is found to be poor. ESA

N91-19763# Oxford Univ. (England). Dept. of Engineering Science.
MODEL DISTRIBUTION IN DECENTRALIZED MULTI-SENSOR DATA FUSION
Timothy M. Berg and Hugh F. Durrant-Whyte 30 Oct. 1990 15 p
(OUEL-1868/90; ETN-91-98963) Avail: NTIS HC/MF A03

The problem of data fusion in decentralized and distributed network of multisensor processing nodes is considered. The network presented is based on a decentralized Kalman filter which needs no central processor; globally optimum estimates are obtained at each node by requiring an underlying centrality of the state space rather than a centralized topology. Each node maintains a local model that is most appropriate to the dynamics of its observations. The combination of model distribution and decentralization yields a robust, parallel processing network with reduced vulnerability and increased performance. Nodes communicate directly with each other node having observations relevant to its own model via internodal transformations. These internodal transformations enable nodes to communicate relevant parts of their state vectors, covariance matrices and local models directly to other interested nodes or to a new node to be initialized. Compatibility is assured because every node's state space is a subspace of a global state space. The internodal state and model transformations are derived with the necessary local model constraints for the discrete, linear, time varying case. The effects of model and organizational choices on such properties as redundancy (survivability), computational burden, communication requirements, efficiency and network expandability are discussed as a first step towards a justifiable design methodology for decentralized architectures and algorithms. ESA

63 CYBERNETICS

Includes feedback and control theory, artificial intelligence, robotics and expert systems.

For related information see also *54 Man/System Technology and Life Support.*

N91-19764# Department of the Navy, Washington, DC.
ARTIFICIAL NEURAL NETWORK IMPLEMENTATION Patent
David K. Andes, inventor (to Navy), Robert A. Licklider, inventor (to Navy), Donald H. Witcher, inventor (to Navy), and Richard M. Swenson, inventor (to Navy) 21 Aug. 1990 13 p Filed 27 Oct. 1988
(AD-D014663; US-Patent-4,951,239; US-Patent-Appl-SN-263455; US-Patent-Class-364-807) Avail: US Patent and Trademark Office CSCL 09/1

An artificial neural network having analog circuits for simultaneous parallel processing using individually variable synaptic input weights was discussed. The processing is implemented with a circuit adapted to vary the weight, which may be stored in a metal oxide field effect transistor, for teaching the network or for Hebbian or delta rule learning by the network itself. GRA

N91-19765*# Tennessee Univ., Tullahoma. Center for Advanced Space Propulsion.
ENGINEERING MONITORING EXPERT SYSTEM'S DEVELOPER Final Report, Aug. 1989 - Dec. 1990
Ching F. Lo Feb. 1991 26 p Submitted for publication
(Grant NAG2-596)
(NASA-CR-187914; NAS 1.26:187914) Avail: NTIS HC/MF A03 CSCL 09B

This research project is designed to apply artificial intelligence technology including expert systems, dynamic interface of neural networks, and hypertext to construct an expert system developer. The developer environment is specifically suited to building expert systems which monitor the performance of ground support equipment for propulsion systems and testing facilities. The expert system developer, through the use of a graphics interface and a rule network, will be transparent to the user during rule constructing and data scanning of the knowledge base. The project will result in a software system that allows its user to build specific monitoring type expert systems which monitor various equipments used for propulsion systems or ground testing facilities and accrues system performance information in a dynamic knowledge base. Author

N91-19766*# National Aeronautics and Space Administration. Lewis Research Center, Cleveland, OH.
TOWARDS PRACTICAL CONTROL DESIGN USING NEURAL COMPUTATION
Terry Troudet, Sanjay Garg, Duane Mattern (Sverdrup Technology, Inc., Brook Park, OH.), and Walter Merrill 1991 9 p Proposed for presentation at the International Joint Conference on Neural Networks, Seattle, WA, 8-12 Jul. 1991; cosponsored by IEEE and International Neural Network Society
(NASA-TM-103785; E-6061; NAS 1.15:103785) Avail: NTIS HC/MF A02 CSCL 09B

The objective is to develop neural network based control design techniques which address the issue of performance/control effort tradeoff. Additionally, the control design needs to address the important issue if achieving adequate performance in the presence of actuator nonlinearities such as position and rate limits. These issues are discussed using the example of aircraft flight control. Given a set of pilot input commands, a feedforward net is trained to control the vehicle within the constraints imposed by the actuators. This is achieved by minimizing an objective function which is the sum of the tracking errors, control input rates and control input deflections. A tradeoff between tracking performance and control smoothness is obtained by varying, adaptively, the weights of the objective function. The neurocontroller performance is evaluated in the presence of actuator dynamics using a simulation of the vehicle. Appropriate selection of the different weights in the objective function resulted in the good tracking of the pilot commands and smooth neurocontrol. An extension of the neurocontroller design approach is proposed to enhance its practicality. Author

N91-19767# Sandia National Labs., Albuquerque, NM.
A HAPTIC SYSTEM FOR A MULTIFINGERED HAND
S. A. Stansfield 1990 15 p Presented at the IEEE Robotics and Automation Conference, Sacramento, CA, 7-12 Apr. 1991
(Contract DE-AC04-76DP-00789)
(DE90-017044; SAND-90-2001C; CONF-910451-1) Avail: NTIS HC/MF A03

In this paper we present a series of haptic exploratory procedures, or EPs, implemented for a multi-fingered, articulated,

sensate robot hand. These EPs are designed to extract specific tactile and kinesthetic information from an object via their purposive invocation by an intelligent robotic system. Taken together, they form an active robotic touch perception system to be used both in extracting information about the environment for internal representation and in acquiring grasps for manipulation. The haptic system presented utilizes an integrated robotic system consisting of a PUMA 560 robot arm, a JPL/Stanford robot hand, with joint torque sensing in the fingers, a wrist force/torque sensor, and a 256 element, spatially-resolved fingertip tactile array. We describe the EPs implemented for this system and provide experimental results which illustrate how they function. A final example demonstrates how the information extracted may be used. DOE

N91-19768# Sandia National Labs., Albuquerque, NM.
PRACTICAL PATH PLANNING AMONG MOVABLE OBSTACLES
Pang C. Chen and Yong K. Hwang Sep. 1990 13 p Presented at the IEEE Robotics and Automation Conference, Sacramento, CA, 7-12 Apr. 1991
(Contract DE-AC04-76DP-00789)
(DE91-000034; SAND-90-2383C; CONF-910451-7) Avail: NTIS HC/MF A03

Path planning among movable obstacles is a practical problem that is in need of a solution. This paper presents an efficient heuristic algorithm that uses a generate-and-test paradigm: a good candidate path is hypothesized by a global planner and subsequently verified by a local planner. In the process of formalizing the problem, we also present a technique for modeling object interactions through contact. Our algorithm has been tested on a variety of examples, and was able to generate solutions within 10 seconds. DOE

N91-19769# Oak Ridge National Lab., TN.
NAVIGATION OF A CAR-LIKE MOBILE ROBOT USING A DECOMPOSITION OF THE ENVIRONMENT IN CONVEX CELLS
H. A. Vasseur, F. G. Pin, and J. R. Taylor (Oak Ridge Y-12 Plant, TN.) 1990 11 p Presented at the IEEE Robotics and Automation Conference, Sacramento, CA, 7-12 Apr. 1991
(Contract DE-AC05-84OR-21400)
(DE91-000709; CONF-910451-9) Avail: NTIS HC/MF A03

Due to their kinematics, car-like mobile robots cannot follow an arbitrary path. Besides obstacle avoidance, the path planning problem for such platforms has to satisfy two additional constraints: a lower bounded radius of turn, and a nonholonomic constraint. When the robot is not circular, precise maneuvering always implies working in the configuration space of the vehicle. Due to the complexity of the problem, the planning of a path involves computer intensive methods, and rarely allows for real time applications. However, in a convex polygonal cell, maneuvering can be completely handled within geometric reasoning. In this simplified environment, joining two configurations may require maneuvers only at the beginning and at the end of the trajectory. The method consists of computing the possible maneuvers either starting from the initial configuration, or arriving at the final configuration. Just a few boundary configurations have to be checked to avoid collision. Maneuvers related to the initial configuration and to the final configuration can be connected by a straight trajectory because of the convexity of the cell, which allows precise maneuvering computation, without using the whole configuration space. We describe a general environment by means of a graph connecting overlapping convex cells. To find a path between two configurations, the graph is searched in order to list the cells that have to be traversed. Then, intermediate configurations are computed inside the intersection of two adjacent cells. Finally, the trajectories generated inside each cell are assembled to produce global collision free paths in complex environments. DOE

N91-19770*# National Aeronautics and Space Administration. Ames Research Center, Moffett Field, CA.
SIMULATING MOTIVATED COGNITION
William B. Gevarter Feb. 1991 19 p
(NASA-TM-102886; A-91015; NAS 1.15:102886) Avail: NTIS HC/MF A03 CSCL 09B

A research effort to develop a sophisticated computer model of human behavior is described. A computer framework of motivated cognition was developed. Motivated cognition focuses on the motivations or affects that provide the context and drive in human cognition and decision making. A conceptual architecture of the human decision-making approach from the perspective of information processing in the human brain is developed in diagrammatic form. A preliminary version of such a diagram is presented. This architecture is then used as a vehicle for successfully constructing a computer program simulation Dweck and Leggett's findings that relate how an individual's implicit theories orient them toward particular goals, with resultant cognitions, affects, and behavior. Author

N91-19771*# Stanford Univ., CA. Dept. of Electrical Engineering.
CASCADING A SYSTOLIC ARRAY AND A FEEDFORWARD NEURAL NETWORK FOR NAVIGATION AND OBSTACLE AVOIDANCE USING POTENTIAL FIELDS
Edward S. Plumer Feb. 1991 23 p
(Grant NGT-50642)
(NASA-CR-177575; A-91066; NAS 1.26:177575) Avail: NTIS HC/MF A03 CSCL 09B

A technique is developed for vehicle navigation and control in the presence of obstacles. A potential function was devised that peaks at the surface of obstacles and has its minimum at the proper vehicle destination. This function is computed using a systolic array and is guaranteed not to have local minima. A feedfoward neural network is then used to control the steering of the vehicle using local potential field information. In this case, the vehicle is a trailer truck backing up. Previous work has demonstrated the capability of a neural network to control steering of such a trailer truck backing to a loading platform, but without obstacles. Now, the neural network was able to learn to navigate a trailer truck around obstacles while backing toward its destination. The network is trained in an obstacle free space to follow the negative gradient of the field, after which the network is able to control and navigate the truck to its target destination in a space of obstacles which may be stationary or movable. Author

N91-19772# Sheffield Univ. (England). Dept. of Control Engineering.
THE APPLICATION OF NEURAL NETWORKS FOR FAULT DIAGNOSIS IN NUCLEAR REACTORS
N. A. Jalel and H. Nicholson Nov. 1990 20 p
(RR-411; ETN-91-98845) Avail: NTIS HC/MF A03

Considerable work has been done in the field of neural networks due to the recent development of effective learning algorithms, and the results of their applications have suggested that they can provide useful tools for solving practical problems. Artificial neural networks are mathematical models of theorized mind and brain activity. They are aimed at exploring and reproducing human information processing tasks such as speech, vision, knowledge processing and control. The possiblity of using artificial neural networks for fault and accident diagnosis in the Loss Of Fluid Test (LOFT) reactor, a small scale pressurized water reactor, is examined and explained. ESA

N91-19773# Technische Univ., Delft (Netherlands).
DESIGN AND IMPLEMENTATION OF AN IMAGE UNDERSTANDING SYSTEM: DADS Ph.D. Thesis
Xiang Sheng Cheng 1990 237 p
(ETN-91-98926) Avail: NTIS HC/MF A11

A general system design, the Distributed and Anomaly Driven System (DADS) is proposed for building up a general image understanding system. Within this framework, the notion of context hierarchy and anomaly are introduced. The first allows the understanding process of a particular problem to be described through intermediate metal objects; the second improves the system performance by assessing various insufficiences of the

current system and adding appropriate anomaly handlers to counter them. Human visual perception is discussed, the DADS design and system framework are presented, and various properties of DADS are summarized. A DADS based application system for interpreting SLAR (Side Looking Airborne Radar) images is presented. An edgeness detector and an interaction based adaptive shrinking algorithm for postprocessing an edgeness image are described. An edge constrained region growing based segmentation approach for extracting tentative regions in a SLAR image is presented. The extraction of crop fields versus non crop fields in a SLAR image is presented. The effectiveness and flexibility of the anomaly driven mechanism is observed and the experimental results of the methods applied to various types of heavily noise corrupted images prove to be good. ESA

N91-19774# Oxford Univ. (England). Dept. of Engineering Science.
TOPOLOGICAL MODELS FOR SPACE AND TIME
M. M. Fleck 1990 35 p
(OUEL-1860/90; ETN-91-98958) Avail: NTIS HC/MF A03

A new class of concrete models for representing situations in space and time is presented. These models are based on space filling call complexes, which make finite precision data easier to reason about and prohibit pathological situations. They also incorporate a new notion of object or region boundaries, in which the boundaries alter the topological structure of the situation. The models are developed mathematically and then applied to outstanding problems in computer vision, high level reasoning, and natural language semantics. Previous models of topological structure were plagued by technical difficulties. Some cannot model sharp changes in properties. Some allow connectivity 'paradoxes'. Some fail to represent topological structure unambiguously. In some, intuitively basic distinctions and obvious inferences require special axioms. By removing such difficulties the new models allow topological structure to be more widely exploited by artificial intelligence algorithms. ESA

N91-20037*# Lehigh Univ., Bethlehem, PA. Dept. of Industrial Engineering.
ROBOT TRACKING SYSTEM IMPROVEMENTS AND VISUAL CALIBRATION OF ORBITER POSITION FOR RADIATOR INSPECTION
Gregory Tonkay *In* NASA, John F. Kennedy Space Center, Research Reports: 1990 NASA/ASEE Summer Faculty Fellowship Program Sep. 1990 p 462-487 (For primary document see N91-20022 11-99)
(Grant NGT-60002)
Avail: NTIS HC/MF A23 CSCL 09B

N91-20038*# Florida Inst. of Tech., Melbourne. Dept. of Chemical Engineering.
MODELING OF FLOW SYSTEMS FOR IMPLEMENTATION UNDER KATE
Jonathan E. Whitlow *In* NASA, John F. Kennedy Space Center, Research Reports: 1990 NASA/ASEE Summer Faculty Fellowship Program Sep. 1990 p 488-520 (For primary document see N91-20022 11-99)
(Grant NGT-60002)
Avail: NTIS HC/MF A23 CSCL 09B

64 NUMERICAL ANALYSIS

Includes iteration, difference equations, and numerical approximation.

N91-19775# Lawrence Livermore National Lab., CA.
THE COST-CONSTRAINED TRAVELING SALESMAN PROBLEM Ph.D. Thesis
P. R. Sokkappa Oct. 1990 113 p
(Contract W-7405-eng-48)
(DE91-004943; UCRL-LR-105145) Avail: NTIS HC/MF A06

The Cost-Constrained Traveling Salesman Problem (CCTSP) is a variant of the well-known Traveling Salesman Problem (TSP). In the TSP, the goal is to find a tour of a given set of cities such that the total cost of the tour is minimized. In the CCTSP, each city is given a value, and a fixed cost-constraint is specified. The objective is to find a subtour of the cities that achieves maximum value without exceeding the cost-constraint. Thus, unlike the TSP, the CCTSP requires both selection and sequencing. As a consequence, most results for the TSP cannot be extended to the CCTSP. We show that the CCTSP is NP-hard and that no K-approximation algorithm or fully polynomial approximation scheme exists, unless P = NP. We also show that several special cases are polynomially solvable. Algorithms for the CCTSP, which outperform previous methods, are developed in three areas: upper bounding methods, exact algorithms, and heuristics. We found that a bounding strategy based on the knapsack problem performs better, both in speed and in the quality of the bounds, than methods based on the assignment problem. Likewise, we found that a branch-and-bound approach using the knapsack bound was superior to a method based on a common branch-and-bound method for the TSP. In our study of heuristic algorithms, we found that, when selecting modes for inclusion in the subtour, it is important to consider the 'neighborhood' of the nodes. A node with low value that brings the subtour near many other nodes may be more desirable than an isolated node of high value. We found two types of repetition to be desirable: repetitions based on randomization in the subtour buildings process, and repetitions encouraging the inclusion of different subsets of the nodes. By varying the number and type of repetitions, we can adjust the computation time required by our method to obtain algorithms that outperform previous methods. DOE

N91-19776# Massachusetts Univ., Amherst.
COMPUTATION AND GRAPHICS IN MATHEMATICAL RESEARCH
D. A. Hoffman and J. Spruck Jan. 1991 29 p
(Contract DE-FG02-86ER-25015)
(DE91-007333; DOE/ER-25015/30) Avail: NTIS HC/MF A03

Research in the following areas is discussed: (1) computer graphics; (2) video animation; (3) software development; and (4) problems in differential geometry, calculus of variations, and mathematical physics. DOE

N91-19777# Stanford Linear Accelerator Center, CA.
INVARIANT TORI OF THE POINCARE RETURN MAP AS SOLUTIONS OF FUNCTIONAL DIFFERENCE EQUATIONS
R. L. Warnock Jan. 1991 5 p Presented at the US-Japan Workshop on Nonlinear Dynamics and Acceleration Mechanisms, Tsukuba, Japan, 22-25 Oct. 1990
(Contract DE-AC03-76SF-00515)
(DE91-007423; SU-SLAC-PUB-5412; CONF-9010270-2) Avail: NTIS HC/MF A01

Functional difference equations characterize the invariant surfaces of the Poincare return map of a general Hamiltonian system. Two different functional equations are derived. The first is analogous to the Hamilton-Jacobi equation and the second is a generalization of Moser's equation. Some properties of the equations, and schemes for solving them numerically, are discussed. DOE

N91-19778# Stanford Linear Accelerator Center, CA.
COMPUTATION OF INVARIANT TORI IN 2 (1/2) DEGREES OF FREEDOM
W. E. Gabella (Colorado Univ., Boulder.), R. D. Ruth, and R. L. Warnock Jan. 1991 6 p Presented at the US-Japan Workshop on Nonlinear Dynamics and Acceleration Mechanisms, Tsukuba, Japan, 22-25 Oct. 1990
(Contract DE-AC03-76SF-00515)
(DE91-007424; SU-SLAC-PUB-5414; CONF-9010270-3) Avail: NTIS HC/MF A02

Approximate invariant tori in phase space are found using a non-perturbative, numerical solution of the Hamilton-Jacobi equation for a nonlinear, time-periodic Hamiltonian. The Hamiltonian is written in the action-angle variables of its solvable part. The

solution of the Hamilton-Jacobi equation is represented as a Fourier series in the angle variables but not in the time variable. The Fourier coefficients of the solution are regarded as the fixed point of a nonlinear map. The fixed point is found using a simple iteration or a Newton-Broyden iteration. The Newton-Broyden method is slower than the simple iteration, but it yields solutions at amplitudes that are significant compared to the dynamic aperture. Invariant tori are found for the dynamics of a charged particle in a storage ring with sextupole magnets. DOE

N91-19779# Oak Ridge National Lab., TN.
BOUNDARY INTEGRAL EQUATIONS AND THE DIRICHLET PROBLEM
L. F. Gray, O. A. Basaran, M. T. Harris, and F. Wohlhuter (Tennessee Univ., Knoxville.) 1990 7 p Presented at the Forum on Advanced Boundary Element Methods and International Conference on Computational Engineering Science, Patras, Greece, 21-25 Apr. 1991
(Contract DE-AC05-84OR-21400)
(DE91-004537; CONF-910498-1) Avail: NTIS HC/MF A02

The standard boundary element method applied to a problem with Dirichlet boundary conditions leads to a Fredholm integral equation of the first kind. A stable second kind equation results from a hypersingular equation formulation of the problem, obtained by differentiating the original boundary integral statement. The evaluation of the hypersingular integral requires that the coefficient function multiplying the hypersingular kernel be differentiable. For two dimensional problems, Overhauser elements are a very convenient basis set for obtaining the necessary smoothness. Test calculations with the Laplace equation demonstrate: (1) the stability of the hypersingular approach for the Dirichlet problem; and (2) that the hypersingular approach yields results that are more accurate than those obtained with the standard approach. DOE

N91-19780# Lawrence Livermore National Lab., CA.
ANALYSIS OF SPHERICAL GEOMETRY FINITE ELEMENT TRANSPORT SOLUTIONS IN THE THICK DIFFUSION LIMIT
T. S. Palmer (Michigan Univ., Ann Arbor.) and M. L. Adams 15 Jan. 1991 13 p Presented at the International Topical Meeting on Advances in Mathematics, Computations and Reactor Physics, Pittsburgh, 28 Apr. - 2 May 1991
(Contract W-7405-eng-48)
(DE91-007598; UCRL-JC-104789; CONF-910414-14) Avail: NTIS HC/MF A03

An asymptotic analysis is performed on a family of discontinuous finite element methods (DFEMs) for spherical geometry transport. It is found that transport methods of this type transition into discrete versions of the spherical geometry diffusion equation in the thick diffusion limit with boundary conditions that may, in general, be inaccurate. A linear DFEM method was designed such that its asymptotic diffusion boundary conditions are accurate. In a related development, the asymptotic diffusion equation is used to accelerate the transport calculation and the iterative scheme is fully described. The results of the analysis are confirmed by numerical testing of the specific case of linear elements. DOE

N91-19781# Lawrence Livermore National Lab., CA.
EVEN- AND ODD-PARITY FINITE-ELEMENT TRANSPORT SOLUTIONS IN THE THICK DIFFUSION LIMIT
M. L. Adams Jan. 1991 12 p Presented at the International Topical Meeting on Advances in Mathematics, Computations and Reactor Physics, Pittsburgh, 28 Apr. - 2 May 1991
(Contract W-7405-eng-48)
(DE91-007618; UCRL-JC-104788; CONF-910414-18) Avail: NTIS HC/MF A03

The behavior was analyzed of odd-parity continuous finite element methods (CFEMs) for problems that contain diffusive regions. It was found that each of these methods produces a solution that, to leading order inside diffusive regions, satisfies a discretization of the diffusion equation. It was further found that these leading order solutions satisfy boundary conditions that can lead to large errors in the interior solution. It was recognized, however, that an odd-purity CFEM solution and an even-parity CFEM solution can be combined to obtain a solution that satisfies very accurate boundary conditions. The analysis holds in 3-D Cartesian geometry, with an arbitrary spatial grid. Numerical results are given from slab-geometry; these invariably agree with the predictions of the analysis. Finally, a rapidly convergent diffusion-synthetic acceleration scheme is introduced for the odd-parity CFEMs, which is believed to be new. DOE

N91-19782# Lawrence Livermore National Lab., CA.
DISCONTINUOUS FINITE-ELEMENT TRANSPORT SOLUTIONS IN THE THICK DIFFUSION LIMIT IN CARTESIAN GEOMETRY
M. L. Adams Jan. 1991 17 p Presented at the International Topical Meeting on Advances in Mathematics, Computations and Reactor Physics, Pittsburgh, 28 Apr. - 2 May 1991
(Contract W-7405-eng-48)
(DE91-007620; UCRL-JC-104787; CONF-910414-17) Avail: NTIS HC/MF A03

The behavior was analyzed of discontinuous finite element methods (DFEMs) for problems that contain diffusive regions. It was found that in slab geometry most of these methods perform quite well, but that the same is not true in XY or XYZ geometry. In these geometries, it was found that there are two distinct sets of DFEMS. Methods in one set produce unphysical solutions in diffusive regions; the other leading order solutions that satisfy discretizations of the correct diffusion equation. It is shown that two simple properties of the finite element weight functions are sufficient to guarantee that a DFEM belongs to the latter set. It is shown, however, that even these DFEMs suffer from several defects: their leading order solutions are in general discontinuous, they satisfy diffusion discretizations that can be ill-behaved, and they may not be accurate given boundary layers that are not resolved by the spatial mesh. The practical significance of these defects are discussed, and it is shown that liberal modification of some DFEMs can eliminate the defects. Numerical results are presented from simple test problems; these fully agree with the analysis. DOE

N91-19783# Lawrence Livermore National Lab., CA.
ANASTASIA: A SOLID MODEL BASED 3D FINITE DIFFERENCE MESH GENERATOR
G. Laguna Nov. 1990 63 p
(Contract W-7405-eng-48)
(DE91-007621; UCRL-MA-105580) Avail: NTIS HC/MF A04

Finite difference (FD) is a method for approximating mathematical functions using regularly spaced samples of the function to be solved. Finite difference methods have proven to be very useful to a broad range of disciplines. One area where finite difference methods are particularly useful is for the estimation of electromagnetic (EM) effects. For instance, finite difference methods can be used to anticipate how the shape of a system will affect an objects resistance to EM attack or its ability to otherwise survive a hostile EM environment. Finite difference analysis codes require as input certain information at regularly spaced sample points. For the applications, each sample point must be associated with the appropriate material properties corresponding to the properties of the material at the physical point. Since all of the sample points are regularly spaced, they can be thought of as a grid or mesh. Anastasia is a software package which allows 3-D finite difference meshes to be generated automatically from a geometric description of the problem known as a solid model. This manual provides the information necessary to be able to use Anastasia to generate meshes. The manual is divided into four major sections. The first section, the introduction, gives some background information about finite difference and mesh generation. The second section examines the methods by which Anastasia generates meshes, including the rationale behind the mesh generation process and techniques required to achieve particular results. The third section describes the usage of Anastasia. The fourth and final section is a collection of Appendices which present a variety of information pertinent to mesh generation with Anastasia. DOE

N91-19784# Oak Ridge National Lab., TN.
THE WEIGHTED-DIFFERENCE FORM OF THE NODAL DIFFUSION METHOD IN CYLINDRICAL GEOMETRY
L. Deleanu, Y. Y. Azmy, and R. T. Primm, III 1991 9 p Presented at the International Topical Meeting on Advances in Mathematics, Computations and Reactor Physics, Pittsburgh, PA, 28 Apr. - 2 May 1991
(Contract DE-AC05-84OR-21400)
(DE91-007849; CONF-910414-21) Avail: NTIS HC/MF A02

A nodal integral method is derived for the neutron diffusion equation in cylindrical, r - z geometry. The final discrete-variable equations that express nodal balance of neutrons and net current continuity across node boundaries, are cast in a five-point, weighted difference form. These equations are identical in form, but with different expressions for the spatial weights, to their counterparts in cartesian geometry. Hence, the iterative procedure previously developed for the latter, is used to solve the newly installed r - z nodal method in the production code BOLD-VENTURE. Preliminary numerical experiments on simple one and two group, fixed source, test problems demonstrate the superior accuracy of the nodal method compared to the finite difference method. DOE

N91-19785# Oak Ridge National Lab., TN.
BAYESIAN APPROXIMATION OF SOLUTIONS TO LINEAR ORDINARY DIFFERENTIAL EQUATIONS
K. J. Herzog, M. D. Morris, and T. J. Mitchell Nov. 1990 29 p
(Contract DE-AC05-84OR-21400)
(DE91-007872; ORNL/TM-11688) Avail: NTIS HC/MF A03

An approach to numerically solving linear ordinary differential equations, based on statistical Bayesian prediction, is described. Preliminary results on the details of choice of correlation parameters and experimental design are given, using first- and second-order example problems. DOE

N91-19786*# National Aeronautics and Space Administration. Lewis Research Center, Cleveland, OH.
SPECTRUM TRANSFORMATION FOR DIVERGENT ITERATIONS
Murli M. Gupta (George Washington Univ., Washington, DC.) Mar. 1991 18 p
(NASA Order C-99066-G)
(NASA-TM-103745; E-5989; ICOMP-91-02; NAS 1.15:103745)
Avail: NTIS HC/MF A03 CSCL 12A

Certain spectrum transformation techniques are described that can be used to transform a diverging iteration into a converging one. Two techniques are considered called spectrum scaling and spectrum enveloping and how to obtain the optimum values of the transformation parameters is discussed. Numerical examples are given to show how this technique can be used to transform diverging iterations into converging ones; this technique can also be used to accelerate the convergence of otherwise convergent iterations. Author

N91-19787# Texas Univ., Austin. Inst. for Fusion Studies.
ACTION PRINCIPLES FOR THE VLASOV EQUATION: FOUR OLD, ONE NEW
Huanchun Ye and P. J. Morrison Jan. 1991 12 p
(Contract DE-FG05-80ET-53088)
(DE91-008177; DOE/ET-53088/435; IFSR-435) Avail: NTIS HC/MF A03

Action principles for the Vlasov equation are presented. Four previously known action principles, which differ by the choice of dynamical variables, are described and the interrelationship between them discussed. A new action principle called the leaf action, which manifestly preserves the Casimir invariants and possess a single function as the dynamical variable, is presented. The relationship to the noncanonical Hamiltonian formalism is also explored. DOE

N91-19788# Academy of Sciences (USSR), Novosibirsk. Inst. Yadernoj Fiziki.
CORRELATIONS OF PSEUDO-RANDOM NUMBERS OF MULTIPLICATIVE SEQUENCE
A. D. Bukin 1989 26 p
(DE91-615076; IYaF-89-86) Avail: NTIS HC/MF A03

An algorithm is suggested for searching with a computer in unit n-dimensional cube the sets of planes where all the points fall whose coordinates are composed of n successive pseudo-random numbers of multiplicative sequence. This effect should be taken into account in Monte Carlo calculations with definite constructive dimension. The parameters of these planes are obtained for three random number generators. DOE

N91-19789# Sheffield Univ. (England). Dept. of Control Engineering.
THE QUALITATIVE ANALYSIS OF NONLINEAR PARAMETERIZED SYSTEMS. PART 1: NONLINEAR SYSTEMS REPRESENTATION AND DYNAMICAL SYSTEMS THEORY
B. R. Haynes (Leeds Polytechnic, England) and S. A. Billings Aug. 1990 44 p Sponsored by Science Research Council, England
(RR-408-Pt-1; ETN-91-98842) Avail: NTIS HC/MF A03

The analysis of parameterized nonlinear models is considered and a new approach is introduced which provides a framework for the global analysis of both continuous and discrete time nonlinear systems. The paper is divided into two parts. An overview of nonlinear system representations and dynamical systems theory is provided in part one, which forms the basis for the results in the second part. The latter introduces a numerically based analysis tool and demonstrates that this provides a flexible framework for the analysis of a diverse range of nonlinear model types. It is shown, by extending the numerical algorithm, that the approach provides a global perspective to the results that is difficult to obtain using analytical methods alone. Simple examples are used to illustrate how the new approach provides both qualitative information and a global perspective over a defined region of the systems parameter space. The method proves to be a powerful tool when used to probe the nonlinear characteristic of a system. ESA

N91-19790# Technische Univ., Eindhoven (Netherlands).
SUBCYCLING IN TRANSIENT FINITE ELEMENT ANALYSIS Ph.D. Thesis
Willem Elisabeth Mar Bruijs 1990 131 p Sponsored in part by Netherlands Organization for Applied Scientific Research
(ISBN-90-9003684-9; ETN-91-98934) Avail: NTIS HC/MF A07

A method called subcycling, which uses different time steps for the numerical integration of one set of mutually coupled ordinary nonlinear differential equations is developed. This implies that smaller elements are treated with smaller time steps than larger elements; for the larger elements, the number of elemental calculations and hence the computational costs will decrease; and local mesh refinement can be allowed without a large increase in the computational costs. One of the first decisions to be made when subcycling is applied, is what element must be treated with what time step. An algorithm that automatically partitions the elements into groups in such a way that the savings are maximal is developed for this purpose. With the aid of a case study, it is shown that the method is conditionally stable. For a one dimensional simulation, it is shown that subcycling results in more accurate solutions than calculations without subcycling. Test calculations are performed to check the accuracy of the subcycling algorithm and to show that subcycling indeed yields computer time savings. ESA

N91-19791# Oxford Univ. (England). Dept. of Engineering Science.
A NOVEL ISOPARAMETRIC FINITE ELEMENT DISPLACEMENT FORMULATION FOR AXISYMMETRIC ANALYSIS OF NEARLY INCOMPRESSIBLE MATERIALS
H. S. Yu (Newcastle Univ., Australia), G. T. Houlsby, and H. J. Burd 1991 33 p
(OUEL-1872/91; SM-114/91; ETN-91-98964) Avail: NTIS HC/MF A03

It is well accepted that severe numerical difficulties arise when

using the conventional displacement method to analyze incompressible or nearly incompressible solids. These effects are caused by the kinematic constraints imposed on the nodal velocities by the constant volume condition. In elastic-plastic analysis, these effects are due to a conflict between the plastic flow rule and the finite element discretization. Although there are several methods proposed to cope with this problem, none are based on the appropriate choice of displacement interpolation functions to minimize the constraints. The theoretical formulation of a six noded isoparameteric displacement finite element, which is well suited for elastic-plastic analysis of axisymmetric constrained solids by using a rational displacement interpolation function, is presented. The proposed displacement interpolation function implies that the displacement in axial direction and the product of the displacement in radial direction and the radius should be treated as two independent basic variables. Alternatively, the proposed displacement interpolation function can also be implemented in a conventional displacement formulation simply by using a modified shape function matrix. The suitability of the proposed formulations is studied theoretically by assessing the number of degrees of freedom per constraint and verified by performing numerical experiments on typical boundary value problems which involve incompressible behavior. ESA

65 STATISTICS AND PROBABILITY

Includes data sampling and smoothing; Monte Carlo method; and stochastic processes.

N91-19792# Maryland Univ., College Park. Lab. for Plasma Research.

THE STUDY OF EFFECTS OF SMALL PERTURBATIONS ON CHAOTIC SYSTEMS

C. Grebogi and J. A. Yorke Dec. 1990 9 p

(Contract DE-FG05-87ER-25036)

(DE91-007320; DOE/ER-25036/4) Avail: NTIS HC/MF A02

This report discusses the following topics on small perturbations on chaotic systems: controlling chaos; shadowing and noise reduction; chaotic scattering; random maps; magnetic dynamo; and aids transmission. DOE

N91-19793# Sandia National Labs., Albuquerque, NM.

PARAMETER ESTIMATION OF STRUCTURAL DYNAMIC MODELS USING EIGENVALUE AND EIGENVECTOR INFORMATION

J. J. Allen and D. R. Martinez Nov. 1990 20 p Presented at the 9th International Modal Analysis Conference, Florence Italy, 14-18 Apr. 1991

(Contract DE-AC04-76DP-00789)

(DE91-004379; SAND-90-2025C; CONF-910494-1) Avail: NTIS HC/MF A03

Structural system identification methods are analytical techniques for reconciling test data with analytical models. The response data frequently used to compare a finite element model and test data are the eigenvalues of the system. However, eigenvalues alone cannot assure an adequate model. Eigenvectors also provide valuable information for the process of updating finite element models. For large order, complex finite element models, ad-hoc procedures have often proven inadequate for model parameter updating. Therefore, parameter estimation techniques such as Bayes estimation or mathematical programming have been applied. Mathematical programming techniques can be use for parameter estimation allowing a very general definition of the objective function and constraints. This paper will present the application of mathematical programming techniques of parameter estimation to the updating of a finite element model of an electronic package. The following topics will be discussed in the paper: the mathematical programming formulation of the parameter estimation problem, which uses both eigenvalue and eigenvector response data, the software implementation of this technique, and the application of this methodology to the estimation of parameters of an electronics package model. Author

N91-19794# Lawrence Livermore National Lab., CA.

RESPONSE MATRIX MONTE CARLO BASED ON A GENERAL GEOMETRY LOCAL CALCULATION FOR ELECTRON TRANSPORT

C. T. Ballinger, J. A. Rathkopf, and W. R. Martin (Michigan Univ., Ann Arbor.) 1991 13 p Presented at the International Topical Meeting on Advances in Mathematics, Computations and Reactor Physics, Pittsburgh, 28 Apr. - 2 May 1991

(Contract W-7405-eng-48)

(DE91-007638; UCRL-JC-105626; CONF-910414-19) Avail: NTIS HC/MF A03

A Response Matrix Monte Carlo (RMMC) method has been developed for solving electron transport problems. This method was born of the need to have a reliable, computationally efficient transport method for low energy electrons (below a few hundred keV) in all materials. Today, condensed history methods are used which reduce the computation time by modeling the combined effect of many collisions but fail at low energy because of the assumptions required to characterize the electron scattering. Analog Monte Carlo simulations are prohibitively expensive since electrons undergo coulombic scattering with little state change after a collision. The RMMC method attempts to combine the accuracy of an analog Monte Carlo simulation with the speed of the condensed history methods. Like condensed history, the RMMC method uses probability distributions functions (PDFs) to describe the energy and direction of the electron after several collisions. However, unlike the condensed history method the PDFs are based on an analog Monte Carlo simulation over a small region. Condensed history theories require assumptions about the electron scattering to derive the PDFs for direction and energy. Thus the RMMC method samples from PDFs which more accurately represent the electron random walk. Results show good agreement between the RMMC method and analog Monte Carlo. DOE

N91-19795# Oak Ridge National Lab., TN.

SIGNIF AND GENFMT, SAS MACROS FOR COMPUTING AND REPORTING SIGNIFICANT DIGITS

B. M. Horwedel and J. E. Horwedel 1991 5 p Presented at the 16th Annual SAS Users Group International Conference, New Orleans, 17-20 Feb. 1991

(Contract DE-AC05-84OR-21400)

(DE91-007702; CONF-910280-2) Avail: NTIS HC/MF A01

Reporting generalized statistics such as mean or standard error with excessive significant digits can be misleading and imply more precision than that found in the original measurements. Measurement data seldom warrant more than two or three significant figures to represent values. An appropriate number of digits is determined by the precision of the reported value. This poster presents two SAS macros that are useful in reporting values with a limited number of significant digits. SIGNIF is a macro that will return a value rounded to a specified number of digits. GENFMT is a macro that will generate a picture format to be used in printing numbers. Examples using SIGNIF and GENFMT are shown. DOE

N91-19796# Technische Hochschule, Darmstadt (Germany, F.R.).

OPTIMAL OBSERVATION DIRECTIONS FOR ESTIMATING A VECTOR

Helmut Wegmann Feb. 1990 14 p

(Preprint-1285; ETN-91-98808) Avail: NTIS HC/MF A03

To estimate a k-dimensional vector mu observations x(sub 1) to x(sub n) with random errors of the projections of mu in n given directions are used. The data can also be applied to test for bias of the observations. The problem discussed is how to choose directions to optimize these statistical procedures. The random variables x(sub 1) to x(sub n) are assumed to be uncorrelated with the same variance and normally distributed. Optimization criteria are: minimizing mean square error of the estimate and maximizing the power of the test. ESA

N91-19797# Sheffield Univ. (England). Dept. of Control Engineering.
ORTHOGONAL LEAST SQUARES PARAMETER ESTIMATION ALGORITHMS FOR NONLINEAR STOCHASTIC SYSTEMS
S. A. Billings and G. N. Jones Oct. 1990 19 p
(Grant SERC-GK/F24177)
(RR-404; ETN-91-98841) Avail: NTIS HC/MF A03

The derivations of orthogonal least squares algorithms based on the principle of Hsia's method and generalized least squares are presented. The advantages of the new algorithm include computational simplicity and the ability to implement a simple term selection routine, based on an error reduction test. Extensions of the case of nonlinear stochastic systems are discussed and the performance of the algorithms is illustrated with the identification of both simulated systems and linear models of an electric are furnace and a gas furnace. ESA

N91-19798# Ecole Nationale Superieure des Telecommunications, Paris (France). Dept. of Signal.
REGULAR UNITARY DILATION OF COMMUTING CONTRACTIONS AND MARKOVIAN REPRESENTATIONS OF GAUSSIAN STATIONARY PROCESSES ON THE SET Z(2)
Philippe Loubaton 1990 39 p
(TELECOM-90-D-009; ISSN-0751-1345; ETN-91-98895) Avail: NTIS HC/MF A03

The concept of regular unitary dilation of a pair of commuting contractions is shown to be intimately related to Markovian like subspaces with respect to a pair of commuting unitary operators. Starting from this observation, a two dimensional Markovian like representation problem is studied geometrically. By using the geometric properties of the state spaces and some elementary properties of the two variable Hardy spaces, the spectral domain description of regular and coregular representations is given. ESA

66 SYSTEMS ANALYSIS

Includes mathematical modeling; network analysis; and operations research.

No abstracts in this category.

67 THEORETICAL MATHEMATICS

Includes topology and number theory.

N91-19799# Technische Univ., Berlin (Germany, F.R.). Fachbereich Mathematik.
APPROXIMATION PROPERTIES OF WAVELET TRANSFORMS Ph.D. Thesis [APPROXIMATIONSEIGENSCHAFTEN DER WAVELET-TRANSFORMATION]
Andreas Rieder 1990 79 p In GERMAN
(ETN-91-98922) Avail: NTIS HC/MF A05

Contrary to the Fourier transformation, the Wavelet transformation represents a signal in the time frequency plane, from the point of view of local affects. After a short summary of group theory, the wavelet transform is continued in Sobolev space. The consequences of theoretical results on one and multidimensional discrete wavelet transforms are discussed. A complete description of wavelet transform in high frequencies and a classification of a number of wavelets are given. The remarks concerning the numerical stability of discrete wavelet transforms are important for the application. ESA

70 PHYSICS (GENERAL)

For precision time and time interval (PTTI) see *35 Instrumentation and Photography;* for geophysics, astrophysics or solar physics see *46 Geophysics, 90 Astrophysics,* or *92 Solar Physics.*

N91-19800# Joint Publications Research Service, Arlington, VA.
JPRS REPORT: SCIENCE AND TECHNOLOGY. USSR: PHYSICS AND MATHEMATICS
31 Oct. 1990 36 p Transl. into ENGLISH from various Russian articles
(JPRS-UPM-90-004) Avail: NTIS HC/MF A03

Abstracts of Soviet literature in various areas of physics and mathematics are compiled. The following subject areas are covered: acoustics, lasers, nuclear physics, optics, spectroscopy, superconductivity, and differential equations. For individual titles, see N91-19801 through N91-19820.

N91-19801# Joint Publications Research Service, Arlington, VA.
LAWS OF HEAT TRANSFER IN THREE-DIMENSIONAL VISCOUS SHOCK LAYER OF STREAM FLOWING PAST BLUNT BODIES AT SOME ANGLES OF ATTACK AND GLIDE Abstract Only **c34**
A. I. Borodin and S. V. Peygin *In its* JPRS Report: Science and Technology. USSR: Physics and Mathematics 31 Oct. 1990 p 1 Transl. into ENGLISH from Inzhenerno-Fizicheskiy Zhurnal (Minsk, USSR), v. 58, no. 2, Feb. 1990 p 200-206 (For primary document see N91-19800 11-70)
Avail: NTIS HC/MF A03

Heat transfer in a three-dimensional thin viscous shock layer of a supersonic stream flowing past blunt bodies is analyzed by solving the applicable system of three dimensionless partial differential transfer equations, specifically for a stream flowing past triaxial ellipsoids of various proportions with the angles of attack and glide included as two additional parameters of the problem. The ellipsoidal body is described in a rectangular Cartesian system of coordinates with the origin at the stagnation point, with two axes of coordinates on the body surface and the third one normal to it. The stagnation point is a singular one for that system of equations and the two sets of coordinates on the body surface are generated, both features being explicated by a change to appropriate new independent and dependent variables. The boundary conditions for the system of equations are adhesion to an impermeable body surface and generalized Rankin-Hugoniot conditions at the shock wave. Such a boundary value problem is solved numerically by the method of finite differences. Calculations on a BESM-6 high-speed computer were made for ellipsoids with both transverse semiaxes b and c varied from 0.3 to 3 (longitudinal semiaxis a=1), the angle of attack varied from 0 to pi/2, the angle of glide varied from 0 to pi/4, and the Reynolds number varied from 100 to 500,000. Author

N91-19802# Joint Publications Research Service, Arlington, VA.
ACOUSTIC STABILIZATION OF LASER BEAM WAVEFRONT IN NONHOMOGENEOUS GASEOUS MEDIUM Abstract Only **c36**
D. O. Lapotko and O. G. Martynenko *In its* JPRS Report: Science and Technology. USSR: Physics and Mathematics 31 Oct. 1990 p 1 Transl. into ENGLISH from Inzhenerno-Fizicheskiy Zhurnal (Minsk, USSR), v. 58, no. 2, Feb. 1990 p 235-238 (For primary document see N91-19800 11-70)
Avail: NTIS HC/MF A03

Use of acoustic flow for stabilization of the laser beam wavefront propagating through a nonisothermal and thus, nonhomogeneous gaseous medium is considered, on account of its low inertia and controllability. An ultrasonic beam generated by a sound source propagates toward an inhomogeneity and, as sound is absorbed in the surrounding gas, there is generated a secondary acoustic flow in the same direction which sweeps the inhomogeneity away from the path of the laser beam and thus, prevents distortion of its wavefront. The effectiveness of such a stabilization is measured in terms of space and time: namely size of the region from which an inhomogeneity must be removed and

length of time from emission of the ultrasonic beam to restoration of the laser beam wavefront. The process is analyzed, considering that the coefficient of sound absorption in an irradiated inhomogeneity can be much smaller than, much larger than, or approximately equal to the coefficient of sound absorption in a homogeneous medium depending on whether the inhomogeneity is removed by acoustic flow within the surrounding homogeneous region, or by acoustic flow developing within the inhomogeneity, or by acoustic flow both within or around the inhomogeneity. Calculations are made for two fundamentally different conditions: an acoustic Reynolds number smaller than one corresponding to linear propagation of sound waves through a medium with linear absorption characteristics; and an acoustic Reynolds number much larger than one corresponding to propagation of intense sound waves through a weakly absorbing medium which distorts them nonlinearly and, as a consequence, absorbs them fast. This method of stabilization was tested experimentally: the light intensity on the axis of a laser beam entering a nonhomogeneous medium being measured from the moment an ultrasonic beam had also entered the medium to the moment the laser beam wavefront was restored. This time span was found to almost coincide with that taken for development of secondary acoustic flow. Author

N91-19803# Joint Publications Research Service, Arlington, VA.
PASSIVE MODE LOCKING IN OPTICALLY PUMPED Al2O3:Ti(3+) LASER Abstract Only **c36**
M. I. Demchuk, A. A. Demidovich, N. I. Zhavoronkov, V. P. Mikhaylov, A. P. Shkadarevich, A. A. Ishchenko, and A. I. Sopin *In its* JPRS Report: Science and Technology. USSR: Physics and Mathematics 31 Oct. 1990 p 3 Transl. into ENGLISH from Kvantovaya Elektronika (Moscow, USSR), v. 17, no. 2, Feb. 1990 p 133 (For primary document see N91-19800 11-70)
Avail: NTIS HC/MF A03

An experiment involving an optically pumped Ti-activated sapphire crystal grown by the Czochralski method demonstrated the feasibility of passive mode locking in such a laser. The crystal, a rod 7 mm in diameter and 80 mm long, was pumped by a gas-discharge lamp with flash pulses of 5 to 100 J energy and 5 microseconds duration above the half-amplitude level, inside an elliptical reflector with a luminophor based ethanol solution of coumarin-30 dye as coolant. The laser cavity was formed by a spherical 100 percent reflectance mirror with a 2.5 m radius and an 85 percent reflectance plane. Three prisms made of TFN optical glass were used for wavelength selection and dyes with the matching spectral characteristics served as passive saturable filters. Passive mode locking and emission of ultrashort 25 ps pulses were achieved, tunable over both 750 to 765 nm and 780 to 790 nm bands with 2780 dye and with 4409 dye respectively. Author

N91-19804# Joint Publications Research Service, Arlington, VA.
POSSIBILITY OF RAISING EFFICIENCY OF FREE-ELECTRON LASER IN LONGITUDINAL MAGNETIC FIELD Abstract Only **c36**
V. A. Bazylev and A. V. Tulupov *In its* JPRS Report: Science and Technology. USSR: Physics and Mathematics 31 Oct. 1990 p 3 Transl. into ENGLISH from Kvantovaya Elektronika (Moscow, USSR), v. 17, no. 2, Feb. 1990 p 156-159 (For primary document see N91-19800 11-70)
Avail: NTIS HC/MF A03

The possibility of further raising the efficiency of a free-electron laser in a longitudinal magnetic field (ubitron) by providing for a single reflection of the electrons at the ponderomotive potential and thus, their single passage through resonance is examined theoretically on the basis of electron motion in both magnetic and wiggler fields. The efficiency of such a laser was already raised by a profiling of its parameters to ensure capture of electrons on closed trajectories near the retarding stage as well as by optimization of the magnetic field. The interaction of electrons and the combination-frequency wave is shown to depend largely on a parameter which determines the electron bunching and in the absence of wiggler profiling characterizes anisochronism. Therefore, as this parameter approaches zero, the efficiency can increase appreciably toward a higher attainable maximum. However, as this parameter approaches infinity, the efficiency remains constant but the phase area of the capture region shrinks toward zero. These conclusions were confirmed by analytical and then numerical solution of a system of two equations describing the evolution of both amplitude and phase of the light wave. Author

N91-19805# Joint Publications Research Service, Arlington, VA.
QUANTUM FLUCTUATIONS IN LASER WITH INTRACAVITY FREQUENCY DOUBLING Abstract Only **c36**
A. I. Zhiliba *In its* JPRS Report: Science and Technology. USSR: Physics and Mathematics 31 Oct. 1990 p 3-4 Transl. into ENGLISH from Optika Atmosfery (Tomsk, USSR), v. 2, no. 10, Oct. 1989 p 1118-1120 (For primary document see N91-19800 11-70)
Avail: NTIS HC/MF A03

A source of light with minimal quantum fluctuations of intensity for ultrasensitive laser spectroscopy is considered; namely, one consisting of an active lasing medium and a frequency-doubling nonlinear crystal inside a common cavity. The ability of such a device to generate simultaneously compressed fundamental and second-harmonic radiation or, under the appropriate optimum condition, only second-harmonic radiation is demonstrated theoretically on the basis of a semiclassical description of the process by a system of two differential equations. Two successive integrations by parts solve this system of equations in the zeroth and then first approximation. A subsequent quantum-electronic description of this device and analysis of its statistical characteristics on the basis of the Fokker-Plank equation indicate the feasibility of attenuating shot noise in the low-frequency range of the radiation power spectrum and thus, in emission of fundamental radiation. Author

N91-19806# Joint Publications Research Service, Arlington, VA.
COPPER VAPOR AS ACTIVE MEDIUM FOR HIGH-POWER OSCILLATOR-AMPLIFIER LASER SYSTEMS Abstract Only **c36**
N. A. Lyabin, V. V. Zubov, and A. D. Chursin *In its* JPRS Report: Science and Technology. USSR: Physics and Mathematics 31 Oct. 1990 p 4 Transl. into ENGLISH from Kvantovaya Elektronika (Moscow, USSR), v. 17, no. 1, Jan. 1990 p 28-31 (For primary document see N91-19800 11-70)
Avail: NTIS HC/MF A03

An experimental study of the GI-201 industrial Cu-vapor laser with electric discharge pumping is presented. The active medium occupying a volume of 350 cc and the 2 cm diameter of the discharge channel were lengthened from 93 cm to 123 cm. A shield consisting of eight copper strips around the Cu-vapor cell lowered the wave impedance. Heating and excitation of the active medium was effected by pulses coming from a TGI1-2500/50 thyratron-rectifier. The results of the study are discussed. Author

N91-19807# Joint Publications Research Service, Arlington, VA.
CHARACTERISTICS OF EXCIMER LASER WITH NARROW EMISSION LINE Abstract Only **c36**
K. A. Valiyev, L. V. Velikov, G. S. Volkov, and D. Yu. Zaroslov *In its* JPRS Report: Science and Technology. USSR: Physics and Mathematics 31 Oct. 1990 p 4-5 Transl. into ENGLISH from Kvantovaya Elektronika (Moscow, USSR), v. 17, no. 1, Jan. 1990 p 43-45 (For primary document see N91-19800 11-70)
Avail: NTIS HC/MF A03

Narrowing the emission line of excimer lasers for ultraviolet photolithography with use of monochromatic objectives is considered as an alternative to the costly manufacturing of polychromatic precision objectives or wide-aperature wide-field mirrors of chromatic aberration. Experiments were performed with an ELI-71 commercial 308 nm XeCl-laser and with a diffraction grating as a dispersive element. The latter was either a reflective one with 2400 lines/mm in an autocollimating position at a 22 degree angle of reflection in the first order, preceded by a beam-widening tetraprism telescope, or a diffraction grating with 2400 lines/mm in a position for grazing incidence at a 5 to 10

degree angle and for the high-reflectance to be located with in the first order of the diffraction pattern. The results of this investigation are presented. Author

N91-19808# Joint Publications Research Service, Arlington, VA.
INTRACAVITY SECOND-HARMONIC GENERATION BY LASER WITH OPTICAL DELAY LINE AND MODE LOCKING Abstract Only **c36**
N. S. Balashov, S. K. Isayev, L. S. Korniyenko, N. V. Kvartsov, L. N. Magdich, V. Yu. Mikhaylov, S. R. Rustamov, and V. V. Firsov *In its* JPRS Report: Science and Technology. USSR: Physics and Mathematics 31 Oct. 1990 p 5 Transl. into ENGLISH from Kvantovaya Elektronika (Moscow, USSR), v. 17, no. 1, Jan. 1990 p 64-66 Original language document was announced in IAA as A90-34616 (For primary document see N91-19800 11-70)
Avail: NTIS HC/MF A03

The operation of a mode-locked garnet laser with intracavity second harmonic generation is investigated experimentally. It is shown that the use of an afocal optical delay line to increase the effective cavity length makes it possible to significantly increase the peak power of ultrashort pulses and to improve the efficiency of intracavity second harmonic generation. Details of the experimental procedure and results are presented. K.S.

N91-19809# Joint Publications Research Service, Arlington, VA.
SOLUTION OF ONE-DIMENSIONAL PROBLEM IN NONLINEAR THEORY OF ELASTICITY WITH STRUCTURED SHOCK WAVE Abstract Only **c39**
A. A. Burenin and Yu. A. Rossikhin *In its* JPRS Report: Science and Technology. USSR: Physics and Mathematics 31 Oct. 1990 p 12 Transl. into ENGLISH from Prikladnaya Mekhanika (Kiev, USSR), v. 26, no. 1, Jan. 1990 p 103-108 (For primary document see N91-19800 11-70)
Avail: NTIS HC/MF A03

A system of wave propagation equations through an isotropic elastic medium is formulated in Euler variables as a one-dimensional nonlinear problem of elasticity in a rectangular Cartesian system of coordinates, assuming that both the velocity function and the stress function are expandable into power series in time t. It is then reduced to a single dimensionless equation, after stress is eliminated from two of the original ones. This equation is solved by the perturbation method with a small parameter and asymptotic expansion, the space variable must be rescaled for internal asymptotic expansions. As the viscosity vanishes, the solution becomes that of a structures shock wave. Author

N91-19810# Joint Publications Research Service, Arlington, VA.
CONSTRUCTING MATHEMATICAL MODEL OF ADAPTIVE ANTI-FLUTTER SYSTEM Abstract Only **c08**
B. O. Kachanov, S. I. Ovcharenko, and A. T. Ponomarev *In its* JPRS Report: Science and Technology. USSR: Physics and Mathematics 31 Oct. 1990 p 12-13 Transl. into ENGLISH from Prikladnaya Mekhanika (Kiev, USSR), v. 26, no. 1, Jan. 1990 p 113-119 (For primary document see N91-19800 11-70)
Avail: NTIS HC/MF A03

A linear mathematical model of an anti-flutter system for aircraft is constructed on the basis of an approximate finite-dimensional mathematical description of perturbed aircraft motion and its stability analysis in accordance with the Mikhaylov's aeroelasticity criterion. For simplification of the iterative calculation process, the aerodynamic and kinematic parameters are assumed to vary harmonically at the stagnation point. To make the system adaptive, the model includes algorithms of identification, estimation, and optimal control based on that simplified aeroelasticity model. Practical application is demonstrated on suppression of symmetric flutter of a hypothetical transport plane during depletion of fuel. It is assumed that the fuel is carried in tanks under the wings and that the rudders have a surface area constituting one quarter of the aileron surface that extend almost to the tip of the wings. Three coefficients most sensitive to fuel depletion were selected for adaptive control by sensitivity analysis of the critical flutter velocity and frequency to variation of coefficients in the model equation. The other coefficients were assumed to remain constant at their design values corresponding to the basic plane load. Author

N91-19811# Joint Publications Research Service, Arlington, VA.
MICROSECOND-PULSE Nd-GLASS LASER WITH MONOPULSE DURATION CONTROL Abstract Only **c36**
B. V. Anikeyev and V. V. Krutyakov *In its* JPRS Report: Science and Technology. USSR: Physics and Mathematics 31 Oct. 1990 p 15 Transl. into ENGLISH from Ukrainskiy Fizicheskiy Zhurnal (Kiev, USSR), v. 35, no. 2, Feb. 1990 p 209-213 (For primary document see N91-19800 11-70)
Avail: NTIS HC/MF A03

A technological pulsed Nd-glass laser with power stabilizing external negative feedback was built for applications such as micro-welding which require flat-top laser monopulses with duration control. Both the beginning and ending of an emission monopulse are controlled by Q-switching an electro-optic shutter which operates on the basis of the longitudinal Pockels effect. Precise control of the pulse-start is achieved by suppression of acoustic waves generated upon impact excitation of the shutter by the piezoelectric effect. This excitation is effectively prevented by damping the laser crystal so that quasi-continuous pulse emission becomes attainable with the maximum pulse duration determined by duration of the pumping pulse. The optical cavity, optically 90 cm long, is formed by two mirrors with 1.0 and 0.40 reflection coefficients respectively. A diaphragm protects the shutter fixture against burns by reducing the diameter of the laser beam to 4 mm. A unique feature of the shutter is an additional polarizer, a Brewster stack of nine plates, which maximizes the contrast. Feedback signals are generated by a coaxial photocell. The laser was tested for performance, including dependence of laser plus feedback kinetics on the rise time of Q-switching pulse and reliability of transition to quasi-continuous monopulse emission. Author

N91-19812# Joint Publications Research Service, Arlington, VA.
BREAKUP OF FEMTOSECOND PULSES DURING AMPLIFICATION IN Er(3+)-DOPED SINGLE-MODE OPTICAL FIBERS Abstract Only **c36**
A. B. Grudinin, Ye. M. Dianov, D. V. Korobkin, A. Yu. Makarenko, A. M. Prokhorov, and I. Yu. Khrushchev *In its* JPRS Report: Science and Technology. USSR: Physics and Mathematics 31 Oct. 1990 p 15-16 Transl. into ENGLISH from Pisma v Zhurnal Eksperimentalnoy i Teoreticheskoy Fiziki (Moscow, USSR), v. 51, no. 3, 10 Feb. 1990 p 121-124 (For primary document see N91-19800 11-70)
Avail: NTIS HC/MF A03

Amplification of femtosecond solitons by stimulated Raman scattering (SRS) in Er(+3)-doped optical fibers is considered. Fibers doped with rare-earth element ions acquire the characteristics of an active laser medium and the duration of femtosecond solitons are comparable with the transverse-relaxation time for the (4)I(sub 13/2)ad (4)I(sub 15/2) transition in an Er(+3) ion. An experiment was performed with an SRS soliton generator and a 35 m long fiber. The result from this experiment are presented. Author

N91-19813# Joint Publications Research Service, Arlington, VA.
He-Ne LASER EMITTING FIVE LINES SIMULTANEOUSLY Abstract Only **c36**
Ya. M. Bondarchuk, R. M. Voznyak, and V. Ye. Privalov *In its* JPRS Report: Science and Technology. USSR: Physics and Mathematics 31 Oct. 1990 p 17 Transl. into ENGLISH from Optika i Spektroskopiya (Leningrad, USSR), v. 67, no. 6, Dec. 1989 p 1418-1419 (For primary document see N91-19800 11-70)
Avail: NTIS HC/MF A03

A multicolor He-Ne laser was developed which emits simultaneously five lines within the visible range of the spectrum. Its approximately 2 m long cavity is formed by two spherical mirrors, a 19-layer coating on each ensuring higher than 0.99 reflection coefficient for 590-710 nm light with a 3,390 nm transmission window. This cavity is almost fully occupied by the active medium

in a bipartite cell with a common cathode between its two arms. Cavity and active medium were so matched to prevent suppression of emission at 640, 635, 629, and 612 nm wavelengths by the emission of 633 nm radiation. The total multicolor emission power with a 72-76 mA current through the cathode is 4.8 mW, split between the five lines in a P(640):P(635):P(633):P(629):p(612) = 0.4:0.1:1:0.1:0.5 ratio. Separate emission of each line is achieved by replacement of one mirror with a Littrow prism. Author

N91-19814# Joint Publications Research Service, Arlington, VA.
ORIGIN OF RESIDUAL SURFACE RESISTANCE OF CERAMIC HIGH-TEMPERATURE SUPERCONDUCTORS Abstract Only **c76**

N. V. Fomin *In its* JPRS Report: Science and Technology. USSR: Physics and Mathematics 31 Oct. 1990 p 17-18 Transl. into ENGLISH from Pisma v Zhurnal Tekhnicheskoy Fiziki (Leningrad, USSR), v. 16, no. 1, 12 Jan. 1990 p 77-79 (For primary document see N91-19800 11-70)
Avail: NTIS HC/MF A03

The results of an experiment that revealed residual surface resistance on a ceramic high temperature superconductor in a microwave field at a temperature near absolute zero are explained. The Bardeen-Cooper-Schrieffer theory is the basis of the explanation of these apparently paradoxical results. The excited states are considered to be separate from the ground state by the energy gap in this theory. The paradox is resolved by taking into account losses in the natural mode of the microwave resonator due to diffuse diffractive scattering of this mode by randomly oriented anisotropic macrograins of the ceramic material. Quantitative theoretical estimates validating this interpretation of the results are made on the basis of a simple model with only two equiprobable orientations of grains whose C-axis either runs perpendicular to the surface parallel to the Z-axis or runs parallel to the X-axis in the Cartesian system of coordinates. Reflection of a normally incident wave by the surface of a ceramic superconductor is analyzed on this basis, assuming that the electric field of this wave lies in the XZ-plane and penetrates a grain of either orientation to a depth much smaller than the grain diameter. A single crystal of a high temperature superconductor is considered. Its optical anisotropy is recognized as a principal result of the interaction between Cooper-pair electrons and the anisotropic crystal. This result is accounted for by extending the London equation to the effective electron tensor mass. Author

N91-19815# Joint Publications Research Service, Arlington, VA.
LIMITING PULSE SIGNAL IN NbN-Si STRUCTURE: SUPERCONDUCTOR FILM ON SUBSTRATE Abstract Only **c76**

Ye. F. Gatsura, A. B. Kozyrev, and T. B. Samoylova *In its* JPRS Report: Science and Technology. USSR: Physics and Mathematics 31 Oct. 1990 p 19 Transl. into ENGLISH from Zhurnal Tekhnicheskoy Fiziki (Leningrad, USSR), v. 60, no. 1, Jan. 1990 p 218-222 (For primary document see N91-19800 11-70)
Avail: NTIS HC/MF A03

An experiment concerning the effect of electromagnetic pulses on an NbN-Si structure consisting of an NbN-film microstrip and a Si single crystal as substrate was studied. NbN films were deposited on SiO2 and Si substrates by ionplasma getter sputtering of a niobium target. The static current-voltage characteristics of the substrates and of the NbN films on SiO2 and Si substrates were measured. Measurements were also made for determining the dependence of the critical superconducting transition temperature, its fluctuation range, and of the R(300 K)/R(17 K) NbN resistance ratio on the thickness of the 750 C NbN films. The results indicate that such structures behave like linear-nonlinear limiters when the NbN film switches from superconducting to normal state with attendant impact ionization of the silicon substrate acting as a discharger. They were tested in a transmission line for pulse response characteristics and the results are presented. Author

N91-19816# Joint Publications Research Service, Arlington, VA.
EFFECT OF PARAMAGNETIC IMPURITIES ON DYNAMICS OF MAGNETIC FLUXES IN SUPERCONDUCTORS Abstract Only **c76**

Yu. I. Gorobets, A. N. Kuchko, and V. I. Finokhin *In its* JPRS Report: Science and Technology. USSR: Physics and Mathematics 31 Oct. 1990 p 20 Transl. into ENGLISH from Ukrainskiy Fizicheskiy Zhurnal (Kiev, USSR), v. 35, no. 1, Jan. 1990 p 131-135 (For primary document see N91-19800 11-70)
Avail: NTIS HC/MF A03

The effect of paramagnetic impurities on the redistribution of magnetic fluxes in a magnetic superconductor with a system of noninteracting paramagnetic ions is analyzed theoretically in terms of electron spin and magnetic flux interactions. A plane N-S interphase boundary is assumed to propagate through the material so that two magnetic fields act on the paramagnetic ions: a constant magnetic one produced by their exchange interaction with the magnetic subsystem in the superconductor and a variable one associated with penetration of the external magnetic field into the superconductor. Interaction of a solitary paramagnetic ion with the resultant magnetic flux and the magnetic subsystem in the superconductor is described by the corresponding interaction Hamiltonia.ı. The following are calculated: (1) the energy transfer to a paramagnetic ion upon crossing the interphase boundary in the approximation of slow ion relaxation; (2) the energy transfer to the entire system of paramagnetic ions proportional to their concentration and to the velocity of the interphase boundary in an asymptotic form which differs for low and high temperatures; (3) the energy lost by a solitary Abrikosov vortex moving at a constant velocity in a type-II superconductor based on the Clem model; and (4) estimates for YBa2Cu3O(d):Fe(+3) ceramic energy transfer. Author

N91-19817# Joint Publications Research Service, Arlington, VA.
PHENOMENOLOGICAL THEORY OF PHASE TRANSITIONS TO NONHOMOGENEOUS NONCOMMENSURATE PHASE WITH SUPERCONDUCTING CURRENT Abstract Only **c76**

A. M. Prokhorov, A. Ya. Braginskiy, Yu. M. Gufan, and Ye. G. Rudashevskiy *In its* JPRS Report: Science and Technology. USSR: Physics and Mathematics 31 Oct. 1990 p 20 Transl. into ENGLISH from Doklady Akademii Nauk SSSR (Moscow, USSR), v. 310, no. 3, 30 Jan. 1990 p 599-603 (For primary document see N91-19800 11-70)
Avail: NTIS HC/MF A03

A phenomenological theory is constructed to describe structural transition of a crystal from a plain highly symmetric phase to a less symmetric one with small-scale but still macroscopic nonhomogeneity. The small group G(sub k) is assumed to remain unchanged while the K(x) vector (x-macroscopic space coordinate characterizing the volume of a crystal sufficiently macroscopic for being associated with density of the Landau nonequilibrium potential) varies within the Brillouin zone along some axis z. As specific examples, 123-phase high temperature superconductor compounds such as Y(RE)Ba2Cu3O(7-d) with an approximately perovskitic primitive crystal structure are considered. Author

N91-19818# Joint Publications Research Service, Arlington, VA.
THERMAL CONDUCTIVITY OF HIGH-TEMPERATURE SUPERCONDUCTORS IN NORMAL STATE Abstract Only **c76**

A. Jezowski, J. Klamut, and J. Trojnar *In its* JPRS Report: Science and Technology. USSR: Physics and Mathematics 31 Oct. 1990 p 21 Transl. into ENGLISH from Fizika Nizkikh Temperatur (Kharkov, USSR), v. 15, no. 10, Oct. 1989 p 1025-1031 (For primary document see N91-19800 11-70)
Avail: NTIS HC/MF A03

Available experimental data on high temperature superconductors are anayzed concerning the thermal conductivity of these materials in the normal state above the superconducting transition temperatures. The materials included here are YBa2Cu3O(7-d) (d = 0.19, 0.46, 0.90), (Sm, Eu, Gd, Ho, Er)-Ba-Cu-O, and Ti-Ba-Ca-Cu-O metal oxides, their thermal conductivity was measured over the 5 to 320 K temperature range. The main conclusions are that only the maximum value of the

thermal conductivity depends on the oxygen content in a metal-like; therefore, superconducting material: it increases with increasing oxygen content while the trend of its temperature dependence above the critical temperature does not. Author

N91-19819# Joint Publications Research Service, Arlington, VA.
SUPERCONDUCTIVITY OF OXIDE FILM ELECTROLYTICALLY DEPOSITED ON SURFACE OF B(1-x)Sb(x) SINGLE CRYSTAL Abstract Only **c76**
V. N. Alfeyev, B. A. Aminov, N. B. Brandt, S. Ya. Vasina, B. B. Damaskin, M. Zigel, V. P. Kuznetsov, O. A. Petriy, Ya. G. Ponomarev, and M. V. Sudakova et al *In its* JPRS Report: Science and Technology. USSR: Physics and Mathematics 31 Oct. 1990 p 21-22 Transl. into ENGLISH from Fizika Nizkikh Temperatur (Kharkov, USSR), v. 15, no. 10, Oct. 1989 p 1099-1101 (For primary document see N91-19800 11-70)
Avail: NTIS HC/MF A03

An experimental study was made of thin oxide films electrolytically deposited on the surface of Bi(1-x)Sb(x) single crystals (x from 0.1 to 0.3) at room temperature, the electrolyte consisting of acetonitrile as solvent with salicylic acid as conductive additive and containing copper ions. The current-voltage characteristics of point junctions produced by mechanical pressure on oxidized surfaces were measured at temperatures ranging from 1.7 K to above 20 K. They were found in most cases to be characteristic of Josephson junctions, with a critical current in the milliampere range at 4.2 K, with Mersero constant-period oscillations of the differential electrical conductance dI/dV near zero voltage in a magnetic field, and with Shapiro plateaus in a microwave field. The critical temperature of superconducting transition corresponding to maximum differential electrical conductance near zero voltage was found to be within 6 to 8 K in most cases and 20 K or higher in some cases. Author

N91-19820# Joint Publications Research Service, Arlington, VA.
COHERENT EFFECTS IN GENERATION OF ULTRASHORT LIGHT PULSES BY SEMICONDUCTOR INJECTION LASER Abstract Only **c36**
E. M. Belenov and P. P. Vasilyev *In its* JPRS Report: Science and Technology. USSR: Physics and Mathematics 31 Oct. 1990 p 26 Transl. into ENGLISH from Zhurnal Eksperimentalnoy i Teoreticheskoy Fiziki (Moscow, USSR), v. 96, no. 5, Nov. 1989 p 1629-1637 (For primary document see N91-19800 11-70)
Avail: NTIS HC/MF A03

Pulsed emission of coherent light by a two-level semiconductor as the active medium of an injection laser with a new kind of Q switching is analyzed. The case considered is that of pulse duration longer than the zero-field polarization relaxation time at the second level T2(O). This relaxation time becomes longer in the presence of an electric field and more so as the field intensity increases so that in a strong field T2(E) may be longer than the pulse duration. Pulses shorter that 5 ps with a power flux density in the GW/sq cm range are considered. This power density is also sufficient for stimulated Raman scattering of active modes during coherent light conversion with suppressed scattering-phase relaxation. The theoretical analysis is based on a system of Maxwell-Bloch equations which describe the dynamics of coherent radiation emission for an injection laser with a very high excess above the threshold inversion. An experiment was performed with an AlGaAs/GaAs heterojunction injection laser and the new method of Q-switching to ensure formation of high power ultrashort pulses. It revealed the conditions and characteristics of stimulated Raman scattering during generation of picosecond pulses. On the basis of these data and theoretical considerations, the feasibility of generating femtosecond pulses in such an injection laser by means of stimulated Raman scattering, which suppresses field oscillations, is predicted. Author

N91-19821# Fermi National Accelerator Lab., Batavia, IL.
LONGITUDINAL PERIODICITY IN SUPERCONDUCTING DIPOLE MAGNETS
M. Kuchnir 25 Jan. 1991 4 p
(Contract DE-AC02-76CH-03000)
(DE91-008421; FNAL-TM-1712) Avail: NTIS HC/MF A01

Recent magnetic measurements sensitive to the persistent currents in superconducting HERA dipole magnets uncovered a longitudinal periodic pattern with a period equal to the pitch of the strands in the cable. Not all the observed facets of this phenomenon have been explained yet. Although the existence of this pattern does not affect the performance of the accelerator, it is of interest to understand its exact source. In this note it is suggested how this pattern could result from differences in the strands making up the cable. More specifically, from differences in their (Jc*D), the average of the product Jc*D of the filaments of a strand, where Jc is the critical current density and D is the diameter of the filament. These strand-to-strand differences in a cable are to be expected from the selection process that probably occurred in the cable manufacture: strands of high and low critical current were mixed in order to maximize cable production yield. DOE

N91-19822# Istituto Elettrotecnico Nazionale (Galileo Ferraris), Turin (Itlay).
[ACTIVITIES REPORT OF THE ISTITUTO ELETTROTECNICO NAZIONALE GALILEO FERRARIS] Annual Report, 1989
Jun. 1990 253 p Partly in ENGLISH and ITALIAN Original contains color illustrations
(ETN-91-98868) Avail: NTIS HC/MF A12

Progess made in the scientific and technical activities peformed at the institute during 1989 is described. There are four main scientific areas covered at IEN. In the field of metrology with regard to time, frequency, electromagnetic, photometric, and acoustic quantities, IEN performs research on primary measurement standards, determines fundamental physical constant, realizes measurement units, maintains reference standards, disseminates measurement units, and represents Italy in international organizations. Their materials section studies magnetic materials, high temperature superconductors, and amorphous thin film semiconductors, and evaluates magnetic, electrical, radiometric, photometric, and acoustic properties of materials for specific applications. In the area of electrical equipment IEN mainly performs research aiming at improving characteristics, reliability and safety of low-voltage devices, and installations. Techniques for image understanding and research on complex system reliability are developed in the computer science field. Abstracts of reports dealing with these areas are presented. Author

71 ACOUSTICS

Includes sound generation, transmission and attenuation. For noise pollution see *45 Environmental Pollution.*

N91-19823*# National Aeronautics and Space Administration. Ames Research Center, Moffett Field, CA.
J-85 JET ENGINE NOISE MEASURED IN THE ONERA S1 WIND TUNNEL AND EXTRAPOLATED TO FAR FIELD
Paul T. Soderman, Alain Julienne (Office National d'Etudes et de Recherches Aerospatiales, Paris, France), and Adolph Atencio, Jr. Washington Jan. 1991 181 p
(NASA-TP-3053; A-89265; NAS 1.60:3053) Avail: NTIS HC/MF A09 CSCL 20A

Noise from a J-85 turbojet with a conical, convergent nozzle was measured in simulated flight in the ONERA S1 Wind Tunnel. Data are presented for several flight speeds up to 130 m/sec and for radiation angles of 40 to 160 degrees relative to the upstream direction. The jet was operated with subsonic and sonic exhaust speeds. A moving microphone on a 2 m sideline was used to survey the radiated sound field in the acoustically treated, closed test section. The data were extrapolated to a 122 m sideline by means of a multiple-sideline source-location method, which was used to identify the acoustic source regions, directivity patterns, and near field effects. The source-location method is described along with its advantages and disadvantages. Results indicate that the effects of simulated flight on J-85 noise are significant. At the

maximum forward speed of 130 m/sec, the peak overall sound levels in the aft quadrant were attentuated approximately 10 dB relative to sound levels of the engine operated statically. As expected, the simulated flight and static data tended to merge in the forward quadrant as the radiation angle approached 40 degrees. There is evidence that internal engine or shock noise was important in the forward quadrant. The data are compared with published predictions for flight effects on pure jet noise and internal engine noise. A new empirical prediction is presented that relates the variation of internally generated engine noise or broadband shock noise to forward speed. Measured near field noise extrapolated to far field agrees reasonably well with data from similar engines tested statically outdoors, in flyover, in a wind tunnel, and on the Bertin Aerotrain. Anomalies in the results for the forward quadrant and for angles above 140 degrees are discussed. The multiple-sideline method proved to be cumbersome in this application, and it did not resolve all of the uncertainties associated with measurements of jet noise close to the jet. The simulation was complicated by wind-tunnel background noise and the propagation of low frequency sound around the circuit. Author

N91-19824*# National Aeronautics and Space Administration. Ames Research Center, Moffett Field, CA.

LARGE-SCALE AEROACOUSTIC RESEARCH FEASIBILITY AND CONCEPTUAL DESIGN OF TEST-SECTION INSERTS FOR THE AMES 80- BY 120-FOOT WIND TUNNEL

Paul T. Soderman and Larry E. Olsen Dec. 1990 50 p
(NASA-TP-3020; A-88007; NAS 1.60:3020) Avail: NTIS HC/MF A03 CSCL 20A

An engineering feasibility study was made of aeroacoustic inserts designed for large-scale acoustic research on aircraft models in the 80 by 120 foot Wind Tunnel at NASA Ames Research Center. The advantages and disadvantages of likely designs were analyzed. Results indicate that the required maximum airspeed leads to the design of a particular insert. Using goals of 200, 150, and 100 knots airspeed, the analysis indicated a 30 x 60 ft open-jet test section, a 40 x 80 ft open jet test section, and a 70 x 100 ft closed test section with enhanced wall lining, respectively. The open-jet inserts would be composed of a nozzle, collector, diffuser, and acoutic wedges incorporated in the existing 80 x 120 test section. The closed test section would be composed of approximately 5 ft acoustic wedges covered by a porous plate attached to the test section walls of the existing 80 x 120. All designs would require a double row of acoustic vanes between the test section and fan drive to attenuate fan noise and, in the case of the open-jet designs, to control flow separation at the diffuser downstream end. The inserts would allow virtually anechoic acoustic studies of large helicopter models, jets, and V/STOL aircraft models in simulated flight. Model scale studies would be necessary to optimize the aerodynamic and acoustic performance of any of the designs. In all designs studied, the existing structure would have to be reinforced. Successful development of acoustically transparent walls, though not strictly necessary to the project, would lead to a porous-wall test section that could be substituted for any of the open-jet designs, and thereby eliminate many aerodynamic and acoustic problems characteristic of open-jet shear layers. The larger size of the facility would make installation and removal of the insert components difficult. Consequently, scheduling of the existing 80 x 120 aerodynamic test section and scheduling of the open-jet test section would likely be made on an annual or longer basis. The enhanced wall-lining insert would likely be permanent. Although the modifications are technically feasible, the economic practicality of the project was not evaluated. Author

N91-19825*# National Aeronautics and Space Administration. Lewis Research Center, Cleveland, OH.

UNSTEADY BLADE PRESSURE MEASUREMENTS FOR THE SR-7A PROPELLER AT CRUISE CONDITIONS

L. J. Heidelberg and M. Nallasamy (Sverdrup Technology, Inc., Brook Park, OH.) 1990 17 p Presented at the 13th Aeroacoustics Conference, Tallahassee, FL, 22-24 Oct. 1990; sponsored by AIAA Previously announced in IAA as A91-12533
(Contract NAS3-24105)
(NASA-TM-103606; E-5754; NAS 1.15:103606; AIAA-90-4022)
Avail: NTIS HC/MF A03 CSCL 20A

The unsteady blade surface pressures were measured on the SR-7A propeller. The freestream Mach no., inflow angle, and advance ratio were varied while measurements were made at nine blade stations. At a freestream Mach no. of 0.8, the data in terms of unsteady pressure coefficient vs. azimuth angle are compared to an unsteady 3-D Euler solution, yielding very encouraging results. The code predicts the shape (phase) of the waveform very well, while the magnitude is over-predicted in many cases. At tunnel Mach nos. below 0.6, an unusually large response on the suction surface at 0.15 chord and 0.88 radius was observed. The behavior of this response suggests the presence of a leading edge vortex. The midchord measuring stations on the suction surface exhibit a response that leads the forcing function while most other locations show a phase lag. Author

N91-19826*# Army Aviation Research and Development Command, Moffett Field, CA. Aeroflightdynamics Directorate.

EULER SOLUTIONS TO NONLINEAR ACOUSTICS OF NON-LIFTING HOVERING ROTOR BLADES

J. D. Baeder Feb. 1991 17 p Presented at the 16th European Rotorcraft Forum, Glasgow, Scotland, 18-21 Sep. 1990
(NASA-TM-103837; A-91063; NAS 1.15:103837; USAAVSCOM-TM-90-A-007) Avail: NTIS HC/MF A03 CSCL 20A

For the first time a computational fluid dynamics (CFD) method is used to calculate directly the high-speed impulsive (HSI) noise of a non-lifting hovering rotor blade out to a distance of over three rotor radii. In order to accurately propagate the acoustic wave in a stable and efficient manner, an implicit upwind-biased Euler method is solved on a grid with points clustered along the line of propagation. A detailed validation of the code is performed for a rectangular rotor blade at tip Mach numbers ranging from 0.88 to 0.92. The agreement with experiment is excellent at both the sonic cylinder and at 2.18 rotor radii. The agreement at 3.09 rotor radii is still very good, showing improvements over the results from the best previous method. Grid sensitivity studies indicate that with special attention to the location of the boundaries a grid with approximately 60,000 points is adequate. This results in a computational time of approximately 40 minutes on a Cray-XMP. The practicality of the method to calculate HSI noise is demonstrated by expanding the scope of the investigation to examine the rectangular blade as well as a highly swept and tapered blade over a tip Mach number range of 0.80 to 0.95. Comparisons with experimental data are excellent and the advantages of planform modifications are clearly evident. New insight is gained into the mechanisms of nonlinear propagation and the minimum distance at which a valid comparison of different rotors can be made: approximately two rotor radii from the center of rotation. Author

N91-19827# Max-Planck-Inst. fuer Stroemungsforschung, Goettingen (Germany, F.R.).

REFLECTIONS ON SOME PROBLEMS CONCERNING THE ROLE OF SUPERFLUID TURBULENCE IN THE PROPAGATION OF SECOND-SOUND PULSES IN He 2

S. K. Nemirovskii (Academy of Sciences, USSR, Novosibirsk) and D. W. Schmidt Apr. 1990 37 p
(MPIS-8/1990; ISSN-0436-1199; ETN-91-98810) Avail: NTIS HC/MF A03

A survey of the present state of knowledge about the role of superfluid turbulence in the propagation of second sound pulsers in He-2 is presented as well as the theory concerning primarily, the initial stages of heat pulse evolution. Research findings which are mostly related to overshoot effects are given. Some ad hoc experimental and theoretical checkups run to clarify some of the questions raised during the survey are also presented. ESA

N91-19828# Messerschmitt-Boelkow-Blohm G.m.b.H., Munich (Germany, F.R.).

NOISE LEVEL REDUCTION INSIDE HELICOPTER CABINS

Eckehard Laudien and George Niesl Sep. 1990 12 p Presented at the 16th European Rotorcraft Forum, Glasgow, Scotland, 18-21 Sep. 1990
(MBB-UD-0578-90-PUB; ETN-91-98828) Avail: NTIS HC/MF A03

A number of measures to reduce the noise level in helicopter cabins are discussed. Laboratory test results of various panellings are presented as well as the insulation capacities of different panel mounts. Experiments in acoustic facilities (anechoic chamber and reverberation room) with the original cabin door and its frame led to an optimization of the transmission losses of door components such as window, sealing, and frame. The reduction of the cabin noise level by adding absorption is illustrated in the case of a honeycomb bulkhead with Helmholtz resonators. These sound absorption elements were designed to damp discrete gearbox frequencies. Resonators were also used for noise attenuation of an oil cooler fan. Cabin noise comfort can be improved by eliminating discrete frequencies. This was achieved in an experimental set up where properly tuned resonators were placed as close as possible to the passenger's ear in the headrest of the seat. In order to reduce structureborne transmission system noise, ground and flight test data of gearbox strut impedance were used for the design of specially tuned vibration absorbers. ESA

N91-19829# Messerschmitt-Boelkow-Blohm G.m.b.H., Munich (Germany, F.R.).
A GRADIENT MICROPHONE FOR LOCATING SOUND TARGETS [GRADIENTENMOKROFON ZUR ORTUNG VON SCHALLZIENLEN]
Oskar Bschorr 1990 12 p In GERMAN Presented at the 7th Tagung Anwendungen der Akustik, Meppen, Fed. Republic of Germany, 11-16 Sep. 1990
(MBB-Z-0341-90-PUB; ETN-91-98838) Avail: NTIS HC/MF A03

The gradient microphone is composed of a hollow sphere, e.g., aluminum, whose inner side is equipped with acceleration recorders. The microphone sphere is submitted to forced vibrations in a sound field, which are recorded by the acceleration sensors. The vectorial vibration velocity is shown to be directly proportional to the local speed vector of the adjacent sound field. In comparison with the conventional pressure actuated microphone, the gradient microphone not only gives the pressure behavior, but also the direction of the sound source. The gradient microphone is insensitive to external disturbances such as electromagnetic irradiation, wind and weather. It can be used for airborne sound as well as for waterborne sound. ESA

N91-19830# Helsinki Univ. of Technology, Espoo (Finland). Low Temperature Lab.
ULTRASONIC INVESTIGATIONS ON SUPERFLUID He-3-A AND He-3-B Ph.D. Thesis
Jukka Kyynaeraeinen 1990 62 p Sponsored by Finnish Cultural Foundation and Magnus Ehrnrooth Foundation
(ISBN-952-90-2241-7; ETN-91-98912) Avail: NTIS HC/MF A04

A rotating nuclear demagnetization cryostat (ROTA2) for attaining submillikelvin temperatures was constructed and a set of experiments, using ultrasound propagation in superfluid He3, was carried out in it. Abstracts of publications relating to the construction, to experiments where the so called real squashing mode in He3-B was studied under rotation, to the effect of rotation on sound propagation in He3-A, to the ultrasonic measurements in high magnetic fields, and to increased sound attenuation in He3-A at very low temperatures, are provided. The concept of superfluidity and super fluids under rotation are described. A phase diagram and an order parameter for He3 are given. The ultrasonic properties of the rotating cryostat are described. Experimental results are presented. The experimental data was obtained using pulsed zero sound propagation in a cylindrical cavity; nonlinear rotation responses were observed in He3-A; the rise of sound attenuation in He3-A; towards low temperatures was shown to arise from the reentrant normal flapping mode, which is excited near the cell boundaries; anisotropic sound attenuation in the field distorted He3-B was measured under rotation. ESA

N91-19831# Technische Univ., Delft (Netherlands). Dept. of Aerospace Engineering.
ELEMENTARY PULSE DIFFRACTION PROBLEMS AND THE GENERATION OF SOUND BY A DIPOLE MOVING ACROSS THE EDGE OF A HALF-PLANE
G. Schouten Nov. 1990 30 p
(LR-565; ETN-91-98939) Avail: NTIS HC/MF A03

The exact solution of the linearized wave equation for the diffracted field of a three dimensional sound pulse incident on the sharp edge of a half plane is constructed in closed form using Sommerfeld's method. From this solution the well known two dimensional equivalent is derived by the method of descent. The transient behavior of two dimensional and three dimensional switch-on sources, leading to steady incompressible potential flow, is obtained by time integrations of the pulse solutions. The characteristic features are discussed and plots of the flow field are presented. The three dimensional switch-on source is the classical result of Cagiard's 1935 paper. The field of a moving source in a branched space is generated by integration of the field of a pulse source. The diffracted field of the moving source can only approximately be obtained and only for relatively low velocity motion. Differentiation of the moving source solution yields the approximation to the field of a moving dipole in a branched space. The pressure (sound) wave generated by a dipole passing near the sharp edge of a half plane is computed as an application of the elementary solutions in a branched space. Spatial plots of the wave profiles and time histories of the pressure are presented. The results are compared with the existing literature and it must be concluded that the above direct approach presents a substantial improvement to the pulse Green's function. ESA

N91-19143*# National Research Council of Canada, Ottawa (Ontario). Inst. for Aerospace Research.
NON-LINEAR GENERATION OF ACOUSTIC NOISE IN THE IAR SPACECRAFT
R. Westley, K. Nguyen, and M. S. Westley *In* NASA, Goddard Space Flight Center, 16th Space Simulation Conference Confirming Spaceworthiness Into the Next Millennium Nov. 1990 p 195-210 (For primary document see N91-19126 11-18)
Avail: NTIS HC/MF A20 CSCL 20A

72 ATOMIC AND MOLECULAR PHYSICS

Includes atomic structure, electron properties, and molecular spectra.

N91-19832 New South Wales Univ., Kensington (Australia). Faculty of Sciences.
PROTON INDUCED X RAY EMISSION ANALYSIS Abstract Only Ph.D. Thesis
Eric Clayton Dec. 1988 3 p
Avail: Issuing Activity

A solid mathematical basis is established for the use of thick target Proton Induced X ray Emission (PIXE) analysis to determine the trace element concentrations in solid samples. With the advent of high resolution Si(Li) detectors there was a revival of interest in the use of characteristic x ray induced by high energy particle beams. It was shown that it is possible to use these x rays to measure very low concentrations of trace elements in samples. Ion beams were used for the analysis of archaeological artefacts using the technique of Particle Induced Gamma ray Emission (PIGME). Because of the necessity to use analysis methods that did not require destruction of the sample, the work involved the use of targets that were thick. In comparison with thin samples, the mathematical foundation for analysis was not well established. After a PIXE spectrum was measured, there are essentially three steps in its interpretation. The first to is analyze the spectrum to extract areas of the peaks which constitute that spectrum. This changes the ratio of the characteristic peak areas and must be modeled in the analysis program. After peak areas were estimated, they are utilized to determine the concentration of the element emitting those x rays. This involves modeling the processes that

results in the emission of x rays and their attenuation in the sample and detector system. Computer programs that allow implementation of a full PIXE analysis for either a thin or thick target are developed. As well as developing the foundation for thick target PIXE analysis, its application is considered in biological monitoring of occupational hazards. In this field questions of accuracy and quality control must be answered. A study in which PIXE analysis is applied to biological samples is considered. Author

N91-19833# Yale Univ., New Haven, CT. Dept. of Mechanical Engineering.
AERODYNAMIC FOCUSING OF PARTICLES AND HEAVY MOLECULES
Juan Fernandez delaMora Jan. 1990 8 p
(Contract DE-FG02-87ER-13750)
(DE91-006922; DOE/ER-13750/2) Avail: NTIS HC/MF A02

By accelerating a gas containing suspended particles or large molecules through a converging nozzle, the suspended species may be focused and therefore used to write fine lines on a surface. Our objective was to study the limits on how narrow this focal region could be as a function of particle size. We find that, for monodisperse particles with masses m(sub p) some 3.6 times 10(exp 5) times larger than the molecular mass m of the carrier gas (diameters above some 100 angstroms, there is no fundamental obstacle to directly write submicron features. However, this conclusion has been verified experimentally only with particles larger than 0.1 m. Experimental, theoretical and numerical studies on the defocusing role of Brownian motion for very small particles or heavy molecules have shown that high resolution (purely aerodynamic) focusing is impossible with volatile molecules whose masses are typically smaller than 1000 Dalton. For these, the minimal focal diameter after optimization appears to be 5(radical)(m/m(sub p)) times the nozzle diameter d(sub n). But combinations of focused lasers and aerodynamic focusing appear as promising for direct writing with molecular precursors. Theoretical and numerical schemes capable of predicting the evolution of the focusing beam, including Brownian motion effects, have been developed, although further numerical work would be desirable. DOE

N91-19834# University of South Florida, Tampa. Dept. of Chemistry.
FRONTIER ORBITAL SYMMETRY CONTROL OF INTERMOLECULAR ELECTRON TRANSFER
B. Stevens Nov. 1990 6 p
(Contract DE-FG05-88ER-13975)
(DE91-005699; DOE/ER-13975/2) Avail: NTIS HC/MF A02

Research continued on the study of intermolecular electron transfer. The following topics are discussed: fluorescence quenching by electron transfer and the modification of quenching dynamics by solvent properties and net free energy change; transient absorption measurements following selective excitation of 1:1 EDA complex isomers; selective quenching of dual fluorescence from linked EDA systems; electron-transfer sensitized cycloreversion of rubrene endoperoxide; and vibronic modification of adiabatic requirements for intermolecular electron transfer. DOE

N91-19835# Brookhaven National Lab., Upton, NY.
INTENSE FIELD NON-RESONANT MULTIPHOTON ABSORPTION OF DIATOMIC MOLECULES
B. Yang, M. Saeed, T. Breeden, and L. F. DiMauro 1991 5 p Presented at the Conference on Short-Wavelength Coherent Radiation: Generation and Application, Monterey, 4-10 Apr. 1991
(Contract DE-AC02-76CH-00016)
(DE91-006920; BNL-45653; CONF-9104164-1) Avail: NTIS HC/MF A01

The results of nonlinear ionization and dissociation of gas-phase diatomic molecules, H2, D2, O2, and Cl2, in an intense (10(exp 11 to -14) W/sq cm) laser field are reported. Measurements include energy and angularly resolved vibrational photoelectron spectroscopy, as well as mass spectroscopy. DOE

N91-19836# Rochester Univ., NY.
PHOTOINDUCED ELECTRON TRANSFER PROCESSES IN HOMOGENEOUS AND MICROHETEROGENEOUS SOLUTIONS
D. G. Whitten Oct. 1990 11 p
(Contract DE-FG02-86ER-13504)
(DE91-007582; DOE/ER-13504/5) Avail: NTIS HC/MF A03

Chemical electron transfer-induced fragmentation of a variety of electron donors was shown to be a quite general process. In previous studies, attention was focused on alpha-Beta aminoalcohols and 1,2-ditertiary amines. In the present year, studies were extended to include pinacols, an richer variety of diamines and amino-ketones. The mechanisms, intermediates involved in these fragmentation reactions, and medium effects were also studied. Studies of pinacols and a variety of diamines show that photooxidative cleavage of 1,2-diheteroatom-containing molecules is a very general process which can occur for several different types of molecules. In order to demonstrate clearly that cation radicals of the heteroatom containing donor can be intermediates in these reactions, the reaction was studied of several different donors with the acceptors, dicyanoanthracene (DCA) and tetracyanoanthracene (TCA) using biphenyl (BP) as a cosensitizer. The second major focus of the work was to look at donors which, undergo reversible redox reactions to give relatively high energy products which are capable of undergoing clean thermal reverse redox reactions but which survive long enough to be potentially useful for other purposes. The reaction explored extensively is the oxidation of tertiary amines to enamines by quinone type molecules such as beta-lapachone. These studies are continued and other reactions are examined which may be more promising in terms of finding a photochemical-thermal redox cycle which can be carried out with little loss of material through competing side reactions. DOE

N91-19837# Iowa State Univ. of Science and Technology, Ames.
LOCALIZATION AND ELECTRON-PHONON INTERACTION IN DISORDERED SYSTEMS Ph.D. Thesis
Yi Wan Jan. 1991 76 p
(Contract W-7405-eng-82)
(DE91-007654; IS-T-1459) Avail: NTIS HC/MF A05

The problem of localization of electrons in the presence of electron-phonon interaction in disordered 1-D system is studied. In the mean-field approximation, the electron-phonon interaction results in a distorted lattice, the Peierls instability. At the same time, a gap opens at the Fermi level in the electron band. It is known that the scattering of electrons by the disorder will destroy the lattice distortion and close the gap. However, there is disagreement on the way this happens and on the nature of the resulting electronic states. Recent progress in the experimental and theoretical studies of the 1-D organic polymer systems has given a great interest in this problem, and has also provided a suitable model for comparison with the theoretical studies. Numerical results are presented for the electron density of states, the effective size of the electronic state and the frequency dependent conductivity, and emphasize the mutual effects of the electron localization and the Peierls distortion. The development based on analytical perturbation theory is reported and some of the available results are compared with those from the numerical studies and experiments. DOE

N91-19838# Argonne National Lab., IL.
VARIATIONAL MONTE CARLO STUDIES OF ELECTROMAGNETIC STRUCTURE OF FEW-BODY NUCLEI
R. Schiavilla 1990 9 p Presented at the Monte Carlo Methods in Theoretical Physics, Elba, Italy, Jul. 1990
(Contract W-31-109-eng-38)
(DE91-007756; CONF-9007198-2) Avail: NTIS HC/MF A02

The electromagnetic structure and dynamic response of A = 2, 3 and 4 nuclei are studied with the Variational Monte Carlo method by using wave functions based on realistic nuclear interactions. Recent results obtained for the elastic form factors of H-2, H-3, He-3 and He-4, the radiative neutron capture on

He-3 at thermal energies, and the reaction He-4(e,e'p) H-3 are reported. DOE

N91-19839# Colorado Univ., Boulder.
NEAR RESONANT ABSORPTION BY ATOMS IN INTENSE FLUCTUATING FIELDS
S. J. Smith 1990 22 p
(Contract DE-FG02-85ER-13421)
(DE91-007911; DOE/ER-13421/9) Avail: NTIS HC/MF A03

We have completed a comprehensive study of the effects of phase/frequency fluctuations in the incident laser field on the fluorescence intensity from the 3S(sub 1/2) (F = 2, M(sub F) = 2) to 3P(sub 3/2) (F = 3, M(sub F) = 3) transition to atomic sodium. The experiments were carried out in an atomic beam apparatus with a laser driving field on which well-characterized synthesized phase-fluctuations were imposed. The mean fluorescence intensity and the fluctuations in the intensity were measured as a function of detuning of the driving field from the resonance frequency of the transition, and for several different laser powers and bandwidths of laser noise. Power spectra of the intensity fluctuations were measured for a wide range of parameters and the effects of correlated amplitude and phase fluctuations were probed. Detailed comparisons between theoretical predictions and experimental measurements were carried out, and a theoretical model was developed to include the effects of residual Doppler broadening and the nonuniform spatial intensity profile of the driving laser. Experimental investigations of effects of laser phase-noise on degenerate four- wave-mixing have been started. DOE

N91-19840# Nebraska Univ., Lincoln. Dept. of Physics and Astronomy.
DYNAMICS OF COLLISION PROCESSES
A. F. Starace Jan. 1991 8 p
(Contract DE-FG02-88ER-13955)
(DE91-007933; DOE/ER-13955/11) Avail: NTIS HC/MF A02

This project is concerned with collision processes that are governed by the dynamics of three interacting charged particles. Results in three broad areas have been obtained over the current project period. First, detailed theoretical analyses have been presented of the projectile energy dependence as well as the target dependence of the electron detachment collision processes, H(-) + T yields H(n = 1,2) + T* + e(-), for targets T = He, Ne, Ar, Kr, and Xe, and for incident H(-) projectile energies of 0.1, 0.5, 1.0, and 1.5 MeV. Inclusion of H(n = 2) final states in the calculations has been shown definitively to give marked improvement in the agreement of theory with experimental data. Second, a large number of processes involving laser-induced detachment of H(-) were studied, i.e., N(gamma) + H(-) yields H(n = 1,2) + e(-), where N = 1,2,3. The use of adiabatic hypersherical wave functions provides in many cases the most detailed treatment of electron correlation effects to date. Particularly noteworthy, for 2-photon detachment of H(-) with excitation of H(n = 2), is our identification of a half-cycle of long-range dipole-field-induced oscillation of the cross section above threshold. Such oscillations have never been observed experimentally. Third, an asymptotic expansion in Sturmian functions of the wave functions for three-body break-up processes was carried out. These expansions lead to polarized orbitals for two-electron systems and to improved dissociation channels for molecular ions. DOE

N91-19841# Boston Univ., MA. Dept. of Physics.
ATOMIC BEAM STUDIES OF THE INTERACTION OF HYDROGEN WITH TRANSITION METAL SURFACES
1990 8 p
(Contract DE-FG02-85ER-45222)
(DE91-007938; DOE/ER-45222/5) Avail: NTIS HC/MF A02

This report presents the investigations of the H/Pd(111) system. Results, equipment and publications are briefly discussed and listed. DOE

N91-19842# Argonne National Lab., IL.
VARIATIONAL MONTE CARLO CALCULATIONS OF NUCLEAR GROUND STATES
R. B. Wiringa 1990 16 p Presented at the Workshop on Monte Carlo Methods in Theoretical Physics, Isola D'Elba, Italy, 27 Jun. - 6 Jul. 1990
(Contract W-31-109-eng-38)
(DE91-007760; CONF-9006314-1) Avail: NTIS HC/MF A03

A major goal in nuclear physics is to understand how nuclear structure comes about from the underlying interactions between nucleons. This requires modelling nuclei as collections of strongly interacting nucleons. Realistic nucleon-nucleon potentials begins and is supplemented with consistent three-nucleon potentials and two-body electroweak current operators, and prediction is made on nuclear ground properties, such as the binding energy, density and momentum distributions, and electromagnetic form factors. Other properties were also predicted of nuclei such as excited states and low energy reactions. DOE

N91-19843# Notre Dame Univ., IN. Radiation Lab.
[RESEARCH CONDUCTED AT THE RADIATION LAB, NOTRE DAME UNIV.] Quarterly Report, 1 Oct. - 31 Dec. 1990
23 Jan. 1991 40 p
(Contract DE-AC02-76ER-00038)
(DE91-007969; DOE/ER-00038/3345; NDRL-3345) Avail: NTIS HC/MF A03

This report, on research preformed at the Radiation Laboratory, University of Notre Dame, contain contributions on such topics as: formation of carbenium ions or yields from carbenes, photochemical oxidations and reductions, photoreactivity of molybdates, radiolysis of water, spin trapping kinetics, pulse radiolysis, photogenerated radical anions, photochemistry of Fe and Re complexes, hyperfine coupling calculations, electron energy loss in hydrocarbons, radiolysis of halophenols, conductivity in lipid monolayers, solitonsin polyacetylene, triplet-triplet annhilation, random walk problems, proton and electron impact on water luminescence quenching, raman spectrum of ozonide ion, time-resolved spectra of supercritical fluids, sequential biphotonic photochemistry, reduction of CO2 with Cu(I) macrocycles,and studies on photosensitizing dyes and on air-water interface problems. DOE

N91-19844# Pennsylvania State Univ., University Park.
ELECTRON TRANSFER, IONIZATION, AND EXCITATION IN ATOMIC COLLISIONS
1991 6 p
(Contract DE-FG02-86ER-13549)
(DE91-008044; DOE/ER-13549/5) Avail: NTIS HC/MF A02

The research being carried out at Penn State by Winter and Alston addresses the fundamental atomic-collision processes of electron transfer, ionization, and excitation. Winter has focussed attention on intermediate and, more recently, higher collision energies -- proton energies of at least about 50 keV -- for which coupled-state approaches are appropriate. Alston has concentrated on perturbative approaches to symmetric ion-ion/atom collisions at high energies and to asymmetric collisions at intermediate to high energies. DOE

N91-19845# Princeton Univ., NJ. Dept. of Physics.
THE PHYSICS OF LASER POLARIZED MUONIC ATOMS
G. D. Cates 1991 31 p
(Contract DE-FG02-90ER-40557)
(DE91-008045; DOE/ER-40557/1) Avail: NTIS HC/MF A03

This past research period we carried out a successful experiment at LAMPF in collaboration with Syracuse University in which we used lasers to produce polarized muonic He-3. Samples of nuclear polarized He-3 were produced by spin-exchange with optically pumped rubidium vapor. Unpolarized muons were stopped in the gas, and became polarized due to their hyperfine interaction with the He-3 nucleus. We determined that a muon polarization of approximately 8 percent results with a He-3 target polarization of 100 percent. The high statistical accuracy of our result gives us a firm handle on a theoretical question of great importance to future work involving muons and polarized He-3. Currently, we are working toward a new experiment at LAMPF, for which we have just submitted a proposal requesting running time this coming summer.

The experiment utilizes a new technique for producing polarized muonic He-3, a technique we believe has the potential for producing practical polarizations that in principle could be as high as 75 percent, and in practice may exceed 25 to 50 percent. We call this new technique direct spin-exchange (DSE) because it is based on spin-exchange collisions between neutral muonic helium and an optically pumped vapor of Rb. It is direct because, in contrast to the technique we used last summer, the He-3 nucleus is not involved in the spin-exchange process. We have proposed the use of DSE to study the induced pseudoscalar form factor of He-3. Finally, we describe an experiment to measure the spin dependent structure function of the neutron at SLAC. Princeton played an important role in the design and proposal of this experiment, including hosting a meeting to explore the technical feasibility of the polarized He-3 target. DOE

N91-19846# Louisiana State Univ., Baton Rouge. Dept. of Physics and Astronomy.

THE STRUCTURE OF NUCLEI FAR FROM BETA STABILITY

E. F. Zganjar 1991 14 p

(Contract DE-FG05-84ER-40159)

(DE91-008140; DOE/ER-40159/174) Avail: NTIS HC/MF A03

This report discusses the structural of nuclei for from beta stability of the following isotopes: thallium isotopes; mercury isotopes; gold isotopes; platinum isotopes; iridium isotopes; the neutron deficient rare-earth, Z = 57-72 region, and the neutron deficient Z = 50-56 region; also discussed are in-beam spectroscopy in the A = 70 region and shape coexistence, intruder states, and EO transitions. DOE

N91-19847# Louisiana State Univ., Baton Rouge. Dept. of Physics and Astronomy.

ELECTRIC MONOPOLE TRANSITIONS AND SHAPE COEXISTENCE IN NUCLEI

E. F. Zganjar and J. L. Wood (Georgia Inst. of Tech., Atlanta.) 1990 10 p Presented at the Nuclear Structure in the '90's, Oak Ridge, TN, 23-27 Apr. 1990 Prepared in cooperation with Georgia Inst. of Tech., Atlanta, GA

(Contracts DE-FG05-84ER-40159; DE-FG05-87ER-40330; DE-AC05-76OR-00033; DE-AC05-84OR-21400)

(DE91-008141; DOE/ER-40159/166; CONF-900450-13) Avail: NTIS HC/MF A02

The region bounded by 78 (le) Z (le) 82, 104 (le) N (le) 114 has attracted considerable attention following the observation by Bonn, et al., that there is a sudden large increase in the charge volume of the Hg isotopes between 187 and 185. The situation was shortly thereafter clarified with the observation of coexisting bands in several even-even Hg isotopes via in-beam reaction, and radioactive decay studies. The latter work also observed electric monopole transitions in these even-even nuclei and precipitated the evolution of the region into a unique example of widely-occurring, nearly-degenerate shape coexistence. More recently, a large number of electric monopole (E0) transitions have been observed in odd-mass nuclei in this region. Such transitions are of limited interest when associated with 0(sup +) (yields) 0(sup +) transitions since in those cases only the monopole component (E0) is possible. Of greater interest are J(sup (pi) yields J(sup (pi) J (ne) 0 transitions which exhibit significant E0 strength. Until recently, few transitions of this type had been observed and E0 was not expected to compete significantly with M1 and E2. A major change in this picture has occurred as a result of investigations at UNISOR of shape coexistence in the Pt, Au, Hg, and Pb isotopes; and evidence correlating the observance of nuclear shape coexistence with the observation of electric monopole transitions continues to accumulate. Some new results are presented here and their implications to studies of superdeformation are discussed. DOE

N91-19848# Brookhaven National Lab., Upton, NY.

SUMMARY OF DISCUSSIONS AT THE HIGH p (SUB T) SESSION

M. J. Tannenbaum Dec. 1990 14 p Presented at the International Workshop on Quark Gluon Plasma Signatures, Strasbourg, France, 1-4 Oct. 1990

(Contract DE-AC02-76CH-00016)

(DE91-008196; BNL-45696; CONF-9010320-1) Avail: NTIS HC/MF A03

A summary of the discussion at the HIGH p(sub T) session is presented. There was a clear consensus at this session that Jets and Jet Phenomena in Relativistic Heavy Ion collisions would best be studied using leading particles, in the same way that these phenomena were originally mapped out in p-p collisions. The new topic of jet quenching in nuclei was extensively discussed. It was clear that this proposed phenomenon could also be studied by measuring fragmentation functions in deeply inelastic lepton-nucleus scattering; but there was controversy over whether the effect should be seen in proton-nucleus reactions. Other hard-scattering phenomena, including mini-jets, single particle inclusive production, the Cronin effect, and direct photon production, are mentioned. DOE

N91-19849# Brookhaven National Lab., Upton, NY.

PHOTOEMISSION STUDIES USING FEMTOSECOND PULSES FOR HIGH BRIGHTNESS ELECTRON BEAMS

T. Srinivasan-Rao, T. Tsang, and J. Fischer Jun. 1990 19 p Presented at the Workshop on Short Pulse High Current Cathodes, Bendor, France, 18-22 Jun. 1990

(Contract DE-AC02-76CH-00016)

(DE91-008436; BNL-45469; CONF-9006242-3) Avail: NTIS HC/MF A03

We present the results of a series of experiments where various metal photocathodes are irradiated with ultrashort laser pulses, whose characteristics are: (lambda) = 625 nm, (tau) = 100 fs, PRR = 89.5 MHz, H(nu) = 2 eV and average power 25 mW in each of the two beams. The quantum efficiency of the metals range from approximately 10(exp -12) to 10(exp -8) at a power density of 100 MW/sq cm at normal incidence. Since all the electrons are emitted due to multiphoton processes, these efficiencies are expected to increase substantially at large intensities. The efficiency at 100 MW/sq cm was increased by using p-polarized light at oblique incidence by approximately 20 x and by mediating the electron emission through surface plasmon excitation by approximately 10(exp 3) x. For the low intensities used in these experiments, the electron pulse duration is almost the same as the laser pulse duration for both the bulk and the surface plasmon mediated photoemission. DOE

N91-19850# Brookhaven National Lab., Upton, NY.

DEVELOPMENT OF HIGH CURRENT ELECTRON SOURCE USING PHOTOEMISSION FROM METALS WITH ULTRASHORT LASER PULSES

T. Tsang, T. Srinivasan-Rao, and J. Fischer Oct. 1990 25 p Presented at the Prospects for A 1 Angstrom Free-Electron Laser (FEL) Workshop, Sag Harbor, ME, 22-27 Apr. 1990

(Contract DE-AC02-76CH-00016)

(DE91-008438; BNL-45481; CONF-9004232-5) Avail: NTIS HC/MF A03

The studies of photoemission from metal photocathodes using picosecond pulses in the UV (4.66 eV) wavelength and femtosecond laser pulses in the visible (2 eV) wavelengths are summarized. To achieve high current density yield from metal photocathodes, multiphoton photoemission using femtosecond laser pulses are suggested. Electron yield improvement incorporating surface photoemission and surface plasmon resonance in metals and metal films are demonstrated. The possibility of the nonlinear photoemission process overtaking the linear process was examined, and some possible complexity identified. To extract the large amount of electrons free of space charge, a pulsed high voltage is designed; the results of the preliminary test are presented. Finally, for the first time, the width of the electron temporal profiles are measured, utilizing the nonlinear photoelectric effect, to below 100 fsec time regime. The results indicated that the electron pulse duration follows the laser pulses and are not limited by the material. DOE

N91-19851# Brookhaven National Lab., Upton, NY.
W(SUB L)W(SUB L) SCATTERING AT THE SSC
J. Bagger (Johns Hopkins Univ., Baltimore, MD.), S. Dawson, and G. Valencia 1990 6 p Presented at the 1990 DPF Summer Study on High Energy Physics, Snowmass, 25 Jun. - 13 Jul. 1990 (Contract DE-AC02-76CH-00016)
(DE91-008442; BNL-45782; CONF-9006267-23) Avail: NTIS HC/MF A02

Higher-order chiral Lagrangians were used to study W(sub L)W(sub L) scattering at the SSC. We analyze a model that is consistent with crossing, unitarity and chiral symmetry, with no resonant behavior at SSC energies. The only signal is a slightly enhanced rate for W(sub L)W(sub L) scattering. The results indicate the level of sensitivity that must be reached before the SSC can be assured of discovering the mechanism for electroweak symmetry breaking. DOE

N91-19852# National Inst. for Fusion Science, Nagoya (Japan).
CROSS SECTION FOR PRODUCTION OF EXCITED HYDROGEN ATOMS FOLLOWING DISSOCIATIVE EXCITATION OF MOLECULAR HYDROGEN BY ELECTRON IMPACT
Takashi Fujimoto, Keiji Sawada, and Kiyoto Takahata Mar. 1990 21 p
(DE91-745035; NIFS-DATA-4) Avail: NTIS HC/MF A03

For the purpose of investigating molecular hydrogen present in plasmas, the production cross section of excited hydrogen atoms due to dissociative excitation of molecular hydrogen by electron collisions was estimated from the emission cross sections of Lyman and Balmer lines. DOE

N91-19853# Rome Univ. (Italy). Dipt. di Fisica.
ELECTROWEAK INTERACTIONS AT LEP
Bruno Borgia (Istituto Nazionale di Fisica Nucleare, Rome, Italy) 22 Nov. 1990 38 p Presented at SLAC Summer Institute, Topical Conference, Stanford, CA, 16-27 Jul. 1990
(Nota-Interna-962; ETN-91-98883) Avail: NTIS HC/MF A03

Four experiments (Aleph, Delphi, L3, and Opal) on electroweak interactions at the LEP (European Large Electron-Positron storage rings) after the analysis of about half of the data collected in 1989 and 1990, are reported. Electroweak aspects of the process where the fermions can be either quarks or leptons are reviewed. The analysis of experimental data is based on the determination of the cross section integrated on the solid angle and the asymmetry of forward-backward leptons in the final state. Attention is given to the center mass energy being fundamental as the determination of the luminosity by which the event rate is normalized to compute the absolute cross section. The Z(0) parameters after combination of the data from all experiments are given. LEP measurements and other electroweak results are consistent with a high top mass of about 150 GeV. ESA

N91-19854# Rome Univ. (Italy). Dipt. di Fisica.
PUNCHTHROUGH IN HADRONIC SHOWERS: A PARAMETERIZATION OF THE TOTAL PROBABILITY
F. Lacava (Istituto Nazionale di Fisica Nucleare, Rome, Italy) 18 Dec. 1990 19 p
(Nota-Interna-968; ETN-91-98888) Avail: NTIS HC/MF A03

The estimation of how hadronic showers are observed in the calorimeters and in the absorbers added in front of muon detectors is useful for hard electron identification in prompt lepton production. The maximum penetration depth of any particle in hadronic showers is called punchthrough and punchthrough probability, at a given depth, is the probability to observe there a signal produced by any particle of the shower. A short discussion of punchthrough in hadronic shower is followed by a compilation of published data on total punchthrough probability. A parameterization, of this probability in terms of two components (hadronic and muonic) is presented. ESA

N91-19855# Technische Univ., Delft (Netherlands).
EXCHANGE CURRENTS IN LOW-ENERGY NUCLEON CAPTURE BY He3 Ph.D. Thesis
Rob Wervelman 1991 88 p Sponsored by Netherlands Organization for Scientific Research
(ETN-91-98917) Avail: NTIS HC/MF A05

Reasons for the need for information on radiative neutron capture (RNC) by few-nucleon systems are described. Absolute cross section measurements on the RNC reactions He-3(n, gamma)He-4 and He-3(n, gamma gamma)He-4 are studied, and are complemented with shell model calculations on the radiative thermal neutron capture reaction by He-3 and on the weak He-3(p,e+nu sub e)He-4 reaction. The latter reaction is of interest as a source of high energy neutrinos emitted by the Sun which may be detectable in the new generation of solar neutrino detectors. Main conclusions from experiments performed at two neutron energies, with subthermal neutrons where s-wave capture is dominant, and with a quasimonochromatic 24.5 keV neutron beam (p-wave capture), are summarized. Conclusions on a theoretical study, where a standard model of nuclear weak and electromagnetic interaction currents, consisting of one body impulse approximation and a two body meson exchange current part, was applied to the process of nucleon capture by He-3, are presented. ESA

N91-19856# Technische Univ., Berlin (Germany, F.R.). Fachbereich Physik.
SEMICONDUCTOR PHOTODIODES AS RADIOMETRIC RECEIVERS IN THE FIELD OF SOFT RADIATION Ph.D. Thesis [HALBLEITER-PHOTODIODEN ALS RADIOMETRISCHE EMPFAENGERNORMALE IM BEREICH WEICHER ROENTGENSTRAHLUNG]
Michael Krumrey 1990 101 p In GERMAN
(ETN-91-98925) Avail: NTIS HC/MF A06

Two independent calibrating processes were developed in order to determine the spectral sensitivity of semiconductor photodiodes as radiometric receivers. A fundamental process allows the calibrating of any detector in photon energy field over 600 eV. The detailed thicknesses of layers and diffusion lengths of the materials concerned could be determined from the measurement of the angle dependence of the photon stream. The detailed mean energy for producing a pair of vacant electron sites was determined by photon stream measurements in computable white synchroton radiation. The semiconductor photodiodes were also examined for surface homogeneity, scattering and temperature stability. It was shown that, for the first time in the field of photon energy above 250 eV, easily operational radiometric receivers were available. ESA

73 NUCLEAR AND HIGH-ENERGY PHYSICS

Includes elementary and nuclear particles; and reactor theory.

For space radiation see *93 Space Radiation.*

N91-19857# Lawrence Livermore National Lab., CA.
POTENTIAL HEALTH RISKS FROM POSTULATED ACCIDENTS INVOLVING THE Pu-238 RTG (RADIOISOTOPE THERMOELECTRIC GENERATOR) ON THE ULYSSES SOLAR EXPLORATION MISSION
M. Goldman, R. C. Nelson, L. Bollinger, and M. D. Hoover (Lovelace Biomedical and Environmental Research Inst., Albuquerque, NM.) 2 Nov. 1990 16 p Presented at the 8th Symposium on Space Nuclear Power Systems, Albuquerque, 6-10 Jan. 1991
(Contract W-7405-eng-48)
(DE91-007142; UCRL-JC-105779; CONF-910116-19) Avail: NTIS HC/MF A03

Potential radiation impacts from launch of the Ulysses solar exploration experiment were evaluated using eight postulated accident scenarios. Lifetime individual dose estimates rarely exceeded 1 mrem. Most of the potential health effects would come from inhalation exposures immediately after an accident, rather than from ingestion of contaminated food or water, or from inhalation of resuspended plutonium from contaminated ground.

For local Florida accidents (that is, during the first minute after launch), an average source term accident was estimated to cause a total added cancer risk of up to 0.2 deaths. For accidents at later times after launch, a worldwide cancer risk of up to three cases was calculated (with a four in a million probability). Upper bound estimates were calculated to be about 10 times higher. DOE

N91-19858# Los Alamos National Lab., NM.
PREDICTED BREMSSTRAHLUNG GENERATION BY ENERGETIC ELECTRON BEAMS
R. J. Faehl, C. M. Snell, and R. K. Keinigs Jan. 1991 57 p
(Contract W-7405-eng-36)
(DE91-007164; LA-11742-MS) Avail: NTIS HC/MF A04

The CYLTRAN photon/electron Monte Carlo code has been employed to predict Bremsstrahlung generation by monoenergetic electron beams from 10 to 1000 MeV. The forward-directed Bremsstrahlung intensity is investigated as a function of beam energy converter thickness, and material. At high energies, the forward extraction efficiency is maximized by using converters that are about 0.1-electron ranges thick. The largest intensities are attained with low-Z converter materials such as beryllium. Because the Bremsstrahlung radiation is strongly forward-directed, low divergence of the incident electron beam is crucial. Under ideal conditions, a 1000-MeV beam can produce intensities up to 10(exp 8) MeV per steradian, per incident electron. DOE

N91-19859# California Univ., Berkeley. Dept. of Astronomy.
HIGH ENERGY PHYSICS AND COSMOLOGY
J. I. Silk 1991 37 p
(Contract DE-FG03-84ER-40161)
(DE91-007369; DOE/ER-40161/T5) Avail: NTIS HC/MF A03

This research will focus on the implications of recent theories and experiments in high energy physics of the evolution of the early universe, and on the constraints that cosmological considerations can place on such theories. Several problems are under investigation, including studies of the nature of dark matter and the signature of annihilations in the galactic halo, where the resulting (gamma)-ray fluxes are potentially observable, and in stars, where stellar evolution may be affected. We will develop constraints on the inflationary predictions of scale-free primordial fluctuations in a universe at critical closure density by studying their linear and non-linear evolution after they re-enter the particle horizon, examining the observable imprint of primordial density fluctuations on the cosmic microwave background radiation in both flat and curved cosmological models, and implications for observations of large-scale galaxy clustering and structure formation theories. We will also study spectral distortions in the microwave background radiation that are produced by exotic particle decays in the very early universe. We expect such astrophysical considerations to provide fruitful insights both into high-energy particle physics and into possible cosmological for the early universe. DOE

N91-19860# Los Alamos National Lab., NM.
ELECTROMAGNETIC ION/ION CYCLOTRON INSTABILITY
D. Winske, M. E. McKean, N. Omidi, and V. Chou (California Univ., San Diego.) 1991 5 p Presented at the 4th International School for Space Simulation, Nara, Japan, 1-5 Apr. 1991
(Contract W-7405-eng-36)
(DE91-004841; LA-UR-90-3859; CONF-9104109-1) Avail: NTIS HC/MF A01

Linear analysis and hybrid simulations are used to investigate the properties of a new electromagnetic ion beam instability. Some applications of the instability in space are also discussed. DOE

N91-19861# California Univ., Berkeley. Lawrence Berkeley Lab.
THE ADVANCED LIGHT SOURCE: A NEW TOOL FOR RESEARCH IN ATOMIC PHYSICS
A. S. Schlachter Sep. 1990 5 p Presented at the 5th International Conference on the Physics of Highly Charged Ions, Giessen, Fed. Republic of Germany, 10-14 Sep. 1990
(Contract DE-AC03-76SF-00098)
(DE91-007739; LBL-29644; CONF-900923-9) Avail: NTIS HC/MF A01

The Advanced Light Source, a third-generation national synchrotron-radiation facility now under construction at the Lawrence Berkeley Laboratory in Berkeley, California, is scheduled to begin serving qualified users across a broad spectrum of research areas in the spring of 1993. Undulators will generate high-brightness, partially coherent, plane polarized, soft-x-ray and ultraviolet (XUV) radiation from below 10 eV to above 2 keV. Wigglers and bend magnets will generate high fluxes of x-rays to photon energies above 10 keV. The ALS will have an extensive research program in which XUV radiation is used to study matter in all its varied gaseous, liquid, and solid forms. DOE

N91-19862# Lawrence Livermore National Lab., CA.
RELATIVISTIC KLYSTRON RESEARCH FOR FUTURE LINEAR COLLIDERS
G. A. Westenskow, T. L. Houck, and R. D. Ryne Jan. 1991 8 p Presented at the OE/LASE 1991: 4th Society of Photo-Optical Instrumentation Engineers (SPIE) International Symposium, Los Angeles, 20-25 Jan. 1991
(Contract W-7405-eng-48)
(DE91-008063; UCRL-JC-106216; CONF-910123-12) Avail: NTIS HC/MF A02

We are continuing our work to develop high-power 11.4-GHz relativistic klystrons suitable for driving future linear colliders. Peak RF power levels of 330 MW have been achieved using an 11.4 GHz, high-gain tube with multiple output structures. In these experiments the RF pulse is of the same duration as the beam current pulse. Experiments have been preformed on two short sections of high-gradient accelerator using the RF power from a relativistic klystron. An average accelerating gradient of 84 MV/m has been achieved with 80-MW of RF power. The use of the front end of the Advanced Test Accelerator at Lawrence Livermore National Laboratory will allow future test of new RF sources and tests of two-beam accelerator concepts. We are ready to test a 3-MV RF generator which uses transverse modulation. DOE

N91-19863# Superconducting Super Collider Lab., Dallas, TX.
STUDIES OF COLD PROTECTION DIODES
R. Carcagno and J. Zeigler Mar. 1990 15 p Presented at the 2nd International Industrialization Symposium on the Super Collider (IISSC), Miami, FL, 14-16 Mar. 1990
(Contract DE-AC02-89ER-40486)
(DE91-008203; SSCL-270; CONF-900348-21) Avail: NTIS HC/MF A03

The feasibility of a passive quench protection system for the superconducting supercollider (SSC) main ring magnets depends on the radiation resistance and reliability of the diodes used as current bypass elements. These diodes would be located inside the magnet cryostat, subjecting them to liquid helium temperature and a relatively high radiation flux. Experimental and theoretical efforts have identified a commercially available diode which appears to be capable of surviving the cryogenic temperature and radiation environment of the accelerator. High current 4 measurements indicate that the usable lifetime of this diode, based on an estimate of the peak junction temperature during a quench pulse, is an order of magnitude greater then than the expected lifetime of the SSC itself. However, an unexpected relationship was discovered between the diode turn-on voltage at 5 K and the most recent reverse voltage or temperature excursion. This turn-on voltage as a function of radiation exposure appears to be erratic and indicates a need for further investigation. DOE

N91-19864# Sheffield Univ. (England). Dept. of Control Engineering.
EXPERT SYSTEMS FOR FAULT DIAGNOSIS IN NUCLEAR REACTOR CONTROL
N. A. Jalel and H. Nicholson Nov. 1990 34 p
(RR-412; ETN-91-98846) Avail: NTIS HC/MF A03

An expert system for accident analysis and fault diagnosis for the Loss Of Fluid Test (LOFT) reactor, a small scale pressurized

water reactor, was developed for a personal computer. The knowledge of the system is presented using a production rule approach with a backward chaining inference engine. The data base of the system includes simulated dependent state variables of the LOFT reactor model. Another system is designed to assist the operator in choosing the appropriate cooling mode and to diagnose the fault in the selected cooling system. The response tree, which is used to provide the link between a list of very specific accident sequences and a set of generic emergency procedures which help the operator in monitoring system status, and to differentiate between different accident sequences and select the correct procedures, is used to build the system knowledge base. Both systems are written in TURBO PROLOG language and can be run on an IBM PC compatible with 640k RAM, 40 Mbyte hard disk and color graphics. ESA

N91-19865# Sheffield Univ. (England). Dept. of Control Engineering.
PETRI NETS AND FAULT DIAGNOSIS IN NUCLEAR REACTORS
N. A. Jalel and H. Nicholson Nov. 1990 19 p
(RR-413; ETN-91-98847) Avail: NTIS HC/MF A03

The possibility of applying Petri nets (Pns) as a modeling tool to represent any fault or accident that might occur in the Loss Of Fluid Test (LOFT), small scale pressurized water reactor, is discussed and analyzed. Pns are developed to assist the nuclear reactor operator in identifying any fault or alarm that might arise in the power station. ESA

N91-19866# Sheffield Univ. (England). Dept. of Control Engineering.
THE USE OF AN OBJECT ORIENTED TECHNIQUE FOR FAULT DIAGNOSIS IN NUCLEAR REACTORS
N. A. Jalel and H. Nicholson Nov. 1990 17 p
(RR-414; ETN-91-98848) Avail: NTIS HC/MF A03

In recent years there has been an increased growth of interest in object oriented programming which is a new approach to software construction having wide application. The possibility of using object oriented programming to build a software package that will assist the nuclear reactor operator in diagnosing any fault or alarms in the Loss Of Fluid Test (LOFT) reactor scale pressurized water reactor, is investigated. ESA

N91-19867# Sheffield Univ. (England). Dept. of Control Engineering.
FAULT DETECTION USING OPTIMAL CONTROL TECHNIQUES
N. A. Jalel and H. Nicholson Nov. 1990 25 p
(RR-419; ETN-91-98851) Avail: NTIS HC/MF A03

The possibility of using optimal control techniques for fault diagnosis is investigated. Two techniques are used. The performance index is used to identify the abnormal behavior in any subsystem of the Loss Of Fluid Test (LOFT) reactor, a small scale pressurized water reactor, and the faulty controller of the LOFT reactor is identified using the Pontryagin maximum principle. ESA

N91-19868# Rome Univ. (Italy). Dipt. di Fisica.
A GLOBAL FIT TO THE Z(0) LINE SHAPE
M. Diemoz and E. Longo (Istituto Nazionale di Fisica Nucleare, Rome, Italy) 14 Dec. 1990 17 p Presented at Perugia Workshop on Phenomenology, Italy, 24-26 Oct. 1990
(Nota-Interna-966; ETN-91-98886) Avail: NTIS HC/MF A03

A global fit to the available LEP (European Large Electron-Positron storage rings) data to determine the parameters of the Z(0) (neutral bosons) resonance is presented. The main sources of systematics uncertainty, coming from the knowledge of the LEP and the four experiments are discussed and their effects are included in the fit. ESA

74 OPTICS

Includes light phenomena; and optical devices.
For lasers see *36 Lasers and Masers.*

N91-19869# Department of the Navy, Washington, DC.
A MODULATED HIGH-POWER OPTICAL SOURCE SPECIFICATION Patent Application
Joseph F. Weller, inventor (to Navy), William K. Burne, inventor (to Navy), and Lew Goldberg, inventor (to Navy) 31 May 1990 23 p
(AD-D014654; US-Patent-Appl-SN-531416) Avail: NTIS HC/MF A03 CSCL 09/5

An apparatus for generating a relatively high-power, modulated optical beam is disclosed. The apparatus comprises a first element for emitting a relatively low-power laser beam at a preselected wavelength, means for focusing the laser beam into a focused beam, a damage-resistant integrated optic modulator responsive to the focused beam for developing a modulated beam, optical means for shaping the modulated beam into a shaped modulated beam, and semiconductor means having a large active area responsive to the shaped, modulated beam for producing a relatively high-power, output modulated beam. In a first embodiment, the semiconductor means is a semiconductor amplifier which amplifies the modulated beam to produce the high-power, modulated output beam. In a second embodiment, the semiconductor means is a semiconductor amplifier with a highly-reflective, coated rear facet for reflecting the amplified focused beam back through the amplifier to produce a twice-amplified, high-power, output modulated beam which is reflected out of the apparatus by a polarizing beam-splitter in the optical means. GRA

N91-19870 Department of the Navy, Washington, DC.
OPTICAL FIBER BACKSCATTER SIGNATURE GENERATOR (OFBSG) Patent
Neil Kamikawa, inventor (to Navy), Arthur Nakagawa, inventor (to Navy), Grant Tanaka, inventor (to Navy), and Ken Yamada, inventor (to Navy) 28 Aug. 1990 18 p Filed 3 May 1989
(AD-D014668; US-Patent-4,952,057; US-Patent-Appl-SN-350172; US-Patent-Class-356-73.1) Avail: US Patent and Trademark Office CSCL 20/6

The optical fiber backscatter signal generator (OFBSG) generates simulated optical fiber backscatter waveform signals that are used to characterize or calibrate an optical time domain reflectometer (OTDR). An OTDR is a commercially available test instrument that measures loss and length of a fiber optic cable by launching an optical signal into the cable and measuring the power that is reflected back (backscattered) into the OTDR. The OFBSG device creates a simulated optical fiber backscattered signal of a virtual cable and couples this signal into the OTDR so that length accuracy, loss accuracy, and dynamic range of the OTDR can be determined. An electrooptical section, a signal generator section and a microprocessor section that is programmable to simulate a variety of cable anomalies, provide adaptability to accommodate a wide variety of OTDRs and, by reason of its sound engineering design, it is capable of being used under adverse conditions such as those encountered in this field. GRA

N91-19871*# Arizona Univ., Tucson. Optical Sciences Center.
HUBBLE SPACE TELESCOPE SECONDARY MIRROR VERTEX RADIUS/CONIC CONSTANT TEST Final Technical Report
Robert Parks 15 Mar. 1991 75 p
(Grant NAG8-863)
(NASA-CR-187989; NAS 1.26:187989) Avail: NTIS HC/MF A04 CSCL 20F

The Hubble Space Telescope backup secondary mirror was tested to determine the vertex radius and conic constant. Three completely independent tests (to the same procedure) were performed. Similar measurements in the three tests were highly consistent. The values obtained for the vertex radius and conic constant were the nominal design values within the error bars associated with the tests. Visual examination of the interferometric

data did not show any measurable zonal figure error in the secondary mirror. Author

N91-19872# Sandia National Labs., Albuquerque, NM.
DESIGN CONSIDERATIONS FOR MULTI COMPONENT MOLECULAR-POLYMERIC NONLINEAR OPTICAL MATERIALS
K. D. Singer, M. G. Kuzyk, T. Fang, W. R. Holland (Bell Telephone Labs., Inc., Princeton, NJ.), and P. A. Cahill 1990 15 p Presented at the NATO Advanced Research Workshop on Organic Molecules for Nonlinear and Photonics, La Rochelle, France, Aug. 1990
(Contract DE-AC04-76DP-00789)
(DE91-006778; SAND-91-0139C; CONF-9008185-1) Avail: NTIS HC/MF A03

We review our work on multi component polymeric nonlinear optical materials. These materials consist of nonlinear optical molecules incorporated in a polymeric host. A cross-linked triazine polymer incorporating a dicyanovinyl terminated azo dye was found to be relatively stable at 85 deg and possess an electro-optic coefficient of 11pm/V. We have also observed the zero dispersion condition in a new anomalous dispersion dye for phase matched second harmonic generation, and expect efficient conversion to the blue. A squarylium dye, ISQ, has been found to possess a large third order nonlinearity, and may display two-level behavior. DOE

N91-19873# Brookhaven National Lab., Upton, NY.
THE SPECIFICATION OF GLANCING INCIDENCE MIRRORS IN TERMS OF SYSTEM PERFORMANCE
E. L. Church and P. Z. Takacs Aug. 1990 5 p Presented at the 15th Congress of the International Commission for Optics: Optics in Complex Systems, Garmisch-Partenkirchen, Fed. Republic of Germany, 5-10 Aug. 1990
(Contract DE-AC02-76CH-00016)
(DE91-007556; BNL-45579; CONF-900834-1) Avail: NTIS HC/MF A01

A simple analytic method was developed of predicting the performance of glancing-incidence mirrors from laboratory measurements of their surface profiles and, conversely, of specifying mirror quality in terms of practical performance requirements. It is called five-factor formula. Its derivation and properties are outlined. DOE

N91-19874# Brookhaven National Lab., Upton, NY.
THE SPECIFICATION OF GLANCING INCIDENCE MIRRORS IN TERMS OF SYSTEM PERFORMANCE
E. L. Church and P. Z. Takacs Sep. 1990 3 p Presented at the 1990 American Society of Photo-Optical Engineers (ASPE) Annual Conference, Rochester, 23-28 Sep. 1990
(Contract DE-AC02-76CH-00016)
(DE91-007564; BNL-45579-Rev; CONF-9009241-2-Rev) Avail: NTIS HC/MF A01

Brookhaven National Laboratory is the site of the National Synchrotron Light Source (NSLS), which uses many high performance mirrors for directing and focussing EUV and x ray radiation. The measurement, testing and specification of these mirrors were studied for a number of years, and some of the interesting general issues encountered are described. The issues discussed are metrology, statistical estimation, scattering, testing and specifications. DOE

N91-19875# National Oceanic and Atmospheric Administration, Boulder, CO. Wave Propagation Lab.
APERTURE-AVERAGING FACTOR FOR OPTICAL PROPAGATION THROUGH THE TURBULENT ATMOSPHERE
J. H. Churnside Nov. 1990 55 p
(PB91-129338; NOAA-TM-ERL-WPL-188) Avail: NTIS HC/MF A04 CSCL 20F

Approximate expressions for the aperture-averaging factor of optical scintillation in the turbulent atmosphere were developed. For large apertures and weak path-integrated turbulence with small inner scale, the variance of signal fluctuations is proportional to the -7/3 power of the ratio of the aperture diameter to the Fresnel zone size. If the inner scale is large, the variance is proportional to the -7/3 power of the ration of the aperture diameter to the inner scale. In strong, path-integrated turbulence, two scales develop. That portion of the variance associated with the smaller scale is proportional to the -2 power of the ration of aperture diameter to the phase coherent length. That portion of the variance associated with the large scale is proportional to the -7/3 power of the aperture diameter to the scattering disk. These simple approximations are within a factor of 2 of the measurements. The probability density function is nearly log normal under most conditions. Author

N91-19876# Messerschmitt-Boelkow-Blohm G.m.b.H., Munich (Germany, F.R.).
FIBER OPTIC INTERFEROMETRIC MEASURING METHOD FOR THE DETERMINATION OF A VERY SMALL POLARIZATION COEFFICIENT
R. Mueller and E. Hartl 1990 6 p In GERMAN; ENGLISH summary Presented at OPTO-7, Nuernberg, Fed. Republic of Germany, 16-18 Oct. 1990
(MBB-UA-1185-90-PUB; ETN-91-98818) Avail: NTIS HC/MF A02

An alternative method for high sensitive measurement of residual polarization using an all fiber interferometric set up is presented. The set up, consisting of a three by three coupler and a polarization preserving fiber loop, and using a passive signal recovery scheme, can be adjusted in such a way that the bias is a very sensitive function of the degree of polarization of the input light. This was used to measure the residual polarization during the fabrication of Lyot depolarizers. By means of this set up, depolarizers were built which reduce the degree of polarization by a factor of 400. In the case of a small input polarization, the residual polarization of such a depolarizer was measured to be greater than 0.0003. This is due to polarization arising in the depolarizer, because of polarization dependent loss. ESA

N91-19877# Messerschmitt-Boelkow-Blohm G.m.b.H., Munich (Germany, F.R.).
LIGHT GUIDE FIBERS [ANMERKUNG: ZU DIESEM VORTRAG GIBT ES NUR VIEWGRAPHS UND KEIN TEXTMANUSKRIPT]
G. Trommer and H. Poisel 1990 37 p In GERMAN Presented at the OPTO 7, Nuernberg, Fed. Republic of Germany, 16-18 Oct. 1990
(MBB-UA-1199-90-PUB; ETN-91-98820) Avail: NTIS HC/MF A03

The transmission properties of light waveguides are given in viewgraphs. Functions are defined. Absorption and dispersion problems are illustrated. Formulas are given for refraction of light, numerical aperture, nondimensional frequency, mode number, and electromagnetic wave. Fiber optic sensors are reviewed, and their advantages are outlined. An index of refraction is given for different dopings. ESA

N91-19878# Technische Univ., Berlin (Germany, F.R.). Fachbereich Physik.
NONLINEAR OPTIC EFFECTS IN LIQUID CRYSTALS Ph.D. Thesis [NICHTLINEARE OPTISCHE EFFEKTE IN FLUESSIGKRISTALLEN]
Rainer MacDonald 1990 167 p In GERMAN Sponsored by DFG
(ETN-91-98923) Avail: NTIS HC/MF A08

Self diffracted effects of laser beams on light induced lenses were studied to examine the static and slowly dynamic nonlinearities on some nematic liquid crystals as a result of reorientation effects. A picosesond laser apparatus and the light induced grate method were used to examine transient dynamic arrangements and reorientation effects. The dynamics of the phenomena in the nematic and isotropic phase of liquid crystals was obtained by time solving measurements of the grate construction and disaggregation. Optical excitation of ultrasonic waves and acoustic grates was produced in the experiments laser pulses. ESA

N91-19879# Naval Research Lab., Washington, DC.
FIBER OPTIC FEED Memorandum Report, 1985 - 1990

P. D. Stilwell, M. G. Parent, and L. Goldberg 6 Nov. 1990 47 p
(AD-A229860; NRL-MR-6741) Avail: NTIS HC/MF A03 CSCL 20/6

This report details a Fiber Optic Feeding (FOF) concept for beamforming in phased arrays. Experimental data is presented which validates the basic underlying assumptions. Elaborations on this basic concept are presented which illustrate the power of this new approach to beamforming. All radar and communications functions have a realization in the architecture, including monopulse, multiple beams (on same or different frequencies), beamspace adaptivity (open or closed loop), and wide-band beam and null forming. It presumes an active antenna aperture but uses TR modules containing no phase shifters. Identical TR modules are used at each of the antenna elements and which require a minimum of digitally controlled components. The architecture is appropriate for arrays on any platform and accommodates sparse and/or conformal designs without the necessity of introducing significant microwave modifications. The approach can use existing state-of-the-art components to affordably implement high performance arrays. Of particular importance is the capability of forming time delay beams from an array without the use of phase shifters. GRA

N91-19137*# CBI Na-Con, Oak Brook, IL.
OPTICAL TESTING CRYOGENIC THERMAL VACUUM FACILITY
Patrick W. Dohogne and Warren A. Carpenter *In* NASA, Goddard Space Flight Center, 16th Space Simulation Conference Confirming Spaceworthiness Into the Next Millennium Nov. 1990 p 113-132 Sponsored in part by AF (For primary document see N91-19126 11-18)
Avail: NTIS HC/MF A20 CSCL 20F

N91-19155*# European Space Agency. European Space Research and Technology Center, ESTEC, Noordwijk (Netherlands).
PROPOSAL FOR A CONCEPTUALLY NEW COMPACT COLLECTING OPTICS FOR POWERFUL LIGHT SOURCES
G. Saenger *In* NASA, Goddard Space Flight Center, 16th Space Simulation Conference Confirming Spaceworthiness Into the Next Millennium Nov. 1990 p 357-375 (For primary document see N91-19126 11-18)
Avail: NTIS HC/MF A20 CSCL 20F

N91-20024*# Towson State Univ., MD. Dept. of Physics.
STUDY OF WAVELENGTH DIVISION MULTIPLEXING AS A MEANS OF INCREASING THE NUMBER OF CHANNELS IN MULTIMODE FIBER OPTIC COMMUNICATION LINKS
Harry Bates *In* NASA, John F. Kennedy Space Center, Research Reports: 1990 NASA/ASEE Summer Faculty Fellowship Program Sep. 1990 p 29-64 (For primary document see N91-20022 11-99)
(Grant NGT-60002)
Avail: NTIS HC/MF A23 CSCL 20F

75 PLASMA PHYSICS

Includes magnetohydrodynamics and plasma fusion.

For ionospheric plasmas see *46 Geophysics*. For space plasmas see *90 Astrophysics*.

N91-19880 Max-Planck-Inst. fuer Physik und Astrophysik, Garching (Germany, F.R.). Inst. fuer Extraterrestrische Physik.
AN ANALYTICAL STUDY OF NEUTRAL EXPANSION, IONIZATION, AND CHARGED PARTICLE ACCELERATION IN A NEUTRAL LITHIUM RELEASE FOR THE PARALLEL ELECTRIC FIELD MEASUREMENT
Masato Nakamura and Koichiro Tsuruda (Tokyo Univ., Japan) Apr. 1990 43 p Previously announced in IAA as A90-30552 Submitted for publication
(MPE-Preprint-180; ETN-91-98604) Copyright Avail: Fachinformationszentrum Karlsruhe, 7514 Leopoldshafen-Eggenstein 2, Fed. Republic of Germany

The acceleration of lithium ions produced from a neutral lithium release experiment is analytically described to study a method of measuring the electric field parallel to the magnetic field in the auroral region. The neutral cloud expansion, ionization and subsequent charged particle acceleration is modeled during a high altitude neutral lithium release, ion flux estimates at several observation points being calculated as a feasibility study of the experiment. The lithium energy-time spectrum obtained during the observation window provides information on magnitude and structure of the parallel electric field. ESA

N91-19881# General Atomic Co., San Diego, CA.
PLASMA BOUNDARY EXPERIMENTS ON D3-D TOKAMAK
M. A. Mahdavi, N. Brooks, G. L. Jackson, A. Langhorn, B. Leikind, S. Lippmann, A. Futch, D. N. Hill, and J. Hogan (Oak Ridge National Lab., TN.) et al Jun. 1990 37 p Presented at the 9th Plasma Surface Interactions in Controlled Fusion Devices Conference, Bournemouth, England, 20-25 May 1990 Prepared in cooperation with Joint European Torus Project, Abingdon, England Submitted for publication
(Contracts DE-AC03-89ER-51114; DE-FG03-89ER-51121; W-7405-eng-48; DE-AC03-84OR-21400; DE-AC03-76DP-00789) (DE91-002429; GA-A-20130; CONF-900505-9) Avail: NTIS HC/MF A03

A survey of the boundary physics research on the DIII-D tokamak and an outline of the DIII-D Advanced Divertor Program (ADP) is presented. We will present results of experiments on impurity control, impurity transport, neutral particle transport, and particle effects on core confinement over a wide range of plasma parameters, I(sub p)(approx lt) 3 MA, (beta)(sub T) (approx lt) 10.7 percent, P(auxiliary) (approx lt) 20 MW. Based on the understanding gained in these studies, we in collaboration with a number of other laboratories have devised a series of experiments (ADP) to modify the core plasma conditions through changes in the edge electric field, neutral recycling, and plasma surface interactions. DOE

N91-19882# National Inst. for Fusion Science, Nagoya (Japan).
SYMPOSIUM ON DEVELOPMENT OF INTENSED PULSED PARTICLE BEAMS AND ITS APPLICATIONS
Kiyoshi Yatsui, ed. Oct. 1990 122 p Symposium held in Nagoya, Japan, 20 Feb. 1990 Submitted for publication
(NIFS-Proc-5; ISSN-0915-6348) Avail: NTIS HC/MF A06

The papers given at this symposium are presented. Some representative titles are as follows: Rayleigh-Taylor Instability in LIB ICF; Two Stage Ion Diode Experiments on Induction Adder; Study of Ablation of Target Material Induced by Pulsed Ion Beam Bombardment; Theoretical Study of Plasma Focus Diode; Reduction of Low Energy Components in Pulse Ion Beam; and Power Plant by LIB Fusion. For individual titles, see N91-19883 through N91-19893.

N91-19883# Nagaoka Technological Univ., Niigata (Japan). Dept. of Electrical Engineering.
RAYLEIGH-TAYLOR INSTABILITY IN LIB ICF
Shigeo Kawata, Toshiaki Sato, and Takayuki Teramoto *In* National Inst. for Fusion Science, Symposium on Development of Intensed Pulsed Particle Beams and Its Applications Oct. 1990 p 1-10 (For primary document see N91-19882 11-75)
Avail: NTIS HC/MF A06

The Rayleigh-Taylor (R-T) Instability is studied in the Light Ion Beam (LIB) Inertial Confinement Fusion (ICF) pellet. The R-T instability is one of the problems in ICF. The nonuniform acceleration field and the radiation effects on the LIB-ICF pellet implosion are studied by linear analyses. By means of these analyses the following results were obtained: (1) The nonuniform acceleration field in space does not change the growth rate (gamma) of the R-T instability (However this nonuniformity may suppress the R-T instability in some particular cases); and (2) The radiation may reduce the growth rate (gamma). Author

N91-19884# Osaka Univ. (Japan). Inst. of Laser Engineering.
TWO-STAGE ION DIODE EXPERIMENTS ON INDUCTION ADDER
S. Miyamoto, Y. Yasuda, M. Yamamoto, T. Honma, A. Zakou, S. Umehara, T. Akiba, K. Imasaki, C. Yamanaka, and S. Nakai *In* National Inst. for Fusion Science, Symposium on Development of Intensed Pulsed Particle Beams and Its Applications Oct. 1990 p 11-19 (For primary document see N91-19882 11-75)
Avail: NTIS HC/MF A06

Two stage ion diode experiment was performed on an induction adder accelerator Reiden-SHVS. The second stage diode is operated in an ion beam injection mode. Enhanced space charge limited current in second stage diode indicates a formation of virtual anode due to the energetic ion beam injection. The beam deflection by virtual anode formation occurred only at inner part of the beam. Two stage charge stripping ion diode is demonstrated. Carbon beam of C(+) and C2(+) are stripped and partially recombined in thin stripping foil and accelerated at second diode. Author

N91-19885# Tokyo Inst. of Tech., Yokahama (Japan). Dept. of Energy Sciences.
EXPERIMENTS TOWARD THE DEVELOPMENT OF NEW PULSED ION DIODES
Kazuhiko Horioka, Naoki Tazima, Yasuhiro Saito, and Koichi Kasuya *In* National Inst. for Fusion Science, Symposium on Development of Intensed Pulsed Particle Beams and Its Applications Oct. 1990 p 21-33 (For primary document see N91-19882 11-75)
Avail: NTIS HC/MF A06

Laser based diagnostic methods are developed to improve the understanding of the behavior of a flashover-type magnetically insulated, pulsed ion diode. Effects of neutral particles on the diode characteristics are examined with laser resonant interferometry. For the quantitative estimation of the particle density, a laser resonance scattering method is also applied. These techniques could allow direct determination of the particle distribution in the diode gap. A new diode which uses actively produced source plasma is developed for the investigation of the anode plasma effect on the diode characteristics. Two types of diode configurations are tested, over a wide range of pulse delays and peak flux of the source plasma injection. Author

N91-19886# Kobe Univ. of Mercantile Marine (Japan). Dept. of Nuclear Engineering.
STUDY ON ABLATION OF TARGET MATERIAL INDUCED BY PULSED ION BEAM BOMBARDMENT
S. Kamihata, A. Kitamura, Y. Furuyama, and T. Nakajima *In* National Inst. for Fusion Science, Symposium on Development of Intensed Pulsed Particle Beams and Its Applications Oct. 1990 p 35-44 (For primary document see N91-19882 11-75)
Avail: NTIS HC/MF A06

Process of ablation due to irradiation of medium power pulsed ion beams (PIB) with a power level of 10(exp 7) to 10(exp 8) w/sq cm, which have been proven useful for material processing, is studied with use of a charge collector method and a collector RBS method. The ablation particles are collected onto a silicon probe surface, which is later subjected to Rutherford Backscattering Spectroscopy (RBS). Preliminary results of measurements on the ablation mass as a function of the ion current density and the target material and on the ion energy include some interesting features, which must be followed by further investigation. Author

N91-19887# Nagaoka Technological Univ., Niigata (Japan). Lab. of Beam Technology.
THEORETICAL STUDY OF PLASMA FOCUS DIODE
Weihua Jiang, Katsumi Masugata, and Kiyoshi Yatsui *In* National Inst. for Fusion Science, Symposium on Development of Intensed Pulsed Particle Beams and Its Applications Oct. 1990 p 45-57 Sponsored in part by Ministry of Education, Science and Culture, Sagamihara, Japan (For primary document see N91-19882 11-75)
Avail: NTIS HC/MF A06

A theoretical model of self magnetically insulated coaxial type ion beam diode, Plasma Focus Diode (PFD), is developed and analyzed in detail. In this theory, self consistant electron current and space charge limited ion current are incorporated. The steady state charge and current distribution inside the diode is calculated for given diode voltage. The calculated diode impedance is compared with the experimental results obtained at the peak power, and good agreement was obtained. Some diode behaviors observed in the experiments are explained by the theory. From the theoretical understanding of PFD, the scaling relations was obtained of diode impedance and the ion current efficiency, and they are used to discuss the possible ways to improve the diode operation. Author

N91-19888# Nagaoka Technological Univ., Niigata (Japan). Lab. of Beam Technology.
PULSE-POWER CHARACTERISTIC OF VIVA-1 (VERSATILE INDUCTIVE VOLTAGE ADDER)
K. Shimiya, Y. Hozumi, T. Aoyama, M. Shigeta, Kiyoshi Shibata (TDK Electronics Co. Ltd., Narita, Japan), Y. Sekimoto, Katsumi Masugata, and Kiyoshi Yatsui *In* National Inst. for Fusion Science, Symposium on Development of Intensed Pulsed Particle Beams and Its Applications Oct. 1990 p 59-67 Sponsored in part by Ministry of Education, Science and Culture, Sagamihara, Japan (For primary document see N91-19882 11-75)
Avail: NTIS HC/MF A06

Versatile Inductive Voltage Adder, (VIVA-1), with high potential gradient was successfully developed to be in operation. It was designed to produce output pulse of 4 MV, 60 ns by adding 2 MV pulses in 2 stages of induction cells, where amorphous cores are installed. Within approx. 40 percent of full charge voltage, pulse power characteristics of Marx generator, pulse forming line (PFL), transmission line (TL), and induction cells were tested for three types of loads: open circuit; dummy load of CuSO4 resistor; and electron diode. In open circuit test, approx. 2.0 MV of output voltage was obtained with good reproducibility. Dependence of output voltage on diode impedance was evaluated by using a dummy load, and good agreement was obtained with that expected. An E-beam diode was operated successfully, and approx. 18 kA of beam current was obtained at diode voltage of approx. 1 MV. Author

N91-19889# Himeji Inst. of Tech. (Japan). Dept. of Electrical Engineering.
REDUCTION OF LOW ENERGY COMPONENTS IN PULSE ION BEAM
M. Sato, Y. Hashimoto, M. Yatsuzuka, and S. Nobuhara *In* National Inst. for Fusion Science, Symposium on Development of Intensed Pulsed Particle Beams and Its Applications Oct. 1990 p 69-77 (For primary document see N91-19882 11-75)
Avail: NTIS HC/MF A06

Reduction of low energy components was tried in pulse ion beams with self crowbar switch in which operation was achieved by expansion of electrode plasmas in a small Magnetically Insulated Transmission Line (MITL). The experiments were carried out with the small MITL (self crowbar switch) and the Inverse Pinch Ion Diode. From the experimental results, the times required for dropping of pulse high voltage were shortened from 40 to 15 ns. As the result of this shortening, the ions accelerated at a relatively low voltage, and the energy ranges of proton beams were reduced from 60 to 30 keV. Author

N91-19890# Himeji Inst. of Tech. (Japan). Dept. of Electrical Engineering.
GENERATION AND FOCUSING OF CARBON ION BEAM BY THE INVERSE PINCH ION DIODE
Y. Hashimoto, M. Sato, M. Yatsuzuka, and S. Nobuhara *In* National Inst. for Fusion Science, Symposium on Development of Intensed Pulsed Particle Beams and Its Applications Oct. 1990 p 79-88 (For primary document see N91-19882 11-75)
Avail: NTIS HC/MF A06

Focusing of intense ion beams was attained with the Inverse Pinch Ion Diode which has a flat anode. The energy of the ion

beam was 180 keV. At the focal point, the ion current density of 0.5 kA/sq cm was obtained and the focusing radius of the ion beam (FWHM) is 10 mm. Focusing of the ion beam is due to the electrostatic field in the Inverse Pinch Ion Diode. Author

N91-19891# Kumamoto Univ. (Japan).
GENERATION OF PULSED ION BEAMS BY AN INDUCTIVE STORAGE PULSED POWER GENERATOR
Sunao Katsuki, Hidenori Akiyama, and Sadao Maeda *In* National Inst. for Fusion Science, Symposium on Development of Intensed Pulsed Particle Beams and Its Applications Oct. 1990 p 89-97 (For primary document see N91-19882 11-75)
Avail: NTIS HC/MF A06

A pulsed power generator by an inductive energy storage system is extremely compact and light in comparison with a conventional pulsed power generator, which consists of a Marx bank and a water pulse forming line. A compact and light pulse power generator is applied to the generation of pulsed ion beams. A thin copper fuse is used an an opening switch, which is necessary in the inductive storage pulsed power generator. A magnetically insulated diode is used for the generation of ion beams. The pulsed ion beams are successfully generated by the inductive storage pulsed power generator for the first time. Author

N91-19892# Tokyo Inst. of Tech., Yokahama (Japan). Dept. of Energy Sciences.
POWER PLANT BY LIB FUSION
Keishiro Niu, Takayuki Aoki, and Hiroya Naramoto *In* National Inst. for Fusion Science, Symposium on Development of Intensed Pulsed Particle Beams and Its Applications Oct. 1990 p 99-107 (For primary document see N91-19882 11-75)
Avail: NTIS HC/MF A06

A fusion power plant of 1 GW electric output is proposed here by using proton beam of 12 MJ for energy driver. The flibe for the coolant in the reactor cavity with a thickness of 50 cm thermalizes the neutrons which produced by fusion reactions and protects the solid wall from being damaged. Tritium breeding radio can exceed unity. An indirect driven target will implode in a spherically symmetric way even in the nonuniform beam irradiation. Author

N91-19893# Tokyo Inst. of Tech., Yokahama (Japan). Dept. of Energy Sciences.
CONTROL OF GAP CLOSURE IN APPLIED-B DIODE
Takayuki Aoki and Keishiro Niu *In* National Inst. for Fusion Science, Symposium on Development of Intensed Pulsed Particle Beams and Its Applications Oct. 1990 p 109-119 Sponsored in part by Ministry of Education, Scien ce and Culture, Sagamihara, Japan (For primary document see N91-19882 11-75)
Avail: NTIS HC/MF A06

The rapid gap closure due to the build-up of the electron sheath is analyzed by a new 1-D particle in cell code. It is found that the diamagnetic effect of the electrons enhances the ion emission from the anode and increases the amount of the ion charge in the diode gap. The ion charge cancels out the electron charge in the sheath, so that the electron density of the sheath increases and the diamagnetism has more effect on the build-up of the sheath toward the anode. Two methods are proposed to control the gap closure. One is to increase the applied magnetic field and another is to limit the flux emitted at the anode surface. In the simulation results, it is shown that these methods improve the impedance characteristics of the diode. Author

N91-19894# National Inst. for Fusion Science, Nagoya (Japan).
He-LIKE SPECTRA THROUGH CHARGE EXCHANGE PROCESSES IN TOKAMAK PLASMAS
T. Kato, K. Masai, Takashi Fujimoto, F. Koike, E. Kallne, E. S. Marmar, and J. E. Rice (Massachusetts Inst. of Tech., Cambridge.) Jan. 1991 37 p
(NIFS-69; ISSN-0915-633X) Avail: NTIS HC/MF A03

Population mechanisms and cascade effects due to charge exchange processes between hydrogen-like ions and neutral hydrogen are investigated for helium-like ions in tokamaks by using a collisional radiative model. Dependences of charge exchange cross sections on both the principal and angular momentum quantum numbers, n and l, are estimated from the observed spectra. Author

N91-19895# Lawrence Livermore National Lab., CA.
UV THOMSON SCATTERING FROM X RAY LASER PLASMAS
B. LaFontaine, H. A. Baldis, D. M. Villeneuve, J. E. Bernard, G. D. Enright, M. D. Rosen, P. E. Young, and D. L. Matthews 3 Jan. 1991 6 p Presented at the 2nd International Colloqium on X-Ray Lasers, York, England, 17-21 Sep. 1990
(Contract W-7405-eng-48)
(DE91-007347; UCRL-JC-105905; CONF-9009266-7) Avail: NTIS HC/MF A02

Plasmas produced by irradiating massive carbon targets with a 1.064 micron, 1.5 ns laser pulse at incident energies of approximately 100 J have been investigated. UV thermal Thomson scattering was used to obtain the electron and ion temperatures, as well as drift velocities. The electron density was obtained by optical interferometry. The results are compared to hydrodynamic computer modeling. DOE

N91-19896# Sandia National Labs., Albuquerque, NM.
US-JAPAN WORKSHOPS: Q-111, DEVELOPMENT OF PLASMA FACING COMPONENTS AND MATERIALS FOR NEXT LARGE FUSION DEVICES, AND Q-112, VACUUM AND FIRST WALL TECHNOLOGY FOR FUSION DEVICES
J. B. Whitley, ed. and A. Miyahara, ed. 1990 464 p Workshop held in La Jolla, CA, 28 Feb. - 2 Mar. 1990
(Contract DE-AC04-76DP-00789)
(DE91-006879; SAND-90-1478C; CONF-9002169) Avail: NTIS HC/MF A20

This report contains papers on the following topics: plasma facing components (PFC) recent experiments on large devices; PFC materials for future plasma devices; neutron effects on carbon materials; innovative concepts for power and particle control; status of high z materials for PFC's; alternate low z plasma facing materials; erosion and hydrogen studies; engineering issues for PFC's; vacuum vessel design for large devices; and testing facilities and test results. DOE

N91-19897# Texas Univ., Austin. Inst. for Fusion Studies.
SUMMARY OF THE INTERNATIONAL DAWSON SYMPOSIUM ON THE PHYSICS OF PLASMAS
T. Tajima Dec. 1990 29 p Symposium held in Los Angeles, CA, 24-25 Sep. 1990
(Contract DE-FG05-80ET-53088)
(DE91-006912; DOE/ET-53088/469; IFSR-469; CONF-9009337-Summ) Avail: NTIS HC/MF A03

The Dawson Symposium was held on September 24 and 25, 1990 in honor of John Dawson's 60th birthday to reflect on various physics of plasma that he had pioneered. The international speakers touched on a wide range of subjects: magnetic fusion, laser fusion, isotope separation, computer simulation, basic plasma physics, accelerators and light sources, space physics, and international scientific collaboration. Highlighted in this article are magnetic fusion and laser fusion investigation that Dawson has been engaged in and the reviews of the present status of their development. The impact of the two-component fusion plasma idea, reactor concepts for advanced fuels, hot electron production by lasers and other nonlinear effects in laser fusion are discussed. Dawson's contributions in the allied areas are also reviewed. DOE

N91-19898# Lawrence Livermore National Lab., CA.
OPTICALLY-IONIZED PLASMA RECOMBINATION X RAY LASERS
P. Amendt, D. C. Eder, S. C. Wilks, M. J. Dunning, and C. J. Keane 18 Jan. 1991 13 p Presented at the OE/LASE 1991: 4th Society of Photo-Optical Instrumentation Engineers International Symposium, Los Angeles, 20-25 Jan. 1991
(Contract W-7405-eng-48)

(DE91-007261; UCRL-JC-106272; CONF-910123-7) Avail: NTIS HC/MF A03

Design studies for recombination x-ray lasers based on plasmas ionized by high intensity, short pulse optical lasers are presented. Transient lasing on n = 3 to n = 2 transitions in lithium-like neon allows for moderately short wavelengths (less than or equal to 100 A) without requiring ionizing intensities associated with relativistic electron quiver energies. The electron energy distribution following the ionizing pulse affects directly the predicted gains for this resonance transition. Efficiencies of 10(exp -6) or greater are found for plasma temperatures in the vicinity of 40 eV. Simulation studies of parametric heating phenomena relating to stimulated Raman and Compton scattering are presented. For electron densities less than about 2.5 x 10(exp 20)/cu cm and peak driver intensity of 2 x 10(exp 17) W/sq cm at 0.25 micron with pulse length of 100 fsec, the amount of electron heating is found to be marginally significant. For lithium-like aluminum, the required relativistic ionizing intensity gives excessive electron heating and reduced efficiency, thereby rendering this scheme impractical for generating shorter wavelength lasing (less than or equal to 50 A) in the transient case. Following the transient lasing phase, a slow hydrodynamic expansion into the surrounding cool plasma is accompanied by quasi-static gain on the n = 4 to n = 3 transition in lithium-like neon. Parametric heating effects on gain optimization in this regime are also discussed. DOE

N91-19899# Los Alamos National Lab., NM.
QUASI-MOLECULAR PROCESSES IN DENSE PLASMAS
S. M. Younger 1991 8 p Presented at the Spring Meeting of the American Physical Society, Washington, DC, 15-18 Apr. 1991
(Contract W-7405-eng-36)
(DE91-007388; LA-UR-91-124; CONF-910427-1) Avail: NTIS HC/MF A02

Quasi-molecular phenomena occur in dense plasmas when the interatomic spacing is comparable to the characteristic wavelength of the electrons. If the electronic states are bound, covalent orbitals arise with different excitation energies, radiative rates, and collisional rates than for isolated ions. For continuum electrons, charge localization near transient clusters of nuclei can influence many scattering and transport processes. Several consequences of quasi-molecular phenomena in plasmas were identified and a possible explanation of high energy features associated with helium-like emissions lines observed in recent inertial fusion experiments was given. DOE

N91-19900# Lawrence Livermore National Lab., CA.
CALCULATION OF EMISSION AND ABSORPTION SPECTRA OF LTE PLASMA BY THE STA (SUPER TRANSITION ARRAY) METHOD
A. Bar-Shalon, J. Oreg, and W. H. Goldstein 11 Jan. 1991 9 p Presented at the International Workshop on Radiative Properties of Hot Dense Matter, Sarasota, 22-26 Oct. 1990
(Contract W-7405-eng-48)
(DE91-007617; UCRL-JC-105957; CONF-9010298-7) Avail: NTIS HC/MF A02

Recent improvements in the Super Transition Array (STA) method for calculating Bound-Bound (BB) and Bound-Free (BF) emission and absorption spectra for Laser Thermal Equilibrium (LTE) plasma are described and illustrated. The method accounts for all possible BB and BF radiative transitions in the plasma. Full detailed first order quantum relativistic treatment is used for calculating transition energies and probabilities. The enormous number of configurations are divided into sets of superconfigurations comprised of a collection of energetically grouped configurations. The contribution of the transition array between two superconfigurations to a specific one-electron transition is then represented by a Gaussian whose moments are calculated accurately using a technique that bypasses the necessity of direct summation over all the levels involved. The calculation of these moments involves the populations of the configurations given by their statistical weights and the Boltzmann factor. For each configuration within the super configuration zeroeth order energies are used in the Boltzmann factor corrected by a super configuration averaged first order term. The structure of the spectrum is increasingly revealed by splitting each STA into a number of smaller STAs. When the spectrum converges it describes the detailed UTA structure, where each configuration-to-configuration array is represented by a separate Gaussian with first order energy in the Boltzmann factor. Convergence is reached with only a few thousand STAs, at most, which makes the calculations practical. It should be pointed out that in this treatment the STA moments are obtained by summing over all level-to-level transitions, rather than configuration-to-configuration average transitions. DOE

N91-19901# Oak Ridge National Lab., TN.
REVIEW OF RECENT STELLARATOR RESULTS IN THE USA, THE USSR, AND JAPAN
J. F. Lyon Dec. 1990 36 p
(Contract DE-AC05-84OR-21400)
(DE91-007798; ORNL/TM-11620) Avail: NTIS HC/MF A03

Stellarators with significant magnetic shear in the United States, the Soviet Union, and Japan are described, and recent results are discussed in terms of their contributions to the physics understanding relevant for stellarator optimization and to toroidal confinement understanding in general. The areas discussed are the properties of stellarators with significant shear, magnetic surfaces, trapped-particle losses, magnetohydrodynamic (MHD) stability, global confinement scaling, local transport, fluctuations, and particle and impurity control. DOE

N91-19902# Oak Ridge National Lab., TN.
PARTICLE-IN-CELL PLASMA SIMULATION CODES ON THE CONNECTION MACHINE
D. W. Walker 1991 38 p Presented at the Meeting on Parallel Methods on Large-Scale Structural Analysis and Physics Applications, Hampton, VA, 5-6 Feb. 1991
(Contract DE-AC05-84OR-21400)
(DE91-007845; CONF-910207-2) Avail: NTIS HC/MF A03

Methods for implementing three-dimensional, electromagnetic, relativistic PIC plasma simulation codes on the Connection Machine (CM-2) are discussed. The gather and scatter phases of the PIC algorithm involve indirect indexing of data, which results in a large amount of communication on the CM-2. Different data decompositions are described that seek to reduce the amount of communication while maintaining good load balance. These methods require the particles to be spatially sorted at the start of each time step, which introduced another form of overhead. The different methods are implemented in CM FORTRAN on the CM-2 and compared. It was found that the general router is slow in performing the communication in the gather and scatter steps, which precludes an efficient CM FORTRAN implementation. An alternative method that uses PARIS calls and the NEWS communication network to pipeline data along the axes of the VP set is suggested as a more efficient algorithm. DOE

N91-19903# Argonne National Lab., IL. Fusion Power Program.
A METHOD FOR DETERMINING POLOIDAL COIL CONFIGURATIONS FOR TOKAMAK DEVICES
K. Evans, Jr. Dec. 1990 65 p
(Contract W-31-109-eng-38)
(DE91-007940; ANL/FPP/TM-156) Avail: NTIS HC/MF A04

This paper presents a method for obtaining the locations and currents of the poloidal coil systems for a tokamak, given an desirable magnetohydrodynamic equilibrium for the device. The method involves a simultaneous minimization of the match to the desired poloidal field and the stored energy in the coils, subject to the constraints necessary to achieve decoupling of the equilibrium and inductive-current-drive (ohmic-heating) systems and to achieve a given coupling of the current-drive system with the plasma. A compendium of mutual and self-inductance formulas as they apply to tokamak systems is presented, as well as examples of how the method has been used in the design of several tokamaks. Finally, a user manual for a computer code that implements this method is provided. DOE

N91-19904# Columbia Univ., New York, NY. Plasma Physics Lab.
EXPERIMENTAL STUDY OF EXTERNAL KINK INSTABILITIES IN THE COLUMBIA HIGH BETA TOKAMAK Ph.D. Thesis
T. H. Ivers 1991 138 p
(Contract DE-FG02-86ER-53222)
(DE91-008116; DOE/ER-53222/105) Avail: NTIS HC/MF A07

The generation of power through controlled thermonuclear fusion reactions in a magnetically confined plasma holds promise as a means of supplying mankind's future energy needs. The device most technologically advanced in pursuit of this goal is the tokamak, a machine in which a current-carrying toroidal plasma is thermally isolated from its surroundings by a strong magnetic field. To be viable, the tokamak reactor must produce a sufficiently large amount of power relative to that needed to sustain the fusion reactions. Plasma instabilities may severely limit this possibility. In this work, I describe experimental measurements of the magnetic structure of large-scale, rapidly-growing instabilities that occur in a tokamak when the current or pressure of the plasma exceeds a critical value relative to the magnetic field, and I compare these measurements with theoretical predictions. DOE

N91-19905# Mississippi State Univ., Mississippi State. Diagnostic Instrumentation and Analysis Lab.
PERFORMANCE CHARACTERISTICS OF AN MHD (MAGNETOHYDRODYNAMIC) PILOT PLANT ELECTROSTATIC PRECIPITATOR
J. S. Lindner, P. R. Jang, W. P. Okhuysen, and J. K. Holt (Tennessee Univ., Tullahoma.) 1991 9 p Presented at the 201st American Chemical Society (ACS) National Meeting, Atlanta, 14-19 Apr. 1991
(Contract DE-AC02-80ET-15601)
(DE91-007218; CONF-910402-8) Avail: NTIS HC/MF A02

In magnetohydrodynamic (MHD) power generation, a seed material, normally K2CO3, is added to enhance the conductivity of the coal-fired gas stream. The plasma is passed through a magnetic field and electricity is produced by the Hall effect. Future large scale MHD facilities are expected to be more efficient than conventional coal-fired power plants not only because of the dc electricity produced but also from increased heat recovery owing to the large (3000 K) combustion temperatures employed. There is; however, a finite cost for the seed material and the resulting K2SO4 particles (SO2 emissions are minimized by combination with seed potassium) must be collected, converted back to K2CO3 or KCO2H, and recycled back to the combustor. The performance characteristics of the MHD electrostatic precipitator (ESP) are therefore, of interest. We describe Mie scattering and electric field measurements on an MHD pilot scale ESP located at the Coal Fire Flow Facility (CFFF) at the University of Tennessee Space Institute. Results are reported for the determination of near-real-time collection efficiencies, the variation of the ESP performance with seed percentage, and initial studies on the extent of particle re-entrainment. DOE

N91-19906# Tennessee Univ. Space Inst., Tullahoma.
THE MAGNETOHYDRODYNAMICS COAL-FIRED FLOW FACILITY
Dec. 1990 51 p
(Contract DE-AC02-79ET-10815)
(DE91-007672; DOE/ET-10815/154) Avail: NTIS HC/MF A04

The purpose of this report is to provide the status of a multi-task research and development program in coal fired MHD/steam combined cycle power production (more detailed information on specific topics is presented in topical reports). Current emphasis is on developing technology for the Steam Bottoming Cycle Program. The approach being taken is to design test components that simulate the most important process variables, such as gas temperature, chemical composition, tube metal temperature, particulate loading, etc., to gain test data needed for scale-up to larger size components. This quarter, a 217 hour coal-fired long-duration test was completed as part of the Proof-of-Concept (POC) test program. The aggregate test time is now 1512 hours of a planned 2000 hours on Eastern coal. The report contains results of testing the newly installed automatic ash/seed handling system and the high pressure sootblower system. The conceptual design for the modifications to the coal processing system to permit operation with Western coal is presented. Results of analysis of superheater test module tube removed after 500 hours of coal-fired testing are summarized. The status of the environmental program is reported. Pollutant measurements from remote monitoring trailers that give the dispersion of stack emissions are presented. Results of advanced measurement systems operated by both UTSI and Mississippi State University during the POC test are summarized. Actions to prepare for the installation of a 20MW(sub t) prototype of the TRW slag rejection combustor first stage are discussed. Contract management and administrative actions completed during the quarter are included. DOE

N91-19907# Sandia National Labs., Albuquerque, NM.
OPTICAL DIAGNOSTICS FOR LOW-TEMPERATURE PLASMAS
W. A. Hareland and R. J. Buss 1990 11 p Presented at the Fall Meeting of the Materials Research Society, Boston, 24 Nov. - 1 Dec. 1990
(Contract DE-AC04-76DP-00789)
(DE91-007896; SAND-90-1754C; CONF-901105-94) Avail: NTIS HC/MF A03

A monochromatic imaging system was used to measure the spatial distribution of excited species in a radiofrequency (RF) plasma etching reactor. The instrument consists of an image intensifier and CCD video camera that are coupled optically to a grating monochromator. The monochromatic imaging instrument has high spectral, spatial, and temporal resolution and is extremely sensitive for measuring low-level light. Monochromatic images of plasma sources are measured at a spectral bandwidth of 2.4 nm over the wavelength region from 350 to 850 nm, and the images are treated by Abel inversion to generate a spatial map of emitting species. Monochromatic images of excited atomic chlorine were measured in a parallel-plate cylindrically symmetric chlorine/helium plasma during the etch of a silicon wafer in reactive-ion etch configuration. We observed a strong correlation between the radial distribution of excited atomic chlorine and the radial etch rate of polysilicon. These studies indicate that the radial etch rate polysilicon. These studies indicate that monochromatic imaging would be a useful diagnostic tool for monitoring etch uniformity during plasma processing of microelectronic components. DOE

N91-19908# General Atomic Co., San Diego, CA.
TOKAMAK IGNITION PROJECTIONS FROM DIMENSIONALLY SIMILAR DISCHARGES
R. E. Waltz, J. C. DeBoo, R. J. Goldston, D. W. Johnson, F. W. Perkins, S. D. Scott, M. C. Zarnstorff, M. N. Rosenbluth, and C. W. Barnes (Los Alamos National Lab., NM.) Nov. 1990 11 p Presented at the 13th International Conference on Plasma Physics and Controlled Nuclear Fusion Research, Washington, DC, 1-6 Oct. 1990
(Contracts DE-AC03-89ER-53277; DE-AC02-76CH-03073)
(DE91-008195; GA-A-20267; IAEA-CN-53/D-4-7;
CONF-901025-40) Avail: NTIS HC/MF A03

Dimensionally similar tokamak discharges with all dimensionless parameters the same except for the relative gyroradius can be scaled to ignition regime discharges of larger size and/or magnetic field analogous with the principles of wind tunnel design. This paper describes the first controlled experiments to determine whether the scaling with relative gyroradius corresponds to transport based on shortwave or longwave length turbulence. DOE

N91-19909# Texas Univ., Austin. Inst. for Fusion Studies.
RELAXED STATES WITH PLASMA FLOW
K. Avinash and J. B. Taylor Jan. 1991 11 p
(Contract DE-FG05-80ET-53088)
(DE91-008199; DOE/ET-53088/472; IFSR-472) Avail: NTIS HC/MF A03

In the theory of relaxation, a plasma reaches a state of minimum energy subject to constant magnetic helicity. In this state, the plasma velocity is zero. Several authors have attempted to extend

the theory, by introducing a number of different helicity invariants, so as to obtain relaxed states with plasma flow. It is shown here that these generalized invariants are special cases of two basic self-helicities: one for electrons and one for ions. The validity of the generalized invariants is discussed and contrasted with that of original magnetic helicity. DOE

N91-19910# Lawrence Livermore National Lab., CA.
MEASUREMENTS OF STARK-BROADENING IN HOT DENSE PLASMA
P. T. Springer, T. S. Perry, R. E. Stewart, C. A. Iglesias, F. J. Serduke, B. G. Wilson, R. W. Lee, J. M. Foster, C. C. Smith, and D. J. Hoarty et al 11 Jan. 1991 10 p Presented at the International Workshop on Radiative Properties of Hot Dense Matter, Sarasota, FL, 22-26 Oct. 1990
(Contract W-7405-eng-48)
(DE91-008504; UCRL-JC-105205; CONF-9010298-5) Avail: NTIS HC/MF A02

We have performed high-resolution measurements of the Stark-broadened line profiles in a magnesium plasma at known density, and compared the measured line profiles with theoretical predictions. In the experiment, a magnesium sample was heated indirectly by x rays from laser-produced plasma. Both the lateral expansion of the exploding foil and the absorption in the helium-like Rydberg series were measured through the use of point projection spectroscopy. The plasma temperature and ionization distribution were determined from the ratio of the helium-like to lithium-like absorption features. For this experiment, a comparison between plasma density derived directly from radiography and by careful examination of Stark profiles was accurate to order 40 percent. The experiment will be repeated under more carefully controlled conditions which should allow a calibration of Stark-broadened profiles with an accuracy of order 10 percent. DOE

N91-19911# Nagoya Univ. (Japan). Plasma Science Center.
NEW METHOD FOR EDGE PLASMA CONTROL BY RF PONDEROMOTIVE FORCE
T. Shoji, R. Conn, A. Grossman, Y. Hirooka, R. Lehmer, W. Leung, L. Schmitz, and G. Tynan Aug. 1990 28 p
(DE91-744823; PSC-9) Avail: NTIS HC/MF A03

A new method to reduce plasma heat flow to a limiter head has been developed with the use of a radio frequency (RF) field barrier. The RF current drawn on the limiter surface produces a ponderomotive potential, psi(sub RF) of the order of the temperature of the plasma near the limiter head in the frequency range omega(sub ci) less than omega much less than omega(sub ce). The limiter head is protected from the plasma by this potential barrier. Experimental proof of the RF limiter concept was attempted using the PISCES-A facility with plasma parameters which are comparable to the edge plasma of typical tokamaks. Production of the RF potential (approximately 20 V) is confirmed by the reflection of an electron beam injected in vacuum with an RF power of approximately 1 kW. Spectroscopic and Langmuir probe measurements show decrease and modification of the edge plasma density by the RF power. As a result of the RF field formation, a remarkable suppression of low frequency fluctuations has been observed at the plasma periphery, which is expected to reduce the plasma transport in the boundary layer. The experimental results are analyzed using numerical particle orbit and fluid drift calculations. Possible application of plasma flow due to (nabla)psi(sub RF) x B(sub o) drift tokamak, a divertor configuration in confinement devices, is discussed. DOE

N91-19912# Japan Atomic Energy Research Inst., Tokyo.
INTRODUCTION TO FUSION
Akio Kitsunezaki Sep. 1990 161 p In JAPANESE; ENGLISH summary
(DE91-744831; JAERI-M-90-150) Avail: NTIS HC/MF A08

The outline of the fusion research and technology is explained for people outside of the fusion research society using non-complex terminology. The principle long range objective and necessity for safety are described in the first chapter. Then, the physics of the magnetic fusion and diagnostics are explained together with engineering research and development for future fusion reactor. Relation of fusion related technology with other field is also described. DOE

N91-19913# Japan Atomic Energy Research Inst., Tokyo.
ELECTRON TEMPERATURE OF Gd PLASMA PRODUCED BY LASER RESONANCE IONIZATION
Koichi Ogura, Takashi Arisawa, Akira Kobana, and Takemasa Shibata Sep. 1990 19 p In JAPANESE; ENGLISH summary
(DE91-744833; JAERI-M-90-162) Avail: NTIS HC/MF A03

In atomic vapor laser isotope separation (AVLIS), it is necessary to extract ions efficiently from plasma produced by laser resonance ionization. It is important to know electron temperature of the plasma, since the aimed isotope ions are accelerated by electric potential of the order of electron temperature in the plasma. The electron temperature of Gd plasma produced by laser resonance ionization was measured by a Langmuir probe. This measured electron temperature is much lower than the released electron energy and is close to the atomic excitation temperature of Gd. This result seems to show that electrons collide with Gd atoms with excited or de-excitated ground or metastable Gd atoms, and the electron temperature becomes close to the atomic excitation temperature. DOE

N91-19914# Japan Atomic Energy Research Inst., Tokyo.
EFFECTS OF PRESSURE PROFILE AND PLASMA SHAPING ON THE n=1 INTERNAL KINK MODE IN JT-60/JT-60U PELLET FUELLED PLASMAS
Takahisa Ozeki and Masafumi Azumi Oct. 1990 28 p
(DE91-744965; JAERI-M-90-170) Avail: NTIS HC/MF A03

The stability of the n=1 internal kink mode in a tokamak is numerically analyzed for plasmas with a centrally peaked pressure profile. These studies are carried out with the strongly peaked pressure inside the q=1 surface, which is based on the experimentally observed plasmas by means of injections of hydrogen-ice pellets in JT-60 tokamak. The effects of peaked pressure and shaping, i.e., elongation and triangularity, are also studied for JT-60U tokamak. The plasma with the strongly peaked pressure profile has higher critical value of poloidal beta defined within the q=1 surface than that with a parabolic pressure profile. Though the beta limit reduces with the increase of the elongation, the plasma with the peaked pressure profile has larger improvement due to the triangularity than that with the parabolic pressure profile. To access the second stability of the n=1 internal kink mode, the plasma with a flat pressure profile and the large minor radius of the q=1 surface is effective. DOE

N91-19915# Institut National des Sciences Appliquees, Lyon (France). Lab. de Physicochimie Industrielle.
A STUDY OF ALKALINE ELEMENT INTERFERENCES IN ANALYTICAL INDUCTIVELY COUPLED PLASMAS Ph.D. Thesis
Sylvie Chomet 1990 254 p In FRENCH; ENGLISH summary
(ISAL-90-0069; ETN-91-98894) Avail: NTIS HC/MF A12

Alkaline elements are known to produce interferences when analyses are realized with an inductively coupled plasma. Their presence in samples can change analyte signals and leads to non negligible errors in analytical results, in atomic emission spectroscopy and mass spectroscopy as well. Authors who studied this problem, do not agree with the nature of the matrix effect, because observed phenomena appear sometimes inconsistent. Thus, alkaline perturbation is often connected to their quality of easily ionized elements. A comparative study of effects induced by the presence of alkaline elements (Na, Cs and Rb) on a large concentration scale -0.0001 to 0.1 mol/l in solutions (of Ca, Mg and Sr, Ba) was performed in inductively coupled argon plasma by optical spectroscopy and mass spectroscopy. Perturbations at low alkaline concentrations (0.0001 mol/l, corresponding to a molar concentration ratio 1:1 to the analyte) were noted. It is underlined that the interference amplitude depends, especially at lower concentrations, on plasma/generator impedence matching. Observed phenomena, similar for mass and optical detections, show that alkaline element effects occur during sample

volatilization/atomization phase i.e., during the thermal step. It appears that the influence of alkaline elements is linked to their great collisional cross sections, a characteristic associated to an increase of the plasma thermal conductivity. ESA

N91-19916# Technische Univ., Eindhoven (Netherlands). Electrical Energy Systems Group.
NOBLE GAS DISK MHD GENERATOR PERFORMANCE WITH UNSTABLE NONEQUILIBRIUM PLASMA Ph.D. Thesis
Plamen Raytchev Karavassilev 1990 153 p
(ISBN-90-9003671-7; ETN-91-98931) Avail: NTIS HC/MF A08

Three disk shaped magnetohydrodynamic (MHD) generators working with hot argon or helium gas seeded with cesium are studied. Experiments are performed using a shock tube as the plasma source and an absorption measurement diagnostic for seed concentration determination. Time resolved measurements of the static pressure and plasma voltage radial distributions, and the radial components of the generated current, are carried out. A Rogowski coil diagnostic is applied to measure the azimuthal current component, and flow velocity information is obtained by streak photographs. Plasma nonuniformities are visualized by fast framing photographs. Plasma optical emission is fast sample rate detected for electron density and temperature determinations. Experimental results are analyzed by the solution of quasi one dimensional gas dynamical equations. The calculated static pressure, azimuthal current and radial component of the flow velocity are fitted to the corresponding mesured counterparts using the values of the effective Hall parameter. A model incorporating the derived semiempirical relationships is formulated and tested for consistency. The middle size generator has better efficiency characteristics than the large size. ESA

76 SOLID-STATE PHYSICS

Includes superconductivity.

For related information, see also *33 Electronics and Electrical Engineering* and *36 Lasers and Masers.*

N91-19917# Department of the Navy, Washington, DC.
METHOD OF PRODUCING SUPERCONDUCTING MATERIALS IN BULK FORM Patent Application
V. Provenzano, inventor (to Navy), M. S. Imam, inventor (to Navy), K. Sadananda, inventor (to Navy), and W. F. Henshaw, inventor (to Navy) 28 Feb. 1990 14 p
(AD-D014656; US-Patent-Appl-SN-489313) Avail: NTIS HC/MF A03 CSCL 13/8

Bulk form of superconducting materials are produced by pouring a melt a O2-containing superconducting material into a heated mold, cooling the mold until solidification begins, removing the cast object from the mold, gradually cooling the cast object to prevent the development of thermal stresses, and then annealing the cast, cooled object to restore O2 to near equilibrium levels. The bulk form produced according to the present invention may be used as a sputtering target in the production of wires, or as a bulk form semiconductor. GRA

N91-19918 Department of the Navy, Washington, DC.
APPARATUS FOR DETERMINING MICROWAVE CHARACTERISTICS OF SUPERCONDUCTIVE MATERIALS USING A RESONANT CAVITY AND CALIBRATION WAVEGUIDES Patent
Donald R. Bowling, inventor (to Navy) and Charles F. Smith, inventor (to Navy) 25 Sep. 1990 13 p Filed 3 Aug. 1989
(AD-D014694; US-Patent-4,959,614; US-Patent-Appl-SN-389233; US-Patent-Class-324-636) Avail: US Patent and Trademark Office CSCL 14/2

Apparatus for determining the electrical characteristics of a superconductive material in a range of microwave frequencies and in a range of cryogenic temperatures has the material incorporated within a resonant cavity mounted on a a cold finger for maintaining the material at a predetermined temperature. A pair of test waveguides extended oppositely of the cavity and terminate in separable waveguide junctions for passage of microwave energy to measure the microwave characteristics of the cavity as affected by the enclosed in a vacuum chamber from which the cold finger extends for connection to controlled temperature cryogenic cooling equipment. The chamber also contains a plurality of calibration waveguides which extend parallel to the test waveguides, each calibration waveguide terminating oppositely in separable junctions. The chamber has plates disposed oppositely of the waveguides and movable transversely in relation to the waveguides without loss of vacuum. GRA

N91-19919# Lawrence Livermore National Lab., CA.
POSITRON LIFETIME STUDIES OF DEFECT STRUCTURES IN Ba(1-x)K(x)BiO3
J. C. OBrien, R. H. Howell, H. B. Radousky, P. A. Sterne, D. G. Hinks, T. J. Folkerts, and R. N. Shelton (California Univ., Davis.) 20 Dec. 1990 8 p Presented at the Fall Meeting of the Materials Research Society, Boston, 24 Nov. - 1 Dec. 1990
(Contracts W-7405-eng-48; W-31-109-eng-38)
(DE91-007341; UCRL-JC-105876; CONF-901105-89) Avail: NTIS HC/MF A02

Temperature-dependent positron lifetime experiments have been performed from room temperature to cryogenic temperatures on Ba(1-x)K(x)BiO3, for x = 0.4 and 0.5. From the temperature dependence of the positron lifetime in the normal state, we observe a clear signature of competition between separate defect populations to trap the positron. Theoretical calculations of lifetimes of free or trapped positrons have been performed on Ba(1-x)K(x)BiO3, to help identify these defects. Lifetime measurements separated by long times have been performed and evidence of aging effects in the sample defect populations is seen in these materials. DOE

N91-19920# Princeton Univ., NJ.
SURFACE CHEMISTRY AT SEMICONDUCTOR-ELECTROLYTE INTERFACES
1990 3 p
(Contract DE-FG02-85ER-13438)
(DE91-005915; DOE/ER-13438/1) Avail: NTIS HC/MF A01

During the past funding period, DOE projects have involved six graduate students. Over the past four months, work on interfacial photoprocesses occurring at II-VI semi-conductors has occupied much of our time, since a recent literature report by Licht has suggests that our prior conclusions might not be correct. As detailed below, we are now able to report that our previous studies stand and that the Licht work contains a major error. In addition to this work, we have now initiated high-speed data collection of photocurrent transients on n-type TiO2 and p-GaP based photoelectrochemical cells with an aim to determining the mechanistic details associated with the photoelectrolysis of water at these interfaces. We are also continuing our work on the photodeposition on plantinum metal on nonconducting substrates and semiconductors as well as our study of ascorbate oxidation at n-type CdS photoelectrodes. This report presents the results obtained over the last year's work. DOE

N91-19921# Lawrence Livermore National Lab., CA.
A PHOTOEMISSION INVESTIGATION OF COMPOUND SEMICONDUCTOR MONODISPERSE CLUSTERS
J. G. Tobin, V. L. Colvin, and A. P. Alivisatos Dec. 1990 10 p Presented at the 37th National American Vacuum Society Symposium, Toronto, Ontario, 8-12 Oct. 1990
(Contract W-7405-eng-48)
(DE91-006707; UCRL-JC-103724; CONF-901035-17) Avail: NTIS HC/MF A02

We have used synchrotron radiation photoemission to probe the valence and core level electronic structure of compound-semiconductor monodisperse clusters (nanocrystals). These clusters exhibited a 10 percent or less variation relative to the mean diameter and were attached to the metal substrates via alkane chains. Direct evidence of gap broadening due to size variation in CdS clusters was observed. The novel utilization of alkane chain attachment is the key to eliminating the otherwise

debilitating problem of sample charging, as occurs with powders. The quality of sample preparation was confirmed by other methods such as transmission electron microscopy, Raman scattering and x ray diffraction. This work provides a direct link between photoemission studies of expitaxial ultra-thin films of compound semiconductors, the photon-spectroscopy measurements of cluster powders and the existing theories of quantum confinement in reduced dimensionality structures. DOE

N91-19922# Sandia National Labs., Albuquerque, NM.
CONSIDERATIONS RELATING TO PULSED-BEAM MODIFICATION OF MATERIALS
S. M. Myers, D. M. Follstaedt, R. J. Bourcier, M. T. Dugger, D. C. McIntyre, and D. J. Rader 1990 11 p Presented at the 3rd International Conference on Intense Ion-Beam Interaction with Matter, Albuquerque, NM, 6-8 Nov. 1990
(Contract DE-AC04-76DP-00789)
(DE91-006771; SAND-90-3233C; CONF-9011175-1) Avail: NTIS HC/MF A03

Ion implantation has been shown to produce unique improvements in the properties of a wide range of materials. This technology has been extensively used for doping of semiconductors, where the required doses and implantation depths are relatively modest and readily achieved with commercial implanters. Other applications of ion implantation currently being pursued at a commercial level include the synthesis of buried second-phase layers in Si and the improvement of metal surface properties such as hardness, friction, wear rate, and corrosion. However, these applications have been severely constrained by the costs of treating large surface areas with the high ion doses required, and by the need to produce modified layers thicker than the range of the sub-MeV ions available from presently available commercial high-flux ion implanters. It therefore seems worthwhile to consider whether pulsed ion accelerators may offer advantages for such applications by providing high ion fluxes at MeV energies. The previously reported applications of pulsed accelerators to materials modification have used sub-MeV ion energies. The purpose of this article is to being these considerations the perspective of materials scientists who use ion implantation. Needed extensions in implantation capabilities are commented on while leaving to others the question of whether these needs can be met with pulsed-beam technology. Further, in order to illustrate the kinds of beneficial materials modifications that can be achieved with implantation, we provide examples from recent work at Sandia National Laboratories, where large improvements have been realized in the tribological properties and strengths of Fe and Al alloys. DOE

N91-19923# Brigham Young Univ., Provo, UT.
INVESTIGATION OF CONDENSED MATTER FUSION
S. E. Jones, M. Berrondo, J. B. Czirr, D. L. Decker, K. Harrison, G. L. Jensen, E. P. Palmer, L. B. Rees, S. Taylor, and H. B. Vanfleet et al Dec. 1990 14 p
(Contract DE-FG02-90ER-12105)
(DE91-007246; DOE/ER-12105/1) Avail: NTIS HC/MF A03

Work on muon-catalyzed fusion led to research on a possible new type of fusion occurring in hydrogen isotopes embedded in metal lattices. While the nuclear-product yields observed to date are so small as to require careful further checking, rates observed over short times appear sufficiently large to suggest that significant neutrons and triton yields could be realized -- if the process could be understood and controlled. During 1990, we have developed two charged-particle detection systems and three new neutron detectors. A segmented, high-efficiency neutron counter was taken 600 m underground in a mine in Colorado for studies of the cosmic-ray background. Significant neutron emissions were observed in this environment in both deuterium-gas-loaded metals and in electrolytic cells, confirming our earlier observations. DOE

N91-19924# Lawrence Livermore National Lab., CA.
PHOTOELECTRON DIFFRACTION OF MAGNETIC ULTRATHIN FILMS: Fe/Cu(001)
J. G. Tobin, M. K. Wagner, X. Q. Guo, and S. Y. Tong (Wisconsin Univ., Milwaukee.) 3 Jan. 1991 9 p Presented at the Fall Meeting of the Materials Research Society, Boston, MA, 24 Nov. - 1 Dec. 1990
(Contract W-7405-eng-48)
(DE91-007254; UCRL-JC-103725; CONF-901105-87) Avail: NTIS HC/MF A02

The preliminary results of an ongoing investigation of Fe/Cu(001) are presented here. Energy dependent photoelectron diffraction, including the spin-dependent variant using the multiplet split Fe3s state, is being used to investigate the nanoscale structures formed by near-monolayer deposits of Fe onto Cu(001). Core-level photoemission from the Fe3p and Fe3s states has been generated using synchrotron radiation as the tunable excitation source. Tentatively, a comparison of the experimental Fe3p cross section measurements with multiple scattering calculations indicates that the Fe is in a fourfold hollow site with a spacing of 3.6(Angstrom) between it and the atom directly beneath it, in the third layer. This is consistent with an FCC structure. The possibility of utilizing spin-dependent photoelectron diffraction to investigate magnetic ultrathin films will be demonstrated, using our preliminary spectra of the multiplet-split Fe3s on near-monolayer Fe/Cu(001). DOE

N91-19925# Oak Ridge National Lab., TN.
THIN FILM AMORPHOUS ELECTROLYTES: THE LI2O-SIO2-P2O5 SYSTEM
J. B. Bates, N. J. Dudney, B. C. Sales, R. A. Zuhr, G. R. Gruzalski, C. F. Luck, and J. D. Robertson (Kentucky Univ., Lexington.) Jan. 1991 11 p Presented at the Fall Meeting of the Materials Research Society, Boston, MA, 24 Nov. - 1 Dec. 1990
(Contract DE-AC05-84OR-21400)
(DE91-007272; CONF-901105-86) Avail: NTIS HC/MF A03

Thin film amorphous electrolytes with compositions xLi-2O:ySiO2:zP2O5 were deposited by single and dual source rf magnetron sputtering and their compositions determined by electron and ion beam techniques. Films containing P but no Si were composed of mainly orthophosphate and some linear chain phosphate anions, whereas single phase films containing Si and P were evidently composed of branched and possible cyclic and extended network structures. Films with Si/P greater than 1 appeared to contain two or more amorphous phases. In the range of compositions investigated, the lithium ion conductivity depends mainly on the lithium ion mobility which is sensitive to the structure of the films. An open circuit voltage from 1 to 3 V measured between blocking metal contacts on the electrolyte thin films suggest that the films might be electrets. DOE

N91-19926# Oak Ridge National Lab., TN.
IN SITU TEM STUDIES OF THE GROWTH OF STRAINED Si(1-X)Ge(X) BY SOLID PHASE EPITAXY
D. C. Paine, D. J. Howard, N. D. Evans, D. W. Greve, and M. Racanelli (Carnegie-Mellon Univ., Pittsburgh, PA.) 1990 6 p Presented at the Fall Meeting of the Materials Research Society, Boston, MA, 24 Nov. - 1 Dec. 1990
(Contracts DE-AC05-84OR-21400; DE-AC05-76OR-00033)
(DE91-007278; CONF-901105-88) Avail: NTIS HC/MF A02

In this paper we report on the epitaxial growth of strained thin films Si(1-x)Ge(x) on Si by solid phase epitaxy. For these solid phase epitaxy experiments, a 180-nm-thick strained-layer of Si(1-x)Ge(x) with x(sub Ge) = 11.6 at. percent was epitaxially grown on group of zone axes (001) Si using chemical vapor deposition. The near surface region of the substrate, including the entire Si(1-x)Ge(x) film, was then amorphized to a depth of 380 nm using a two step process of 100 keV, followed by 200 keV, Si-29 ion implantation. The epitaxial regrowth of the alloy was studied with in situ TEM (transmission electron microscopy) heating techniques which enabled an evaluation of the activation energy for strained solid phase epitaxial regrowth. We report that the activation energy for Si(1-x)Ge(x) (x = 11.6 at. percent) strained-layer regrowth is 3.2 eV while that for unstrained regrowth of pure Si is 2.68 eV and that regrowth in the alloy is slower than in pure Si over the temperature range 490 to 600 C. DOE

N91-19927# Lawrence Livermore National Lab., CA.
APPLICATION OF MeV IONS TO THE ANALYSIS AND MODIFICATION OF HIGH TEMPERATURE SUPERCONDUCTING MATERIALS
T. A. Tombrello 2 Nov. 1990 18 p
(Contract W-7405-eng-48)
(DE91-007317; UCRL-CR-105373) Avail: NTIS HC/MF A03

In analyzing the composition of high (Tc) superconducting materials using heavy-ion RBS we discovered that the electronic excitation of the target caused mixing to occur. To study this effect we made superlattice structures of alternating thin layers of Ba2YCu3O(6+x) and BaF2. At this point in the process some mixing has occurred, but the individual layers are still visible. However, as the bombardment continued the layers were mixed together. It may well be that one can use this phenomenon to produce high (Tc) materials with a wide range of compositions. In this report, we discuss modifications to the high (Tc) superconductors and the subsequent analysis. DOE

N91-19928# Los Alamos National Lab., NM.
FREE ENERGY SIMULATION OF GRAIN BOUNDARY SEGREGATION THE THERMODYNAMICS IN Ni(3-x)Al(1+x)
R. Najafabadi, H. Y. Wang, D. J. Srolovitz (Michigan Univ., Ann Arbor.), and R. LeSar 1990 9 p Presented at the Fall Meeting of the Materials Research Society, Boston, MA, 24 Nov. - 1 Dec. 1990
(Contract W-7405-eng-36)
(DE91-007473; LA-UR-91-276; CONF-901105-90) Avail: NTIS HC/MF A02

The free energy simulation method is employed to study segregation to Sigma 5 and Sigma 13 set of planes (001) twist grain boundaries and their free energies in ordered Ni(3-x)Al(1+x). In the temperature range studied (300 to 900 K), it is shown that there is almost no segregation, strong Al segregation, and weak Ni segregation to the grain boundary for the stoichiometric, Al-rich and Ni-rich bulk compositions respectively. It is also shown that the segregation is limited to a few set of planes (002) around the grain boundary and its magnitude decreases with increasing temperature. For Al-rich bulk composition, it is demonstrated that segregation at low temperature substantially lowers the grain boundary free energy. DOE

N91-19929# Brookhaven National Lab., Upton, NY.
THE CHARACTERIZATION OF INTERFACE ROUGHNESS AND OTHER DEFECTS IN MULTILAYERS BY X RAY SCATTERING
S. K. Sinha, M. K. Sanyal, A. Gibaud, S. K. Satija, C. F. Majlrzak, and H. Homma (State Univ. of New York, Brooklyn.) 1990 5 p Presented at the NATO Advanced Study Institute on Science and Technology of Nanostructured Magnetic Materials, Crete, Greece, 25 Jun. - 7 Jul. 1990
(Contract DE-AC02-76CH-00016)
(DE91-007558; BNL-45732; CONF-900688-1) Avail: NTIS HC/MF A01

Some theoretical and experimental results are presented on the characterization of roughness in thin films and multilayers by scattering techniques. Particular attention is focused on the difference between specular and diffuse scattering and on correlated roughness between interfaces. DOE

N91-19930# California Univ., Berkeley. Lawrence Berkeley Lab.
PHASE TRANSITIONS AND EQUATION OF STATE OF CsI UNDER HIGH PRESSURE AND THE DEVELOPMENT OF A FOCUSING SYSTEM FOR X RAYS Ph.D. Thesis
Yan Wu Nov. 1990 195 p
(Contract DE-AC03-76SF-00098)
(DE91-007646; LBL-29844) Avail: NTIS HC/MF A09

The phase transitions and equation of state of ionic solid cesium iodide were studied under high pressure and room temperature in a diamond anvil cell. The studies were carried out using both energy dispersive and angular dispersive diffraction methods on synchrotron radiation sources over the pressure range from atmospheric pressure to over 300 gigapascals (3 million atmospheres). CsI undergoes a distinct phase transition at about 40 GPa, a pressure that is much lower than the reported insulator-metal transition at 110 GPa, from the atmospheric pressure B2(CsCl) structure to an orthorhombic structure. At higher pressures, a continuous distortion in the structure was observed with a final structure similar to a hcp lattice under ultra high pressure. No volume discontinuity was observed at the insulator-metal transition. The newly found transition sequence is different from the result of previous static compression studies. The current structure has a smaller unit cell volume than the previous assignment. This has resolved a long existing controversy among the previous static compression studies, the dynamic compression studies, and the theoretical studies. The current results also explain the apparent discrepancy between the present study and the previous static studies. The development is also presented of a focusing system for high energy x rays (less than 12 keV) that is particularly suited for high pressure diffraction studies. This system uses a pair of multilayer coated spherical mirrors in a Kirkpatrick-Baez geometry. A focused beam size less than 10 micron in diameter can be readily achieved with sufficient intensity to perform diffraction studies. DOE

N91-19931# California Univ., Berkeley. Lawrence Berkeley Lab.
THIN FILM REACTIONS ON ALLOY SEMICONDUCTOR SUBSTRATES Ph.D. Thesis
D. A. Olson Nov. 1990 161 p
(Contract DE-AC03-76SF-00098)
(DE91-007651; LBL-29837) Avail: NTIS HC/MF A08

The interactions between Pt and In(.53)Ga(.47)As were studied. In(.53)Ga(.47)As substrates with 70 nm Pt films were encapsulated in SiO2, and annealed up to 600 C in flowing forming gas. The composition and morphology of the reaction product phases were studied using x ray diffraction, Auger depth profiling, and transmission electron microscopy. The reaction kinetics were examined with Rutherford Backscattering. Results show that Pt/In(.53)Ga(.47)As reacts to form many of the reaction products encountered in the Pt/GaAs and Pt/InP reactions: PtGa, Pt3Ga, and PtAs2. In addition, a ternary phase, Pt(In:Ga)2, develops, which is a solid solution between PtIn2 and PtGa2. The amount of Ga in the ternary phase increases with annealing temperature, which causes a decrease in the lattice parameter of the phase. The reaction products show a tendency to form layered structures, especially for higher temperatures and longer annealing times. Unlike the binary case, the PtAs2, phase is randomly oriented on the substrate, and is intermingle with a significant amount of Pt(In:Ga)2. Following Pt/In(.53)Ga(.47)As reactions, two orientation relationships between the Pt(In:Ga)2 product phase and the substrate were observed, despite the large mismatch with the substrate (approx. 8 percent). For many metal/compound semiconductor interactions, the reaction rate is diffusion limited, i.e., exhibits a parabolic dependence on time. An additional result was the development of an In-rich layer beneath the reacted layer. The Auger depth profile showed a substantial increase in the sample at this layer. This is a significant result for the production of ohmic contacts, as the Schottky barrier height in this system lower for higher In concentrations. DOE

N91-19932# Sandia National Labs., Albuquerque, NM.
COMPOUND SEMICONDUCTORS, STRAINED LAYER EPITAXY, AND THE INFORMATION AGE
V. Narayanamurti 1990 19 p Presented at the SPIE International Conference on Physics Concepts of Materials for Novel Optoelectronic Device Applications, Aachen, Fed. Republic of Germany, 27 Oct. - 2 Nov. 1990
(Contract DE-AC04-76DP-00789)
(DE91-007735; SAND-91-0362C; CONF-901047-1) Avail: NTIS HC/MF A03

The semiconductor laser has spawned a new technological revolution - the so-called photonics revolution. When combined with advances in electronics, this new technology will usher in the dawning of the information age. Advances in optoelectronics will

be spurred by new advances in band gap engineering. Recent progress in this area, with particular emphasis on new devices formed by strained-layer epitaxy, is reviewed. DOE

N91-19933# California Univ., Berkeley. Lawrence Berkeley Lab.
SOME ROLES FOR TEM IN THE DEVELOPMENT OF NEW MATERIALS
K. H. Westmacott Apr. 1990 11 p Presented at the 3rd International New Materials Conference, Osaka, Japan, 1-5 Oct. 1990
(Contract DE-AC03-76SF-00098)
(DE91-007742; LBL-29589; CONF-9010135-1) Avail: NTIS HC/MF A03

A fundamental understanding of the growth mechanism of epitaxial metal films on semiconductor substrates has important implications in a number of key technological areas. Of equal importance is a thorough knowledge and understanding of the interface structure and its relationship to properties. High voltage transmission electron microscopy using both conventional and high resolution imaging and diffraction provides a powerful tool for addressing important questions relating to thin film growth and interface structure. In the present contribution some recent applications of advanced TEM techniques to fundamental issues will be discussed. In each case studies of interface structures have revealed interesting effects of relevance to a broad range of problems. DOE

N91-19934# California Univ., Berkeley. Lawrence Berkeley Lab.
PART 1: THE EFFECT OF LATTICE DEFECTS ON THE SINTERING OF LITHIUM FLUORIDE; PART 2: THE MORPHOLOGY OF CALCIUM OXIDE FROM CALCIUM CARBONATE DECOMPOSITION Ph.D. Thesis
D. M. Fenwick Sep. 1990 64 p
(Contract DE-AC03-76SF-00098)
(DE91-007743; LBL-28303) Avail: NTIS HC/MF A04

Our motivation for studying the effect of lattice defects on sintering kinetics came from a theory by Searcy concerning surface melting of solids. Surface melting has been shown to occur in ice, argon, and lead at temperatures below the melting point. While surface melting of this sort is an equilibrium phenomenon, Searcy has predicted that surface melting may also occur in a non-equilibrium situation when a solid is being rapidly heated and has a below-equilibrium concentration of vacancies for the temperature reached. To test the surface melting theory we have compared the density changes of two different types of powder compacts of lithium fluoride after subjecting both to the same fast-firing heat treatment. One type of compact consisted of powder originating from a crystal which he had quenched from a high temperature, and the other consisted of powder from a crystal which we had annealed at a lower temperature. When calcite is decomposed in vacuum, CaO is sometimes found in two distinguishable layers. Both layers are comprised of fairly uniformly sized, cylindrical rods on the order of 10 nm in diameter with the normal NaCl-type crystal structure. The outer layer consists of approximately 1 micron diameter bundles of rods separated by approximately 1 micron wide cracks. The second layer, adjacent to any undecomposed calcite (the intermediate layer) probably consists of rods which are relatively evenly spaced. Because sintering is negligible when calcite decomposition occurs below 700 C in a vacuum of 10(exp -3) torr or less, the outer layer is probably formed by a diffusionless, cooperative re-packing of CaO rods first formed with the uniform spacing characteristic of the intermediate layer. DOE

N91-19935*# National Aeronautics and Space Administration. Lewis Research Center, Cleveland, OH.
STUDY OF InGaAs BASED MODFET STRUCTURES USING VARIABLE ANGLE SPECTROSCOPIC ELLIPSOMETRY
S. A. Alterovitz, R. M. Sieg, H. D. Yao, P. G. Snyder, J. A. Woollam, J. Pamulapati, P. K. Bhattacharya, and P. A. Sekula-Moise (Spire Corp., Bedford, MA.) 1991 13 p Presented at the International Conference on Metallurical Coatings and Thin Films, San Diego, CA, 22-26 Apr. 1991; sponsored by American Vacuum Society
(NASA-TM-103792; E-6069; NAS 1.15:103792) Avail: NTIS HC/MF A03 CSCL 20L

Variable angle spectroscopic ellipsometry was used to estimate the thicknesses of all layers within the optical penetration depth of InGaAs based MODFET structures. Strained and unstrained InGaAs channels were made by MBE on InP substrates and by MOCVD on GaAs substrates. In most cases, ellipsometrically determined thicknesses were within 10 percent of the growth calibration results. The MBE made InGaAs strained layers showed large strain effects, indicating a probable shift in the critical points of their dielectric function toward the InP lattice matched concentration. Author

N91-19936# Sandia National Labs., Albuquerque, NM.
ELECTRONIC CHARGE DENSITY AND BONDING IN ALPHA-BORON: AN EXPERIMENTAL-THEORETICAL COMPARISON
A. C. Switendick and B. Morosin 1990 7 p Presented at the 10th International Symposium on Boron, Borides and Related Compounds, Albuquerque, 27-30 Aug. 1990
(Contract DE-AC04-76DP-00789)
(DE91-006629; SAND-90-3269C; CONF-900870-6) Avail: NTIS HC/MF A02

Improved crystal structure parameters are reported for alpha-boron. Plots showing comparison of theoretical and experimental valence charge densities for two crystalline planes are given. Comparisons of the strengths of various inter- and intraicosahedral bonds are reported in terms of the maximum charge density associated with the line joining the atoms. DOE

N91-19937# Oak Ridge National Lab., TN.
X RAY DETERMINATION OF SITE OCCUPATION PARAMETERS IN ORDERED TERNARIES Cu(Au(x)M(1-x))M = Ni,Pd
R. Kumar, C. J. Sparks, E. D. Specht, P. Zschack, G. E. Ice, T. Shiraishi, and K. Hisatsune (Nagasaki Univ., Japan) 1990 6 p Presented at the Fall Meeting of the Materials Research Society, Boston, 24 Nov. - 1 Dec. 1990
(Contract DE-AC05-84OR-21400)
(DE91-007861; CONF-901105-95) Avail: NTIS HC/MF A02

X ray scattering data obtained for multiple wavelengths with synchrotron radiation were analyzed by the Rietveld method to determine Ni and Pd distributions on the Cu(000) and Au(1/2 1/2 1/2) sites in the CuAuI tetragonal P4/mmm structure. Alloys of CuAu(x)M(1-x) containing 6 at. percent Ni or 10 and 25 at. percent Pd were processed to obtain maximum ordering. Nickel is predominantly found on the Cu size and most all the Pd is found on the Au site. The uncertainty in site occupation parameters is discussed for various contributions which affect powder intensity measurements. For highly absorbing materials, an observed powder roughness effect decreases the low angle (2 theta) intensities relative to the high 2 theta intensities. This effect reduces the reliability of the thermal parameters and obscure a proper description of the thermal motion of the two sublattices. Corrections to the x ray intensity data for surface roughness/porosity effects reduce uncertainties to about = or - 1 at. percent on the refined value of the site occupations. This use of variable wavelength x rays with simultaneous refinement of the corresponding data is capable of distinguishing site occupations even between two elements of almost equal scattering factor as, for example, Cu and Ni atoms in this investigation. Chemical phase stability is related to the site occupation parameters. DOE

N91-19938# Northwestern Univ., Evanston, IL. Dept. of Materials Science and Engineering.
PLASMA, PHOTON, AND BEAM SYNTHESIS OF DIAMOND FILMS AND MULTILAYERED STRUCTURES
R. P. H. Chang 1990 5 p
(Contract DE-FG02-87ER-45314)
(DE91-007934; DOE/ER-45314/3) Avail: NTIS HC/MF A01

Three major areas of fundamental research on diamond thin

films have been carried out successfully during the last period 1989 to 1990. By controlling the nucleation process we have learned that very smooth and transparent films can be grown at low temperatures. We have carefully studied the chemistry of iron surfaces and learned how to nucleate and grow diamond films on them. In addition, we have devised a means of growing composite diamond film which is flexible. Diamond films can be doped to conduct electricity. We have made careful studies on the physical and optical properties of Boron doped diamond films. DOE

N91-19939# Northwestern Univ., Evanston, IL. Dept. of Chemical Engineering.
SOLID STATE, SURFACE, AND CATALYTIC STUDIES OF OXIDES
H. H. Kung 1 Feb. 1991 7 p
(Contract DE-FG02-87ER-13725)
(DE91-007979; DOE/ER-13725/4) Avail: NTIS HC/MF A02

Work conducted in this period can be grouped into three projects, all of which deals with the selective oxidative dehydrogenation of butane and propane: investigation of the reasons for the differences in the observations reported by us, which showed that magnesium orthovanadate Mg3(VO4)2 is the selective phase for the oxidative dehydrogenation of butane and propane, and those by Volta and coworkers which showed that the orthovanadate is nonselective for propane and the selective phase is magnesium pyrovanadate. Investigation of the effect of reducibility of the cations in the orthovanadate structure on the selectivity in the oxidative dehydrogenation reaction. Investigation of the effect of support. DOE

N91-19940# Lehigh Univ., Bethlehem, PA.
HIGH RESOLUTION MICROSTRUCTURAL AND MICROCHEMICAL ANALYSIS OF ZIRCONIA EUTECTIC INTERFACES
M. R. Notis 1991 4 p
(Contract DE-FG02-84ER-45150)
(DE91-008032; DOE/ER-45150/6) Avail: NTIS HC/MF A01

The research performed here is of significance with respect to new materials technology and in fundamental materials science. The materials being studied, zirconia-based ceramics and eutectics, have application as sensors, as catalyst supports, as substrate materials for high-(Tc) superconductors, and as structural ceramics because of their unusual high-toughness behavior. The work performed on precipitation/coarsening in ternary zirconia ceramics highlights the driving forces which control coarsening kinetics and morphology, and hence which effect mechanical properties during long-time aging. The work performed on microscopy of interphase interfaces in zirconia lamellar eutectics represents the most in-depth study available to date concerning the structure of, and relaxation processes which take place at, interfaces in ceramic materials. DOE

N91-19941# Argonne National Lab., IL.
SILVER-SHEATHED MULTIFILAMENT WIRES
C. T. Wu (Illinois Inst. of Tech., Chicago.), K. C. Goretta, D. Shi, M. T. Lanagan, and R. B. Poeppel Jan. 1991 9 p Presented at the High-Temperature Superconductors: Processing and Microstructure Property Relationships, New Orleans, 17-21 Feb. 1991
(Contract W-31-109-eng-38)
(DE91-008107; CONF-910212-2) Avail: NTIS HC/MF A02

The process for manufacturing Ag-sheathed multifilament superconducting wires was investigated. Bi2Sr(1.7)CaCu2O(x), Pb-doped Bi2Sr2Ca2Cu3O(x), or YBa2Cu3O(x) powders were packed into Ag tubes and swaged into long wires. Pieces were cut from each wire, packed into a second Ag tube and swaged or rolled into multifilament wires. Each wire was then sintered to produce a superconductor. Processing considerations included the sheath workability, effects of compacting and residual stresses, and heat treatment schedules. The superconducting properties of the Bi-based wires were superior to those of the YBa2Cu3O(x) wires at 4.2 K, but not at 77 K. DOE

N91-19942# Sandia National Labs., Albuquerque, NM.
PHASE FORMATION IN THE Tl-Ca-BaCu-O SYSTEM
T. L. Aselage, J. A. Voigt, E. L. Venturini, W. F. Hammetter, S. B. VanDeusen, D. L. Lamppa, R. G. Tissot, M. O. Eatough, and K. D. Keefer (Cincinnati Univ., OH.) 1990 17 p Presented at the 2nd International Ceramic Science and Technology Congress, Orlando, FL, 12-15 Nov. 1990
(Contract DE-AC04-76DP-00789)
(DE91-008184; SAND-90-2754C; CONF-901125-10) Avail: NTIS HC/MF A03

The formation of phases in the Tl-Ca-Ba-Cu-O system under conditions approaching equilibrium has been investigated. The oxygen pressure (approximately 3 atm) and sample temperature (890 C) were held constant, and the Tl2O vapor pressure over the sample was controlled by controlling the temperature of a Tl2O3 source. High source temperature (greater than 825 C) resulted in the formation of Tl-rich, non-superconducting phases. A range of lower source temperatures (725 to 800 C) were found for which the superconducting 2122 and 2223 phases appear to be stable. These phases decomposed with source temperature below about 725 C. Transition temperatures of the superconducting phases in multiphase samples are sharp (123 K for 2223, 100 K for 2122), and do not depend on the Ca:Ba:Cu ratio of the sample. Because of contamination of the samples with BaCO3, the dependence of phase formation and properties on stoichiometry could not be determined. DOE

N91-19943# Academy of Sciences (USSR), Gorky.
DIFFUSE X RAY SCATTERING YBa2Cu3O(6.95) MONOCRYSTAL
G. A. Emelchenko, V. A. Tatarchenko, V. P. Plakhtij, Yu. P. Chernenkov, and A. B. Stratilatov 1988 11 p In RUSSIAN; ENGLISH summary
(DE91-615182; LIYF-1451) Avail: NTIS HC/MF A03

The diffuse scattering of x rays in the single crystal of YBa2Cu3O(6.95) is studied. It is shown that the doubling of the lattice period (a or b) most probably is caused by the quasi-2D ordering of the copper and oxygen valences. The ordering of the oxygen atoms O(4) in the volume about 10(exp -3) of the whole crystal volume is not excluded. DOE

N91-19944# Academy of Sciences (USSR), Gorky.
HIGHER HARMONICS OF MAGNETIZATION IN THE CRITICAL STATE OF CERAMIC HIGH Tc SUPERCONDUCTORS
S. L. Ginzburg, I. D. Luzyanin, V. P. Khavronin, and G. Yu. Logvinova 1989 12 p
(DE91-615506; LIYF-1524) Avail: NTIS HC/MF A03

The study of field dependence of dynamic susceptibility of the first and higher harmonics in ultra-low fields is performed. The results show the satisfactory fit with the conclusions of the critical state theory of low field electrodynamics of high-Tc superconductors. DOE

N91-19945# Academy of Sciences (USSR), Gorky.
MAGNETISM AND SUPERCONDUCTIVITY IN YBa2Cu3O(6+x) AT 0.3 LESS THAN OR EQUAL TO x LESS THAN OR EQUAL TO 0.4
S. G. Barsov, A. A. Vasilev, A. L. Getalov, V. P. Koptev, L. A. Kuzmin, S. M. Mikirtychyants, G. V. Shcherbakov, R. K. Nikolaev, N. S. Sidorov, and V. K. Fedotov 1989 9 p In RUSSIAN
(DE91-615507; LIYF-1552) Avail: NTIS HC/MF A02

The investigations of the magnetic and superconducting properties in YBa2Cu3O(6.37) ceramic sample are performed. It is shown that irreversible phenomena take place at T=4.7 K when the magnetic correlations occupy not less than 95 percent of the total sample volume. These results are compared with ones for antiferromagnetic YBa2Cu3O(6.35) and superconducting YBa2Cu-3O(6.4) samples. DOE

N91-19946# Max-Planck-Inst. fuer Radioastronomie, Bonn (Germany, F.R.).
QUANTUM OPTICS REVEALS THE NATURE OF SUPERCONDUCTIVITY

Harald H. Groebke 1990 28 p Presented at Lausanne Univ. Institute de Physique Experimentale Autumn Seminar, Lausanne, Switzerland, Oct. 1990
(TR-69; ETN-91-98809) Avail: NTIS HC/MF A03

The use of the electron state vector was recently shown to resolve the difficulties with the interpretation of photoelectron spectra. A method of obtaining the complete Hamilton operator in harmony with the Pauli exclusion principle is described; thus, the foundation for a rigorous new theory of superconductivity without electron pairing is created. Starting from first principles of quantum field theory, the characteristic effects of superconductivity are described consistently with most of them being the superposition of single electron effects. The phase coherence in a system of superconduction electrons is explained by the coupling to a slaving boson field. A paper on the theory of photon assisted tunneling is included. ESA

N91-19947# Technische Univ., Delft (Netherlands).
CLASSICAL AND QUANTUM CHARGE DYNAMICS IN SMALL TUNNEL JUNCTIONS Ph.D. Thesis
Lambert Johan Geerligs 1990 168 p Sponsored by Stichting voor Fundamenteel Onderzoek der Materie
(ETN-91-98916) Avail: NTIS HC/MF A08

An experimental study of the effects of a small capacitance on the electrical conduction in systems of small tunnel junctions is presented. In zero magnetic field, the characteristics of the junctions with superconducting electrodes are studied. In normal and superconducting state the characteristics of arrays of high resistance junctions show clear Coulomb blockade of single electron and Cooper pair tunneling respectively. A frequency controlled turnstile device for single electrons based on a small array of high resistance junctions was operated. Limitations to the accuracy of the yielded charge or current source are discussed. Some possible mechanisms to operate a turnstile device for Cooper pairs are discussed. The effects of finite barrier transparency on charge dynamics are studied for junctions with well defined capacitance (i.e. those incorporated in arrays). ESA

N91-19948# Technische Univ., Berlin (Germany, F.R.). Fachbereich Elektrotechnik.
MUTUAL INFLUENCE OF DOPING AND OXIDATION IN HIGHLY DOPED SILICON Ph.D. Thesis [GEGENSEITIGE BEEINFLUGSUNG VON DOTEIRUNG UND OXIDATION BEI HOCHDOTIERTEM SILIZIUM]
Erich Biermann 1990 117 p In GERMAN
(ETN-91-98924) Avail: NTIS HC/MF A06

Arsenic was used as a doping material. The oxidation took place in a wet atmosphere, at normal pressure and temperature of 700, 800, and 900 C. The oxidation rate of highly doped silicon is, in general, higher than for nondoped ones. The Ho and Plummer formula is used in simulation programs, in order to take this effect into consideration. The increase in oxidation rate is attributed to the higher electron concentration and the consecutive displacement of Fermi levels in doped silicon. A direct measurement of the electrical activity of the doping material piling showed that the redistributed doping material is not electrically active at 700 and 800 C. At 900 C, one part of the doping material is activated. The influence of the strong mechanical stresses of materials on surface reaction rate is to be particularly noticed. ESA

N91-19949# Technische Univ., Eindhoven (Netherlands).
INDIUM TIN OXIDE FOR SOLID-STATE IMAGE SENSORS Ph.D. Thesis
Christianus Hermanus Weijtens 1990 201 p
(ETN-91-98932) Avail: NTIS HC/MF A10

Solid State Image Sensors (SSIS) which convert light into an electrical signal are introduced and transparent conductive materials and their deposition methods are reviewed as a solution to imager problems. The development of basic tools to enable replacement of poly-Si by Indium Tin Oxide (ITO) in SSIS is addressed. The installation and optimization of deposition equipment, the development of deposition and process technology of ITO, and the implementation and application of ITO in an image sensor are studied. Deposition rate and homogeneity and morphology and parameters like gas composition, power, pressure and substrate temperature are considered. Scope is limited to a first generation frame transfer imager with only one ITO layer although some concepts of an all ITO imager are discussed. The sensor used is a redesign of the accordion imager. All requirements imposed on ITO were met and the usefulness of the developed technology was demonstrated by implementing ITO in an imager. The characteristics of a constructed frame-transfer image sensor in which half the gates in the light sensitive part were replaced by ITO gates are discussed. ESA

N91-19814# Joint Publications Research Service, Arlington, VA.
ORIGIN OF RESIDUAL SURFACE RESISTANCE OF CERAMIC HIGH-TEMPERATURE SUPERCONDUCTORS Abstract Only
N. V. Fomin *In its* JPRS Report: Science and Technology. USSR: Physics and Mathematics 31 Oct. 1990 p 17-18 Transl. into ENGLISH from Pisma v Zhurnal Tekhnicheskoy Fiziki (Leningrad, USSR), v. 16, no. 1, 12 Jan. 1990 p 77-79 (For primary document see N91-19800 11-70)
Avail: NTIS HC/MF A03

N91-19815# Joint Publications Research Service, Arlington, VA.
LIMITING PULSE SIGNAL IN NbN-Si STRUCTURE: SUPERCONDUCTOR FILM ON SUBSTRATE Abstract Only
Ye. F. Gatsura, A. B. Kozyrev, and T. B. Samoylova *In its* JPRS Report: Science and Technology. USSR: Physics and Mathematics 31 Oct. 1990 p 19 Transl. into ENGLISH from Zhurnal Tekhnicheskoy Fiziki (Leningrad, USSR), v. 60, no. 1, Jan. 1990 p 218-222 (For primary document see N91-19800 11-70)
Avail: NTIS HC/MF A03

N91-19816# Joint Publications Research Service, Arlington, VA.
EFFECT OF PARAMAGNETIC IMPURITIES ON DYNAMICS OF MAGNETIC FLUXES IN SUPERCONDUCTORS Abstract Only
Yu. I. Gorobets, A. N. Kuchko, and V. I. Finokhin *In its* JPRS Report: Science and Technology. USSR: Physics and Mathematics 31 Oct. 1990 p 20 Transl. into ENGLISH from Ukrainskiy Fizicheskiy Zhurnal (Kiev, USSR), v. 35, no. 1, Jan. 1990 p 131-135 (For primary document see N91-19800 11-70)
Avail: NTIS HC/MF A03

N91-19817# Joint Publications Research Service, Arlington, VA.
PHENOMENOLOGICAL THEORY OF PHASE TRANSITIONS TO NONHOMOGENEOUS NONCOMMENSURATE PHASE WITH SUPERCONDUCTING CURRENT Abstract Only
A. M. Prokhorov, A. Ya. Braginskiy, Yu. M. Gufan, and Ye. G. Rudashevskiy *In its* JPRS Report: Science and Technology. USSR: Physics and Mathematics 31 Oct. 1990 p 20 Transl. into ENGLISH from Doklady Akademii Nauk SSSR (Moscow, USSR), v. 310, no. 3, 30 Jan. 1990 p 599-603 (For primary document see N91-19800 11-70)
Avail: NTIS HC/MF A03

N91-19818# Joint Publications Research Service, Arlington, VA.
THERMAL CONDUCTIVITY OF HIGH-TEMPERATURE SUPERCONDUCTORS IN NORMAL STATE Abstract Only
A. Jezowski, J. Klamut, and J. Trojnar *In its* JPRS Report: Science and Technology. USSR: Physics and Mathematics 31 Oct. 1990 p 21 Transl. into ENGLISH from Fizika Nizkikh Temperatur (Kharkov, USSR), v. 15, no. 10, Oct. 1989 p 1025-1031 (For primary document see N91-19800 11-70)
Avail: NTIS HC/MF A03

N91-19819# Joint Publications Research Service, Arlington, VA.
SUPERCONDUCTIVITY OF OXIDE FILM ELECTROLYTICALLY DEPOSITED ON SURFACE OF B(1-x)Sb(x) SINGLE CRYSTAL Abstract Only
V. N. Alfeyev, B. A. Aminov, N. B. Brandt, S. Ya. Vasina, B. B. Damaskin, M. Zigel, V. P. Kuznetsov, O. A. Petriy, Ya. G. Ponomarev, and M. V. Sudakova et al *In its* JPRS Report: Science and Technology. USSR: Physics and Mathematics 31 Oct. 1990 p 21-22 Transl. into ENGLISH from Fizika Nizkikh

Temperatur (Kharkov, USSR), v. 15, no. 10, Oct. 1989 p 1099-1101 (For primary document see N91-19800 11-70)
Avail: NTIS HC/MF A03

77 THERMODYNAMICS AND STATISTICAL PHYSICS

Includes quantum mechanics; theoretical physics; and Bose and Fermi statistics.

For related information see also *25 Inorganic and Physical Chemistry* and *34 Fluid Mechanics and Heat Transfer.*

N91-19950# Oak Ridge National Lab., TN.
LOSS ANALYSIS OF THE THERMODYNAMIC CYCLE OF MAGNETIC HEAT PUMPS
F. C. Chen, R. W. Murphy, V. C. Mei, G. L. Chen, J. W. Lue, and M. S. Lubell Feb. 1991 85 p
(Contract DE-AC05-84OR-21400)
(DE91-007669; ORNL/TM-11608) Avail: NTIS HC/MF A05

The needs for developing non-ozone-depleting, no-greenhouse-effect heat pump systems and for exploring the potential of new high-temperature superconducting materials have prompted a renewed interest in the study of magnetic heat pumps. The new materials can provide the high magnetic field that an effective superconducting magnetic heat pump requires, and magnetic heat pumps do not use freon for a working fluid. Traditionally, magnetic heat pump concepts have been successfully developed and used for refrigeration applications at temperatures near absolute zero degree. In these cases, a temperature lift of a few degrees in a cryogenic environment is sufficient and can be easily achieved by a simple magnetic heat pump cycle. The working media are usually the chemical compounds of gadolinium. To extend magnetic heat pumping to other temperature ranges and other types of applications in which the temperature lift is more than just a few degrees requires more involved cycle processes dependent upon the thermomagnetic properties of the working media and the availability of a high magnetic field. This report documents our efforts to study the thermophysics of magnetic heat pumps, including a survey of literature, a study of thermodynamic cycles and cycle thermal losses, and an analysis of pulse magnets. The regenerative cycle has been identified as the most efficient, with a maximum of 42 percent loss in coefficient of performance at 260 K cooling temperature and a maximum of 15 percent loss in capacity at 232 K cooling temperature for the constant field (magnetic Ericsson) cycle, between 200 and 320 K, as compared with the ideal regenerative cycle with gadolinium as the core material. DOE

N91-19951# California Univ., Berkeley. Lawrence Berkeley Lab.
SYMMETRIES ON THE SPACE OF (2,2) SUPERSTRING VACUA AND AUTOMORPHISM GROUPS OF CALABI-YAU MANIFOLDS
A. Giveon and D. J. Smit Aug. 1990 35 p Presented at the International Seminar on Common Threads in Mathematics and Quantum Field Theory, Kyoto, Japan, 10-22 May 1990
(Contract DE-AC03-76SF-00098)
(DE91-008218; LBL-29470; CONF-9005316-1; UCB-PTH-90/37)
Avail: NTIS HC/MF A03

Symmetry groups on the space of (2,2) string vacua for c = 3, 6, and 9 are discussed in the context of orbifoldized Landau-Ginzburg theories. A general method for finding the maximal symmetry groups on the moduli space of untwisted marginal operators is presented by studying symmetries on the resolution of isolated singularities of superpotentials. Stabilizing subgroups of such symmetry groups are shown to correspond with automorphism groups of Calabi-Yau manifolds. In addition to our earlier work on this subject, we present some new examples for c = 9 (2,2) vacua. Subsequently we discuss modular transformations that relate small volume target-spaces to large ones. DOE

80 SOCIAL SCIENCES (GENERAL)

Includes educational matters.

No abstracts in this category.

81 ADMINISTRATION AND MANAGEMENT

Includes management planning and research.

N91-19952# National Academy of Sciences - National Research Council, Washington, DC.
REPORT OF A WORKSHOP ON DISTRIBUTED DECISION MAKING
1990 70 p Workshop held 3-5 Dec. 1986, Washington, D.C.
(Contracts N00014-85-6-0093; MDA903-88-C-0031; MDA903-89-K-0074)
(LC-89-64440; ISBN-0309-04199-6) Avail: NTIS HC/MF A04

The Committee on Human Factors of the National Research Council presents a report on a workshop on distributed decision making. This is defined as the task faced by organizations in which the information and responsibility for decision making is distributed among individuals within the organization, who are often distributed geographically. The Committee recognized that, although the term was new, the problem is an old one that has been given important new aspects and complications by advances in modern technology. Topics discussed include systems design, theories for distributed decision making, alternate definitions, appropriate applications, human factors, and required institutional structures for research on distributed decision making. A number of research projects are suggested. J.P.S.

N91-19953# Department of Energy, Washington, DC. Materials Sciences Div.
MATERIALS SCIENCES PROGRAMS Report, FY 1990
Jan. 1991 164 p
(DE91-007601; DOE/ER-0483P) Avail: NTIS HC/MF A08

The purpose of this report is to provide a convenient compilation and index of the DOE Materials Sciences Division programs. This compilation is primarily intended for use by administrators, managers, and scientists to help coordinate research. The report is divided into seven sections. Section A contains all Laboratory projects, Section B has all contract research projects, Section C has projects funded under the Small Business Innovation Research Program, Sections D and E have information on DOE collaborative research centers, Section F gives distribution of funding, and Section G has various indexes. DOE

N91-19954# Royal Military Coll. of Science, Shrivenham (England).
THE IMPACT OF THE NEW MANAGEMENT STRATEGY ON SENIOR OPERATIONAL COMMANDERS AT GROUP LEVEL WITHIN ROYAL AIR FORCE STRIKE COMMAND M.S. Thesis
J. McHale Dec. 1989 151 p
(Rept-89SDM/McHALE/03-MDA; ETN-91-98856) Copyright
Avail: NTIS HC/MF A08

The government's introduction of a financial management initiative has affected the way all government departments do business. The Ministry of Defence for its part is introducing a new management strategy to meet the objectives of the aforementioned initiative. A study which examines how this strategy will be implemented within the Royal Air Force Strike Command group structure is presented. A methodological approach is adopted to analyze how the groups currently operate. Some consideration is given as to how the groups will need to operate when the new management strategy is implemented in April 1992. A number of alternative options for changing the organizational structure of the Command under the strategy are offered. They are considered

from both a theoretical and practical viewpoint before an option is proposed. The implementation of the proposed option is discussed. ESA

82 DOCUMENTATION AND INFORMATION SCIENCE

Includes information management; information storage and retrieval technology; technical writing; graphic arts; and micrography.

For computer documentation see *61 Computer Programming and Software.*

N91-19955# General Accounting Office, Washington, DC.
SPACE OPERATIONS: NASA IS NOT ARCHIVING ALL POTENTIALLY VALUABLE DATA
1991 53 p
(GAO/IMTEC-91-3) Avail: NTIS HC/MF A04

The Government Accounting Office (GAO) presents to the House Committee on Science, Space, and Technology the GAO findings on the National Aeronautics and Space Administration's (NASA's) handling of space science data, including its selection, management, and dissemination. In particular, GAO was to determine if NASA: (1) was archiving all of its valuable space science data, and (2) had a mechanism in place to allow scientists to provide input on what data should be archived. GAO found that NASA's 1978 policy does not require original or certain research and scientific data to be archived, and missions do not prepare requisite plans for data management, archiving, and disposition. NASA's existing network of committees, advisory panels, and working groups gives scientists an opportunity to provide input on the planning, development, and operation of mission data processing systems. However, their participation is not required and either may not occur or their recommendations may not be implemented. NASA is taking steps to expand the role of outside scientists in the management and archiving of space science data. GAO recommends that NASA take appropriate action to ensure that any valuable missing data from past missions is archived; revise data management policy to ensure that all valuable data are archived; and identify areas where the participation of scientists in data management and archiving activities should be strengthened. Details on the investigation and recommendations are provided. J.P.S.

N91-19956 North Carolina Univ., Chapel Hill.
IMPROVED SYNTACTIC DISAMBIGUATION IN THE FASIT AUTOMATIC INDEXING ENVIRONMENT Ph.D. Thesis
Robert Edward Burgin 1990 221 p
Avail: Univ. Microfilms Order No. DA9034682

The development, implementation, and evaluation of an improved disambiguation mechanism within the FASIT automatic indexing system are examined. The enhanced disambiguation mechanism relies on a recursive transition network to improve the indexing representation produced by FASIT by enhancing the system's ability to disambiguate syntatic tags assigned to the words of a text and thereby to improve retrieval results. FASIT with the recursive transition network was compared with FASIT alone and with single-term indexing on retrieval effectiveness in experiments with two databases. Both versions of FASIT showed noticeable improvement over single-term indexing with a database of articles on cystic fibrosis, and both showed material improvement over single-term indexing with a subset of the Inspec database. However, in neither case did FASIT with the enhanced disambiguation mechansism provide even noticeable improvement over FASIT alone. The failure of FASIT with the recursive transition network to improve upon the retrieval results of FASIT alone appeared to be due primarily to the interaction of two factors: the inability of the recursive transition network to correctly disambiguate more than 40 percent of the sentences requiring further disambiguation; and the stepwise reduction of the effectiveness of further disambiguation in the FASIT environment. A retrieval experiment using a complete manual disambiguation of a sample of documents from the cystic fibrosis database produced no noticable difference between FASIT alone and FASIT with the manual disambiguation. Dissert. Abstr.

N91-19957# Iona Coll., New Rochelle, NY. Machine Intelligence Inst.
THE DEVELOPMENT OF STRUCTURE FOR THE REPRESENTATION AND MANIPULATION OF SOPHISTICATED KNOWLEDGE IN INTELLIGENT SYSTEMS Final Technical Report, 1 Apr. 1989 - 31 Mar. 1990
Ronald R. Yager 31 Mar. 1990 9 p
(Grant AF-AFOSR-0126-87; AF Proj. 2304)
(AD-A229114; AFOSR-90-1112TR) Avail: NTIS HC/MF A02
CSCL 12/9

The central focus of the research was the development of a unified theory for reasoning under uncertainty in knowledge base systems. In particular an effort was made to bring together the concepts of fuzziness, lack of specificity, randomness, and monotonicity, under one framework. A number of issues relating to this goal were investigated. This effort resulted in 56 submitted papers of which 49 have been published and 7 are to appear in the near future. GRA

N91-19958# Fermi National Accelerator Lab., Batavia, IL.
TABLE OF TABLES: A DATABASE DESIGN TOOL FOR SYBASE
B. C. Brown, K. Coulter, H. D. Glass, R. Glosson, R. W. Hanft, D. J. Harding, K. Trombly-Freytag, D. G. C. Walbridge, D. B. Wallis, and M. E. Allen (Superconducting Super Collider Lab., Dallas, TX.) Jan. 1991 48 p
(Contract DE-AC02-76CH-03000)
(DE91-007257; FNAL-TM-1707) Avail: NTIS HC/MF A03

The 'Table of Tables' application system captures in a set of SYBASE tables the basic design specification for a database schema. Specification of tables, columns (including the related defaults and rules for the stored values) and keys are provided. The feature which makes this application specifically useful for SYBASE is the ability to automatically generate SYBASE triggers. A description field is provided for each database object. Based on the data stored, SQL scripts for creating complete schema including the tables, their defaults and rules, their indexes, and their SYBASE triggers, are written by TOT. Insert, update and delete triggers are generated from TOT to guarantee integrity of data relations when tables are connected by single column foreign keys. The application is written in SYBASE's APT-SQL and includes a forms based data entry system. Using the features of TOT we can create a complete database schema for which the data integrity specified by our design is guaranteed by the SYBASE triggers generated by TOT. DOE

N91-19959*# National Aeronautics and Space Administration. Lyndon B. Johnson Space Center, Houston, TX.
THE 1989 JSC BIBLIOGRAPHY OF SCIENTIFIC AND TECHNICAL PAPERS
Nancy Hutchins, comp. Jan. 1991 240 p
(NASA-TM-102173; S-621; NAS 1.15:102173) Avail: NTIS HC/MF A11 CSCL 05B

This document is a compilation of Lyndon B. Johnson Space Center contributions to the scientific and technical literature in aerospace and life sciences made during calendar year 1989. Citations include NASA formal series reports, journal articles, conference and symposium presentations, papers published in proceedings or other collective works, and seminar and workshop results. Author

N91-19960# Sandia National Labs., Albuquerque, NM.
ANALYZING PRODUCT TEST DATA IN A RELATIONAL DATABASE USING SAS SOFTWARE
J. L. Orman 1991 33 p Presented at the 16th Annual SAS Users Group International Conference, New Orleans, 17-20 Feb. 1991
(Contract DE-AC04-76DP-00789)

(DE91-007734; SAND-91-0312C; CONF-910280-1) Avail: NTIS HC/MF A03

SAS software is being used to analyze product test data stored in an INGRES relational database. The database has been implemented at Allied-Signal in Kansas City on a Digital Equipment Corporation (DEC) VAX computer. The INGRES application development has been a joint project between Sandia National Laboratories and Allied-Signal. Application screens have been developed so that the user can query the database for selected data. Fourth generation language procedures are used to retrieve all data requested. FORTRAN and VAX/VMS DCL (DIGITAL Control Language) procedures are invoked from the application to create SAS data sets and dynamically build SAS programs that are executed to build custom reports or graphically display the retrieved test data along with control and specification limits. A retrieval screen has also been developed which invokes SAS software to calculate the mean and standard deviation of the retrieved data. These parameters are passed back into the application for display and may then be used as an aid in setting new control limits for future test runs. Screens have been developed to provide an interface for the user to select from a library of SAS programs, edit the selected program, and run the program with a user-defined SAS data set as input. This paper will give a brief description of the application screens and provide details of how information is passed between the application and SAS programs. DOE

N91-19961# Oak Ridge National Lab., TN.
ENVIRONMENTAL SCIENCES DIVISION COMPUTING AND GEOGRAPHIC INFORMATION SYSTEM FACILITY USER HANDBOOK
R. A. McCord Dec. 1990 123 p
(Contract DE-AC05-84OR-21400)
(DE91-007820; ORNL/TM-11711) Avail: NTIS HC/MF A06

The Environmental Sciences Division (ESD) at Oak Ridge National Laboratory (ORNL) operates a Computing and Geographic Information System Facility as a tool for its environmental research. This facility provides ESD staff and guests with three major computing functions: (1) a remote batch station (RBS) for processing print and plot output from other ORNL systems, (2) a geographic information system (GIS) for mapping and spatial analysis of environmental problems, and (3) an ethernet network for high-speed communications, file sharing, and printer sharing services. This handbook provides an overview of the components of the facility. The overview includes the staff, computers, peripherals, and communications. Generic descriptions of the user commands to send print and plot output to the ESD RBS are also provided. Information and guidelines are presented for the direct use of the ESD VAX and GIS. The unique operational aspects of this VAX installation (e.g. queue names, device names, local commands, and telecommunications pathways) are documented. The ESD GIS is and application of the direct VAX users. Because special GIS commands have been developed by ESD staff, these commands are documented in more detail in a series of appendixes. Computer security, authorization, disk management, backup, and facility access policies and procedures are described to clarify the users expectations and responsibilities while utilizing the ESD systems. The network service functions of the ESD VAXes are described for the direct users and members of the ESD PC-VAX network. Explanations of commands for file transfer and remote system access are included. Remote disk sharing and remote printer sharing services for personal computers are also described. DOE

N91-19962*# National Aeronautics and Space Administration, Washington, DC.
NASA THESAURUS SUPPLEMENT: A FOUR PART CUMULATIVE SUPPLEMENT TO THE 1988 EDITION OF THE NASA THESAURUS (SUPPLEMENT 5) Semiannual Report
Mar. 1991 49 p
(NASA-SP-7064-Suppl-5; NAS 1.21:7064-Suppl-5) Avail: NTIS HC/MF A03 CSCL 05B

The four-part cumulative supplement to the 1988 edition of the NASA Thesaurus includes the Hierarchical Listing (Part 1), Access Vocabulary (Part 2), Definitions (Part 3), and Changes (Part 4). The semiannual supplement gives complete hierarchies and accepted upper/lowercase forms for new terms. Author

N91-19963# Superconducting Super Collider Lab., Dallas, TX.
PROTOTYPE DOCUMENT TRACKING AND STORAGE SYSTEM FOR THE SUPERCONDUCTING SUPER COLLIDER LABORATORY (SSCL)
N. E. Wells Oct. 1990 4 p Presented at the Symposium on Detector Research and Development for the Superconducting Super Collider, Fort Worth, TX, 15-18 Oct. 1990
(Contract DE-AC02-89ER-40486)
(DE91-008204; SSCL-338; CONF-9010212-33) Avail: NTIS HC/MF A01

The design and development of the detectors for the SSCL will be facilitated by a central system to track and store the design documents and drawings. Collaborators and SSCL personnel need a single system that they can access from a terminal on their desk and be able to locate and view the latest version of a document. The SSCL is developing a prototype system to track documents and drawings, and to make them accessible via the local and wide-area networks. The prototype will be used to refine the requirements and to develop the procedures for a larger system that will be acquired later. This paper discusses the system requirements, architecture, and status. DOE

N91-19964# Sandia National Labs., Albuquerque, NM.
AN ARCHITECTURE FOR ACCOMMODATING REFERENCEABILITY AMONG INTELLIGENT ELECTRONIC DOCUMENTS
R. C. Hall 1991 12 p Presented at the Southwest Regional INGRES Users Association Meeting, Albuquerque, NM, 28 Feb. - 1 Mar. 1991
(Contract DE-AC04-76DP-00789)
(DE91-008250; SAND-91-0414C; CONF-910276-2-Vugraphs)
Avail: NTIS HC/MF A03

This presentation identifies an architecture for compiling and representing electronic documents in a framework which accommodates knowledge about how the documents are composed, organized, and correlated. A general concept of referenceability is employed. While the concept is relevant to a wide range of application areas, it is described in familiar terms of an electronic document comprised of related textual information and graphics. The concept is applicable to all classes of objects which, together with their references, constitute the electronic document. The documents may themselves contain references to other documents, as well as to constituent object classes such as textual components, figures, footnotes, subject indexes, and the like. The objects and references can be dynamically combined according to a total logical structure representable within a window environment. The framework supports automatic resolution of references and display of related document objects through intercommunicating windows which constitute a relevant user view of a document. DOE

N91-19965# Sandia National Labs., Albuquerque, NM.
ANALYZING PRODUCT TEST DATA IN AN INGRES DATABASE USING SAS SOFTWARE
J. L. Orman 1991 19 p Presented at the Southwest Regional INGRES Users Association Meeting, Albuquerque, NM, 28 Feb. - 1 Mar. 1991
(Contract DE-AC04-76DP-00789)
(DE91-008251; SAND-91-0431C; CONF-910276-3-Vugraphs)
Avail: NTIS HC/MF A03

SAS software is being used to analyze product test data stored in an INGRES database. The database has been implemented at Allied-Signal in Kansas City on a DEC VAX computer. The INGRES application development was a joint project between Sandia National Labs and Allied-Signal. INGRES ABF/4GL was used to develop application screens so that the user can query the database for selected data. Fourth generation language procedures are used to retrieve all data requested. FORTRAN

and VAX/VMS DCL (DIGITAL Control Language) procedures are invoked from the application to create SAS data sets and dynamically build SAS programs that are executed to build custom reports or graphically display the retrieved test data along with control and specification limits. A retrieval screen was also developed which invokes SAS software to calculate the mean and standard deviation of the retrieved data. These parameters are passed back into the application for display and may then be used as an aid in setting new control limits for future test runs. Screens were developed to provide an interface for the user to select from a library of SAS programs, edit the selected program, and run the program with a user-defined SAS data set as input. A brief description is given of the application screens and provide details of how information is passed between the INGRES application and SAS programs. DOE

83 ECONOMICS AND COST ANALYSIS

Includes cost effectiveness studies.

No abstracts in this category.

84 LAW, POLITICAL SCIENCE AND SPACE POLICY

Includes NASA appropriation hearings; aviation law; space law and policy; international law; international cooperation; and patent policy.

N91-19966# Committee on Appropriations (U.S. Senate).
DEPARTMENTS OF VETERANS AFFAIRS AND HOUSING AND URBAN DEVELOPMENT, AND INDEPENDENT AGENCIES APPROPRIATION BILL, 1991
Barbara Mikulski Washington GPO 1990 178 p Report to accompany H.R. 5158 presented by the Committee on Appropriations, 101st Congress, 2d Session, 26 Sep. 1990
(S-Rept-101-474; GPO-34-529) Avail: Document Room, Senate, Washington, DC 20510 HC free

The Senate Committee on Appropriations presents, with various amendments and an explanation of the contents, the bill making appropriations for the Departments of Veterans Affairs and Housing and Urban Development, and for sundry independent agencies, boards, commissions, corporations, and offices, for the fiscal year ending 30 September 1991. For individual titles, see N91-19967 through N91-19967.

N91-19967# Committee on Appropriations (U.S. Senate).
NATIONAL AERONAUTICS AND SPACE ADMINISTRATION
In its Departments of Veterans Affairs and Housing and Urban Development, and Independent Agencies Appropriation Bill, 1991 1990 p 128-146 (For primary document see N91-19966 11-84)
Avail: Document Room, Senate, Washington, DC 20510 HC free

Following a general description of NASA's structure and a summary of each center's activities, NASA's mission and its objectives are presented. The Senate Committee on Appropriations lists its recommendations for funding. It also recommends cuts in several specific programs. J.P.S.

N91-19968# Committee on Science, Space and Technology (U.S. House).
COMMERCIAL SPACE LAUNCH ACT IMPLEMENTATION
Washington GPO 1990 245 p Hearing before the Committee on Science, Space, and Technology, 101st Congress, 1st Session, No. 98, 9 Nov. 1989
(GPO-27-944) Avail: Subcommittee on Space Science and Applications, House of Representatives, Washington, DC 20515 HC free; also available SOD HC $7.00 as 552-070-08309-0

Hearings before the House Subcommittee on Space Science and Applications of the Committee on Science, Space, and Technology are presented on the implementation of the Commercial Space Launch Act. The stability, support, guidelines, and provision of launch services by government agencies for companies engaged in commerce in space is examined. J.P.S.

N91-19969# Committee on Appropriations (U.S. Senate).
PROBLEMS AT NATIONAL AERONAUTICS AND SPACE ADMINISTRATION
Washington GPO 1991 63 p Special hearing before the Committee on Appropriations, 101st Congress, 2d Session, 18 Jul. 1990
(S-Hrg-101-1146; GPO-36-778) Avail: Committee on Appropriations, Senate, Washington, DC 20510 HC free; also available SOD HC $2.00 as 552-707-09795-3

Hearings before the Subcommittee on Veterans Affairs, Housing and Urban Development, and Independent Agencies of the Senate Committee on Appropriations are presented on problems at the National Aeronautics and Space Administration (NASA). The hearing focused on the Hubble telescope, the space shuttle, and the space station and effects that problems with these projects have on the Federal budget. The management structure of NASA was discussed and the need for adequate support not only for space operations but also for research. Various broad issues were discussed as they pertain to the Subcommittee's stated goal of an affordable, achievable space program. Senator Garn noted that the identification and open discussion of problems with space projects when they are in the design stage is a necessary step for a successful mission. He stressed that the identification and discussion of problems that need to be corrected before liftoff is not pointing a finger at NASA's failures, as media personnel seem to perceive it, but is a normal and essential procedure which should be understood as such by the American taxpayers. J.P.S.

85 URBAN TECHNOLOGY AND TRANSPORTATION

Includes applications of space technology to urban problems; technology transfer; technology assessment; and surface and mass transportation.

For related information see also *03 Air Transportation and Safety, 16 Space Transportation,* and *44 Energy Production and Conversion.*

N91-19970# Office of Science and Technology, Washington, DC.
US TECHNOLOGY POLICY: EXECUTIVE OFFICE OF THE PRESIDENT
26 Sep. 1990 17 p
(PB91-119677) Avail: NTIS HC/MF A03 CSCL 05A

A statement of the Administration's technology policy is presented. Many facets of technology policy are brought together, and it is shown how they fit into a comprehensive framework. The goals and strategies of this policy are discussed. The program implementation proposed in the Administration's Fiscal Year 1991 budget submittal to Congress is presented. Areas associated with classified national security technologies are not included. A nation's technology policy is based on the broad principles that govern the allocation of its technological resources. Competitive market forces determine, for the most part, an optimal allocation of U.S. technological resources. Government can nonetheless play an important role by supplementing and complimenting those forces. Y.S.

88 SPACE SCIENCES (GENERAL)

N91-19971# Max-Planck-Inst. fuer Physik und Astrophysik, Garching (Germany, F.R.). Inst. fuer Extraterrestrische Physik.
[ACTIVITIES REPORT OF THE INSTITUTE FOR EXTRATERRESTRIAL PHYSICS] Report, 1988-1990
Sep. 1990 101 p
(MPE-222; ISSN-0178-7101; ETN-91-98806) Copyright Avail: NTIS HC/MF A06

This report, directed at fellow scientists, emphasizes the physical aspects of the Institute. Details of the preceding year, ongoing activities and plans for the future are given. Space and astrophysical research work is described under the headings: the solar system; life cycle of stars; interstellar medium; extragalactic astrophysics; laboratory astrophysics; first results from ROSAT (Roentgen Satellite). The present knowledge of the particular field and the work done at the Institute are described. ESA

89 ASTRONOMY

Includes radio, gamma-ray, and infrared astronomy, and astrometry.

N91-19972 Department of the Navy, Washington, DC.
METHOD FOR DETERMINING ASTRONOMIC AZIMUTH Patent
Alan G. Evans, inventor (to Navy) and William L. Stein, inventor (to Navy) 4 Sep. 1990 5 p Filed 5 Jul. 1989
(AD-D014677; US-Patent-4,954,833; US-Patent-Appl-SN-376278; US-Patent-Class-342-357) Avail: US Patent and Trademark Office CSCL 08/5

An improved method is disclosed for fixing position of a land based target site with respect to a reference site in the natural coordinate frame comprising the steps of determining geodetic azimuth between the target site and the reference target using Global Positioning System (GPS) satellites and relative positioning survey techniques; then calculating a relationship using gravity vertical deflections; and then converting the geodetic azimuth to astronomic azimuth. This method has several advantages over conventional methods of targeting, including speed, the ability to work in all weather conditions, and improved accuracy. GRA

N91-19973*# Smithsonian Astrophysical Observatory, Cambridge, MA.
A BALLOON-BORNE 102-cm TELESCOPE FOR FAR-INFRARED ASTRONOMY Final Report
Giovanni G. Fazio Dec. 1990 23 p
(Grant NAGw-17)
(NASA-CR-187778; NAS 1.26:187778) Avail: NTIS HC/MF A03 CSCL 03A

In the early 1970's, the Smithsonian Astrophysical Observatory and the University of Arizona engaged in a cooperative program to develop a balloon-borne 102-cm telescope capable of carrying out far infrared (40 to 250 micron) observations of astronomical interest above the earth's atmosphere. Since 1972, the telescope has flown and successfully recovered a total of nineteen times. Thirteen of the flights produced high-quality astronomical data, resulting in more than 92.5 hours of photometric and spectroscopic observations of numerous objects, such as H 2 regions, dark clouds, molecular clouds, a planetary nebula, a galaxy, the galactic center, the planets, and an asteroid. From the launch site in Palestine, Texas, sources as far south as -50 degrees declination were observed. The balloon-borne telescope was one of the most sensitive instruments ever used for observation in the far infrared region of the spectrum. It was most productive in producing high resolution maps of large areas (typically square degrees) centered on known H 2 regions, molecular clouds, and dark cloud complexes. In many cases, these scans produced the first far infrared maps of these regions, and many new sources were discovered. The results have led to a better understanding of the distribution of gas and dust in these regions, the evolution of H 2 regions, and the processes of star formation in giant molecular clouds. The following topics are presented: (1) the focal plane instrumentation; (2) the history and flight record; (3) scientific results and publications; (4) eduational aspects; and (5) future planes. Author

N91-19974# Committee on Commerce, Science, and Transportation (U.S. Senate).
HUBBLE SPACE TELESCOPE AND THE SPACE SHUTTLE PROBLEMS
Washington GPO 1990 59 p Hearing before the Committee on Commerce, Science, and Transportation, 101st Congress, 2d Session, 10 Jul. 1990
(S-Hrg-101-1087; GPO-36-688) Avail: Subcommittee on Science, Technology, and Space, Senate, Washington, DC 20510 HC free; also available SOD HC $2.00 as 552-070-09632-9

Hearings before the Subcommittee on Science, Technology, and Space of the Senate Committee on Commerce, Science, and Transportation are presented on oversight on recent problems with the Hubble space telescope and the space shuttle. The question of testing versus a test's costs, risks, and information yield are discussed as well as, lessons learned in management. The Subcommittee reviewed NASA's quality control procedures, the adequacy of Congressional and Office of Management and Budget support, and government's verification responsibilities. Oral and written testimony from NASA management and pertinent contractors is included. J.P.S.

N91-19975*# California Inst. of Tech., Pasadena.
[HIGH RESOLUTION INFRARED ASTRONOMY SATELLITE OBSERVATIONS OF A SELECTED SPIRAL GALAXY]
S. R. Kulkarni 1991 44 p
(Grant NAG5-1164)
(NASA-CR-188019; NAS 1.26:188019) Avail: NTIS HC/MF A03 CSCL 03A

The H I, infrared, CO, H alpha and H beta band observations of M51, the prototypical grand-design spiral galaxy, are used to study the consequences of star formation for the distribution of H I and dust. Using the new Very Large Array (VLA) map of 21 cm emission, the Owens Valley Radio Observatory CO mosaic map, and an H alpha imate, new tests were performed with the idea of Tilanus and Allen that the H I is largely a photodissociation product in star-forming regions. It is confirmed that the H I spiral arms are generally coincident with the H II region arms, and offset downstream from the CO arms. The radial distributions of total gas, H alpha and H I surface density have a simple explanation in the dissociation picture. The distributions also demonstrate how the surface density of H I might be related to the star formation efficiency in molecule-rich galaxies. The large width of the H I regions along the arms compared to that of the giant H II regions can be understood in terms of a simple calculation of the expected size of an H I region associated with a typical giant H II region. The longer lifetime of the stars producing dissociating radiation vs. those producing ionizing radiation and the relatively long molecular formation timescale will also contribute to the greater width of the H I arms if stars are continuously forming on the arms. The lack of detailed coincidence of the H I and H II regions along the inner arms has a variety of possible explanations. Two simple tests were performed to probe the origins of the IRAS emission in M51. First, it was found that the infrared excess (IFE) of M51 is 24, suggesting that a substantial fraction of the infrared emission arises from dust heated by photons which do not originate in massive star-formaing regions. Second, radial cuts through the IRAS bands show that at 12, 25, and 60 microns, the arm-interarm contrast of the IRAS emission is substantially less than that of the H alpha emission, providing further evidence for the explanation and for the existence of a broadly distributed dust component. Deconvolved IRAS maps have improved resolution but do not change this finding. Author

N91-19976 Max-Planck-Inst. fuer Physik und Astrophysik, Garching (Germany, F.R.). Inst. fuer Extraterrestrische Physik.
DETECTION OF AN ISOTOPIC SHORT SUBMILLIMETER CO LINE: COLUMN DENSITIES OF WARM GAS IN MOLECULAR CLOUDS
U. U. Graf, R. Genzel, A. I. Harris, R. E. Hills, A. P. G. Russel (Joint Astronomy Centre, Hilo, HI.), and J. Stutzki Mar. 1990 22 p Previously announced in IAA as A90-42865 Submitted for publication
(MPE-Preprint-178; ETN-91-98602) Copyright Avail: Fachinformationszentrum Karlsruhe, 7514
Leopoldshafen-Eggenstein 2, Fed. Republic of Germany

The first astronomical detection of the transition of J from 6 to 5 in isotopic CO-13 emission at 661 GHz from the molecular clouds in Orion A and in NGC 2024 is reported. Large column densities of warm, dense, molecular gas are reported in star formation regions, and correspond to greater than 30 percent of the molecular gas mass in this region. They are difficult to explain by present theoretical heating models where the lines and narrow shock heating is unlikely. The correlation of warm CO column density with UV intensity is indicated and favors heating by UV radiation. However, present photodissociation region models fail to predict the large quantities of warm gas detected. ESA

N91-19977 Max-Planck-Inst. fuer Physik und Astrophysik, Garching (Germany, F.R.). Inst. fuer Extraterrestrische Physik.
OBSERVATIONS OF CO ISOTOPIC EMISSION AND THE FAR-INFRARED CONTINUUM OF CENTAURUS A
A. Eckart, M. Cameron, H. Rothermel, W. Wild, H. Zinnecker, G. Rydbeck, M. Olberg, and T. Wiklind (Onsala Space Observatory, Sweden) Apr. 1990 42 p Submitted for publication Sponsored in part by the Royal Society
(MPE-Preprint-183; ETN-91-98607) Copyright Avail: Fachinformationszentrum Karlsruhe, 7514
Leopoldshafen-Eggenstein 2, Fed. Republic of Germany

CO isotopic emission and the far infrared continuum of Centaurus A are examined with the Swedish ESO Submillimeter Telecope (SEST) and the Chopped Photometric Channel (CPC) instrument onboard the Infrared Astronomical Satellite (IRAS). The physical properties of the molecular disk in Centaurus A seem to be very comparable to those of nearby galaxies showing starburst activity, and it appears that most of the peculiarities that are attributed to Centaurus A are probably a mere consequence of its proximity. ESA

N91-19978 Max-Planck-Inst. fuer Physik und Astrophysik, Garching (Germany, F.R.). Inst. fuer Extraterrestrische Physik.
SEARCH FOR THE OPTICAL SIGNATURES OF A PULSAR IN SN1987A
H. Oegelman, C. Gouiffes, T. Augusteijn, H. Pedersen, F. Gutierrez, G. Hasinger, J. Melnick, W. Pietsch, and C. Santini (European Southern Observatory, Garching, Germany, F.R.) Jul. 1990 16 p Previously announced in IAA as A91-14687 Submitted for publication
(MPE-Preprint-188; ETN-91-98612) Copyright Avail: Max-Planck-Institut fuer Physik und Astrophysik, 8046 Garching-bei-Muenchen, Fed. Republic of Germany

Pulsed optical emission from the putative pulsar in SN1987A is searched for, using various ESO telescopes and a fast photometer. In none of the fast Fourier transform outputs of individual nights was an outstanding power in excess of the expected tail of the noise distribution found. The lowest 2 sigma upper limits reached on March and April 1990 correspond to about 3, 4, and 10 microJy (22.5, 22.2 and 21.5 magnitudes) for frequencies above 0.1 Hz up to 50, 500 and 5000 Hz respectively. These limits imply that the pulsar either emits less optical power than the Crab pulsar and the 50 ms pulsar PSR 0540-69 in large magellanic cloud, or it has an unfavorable disposition. Combination of the power outputs of different nights further decrease these upper limits by approximately 0.3 magnitudes. ESA

N91-19979*# National Aeronautics and Space Administration, Washington, DC.
A SCIENTIFIC PROGRAM FOR INFRARED, SUBMILLIMETER AND RADIO ASTRONOMY FROM SPACE: A REPORT BY THE MANAGEMENT OPERATIONS WORKING GROUP
Jun. 1989 54 p Original contains color illustrations
(NASA-TM-103333; NAS 1.15:103333) Avail: NTIS HC/MF A04; 9 functional color pages CSCL 03A

Important and fundamental scientific progress can be attained through space observations in the wavelengths longward of 1 micron. The formation of galaxies, stars, and planets, the origin of quasars and the nature of active galactic nuclei, the large scale structure of the Universe, and the problem of the missing mass, are among the major scientific issues that can be addressed by these observations. Significant advances in many areas of astrophysics can be made over the next 20 years by implementing the outlined program. This program combines large observatories with smaller projects to create an overall scheme that emphasized complementarity and synergy, advanced technology, community support and development, and the training of the next generation of scientists. Key aspects of the program include: the Space Infrared Telescope Facility; the Stratospheric Observatory for Infrared Astronomy; a robust program of small missions; and the creation of the technology base for future major observatories. Y.S.

N91-19980*# Alabama Univ., Huntsville. Dept. of Physics.
GAMMA RAY ASTRONOMY Final Technical Report, 13 Jun. 1990 - 12 Apr. 1991
William S. Paciesas 27 Mar. 1991 19 p
(Contract NAS8-36955)
(NASA-CR-188031; NAS 1.26:188031) Avail: NTIS HC/MF A03 CSCL 03A

Miscellaneous tasks related to the development of the Burst and Transient Source Experiment on the Gamma Ray Observatory and to collection, analysis, and interpretation of data from the MSFC Very Low Frequency transient monitoring program were performed. The results are summarized and relevant references are included. Author

N91-19981# Messerschmitt-Boelkow-Blohm G.m.b.H., Ottobrunn (Germany, F.R.). Unternehmensbereich Hubschrauber.
THERMAL INSULATION OF A CRYOGENIC TANK FOR A SPACE TELESCOPE USING A PRETENSIONED SUSPENSION OF FIBER REINFORCED COMPOSITE (FRC)
Bernd Bongers, Otmar Haider, and Wolfgang Tauber Sep. 1990 8 p Presented at the 4th European Conference on Composite Materials, Stuttgart, Fed. Republic of Germany, 25-28 Sep. 1990
(MBB-UD-0571-90-PUB; ETN-91-98821) Avail: NTIS HC/MF A02

For the thermal insulation of cryogenic tanks in satellite applications Fiber Reinforced Composite (FRC) materials are preferable because of their low thermal conductivity and high tensile strength compared to metallic materials. At the Infrared Space Observatory (ISO) satellite the main Liquid Helium (LHe) tank is suspended by one spatial framework and eight pretensioned chain strands at each side. Frameworks and chain strands are acting as a thermal barrier and therefore made of FRC. To meet the various and, in parts contractive requirements, sophisticated design approaches are chosen for the structural parts. ESA

90 ASTROPHYSICS

Includes cosmology; celestial mechanics; space plasmas; and interstellar and interplanetary gases and dust.
For related information see also *75 Plasma Physics.*

N91-19982 Max-Planck-Inst. fuer Physik und Astrophysik, Garching (Germany, F.R.). Inst. fuer Extraterrestrische Physik.
FLUORESCENT HD EMISSION FROM PHOTODISSOCIATION REGIONS
Amiel Sternberg Mar. 1990 43 p Previously announced in

IAA as A90-48914 Submitted for publication Sponsored in part by Minerva Society Research Fellowship
(MPE-Preprint-177; ETN-91-98601) Copyright Avail: Fachinformationszentrum Karlsruhe, 7514
Leopoldshafen-Eggenstein 2, Fed. Republic of Germany

Computations are presented of the infrared fluorescent HD emission spectrum that is produced in cold, isothermal, static photodissociation regions at the surfaces of interstellar molecular clouds exposed to UV radiation. A scaling equation is derived which relates the HD line intensities to the gas density, the intensity of the incident UV radiation, the grain surface molecular formation rate coefficient, and the cosmic ray ionization rate. Fluorescent HD emission lines may be detectable from dense photodissociation regions with hydrogen densities equal to approximately 5,000,000/cu cm which are exposed to intense UV fields. ESA

N91-19983# Lawrence Livermore National Lab., CA.
SOME LIMITATIONS OF DETAILED BALANCE FOR INVERSE REACTION CALCULATIONS IN THE ASTROPHYSICAL P-PROCESS
D. G. Gardner and M. A. Gardner Dec. 1990 12 p Presented at the 7th International Symposium on Capture Gamma-Ray Spectroscopy and Related Topics, Pacific Grove, 14-19 Oct. 1990
(Contract W-7405-eng-48)
(DE91-007258; UCRL-JC-104716; CONF-901057-28) Avail: NTIS HC/MF A03

P-Process modeling of some rare but stable proton-rich nuclei requires knowledge of a variety of neutron, charged particle, and photonuclear reaction rates at temperatures of 2 to 3 x 10(exp 9) K. Detailed balance is usually invoked to obtain the stellar photonuclear rates, in spite of a number of well-known constraints. We attempt to calculate directly the stellar rates for (gamma ,n) and (gamma, alpha) reactions on Eu-151. These are compared with stellar rates obtained from detailed balance, using the same input parameters for the stellar (n, gamma) and (alpha, gamma) reactions on Eu-150 and Pm-147, respectively. The two methods yielded somewhat different results, which will be discussed along with some sensitivity studies. DOE

N91-19984# Lawrence Livermore National Lab., CA.
PRIMORDIAL NUCLEOSYNTHESIS: BEYOND THE STANDARD MODEL
R. A. Malaney Jan. 1991 29 p Presented at the International Symposium on Nuclear Astrophysics: Nuclei in the Cosmos, Vienna, Austria, 18-22 Jun. 1990
(Contract W-7405-eng-48)
(DE91-007264; UCRL-JC-105971; CONF-9006212-5) Avail: NTIS HC/MF A03

Non-standard primordial nucleosynthesis merits continued study for several reasons. First and foremost are the important implications determined from primordial nucleosynthesis regarding the composition of the matter in the universe. Second, the production and the subsequent observation of the primordial isotopes is the most direct experimental link with the early (t is less than or approximately 1 sec) universe. Third, studies of primordial nucleosynthesis allow for important, and otherwise unattainable, constraints on many aspects of particle physics. Finally, there is tentative evidence which suggests that the Standard Big Bang (SBB) model is incorrect in that it cannot reproduce the inferred primordial abundances for a single value of the baryon-to-photon ratio. Reviewed here are some aspects of non-standard primordial nucleosynthesis which mostly overlap with the authors own personal interest. A short discussion of the SBB nucleosynthesis theory is presented, high-lighting some recent related developments. Next discussed is how recent observations of helium and lithium abundances may indicate looming problems for the SBB model. Then discussed is how the QCD phase transition, neutrinos, and cosmic strings can influence primordial nucleosynthesis. A short discussion of the multitude of other non-standard nucleosynthesis models found in the literature is finally presented and some comments made on possible progress in the future. DOE

N91-19985# Lawrence Livermore National Lab., CA.
TWO POSSIBLE PROBLEMS FOR STANDARD BIG BANG NUCLEOSYNTHESIS
R. A. Malaney Jan. 1990 6 p Presented at the International Conference on Trends in Astroparticle Physics, Santa Monica, 26 Nov. - 1 Dec. 1990
(Contract W-7405-eng-48)
(DE91-007342; UCRL-JC-105970; CONF-901141-1) Avail: NTIS HC/MF A02

A great deal of effort has gone into the determination of the primordial abundances of the light isotopes as inferred from observation. Here we will discuss just two aspects of these observational studies, which tentatively suggest that the storm clouds may be gathering for the SBB (standard big bang) nucleosynthesis model. The first of these is the determination of the primordial He-4 abundance. DOE

N91-19986# Los Alamos National Lab., NM.
ORIGIN OF REGULARITIES IN THE REDSHIFT DISTRIBUTIONS OF DISTANT GALAXIES AND QUASARS
L. M. Ozernoy Feb. 1991 10 p
(Contract W-7405-eng-36)
(DE91-007889; LA-12017-MS) Avail: NTIS HC/MF A02

A model in which inhomogeneities originated during inflation and transformed eventually into density peaks with maximum wavelength equal to the horizon size at the decoupling epoch (z sub dec approx. 10(exp 3)) would give at the present for very large scale structure a periodic distribution: 1n (1 + z) approx. 0.04n + 0.04, n = 0, 1, 2, ... This formula in which the true phase is replaced by its characteristic value fits the data on redshift distribution of distant galaxies fairly well. Some relevant implications are discussed, such as (1) difference between the constants of periodicity C (equivalent to) Delta ln (1 + z): C(sub G) for distant galaxies and C(sub Q) for quasars, and (2) a recent finding that quasars close on the sky to low redshifted galaxies show a higher concentration toward peaks in the quasar redshift distribution than do quasars in general. DOE

N91-19987# Moscow State Univ. (USSR). Nauchno-Issledovatel'skij Inst. Yadernoj Fiziki.
SIXQUARKS IN NEUTRON STARS
Yu. V. Kuzmin 1989 15 p In RUSSIAN
(DE91-615472; NIIYaF-MGU-89-16/93) Avail: NTIS HC/MF A03

Neutron star parameters are calculated with regard to the existence of recently discovered sixquarks-narrow dibaryon resonances. It is shown that as compared to the previous calculations, the maximum masses and radii of neutron stars are notably reduced, compact objects of very low masses appear to be stable. It is shown that at the certain stage of the star collapse an instability occurs which leads to the second type Supernova flare. It is also shown that in a certain pressure interval two phases exist: neutron and neutron-sixquark ones, and the first type Supernova flares can be interpreted as a phase transition in the external layers of the neutron stars. DOE

N91-19988# Hiroshima Univ., Takehara (Japan). Research Inst. for Theoretical Physics.
OBSERVATIONAL RELATIONS IN MODEL UNIVERSES DOMINATED BY DOMAIN-WALL-LIKE MATTER
Kenji Tomita and Kazuya Watanabe May 1990 12 p
(DE91-744969; RRK-90-11) Avail: NTIS HC/MF A03

In model universes dominated by defected matter such as domain walls, observational relations among apparent magnitudes of galaxies, redshifts and number counts are considered. It is shown that the ratio of the mean negative pressure to the mean density plays a role similar to the positive cosmological constant, and that the domain-wall-dominated model may be consistent with the recent number count observations. DOE

N91-19989# Kyoto Univ., Uji (Japan). Inst. for Theoretical Physics.
QUASI-NONLINEAR THEORY OF COSMOLOGICAL SELF-GRAVITATING SYSTEMS
Yasushi Suto and Misao Sasaki Jun. 1990 10 p
(DE91-744971; YITP/U-90-13) Avail: NTIS HC/MF A02

Nonlinear effects of self-gravitating systems in cosmology are considered on the basis of perturbation theory. In particular, several cases are examined in which evolution of power-spectrum of density fluctuations can be analytically calculated. In some cases, nonlinearity suppresses the growth of fluctuations relative to linear theory, and the power transfer via nonlinear mode-coupling is sensitive to the specific shape of the underlying fluctuation spectrum. The result is in good agreement with recent numerical simulations. DOE

N91-19990# Kyoto Univ., Uji (Japan). Inst. for Theoretical Physics.
STATISTICS OF PEAKS IN COSMOLOGICAL NONLINEAR DENSITY FIELDS
Tatsushi Suginohara (Tokyo Univ., Japan) and Yasushi Suto Jun. 1990 15 p
(DE91-744972; YITP/U-90-14) Avail: NTIS HC/MF A03

Distribution of the high-density peaks in the universe is examined using N-body simulations. Nonlinear evolution of the underlying density field significantly changes the statistical properties of the peaks, compared with the analytic results valid for the random Gaussian field. In particular, the abundances and correlations of the initial density peaks are discussed in the context of biased galaxy formation theory. DOE

N91-19991# Kyoto Univ., Uji (Japan). Inst. for Theoretical Physics.
HOW MANY TIMES DO WE HAVE IN QUANTUM GRAVITY
Akio Hosoya (Tokyo Inst. of Tech., Japan) and Jiro Soda Jul. 1990 10 p
(DE91-744973; YITP/U-90-15) Avail: NTIS HC/MF A02

Apparently, there are infinite number of time-like variables in the Wheeler-DeWitt equation in quantum gravity. This gives rise to an obvious conceptual difficulty and further becomes an obstacle if one wants to canonically third quantize the universe. In this paper, adopting York's gauge in the path-integral approach, quantum geometrodynamics is formulated so that it contains only a single time-like variable corresponding to the total volume of the universe. DOE

N91-19992# Kyoto Univ., Uji (Japan). Inst. for Theoretical Physics.
GRAVITATIONAL LENS EFFECT OF WALL-LIKE OBJECTS AND ITS COSMOLOGICAL IMPLICATIONS
Kenji Tomita Aug. 1990 20 p
(DE91-744976; YITP/U-90-18) Avail: NTIS HC/MF A03

First the gravitational deflection angle of light rays passing through a disk consisting of pressureless matter was derived, and it was shown that it behaves like a convex lens. Next the two-ray difference of deflection angles was derived by help of the Raychaudhuri equation, in the cases when the wall-like objects are dust walls and domain-walls. Moreover, the two-ray difference of deflection angles was derived in a low mass-density regions lying between wall-like objects. This region plays a role of a concave lens, but it is shown that its effect is minor, compared with the effect of wall-like objects. On the basis of these deflection angle differences, the gravitational lens effect of uniform wall-like objects which may exist homogeneously on the cosmological scale was considered and it was shown that, in the case when the wall-like objects appear at the epoch of $z = 5$, the measured angles of the cosmic background radiation may be increased about 3 to 2 times owing to the integrated convex lens effect and so its measured anisotropy may be smaller by a factor of about 10 to 6 than the intrinsic one. DOE

N91-19993# Onsala Space Observatory (Sweden).
PROCEEDINGS OF THE SYMPOSIUM ASTROPHYSICAL PROCESSES AND STRUCTURES IN THE UNIVERSE
A. Hjalmarson, M. Lindqvist, L. A. Nyman, H. Olofsson, and A. Winnberg Oct. 1990 28 p Proceedings held in Uppsala, Sweden, 17-21 Jun. 1990
(PB91-123653) Avail: NTIS HC/MF A03 CSCL 03B

The following topics are covered: (1) interstellar molecules and astrophysics; (2) circumstellar chemistry of oxygen-rich stars; (3) mass loss and red giant evolution; (4) VLBI observations at 18 cm and 3 mm of the quasar 3C345; and (5) a model galaxy with two long-lived spiral arms. Author

N91-19994# Onsala Space Observatory (Sweden).
PROCEEDINGS OF 146TH IAU SYMPOSIUM ON DYNAMICS OF GALAXIES AND MOLECULAR CLOUD DISTRIBUTION
L. E. B. Johansson, T. Wiklind, G. Rydbeck, S. Aalto, and H. Olofsson Oct. 1990 27 p Proceedings held in Paris, France, Jun. 1990
(PB91-123661) Avail: NTIS HC/MF A03 CSCL 03B

The following topics were covered: (1) interstellar gas in the Magellanic clouds (SEST observations of CO and other molecules); (2) CO in early type galaxies; (3) properties of the molecular arms in the galaxies M51, M101, and IC342; (4) molecular clouds in NGC 3256; (5) the (12)CO/(13)CO intensity ratio in external galaxies; (6) CO(J = 1-0) observations of M101; and (7) a galaxy model with a long-lived two-arm spiral structure. Author

N91-19996*# Arizona Univ., Tucson. Lunar and Planetary Lab.
IMPACT PROCESSES IN THE SOLAR SYSTEM: NEW UNDERSTANDINGS THROUGH NUMERICAL MODELING
E. Asphaug, H. J. Melosh, and E. Ryan (Planetary Science Inst., Tucson, AZ.) *In* Lunar and Planetary Inst., 22nd Lunar and Planetary Science Conference 1991 p 1-5 (For primary document see N91-19995 11-91)
Avail: NTIS HC/MF A04 CSCL 03B

N91-19998*# Washington Univ., Saint Louis, MO. Dept. of Physics.
INSTELLAR GRAINS WITHIN INTERSTELLAR GRAINS
Thomas J. Bernatowicz, Sachiko Amari, Ernst K. Zinner, and Roy S. Lewis (Chicago Univ., IL.) *In* Lunar and Planetary Inst., 22nd Lunar and Planetary Science Conference 1991 p 11-13 (For primary document see N91-19995 11-91)
Avail: NTIS HC/MF A04 CSCL 03B

N91-19999*# National Aeronautics and Space Administration. Goddard Space Flight Center, Greenbelt, MD.
K/T AGE FOR THE POPIGAI IMPACT EVENT
A. L. Deino, J. B. Garvin, and S. Montanari (California Univ., Berkeley.) *In* Lunar and Planetary Inst., 22nd Lunar and Planetary Science Conference 1991 p 15-16 (For primary document see N91-19995 11-91)
Avail: NTIS HC/MF A04 CSCL 03B

N91-20006*# California Inst. of Tech., Pasadena. Div. of Geological and Planetary Sciences.
STABLE HYDROGEN AND CARBON ISOTOPE RATIOS OF EXTRACTABLE HYDROCARBONS IN THE MURCHISON METEORITE
R. V. Krishnamurthy, S. Epstein, S. Pizzarello, J. R. Cronin, and G. U. Yuen (Arizona State Univ., Tempe.) *In* Lunar and Planetary Inst., 22nd Lunar and Planetary Science Conference 1991 p 39-40 (For primary document see N91-19995 11-91)
Avail: NTIS HC/MF A04 CSCL 03B

N91-20012*# Los Alamos National Lab., NM.
EFFECTS OF A GIANT IMPACT ON URANUS
W. L. Slattery, W. Benz, and A. G. W. Cameron (Harvard-Smithsonian Center for Astrophysics, Cambridge, MA.) *In* Lunar and Planetary Inst., 22nd Lunar and Planetary Science Conference 1991 p 59-61 (For primary document see N91-19995 11-91)
Avail: NTIS HC/MF A04 CSCL 03B

N91-20013*# Washington Univ., Saint Louis, MO. Dept. of Physics.
COSMIC DUST: LABORATORY ANALYSES OF EXTREMELY SMALL PARTICLES
Frank J. Stadermann *In* Lunar and Planetary Inst., 22nd Lunar and Planetary Science Conference 1991 p 63-65 (For primary document see N91-19995 11-91)
Avail: NTIS HC/MF A04 CSCL 03B

N91-20014*# Geological Survey, Flagstaff, AZ.
WHAT WERE THE EFFECTS OF THE FORMATION OF THE BOREALIS BASIN, MARS
Kenneth L. Tanaka *In* Lunar and Planetary Inst., 22nd Lunar and Planetary Science Conference 1991 p 67-69 (For primary document see N91-19995 11-91)
Avail: NTIS HC/MF A04 CSCL 03B

91 LUNAR AND PLANETARY EXPLORATION

Includes planetology; and manned and unmanned flights. For spacecraft design or space stations see *18 Spacecraft Design, Testing and Performance.*

N91-19995*# Lunar and Planetary Inst., Houston, TX.
TWENTY-SECOND LUNAR AND PLANETARY SCIENCE CONFERENCE Press Abstracts
1991 69 p Sponsored by NASA. Johnson Space Center (NASA-CR-187971; NAS 1.26:187971; LPI-Contrib-758) Avail: NTIS HC/MF A04 CSCL 03B

The papers in this collection were written for general presentation, avoiding jargon and unnecessarily complex terms. Some of the topics covered include: planetary evolution, planetary satellites, planetary composition, planetary surfaces, planetary geology, volcanology, meteorite impacts and composition, and cosmic dust. Particular emphasis is placed on Mars and the Moon. For individual titles, see N91-19996 through N91-20014.

N91-19996*# Arizona Univ., Tucson. Lunar and Planetary Lab.
IMPACT PROCESSES IN THE SOLAR SYSTEM: NEW UNDERSTANDINGS THROUGH NUMERICAL MODELING **c90**
E. Asphaug, H. J. Melosh, and E. Ryan (Planetary Science Inst., Tucson, AZ.) *In* Lunar and Planetary Inst., 22nd Lunar and Planetary Science Conference 1991 p 1-5 (For primary document see N91-19995 11-91)
Avail: NTIS HC/MF A04 CSCL 03B

A collision of two rocky objects circling the sun in space, each roughly the size and mass of a large mountain range, was modeled. A fragmentation hydrocode was developed to perform dynamical computations of collisional outcomes. Explosive framentation and fluid dynamics were used and drawn together into a single application. To model a solid, certain material parameters, such as density, elasticity, rigidity, and energies of melting and vaporization were input. These parameters are well-known for a variety of important materials, such as ice, iron, granite, and basalt. Another important parameter used is the distribution of initial flaws within the material. Y.S.

N91-19997*# Arizona Univ., Tucson. Dept. of Planetary Sciences.
ANCIENT OCEANS AND MARTIAN PALEOHYDROLOGY
Victor R. Baker, Robert G. Strom, Virginia C. Gulick, Jeffrey S. Kargel, Goro Komatsu, and Vishwas S. Kale *In* Lunar and Planetary Inst., 22nd Lunar and Planetary Science Conference 1991 p 7-10 (For primary document see N91-19995 11-91)
Avail: NTIS HC/MF A04 CSCL 03B

The global model of ocean formation on Mars is discussed. The studies of impact crater densities on certain Martian landforms show that late in Martian history there could have been coincident formation of: (1) glacial features in the Southern Hemisphere; (2) ponded water and related ice features in the northern plains; (3) fluvial runoff on Martian uplands; and (4) active ice-related mass-movement. This model of transient ocean formation ties these diverse observations together in a long-term cyclic scheme of global planetary operation. Y.S.

N91-19998*# Washington Univ., Saint Louis, MO. Dept. of Physics.
INSTELLAR GRAINS WITHIN INTERSTELLAR GRAINS **c90**
Thomas J. Bernatowicz, Sachiko Amari, Ernst K. Zinner, and Roy S. Lewis (Chicago Univ., IL.) *In* Lunar and Planetary Inst., 22nd Lunar and Planetary Science Conference 1991 p 11-13 (For primary document see N91-19995 11-91)
Avail: NTIS HC/MF A04 CSCL 03B

The discovery of crystals of titanium carbide in an interstellar graphite spherule is reported. The new species is particularly interesting in that it came in a protective wrapping (the graphite spherule) which eliminated the possibility of chemical alteration during its residence in the interstellar medium and in the meteorite in which it was discovered. Y.S.

N91-19999*# National Aeronautics and Space Administration. Goddard Space Flight Center, Greenbelt, MD.
K/T AGE FOR THE POPIGAI IMPACT EVENT **c90**
A. L. Deino, J. B. Garvin, and S. Montanari (California Univ., Berkeley.) *In* Lunar and Planetary Inst., 22nd Lunar and Planetary Science Conference 1991 p 15-16 (For primary document see N91-19995 11-91)
Avail: NTIS HC/MF A04 CSCL 03B

The multi-ringed POPIGAI structure, with an outer ring diameter of over 100 km, is the largest impact feature currently recognized on Earth with an Phanerozoic age. The target rocks in this relatively unglaciated region consist of upper Proterozoic through Mesozoic platform sediments and igneous rocks overlying Precambrian crystalline basement. The reported absolute age of the Popigai impact event ranges from 30.5 to 39 Ma. With the intent of refining this age estimate, a melt-breccia (suevite) sample from the inner regions of the Popigai structure was prepared for total fusion and step-wise heating Ar-40/Ar-39 analysis. Although the total fusion and step-heating experiments suggest some degree of age heterogeneity, the recurring theme is an age of around 64 to 66 Ma. Y.S.

N91-20000*# Arizona State Univ., Tempe.
LUNAR MARIA AND RELATED DEPOSITS: PRELIMINARY GALILEO IMAGING RESULTS
R. Greeley, M. Belton, L. Bolef, M. Carr, C. Chapman, M. Davies, L. Doose, F. Fanale, L. Gaddis, and R. Greenberg (Arizona Univ., Tucson.) et al *In* Lunar and Planetary Inst., 22nd Lunar and Planetary Science Conference 1991 p 17-18 (For primary document see N91-19995 11-91)
Avail: NTIS HC/MF A04 CSCL 03B

During the Earth-Moon flyby the Galileo Solid State Imaging system obtained new information on lunar media. Imaging data in spectral bands from 0.4 tc 1.0 micron wavelength provide color data for deposits on the western limb. General objectives were to determine the composition and stratigraphy of mare and related deposits for areas not previously seen well in color, and to compare the results with well-studied nearside maria. Initial results from images reduced with preliminary calibrations show that Galileo spectral reflectance data are consistent with previous earthbased observations. Y.S.

N91-20001*# National Astronomy and Ionosphere Center, Arecibo, Puerto Rico.
MARS RADAR MAPPING: STRONG DEPOLARIZED ECHOES FROM THE ELYSIUM/AMAZONIS OUTFLOW CHANNEL COMPLEX
J. K. Harmon, M. P. Sulzer, and P. Perillat *In* Lunar and Planetary Inst., 22nd Lunar and Planetary Science Conference 1991 p 19-21 (For primary document see N91-19995 11-91)
Avail: NTIS HC/MF A04 CSCL 03B

A new technique was used to make radar maps of Mars with the Arecibo radiotelescope. The observations were made during the 1990 opposition (close approach) of Mars. Among the most

interesting of the preliminary results is the discovery of strong depolarized echoes from the enormous Elysium/Amazonis outflow channel complex. These strong echoes may represent rough-surface scattering off the youngest lava flows on Mars. Y.S.

N91-20002*# National Aeronautics and Space Administration, Washington, DC.
ORIENTALE AND SOUTH POLE-AITKEN BASINS ON THE MOON: PRELIMINARY GALILEO IMAGING RESULTS
J. Head, E. Fischer, S. Murchie, C. Pieters, J. Plutchak, J. Sunshine, M. Belton, M. Carr, C. Chapman, and M. Davies (RAND Corp., Santa Monica, CA.) et al *In* Lunar and Planetary Inst., 22nd Lunar and Planetary Science Conference 1991 p 23-26 Prepared in cooperation with Hawaii Univ., Honolulu, Arizona State Univ., Tempe; Arizona Univ., Tucson; Cornell Univ., Ithaca, NY; Deutsche Forschungsanstalt Luft- and Raumfahrt, Oberpfaffenhofen; JPL, Pasadena, CA; Geological Survey, Flagstaff, AZ (For primary document see N91-19995 11-91)
Avail: NTIS HC/MF A04 CSCL 03B

During the Earth-Moon flyby the Galileo Solid State Imaging System obtained new information on the landscape and physical geology of the Moon. Multicolor Galileo images of the Moon reveal variations in color properties of the lunar surface. Using returned lunar samples as a key, the color differences can be interpreted in terms of variations in the mineral makeup of the lunar rocks and soil. The combined results of Apollo landings and multicolor images from Galileo allow extrapolation of surface composition to areas distant from the landing sites, including the far side invisible from Earth. Y.S.

N91-20003*# Toledo Univ., OH.
HUBBLE SPACE TELESCOPE OBSERVATIONS OF MARS
Philip B. James, Todd Clancy, Steve Lee, Ralph Kahn, Richard Zurek, Leonard Martin, and Robert Singer (Arizona Univ., Tucson.) *In* Lunar and Planetary Inst., 22nd Lunar and Planetary Science Conference 1991 p 27-29 (For primary document see N91-19995 11-91)
Avail: NTIS HC/MF A04 CSCL 03B

Hubble Space Telescope (HST) afforded the possibility of resolving features as small as 100 km on the Martian surface even when it is at the far point of its orbit. Therefore it is ideally suited for monitoring seasonal changes on the red planet. The objectives research include: the study of Martian dust storms; use of images obtained through different filters to study the spectral reflectance of regions on the Martian surface; use of ultraviolet images and spectra to measure the amount of ozone in the planet's atmosphere as a function of location of the planet; use of images to study changes in the albedo of the Mars surface; and use of Planetary Camera images to study Martian clouds and to measure the opacity of the atmosphere. Y.S.

N91-20004*# Geological Survey, Denver, CO.
EVIDENCE FOR AMMONIUM-BEARING MINERALS IN CERES
T. V. V. King, R. N. Clark, W. M. Calvin, D. M. Sherman, G. A. Swayze, and R. H. Brown (Jet Propulsion Lab., California Inst. of Tech., Pasadena.) *In* Lunar and Planetary Inst., 22nd Lunar and Planetary Science Conference 1991 p 31-33 (For primary document see N91-19995 11-91)
Avail: NTIS HC/MF A04 CSCL 03B

Evidence for ammonium-bearing minerals was found on the surface of the largest asteroid Ceres. The presence of ammonium-bearing clays suggests that Ceres has experienced a period of alteration by substantial amounts of an ammonium-bearing fluid. The presence of the ammonium-bearing clays does not preclude Ceres maintaining a volatile inventory in the core or in a volatile-rich zone at some distance below the surface. Telescopic observations of Ceres, using the 3.0 meter NASA Infrared telescope facility prompted this reevaluation of its surface mineralogy. Y.S.

N91-20005*# Geological Survey, Flagstaff, AZ.
TRITON: A HOT POTATO
R. L. Kirk and R. H. Brown (Jet Propulsion Lab., California Inst. of Tech., Pasadena.) *In* Lunar and Planetary Inst., 22nd Lunar and Planetary Science Conference 1991 p 35-38 (For primary document see N91-19995 11-91)
Avail: NTIS HC/MF A04 CSCL 03B

The effect of sunlight on the surface of Triton was studied. Widely disparate models of the active geysers observed during Voyager 2 flyby were proposed, with a solar energy source almost their only feature. Yet Triton derives more of its heat from internal sources (energy released by the radioactive decay) than any other icy satellite. The effect of this relatively large internal heat on the observable behavior of volatiles on Triton's surface is investigated. The following subject areas are covered: the Global Energy Budget; insulation polar caps; effect on frost stability; mantle convection; and cryovolcanism. Y.S.

N91-20006*# California Inst. of Tech., Pasadena. Div. of Geological and Planetary Sciences.
STABLE HYDROGEN AND CARBON ISOTOPE RATIOS OF EXTRACTABLE HYDROCARBONS IN THE MURCHISON METEORITE **c90**
R. V. Krishnamurthy, S. Epstein, S. Pizzarello, J. R. Cronin, and G. U. Yuen (Arizona State Univ., Tempe.) *In* Lunar and Planetary Inst., 22nd Lunar and Planetary Science Conference 1991 p 39-40 (For primary document see N91-19995 11-91)
Avail: NTIS HC/MF A04 CSCL 03B

A fairly fool-proof method to ensure that the compounds isolated from meteorites are truly part of the meteorites and not an artifact introduced by exposure to the terrestrial environment, storage, or handling is presented. The stable carbon and hydrogen isotope ratios in several of the chemical compounds extracted from the Murchison meteorite were measured. The results obtained by studying the amino acids in this meteorite gave very unusual hydrogen and carbon isotope ratios. The technique was extended to the different classes of hydrocarbons and the hydrocarbons were isolated using a variety of separation techniques. The results and methods used in this investigation are described in this two page paper. K.S.

N91-20007*# National Aeronautics and Space Administration. Lyndon B. Johnson Space Center, Houston, TX.
RELATIVE CHRONOLOGY OF MARTIAN VOLCANOES
R. Landheim (Louisiana Tech Univ., Ruston.) and N. G. Barlow *In* Lunar and Planetary Inst., 22nd Lunar and Planetary Science Conference 1991 p 41-43 (For primary document see N91-19995 11-91)
Avail: NTIS HC/MF A04 CSCL 03B

Impact cratering is one of the major geological processes that has affected the Martian surface throughout the planet's history. The frequency of craters within particular size ranges provides information about the formation ages and obliterative episodes of Martian geologic units. The Barlow chronology was extended by measuring small craters on the volcanoes and a number of standard terrain units. Inclusions of smaller craters in units previously analyzed by Barlow allowed for a more direct comparison between the size-frequency distribution data for volcanoes and established chronology. During this study, 11,486 craters were mapped and identified in the 1.5 to 8 km diameter range in selected regions of Mars. The results are summarized in this three page report and give a more precise estimate of the relative chronology of the Martian volcanoes. Also, the results of this study lend further support to the increasing evidence that volcanism has been a dominant geologic force throughout Martian history. K.S.

N91-20008*# Kent Univ., Canterbury (England). Physics Lab.
SPACE DEBRIS: ORBITAL MICROPARTICULATES IMPACTING LDEF EXPERIMENTS FAVOUR A NATURAL EXTRATERRESTRIAL ORIGIN **c18**
Tony McDonnell *In* Lunar and Planetary Inst., 22nd Lunar and Planetary Science Conference 1991 p 45-48 (For primary document see N91-19995 11-91)
Avail: NTIS HC/MF A04 CSCL 22B

The results of work carried out at the Unit for Space Sciences at the University of Kent at Canterbury, United Kingdom, on the

micrometeoroid and space debris environment of near Earth space are described. The primary data for the research program is supplied by an examination of several types of exposed surface from the NASA Long Duration Exposure Facility (LDEF), including an experiment dedicated to the detection of micrometeoroids and space debris provided by the University. Author

N91-20009*# National Aeronautics and Space Administration. Lyndon B. Johnson Space Center, Houston, TX.
EXPERIMENTAL REDUCTION OF SIMULATED LUNAR GLASS BY CARBON AND HYDROGEN AND IMPLICATIONS FOR LUNAR BASE OXYGEN PRODUCTION
David S. McKay, Richard V. Morris, and Amy J. Jurewicz (Lockheed Corp., Houston, TX.) *In* Lunar and Planetary Inst., 22nd Lunar and Planetary Science Conference 1991 p 49-52 (For primary document see N91-19995 11-91)
Avail: NTIS HC/MF A04 CSCL 03B

The most abundant element in lunar rocks and soils is oxygen which makes up approximately 45 percent by weight of the typical lunar samples returned during the Apollo missions. This oxygen is not present as a gas but is tightly bound to other elements in mineral or glass. When people return to the Moon to explore and live, the extraction of this oxygen at a lunar outpost may be a major goal during the early years of operation. Among the most studied processes for oxygen extraction is the reduction of ilmenite by hydrogen gas to form metallic iron, titanium oxide, and oxygen. A related process is proposed which overcomes some of the disadvantages of ilmenite reduction. It is proposed that oxygen can be extracted by direct reduction of native lunar pyroclactic glass using either carbon, carbon monoxide, or hydrogen. In order to evaluate the feasibility of this proposed process a series of experiments on synthetic lunar glass are presented. The results and a discussion of the experiments are presented. K.S.

N91-20010*# Notre Dame Univ., IN. Dept of Earth Sciences.
WANTED: LUNAR DETECTIVES TO UNRAVEL THE MYSTERIES OF THE MOON! CRIME TO BE SOLVED: MASS EXTINCTIONS ON THE MOON BY METEORITE IMPACT!
Clive R. Neal and Lawrence A. Taylor (Tennessee Univ., Knoxville.) *In* Lunar and Planetary Inst., 22nd Lunar and Planetary Science Conference 1991 p 53-56 (For primary document see N91-19995 11-91)
Avail: NTIS HC/MF A04 CSCL 03B

The criteria and clues for identifying meteorite contamination are outlined to aid in the quest for more knowledge regarding the evolution of the Moon and the early Earth. The Warren and Wasson seven criteria for establishing the pristine nature of highland rocks are presented. Other topics covered include iron/nickel metals, monomict nature, and lunar glasses. The major conclusion is that pristinity should not be the primary consideration in the study of lunar rocks. The most important criterion to establish is whether or not the lunar sample contains more than one lunar rock type. Even if a sample is non-pristine, as long as only one lunar rock type is present, petrogenetic interpretation can still be carried out. K.S.

N91-20011*# Jet Propulsion Lab., California Inst. of Tech., Pasadena.
MAGELLAN: PRELIMINARY DESCRIPTION OF VENUS SURFACE GEOLOGIC UNITS
R. S. Saunders, R. Arvidson, J. W. Head, III, G. G. Schaber, S. C. Solomon, E. R. Stofan, Alexander T. Basilevsky, J. E. Guest, G. E. McGill, and H. J. Moore (Geological Survey, Flagstaff, AZ.) *In* Lunar and Planetary Inst., 22nd Lunar and Planetary Science Conference 1991 p 57-58 (For primary document see N91-19995 11-91)
Avail: NTIS HC/MF A04 CSCL 03B

Observations from approximately one-half of the Magellan nominal eight-month mission to map Venus are summarized. Preliminary compilation of initial geologic observations of the planet reveals a surface dominated by plains that are characterized by extensive and intensive volcanism and tectonic deformation. Four broad categories of units have been identified: plains units, linear belts, surficial units, and terrain units. Author

N91-20012*# Los Alamos National Lab., NM.
EFFECTS OF A GIANT IMPACT ON URANUS **c90**
W. L. Slattery, W. Benz, and A. G. W. Cameron (Harvard-Smithsonian Center for Astrophysics, Cambridge, MA.) *In* Lunar and Planetary Inst., 22nd Lunar and Planetary Science Conference 1991 p 59-61 (For primary document see N91-19995 11-91)
Avail: NTIS HC/MF A04 CSCL 03B

The effects of a giant impact on Uranus with respect to the axis tilt of Uranus and its satellites are discussed. The simulations of possible giant impacts were carried out using Cray supercomputers. The technique used is called smooth particle hydrodynamics (SPH). In this technique, the material in the proto-Uranus planet and in the impactor is divided into a large number of particles which can overlap one another so that local averages over these particles determine density and pressure in the problem, and the particles themselves have their own temperatures and internal energies. During the course of the simulation, these particles move around under the influence of the forces acting on them: gravity and pressure gradients. The results of model simulations are presented. K.S.

N91-20013*# Washington Univ., Saint Louis, MO. Dept. of Physics.
COSMIC DUST: LABORATORY ANALYSES OF EXTREMELY SMALL PARTICLES **c90**
Frank J. Stadermann *In* Lunar and Planetary Inst., 22nd Lunar and Planetary Science Conference 1991 p 63-65 (For primary document see N91-19995 11-91)
Avail: NTIS HC/MF A04 CSCL 03B

A discussion of cosmic dust, its classification, the usefulness of its analysis, and problems associated with its analysis is presented. All measurements on stratospheric dust particles presented here were made with secondary ion mass spectrometry (SIMS). The SIMS technique turns out to be an extremely useful tool in the study of very small particles and made a number of firsts possible. The isotopic composition of cosmic dust particles were measured for the first time. It was also the first time that it was possible to measure the abundances of the rare earth elements in these particles. However, the most important advance this work represents is that both trace elemental and isotopic abundances were successfully measured in the same particles. Thus, for the first time, it is possible to compare isotopic and trace element abundance data of the same cosmic dust particles. K.S.

N91-20014*# Geological Survey, Flagstaff, AZ.
WHAT WERE THE EFFECTS OF THE FORMATION OF THE BOREALIS BASIN, MARS **c90**
Kenneth L. Tanaka *In* Lunar and Planetary Inst., 22nd Lunar and Planetary Science Conference 1991 p 67-69 (For primary document see N91-19995 11-91)
Avail: NTIS HC/MF A04 CSCL 03B

The progress that has been made in the study of the Borealis basin in the Northern Hemisphere of Mars is presented in this two page report. The effect of the runoff of ground water into the Borealis basin on the climate of Mars is discussed. K.S.

N91-20015*# National Aeronautics and Space Administration. Lewis Research Center, Cleveland, OH.
CHEMICAL APPROACHES TO CARBON DIOXIDE UTILIZATION FOR MANNED MARS MISSIONS
Aloysius F. Hepp, Geoffrey A. Landis, and Clifford P. Kubiak (Purdue Univ., West Lafayette, IN.) 1991 22 p Presented at the 2nd Annual Symposium of the UA/NASA Space Engineering Research Center, Tucson, AZ, 7-10 Jan. 1991
(Contract NAS3-25266)
(NASA-TM-103728; E-5962; NAS 1.15:103728) Avail: NTIS HC/MF A03 CSCL 03B

Use of resources available in situ is a critical enabling technology for a permanent human presence in space. A permanent presence

on Mars, e.g., requires a large infrastructure to sustain life under hostile conditions. As a resource on Mars, atmospheric CO2 is as follows: abundant; available at all points on the surface; of known presence; chemically simple; and can be obtained by simple compression. Many studies focus on obtaining O2 and the various uses for O2 including life support and fuel; discussion of CO, the coproduct from CO2 fixation revolves around its uses as a fuel, being oxidized back to CO2. Several new proposals are studied for CO2 fixation through chemical, photochemical, and photoelectrochemical means. For example, the reduction of CO2 to hydrocarbons such as acetylene (C2H2) can be accomplished with H2. C2H2 has a theoretical vacuum specific impulse of approx. 375 secs. Potential uses were also studied of CO2, as obtained or further reduced to carbon, as a reducing agent in metal oxide processing to form metals or metal carbides for use as structural or power materials; the CO2 can be recycled to generate O2 and CO. Author

92 SOLAR PHYSICS

Includes solar activity, solar flares, solar radiation and sunspots.

For related information see *93 Space Radiation.*

N91-20016# Moscow State Univ. (USSR). Nauchno-Issledovatel'skij Inst. Yadernoj Fiziki.
NEUTRON PROPAGATION FROM SOLAR FLARE IN THE SOLAR ATMOSPHERE
B. M. Kuzhevskij and E. V. Troitskaya 1989 28 p In RUSSIAN
(DE91-615465; NIIYaF-MGU-89-28/105) Avail: NTIS HC/MF A03

Some characteristics of neutron propagation caused by instantaneous point source in the atmosphere of the Sun are calculated. Calculation is performed in different approximations. Effect of the form of substance concentration dependence on the height on the thermal neutron depth distribution density is revealed. It is found that 90 percent of neutrons give their energy to the environment in the depth interval of the order of several hundred kilometers. Shares of neutron quantity, escaping from the solar atmosphere to the surrounding space, are calculated. DOE

N91-20017# National Geophysical Data Center, Boulder, CO.
SOLAR-GEOPHYSICAL DATA NUMBER 554, OCTOBER 1990. PART 2 (COMPREHENSIVE REPORTS): DATA FOR APRIL 1990 AND MISCELLANEOUS. EXPLANATION OF DATA REPORTS ISSUED AS NUMBER 515 (SUPPLEMENT) JULY 1987
H. E. Coffey Oct. 1990 78 p
(PB91-124586; SGD-554-Pt-2) Avail: NTIS HC/MF A05 CSCL 03B

The following solar-geophysical data for april 1990 are compiled: solar flares; solar radio bursts at fixed frequencies; solar x ray radiation from GOES satellites; mass ejections from the sun; and active prominences and filaments. Author

N91-20018# National Geophysical Data Center, Boulder, CO.
SOLAR-GEOPHYSICAL DATA NUMBER 554, OCTOBER 1990. PART 1 (PROMPT REPORTS): DATA FOR SEPTEMBER, AUGUST 1990, AND LATE DATA. EXPLANATION OF DATA REPORTS ISSUED AS NUMBER 515 (SUPPLEMENT) JULY 1987
H. E. Coffey Oct. 1990 189 p
(PB91-124594; SGD-554-Pt-1) Avail: NTIS HC/MF A09 CSCL 03B

The solar-geophysical data for 1990 are compiled. Data for September (solar-terrestrial environment, IUWDS alert periods, solar activity indices, solar flares, solar radio emission, and Stanford mean solar magnetic field), August (solar active regions, sudden ionospheric disturbances, solar radio spectral observations, cosmic ray measurements by neutron monitor, and geomagnetic indices), and some late data are presented. Author

N91-20019# Rome Univ. (Italy). Dipt. di Fisica.
THE ROME NEUTRON MONITOR DATA FOR FOUR GROUND-LEVEL ENHANCEMENTS OBSERVED BY THE WORLD-WIDE STATION NETWORK IN 1990
G. Villoresi, N. L. Zangrilli, F. Signoretti, F. Re (Istituto Nazionale di Fisica Nucleare, Rome, Italy), and N. Iucci 17 Dec. 1990 37 p
(Nota-Interna-967; ETN-91-98887) Avail: NTIS HC/MF A03

Four solar flare particle events were detected by the ground based network of neutron monitors during May 1990 in the ascending solar activity phase. The data of the 17-NM64 neutron monitor run for periods in which the ground level enhancements are observed by the station network are presented. The data are given in the table form suggested at the XXI (XUV/X-ray Imager (Orbiting Solar Laboratory)) international cosmic ray conference in order to produce uniform data sets from the various cosmic ray detectors. For each event some preliminary information on the related flares are given; data plots are given; different time scales are used for a better visualization of the events. A discussion on the presented data is given. ESA

93 SPACE RADIATION

Includes cosmic radiation; and inner and outer earth's radiation belts.

For biological effects of radiation see *52 Aerospace Medicine.* For theory see *73 Nuclear and High-Energy Physics.*

N91-20020# Moscow State Univ. (USSR). Nauchno-Issledovatel'skij Inst. Yadernoj Fiziki.
EXPERIMENTAL DATA ON STUDY OF COSMIC RAY PARTICLES IN THE E GREATER THAN OR EQUAL TO 2 TeV ENERGY RANGE AT THE COSMOS-1713 SATELLITE WITH THE SOKOL-2 DEVICE
I. P. Ivanenko, I. D. Rapoport, and V. Ya. Shestoperov 1989 42 p In RUSSIAN
(DE91-615479; NIIYaF-MGU-89-29/106) Avail: NTIS HC/MF A03

Primary data of results of experiment on studying the cosmic ray particles with energy in the range exceeding 2 TeV at the Cosmos-1713 satellite using the Sokol-2 equipment are presented in the tabular form. A brief description of the equipment is given. DOE

N91-20021# Moscow State Univ. (USSR). Nauchno-Issledovatel'skij Inst. Yadernoj Fiziki.
COSMIC RAY CHARGED COMPONENT VARIATIONS AT SEA LEVEL
T. N. Charakhchyan, V. P. Okhlopkov, A. F. Krasotkin, N. S. Svirzhevskij, and L. A. Charakhchyan 1989 29 p In RUSSIAN
(DE91-615480; NIIYaF-MGU-89-65/142) Avail: NTIS HC/MF A03

Results of measuring the cosmic ray charged component using devices installed at the Olen'ya station (the Murmansk region), in Dolgoprudny town (the Moscow region), and in Mirny (Antarctic continent) are investigated. The analysis has shown that apart from solar origin and seasonal variations there are annual variations of cosmic ray charged component. By results of comparing annual variations of the charged component on the Earth surface to data of neutron and muon components a conclusion is made that annual variations of the charge component on the Earth surface appear to be a manifestation of cosmic ray zonal modulation and are not connected with variations of galactic cosmic rays. DOE

99 GENERAL

N91-20022*# National Aeronautics and Space Administration. John F. Kennedy Space Center, Cocoa Beach, FL.
RESEARCH REPORTS: 1990 NASA/ASEE SUMMER FACULTY FELLOWSHIP PROGRAM Final Report, Jun. - Aug. 1990
Loren A. Anderson, ed. (University of Central Florida, Orlando.) and Mark A. Beymer, ed. Sep. 1990 526 p Fellowship program held in Merritt Island, FL, 4 Jun. - 10 Aug. 1990; sponsored by NASA, Washington and ASEE
(Grant NGT-60002)
(NASA-CR-187638; NAS 1.26:187638) Avail: NTIS HC/MF A23 CSCL 05I

A collection of technical reports on research conducted by the participants in this program is presented. The topics covered include: human-computer interface software, multimode fiber optic communication links, electrochemical impedance spectroscopy, rocket-triggered lightning, robotics, a flammability study of thin polymeric film materials, a vortex shedding flowmeter, modeling of flow systems, monomethyl hydrazine vapor detection, a rocket noise filter system using digital filters, computer programs, lower body negative pressure, closed ecological systems, and others. Several reports with respect to space shuttle orbiters are presented. For individual titles, see N91-20023 through N91-20038.

N91-20023*# California State Univ., Fresno. Dept. of Computer Science.
FORMAL SPECIFICATION OF HUMAN-COMPUTER INTERFACES **c61**
Brent Auernheimer *In* NASA, John F. Kennedy Space Center, Research Reports: 1990 NASA/ASEE Summer Faculty Fellowship Program Sep. 1990 p 1-28 (For primary document see N91-20022 11-99)
(Grant NGT-60002)
Avail: NTIS HC/MF A23 CSCL 09B

A high-level formal specification of a human computer interface is described. Previous work is reviewed and the ASLAN specification language is described. Top-level specifications written in ASLAN for a library and a multiwindow interface are discussed. Author

N91-20024*# Towson State Univ., MD. Dept. of Physics.
STUDY OF WAVELENGTH DIVISION MULTIPLEXING AS A MEANS OF INCREASING THE NUMBER OF CHANNELS IN MULTIMODE FIBER OPTIC COMMUNICATION LINKS **c74**
Harry Bates *In* NASA, John F. Kennedy Space Center, Research Reports: 1990 NASA/ASEE Summer Faculty Fellowship Program Sep. 1990 p 29-64 (For primary document see N91-20022 11-99)
(Grant NGT-60002)
Avail: NTIS HC/MF A23 CSCL 20F

A number of optical communication lines are now in use at the Kennedy Space Center (KSC) for the transmission of voice, computer data, and video signals. Presently, all of these channels utilize a single carrier wavelength centered near 1300 nm. The theoretical bandwidth of the fiber far exceeds the utilized capacity. Yet, practical considerations limit the usable bandwidth. The fibers have the capability of transmitting a multiplicity of signals simultaneously in each of two separate bands (1300 and 1550 nm). Thus, in principle, the number of transmission channels can be increased without installing new cable if some means of wavelength division multiplexing (WDM) can be utilized. The main goal of these experiments was to demonstrate that a factor of 2 increase in bandwidth utilization can share the same fiber in both a unidirectional configuration and a bidirectional mode of operation. Both signal and multimode fiber are installed at KSC. The great majority is multimode; therefore, this effort concentrated on multimode systems. Author

N91-20025*# Randolph-Macon Coll., Ashland, VA. Dept. of Chemistry.
ELECTROCHEMICAL IMPEDANCE SPECTROSCOPY OF METAL ALLOYS IN THE SPACE TRANSPORTATION SYSTEM LAUNCH ENVIRONMENT **c26**
Luz Calle *In* NASA, John F. Kennedy Space Center, Research Reports: 1990 NASA/ASEE Summer Faculty Fellowship Program Sep. 1990 p 65-114 (For primary document see N91-20022 11-99)
(Grant NGT-60002)
Avail: NTIS HC/MF A23 CSCL 11F

AC impedance measurements were performed to investigate the corrosion resistance of 18 alloys under conditions similar to the Space Transportation System (STS) launch environment. The alloys were: (1) zirconium 702; (2) Hastelloy C-22, C-276, C-4, and B-2; (3) Inconel 600 and 825; (4) Ferralium 255; (5) Inco Alloy G-3; (6) 20Cb-3; (7) SS 904L, 304LN, 316L, 317L, and 304L; (8) ES 2205; and (9) Monel 400. AC impedance data were gathered for each alloy at various immersion times in 3.55 percent NaCl-0.1N HCl. Polarization resistance values were obtained for the Nyguist plots at each immersion time using the EQUIVALENT CIRCUIT software package available with the 388 electrochemical impedance software. Hastelloy C-22 showed the highest overall values for polarization resistance while Monel 400 and Inconel 600 had the lowest overall values. There was good general correlation between the corrosion performance of the alloys at the beach corrosion testing site, and the expected rate of corrosion as predicted based on the polarization resistance values obtained. The data indicate that electrochemical impedance spectroscopy can be used to predict the corrosion performance of metal alloys. Author

N91-20026*# Massachusetts Univ., Amherst. Dept. of Plant and Soil Sciences.
CARBON DIOXIDE AND WATER EXCHANGE OF A SOYBEAN STAND GROWN IN THE BIOMASS PRODUCTION CHAMBER **c51**
Kenneth A. Corey *In* NASA, John F. Kennedy Space Center, Research Reports: 1990 NASA/ASEE Summer Faculty Fellowship Program Sep. 1990 p 115-141 (For primary document see N91-20022 11-99)
(Grant NGT-60002)
Avail: NTIS HC/MF A23 CSCL 06C

Soybean plants were grown under metal halide lamps in NASA's biomass production chamber (BPC). Experiments were conducted to determine whole stand rates of carbon dioxide exchange and transpiration as influenced by time of day, CO2 concentration, irradiance, and temperature. Plants were grown at a population of 24 plants/sq m, a daily cycle of 12 hr light/12 hr dark, and average temperature regime of 26 C light/20 C dark, and a CO2 concentration enriched and maintained at 1000 ppm during the photoperiod. A distinct diurnal pattern in the rate of stand transpiration was measured at both ambient and enriched (1000 ppm) concentration of CO2. Data generated in this study represent true whole stand responses to key developmental and environmental variables and will be valuable in database construction for future working CELSS. Crop growth studies in the BPC were conducted with a high degree of environmental control, gas tightness during growth, and have used large plant stands. These characteristics have placed it in a unique position internationally as a research tool and as a preprototype subcomponent to a fully integrated CELSS. The results from the experiments are presented. Author

N91-20027*# Auburn Univ., AL. Dept. of Aerospace Engineering.
ROCKET-TRIGGERED LIGHTNING STRIKES AND FOREST FIRE IGNITION **c47**
James Fenner *In* NASA, John F. Kennedy Space Center, Research Reports: 1990 NASA/ASEE Summer Faculty Fellowship Program Sep. 1990 p 142-168 (For primary document see N91-20022 11-99)

(Grant NGT-60002)
Avail: NTIS HC/MF A23 CSCL 04B

The following are presented: (1) background information on the rocket-triggered lightning project an Kennedy Space Center (KSC); (2) a summary of the forecasting problem; (3) the facilities and equipment available for undertaking field experiments at KSC; (4) previous research activity performed; (5) a description of the atmospheric science field laboratory near Mosquito Lagoon on the KSC complex; (6) methods of data acquisition; and (7) present results. New sources of data for the 1990 field experiment include measuring the electric field in the lower few thousand feet of the atmosphere by suspending field measuring devices below a tethered balloon, and measuring the electric field intensity in clouds and in the atmosphere with aircraft. The latter program began in July of 1990. Also, future prospects for both triggered lightning and forest fire research at KSC are listed. Author

N91-20028*# Savannah State Coll., GA. Dept. of Engineering Technology.
AN EXPANSION PLAN FOR THE 60 Hz POWER DISTRIBUTION SYSTEM AT KSC: LC-39 SUBSTATIONS LOAD ALLOCATION PLAN c33
Alex Kalu *In* NASA, John F. Kennedy Space Center, Research Reports: 1990 NASA/ASEE Summer Faculty Fellowship Program Sep. 1990 p 169-196 (For primary document see N91-20022 11-99)
(Grant NGT-60002)
Avail: NTIS HC/MF A23 CSCL 10B

The increasing load density in the LC-39 area of Kennedy Space Center (KSC) can be met by either modifying the existing substation and increasing its capacity or by planning an additional new substation. Evidence that the later approach is more economical, enhances the system reliability, and would produce more satisfactory performance indices is provided. Network theory is the basis for the optimal location determination of the proposed substation. A load reallocation plan which minimizes investment cost and power losses and meets other desirable system features is drafted. The report should be useful to the system designer and can be a useful guideline for future facility planners. Author

N91-20029*# Memphis State Univ., TN. Dept. of Mechanical Engineering.
STUDY OF THE AVAILABLE FINITE ELEMENT SOFTWARE PACKAGES AT KSC c61
Chu-Ho Lu *In* NASA, John F. Kennedy Space Center, Research Reports: 1990 NASA/ASEE Summer Faculty Fellowship Program Sep. 1990 p 197-221 (For primary document see N91-20022 11-99)
(Grant NGT-60002)
Avail: NTIS HC/MF A23 CSCL 09B

The interaction among the three finite element software packages, SDRCI/I-DEAS, MSC/NASTRAN, and I/FEM, used at NASA, Kennedy Space Center is addressed. The procedures for using more than one of these application software packages to model and analyze a structure design are discussed. Design and stress analysis of a solid rocket booster fixture is illustrated by using four different combinations of the three software packages. Their results are compared and show small yet acceptable differences. Author

N91-20030*# North Carolina Univ., Greensboro. Dept. of Mathematics and Statistics.
CAROTID-CARDIAC BAROREFLEX INFLUENCE ON FOREARM VASCULAR RESISTANCE DURING LOW LEVEL LBNP c52
David Ludwig *In* NASA, John F. Kennedy Space Center, Research Reports: 1990 NASA/ASEE Summer Faculty Fellowship Program Sep. 1990 p 222-243 (For primary document see N91-20022 11-99)
(Grant NGT-60002)
Avail: NTIS HC/MF A23 CSCL 06P

Twelve healthy males were tested at low levels of lower body negative pressure (LBNP) with and without artificial stimulation of the carotid-cardiac baroreceptors. The carotid-cardiac baroreceptors were stimulated by applying a pressure of 10 mmHg to the carotid artery via a pressurized neck chamber. During the procedure, forearm blood flow (FBF) and forearm vascular resistance (FVR) were measured using a Whitney mercury silastic strain gauge technique. FBF decreased while FVR increased with increased intensity of LBNP. Both FBF and FVR were unaffected by carotid-cardiac baroreceptor stimulation. Author

N91-20031*# Indiana Univ.-Purdue Univ., Fort Wayne.
ROCKET NOISE FILTERING SYSTEM USING DIGITAL FILTERS c20
David Mauritzen *In* NASA, John F. Kennedy Space Center, Research Reports: 1990 NASA/ASEE Summer Faculty Fellowship Program Sep. 1990 p 244-275 (For primary document see N91-20022 11-99)
(Grant NGT-60002)
Avail: NTIS HC/MF A23 CSCL 21H

A set of digital filters is designed to filter rocket noise to various bandwidths. The filters are designed to have constant group delay and are implemented in software on a general purpose computer. The Parks-McClellan algorithm is used. Preliminary tests are performed to verify the design and implementation. An analog filter which was previously employed is also simulated. Author

N91-20032*# Puerto Rico Univ., Mayaguez. Coll. of Engineering.
LOW LEVEL VAPOR VERIFICATION OF MONOMETHYL HYDRAZINE c25
Narinder Mehta *In* NASA, John F. Kennedy Space Center, Research Reports: 1990 NASA/ASEE Summer Faculty Fellowship Program Sep. 1990 p 276-307 (For primary document see N91-20022 11-99)
(Grant NGT-60002)
Avail: NTIS HC/MF A23 CSCL 07D

The vapor scrubbing system and the coulometric test procedure for the low level vapor verification of monomethyl hydrazine (MMH) are evaluated. Experimental data on precision, efficiency of the scrubbing liquid, instrument response, detection and reliable quantitation limits, stability of the vapor scrubbed solution, and interference were obtained to assess the applicability of the method for the low ppb level detection of the analyte vapor in air. The results indicated that the analyte vapor scrubbing system and the coulometric test procedure can be utilized for the quantitative detection of low ppb level vapor of MMH in air. Author

N91-20033*# Norwalk State Technical Coll., CT. Dept. of Mathematics/Science.
CORRELATION OF LEAK RATES OF VARIOUS FLUIDS WITH THE LEAK RATE OF AN INERT GAS IN THE SAME CONFIGURATION c34
Howard Schleier *In* NASA, John F. Kennedy Space Center, Research Reports: 1990 NASA/ASEE Summer Faculty Fellowship Program Sep. 1990 p 308-338 (For primary document see N91-20022 11-99)
(Grant NGT-60002)
Avail: NTIS HC/MF A23 CSCL 20D

NASA is interested in field testing for possible leakage in their fueling systems; however, many fuels are hazardous to the extent that personnel cannot be on hand when the system is being monitored. It is proposed that an inert material such as helium be used on the field test, and that those results be calibrated to simulate the actual process. A technique such as this would allow personnel to be on site during the testing and use techniques to determine the behavior of the system that could not be used otherwise. This endeavor attempts to develop such a correlation. The results show promise, but more refinement and data are needed. Author

N91-20034*# South Carolina Univ., Columbia. Dept. of Physics.
A FLAMMABILITY STUDY OF THIN PLASTIC FILM MATERIALS c27
S. Ballou Skinner *In* NASA, John F. Kennedy Space Center,

Research Reports: 1990 NASA/ASEE Summer Faculty Fellowship Program Sep. 1990 p 339-379 (For primary document see N91-20022 11-99)
(Grant NGT-60002)
Avail: NTIS HC/MF A23 CSCL 11C

The Materials Science Laboratory at the Kennedy Space Center presently conducts flammability tests on thin plastic film materials by using a small needle rake method. Flammability data from twenty-two thin plastic film materials were obtained and cross-checked by using three different testing methods: (1) the presently used small needle rake; (2) the newly developed large needle rake; and (3) the previously used frame. In order to better discern the melting-burning phenomenon of thin plastic film material, five additional specific experiments were performed. These experiments determined the following: (1) the heat sink effect of each testing method; (2) the effect of the burn angle on the burn length or melting/shrinkage length; (3) the temperature profile above the ignition source; (4) the melting point and the fire point of each material; and (5) the melting/burning profile of each material via infrared (IR) imaging. The results of these experimentations are presented. Author

N91-20035*# State Univ. of New York, Farmingdale. Dept. of Mechanical Engineering Technology.
SOME ASPECTS OF ROBOTICS CALIBRATION, DESIGN AND CONTROL **c37**
Hazem Tawfik *In* NASA, John F. Kennedy Space Center, Research Reports: 1990 NASA/ASEE Summer Faculty Fellowship Program Sep. 1990 p 380-431 (For primary document see N91-20022 11-99)
(Grant NGT-60002)
Avail: NTIS HC/MF A23 CSCL 13I

The main objective is to introduce techniques in the areas of testing and calibration, design, and control of robotic systems. A statistical technique is described that analyzes a robot's performance and provides quantitative three-dimensional evaluation of its repeatability, accuracy, and linearity. Based on this analysis, a corrective action should be taken to compensate for any existing errors and enhance the robot's overall accuracy and performance. A comparison between robotics simulation software packages that were commercially available (SILMA, IGRIP) and that of Kennedy Space Center (ROBSIM) is also included. These computer codes simulate the kinematics and dynamics patterns of various robot arm geometries to help the design engineer in sizing and building the robot manipulator and control system. A brief discussion on an adaptive control algorithm is provided. Author

N91-20036*# California State Univ., Sacramento. Dept. of Mechanical Engineering.
LOW FLOW VORTEX SHEDDING FLOWMETER FOR HYPERGOLICS/ALL MEDIA **c34**
Ngo Thinh *In* NASA, John F. Kennedy Space Center, Research Reports: 1990 NASA/ASEE Summer Faculty Fellowship Program Sep. 1990 p 432-461 (For primary document see N91-20022 11-99)
(Grant NGT-60002)
Avail: NTIS HC/MF A23 CSCL 20D

A family of vortex shedding flowmeters for flow measurement of hypergols that requires a long term operation without removal from system lines was further developed. A family of vortex shedding flowmeters without moving parts was designed. The test loop to evaluate the meters for the Freon flow, which simulates the hypergolic fluids, was modified and reconstructed. Preliminary results were obtained on the output frequency characteristics of an 1/2 inch flowmeter as a function of the flow rate. Author

N91-20037*# Lehigh Univ., Bethlehem, PA. Dept. of Industrial Engineering.
ROBOT TRACKING SYSTEM IMPROVEMENTS AND VISUAL CALIBRATION OF ORBITER POSITION FOR RADIATOR INSPECTION **c63**
Gregory Tonkay *In* NASA, John F. Kennedy Space Center, Research Reports: 1990 NASA/ASEE Summer Faculty Fellowship Program Sep. 1990 p 462-487 (For primary document see N91-20022 11-99)
(Grant NGT-60002)
Avail: NTIS HC/MF A23 CSCL 09B

The following separate topics are addressed: (1) improving a robotic tracking system; and (2) providing insights into orbiter position calibration for radiator inspection. The objective of the tracking system project was to provide the capability to track moving targets more accurately by adjusting parameters in the control system and implementing a predictive algorithm. A computer model was developed to emulate the tracking system. Using this model as a test bed, a self-tuning algorithm was developed to tune the system gains. The model yielded important findings concerning factors that affect the gains. The self-tuning algorithms will provide the concepts to write a program to automatically tune the gains in the real system. The section concerning orbiter position calibration provides a comparison to previous work that had been performed for plant growth. It provided the conceptualized routines required to visually determine the orbiter position and orientation. Furthermore, it identified the types of information which are required to flow between the robot controller and the vision system. Author

N91-20038*# Florida Inst. of Tech., Melbourne. Dept. of Chemical Engineering.
MODELING OF FLOW SYSTEMS FOR IMPLEMENTATION UNDER KATE **c63**
Jonathan E. Whitlow *In* NASA, John F. Kennedy Space Center, Research Reports: 1990 NASA/ASEE Summer Faculty Fellowship Program Sep. 1990 p 488-520 (For primary document see N91-20022 11-99)
(Grant NGT-60002)
Avail: NTIS HC/MF A23 CSCL 09B

The modeling of flow systems is a task currently being investigated at Kennedy Space Center in parallel with the development of the KATE artificial intelligence system used for monitoring diagnosis and control. Various aspects of the modeling issues are focussed on with particular emphasis on a water system scheduled for demonstration within the KATE environment in September of this year. LISP procedures were written to solve the continuity equations for three internal pressure nodes using Newton's method for simultaneous nonlinear equations. Author

N91-20039*# National Aeronautics and Space Administration. Ames Research Center, Moffett Field, CA.
RESEARCH AND TECHNOLOGY, 1989
Nov. 1990 238 p Original contains color illustrations
(NASA-TM-102264; A-90030; NAS 1.15:102264) Avail: NTIS HC/MF A11; 14 functional color pages CSCL 05A

Selected research and technology activities at Ames Research Center, including the Moffett Field site and the Dryden Flight Research Facility, are summarized. These accomplishments exemplify the Center's varied and highly productive research efforts for 1989. Author

Typical Subject Index Listing

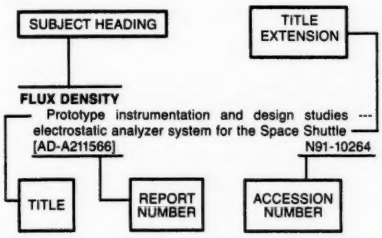

The subject heading is a key to the subject content of the document. Titles, report numbers, and accession numbers of pertinent documents are provided under each subject heading. When the title is insufficiently descriptive of the document content, a title extension has been added, separated from the title by three hyphens. The report number helps to indicate the type of document cited (e.g., NASA report, NASA translation, NASA contractor report). The accession number is the number by which the document abstracts are arranged in this journal and by which the document is sold or requested. The titles, with title extensions if present, are arranged under each subject heading in ascending accession number order. The subject headings have been selected from the latest revision of the *NASA Thesaurus* (NASA SP-7064).

A

ABLATION
Study on ablation of target material induced by pulsed ion beam bombardment N91-19886

ABSORPTANCE
Progress toward the development of dual junction GaAs/Ge solar cells N91-19184

ABSORPTION CROSS SECTIONS
NO2 absorption cross-section in the 440 to 460 nm region at 298 and 220 K
[NOTA-INTERNA-964] N91-19550

ABSORPTION SPECTRA
NO2 absorption cross-section in the 440 to 460 nm region at 298 and 220 K
[NOTA-INTERNA-964] N91-19550
Calculation of emission and absorption spectra of LTE plasma by the STA (Super Transition Array) method
[DE91-007617] N91-19900

ABSORPTION SPECTROSCOPY
X ray absorption spectroscopy of oxide films on metals
[DE91-008100] N91-19278

ABSTRACTS
JPRS report: Science and technology. USSR: Life sciences
[JPRS-ULS-91-001] N91-19567
JPRS report: Science and technology. USSR: Physics and mathematics
[JPRS-UPM-90-004] N91-19800
Activities report of the Istituto Elettrotecnico Nazionale Galileo Ferraris
[ETN-91-98868] N91-19822

ABUNDANCE
Two possible problems for standard big bang nucleosynthesis
[DE91-007342] N91-19985

ACCELERATED LIFE TESTS
Low cost space power generation N91-19212

ACCELERATION (PHYSICS)
Pneumatic launcher
[AD-D014658] N91-19116
Launching projectiles with hydrogen gas generated from titanium-water reactions
[AD-D014653] N91-19171

ACCELERATION STRESSES (PHYSIOLOGY)
Hypergravity and bone mineralization N91-19650

ACCELERATION TOLERANCE
Gravitation receptor reaction in response to effect of acceleration N91-19569

ACCELEROMETERS
The development of a rugged accelerometer
[DE91-007731] N91-19407

ACCIDENTS
Potential health risks from postulated accidents involving the Pu-238 RTG (Radioisotope Thermoelectric Generator) on the Ulysses solar exploration mission
[DE91-007142] N91-19857

ACCUMULATORS
Pneumatic launcher
[AD-D014658] N91-19116
An energy recovery system for a quasi-optical gyrotron
[DE91-008317] N91-19357

ACETATES
Extrudable PBX molding powder
[AD-D014667] N91-19312

ACID RAIN
Throughfall and foliar extraction
[DE91-007184] N91-19535
The NAPAP assessment of damages to materials from acid deposition
[DE91-008086] N91-19542

ACIDITY
The NAPAP assessment of damages to materials from acid deposition
[DE91-008086] N91-19542

ACOUSTIC ATTENUATION
Quantum fluctuations in laser with intracavity frequency doubling N91-19805

ACOUSTIC MEASUREMENT
Large-scale aeroacoustic research feasibility and conceptual design of test-section inserts for the Ames 80-by 120-foot wind tunnel
[NASA-TP-3020] N91-19824

ACOUSTIC PROPERTIES
Large-scale aeroacoustic research feasibility and conceptual design of test-section inserts for the Ames 80-by 120-foot wind tunnel
[NASA-TP-3020] N91-19824
Euler solutions to nonlinear acoustics of non-lifting hovering rotor blades
[NASA-TM-103837] N91-19826

ACOUSTIC SCATTERING
Very low frequency seismo-acoustic scattering from a rough seafloor
[AD-A227947] N91-19564

ACOUSTICS
Mechanical behavior of a ceramic matrix composite material
[NASA-CR-187072] N91-19461
A gradient microphone for locating sound targets
[MBB-Z-0341-90-PUB] N91-19829

ACOUSTO-OPTICS
Acoustic stabilization of laser beam wavefront in nonhomogeneous gaseous medium N91-19802

ACRYLIC RESINS
The mechanical behavior of microcellular foams
[DE91-006775] N91-19291

ACTIVATION ENERGY
Chemical activation of molecules by metals: Experimental studies of electron distributions and bonding
[DE91-007695] N91-19275

ACTIVE CONTROL
Active damping application to the shuttle RMS
[NASA-TM-102763] N91-19471

ACTUATORS
Design and first tests of individual blade control actuators
[MBB-UD-0577-90-PUB] N91-19087
Towards practical control design using neural computation
[NASA-TM-103785] N91-19766

ADA (PROGRAMMING LANGUAGE)
The role of software engineering in the space station program N91-19729
Lessons learned from an Ada conversion project N91-19730
QUEST/Ada (query utility environment for software testing of Ada: The development of a program analysis environment for Ada, task 1, phase 3
[NASA-CR-187983] N91-19735

ADAPTATION
Coordination of eye, head and arm movements in weightlessness N91-19588
Postural changes following sensory reinterpretation as an analog to spaceflight N91-19610
The biological and medical programme of the manned Aragatz mission on the Mir Space Station N91-19617
Human and animal results on vestibular research in space: VERIS N91-19642
Bone adaptation to real and simulated microgravity N91-19643
Adaptive responses in monkeys during two week space flight N91-19645

ADAPTIVE CONTROL
System identification for nonlinear control using neural networks N91-19039
Constructing mathematical model of adaptive anti-flutter system N91-19810

ADDITIVES
Plasma, photon, and beam synthesis of diamond films and multilayered structures
[DE91-007934] N91-19938
Mutual influence of doping and oxidation in highly doped silicon
[ETN-91-98924] N91-19948

ADHESION
Reduced lymphocyte activation in space: Role of cell-substratum interactions N91-19621

ADHESIVE BONDING
Modeling and analysis of orthotropic plate with circular cutout and adhesive bonded patch
[AD-A229866] N91-19496

ADHESIVES
Spaceflight performance of several types of silicon solar cells on the LIPS 3 satellite N91-19213
Modeling and analysis of orthotropic plate with circular cutout and adhesive bonded patch
[AD-A229866] N91-19496

AEOLIAN TONES
Aeolian removal of dust types from photovoltaic surfaces on Mars N91-19156
Computational comparison of efficacies of aeolian vibration damping devices for multiconductor overhead power lines
[BU-411] N91-19487

AEROACOUSTICS
Inflight source noise of an advanced full-scale single-rotation propeller
[NASA-TM-103687] N91-19045
Unified aeroacoustics analysis for high speed turboprop aerodynamics and noise. Volume 1: Development of theory for blade loading, wakes, and noise
[NASA-CR-4329] N91-19049
Large-scale aeroacoustic research feasibility and conceptual design of test-section inserts for the Ames 80-by 120-foot wind tunnel
[NASA-TP-3020] N91-19824

AERODYNAMIC BALANCE
An experimental study of a sting-mounted single-slot circulation control wing
[AD-A229867] N91-19111

AERODYNAMIC CHARACTERISTICS
Prediction of ice shapes and their effect on airfoil performance
[NASA-TM-103701] N91-19047
Large-scale aeroacoustic research feasibility and conceptual design of test-section inserts for the Ames 80-by 120-foot wind tunnel
[NASA-TP-3020] N91-19824

AERODYNAMIC COEFFICIENTS
Cascade flutter analysis with transient response aerodynamics
[NASA-TM-103746] N91-19475
AERODYNAMIC CONFIGURATIONS
The effect of body shape on the development of vortex asymmetry in the flow past slender bodies
[BU-413] N91-19068
AERODYNAMIC DRAG
Prediction of ice shapes and their effect on airfoil performance
[NASA-TM-103701] N91-19047
A novel potential/viscous flow coupling technique for computing helicopter flow fields
[NASA-CR-177568] N91-19060
AERODYNAMIC FORCES
A flight-dynamic helicopter mathematical model with a single flap-lag-torsion main rotor
[NASA-TM-102267] N91-19041
An experimental study of a sting-mounted single-slot circulation control wing
[AD-A229867] N91-19111
AERODYNAMIC LOADS
Modal analysis of UH-60A instrumented rotor blades
[NASA-TM-4239] N91-19052
The effect of steady aerodynamic loading on the flutter stability of turbomachinery blading
[NASA-CR-187055] N91-19479
AERODYNAMIC NOISE
Non-linear generation of acoustic noise in the IAR spacecraft N91-19143
Unsteady blade pressure measurements for the SR-7A propeller at cruise conditions
[NASA-TM-103606] N91-19825
Elementary pulse diffraction problems and the generation of sound by a dipole moving across the edge of a half-plane
[LR-565] N91-19831
AERODYNAMIC STABILITY
Constructing mathematical model of adaptive anti-flutter system N91-19810
AERODYNAMICS
Dedication of National Institute for Aviation Research
[NIAR-90-21] N91-19040
Aerodynamic focusing of particles and heavy molecules
[DE91-006922] N91-19833
AEROELASTICITY
The effect of steady aerodynamic loading on the flutter stability of turbomachinery blading
[NASA-CR-187055] N91-19479
Constructing mathematical model of adaptive anti-flutter system N91-19810
AERONAUTICAL ENGINEERING
Enhancing space transportation: The NASA program to develop electric propulsion
[NASA-TM-4244] N91-19181
AEROSOLS
Theory of CW lidar aerosol backscatter measurements and development of a 2.1 microns solid-state pulsed laser radar for aerosol backscatter profiling
[NASA-CR-4347] N91-19498
SBUV/2 comparisons with ground-based and SBUV spacecraft data N91-19521
Umkehr work N91-19522
The relationship between aerosol and drop size distributions in the marine atmosphere
[DE91-006514] N91-19553
Aerosol formation in atmospheric mixtures
[PB91-129114] N91-19560
AEROSPACE ENGINEERING
The OAST space power program N91-19183
NDE standards for high temperature materials
[NASA-TM-103761] N91-19464
AEROSPACE ENVIRONMENTS
High vacuum facility for hydrazine thruster testing N91-19134
The effect of the low Earth orbit environment on space solar cells
[NASA-TM-103735] N91-19165
Strategy in space flight experiments N91-19220
In-space experiment on thermoacoustic convection heat transfer phenomenon-experiment definition
[NASA-CR-187070] N91-19378
New experimental approach in quality factor and dose equivalent determination during a long term manned space mission N91-19679
AEROSPACE INDUSTRY
Space Vehicle Flight Mechanics
[AGARD-AR-294] N91-19124
Application of functional gradient materials in the aerospace industry
[MBB-Z-0320-90-PUB] N91-19311
Commercial Space Launch Act implementation
[GPO-27-944] N91-19968
AEROSPACE MEDICINE
Reactivity of exhausted human skeletal muscle fibers following prolonged antiorthostatic hypokinesia N91-19568
Fourth European Symposium on Life Sciences Research in Space
[ESA-SP-307] N91-19572
Life sciences in ESA TRP activity N91-19589
The biological and medical programme of the manned Aragatz mission on the Mir Space Station N91-19617
USSR Space Life Sciences Digest. Index to issues 26-29
[NASA-CR-3922(35)] N91-19700
AEROSPACE SAFETY
COLD-SAT feasibility study safety analysis
[NASA-CR-187042] N91-19167
Low level vapor verification of monomethyl hydrazine N91-20032
AEROSPACE SCIENCES
NASA Thesaurus supplement: A four part cumulative supplement to the 1988 edition of the NASA Thesaurus (supplement 5)
[NASA-SP-7064-SUPPL-5] N91-19962
AEROSPACE SYSTEMS
Space reactor/Stirling cycle systems for high power lunar application
[NASA-TM-103698] N91-19112
AEROSPACE VEHICLES
Hypervelocity impact physics
[NASA-CR-4343] N91-19164
AEROTHERMODYNAMICS
Techniques for hot structures testing
[NASA-TM-101727] N91-19080
AGING (BIOLOGY)
Microgravity, hypergravity, and aging: A unifying hypothesis N91-19633
AGING (MATERIALS)
Effect of fiber reinforcements on thermo-oxidative stability and mechanical properties of polymer matrix composites
[NASA-TM-103648] N91-19234
AH-1G HELICOPTER
Development and applications of a multi-level strain energy method for detecting finite element modeling errors
[NASA-CR-187447] N91-19478
AIR
The application of simulation model for the flow induced by air bubble plume in thermally stratified reservoirs
[DE91-003064] N91-19380
AIR DATA SYSTEMS
Preliminary results from an airdata enhancement algorithm with application to high-angle-of-attack flight
[NASA-TM-101737] N91-19095
AIR FLOW
Identification of flow and volume parameters in multizone systems using a single gas tracer technique
[DE91-006894] N91-19368
A modelling of unsteady air flow in the resonance charging system of high speed diesel engines
[ACTA-POLYTEC-SCAND-ME-97] N91-19454
A non-linear method for the calculation of the power output of a rotating wind turbine
[BU-416] N91-19512
Wavelets and turbulence on the sea surface
[AD-A229862] N91-19565
AIR NAVIGATION
Investigation of air transportation technology at Ohio University, 1989-1990 N91-19028
AIR POLLUTION
Remote detection of organics using Fourier transform infrared spectroscopy
[DE91-006045] N91-19253
The dilemma of fossil fuel use and global climate change
[DE91-007859] N91-19533
Throughfall and foliar extraction
[DE91-007184] N91-19535
Analysis of high frequency surface-induced concentration fluctuations
[DE91-007561] N91-19538
Estimating lightning-generated NOx emissions for regional air pollution models
[PB91-131664] N91-19546
AIR SAMPLING
Screening volatile organics by direct sampling ion trap and glow discharge mass spectrometry
[DE91-007708] N91-19258
AIR TRAFFIC
Air traffic simulation with a view to system interpretation N91-19110
AIR TRAFFIC CONTROL
Automatic speech recognition in air traffic control: A human factors perspective N91-19025
Investigation of air transportation technology at Ohio University, 1989-1990 N91-19028
Aircraft standstill, requirements for ground handling from the point of view of aircraft operation N91-19109
AIR TRAFFIC CONTROLLERS (PERSONNEL)
BUBBLES: An automated decision support system for final approach controllers N91-19027
AIR TRANSPORTATION
Joint University Program for Air Transportation Research, 1989-1990
[NASA-CP-3095] N91-19024
Investigation of air transportation technology at Ohio University, 1989-1990 N91-19028
Investigation of air transportation technology at Princeton University, 1989-1990 N91-19033
The 1990-1991 aviation system capacity plan
[AD-A229863] N91-19075
Aircrafts, requirements for ground installations from the aircraft point of view N91-19108
Air traffic simulation with a view to system interpretation N91-19110
AIR WATER INTERACTIONS
Air/sea temperature probe
[AD-D014674] N91-19397
Thermohaline circulations and global climate change
[DE91-007458] N91-19537
Wavelets and turbulence on the sea surface
[AD-A229862] N91-19565
Research conducted at the Radiation Lab, Notre Dame Univ.
[DE91-007969] N91-19843
AIRBORNE/SPACEBORNE COMPUTERS
I'm all 'light' Jack
[MBB-UD-0576-90-PUB] N91-19101
Space Shuttle: NASA should implement independent oversight of software development
[GAO/IMTEC-91-20] N91-19119
AIRCRAFT BRAKES
TF89 design project airbrake and arrester hook design
[ETN-91-98853] N91-19092
AIRCRAFT CONFIGURATIONS
Introduction of the M-85 high-speed rotorcraft concept
[NASA-TM-102871] N91-19078
AIRCRAFT CONSTRUCTION MATERIALS
Research on advanced NDE methods for aerospace structures
[AD-A226858] N91-19460
AIRCRAFT CONTROL
Progress on intelligent guidance and control for wind shear encounter N91-19034
Neural networks in nonlinear aircraft control N91-19037
Constructing mathematical model of adaptive anti-flutter system N91-19810
AIRCRAFT DESIGN
An experimental study of the turbulent boundary layer on a transport wing in subsonic and transonic flow
[NASA-TM-102206] N91-19062
TF89 design project airbrake and arrester hook design
[ETN-91-98853] N91-19092
Air traffic simulation with a view to system interpretation N91-19110
Space Vehicle Flight Mechanics
[AGARD-AR-294] N91-19124
An expert system for laminated plate design using composite materials
[BU-406] N91-19245
Development and applications of a multi-level strain energy method for detecting finite element modeling errors
[NASA-CR-187447] N91-19478
AIRCRAFT ENGINES
Propulsion system concept for the Eurofar tilt rotor aircraft
[MBB-UD-0573-90-PUB] N91-19084
AIRCRAFT GUIDANCE
Progress on intelligent guidance and control for wind shear encounter N91-19034
AIRCRAFT MANEUVERS
Preliminary results from an airdata enhancement algorithm with application to high-angle-of-attack flight
[NASA-TM-101737] N91-19095
AIRCRAFT MODELS
TF89 design project airbrake and arrester hook design
[ETN-91-98853] N91-19092
AIRCRAFT NOISE
Inflight source noise of an advanced full-scale single-rotation propelier
[NASA-TM-103687] N91-19045
Unified aeroacoustics analysis for high speed turboprop aerodynamics and noise. Volume 1: Development of theory for blade loading, wakes, and noise
[NASA-CR-4329] N91-19049
BO 108 development status and prospects
[MBB-UD-0574-90-PUB] N91-19085

AIRCRAFT PARTS
Life and dynamic capacity modeling for aircraft transmissions
[NASA-CR-4341] N91-19438
AIRCRAFT PERFORMANCE
Joint University Program for Air Transportation Research, 1989-1990
[NASA-CP-3095] N91-19024
AIRCRAFT RELIABILITY
BO 108 development status and prospects
[MBB-UD-0574-90-PUB] N91-19085
AIRCRAFT SAFETY
Progress on intelligent guidance and control for wind shear encounter N91-19034
Dedication of National Institute for Aviation Research
[NIAR-90-21] N91-19040
BO 108 development status and prospects
[MBB-UD-0574-90-PUB] N91-19085
AIRCRAFT STRUCTURES
Techniques for hot structures testing
[NASA-TM-101727] N91-19080
Thermoelastic vibration test techniques
[NASA-TM-101742] N91-19083
Smoothness criteria for runway rehabilitation and overlays
[DOT/FAA/RD-90/23] N91-19102
Strength test of CFRP box beam model
[NAL-TR-1057] N91-19469
AIRCRAFT TIRES
Dynamic behavior of pneumatic tyres
[BU-412] N91-19453
AIRFOILS
Icing characteristics of a natural-laminar-flow, a medium-speed, and a swept, medium-speed airfoil
[NASA-TM-103693] N91-19046
Prediction of ice shapes and their effect on airfoil performance
[NASA-TM-103701] N91-19047
Acoustic radiation from lifting airfoils in compressible subsonic flow
[NASA-TM-103650] N91-19053
Wind tunnel wall effects in a linear oscillating cascade
[NASA-TM-103690] N91-19098
AIRFRAMES
Use of system identification techniques for improving airframe finite element models using test data
[NASA-CR-188041] N91-19750
AIRPORT PLANNING
Airport apron research and development
[MBB-Z-0168-90-PUB] N91-19106
AIRPORTS
The 1990-1991 aviation system capacity plan
[AD-A229863] N91-19075
Smoothness criteria for runway rehabilitation and overlays
[DOT/FAA/RD-90/23] N91-19102
Airport apron research and development
[MBB-Z-0168-90-PUB] N91-19106
Airport system technical aspects N91-19107
Aircrafts, requirements for ground installations from the aircraft point of view N91-19108
Air traffic simulation with a view to system interpretation N91-19110
AIRSPACE
The 1990-1991 aviation system capacity plan
[AD-A229863] N91-19075
Air traffic simulation with a view to system interpretation N91-19110
ALASKA
Outer continental shelf environmental assessment program, volume 70
[PB91-129288] N91-19548
ALBEDO
SBUV/2 in-orbit performance N91-19517
ALCOHOLS
Comprehensive mechanisms for combustion chemistry: An experimental and numerical study with emphasis on applied sensitivity analysis
[DE91-008030] N91-19262
ALDEHYDES
Comprehensive mechanisms for combustion chemistry: An experimental and numerical study with emphasis on applied sensitivity analysis
[DE91-008030] N91-19262
ALGAE
Unicellular algae in space. 1: Preparatory tests N91-19639
Unicellular algae in space. 2: Sounding-rocket experiment N91-19640
Unicellular algae in space. 3: Addendum N91-19641
ALGEBRA
A theoretical solution for the buckling of sandwich panels with laminated face plates using a computer algebra system
[BU-407] N91-19486
ALGORITHMS
A proposed Kalman filter algorithm for estimation of unmeasured output variables for an F100 turbofan engine
[NASA-TM-4234] N91-19099
Digital optical computers at the optoelectronic computing systems center
[NASA-CR-187520] N91-19345
Laboratory testing of the Sonnenschein charger, Part number DTL 12040
[DE91-006543] N91-19346
SBUV/2 comparisons with ground-based and SBUV spacecraft data N91-19521
Umkehr work N91-19522
Design, implementation and evaluation of new fully automated algorithms for the extraction of cardiac parameters from 3D, 2D and M-mode echocardiograms N91-19582
Advanced sequencing technology
[DE91-008031] N91-19706
Complete exchange on the iPSC-860
[NASA-CR-187498] N91-19715
Multiphase complete exchange on a circuit switched hypercube
[NASA-CR-187499] N91-19716
Algorithms for a very high speed universal noiseless coding module
[NASA-CR-187974] N91-19733
On the optimality of code options for a universal noiseless coder
[NASA-CR-187973] N91-19734
Rational model identification using an extended least squares algorithm
[RR-388] N91-19753
The qualitative analysis of nonlinear parameterised systems. Part 2: A method for the global analysis of nonlinear systems
[RR-400-PT-2] N91-19754
Model distribution in decentralized multi-sensor data fusion
[OUEL-1868/90] N91-19763
Practical path planning among movable obstacles
[DE91-000034] N91-19768
Cascading a systolic array and a feedforward neural network for navigation and obstacle avoidance using potential fields
[NASA-CR-177575] N91-19771
Design and implementation of an image understanding system: DADS
[ETN-91-98926] N91-19773
The cost-constrained traveling salesman problem
[DE91-004943] N91-19775
The qualitative analysis of nonlinear parameterized systems. Part 1: Nonlinear systems representation and dynamical systems theory
[RR-408-PT-1] N91-19789
Subcycling in transient finite element analysis
[ISBN-90-9003684-9] N91-19790
Orthogonal least squares parameter estimation algorithms for nonlinear stochastic systems
[RR-404] N91-19797
Rocket noise filtering system using digital filters N91-20031
Robot tracking system improvements and visual calibration of orbiter position for radiator inspection N91-20037
ALIGNMENT
Local synthesis and tooth contact analysis of face-milled spiral bevel gears
[NASA-CR-4342] N91-19439
ALKALI METALS
Alkali metal corrosion of alumina: Thermodynamics, phase diagrams and testing
[ETN-91-98933] N91-19286
ALKALIES
A study of alkaline element interferences in analytical inductively coupled plasmas
[ISAL-90-0069] N91-19915
ALKALINE EARTH COMPOUNDS
Direct conversion of methane to C2's and liquid fuels
[DE91-007545] N91-19318
ALLOCATIONS
National Aeronautics and Space Administration N91-19967
ALLOYING
Gas entrapment and evolution in aluminium alloys produced by powder metallurgy
[ETN-91-98918] N91-19285
ALLOYS
Microbiologically influenced corrosion in copper and nickel seawater piping systems
[AD-A229874] N91-19287
The effect of elastic stress on Ostwald ripening phenomena
[DE91-008034] N91-19484
Electrochemical impedance spectroscopy of metal alloys in the space transportation system launch environment N91-20025
ALPHA PARTICLES
Evaluation of a Photo-Electron Rejecting Alpha Liquid Scintillation (PERALS) spectrometer for the measurement of alpha-emitting radionuclides
[DE91-005652] N91-19399
ALTERNATIVES
Efficient connecting networks using directed links
[ETN-91-98855] N91-19762
ALTITUDE SIMULATION
The development of a ram air decelerator for the recovery of artillery shells
[DE91-007732] N91-19064
ALUMINIDES
Low-density, high-strength intermetallic matrix composites by XD (trademark) synthesis
[NASA-TM-103724] N91-19233
ALUMINUM
Thermoelastic vibration test techniques
[NASA-TM-101742] N91-19083
Characterization of ion-implanted aluminum and iron by spectroscopic ellipsometry
[DE91-008371] N91-19283
XANES investigation of pH effects during cerium-sealing of anodized aluminum
[DE91-008101] N91-19302
Recombination x ray laser experiments using exploding ribbon Al targets
[DE91-007146] N91-19429
ALUMINUM ALLOYS
Bulging of fatigue cracks in a pressurized aircraft fuselage
[LR-647] N91-19094
Minimum weight optimization of composite laminated struts
[BU-409] N91-19246
Stress corrosion cracking of Al-Li-Cu-Zr alloy 2090 in aqueous Cl(-) and mixed CO3(2-)/Cl(-) environments
[DE91-007064] N91-19269
Effects of radiolytic tritium decay on the thermodynamic behavior of LaNi(4.25)Al(0.75) tritides
[DE91-007961] N91-19277
Gas entrapment and evolution in aluminium alloys produced by powder metallurgy
[ETN-91-98918] N91-19285
Texture and microstructure development in Al-2 percent Mg during high-temperature deformation
[DE91-007355] N91-19480
Crack opening stress measurements of surface cracks in 7075-T6 Al alloy plate specimens through electron fractography
[LR-641] N91-19492
Design and testing of a circumferential and longitudinal joint of the A320 fuselage section 13/14 in GLARE
[LR-645] N91-19494
Considerations relating to pulsed-beam modification of materials
[DE91-006771] N91-19922
Free energy simulation of grain boundary segregation the thermodynamics in Ni(3-x)Al(1+x)
[DE91-007473] N91-19928
Some roles for TEM in the development of new materials
[DE91-007742] N91-19933
ALUMINUM GALLIUM ARSENIDES
Status of GaAs/Ge solar cells N91-19185
Graded-bandgap AlGaAs solar cells for AlGaAs/Ge cascade cells N91-19186
AlGaAs top solar cell for mechanical attachment in a multi-junction tandem concentrator solar cell stack N91-19187
Progress in GaAs/CuInSe2 tandem junction solar cells N91-19190
GaAs solar cell photoresponse modeling using PC-1D V2.1 N91-19193
ALUMINUM OXIDES
Tribological properties of Ag/Ti films on Al2O3 ceramic substrates
[NASA-TM-103784] N91-19224
Alkali metal corrosion of alumina: Thermodynamics, phase diagrams and testing
[ETN-91-98933] N91-19286
Ceramic fabrication R and D
[DE91-006537] N91-19298
Passive mode locking in optically pumped Al2O3:Ti(3+) laser N91-19803
AMBIENT TEMPERATURE
Special requirements in the design of a sensor test and integration laboratory N91-19141
AMINES
Photoinduced electron transfer processes in homogeneous and microheterogeneous solutions
[DE91-007582] N91-19836

AMMONIA
Control of catalytic hydrotreating selectivity with ammonia
[DE91-005511] N91-19250
Evidence for ammonium-bearing minerals in Ceres N91-20004

AMORPHOUS MATERIALS
Thin film amorphous electrolytes: The Li2O-SiO2-P2O5 system
[DE91-007272] N91-19925

AMORPHOUS SILICON
Annealing characteristics of irradiated hydrogenated amorphous silicon solar cells N91-19214
Integral bypass diodes in an amorphous silicon alloy photovoltaic module N91-19218

AMPLIFIERS
Alternate approach for obtaining dynamic range in monopulse guidance systems
[AD-D014644] N91-19100
High pulse repetition frequency radar early warning receiver
[AD-D014655] N91-19328
Intense microwave generation using free-electron lasers
[DE91-007262] N91-19417
A modulated high-power optical source specification
[AD-D014654] N91-19869

ANALOGIES
Modal analysis of UH-60A instrumented rotor blades
[NASA-TM-4239] N91-19052

ANALYSIS (MATHEMATICS)
Large-scale computing in the energy research programs
[DE91-007907] N91-19748

ANECHOIC CHAMBERS
Noise level reduction inside helicopter cabins
[MBB-UD-0578-90-PUB] N91-19828

ANELASTICITY
Internal friction peaks due to interstitials in bcc alloys
[DE91-007411] N91-19272

ANGLE OF ATTACK
Prediction of ice shapes and their effect on airfoil performance
[NASA-TM-103701] N91-19047
F-18 high alpha research vehicle surface pressures: Initial in-flight results and correlation with flow visualization and wind-tunnel data
[NASA-TM-101724] N91-19051
Preliminary results from an airdata enhancement algorithm with application to high-angle-of-attack flight
[NASA-TM-101737] N91-19095
Laws of heat transfer in three-dimensional viscous shock layer of stream flowing past blunt bodies at some angles of attack and glide N91-19801

ANGULAR MOMENTUM
Conservation of energy, momentum, and angular momentum in Lagrangian staggered-grid hydrodynamics
[DE91-008059] N91-19381

ANIMALS
Microgravity and development of aquatic animals N91-19625
Human and animal results on vestibular research in space: VERIS N91-19642
The 1989-1990 NASA space biology accomplishments
[NASA-TM-4258] N91-19697

ANIMATION
Computation and graphics in mathematical research
[DE91-007333] N91-19776

ANNEALING
Thermal annealing of GaAs concentrator solar cells N91-19195
Burst annealing of high temperature GaAs solar cells N91-19196
Annealing characteristics of irradiated hydrogenated amorphous silicon solar cells N91-19214
Method of producing superconducting materials in bulk form
[AD-D014656] N91-19917

ANNUAL VARIATIONS
Cosmic ray charged component variations at sea level
[DE91-615480] N91-20021

ANNULAR FLOW
Three-component laser anemometer measurement systems
[NASA-TP-3080] N91-19057

ANODES
Investigation of anodic and chemical oxides grown on p-type InP with applications to surface passivation for n(+)-p solar cell fabrication N91-19208

ANODIZING
XANES investigation of pH effects during cerium-sealing of anodized aluminum
[DE91-008101] N91-19302

ANOMALIES
Design and implementation of an image understanding system: DADS
[ETN-91-98926] N91-19773
J-85 jet engine noise measured in the ONERA S1 wind tunnel and extrapolated to far field
[NASA-TP-3053] N91-19823

ANTENNA ARRAYS
Fiber optic feed
[AD-A229860] N91-19879

ANTENNA COMPONENTS
Fiber optic feed
[AD-A229860] N91-19879

ANTENNA DESIGN
C-band antennas for regional communication systems
[MBB-UK-0107-90-PUB] N91-19336

ANTHROPOMETRY
Vertebral column length changes during simulated microgravity N91-19604
Responses of women to orthostatic and exercise stresses
[NASA-TP-3043] N91-19711
Army-NASA aircrew/aircraft integration program (A3I) software detailed design document, phase 3
[NASA-CR-177557] N91-19714

ANTIBIOTICS
Growth rate of bacteria without and with antibiotic at different levels of gravity N91-19632

ANTIFERROMAGNETISM
Magnetism and superconductivity in YBa2Cu3O(6+x) at 0.3 less than or equal to x less than or equal to 0.4
[DE91-615507] N91-19945

ANTIMONY COMPOUNDS
Superconductivity of oxide film electrolytically deposited on surface of B(1-x)Sb(x) single crystal N91-19819

ANTIREFLECTION COATINGS
Progress toward the development of dual junction GaAs/Ge solar cells N91-19184

APERTURES
Aperture-averaging factor for optical propagation through the turbulent atmosphere
[PB91-129338] N91-19875
Fiber optic feed
[AD-A229860] N91-19879

APPLICATIONS PROGRAMS (COMPUTERS)
New computer codes for the structural analysis of composite helicopter structures
[MBB-UD-0580-90-PUB] N91-19089
Computational simulation of hot composites structures
[NASA-TM-103681] N91-19230
A finite element conjugate gradient FFT method for scattering N91-19306
Local synthesis and tooth contact analysis of face-milled spiral bevel gears
[NASA-CR-4342] N91-19439
A theoretical solution for the buckling of sandwich panels with laminated face plates using a computer algebra system
[BU-407] N91-19486
COMPLEAT (community-oriented model for planning least-cost energy alternatives and technologies): A planning tool for publicly owned electric utilities
[DE91-006955] N91-19511
ARCHY (analysis and reverse engineering of code using hierarchy and Yourdon): A tool for FORTRAN code maintenance and development
[DE91-007241] N91-19720
Some neutronics and thermal-hydraulics codes for reactor analysis using personal computers
[DE91-006591] N91-19743
Software for the ODRENOK microcomputer. Program package for graphics editing
[DE91-614980] N91-19752
Research reports: 1990 NASA/ASEE Summer Faculty Fellowship Program
[NASA-CR-187638] N91-20022
Study of the available finite element software packages at KSC N91-20029
Some aspects of robotics calibration, design and control N91-20035

APPROACH CONTROL
BUBBLES: An automated decision support system for final approach controllers N91-19027

APPROPRIATIONS
Departments of Veterans Affairs and Housing and Urban Development, and Independent Agencies Appropriation Bill, 1991
[S-REPT-101-474] N91-19966
National Aeronautics and Space Administration N91-19967
Problems at National Aeronautics and Space Administration
[S-HRG-101-1146] N91-19969

APPROXIMATION
Bayesian approximation of solutions to linear ordinary differential equations
[DE91-007872] N91-19785
Approximation properties of wavelet transforms
[ETN-91-98922] N91-19799
Aperture-averaging factor for optical propagation through the turbulent atmosphere
[PB91-129338] N91-19875

ARC JET ENGINES
High power arcjet
[NASA-CR-187986] N91-19173

ARC WELDING
Effects of irradiation on crack-arrest toughness of two high-copper welds
[DE91-007189] N91-19270
Performance of underwater weldments
[PB91-129254] N91-19452

ARCHITECTURE (COMPUTERS)
Digital optical computers at the optoelectronic computing systems center
[NASA-CR-187520] N91-19345
Performance measurements of the first RAID prototype
[NASA-CR-187958] N91-19718
A valiant little terminal: A VLT user's manual
[DE91-007295] N91-19719
ARCHY (analysis and reverse engineering of code using hierarchy and Yourdon): A tool for FORTRAN code maintenance and development
[DE91-007241] N91-19720
Finding the object proceedings addendum
[DE91-006724] N91-19738
Development of a numerical computer code and circuit element models for simulation of firing systems
[DE91-007162] N91-19739
A structured representation for parallel algorithm design on multicomputers
[DE91-006674] N91-19744
PHIGS PLUS for scientific graphics
[DE91-007615] N91-19747
Summer institute in parallel programming
[DE91-007922] N91-19760
Particle-in-cell plasma simulation codes on the connection machine
[DE91-007845] N91-19902
Analyzing product test data in a relational database using SAS software
[DE91-007734] N91-19960
Prototype document tracking and storage system for the Superconducting Super Collider Laboratory (SSCL)
[DE91-008204] N91-19963
An architecture for accommodating referenceability among intelligent electronic documents
[DE91-008250] N91-19964

ARGON
A study of alkaline element interferences in analytical inductively coupled plasmas
[ISAL-90-0069] N91-19915
Noble gas disk MHD generator performance with unstable nonequilibrium plasma
[ISBN-90-9003671-7] N91-19916

ARGON PLASMA
He-like spectra through charge exchange processes in tokamak plasmas
[NIFS-69] N91-19894

ARM (ANATOMY)
Coordination of eye, head and arm movements in weightlessness N91-19588

ARMED FORCES (FOREIGN)
The impact of the new management strategy on senior operational commanders at group level within Royal Air Force Strike Command
[REPT-89SDM/MCHALE/03-MDA] N91-19954

ARRESTING GEAR
TF89 design project airbrake and arrester hook design
[ETN-91-98853] N91-19092

ARSENIC
Mutual influence of doping and oxidation in highly doped silicon
[ETN-91-98924] N91-19948

ARTERIES
Simulated absence of gravity impairs arterial baroreceptor control of heart rate in man N91-19599
Carotid-cardiac baroreflex influence on forearm vascular resistance during low level LBNP N91-20030

ARTIFICIAL INTELLIGENCE
Uncertainty reasoning applied to the assessment of composite material for structural design
[BU-405] N91-19244
Artificial neural network implementation
[AD-D014663] N91-19764
A haptic system for a multifingered hand
[DE90-017044] N91-19767

Navigation of a car-like mobile robot using a decomposition of the environment in convex cells
[DE91-000709] N91-19769
Simulating motivated cognition
[NASA-TM-102886] N91-19770
Topological models for space and time
[OUEL-1860/90] N91-19774
Modeling of flow systems for implementation under KATE N91-20038

ARTIFICIAL SATELLITES
COLD-SAT feasibility study safety analysis
[NASA-CR-187042] N91-19167

ARTILLERY
The development of a ram air decelerator for the recovery of artillery shells
[DE91-007732] N91-19064

ASCENT
Atmospheric environment for space shuttle (STS-41) launch
[NASA-TM-103525] N91-19529

ASSESSMENTS
Uncertainty reasoning applied to the assessment of composite material for structural design
[BU-405] N91-19244

ASTEROIDS
Evidence for ammonium-bearing minerals in Ceres N91-20004

ASTRONAUT PERFORMANCE
Central and peripheral cardiovascular responses to electrically induced and voluntary leg exercise N91-19687

ASTRONAUTS
Physiological criteria and requirement of biomass production under controlled ecological life support systems N91-19659

ASTRONOMICAL MODELS
High energy physics and cosmology
[DE91-007369] N91-19859
Two possible problems for standard big bang nucleosynthesis
[DE91-007342] N91-19985
Origin of regularities in the redshift distributions of distant galaxies and quasars
[DE91-007889] N91-19986
Observational relations in model universes dominated by domain-wall-like matter
[DE91-744969] N91-19988
Gravitational lens effect of wall-like objects and its cosmological implications
[DE91-744976] N91-19992

ASTROPHYSICS
Activities report of the Institute for Extraterrestrial Physics
[MPE-222] N91-19971
A scientific program for infrared, submillimeter and radio astronomy from space: A report by the Management Operations Working Group
[NASA-TM-103333] N91-19979
Some limitations of detailed balance for inverse reaction calculations in the astrophysical P-process
[DE91-007258] N91-19983
Proceedings of the symposium Astrophysical Processes and Structures in the Universe
[PB91-123653] N91-19993

ASYMMETRY
The effect of body shape on the development of vortex asymmetry in the flow past slender bodies
[BU-413] N91-19068

ASYMPTOTIC METHODS
Analytical solutions with Generalized Impedance Boundary Conditions (GIBC) N91-19307

ASYMPTOTIC SERIES
Dynamics of collision processes
[DE91-007933] N91-19840

ATMOSPHERIC CHEMISTRY
Regional Oxidant Model Multi-Processor (ROMMP)
[PB91-131680] N91-19547
Aerosol formation in atmospheric mixtures
[PB91-129114] N91-19560

ATMOSPHERIC COMPOSITION
Umkehr work N91-19522
Calibration of long term satellite ozone data sets using the space shuttle N91-19524
Atmospheric environment for space shuttle (STS-41) launch
[NASA-TM-103525] N91-19529
Evaluation of significant anthropogenic sources of radiatively important trace gases
[PB91-127753] N91-19545
ICRCCM (intercomparison of radiation codes used in climate models). Phase 2: Verification and calibration of radiation codes in climate models
[DE91-007323] N91-19555
Aerosol formation in atmospheric mixtures
[PB91-129114] N91-19560
Chemical approaches to carbon dioxide utilization for manned Mars missions
[NASA-TM-103728] N91-20015

ATMOSPHERIC EFFECTS
Effects of atmosphere and heating rate during processing of a ceramic superconductor
[DE91-007761] N91-19299

ATMOSPHERIC ELECTRICITY
Rocket-triggered lightning strikes and forest fire ignition N91-20027

ATMOSPHERIC GENERAL CIRCULATION MODELS
Zonal statistics in (General Circulation Model) GCM/GCM/data intercomparisons
[DE91-006706] N91-19530
Natural and anthropogenic climate change
[DE91-007363] N91-19532

ATMOSPHERIC IONIZATION
Studies of atmospheric molecules by multiphoton spectroscopy
[DE91-006738] N91-19554

ATMOSPHERIC MODELS
Analysis of workload and load balancing issues in the NCAR community climate model
[DE91-008052] N91-19534
Estimating lightning-generated NOx emissions for regional air pollution models
[PB91-131664] N91-19546
Cloud forcing: A modeling perspective
[DE91-007215] N91-19551
ICRCCM (intercomparison of radiation codes used in climate models). Phase 2: Verification and calibration of radiation codes in climate models
[DE91-007323] N91-19555
Energy sciences supercomputing 1990
[DE91-007188] N91-19740

ATMOSPHERIC MOISTURE
Design, performance evaluation, and investigation of the theoretical capabilities of the NASA Millimeter-wave Imaging Radiometer (MIR)
[NASA-CR-187984] N91-19398

ATMOSPHERIC OPTICS
Aperture-averaging factor for optical propagation through the turbulent atmosphere
[PB91-129338] N91-19875

ATMOSPHERIC RADIATION
Cloud forcing: A modeling perspective
[DE91-007215] N91-19551
ICRCCM (intercomparison of radiation codes used in climate models). Phase 2: Verification and calibration of radiation codes in climate models
[DE91-007323] N91-19555

ATMOSPHERIC SOUNDING
Rocket-triggered lightning strikes and forest fire ignition N91-20027

ATMOSPHERIC TEMPERATURE
Air/sea temperature probe
[AD-D014674] N91-19397

ATMOSPHERIC TURBULENCE
Aperture-averaging factor for optical propagation through the turbulent atmosphere
[PB91-129338] N91-19875

ATOMIC BEAMS
Atomic beam studies of the interaction of hydrogen with transition metal surfaces
[DE91-007938] N91-19841

ATOMIC COLLISIONS
Electron transfer, ionization, and excitation in atomic collisions
[DE91-008044] N91-19844

ATOMIC PHYSICS
The advanced light source: A new tool for research in atomic physics
[DE91-007739] N91-19861
Quasi-molecular processes in dense plasmas
[DE91-007388] N91-19899

ATOMIC STRUCTURE
Theoretical investigation of phase stability in non-magnetic Fe-V substitutional alloys
[DE91-006711] N91-19268
Electric monopole transitions and shape coexistence in nuclei
[DE91-008141] N91-19847
Quasi-molecular processes in dense plasmas
[DE91-007388] N91-19899

ATOMIZERS
Cryogenic liquid-jet breakup in two-fluid atomizers
[NASA-TM-103734] N91-19402

ATOMIZING
LOX/hydrogen coaxial injector atomization test program
[NASA-CR-187037] N91-19117

ATROPHY
Muscle function impairment following lower limb unloading in men N91-19616
Contractile protein changes induced by hindlimb suspension in rat skeletal muscle N91-19646

ATTITUDE (INCLINATION)
Integrated inertial/GPS N91-19032
Determinants of spatial orientation in weightlessness N91-19605
Vertically moving visual stimuli and vertical vection: A tool against space motion sickness N91-19606
The reference systems for tactile perception and for the orientation with respect to body N91-19691
Gaze control and spatial memory in weightlessness N91-19692

AUGER SPECTROSCOPY
Chemical activation of molecules by metals: Experimental studies of electron distributions and bonding
[DE91-007695] N91-19275

AURORA 7
An analytical study of neutral expansion, ionization, and charged particle acceleration in a neutral lithium release for the parallel electric field measurement
[MPE-PREPRINT-180] N91-19880

AURORAS
Association of an auroral surge with plasma sheet recovery and the retreat of the substorm neutral line
[DE91-007351] N91-19552

AUTOMATIC CONTROL
BUBBLES: An automated decision support system for final approach controllers N91-19027
Automatic control study of the icing research tunnel refrigeration system
[NASA-TM-4257] N91-19115
Modeling of flow systems for implementation under KATE N91-20038

AUTOMATIC TEST EQUIPMENT
Robot tracking system improvements and visual calibration of orbiter position for radiator inspection N91-20037

AUTOMORPHISMS
Symmetries on the space of (2,2) superstring vacua and automorphism groups of Calabi-Yau manifolds
[DE91-008218] N91-19951

AUTONOMOUS NAVIGATION
DEMO 89: The initial experiment with the HERMIES-3 robot
[DE90-017765] N91-19447
Practical path planning among movable obstacles
[DE91-000034] N91-19768
Navigation of a car-like mobile robot using a decomposition of the environment in convex cells
[DE91-000709] N91-19769

AVIONICS
Joint University Program for Air Transportation Research, 1989-1990
[NASA-CP-3095] N91-19024
System design for the Tiger helicopter
[MBB-UD-0581-90-PUB] N91-19090
Computer Aided System Design and Simulation
[AGARD-AR-283] N91-19731

AXES OF ROTATION
Effects of a giant impact on Uranus N91-20012

AXISYMMETRIC FLOW
A numerical method for solving steady 2D and axisymmetrical viscoelastic flow problems with an application to inertia effects in contraction flows
[MEMT-11] N91-19394

AZIMUTH
Method for determining astronomic azimuth
[AD-D014677] N91-19972

B

BACKGROUND RADIATION
Gravitational lens effect of wall-like objects and its cosmological implications
[DE91-744976] N91-19992

BACKSCATTERING
Slope modulation of the radar backscatter by sea waves
[BCRS-88-05] N91-19327
Radar backscatter from the sea controlled experiments
[AD-A229847] N91-19340
Effects of soil and canopy characteristics on microwave backscattering of vegetation
[NASA-CR-188022] N91-19497
Theory of CW lidar aerosol backscatter measurements and development of a 2.1 microns solid-state pulsed laser radar for aerosol backscatter profiling
[NASA-CR-4347] N91-19498
NOAA-9 Solar Backscatter Ultraviolet (SBUV/2) Instrument and Derived Ozone Data: Review
[NOAA-TR-NESDIS-53] N91-19514
Data status and availability N91-19515
An assessment of instrument performance for the NOAA-9 SBUV/2 N91-19516
SBUV/2 in-orbit performance N91-19517

A status report on the analysis of the NOAA-9 SBUV/2 sweep mode solar irradiance data N91-19518
NOAA-9 SBUV/2 ozone sounding accuracy: Presentation summary N91-19519
A technique for directly comparing radiances from two satellites N91-19520
SBUV/2 comparisons with ground-based and SBUV spacecraft data N91-19521
Initial estimate of NOAA-9 SBUV/2 total ozone drift: Based on comparison with re-calibrated TOMS measurements and pair justification of SBUV/2 N91-19523
Total ozone, ozonesonde, and Umkehr observations for satellite ozone data validation N91-19525
Analysis of SBUV/2 measurements of solar UV irradiance variations N91-19526
Optical Fiber Backscatter Signature Generator (OFBSG) [AD-D014668] N91-19870

BACKWARD WAVE TUBES
A program of high power microwave source research and development from 8 GHz to 600 GHz [DE91-008320] N91-19358

BACTERIA
Spatial and temporal relationships between localized microbial metabolic activity and electrochemical activity of steel [DE91-008102] N91-19279
Microbiologically influenced corrosion in copper and nickel seawater piping systems [AD-A229874] N91-19287
Growth rate of bacteria without and with antibiotic at different levels of gravity N91-19632

BACTERIOPHAGES
Physiological genetics of denitrification: A route to conserving fixed nitrogen [DE91-008157] N91-19707

BALLISTIC TRAJECTORIES
Launching projectiles with hydrogen gas generated from titanium-water reactions [AD-D014653] N91-19171

BALLOON-BORNE INSTRUMENTS
A balloon-borne 102-cm telescope for far-infrared astronomy [NASA-CR-187778] N91-19973

BANACH SPACE
Regular unitary dilation of commuting contractions and Markovian representations of Gaussian stationary processes on the set Z(2) [TELECOM-90-D-009] N91-19798

BANDWIDTH
Rocket noise filtering system using digital filters N91-20031

BARIUM COMPOUNDS
Direct conversion of methane to C2's and liquid fuels [DE91-005729] N91-19313

BARIUM OXIDES
Positron lifetime studies of defect structures in Ba(1-x)K(x)BiO3 [DE91-007341] N91-19919
Phase formation in the Tl-Ca-BaCu-O system [DE91-008184] N91-19942

BARORECEPTORS
Simulated absence of gravity impairs arterial baroreceptor control of heart rate in man N91-19599
Carotid-cardiac baroreflex influence on forearm vascular resistance during low level LBNP N91-20030

BARS
Non-homogeneous bars under tension, pure bending, and temperature loads [MBB-UD-0572-90-PUB] N91-19485

BATTERY CHARGERS
Laboratory testing of the Sonnenschein charger, Part number DTL 12040 [DE91-006543] N91-19346

BAYES THEOREM
Bayesian approximation of solutions to linear ordinary differential equations [DE91-007872] N91-19785

BCS THEORY
Origin of residual surface resistance of ceramic high-temperature superconductors N91-19814

BEAM CURRENTS
Pulse-power characteristic of VIVA-1 (Versatile Inductive Voltage Adder) N91-19888

BEAM INJECTION
Two-stage ion diode experiments on induction adder N91-19884

BEAM INTERACTIONS
Atomic beam studies of the interaction of hydrogen with transition metal surfaces [DE91-007938] N91-19841

BEAM SPLITTERS
Laser Tracker 2: Sandia National Laboratories' second generation laser tracking system [DE91-007711] N91-19424

BEAMS (SUPPORTS)
A variational approach to magneto-elastic buckling problems [ETN-91-98929] N91-19338

BEARING (DIRECTION)
Graviorientation in photosynthetic flagellates N91-19673

BEARINGLESS ROTORS
Development of bearingless tail rotors [MBB-UD-0575-90-PUB] N91-19086

BEARINGS
Vibration transmission through rolling element bearings in geared rotor systems [NASA-CR-4334] N91-19435

BED REST
Effect of running and head down tilt bedrest on lymphocyte reactivity N91-19598

BEHAVIOR
Gravitaxis in Physarum polycephalum N91-19678

BEND TESTS
Flexure fatigue tests for composites N91-19227
Flexural testing and evaluation methods of advanced composite materials N91-19228
Nonlinear analysis and redesign of the mixed-mode bending delamination test [NASA-TM-102777] N91-19482

BENDING
Flexure fatigue tests for composites N91-19227
Nonlinear analysis and redesign of the mixed-mode bending delamination test [NASA-TM-102777] N91-19482
Non-homogeneous bars under tension, pure bending, and temperature loads [MBB-UD-0572-90-PUB] N91-19485

BENDING FATIGUE
Flexural testing and evaluation methods of advanced composite materials N91-19228

BERYLLIUM ALLOYS
Radiation-induced changes in electrical conductivity of a wide range of copper alloys [DE91-007200] N91-19271
An evaluation of the fatigue crack growth and fracture toughness properties of beryllium-copper alloy CDA172 [NASA-TM-102166] N91-19274

BIAS
Relation between perception of vertical axis rotation and vestibulo-ocular reflex symmetry [NASA-CR-187997] N91-19710

BIBLIOGRAPHIES
USSR Space Life Sciences Digest. Index to issues 26-29 [NASA-CR-3922(35)] N91-19700
The 1989 JSC bibliography of scientific and technical papers [NASA-TM-102173] N91-19959

BIG BANG COSMOLOGY
Two possible problems for standard big bang nucleosynthesis [DE91-007342] N91-19985

BIMETALS
Chemical interactions in multimetal/zeolite catalysts [DE91-007978] N91-19261

BIOASSAY
Microbiological assay using bioluminescent organism [AD-D014651] N91-19249
An introduction to biological dosimetry [DE91-007125] N91-19698

BIOASTRONAUTICS
USSR Space Life Sciences Digest. Index to issues 26-29 [NASA-CR-3922(35)] N91-19700

BIOCHEMISTRY
The biochemical and physiological variables in motion sickness followed modified neuroendocrine activity N91-19607
Physiological genetics of denitrification: A route to conserving fixed nitrogen [DE91-008157] N91-19707

BIOCONVERSION
A summary of the status of biomass conversion technologies and opportunities for their use in developing countries [DE91-006341] N91-19506

BIOINSTRUMENTATION
Spatial and temporal variation in biomonitoring data [DE91-007843] N91-19539

BIOLOGICAL EFFECTS
The biological and medical programme of the manned Aragatz mission on the Mir Space Station N91-19617
Gravity effects on cells N91-19618
Developmental biology and microgravity N91-19622
An introduction to biological dosimetry [DE91-007125] N91-19698
Biological effects of extremely low-frequency electromagnetic fields: In vivo studies [DE91-007899] N91-19704

BIOLOGICAL EVOLUTION
Extraterrestrial organic molecules and the emergence of life on Earth N91-19681

BIOLUMINESCENCE
Microbiological assay using bioluminescent organism [AD-D014651] N91-19249

BIOMASS
Physiological criteria and requirement of biomass production under controlled ecological life support systems N91-19659
Tuning the efficiencies of plant lighting systems: From primary energy to edible biomass: The LED as an alternative light source N91-19660
Carbon dioxide and water exchange of a soybean stand grown in the biomass production chamber N91-20026

BIOMASS ENERGY PRODUCTION
A summary of the status of biomass conversion technologies and opportunities for their use in developing countries [DE91-006341] N91-19506

BIOMETRICS
Ultrasound investigation of the cardiovascular system during the 25 days French-Soviet spaceflight (26 November - 21 December 1988) N91-19577
Measurement of eye movements in space-related research environments N91-19591

BIOREACTORS
Preliminary study of a membrane bioreactor for cell culture in space N91-19627
Plant biotechnology in space: Facts and speculations N91-19664

BIOSATELLITES
Preliminary studies before defining a payload adapted to the primate model N91-19648
Review of EEG studies in non human primates exposed to microgravity N91-19649

BIOTECHNOLOGY
Fourth European Symposium on Life Sciences Research in Space [ESA-SP-307] N91-19572
Biolab on Columbus: A facility for basic science and biotechnology N91-19658
Cells in space: Sounding rocket facilities for cell biology and biotechnology in microgravity N91-19661
Plant biotechnology in space: Facts and speculations N91-19664

BIPOLARITY
Sodium/metal chloride program conceptual design study [DE91-007216] N91-19353

BISMUTH COMPOUNDS
Superconductivity of oxide film electrolytically deposited on surface of B(1-x)Sb(x) single crystal N91-19819

BISMUTH OXIDES
Positron lifetime studies of defect structures in Ba(1-x)K(x)BiO3 [DE91-007341] N91-19919

BLACK BODY RADIATION
Gravitational lens effect of wall-like objects and its cosmological implications [DE91-744976] N91-19992

BLADE TIPS
Euler solutions to nonlinear acoustics of non-lifting hovering rotor blades [NASA-TM-103837] N91-19826

BLOOD CELLS
Free flow electrophoresis experiment TEPE 3 on TEXUS 24 N91-19654

BLOOD PLASMA
Fluid shifts and regulation of plasma volume in humans during 12 hours of head-out water immersion N91-19602
Volume regulating hormones, fluid and electrolyte modifications during the Aragatz Mission (Mir station) N91-19689

BLOOD PRESSURE
Blood pressure regulation in parabolic flight N91-19575
Blood pressure maturation curve in normotensive rats during growth in simulated microgravitational environment N91-19644
Carotid-cardiac baroreflex influence on forearm vascular resistance during low level LBNP N91-20030

BLOOD VOLUME
Medex: A useful tool for counteracting orthostatic intolerance resulting from body fluid loss under microgravity N91-19585
Time courses of endurance performance parameters following 500 ml blood withdrawal N91-19586
A new principle for dynamic fluid shift investigations in astronauts N91-19600
Fluid shifts and regulation of plasma volume in humans during 12 hours of head-out water immersion N91-19602

Influence on natriuresis of prolonged (12 h) water immersion on central hemodynamics and endocrine elements in humans N91-19612
Volume regulating hormones, fluid and electrolyte modifications during the Aragatz Mission (Mir station) N91-19689

BLUNT BODIES
The behaviour of flux-difference and flux-vector splitting methods in explicit schemes for hypersonic blunt body flow
[LR-643] N91-19069
Laws of heat transfer in three-dimensional viscous shock layer of stream flowing past blunt bodies at some angles of attack and glide N91-19801

BODIES OF REVOLUTION
Task reports on developing techniques for scattering by 3D composite structures and to generate new solutions in diffraction theory using higher order boundary conditions
[NASA-CR-188057] N91-19305
A finite element conjugate gradient FFT method for scattering N91-19306

BODY CENTERED CUBIC LATTICES
Internal friction peaks due to interstitials in bcc alloys
[DE91-007411] N91-19272

BODY FLUIDS
Medex: A useful tool for counteracting orthostatic intolerance resulting from body fluid loss under microgravity N91-19585
A new principle for dynamic fluid shift investigations in astronauts N91-19600
Fluid shifts and regulation of plasma volume in humans during 12 hours of head-out water immersion N91-19602
Visualisation of fluid shifts within the body during a parabolic flight by measurements of electrical bio-impedance N91-19688

BODY-WING CONFIGURATIONS
An experimental study of the turbulent boundary layer on a transport wing in subsonic and transonic flow
[NASA-TM-102206] N91-19062

BOLTED JOINTS
Experimental determination of satellite bolted joints thermal resistance N91-19157
Bolted joints in a laminated composite strut design expert system
[BU-415] N91-19488

BOLTZMANN TRANSPORT EQUATION
Contributions to the Non Equilibrium Molecular Dynamics (NEMD) computer simulation for transport processes in simple fluids
[ETN-91-98921] N91-19393

BOMBS (ORDNANCE)
Wire-free arming system for an aircraft-delivered bomb
[AD-D014611] N91-19076
Alternate approach for obtaining dynamic range in monopulse guidance systems
[AD-D014644] N91-19100

BONDING
Electronic charge density and bonding in alpha-boron: An experimental-theoretical comparison
[DE91-006629] N91-19936

BONE DEMINERALIZATION
Skeletal adaptation in altered gravity environments N91-19603
Assessment of bone turnover in humans after space flight and hypokinesia N91-19608
Bone adaptation to real and simulated microgravity N91-19643

BONE MARROW
An assay for bone cell differentiation in vitro as a tool for microgravity studies in space N91-19637
Cosmos: 1989 immunology studies
[NASA-CR-188046] N91-19701

BONE MINERAL CONTENT
Hypergravity and bone mineralization N91-19650
Aragatz Mission: Bone densitometric results obtained with the SCOOP miniscanner N91-19690

BONES
Assessment of bone turnover in humans after space flight and hypokinesia N91-19608
Bone adaptation to real and simulated microgravity N91-19643
Hypergravity and bone mineralization N91-19650

BORN APPROXIMATION
Examinations of inverse scattering problem for the scalar Helmholtz equation in the field of first order approximations for potentials with compact supports and safe real wave numbers
[ETN-91-98949] N91-19339

BORON
Electronic charge density and bonding in alpha-boron: An experimental-theoretical comparison
[DE91-006629] N91-19936
Plasma, photon, and beam synthesis of diamond films and multilayered structures
[DE91-007934] N91-19938

BORON CARBIDES
Low temperature properties of boron carbides
[DE91-008172] N91-19243

BORON NITRIDES
Atomic oxygen effects on boron nitride and silicon nitride: A comparison of ground based and space flight data N91-19146

BOSONS
Electroweak interactions at LEP
[NOTA-INTERNA-962] N91-19853
A global fit to the Z(0) line shape
[NOTA-INTERNA-966] N91-19868

BOUNDARIES
Plasma boundary experiments on D3-D tokamak
[DE91-002429] N91-19881

BOUNDARY CONDITIONS
Panel methods: An introduction
[NASA-TP-2995] N91-19058
Task reports on developing techniques for scattering by 3D composite structures and to generate new solutions in diffraction theory using higher order boundary conditions
[NASA-CR-188057] N91-19305
Analytical solutions with Generalized Impedance Boundary Conditions (GIBC) N91-19307
The method of lines in analyzing solids containing cracks
[NASA-TM-103626] N91-19477

BOUNDARY ELEMENT METHOD
Boundary integral equations and the Dirichlet problem
[DE91-004537] N91-19779

BOUNDARY INTEGRAL METHOD
Boundary integral equations and the Dirichlet problem
[DE91-004537] N91-19779

BOUNDARY LAYER CONTROL
Turbulent boundary layer separation over a rearward facing ramp and its control through mechanical excitation
[NASA-TM-103702] N91-19370

BOUNDARY LAYER FLOW
The effect of small streamwise velocity distortion on the boundary layer flow over a thin flat plate with application to boundary layer stability theory
[NASA-TM-103668] N91-19372

BOUNDARY LAYER SEPARATION
Stress corrosion cracking of Al-Li-Cu-Zr alloy 2090 in aqueous Cl(-) and mixed CO3(2-)/Cl(-) environments
[DE91-007064] N91-19269
Turbulent boundary layer separation over a rearward facing ramp and its control through mechanical excitation
[NASA-TM-103702] N91-19370

BOUNDARY LAYER STABILITY
A finite Reynolds number approach for the prediction of boundary layer receptivity in localized regions
[NASA-TM-102781] N91-19061
The effect of small streamwise velocity distortion on the boundary layer flow over a thin flat plate with application to boundary layer stability theory
[NASA-TM-103668] N91-19372

BOUNDARY LAYER TRANSITION
A finite Reynolds number approach for the prediction of boundary layer receptivity in localized regions
[NASA-TM-102781] N91-19061
Critical-layer nonlinearity in the resonance growth of three-dimensional waves in boundary layers
[NASA-TM-103639] N91-19373

BOUNDARY LAYERS
Prediction of ice shapes and their effect on airfoil performance
[NASA-TM-103701] N91-19047

BOUNDARY VALUE PROBLEMS
Traveling time effects in a channel flow
[MPIS-10/1990] N91-19384
The method of lines in analyzing solids containing cracks
[NASA-TM-103626] N91-19477
Laws of heat transfer in three-dimensional viscous shock layer of stream flowing past blunt bodies at some angles of attack and glide N91-19801

BRADYCARDIA
Simulated absence of gravity impairs arterial baroreceptor control of heart rate in man N91-19599

BRAGG ANGLE
Radar backscatter from the sea controlled experiments
[AD-A229847] N91-19340

BRAIN
Morphological, electronmicroscopical and biochemical aspects of hyper-gravity conditions during early ontogenetic development of Cichlid fish N91-19638

BRAKES (FOR ARRESTING MOTION)
The development of a ram air decelerator for the recovery of artillery shells
[DE91-007732] N91-19064

BRANCHING (MATHEMATICS)
The qualitative analysis of nonlinear parameterized systems. Part 1: Nonlinear systems representation and dynamical systems theory
[RR-408-PT-1] N91-19789

BRAYTON CYCLE
Microtube strip heat exchanger
[DE91-005741] N91-19504

BRAZILIAN SPACE PROGRAM
SCD 02 thermal design N91-19129
SCD1 thermal design and test result analysis N91-19130

BREATHING
Lung volumes, chest wall configuration, and pattern of breathing in microgravity N91-19574

BRECCIA
K/T age for the popigai impact event N91-19999

BREMSSTRAHLUNG
Predicted Bremsstrahlung generation by energetic electron beams
[DE91-007164] N91-19858

BRIGHTNESS
Photoemission studies using femtosecond pulses for high brightness electron beams
[DE91-008436] N91-19849

BRILLOUIN ZONES
Phenomenological theory of phase transitions to nonhomogeneous noncommensurate phase with superconducting current N91-19817

BROADBAND
A pocket-size broadband electric field detection and storage device
[DE91-007710] N91-19406

BROADCASTING
The provision of circuits to outside broadcast locations using spectrum within the UHF broadcasting bands
[BBC-RD-1990/12] N91-19329

BROKEN SYMMETRY
W(sub L)W(sub L) scattering at the SSC
[DE91-008442] N91-19851

BUBBLES
Numerical and physical modelling of bubbly flow phenomena
[DE91-007461] N91-19377
The application of simulation model for the flow induced by air bubble plume in thermally stratified reservoirs
[DE91-003064] N91-19380
Vascular gas bubbles or decompression sickness: What is the proper endpoint for evaluating decompression procedures N91-19590

BUCKLING
Single-strain-gage force/stiffness buckling prediction techniques on a hat-stiffened panel
[NASA-TM-101733] N91-19077
A theoretical solution for the buckling of sandwich panels with laminated face plates using a computer algebra system
[BU-407] N91-19486
Finite strip elements in thin plate buckling analysis
[LR-642] N91-19493

BULGING
Bulging of fatigue cracks in a pressurized aircraft fuselage
[ETN-91-98927] N91-19489

BUOYANCY
Heat transfer in rotating serpentine passages with trips normal to the flow
[NASA-TM-103758] N91-19443

BUS CONDUCTORS
Computational comparison of efficacies of aeolian vibration damping devices for multiconductor overhead power lines
[BU-411] N91-19487

BY-PRODUCTS
Direct conversion of methane to C2's
[DE91-005730] N91-19251

BYPASSES
Integral bypass diodes in an amorphous silicon alloy photovoltaic module N91-19218

C

C (PROGRAMMING LANGUAGE)
Data acquisition and analysis on the two-color laser transmissometer system
[DE91-007235] N91-19420

C BAND
C-band antennas for regional communication systems
[MBB-UK-0107-90-PUB] N91-19336

Effects of soil and canopy characteristics on microwave backscattering of vegetation
[NASA-CR-188022] N91-19497

CADMIUM SULFIDES
A photoemission investigation of compound semiconductor monodisperse clusters
[DE91-006707] N91-19921

CALCIUM CARBONATES
Part 1: The effect of lattice defects on the sintering of lithium fluoride; Part 2: The morphology of calcium oxide from calcium carbonate decomposition
[DE91-007743] N91-19934

CALCIUM METABOLISM
Skeletal adaptation in altered gravity environments N91-19603

CALCIUM OXIDES
Direct conversion of methane to C2's and liquid fuels
[DE91-005729] N91-19313
Part 1: The effect of lattice defects on the sintering of lithium fluoride; Part 2: The morphology of calcium oxide from calcium carbonate decomposition
[DE91-007743] N91-19934
Phase formation in the Tl-Ca-BaCu-O system
[DE91-008184] N91-19942

CALCULUS OF VARIATIONS
Computation and graphics in mathematical research
[DE91-007333] N91-19776

CALIBRATING
Boeing infrared sensor (BIRS) calibration facility N91-19138
Rotating pressure measurement system using an on board calibration standard
[NASA-TM-103676] N91-19401
Laser Doppler velocimetry for continuous flow solar-pumped iodine laser system
[NASA-TM-104029] N91-19415
An assessment of instrument performance for the NOAA-9 SBUV/2 N91-19516
Initial estimate of NOAA-9 SBUV/2 total ozone drift: Based on comparison with re-calibrated TOMS measurements and pair justification of SBUV/2 N91-19523
Calibration of long term satellite ozone data sets using the space shuttle N91-19524
Total ozone, ozonesonde, and Umkehr observations for satellite ozone data validation N91-19525
Ozone measurements from the NOAA-9 and the Nimbus-7 satellites: Implications of short and long term variabilities N91-19527
Apparatus for determining microwave characteristics of superconductive materials using a resonant cavity and calibration waveguides
[AD-D014694] N91-19918
Some aspects of robotics calibration, design and control N91-20035

CALORIMETERS
A calorimeter design for high energy PP colliders
[NOTA-INTERNA-965] N91-19410

CAMERAS
Measurements with a 35 psec gate time microchannelplate camera
[DE91-006701] N91-19400

CANCER
Research in radiobiology: Work in progress in immunobiology of experimental host-tumor relationships
[DE91-007936] N91-19705

CANOPIES (VEGETATION)
Effects of soil and canopy characteristics on microwave backscattering of vegetation
[NASA-CR-188022] N91-19497
Throughfall and foliar extraction
[DE91-007184] N91-19535
Analysis of high frequency surface-induced concentration fluctuations
[DE91-007561] N91-19538

CANS
Multi-dimensional modeling of a thermal energy storage canister
[NASA-TM-103731] N91-19177

CAPACITANCE
Classical and quantum charge dynamics in small tunnel junctions
[ETN-91-98916] N91-19947

CAPACITANCE-VOLTAGE CHARACTERISTICS
Classical and quantum charge dynamics in small tunnel junctions
[ETN-91-98916] N91-19947

CAPACITORS
Unique Signal Override Plug (USOP) electromagnetic test report
[DE91-004996] N91-19330
Capattery double layer capacitor life performance
[DE91-006639] N91-19344

CAPE KENNEDY LAUNCH COMPLEX
Research reports: 1990 NASA/ASEE Summer Faculty Fellowship Program
[NASA-CR-187638] N91-20022
Rocket-triggered lightning strikes and forest fire ignition N91-20027
An expansion plan for the 60 Hz power distribution system at KSC: LC-39 substations load allocation plan N91-20028

CAPTURE EFFECT
Exchange currents in low-energy nucleon capture by He3
[ETN-91-98917] N91-19855

CARBENES
Research conducted at the Radiation Lab, Notre Dame Univ.
[DE91-007969] N91-19843

CARBON
Direct conversion of methane to C2's and liquid fuels
[DE91-007545] N91-19318
Generation and focusing of carbon ion beam by the inverse pinch ion diode N91-19890

CARBON CYCLE
Mechanisms controlling the production and transport of methane, carbon dioxide, and dissolved solutes within a large boreal peat basin
[DE91-008115] N91-19543

CARBON DIOXIDE
Monitoring the response of the upper troposphere/lower stratosphere to a greenhouse gas scenario
[DE91-007976] N91-19541
Mechanisms controlling the production and transport of methane, carbon dioxide, and dissolved solutes within a large boreal peat basin
[DE91-008115] N91-19543
Studies of atmospheric molecules by multiphoton spectroscopy
[DE91-006738] N91-19554
Carbon dioxide and water exchange of a soybean stand grown in the biomass production chamber N91-20026

CARBON DIOXIDE CONCENTRATION
The dilemma of fossil fuel use and global climate change
[DE91-007859] N91-19533
Thermohaline circulations and global climate change
[DE91-007458] N91-19537
Analysis of high frequency surface-induced concentration fluctuations
[DE91-007561] N91-19538
Chemical approaches to carbon dioxide utilization for manned Mars missions
[NASA-TM-103728] N91-20015

CARBON FIBER REINFORCED PLASTICS
Flexural testing and evaluation methods of advanced composite materials N91-19228
Effect of fiber reinforcements on thermo-oxidative stability and mechanical properties of polymer matrix composites
[NASA-TM-103648] N91-19234
Strength test of CFRP box beam model
[NAL-TR-1057] N91-19469

CARBON FIBERS
Prospects for using carbon-carbon composites for EMI shielding
[NASA-TM-103677] N91-19231

CARBON ISOTOPES
Stable hydrogen and carbon isotope ratios of extractable hydrocarbons in the Murchison meteorite N91-20006

CARBON MONOXIDE
Comprehensive mechanisms for combustion chemistry: An experimental and numerical study with emphasis on applied sensitivity analysis
[DE91-008030] N91-19262
Proceedings of 146th IAU Symposium on Dynamics of Galaxies and Molecular Cloud Distribution
[PB91-123661] N91-19994

CARBON STEELS
A study of carbon steel corrosion inhibition by phosphate ions and by an organic buffer using a scanning vibrating electrode
[DE91-008103] N91-19280

CARBON TETRACHLORIDE
Frontier orbital symmetry control of intermolecular electron transfer
[DE91-005699] N91-19834

CARBON 13
Detection of an isotopic short submillimeter CO line: Column densities of warm gas in molecular clouds
[MPE-PREPRINT-178] N91-19976

CARBON-CARBON COMPOSITES
Prospects for using carbon-carbon composites for EMI shielding
[NASA-TM-103677] N91-19231

CARBONATES
Molten carbonate fuel cell technology improvement
[DE91-005540] N91-19505
Performance characteristics of an MHD (Magnetohydrodynamic) pilot plant electrostatic precipitator
[DE91-007218] N91-19905

CARDIAC OUTPUT
Ultrasound investigation of the cardiovascular system during the 25-days Soviet-French flight: Cardiac aspects N91-19578

CARDIOVASCULAR SYSTEM
Blood pressure regulation in parabolic flight N91-19575
Ultrasound investigation of the cardiovascular system during the 25 days French-Soviet spaceflight (26 November - 21 December 1988) N91-19577
Ultrasound investigation of the cardiovascular system during the 25-days Soviet-French flight: Cardiac aspects N91-19578
Influence of various parameters on the V'O2 frequency response of the body. A theoretical study on the basis of a nonlinear model N91-19594
Carotid-cardiac baroreflex influence on forearm vascular resistance during low level LBNP N91-20030

CARRIER DENSITY (SOLID STATE)
Key factors limiting the open circuit voltage of n(+)pp(+) indium phosphide solar cells N91-19206

CARRIER FREQUENCIES
Collision detection system
[AD-D014645] N91-19072

CARTESIAN COORDINATES
Even- and odd-parity finite-element transport solutions in the thick diffusion limit
[DE91-007618] N91-19781
Discontinuous finite-element transport solutions in the thick diffusion limit in Cartesian geometry
[DE91-007620] N91-19782

CARTILAGE
Altered cartilage differentiation in tibial epiphyseal plates of Cosmos rats N91-19628

CASCADE FLOW
Cascade flutter analysis with transient response aerodynamics
[NASA-TM-103746] N91-19475
The effect of steady aerodynamic loading on the flutter stability of turbomachinery blading
[NASA-CR-187055] N91-19479

CASTING
Gelcast zirconia-alumina composites
[DE91-007835] N91-19239
Method of producing superconducting materials in bulk form
[AD-D014656] N91-19917

CATALYSIS
Reactivity of pi-complexes of Ti, V, and Nb towards dithioacetic acid: Synthesis and structure of novel metal sulfur-containing complexes
[NASA-TM-103666] N91-19256
Solid state, surface, and catalytic studies of oxides
[DE91-007979] N91-19939

CATALYSTS
Direct conversion of methane to C2's
[DE91-005730] N91-19251
Reactivity of pi-complexes of Ti, V, and Nb towards dithioacetic acid: Synthesis and structure of novel metal sulfur-containing complexes
[NASA-TM-103666] N91-19256
Methane to methanol conversion by direct partial oxidation
[DE91-007352] N91-19257
Chemical interactions in multimetal/zeolite catalysts
[DE91-007978] N91-19261
Direct conversion of methane to C2's and liquid fuels
[DE91-005729] N91-19313
Direct conversion of methane to C2's and liquid fuels
[DE91-007545] N91-19318

CATALYTIC ACTIVITY
Control of catalytic hydrotreating selectivity with ammonia
[DE91-005511] N91-19250
Mechanisms and controlling characteristics of the catalytic oxidation of methane
[DE91-008033] N91-19263

CAUSES
Extraterrestrial organic molecules and the emergence of life on Earth N91-19681

CAVITATION FLOW
Two reference time scales for studying the dynamic cavitation of liquid films
[NASA-TM-103673] N91-19369

CAVITIES
Experimental investigation of porous-floor effects on cavity flow fields at supersonic speeds
[NASA-TP-3032] N91-19042
Calculations of separated 3-D flows with a pressure-staggered Navier-Stokes equations solver
[NASA-CR-187065] N91-19367

CAVITY RESONATORS
Modeling a ferrite-tuned RF cavity
[DE91-008235] N91-19356
Time-dependent multimode simulation of gyrotron oscillators
[AD-A229861] N91-19413
Hole coupling resonator for free electron lasers
[DE91-007745] N91-19426
Apparatus for determining microwave characteristics of superconductive materials using a resonant cavity and calibration waveguides
[AD-D014694] N91-19918
CELL DIVISION
Plant protoplast development on Biokosmos 9 N91-19674
CELL MEMBRANES (BIOLOGY)
Electrofusion and regeneration of protoplasts from sunflower (Helianthus annuus L.) N91-19675
CELLS (BIOLOGY)
Tools for the preparation, performance and evaluation of life sciences experiments N91-19609
Gravity effects on cells N91-19618
Preliminary study of a membrane bioreactor for cell culture in space N91-19627
Altered cartilage differentiation in tibial epiphyseal plates of Cosmos rats N91-19628
Cellular functions of Paramecium under different gravity conditions N91-19631
Growth rate of bacteria without and with antibiotic at different levels of gravity N91-19632
An assay for bone cell differentiation in vitro as a tool for microgravity studies in space N91-19637
Unicellular algae in space. 1: Preparatory tests N91-19639
A new approach to electrophoresis in space N91-19653
Cells in space: Sounding rocket facilities for cell biology and biotechnology in microgravity N91-19661
Plastids and gravity perception N91-19668
Gravitational effects on subcellular structures of plant cells N91-19669
Plant protoplast development on Biokosmos 9 N91-19674
Responses of Physarum polycephalum to varying light levels during fast clinostat rotation: A scientific preparation of an ESA biorack experiment during the IML-1 mission N91-19676
Gravitaxis in Physarum polycephalum N91-19678
Biological action of single accelerated heavy ions on individual yeast cells N91-19683
Predictions of cell damage rates for Lifesat missions
[NASA-TM-102170] N91-19699
Cosmos: 1989 immunology studies
[NASA-CR-188046] N91-19701
Subcellular signal transduction systems in the cellular trauma of ischemia
[AD-A229876] N91-19709
CENTAURUS CONSTELLATION
Observations of CO isotopic emission and the far-infrared continuum of Centaurus A
[MPE-PREPRINT-183] N91-19977
CENTERBODIES
Development of a perturbation generator for vortex stability studies
[NASA-CR-188051] N91-19379
CENTRAL PROCESSING UNITS
Performance measurements of the first RAID prototype
[NASA-CR-187958] N91-19718
CENTRIFUGAL COMPRESSORS
Rotating pressure measurement system using an on board calibration standard
[NASA-TM-103676] N91-19401
CENTRIFUGAL FORCE
Effect of the centrifuge forces on pregnant rats N91-19629
CENTRIFUGES
The slow-rotating centrifuge microscope (NIZEMI): A new research tool for terrestrial and space-related gravitational biology N91-19663
CENTRIFUGING STRESS
Gravitation receptor reaction in response to effect of acceleration N91-19569
CERAMIC MATRIX COMPOSITES
Ceramic composites for rocket engine turbines
[NASA-TM-103743] N91-19235
The application of neutron diffraction time-of-flight measurements to the study of strain in composites
[DE91-008106] N91-19242
Structural reliability analysis of laminated CMC components
[NASA-TM-103685] N91-19292
Thermal shock of fiber reinforced ceramic matrix composites
[NASA-TM-103777] N91-19295
Mechanical behavior of a ceramic matrix composite material
[NASA-CR-187072] N91-19461
NDE standards for high temperature materials
[NASA-TM-103761] N91-19464
CERAMICS
Tribological properties of Ag/Ti films on Al2O3 ceramic substrates
[NASA-TM-103784] N91-19224
Hot isostatic pressing of high performance glass-ceramic to nickel- and iron-based metal components
[DE91-008130] N91-19281
Ceramic fabrication R and D
[DE91-006537] N91-19298
Effects of atmosphere and heating rate during processing of a ceramic superconductor
[DE91-007761] N91-19299
Ceramic Technology for Advanced Heat Engines project database
[DE91-007772] N91-19300
Assessment of tamper-revealing ceramic seals
[DE91-007793] N91-19301
Crystallization and properties of Sr-Ba aluminosilicate glass-ceramic matrices
[NASA-TM-103764] N91-19308
Excimer laser surface processing for tribological applications in metals and ceramics
[DE91-002324] N91-19428
Mechanical behavior of a ceramic matrix composite material
[NASA-CR-187072] N91-19461
Property and microstructural nonuniformity in the yttrium-barium-copper-oxide superconductor determined from electrical, magnetic, and ultrasonic measurements
[NASA-TM-103732] N91-19463
NDE standards for high temperature materials
[NASA-TM-103761] N91-19464
Origin of residual surface resistance of ceramic high-temperature superconductors N91-19814
High resolution microstructural and microchemical analysis of zirconia eutectic interfaces
[DE91-008032] N91-19940
CESIUM
Noble gas disk MHD generator performance with unstable nonequilibrium plasma
[ISBN-90-9003671-7] N91-19916
CESIUM IODIDES
Phase transitions and equation of state of CsI under high pressure and the development of a focusing system for x rays
[DE91-007646] N91-19930
CHALCOGENIDES
Synthesis and structures of metal chalcogenide precursors
[NASA-TM-103665] N91-19296
CHANNEL FLOW
Traveling time effects in a channel flow
[MPIS-10/1990] N91-19384
CHANNELS (DATA TRANSMISSION)
Study of wavelength division multiplexing as a means of increasing the number of channels in multimode fiber optic communication links N91-20024
CHAOS
The study of effects of small perturbations on chaotic systems
[DE91-007320] N91-19792
CHARGE EXCHANGE
He-like spectra through charge exchange processes in tokamak plasmas
[NIFS-69] N91-19894
CHARGE TRANSFER
Theoretical investigation of phase stability in non-magnetic Fe-V substitutional alloys
[DE91-006711] N91-19268
CHARGED PARTICLES
Computation of invariant tori in 2 (1/2) degrees of freedom
[DE91-007424] N91-19778
Dynamics of collision processes
[DE91-007933] N91-19840
Some limitations of detailed balance for inverse reaction calculations in the astrophysical P-process
[DE91-007258] N91-19983
Cosmic ray charged component variations at sea level
[DE91-615480] N91-20021
CHARPY IMPACT TEST
Performance of underwater weldments
[PB91-129254] N91-19452
CHEMICAL ANALYSIS
Thermal properties of polyisocyanurate foam board insulation blown with CFC-11 substitutes
[DE90-016047] N91-19240
Mechanisms controlling the production and transport of methane, carbon dioxide, and dissolved solutes within a large boreal peat basin
[DE91-008115] N91-19543
High resolution microstructural and microchemical analysis of zirconia eutectic interfaces
[DE91-008032] N91-19940
CHEMICAL BONDS
Chemical activation of molecules by metals: Experimental studies of electron distributions and bonding
[DE91-007695] N91-19275
X ray absorption spectroscopy of oxide films on metals
[DE91-008100] N91-19278
Electronic charge density and bonding in alpha-boron: An experimental-theoretical comparison
[DE91-006629] N91-19936
CHEMICAL COMPOSITION
Investigation of anodic and chemical oxides grown on p-type InP with applications to surface passivation for n(+)-p solar cell fabrication N91-19208
Mechanisms controlling the production and transport of methane, carbon dioxide, and dissolved solutes within a large boreal peat basin
[DE91-008115] N91-19543
Thin film amorphous electrolytes: The Li2O-SiO2-P2O5 system
[DE91-007272] N91-19925
Application of MeV ions to the analysis and modification of high temperature superconducting materials
[DE91-007317] N91-19927
Primordial nucleosynthesis: Beyond the standard model
[DE91-007264] N91-19984
Stable hydrogen and carbon isotope ratios of extractable hydrocarbons in the Murchison meteorite N91-20006
Cosmic dust: Laboratory analyses of extremely small particles N91-20013
CHEMICAL ENERGY
The OAST space power program N91-19183
CHEMICAL PROPERTIES
Polymer characterization using the time-resolved phosphorescence of singlet oxygen as a spectroscopic probe
[DE91-001269] N91-19303
CHEMICAL PROPULSION
Advanced chemical propulsion at NASA Lewis: Metallized and high energy density propellants
[NASA-TM-103771] N91-19175
CHEMICAL REACTIONS
Studies of combustion kinetics and mechanisms
[DE91-007829] N91-19259
Chemical interactions in multimetal/zeolite catalysts
[DE91-007978] N91-19261
Mechanisms and controlling characteristics of the catalytic oxidation of methane
[DE91-008033] N91-19263
Basic research model of natural gas combustion in turbulent flow
[PB91-130260] N91-19264
Direct conversion of methane to C2's and liquid fuels
[DE91-007545] N91-19318
CHEMICAL REACTORS
Methane to methanol conversion by direct partial oxidation
[DE91-007352] N91-19257
CHEMILUMINESCENCE
Advanced sequencing technology
[DE91-008031] N91-19706
CHEMISORPTION
Mechanisms and controlling characteristics of the catalytic oxidation of methane
[DE91-008033] N91-19263
Hydrogen storage in metal hydrides
[DE91-746267] N91-19316
CHEST
Lung volumes, chest wall configuration, and pattern of breathing in microgravity N91-19574
CHIPS (ELECTRONICS)
Unique Signal Override Plug (USOP) electromagnetic test report
[DE91-004996] N91-19330
Algorithms for a very high speed universal noiseless coding module
[NASA-CR-187974] N91-19733
CHIRAL DYNAMICS
W(sub L)W(sub L) scattering at the SSC
[DE91-008442] N91-19851
CHLORELLA
Towards bioregenerative life support systems N91-19655
CHLORIDES
Direct conversion of methane to C2's and liquid fuels
[DE91-007545] N91-19318
Sodium/metal chloride program conceptual design study
[DE91-007216] N91-19353

CHROMIUM
Control of texture and defect structure for hot-filament-assisted CVD (Chemical Vapor Deposition) diamond Films
[DE91-008373] N91-19310
CIRCADIAN RHYTHMS
Physiology of body water and salt regulation. Part 1: Circadian rhythms of endocrine systems and urinary electrolyte excretion in humans N91-19592
CIRCUITS
Wire-free arming system for an aircraft-delivered bomb
[AD-D014611] N91-19076
An approach for configuring space photovoltaic tandem arrays based on cell layer performance N91-19197
Application of non-cyanide gold for selective plating of microelectronic circuits
[DE91-007729] N91-19276
The provision of circuits to outside broadcast locations using spectrum within the UHF broadcasting bands
[BBC-RD-1990/12] N91-19329
Complete exchange on the iPSC-860
[NASA-CR-187498] N91-19715
Multiphase complete exchange on a circuit switched hypercube
[NASA-CR-187499] N91-19716
CIRCULAR CYLINDERS
Research on bluff-body vortex wakes
[AD-A229875] N91-19071
CIVIL AVIATION
Aircrafts, requirements for ground installations from the aircraft point of view N91-19108
CLAYS
Evidence for ammonium-bearing minerals in Ceres N91-20004
CLEANING
The effect of process conditions on the performance of epitaxial InP solar cells N91-19204
CLEANLINESS
Contamination control program for the Cosmic Background Explorer: An overview N91-19152
Magnetic cleanliness verification approach on tethered satellite N91-19158
CLIMATE
Climatic water budgets, effective moisture, and elevation in the Southern Sierra Nevada, California, 1951-1980
[PB91-127878] N91-19500
Zonal statistics in (General Circulation Model) GCM/GCM/data intercomparisons
[DE91-006706] N91-19530
Analysis of workload and load balancing issues in the NCAR community climate model
[DE91-008052] N91-19534
Overview of climate information needs for ecological effects models
[PB91-125898] N91-19549
ICRCCM (intercomparison of radiation codes used in climate models). Phase 2: Verification and calibration of radiation codes in climate models
[DE91-007323] N91-19555
Energy sciences supercomputing 1990
[DE91-007188] N91-19740
CLIMATE CHANGE
Total ozone, ozonesonde, and Umkehr observations for satellite ozone data validation N91-19525
Global change: What you can do
[S-HRG-101-1160] N91-19528
Natural and anthropogenic climate change
[DE91-007363] N91-19532
The dilemma of fossil fuel use and global climate change
[DE91-007859] N91-19533
Thermohaline circulations and global climate change
[DE91-007458] N91-19537
Statistical examination of climatological data relevant to global temperature variation
[DE91-007881] N91-19540
Monitoring the response of the upper troposphere/lower stratosphere to a greenhouse gas scenario
[DE91-007976] N91-19541
Overview of climate information needs for ecological effects models
[PB91-125898] N91-19549
What were the effects of the formation of the Borealis basin, Mars N91-20014
CLIMATOLOGY
Climatic water budgets, effective moisture, and elevation in the Southern Sierra Nevada, California, 1951-1980
[PB91-127878] N91-19500
Statistical examination of climatological data relevant to global temperature variation
[DE91-007881] N91-19540
CLIMBING FLIGHT
Icing characteristics of a natural-laminar-flow, a medium-speed, and a swept, medium-speed airfoil
[NASA-TM-103693] N91-19046
CLOSED CYCLES
Microtube strip heat exchanger
[DE91-005741] N91-19504
CLOSED ECOLOGICAL SYSTEMS
Towards bioregenerative life support systems N91-19655
Plant production as part of a Controlled Ecological Life Support System (CELSS) N91-19656
A ground based module for experimentations of cultivations and recycling in a closed environment N91-19657
Physiological criteria and requirement of biomass production under controlled ecological life support systems N91-19659
Productivity and photosynthesis of selected crop plants under orbital light conditions: An approach to solar powered CELSS N91-19662
Carbon dioxide and water exchange of a soybean stand grown in the biomass production chamber N91-20026
CLOUD COVER
Cloud forcing: A modeling perspective
[DE91-007215] N91-19551
CLOUD PHYSICS
Cloud forcing: A modeling perspective
[DE91-007215] N91-19551
CLOUDS (METEOROLOGY)
The relationship between aerosol and drop size distributions in the marine atmosphere
[DE91-006514] N91-19553
COAL GASIFICATION
Molten carbonate fuel cell technology improvement
[DE91-005540] N91-19505
COAL UTILIZATION
Plasma assisted NO(x) reduction in existing coal combustors
[DE91-007380] N91-19536
Performance characteristics of an MHD (Magnetohydrodynamic) pilot plant electrostatic precipitator
[DE91-007218] N91-19905
The magnetohydrodynamics coal-fired flow facility
[DE91-007672] N91-19906
COBALT OXIDES
Direct conversion of methane to C2's and liquid fuels
[DE91-005729] N91-19313
COCKPITS
Flight simulation for wind shear encounter N91-19035
Army-NASA aircrew/aircraft integration program (A3I) software detailed design document, phase 3
[NASA-CR-177557] N91-19714
Noise level reduction inside helicopter cabins
[MBB-UD-0578-90-PUB] N91-19828
CODERS
Algorithms for a very high speed universal noiseless coding module
[NASA-CR-187974] N91-19733
On the optimality of code options for a universal noiseless coder
[NASA-CR-187973] N91-19734
CODING
On the optimality of code options for a universal noiseless coder
[NASA-CR-187973] N91-19734
COEFFICIENTS
Analytical solutions with Generalized Impedance Boundary Conditions (GIBC) N91-19307
COGNITION
The temporal logic of the tower chief system N91-19026
Analyzing thought-related electroencephalographic data using nonlinear techniques N91-19031
Simulating motivated cognition
[NASA-TM-102886] N91-19770
COGNITIVE PSYCHOLOGY
Effects of high temperature and humidity on mental state and metabolism N91-19571
COHERENT RADIATION
Method for making holograms with coherent radiation from a stabilized laser diode that has been actively cooled
[AD-D014673] N91-19396
COLD PLASMAS
Optical diagnostics for low-temperature plasmas
[DE91-007896] N91-19907
COLLAGENS
Altered cartilage differentiation in tibial epiphyseal plates of Cosmos rats N91-19628
COLLISION AVOIDANCE
Collision detection system
[AD-D014645] N91-19072
DEMO 89: The initial experiment with the HERMIES-3 robot
[DE90-017765] N91-19447
Practical path planning among movable obstacles
[DE91-000034] N91-19768
COLLISIONS
Soft x-ray laser gain prediction at high density for the nitrogen isoelectronic sequence
[DE91-007616] N91-19416
Dynamics of collision processes
[DE91-007933] N91-19840
Impact processes in the Solar System: New understandings through numerical modeling N91-19996
COLLOIDS
Gelcast zirconia-alumina composites
[DE91-007835] N91-19239
COLUMBUS SPACE STATION
Biolab on Columbus: A facility for basic science and biotechnology N91-19658
COLUMNS (PROCESS ENGINEERING)
Response of a solidly rotating amphora-type liquid column to axial excitation
[LRT-WE-9-FB-06(1990)] N91-19386
COMBUSTIBLE FLOW
Basic research model of natural gas combustion in turbulent flow
[PB91-130260] N91-19264
COMBUSTION
The magnetohydrodynamics coal-fired flow facility
[DE91-007672] N91-19906
COMBUSTION CHAMBERS
Rapid mix concepts for low emission combustors in gas turbine engines
[NASA-CR-185292] N91-19048
Solid fuel combustion chamber
[LR-648] N91-19222
Two-dimensional non-reacting jet-gas mixing in an MHD (magnetohydrodynamic) second stage combustor
[DE91-006015] N91-19252
Plasma assisted NO(x) reduction in existing coal combustors
[DE91-007380] N91-19536
The magnetohydrodynamics coal-fired flow facility
[DE91-007672] N91-19906
COMBUSTION CHEMISTRY
Comprehensive mechanisms for combustion chemistry: An experimental and numerical study with emphasis on applied sensitivity analysis
[DE91-008030] N91-19262
COMBUSTION PHYSICS
Studies of combustion kinetics and mechanisms
[DE91-007829] N91-19259
A flammability study of thin plastic film materials N91-20034
COMMERCIAL AIRCRAFT
Aircrafts, requirements for ground installations from the aircraft point of view N91-19108
COMMUNICATION
World weather watch: Regional association 4: Hurricane operational plan, supplement 2
[WMO-524-SUPPL-2] N91-19563
COMMUNICATION NETWORKS
Digital optical computers at the optoelectronic computing systems center
[NASA-CR-187520] N91-19345
Complete exchange on the iPSC-860
[NASA-CR-187498] N91-19715
Prototype document tracking and storage system for the Superconducting Super Collider Laboratory (SSCL)
[DE91-008204] N91-19963
Study of wavelength division multiplexing as a means of increasing the number of channels in multimode fiber optic communication links N91-20024
COMMUNICATION SATELLITES
Project Hitch Hiker: A feasibility study for a small telecommunication satellite
[LR-644] N91-19169
COMMUNICATION THEORY
Advanced sequencing technology
[DE91-008031] N91-19706
COMMUTATORS
Action principles for the Vlasov equation: Four old, one new
[DE91-008177] N91-19787
COMMUTER AIRCRAFT
Feasibility of an onboard wake vortex avoidance system
[NASA-CR-187521] N91-19074
COMPARISON
Computational comparison of efficacies of aeolian vibration damping devices for multiconductor overhead power lines
[BU-411] N91-19487
COMPLEX COMPOUNDS
Late transition metal (mu)-oxo and (mu)-imido complexes
[DE91-005349] N91-19267
Chemical activation of molecules by metals: Experimental studies of electron distributions and bonding
[DE91-007695] N91-19275

COMPLEX SYSTEMS
Robust fault diagnosis of physical systems in operation
[NASA-TM-102767] N91-19073
COMPONENT RELIABILITY
Life and dynamic capacity modeling for aircraft transmissions
[NASA-CR-4341] N91-19438
COMPOSITE MATERIALS
Development of bearingless tail rotors
[MBB-UD-0575-90-PUB] N91-19086
An overview of self-consistent methods for fiber-reinforced composites
[NASA-TM-103713] N91-19232
Gelcast zirconia-alumina composites
[DE91-007835] N91-19239
Constitutive models for composites based on numerical micromechanics
[ISBN-90-9003733-0] N91-19248
COMPOSITE STRUCTURES
New computer codes for the structural analysis of composite helicopter structures
[MBB-UD-0580-90-PUB] N91-19089
Computational simulation of hot composites structures
[NASA-TM-103681] N91-19230
Composite materials for space applications
[NASA-CR-187472] N91-19238
Development of a fatigue-life methodology for composite structures subjected to out-of-plane load components
[NASA-TM-102885] N91-19241
Minimum weight optimization of composite laminated struts
[BU-409] N91-19246
Composite flexible insulation for thermal protection of space vehicles
[NASA-TM-103836] N91-19304
Task reports on developing techniques for scattering by 3D composite structures and to generate new solutions in diffraction theory using higher order boundary conditions
[NASA-CR-188057] N91-19305
A finite element conjugate gradient FFT method for scattering N91-19306
Strength test of CFRP box beam model
[NAL-TR-1057] N91-19469
Bolted joints in a laminated composite strut design expert system
[BU-415] N91-19488
COMPRESSIBLE FLOW
Multigrid solution of compressible turbulent flow on unstructured meshes using a two-equation model
[NASA-CR-187513] N91-19043
Acoustic radiation from lifting airfoils in compressible subsonic flow
[NASA-TM-103650] N91-19053
COMPRESSION LOADS
Finite strip elements in thin plate buckling analysis
[LR-642] N91-19493
COMPRESSOR BLADES
The effect of steady aerodynamic loading on the flutter stability of turbomachinery blading
[NASA-CR-187055] N91-19479
COMPRESSORS
The magnetohydrodynamics coal-fired flow facility
[DE91-007672] N91-19906
COMPTON EFFECT
Optically-ionized plasma recombination x ray lasers
[DE91-007261] N91-19898
COMPUTATION
Computational comparison of efficacies of aeolian vibration damping devices for multiconductor overhead power lines
[BU-411] N91-19487
Subcycling in transient finite element analysis
[ISBN-90-9003684-9] N91-19790
COMPUTATIONAL FLUID DYNAMICS
Rapid mix concepts for low emission combustors in gas turbine engines
[NASA-CR-185292] N91-19048
Implementation of control point form of algebraic grid-generation technique
[NASA-TM-103748] N91-19054
A novel potential/viscous flow coupling technique for computing helicopter flow fields
[NASA-CR-177568] N91-19060
The behaviour of flux-difference and flux-vector splitting methods in explicit schemes for hypersonic blunt body flow
[LR-643] N91-19069
Parallel processing for panel methods
[BU-414] N91-19391
Euler solutions to nonlinear acoustics of non-lifting hovering rotor blades
[NASA-TM-103837] N91-19826
COMPUTATIONAL GRIDS
Implementation of control point form of algebraic grid-generation technique
[NASA-TM-103748] N91-19054
Calculations of separated 3-D flows with a pressure-staggered Navier-Stokes equations solver
[NASA-CR-187065] N91-19367
Anastasia: A solid model based 3D finite difference mesh generator
[DE91-007621] N91-19783
Correlations of pseudo-random numbers of multiplicative sequence
[DE91-615076] N91-19788
Subcycling in transient finite element analysis
[ISBN-90-9003684-9] N91-19790
COMPUTER AIDED DESIGN
Investigation of air transportation technology at Princeton University, 1989-1990 N91-19033
New computer codes for the structural analysis of composite helicopter structures
[MBB-UD-0580-90-PUB] N91-19089
TF89 design project airbrake and arrester hook design
[ETN-91-98853] N91-19092
Uncertainty reasoning applied to the assessment of composite material for structural design
[BU-405] N91-19244
An expert system for laminated plate design using composite materials
[BU-406] N91-19245
Two-dimensional non-reacting jet-gas mixing in an MHD (magnetohydrodynamic) second stage combustor
[DE91-006015] N91-19252
Structural reliability analysis of laminated CMC components
[NASA-TM-103685] N91-19292
Coplanar waveguide EEsoF MICAD macros make circuit layout easy
[NASA-TM-103272] N91-19332
Methods for combining a theoretical and an empirical approach in modelling pressure and flow control valves for CAE-programs for fluid power circuits
[ACTA-POLYTEC-SCAND-ME-96] N91-19392
A theoretical solution for the buckling of sandwich panels with laminated face plates using a computer algebra system
[BU-407] N91-19486
Design and testing of a circumferential and longitudinal joint of the A320 fuselage section 13/14 in GLARE
[LR-645] N91-19494
Army-NASA aircrew/aircraft integration program (A3I) software detailed design document, phase 3
[NASA-CR-177557] N91-19714
Computer Aided System Design and Simulation
[AGARD-AR-283] N91-19731
Table of tables: A database design tool for SYBASE
[DE91-007257] N91-19958
Study of the available finite element software packages at KSC N91-20029
COMPUTER AIDED MANUFACTURING
Dedication of National Institute for Aviation Research
[NIAR-90-21] N91-19040
Technology modernization assessment flexible automation
[DE91-005620] N91-19751
Software for the ODRENOK microcomputer. Program package for graphics editing
[DE91-614980] N91-19752
COMPUTER AIDED TOMOGRAPHY
Three-dimensional computed tomography from interferometric measurements within a narrow cone of views
[NASA-TM-103257] N91-19404
Nuclear-spectroscopy computerized tomography scanners
[DE91-008447] N91-19466
Multiple energy computed tomography for neuroradiology with monochromatic x rays from the national synchrotron light source
[DE91-008108] N91-19712
COMPUTER GRAPHICS
Implementation of control point form of algebraic grid-generation technique
[NASA-TM-103748] N91-19054
A valiant little terminal: A VLT user's manual
[DE91-007295] N91-19719
Real-time application of advanced three-dimensional graphic techniques for research aircraft simulation
[NASA-TM-101730] N91-19742
Techniques for interactive 3-D scientific visualization
[DE91-007122] N91-19745
PHIGS PLUS for scientific graphics
[DE91-007615] N91-19747
Software for the ODRENOK microcomputer. Program package for graphics editing
[DE91-614980] N91-19752
Computation and graphics in mathematical research
[DE91-007333] N91-19776
Formal specification of human-computer interfaces N91-20023
COMPUTER INFORMATION SECURITY
Computers at risk: Safe computing in the information age
[LC-90-22329] N91-19721
Environmental Sciences Division computing and geographic information system facility user handbook
[DE91-007820] N91-19961
COMPUTER NETWORKS
Regional Oxidant Model Multi-Processor (ROMMP)
[PB91-131680] N91-19547
Software development environments: Status and trends N91-19723
Large-scale computing in the energy research programs
[DE91-007907] N91-19748
The PVM (Parallel Virtual Machine) system: Supercomputer level concurrent computation on a network of IBM RS/6000 power stations
[DE91-007844] N91-19757
Convergence of linear programming using a Hopfield net
[DE91-007870] N91-19758
Efficient connecting networks using directed links
[ETN-91-98855] N91-19762
Cascading a systolic array and a feedforward neural network for navigation and obstacle avoidance using potential fields
[NASA-CR-177575] N91-19771
Environmental Sciences Division computing and geographic information system facility user handbook
[DE91-007820] N91-19961
COMPUTER PROGRAMMING
Sandia technology: Engineering and science applications
[DE91-006760] N91-19322
Empirical studies of software design: Implications for SSEs N91-19728
The role of software engineering in the space station program N91-19729
QUEST/Ada (query utility environment for software testing of Ada: The development of a program analysis environment for Ada, task 1, phase 3
[NASA-CR-187983] N91-19735
Software reliability through fault-avoidance and fault-tolerance
[NASA-CR-187998] N91-19741
The PVM (Parallel Virtual Machine) system: Supercomputer level concurrent computation on a network of IBM RS/6000 power stations
[DE91-007844] N91-19757
The use of an object oriented technique for fault diagnosis in nuclear reactors
[RR-414] N91-19866
COMPUTER PROGRAMS
Rapid mix concepts for low emission combustors in gas turbine engines
[NASA-CR-185292] N91-19048
Free wake analysis of hover performance using a new influence coefficient method
[NASA-CR-4309] N91-19050
Implementation of control point form of algebraic grid-generation technique
[NASA-TM-103748] N91-19054
Panel methods: An introduction
[NASA-TP-2995] N91-19058
Robust fault diagnosis of physical systems in operation
[NASA-TM-102767] N91-19073
State estimation applications in aircraft flight-data analysis: A user's manual for SMACK
[NASA-RP-1252] N91-19082
Space Shuttle: NASA should implement independent oversight of software development
[GAO/IMTEC-91-20] N91-19119
GaAs solar cell photoresponse modeling using PC-1D V2.1 N91-19193
METCAN updates for high temperature composite behavior: Simulation/verification
[NASA-TM-103682] N91-19229
Data acquisition and analysis on the two-color laser transmissometer system
[DE91-007235] N91-19420
Life and dynamic capacity modeling for aircraft transmissions
[NASA-CR-4341] N91-19438
System description document for the Anthrobot-2: A dexterous robot hand
[NASA-TM-104535] N91-19449
On the vectorization and parallelization of the shooting method using the convex C-240
[LR-639] N91-19491

Finite strip elements in thin plate buckling analysis
[LR-642] N91-19493
Simultaneous tracking of flagellates in real time by image analysis N91-19677
Test analysis program evaluation: Item statistics as feedback to test developers
[AD-A229851] N91-19713
Mission operations directorate: Facility and support systems division N91-19726
Tool and data interoperability in the SSE system N91-19727
Lessons learned from an Ada conversion project N91-19730
QUEST/Ada (query utility environment for software testing of Ada: The development of a program analysis environment for Ada, task 1, phase 3
[NASA-CR-187983] N91-19735
Development of a numerical computer code and circuit element models for simulation of firing systems
[DE91-007162] N91-19739
Structured software design for an on-line laser-based particle size distribution instrument
[DE91-007234] N91-19746
Dynamic applications of ABAQUS
[OUEL-1853/90] N91-19755
Formal proof of the AVM-1 microprocessor using the concept of generic interpreters
[NASA-CR-187491] N91-19756
SIGNIF and GENFMT, SAS macros for computing and reporting significant digits
[DE91-007702] N91-19795
Proton induced x ray emission analysis N91-19832
Particle-in-cell plasma simulation codes on the connection machine
[DE91-007845] N91-19902
Table of tables: A database design tool for SYBASE
[DE91-007257] N91-19958
Analyzing product test data in a relational database using SAS software
[DE91-007734] N91-19960
Formal specification of human-computer interfaces N91-20023

COMPUTER STORAGE DEVICES
Solid state electronic emulator of a multiple track motor driven rotating magnetic memory
[AD-D014705] N91-19437
Enhanced crosstie random access memory element and process for the fabrication thereof
[AD-D014723] N91-19717

COMPUTER SYSTEMS DESIGN
Assessing the impact of large-scale computing on the size and complexity of first-principles electromagnetic models
[DE91-007491] N91-19333
Laser Tracker 2: Sandia National Laboratories' second generation laser tracking system
[DE91-007711] N91-19424
Computers at risk: Safe computing in the information age
[LC-90-22329] N91-19721
The next generation N91-19724
Empirical studies of software design: Implications for SSEs N91-19728
Development of a numerical computer code and circuit element models for simulation of firing systems
[DE91-007162] N91-19739
Design and implementation of an image understanding system: DADS
[ETN-91-98926] N91-19773

COMPUTER SYSTEMS PERFORMANCE
Assessing the impact of large-scale computing on the size and complexity of first-principles electromagnetic models
[DE91-007491] N91-19333
Performance measurements of the first RAID prototype
[NASA-CR-187958] N91-19718
RICIS 1988 Symposium Proceedings. Presentation appendix
[NASA-CR-188077] N91-19722
Software development environments: Status and trends N91-19723
The next generation N91-19724
PHIGS PLUS for scientific graphics
[DE91-007615] N91-19747
Convergence of linear programming using a Hopfield net
[DE91-007870] N91-19758
An architecture for accommodating referenceability among intelligent electronic documents
[DE91-008250] N91-19964
Analyzing product test data in an INGRES database using SAS software
[DE91-008251] N91-19965

COMPUTER SYSTEMS PROGRAMS
Space Shuttle: NASA should implement independent oversight of software development
[GAO/IMTEC-91-20] N91-19119
Software reliability through fault-avoidance and fault-tolerance
[NASA-CR-187998] N91-19741

COMPUTER TECHNIQUES
Investigation of air transportation technology at Princeton University, 1989-1990 N91-19033
Test analysis program evaluation: Item statistics as feedback to test developers
[AD-A229851] N91-19713
A valiant little terminal: A VLT user's manual
[DE91-007295] N91-19719
Environmental Sciences Division computing and geographic information system facility user handbook
[DE91-007820] N91-19961

COMPUTER VISION
Simple object recognition by neural networks: Application of the Hough transform
[RR-410] N91-19761
Design and implementation of an image understanding system: DADS
[ETN-91-98926] N91-19773
Topological models for space and time
[OUEL-1860/90] N91-19774
Activities report of the Istituto Elettrotecnico Nazionale Galileo Ferraris
[ETN-91-98868] N91-19822
Robot tracking system improvements and visual calibration of orbiter position for radiator inspection N91-20037

COMPUTERIZED SIMULATION
Rapid mix concepts for low emission combustors in gas turbine engines
[NASA-CR-185292] N91-19048
Smoothness criteria for runway rehabilitation and overlays
[DOT/FAA/RD-90/23] N91-19102
A multi-vehicle space carrier fleet cost model for a multi-mission scenario
[ILR-MITT-240(1990)] N91-19120
Flow fields of low pressure vent exhausts N91-19135
Multi-dimensional modeling of a thermal energy storage canister
[NASA-TM-103731] N91-19177
InP/Ga0.47In0.53As monolithic, two-junction, three-terminal tandem solar cells N91-19191
Phase equilibrium modeling for high temperature metallization on GaAs solar cells N91-19192
Viability study of photovoltaic systems added to terrestrial electric vehicles
[DE91-007689] N91-19355
Modeling a ferrite-tuned RF cavity
[DE91-008235] N91-19356
Filtering analysis of a direct numerical simulation of the turbulent Rayleigh-Benard problem
[NASA-CR-187488] N91-19366
Contributions to the Non Equilibrium Molecular Dynamics (NEMD) computer simulation for transport processes in simple fluids
[ETN-91-98921] N91-19393
Theory of the ion-channel laser
[DE91-007643] N91-19423
Phase stability of a standing-wave free-electron laser
[DE91-008068] N91-19427
Oxygen-enriched diesel engine performance: A comparison of analytical and experimental results
[DE91-006491] N91-19440
Mechanisms controlling the production and transport of methane, carbon dioxide, and dissolved solutes within a large boreal peat basin
[DE91-008115] N91-19543
Regional Oxidant Model Multi-Processor (ROMMP)
[PB91-131680] N91-19547
Simulation expert system for physiological mechanisms of the space motion sickness N91-19596
Army-NASA aircrew/aircraft integration program (A3I) software detailed design document, phase 3
[NASA-CR-177557] N91-19714
The role of software engineering in the space station program N91-19729
Development of a numerical computer code and circuit element models for simulation of firing systems
[DE91-007162] N91-19739
Real-time application of advanced three-dimensional graphic techniques for research aircraft simulation
[NASA-TM-101730] N91-19742
Techniques for interactive 3-D scientific visualization
[DE91-007122] N91-19745
The PVM (Parallel Virtual Machine) system: Supercomputer level concurrent computation on a network of IBM RS/6000 power stations
[DE91-007844] N91-19757
Simulating motivated cognition
[NASA-TM-102886] N91-19770
Subcycling in transient finite element analysis
[ISBN-90-9003684-9] N91-19790
Particle-in-cell plasma simulation codes on the connection machine
[DE91-007845] N91-19902
Statistics of peaks in cosmological nonlinear density fields
[DE91-744972] N91-19990
Impact processes in the Solar System: New understandings through numerical modeling N91-19996

COMPUTERS
Environmental Sciences Division computing and geographic information system facility user handbook
[DE91-007820] N91-19961

CONCENTRATORS
Mini-dome Fresnel lens photovoltaic concentrator development N91-19219

CONCURRENT PROCESSING
QUEST/Ada (query utility environment for software testing of Ada: The development of a program analysis environment for Ada, task 1, phase 3
[NASA-CR-187983] N91-19735
The PVM (Parallel Virtual Machine) system: Supercomputer level concurrent computation on a network of IBM RS/6000 power stations
[DE91-007844] N91-19757

CONDENSED MATTER PHYSICS
Investigation of condensed matter fusion
[DE91-007246] N91-19923

CONDENSING
The relationship between aerosol and drop size distributions in the marine atmosphere
[DE91-006514] N91-19553

CONDUCTORS
Indium tin oxide for solid-state image sensors
[ETN-91-98932] N91-19949

CONFERENCES
The 5th Annual NASA Spacecraft Control Laboratory Experiment (SCOLE) Workshop, part 2
[NASA-CP-10057-PT-2] N91-19122
Sixteenth Space Simulation Conference Confirming Spaceworthiness Into the Next Millennium
[NASA-CP-3096] N91-19126
Space Photovoltaic Research and Technology, 1989
[NASA-CP-3107] N91-19182
Proceedings of the Workshop Prospects for a 1 Angstrom Free-Electron Laser
[DE91-007631] N91-19422
The National Energy Strategy: The role of geothermal technology development. Proceedings
[DE91-004623] N91-19503
NOAA-9 Solar Backscatter Ultraviolet (SBUV/2) Instrument and Derived Ozone Data: Review
[NOAA-TR-NESDIS-53] N91-19514
Fourth European Symposium on Life Sciences Research in Space
[ESA-SP-307] N91-19572
Computer Aided System Design and Simulation
[AGARD-AR-283] N91-19731
Finding the object proceedings addendum
[DE91-006724] N91-19738
Large-scale computing in the energy research programs
[DE91-007907] N91-19748
Summer institute in parallel programming
[DE91-007922] N91-19760
Symposium on Development of Intensed Pulsed Particle Beams and Its Applications
[NIFS-PROC-5] N91-19882
US-Japan workshops: Q-111, Development of Plasma Facing Components and Materials for Next Large Fusion Devices, and Q-112, Vacuum and First Wall Technology for Fusion Devices
[DE91-006879] N91-19896
Summary of the International Dawson Symposium on The Physics of Plasmas
[DE91-006912] N91-19897
The 1989 JSC bibliography of scientific and technical papers
[NASA-TM-102173] N91-19959
Proceedings of the symposium Astrophysical Processes and Structures in the Universe
[PB91-123653] N91-19993
Proceedings of 146th IAU Symposium on Dynamics of Galaxies and Molecular Cloud Distribution
[PB91-123661] N91-19994
Twenty-Second Lunar and Planetary Science Conference
[NASA-CR-187971] N91-19995

CONFIGURATION MANAGEMENT
The temporal logic of the tower chief system N91-19026

CONGRESSIONAL REPORTS
Space Shuttle: NASA should implement independent oversight of software development
[GAO/IMTEC-91-20] N91-19119
Global change: What you can do
[S-HRG-101-1160] N91-19528
Space operations: NASA is not archiving all potentially valuable data
[GAO/IMTEC-91-3] N91-19955
Departments of Veterans Affairs and Housing and Urban Development, and Independent Agencies Appropriation Bill, 1991
[S-REPT-101-474] N91-19966
National Aeronautics and Space Administration
N91-19967
Commercial Space Launch Act implementation
[GPO-27-944] N91-19968
Problems at National Aeronautics and Space Administration
[S-HRG-101-1146] N91-19969
Hubble Space Telescope and the space shuttle problems
[S-HRG-101-1087] N91-19974
CONICAL INLETS
Fluid mixing device having a conical inlet and a noncircular outlet
[AD-D014708] N91-19364
CONICAL NOZZLES
High power arcjet
[NASA-CR-187986] N91-19173
CONJUGATE GRADIENT METHOD
Task reports on developing techniques for scattering by 3D composite structures and to generate new solutions in diffraction theory using higher order boundary conditions
[NASA-CR-188057] N91-19305
A finite element conjugate gradient FFT method for scattering N91-19306
CONNECTORS
Load bearing connective damper
[AD-D014676] N91-19468
CONSERVATION
Global change: What you can do
[S-HRG-101-1160] N91-19528
CONSERVATION LAWS
Conservation of energy, momentum, and angular momentum in Lagrangian staggered-grid hydrodynamics
[DE91-008059] N91-19381
CONSTITUTIVE EQUATIONS
A numerical method for solving steady 2D and axisymmetrical viscoelastic flow problems with an application to inertia effects in contraction flows
[MEMT-11] N91-19394
CONSTRUCTION MATERIALS
Crashworthiness investigations in the preliminary design phase of the NH90
[MBB-UD-0579-90-PUB] N91-19088
CONSUMABLES (SPACECREW SUPPLIES)
Plant production as part of a Controlled Ecological Life Support System (CELSS) N91-19656
CONTAMINANTS
An outgassing model of non-metallic materials for the ascent of a Titan 4 launch vehicle N91-19132
CONTAMINATION
Flow fields of low pressure vent exhausts N91-19135
The space simulation facilities at IAL SPACE N91-19151
Wanted: Lunar detectives to unravel the mysteries of the Moon! Crime to be solved: Mass extinctions on the Moon by meteorite impact! N91-20010
CONTINENTAL SHELVES
Outer continental shelf environmental assessment program, volume 70
[PB91-129288] N91-19548
CONTINUITY EQUATION
Traveling time effects in a channel flow
[MPIS-10/1990] N91-19384
CONTINUOUS RADIATION
Time-dependent multimode simulation of gyrotron oscillators
[AD-A229861] N91-19413
Theory of CW lidar aerosol backscatter measurements and development of a 2.1 microns solid-state pulsed laser radar for aerosol backscatter profiling
[NASA-CR-4347] N91-19498
CONTINUOUS WAVE LASERS
FALCON reactor-pumped laser description and program overview
[DE91-008185] N91-19431
Investigation at two wavelengths of a modulated He-Xe rare gas laser
[AD-A229852] N91-19434
CONTINUUM FLOW
Laser Doppler velocimetry for continuous flow solar-pumped iodine laser system
[NASA-TM-104029] N91-19415
CONTINUUM MECHANICS
Continuum damage mechanisms with an application to fatigue
[ISBN-90-9003688-1] N91-19490
CONTINUUM MODELING
Continuum damage mechanisms with an application to fatigue
[ISBN-90-9003688-1] N91-19490
CONTINUUMS
Quasi-molecular processes in dense plasmas
[DE91-007388] N91-19899
CONTRACT MANAGEMENT
Hubble Space Telescope and the space shuttle problems
[S-HRG-101-1087] N91-19974
CONTROL SIMULATION
Solid state electronic emulator of a multiple track motor driven rotating magnetic memory
[AD-D014705] N91-19437
CONTROL STABILITY
An experimental study of a sting-mounted single-slot circulation control wing
[AD-A229867] N91-19111
CONTROL SYSTEMS DESIGN
Investigation of air transportation technology at Princeton University, 1989-1990 N91-19033
Stochastic robustness: Towards a comprehensive robustness tool N91-19036
Stochastic satbility and performance robustness of linear multivariable systems N91-19038
System identification for nonlinear control using neural networks N91-19039
Design and first tests of individual blade control actuators
[MBB-UD-0577-90-PUB] N91-19087
A proposed Kalman filter algorithm for estimation of unmeasured output variables for an F100 turbofan engine
[NASA-TM-4234] N91-19099
The 5th Annual NASA Spacecraft Control Laboratory Experiment (SCOLE) Workshop, part 2
[NASA-CP-10057-PT-2] N91-19122
Control and mechanism interaction for ground-based testing of space structures N91-19125
Computer controlled MHD power consolidation and pulse generation system
[DE91-006793] N91-19347
A rigid body model and decoupled control architecture for two manipulators holding a complex object
[DE91-007827] N91-19444
A new wheel control system for the omnidirectional HERMIES-3 robot
[DE90-017764] N91-19446
Active damping application to the shuttle RMS
[NASA-TM-102763] N91-19471
Some control problems with broad range variable speed for horizontal axis wind turbines
[FFA-TN-1990-37] N91-19513
Computer Aided System Design and Simulation
[AGARD-AR-283] N91-19731
Towards practical control design using neural computation
[NASA-TM-103785] N91-19766
Constructing mathematical model of adaptive anti-flutter system N91-19810
Some aspects of robotics calibration, design and control N91-20035
Robot tracking system improvements and visual calibration of orbiter position for radiator inspection N91-20037
CONTROL THEORY
Joint University Program for Air Transportation Research, 1989-1990
[NASA-CP-3095] N91-19024
Stochastic robustness: Towards a comprehensive robustness tool N91-19036
Neural networks in nonlinear aircraft control N91-19037
System identification for nonlinear control using neural networks N91-19039
Implementation of control point form of algebraic grid-generation technique
[NASA-TM-103748] N91-19054
Development of a vibration isolation prototype system for microgravity space experiments
[NASA-TM-103664] N91-19324
CONTROL VALVES
Automatic control study of the icing research tunnel refrigeration system
[NASA-TM-4257] N91-19115
Methods for combining a theoretical and an empirical approach in modelling pressure and flow control valves for CAE-programs for fluid power circuits
[ACTA-POLYTEC-SCAND-ME-96] N91-19392
CONTROLLED FUSION
US-Japan workshops: Q-111, Development of Plasma Facing Components and Materials for Next Large Fusion Devices, and Q-112, Vacuum and First Wall Technology for Fusion Devices
[DE91-006879] N91-19896
Summary of the International Dawson Symposium on The Physics of Plasmas
[DE91-006912] N91-19897
Experimental study of external kink instabilities in the Columbia high beta tokamak
[DE91-008116] N91-19904
Introduction to fusion
[DE91-744831] N91-19912
CONTROLLERS
System identification for nonlinear control using neural networks N91-19039
Automatic control study of the icing research tunnel refrigeration system
[NASA-TM-4257] N91-19115
CONVECTION
Systems near the onset and in the well-developed regimes of turbulence
[DE91-008148] N91-19382
CONVECTIVE HEAT TRANSFER
Development of a laser-induced heat flux technique for measurement of convective heat transfer coefficients in a supersonic flowfield
[NASA-TM-103778] N91-19063
in-space experiment on thermoacoustic convection heat transfer phenomenon-experiment definition
[NASA-CR-187070] N91-19378
Heat transfer in rotating serpentine passages with trips normal to the flow
[NASA-TM-103758] N91-19443
CONVERGENCE
Assessing the impact of large-scale computing on the size and complexity of first-principles electromagnetic models
[DE91-007491] N91-19333
Convergence of linear programming using a Hopfield net
[DE91-007870] N91-19758
Spectrum transformation for divergent iterations
[NASA-TM-103745] N91-19786
CONVERGENT-DIVERGENT NOZZLES
Correlation of leak rates of various fluids with the leak rate of an inert gas in the same configuration N91-20033
CONVEXITY
Wind tunnel wall effects in a linear oscillating cascade
[NASA-TM-103690] N91-19098
COOLING
Cool-down and frozen start-up behavior of a grooved water heat pipe
[NASA-CR-187053] N91-19376
Method of producing superconducting materials in bulk form
[AD-D014656] N91-19917
COOLING FLOWS (ASTROPHYSICS)
Thermal instabilities in cooling flows: The evolution of nearly spherical perturbations
[MPE-PREPRINT-176] N91-19365
COOLING SYSTEMS
Heat transfer in rotating serpentine passages with trips normal to the flow
[NASA-TM-103758] N91-19443
COORDINATES
Correlations of pseudo-random numbers of multiplicative sequence
[DE91-615076] N91-19788
COORDINATION
Coordination of eye, head and arm movements in weightlessness N91-19588
COPOLYMERS
Low cost space power generation N91-19212
Extrudable PBX molding powder
[AD-D014667] N91-19312
COPPER
Microbiologically influenced corrosion in copper and nickel seawater piping systems
[AD-A229874] N91-19287
Copper vapor as active medium for high-power oscillator-amplifier laser systems N91-19806
Photoelectron diffraction of magnetic ultrathin films: Fe/Cu(001)
[DE91-007254] N91-19924
COPPER ALLOYS
Chemical interactions in multimetal/zeolite catalysts
[DE91-007978] N91-19261
Stress corrosion cracking of Al-Li-Cu-Zr alloy 2090 in aqueous Cl(-) and mixed CO3(2-)/Cl(-) environments
[DE91-007064] N91-19269
Radiation-induced changes in electrical conductivity of a wide range of copper alloys
[DE91-007200] N91-19271

An evaluation of the fatigue crack growth and fracture toughness properties of beryllium-copper alloy CDA172
[NASA-TM-102166] N91-19274
X ray determination of site occupation parameters in ordered ternaries Cu(Au(x)M(1-x))M = Ni,Pd
[DE91-007861] N91-19937

COPPER OXIDES
Phase formation in the Tl-Ca-BaCu-O system
[DE91-008184] N91-19942

CORES
Method of producing glass fiber with cores of a different material
[AD-D014664] N91-19288

CORIOLIS EFFECT
Heat transfer in rotating serpentine passages with trips normal to the flow
[NASA-TM-103758] N91-19443
Vestibular tests on UK astronaut candidates for an Anglo/Russian space flight (Juno Mission) N91-19613

COROTATION
Finite element analysis of geometrically non-linear problems using a corotational large rotation formulation
[SU-ATN-9001] N91-19470

CORRECTION
Calculations of separated 3-D flows with a pressure-staggered Navier-Stokes equations solver
[NASA-CR-187065] N91-19367

CORRELATION
Correlations of pseudo-random numbers of multiplicative sequence
[DE91-615076] N91-19788
Correlation of leak rates of various fluids with the leak rate of an inert gas in the same configuration N91-20033

CORROSION
Spatial and temporal relationships between localized microbial metabolic activity and electrochemical activity of steel
[DE91-008102] N91-19279
Alkali metal corrosion of alumina: Thermodynamics, phase diagrams and testing
[ETN-91-98933] N91-19286
Microbiologically influenced corrosion in copper and nickel seawater piping systems
[AD-A229874] N91-19287
DHE (Downhole Heat Exchangers)
[DE91-006620] N91-19509
The NAPAP assessment of damages to materials from acid deposition
[DE91-008086] N91-19542

CORROSION PREVENTION
A study of carbon steel corrosion inhibition by phosphate ions and by an organic buffer using a scanning vibrating electrode
[DE91-008103] N91-19280

CORROSION RESISTANCE
A study of carbon steel corrosion inhibition by phosphate ions and by an organic buffer using a scanning vibrating electrode
[DE91-008103] N91-19280
XANES investigation of pH effects during cerium-sealing of anodized aluminum
[DE91-008101] N91-19302
Molten carbonate fuel cell technology improvement
[DE91-005540] N91-19505
Electrochemical impedance spectroscopy of metal alloys in the space transportation system launch environment N91-20025

CORROSION TESTS
Alkali metal corrosion of alumina: Thermodynamics, phase diagrams and testing
[ETN-91-98933] N91-19286

COSMIC BACKGROUND EXPLORER SATELLITE
The test facility requirements for the thermal vacuum thermal balance test of the Cosmic Background Explorer Observatory N91-19128
Contamination control program for the Cosmic Background Explorer: An overview N91-19152

COSMIC DUST
Extraterrestrial organic molecules and the emergence of life on Earth N91-19681
Defective embryogenesis of Arabidopsis induced by cosmic HZE-particles N91-19682
Cosmic dust: Laboratory analyses of extremely small particles N91-20013

COSMIC RAYS
Solar-geophysical data Number 554, October 1990. Part 1 (prompt reports): Data for September, August 1990, and late data. Explanation of data reports issued as Number 515 (supplement) July 1987
[PB91-124594] N91-20018

COSMOLOGY
High energy physics and cosmology
[DE91-007369] N91-19859
Primordial nucleosynthesis: Beyond the standard model
[DE91-007264] N91-19984
Observational relations in model universes dominated by domain-wall-like matter
[DE91-744969] N91-19988
Quasi-nonlinear theory of cosmological self-gravitating systems
[DE91-744971] N91-19989
Statistics of peaks in cosmological nonlinear density fields
[DE91-744972] N91-19990
Gravitational lens effect of wall-like objects and its cosmological implications
[DE91-744976] N91-19992

COSMONAUTS
Medical results of the fourth prime expedition on the orbital station Mir N91-19576

COSMOS SATELLITES
Experimental data on study of cosmic ray particles in the E greater than or equal to 2 TeV energy range at the Cosmos-1713 satellite with the Sokol-2 device
[DE91-615479] N91-20020

COST ANALYSIS
Project of a cost analysis model for the acquisition of a permanent lunar base
[ILR-MITT-245(1990)] N91-19114
The design of future central receiver power plants based on lessons learned from the Solar One Pilot Plant
[DE91-005224] N91-19510
COMPLEAT (community-oriented model for planning least-cost energy alternatives and technologies): A planning tool for publicly owned electric utilities
[DE91-006955] N91-19511
An expansion plan for the 60 Hz power distribution system at KSC: LC-39 substations load allocation plan N91-20028

COST EFFECTIVENESS
A multi-vehicle space carrier fleet cost model for a multi-mission scenario
[ILR-MITT-240(1990)] N91-19120
Cycling space ship transportation device for continuous link between Earth and Mars
[ILR-MITT-247(1990)] N91-19121
Alternative strategies for the maintenance of geostationary space power plants
[ILR-MITT-249(1990)] N91-19170
Key issues in space nuclear power
[NASA-TM-103656] N91-19179
Solid state electronic emulator of a multiple track motor driven rotating magnetic memory
[AD-D014705] N91-19437

COST ESTIMATES
Performance, size, mass, and cost estimates for projected 1kW EOL Si, InP, and GaAs arrays N91-19199

COST REDUCTION
Key issues in space nuclear power
[NASA-TM-103656] N91-19179
Indium phosphide solar cells N91-19221

COSTS
The cost-constrained traveling salesman problem
[DE91-004943] N91-19775
National Aeronautics and Space Administration N91-19967

COULOMETERS
Low level vapor verification of monomethyl hydrazine N91-20032

COUNTER ROTATION
Unified aeroacoustics analysis for high speed turboprop aerodynamics and noise. Volume 1: Development of theory for blade loading, wakes, and noise
[NASA-CR-4329] N91-19049

COUNTERMEASURES
Central and peripheral cardiovascular responses to electrically induced and voluntary leg exercise N91-19687
Weightlessness countermeasures and human physiology in space: A potential conflict N91-19695

COUPLING
On the joint inversion of geophysical data for models of the coupled core-mantle system
[NASA-TM-104536] N91-19557

CRACK OPENING DISPLACEMENT
Crack opening stress measurements of surface cracks in 7075-T6 Al alloy plate specimens through electron fractography
[LR-641] N91-19492

CRACK PROPAGATION
Effects of irradiation on crack-arrest toughness of two high-copper welds
[DE91-007189] N91-19270
Behavior of surface and corner cracks subjected to tensile and bending loads in Ti-6Al-4V alloy
[NASA-TM-102165] N91-19273
An evaluation of the fatigue crack growth and fracture toughness properties of beryllium-copper alloy CDA172
[NASA-TM-102166] N91-19274
Comparison of dynamic fatigue behavior between SiC whisker-reinforced composite and monolithic silicon nitrides
[NASA-TM-103707] N91-19293
The correlation of transient crack growth under small-scale-creep conditions N91-19467
An on-line real-time system for fatigue crack growth monitoring
[DE91-007931] N91-19483

CRACKING (FRACTURING)
Bulging of fatigue cracks in a pressurized aircraft fuselage
[LR-647] N91-19094
Bulging of fatigue cracks in a pressurized aircraft fuselage
[ETN-91-98927] N91-19489
Crack opening stress measurements of surface cracks in 7075-T6 Al alloy plate specimens through electron fractography
[LR-641] N91-19492

CRACKS
An on-line real-time system for fatigue crack growth monitoring
[DE91-007931] N91-19483

CRASHWORTHINESS
Crashworthiness investigations in the preliminary design phase of the NH90
[MBB-UD-0579-90-PUB] N91-19088

CRATERING
Relative chronology of Martian volcanoes N91-20007

CRAY COMPUTERS
A stochastic performance model for the neutron diffusion nodal method on a multiuser parallel supercomputer
[DE90-017015] N91-19749

CREEP ANALYSIS
A study on prediction of life due to creep behavior in CF/EPOXY and CF/PEEK laminates N91-19226

CREEP PROPERTIES
A study on prediction of life due to creep behavior in CF/EPOXY and CF/PEEK laminates N91-19226
The correlation of transient crack growth under small-scale-creep conditions N91-19467

CREEP TESTS
A study on prediction of life due to creep behavior in CF/EPOXY and CF/PEEK laminates N91-19226

CREW WORKSTATIONS
Army-NASA aircrew/aircraft integration program (A3I) software detailed design document, phase 3
[NASA-CR-177557] N91-19714

CRITICAL FLOW
Critical-layer nonlinearity in the resonance growth of three-dimensional waves in boundary layers
[NASA-TM-103639] N91-19373

CRITICAL TEMPERATURE
Thermal conductivity of high-temperature superconductors in normal state N91-19818

CROP GROWTH
Carbon dioxide and water exchange of a soybean stand grown in the biomass production chamber N91-20026

CRYOGENIC COOLING
Loss analysis of the thermodynamic cycle of magnetic heat pumps
[DE91-007669] N91-19950

CRYOGENIC EQUIPMENT
IAL SPACE: A test laboratory for the ISO cryogenic payload N91-19142
The space simulation facilities at IAL SPACE N91-19151
Integrated Cryogenic Experiment (ICE) microsphere investigation
[NASA-CR-177538] N91-19323
Thermal insulation of a cryogenic tank for a space telescope using a pretensioned suspension of Fiber Reinforced Composite (FRC)
[MBB-UD-0571-90-PUB] N91-19981

CRYOGENIC FLUID STORAGE
COLD-SAT feasibility study safety analysis
[NASA-CR-187042] N91-19167
In-space experiment on thermoacoustic convection heat transfer phenomenon-experiment definition
[NASA-CR-187070] N91-19378

CRYOGENIC FLUIDS
Cryogenic liquid-jet breakup in two-fluid atomizers
[NASA-TM-103734] N91-19402

CRYOGENIC ROCKET PROPELLANTS
Conceptual study of on orbit production of cryogenic propellants by water electrolysis
[NASA-TM-103730] N91-19317

CRYOGENIC STORAGE
Integrated Cryogenic Experiment (ICE) microsphere investigation
[NASA-CR-177538] N91-19323

CRYOGENIC TEMPERATURE
Thermal control for the ground simulation of a space IR sensor system N91-19140
Origin of residual surface resistance of ceramic high-temperature superconductors N91-19814
Studies of cold protection diodes
[DE91-008203] N91-19863
CRYOGENICS
Debris/ice/TPS assessment and photographic analysis for shuttle mission STS-35
[NASA-TM-103816] N91-19118
Development of components and subsystems for low noise receivers at micro- and millimeter waves
[S-187] N91-19363
Microtube strip heat exchanger
[DE91-005741] N91-19504
CRYOSTATS
Ultrasonic investigations on superfluid He-3-A and He-3-B
[ISBN-952-90-2241-7] N91-19830
CRYSTAL DEFECTS
Phenomena affecting morphology of microporous poly(acrylonitrile) prepared via phase separation from solution
[DE91-004501] N91-19297
Control of texture and defect structure for hot-filament-assisted CVD (Chemical Vapor Deposition) diamond Films
[DE91-008373] N91-19310
Solid State Photovoltaic Research Branch
[DE91-002128] N91-19502
Positron lifetime studies of defect structures in Ba(1-x)K(x)BiO3
[DE91-007341] N91-19919
Part 1: The effect of lattice defects on the sintering of lithium fluoride; Part 2: The morphology of calcium oxide from calcium carbonate decomposition
[DE91-007743] N91-19934
CRYSTAL DISLOCATIONS
Effect of dislocations on the open-circuit voltage, short-circuit current and efficiency of heteroepitaxial indium phosphide solar cells
[NASA-TM-103762] N91-19354
CRYSTAL GROWTH
Ultrafine refractory particle formation in counterflow diffusion flames
[DE91-007693] N91-19260
Phenomena affecting morphology of microporous poly(acrylonitrile) prepared via phase separation from solution
[DE91-004501] N91-19297
Growth kinetics of physical vapor transport processes: Crystal growth of the optoelectronic material mercurous chloride
[NASA-TM-103788] N91-19320
The effect of elastic stress on Ostwald ripening phenomena
[DE91-008034] N91-19484
Solid State Photovoltaic Research Branch
[DE91-002128] N91-19502
CRYSTAL LATTICES
Localization and electron-phonon interaction in disordered systems
[DE91-007654] N91-19837
Investigation of condensed matter fusion
[DE91-007246] N91-19923
Part 1: The effect of lattice defects on the sintering of lithium fluoride; Part 2: The morphology of calcium oxide from calcium carbonate decomposition
[DE91-007743] N91-19934
Diffuse x ray scattering YBa2Cu3O(6.95) monocrystal
[DE91-615182] N91-19943
CRYSTAL OPTICS
Nonlinear optic effects in liquid crystals
[ETN-91-98923] N91-19878
CRYSTAL STRUCTURE
The application of neutron diffraction time-of-flight measurements to the study of strain in composites
[DE91-008106] N91-19242
Ellipsometric study of InGaAs MODFET material
[NASA-TM-103286] N91-19351
Texture and microstructure development in Al-2 percent Mg during high-temperature deformation
[DE91-007355] N91-19480
Phenomenological theory of phase transitions to nonhomogeneous noncommensurate phase with superconducting current N91-19817
Phase transitions and equation of state of CsI under high pressure and the development of a focusing system for x rays
[DE91-007646] N91-19930
Electronic charge density and bonding in alpha-boron: An experimental-theoretical comparison
[DE91-006629] N91-19936
X ray determination of site occupation parameters in ordered ternaries Cu(Au(x)M(1-x))M = Ni,Pd
[DE91-007861] N91-19937
Diffuse x ray scattering YBa2Cu3O(6.95) monocrystal
[DE91-615182] N91-19943
CRYSTAL SURFACES
Part 1: The effect of lattice defects on the sintering of lithium fluoride; Part 2: The morphology of calcium oxide from calcium carbonate decomposition
[DE91-007743] N91-19934
CRYSTALLINITY
Investigation of anodic and chemical oxides grown on p-type InP with applications to surface passivation for n(+)-p solar cell fabrication N91-19208
Hot isostatic pressing of high performance glass-ceramic to nickel- and iron-based metal components
[DE91-008130] N91-19281
CRYSTALLIZATION
Hot isostatic pressing of high performance glass-ceramic to nickel- and iron-based metal components
[DE91-008130] N91-19281
Phenomena affecting morphology of microporous poly(acrylonitrile) prepared via phase separation from solution
[DE91-004501] N91-19297
Crystallization and properties of Sr-Ba aluminosilicate glass-ceramic matrices
[NASA-TM-103764] N91-19308
CRYSTALS
Growth kinetics of physical vapor transport processes: Crystal growth of the optoelectronic material mercurous chloride
[NASA-TM-103788] N91-19320
The provision of circuits to outside broadcast locations using spectrum within the UHF broadcasting bands
[BBC-RD-1990/12] N91-19329
Instellar grains within interstellar grains N91-19998
CULTURE TECHNIQUES
Preliminary study of a membrane bioreactor for cell culture in space N91-19627
Human dermal fibroblast sensitivity to hypergravity N91-19630
An assay for bone cell differentiation in vitro as a tool for microgravity studies in space N91-19637
Towards bioregenerative life support systems N91-19655
Plant biotechnology in space: Facts and speculations N91-19664
CURRENT DENSITY
Photoemission studies using femtosecond pulses for high brightness electron beams
[DE91-008436] N91-19849
Study on ablation of target material induced by pulsed ion beam bombardment N91-19886
Generation and focusing of carbon ion beam by the inverse pinch ion diode N91-19890
CURRENT DISTRIBUTION
Theoretical study of plasma focus diode N91-19887
CURVATURE
Free vibration of hexagonal panels supported at discrete points
[NASA-TM-102688] N91-19166
CURVE FITTING
A study on prediction of life due to creep behavior in CF/EPOXY and CF/PEEK laminates N91-19226
CYANIDES
Application of non-cyanide gold for selective plating of microelectronic circuits
[DE91-007729] N91-19276
CYCLOTRON RESONANCE DEVICES
An energy recovery system for a quasi-optical gyrotron
[DE91-008317] N91-19357
Time-dependent multimode simulation of gyrotron oscillators
[AD-A229861] N91-19413
CYCLOTRONS
Electromagnetic ion/ion cyclotron instability
[DE91-004841] N91-19860
CYLINDRICAL BODIES
Analytical solutions with Generalized Impedance Boundary Conditions (GIBC) N91-19307
CYLINDRICAL SHELLS
On the vectorization and parallelization of the shooting method using the convex C-240
[LR-639] N91-19491
CYLINDRICAL TANKS
Experimental studies on a nonlinear hydroelastic vibration of circular cylindrical tanks
[LRT-WE-9-FB-10(1990)] N91-19387
CYTOLOGY
Lymphocytes on sounding rockets N91-19620
Developmental biology and microgravity N91-19622
Unicellular algae in space. 2: Sounding-rocket experiment N91-19640
CYTOPLASM
Human dermal fibroblast sensitivity to hypergravity N91-19630
CZOCHRALSKI METHOD
Passive mode locking in optically pumped Al2O3:Ti(3+) laser N91-19803

D

D LINES
Fluorescent HD emission from photodissociation regions
[MPE-PREPRINT-177] N91-19982
DAMAGE
Smoothness criteria for runway rehabilitation and overlays
[DOT/FAA/RD-90/23] N91-19102
Debris/ice/TPS assessment and photographic analysis for shuttle mission STS-35
[NASA-TM-103816] N91-19118
Recent advances in the ITO/InP solar cell N91-19202
Semiconductor structural damage attendant to contact formation in III-V solar cells N91-19203
Continuum damage mechanisms with an application to fatigue
[ISBN-90-9003688-1] N91-19490
Effects of hyperbaric oxygenation on central hemodynamics and oxygen consumption in severe physical trauma N91-19570
DAMAGE ASSESSMENT
S87 close air support aircraft fatigue analysis
[ETN-91-98854] N91-19093
Radiation damage studies on hybrid preamplifiers
[DE91-008411] N91-19359
Neutron radiation damage studies on silicon detectors
[DE91-008441] N91-19361
The NAPAP assessment of damages to materials from acid deposition
[DE91-008086] N91-19542
DAMPING
Dynamic behavior of pneumatic tyres
[BU-412] N91-19453
Active damping application to the shuttle RMS
[NASA-TM-102763] N91-19471
Lag-stabilized force feedback damping
[DE91-007572] N91-19481
DATA ACQUISITION
Analyzing thought-related electroencephalographic data using nonlinear techniques N91-19031
Rotating pressure measurement system using an on board calibration standard
[NASA-TM-103676] N91-19401
Data acquisition and analysis on the two-color laser transmissometer system
[DE91-007235] N91-19420
Space operations: NASA is not archiving all potentially valuable data
[GAO/IMTEC-91-3] N91-19955
DATA BASE MANAGEMENT SYSTEMS
Ceramic Technology for Advanced Heat Engines project database
[DE91-007772] N91-19300
Radar backscatter from the sea controlled experiments
[AD-A229847] N91-19340
ARCHY (analysis and reverse engineering of code using hierarchy and Yourdon): A tool for FORTRAN code maintenance and development
[DE91-007241] N91-19720
Table of tables: A database design tool for SYBASE
[DE91-007257] N91-19958
An architecture for accommodating referenceability among intelligent electronic documents
[DE91-008250] N91-19964
Analyzing product test data in an INGRES database using SAS software
[DE91-008251] N91-19965
DATA BASES
Satellite servicing economic study
[NASA-CR-184112] N91-19162
Satellite servicing economic study
[NASA-CR-184113] N91-19163
Hypervelocity impact physics
[NASA-CR-4343] N91-19164
Composite materials for space applications
[NASA-CR-187472] N91-19238
Ceramic fabrication R and D
[DE91-006537] N91-19298
Responses of women to orthostatic and exercise stresses
[NASA-TP-3043] N91-19711
Table of tables: A database design tool for SYBASE
[DE91-007257] N91-19958

Analyzing product test data in a relational database using SAS software
[DE91-007734] N91-19960
Prototype document tracking and storage system for the Superconducting Super Collider Laboratory (SSCL)
[DE91-008204] N91-19963
Analyzing product test data in an INGRES database using SAS software
[DE91-008251] N91-19965

DATA CONVERSION ROUTINES
Transferable Output ASCII Data (TOAD) gateway: Version 1.0 user's guide
[NASA-CR-187489] N91-19737

DATA CORRELATION
Total ozone, ozonesonde, and Umkehr observations for satellite ozone data validation N91-19525
Zonal statistics in (General Circulation Model) GCM/GCM/data intercomparisons
[DE91-006706] N91-19530

DATA LINKS
Study of wavelength division multiplexing as a means of increasing the number of channels in multimode fiber optic communication links N91-20024

DATA MANAGEMENT
Transferable Output ASCII Data (TOAD) gateway: Version 1.0 user's guide
[NASA-CR-187489] N91-19737
Space operations: NASA is not archiving all potentially valuable data
[GAO/IMTEC-91-3] N91-19955
Analyzing product test data in a relational database using SAS software
[DE91-007734] N91-19960

DATA PROCESSING
Data acquisition and analysis on the two-color laser transmissometer system
[DE91-007235] N91-19420
Data status and availability N91-19515
Analyzing product test data in a relational database using SAS software
[DE91-007734] N91-19960
Rocket noise filtering system using digital filters N91-20031

DATA PROCESSING EQUIPMENT
Solid state electronic emulator of a multiple track motor driven rotating magnetic memory
[AD-D014705] N91-19437

DATA RETRIEVAL
Analyzing product test data in an INGRES database using SAS software
[DE91-008251] N91-19965

DATA SIMULATION
Overview of climate information needs for ecological effects models
[PB91-125898] N91-19549

DATA SMOOTHING
State estimation applications in aircraft flight-data analysis: A user's manual for SMACK
[NASA-RP-1252] N91-19082

DATA STORAGE
Space operations: NASA is not archiving all potentially valuable data
[GAO/IMTEC-91-3] N91-19955

DATA SYSTEMS
Investigation of air transportation technology at Ohio University, 1989-1990 N91-19028
Rotating pressure measurement system using an on board calibration standard
[NASA-TM-103676] N91-19401

DATA TRANSMISSION
I'm all 'light' Jack
[MBB-UD-0576-90-PUB] N91-19101
Multiphase complete exchange on a circuit switched hypercube
[NASA-CR-187499] N91-19716

DEBRIS
Debris/ice/TPS assessment and photographic analysis for shuttle mission STS-35
[NASA-TM-103816] N91-19118
Hypervelocity impact physics
[NASA-CR-4343] N91-19164

DECISION MAKING
Simulating motivated cognition
[NASA-TM-102886] N91-19770
Report of a workshop on Distributed Decision Making
[LC-89-64440] N91-19952
Space operations: NASA is not archiving all potentially valuable data
[GAO/IMTEC-91-3] N91-19955

DECODERS
On the optimality of code options for a universal noiseless coder
[NASA-CR-187973] N91-19734

DECODING
Algorithms for a very high speed universal noiseless coding module
[NASA-CR-187974] N91-19733

DECOMPRESSION SICKNESS
Vascular gas bubbles or decompression sickness: What is the proper endpoint for evaluating decompression procedures N91-19590

DECONDITIONING
Pedalling in space to simulate gravity: The twin-bike system N91-19583
Medex: A useful tool for counteracting orthostatic intolerance resulting from body fluid loss under microgravity N91-19585

DECOUPLING
A method for determining poloidal coil configurations for tokamak devices
[DE91-007940] N91-19903

DEDUCTION
The temporal logic of the tower chief system N91-19026

DEFECTS
The effect of process conditions on the performance of epitaxial InP solar cells N91-19204
A comparative study of performance parameters of n(+)-p InP solar cells made by closed-ampoule sulfur diffusion into Cd- and Zn-doped p-type InP substrates N91-19209
Annealing characteristics of irradiated hydrogenated amorphous silicon solar cells N91-19214
Research on advanced NDE methods for aerospace structures
[AD-A226858] N91-19460
Mechanical behavior of a ceramic matrix composite material
[NASA-CR-187072] N91-19461
Positron lifetime studies of defect structures in Ba(1-x)K(x)BiO3
[DE91-007341] N91-19919
The characterization of interface roughness and other defects in multilayers by x ray scattering
[DE91-007558] N91-19929

DEFLECTION
Method for determining astronomic azimuth
[AD-D014677] N91-19972

DEFORMATION
Texture and microstructure development in Al-2 percent Mg during high-temperature deformation
[DE91-007355] N91-19480
The structure of nuclei far from beta stability
[DE91-008140] N91-19846

DEGASSING
Gas entrapment and evolution in aluminium alloys produced by powder metallurgy
[ETN-91-98918] N91-19285

DEGRADATION
Ongoing development of a computer jobstream to predict helicopter main rotor performance in icing conditions
[NASA-CR-187076] N91-19056
A flight experiment to determine GPS photochemical contamination accumulation rates N91-19159
Spaceflight performance of several types of silicon solar cells on the LIPS 3 satellite N91-19213
An assessment of instrument performance for the NOAA-9 SBUV/2 N91-19516

DEGREES OF FREEDOM
Computation of invariant tori in 2 (1/2) degrees of freedom
[DE91-007424] N91-19778

DEHYDRATION
Medex: A useful tool for counteracting orthostatic intolerance resulting from body fluid loss under microgravity N91-19585

DEHYDROGENATION
Control of catalytic hydrotreating selectivity with ammonia
[DE91-005511] N91-19250

DELAMINATING
The full-scale process and design changes for elimination of insulation edge separations and voids in tang flap area
[NASA-CR-184110] N91-19172
Development of a fatigue-life methodology for composite structures subjected to out-of-plane load components
[NASA-TM-102885] N91-19241
Nonlinear analysis and redesign of the mixed-mode bending delamination test
[NASA-TM-102777] N91-19482

DELAY LINES
Intracavity second-harmonic generation by laser with optical delay line and mode locking N91-19808

DELTA LAUNCH VEHICLE
A unique approach to space thermal simulation N91-19153

DEMAGNETIZATION
Ultrasonic investigations on superfluid He-3-A and He-3-B
[ISBN-952-90-2241-7] N91-19830

DENITROGENATION
Control of catalytic hydrotreating selectivity with ammonia
[DE91-005511] N91-19250

DENSE PLASMAS
Quasi-molecular processes in dense plasmas
[DE91-007388] N91-19899
Measurements of stark-broadening in hot dense plasma
[DE91-008504] N91-19910

DENSITOMETERS
Aragatz Mission: Bone densitometric results obtained with the SCOOP miniscanner N91-19690

DENSITY (NUMBER/VOLUME)
Electronic charge density and bonding in alpha-boron: An experimental-theoretical comparison
[DE91-006629] N91-19936

DEOXYRIBONUCLEIC ACID
Protein purification in multicompartment electrolyzers for crystal growth of r-DNA products in microgravity N91-19665
Advanced sequencing technology
[DE91-008031] N91-19706

DEPLOYMENT
The design and flight testing of a high-performance low-cost parachute system for a 1000 lb payload
[DE91-007733] N91-19065

DEPOLARIZATION
Fiber optic interferometric measuring method for the determination of a very small polarization coefficient
[MBB-UA-1185-90-PUB] N91-19876

DEPOSITION
An outgassing model of non-metallic materials for the ascent of a Titan 4 launch vehicle N91-19132
A flight experiment to determine GPS photochemical contamination accumulation rates N91-19159
Simulation of Martian dust accumulation on surfaces N91-19160
Application of functional gradient materials in the aerospace industry
[MBB-Z-0320-90-PUB] N91-19311
Throughfall and foliar extraction
[DE91-007184] N91-19535
Plasma, photon, and beam synthesis of diamond films and multilayered structures
[DE91-007934] N91-19938

DEPOSITS
Microbiologically influenced corrosion in copper and nickel seawater piping systems
[AD-A229874] N91-19287

DESALINIZATION
Design and cost of near-term OTEC (Ocean Thermal Energy Conversion) plants for the production of desalinated water and electric power
[DE91-006406] N91-19508

DESIGN ANALYSIS
New computer codes for the structural analysis of composite helicopter structures
[MBB-UD-0580-90-PUB] N91-19089
The full-scale process and design changes for elimination of insulation edge separations and voids in tang flap area
[NASA-CR-184110] N91-19172
Ceramic fabrication R and D
[DE91-006537] N91-19298
High power, high frequency lasertron RF sources
[DE91-006007] N91-19414
ETARA PC version 3.3 user's guide: Reliability, availability, maintainability simulation model
[NASA-TM-103751] N91-19462
Centrifuge Facility Conceptual System Study. Volume 1: Facility overview and habitats
[NASA-TM-102860] N91-19566
Some neutronics and thermal-hydraulics codes for reactor analysis using personal computers
[DE91-006591] N91-19743
Study of the available finite element software packages at KSC N91-20029
Rocket noise filtering system using digital filters N91-20031

DESORPTION
The effect of process conditions on the performance of epitaxial InP solar cells N91-19204

DESULFURIZING
Reactivity of pi-complexes of Ti, V, and Nb towards dithioacetic acid: Synthesis and structure of novel metal sulfur-containing complexes
[NASA-TM-103666] N91-19256

DETECTION
Collision detection system
[AD-D014645] N91-19072

Feasibility of an onboard wake vortex avoidance system
[NASA-CR-187521] N91-19074
Indium tin oxide for solid-state image sensors
[ETN-91-98932] N91-19949
Low level vapor verification of monomethyl hydrazine N91-20032

DIAGNOSIS
Robust fault diagnosis of physical systems in operation
[NASA-TM-102767] N91-19073

DIAMONDS
Control of texture and defect structure for hot-filament-assisted CVD (Chemical Vapor Deposition) diamond Films
[DE91-008373] N91-19310
Plasma, photon, and beam synthesis of diamond films and multilayered structures
[DE91-007934] N91-19938

DIATOMIC MOLECULES
Intense field non-resonant multiphoton absorption of diatomic molecules
[DE91-006920] N91-19835

DIELECTRIC PROPERTIES
Study of InGaAs based MODFET structures using variable angle spectroscopic ellipsometry
[NASA-TM-103792] N91-19935

DIELECTRICS
High power, high frequency lasertron RF sources
[DE91-006007] N91-19414

DIESEL ENGINES
Oxygen-enriched diesel engine performance: A comparison of analytical and experimental results
[DE91-006491] N91-19440
A modelling of unsteady air flow in the resonance charging system of high speed diesel engines
[ACTA-POLYTEC-SCAND-ME-97] N91-19454

DIFFERENCE EQUATIONS
Invariant tori of the Poincare return map as solutions of functional difference equations
[DE91-007423] N91-19777

DIFFERENTIAL EQUATIONS
Bayesian approximation of solutions to linear ordinary differential equations
[DE91-007872] N91-19785

DIFFERENTIAL GEOMETRY
Computation and graphics in mathematical research
[DE91-007333] N91-19776

DIFFERENTIATION (BIOLOGY)
Does gravity play a role in the morphological development and function of the gravity sensory organ of vertebrates. DLR contribution to the D-2 project graviperception and neuronal plasticity, its technical realization and experimental execution N91-19635
An assay for bone cell differentiation in vitro as a tool for microgravity studies in space N91-19637

DIFFRACTION
Some roles for TEM in the development of new materials
[DE91-007742] N91-19933

DIFFUSE RADIATION
Contamination control program for the Cosmic Background Explorer: An overview N91-19152

DIFFUSION
A comparative study of performance parameters of n(+)-p InP solar cells made by closed-ampoule sulfur diffusion into Cd- and Zn-doped p-type InP substrates N91-19209
A stochastic performance model for the neutron diffusion nodal method on a multiuser parallel supercomputer
[DE90-017015] N91-19749

DIFFUSION FLAMES
Ultrafine refractory particle formation in counterflow diffusion flames
[DE91-007693] N91-19260

DIFFUSION LENGTH
GaP betavoltaic cells as a power source N91-19211

DIGITAL COMPUTERS
Time-frequency domain analysis of vibration signals for machinery diagnostics. 1: Introduction to the Wigner-Ville distribution
[OUEL-1859/90] N91-19495

DIGITAL FILTERS
Rocket noise filtering system using digital filters N91-20031

DIGITAL SIMULATION
Automatic control study of the icing research tunnel refrigeration system
[NASA-TM-4257] N91-19115

DIGITAL SYSTEMS
The provision of circuits to outside broadcast locations using spectrum within the UHF broadcasting bands
[BBC-RD-1990/12] N91-19329

DIGITAL TECHNIQUES
Research on advanced NDE methods for aerospace structures
[AD-A226858] N91-19460

DIGITALIS
Regeneration and characterization of protoplast-derived cell lines from Digitalis lanata EHRH. and Digitalis purpurea L. suspension cultures after electrofusion under microgravity conditions N91-19652

DIGITS
SIGNIF and GENFMT, SAS macros for computing and reporting significant digits
[DE91-007702] N91-19795

DIMERS
Late transition metal (mu)-oxo and (mu)-imido complexes
[DE91-005349] N91-19267

DIODES
Integral bypass diodes in an amorphous silicon alloy photovoltaic module N91-19218
Studies of cold protection diodes
[DE91-008203] N91-19863

DIPOLES
Elementary pulse diffraction problems and the generation of sound by a dipole moving across the edge of a half-plane
[LR-565] N91-19831

DIRICHLET PROBLEM
Boundary integral equations and the Dirichlet problem
[DE91-004537] N91-19779

DISEASES
Advanced sequencing technology
[DE91-008031] N91-19706

DISKS (SHAPES)
Noble gas disk MHD generator performance with unstable nonequilibrium plasma
[ISBN-90-9003671-7] N91-19916

DISPLACEMENT
A novel isoparametric finite element displacement formulation for axisymmetric analysis of nearly incompressible materials
[OUEL-1872/91] N91-19791

DISPLAY DEVICES
Flight simulation for wind shear encounter N91-19035
Proposed draft military handbook presenting requirements for an Electronic Display System (EDS) for Interactive Electronic Technical Manuals (IETMs)
[AD-A227471] N91-19342
Real-time application of advanced three-dimensional graphic techniques for research aircraft simulation
[NASA-TM-101730] N91-19742
Techniques for interactive 3-D scientific visualization
[DE91-007122] N91-19745
Formal specification of human-computer interfaces N91-20023

DISTORTION
A test fixture for measuring high-temperature hypersonic-engine seal performance
[NASA-TM-103658] N91-19442

DISTRIBUTED PARAMETER SYSTEMS
Model distribution in decentralized multi-sensor data fusion
[OUEL-1868/90] N91-19763

DISTRIBUTED PROCESSING
DEMO 89: The initial experiment with the HERMIES-3 robot
[DE90-017765] N91-19447
Tool and data interoperability in the SSE system N91-19727

DISTRIBUTION (PROPERTY)
The selection of window functions for the calculation of time domain averages on the vibration of the individual gears in an epicyclic gearbox
[OUEL-1818/90] N91-19457

DISTRIBUTION FUNCTIONS
The selection of window functions for the calculation of time domain averages on the vibration of the individual gears in an epicyclic gearbox
[OUEL-1818/90] N91-19457

DIVERGENCE
Spectrum transformation for divergent iterations
[NASA-TM-103745] N91-19786

DOCUMENT STORAGE
Prototype document tracking and storage system for the Superconducting Super Collider Laboratory (SSCL)
[DE91-008204] N91-19963

DOCUMENTATION
The 1989 JSC bibliography of scientific and technical papers
[NASA-TM-102173] N91-19959

DOCUMENTS
Proposed draft military handbook presenting requirements for an Electronic Display System (EDS) for Interactive Electronic Technical Manuals (IETMs)
[AD-A227471] N91-19342
Improved syntactic disambiguation in the FASIT automatic indexing environment N91-19956

DOGS
Effects of hyperbaric oxygenation on central hemodynamics and oxygen consumption in severe physical trauma N91-19570
Gravity dependence of pleural liquid turnover N91-19651

DOMAIN WALL
Observational relations in model universes dominated by domain-wall-like matter
[DE91-744969] N91-19988

DONOR MATERIALS
Photoinduced electron transfer processes in homogeneous and microheterogeneous solutions
[DE91-007582] N91-19836

DOPED CRYSTALS
Breakup of femtosecond pulses during amplification in Er(3+)-doped single-mode optical fibers N91-19812
Mutual influence of doping and oxidation in highly doped silicon
[ETN-91-98924] N91-19948

DOPPLER EFFECT
Collision detection system
[AD-D014645] N91-19072
Near resonant absorption by atoms in intense fluctuating fields
[DE91-007911] N91-19839

DOSIMETERS
A pocket-size broadband electric field detection and storage device
[DE91-007710] N91-19406
New experimental approach in quality factor and dose equivalent determination during a long term manned space mission N91-19679
An introduction to biological dosimetry
[DE91-007125] N91-19698

DOWNWASH
A flight-dynamic helicopter mathematical model with a single flap-lag-torsion main rotor
[NASA-TM-102267] N91-19041
A new methodology for free wake analysis using curved vortex elements
[NASA-CR-3958] N91-19067

DRAG
Icing characteristics of a natural-laminar-flow, a medium-speed, and a swept, medium-speed airfoil
[NASA-TM-103693] N91-19046
Research on bluff-body vortex wakes
[AD-A229875] N91-19071

DRAG CHUTES
The design and flight testing of a high-performance low-cost parachute system for a 1000 lb payload
[DE91-007733] N91-19065

DRAINAGE
What were the effects of the formation of the Borealis basin, Mars N91-20014

DRIFT (INSTRUMENTATION)
The apparent strain stability and repeatability of a BCL3 resistance strain gage
[NASA-CR-187056] N91-19403

DROP SIZE
LOX/hydrogen coaxial injector atomization test program
[NASA-CR-187037] N91-19117
Cryogenic liquid-jet breakup in two-fluid atomizers
[NASA-TM-103734] N91-19402

DRUGS
Plant biotechnology in space: Facts and speculations N91-19664

DUCTILITY
The 70 percent tungsten heavy alloys: Processing and properties
[DE91-008259] N91-19282

DUCTS
Calculations of separated 3-D flows with a pressure-staggered Navier-Stokes equations solver
[NASA-CR-187065] N91-19367

DURABILITY
Low cost space power generation N91-19212
Effects of training with reduced perfusion pressure on performance and muscle fiber characteristics N91-19615

DUST
Aeolian removal of dust types from photovoltaic surfaces on Mars N91-19156
Simulation of Martian dust accumulation on surfaces N91-19160
High resolution infrared astronomy satellite observations of a selected spiral galaxy
[NASA-CR-188019] N91-19975

DUST STORMS
Aeolian removal of dust types from photovoltaic surfaces on Mars N91-19156

DYE LASERS
Passive mode locking in optically pumped Al2O3:Ti(3+) laser N91-19803
DYES
Design considerations for multi component molecular-polymeric nonlinear optical materials [DE91-006778] N91-19872
DYNAMIC CHARACTERISTICS
Control and mechanism interaction for ground-based testing of space structures N91-19125
Free vibration of hexagonal panels supported at discrete points [NASA-TM-102688] N91-19166
Comparison of dynamic fatigue behavior between SiC whisker-reinforced composite and monolithic silicon nitrides [NASA-TM-103707] N91-19293
Dynamic behavior of pneumatic tyres [BU-412] N91-19453
Atomic beam studies of the interaction of hydrogen with transition metal surfaces [DE91-007938] N91-19841
DYNAMIC CONTROL
Texture and microstructure development in Al-2 percent Mg during high-temperature deformation [DE91-007355] N91-19480
DYNAMIC LOADS
Two reference time scales for studying the dynamic cavitation of liquid films [NASA-TM-103673] N91-19369
DYNAMIC MODELS
A flight-dynamic helicopter mathematical model with a single flap-lag-torsion main rotor [NASA-TM-102267] N91-19041
A simple dynamic engine model for use in a real-time aircraft simulation with thrust vectoring [NASA-TM-4240] N91-19079
A rigid body model and decoupled control architecture for two manipulators holding a complex object [DE91-007827] N91-19444
Army-NASA aircrew/aircraft integration program (A3I) software detailed design document, phase 3 [NASA-CR-177557] N91-19714
Parameter estimation of structural dynamic models using Eigenvalue and Eigenvector information [DE91-004379] N91-19793
DYNAMIC PRESSURE
Development of a piezoelectric polymer film pressure transducer for low frequency and dynamic pressure measurement [AD-A229848] N91-19412
DYNAMIC RESPONSE
Control and mechanism interaction for ground-based testing of space structures N91-19125
DYNAMIC STRUCTURAL ANALYSIS
The 5th Annual NASA Spacecraft Control Laboratory Experiment (SCOLE) Workshop, part 2 [NASA-CP-10057-PT-2] N91-19122
Control and mechanism interaction for ground-based testing of space structures N91-19125
Finite element analysis of geometrically non-linear problems using a corotational large rotation formulation [SU-ATN-9001] N91-19470
Active damping application to the shuttle RMS [NASA-TM-102763] N91-19471
Modal identification of a deployable space truss [NASA-TM-102720] N91-19474
Dynamic applications of ABAQUS [OUEL-1853/90] N91-19755
Parameter estimation of structural dynamic models using Eigenvalue and Eigenvector information [DE91-004379] N91-19793
DYNAMIC TESTS
Detailed modal testing of a solid rocket motor using a portable test system N91-19144
Innovations in dynamic test restraint systems N91-19145
DYNAMICAL SYSTEMS
The qualitative analysis of nonlinear parameterised systems. Part 2: A method for the global analysis of nonlinear systems [RR-400-PT-2] N91-19754
The qualitative analysis of nonlinear parameterized systems. Part 1: Nonlinear systems representation and dynamical systems theory [RR-408-PT-1] N91-19789

E

EARTH (PLANET)
Cycling space ship transportation device for continuous link between Earth and Mars [ILR-MITT-247(1990)] N91-19121
EARTH ATMOSPHERE
Evaluation of significant anthropogenic sources of radiatively important trace gases [PB91-127753] N91-19545
ICRCCM (intercomparison of radiation codes used in climate models). Phase 2: Verification and calibration of radiation codes in climate models [DE91-007323] N91-19555
EARTH CORE
On the joint inversion of geophysical data for models of the coupled core-mantle system [NASA-TM-104536] N91-19557
EARTH CRUST
Very low frequency seismo-acoustic scattering from a rough seafloor [AD-A227947] N91-19564
EARTH ENVIRONMENT
Environmental surveillance data report for the first quarter of 1990 [DE91-008552] N91-19544
EARTH MAGNETOSPHERE
Association of an auroral surge with plasma sheet recovery and the retreat of the substorm neutral line [DE91-007351] N91-19552
EARTH MANTLE
On the joint inversion of geophysical data for models of the coupled core-mantle system [NASA-TM-104536] N91-19557
EARTH ORBITAL ENVIRONMENTS
Space environmental effects on spacecraft thermal control coatings N91-19148
Low Earth orbital atomic oxygen and ultraviolet radiation effects on polymers [NASA-TM-103711] N91-19294
EARTH ORBITS
Atomic oxygen effects on boron nitride and silicon nitride: A comparison of ground based and space flight data N91-19146
Space environmental effects on spacecraft thermal control coatings N91-19148
Conceptual study of on orbit production of cryogenic propellants by water electrolysis [NASA-TM-103730] N91-19317
EARTH RADIATION BUDGET
Cloud forcing: A modeling perspective [DE91-007215] N91-19551
EARTH SURFACE
Solid earth science in the 1990s. Volume 1: Program plan [NASA-TM-4256-VOL-1] N91-19499
K/T age for the popigai impact event N91-19999
Cosmic ray charged component variations at sea level [DE91-615480] N91-20021
EARTHQUAKES
Lecture notes on nonlinear inversion and tomography [DE91-008238] N91-19558
ECHOCARDIOGRAPHY
Ultrasound investigation of the cardiovascular system during the 25-days Soviet-French flight: Cardiac aspects N91-19578
Design, implementation and evaluation of new fully automated algorithms for the extraction of cardiac parameters from 3D, 2D and M-mode echocardiograms N91-19582
ECONOMIC ANALYSIS
Direct conversion of methane to C2's [DE91-005730] N91-19251
Viability study of photovoltaic systems added to terrestrial electric vehicles [DE91-007689] N91-19355
COMPLEAT (community-oriented model for planning least-cost energy alternatives and technologies): A planning tool for publicly owned electric utilities [DE91-006955] N91-19511
ECONOMICS
Satellite servicing economic study [NASA-CR-184112] N91-19162
Satellite servicing economic study [NASA-CR-184113] N91-19163
Optimization and performance of Space Station Freedom solar cells N91-19215
Design and cost of near-term OTEC (Ocean Thermal Energy Conversion) plants for the production of desalinated water and electric power [DE91-006406] N91-19508
ECOSYSTEMS
Climatic water budgets, effective moisture, and elevation in the Southern Sierra Nevada, California, 1951-1980 [PB91-127878] N91-19500
Overview of climate information needs for ecological effects models [PB91-125898] N91-19549
EDGE DETECTION
Design and implementation of an image understanding system: DADS [ETN-91-98926] N91-19773
EDITING
Software for the ODRENOK microcomputer. Program package for graphics editing [DE91-614980] N91-19752
EDUCATION
Weightlessness countermeasures and human physiology in space: A potential conflict N91-19695
EFFERENT NERVOUS SYSTEMS
Medical results of the fourth prime expedition on the orbital station Mir N91-19576
EGGS
Fertilization of Xenopus eggs in space N91-19624
EIGENVALUES
Parameter estimation of structural dynamic models using Eigenvalue and Eigenvector information [DE91-004379] N91-19793
EIGENVECTORS
Parameter estimation of structural dynamic models using Eigenvalue and Eigenvector information [DE91-004379] N91-19793
ELASTIC BUCKLING
A variational approach to magneto-elastic buckling problems [ETN-91-98929] N91-19338
ELASTIC DEFORMATION
The effect of elastic stress on Ostwald ripening phenomena [DE91-008034] N91-19484
ELASTIC MEDIA
Solution of one-dimensional problem in nonlinear theory of elasticity with structured shock wave N91-19809
ELASTIC PROPERTIES
An overview of self-consistent methods for fiber-reinforced composites [NASA-TM-103713] N91-19232
The effect of elastic stress on Ostwald ripening phenomena [DE91-008034] N91-19484
Solution of one-dimensional problem in nonlinear theory of elasticity with structured shock wave N91-19809
ELASTOPLASTICITY
The method of lines in analyzing solids containing cracks [NASA-TM-103626] N91-19477
ELBOW (ANATOMY)
Isokinetic force velocity and electromyographic characteristic of knee and elbow extensor and flexor muscles in the 0-g environment N91-19584
ELECTRIC ARCS
Heat transport during gas tungsten arc welding [ETN-91-98919] N91-19455
ELECTRIC AUTOMOBILES
Methanol reformers for fuel cell powered vehicles: Some design considerations [DE91-006465] N91-19314
ELECTRIC BATTERIES
Laboratory testing of the Sonnenschein charger, Part number DTL 12040 [DE91-006543] N91-19346
Exploratory battery technology development and testing report for 1989 [DE91-006753] N91-19352
Sodium/metal chloride program conceptual design study [DE91-007216] N91-19353
ELECTRIC CHARGE
Electronic charge density and bonding in alpha-boron: An experimental-theoretical comparison [DE91-006629] N91-19936
Classical and quantum charge dynamics in small tunnel junctions [ETN-91-98916] N91-19947
ELECTRIC CONDUCTORS
Electromagnetic penetration through narrow slots in conducting surfaces and coupling to structures on the shadow side [DE91-007155] N91-19331
ELECTRIC CURRENT
Electromagnetic penetration through narrow slots in conducting surfaces and coupling to structures on the shadow side [DE91-007155] N91-19331
ELECTRIC DISCHARGES
Progressive feature of stepped leader on Japan sea coast in winter (basic data to establish shielding theory for lightning) [DE91-742133] N91-19561
Development of a numerical computer code and circuit element models for simulation of firing systems [DE91-007162] N91-19739
Copper vapor as active medium for high-power oscillator-amplifier laser systems N91-19806
ELECTRIC FIELDS
A pocket-size broadband electric field detection and storage device [DE91-007710] N91-19406

Baroelectric effect in the present of gravitational forces
[DE91-615469] N91-19559
An analytical study of neutral expansion, ionization, and charged particle acceleration in a neutral lithium release for the parallel electric field measurement
[MPE-PREPRINT-180] N91-19880
Generation and focusing of carbon ion beam by the inverse pinch ion diode N91-19890
Rocket-triggered lightning strikes and forest fire ignition N91-20027

ELECTRIC GENERATORS
Wire-free arming system for an aircraft-delivered bomb
[AD-D014611] N91-19076

ELECTRIC MOTOR VEHICLES
Viability study of photovoltaic systems added to terrestrial electric vehicles
[DE91-007689] N91-19355

ELECTRIC NETWORKS
Development of a numerical computer code and circuit element models for simulation of firing systems
[DE91-007162] N91-19739
An expansion plan for the 60 Hz power distribution system at KSC: LC-39 substations load allocation plan N91-20028

ELECTRIC POTENTIAL
Progress toward the development of dual junction GaAs/Ge solar cells N91-19184
Capattery double layer capacitor life performance
[DE91-006639] N91-19344
Heat transport during gas tungsten arc welding
[ETN-91-98919] N91-19455
Molten carbonate fuel cell technology improvement
[DE91-005540] N91-19505

ELECTRIC POWER
COMPLEAT (community-oriented model for planning least-cost energy alternatives and technologies): A planning tool for publicly owned electric utilities
[DE91-006955] N91-19511

ELECTRIC POWER PLANTS
Alternative strategies for the maintenance of geostationary space power plants
[ILR-MITT-249(1990)] N91-19170
Design and cost of near-term OTEC (Ocean Thermal Energy Conversion) plants for the production of desalinated water and electric power
[DE91-006406] N91-19508

ELECTRIC POWER SUPPLIES
ETARA PC version 3.3 user's guide: Reliability, availability, maintainability simulation model
[NASA-TM-103751] N91-19462
An expansion plan for the 60 Hz power distribution system at KSC: LC-39 substations load allocation plan N91-20028

ELECTRIC PROPULSION
Enhancing space transportation: The NASA program to develop electric propulsion
[NASA-TM-4244] N91-19181
Dual-purpose self-deliverable lunar surface PV electrical power system N91-19200
Methanol reformers for fuel cell powered vehicles: Some design considerations
[DE91-006465] N91-19314

ELECTRIC ROCKET ENGINES
Enhancing space transportation: The NASA program to develop electric propulsion
[NASA-TM-4244] N91-19181

ELECTRICAL ENGINEERING
Electromagnetic compatibility in high-voltage engineering
[ISBN-90-9002929-X] N91-19337
Activities report of the Istituto Elettrotecnico Nazionale Galileo Ferraris
[ETN-91-98868] N91-19822

ELECTRICAL IMPEDANCE
Task reports on developing techniques for scattering by 3D composite structures and to generate new solutions in diffraction theory using higher order boundary conditions
[NASA-CR-188057] N91-19305
Analytical solutions with Generalized Impedance Boundary Conditions (GIBC) N91-19307
Visualisation of fluid shifts within the body during a parabolic flight by measurements of electrical bio-impedance N91-19688
Electrochemical impedance spectroscopy of metal alloys in the space transportation system launch environment N91-20025

ELECTRICAL MEASUREMENT
Gravity perception by non-specialized structures N91-19636
Superconductivity of oxide film electrolytically deposited on surface of B(1-x)Sb(x) single crystal N91-19819

ELECTRICAL PROPERTIES
Neutron radiation damage studies on silicon detectors
[DE91-008441] N91-19361
Property and microstructural nonuniformity in the yttrium-barium-copper-oxide superconductor determined from electrical, magnetic, and ultrasonic measurements
[NASA-TM-103732] N91-19463
Solid State Photovoltaic Research Branch
[DE91-002128] N91-19502
Apparatus for determining microwave characteristics of superconductive materials using a resonant cavity and calibration waveguides
[AD-D014694] N91-19918
Thin film amorphous electrolytes: The Li2O-SiO2-P2O5 system
[DE91-007272] N91-19925

ELECTRICAL RESISTANCE
Atomic oxygen effects on boron nitride and silicon nitride: A comparison of ground based and space flight data N91-19146
Origin of residual surface resistance of ceramic high-temperature superconductors N91-19814

ELECTRICAL RESISTIVITY
Semiconductor structural damage attendant to contact formation in III-V solar cells N91-19203
Determination of series resistance of indium phosphide solar cells N91-19207
Radiation-induced changes in electrical conductivity of a wide range of copper alloys
[DE91-007200] N91-19271
Measurement of electromagnetic fields over a small electrolytic tank
[DE91-007500] N91-19334
Classical and quantum charge dynamics in small tunnel junctions
[ETN-91-98916] N91-19947

ELECTRO-OPTICS
Sandia technology: Engineering and science applications
[DE91-006760] N91-19322
Characterization of devices, circuits, and high-temperature superconductor transmission lines by electro-optic testing
[NASA-CR-187950] N91-19343
Compound semiconductors, strained layer epitaxy, and the information age
[DE91-007735] N91-19932

ELECTROCHEMICAL CELLS
Surface chemistry at semiconductor-electrolyte interfaces
[DE91-005915] N91-19920

ELECTROCHEMISTRY
Theory of bulk and interface constant phase elements in electrode-electrolyte systems
[DE91-007181] N91-19255
Spatial and temporal relationships between localized microbial metabolic activity and electrochemical activity of steel
[DE91-008102] N91-19279
Electrochemical impedance spectroscopy of metal alloys in the space transportation system launch environment N91-20025

ELECTRODEPOSITION
Application of non-cyanide gold for selective plating of microelectronic circuits
[DE91-007729] N91-19276
Superconductivity of oxide film electrolytically deposited on surface of B(1-x)Sb(x) single crystal N91-19819

ELECTRODES
Theory of bulk and interface constant phase elements in electrode-electrolyte systems
[DE91-007181] N91-19255
A study of carbon steel corrosion inhibition by phosphate ions and by an organic buffer using a scanning vibrating electrode
[DE91-008103] N91-19280
Measurement of electromagnetic fields over a small electrolytic tank
[DE91-007500] N91-19334

ELECTRODYNAMICS
Higher harmonics of magnetization in the critical state of ceramic high Tc superconductors
[DE91-615506] N91-19944

ELECTROENCEPHALOGRAPHY
Analyzing thought-related electroencephalographic data using nonlinear techniques N91-19031
Review of EEG studies in non human primates exposed to microgravity N91-19649

ELECTROLYSIS
Conceptual study of on orbit production of cryogenic propellants by water electrolysis
[NASA-TM-103730] N91-19317

ELECTROLYTES
Measurement of electromagnetic fields over a small electrolytic tank
[DE91-007500] N91-19334
Sodium/metal chloride program conceptual design study
[DE91-007216] N91-19353
Molten carbonate fuel cell technology improvement
[DE91-005540] N91-19505
Physiology of body water and salt regulation. Part 2: Volume and electrolyte homeostasis after an acute saline infusion N91-19593
Thin film amorphous electrolytes: The Li2O-SiO2-P2O5 system
[DE91-007272] N91-19925

ELECTROMAGNETIC ABSORPTION
NO2 absorption cross-section in the 440 to 460 nm region at 298 and 220 K
[NOTA-INTERNA-964] N91-19550

ELECTROMAGNETIC COMPATIBILITY
Electromagnetic compatibility in high-voltage engineering
[ISBN-90-9002929-X] N91-19337

ELECTROMAGNETIC COUPLING
Electromagnetic penetration through narrow slots in conducting surfaces and coupling to structures on the shadow side
[DE91-007155] N91-19331

ELECTROMAGNETIC FIELDS
Electromagnetic penetration through narrow slots in conducting surfaces and coupling to structures on the shadow side
[DE91-007155] N91-19331
Assessing the impact of large-scale computing on the size and complexity of first-principles electromagnetic models
[DE91-007491] N91-19333
Measurement of electromagnetic fields over a small electrolytic tank
[DE91-007500] N91-19334
High power, high frequency lasertron RF sources
[DE91-006007] N91-19414
Biological effects of extremely low-frequency electromagnetic fields: In vivo studies
[DE91-007899] N91-19704

ELECTROMAGNETIC INTERACTIONS
Exchange currents in low-energy nucleon capture by He3
[ETN-91-98917] N91-19855

ELECTROMAGNETIC INTERFERENCE
Prospects for using carbon-carbon composites for EMI shielding
[NASA-TM-103677] N91-19231
Electromagnetic compatibility in high-voltage engineering
[ISBN-90-9002929-X] N91-19337
The development of a rugged accelerometer
[DE91-007731] N91-19407

ELECTROMAGNETIC MEASUREMENT
An analytical study of neutral expansion, ionization, and charged particle acceleration in a neutral lithium release for the parallel electric field measurement
[MPE-PREPRINT-180] N91-19880

ELECTROMAGNETIC PULSES
Computer controlled MHD power consolidation and pulse generation system
[DE91-006793] N91-19347
Limiting pulse signal in NbN-Si structure: Superconductor film on substrate N91-19815

ELECTROMAGNETIC SCATTERING
Task reports on developing techniques for scattering by 3D composite structures and to generate new solutions in diffraction theory using higher order boundary conditions
[NASA-CR-188057] N91-19305
A finite element conjugate gradient FFT method for scattering N91-19306
Analytical solutions with Generalized Impedance Boundary Conditions (GIBC) N91-19307

ELECTROMAGNETIC SHIELDING
Prospects for using carbon-carbon composites for EMI shielding
[NASA-TM-103677] N91-19231

ELECTROMAGNETIC SPECTRA
The evolution and limits of spectral bandwidth in free electron lasers
[DE91-007737] N91-19425

ELECTROMAGNETIC WAVE TRANSMISSION
Unique Signal Override Plug (USOP) electromagnetic test report
[DE91-004996] N91-19330
Theory of the ion-channel laser
[DE91-007643] N91-19423

ELECTROMAGNETISM
Activities report of the Istituto Elettrotecnico Nazionale Galileo Ferraris
[ETN-91-98868] N91-19822

ELECTROMYOGRAPHY
Isokinetic force velocity and electromyographic characteristic of knee and elbow extensor and flexor muscles in the 0-g environment N91-19584

ELECTRON BEAMS
High power, high frequency lasertron RF sources
[DE91-006007] N91-19414
Intense microwave generation using free-electron lasers
[DE91-007262] N91-19417
The evolution and limits of spectral bandwidth in free electron lasers
[DE91-007737] N91-19425
Photoemission studies using femtosecond pulses for high brightness electron beams
[DE91-008436] N91-19849
Predicted Bremsstrahlung generation by energetic electron beams
[DE91-007164] N91-19858

ELECTRON BOMBARDMENT
Study on ablation of target material induced by pulsed ion beam bombardment N91-19886

ELECTRON DENSITY (CONCENTRATION)
Localization and electron-phonon interaction in disordered systems
[DE91-007654] N91-19837
Plasma boundary experiments on D3-D tokamak
[DE91-002429] N91-19881
Control of gap closure in applied-B diode N91-19893

ELECTRON DIFFRACTION
Photoelectron diffraction of magnetic ultrathin films: Fe/Cu(001)
[DE91-007254] N91-19924

ELECTRON ENERGY
Soft x-ray laser gain prediction at high density for the nitrogen isoelectronic sequence
[DE91-007616] N91-19416
Electron temperature of Gd plasma produced by laser resonance ionization
[DE91-744833] N91-19913

ELECTRON IMPACT
Cross section for production of excited hydrogen atoms following dissociative excitation of molecular hydrogen by electron impact
[DE91-745035] N91-19852

ELECTRON IRRADIATION
The effect of process conditions on the performance of epitaxial InP solar cells N91-19204

ELECTRON MICROSCOPY
In situ TEM studies of the growth of strained Si(1-x)Ge(x) by solid phase epitaxy
[DE91-007278] N91-19926
Some roles for TEM in the development of new materials
[DE91-007742] N91-19933

ELECTRON MOBILITY
Possibility of raising efficiency of free-electron laser in longitudinal magnetic field N91-19804

ELECTRON PARAMAGNETIC RESONANCE
Low temperature properties of boron carbides
[DE91-008172] N91-19243

ELECTRON PHONON INTERACTIONS
Localization and electron-phonon interaction in disordered systems
[DE91-007654] N91-19837

ELECTRON RECOMBINATION
Recombination x ray laser experiments using exploding ribbon Al targets
[DE91-007146] N91-19429

ELECTRON SCATTERING
Response matrix Monte Carlo based on a general geometry local calculation for electron transport
[DE91-007638] N91-19794
Dynamics of collision processes
[DE91-007933] N91-19840
Optically-ionized plasma recombination x ray lasers
[DE91-007261] N91-19898

ELECTRON SOURCES
Development of high current electron source using photoemission from metals with ultrashort laser pulses
[DE91-008438] N91-19850

ELECTRON SPIN
Effect of paramagnetic impurities on dynamics of magnetic fluxes in superconductors N91-19816

ELECTRON STATES
Localization and electron-phonon interaction in disordered systems
[DE91-007654] N91-19837

ELECTRON TRAJECTORIES
An energy recovery system for a quasi-optical gyrotron
[DE91-008317] N91-19357

ELECTRON TRANSFER
Response matrix Monte Carlo based on a general geometry local calculation for electron transport
[DE91-007638] N91-19794
Frontier orbital symmetry control of intermolecular electron transfer
[DE91-005699] N91-19834
Photoinduced electron transfer processes in homogeneous and microheterogeneous solutions
[DE91-007582] N91-19836
Electron transfer, ionization, and excitation in atomic collisions
[DE91-008044] N91-19844

ELECTRON TUNNELING
Classical and quantum charge dynamics in small tunnel junctions
[ETN-91-98916] N91-19947

ELECTRON-POSITRON PLASMAS
Electroweak interactions at LEP
[NOTA-INTERNA-962] N91-19853
A global fit to the Z(0) line shape
[NOTA-INTERNA-966] N91-19868

ELECTRONIC EQUIPMENT
Proposed draft military handbook presenting requirements for an Electronic Display System (EDS) for Interactive Electronic Technical Manuals (IETMs)
[AD-A227471] N91-19342
Central and peripheral cardiovascular responses to electrically induced and voluntary leg exercise N91-19687

ELECTRONIC PACKAGING
Parameter estimation of structural dynamic models using Eigenvalue and Eigenvector information
[DE91-004379] N91-19793

ELECTRONS
Relaxed states with plasma flow
[DE91-008199] N91-19909

ELECTROPHORESIS
Free flow electrophoresis experiment TEPE 3 on Texus 24
[MBB-UO-0130-90-PUB] N91-19321
A new approach to electrophoresis in space N91-19653
Free flow electrophoresis experiment TEPE 3 on TEXUS 24 N91-19654

ELECTROSTATIC PRECIPITATORS
Performance characteristics of an MHD (Magnetohydrodynamic) pilot plant electrostatic precipitator
[DE91-007218] N91-19905

ELECTROSTATICS
Baroelectric effect in the present of gravitational forces
[DE91-615469] N91-19559

ELEMENTARY PARTICLES
Summary of discussions at the HIGH p (sub T) session
[DE91-008196] N91-19848

ELLIPSOMETRY
Characterization of ion-implanted aluminum and iron by spectroscopic ellipsometry
[DE91-008371] N91-19283
Ellipsometric study of InGaAs MODFET material
[NASA-TM-103286] N91-19351
Study of InGaAs based MODFET structures using variable angle spectroscopic ellipsometry
[NASA-TM-103792] N91-19935

ELONGATION
Vertebral column length changes during simulated microgravity N91-19604

EMBEDDED COMPUTER SYSTEMS
Computers at risk: Safe computing in the information age
[LC-90-22329] N91-19721

EMBRYOLOGY
Developmental biology and microgravity N91-19622
Defective embryogenesis of Arabidopsis induced by cosmic HZE-particles N91-19682

EMBRYOS
Effect of the centrifuge forces on pregnant rats N91-19629

EMERGENCIES
Expert systems for fault diagnosis in nuclear reactor control
[RR-412] N91-19864

EMISSION
Alternative fuels for heavy duty engines: Status of fleet trials
[DE91-006799] N91-19315
Environmental surveillance data report for the first quarter of 1990
[DE91-008552] N91-19544

EMISSION SPECTRA
Characteristics of excimer laser with narrow emission line N91-19807
He-Ne laser emitting five lines simultaneously N91-19813
Cross section for production of excited hydrogen atoms following dissociative excitation of molecular hydrogen by electron impact
[DE91-745035] N91-19852
Calculation of emission and absorption spectra of LTE plasma by the STA (Super Transition Array) method
[DE91-007617] N91-19900

EMITTANCE
Microbiological assay using bioluminescent organism
[AD-D014651] N91-19249

END EFFECTORS
System description document for the Anthrobot-2: A dexterous robot hand
[NASA-TM-104535] N91-19449
A haptic system for a multifingered hand
[DE90-017044] N91-19767

ENDOCRINE SYSTEMS
Head-down tilt test and space-related endocrine physiology N91-19614

ENDOPLASMIC RETICULUM
Gravitational effects on subcellular structures of plant cells N91-19669

ENERGETIC PARTICLES
Experimental data on study of cosmic ray particles in the E greater than or equal to 2 TeV energy range at the Cosmos-1713 satellite with the Sokol-2 device
[DE91-615479] N91-20020

ENERGY ABSORPTION
Innovations in dynamic test restraint systems N91-19145
Near resonant absorption by atoms in intense fluctuating fields
[DE91-007911] N91-19839

ENERGY CONSERVATION
Conservation of energy, momentum, and angular momentum in Lagrangian staggered-grid hydrodynamics
[DE91-008059] N91-19381

ENERGY CONSUMPTION
Air traffic simulation with a view to system interpretation N91-19110

ENERGY CONVERSION
The OAST space power program N91-19183

ENERGY CONVERSION EFFICIENCY
Progress toward the development of dual junction GaAs/Ge solar cells N91-19184
Progress toward a 30 percent-efficient, monolithic, three-junction, two-terminal concentrator solar cell for space applications N91-19188
Tandem concentrator solar cells with 30 percent (AMO) power conversion efficiency N91-19189
InP/Ga0.47In0.53As monolithic, two-junction, three-terminal tandem solar cells N91-19191
Review of thin film solar cell technology and applications for ultra-light spacecraft solar arrays N91-19198
Determination of series resistance of indium phosphide solar cells N91-19207
A comparative study of performance parameters of n(+)-p InP solar cells made by closed-ampoule sulfur diffusion into Cd- and Zn-doped p-type InP substrates N91-19209
GaP betavoltaic cells as a power source N91-19211
Effect of dislocations on the open-circuit voltage, short-circuit current and efficiency of heteroepitaxial indium phosphide solar cells
[NASA-TM-103762] N91-19354
A summary of the status of biomass conversion technologies and opportunities for their use in developing countries
[DE91-006341] N91-19506
Some control problems with broad range variable speed for horizontal axis wind turbines
[FFA-TN-1990-37] N91-19513
Tuning the efficiencies of plant lighting systems: From primary energy to edible biomass: The LED as an alternative light source N91-19660
Possibility of raising efficiency of free-electron laser in longitudinal magnetic field N91-19804

ENERGY DISSIPATION
Filtering analysis of a direct numerical simulation of the turbulent Rayleigh-Benard problem
[NASA-CR-187488] N91-19366

ENERGY DISTRIBUTION
An expansion plan for the 60 Hz power distribution system at KSC: LC-39 substations load allocation plan N91-20028

ENERGY GAPS (SOLID STATE)
Graded-bandgap AlGaAs solar cells for AlGaAs/Ge cascade cells N91-19186
Progress in GaAs/CuInSe2 tandem junction solar cells N91-19190
InP/Ga0.47In0.53As monolithic, two-junction, three-terminal tandem solar cells N91-19191
Key factors limiting the open circuit voltage of n(+)pp(+) indium phosphide solar cells N91-19206
Radioisotope thermal photovoltaic application of the GaSb solar cell N91-19210
Localization and electron-phonon interaction in disordered systems
[DE91-007654] N91-19837

ENERGY POLICY
The National Energy Strategy: The role of geothermal technology development. Proceedings
[DE91-004623] N91-19503
ENERGY REQUIREMENTS
Sodium/metal chloride program conceptual design study
[DE91-007216] N91-19353
ENERGY STORAGE
Hydrogen storage in metal hydrides
[DE91-746267] N91-19316
Generation of pulsed ion beams by an inductive storage pulsed power generator N91-19891
ENERGY TECHNOLOGY
Feasibility of solar power for Mars N91-19201
COMPLEAT (community-oriented model for planning least-cost energy alternatives and technologies): A planning tool for publicly owned electric utilities
[DE91-006955] N91-19511
Large-scale computing in the energy research programs
[DE91-007907] N91-19748
Introduction to fusion
[DE91-744831] N91-19912
Materials sciences programs
[DE91-007601] N91-19953
ENERGY TRANSFER
GaP betavoltaic cells as a power source N91-19211
Interferometry, streak photography, and stereo photography of laser-driven miniature flying plates
[DE91-007493] N91-19405
A study of alkaline element interferences in analytical inductively coupled plasmas
[ISAL-90-0069] N91-19915
ENGINE DESIGN
Propulsion system concept for the Eurofar tilt rotor aircraft
[MBB-UD-0573-90-PUB] N91-19084
The selection of convertible engines with current gas generator technology for high speed rotorcraft
[NASA-TM-103774] N91-19097
High temperature NASP engine seal development
[NASA-TM-103716] N91-19441
A test fixture for measuring high-temperature hypersonic-engine seal performance
[NASA-TM-103658] N91-19442
ENGINE FAILURE
Monitoring techniques for the X-29A aircraft's high-speed rotating power takeoff shaft
[NASA-TM-101731] N91-19081
ENGINE MONITORING INSTRUMENTS
The application of aero gas turbine engine monitoring systems to military aircraft
[ETN-91-98852] N91-19096
ENGINE NOISE
J-85 jet engine noise measured in the ONERA S1 wind tunnel and extrapolated to far field
[NASA-TP-3053] N91-19823
ENGINE TESTS
Detailed modal testing of a solid rocket motor using a portable test system N91-19144
Orbital transfer vehicle oxygen turbopump technology. Volume 1: Design, fabrication, and hydrostatic bearing testing
[NASA-CR-185175] N91-19174
ENGINES
Ceramic Technology for Advanced Heat Engines project database
[DE91-007772] N91-19300
ENRICHMENT
Oxygen-enriched diesel engine performance: A comparison of analytical and experimental results
[DE91-006491] N91-19440
ENTRAPMENT
Gas entrapment and evolution in aluminium alloys produced by powder metallurgy
[ETN-91-98918] N91-19285
ENVIRONMENT EFFECTS
A status report on the analysis of the NOAA-9 SBUV/2 sweep mode solar irradiance data N91-19518
Natural and anthropogenic climate change
[DE91-007363] N91-19532
The NAPAP assessment of damages to materials from acid deposition
[DE91-008086] N91-19542
Outer continental shelf environmental assessment program, volume 70
[PB91-129288] N91-19548
ENVIRONMENT MODELS
Throughfall and foliar extraction
[DE91-007184] N91-19535
Estimating lightning-generated NOx emissions for regional air pollution models
[PB91-131664] N91-19546
Overview of climate information needs for ecological effects models
[PB91-125898] N91-19549
ENVIRONMENT POLLUTION
Airport system technical aspects N91-19107
Global change: What you can do
[S-HRG-101-1160] N91-19528
ENVIRONMENT PROTECTION
Environmental surveillance data report for the first quarter of 1990
[DE91-008552] N91-19544
ENVIRONMENT SIMULATION
Pedalling in space to simulate gravity: The twin-bike system N91-19583
Mutation induction in dried yeast cells after irradiation with selected UVC- and UVB- wavelengths compared to simulated sunlight N91-19686
Electrochemical impedance spectroscopy of metal alloys in the space transportation system launch environment N91-20025
ENVIRONMENTAL MONITORING
A review of fiber optic and related technologies for environmental sensing applications
[DE91-007736] N91-19409
Total ozone, ozonesonde, and Umkehr observations for satellite ozone data validation N91-19525
Environmental surveillance data report for the first quarter of 1990
[DE91-008552] N91-19544
ENVIRONMENTAL QUALITY
Global change: What you can do
[S-HRG-101-1160] N91-19528
ENVIRONMENTAL TESTS
Stress corrosion cracking of Al-Li-Cu-Zr alloy 2090 in aqueous Cl(-) and mixed CO3(2-)/Cl(-) environments
[DE91-007064] N91-19269
ENZYME ACTIVITY
Subcellular signal transduction systems in the cellular trauma of ischemia
[AD-A229876] N91-19709
ENZYMES
Regeneration and characterization of protoplast-derived cell lines from Digitalis lanata EHRH. and Digitalis purpurea L. suspension cultures after electrofusion under microgravity conditions N91-19652
Physiological genetics of denitrification: A route to conserving fixed nitrogen
[DE91-008157] N91-19707
EPIDERMIS
Epidermal growth factor induced signal transduction in A431 cells is influenced by altered gravity conditions N91-19623
EPITAXY
Effect of dislocations on the open-circuit voltage, short-circuit current and efficiency of heteroepitaxial indium phosphide solar cells
[NASA-TM-103762] N91-19354
In situ TEM studies of the growth of strained Si(1-x)Ge(x) by solid phase epitaxy
[DE91-007278] N91-19926
EQUATIONS OF MOTION
Basic research model of natural gas combustion in turbulent flow
[PB91-130260] N91-19264
Conservation of energy, momentum, and angular momentum in Lagrangian staggered-grid hydrodynamics
[DE91-008059] N91-19381
Traveling time effects in a channel flow
[MPIS-10/1990] N91-19384
Notes on the unsteady rectilinear motion of a perfect gas. 10: On the influence of gravity upon the expansion of an ideal gas with gamma = 3
[LR-640] N91-19395
EQUATIONS OF STATE
Model distribution in decentralized multi-sensor data fusion
[OUEL-1868/90] N91-19763
Phase transitions and equation of state of CsI under high pressure and the development of a focusing system for x rays
[DE91-007646] N91-19930
EQUILIBRIUM EQUATIONS
Continuum damage mechanisms with an application to fatigue
[ISBN-90-9003688-1] N91-19490
ERBIUM
Breakup of femtosecond pulses during amplification in Er(3+)-doped single-mode optical fibers N91-19812
ERGOMETERS
Isokinetic force velocity and electromyographic characteristic of knee and elbow extensor and flexor muscles in the 0-g environment N91-19584
Oxygen uptake during concentric and eccentric resistive exercise using a new gravity-independent ergometer N91-19587
ERROR ANALYSIS
Automatic speech recognition in air traffic control: A human factors perspective N91-19025
Robust fault diagnosis of physical systems in operation
[NASA-TM-102767] N91-19073
Development and applications of a multi-level strain energy method for detecting finite element modeling errors
[NASA-CR-187447] N91-19478
Software reliability through fault-avoidance and fault-tolerance
[NASA-CR-187998] N91-19741
The application of neural networks for fault diagnosis in nuclear reactors
[RR-411] N91-19772
Optimal observation directions for estimating a vector
[PREPRINT-1285] N91-19796
Expert systems for fault diagnosis in nuclear reactor control
[RR-412] N91-19864
Petri nets and fault diagnosis in nuclear reactors
[RR-413] N91-19865
The use of an object oriented technique for fault diagnosis in nuclear reactors
[RR-414] N91-19866
Fault detection using optimal control techniques
[RR-419] N91-19867
Hubble Space Telescope secondary mirror vertex radius/conic constant test
[NASA-CR-187989] N91-19871
ERRORS
Modeling selective availability of the NAVSTAR global positioning system N91-19030
Integrated inertial/GPS N91-19032
Umkehr work N91-19522
ESTIMATING
Estimating lightning-generated NOx emissions for regional air pollution models
[PB91-131664] N91-19546
ETCHING
Optical diagnostics for low-temperature plasmas
[DE91-007896] N91-19907
EULER EQUATIONS OF MOTION
Solution of one-dimensional problem in nonlinear theory of elasticity with structured shock wave N91-19809
Euler solutions to nonlinear acoustics of non-lifting hovering rotor blades
[NASA-TM-103837] N91-19826
EULER-LAGRANGE EQUATION
W(sub L)W(sub L) scattering at the SSC
[DE91-008442] N91-19851
EUROPE
Propulsion system concept for the Eurofar tilt rotor aircraft
[MBB-UD-0573-90-PUB] N91-19084
EUROPEAN SPACE AGENCY
Space research for the sake of all
[ETN-91-98807] N91-19113
EUROPEAN SPACE PROGRAMS
Space research for the sake of all
[ETN-91-98807] N91-19113
EUTECTICS
High resolution microstructural and microchemical analysis of zirconia eutectic interfaces
[DE91-008032] N91-19940
EVAPORATORS
Results of scoping tests for open-cycle OTEC (Ocean Thermal Energy Conversion) components operating with seawater
[DE89-009514] N91-19501
EVEN-EVEN NUCLEI
Electric monopole transitions and shape coexistence in nuclei
[DE91-008141] N91-19847
EVOLUTION (DEVELOPMENT)
Thermal instabilities in cooling flows: The evolution of nearly spherical perturbations
[MPE-PREPRINT-176] N91-19365
Fertilization of Xenopus eggs in space N91-19624
Blood pressure maturation curve in normotensive rats during growth in simulated microgravitational environment N91-19644
Plant protoplast development on Biokosmos 9 N91-19674
EXCIMER LASERS
Excimer laser surface processing for tribological applications in metals and ceramics
[DE91-002324] N91-19428
Characteristics of excimer laser with narrow emission line N91-19807
EXCITATION
Response of a differently axially excited viscous liquid layer in zero-gravity
[LRT-WE-9-FB-12(1990)] N91-19389

Response of a viscous liquid layer to pitch- and roll-excitation in zero-gravity environment
[LRT-WE-9-FB-13(1990)] N91-19390
Dynamics of collision processes
[DE91-007933] N91-19840
Electron transfer, ionization, and excitation in atomic collisions
[DE91-008044] N91-19844
Quasi-molecular processes in dense plasmas
[DE91-007388] N91-19899

EXCRETION
Physiology of body water and salt regulation. Part 1: Circadian rhythms of endocrine systems and urinary electrolyte excretion in humans N91-19592

EXHAUST EMISSION
Results from the third year of operation of the Federal methanol fleet at Argonne National Laboratory
[DE91-007822] N91-19451
Exhaust emissions from heavy duty vehicles
[DE91-006798] N91-19531
The NAPAP assessment of damages to materials from acid deposition
[DE91-008086] N91-19542

EXHAUST GASES
Exhaust emissions from heavy duty vehicles
[DE91-006798] N91-19531

EXOBIOLOGY
Fourth European Symposium on Life Sciences Research in Space
[ESA-SP-307] N91-19572
Life sciences in ESA TRP activity N91-19589
Hindlimb suspension of rabbit for one week: Myofibrillar damage in the soleus may depend on long-lasting shortening and periodic contraction against no load N91-19647
Preliminary studies before defining a payload adapted to the primate model N91-19648
Review of EEG studies in non human primates exposed to microgravity N91-19649
Regeneration and characterization of protoplast-derived cell lines from Digitalis lanata EHRH. and Digitalis purpurea L. suspension cultures after electrofusion under microgravity conditions N91-19652
Biolab on Columbus: A facility for basic science and biotechnology N91-19658
Cells in space: Sounding rocket facilities for cell biology and biotechnology in microgravity N91-19661
The slow-rotating centrifuge microscope (NIZEMI): A new research tool for terrestrial and space-related gravitational biology N91-19663
Protein purification in multicompartment electrolyzers for crystal growth of r-DNA products in microgravity N91-19665
Graviperception in plants N91-19667
Gravitational effects on subcellular structures of plant cells N91-19669
Plant development in space: Observations on root formation and growth N91-19670
Plant growth under microgravity conditions: Experiments and problems N91-19671
Potentials, message and challenges of life science research in space N91-19696
The 1989-1990 NASA space biology accomplishments
[NASA-TM-4258] N91-19697
Predictions of cell damage rates for Lifesat missions
[NASA-TM-102170] N91-19699
USSR Space Life Sciences Digest. Index to issues 26-29
[NASA-CR-3922(35)] N91-19700
Experimental equipment for space biology
[MBB-UO-0096-90-PUB] N91-19708

EXPERIMENT DESIGN
Preliminary studies before defining a payload adapted to the primate model N91-19648

EXPERIMENTATION
Tools for the preparation, performance and evaluation of life sciences experiments N91-19609

EXPERT SYSTEMS
Joint University Program for Air Transportation Research, 1989-1990
[NASA-CP-3095] N91-19024
Progress on intelligent guidance and control for wind shear encounter N91-19034
Robust fault diagnosis of physical systems in operation
[NASA-TM-102767] N91-19073
An expert system for laminated plate design using composite materials
[BU-406] N91-19245
A knowledge based expert system for laminated composite strut design
[BU-410] N91-19247
Bolted joints in a laminated composite strut design expert system
[BU-415] N91-19488
Simulation expert system for physiological mechanisms of the space motion sickness N91-19596
Engineering monitoring expert system's developer
[NASA-CR-187914] N91-19765
Expert systems for fault diagnosis in nuclear reactor control
[RR-412] N91-19864
The development of structure for the representation and manipulation of sophisticated knowledge in intelligent systems
[AD-A229114] N91-19957
Modeling of flow systems for implementation under KATE N91-20038

EXPLORATION
An evaluation of co-planar lineament analysis and some thoughts on using surface geological data to predict sub-surface geology
[DE90-009687] N91-19556

EXPLOSIONS
Impact processes in the Solar System: New understandings through numerical modeling N91-19996

EXPLOSIVES
Designing for explosive safety: The Explosive Components Facility at Sandia National Laboratories
[DE91-006432] N91-19103

EXPOSURE
Spaceflight performance of several types of silicon solar cells on the LIPS 3 satellite N91-19213
Microbiologically influenced corrosion in copper and nickel seawater piping systems
[AD-A229874] N91-19287

EXTERNAL TANKS
Debris/ice/TPS assessment and photographic analysis for shuttle mission STS-35
[NASA-TM-103816] N91-19118

EXTRACTION
Radar-measured height profiles of Cn(2) and turbulence dissipation rate compared with radiosonde data during October 1989 at Denver
[PB91-125500] N91-19562

EXTRATERRESTRIAL ENVIRONMENTS
Activities report of the Institute for Extraterrestrial Physics
[MPE-222] N91-19971

EXTRATERRESTRIAL MATTER
Extraterrestrial organic molecules and the emergence of life on Earth N91-19681

EXTRATERRESTRIAL RADIATION
Biological action of single accelerated heavy ions on individual yeast cells N91-19683
Predictions of cell damage rates for Lifesat missions
[NASA-TM-102170] N91-19699

EXTRUDING
Extrudable PBX molding powder
[AD-D014667] N91-19312

EYE MOVEMENTS
Ocular roll under changing z-axis acceleration and neck position N91-19580
Coordination of eye, head and arm movements in weightlessness N91-19588

F

F-18 AIRCRAFT
F-18 high alpha research vehicle surface pressures: Initial in-flight results and correlation with flow visualization and wind-tunnel data
[NASA-TM-101724] N91-19051
Summary of in-flight flow visualization obtained from the NASA high alpha research vehicle
[NASA-TM-101734] N91-19055
A simple dynamic engine model for use in a real-time aircraft simulation with thrust vectoring
[NASA-TM-4240] N91-19079
Preliminary results from an airdata enhancement algorithm with application to high-angle-of-attack flight
[NASA-TM-101737] N91-19095

FABRICATION
Graded-bandgap AlGaAs solar cells for AlGaAs/Ge cascade cells N91-19186
Tandem concentrator solar cells with 30 percent (AMO) power conversion efficiency N91-19189
Progress in GaAs/CuInSe2 tandem junction solar cells N91-19190
Key factors limiting the open circuit voltage of n(+)pp(+) indium phosphide solar cells N91-19206
Investigation of anodic and chemical oxides grown on p-type InP with applications to surface passivation for n(+)-p solar cell fabrication N91-19208
A comparative study of performance parameters of n(+)-p InP solar cells made by closed-ampoule sulfur diffusion into Cd- and Zn-doped p-type InP substrates N91-19209
Thermal cycle testing of Space Station Freedom solar array blanket coupons N91-19216
Rigid mullitewhisker felt and method of preparation
[AD-D014648] N91-19225
Concurrent micromechanical tailoring and fabrication process optimization for metal-matrix composites
[NASA-TM-103670] N91-19237
Composite materials for space applications
[NASA-CR-187472] N91-19238
Ultrafine refractory particle formation in counterflow diffusion flames
[DE91-007693] N91-19260
Hot isostatic pressing of high performance glass-ceramic to nickel- and iron-based metal components
[DE91-008130] N91-19281
Ceramic fabrication R and D
[DE91-006537] N91-19298
Assessment of tamper-revealing ceramic seals
[DE91-007793] N91-19301
Measured performance of the half-scale accurate antenna reflector
[NASA-CR-187047] N91-19350

FAIL-SAFE SYSTEMS
Pneumatic launcher
[AD-D014658] N91-19116

FAILURE
Integrated inertial/GPS N91-19032
Hypervelocity impact physics
[NASA-CR-4343] N91-19164

FAILURE ANALYSIS
Flexural testing and evaluation methods of advanced composite materials N91-19228
Mechanical behavior of a ceramic matrix composite material
[NASA-CR-187072] N91-19461
Probabilistic simulation of uncertainties in thermal structures
[NASA-TM-103680] N91-19472

FAILURE MODES
Thermal cycle testing of Space Station Freedom solar array blanket coupons N91-19216

FAR FIELDS
Using a modified Hewlett Packard 8410 network analyzer as an automated farfield antenna range receiver
[NASA-TM-103700] N91-19349
J-85 jet engine noise measured in the ONERA S1 wind tunnel and extrapolated to far field
[NASA-TP-3053] N91-19823

FAR INFRARED RADIATION
A balloon-borne 102-cm telescope for far-infrared astronomy
[NASA-CR-187778] N91-19973

FARADAY EFFECT
Elementary considerations on the gas dynamic design parameters of a MHD Faraday generator in relation to a gas turbine cycle
[LR-564] N91-19456

FAST FOURIER TRANSFORMATIONS
A finite element conjugate gradient FFT method for scattering N91-19306

FATIGUE (BIOLOGY)
Time courses of endurance performance parameters following 500 ml blood withdrawal N91-19586

FATIGUE (MATERIALS)
Bulging of fatigue cracks in a pressurized aircraft fuselage
[LR-647] N91-19094
Flexure fatigue tests for composites N91-19227
A knowledge based expert system for laminated composite strut design
[BU-410] N91-19247
Behavior of surface and corner cracks subjected to tensile and bending loads in Ti-6Al-4V alloy
[NASA-TM-102165] N91-19273
Comparison of dynamic fatigue behavior between SiC whisker-reinforced composite and monolithic silicon nitrides
[NASA-TM-103707] N91-19293
An on-line real-time system for fatigue crack growth monitoring
[DE91-007931] N91-19483
Bulging of fatigue cracks in a pressurized aircraft fuselage
[ETN-91-98927] N91-19489
Continuum damage mechanisms with an application to fatigue
[ISBN-90-9003688-1] N91-19490

FATIGUE LIFE
S87 close air support aircraft fatigue analysis
[ETN-91-98854] N91-19093
Development of a fatigue-life methodology for composite structures subjected to out-of-plane load components
[NASA-TM-102885] N91-19241
Application of thermal life prediction model to high-temperature aerospace alloys B1900+Hf and Haynes 188
[NASA-TM-4226] N91-19473

FATIGUE TESTS
Flexure fatigue tests for composites N91-19227
Flexural testing and evaluation methods of advanced composite materials N91-19228
Development of a fatigue-life methodology for composite structures subjected to out-of-plane load components
[NASA-TM-102885] N91-19241
Application of high speed photography to the study of high strain rate materials testing
[OUEL-1852/90] N91-19411
Strength test of CFRP box beam model
[NAL-TR-1057] N91-19469
FAULT TOLERANCE
Software reliability through fault-avoidance and fault-tolerance
[NASA-CR-187998] N91-19741
FEASIBILITY ANALYSIS
Project Hitch Hiker: A feasibility study for a small telecommunication satellite
[LR-644] N91-19169
Low-density, high-strength intermetallic matrix composites by XD (trademark) synthesis
[NASA-TM-103724] N91-19233
FALCON reactor-pumped laser description and program overview
[DE91-008185] N91-19431
Plasma assisted NO(x) reduction in existing coal combustors
[DE91-007380] N91-19536
Experimental reduction of simulated lunar glass by carbon and hydrogen and implications for lunar base oxygen production N91-20009
FEDERAL BUDGETS
Departments of Veterans Affairs and Housing and Urban Development, and Independent Agencies Appropriation Bill, 1991
[S-REPT-101-474] N91-19966
National Aeronautics and Space Administration N91-19967
Problems at National Aeronautics and Space Administration
[S-HRG-101-1146] N91-19969
FEEDBACK
Test analysis program evaluation: item statistics as feedback to test developers
[AD-A229851] N91-19713
FEEDBACK CIRCUITS
Alternate approach for obtaining dynamic range in monopulse guidance systems
[AD-D014644] N91-19100
FEEDBACK CONTROL
A novel potential/viscous flow coupling technique for computing helicopter flow fields
[NASA-CR-177568] N91-19060
Lag-stabilized force feedback damping
[DE91-007572] N91-19481
Microsecond-pulse Nd-glass laser with monopulse duration control N91-19811
Fiber optic feed
[AD-A229860] N91-19879
FEEDFORWARD CONTROL
Towards practical control design using neural computation
[NASA-TM-103785] N91-19766
FEMALES
Responses of women to orthostatic and exercise stresses
[NASA-TP-3043] N91-19711
FERRITES
Modeling a ferrite-tuned RF cavity
[DE91-008235] N91-19356
FERTILIZATION
Fertilization of Xenopus eggs in space N91-19624
Microgravity and development of aquatic animals N91-19625
FETUSES
Hypergravity and bone mineralization N91-19650
FIBER COMPOSITES
New computer codes for the structural analysis of composite helicopter structures
[MBB-UD-0580-90-PUB] N91-19089
Investigation of ATP blades, part 3
[DE91-750104] N91-19105
An overview of self-consistent methods for fiber-reinforced composites
[NASA-TM-103713] N91-19232
Effect of fiber reinforcements on thermo-oxidative stability and mechanical properties of polymer matrix composites
[NASA-TM-103648] N91-19234
The application of neutron diffraction time-of-flight measurements to the study of strain in composites
[DE91-008106] N91-19242
Uncertainty reasoning applied to the assessment of composite material for structural design
[BU-405] N91-19244
An expert system for laminated plate design using composite materials
[BU-406] N91-19245
A knowledge based expert system for laminated composite strut design
[BU-410] N91-19247
Mechanical behavior of a ceramic matrix composite material
[NASA-CR-187072] N91-19461
Non-homogeneous bars under tension, pure bending, and temperature loads
[MBB-UD-0572-90-PUB] N91-19485
Thermal insulation of a cryogenic tank for a space telescope using a pretensioned suspension of Fiber Reinforced Composite (FRC)
[MBB-UD-0571-90-PUB] N91-19981
FIBER OPTICS
A review of fiber optic and related technologies for environmental sensing applications
[DE91-007736] N91-19409
Optical Fiber Backscatter Signature Generator (OFBSG)
[AD-D014668] N91-19870
Fiber optic interferometric measuring method for the determination of a very small polarization coefficient
[MBB-UA-1185-90-PUB] N91-19876
Fiber optic feed
[AD-A229860] N91-19879
Study of wavelength division multiplexing as a means of increasing the number of channels in multimode fiber optic communication links N91-20024
FIBER ORIENTATION
An overview of self-consistent methods for fiber-reinforced composites
[NASA-TM-103713] N91-19232
FIBERS
Reactivity of exhausted human skeletal muscle fibers following prolonged antiorthostatic hypokinesia N91-19568
FIBROBLASTS
Human dermal fibroblast sensitivity to hypergravity N91-19630
FIELD COILS
A method for determining poloidal coil configurations for tokamak devices
[DE91-007940] N91-19903
FIELD EFFECT TRANSISTORS
Monolithic radiation hard charge sensitive preamplifier using junction field effect transistors
[DE91-008437] N91-19360
FIELD STRENGTH
Near resonant absorption by atoms in intense fluctuating fields
[DE91-007911] N91-19839
FIELD THEORY (PHYSICS)
Symmetries on the space of (2,2) superstring vacua and automorphism groups of Calabi-Yau manifolds
[DE91-008218] N91-19951
FIGHTER AIRCRAFT
S87 close air support aircraft fatigue analysis
[ETN-91-98854] N91-19093
FILAMENTS
Silver-sheathed multifilament wires
[DE91-008107] N91-19941
FINANCIAL MANAGEMENT
The impact of the new management strategy on senior operational commanders at group level within Royal Air Force Strike Command
[REPT-89SDM/MCHALE/03-MDA] N91-19954
FINITE DIFFERENCE THEORY
Electromagnetic penetration through narrow slots in conducting surfaces and coupling to structures on the shadow side
[DE91-007155] N91-19331
Very low frequency seismo-acoustic scattering from a rough seafloor
[AD-A227947] N91-19564
Anastasia: A solid model based 3D finite difference mesh generator
[DE91-007621] N91-19783
The weighted-difference form of the nodal diffusion method in cylindrical geometry
[DE91-007849] N91-19784
FINITE ELEMENT METHOD
Modal analysis of UH-60A instrumented rotor blades
[NASA-TM-4239] N91-19052
TF89 design project airbrake and arrester hook design
[ETN-91-98853] N91-19092
Flexural testing and evaluation methods of advanced composite materials N91-19228
A finite element conjugate gradient FFT method for scattering N91-19306
Vibration transmission through rolling element bearings in geared rotor systems
[NASA-CR-4334] N91-19435
Minimum-time trajectory control of a two-link flexible robotic manipulator
[DE91-001261] N91-19448
Finite element analysis of geometrically non-linear problems using a corotational large rotation formulation
[SU-ATN-9001] N91-19470
Probabilistic simulation of uncertainties in thermal structures
[NASA-TM-103680] N91-19472
Development and applications of a multi-level strain energy method for detecting finite element modeling errors
[NASA-CR-187447] N91-19478
Finite strip elements in thin plate buckling analysis
[LR-642] N91-19493
Use of system identification techniques for improving airframe finite element models using test data
[NASA-CR-188041] N91-19750
Dynamic applications of ABAQUS
[OUEL-1853/90] N91-19755
Analysis of spherical geometry finite element transport solutions in the thick diffusion limit
[DE91-007598] N91-19780
Even- and odd-parity finite-element transport solutions in the thick diffusion limit
[DE91-007618] N91-19781
Discontinuous finite-element transport solutions in the thick diffusion limit in Cartesian geometry
[DE91-007620] N91-19782
A novel isoparametric finite element displacement formulation for axisymmetric analysis of nearly incompressible materials
[OUEL-1872/91] N91-19791
Parameter estimation of structural dynamic models using Eigenvalue and Eigenvector information
[DE91-004379] N91-19793
Study of the available finite element software packages at KSC N91-20029
FINITE VOLUME METHOD
Subcycling in transient finite element analysis
[ISBN-90-9003684-9] N91-19790
FIRE POINT
A flammability study of thin plastic film materials N91-20034
FISHES
Morphological, electronmicroscopical and biochemical aspects of hyper-gravity conditions during early ontogenetic development of Cichlid fish N91-19638
FITTING
A global fit to the Z(0) line shape
[NOTA-INTERNA-966] N91-19868
FIXED WINGS
Introduction of the M-85 high-speed rotorcraft concept
[NASA-TM-102871] N91-19078
FIXTURES
Study of the available finite element software packages at KSC N91-20029
FLAGELLATA
Graviorientation in photosynthetic flagellates N91-19673
Simultaneous tracking of flagellates in real time by image analysis N91-19677
FLAMES
Basic research model of natural gas combustion in turbulent flow
[PB91-130260] N91-19264
FLAMMABILITY
A flammability study of thin plastic film materials N91-20034
FLAPPING
A flight-dynamic helicopter mathematical model with a single flap-lag-torsion main rotor
[NASA-TM-102267] N91-19041
FLAT PLATES
Development of a laser-induced heat flux technique for measurement of convective heat transfer coefficients in a supersonic flowfield
[NASA-TM-103778] N91-19063
Research on bluff-body vortex wakes
[AD-A229875] N91-19071
Wind tunnel wall effects in a linear oscillating cascade
[NASA-TM-103690] N91-19098
FLAT SURFACES
Free vibration of hexagonal panels supported at discrete points
[NASA-TM-102688] N91-19166
FLEXIBILITY
Progress in GaAs/CuInSe2 tandem junction solar cells N91-19190
FLEXIBLE SPACECRAFT
The 5th Annual NASA Spacecraft Control Laboratory Experiment (SCOLE) Workshop, part 2
[NASA-CP-10057-PT-2] N91-19122
FLEXING
Flexure fatigue tests for composites N91-19227

FLEXORS
Isokinetic force velocity and electromyographic characteristic of knee and elbow extensor and flexor muscles in the 0-g environment N91-19584
FLIGHT CHARACTERISTICS
Introduction of the M-85 high-speed rotorcraft concept [NASA-TM-102871] N91-19078
BO 108 development status and prospects [MBB-UD-0574-90-PUB] N91-19085
Space Vehicle Flight Mechanics [AGARD-AR-294] N91-19124
FLIGHT CONTROL
Integrated inertial/GPS N91-19032
Investigation of air transportation technology at Princeton University, 1989-1990 N91-19033
Dedication of National Institute for Aviation Research [NIAR-90-21] N91-19040
I'm all 'light' Jack [MBB-UD-0576-90-PUB] N91-19101
FLIGHT MANAGEMENT SYSTEMS
Space Shuttle: NASA should implement independent oversight of software development [GAO/IMTEC-91-20] N91-19119
FLIGHT MECHANICS
Space Vehicle Flight Mechanics [AGARD-AR-294] N91-19124
FLIGHT OPERATIONS
Monitoring techniques for the X-29A aircraft's high-speed rotating power takeoff shaft [NASA-TM-101731] N91-19081
Aircraft standstill, requirements for ground handling from the point of view of aircraft operation N91-19109
FLIGHT SIMULATION
Flight simulation for wind shear encounter N91-19035
Space Vehicle Flight Mechanics [AGARD-AR-294] N91-19124
FLIGHT SIMULATORS
Flight simulation for wind shear encounter N91-19035
FLIGHT TESTS
Inflight source noise of an advanced full-scale single-rotation propeller [NASA-TM-103687] N91-19045
F-18 high alpha research vehicle surface pressures: Initial in-flight results and correlation with flow visualization and wind-tunnel data [NASA-TM-101724] N91-19051
The design and flight testing of a high-performance low-cost parachute system for a 1000 lb payload [DE91-007733] N91-19065
Techniques for hot structures testing [NASA-TM-101727] N91-19080
BO 108 development status and prospects [MBB-UD-0574-90-PUB] N91-19085
Design and first tests of individual blade control actuators [MBB-UD-0577-90-PUB] N91-19087
MBB's involvement in military helicopter programmes [MBB-UD-0588-90-PUB] N91-19091
Preliminary results from an airdata enhancement algorithm with application to high-angle-of-attack flight [NASA-TM-101737] N91-19095
I'm all 'light' Jack [MBB-UD-0576-90-PUB] N91-19101
Strategy in space flight experiments N91-19220
Vibration and thermal vacuum qualification test results for a low-voltage tungsten-halogen light [NASA-CR-187050] N91-19325
Active damping application to the shuttle RMS [NASA-TM-102763] N91-19471
Real-time application of advanced three-dimensional graphic techniques for research aircraft simulation [NASA-TM-101730] N91-19742
FLOW CHARACTERISTICS
Identification of flow and volume parameters in multizone systems using a single gas tracer technique [DE91-006894] N91-19368
FLOW DISTRIBUTION
Experimental investigation of porous-floor effects on cavity flow fields at supersonic speeds [NASA-TP-3032] N91-19042
Improved visualization of flow field measurements [NASA-TM-103679] N91-19044
Unified aeroacoustics analysis for high speed turboprop aerodynamics and noise. Volume 1: Development of theory for blade loading, wakes, and noise [NASA-CR-4329] N91-19049
Summary of in-flight flow visualization obtained from the NASA high alpha research vehicle [NASA-TM-101734] N91-19055
Solar rocket plume/mirror interactions [NASA-CR-185300] N91-19059
A novel potential/viscous flow coupling technique for computing helicopter flow fields [NASA-CR-177568] N91-19060
A finite Reynolds number approach for the prediction of boundary layer receptivity in localized regions [NASA-TM-102781] N91-19061
An experimental study of the turbulent boundary layer on a transport wing in subsonic and transonic flow [NASA-TM-102206] N91-19062
Development of a laser-induced heat flux technique for measurement of convective heat transfer coefficients in a supersonic flowfield [NASA-TM-103778] N91-19063
Result of ONERA standard model test in 2m x 2m transonic wind tunnel [DE91-750115] N91-19066
The behaviour of flux-difference and flux-vector splitting methods in explicit schemes for hypersonic blunt body flow [LR-643] N91-19069
Pitot measurements in the exhaust of a cluster of four small scale supersonic nozzles [OUEL-1862/90] N91-19070
Wind tunnel wall effects in a linear oscillating cascade [NASA-TM-103690] N91-19098
High vacuum facility for hydrazine thruster testing N91-19134
Flow fields of low pressure vent exhausts N91-19135
Experimental investigation of a single flush-mounted hypermixing nozzle [NASA-TM-103726] N91-19374
A 2-D oscillating flow analysis in Stirling engine heat exchangers [NASA-TM-103781] N91-19375
Rotating pressure measurement system using an on board calibration standard [NASA-TM-103676] N91-19401
Microtube strip heat exchanger [DE91-005741] N91-19504
Unsteady blade pressure measurements for the SR-7A propeller at cruise conditions [NASA-TM-103606] N91-19825
FLOW EQUATIONS
Multigrid solution of compressible turbulent flow on unstructured meshes using a two-equation model [NASA-CR-187513] N91-19043
Heat transfer in rotating serpentine passages with trips normal to the flow [NASA-TM-103758] N91-19443
A non-linear method for the calculation of the power output of a rotating wind turbine [BU-416] N91-19512
FLOW GEOMETRY
A non-linear method for the calculation of the power output of a rotating wind turbine [BU-416] N91-19512
FLOW MEASUREMENT
Low flow vortex shedding flowmeter for hypergolics/all media N91-20036
FLOW STABILITY
Turbulent boundary layer separation over a rearward facing ramp and its control through mechanical excitation [NASA-TM-103702] N91-19370
Development of a perturbation generator for vortex stability studies [NASA-CR-188051] N91-19379
FLOW THEORY
The effect of steady aerodynamic loading on the flutter stability of turbomachinery blading [NASA-CR-187055] N91-19479
FLOW VELOCITY
Improved visualization of flow field measurements [NASA-TM-103679] N91-19044
Development of a perturbation generator for vortex stability studies [NASA-CR-188051] N91-19379
Traveling time effects in a channel flow [MPIS-10/1990] N91-19384
Calculation of pulsating liquid free jets [MPIS-15/1990] N91-19385
Laser Doppler velocimetry for continuous flow solar-pumped iodine laser system [NASA-TM-104029] N91-19415
Heat transport during gas tungsten arc welding [ETN-91-98919] N91-19455
FLOW VISUALIZATION
Improved visualization of flow field measurements [NASA-TM-103679] N91-19044
Summary of in-flight flow visualization obtained from the NASA high alpha research vehicle [NASA-TM-101734] N91-19055
Pitot measurements in the exhaust of a cluster of four small scale supersonic nozzles [OUEL-1862/90] N91-19070
FLOWMETERS
Laser Doppler velocimetry for continuous flow solar-pumped iodine laser system [NASA-TM-104029] N91-19415
Low flow vortex shedding flowmeter for hypergolics/all media N91-20036
FLUCTUATION THEORY
Quantum fluctuations in laser with intracavity frequency doubling N91-19805
FLUENCE
GaP betavoltaic cells as a power source N91-19211
FLUID DYNAMICS
Systems near the onset and in the well-developed regimes of turbulence [DE91-008148] N91-19382
Contributions to the Non Equilibrium Molecular Dynamics (NEMD) computer simulation for transport processes in simple fluids [ETN-91-98921] N91-19393
Three-dimensional computed tomography from interferometric measurements within a narrow cone of views [NASA-TM-103257] N91-19404
Impact processes in the Solar System: New understandings through numerical modeling N91-19996
FLUID FILMS
Two reference time scales for studying the dynamic cavitation of liquid films [NASA-TM-103673] N91-19369
FLUID FLOW
Numerical and physical modelling of bubbly flow phenomena [DE91-007461] N91-19377
A numerical method for solving steady 2D and axisymmetrical viscoelastic flow problems with an application to inertia effects in contraction flows [MEMT-11] N91-19394
Lessons learned from the design and operation of steam generators for high temperature gas-cooled reactors [DE91-006139] N91-19450
The study of effects of small perturbations on chaotic systems [DE91-007320] N91-19792
Modeling of flow systems for implementation under KATE N91-20038
FLUID INJECTION
DHE (Downhole Heat Exchangers) [DE91-006620] N91-19509
FLUID JETS
Cryogenic liquid-jet breakup in two-fluid atomizers [NASA-TM-103734] N91-19402
FLUID MANAGEMENT
Modeling of flow systems for implementation under KATE N91-20038
FLUID MECHANICS
A summary of existing and planned experiment hardware for low-gravity fluids research [NASA-TM-103706] N91-19371
FLUID POWER
Methods for combining a theoretical and an empirical approach in modelling pressure and flow control valves for CAE-programs for fluid power circuits [ACTA-POLYTEC-SCAND-ME-96] N91-19392
FLUID PRESSURE
Gravity dependence of pleural liquid turnover N91-19651
FLUORESCENCE
Fluorescent lifetime measurements of rare Earth elements in gallium arsenide [AD-A229865] N91-19265
Near resonant absorption by atoms in intense fluctuating fields [DE91-007911] N91-19839
FLUTTER
The effect of steady aerodynamic loading on the flutter stability of turbomachinery blading [NASA-CR-187055] N91-19479
Constructing mathematical model of adaptive anti-flutter system N91-19810
FLUTTER ANALYSIS
Cascade flutter analysis with transient response aerodynamics [NASA-TM-103746] N91-19475
FLUX VECTOR SPLITTING
The behaviour of flux-difference and flux-vector splitting methods in explicit schemes for hypersonic blunt body flow [LR-643] N91-19069
FLYBY MISSIONS
Lunar maria and related deposits: Preliminary Galileo imaging results N91-20000
Orientale and South Pole-Aitken basins on the Moon: Preliminary Galileo imaging results N91-20002
Triton: A hot potato N91-20005
FOAMS
Thermal properties of polyisocyanurate foam board insulation blown with CFC-11 substitutes [DE90-016047] N91-19240
The mechanical behavior of microcellular foams [DE91-006775] N91-19291

FOCAL PLANE DEVICES
A balloon-borne 102-cm telescope for far-infrared astronomy
[NASA-CR-187778] N91-19973
FOCUSING
Aerodynamic focusing of particles and heavy molecules
[DE91-006922] N91-19833
The specification of glancing incidence mirrors in terms of system performance
[DE91-007564] N91-19874
FOOD PRODUCTION (IN SPACE)
Plant production as part of a Controlled Ecological Life Support System (CELSS) N91-19656
A ground based module for experimentations of cultivations and recycling in a closed environment N91-19657
Physiological criteria and requirement of biomass production under controlled ecological life support systems N91-19659
Productivity and photosynthesis of selected crop plants under orbital light conditions: An approach to solar powered CELSS N91-19662
Carbon dioxide and water exchange of a soybean stand grown in the biomass production chamber N91-20026
FORCED VIBRATION
A gradient microphone for locating sound targets
[MBB-Z-0341-90-PUB] N91-19829
FOREARM
Carotid-cardiac baroreflex influence on forearm vascular resistance during low level LBNP N91-20030
FOREBODIES
F-18 high alpha research vehicle surface pressures: Initial in-flight results and correlation with flow visualization and wind-tunnel data
[NASA-TM-101724] N91-19051
FORECASTING
Key issues in space nuclear power
[NASA-TM-103656] N91-19179
FOREST FIRES
Rocket-triggered lightning strikes and forest fire ignition N91-20027
FORESTS
Throughfall and foliar extraction
[DE91-007184] N91-19535
FORM FACTORS
Variational Monte Carlo studies of electromagnetic structure of few-body nuclei
[DE91-007756] N91-19838
FORMING TECHNIQUES
Extrudable PBX molding powder
[AD-D014667] N91-19312
FORTRAN
ARCHY (analysis and reverse engineering of code using hierarchy and Yourdon): A tool for FORTRAN code maintenance and development
[DE91-007241] N91-19720
FOSSIL FUELS
The dilemma of fossil fuel use and global climate change
[DE91-007859] N91-19533
FOURIER TRANSFORMATION
Remote detection of organics using Fourier transform infrared spectroscopy
[DE91-006045] N91-19253
The evolution and limits of spectral bandwidth in free electron lasers
[DE91-007737] N91-19425
FRACTOGRAPHY
Comparison of dynamic fatigue behavior between SiC whisker-reinforced composite and monolithic silicon nitrides
[NASA-TM-103707] N91-19293
Crack opening stress measurements of surface cracks in 7075-T6 Al alloy plate specimens through electron fractography
[LR-641] N91-19492
FRACTURE MECHANICS
S87 close air support aircraft fatigue analysis
[ETN-91-98854] N91-19093
An evaluation of the fatigue crack growth and fracture toughness properties of beryllium-copper alloy CDA172
[NASA-TM-102166] N91-19274
Performance of underwater weldments
[PB91-129254] N91-19452
The method of lines in analyzing solids containing cracks
[NASA-TM-103626] N91-19477
Nonlinear analysis and redesign of the mixed-mode bending delamination test
[NASA-TM-102777] N91-19482
FRACTURE STRENGTH
Flexural testing and evaluation methods of advanced composite materials N91-19228
Behavior of surface and corner cracks subjected to tensile and bending loads in Ti-6Al-4V alloy
[NASA-TM-102165] N91-19273
An evaluation of the fatigue crack growth and fracture toughness properties of beryllium-copper alloy CDA172
[NASA-TM-102166] N91-19274
Comparison of dynamic fatigue behavior between SiC whisker-reinforced composite and monolithic silicon nitrides
[NASA-TM-103707] N91-19293
Performance of underwater weldments
[PB91-129254] N91-19452
The method of lines in analyzing solids containing cracks
[NASA-TM-103626] N91-19477
Nonlinear analysis and redesign of the mixed-mode bending delamination test
[NASA-TM-102777] N91-19482
FRACTURING
The correlation of transient crack growth under small-scale-creep conditions N91-19467
FRAGMENTATION
Impact processes in the Solar System: New understandings through numerical modeling N91-19996
FREDHOLM EQUATIONS
Boundary integral equations and the Dirichlet problem
[DE91-004537] N91-19779
FREE ELECTRON LASERS
A program of high power microwave source research and development from 8 GHz to 600 GHz
[DE91-008320] N91-19358
Intense microwave generation using free-electron lasers
[DE91-007262] N91-19417
Simulation of a standing-wave free-electron laser
[DE91-007330] N91-19418
Proceedings of the Workshop Prospects for a 1 Angstrom Free-Electron Laser
[DE91-007631] N91-19422
Theory of the ion-channel laser
[DE91-007643] N91-19423
The evolution and limits of spectral bandwidth in free electron lasers
[DE91-007737] N91-19425
Hole coupling resonator for free electron lasers
[DE91-007745] N91-19426
Phase stability of a standing-wave free-electron laser
[DE91-008068] N91-19427
Summary of the working group on transverse emissions from photocathodes
[DE91-008414] N91-19432
Possibility of raising efficiency of free-electron laser in longitudinal magnetic field N91-19804
Development of high current electron source using photoemission from metals with ultrashort laser pulses
[DE91-008438] N91-19850
FREE ENERGY
Free energy simulation of grain boundary segregation the thermodynamics in Ni(3-x)Al(1+x)
[DE91-007473] N91-19928
FREE FLOW
Free wake analysis of hover performance using a new influence coefficient method
[NASA-CR-4309] N91-19050
A new methodology for free wake analysis using curved vortex elements
[NASA-CR-3958] N91-19067
Free flow electrophoresis experiment TEPE 3 on Texus 24
[MBB-UO-0130-90-PUB] N91-19321
The effect of small streamwise velocity distortion on the boundary layer flow over a thin flat plate with application to boundary layer stability theory
[NASA-TM-103668] N91-19372
Free flow electrophoresis experiment TEPE 3 on TEXUS 24 N91-19654
FREE JETS
Calculation of pulsating liquid free jets
[MPIS-15/1990] N91-19385
FREE RADICALS
Plasma assisted NO(x) reduction in existing coal combustors
[DE91-007380] N91-19536
FREE VIBRATION
Free vibration of hexagonal panels supported at discrete points
[NASA-TM-102688] N91-19166
FREEZING
Cool-down and frozen start-up behavior of a grooved water heat pipe
[NASA-CR-187053] N91-19376
FRENCH SPACE PROGRAM
The biological and medical programme of the manned Aragatz mission on the Mir Space Station N91-19617
FREQUENCIES
Method for making holograms with coherent radiation from a stabilized laser diode that has been actively cooled
[AD-D014673] N91-19396
FREQUENCY ASSIGNMENT
The provision of circuits to outside broadcast locations using spectrum within the UHF broadcasting bands
[BBC-RD-1990/12] N91-19329
FREQUENCY MODULATION
The evolution and limits of spectral bandwidth in free electron lasers
[DE91-007737] N91-19425
FREQUENCY MULTIPLIERS
Quantum fluctuations in laser with intracavity frequency doubling N91-19805
FRESNEL LENSES
Mini-dome Fresnel lens photovoltaic concentrator development N91-19219
FRICTION
Considerations relating to pulsed-beam modification of materials
[DE91-006771] N91-19922
FRICTION REDUCTION
Tribological properties of Ag/Ti films on Al2O3 ceramic substrates
[NASA-TM-103784] N91-19224
FROGS
Morphological, electronmicroscopical and biochemical aspects of hyper-gravity conditions during early ontogenetic development of Cichlid fish N91-19638
FRUITS
Genetic risk and physiological stress induced by heavy ions N91-19680
Defective embryogenesis of Arabidopsis induced by cosmic HZE-particles N91-19682
FUEL CAPSULES
Rayleigh-Taylor instability in LIB ICF N91-19883
FUEL CELL POWER PLANTS
Methanol reformers for fuel cell powered vehicles: Some design considerations
[DE91-006465] N91-19314
FUEL CELLS
Methanol reformers for fuel cell powered vehicles: Some design considerations
[DE91-006465] N91-19314
Molten carbonate fuel cell technology improvement
[DE91-005540] N91-19505
Thermal-hydraulic model of a solid-oxide fuel cell
[DE91-006393] N91-19507
FUEL COMBUSTION
Basic research model of natural gas combustion in turbulent flow
[PB91-130260] N91-19264
Oxygen-enriched diesel engine performance: A comparison of analytical and experimental results
[DE91-006491] N91-19440
Evaluation of significant anthropogenic sources of radiatively important trace gases
[PB91-127753] N91-19545
FUEL CONSUMPTION
Cycling space ship transportation device for continuous link between Earth and Mars
[ILR-MITT-247(1990)] N91-19121
FUEL SPRAYS
LOX/hydrogen coaxial injector atomization test program
[NASA-CR-187037] N91-19117
Cryogenic liquid-jet breakup in two-fluid atomizers
[NASA-TM-103734] N91-19402
FUEL SYSTEMS
Correlation of leak rates of various fluids with the leak rate of an inert gas in the same configuration N91-20033
FUMIGATION
Analysis of high frequency surface-induced concentration fluctuations
[DE91-007561] N91-19538
FUNCTIONAL DESIGN SPECIFICATIONS
Phase equilibrium modeling for high temperature metallization on GaAs solar cells N91-19192
The Advanced Photovoltaic Solar Array (APSA) technology status and performance N91-19217
System description document for the Anthrobot-2: A dexterous robot hand
[NASA-TM-104535] N91-19449
Centrifuge Facility Conceptual System Study. Volume 1: Facility overview and habitats
[NASA-TM-102860] N91-19566
FUNCTIONS
C-statistic fitting routines: User's manual and reference guide
[NASA-CR-187992] N91-19736

FUNGI
Responses of Physarum polycephalum to varying light levels during fast clinostat rotation: A scientific preparation of an ESA biorack experiment during the IML-1 mission N91-19676
Gravitaxis in Physarum polycephalum N91-19678
FUSELAGES
Bulging of fatigue cracks in a pressurized aircraft fuselage
[LR-647] N91-19094
Bulging of fatigue cracks in a pressurized aircraft fuselage
[ETN-91-98927] N91-19489
Design and testing of a circumferential and longitudinal joint of the A320 fuselage section 13/14 in GLARE
[LR-645] N91-19494
FUSES (ORDNANCE)
Wire-free arming system for an aircraft-delivered bomb
[AD-D014611] N91-19076
FUSION REACTORS
Development of KrF lasers for inertial confinement fusion
[DE91-007349] N91-19419
Energy sciences supercomputing 1990
[DE91-007188] N91-19740
US-Japan workshops: Q-111, Development of Plasma Facing Components and Materials for Next Large Fusion Devices, and Q-112, Vacuum and First Wall Technology for Fusion Devices
[DE91-006879] N91-19896
Summary of the International Dawson Symposium on The Physics of Plasmas
[DE91-006912] N91-19897
Introduction to fusion
[DE91-744831] N91-19912
FUZZY SETS
The development of structure for the representation and manipulation of sophisticated knowledge in intelligent systems
[AD-A229114] N91-19957

G

GADOLINIUM
Electron temperature of Gd plasma produced by laser resonance ionization
[DE91-744833] N91-19913
GALACTIC CLUSTERS
Thermal instabilities in cooling flows: The evolution of nearly spherical perturbations
[MPE-PREPRINT-176] N91-19365
GALACTIC COSMIC RAYS
Cosmic ray charged component variations at sea level
[DE91-615480] N91-20021
GALACTIC EVOLUTION
High energy physics and cosmology
[DE91-007369] N91-19859
Statistics of peaks in cosmological nonlinear density fields
[DE91-744972] N91-19990
GALACTIC STRUCTURE
Proceedings of the symposium Astrophysical Processes and Structures in the Universe
[PB91-123653] N91-19993
Proceedings of 146th IAU Symposium on Dynamics of Galaxies and Molecular Cloud Distribution
[PB91-123661] N91-19994
GALAXIES
Origin of regularities in the redshift distributions of distant galaxies and quasars
[DE91-007889] N91-19986
Proceedings of 146th IAU Symposium on Dynamics of Galaxies and Molecular Cloud Distribution
[PB91-123661] N91-19994
GALILEO SPACECRAFT
Lunar maria and related deposits: Preliminary Galileo imaging results N91-20000
Orientale and South Pole-Aitken basins on the Moon: Preliminary Galileo imaging results N91-20002
GALLIUM ARSENIDE LASERS
Coherent effects in generation of ultrashort light pulses by semiconductor injection laser N91-19820
GALLIUM ARSENIDES
Progress toward the development of dual junction GaAs/Ge solar cells N91-19184
Status of GaAs/Ge solar cells N91-19185
Graded-bandgap AlGaAs solar cells for AlGaAs/Ge cascade cells N91-19186
Progress in GaAs/CuInSe2 tandem junction solar cells N91-19190
Phase equilibrium modeling for high temperature metallization on GaAs solar cells N91-19192
GaAs solar cell photoresponse modeling using PC-1D V2.1 N91-19193
High-efficiency, radiation-resistant GaAs space cells N91-19194
Thermal annealing of GaAs concentrator solar cells N91-19195
Burst annealing of high temperature GaAs solar cells N91-19196
Effects of proton irradiation on the performance of InP/GaAs solar cells N91-19205
Fluorescent lifetime measurements of rare Earth elements in gallium arsenide
[AD-A229865] N91-19265
Ellipsometric study of InGaAs MODFET material
[NASA-TM-103286] N91-19351
Thin film reactions on alloy semiconductor substrates
[DE91-007651] N91-19931
Study of InGaAs based MODFET structures using variable angle spectroscopic ellipsometry
[NASA-TM-103792] N91-19935
GALLIUM PHOSPHIDES
Surface chemistry at semiconductor-electrolyte interfaces
[DE91-005915] N91-19920
GAMETOCYTES
Unicellular algae in space. 2: Sounding-rocket experiment N91-19640
GAMMA RAY ASTRONOMY
Gamma ray astronomy
[NASA-CR-188031] N91-19980
GAMMA RAY BURSTS
Gamma ray astronomy
[NASA-CR-188031] N91-19980
GAMMA RAY OBSERVATORY
Gamma ray astronomy
[NASA-CR-188031] N91-19980
GAMMA RAYS
Some limitations of detailed balance for inverse reaction calculations in the astrophysical P-process
[DE91-007258] N91-19983
GARNETS
Intracavity second-harmonic generation by laser with optical delay line and mode locking N91-19808
GAS CHROMATOGRAPHY
Finnigan ion trap mass spectrometer detection limits and thermal energy analyzer interface status report and present capabilities
[DE91-006220] N91-19254
GAS DETECTORS
Low level vapor verification of monomethyl hydrazine N91-20032
GAS DISSOCIATION
Intense field non-resonant multiphoton absorption of diatomic molecules
[DE91-006920] N91-19835
GAS DYNAMICS
Correlation of leak rates of various fluids with the leak rate of an inert gas in the same configuration N91-20033
GAS EVOLUTION
Gas entrapment and evolution in aluminium alloys produced by powder metallurgy
[ETN-91-98918] N91-19285
GAS EXCHANGE
Effects of short-lasting weightlessness on gas exchange during light exercise N91-19573
Carbon dioxide and water exchange of a soybean stand grown in the biomass production chamber N91-20026
GAS EXPANSION
Notes on the unsteady rectilinear motion of a perfect gas. 10: On the influence of gravity upon the expansion of an ideal gas with gamma = 3
[LR-640] N91-19395
GAS FLOW
The behaviour of flux-difference and flux-vector splitting methods in explicit schemes for hypersonic blunt body flow
[LR-643] N91-19069
Two-dimensional non-reacting jet-gas mixing in an MHD (magnetohydrodynamic) second stage combustor
[DE91-006015] N91-19252
Basic research model of natural gas combustion in turbulent flow
[PB91-130260] N91-19264
Cryogenic liquid-jet breakup in two-fluid atomizers
[NASA-TM-103734] N91-19402
Heat transport during gas tungsten arc welding
[ETN-91-98919] N91-19455
GAS GENERATORS
The selection of convertible engines with current gas generator technology for high speed rotorcraft
[NASA-TM-103774] N91-19097
Lessons learned from the design and operation of steam generators for high temperature gas-cooled reactors
[DE91-006139] N91-19450
GAS IONIZATION
Studies of atmospheric molecules by multiphoton spectroscopy
[DE91-006738] N91-19554
GAS LASERS
Investigation at two wavelengths of a modulated He-Xe rare gas laser
[AD-A229852] N91-19434
GAS PRESSURE
A test fixture for measuring high-temperature hypersonic-engine seal performance
[NASA-TM-103658] N91-19442
GAS TUNGSTEN ARC WELDING
Heat transport during gas tungsten arc welding
[ETN-91-98919] N91-19455
GAS TURBINE ENGINES
Rapid mix concepts for low emission combustors in gas turbine engines
[NASA-CR-185292] N91-19048
The application of aero gas turbine engine monitoring systems to military aircraft
[ETN-91-98852] N91-19096
GAS TURBINES
Elementary considerations on the gas dynamic design parameters of a MHD Faraday generator in relation to a gas turbine cycle
[LR-564] N91-19456
GASEOUS DIFFUSION
Synthesis and analysis of novel polymers with potential for providing both high permselectivity and permeability in gas separation applications
[DE91-008283] N91-19309
GASES
Vascular gas bubbles or decompression sickness: What is the proper endpoint for evaluating decompression procedures N91-19590
GAUGE INVARIANCE
How many times do we have in quantum gravity
[DE91-744973] N91-19991
GAUGE THEORY
Energy sciences supercomputing 1990
[DE91-007188] N91-19740
GEAR TEETH
Local synthesis and tooth contact analysis of face-milled spiral bevel gears
[NASA-CR-4342] N91-19439
GEARS
Life and dynamic capacity modeling for aircraft transmissions
[NASA-CR-4341] N91-19438
Local synthesis and tooth contact analysis of face-milled spiral bevel gears
[NASA-CR-4342] N91-19439
The selection of window functions for the calculation of time domain averages on the vibration of the individual gears in an epicyclic gearbox
[OUEL-1818/90] N91-19457
GELLED ROCKET PROPELLANTS
Advanced chemical propulsion at NASA Lewis: Metallized and high energy density propellants
[NASA-TM-103771] N91-19175
GELS
Gelcast zirconia-alumina composites
[DE91-007835] N91-19239
Advanced sequencing technology
[DE91-008031] N91-19706
GENE EXPRESSION
Advanced sequencing technology
[DE91-008031] N91-19706
GENETIC ENGINEERING
Electrofusion and regeneration of protoplasts from sunflower (Helianthus annuus L.) N91-19675
Characterization of a defective interfering RNA that contains a mosaic of a plant viral genome
[DE91-007897] N91-19702
Characterization of a defective interfering RNA that contains a mosaic of a plant viral genome
[DE91-007898] N91-19703
GENETICS
Genetic risk and physiological stress induced by heavy ions N91-19680
Defective embryogenesis of Arabidopsis induced by cosmic HZE-particles N91-19682
Characterization of a defective interfering RNA that contains a mosaic of a plant viral genome
[DE91-007897] N91-19702
Characterization of a defective interfering RNA that contains a mosaic of a plant viral genome
[DE91-007898] N91-19703
Physiological genetics of denitrification: A route to conserving fixed nitrogen
[DE91-008157] N91-19707
GEOCHRONOLOGY
Relative chronology of Martian volcanoes N91-20007

GEODESIC LINES
Visual navigation around curved obstacles
[OUEL-1861/90] N91-19458
GEODETIC ACCURACY
Method for determining astronomic azimuth
[AD-D014677] N91-19972
GEODYNAMICS
Solid earth science in the 1990s. Volume 1: Program plan
[NASA-TM-4256-VOL-1] N91-19499
GEOGRAPHIC INFORMATION SYSTEMS
Environmental Sciences Division computing and geographic information system facility user handbook
[DE91-007820] N91-19961
GEOLOGY
Solid earth science in the 1990s. Volume 1: Program plan
[NASA-TM-4256-VOL-1] N91-19499
DHE (Downhole Heat Exchangers)
[DE91-006620] N91-19509
An evaluation of co-planar lineament analysis and some thoughts on using surface geological data to predict sub-surface geology
[DE90-009687] N91-19556
GEOMAGNETISM
On the joint inversion of geophysical data for models of the coupled core-mantle system
[NASA-TM-104536] N91-19557
Solar-geophysical data Number 554, October 1990. Part 1 (prompt reports): Data for September, August 1990, and late data. Explanation of data reports issued as Number 515 (supplement) July 1987
[PB91-124594] N91-20018
GEOMETRICAL THEORY OF DIFFRACTION
Task reports on developing techniques for scattering by 3D composite structures and to generate new solutions in diffraction theory using higher order boundary conditions
[NASA-CR-188057] N91-19305
Analytical solutions with Generalized Impedance Boundary Conditions (GIBC) N91-19307
GEOMORPHOLOGY
Magellan: Preliminary description of Venus surface geologic units N91-20011
GEOPHYSICS
Ozone measurements from the NOAA-9 and the Nimbus-7 satellites: Implications of short and long term variabilities N91-19527
On the joint inversion of geophysical data for models of the coupled core-mantle system
[NASA-TM-104536] N91-19557
Solar-geophysical data Number 554, October 1990. Part 2 (comprehensive reports): Data for April 1990 and miscellaneous. Explanation of data reports issued as Number 515 (supplement) July 1987
[PB91-124586] N91-20017
Solar-geophysical data Number 554, October 1990. Part 1 (prompt reports): Data for September, August 1990, and late data. Explanation of data reports issued as Number 515 (supplement) July 1987
[PB91-124594] N91-20018
GEOPOTENTIAL
Solid earth science in the 1990s. Volume 1: Program plan
[NASA-TM-4256-VOL-1] N91-19499
GEOSYNCHRONOUS ORBITS
Space simulation test for thermal control materials N91-19149
GEOTHERMAL ENERGY CONVERSION
The National Energy Strategy: The role of geothermal technology development. Proceedings
[DE91-004623] N91-19503
GEOTHERMAL ENERGY EXTRACTION
The National Energy Strategy: The role of geothermal technology development. Proceedings
[DE91-004623] N91-19503
GEOTHERMAL ENERGY UTILIZATION
The National Energy Strategy: The role of geothermal technology development. Proceedings
[DE91-004623] N91-19503
GEOTHERMAL RESOURCES
The National Energy Strategy: The role of geothermal technology development. Proceedings
[DE91-004623] N91-19503
GEOTHERMAL TECHNOLOGY
The National Energy Strategy: The role of geothermal technology development. Proceedings
[DE91-004623] N91-19503
DHE (Downhole Heat Exchangers)
[DE91-006620] N91-19509
GERMAN SPACE PROGRAM
Space research for the sake of all
[ETN-91-98807] N91-19113
Free flow electrophoresis experiment TEPE 3 on Texus 24
[MBB-UO-0130-90-PUB] N91-19321
GERMANIDES
In situ TEM studies of the growth of strained Si(1-x)Ge(x) by solid phase epitaxy
[DE91-007278] N91-19926
GERMANIUM
Progress toward the development of dual junction GaAs/Ge solar cells N91-19184
Status of GaAs/Ge solar cells N91-19185
GERMANIUM ALLOYS
Some roles for TEM in the development of new materials
[DE91-007742] N91-19933
GERMINATION
Genetic risk and physiological stress induced by heavy ions N91-19680
GET AWAY SPECIALS (STS)
Development of a miniature biology facility N91-19666
GEYSERS
Triton: A hot potato N91-20005
GLASS
Hot isostatic pressing of high performance glass-ceramic to nickel- and iron-based metal components
[DE91-008130] N91-19281
Crystallization and properties of Sr-Ba aluminosilicate glass-ceramic matrices
[NASA-TM-103764] N91-19308
Experimental reduction of simulated lunar glass by carbon and hydrogen and implications for lunar base oxygen production N91-20009
GLASS FIBERS
Method of producing glass fiber with cores of a different material
[AD-D014664] N91-19288
Design and testing of a circumferential and longitudinal joint of the A320 fuselage section 13/14 in GLARE
[LR-645] N91-19494
GLASS LASERS
Microsecond-pulse Nd-glass laser with monopulse duration control N91-19811
GLIDING
Laws of heat transfer in three-dimensional viscous shock layer of stream flowing past blunt bodies at some angles of attack and glide N91-19801
GLOBAL POSITIONING SYSTEM
Investigation of air transportation technology at Ohio University, 1989-1990 N91-19028
Ridge regression signal processing N91-19029
Modeling selective availability of the NAVSTAR global positioning system N91-19030
Integrated inertial/GPS N91-19032
Aircraft standstill, requirements for ground handling from the point of view of aircraft operation N91-19109
A flight experiment to determine GPS photochemical contamination accumulation rates N91-19159
Method for determining astronomic azimuth
[AD-D014677] N91-19972
GLOBAL WARMING
Global change: What you can do
[S-HRG-101-1160] N91-19528
The dilemma of fossil fuel use and global climate change
[DE91-007859] N91-19533
Thermohaline circulations and global climate change
[DE91-007458] N91-19537
Statistical examination of climatological data relevant to global temperature variation
[DE91-007881] N91-19540
GLOW DISCHARGES
Screening volatile organics by direct sampling ion trap and glow discharge mass spectrometry
[DE91-007708] N91-19258
GLUCOSIDES
Regeneration and characterization of protoplast-derived cell lines from Digitalis lanata EHRH. and Digitalis purpurea L. suspension cultures after electrofusion under microgravity conditions N91-19652
GOALS
An approach for configuring space photovoltaic tandem arrays based on cell layer performance N91-19197
GOLD ALLOYS
X ray determination of site occupation parameters in ordered ternaries Cu(Au(x)M(1-x))M = Ni,Pd
[DE91-007861] N91-19937
GOLD COATINGS
Application of non-cyanide gold for selective plating of microelectronic circuits
[DE91-007729] N91-19276
GOVERNMENTS
US technology policy: Executive Office of the President
[PB91-119677] N91-19970
GRADIENTS
A gradient microphone for locating sound targets
[MBB-Z-0341-90-PUB] N91-19829
GRAIN BOUNDARIES
The correlation of transient crack growth under small-scale-creep conditions N91-19467
Free energy simulation of grain boundary segregation the thermodynamics in Ni(3-x)Al(1+x)
[DE91-007473] N91-19928
GRAPH THEORY
Efficient connecting networks using directed links
[ETN-91-98855] N91-19762
GRAPHITE
Instellar grains within interstellar grains N91-19998
GRAPHITE-EPOXY COMPOSITES
Monitoring techniques for the X-29A aircraft's high-speed rotating power takeoff shaft
[NASA-TM-101731] N91-19081
A study on prediction of life due to creep behavior in CF/EPOXY and CF/PEEK laminates N91-19226
Probabilistic micromechanics and macromechanics of polymer matrix composites
[NASA-TM-103669] N91-19236
GRAPHS (CHARTS)
Real-time application of advanced three-dimensional graphic techniques for research aircraft simulation
[NASA-TM-101730] N91-19742
GRATINGS (SPECTRA)
Characteristics of excimer laser with narrow emission line N91-19807
Nonlinear optic effects in liquid crystals
[ETN-91-98923] N91-19878
GRAVIRECEPTORS
Gravitation receptor reaction in response to effect of acceleration N91-19569
Graviperception in plants N91-19667
GRAVITATION
Gravity perception by non-specialized structures N91-19636
How many times do we have in quantum gravity
[DE91-744973] N91-19991
GRAVITATIONAL COLLAPSE
Sixquarks in neutron stars
[DE91-615472] N91-19987
GRAVITATIONAL EFFECTS
Multi-dimensional modeling of a thermal energy storage canister
[NASA-TM-103731] N91-19177
Free flow electrophoresis experiment TEPE 3 on Texus 24
[MBB-UO-0130-90-PUB] N91-19321
Development of a vibration isolation prototype system for microgravity space experiments
[NASA-TM-103664] N91-19324
Notes on the unsteady rectilinear motion of a perfect gas. 10: On the influence of gravity upon the expansion of an ideal gas with gamma = 3
[LR-640] N91-19395
Effects of short-lasting weightlessness on gas exchange during light exercise N91-19573
Blood pressure regulation in parabolic flight N91-19575
Vestibular function in altered states of gravity N91-19579
Determinants of spatial orientation in weightlessness N91-19605
Gravity effects on cells N91-19618
Developmental biology and microgravity N91-19622
Epidermal growth factor induced signal transduction in A431 cells is influenced by altered gravity conditions N91-19623
Fertilization of Xenopus eggs in space N91-19624
Effect of hyper-gravity on the swimming behavior of aquatic vertebrates N91-19626
Altered cartilage differentiation in tibial epiphyseal plates of Cosmos rats N91-19628
Effect of the centrifuge forces on pregnant rats N91-19629
Human dermal fibroblast sensitivity to hypergravity N91-19630
Cellular functions of Paramecium under different gravity conditions N91-19631
Growth rate of bacteria without and with antibiotic at different levels of gravity N91-19632
Microgravity, hypergravity, and aging: A unifying hypothesis N91-19633
Does gravity play a role in the morphological development and function of the gravity sensory organ of vertebrates. DLR contribution to the D-2 project graviperception and neuronal plasticity, its technical realization and experimental execution N91-19635
Gravity perception by non-specialized structures N91-19636
An assay for bone cell differentiation in vitro as a tool for microgravity studies in space N91-19637
Morphological, electronmicroscopical and biochemical aspects of hyper-gravity conditions during early ontogenetic development of Cichlid fish N91-19638

Unicellular algae in space. 1: Preparatory tests N91-19639
Unicellular algae in space. 2: Sounding-rocket experiment N91-19640
Unicellular algae in space. 3: Addendum N91-19641
Human and animal results on vestibular research in space: VERIS N91-19642
Bone adaptation to real and simulated microgravity N91-19643
Blood pressure maturation curve in normotensive rats during growth in simulated microgravitational environment N91-19644
Adaptive responses in monkeys during two week space flight N91-19645
Contractile protein changes induced by hindlimb suspension in rat skeletal muscle N91-19646
The slow-rotating centrifuge microscope (NIZEMI): A new research tool for terrestrial and space-related gravitational biology N91-19663
Effect of gravity on the distribution of electron dense chromatin in the nucleus of root statocytes N91-19672
Graviorientation in photosynthetic flagellates N91-19673
Plant protoplast development on Biokosmos 9 N91-19674
Electrofusion and regeneration of protoplasts from sunflower (Helianthus annuus L.) N91-19675
Simultaneous tracking of flagellates in real time by image analysis N91-19677
Gravitaxis in Physarum polycephalum N91-19678
The reference systems for tactile perception and for the orientation with respect to body N91-19691
Mental rotation of three-dimensional shapes in microgravity N91-19694
Predictions of cell damage rates for Lifesat missions [NASA-TM-102170] N91-19699

GRAVITATIONAL FIELDS
Notes on the unsteady rectilinear motion of a perfect gas. 10: On the influence of gravity upon the expansion of an ideal gas with gamma = 3 [LR-640] N91-19395
Baroelectric effect in the present of gravitational forces [DE91-615469] N91-19559
Quasi-nonlinear theory of cosmological self-gravitating systems [DE91-744971] N91-19989

GRAVITATIONAL LENSES
Gravitational lens effect of wall-like objects and its cosmological implications [DE91-744976] N91-19992

GRAVITATIONAL PHYSIOLOGY
Gravitation receptor reaction in response to effect of acceleration N91-19569
Microgravity and development of aquatic animals N91-19625
Preliminary study of a membrane bioreactor for cell culture in space N91-19627
Preliminary studies before defining a payload adapted to the primate model N91-19648
Hypergravity and bone mineralization N91-19650
Gravity dependence of pleural liquid turnover N91-19651
The slow-rotating centrifuge microscope (NIZEMI): A new research tool for terrestrial and space-related gravitational biology N91-19663
Development of a miniature biology facility N91-19666
Graviperception in plants N91-19667
Plastids and gravity perception N91-19668
Gravitational effects on subcellular structures of plant cells N91-19669
Plant development in space: Observations on root formation and growth N91-19670
Plant growth under microgravity conditions: Experiments and problems N91-19671
The 1989-1990 NASA space biology accomplishments [NASA-TM-4258] N91-19697

GRAVITROPISM
Plastids and gravity perception N91-19668

GRAZING INCIDENCE
The specification of glancing incidence mirrors in terms of system performance [DE91-007556] N91-19873
The specification of glancing incidence mirrors in terms of system performance [DE91-007564] N91-19874

GREENHOUSE EFFECT
Natural and anthropogenic climate change [DE91-007363] N91-19532
The dilemma of fossil fuel use and global climate change [DE91-007859] N91-19533
Thermohaline circulations and global climate change [DE91-007458] N91-19537
Monitoring the response of the upper troposphere/lower stratosphere to a greenhouse gas scenario [DE91-007976] N91-19541
Evaluation of significant anthropogenic sources of radiatively important trace gases [PB91-127753] N91-19545

GRID GENERATION (MATHEMATICS)
Implementation of control point form of algebraic grid-generation technique [NASA-TM-103748] N91-19054
Anastasia: A solid model based 3D finite difference mesh generator [DE91-007621] N91-19783

GROUND BASED CONTROL
Airport system technical aspects N91-19107

GROUND HANDLING
Aircraft standstill, requirements for ground handling from the point of view of aircraft operation N91-19109

GROUND OPERATIONAL SUPPORT SYSTEM
Monitoring techniques for the X-29A aircraft's high-speed rotating power takeoff shaft [NASA-TM-101731] N91-19081

GROUND STATE
Variational Monte Carlo calculations of nuclear ground states [DE91-007760] N91-19842

GROUND SUPPORT EQUIPMENT
Airport apron research and development [MBB-Z-0168-90-PUB] N91-19106
Engineering monitoring expert system's developer [NASA-CR-187914] N91-19765
An expansion plan for the 60 Hz power distribution system at KSC: LC-39 substations load allocation plan N91-20028

GROUND TESTS
Control and mechanism interaction for ground-based testing of space structures N91-19125

GROUND WATER
Mechanisms controlling the production and transport of methane, carbon dioxide, and dissolved solutes within a large boreal peat basin [DE91-008115] N91-19543
What were the effects of the formation of the Borealis basin, Mars N91-20014

GROUP DYNAMICS
Report of a workshop on Distributed Decision Making [LC-89-64440] N91-19952

GROUP THEORY
Approximation properties of wavelet transforms [ETN-91-98922] N91-19799
Symmetries on the space of (2,2) superstring vacua and automorphism groups of Calabi-Yau manifolds [DE91-008218] N91-19951

GROWTH
Plant protoplast development on Biokosmos 9 N91-19674

GUIDANCE (MOTION)
Joint University Program for Air Transportation Research, 1989-1990 [NASA-CP-3095] N91-19024
Alternate approach for obtaining dynamic range in monopulse guidance systems [AD-D014644] N91-19100

GUIDE VANES
Turbulent boundary layer separation over a rearward facing ramp and its control through mechanical excitation [NASA-TM-103702] N91-19370

GUINEA PIGS
Gravitation receptor reaction in response to effect of acceleration N91-19569

GULF OF ALASKA
Outer continental shelf environmental assessment program, volume 70 [PB91-129288] N91-19548

GUN PROPELLANTS
Launching projectiles with hydrogen gas generated from titanium-water reactions [AD-D014653] N91-19171

GUNS (ORDNANCE)
Effects of hyperbaric oxygenation on central hemodynamics and oxygen consumption in severe physical trauma N91-19570

GUST LOADS
Acoustic radiation from lifting airfoils in compressible subsonic flow [NASA-TM-103650] N91-19053

GYROFREQUENCY
Tokamak ignition projections from dimensionally similar discharges [DE91-008195] N91-19908

H

H I REGIONS
High resolution infrared astronomy satellite observations of a selected spiral galaxy [NASA-CR-188019] N91-19975

H II REGIONS
High resolution infrared astronomy satellite observations of a selected spiral galaxy [NASA-CR-188019] N91-19975

H LINES
Fluorescent HD emission from photodissociation regions [MPE-PREPRINT-177] N91-19982

HABITATS
Centrifuge Facility Conceptual System Study. Volume 1: Facility overview and habitats [NASA-TM-102860] N91-19566

HADRONS
Punchthrough in hadronic showers: A parameterization of the total probability [NOTA-INTERNA-968] N91-19854

HALF PLANES
Elementary pulse diffraction problems and the generation of sound by a dipole moving across the edge of a half-plane [LR-565] N91-19831

HALOGENS
Vibration and thermal vacuum qualification test results for a low-voltage tungsten-halogen light [NASA-CR-187050] N91-19325

HAMILTON-JACOBI EQUATION
Invariant tori of the Poincare return map as solutions of functional difference equations [DE91-007423] N91-19777
Computation of invariant tori in 2 (1/2) degrees of freedom [DE91-007424] N91-19778

HAMILTONIAN FUNCTIONS
Theoretical investigation of phase stability in non-magnetic Fe-V substitutional alloys [DE91-006711] N91-19268
Invariant tori of the Poincare return map as solutions of functional difference equations [DE91-007423] N91-19777
Computation of invariant tori in 2 (1/2) degrees of freedom [DE91-007424] N91-19778
Action principles for the Vlasov equation: Four old, one new [DE91-008177] N91-19787
Quantum optics reveals the nature of superconductivity [TR-69] N91-19946

HANDBOOKS
Spaceflight performance of several types of silicon solar cells on the LIPS 3 satellite N91-19213
Proposed draft military handbook presenting requirements for an Electronic Display System (EDS) for Interactive Electronic Technical Manuals (IETMs) [AD-A227471] N91-19342

HARDNESS
Considerations relating to pulsed-beam modification of materials [DE91-006771] N91-19922

HARDWARE
A summary of existing and planned experiment hardware for low-gravity fluids research [NASA-TM-103706] N91-19371

HARMONIC EXCITATION
Liquid sloshing response in a spinning container due to pitching excitation [LRT-WE-9-FB-11(1990)] N91-19388

HARMONIC GENERATIONS
Intracavity second-harmonic generation by laser with optical delay line and mode locking N91-19808
Design considerations for multi component molecular-polymeric nonlinear optical materials [DE91-006778] N91-19872

HARMONIC OSCILLATION
Wind tunnel wall effects in a linear oscillating cascade [NASA-TM-103690] N91-19098

HARMONICS
Higher harmonics of magnetization in the critical state of ceramic high Tc superconductors [DE91-615506] N91-19944

HEAD (ANATOMY)
Multiple energy computed tomography for neuroradiology with monochromatic x rays from the national synchrotron light source [DE91-008108] N91-19712

HEAD DOWN TILT
Effect of running and head down tilt bedrest on lymphocyte reactivity N91-19598

Assessment of bone turnover in humans after space flight and hypokinesia N91-19608
Head-down tilt test and space-related endocrine physiology N91-19614

HEAD MOVEMENT
Coordination of eye, head and arm movements in weightlessness N91-19588

HEART RATE
Ultrasound investigation of the cardiovascular system during the 25-days Soviet-French flight: Cardiac aspects N91-19578

HEAT BALANCE
Thermal balance testing of the Anik-E spacecraft N91-19131

HEAT EXCHANGERS
High temperature tensile properties of nickel-base superalloys for intermediate heat exchangers of high temperature gas-cooled reactors [DE91-744958] N91-19284
A 2-D oscillating flow analysis in Stirling engine heat exchangers [NASA-TM-103781] N91-19375
Microtube strip heat exchanger [DE91-005741] N91-19504
DHE (Downhole Heat Exchangers) [DE91-006620] N91-19509

HEAT FLUX
Development of a laser-induced heat flux technique for measurement of convective heat transfer coefficients in a supersonic flowfield [NASA-TM-103778] N91-19063
Thermal balance testing of the Anik-E spacecraft N91-19131
Systems near the onset and in the well-developed regimes of turbulence [DE91-008148] N91-19382

HEAT MEASUREMENT
Development of a laser-induced heat flux technique for measurement of convective heat transfer coefficients in a supersonic flowfield [NASA-TM-103778] N91-19063
Heat transport during gas tungsten arc welding [ETN-91-98919] N91-19455

HEAT PIPES
Cool-down and frozen start-up behavior of a grooved water heat pipe [NASA-CR-187053] N91-19376

HEAT PUMPS
Loss analysis of the thermodynamic cycle of magnetic heat pumps [DE91-007669] N91-19950

HEAT RESISTANT ALLOYS
High temperature tensile properties of nickel-base superalloys for intermediate heat exchangers of high temperature gas-cooled reactors [DE91-744958] N91-19284
Application of thermal life prediction model to high-temperature aerospace alloys B1900+Hf and Haynes 188 [NASA-TM-4226] N91-19473

HEAT SHIELDING
The test facility requirements for the thermal vacuum thermal balance test of the Cosmic Background Explorer Observatory N91-19128
Composite flexible insulation for thermal protection of space vehicles [NASA-TM-103836] N91-19304

HEAT SOURCES
Radioisotope thermal photovoltaic application of the GaSb solar cell N91-19210
Triton: A hot potato N91-20005

HEAT STORAGE
Multi-dimensional modeling of a thermal energy storage canister [NASA-TM-103731] N91-19177

HEAT TRANSFER
The performance of multilayer insulation in a rapidly depressurizing environment N91-19133
Experimental determination of satellite bolted joints thermal resistance N91-19157
Multi-dimensional modeling of a thermal energy storage canister [NASA-TM-103731] N91-19177
Oxygen-enriched diesel engine performance: A comparison of analytical and experimental results [DE91-006491] N91-19440
Heat transport during gas tungsten arc welding [ETN-91-98919] N91-19455
Results of scoping tests for open-cycle OTEC (Ocean Thermal Energy Conversion) components operating with seawater [DE89-009514] N91-19501
Thermal-hydraulic model of a solid-oxide fuel cell [DE91-006393] N91-19507
The design of future central receiver power plants based on lessons learned from the Solar One Pilot Plant [DE91-005224] N91-19510
Laws of heat transfer in three-dimensional viscous shock layer of stream flowing past blunt bodies at some angles of attack and glide N91-19801

HEAT TRANSFER COEFFICIENTS
Development of a laser-induced heat flux technique for measurement of convective heat transfer coefficients in a supersonic flowfield [NASA-TM-103778] N91-19063

HEAT TRANSMISSION
DHE (Downhole Heat Exchangers) [DE91-006620] N91-19509
New method for edge plasma control by RF ponderomotive force [DE91-744823] N91-19911

HEAT TREATMENT
Semiconductor structural damage attendant to contact formation in III-V solar cells N91-19203
Rigid mullitewhisker felt and method of preparation [AD-D014648] N91-19225
Crystallization and properties of Sr-Ba aluminosilicate glass-ceramic matrices [NASA-TM-103764] N91-19308

HEATING
Effects of atmosphere and heating rate during processing of a ceramic superconductor [DE91-007761] N91-19299

HEAVY IONS
Genetic risk and physiological stress induced by heavy ions N91-19680
Defective embryogenesis of Arabidopsis induced by cosmic HZE-particles N91-19682
Biological action of single accelerated heavy ions on individual yeast cells N91-19683
Arabidopsis thaliana (Heynh.) pollen: A new tool in heavy ions radiation N91-19685
Summary of discussions at the HIGH p (sub T) session [DE91-008196] N91-19848
Application of MeV ions to the analysis and modification of high temperature superconducting materials [DE91-007317] N91-19927

HELICAL FLOW
Relaxed states with plasma flow [DE91-008199] N91-19909

HELICOPTER CONTROL
Development of bearingless tail rotors [MBB-UD-0575-90-PUB] N91-19086
Design and first tests of individual blade control actuators [MBB-UD-0577-90-PUB] N91-19087
I'm all 'light' Jack [MBB-UD-0576-90-PUB] N91-19101

HELICOPTER DESIGN
BO 108 development status and prospects [MBB-UD-0574-90-PUB] N91-19085
Crashworthiness investigations in the preliminary design phase of the NH90 [MBB-UD-0579-90-PUB] N91-19088
New computer codes for the structural analysis of composite helicopter structures [MBB-UD-0580-90-PUB] N91-19089
System design for the Tiger helicopter [MBB-UD-0581-90-PUB] N91-19090
Noise level reduction inside helicopter cabins [MBB-UD-0578-90-PUB] N91-19828

HELICOPTER PERFORMANCE
Free wake analysis of hover performance using a new influence coefficient method [NASA-CR-4309] N91-19050
BO 108 development status and prospects [MBB-UD-0574-90-PUB] N91-19085

HELICOPTER TAIL ROTORS
Development of bearingless tail rotors [MBB-UD-0575-90-PUB] N91-19086
Design and first tests of individual blade control actuators [MBB-UD-0577-90-PUB] N91-19087

HELICOPTER WAKES
Free wake analysis of hover performance using a new influence coefficient method [NASA-CR-4309] N91-19050
A new methodology for free wake analysis using curved vortex elements [NASA-CR-3958] N91-19067

HELICOPTERS
A flight-dynamic helicopter mathematical model with a single flap-lag-torsion main rotor [NASA-TM-102267] N91-19041
Ongoing development of a computer jobstream to predict helicopter main rotor performance in icing conditions [NASA-CR-187076] N91-19056
A novel potential/viscous flow coupling technique for computing helicopter flow fields [NASA-CR-177568] N91-19060
Introduction of the M-85 high-speed rotorcraft concept [NASA-TM-102871] N91-19078
BO 108 development status and prospects [MBB-UD-0574-90-PUB] N91-19085
System design for the Tiger helicopter [MBB-UD-0581-90-PUB] N91-19090
I'm all 'light' Jack [MBB-UD-0576-90-PUB] N91-19101

HELIUM
Noble gas disk MHD generator performance with unstable nonequilibrium plasma [ISBN-90-9003671-7] N91-19916

HELIUM ISOTOPES
Effects of radiolytic tritium decay on the thermodynamic behavior of LaNi(4.25)Al(0.75) tritides [DE91-007961] N91-19277
Superconducting instrumentation for critical He-4 measurements in space [DE91-007894] N91-19408
Reflections on some problems concerning the role of superfluid turbulence in the propagation of second-sound pulses in He 2 [MPIS-8/1990] N91-19827
Ultrasonic investigations on superfluid He-3-A and He-3-B [ISBN-952-90-2241-7] N91-19830
Variational Monte Carlo studies of electromagnetic structure of few-body nuclei [DE91-007756] N91-19838
The physics of laser polarized muonic atoms [DE91-008045] N91-19845
Exchange currents in low-energy nucleon capture by He3 [ETN-91-98917] N91-19855

HELIUM-NEON LASERS
Laser Doppler velocimetry for continuous flow solar-pumped iodine laser system [NASA-TM-104029] N91-19415
He-Ne laser emitting five lines simultaneously N91-19813

HELMHOLTZ RESONATORS
Noise level reduction inside helicopter cabins [MBB-UD-0578-90-PUB] N91-19828

HELMHOLTZ VORTICITY EQUATION
Examinations of inverse scattering problem for the scalar Helmholtz equation in the field of first order approximations for potentials with compact supports and safe real wave numbers [ETN-91-98949] N91-19339

HEMODYNAMIC RESPONSES
Effects of hyperbaric oxygenation on central hemodynamics and oxygen consumption in severe physical trauma N91-19570

HEMODYNAMICS
Influence on natriuresis of prolonged (12 h) water immersion on central hemodynamics and endocrine elements in humans N91-19612

HETEROJUNCTIONS
Coherent effects in generation of ultrashort light pulses by semiconductor injection laser N91-19820

HEURISTIC METHODS
Investigation of air transportation technology at Princeton University, 1989-1990 N91-19033
Practical path planning among movable obstacles [DE91-000034] N91-19768

HIERARCHIES
ARCHY (analysis and reverse engineering of code using hierarchy and Yourdon): A tool for FORTRAN code maintenance and development [DE91-007241] N91-19720
Design and implementation of an image understanding system: DADS [ETN-91-98926] N91-19773

HIGH CURRENT
Development of high current electron source using photoemission from metals with ultrashort laser pulses [DE91-008438] N91-19850

HIGH ENERGY INTERACTIONS
Large-scale computing in the energy research programs [DE91-007907] N91-19748
Electron transfer, ionization, and excitation in atomic collisions [DE91-008044] N91-19844
Summary of discussions at the HIGH p (sub T) session [DE91-008196] N91-19848
High energy physics and cosmology [DE91-007369] N91-19859

HIGH ENERGY PROPELLANTS
Advanced chemical propulsion at NASA Lewis: Metallized and high energy density propellants [NASA-TM-103771] N91-19175

HIGH FREQUENCIES
High power, high frequency lasertron RF sources
[DE91-006007] N91-19414
Analysis of high frequency surface-induced concentration fluctuations
[DE91-007561] N91-19538
A study of alkaline element interferences in analytical inductively coupled plasmas
[ISAL-90-0069] N91-19915
HIGH GRAVITY ENVIRONMENTS
Effect of hyper-gravity on the swimming behavior of aquatic vertebrates N91-19626
Human dermal fibroblast sensitivity to hypergravity N91-19630
Cellular functions of Paramecium under different gravity conditions N91-19631
Growth rate of bacteria without and with antibiotic at different levels of gravity N91-19632
Microgravity, hypergravity, and aging: A unifying hypothesis N91-19633
Increased mitogenic response in lymphocytes from chronically centrifuged mice N91-19634
Morphological, electronmicroscopical and biochemical aspects of hyper-gravity conditions during early ontogenetic development of Cichlid fish N91-19638
Hypergravity and bone mineralization N91-19650
Pupil size in parabolic flight N91-19693
HIGH LEVEL LANGUAGES
Formal proof of the AVM-1 microprocessor using the concept of generic interpreters
[NASA-CR-187491] N91-19756
HIGH POWER LASERS
FALCON reactor-pumped laser description and program overview
[DE91-008185] N91-19431
Copper vapor as active medium for high-power oscillator-amplifier laser systems N91-19806
HIGH PRESSURE OXYGEN
Orbital transfer vehicle oxygen turbopump technology. Volume 1: Design, fabrication, and hydrostatic bearing testing
[NASA-CR-185175] N91-19174
HIGH RESOLUTION
Focusing infrared laser beams on targets in space without using adaptive optics
[DE91-007518] N91-19421
High resolution microstructural and microchemical analysis of zirconia eutectic interfaces
[DE91-008032] N91-19940
High resolution infrared astronomy satellite observations of a selected spiral galaxy
[NASA-CR-188019] N91-19975
HIGH REYNOLDS NUMBER
Critical-layer nonlinearity in the resonance growth of three-dimensional waves in boundary layers
[NASA-TM-103639] N91-19373
HIGH SPEED
Unified aeroacoustics analysis for high speed turboprop aerodynamics and noise. Volume 1: Development of theory for blade loading, wakes, and noise
[NASA-CR-4329] N91-19049
Introduction of the M-85 high-speed rotorcraft concept
[NASA-TM-102871] N91-19078
Monitoring techniques for the X-29A aircraft's high-speed rotating power takeoff shaft
[NASA-TM-101731] N91-19081
The selection of convertible engines with current gas generator technology for high speed rotorcraft
[NASA-TM-103774] N91-19097
Digital optical computers at the optoelectronic computing systems center
[NASA-CR-187520] N91-19345
HIGH SPEED PHOTOGRAPHY
Debris/ice/TPS assessment and photographic analysis for shuttle mission STS-35
[NASA-TM-103816] N91-19118
Application of high speed photography to the study of high strain rate materials testing
[OUEL-1852/90] N91-19411
HIGH STRENGTH ALLOYS
Hot isostatic pressing of high performance glass-ceramic to nickel- and iron-based metal components
[DE91-008130] N91-19281
HIGH TEMPERATURE
Phase equilibrium modeling for high temperature metallization on GaAs solar cells N91-19192
Burst annealing of high temperature GaAs solar cells N91-19196
Theoretical investigation of phase stability in non-magnetic Fe-V substitutional alloys
[DE91-006711] N91-19268
High temperature tensile properties of nickel-base superalloys for intermediate heat exchangers of high temperature gas-cooled reactors
[DE91-744958] N91-19284
Nickel-like x ray lasers
[DE91-008502] N91-19433
A test fixture for measuring high-temperature hypersonic-engine seal performance
[NASA-TM-103658] N91-19442
NDE standards for high temperature materials
[NASA-TM-103761] N91-19464
Texture and microstructure development in Al-2 percent Mg during high-temperature deformation
[DE91-007355] N91-19480
Effects of high temperature and humidity on mental state and metabolism N91-19571
HIGH TEMPERATURE GAS COOLED REACTORS
High temperature tensile properties of nickel-base superalloys for intermediate heat exchangers of high temperature gas-cooled reactors
[DE91-744958] N91-19284
Lessons learned from the design and operation of steam generators for high temperature gas-cooled reactors
[DE91-006139] N91-19450
HIGH TEMPERATURE PLASMAS
Measurements of stark-broadening in hot dense plasma
[DE91-008504] N91-19910
HIGH TEMPERATURE SUPERCONDUCTORS
Effects of atmosphere and heating rate during processing of a ceramic superconductor
[DE91-007761] N91-19299
Property and microstructural nonuniformity in the yttrium-barium-copper-oxide superconductor determined from electrical, magnetic, and ultrasonic measurements
[NASA-TM-103732] N91-19463
Origin of residual surface resistance of ceramic high-temperature superconductors N91-19814
Phenomenological theory of phase transitions to nonhomogeneous noncommensurate phase with superconducting current N91-19817
Thermal conductivity of high-temperature superconductors in normal state N91-19818
Activities report of the Istituto Elettrotecnico Nazionale Galileo Ferraris
[ETN-91-98868] N91-19822
Application of MeV ions to the analysis and modification of high temperature superconducting materials
[DE91-007317] N91-19927
Silver-sheathed multifilament wires
[DE91-008107] N91-19941
Phase formation in the Tl-Ca-BaCu-O system
[DE91-008184] N91-19942
Higher harmonics of magnetization in the critical state of ceramic high Tc superconductors
[DE91-615506] N91-19944
Magnetism and superconductivity in YBa2Cu3O(6+x) at 0.3 less than or equal to x less than or equal to 0.4
[DE91-615507] N91-19945
Classical and quantum charge dynamics in small tunnel junctions
[ETN-91-98916] N91-19947
Loss analysis of the thermodynamic cycle of magnetic heat pumps
[DE91-007669] N91-19950
HIGH TEMPERATURE TESTS
Techniques for hot structures testing
[NASA-TM-101727] N91-19080
HIGH VOLTAGES
Electromagnetic compatibility in high-voltage engineering
[ISBN-90-9002929-X] N91-19337
HISTOCHEMICAL ANALYSIS
Reactivity of exhausted human skeletal muscle fibers following prolonged antiorthostatic hypokinesia N91-19568
HISTORIES
Responses of women to orthostatic and exercise stresses
[NASA-TP-3043] N91-19711
HOLOGRAPHY
Method for making holograms with coherent radiation from a stabilized laser diode that has been actively cooled
[AD-D014673] N91-19396
Three-dimensional computed tomography from interferometric measurements within a narrow cone of views
[NASA-TM-103257] N91-19404
Nickel-like x ray lasers
[DE91-008502] N91-19433
HOMEOSTASIS
Physiology of body water and salt regulation. Part 2: Volume and electrolyte homeostasis after an acute saline infusion N91-19593
HOOKS
TF89 design project airbrake and arrester hook design
[ETN-91-98853] N91-19092
HORMONES
Physiology of body water and salt regulation. Part 2: Volume and electrolyte homeostasis after an acute saline infusion N91-19593
The biochemical and physiological variables in motion sickness followed modified neuroendocrine activity N91-19607
Influence on natriuresis of prolonged (12 h) water immersion on central hemodynamics and endocrine elements in humans N91-19612
Volume regulating hormones, fluid and electrolyte modifications during the Aragatz Mission (Mir station) N91-19689
HOT ISOSTATIC PRESSING
Hot isostatic pressing of high performance glass-ceramic to nickel- and iron-based metal components
[DE91-008130] N91-19281
Crystallization and properties of Sr-Ba aluminosilicate glass-ceramic matrices
[NASA-TM-103764] N91-19308
HOVERING
Introduction of the M-85 high-speed rotorcraft concept
[NASA-TM-102871] N91-19078
Euler solutions to nonlinear acoustics of non-lifting hovering rotor blades
[NASA-TM-103837] N91-19826
HOVERING STABILITY
Free wake analysis of hover performance using a new influence coefficient method
[NASA-CR-4309] N91-19050
HTPB PROPELLANTS
Solid fuel combustion chamber
[LR-648] N91-19222
HUBBLE SPACE TELESCOPE
Hubble Space Telescope secondary mirror vertex radius/conic constant test
[NASA-CR-187989] N91-19871
Hubble Space Telescope and the space shuttle problems
[S-HRG-101-1087] N91-19974
Hubble Space Telescope observations of Mars N91-20003
HUMAN BEHAVIOR
Simulating motivated cognition
[NASA-TM-102886] N91-19770
HUMAN BEINGS
Reactivity of exhausted human skeletal muscle fibers following prolonged antiorthostatic hypokinesia N91-19568
Effects of high temperature and humidity on mental state and metabolism N91-19571
Human and animal results on vestibular research in space: VERIS N91-19642
HUMAN FACTORS ENGINEERING
Automatic speech recognition in air traffic control: A human factors perspective N91-19025
Skeletal adaptation in altered gravity environments N91-19603
Army-NASA aircrew/aircraft integration program (A3I) software detailed design document, phase 3
[NASA-CR-177557] N91-19714
HUMAN PERFORMANCE
Test analysis program evaluation: Item statistics as feedback to test developers
[AD-A229851] N91-19713
Army-NASA aircrew/aircraft integration program (A3I) software detailed design document, phase 3
[NASA-CR-177557] N91-19714
HUMAN REACTIONS
Report of a workshop on Distributed Decision Making
[LC-89-64440] N91-19952
HUMIDITY
Effects of high temperature and humidity on mental state and metabolism N91-19571
HURRICANES
World weather watch: Regional association 4: Hurricane operational plan, supplement 2
[WMO-524-SUPPL-2] N91-19563
HYDRAULIC CONTROL
Methods for combining a theoretical and an empirical approach in modelling pressure and flow control valves for CAE-programs for fluid power circuits
[ACTA-POLYTEC-SCAND-ME-96] N91-19392
HYDRAZINE ENGINES
High vacuum facility for hydrazine thruster testing N91-19134
HYDROCARBON COMBUSTION
Studies of combustion kinetics and mechanisms
[DE91-007829] N91-19259
HYDRODYNAMICS
Conservation of energy, momentum, and angular momentum in Lagrangian staggered-grid hydrodynamics
[DE91-008059] N91-19381
Wavelets and turbulence on the sea surface
[AD-A229862] N91-19565

Optically-ionized plasma recombination x ray lasers
[DE91-007261] N91-19898
Effects of a giant impact on Uranus N91-20012

HYDROELASTICITY
Experimental studies on a nonlinear hydroelastic vibration of circular cylindrical tanks
[LRT-WE-9-FB-10(1990)] N91-19387

HYDROGEN
Orbital transfer vehicle oxygen turbopump technology. Volume 1: Design, fabrication, and hydrostatic bearing testing
[NASA-CR-185175] N91-19174
Comprehensive mechanisms for combustion chemistry: An experimental and numerical study with emphasis on applied sensitivity analysis
[DE91-008030] N91-19262
Hydrogen storage in metal hydrides
[DE91-746267] N91-19316
Atomic beam studies of the interaction of hydrogen with transition metal surfaces
[DE91-007938] N91-19841

HYDROGEN ATOMS
Cross section for production of excited hydrogen atoms following dissociative excitation of molecular hydrogen by electron impact
[DE91-745035] N91-19852

HYDROGEN EMBRITTLEMENT
The 70 percent tungsten heavy alloys: Processing and properties
[DE91-008259] N91-19282

HYDROGEN ISOTOPES
Variational Monte Carlo studies of electromagnetic structure of few-body nuclei
[DE91-007756] N91-19838
Investigation of condensed matter fusion
[DE91-007246] N91-19923
Stable hydrogen and carbon isotope ratios of extractable hydrocarbons in the Murchison meteorite N91-20006

HYDROGEN PRODUCTION
Launching projectiles with hydrogen gas generated from titanium-water reactions
[AD-D014653] N91-19171

HYDROGENATION
Annealing characteristics of irradiated hydrogenated amorphous silicon solar cells N91-19214
Control of catalytic hydrotreating selectivity with ammonia
[DE91-005511] N91-19250
Chemical approaches to carbon dioxide utilization for manned Mars missions
[NASA-TM-103728] N91-20015

HYDROLOGY
Natural and anthropogenic climate change
[DE91-007363] N91-19532

HYDROTHERMAL SYSTEMS
The National Energy Strategy: The role of geothermal technology development. Proceedings
[DE91-004623] N91-19503

HYDROXYL COMPOUNDS
Reduced lymphocyte activation in space: Role of cell-substratum interactions N91-19621
Regeneration and characterization of protoplast-derived cell lines from Digitalis lanata EHRH. and Digitalis purpurea L. suspension cultures after electrofusion under microgravity conditions N91-19652

HYPERCUBE MULTIPROCESSORS
DEMO 89: The initial experiment with the HERMIES-3 robot
[DE90-017765] N91-19447
Complete exchange on the iPSC-860
[NASA-CR-187498] N91-19715
Multiphase complete exchange on a circuit switched hypercube
[NASA-CR-187499] N91-19716

HYPERFINE STRUCTURE
Research conducted at the Radiation Lab, Notre Dame Univ.
[DE91-007969] N91-19843

HYPERGOLIC ROCKET PROPELLANTS
Low flow vortex shedding flowmeter for hypergolics/all media N91-20036

HYPERSONIC FLIGHT
Space Vehicle Flight Mechanics
[AGARD-AR-294] N91-19124

HYPERSONIC FLOW
The behaviour of flux-difference and flux-vector splitting methods in explicit schemes for hypersonic blunt body flow
[LR-643] N91-19069

HYPERSONIC VEHICLES
Single-strain-gage force/stiffness buckling prediction techniques on a hat-stiffened panel
[NASA-TM-101733] N91-19077
High temperature NASP engine seal development
[NASA-TM-103716] N91-19441

HYPERSONICS
A test fixture for measuring high-temperature hypersonic-engine seal performance
[NASA-TM-103658] N91-19442

HYPERVELOCITY IMPACT
Hypervelocity impact physics
[NASA-CR-4343] N91-19164
Space debris: Orbital microparticulates impacting LDEF experiments favour a natural extraterrestrial origin N91-20008

HYPOKINESIA
Reactivity of exhausted human skeletal muscle fibers following prolonged antiorthostatic hypokinesia N91-19568
Assessment of bone turnover in humans after space flight and hypokinesia N91-19608
Bone adaptation to real and simulated microgravity N91-19643

HYPOVOLEMIA
Ultrasound investigation of the cardiovascular system during the 25 days French-Soviet spaceflight (26 November - 21 December 1988) N91-19577
Ultrasound investigation of the cardiovascular system during the 25-days Soviet-French flight: Cardiac aspects N91-19578

HYPOXIA
Subcellular signal transduction systems in the cellular trauma of ischemia
[AD-A229876] N91-19709

I

ICE
Debris/ice/TPS assessment and photographic analysis for shuttle mission STS-35
[NASA-TM-103816] N91-19118

ICE FORMATION
Icing characteristics of a natural-laminar-flow, a medium-speed, and a swept, medium-speed airfoil
[NASA-TM-103693] N91-19046
Prediction of ice shapes and their effect on airfoil performance
[NASA-TM-103701] N91-19047
Ongoing development of a computer jobstream to predict helicopter main rotor performance in icing conditions
[NASA-CR-187076] N91-19056
Automatic control study of the icing research tunnel refrigeration system
[NASA-TM-4257] N91-19115

IDEAL GAS
Notes on the unsteady rectilinear motion of a perfect gas. 10: On the influence of gravity upon the expansion of an ideal gas with gamma = 3
[LR-640] N91-19395

IGNEOUS ROCKS
K/T age for the popigai impact event N91-19999

IGNITION
High vacuum facility for hydrazine thruster testing N91-19134
High power arcjet
[NASA-CR-187986] N91-19173
Tokamak ignition projections from dimensionally similar discharges
[DE91-008195] N91-19908

IMAGE ANALYSIS
Application of high speed photography to the study of high strain rate materials testing
[OUEL-1852/90] N91-19411
Simultaneous tracking of flagellates in real time by image analysis N91-19677
Biological action of single accelerated heavy ions on individual yeast cells N91-19683
Design and implementation of an image understanding system: DADS
[ETN-91-98926] N91-19773

IMAGE CONTRAST
Radar backscatter from the sea controlled experiments
[AD-A229847] N91-19340

IMAGE ENHANCEMENT
Research on advanced NDE methods for aerospace structures
[AD-A226858] N91-19460

IMAGE PROCESSING
Improved visualization of flow field measurements
[NASA-TM-103679] N91-19044
Research on advanced NDE methods for aerospace structures
[AD-A226858] N91-19460
Design, implementation and evaluation of new fully automated algorithms for the extraction of cardiac parameters from 3D, 2D and M-mode echocardiograms N91-19582
Mental rotation of three-dimensional shapes in microgravity N91-19694
A haptic system for a multifingered hand
[DE90-017044] N91-19767
Design and implementation of an image understanding system: DADS
[ETN-91-98926] N91-19773

IMAGES
SIGNIF and GENFMT, SAS macros for computing and reporting significant digits
[DE91-007702] N91-19795
Indium tin oxide for solid-state image sensors
[ETN-91-98932] N91-19949

IMAGING TECHNIQUES
Focusing infrared laser beams on targets in space without using adaptive optics
[DE91-007518] N91-19421
Laser Tracker 2: Sandia National Laboratories' second generation laser tracking system
[DE91-007711] N91-19424
Research on advanced NDE methods for aerospace structures
[AD-A226858] N91-19460
Lunar maria and related deposits: Preliminary Galileo imaging results N91-20000
Orientale and South Pole-Aitken basins on the Moon: Preliminary Galileo imaging results N91-20002

IMIDES
Late transition metal (mu)-oxo and (mu)-imido complexes
[DE91-005349] N91-19267

IMMUNITY
Reduced lymphocyte activation in space: Role of cell-substratum interactions N91-19621

IMMUNOLOGY
Cosmos: 1989 immunology studies
[NASA-CR-188046] N91-19701
Research in radiobiology: Work in progress in immunobiology of experimental host-tumor relationships
[DE91-007936] N91-19705

IMPACT STRENGTH
Investigation of ATP blades, part 3
[DE91-750104] N91-19105

IMPACT TESTS
Investigation of ATP blades, part 3
[DE91-750104] N91-19105

IMPEDANCE
Theoretical study of plasma focus diode N91-19887

IMPEDANCE MEASUREMENT
Visualisation of fluid shifts within the body during a parabolic flight by measurements of electrical bio-impedance N91-19688

IMPINGEMENT
Icing characteristics of a natural-laminar-flow, a medium-speed, and a swept, medium-speed airfoil
[NASA-TM-103693] N91-19046

IMPLOSIONS
Rayleigh-Taylor instability in LIB ICF N91-19883

IMPULSE GENERATORS
Wire-free arming system for an aircraft-delivered bomb
[AD-D014611] N91-19076

IMPURITIES
Parallel processing for a 1-D time-dependent solution to impurity rate equations for fusion plasma simulations
[DE90-015857] N91-19759
Effect of paramagnetic impurities on dynamics of magnetic fluxes in superconductors N91-19816
Plasma boundary experiments on D3-D tokamak
[DE91-002429] N91-19881

INCOMPRESSIBILITY
A novel isoparametric finite element displacement formulation for axisymmetric analysis of nearly incompressible materials
[OUEL-1872/91] N91-19791

INCOMPRESSIBLE FLUIDS
Response of a solidly rotating amphora-type liquid column to axial excitation
[LRT-WE-9-FB-06(1990)] N91-19386
A numerical method for solving steady 2D and axisymmetrical viscoelastic flow problems with an application to inertia effects in contraction flows
[MEMT-11] N91-19394

INDEXES (DOCUMENTATION)
Improved syntactic disambiguation in the FASIT automatic indexing environment N91-19956
NASA Thesaurus supplement: A four part cumulative supplement to the 1988 edition of the NASA Thesaurus (supplement 5)
[NASA-SP-7064-SUPPL-5] N91-19962

INDIUM
Recent advances in the ITO/InP solar cell N91-19202

INDIUM ALLOYS
Indium tin oxide for solid-state image sensors
[ETN-91-98932] N91-19949

INDIUM ARSENIDES
Ellipsometric study of InGaAs MODFET material
[NASA-TM-103286] N91-19351
Thin film reactions on alloy semiconductor substrates
[DE91-007651] N91-19931
Study of InGaAs based MODFET structures using variable angle spectroscopic ellipsometry
[NASA-TM-103792] N91-19935
INDIUM PHOSPHIDES
Recent advances in the ITO/InP solar cell N91-19202
The effect of process conditions on the performance of epitaxial InP solar cells N91-19204
Effects of proton irradiation on the performance of InP/GaAs solar cells N91-19205
Key factors limiting the open circuit voltage of n(+)pp(+) indium phosphide solar cells N91-19206
Determination of series resistance of indium phosphide solar cells N91-19207
Indium phosphide solar cells N91-19221
Effect of dislocations on the open-circuit voltage, short-circuit current and efficiency of heteroepitaxial indium phosphide solar cells
[NASA-TM-103762] N91-19354
INELASTIC SCATTERING
Summary of discussions at the HIGH p (sub T) session
[DE91-008196] N91-19848
INERTIAL CONFINEMENT FUSION
Development of KrF lasers for inertial confinement fusion
[DE91-007349] N91-19419
Upgrade of the LLNL Nova laser for inertial confinement fusion
[DE91-008060] N91-19430
Symposium on Development of Intensed Pulsed Particle Beams and Its Applications
[NIFS-PROC-5] N91-19882
Rayleigh-Taylor instability in LIB ICF N91-19883
Two-stage ion diode experiments on induction adder N91-19884
Power plant by LIB fusion N91-19892
INERTIAL NAVIGATION
Integrated inertial/GPS N91-19032
INFLUENCE COEFFICIENT
Free wake analysis of hover performance using a new influence coefficient method
[NASA-CR-4309] N91-19050
Cascade flutter analysis with transient response aerodynamics
[NASA-TM-103746] N91-19475
INFORMATION PROCESSING (BIOLOGY)
Postural changes following sensory reinterpretation as an analog to spaceflight N91-19610
INFORMATION RETRIEVAL
Finding the object proceedings addendum
[DE91-006724] N91-19738
NASA Thesaurus supplement: A four part cumulative supplement to the 1988 edition of the NASA Thesaurus (supplement 5)
[NASA-SP-7064-SUPPL-5] N91-19962
Prototype document tracking and storage system for the Superconducting Super Collider Laboratory (SSCL)
[DE91-008204] N91-19963
INFORMATION SYSTEMS
RICIS 1988 Symposium Proceedings. Presentation appendix
[NASA-CR-188077] N91-19722
Finding the object proceedings addendum
[DE91-006724] N91-19738
Prototype document tracking and storage system for the Superconducting Super Collider Laboratory (SSCL)
[DE91-008204] N91-19963
An architecture for accommodating referenceability among intelligent electronic documents
[DE91-008250] N91-19964
Formal specification of human-computer interfaces N91-20023
INFRARED ASTRONOMY
A balloon-borne 102-cm telescope for far-infrared astronomy
[NASA-CR-187778] N91-19973
A scientific program for infrared, submillimeter and radio astronomy from space: A report by the Management Operations Working Group
[NASA-TM-103333] N91-19979
INFRARED ASTRONOMY SATELLITE
High resolution infrared astronomy satellite observations of a selected spiral galaxy
[NASA-CR-188019] N91-19975
Observations of CO isotopic emission and the far-infrared continuum of Centaurus A
[MPE-PREPRINT-183] N91-19977
INFRARED DETECTORS
Boeing infrared sensor (BIRS) calibration facility N91-19138
Infrared sensor test methodology and facilities N91-19139
Thermal control for the ground simulation of a space IR sensor system N91-19140
INFRARED IMAGERY
Focusing infrared laser beams on targets in space without using adaptive optics
[DE91-007518] N91-19421
INFRARED LASERS
Focusing infrared laser beams on targets in space without using adaptive optics
[DE91-007518] N91-19421
Investigation at two wavelengths of a modulated He-Xe rare gas laser
[AD-A229852] N91-19434
INFRARED RADAR
Theory of CW lidar aerosol backscatter measurements and development of a 2.1 microns solid-state pulsed laser radar for aerosol backscatter profiling
[NASA-CR-4347] N91-19498
INFRARED RADIATION
Thermal balance testing of the Anik-E spacecraft N91-19131
Theory of CW lidar aerosol backscatter measurements and development of a 2.1 microns solid-state pulsed laser radar for aerosol backscatter profiling
[NASA-CR-4347] N91-19498
INFRARED SPACE OBSERVATORY (ISO)
IAL SPACE: A test laboratory for the ISO cryogenic payload N91-19142
INFRARED SPECTRA
Fluorescent HD emission from photodissociation regions
[MPE-PREPRINT-177] N91-19982
INFRARED SPECTROSCOPY
Remote detection of organics using Fourier transform infrared spectroscopy
[DE91-006045] N91-19253
INFRARED TELESCOPES
A scientific program for infrared, submillimeter and radio astronomy from space: A report by the Management Operations Working Group
[NASA-TM-103333] N91-19979
Evidence for ammonium-bearing minerals in Ceres N91-20004
INHIBITORS
Subcellular signal transduction systems in the cellular trauma of ischemia
[AD-A229876] N91-19709
INJECTION LASERS
Coherent effects in generation of ultrashort light pulses by semiconductor injection laser N91-19820
INJECTORS
LOX/hydrogen coaxial injector atomization test program
[NASA-CR-187037] N91-19117
INLET FLOW
Turbulent boundary layer separation over a rearward facing ramp and its control through mechanical excitation
[NASA-TM-103702] N91-19370
INSERTS
Large-scale aeroacoustic research feasibility and conceptual design of test-section inserts for the Ames 80-by 120-foot wind tunnel
[NASA-TP-3020] N91-19824
INSPECTION
Debris/ice/TPS assessment and photographic analysis for shuttle mission STS-35
[NASA-TM-103816] N91-19118
INSTALLING
Large-scale aeroacoustic research feasibility and conceptual design of test-section inserts for the Ames 80-by 120-foot wind tunnel
[NASA-TP-3020] N91-19824
INSTRUMENT PACKAGES
A flight experiment to determine GPS photochemical contamination accumulation rates N91-19159
INSULATION
The full-scale process and design changes for elimination of insulation edge separations and voids in tang flap area
[NASA-CR-184110] N91-19172
Composite flexible insulation for thermal protection of space vehicles
[NASA-TM-103836] N91-19304
Integrated Cryogenic Experiment (ICE) microsphere investigation
[NASA-CR-177538] N91-19323
INTEGRAL EQUATIONS
Electromagnetic penetration through narrow slots in conducting surfaces and coupling to structures on the shadow side
[DE91-007155] N91-19331
INTEGRATED CIRCUITS
Coplanar waveguide EEsoF MICAD macros make circuit layout easy
[NASA-TM-103272] N91-19332
INTERFACES
Theory of bulk and interface constant phase elements in electrode-electrolyte systems
[DE91-007181] N91-19255
The characterization of interface roughness and other defects in multilayers by x ray scattering
[DE91-007558] N91-19929
INTERFERENCE IMMUNITY
Prospects for using carbon-carbon composites for EMI shielding
[NASA-TM-103677] N91-19231
INTERFEROMETRY
Three-dimensional computed tomography from interferometric measurements within a narrow cone of views
[NASA-TM-103257] N91-19404
Interferometry, streak photography, and stereo photography of laser-driven miniature flying plates
[DE91-007493] N91-19405
Fiber optic interferometric measuring method for the determination of a very small polarization coefficient
[MBB-UA-1185-90-PUB] N91-19876
INTERMETALLICS
Low-density, high-strength intermetallic matrix composites by XD (trademark) synthesis
[NASA-TM-103724] N91-19233
Effects of radiolytic tritium decay on the thermodynamic behavior of LaNi(4.25)Al(0.75) tritides
[DE91-007961] N91-19277
NDE standards for high temperature materials
[NASA-TM-103761] N91-19464
INTERNAL ENERGY
Triton: A hot potato N91-20005
INTERNAL FRICTION
Internal friction peaks due to interstitials in bcc alloys
[DE91-007411] N91-19272
INTERNATIONAL COOPERATION
Review of recent stellarator results in the USA, the USSR, and Japan
[DE91-007798] N91-19901
INTERPLANETARY SPACECRAFT
Cycling space ship transportation device for continuous link between Earth and Mars
[ILR-MITT-247(1990)] N91-19121
INTERPOLATION
Calculations of separated 3-D flows with a pressure-staggered Navier-Stokes equations solver
[NASA-CR-187065] N91-19367
INTERSTELLAR GAS
Proceedings of 146th IAU Symposium on Dynamics of Galaxies and Molecular Cloud Distribution
[PB91-123661] N91-19994
INTERSTELLAR MATTER
Activities report of the Institute for Extraterrestrial Physics
[MPE-222] N91-19971
Fluorescent HD emission from photodissociation regions
[MPE-PREPRINT-177] N91-19982
Proceedings of the symposium Astrophysical Processes and Structures in the Universe
[PB91-123653] N91-19993
Instellar grains within interstellar grains N91-19998
Stable hydrogen and carbon isotope ratios of extractable hydrocarbons in the Murchison meteorite N91-20006
INTERSTITIALS
Internal friction peaks due to interstitials in bcc alloys
[DE91-007411] N91-19272
INTRUSION
Computers at risk: Safe computing in the information age
[LC-90-22329] N91-19721
INVARIANCE
Computation of invariant tori in 2 (1/2) degrees of freedom
[DE91-007424] N91-19778
Relaxed states with plasma flow
[DE91-008199] N91-19909
INVERSE SCATTERING
Examinations of inverse scattering problem for the scalar Helmholtz equation in the field of first order approximations for potentials with compact supports and safe real wave numbers
[ETN-91-98949] N91-19339
INVERSIONS
On the joint inversion of geophysical data for models of the coupled core-mantle system
[NASA-TM-104536] N91-19557
INVISCID FLOW
Panel methods: An introduction
[NASA-TP-2995] N91-19058

The effect of body shape on the development of vortex asymmetry in the flow past slender bodies
[BU-413] N91-19068

IODINE LASERS
Laser Doppler velocimetry for continuous flow solar-pumped iodine laser system
[NASA-TM-104029] N91-19415

ION BEAMS
Advances in atomic oxygen simulation N91-19147
Proton induced x ray emission analysis N91-19832
Electromagnetic ion/ion cyclotron instability
[DE91-004841] N91-19860
Symposium on Development of Intensed Pulsed Particle Beams and Its Applications
[NIFS-PROC-5] N91-19882
Rayleigh-Taylor instability in LIB ICF N91-19883
Two-stage ion diode experiments on induction adder N91-19884
Experiments toward the development of new pulsed ion diodes N91-19885
Study on ablation of target material induced by pulsed ion beam bombardment N91-19886
Theoretical study of plasma focus diode N91-19887
Pulse-power characteristic of VIVA-1 (Versatile Inductive Voltage Adder) N91-19888
Reduction of low energy components in pulse ion beam N91-19889
Generation and focusing of carbon ion beam by the inverse pinch ion diode N91-19890
Generation of pulsed ion beams by an inductive storage pulsed power generator N91-19891
Power plant by LIB fusion N91-19892
Control of gap closure in applied-B diode N91-19893

ION CURRENTS
Study on ablation of target material induced by pulsed ion beam bombardment N91-19886

ION CYCLOTRON RADIATION
Electromagnetic ion/ion cyclotron instability
[DE91-004841] N91-19860

ION ENGINES
Solar electric propulsion for Mars transport vehicles
[NASA-TM-103234] N91-19178
Enhancing space transportation: The NASA program to develop electric propulsion
[NASA-TM-4244] N91-19181

ION IMPLANTATION
The effect of process conditions on the performance of epitaxial InP solar cells N91-19204
Characterization of ion-implanted aluminum and iron by spectroscopic ellipsometry
[DE91-008371] N91-19283
Solid State Photovoltaic Research Branch
[DE91-002128] N91-19502
Considerations relating to pulsed-beam modification of materials
[DE91-006771] N91-19922

ION INJECTION
Plasma assisted NO(x) reduction in existing coal combustors
[DE91-007380] N91-19536

ION PROPULSION
A 5-kW xenon ion thruster lifetest
[NASA-TM-103191] N91-19180
Dual-purpose self-deliverable lunar surface PV electrical power system N91-19200

ION SOURCES
Finnigan ion trap mass spectrometer detection limits and thermal energy analyzer interface status report and present capabilities
[DE91-006220] N91-19254

ION TRAPS (INSTRUMENTATION)
Finnigan ion trap mass spectrometer detection limits and thermal energy analyzer interface status report and present capabilities
[DE91-006220] N91-19254

IONIC COLLISIONS
Electron transfer, ionization, and excitation in atomic collisions
[DE91-008044] N91-19844
Summary of discussions at the HIGH p (sub T) session
[DE91-008196] N91-19848

IONIZATION
Soft x-ray laser gain prediction at high density for the nitrogen isoelectronic sequence
[DE91-007616] N91-19416
Intense field non-resonant multiphoton absorption of diatomic molecules
[DE91-006920] N91-19835
Electron transfer, ionization, and excitation in atomic collisions
[DE91-008044] N91-19844

IONS
A study of carbon steel corrosion inhibition by phosphate ions and by an organic buffer using a scanning vibrating electrode
[DE91-008103] N91-19280
He-like spectra through charge exchange processes in tokamak plasmas
[NIFS-69] N91-19894
Relaxed states with plasma flow
[DE91-008199] N91-19909

IRON
Characterization of ion-implanted aluminum and iron by spectroscopic ellipsometry
[DE91-008371] N91-19283
Microbiologically influenced corrosion in copper and nickel seawater piping systems
[AD-A229874] N91-19287
Photoelectron diffraction of magnetic ultrathin films: Fe/Cu(001)
[DE91-007254] N91-19924

IRON ALLOYS
Considerations relating to pulsed-beam modification of materials
[DE91-006771] N91-19922

IRRADIANCE
Analysis of SBUV/2 measurements of solar UV irradiance variations N91-19526

IRRADIATION
High-efficiency, radiation-resistant GaAs space cells N91-19194
Thermal annealing of GaAs concentrator solar cells N91-19195
Effects of irradiation on crack-arrest toughness of two high-copper welds
[DE91-007189] N91-19270
Radiation-induced changes in electrical conductivity of a wide range of copper alloys
[DE91-007200] N91-19271

ISCHEMIA
Effects of training with reduced perfusion pressure on performance and muscle fiber characteristics N91-19615
Subcellular signal transduction systems in the cellular trauma of ischemia
[AD-A229876] N91-19709

ISOELECTRONIC SEQUENCE
Soft x-ray laser gain prediction at high density for the nitrogen isoelectronic sequence
[DE91-007616] N91-19416

ISOPARAMETRIC FINITE ELEMENTS
A novel isoparametric finite element displacement formulation for axisymmetric analysis of nearly incompressible materials
[OUEL-1872/91] N91-19791

ISOTOPES
Cosmic dust: Laboratory analyses of extremely small particles N91-20013

ISOTROPY
Solution of one-dimensional problem in nonlinear theory of elasticity with structured shock wave N91-19809

ITERATION
A novel potential/viscous flow coupling technique for computing helicopter flow fields
[NASA-CR-177568] N91-19060
The next generation N91-19724
Design and implementation of an image understanding system: DADS
[ETN-91-98926] N91-19773
Spectrum transformation for divergent iterations
[NASA-TM-103745] N91-19786

ITERATIVE SOLUTION
On the joint inversion of geophysical data for models of the coupled core-mantle system
[NASA-TM-104536] N91-19557
The weighted-difference form of the nodal diffusion method in cylindrical geometry
[DE91-007849] N91-19784

J

J-85 ENGINE
J-85 jet engine noise measured in the ONERA S1 wind tunnel and extrapolated to far field
[NASA-TP-3053] N91-19823

JET AIRCRAFT
Aircrafts, requirements for ground installations from the aircraft point of view N91-19108

JET FLOW
Calculation of pulsating liquid free jets
[MPIS-15/1990] N91-19385

JET IMPINGEMENT
Solar rocket plume/mirror interactions
[NASA-CR-185300] N91-19059

JET MIXING FLOW
Rapid mix concepts for low emission combustors in gas turbine engines
[NASA-CR-185292] N91-19048
Two-dimensional non-reacting jet-gas mixing in an MHD (magnetohydrodynamic) second stage combustor
[DE91-006015] N91-19252
Fluid mixing device having a conical inlet and a noncircular outlet
[AD-D014708] N91-19364
Experimental investigation of a single flush-mounted hypermixing nozzle
[NASA-TM-103726] N91-19374

JETS
Summary of discussions at the HIGH p (sub T) session
[DE91-008196] N91-19848

JFET
Monolithic radiation hard charge sensitive preamplifier using junction field effect transistors
[DE91-008437] N91-19360

JOINTS (JUNCTIONS)
Design and testing of a circumferential and longitudinal joint of the A320 fuselage section 13/14 in GLARE
[LR-645] N91-19494
Modeling and analysis of orthotropic plate with circular cutout and adhesive bonded patch
[AD-A229866] N91-19496

JOURNAL BEARINGS
Two reference time scales for studying the dynamic cavitation of liquid films
[NASA-TM-103673] N91-19369

JUNCTION DIODES
Classical and quantum charge dynamics in small tunnel junctions
[ETN-91-98916] N91-19947

K

K-EPSILON TURBULENCE MODEL
Multigrid solution of compressible turbulent flow on unstructured meshes using a two-equation model
[NASA-CR-187513] N91-19043
A 2-D oscillating flow analysis in Stirling engine heat exchangers
[NASA-TM-103781] N91-19375

KALMAN FILTERS
Ridge regression signal processing N91-19029
A proposed Kalman filter algorithm for estimation of unmeasured output variables for an F100 turbofan engine
[NASA-TM-4234] N91-19099
Model distribution in decentralized multi-sensor data fusion
[OUEL-1868/90] N91-19763

KERNEL FUNCTIONS
Boundary integral equations and the Dirichlet problem
[DE91-004537] N91-19779

KINEMATICS
State estimation applications in aircraft flight-data analysis: A user's manual for SMACK
[NASA-RP-1252] N91-19082
A rigid body model and decoupled control architecture for two manipulators holding a complex object
[DE91-007827] N91-19444

KINETIC ENERGY
Filtering analysis of a direct numerical simulation of the turbulent Rayleigh-Benard problem
[NASA-CR-187488] N91-19366
Summary of the working group on transverse emissions from photocathodes
[DE91-008414] N91-19432

KINETICS
Theoretical investigation of phase stability in non-magnetic Fe-V substitutional alloys
[DE91-006711] N91-19268
Growth kinetics of physical vapor transport processes: Crystal growth of the optoelectronic material mercurous chloride
[NASA-TM-103788] N91-19320
Influence of various parameters on the V'O2 frequency response of the body. A theoretical study on the basis of a nonlinear model N91-19594
Intra-individual variability V'O2 frequency responses in physically active subjects N91-19601

KLYSTRONS
Relativistic klystron research for future linear colliders
[DE91-008063] N91-19862

KNEE (ANATOMY)
Isokinetic force velocity and electromyographic characteristic of knee and elbow extensor and flexor muscles in the 0-g environment N91-19584

KNOWLEDGE BASES (ARTIFICIAL INTELLIGENCE)
Modeling of flow systems for implementation under KATE N91-20038

KNOWLEDGE REPRESENTATION
The development of structure for the representation and manipulation of sophisticated knowledge in intelligent systems
[AD-A229114] N91-19957
KRYPTON FLUORIDE LASERS
Development of KrF lasers for inertial confinement fusion
[DE91-007349] N91-19419

L

LABORATORIES
Exploratory battery technology development and testing report for 1989
[DE91-006753] N91-19352
Prototype document tracking and storage system for the Superconducting Super Collider Laboratory (SSCL)
[DE91-008204] N91-19963
LAMINAR FLOW
Icing characteristics of a natural-laminar-flow, a medium-speed, and a swept, medium-speed airfoil
[NASA-TM-103693] N91-19046
A finite Reynolds number approach for the prediction of boundary layer receptivity in localized regions
[NASA-TM-102781] N91-19061
LAMINATES
Bulging of fatigue cracks in a pressurized aircraft fuselage
[LR-647] N91-19094
A study on prediction of life due to creep behavior in CF/EPOXY and CF/PEEK laminates N91-19226
METCAN updates for high temperature composite behavior: Simulation/verification
[NASA-TM-103682] N91-19229
Probabilistic micromechanics and macromechanics of polymer matrix composites
[NASA-TM-103669] N91-19236
Development of a fatigue-life methodology for composite structures subjected to out-of-plane load components
[NASA-TM-102885] N91-19241
An expert system for laminated plate design using composite materials
[BU-406] N91-19245
Minimum weight optimization of composite laminated struts
[BU-409] N91-19246
A knowledge based expert system for laminated composite strut design
[BU-410] N91-19247
Structural reliability analysis of laminated CMC components
[NASA-TM-103685] N91-19292
Piezoelectric sandwich polymer transducer
[AD-D014650] N91-19341
Bolted joints in a laminated composite strut design expert system
[BU-415] N91-19488
Design and testing of a circumferential and longitudinal joint of the A320 fuselage section 13/14 in GLARE
[LR-645] N91-19494
LANDING
Collision detection system
[AD-D014645] N91-19072
LANDING SITES
Feasibility of solar power for Mars N91-19201
LANTHANUM ALLOYS
Effects of radiolytic tritium decay on the thermodynamic behavior of LaNi(4.25)Al(0.75) tritides
[DE91-007961] N91-19277
LANTHANUM OXIDES
Direct conversion of methane to C2's and liquid fuels
[DE91-005729] N91-19313
LAPLACE EQUATION
Boundary integral equations and the Dirichlet problem
[DE91-004537] N91-19779
LARGE SPACE STRUCTURES
The 5th Annual NASA Spacecraft Control Laboratory Experiment (SCOLE) Workshop, part 2
[NASA-CP-10057-PT-2] N91-19122
Control and mechanism interaction for ground-based testing of space structures N91-19125
Hypervelocity impact physics
[NASA-CR-4343] N91-19164
Modal identification of a deployable space truss
[NASA-TM-102720] N91-19474
LARVAE
Effect of hyper-gravity on the swimming behavior of aquatic vertebrates N91-19626
LASER ANEMOMETERS
Improved visualization of flow field measurements
[NASA-TM-103679] N91-19044
Three-component laser anemometer measurement systems
[NASA-TP-3080] N91-19057
LASER APPLICATIONS
Sandia technology: Engineering and science applications
[DE91-006760] N91-19322
High power, high frequency lasertron RF sources
[DE91-006007] N91-19414
Laser Tracker 2: Sandia National Laboratories' second generation laser tracking system
[DE91-007711] N91-19424
Structured software design for an on-line laser-based particle size distribution instrument
[DE91-007234] N91-19746
Breakup of femtosecond pulses during amplification in Er(3+)-doped single-mode optical fibers N91-19812
LASER BEAMS
Interferometry, streak photography, and stereo photography of laser-driven miniature flying plates
[DE91-007493] N91-19405
Focusing infrared laser beams on targets in space without using adaptive optics
[DE91-007518] N91-19421
Laser Tracker 2: Sandia National Laboratories' second generation laser tracking system
[DE91-007711] N91-19424
Acoustic stabilization of laser beam wavefront in nonhomogeneous gaseous medium N91-19802
Microsecond-pulse Nd-glass laser with monopulse duration control N91-19811
A modulated high-power optical source specification
[AD-D014654] N91-19869
Nonlinear optic effects in liquid crystals
[ETN-91-98923] N91-19878
LASER CAVITIES
Hole coupling resonator for free electron lasers
[DE91-007745] N91-19426
Quantum fluctuations in laser with intracavity frequency doubling N91-19805
Intracavity second-harmonic generation by laser with optical delay line and mode locking N91-19808
He-Ne laser emitting five lines simultaneously N91-19813
LASER DOPPLER VELOCIMETERS
Three-component laser anemometer measurement systems
[NASA-TP-3080] N91-19057
Laser Doppler velocimetry for continuous flow solar-pumped iodine laser system
[NASA-TM-104029] N91-19415
LASER FUSION
Development of KrF lasers for inertial confinement fusion
[DE91-007349] N91-19419
Upgrade of the LLNL Nova laser for inertial confinement fusion
[DE91-008060] N91-19430
Summary of the International Dawson Symposium on The Physics of Plasmas
[DE91-006912] N91-19897
LASER INTERFEROMETRY
Three-component laser anemometer measurement systems
[NASA-TP-3080] N91-19057
Experiments toward the development of new pulsed ion diodes N91-19885
LASER MODE LOCKING
Passive mode locking in optically pumped Al2O3:Ti(3+) laser N91-19803
Intracavity second-harmonic generation by laser with optical delay line and mode locking N91-19808
LASER OUTPUTS
Soft x-ray laser gain prediction at high density for the nitrogen isoelectronic sequence
[DE91-007616] N91-19416
Hole coupling resonator for free electron lasers
[DE91-007745] N91-19426
Investigation at two wavelengths of a modulated He-Xe rare gas laser
[AD-A229852] N91-19434
Possibility of raising efficiency of free-electron laser in longitudinal magnetic field N91-19804
Quantum fluctuations in laser with intracavity frequency doubling N91-19805
Near resonant absorption by atoms in intense fluctuating fields
[DE91-007911] N91-19839
Electron temperature of Gd plasma produced by laser resonance ionization
[DE91-744833] N91-19913
LASER PLASMAS
Measurements with a 35 psec gate time microchannelplate camera
[DE91-006701] N91-19400
Recombination x ray laser experiments using exploding ribbon Al targets
[DE91-007146] N91-19429
Nickel-like x ray lasers
[DE91-008502] N91-19433
UV Thomson scattering from x ray laser plasmas
[DE91-007347] N91-19895
Electron temperature of Gd plasma produced by laser resonance ionization
[DE91-744833] N91-19913
LASER PUMPING
Development of KrF lasers for inertial confinement fusion
[DE91-007349] N91-19419
Recombination x ray laser experiments using exploding ribbon Al targets
[DE91-007146] N91-19429
Nickel-like x ray lasers
[DE91-008502] N91-19433
The physics of laser polarized muonic atoms
[DE91-008045] N91-19845
LASER SPECTROSCOPY
Studies of atmospheric molecules by multiphoton spectroscopy
[DE91-006738] N91-19554
Quantum fluctuations in laser with intracavity frequency doubling N91-19805
LASER STABILITY
Hole coupling resonator for free electron lasers
[DE91-007745] N91-19426
Acoustic stabilization of laser beam wavefront in nonhomogeneous gaseous medium N91-19802
LASER TARGETS
Focusing infrared laser beams on targets in space without using adaptive optics
[DE91-007518] N91-19421
Recombination x ray laser experiments using exploding ribbon Al targets
[DE91-007146] N91-19429
Upgrade of the LLNL Nova laser for inertial confinement fusion
[DE91-008060] N91-19430
LASERS
Near resonant absorption by atoms in intense fluctuating fields
[DE91-007911] N91-19839
LASING
Optically-ionized plasma recombination x ray lasers
[DE91-007261] N91-19898
LATTICE PARAMETERS
Theoretical investigation of phase stability in non-magnetic Fe-V substitutional alloys
[DE91-006711] N91-19268
LAUNCH VEHICLES
Innovations in dynamic test restraint systems N91-19145
Commercial Space Launch Act implementation
[GPO-27-944] N91-19968
LAUNCHERS
Pneumatic launcher
[AD-D014658] N91-19116
LAY-UP
Probabilistic micromechanics and macromechanics of polymer matrix composites
[NASA-TM-103669] N91-19236
LEAD ACID BATTERIES
Laboratory testing of the Sonnenschein charger, Part number DTL 12040
[DE91-006543] N91-19346
LEADING EDGES
F-18 high alpha research vehicle surface pressures: Initial in-flight results and correlation with flow visualization and wind-tunnel data
[NASA-TM-101724] N91-19051
The effect of small streamwise velocity distortion on the boundary layer flow over a thin flat plate with application to boundary layer stability theory
[NASA-TM-103668] N91-19372
LEAKAGE
A test fixture for measuring high-temperature hypersonic-engine seal performance
[NASA-TM-103658] N91-19442
Correlation of leak rates of various fluids with the leak rate of an inert gas in the same configuration N91-20033
LEAST SQUARES METHOD
Performance monitoring in nonlinear adaptive noise cancellation
[RR-409] N91-19362
Lecture notes on nonlinear inversion and tomography
[DE91-008238] N91-19558
Rational model identification using an extended least squares algorithm
[RR-388] N91-19753
Orthogonal least squares parameter estimation algorithms for nonlinear stochastic systems
[RR-404] N91-19797

LEGUMINOUS PLANTS
Productivity and photosynthesis of selected crop plants under orbital light conditions: An approach to solar powered CELSS N91-19662
LENSES
Nonlinear optic effects in liquid crystals [ETN-91-98923] N91-19878
LETHALITY
Genetic risk and physiological stress induced by heavy ions N91-19680
Defective embryogenesis of Arabidopsis induced by cosmic HZE-particles N91-19682
LEUKOCYTES
Cosmos: 1989 immunology studies [NASA-CR-188046] N91-19701
LEVERS
Nonlinear analysis and redesign of the mixed-mode bending delamination test [NASA-TM-102777] N91-19482
LIBRARIES
Formal specification of human-computer interfaces N91-20023
LIFE (DURABILITY)
Computational simulation of hot composites structures [NASA-TM-103681] N91-19230
Life and dynamic capacity modeling for aircraft transmissions [NASA-CR-4341] N91-19438
Application of thermal life prediction model to high-temperature aerospace alloys B1900+Hf and Haynes 188 [NASA-TM-4226] N91-19473
Positron lifetime studies of defect structures in Ba(1-x)K(x)BiO3 [DE91-007341] N91-19919
LIFE CYCLE COSTS
Project of a cost analysis model for the acquisition of a permanent lunar base [ILR-MITT-245(1990)] N91-19114
LIFE SCIENCES
Centrifuge Facility Conceptual System Study. Volume 1: Facility overview and habitats [NASA-TM-102860] N91-19566
JPRS report: Science and technology. USSR: Life sciences [JPRS-ULS-91-001] N91-19567
Fourth European Symposium on Life Sciences Research in Space [ESA-SP-307] N91-19572
Life sciences in ESA TRP activity N91-19589
Tools for the preparation, performance and evaluation of life sciences experiments N91-19609
Potentials, message and challenges of life science research in space N91-19696
Predictions of cell damage rates for Lifesat missions [NASA-TM-102170] N91-19699
USSR Space Life Sciences Digest. Index to issues 26-29 [NASA-CR-3922(35)] N91-19700
LIFE SUPPORT SYSTEMS
Fourth European Symposium on Life Sciences Research in Space [ESA-SP-307] N91-19572
Tuning the efficiencies of plant lighting systems: From primary energy to edible biomass: The LED as an alternative light source N91-19660
Development of a miniature biology facility N91-19666
Experimental equipment for space biology [MBB-UO-0096-90-PUB] N91-19708
LIFT
Acoustic radiation from lifting airfoils in compressible subsonic flow [NASA-TM-103650] N91-19053
LIFT DRAG RATIO
An experimental study of a sting-mounted single-slot circulation control wing [AD-A229867] N91-19111
LIGANDS
Late transition metal (mu)-oxo and (mu)-imido complexes [DE91-005349] N91-19267
LIGHT (VISIBLE RADIATION)
A status report on the analysis of the NOAA-9 SBUV/2 sweep mode solar irradiance data N91-19518
Responses of Physarum polycephalum to varying light levels during fast clinostat rotation: A scientific preparation of an ESA biorack experiment during the IML-1 mission N91-19676
LIGHT AMPLIFIERS
Copper vapor as active medium for high-power oscillator-amplifier laser systems N91-19806
LIGHT BEAMS
A modulated high-power optical source specification [AD-D014654] N91-19869
LIGHT EMITTING DIODES
Tuning the efficiencies of plant lighting systems: From primary energy to edible biomass: The LED as an alternative light source N91-19660
LIGHT IONS
Power plant by LIB fusion N91-19892
LIGHT MODULATION
Investigation at two wavelengths of a modulated He-Xe rare gas laser [AD-A229852] N91-19434
A modulated high-power optical source specification [AD-D014654] N91-19869
LIGHT SCATTERING
Light guide fibers [MBB-UA-1199-90-PUB] N91-19877
LIGHT SOURCES
Proposal for a conceptually new compact collecting optics for powerful light sources N91-19155
Radioluminescent polymer lights [DE91-005521] N91-19290
The advanced light source: A new tool for research in atomic physics [DE91-007739] N91-19861
The specification of glancing incidence mirrors in terms of system performance [DE91-007556] N91-19873
LIGHT TRANSMISSION
Light guide fibers [MBB-UA-1199-90-PUB] N91-19877
LIGHTING EQUIPMENT
Tuning the efficiencies of plant lighting systems: From primary energy to edible biomass: The LED as an alternative light source N91-19660
LIGHTNING
Progressive feature of stepped leader on Japan sea coast in winter (basic data to establish shielding theory for lightning) [DE91-742133] N91-19561
Rocket-triggered lightning strikes and forest fire ignition N91-20027
LIMITERS (FUSION REACTORS)
New method for edge plasma control by RF ponderomotive force [DE91-744823] N91-19911
LINE SHAPE
A global fit to the Z(0) line shape [NOTA-INTERNA-966] N91-19868
LINE SPECTRA
Characteristics of excimer laser with narrow emission line N91-19807
He-Ne laser emitting five lines simultaneously N91-19813
LINEAR ACCELERATORS
Intense microwave generation using free-electron lasers [DE91-007262] N91-19417
Relativistic klystron research for future linear colliders [DE91-008063] N91-19862
LINEAR ENERGY TRANSFER (LET)
LDEF Experiment P0006 Linear Energy Transfer Spectrum Measurement (LETSME) quick look report [NASA-CR-184115] N91-19223
LINEAR EQUATIONS
Bayesian approximation of solutions to linear ordinary differential equations [DE91-007872] N91-19785
LINEAR FILTERS
Performance monitoring in nonlinear adaptive noise cancellation [RR-409] N91-19362
LINEAR PROGRAMMING
Convergence of linear programming using a Hopfield net [DE91-007870] N91-19758
LINEAR SYSTEMS
Stochastic satbility and performance robustness of linear multivariable systems N91-19038
LININGS
Large-scale aeroacoustic research feasibility and conceptual design of test-section inserts for the Ames 80-by 120-foot wind tunnel [NASA-TP-3020] N91-19824
LIQUID ATOMIZATION
Cryogenic liquid-jet breakup in two-fluid atomizers [NASA-TM-103734] N91-19402
LIQUID CRYSTALS
Solid State Photovoltaic Research Branch [DE91-002128] N91-19502
Nonlinear optic effects in liquid crystals [ETN-91-98923] N91-19878
LIQUID FUELS
Direct conversion of methane to C2's and liquid fuels [DE91-005729] N91-19313
Direct conversion of methane to C2's and liquid fuels [DE91-007545] N91-19318
LIQUID HELIUM
Integrated Cryogenic Experiment (ICE) microsphere investigation [NASA-CR-177538] N91-19323
Reflections on some problems concerning the role of superfluid turbulence in the propagation of second-sound pulses in He 2 [MPIS-8/1990] N91-19827
Ultrasonic investigations on superfluid He-3-A and He-3-B [ISBN-952-90-2241-7] N91-19830
LIQUID HYDROGEN
COLD-SAT feasibility study safety analysis [NASA-CR-187042] N91-19167
LIQUID NITROGEN
Cryogenic liquid-jet breakup in two-fluid atomizers [NASA-TM-103734] N91-19402
LIQUID OXYGEN
Orbital transfer vehicle oxygen turbopump technology. Volume 1: Design, fabrication, and hydrostatic bearing testing [NASA-CR-185175] N91-19174
LIQUID PROPELLANT ROCKET ENGINES
LOX/hydrogen coaxial injector atomization test program [NASA-CR-187037] N91-19117
LIQUID SLOSHING
Liquid sloshing in cargo tanks. Liquid slosh loading in slack ship tanks: Forces on internal structure and pressures [PB91-129262] N91-19383
Experimental studies on a nonlinear hydroelastic vibration of circular cylindrical tanks [LRT-WE-9-FB-10(1990)] N91-19387
Liquid sloshing response in a spinning container due to pitching excitation [LRT-WE-9-FB-11(1990)] N91-19388
LIQUID SURFACES
Response of a viscous liquid layer to pitch- and roll-excitation in zero-gravity environment [LRT-WE-9-FB-13(1990)] N91-19390
LIQUID WASTES
Environmental surveillance data report for the first quarter of 1990 [DE91-008552] N91-19544
LIQUID-SOLID INTERFACES
Surface chemistry at semiconductor-electrolyte interfaces [DE91-005915] N91-19920
High resolution microstructural and microchemical analysis of zirconia eutectic interfaces [DE91-008032] N91-19940
LITERATURE
The 1989 JSC bibliography of scientific and technical papers [NASA-TM-102173] N91-19959
LITHIUM ALLOYS
Stress corrosion cracking of Al-Li-Cu-Zr alloy 2090 in aqueous Cl(-) and mixed CO3(2-)/Cl(-) environments [DE91-007064] N91-19269
LITHIUM FLUORIDES
Part 1: The effect of lattice defects on the sintering of lithium fluoride; Part 2: The morphology of calcium oxide from calcium carbonate decomposition [DE91-007743] N91-19934
LITHIUM OXIDES
Thin film amorphous electrolytes: The Li2O-SiO2-P2O5 system [DE91-007272] N91-19925
LOAD DISTRIBUTION (FORCES)
Behavior of surface and corner cracks subjected to tensile and bending loads in Ti-6Al-4V alloy [NASA-TM-102165] N91-19273
LOADS (FORCES)
Load bearing connective damper [AD-D014676] N91-19468
LOCOMOTION
Gravitaxis in Physarum polycephalum N91-19678
LOGIC PROGRAMMING
Formal specification of human-computer interfaces N91-20023
LONG DURATION EXPOSURE FACILITY
The effect of the low Earth orbit environment on space solar cells [NASA-TM-103735] N91-19165
LDEF Experiment P0006 Linear Energy Transfer Spectrum Measurement (LETSME) quick look report [NASA-CR-184115] N91-19223
Space debris: Orbital microparticulates impacting LDEF experiments favour a natural extraterrestrial origin N91-20008
LONG DURATION SPACE FLIGHT
Experiment lymphocytes of Aragatz mission: Influence of the space flight on human T lymphocyte and monocyte functions N91-19619

New experimental approach in quality factor and dose equivalent determination during a long term manned space mission N91-19679
Aragatz Mission: Bone densitometric results obtained with the SCOOP miniscanner N91-19690
Weightlessness countermeasures and human physiology in space: A potential conflict N91-19695

LONG WAVE RADIATION
Boeing infrared sensor (BIRS) calibration facility N91-19138

LOW ALTITUDE
Progress on intelligent guidance and control for wind shear encounter N91-19034

LOW COST
The design and flight testing of a high-performance low-cost parachute system for a 1000 lb payload [DE91-007733] N91-19065
Low cost space power generation N91-19212

LOW CURRENTS
Elementary considerations on the gas dynamic design parameters of a MHD Faraday generator in relation to a gas turbine cycle [LR-564] N91-19456

LOW FREQUENCIES
Critical-layer nonlinearity in the resonance growth of three-dimensional waves in boundary layers [NASA-TM-103639] N91-19373
Development of a piezoelectric polymer film pressure transducer for low frequency and dynamic pressure measurement [AD-A229848] N91-19412
Biological effects of extremely low-frequency electromagnetic fields: In vivo studies [DE91-007899] N91-19704

LOW NOISE
Development of components and subsystems for low noise receivers at micro- and millimeter waves [S-187] N91-19363

LOW PASS FILTERS
Filtering analysis of a direct numerical simulation of the turbulent Rayleigh-Benard problem [NASA-CR-187488] N91-19366

LOW TEMPERATURE
Low temperature properties of boron carbides [DE91-008172] N91-19243

LOW VOLTAGE
Vibration and thermal vacuum qualification test results for a low-voltage tungsten-halogen light [NASA-CR-187050] N91-19325

LOWER BODY NEGATIVE PRESSURE
A new principle for dynamic fluid shift investigations in astronauts N91-19600
Carotid-cardiac baroreflex influence on forearm vascular resistance during low level LBNP N91-20030

LUBRICATING OILS
Results from the third year of operation of the Federal methanol fleet at Argonne National Laboratory [DE91-007822] N91-19451

LUGS
S87 close air support aircraft fatigue analysis [ETN-91-98854] N91-19093

LUMINAIRES
Vibration and thermal vacuum qualification test results for a low-voltage tungsten-halogen light [NASA-CR-187050] N91-19325

LUMINESCENCE
Florida radioluminescent taxiway light development program [DE91-005650] N91-19104
Radioluminescent polymer lights [DE91-005521] N91-19290

LUMINOSITY
Electroweak interactions at LEP [NOTA-INTERNA-962] N91-19853

LUNAR BASES
Space reactor/Stirling cycle systems for high power lunar application [NASA-TM-103698] N91-19112
Project of a cost analysis model for the acquisition of a permanent lunar base [ILR-MITT-245(1990)] N91-19114
Experimental reduction of simulated lunar glass by carbon and hydrogen and implications for lunar base oxygen production N91-20009

LUNAR EVOLUTION
Wanted: Lunar detectives to unravel the mysteries of the Moon! Crime to be solved: Mass extinctions on the Moon by meteorite impact! N91-20010

LUNAR GEOLOGY
Orientale and South Pole-Aitken basins on the Moon: Preliminary Galileo imaging results N91-20002
Wanted: Lunar detectives to unravel the mysteries of the Moon! Crime to be solved: Mass extinctions on the Moon by meteorite impact! N91-20010

LUNAR MARIA
Lunar maria and related deposits: Preliminary Galileo imaging results N91-20000
Orientale and South Pole-Aitken basins on the Moon: Preliminary Galileo imaging results N91-20002

LUNAR ROCKS
Experimental reduction of simulated lunar glass by carbon and hydrogen and implications for lunar base oxygen production N91-20009
Wanted: Lunar detectives to unravel the mysteries of the Moon! Crime to be solved: Mass extinctions on the Moon by meteorite impact! N91-20010

LUNAR SOIL
Experimental reduction of simulated lunar glass by carbon and hydrogen and implications for lunar base oxygen production N91-20009

LUNAR SURFACE
Dual-purpose self-deliverable lunar surface PV electrical power system N91-19200
Orientale and South Pole-Aitken basins on the Moon: Preliminary Galileo imaging results N91-20002

LUNAR SURFACE VEHICLES
Dual-purpose self-deliverable lunar surface PV electrical power system N91-19200

LUNGS
Lung volumes, chest wall configuration, and pattern of breathing in microgravity N91-19574

LYMPH
Gravity dependence of pleural liquid turnover N91-19651

LYMPHOCYTES
Effect of running and head down tilt bedrest on lymphocyte reactivity N91-19598
Experiment lymphocytes of Aragatz mission: Influence of the space flight on human T lymphocyte and monocyte functions N91-19619
Lymphocytes on sounding rockets N91-19620
Reduced lymphocyte activation in space: Role of cell-substratum interactions N91-19621
Increased mitogenic response in lymphocytes from chronically centrifuged mice N91-19634

M

MACH NUMBER
Experimental investigation of porous-floor effects on cavity flow fields at supersonic speeds [NASA-TP-3032] N91-19042
F-18 high alpha research vehicle surface pressures: Initial in-flight results and correlation with flow visualization and wind-tunnel data [NASA-TM-101724] N91-19051
Experimental investigation of a single flush-mounted hypermixing nozzle [NASA-TM-103726] N91-19374

MACHINE TOOLS
Local synthesis and tooth contact analysis of face-milled spiral bevel gears [NASA-CR-4342] N91-19439

MACROPHAGES
Subcellular signal transduction systems in the cellular trauma of ischemia [AD-A229876] N91-19709

MAGELLAN PROJECT (NASA)
Magellan: Preliminary description of Venus surface geologic units N91-20011

MAGELLAN SPACECRAFT (NASA)
Solar thermal vacuum tests of Magellan spacecraft N91-19127

MAGELLANIC CLOUDS
Proceedings of 146th IAU Symposium on Dynamics of Galaxies and Molecular Cloud Distribution [PB91-123661] N91-19994

MAGNESIUM ALLOYS
Texture and microstructure development in Al-2 percent Mg during high-temperature deformation [DE91-007355] N91-19480

MAGNESIUM OXIDES
Direct conversion of methane to C2's and liquid fuels [DE91-005729] N91-19313

MAGNETIC DIPOLES
Longitudinal periodicity in superconducting dipole magnets [DE91-008421] N91-19821
Elementary pulse diffraction problems and the generation of sound by a dipole moving across the edge of a half-plane [LR-565] N91-19831

MAGNETIC DISKS
Performance measurements of the first RAID prototype [NASA-CR-187958] N91-19718

MAGNETIC FIELD CONFIGURATIONS
Longitudinal periodicity in superconducting dipole magnets [DE91-008421] N91-19821
Experimental study of external kink instabilities in the Columbia high beta tokamak [DE91-008116] N91-19904
Relaxed states with plasma flow [DE91-008199] N91-19909

MAGNETIC FIELDS
Heterogeneous magnetoresistant layer [AD-D014665] N91-19289
An energy recovery system for a quasi-optical gyrotron [DE91-008317] N91-19357
Association of an auroral surge with plasma sheet recovery and the retreat of the substorm neutral line [DE91-007351] N91-19552
Possibility of raising efficiency of free-electron laser in longitudinal magnetic field N91-19804
Summary of the International Dawson Symposium on The Physics of Plasmas [DE91-006912] N91-19897
Higher harmonics of magnetization in the critical state of ceramic high Tc superconductors [DE91-615506] N91-19944
Magnetism and superconductivity in YBa2Cu3O(6+x) at 0.3 less than or equal to x less than or equal to 0.4 [DE91-615507] N91-19945

MAGNETIC FILMS
Photoelectron diffraction of magnetic ultrathin films: Fe/Cu(001) [DE91-007254] N91-19924

MAGNETIC FLUX
Magneto-elastic behaviour of steels for naval applications [MRL-TR-90-27] N91-19266
Elementary considerations on the gas dynamic design parameters of a MHD Faraday generator in relation to a gas turbine cycle [LR-564] N91-19456
Effect of paramagnetic impurities on dynamics of magnetic fluxes in superconductors N91-19816

MAGNETIC INDUCTION
Two-stage ion diode experiments on induction adder N91-19884
Pulse-power characteristic of VIVA-1 (Versatile Inductive Voltage Adder) N91-19888

MAGNETIC LEVITATION VEHICLES
Safety of high speed magnetic levitation transportation systems. Preliminary safety review of the transrapid maglev system [PB91-129684] N91-19326

MAGNETIC MATERIALS
Activities report of the Istituto Elettrotecnico Nazionale Galileo Ferraris [ETN-91-98868] N91-19822

MAGNETIC MEASUREMENT
Longitudinal periodicity in superconducting dipole magnets [DE91-008421] N91-19821

MAGNETIC PROPERTIES
Property and microstructural nonuniformity in the yttrium-barium-copper-oxide superconductor determined from electrical, magnetic, and ultrasonic measurements [NASA-TM-103732] N91-19463
Magnetism and superconductivity in YBa2Cu3O(6+x) at 0.3 less than or equal to x less than or equal to 0.4 [DE91-615507] N91-19945

MAGNETIC PUMPING
Loss analysis of the thermodynamic cycle of magnetic heat pumps [DE91-007669] N91-19950

MAGNETIC SIGNALS
Wire-free arming system for an aircraft-delivered bomb [AD-D014611] N91-19076

MAGNETIC STORAGE
Solid state electronic emulator of a multiple track motor driven rotating magnetic memory [AD-D014705] N91-19437

MAGNETIC SUSPENSION
Development of a vibration isolation prototype system for microgravity space experiments [NASA-TM-103664] N91-19324

MAGNETIC TAPES
Laser Tracker 2: Sandia National Laboratories' second generation laser tracking system [DE91-007711] N91-19424

MAGNETIZATION
Magneto-elastic behaviour of steels for naval applications [MRL-TR-90-27] N91-19266
Higher harmonics of magnetization in the critical state of ceramic high Tc superconductors [DE91-615506] N91-19944

Magnetism and superconductivity in YBa2Cu3O(6+x) at 0.3 less than or equal to x less than or equal to 0.4
[DE91-615507] N91-19945

MAGNETOHYDRODYNAMIC FLOW
Relaxed states with plasma flow
[DE91-008199] N91-19909
New method for edge plasma control by RF ponderomotive force
[DE91-744823] N91-19911

MAGNETOHYDRODYNAMIC GENERATORS
Two-dimensional non-reacting jet-gas mixing in an MHD (magnetohydrodynamic) second stage combustor
[DE91-006015] N91-19252
Computer controlled MHD power consolidation and pulse generation system
[DE91-006793] N91-19347
Elementary considerations on the gas dynamic design parameters of a MHD Faraday generator in relation to a gas turbine cycle
[LR-564] N91-19456
Performance characteristics of an MHD (Magnetohydrodynamic) pilot plant electrostatic precipitator
[DE91-007218] N91-19905
Noble gas disk MHD generator performance with unstable nonequilibrium plasma
[ISBN-90-9003671-7] N91-19916

MAGNETOHYDRODYNAMIC STABILITY
Theory of the ion-channel laser
[DE91-007643] N91-19423
Electromagnetic ion/ion cyclotron instability
[DE91-004841] N91-19860
Review of recent stellarator results in the USA, the USSR, and Japan
[DE91-007798] N91-19901
A method for determining poloidal coil configurations for tokamak devices
[DE91-007940] N91-19903
Experimental study of external kink instabilities in the Columbia high beta tokamak
[DE91-008116] N91-19904
Effects of pressure profile and plasma shaping on the n=1 internal kink mode in JT-60/JT-60U pellet fuelled plasmas
[DE91-744965] N91-19914
Noble gas disk MHD generator performance with unstable nonequilibrium plasma
[ISBN-90-9003671-7] N91-19916

MAGNETOHYDRODYNAMICS
Energy sciences supercomputing 1990
[DE91-007188] N91-19740
Performance characteristics of an MHD (Magnetohydrodynamic) pilot plant electrostatic precipitator
[DE91-007218] N91-19905
The magnetohydrodynamics coal-fired flow facility
[DE91-007672] N91-19906

MAGNETOMETERS
Magnetic cleanliness verification approach on tethered satellite N91-19158
Heterogeneous magnetoresistant layer
[AD-D014665] N91-19289

MAGNETOPLASMADYNAMICS
Enhancing space transportation: The NASA program to develop electric propulsion
[NASA-TM-4244] N91-19181

MAGNETOSTRICTION
Heterogeneous magnetoresistant layer
[AD-D014665] N91-19289
A variational approach to magneto-elastic buckling problems
[ETN-91-98929] N91-19338

MAGNETRON SPUTTERING
Application of functional gradient materials in the aerospace industry
[MBB-Z-0320-90-PUB] N91-19311

MAINTENANCE
Alternative strategies for the maintenance of geostationary space power plants
[ILR-MITT-249(1990)] N91-19170
Results from the third year of operation of the Federal methanol fleet at Argonne National Laboratory
[DE91-007822] N91-19451
Modeling and analysis of orthotropic plate with circular cutout and adhesive bonded patch
[AD-A229866] N91-19496
DHE (Downhole Heat Exchangers)
[DE91-006620] N91-19509
ARCHY (analysis and reverse engineering of code using hierarchy and Yourdon): A tool for FORTRAN code maintenance and development
[DE91-007241] N91-19720

MAN ENVIRONMENT INTERACTIONS
A status report on the analysis of the NOAA-9 SBUV/2 sweep mode solar irradiance data N91-19518
Evaluation of significant anthropogenic sources of radiatively important trace gases
[PB91-127753] N91-19545

MAN MACHINE SYSTEMS
Automatic speech recognition in air traffic control: A human factors perspective N91-19025
Army-NASA aircrew/aircraft integration program (A3I) software detailed design document, phase 3
[NASA-CR-177557] N91-19714

MAN-COMPUTER INTERFACE
Analyzing thought-related electroencephalographic data using nonlinear techniques N91-19031
A valiant little terminal: A VLT user's manual
[DE91-007295] N91-19719
Formal specification of human-computer interfaces N91-20023

MANAGEMENT METHODS
The OAST space power program N91-19183

MANAGEMENT PLANNING
COMPLEAT (community-oriented model for planning least-cost energy alternatives and technologies): A planning tool for publicly owned electric utilities
[DE91-006955] N91-19511

MANAGEMENT SYSTEMS
The temporal logic of the tower chief system N91-19026
Problems at National Aeronautics and Space Administration
[S-HRG-101-1146] N91-19969

MANIFOLDS (MATHEMATICS)
Symmetries on the space of (2,2) superstring vacua and automorphism groups of Calabi-Yau manifolds
[DE91-008218] N91-19951

MANIPULATORS
A rigid body model and decoupled control architecture for two manipulators holding a complex object
[DE91-007827] N91-19444
Minimum-time trajectory control of a two-link flexible robotic manipulator
[DE91-001261] N91-19448
System description document for the Anthrobot-2: A dexterous robot hand
[NASA-TM-104535] N91-19449
Real-time sensor-based approach to the improvement of transitions of robot manipulator controls
[OUEL-1866/90] N91-19459

MANNED SPACE FLIGHT
New experimental approach in quality factor and dose equivalent determination during a long term manned space mission N91-19679

MANUALS
Proposed draft military handbook presenting requirements for an Electronic Display System (EDS) for Interactive Electronic Technical Manuals (IETMs)
[AD-A227471] N91-19342
Improved syntactic disambiguation in the FASIT automatic indexing environment N91-19956
Environmental Sciences Division computing and geographic information system facility user handbook
[DE91-007820] N91-19961

MANUFACTURING
Silver-sheathed multifilament wires
[DE91-008107] N91-19941

MANY BODY PROBLEM
Statistics of peaks in cosmological nonlinear density fields
[DE91-744972] N91-19990

MAPPING
Design, performance evaluation, and investigation of the theoretical capabilities of the NASA Millimeter-wave Imaging Radiometer (MIR)
[NASA-CR-187984] N91-19398
An evaluation of co-planar lineament analysis and some thoughts on using surface geological data to predict sub-surface geology
[DE90-009687] N91-19556

MARINE BIOLOGY
Microgravity and development of aquatic animals N91-19625
Effect of hyper-gravity on the swimming behavior of aquatic vertebrates N91-19626

MARKETING
Direct conversion of methane to C2's
[DE91-005730] N91-19251

MARKOV PROCESSES
Regular unitary dilation of commuting contractions and Markovian representations of Gaussian stationary processes on the set Z(2)
[TELECOM-90-D-009] N91-19798

MARS (PLANET)
Cycling space ship transportation device for continuous link between Earth and Mars
[ILR-MITT-247(1990)] N91-19121
Twenty-Second Lunar and Planetary Science Conference
[NASA-CR-187971] N91-19995
Ancient oceans and Martian paleohydrology N91-19997
Relative chronology of Martian volcanoes N91-20007
What were the effects of the formation of the Borealis basin, Mars N91-20014

MARS ATMOSPHERE
Hubble Space Telescope observations of Mars N91-20003
Chemical approaches to carbon dioxide utilization for manned Mars missions
[NASA-TM-103728] N91-20015

MARS CRATERS
Relative chronology of Martian volcanoes N91-20007

MARS ENVIRONMENT
Simulation of Martian dust accumulation on surfaces N91-19160
Hubble Space Telescope observations of Mars N91-20003

MARS PROBES
Solar electric propulsion for Mars transport vehicles
[NASA-TM-103234] N91-19178

MARS SURFACE
Aeolian removal of dust types from photovoltaic surfaces on Mars N91-19156
Simulation of Martian dust accumulation on surfaces N91-19160
Feasibility of solar power for Mars N91-19201
Ancient oceans and Martian paleohydrology N91-19997
Mars radar mapping: Strong depolarized echoes from the Elysium/Amazonis outflow channel complex N91-20001
Hubble Space Telescope observations of Mars N91-20003
Relative chronology of Martian volcanoes N91-20007
What were the effects of the formation of the Borealis basin, Mars N91-20014

MARS VOLCANOES
Relative chronology of Martian volcanoes N91-20007

MASS
Performance, size, mass, and cost estimates for projected 1kW EOL Si, InP, and GaAs arrays N91-19199

MASS SPECTROMETERS
Finnigan ion trap mass spectrometer detection limits and thermal energy analyzer interface status report and present capabilities
[DE91-006220] N91-19254

MASS SPECTROSCOPY
Screening volatile organics by direct sampling ion trap and glow discharge mass spectrometry
[DE91-007708] N91-19258
A study of alkaline element interferences in analytical inductively coupled plasmas
[ISAL-90-0069] N91-19915
Cosmic dust: Laboratory analyses of extremely small particles N91-20013

MASS TRANSFER
Thermal-hydraulic model of a solid-oxide fuel cell
[DE91-006393] N91-19507

MASSIVELY PARALLEL PROCESSORS
Particle-in-cell plasma simulation codes on the connection machine
[DE91-007845] N91-19902

MATERIALS SCIENCE
Materials sciences programs
[DE91-007601] N91-19953

MATERIALS TESTS
A flammability study of thin plastic film materials N91-20034

MATHEMATICAL LOGIC
Topological models for space and time
[OUEL-1860/90] N91-19774

MATHEMATICAL MODELS
A flight-dynamic helicopter mathematical model with a single flap-lag-torsion main rotor
[NASA-TM-102267] N91-19041
Multigrid solution of compressible turbulent flow on unstructured meshes using a two-equation model
[NASA-CR-187513] N91-19043
The effect of body shape on the development of vortex asymmetry in the flow past slender bodies
[BU-413] N91-19068
Project of a cost analysis model for the acquisition of a permanent lunar base
[ILR-MITT-245(1990)] N91-19114
LOX/hydrogen coaxial injector atomization test program
[NASA-CR-187037] N91-19117
The 5th Annual NASA Spacecraft Control Laboratory Experiment (SCOLE) Workshop, part 2
[NASA-CP-10057-PT-2] N91-19122
Thermal control for the ground simulation of a space IR sensor system N91-19140
Magnetic cleanliness verification approach on tethered satellite N91-19158

Alternative strategies for the maintenance of geostationary space power plants
[ILR-MITT-249(1990)] N91-19170
Multi-dimensional modeling of a thermal energy storage canister
[NASA-TM-103731] N91-19177
GaAs solar cell photoresponse modeling using PC-1D V2.1 N91-19193
Determination of series resistance of indium phosphide solar cells N91-19207
Constitutive models for composites based on numerical micromechanics
[ISBN-90-9003733-0] N91-19248
Control of catalytic hydrotreating selectivity with ammonia
[DE91-005511] N91-19250
Basic research model of natural gas combustion in turbulent flow
[PB91-130260] N91-19264
Assessing the impact of large-scale computing on the size and complexity of first-principles electromagnetic models
[DE91-007491] N91-19333
Measurement of electromagnetic fields over a small electrolytic tank
[DE91-007500] N91-19334
Sodium/metal chloride program conceptual design study
[DE91-007216] N91-19353
Viability study of photovoltaic systems added to terrestrial electric vehicles
[DE91-007689] N91-19355
Identification of flow and volume parameters in multizone systems using a single gas tracer technique
[DE91-006894] N91-19368
Numerical and physical modelling of bubbly flow phenomena
[DE91-007461] N91-19377
Liquid sloshing in cargo tanks. Liquid slosh loading in slack ship tanks: Forces on internal structure and pressures
[PB91-129262] N91-19383
Calculation of pulsating liquid free jets
[MPIS-15/1990] N91-19385
Methods for combining a theoretical and an empirical approach in modelling pressure and flow control valves for CAE-programs for fluid power circuits
[ACTA-POLYTEC-SCAND-ME-96] N91-19392
Simulation of a standing-wave free-electron laser
[DE91-007330] N91-19418
Phase stability of a standing-wave free-electron laser
[DE91-008068] N91-19427
Local synthesis and tooth contact analysis of face-milled spiral bevel gears
[NASA-CR-4342] N91-19439
A modelling of unsteady air flow in the resonance charging system of high speed diesel engines
[ACTA-POLYTEC-SCAND-ME-97] N91-19454
Application of thermal life prediction model to high-temperature aerospace alloys B1900+Hf and Haynes 188
[NASA-TM-4226] N91-19473
Thermal-hydraulic model of a solid-oxide fuel cell
[DE91-006393] N91-19507
COMPLEAT (community-oriented model for planning least-cost energy alternatives and technologies): A planning tool for publicly owned electric utilities
[DE91-006955] N91-19511
A non-linear method for the calculation of the power output of a rotating wind turbine
[BU-416] N91-19512
Cloud forcing: A modeling perspective
[DE91-007215] N91-19551
Influence of various parameters on the V'O2 frequency response of the body. A theoretical study on the basis of a nonlinear model N91-19594
A stochastic performance model for the neutron diffusion nodal method on a multiuser parallel supercomputer
[DE90-017015] N91-19749
Use of system identification techniques for improving airframe finite element models using test data
[NASA-CR-188041] N91-19750
Rational model identification using an extended least squares algorithm
[RR-388] N91-19753
Topological models for space and time
[OUEL-1860/90] N91-19774
The cost-constrained traveling salesman problem
[DE91-004943] N91-19775
Anastasia: A solid model based 3D finite difference mesh generator
[DE91-007621] N91-19783
A novel isoparametric finite element displacement formulation for axisymmetric analysis of nearly incompressible materials
[OUEL-1872/91] N91-19791
The study of effects of small perturbations on chaotic systems
[DE91-007320] N91-19792
Constructing mathematical model of adaptive anti-flutter system N91-19810
Near resonant absorption by atoms in intense fluctuating fields
[DE91-007911] N91-19839
The specification of glancing incidence mirrors in terms of system performance
[DE91-007556] N91-19873
Free energy simulation of grain boundary segregation the thermodynamics in Ni(3-x)Al(1+x)
[DE91-007473] N91-19928
Primordial nucleosynthesis: Beyond the standard model
[DE91-007264] N91-19984
Statistics of peaks in cosmological nonlinear density fields
[DE91-744972] N91-19990
Impact processes in the Solar System: New understandings through numerical modeling N91-19996

MATHEMATICAL PROGRAMMING
Parameter estimation of structural dynamic models using Eigenvalue and Eigenvector information
[DE91-004379] N91-19793
The development of structure for the representation and manipulation of sophisticated knowledge in intelligent systems
[AD-A229114] N91-19957

MATHEMATICS
JPRS report: Science and technology. USSR: Physics and mathematics
[JPRS-UPM-90-004] N91-19800

MATRICES (MATHEMATICS)
Response matrix Monte Carlo based on a general geometry local calculation for electron transport
[DE91-007638] N91-19794

MATRIX MATERIALS
Probabilistic micromechanics and macromechanics of polymer matrix composites
[NASA-TM-103669] N91-19236
Comparison of dynamic fatigue behavior between SiC whisker-reinforced composite and monolithic silicon nitrides
[NASA-TM-103707] N91-19293

MEAN SQUARE VALUES
Optimal observation directions for estimating a vector
[PREPRINT-1285] N91-19796

MEASUREMENT
Fiber optic interferometric measuring method for the determination of a very small polarization coefficient
[MBB-UA-1185-90-PUB] N91-19876

MEASURING INSTRUMENTS
Using a modified Hewlett Packard 8410 network analyzer as an automated farfield antenna range receiver
[NASA-TM-103700] N91-19349
Rotating pressure measurement system using an on board calibration standard
[NASA-TM-103676] N91-19401
Measurement of eye movements in space-related research environments N91-19591

MECHANICAL PROPERTIES
Status of GaAs/Ge solar cells N91-19185
Effect of fiber reinforcements on thermo-oxidative stability and mechanical properties of polymer matrix composites
[NASA-TM-103648] N91-19234
Composite materials for space applications
[NASA-CR-187472] N91-19238
The mechanical behavior of microcellular foams
[DE91-006775] N91-19291
Crystallization and properties of Sr-Ba aluminosilicate glass-ceramic matrices
[NASA-TM-103764] N91-19308
Application of high speed photography to the study of high strain rate materials testing
[OUEL-1852/90] N91-19411
Mechanical behavior of a ceramic matrix composite material
[NASA-CR-187072] N91-19461

MELTING
Part 1: The effect of lattice defects on the sintering of lithium fluoride; Part 2: The morphology of calcium oxide from calcium carbonate decomposition
[DE91-007743] N91-19934

MELTING POINTS
A flammability study of thin plastic film materials N91-20034

MEMBRANE STRUCTURES
Gravity perception by non-specialized structures N91-19636

MEMBRANES
Preliminary study of a membrane bioreactor for cell culture in space N91-19627

MEMORY (COMPUTERS)
Capattery double layer capacitor life performance
[DE91-006639] N91-19344
Enhanced crosstie random access memory element and process for the fabrication thereof
[AD-D014723] N91-19717

MENTAL PERFORMANCE
Effects of high temperature and humidity on mental state and metabolism N91-19571

MESSAGE PROCESSING
Complete exchange on the iPSC-860
[NASA-CR-187498] N91-19715

METABOLISM
Spatial and temporal relationships between localized microbial metabolic activity and electrochemical activity of steel
[DE91-008102] N91-19279
Effects of high temperature and humidity on mental state and metabolism N91-19571
Medical results of the fourth prime expedition on the orbital station Mir N91-19576
Influence of various parameters on the V'O2 frequency response of the body. A theoretical study on the basis of a nonlinear model N91-19594
Adaptive responses in monkeys during two week space flight N91-19645

METAL FIBERS
Method of producing glass fiber with cores of a different material
[AD-D014664] N91-19288

METAL FILMS
Some roles for TEM in the development of new materials
[DE91-007742] N91-19933

METAL HYDRIDES
Hydrogen storage in metal hydrides
[DE91-746267] N91-19316

METAL IONS
Control of texture and defect structure for hot-filament-assisted CVD (Chemical Vapor Deposition) diamond Films
[DE91-008373] N91-19310

METAL MATRIX COMPOSITES
METCAN updates for high temperature composite behavior: Simulation/verification
[NASA-TM-103682] N91-19229
Computational simulation of hot composites structures
[NASA-TM-103681] N91-19230
Low-density, high-strength intermetallic matrix composites by XD (trademark) synthesis
[NASA-TM-103724] N91-19233
Concurrent micromechanical tailoring and fabrication process optimization for metal-matrix composites
[NASA-TM-103670] N91-19237
The application of neutron diffraction time-of-flight measurements to the study of strain in composites
[DE91-008106] N91-19242

METAL OXIDES
Direct conversion of methane to C2's and liquid fuels
[DE91-007545] N91-19318
Thermal conductivity of high-temperature superconductors in normal state N91-19818

METAL PLATES
Interferometry, streak photography, and stereo photography of laser-driven miniature flying plates
[DE91-007493] N91-19405

METAL POWDER
Synthesis and structures of metal chalcogenide precursors
[NASA-TM-103665] N91-19296

METAL PROPELLANTS
Advanced chemical propulsion at NASA Lewis: Metallized and high energy density propellants
[NASA-TM-103771] N91-19175
Solid fuel combustion chamber
[LR-648] N91-19222

METAL SURFACES
Reactivity of pi-complexes of Ti, V, and Nb towards dithioacetic acid: Synthesis and structure of novel metal sulfur-containing complexes
[NASA-TM-103666] N91-19256
Spatial and temporal relationships between localized microbial metabolic activity and electrochemical activity of steel
[DE91-008102] N91-19279
Atomic beam studies of the interaction of hydrogen with transition metal surfaces
[DE91-007938] N91-19841
Considerations relating to pulsed-beam modification of materials
[DE91-006771] N91-19922

METAL VAPOR LASERS
Copper vapor as active medium for high-power oscillator-amplifier laser systems N91-19806

METAL VAPORS
The physics of laser polarized muonic atoms [DE91-008045] N91-19845
METALLIZING
Phase equilibrium modeling for high temperature metallization on GaAs solar cells N91-19192
Semiconductor structural damage attendant to contact formation in III-V solar cells N91-19203
METALS
Excimer laser surface processing for tribological applications in metals and ceramics [DE91-002324] N91-19428
METASTABLE STATE
Theoretical investigation of phase stability in non-magnetic Fe-V substitutional alloys [DE91-006711] N91-19268
METEORITE CRATERS
K/T age for the popigai impact event N91-19999
METEORITES
Wanted: Lunar detectives to unravel the mysteries of the Moon! Crime to be solved: Mass extinctions on the Moon by meteorite impact! N91-20010
METEORITIC COMPOSITION
Stable hydrogen and carbon isotope ratios of extractable hydrocarbons in the Murchison meteorite N91-20006
Wanted: Lunar detectives to unravel the mysteries of the Moon! Crime to be solved: Mass extinctions on the Moon by meteorite impact! N91-20010
METEORITIC DAMAGE
Effects of a giant impact on Uranus N91-20012
METEOROIDS
Hypervelocity impact physics [NASA-CR-4343] N91-19164
METEOROLOGICAL PARAMETERS
Atmospheric environment for space shuttle (STS-41) launch [NASA-TM-103525] N91-19529
Overview of climate information needs for ecological effects models [PB91-125898] N91-19549
METEOROLOGICAL RADAR
World weather watch: Regional association 4: Hurricane operational plan, supplement 2 [WMO-524-SUPPL-2] N91-19563
METEOROLOGY
Atmospheric environment for space shuttle (STS-41) launch [NASA-TM-103525] N91-19529
METHANE
Direct conversion of methane to C2's [DE91-005730] N91-19251
Methane to methanol conversion by direct partial oxidation [DE91-007352] N91-19257
Mechanisms and controlling characteristics of the catalytic oxidation of methane [DE91-008033] N91-19263
Direct conversion of methane to C2's and liquid fuels [DE91-005729] N91-19313
Direct conversion of methane to C2's and liquid fuels [DE91-007545] N91-19318
Mechanisms controlling the production and transport of methane, carbon dioxide, and dissolved solutes within a large boreal peat basin [DE91-008115] N91-19543
METHYL ALCOHOL
Methane to methanol conversion by direct partial oxidation [DE91-007352] N91-19257
Methanol reformers for fuel cell powered vehicles: Some design considerations [DE91-006465] N91-19314
Alternative fuels for heavy duty engines: Status of fleet trials [DE91-006799] N91-19315
Results from the third year of operation of the Federal methanol fleet at Argonne National Laboratory [DE91-007822] N91-19451
Exhaust emissions from heavy duty vehicles [DE91-006798] N91-19531
METHYLHYDRAZINE
Low level vapor verification of monomethyl hydrazine N91-20032
METROLOGY
Principle and realization of the instrument used for the CIRCE experiment on board the Mir station N91-19684
Activities report of the Istituto Elettrotecnico Nazionale Galileo Ferraris [ETN-91-98868] N91-19822
MICE
Increased mitogenic response in lymphocytes from chronically centrifuged mice N91-19634
Hypergravity and bone mineralization N91-19650
MICROANALYSIS
High resolution microstructural and microchemical analysis of zirconia eutectic interfaces [DE91-008032] N91-19940
MICROBIOLOGY
Microbiological assay using bioluminescent organism [AD-D014651] N91-19249
MICROBURSTS (METEOROLOGY)
Investigation of air transportation technology at Princeton University, 1989-1990 N91-19033
MICROCHANNEL PLATES
Measurements with a 35 psec gate time microchannelplate camera [DE91-006701] N91-19400
MICROELECTRONICS
Application of non-cyanide gold for selective plating of microelectronic circuits [DE91-007729] N91-19276
Sandia technology: Engineering and science applications [DE91-006760] N91-19322
Optical diagnostics for low-temperature plasmas [DE91-007896] N91-19907
MICROGRAVITY APPLICATIONS
Microgravity strategic plan, 1988 [NASA-TM-103397] N91-19319
A new approach to electrophoresis in space N91-19653
Free flow electrophoresis experiment TEPE 3 on TEXUS 24 N91-19654
Plant biotechnology in space: Facts and speculations N91-19664
Protein purification in multicompartment electrolyzers for crystal growth of r-DNA products in microgravity N91-19665
The 1989-1990 NASA space biology accomplishments [NASA-TM-4258] N91-19697
MICROMECHANICS
Probabilistic micromechanics and macromechanics of polymer matrix composites [NASA-TM-103669] N91-19236
Concurrent micromechanical tailoring and fabrication process optimization for metal-matrix composites [NASA-TM-103670] N91-19237
Constitutive models for composites based on numerical micromechanics [ISBN-90-9003733-0] N91-19248
MICROMETEOROIDS
Hypervelocity impact physics [NASA-CR-4343] N91-19164
Space debris: Orbital microparticulates impacting LDEF experiments favour a natural extraterrestrial origin N91-20008
Cosmic dust: Laboratory analyses of extremely small particles N91-20013
MICROORGANISMS
Simultaneous tracking of flagellates in real time by image analysis N91-19677
MICROPARTICLES
Integrated Cryogenic Experiment (ICE) microsphere investigation [NASA-CR-177538] N91-19323
MICROPHONES
A gradient microphone for locating sound targets [MBB-Z-0341-90-PUB] N91-19829
MICROPOROSITY
Phenomena affecting morphology of microporous poly(acrylonitrile) prepared via phase separation from solution [DE91-004501] N91-19297
MICROPROCESSORS
The FORCE: A highly portable parallel programming language [NASA-CR-187928] N91-19732
Formal proof of the AVM-1 microprocessor using the concept of generic interpreters [NASA-CR-187491] N91-19756
MICROSCOPES
The slow-rotating centrifuge microscope (NIZEMI): A new research tool for terrestrial and space-related gravitational biology N91-19663
MICROSTRIP TRANSMISSION LINES
Soliton Microwave Generator [DE91-008277] N91-19335
MICROSTRUCTURE
Constitutive models for composites based on numerical micromechanics [ISBN-90-9003733-0] N91-19248
Ultrafine refractory particle formation in counterflow diffusion flames [DE91-007693] N91-19260
The 70 percent tungsten heavy alloys: Processing and properties [DE91-008259] N91-19282
Property and microstructural nonuniformity in the yttrium-barium-copper-oxide superconductor determined from electrical, magnetic, and ultrasonic measurements [NASA-TM-103732] N91-19463
Texture and microstructure development in Al-2 percent Mg during high-temperature deformation [DE91-007355] N91-19480
The effect of elastic stress on Ostwald ripening phenomena [DE91-008034] N91-19484
High resolution microstructural and microchemical analysis of zirconia eutectic interfaces [DE91-008032] N91-19940
Silver-sheathed multifilament wires [DE91-008107] N91-19941
MICROWAVE AMPLIFIERS
An energy recovery system for a quasi-optical gyrotron [DE91-008317] N91-19357
MICROWAVE ANTENNAS
C-band antennas for regional communication systems [MBB-UK-0107-90-PUB] N91-19336
Using a modified Hewlett Packard 8410 network analyzer as an automated farfield antenna range receiver [NASA-TM-103700] N91-19349
MICROWAVE EQUIPMENT
Using a modified Hewlett Packard 8410 network analyzer as an automated farfield antenna range receiver [NASA-TM-103700] N91-19349
MICROWAVE FREQUENCIES
Effects of soil and canopy characteristics on microwave backscattering of vegetation [NASA-CR-188022] N91-19497
Apparatus for determining microwave characteristics of superconductive materials using a resonant cavity and calibration waveguides [AD-D014694] N91-19918
MICROWAVE IMAGERY
Design, performance evaluation, and investigation of the theoretical capabilities of the NASA Millimeter-wave Imaging Radiometer (MIR) [NASA-CR-187984] N91-19398
MICROWAVE OSCILLATORS
A program of high power microwave source research and development from 8 GHz to 600 GHz [DE91-008320] N91-19358
MICROWAVE POWER BEAMING
Soliton Microwave Generator [DE91-008277] N91-19335
MICROWAVE TRANSMISSION
Soliton Microwave Generator [DE91-008277] N91-19335
MICROWAVES
Coplanar waveguide EEsoF MICAD macros make circuit layout easy [NASA-TM-103272] N91-19332
Measured performance of the half-scale accurate antenna reflector [NASA-CR-187047] N91-19350
A program of high power microwave source research and development from 8 GHz to 600 GHz [DE91-008320] N91-19358
Development of components and subsystems for low noise receivers at micro- and millimeter waves [S-187] N91-19363
Intense microwave generation using free-electron lasers [DE91-007262] N91-19417
Simulation of a standing-wave free-electron laser [DE91-007330] N91-19418
Origin of residual surface resistance of ceramic high-temperature superconductors N91-19814
MILITARY AIRCRAFT
The application of aero gas turbine engine monitoring systems to military aircraft [ETN-91-98852] N91-19096
MILITARY AVIATION
The impact of the new management strategy on senior operational commanders at group level within Royal Air Force Strike Command [REPT-89SDM/MCHALE/03-MDA] N91-19954
MILITARY HELICOPTERS
MBB's involvement in military helicopter programmes [MBB-UD-0588-90-PUB] N91-19091
MILITARY OPERATIONS
The impact of the new management strategy on senior operational commanders at group level within Royal Air Force Strike Command [REPT-89SDM/MCHALE/03-MDA] N91-19954
MILITARY TECHNOLOGY
Proposed draft military handbook presenting requirements for an Electronic Display System (EDS) for Interactive Electronic Technical Manuals (IETMs) [AD-A227471] N91-19342

MILLIMETER WAVES
Development of components and subsystems for low noise receivers at micro- and millimeter waves
[S-187] N91-19363
MIR SPACE STATION
The biological and medical programme of the manned Aragatz mission on the Mir Space Station N91-19617
MIRRORS
Solar rocket plume/mirror interactions
[NASA-CR-185300] N91-19059
Hubble Space Telescope secondary mirror vertex radius/conic constant test
[NASA-CR-187989] N91-19871
The specification of glancing incidence mirrors in terms of system performance
[DE91-007556] N91-19873
The specification of glancing incidence mirrors in terms of system performance
[DE91-007564] N91-19874
MISSILE SYSTEMS
Launching projectiles with hydrogen gas generated from titanium-water reactions
[AD-D014653] N91-19171
MISSILES
Sandia technology: Engineering and science applications
[DE91-006760] N91-19322
MIXED OXIDES
Property and microstructural nonuniformity in the yttrium-barium-copper-oxide superconductor determined from electrical, magnetic, and ultrasonic measurements
[NASA-TM-103732] N91-19463
Phenomenological theory of phase transitions to nonhomogeneous noncommensurate phase with superconducting current N91-19817
Thermal conductivity of high-temperature superconductors in normal state N91-19818
Phase formation in the Tl-Ca-BaCu-O system
[DE91-008184] N91-19942
MIXERS
Rapid mix concepts for low emission combustors in gas turbine engines
[NASA-CR-185292] N91-19048
Fluid mixing device having a conical inlet and a noncircular outlet
[AD-D014708] N91-19364
MODAL RESPONSE
Thermoelastic vibration test techniques
[NASA-TM-101742] N91-19083
Modal identification of a deployable space truss
[NASA-TM-102720] N91-19474
MODE (STATISTICS)
Modal analysis of UH-60A instrumented rotor blades
[NASA-TM-4239] N91-19052
MODEL REFERENCE ADAPTIVE CONTROL
Minimum-time trajectory control of a two-link flexible robotic manipulator
[DE91-001261] N91-19448
MODFETS
Ellipsometric study of InGaAs MODFET material
[NASA-TM-103286] N91-19351
Study of InGaAs based MODFET structures using variable angle spectroscopic ellipsometry
[NASA-TM-103792] N91-19935
MODULATORS
A modulated high-power optical source specification
[AD-D014654] N91-19869
MODULES
Centrifuge Facility Conceptual System Study. Volume 1: Facility overview and habitats
[NASA-TM-102860] N91-19566
MOISTURE
Climatic water budgets, effective moisture, and elevation in the Southern Sierra Nevada, California, 1951-1980
[PB91-127878] N91-19500
MOLDING MATERIALS
Extrudable PBX molding powder
[AD-D014667] N91-19312
MOLECULAR BEAM EPITAXY
Compound semiconductors, strained layer epitaxy, and the information age
[DE91-007735] N91-19932
MOLECULAR BEAMS
Aerodynamic focusing of particles and heavy molecules
[DE91-006922] N91-19833
MOLECULAR BIOLOGY
Physiological genetics of denitrification: A route to conserving fixed nitrogen
[DE91-008157] N91-19707
MOLECULAR CLOUDS
Detection of an isotopic short submillimeter CO line: Column densities of warm gas in molecular clouds
[MPE-PREPRINT-178] N91-19976
Fluorescent HD emission from photodissociation regions
[MPE-PREPRINT-177] N91-19982
Proceedings of 146th IAU Symposium on Dynamics of Galaxies and Molecular Cloud Distribution
[PB91-123661] N91-19994
MOLECULAR EXCITATION
Cross section for production of excited hydrogen atoms following dissociative excitation of molecular hydrogen by electron impact
[DE91-745035] N91-19852
MOLECULAR FLOW
The performance of multilayer insulation in a rapidly depressurizing environment N91-19133
Contributions to the Non Equilibrium Molecular Dynamics (NEMD) computer simulation for transport processes in simple fluids
[ETN-91-98921] N91-19393
MOLECULES
Extraterrestrial organic molecules and the emergence of life on Earth N91-19681
Aerodynamic focusing of particles and heavy molecules
[DE91-006922] N91-19833
MOLTEN SALTS
The design of future central receiver power plants based on lessons learned from the Solar One Pilot Plant
[DE91-005224] N91-19510
MOLYBDATES
Research conducted at the Radiation Lab, Notre Dame Univ.
[DE91-007969] N91-19843
MOLYBDENUM COMPOUNDS
Ceramic fabrication R and D
[DE91-006537] N91-19298
MONITORS
A review of fiber optic and related technologies for environmental sensing applications
[DE91-007736] N91-19409
An on-line real-time system for fatigue crack growth monitoring
[DE91-007931] N91-19483
Analysis of SBUV/2 measurements of solar UV irradiance variations N91-19526
Visualisation of fluid shifts within the body during a parabolic flight by measurements of electrical bio-impedance N91-19688
Engineering monitoring expert system's developer
[NASA-CR-187914] N91-19765
MONKEYS
Adaptive responses in monkeys during two week space flight N91-19645
Preliminary studies before defining a payload adapted to the primate model N91-19648
Review of EEG studies in non human primates exposed to microgravity N91-19649
MONOCHROMATIC RADIATION
Mutation induction in dried yeast cells after irradiation with selected UVC- and UVB- wavelengths compared to simulated sunlight N91-19686
MONOCHROMATORS
Multiple energy computed tomography for neuroradiology with monochromatic x rays from the national synchrotron light source
[DE91-008108] N91-19712
MONOPOLES
Electric monopole transitions and shape coexistence in nuclei
[DE91-008141] N91-19847
MONOPULSE RADAR
Alternate approach for obtaining dynamic range in monopulse guidance systems
[AD-D014644] N91-19100
MONTE CARLO METHOD
Stochastic robustness: Towards a comprehensive robustness tool N91-19036
ETARA PC version 3.3 user's guide: Reliability, availability, maintainability simulation model
[NASA-TM-103751] N91-19462
Correlations of pseudo-random numbers of multiplicative sequence
[DE91-615076] N91-19788
Response matrix Monte Carlo based on a general geometry local calculation for electron transport
[DE91-007638] N91-19794
Variational Monte Carlo studies of electromagnetic structure of few-body nuclei
[DE91-007756] N91-19838
Variational Monte Carlo calculations of nuclear ground states
[DE91-007760] N91-19842
Predicted Bremsstrahlung generation by energetic electron beams
[DE91-007164] N91-19858
MOON
Twenty-Second Lunar and Planetary Science Conference
[NASA-CR-187971] N91-19995
MORPHOLOGY
Comparative morphology of configurations with reduced part count derived from the octahedral-tetrahedral truss
[NASA-TM-102768] N91-19168
Ultrafine refractory particle formation in counterflow diffusion flames
[DE91-007693] N91-19260
Control of texture and defect structure for hot-filament-assisted CVD (Chemical Vapor Deposition) diamond Films
[DE91-008373] N91-19310
Increased mitogenic response in lymphocytes from chronically centrifuged mice N91-19634
Does gravity play a role in the morphological development and function of the gravity sensory organ of vertebrates. DLR contribution to the D-2 project graviperception and neuronal plasticity, its technical realization and experimental execution N91-19635
Morphological, electronmicroscopical and biochemical aspects of hyper-gravity conditions during early ontogenetic development of Cichlid fish N91-19638
MOSAICS
Characterization of a defective interfering RNA that contains a mosaic of a plant viral genome
[DE91-007897] N91-19702
MOTION PICTURES
Laser Tracker 2: Sandia National Laboratories' second generation laser tracking system
[DE91-007711] N91-19424
MOTION SICKNESS
Simulation expert system for physiological mechanisms of the space motion sickness N91-19596
The biochemical and physiological variables in motion sickness followed modified neuroendocrine activity N91-19607
Standardization of motion sickness induced by left-right and up-down reversing prisms N91-19611
Vestibular tests on UK astronaut candidates for an Anglo/Russian space flight (Juno Mission) N91-19613
MOTION SIMULATION
Simulation expert system for physiological mechanisms of the space motion sickness N91-19596
The biochemical and physiological variables in motion sickness followed modified neuroendocrine activity N91-19607
Standardization of motion sickness induced by left-right and up-down reversing prisms N91-19611
MOTIVATION
Simulating motivated cognition
[NASA-TM-102886] N91-19770
MULLITES
Rigid mullitewhisker felt and method of preparation
[AD-D014648] N91-19225
MULTIGRID METHODS
Multigrid solution of compressible turbulent flow on unstructured meshes using a two-equation model
[NASA-CR-187513] N91-19043
MULTILAYER INSULATION
The performance of multilayer insulation in a rapidly depressurizing environment N91-19133
Multipurpose hardened spacecraft insulation N91-19136
MULTIPHOTON ABSORPTION
Studies of atmospheric molecules by multiphoton spectroscopy
[DE91-006738] N91-19554
Intense field non-resonant multiphoton absorption of diatomic molecules
[DE91-006920] N91-19835
MULTIPLEXING
Solid state electronic emulator of a multiple track motor driven rotating magnetic memory
[AD-D014705] N91-19437
MULTIPROCESSING (COMPUTERS)
Regional Oxidant Model Multi-Processor (ROMMP)
[PB91-131680] N91-19547
A new generation of real-time DOS technology for mission-oriented system integration and operation N91-19725
The FORCE: A highly portable parallel programming language
[NASA-CR-187928] N91-19732
A structured representation for parallel algorithm design on multicomputers
[DE91-006674] N91-19744
The PVM (Parallel Virtual Machine) system: Supercomputer level concurrent computation on a network of IBM RS/6000 power stations
[DE91-007844] N91-19757
MUONS
The physics of laser polarized muonic atoms
[DE91-008045] N91-19845

MURCHISON METEORITE
Stable hydrogen and carbon isotope ratios of extractable hydrocarbons in the Murchison meteorite N91-20006
MUSCLES
Reactivity of exhausted human skeletal muscle fibers following prolonged antiorthostatic hypokinesia N91-19568
Body proprioceptive references in weightlessness as studied by muscle tendon vibration N91-19581
Contractile protein changes induced by hindlimb suspension in rat skeletal muscle N91-19646
Hindlimb suspension of rabbit for one week: Myofibrillar damage in the soleus may depend on long-lasting shortening and periodic contraction against no load N91-19647
Central and peripheral cardiovascular responses to electrically induced and voluntary leg exercise N91-19687
MUSCULAR STRENGTH
Oxygen uptake during concentric and eccentric resistive exercise using a new gravity-independent ergometer N91-19587
Effects of training with reduced perfusion pressure on performance and muscle fiber characteristics N91-19615
Muscle function impairment following lower limb unloading in men N91-19616
MUSCULOSKELETAL SYSTEM
Reactivity of exhausted human skeletal muscle fibers following prolonged antiorthostatic hypokinesia N91-19568
Effects of hyperbaric oxygenation on central hemodynamics and oxygen consumption in severe physical trauma N91-19570
Is physiological tremor (microvibration) influenced by microgravity N91-19595
Contractile protein changes induced by hindlimb suspension in rat skeletal muscle N91-19646
MUTATIONS
Arabidopsis thaliana (Heynh.) pollen: A new tool in heavy ions radiation N91-19685
Mutation induction in dried yeast cells after irradiation with selected UVC- and UVB- wavelengths compared to simulated sunlight N91-19686

N

N-TYPE SEMICONDUCTORS
Surface chemistry at semiconductor-electrolyte interfaces
[DE91-005915] N91-19920
NACELLES
Propulsion system concept for the Eurofar tilt rotor aircraft
[MBB-UD-0573-90-PUB] N91-19084
NASA PROGRAMS
Advanced chemical propulsion at NASA Lewis: Metallized and high energy density propellants
[NASA-TM-103771] N91-19175
Solid earth science in the 1990s. Volume 1: Program plan
[NASA-TM-4256-VOL-1] N91-19499
The 1989-1990 NASA space biology accomplishments
[NASA-TM-4258] N91-19697
Space operations: NASA is not archiving all potentially valuable data
[GAO/IMTEC-91-3] N91-19955
Departments of Veterans Affairs and Housing and Urban Development, and Independent Agencies Appropriation Bill, 1991
[S-REPT-101-474] N91-19966
National Aeronautics and Space Administration N91-19967
Problems at National Aeronautics and Space Administration
[S-HRG-101-1146] N91-19969
Research reports: 1990 NASA/ASEE Summer Faculty Fellowship Program
[NASA-CR-187638] N91-20022
Research and technology, 1989
[NASA-TM-102264] N91-20039
NASA SPACE PROGRAMS
Space station: The next logical step
[NASA-TM-103398] N91-19123
NASTRAN
Modal analysis of UH-60A instrumented rotor blades
[NASA-TM-4239] N91-19052
Development and applications of a multi-level strain energy method for detecting finite element modeling errors
[NASA-CR-187447] N91-19478
NATIONAL AEROSPACE PLANE PROGRAM
High temperature NASP engine seal development
[NASA-TM-103716] N91-19441
A test fixture for measuring high-temperature hypersonic-engine seal performance
[NASA-TM-103658] N91-19442
NATIONAL AIRSPACE SYSTEM
Ridge regression signal processing N91-19029
NATURAL GAS
Basic research model of natural gas combustion in turbulent flow
[PB91-130260] N91-19264
An evaluation of co-planar lineament analysis and some thoughts on using surface geological data to predict sub-surface geology
[DE90-009687] N91-19556
NATURAL SATELLITES
Twenty-Second Lunar and Planetary Science Conference
[NASA-CR-187971] N91-19995
NAVIER-STOKES EQUATION
Calculations of separated 3-D flows with a pressure-staggered Navier-Stokes equations solver
[NASA-CR-187065] N91-19367
NAVIGATION
Joint University Program for Air Transportation Research, 1989-1990
[NASA-CP-3095] N91-19024
Design and control of a fully omnidirectional and holonomic wheeled platform for robotic vehicles
[DE90-017746] N91-19445
A new wheel control system for the omnidirectional HERMIES-3 robot
[DE90-017764] N91-19446
Visual navigation around curved obstacles
[OUEL-1861/90] N91-19458
NAVIGATION INSTRUMENTS
Integrated inertial/GPS N91-19032
NAVSTAR SATELLITES
Modeling selective availability of the NAVSTAR global positioning system N91-19030
NEAR FIELDS
Measured performance of the half-scale accurate antenna reflector
[NASA-CR-187047] N91-19350
NECK (ANATOMY)
Ocular roll under changing z-axis acceleration and neck position N91-19580
Multiple energy computed tomography for neuroradiology with monochromatic x rays from the national synchrotron light source
[DE91-008108] N91-19712
NEODYMIUM LASERS
Microsecond-pulse Nd-glass laser with monopulse duration control N91-19811
NETWORK ANALYSIS
Characterization of devices, circuits, and high-temperature superconductor transmission lines by electro-optic testing
[NASA-CR-187950] N91-19343
Using a modified Hewlett Packard 8410 network analyzer as an automated farfield antenna range receiver
[NASA-TM-103700] N91-19349
Development of a numerical computer code and circuit element models for simulation of firing systems
[DE91-007162] N91-19739
Model distribution in decentralized multi-sensor data fusion
[OUEL-1868/90] N91-19763
An expansion plan for the 60 Hz power distribution system at KSC: LC-39 substations load allocation plan N91-20028
NETWORK CONTROL
Computers at risk: Safe computing in the information age
[LC-90-22329] N91-19721
Towards practical control design using neural computation
[NASA-TM-103785] N91-19766
NEURAL NETS
Investigation of air transportation technology at Princeton University, 1989-1990 N91-19033
Neural networks in nonlinear aircraft control N91-19037
System identification for nonlinear control using neural networks N91-19039
Sandia technology: Engineering and science applications
[DE91-006760] N91-19322
Simple object recognition by neural networks: Application of the Hough transform
[RR-410] N91-19761
Artificial neural network implementation
[AD-D014663] N91-19764
Engineering monitoring expert system's developer
[NASA-CR-187914] N91-19765
Towards practical control design using neural computation
[NASA-TM-103785] N91-19766
Cascading a systolic array and a feedforward neural network for navigation and obstacle avoidance using potential fields
[NASA-CR-177575] N91-19771
The application of neural networks for fault diagnosis in nuclear reactors
[RR-411] N91-19772
The development of structure for the representation and manipulation of sophisticated knowledge in intelligent systems
[AD-A229114] N91-19957
NEUROLOGY
Neurological findings after 72 hours water immersion N91-19597
NEUROPHYSIOLOGY
Is physiological tremor (microvibration) influenced by microgravity N91-19595
Morphological, electronmicroscopical and biochemical aspects of hyper-gravity conditions during early ontogenetic development of Cichlid fish N91-19638
NEUTRAL ATOMS
Advances in atomic oxygen simulation N91-19147
NEUTRAL PARTICLES
Experiments toward the development of new pulsed ion diodes N91-19885
NEUTRON BEAMS
Exchange currents in low-energy nucleon capture by He3
[ETN-91-98917] N91-19855
NEUTRON COUNTERS
Investigation of condensed matter fusion
[DE91-007246] N91-19923
The Rome neutron monitor data for four ground-level enhancements observed by the world-wide station network in 1990
[NOTA-INTERNA-967] N91-20019
NEUTRON DIFFRACTION
The application of neutron diffraction time-of-flight measurements to the study of strain in composites
[DE91-008106] N91-19242
NEUTRON DISTRIBUTION
Neutron propagation from solar flare in the solar atmosphere
[DE91-615465] N91-20016
NEUTRON PHYSICS
Some neutronics and thermal-hydraulics codes for reactor analysis using personal computers
[DE91-006591] N91-19743
NEUTRON STARS
Sixquarks in neutron stars
[DE91-615472] N91-19987
NEUTRONS
Neutron radiation damage studies on silicon detectors
[DE91-008441] N91-19361
A stochastic performance model for the neutron diffusion nodal method on a multiuser parallel supercomputer
[DE90-017015] N91-19749
Variational Monte Carlo studies of electromagnetic structure of few-body nuclei
[DE91-007756] N91-19838
Some limitations of detailed balance for inverse reaction calculations in the astrophysical P-process
[DE91-007258] N91-19983
Neutron propagation from solar flare in the solar atmosphere
[DE91-615465] N91-20016
NICKEL
Microbiologically influenced corrosion in copper and nickel seawater piping systems
[AD-A229874] N91-19287
NICKEL ALLOYS
Chemical interactions in multimetal/zeolite catalysts
[DE91-007978] N91-19261
Effects of radiolytic tritium decay on the thermodynamic behavior of LaNi(4.25)Al(0.75) tritides
[DE91-007961] N91-19277
High temperature tensile properties of nickel-base superalloys for intermediate heat exchangers of high temperature gas-cooled reactors
[DE91-744958] N91-19284
Free energy simulation of grain boundary segregation the thermodynamics in Ni(3-x)Al(1+x)
[DE91-007473] N91-19928
X ray determination of site occupation parameters in ordered ternaries Cu(Au(x)M(1-x))M = Ni,Pd
[DE91-007861] N91-19937
NIOBIUM ALLOYS
Reactivity of pi-complexes of Ti, V, and Nb towards dithioacetic acid: Synthesis and structure of novel metal sulfur-containing complexes
[NASA-TM-103666] N91-19256
Internal friction peaks due to interstitials in bcc alloys
[DE91-007411] N91-19272
NIOBIUM COMPOUNDS
Limiting pulse signal in NbN-Si structure: Superconductor film on substrate N91-19815

NITRIDES
Limiting pulse signal in NbN-Si structure: Superconductor film on substrate N91-19815
NITROGEN OXIDES
Rapid mix concepts for low emission combustors in gas turbine engines
[NASA-CR-185292] N91-19048
Plasma assisted NO(x) reduction in existing coal combustors
[DE91-007380] N91-19536
Estimating lightning-generated NOx emissions for regional air pollution models
[PB91-131664] N91-19546
NO2 absorption cross-section in the 440 to 460 nm region at 298 and 220 K
[NOTA-INTERNA-964] N91-19550
NITROGEN PLASMA
Plasma assisted NO(x) reduction in existing coal combustors
[DE91-007380] N91-19536
NITROGEN POLYMERS
Synthesis and analysis of novel polymers with potential for providing both high permselectivity and permeability in gas separation applications
[DE91-008283] N91-19309
NITROUS OXIDES
Physiological genetics of denitrification: A route to conserving fixed nitrogen
[DE91-008157] N91-19707
NOAA 9 SATELLITE
NOAA-9 Solar Backscatter Ultraviolet (SBUV/2) Instrument and Derived Ozone Data: Review
[NOAA-TR-NESDIS-53] N91-19514
NOISE GENERATORS
Non-linear generation of acoustic noise in the IAR spacecraft N91-19143
NOISE REDUCTION
Performance monitoring in nonlinear adaptive noise cancellation
[RR-409] N91-19362
Noise level reduction inside helicopter cabins
[MBB-UD-0578-90-PUB] N91-19828
NOISE SPECTRA
Non-linear generation of acoustic noise in the IAR spacecraft N91-19143
NONDESTRUCTIVE TESTS
Characterization of ion-implanted aluminum and iron by spectroscopic ellipsometry
[DE91-008371] N91-19283
Research on advanced NDE methods for aerospace structures
[AD-A226858] N91-19460
Mechanical behavior of a ceramic matrix composite material
[NASA-CR-187072] N91-19461
NDE standards for high temperature materials
[NASA-TM-103761] N91-19464
The challenge of standards for emerging NDT methods
[DE91-007834] N91-19465
Nuclear-spectroscopy computerized tomography scanners
[DE91-008447] N91-19466
NONEQUILIBRIUM FLOW
Contributions to the Non Equilibrium Molecular Dynamics (NEMD) computer simulation for transport processes in simple fluids
[ETN-91-98921] N91-19393
NONLINEAR EQUATIONS
Finite element analysis of geometrically non-linear problems using a corotational large rotation formulation
[SU-ATN-9001] N91-19470
Solution of one-dimensional problem in nonlinear theory of elasticity with structured shock wave N91-19809
NONLINEAR OPTICS
Design considerations for multi component molecular-polymeric nonlinear optical materials
[DE91-006778] N91-19872
Nonlinear optic effects in liquid crystals
[ETN-91-98923] N91-19878
NONLINEAR SYSTEMS
System identification for nonlinear control using neural networks N91-19039
Performance monitoring in nonlinear adaptive noise cancellation
[RR-409] N91-19362
Time-frequency domain analysis of vibration signals for machinery diagnostics. 1: Introduction to the Wigner-Ville distribution
[OUEL-1859/90] N91-19495
The qualitative analysis of nonlinear parameterised systems. Part 2: A method for the global analysis of nonlinear systems
[RR-400-PT-2] N91-19754
The qualitative analysis of nonlinear parameterized systems. Part 1: Nonlinear systems representation and dynamical systems theory
[RR-408-PT-1] N91-19789
Orthogonal least squares parameter estimation algorithms for nonlinear stochastic systems
[RR-404] N91-19797
Quasi-nonlinear theory of cosmological self-gravitating systems
[DE91-744971] N91-19989
NONLINEARITY
Analyzing thought-related electroencephalographic data using nonlinear techniques N91-19031
Neural networks in nonlinear aircraft control N91-19037
System identification for nonlinear control using neural networks N91-19039
Non-linear generation of acoustic noise in the IAR spacecraft N91-19143
Critical-layer nonlinearity in the resonance growth of three-dimensional waves in boundary layers
[NASA-TM-103639] N91-19373
Euler solutions to nonlinear acoustics of non-lifting hovering rotor blades
[NASA-TM-103837] N91-19826
Intense field non-resonant multiphoton absorption of diatomic molecules
[DE91-006920] N91-19835
Quasi-nonlinear theory of cosmological self-gravitating systems
[DE91-744971] N91-19989
Statistics of peaks in cosmological nonlinear density fields
[DE91-744972] N91-19990
NONUNIFORMITY
Property and microstructural nonuniformity in the yttrium-barium-copper-oxide superconductor determined from electrical, magnetic, and ultrasonic measurements
[NASA-TM-103732] N91-19463
NOVA LASER SYSTEM
Upgrade of the LLNL Nova laser for inertial confinement fusion
[DE91-008060] N91-19430
NOZZLE FLOW
Solar rocket plume/mirror interactions
[NASA-CR-185300] N91-19059
Calculation of pulsating liquid free jets
[MPIS-15/1990] N91-19385
Correlation of leak rates of various fluids with the leak rate of an inert gas in the same configuration N91-20033
NOZZLE GEOMETRY
Experimental investigation of a single flush-mounted hypermixing nozzle
[NASA-TM-103726] N91-19374
NUCLEAR ELECTRIC PROPULSION
Enhancing space transportation: The NASA program to develop electric propulsion
[NASA-TM-4244] N91-19181
NUCLEAR FISSION
FALCON reactor-pumped laser description and program overview
[DE91-008185] N91-19431
NUCLEAR FUELS
Evaluation of a Photo-Electron Rejecting Alpha Liquid Scintillation (PERALS) spectrometer for the measurement of alpha-emitting radionuclides
[DE91-005652] N91-19399
NUCLEAR FUSION
Large-scale computing in the energy research programs
[DE91-007907] N91-19748
Power plant by LIB fusion N91-19892
Summary of the International Dawson Symposium on The Physics of Plasmas
[DE91-006912] N91-19897
Introduction to fusion
[DE91-744831] N91-19912
Investigation of condensed matter fusion
[DE91-007246] N91-19923
Primordial nucleosynthesis: Beyond the standard model
[DE91-007264] N91-19984
Two possible problems for standard big bang nucleosynthesis
[DE91-007342] N91-19985
NUCLEAR INTERACTIONS
Variational Monte Carlo studies of electromagnetic structure of few-body nuclei
[DE91-007756] N91-19838
Exchange currents in low-energy nucleon capture by He3
[ETN-91-98917] N91-19855
NUCLEAR PHYSICS
Large-scale computing in the energy research programs
[DE91-007907] N91-19748
NUCLEAR POWER PLANTS
Power plant by LIB fusion N91-19892
NUCLEAR POWER REACTORS
Key issues in space nuclear power
[NASA-TM-103656] N91-19179
NUCLEAR PUMPED LASERS
FALCON reactor-pumped laser description and program overview
[DE91-008185] N91-19431
NUCLEAR PUMPING
FALCON reactor-pumped laser description and program overview
[DE91-008185] N91-19431
NUCLEAR REACTOR CONTROL
Petri nets and fault diagnosis in nuclear reactors
[RR-413] N91-19865
The use of an object oriented technique for fault diagnosis in nuclear reactors
[RR-414] N91-19866
Fault detection using optimal control techniques
[RR-419] N91-19867
NUCLEAR REACTORS
Space reactor/Stirling cycle systems for high power lunar application
[NASA-TM-103698] N91-19112
Radiation-induced changes in electrical conductivity of a wide range of copper alloys
[DE91-007200] N91-19271
The development of a rugged accelerometer
[DE91-007731] N91-19407
FALCON reactor-pumped laser description and program overview
[DE91-008185] N91-19431
An on-line real-time system for fatigue crack growth monitoring
[DE91-007931] N91-19483
The application of neural networks for fault diagnosis in nuclear reactors
[RR-411] N91-19772
Expert systems for fault diagnosis in nuclear reactor control
[RR-412] N91-19864
Particle-in-cell plasma simulation codes on the connection machine
[DE91-007845] N91-19902
NUCLEAR STRUCTURE
Variational Monte Carlo calculations of nuclear ground states
[DE91-007760] N91-19842
The structure of nuclei far from beta stability
[DE91-008140] N91-19846
Electric monopole transitions and shape coexistence in nuclei
[DE91-008141] N91-19847
NUCLEAR WEAPONS
The development of a ram air decelerator for the recovery of artillery shells
[DE91-007732] N91-19064
Sandia technology: Engineering and science applications
[DE91-006760] N91-19322
NUCLEATION
The relationship between aerosol and drop size distributions in the marine atmosphere
[DE91-006514] N91-19553
NUCLEI (CYTOLOGY)
Effect of gravity on the distribution of electron dense chromatin in the nucleus of root statocytes N91-19672
NUCLEI (NUCLEAR PHYSICS)
The structure of nuclei far from beta stability
[DE91-008140] N91-19846
NUCLEON-NUCLEON INTERACTIONS
Variational Monte Carlo calculations of nuclear ground states
[DE91-007760] N91-19842
NUCLEONS
Exchange currents in low-energy nucleon capture by He3
[ETN-91-98917] N91-19855
NUMERICAL CONTROL
Computer controlled MHD power consolidation and pulse generation system
[DE91-006793] N91-19347
NUMERICAL STABILITY
Boundary integral equations and the Dirichlet problem
[DE91-004537] N91-19779

O

OBJECT PROGRAMS
Finding the object proceedings addendum
[DE91-006724] N91-19738
Simple object recognition by neural networks: Application of the Hough transform
[RR-410] N91-19761
The use of an object oriented technique for fault diagnosis in nuclear reactors
[RR-414] N91-19866
OBSTACLE AVOIDANCE
Navigation of a car-like mobile robot using a decomposition of the environment in convex cells
[DE91-000709] N91-19769
Cascading a systolic array and a feedforward neural network for navigation and obstacle avoidance using potential fields
[NASA-CR-177575] N91-19771
OCEAN BOTTOM
Very low frequency seismo-acoustic scattering from a rough seafloor
[AD-A227947] N91-19564
OCEAN CURRENTS
Thermohaline circulations and global climate change
[DE91-007458] N91-19537
OCEAN MODELS
Ancient oceans and Martian paleohydrology
N91-19997
OCEAN SURFACE
Slope modulation of the radar backscatter by sea waves
[BCRS-88-05] N91-19327
Wavelets and turbulence on the sea surface
[AD-A229862] N91-19565
OCEAN TEMPERATURE
Air/sea temperature probe
[AD-D014674] N91-19397
OCEAN THERMAL ENERGY CONVERSION
Results of scoping tests for open-cycle OTEC (Ocean Thermal Energy Conversion) components operating with seawater
[DE89-009514] N91-19501
Design and cost of near-term OTEC (Ocean Thermal Energy Conversion) plants for the production of desalinated water and electric power
[DE91-006406] N91-19508
OCEANOGRAPHY
Radar backscatter from the sea controlled experiments
[AD-A229847] N91-19340
OCEANS
Radar backscatter from the sea controlled experiments
[AD-A229847] N91-19340
Ancient oceans and Martian paleohydrology
N91-19997
ON-LINE SYSTEMS
Structured software design for an on-line laser-based particle size distribution instrument
[DE91-007234] N91-19746
ONE DIMENSIONAL FLOW
Traveling time effects in a channel flow
[MPIS-10/1990] N91-19384
OPEN CIRCUIT VOLTAGE
Key factors limiting the open circuit voltage of n(+)pp(+) indium phosphide solar cells N91-19206
Effect of dislocations on the open-circuit voltage, short-circuit current and efficiency of heteroepitaxial indium phosphide solar cells
[NASA-TM-103762] N91-19354
OPERATING SYSTEMS (COMPUTERS)
Performance measurements of the first RAID prototype
[NASA-CR-187958] N91-19718
A new generation of real-time DOS technology for mission-oriented system integration and operation
N91-19725
OPERATING TEMPERATURE
SCD 02 thermal design N91-19129
NDE standards for high temperature materials
[NASA-TM-103761] N91-19464
OPTICAL COMMUNICATION
I'm all 'light' Jack
[MBB-UD-0576-90-PUB] N91-19101
Digital optical computers at the optoelectronic computing systems center
[NASA-CR-187520] N91-19345
Study of wavelength division multiplexing as a means of increasing the number of channels in multimode fiber optic communication links N91-20024
OPTICAL COMPUTERS
Digital optical computers at the optoelectronic computing systems center
[NASA-CR-187520] N91-19345
OPTICAL EMISSION SPECTROSCOPY
A study of alkaline element interferences in analytical inductively coupled plasmas
[ISAL-90-0069] N91-19915
Search for the optical signatures of a pulsar in SN1987A
[MPE-PREPRINT-188] N91-19978
OPTICAL EQUIPMENT
The challenge of standards for emerging NDT methods
[DE91-007834] N91-19465
Compound semiconductors, strained layer epitaxy, and the information age
[DE91-007735] N91-19932
OPTICAL FIBERS
The development of a rugged accelerometer
[DE91-007731] N91-19407
Breakup of femtosecond pulses during amplification in Er(3+)-doped single-mode optical fibers N91-19812
Optical Fiber Backscatter Signature Generator (OFBSG)
[AD-D014668] N91-19870
Light guide fibers
[MBB-UA-1199-90-PUB] N91-19877
OPTICAL MATERIALS
Design considerations for multi component molecular-polymeric nonlinear optical materials
[DE91-006778] N91-19872
OPTICAL PROPERTIES
Characterization of ion-implanted aluminum and iron by spectroscopic ellipsometry
[DE91-008371] N91-19283
Radar backscatter from the sea controlled experiments
[AD-A229847] N91-19340
Plasma, photon, and beam synthesis of diamond films and multilayered structures
[DE91-007934] N91-19938
OPTICAL RADAR
Theory of CW lidar aerosol backscatter measurements and development of a 2.1 microns solid-state pulsed laser radar for aerosol backscatter profiling
[NASA-CR-4347] N91-19498
OPTICAL RESONANCE
Electron temperature of Gd plasma produced by laser resonance ionization
[DE91-744833] N91-19913
OPTICAL TRACKING
Laser Tracker 2: Sandia National Laboratories' second generation laser tracking system
[DE91-007711] N91-19424
Gaze control and spatial memory in weightlessness
N91-19692
OPTICAL WAVEGUIDES
Light guide fibers
[MBB-UA-1199-90-PUB] N91-19877
OPTICS
Optical testing cryogenic thermal vacuum facility
N91-19137
OPTIMAL CONTROL
Radar backscatter from the sea controlled experiments
[AD-A229847] N91-19340
Constructing mathematical model of adaptive anti-flutter system N91-19810
Fault detection using optimal control techniques
[RR-419] N91-19867
OPTIMIZATION
Optimization and performance of Space Station Freedom solar cells N91-19215
Concurrent micromechanical tailoring and fabrication process optimization for metal-matrix composites
[NASA-TM-103670] N91-19237
Minimum weight optimization of composite laminated struts
[BU-409] N91-19246
Bolted joints in a laminated composite strut design expert system
[BU-415] N91-19488
On the optimality of code options for a universal noiseless coder
[NASA-CR-187973] N91-19734
Structured software design for an on-line laser-based particle size distribution instrument
[DE91-007234] N91-19746
Optimal observation directions for estimating a vector
[PREPRINT-1285] N91-19796
OPTOELECTRONIC DEVICES
Growth kinetics of physical vapor transport processes: Crystal growth of the optoelectronic material mercurous chloride
[NASA-TM-103788] N91-19320
ORBIT TRANSFER VEHICLES
Transfer orbit stage mechanisms thermal vacuum test
N91-19161
Orbital transfer vehicle oxygen turbopump technology. Volume 1: Design, fabrication, and hydrostatic bearing testing
[NASA-CR-185175] N91-19174
Composite flexible insulation for thermal protection of space vehicles
[NASA-TM-103836] N91-19304
ORDER-DISORDER TRANSFORMATIONS
Localization and electron-phonon interaction in disordered systems
[DE91-007654] N91-19837
ORGANIC COMPOUNDS
Remote detection of organics using Fourier transform infrared spectroscopy
[DE91-006045] N91-19253
Polymer characterization using the time-resolved phosphorescence of singlet oxygen as a spectroscopic probe
[DE91-001269] N91-19303
Extraterrestrial organic molecules and the emergence of life on Earth N91-19681
ORGANOMETALLIC COMPOUNDS
Chemical activation of molecules by metals: Experimental studies of electron distributions and bonding
[DE91-007695] N91-19275
ORTHOGONAL FUNCTIONS
Orthogonal least squares parameter estimation algorithms for nonlinear stochastic systems
[RR-404] N91-19797
ORTHOSTATIC TOLERANCE
Reactivity of exhausted human skeletal muscle fibers following prolonged antiorthostatic hypokinesia
N91-19568
Medex: A useful tool for counteracting orthostatic intolerance resulting from body fluid loss under microgravity N91-19585
ORTHOTROPIC PLATES
Modeling and analysis of orthotropic plate with circular cutout and adhesive bonded patch
[AD-A229866] N91-19496
OSCILLATING CYLINDERS
Research on bluff-body vortex wakes
[AD-A229875] N91-19071
OSCILLATING FLOW
Research on bluff-body vortex wakes
[AD-A229875] N91-19071
A 2-D oscillating flow analysis in Stirling engine heat exchangers
[NASA-TM-103781] N91-19375
Calculation of pulsating liquid free jets
[MPIS-15/1990] N91-19385
OSCILLATIONS
Dynamics of collision processes
[DE91-007933] N91-19840
OSCILLATORS
Development of components and subsystems for low noise receivers at micro- and millimeter waves
[S-187] N91-19363
Time-dependent multimode simulation of gyrotron oscillators
[AD-A229861] N91-19413
Theory of CW lidar aerosol backscatter measurements and development of a 2.1 microns solid-state pulsed laser radar for aerosol backscatter profiling
[NASA-CR-4347] N91-19498
Copper vapor as active medium for high-power oscillator-amplifier laser systems N91-19806
OSTEOPOROSIS
Bone adaptation to real and simulated microgravity
N91-19643
Aragatz Mission: Bone densitometric results obtained with the SCOOP miniscanner N91-19690
OUTGASSING
An outgassing model of non-metallic materials for the ascent of a Titan 4 launch vehicle N91-19132
OXIDATION
Advances in atomic oxygen simulation N91-19147
Investigation of anodic and chemical oxides grown on p-type InP with applications to surface passivation for n(+)-p solar cell fabrication N91-19208
Methane to methanol conversion by direct partial oxidation
[DE91-007352] N91-19257
Comprehensive mechanisms for combustion chemistry: An experimental and numerical study with emphasis on applied sensitivity analysis
[DE91-008030] N91-19262
Mechanisms and controlling characteristics of the catalytic oxidation of methane
[DE91-008033] N91-19263
Solid state, surface, and catalytic studies of oxides
[DE91-007979] N91-19939
Mutual influence of doping and oxidation in highly doped silicon
[ETN-91-98924] N91-19948

OXIDATION RESISTANCE
Effect of fiber reinforcements on thermo-oxidative stability and mechanical properties of polymer matrix composites
[NASA-TM-103648] N91-19234
OXIDATION-REDUCTION REACTIONS
Photoinduced electron transfer processes in homogeneous and microheterogeneous solutions
[DE91-007582] N91-19836
OXIDE FILMS
X ray absorption spectroscopy of oxide films on metals
[DE91-008100] N91-19278
Superconductivity of oxide film electrolytically deposited on surface of B(1-x)Sb(x) single crystal N91-19819
OXIDES
Investigation of anodic and chemical oxides grown on p-type InP with applications to surface passivation for n(+)-p solar cell fabrication N91-19208
XANES investigation of pH effects during cerium-sealing of anodized aluminum
[DE91-008101] N91-19302
Solid state, surface, and catalytic studies of oxides
[DE91-007979] N91-19939
OXIDIZERS
Regional Oxidant Model Multi-Processor (ROMMP)
[PB91-131680] N91-19547
OXYGEN
Orbital transfer vehicle oxygen turbopump technology. Volume 1: Design, fabrication, and hydrostatic bearing testing
[NASA-CR-185175] N91-19174
Studies of combustion kinetics and mechanisms
[DE91-007829] N91-19259
Comprehensive mechanisms for combustion chemistry: An experimental and numerical study with emphasis on applied sensitivity analysis
[DE91-008030] N91-19262
Polymer characterization using the time-resolved phosphorescence of singlet oxygen as a spectroscopic probe
[DE91-001269] N91-19303
Oxygen-enriched diesel engine performance: A comparison of analytical and experimental results
[DE91-006491] N91-19440
OXYGEN ATOMS
Atomic oxygen effects on boron nitride and silicon nitride: A comparison of ground based and space flight data N91-19146
Advances in atomic oxygen simulation N91-19147
Low Earth orbital atomic oxygen and ultraviolet radiation effects on polymers
[NASA-TM-103711] N91-19294
OXYGEN COMPOUNDS
Late transition metal (mu)-oxo and (mu)-imido complexes
[DE91-005349] N91-19267
OXYGEN CONSUMPTION
Effects of hyperbaric oxygenation on central hemodynamics and oxygen consumption in severe physical trauma N91-19570
Oxygen uptake during concentric and eccentric resistive exercise using a new gravity-independent ergometer N91-19587
Influence of various parameters on the V'O2 frequency response of the body. A theoretical study on the basis of a nonlinear model N91-19594
Intra-individual variability V'O2 frequency responses in physically active subjects N91-19601
OXYGEN PRODUCTION
Physiological criteria and requirement of biomass production under controlled ecological life support systems N91-19659
Experimental reduction of simulated lunar glass by carbon and hydrogen and implications for lunar base oxygen production N91-20009
OXYGENATION
Mechanisms and controlling characteristics of the catalytic oxidation of methane
[DE91-008033] N91-19263
Effects of hyperbaric oxygenation on central hemodynamics and oxygen consumption in severe physical trauma N91-19570
OZONE
NOAA-9 Solar Backscatter Ultraviolet (SBUV/2) Instrument and Derived Ozone Data: Review
[NOAA-TR-NESDIS-53] N91-19514
Data status and availability N91-19515
An assessment of instrument performance for the NOAA-9 SBUV/2 N91-19516
SBUV/2 in-orbit performance N91-19517
A status report on the analysis of the NOAA-9 SBUV/2 sweep mode solar irradiance data N91-19518
NOAA-9 SBUV/2 ozone sounding accuracy: Presentation summary N91-19519
SBUV/2 comparisons with ground-based and SBUV spacecraft data N91-19521
Umkehr work N91-19522
Initial estimate of NOAA-9 SBUV/2 total ozone drift: Based on comparison with re-calibrated TOMS measurements and pair justification of SBUV/2 N91-19523
Calibration of long term satellite ozone data sets using the space shuttle N91-19524
Total ozone, ozonesonde, and Umkehr observations for satellite ozone data validation N91-19525
Ozone measurements from the NOAA-9 and the Nimbus-7 satellites: Implications of short and long term variabilities N91-19527
Aerosol formation in atmospheric mixtures
[PB91-129114] N91-19560
OZONE DEPLETION
Calibration of long term satellite ozone data sets using the space shuttle N91-19524

P

P-TYPE SEMICONDUCTORS
Surface chemistry at semiconductor-electrolyte interfaces
[DE91-005915] N91-19920
PALLADIUM ALLOYS
Chemical interactions in multimetal/zeolite catalysts
[DE91-007978] N91-19261
Mechanisms and controlling characteristics of the catalytic oxidation of methane
[DE91-008033] N91-19263
X ray determination of site occupation parameters in ordered ternaries Cu(Au(x)M(1-x))M = Ni,Pd
[DE91-007861] N91-19937
PANEL METHOD (FLUID DYNAMICS)
Panel methods: An introduction
[NASA-TP-2995] N91-19058
Parallel processing for panel methods
[BU-414] N91-19391
PANELS
Single-strain-gage force/stiffness buckling prediction techniques on a hat-stiffened panel
[NASA-TM-101733] N91-19077
Free vibration of hexagonal panels supported at discrete points
[NASA-TM-102688] N91-19166
A theoretical solution for the buckling of sandwich panels with laminated face plates using a computer algebra system
[BU-407] N91-19486
PARABOLIC FLIGHT
Lung volumes, chest wall configuration, and pattern of breathing in microgravity N91-19574
Blood pressure regulation in parabolic flight N91-19575
Vestibular function in altered states of gravity N91-19579
Measurement of eye movements in space-related research environments N91-19591
Visualisation of fluid shifts within the body during a parabolic flight by measurements of electrical bio-impedance N91-19688
Pupil size in parabolic flight N91-19693
PARACHUTES
The design and flight testing of a high-performance low-cost parachute system for a 1000 lb payload
[DE91-007733] N91-19065
PARALLEL COMPUTERS
Multiphase complete exchange on a circuit switched hypercube
[NASA-CR-187499] N91-19716
PARALLEL PROCESSING (COMPUTERS)
Parallel processing for panel methods
[BU-414] N91-19391
On the vectorization and parallelization of the shooting method using the convex C-240
[LR-639] N91-19491
Analysis of workload and load balancing issues in the NCAR community climate model
[DE91-008052] N91-19534
Regional Oxidant Model Multi-Processor (ROMMP)
[PB91-131680] N91-19547
Energy sciences supercomputing 1990
[DE91-007188] N91-19740
A stochastic performance model for the neutron diffusion nodal method on a multiuser parallel supercomputer
[DE90-017015] N91-19749
Parallel processing for a 1-D time-dependent solution to impurity rate equations for fusion plasma simulations
[DE90-015857] N91-19759
Model distribution in decentralized multi-sensor data fusion
[OUEL-1868/90] N91-19763
Artificial neural network implementation
[AD-D014663] N91-19764
PARALLEL PROGRAMMING
The FORCE: A highly portable parallel programming language
[NASA-CR-187928] N91-19732
A structured representation for parallel algorithm design on multicomputers
[DE91-006674] N91-19744
Summer institute in parallel programming
[DE91-007922] N91-19760
PARAMAGNETISM
Effect of paramagnetic impurities on dynamics of magnetic fluxes in superconductors N91-19816
PARAMECIA
Cellular functions of Paramecium under different gravity conditions N91-19631
PARAMETER IDENTIFICATION
Parameter estimation of structural dynamic models using Eigenvalue and Eigenvector information
[DE91-004379] N91-19793
Orthogonal least squares parameter estimation algorithms for nonlinear stochastic systems
[RR-404] N91-19797
PARAMETERIZATION
The relationship between aerosol and drop size distributions in the marine atmosphere
[DE91-006514] N91-19553
The qualitative analysis of nonlinear parameterised systems. Part 2: A method for the global analysis of nonlinear systems
[RR-400-PT-2] N91-19754
The qualitative analysis of nonlinear parameterized systems. Part 1: Nonlinear systems representation and dynamical systems theory
[RR-408-PT-1] N91-19789
Punchthrough in hadronic showers: A parameterization of the total probability
[NOTA-INTERNA-968] N91-19854
PARTIAL DIFFERENTIAL EQUATIONS
The method of lines in analyzing solids containing cracks
[NASA-TM-103626] N91-19477
PARTICLE ACCELERATORS
A calorimeter design for high energy PP colliders
[NOTA-INTERNA-965] N91-19410
PARTICLE BEAMS
Aerodynamic focusing of particles and heavy molecules
[DE91-006922] N91-19833
PARTICLE COLLISIONS
A calorimeter design for high energy PP colliders
[NOTA-INTERNA-965] N91-19410
Relativistic klystron research for future linear colliders
[DE91-008063] N91-19862
PARTICLE DIFFUSION
The weighted-difference form of the nodal diffusion method in cylindrical geometry
[DE91-007849] N91-19784
PARTICLE EMISSION
Proton induced x ray emission analysis N91-19832
Observations of CO isotopic emission and the far-infrared continuum of Centaurus A
[MPE-PREPRINT-183] N91-19977
PARTICLE IN CELL TECHNIQUE
Control of gap closure in applied-B diode N91-19893
PARTICLE INTERACTIONS
Neutron propagation from solar flare in the solar atmosphere
[DE91-615465] N91-20016
PARTICLE MOTION
Possibility of raising efficiency of free-electron laser in longitudinal magnetic field N91-19804
PARTICLE PRODUCTION
Punchthrough in hadronic showers: A parameterization of the total probability
[NOTA-INTERNA-968] N91-19854
PARTICLE SIZE DISTRIBUTION
Ultrafine refractory particle formation in counterflow diffusion flames
[DE91-007693] N91-19260
Data acquisition and analysis on the two-color laser transmissometer system
[DE91-007235] N91-19420
The relationship between aerosol and drop size distributions in the marine atmosphere
[DE91-006514] N91-19553
Structured software design for an on-line laser-based particle size distribution instrument
[DE91-007234] N91-19746
PARTICLE THEORY
Punchthrough in hadronic showers: A parameterization of the total probability
[NOTA-INTERNA-968] N91-19854

PARTICULATES
Low-density, high-strength intermetallic matrix composites by XD (trademark) synthesis
[NASA-TM-103724] N91-19233
PASSENGERS
Airport system technical aspects N91-19107
PASSIVITY
Radiation resistance of thin-film solar cells for space photovoltaic power
[NASA-TM-103715] N91-19176
A comparative study of performance parameters of n(+)-p InP solar cells made by closed-ampoule sulfur diffusion into Cd- and Zn-doped p-type InP substrates N91-19209
Stress corrosion cracking of Al-Li-Cu-Zr alloy 2090 in aqueous Cl(-) and mixed CO3(2-)/Cl(-) environments
[DE91-007064] N91-19269
PATTERN RECOGNITION
Simple object recognition by neural networks: Application of the Hough transform
[RR-410] N91-19761
A haptic system for a multifingered hand
[DE90-017044] N91-19767
Design and implementation of an image understanding system: DADS
[ETN-91-98926] N91-19773
PAYLOADS
The design and flight testing of a high-performance low-cost parachute system for a 1000 lb payload
[DE91-007733] N91-19065
PEEK
A study on prediction of life due to creep behavior in CF/EPOXY and CF/PEEK laminates N91-19226
PERCEPTION
Gravitaxis in Physarum polycephalum N91-19678
The reference systems for tactile perception and for the orientation with respect to body N91-19691
PERCEPTUAL ERRORS
Relation between perception of vertical axis rotation and vestibulo-ocular reflex symmetry
[NASA-CR-187997] N91-19710
PERFORMANCE PREDICTION
Ongoing development of a computer jobstream to predict helicopter main rotor performance in icing conditions
[NASA-CR-187076] N91-19056
GaAs solar cell photoresponse modeling using PC-1D V2.1 N91-19193
An approach for configuring space photovoltaic tandem arrays based on cell layer performance N91-19197
Key factors limiting the open circuit voltage of n(+)pp(+) indium phosphide solar cells N91-19206
Analysis of workload and load balancing issues in the NCAR community climate model
[DE91-008052] N91-19534
PERFORMANCE TESTS
A 5-kW xenon ion thruster lifetest
[NASA-TM-103191] N91-19180
Thermal annealing of GaAs concentrator solar cells N91-19195
An approach for configuring space photovoltaic tandem arrays based on cell layer performance N91-19197
Effects of proton irradiation on the performance of InP/GaAs solar cells N91-19205
Spaceflight performance of several types of silicon solar cells on the LIPS 3 satellite N91-19213
Optimization and performance of Space Station Freedom solar cells N91-19215
Thermal cycle testing of Space Station Freedom solar array blanket coupons N91-19216
Vibration and thermal vacuum qualification test results for a low-voltage tungsten-halogen light
[NASA-CR-187050] N91-19325
Laboratory testing of the Sonnenschein charger, Part number DTL 12040
[DE91-006543] N91-19346
Design, performance evaluation, and investigation of the theoretical capabilities of the NASA Millimeter-wave Imaging Radiometer (MIR)
[NASA-CR-187984] N91-19398
Data acquisition and analysis on the two-color laser transmissometer system
[DE91-007235] N91-19420
Performance of underwater weldments
[PB91-129254] N91-19452
NOAA-9 Solar Backscatter Ultraviolet (SBUV/2) Instrument and Derived Ozone Data: Review
[NOAA-TR-NESDIS-53] N91-19514
An assessment of instrument performance for the NOAA-9 SBUV/2 N91-19516
Test analysis program evaluation: Item statistics as feedback to test developers
[AD-A229851] N91-19713
Hubble Space Telescope secondary mirror vertex radius/conic constant test
[NASA-CR-187989] N91-19871
The magnetohydrodynamics coal-fired flow facility
[DE91-007672] N91-19906
Correlation of leak rates of various fluids with the leak rate of an inert gas in the same configuration N91-20033
PERIODIC VARIATIONS
Longitudinal periodicity in superconducting dipole magnets
[DE91-008421] N91-19821
PERMEABILITY
Synthesis and analysis of novel polymers with potential for providing both high permselectivity and permeability in gas separation applications
[DE91-008283] N91-19309
Modeling a ferrite-tuned RF cavity
[DE91-008235] N91-19356
PEROVSKITES
Method of producing superconducting materials in bulk form
[AD-D014656] N91-19917
PERSONAL COMPUTERS
Some neutronics and thermal-hydraulics codes for reactor analysis using personal computers
[DE91-006591] N91-19743
SIGNIF and GENFMT, SAS macros for computing and reporting significant digits
[DE91-007702] N91-19795
PERTURBATION
Thermal instabilities in cooling flows: The evolution of nearly spherical perturbations
[MPE-PREPRINT-176] N91-19365
Development of a perturbation generator for vortex stability studies
[NASA-CR-188051] N91-19379
Traveling time effects in a channel flow
[MPIS-10/1990] N91-19384
The study of effects of small perturbations on chaotic systems
[DE91-007320] N91-19792
PERTURBATION THEORY
Theoretical investigation of phase stability in non-magnetic Fe-V substitutional alloys
[DE91-006711] N91-19268
W(sub L)W(sub L) scattering at the SSC
[DE91-008442] N91-19851
Quasi-nonlinear theory of cosmological self-gravitating systems
[DE91-744971] N91-19989
PETN
Extrudable PBX molding powder
[AD-D014667] N91-19312
PETRI NETS
Petri nets and fault diagnosis in nuclear reactors
[RR-413] N91-19865
PH
XANES investigation of pH effects during cerium-sealing of anodized aluminum
[DE91-008101] N91-19302
PHASE DIAGRAMS
Alkali metal corrosion of alumina: Thermodynamics, phase diagrams and testing
[ETN-91-98933] N91-19286
Thin film reactions on alloy semiconductor substrates
[DE91-007651] N91-19931
PHASE SEPARATION (MATERIALS)
Phenomena affecting morphology of microporous poly(acrylonitrile) prepared via phase separation from solution
[DE91-004501] N91-19297
PHASE SHIFT CIRCUITS
Fiber optic feed
[AD-A229860] N91-19879
PHASE TRANSFORMATIONS
Phase equilibrium modeling for high temperature metallization on GaAs solar cells N91-19192
The apparent strain stability and repeatability of a BCL3 resistance strain gage
[NASA-CR-187056] N91-19403
Phenomenological theory of phase transitions to nonhomogeneous noncommensurate phase with superconducting current N91-19817
Phase transitions and equation of state of CsI under high pressure and the development of a focusing system for x rays
[DE91-007646] N91-19930
Phase formation in the Tl-Ca-BaCu-O system
[DE91-008184] N91-19942
PHASED ARRAYS
Fiber optic feed
[AD-A229860] N91-19879
PHOSPHATES
A study of carbon steel corrosion inhibition by phosphate ions and by an organic buffer using a scanning vibrating electrode
[DE91-008103] N91-19280
PHOSPHORESCENCE
Polymer characterization using the time-resolved phosphorescence of singlet oxygen as a spectroscopic probe
[DE91-001269] N91-19303
PHOSPHORUS OXIDES
Thin film amorphous electrolytes: The Li2O-SiO2-P2O5 system
[DE91-007272] N91-19925
PHOTOCATHODES
Proceedings of the Workshop Prospects for a 1 Angstrom Free-Electron Laser
[DE91-007631] N91-19422
PHOTOCHEMICAL REACTIONS
A flight experiment to determine GPS photochemical contamination accumulation rates N91-19159
Calibration of long term satellite ozone data sets using the space shuttle N91-19524
Regional Oxidant Model Multi-Processor (ROMMP)
[PB91-131680] N91-19547
Research conducted at the Radiation Lab, Notre Dame Univ.
[DE91-007969] N91-19843
PHOTODIODES
Semiconductor photodiodes as radiometric receivers in the field of soft radiation
[ETN-91-98925] N91-19856
PHOTODISSOCIATION
A status report on the analysis of the NOAA-9 SBUV/2 sweep mode solar irradiance data N91-19518
Fluorescent HD emission from photodissociation regions
[MPE-PREPRINT-177] N91-19982
PHOTOELECTRIC EFFECT
High power, high frequency lasertron RF sources
[DE91-006007] N91-19414
PHOTOELECTRIC EMISSION
Photoemission studies using femtosecond pulses for high brightness electron beams
[DE91-008436] N91-19849
Development of high current electron source using photoemission from metals with ultrashort laser pulses
[DE91-008438] N91-19850
A photoemission investigation of compound semiconductor monodisperse clusters
[DE91-006707] N91-19921
PHOTOELECTROCHEMICAL DEVICES
Surface chemistry at semiconductor-electrolyte interfaces
[DE91-005915] N91-19920
PHOTOELECTRON SPECTROSCOPY
Chemical activation of molecules by metals: Experimental studies of electron distributions and bonding
[DE91-007695] N91-19275
PHOTOELECTRONS
Photoelectron diffraction of magnetic ultrathin films: Fe/Cu(001)
[DE91-007254] N91-19924
PHOTOGRAPHS
Debris/ice/TPS assessment and photographic analysis for shuttle mission STS-35
[NASA-TM-103816] N91-19118
PHOTOIONIZATION
Recombination x ray laser experiments using exploding ribbon Al targets
[DE91-007146] N91-19429
Studies of atmospheric molecules by multiphoton spectroscopy
[DE91-006738] N91-19554
Electron temperature of Gd plasma produced by laser resonance ionization
[DE91-744833] N91-19913
PHOTOLITHOGRAPHY
Characteristics of excimer laser with narrow emission line N91-19807
PHOTOLUMINESCENCE
Graded-bandgap AlGaAs solar cells for AlGaAs/Ge cascade cells N91-19186
PHOTOLYSIS
Research conducted at the Radiation Lab, Notre Dame Univ.
[DE91-007969] N91-19843
PHOTONICS
Compound semiconductors, strained layer epitaxy, and the information age
[DE91-007735] N91-19932
PHOTONS
Dynamics of collision processes
[DE91-007933] N91-19840
PHOTONUCLEAR REACTIONS
Some limitations of detailed balance for inverse reaction calculations in the astrophysical P-process
[DE91-007258] N91-19983

PHOTOOXIDATION
Aerosol formation in atmospheric mixtures
[PB91-129114] N91-19560
Photoinduced electron transfer processes in homogeneous and microheterogeneous solutions
[DE91-007582] N91-19836
PHOTOSYNTHESIS
Physiological criteria and requirement of biomass production under controlled ecological life support systems N91-19659
Tuning the efficiencies of plant lighting systems: From primary energy to edible biomass: The LED as an alternative light source N91-19660
Productivity and photosynthesis of selected crop plants under orbital light conditions: An approach to solar powered CELSS N91-19662
Graviorientation in photosynthetic flagellates N91-19673
PHOTOVOLTAIC CELLS
Aeolian removal of dust types from photovoltaic surfaces on Mars N91-19156
Space Photovoltaic Research and Technology, 1989
[NASA-CP-3107] N91-19182
Progress in GaAs/CuInSe2 tandem junction solar cells N91-19190
An approach for configuring space photovoltaic tandem arrays based on cell layer performance N91-19197
Dual-purpose self-deliverable lunar surface PV electrical power system N91-19200
Feasibility of solar power for Mars N91-19201
Recent advances in the ITO/InP solar cell N91-19202
Thermal cycle testing of Space Station Freedom solar array blanket coupons N91-19216
The Advanced Photovoltaic Solar Array (APSA) technology status and performance N91-19217
Integral bypass diodes in an amorphous silicon alloy photovoltaic module N91-19218
Mini-dome Fresnel lens photovoltaic concentrator development N91-19219
Viability study of photovoltaic systems added to terrestrial electric vehicles
[DE91-007689] N91-19355
PHOTOVOLTAIC CONVERSION
Space Photovoltaic Research and Technology, 1989
[NASA-CP-3107] N91-19182
The OAST space power program N91-19183
Feasibility of solar power for Mars N91-19201
PHOTOVOLTAIC EFFECT
Radiation resistance of thin-film solar cells for space photovoltaic power
[NASA-TM-103715] N91-19176
Solid State Photovoltaic Research Branch
[DE91-002128] N91-19502
PHYSICAL EXERCISE
Effects of short-lasting weightlessness on gas exchange during light exercise N91-19573
Pedalling in space to simulate gravity: The twin-bike system N91-19583
Oxygen uptake during concentric and eccentric resistive exercise using a new gravity-independent ergometer N91-19587
Influence of various parameters on the V'O2 frequency response of the body. A theoretical study on the basis of a nonlinear model N91-19594
Effects of training with reduced perfusion pressure on performance and muscle fiber characteristics N91-19615
Central and peripheral cardiovascular responses to electrically induced and voluntary leg exercise N91-19687
Responses of women to orthostatic and exercise stresses
[NASA-TP-3043] N91-19711
PHYSICAL FACTORS
Numerical and physical modelling of bubbly flow phenomena
[DE91-007461] N91-19377
PHYSICAL FITNESS
Time courses of endurance performance parameters following 500 ml blood withdrawal N91-19586
Intra-individual variability V'O2 frequency responses in physically active subjects N91-19601
Weightlessness countermeasures and human physiology in space: A potential conflict N91-19695
PHYSICS
JPRS report: Science and technology. USSR: Physics and mathematics
[JPRS-UPM-90-004] N91-19800
PHYSIOLOGICAL EFFECTS
Fourth European Symposium on Life Sciences Research in Space
[ESA-SP-307] N91-19572
Head-down tilt test and space-related endocrine physiology N91-19614
Muscle function impairment following lower limb unloading in men N91-19616
The biological and medical programme of the manned Aragatz mission on the Mir Space Station N91-19617
Experiment lymphocytes of Aragatz mission: Influence of the space flight on human T lymphocyte and monocyte functions N91-19619
Lymphocytes on sounding rockets N91-19620
Hindlimb suspension of rabbit for one week: Myofibrillar damage in the soleus may depend on long-lasting shortening and periodic contraction against no load N91-19647
Preliminary studies before defining a payload adapted to the primate model N91-19648
Hypergravity and bone mineralization N91-19650
Graviperception in plants N91-19667
Plant development in space: Observations on root formation and growth N91-19670
Arabidopsis thaliana (Heynh.) pollen: A new tool in heavy ions radiation N91-19685
Weightlessness countermeasures and human physiology in space: A potential conflict N91-19695
PHYSIOLOGICAL RESPONSES
Gravitation receptor reaction in response to effect of acceleration N91-19569
Subcellular signal transduction systems in the cellular trauma of ischemia
[AD-A229876] N91-19709
PHYSIOLOGY
Fourth European Symposium on Life Sciences Research in Space
[ESA-SP-307] N91-19572
Physiology of body water and salt regulation. Part 1: Circadian rhythms of endocrine systems and urinary electrolyte excretion in humans N91-19592
Physiology of body water and salt regulation. Part 2: Volume and electrolyte homeostasis after an acute saline infusion N91-19593
The biochemical and physiological variables in motion sickness followed modified neuroendocrine activity N91-19607
Biological effects of extremely low-frequency electromagnetic fields: In vivo studies
[DE91-007899] N91-19704
Responses of women to orthostatic and exercise stresses
[NASA-TP-3043] N91-19711
PIEZOELECTRIC TRANSDUCERS
Piezoelectric sandwich polymer transducer
[AD-D014650] N91-19341
Development of a piezoelectric polymer film pressure transducer for low frequency and dynamic pressure measurement
[AD-A229848] N91-19412
PIEZOELECTRICITY
The development of a rugged accelerometer
[DE91-007731] N91-19407
Development of a piezoelectric polymer film pressure transducer for low frequency and dynamic pressure measurement
[AD-A229848] N91-19412
PILOT PLANTS
Data acquisition and analysis on the two-color laser transmissometer system
[DE91-007235] N91-19420
Performance characteristics of an MHD (Magnetohydrodynamic) pilot plant electrostatic precipitator
[DE91-007218] N91-19905
PIPE FLOW
Modeling of flow systems for implementation under KATE N91-20038
PITOT TUBES
Pitot measurements in the exhaust of a cluster of four small scale supersonic nozzles
[OUEL-1862/90] N91-19070
PLANETARY COMPOSITION
Twenty-Second Lunar and Planetary Science Conference
[NASA-CR-187971] N91-19995
PLANETARY EVOLUTION
Twenty-Second Lunar and Planetary Science Conference
[NASA-CR-187971] N91-19995
Effects of a giant impact on Uranus N91-20012
What were the effects of the formation of the Borealis basin, Mars N91-20014
PLANETARY GEOLOGY
Twenty-Second Lunar and Planetary Science Conference
[NASA-CR-187971] N91-19995
Ancient oceans and Martian paleohydrology N91-19997
Relative chronology of Martian volcanoes N91-20007
PLANETARY MAGNETIC FIELDS
An analytical study of neutral expansion, ionization, and charged particle acceleration in a neutral lithium release for the parallel electric field measurement
[MPE-PREPRINT-180] N91-19880
PLANETARY MAPPING
Mars radar mapping: Strong depolarized echoes from the Elysium/Amazonis outflow channel complex N91-20001
Magellan: Preliminary description of Venus surface geologic units N91-20011
PLANETARY STRUCTURE
Solid earth science in the 1990s. Volume 1: Program plan
[NASA-TM-4256-VOL-1] N91-19499
PLANETARY SURFACES
Twenty-Second Lunar and Planetary Science Conference
[NASA-CR-187971] N91-19995
PLANNING
World weather watch: Regional association 4: Hurricane operational plan, supplement 2
[WMO-524-SUPPL-2] N91-19563
PLANT DESIGN
The design of future central receiver power plants based on lessons learned from the Solar One Pilot Plant
[DE91-005224] N91-19510
PLANT ROOTS
Plant development in space: Observations on root formation and growth N91-19670
Effect of gravity on the distribution of electron dense chromatin in the nucleus of root statocytes N91-19672
PLANTS (BOTANY)
Plant production as part of a Controlled Ecological Life Support System (CELSS) N91-19656
A ground based module for experimentations of cultivations and recycling in a closed environment N91-19657
Physiological criteria and requirement of biomass production under controlled ecological life support systems N91-19659
Tuning the efficiencies of plant lighting systems: From primary energy to edible biomass: The LED as an alternative light source N91-19660
Plant biotechnology in space: Facts and speculations N91-19664
Development of a miniature biology facility N91-19666
Graviperception in plants N91-19667
Plastids and gravity perception N91-19668
Gravitational effects on subcellular structures of plant cells N91-19669
Plant development in space: Observations on root formation and growth N91-19670
Plant growth under microgravity conditions: Experiments and problems N91-19671
The 1989-1990 NASA space biology accomplishments
[NASA-TM-4258] N91-19697
Characterization of a defective interfering RNA that contains a mosaic of a plant viral genome
[DE91-007897] N91-19702
PLASMA CONTROL
Plasma boundary experiments on D3-D tokamak
[DE91-002429] N91-19881
Control of gap closure in applied-B diode N91-19893
US-Japan workshops: Q-111, Development of Plasma Facing Components and Materials for Next Large Fusion Devices, and Q-112, Vacuum and First Wall Technology for Fusion Devices
[DE91-006879] N91-19896
Summary of the International Dawson Symposium on The Physics of Plasmas
[DE91-006912] N91-19897
Experimental study of external kink instabilities in the Columbia high beta tokamak
[DE91-008116] N91-19904
Tokamak ignition projections from dimensionally similar discharges
[DE91-008195] N91-19908
New method for edge plasma control by RF ponderomotive force
[DE91-744823] N91-19911
Introduction to fusion
[DE91-744831] N91-19912
PLASMA DIAGNOSTICS
Measurements with a 35 psec gate time microchannelplate camera
[DE91-006701] N91-19400
UV Thomson scattering from x ray laser plasmas
[DE91-007347] N91-19895
A method for determining poloidal coil configurations for tokamak devices
[DE91-007940] N91-19903
Optical diagnostics for low-temperature plasmas
[DE91-007896] N91-19907

Measurements of stark-broadening in hot dense plasma
[DE91-008504] N91-19910
Introduction to fusion
[DE91-744831] N91-19912

PLASMA DIFFUSION
Analysis of spherical geometry finite element transport solutions in the thick diffusion limit
[DE91-007598] N91-19780
Even- and odd-parity finite-element transport solutions in the thick diffusion limit
[DE91-007618] N91-19781
Discontinuous finite-element transport solutions in the thick diffusion limit in Cartesian geometry
[DE91-007620] N91-19782

PLASMA DIODES
Symposium on Development of Intensed Pulsed Particle Beams and Its Applications
[NIFS-PROC-5] N91-19882
Two-stage ion diode experiments on induction adder N91-19884
Experiments toward the development of new pulsed ion diodes N91-19885
Theoretical study of plasma focus diode N91-19887
Pulse-power characteristic of VIVA-1 (Versatile Inductive Voltage Adder) N91-19888
Reduction of low energy components in pulse ion beam N91-19889
Generation and focusing of carbon ion beam by the inverse pinch ion diode N91-19890
Generation of pulsed ion beams by an inductive storage pulsed power generator N91-19891
Control of gap closure in applied-B diode N91-19893

PLASMA DRIFT
New method for edge plasma control by RF ponderomotive force
[DE91-744823] N91-19911

PLASMA ELECTRODES
Reduction of low energy components in pulse ion beam N91-19889

PLASMA EQUILIBRIUM
Calculation of emission and absorption spectra of LTE plasma by the STA (Super Transition Array) method
[DE91-007617] N91-19900
Noble gas disk MHD generator performance with unstable nonequilibrium plasma
[ISBN-90-9003671-7] N91-19916

PLASMA FOCUS
Symposium on Development of Intensed Pulsed Particle Beams and Its Applications
[NIFS-PROC-5] N91-19882
Theoretical study of plasma focus diode N91-19887

PLASMA HEATING
A program of high power microwave source research and development from 8 GHz to 600 GHz
[DE91-008320] N91-19358
Plasma boundary experiments on D3-D tokamak
[DE91-002429] N91-19881
Optically-ionized plasma recombination x ray lasers
[DE91-007261] N91-19898

PLASMA LAYERS
Association of an auroral surge with plasma sheet recovery and the retreat of the substorm neutral line
[DE91-007351] N91-19552

PLASMA PHYSICS
Summary of the International Dawson Symposium on The Physics of Plasmas
[DE91-006912] N91-19897

PLASMA PINCH
Generation and focusing of carbon ion beam by the inverse pinch ion diode N91-19890

PLASMA PROPULSION
Enhancing space transportation: The NASA program to develop electric propulsion
[NASA-TM-4244] N91-19181

PLASMA SHEATHS
Control of gap closure in applied-B diode N91-19893

PLASMA TEMPERATURE
New method for edge plasma control by RF ponderomotive force
[DE91-744823] N91-19911
Electron temperature of Gd plasma produced by laser resonance ionization
[DE91-744833] N91-19913

PLASMA TURBULENCE
Relaxed states with plasma flow
[DE91-008199] N91-19909

PLASMAS (PHYSICS)
Energy sciences supercomputing 1990
[DE91-007188] N91-19740
Parallel processing for a 1-D time-dependent solution to impurity rate equations for fusion plasma simulations
[DE90-015857] N91-19759
Plasma boundary experiments on D3-D tokamak
[DE91-002429] N91-19881
Optically-ionized plasma recombination x ray lasers
[DE91-007261] N91-19898
Particle-in-cell plasma simulation codes on the connection machine
[DE91-007845] N91-19902
Effects of pressure profile and plasma shaping on the n=1 internal kink mode in JT-60/JT-60U pellet fuelled plasmas
[DE91-744965] N91-19914
A study of alkaline element interferences in analytical inductively coupled plasmas
[ISAL-90-0069] N91-19915
Noble gas disk MHD generator performance with unstable nonequilibrium plasma
[ISBN-90-9003671-7] N91-19916

PLASTIC PROPELLANTS
Extrudable PBX molding powder
[AD-D014667] N91-19312

PLASTIC PROPERTIES
Texture and microstructure development in Al-2 percent Mg during high-temperature deformation
[DE91-007355] N91-19480

PLATES (STRUCTURAL MEMBERS)
An expert system for laminated plate design using composite materials
[BU-406] N91-19245

PLATFORMS
Design and control of a fully omnidirectional and holonomic wheeled platform for robotic vehicles
[DE90-017746] N91-19445

PLATINUM ALLOYS
Chemical interactions in multimetal/zeolite catalysts
[DE91-007978] N91-19261

PLEURAE
Gravity dependence of pleural liquid turnover N91-19651

PLUMES
Solar rocket plume/mirror interactions
[NASA-CR-185300] N91-19059
Pitot measurements in the exhaust of a cluster of four small scale supersonic nozzles
[OUEL-1862/90] N91-19070
High vacuum facility for hydrazine thruster testing N91-19134
Flow fields of low pressure vent exhausts N91-19135
The application of simulation model for the flow induced by air bubble plume in thermally stratified reservoirs
[DE91-003064] N91-19380

PLY ORIENTATION
Dynamic behavior of pneumatic tyres
[BU-412] N91-19453

PNEUMATIC EQUIPMENT
Pneumatic launcher
[AD-D014658] N91-19116
Transfer orbit stage mechanisms thermal vacuum test N91-19161

PNEUMATICS
Pneumatic launcher
[AD-D014658] N91-19116

POINCARE PROBLEM
Invariant tori of the Poincare return map as solutions of functional difference equations
[DE91-007423] N91-19777

POLAR REGIONS
Ozone measurements from the NOAA-9 and the Nimbus-7 satellites: Implications of short and long term variabilities N91-19527

POLARIZATION (CHARGE SEPARATION)
Fiber optic interferometric measuring method for the determination of a very small polarization coefficient
[MBB-UA-1185-90-PUB] N91-19876

POLARIZATION (SPIN ALIGNMENT)
The physics of laser polarized muonic atoms
[DE91-008045] N91-19845

POLARIZED LIGHT
A modulated high-power optical source specification
[AD-D014654] N91-19869

POLICIES
Space operations: NASA is not archiving all potentially valuable data
[GAO/IMTEC-91-3] N91-19955
US technology policy: Executive Office of the President
[PB91-119677] N91-19970

POLLEN
Arabidopsis thaliana (Heynh.) pollen: A new tool in heavy ions radiation N91-19685

POLLUTION MONITORING
Remote detection of organics using Fourier transform infrared spectroscopy
[DE91-006045] N91-19253

POLLUTION TRANSPORT
Throughfall and foliar extraction
[DE91-007184] N91-19535

POLYACRYLONITRILE
Phenomena affecting morphology of microporous poly(acrylonitrile) prepared via phase separation from solution
[DE91-004501] N91-19297

POLYCARBONATES
Synthesis and analysis of novel polymers with potential for providing both high permselectivity and permeability in gas separation applications
[DE91-008283] N91-19309

POLYESTERS
Synthesis and analysis of novel polymers with potential for providing both high permselectivity and permeability in gas separation applications
[DE91-008283] N91-19309

POLYMER CHEMISTRY
Low Earth orbital atomic oxygen and ultraviolet radiation effects on polymers
[NASA-TM-103711] N91-19294
Synthesis and analysis of novel polymers with potential for providing both high permselectivity and permeability in gas separation applications
[DE91-008283] N91-19309

POLYMER MATRIX COMPOSITES
Effect of fiber reinforcements on thermo-oxidative stability and mechanical properties of polymer matrix composites
[NASA-TM-103648] N91-19234
Probabilistic micromechanics and macromechanics of polymer matrix composites
[NASA-TM-103669] N91-19236

POLYMERIC FILMS
Low Earth orbital atomic oxygen and ultraviolet radiation effects on polymers
[NASA-TM-103711] N91-19294
Development of a piezoelectric polymer film pressure transducer for low frequency and dynamic pressure measurement
[AD-A229848] N91-19412
A flammability study of thin plastic film materials N91-20034

POLYMERIZATION
Gelcast zirconia-alumina composites
[DE91-007835] N91-19239
Synthesis and analysis of novel polymers with potential for providing both high permselectivity and permeability in gas separation applications
[DE91-008283] N91-19309

POLYMERS
Radioluminescent polymer lights
[DE91-005521] N91-19290
Polymer characterization using the time-resolved phosphorescence of singlet oxygen as a spectroscopic probe
[DE91-001269] N91-19303
Design considerations for multi component molecular-polymeric nonlinear optical materials
[DE91-006778] N91-19872

POLYNOMIALS
The cost-constrained traveling salesman problem
[DE91-004943] N91-19775

POLYSTYRENE
The mechanical behavior of microcellular foams
[DE91-006775] N91-19291

POLYURETHANE RESINS
The mechanical behavior of microcellular foams
[DE91-006775] N91-19291

PONDEROMOTIVE FORCES
New method for edge plasma control by RF ponderomotive force
[DE91-744823] N91-19911

POPULATION INVERSION
He-like spectra through charge exchange processes in tokamak plasmas
[NIFS-69] N91-19894

POROSITY
Experimental investigation of porous-floor effects on cavity flow fields at supersonic speeds
[NASA-TP-3032] N91-19042
Rigid mullitewhisker felt and method of preparation
[AD-D014648] N91-19225

POROUS MATERIALS
Phenomena affecting morphology of microporous poly(acrylonitrile) prepared via phase separation from solution
[DE91-004501] N91-19297

PORTABLE EQUIPMENT
Lessons learned from an Ada conversion project N91-19730

POSITION (LOCATION)
Method for determining astronomic azimuth
[AD-D014677] N91-19972

POSITION INDICATORS
Aircraft standstill, requirements for ground handling from the point of view of aircraft operation N91-19109

POSITRONS
Positron lifetime studies of defect structures in Ba(1-x)K(x)BiO3
[DE91-007341] N91-19919
POSTFLIGHT ANALYSIS
State estimation applications in aircraft flight-data analysis: A user's manual for SMACK
[NASA-RP-1252] N91-19082
POSTURE
Body proprioceptive references in weightlessness as studied by muscle tendon vibration N91-19581
Postural changes following sensory reinterpretation as an analog to spaceflight N91-19610
POTABLE WATER
Design and cost of near-term OTEC (Ocean Thermal Energy Conversion) plants for the production of desalinated water and electric power
[DE91-006406] N91-19508
POTASSIUM COMPOUNDS
Performance characteristics of an MHD (Magnetohydrodynamic) pilot plant electrostatic precipitator
[DE91-007218] N91-19905
POTENTIAL FIELDS
Cascading a systolic array and a feedforward neural network for navigation and obstacle avoidance using potential fields
[NASA-CR-177575] N91-19771
POTENTIAL FLOW
Panel methods: An introduction
[NASA-TP-2995] N91-19058
A novel potential/viscous flow coupling technique for computing helicopter flow fields
[NASA-CR-177568] N91-19060
Examinations of inverse scattering problem for the scalar Helmholtz equation in the field of first order approximations for potentials with compact supports and safe real wave numbers
[ETN-91-98949] N91-19339
POTENTIAL GRADIENTS
Pulse-power characteristic of VIVA-1 (Versatile Inductive Voltage Adder) N91-19888
POTENTIAL THEORY
Cascade flutter analysis with transient response aerodynamics
[NASA-TM-103746] N91-19475
POWDER (PARTICLES)
Rigid mullitewhisker felt and method of preparation
[AD-D014648] N91-19225
Ultrafine refractory particle formation in counterflow diffusion flames
[DE91-007693] N91-19260
Crystallization and properties of Sr-Ba aluminosilicate glass-ceramic matrices
[NASA-TM-103764] N91-19308
Silver-sheathed multifilament wires
[DE91-008107] N91-19941
POWDER METALLURGY
Low-density, high-strength intermetallic matrix composites by XD (trademark) synthesis
[NASA-TM-103724] N91-19233
The 70 percent tungsten heavy alloys: Processing and properties
[DE91-008259] N91-19282
Gas entrapment and evolution in aluminium alloys produced by powder metallurgy
[ETN-91-98918] N91-19285
POWER EFFICIENCY
Tandem concentrator solar cells with 30 percent (AMO) power conversion efficiency N91-19189
High power, high frequency lasertron RF sources
[DE91-006007] N91-19414
POWER LINES
Computational comparison of efficacies of aeolian vibration damping devices for multiconductor overhead power lines
[BU-411] N91-19487
PREAMPLIFIERS
Radiation damage studies on hybrid preamplifiers
[DE91-008411] N91-19359
Monolithic radiation hard charge sensitive preamplifier using junction field effect transistors
[DE91-008437] N91-19360
PRECAMBRIAN PERIOD
K/T age for the popigai impact event N91-19999
PREDICTION ANALYSIS TECHNIQUES
Prediction of ice shapes and their effect on airfoil performance
[NASA-TM-103701] N91-19047
Single-strain-gage force/stiffness buckling prediction techniques on a hat-stiffened panel
[NASA-TM-101733] N91-19077
ETARA PC version 3.3 user's guide: Reliability, availability, maintainability simulation model
[NASA-TM-103751] N91-19462
Application of thermal life prediction model to high-temperature aerospace alloys B1900+Hf and Haynes 188
[NASA-TM-4226] N91-19473
PREDICTIONS
Application of thermal life prediction model to high-temperature aerospace alloys B1900+Hf and Haynes 188
[NASA-TM-4226] N91-19473
Predicted Bremsstrahlung generation by energetic electron beams
[DE91-007164] N91-19858
PREGNANCY
Effect of the centrifuge forces on pregnant rats N91-19629
PRELAUNCH TESTS
Hubble Space Telescope and the space shuttle problems
[S-HRG-101-1087] N91-19974
PREPROCESSING
Algorithms for a very high speed universal noiseless coding module
[NASA-CR-187974] N91-19733
PRESIDENTIAL REPORTS
US technology policy: Executive Office of the President
[PB91-119677] N91-19970
PRESSURE DISTRIBUTION
F-18 high alpha research vehicle surface pressures: Initial in-flight results and correlation with flow visualization and wind-tunnel data
[NASA-TM-101724] N91-19051
Result of ONERA standard model test in 2m x 2m transonic wind tunnel
[DE91-750115] N91-19066
Multipurpose hardened spacecraft insulation N91-19136
Development of a piezoelectric polymer film pressure transducer for low frequency and dynamic pressure measurement
[AD-A229848] N91-19412
Effects of pressure profile and plasma shaping on the n=1 internal kink mode in JT-60/JT-60U pellet fuelled plasmas
[DE91-744965] N91-19914
PRESSURE EFFECTS
The performance of multilayer insulation in a rapidly depressurizing environment N91-19133
Unsteady blade pressure measurements for the SR-7A propeller at cruise conditions
[NASA-TM-103606] N91-19825
Effects of pressure profile and plasma shaping on the n=1 internal kink mode in JT-60/JT-60U pellet fuelled plasmas
[DE91-744965] N91-19914
Phase transitions and equation of state of CsI under high pressure and the development of a focusing system for x rays
[DE91-007646] N91-19930
PRESSURE GRADIENTS
An experimental study of the turbulent boundary layer on a transport wing in subsonic and transonic flow
[NASA-TM-102206] N91-19062
Elementary considerations on the gas dynamic design parameters of a MHD Faraday generator in relation to a gas turbine cycle
[LR-564] N91-19456
PRESSURE MEASUREMENT
Rotating pressure measurement system using an on board calibration standard
[NASA-TM-103676] N91-19401
Development of a piezoelectric polymer film pressure transducer for low frequency and dynamic pressure measurement
[AD-A229848] N91-19412
Blood pressure regulation in parabolic flight N91-19575
Unsteady blade pressure measurements for the SR-7A propeller at cruise conditions
[NASA-TM-103606] N91-19825
PRESSURE RATIO
Pitot measurements in the exhaust of a cluster of four small scale supersonic nozzles
[OUEL-1862/90] N91-19070
PRESSURE REGULATORS
Methods for combining a theoretical and an empirical approach in modelling pressure and flow control valves for CAE-programs for fluid power circuits
[ACTA-POLYTEC-SCAND-ME-96] N91-19392
PRESSURE SENSORS
Development of a piezoelectric polymer film pressure transducer for low frequency and dynamic pressure measurement
[AD-A229848] N91-19412
PRESSURE VESSELS
Effects of irradiation on crack-arrest toughness of two high-copper welds
[DE91-007189] N91-19270
PRESSURIZED CABINS
Bulging of fatigue cracks in a pressurized aircraft fuselage
[ETN-91-98927] N91-19489
PRESSURIZED WATER REACTORS
Petri nets and fault diagnosis in nuclear reactors
[RR-413] N91-19865
The use of an object oriented technique for fault diagnosis in nuclear reactors
[RR-414] N91-19866
Fault detection using optimal control techniques
[RR-419] N91-19867
PRIMARY COSMIC RAYS
Experimental data on study of cosmic ray particles in the E greater than or equal to 2 TeV energy range at the Cosmos-1713 satellite with the Sokol-2 device
[DE91-615479] N91-20020
PRINTED CIRCUITS
Software for the ODRENOK microcomputer. Program package for graphics editing
[DE91-614980] N91-19752
PRINTING
SIGNIF and GENFMT, SAS macros for computing and reporting significant digits
[DE91-007702] N91-19795
PRISMS
Standardization of motion sickness induced by left-right and up-down reversing prisms N91-19611
PRIVACY
Computers at risk: Safe computing in the information age
[LC-90-22329] N91-19721
PROBABILITY DISTRIBUTION FUNCTIONS
Free vibration of hexagonal panels supported at discrete points
[NASA-TM-102688] N91-19166
Response matrix Monte Carlo based on a general geometry local calculation for electron transport
[DE91-007638] N91-19794
PROBABILITY THEORY
Probabilistic micromechanics and macromechanics of polymer matrix composites
[NASA-TM-103669] N91-19236
Probabilistic simulation of uncertainties in thermal structures
[NASA-TM-103680] N91-19472
Punchthrough in hadronic showers: A parameterization of the total probability
[NOTA-INTERNA-968] N91-19854
The specification of glancing incidence mirrors in terms of system performance
[DE91-007564] N91-19874
PROBES
Polymer characterization using the time-resolved phosphorescence of singlet oxygen as a spectroscopic probe
[DE91-001269] N91-19303
PROBLEM SOLVING
Robust fault diagnosis of physical systems in operation
[NASA-TM-102767] N91-19073
Report of a workshop on Distributed Decision Making
[LC-89-64440] N91-19952
PROCESS CONTROL (INDUSTRY)
The effect of process conditions on the performance of epitaxial InP solar cells N91-19204
PRODUCT DEVELOPMENT
Method of producing superconducting materials in bulk form
[AD-D014656] N91-19917
PRODUCTION MANAGEMENT
Technology modernization assessment flexible automation
[DE91-005620] N91-19751
PRODUCTIVITY
Productivity and photosynthesis of selected crop plants under orbital light conditions: An approach to solar powered CELSS N91-19662
PROGRAM VERIFICATION (COMPUTERS)
Space Shuttle: NASA should implement independent oversight of software development
[GAO/IMTEC-91-20] N91-19119
QUEST/Ada (query utility environment for software testing of Ada: The development of a program analysis environment for Ada, task 1, phase 3
[NASA-CR-187983] N91-19735
PROGRAMMING LANGUAGES
Uncertainty reasoning applied to the assessment of composite material for structural design
[BU-405] N91-19244

The FORCE: A highly portable parallel programming language
[NASA-CR-187928] N91-19732
Formal specification of human-computer interfaces N91-20023

PROJECT MANAGEMENT
Microgravity strategic plan, 1988
[NASA-TM-103397] N91-19319
QUEST/Ada (query utility environment for software testing of Ada: The development of a program analysis environment for Ada, task 1, phase 3
[NASA-CR-187983] N91-19735
Materials sciences programs
[DE91-007601] N91-19953

PROJECT PLANNING
Microgravity strategic plan, 1988
[NASA-TM-103397] N91-19319
Solid earth science in the 1990s. Volume 1: Program plan
[NASA-TM-4256-VOL-1] N91-19499
COMPLEAT (community-oriented model for planning least-cost energy alternatives and technologies): A planning tool for publicly owned electric utilities
[DE91-006955] N91-19511

PROJECTILES
The development of a ram air decelerator for the recovery of artillery shells
[DE91-007732] N91-19064
Launching projectiles with hydrogen gas generated from titanium-water reactions
[AD-D014653] N91-19171
Effects of hyperbaric oxygenation on central hemodynamics and oxygen consumption in severe physical trauma N91-19570

PROJECTS
Project of a cost analysis model for the acquisition of a permanent lunar base
[ILR-MITT-245(1990)] N91-19114

PROP-FAN TECHNOLOGY
Inflight source noise of an advanced full-scale single-rotation propeller
[NASA-TM-103687] N91-19045
The selection of convertible engines with current gas generator technology for high speed rotorcraft
[NASA-TM-103774] N91-19097

PROPELLANT PROPERTIES
Detailed modal testing of a solid rocket motor using a portable test system N91-19144

PROPELLER BLADES
Unsteady blade pressure measurements for the SR-7A propeller at cruise conditions
[NASA-TM-103606] N91-19825

PROPELLER FANS
Inflight source noise of an advanced full-scale single-rotation propeller
[NASA-TM-103687] N91-19045
The selection of convertible engines with current gas generator technology for high speed rotorcraft
[NASA-TM-103774] N91-19097

PROPELLERS
Inflight source noise of an advanced full-scale single-rotation propeller
[NASA-TM-103687] N91-19045

PROPHYLAXIS
Medical results of the fourth prime expedition on the orbital station Mir N91-19576

PROPORTIONAL COUNTERS
Principle and realization of the instrument used for the CIRCE experiment on board the Mir station N91-19684

PROPRIOCEPTION
Body proprioceptive references in weightlessness as studied by muscle tendon vibration N91-19581

PROPRIOCEPTORS
Ocular roll under changing z-axis acceleration and neck position N91-19580
Body proprioceptive references in weightlessness as studied by muscle tendon vibration N91-19581

PROPULSION
Dedication of National Institute for Aviation Research
[NIAR-90-21] N91-19040

PROPULSION SYSTEM CONFIGURATIONS
Propulsion system concept for the Eurofar tilt rotor aircraft
[MBB-UD-0573-90-PUB] N91-19084
The selection of convertible engines with current gas generator technology for high speed rotorcraft
[NASA-TM-103774] N91-19097
Solar electric propulsion for Mars transport vehicles
[NASA-TM-103234] N91-19178

PROPULSION SYSTEM PERFORMANCE
The selection of convertible engines with current gas generator technology for high speed rotorcraft
[NASA-TM-103774] N91-19097
Engineering monitoring expert system's developer
[NASA-CR-187914] N91-19765

PROTEIN CRYSTAL GROWTH
Protein purification in multicompartment electrolyzers for crystal growth of r-DNA products in microgravity N91-19665

PROTEINS
Contractile protein changes induced by hindlimb suspension in rat skeletal muscle N91-19646
A new approach to electrophoresis in space N91-19653
Physiological genetics of denitrification: A route to conserving fixed nitrogen
[DE91-008157] N91-19707
Subcellular signal transduction systems in the cellular trauma of ischemia
[AD-A229876] N91-19709

PROTON BEAMS
Power plant by LIB fusion N91-19892

PROTON IRRADIATION
Effects of proton irradiation on the performance of InP/GaAs solar cells N91-19205
Annealing characteristics of irradiated hydrogenated amorphous silicon solar cells N91-19214

PROTONS
Proton induced x ray emission analysis N91-19832

PROTOPLASTS
Regeneration and characterization of protoplast-derived cell lines from Digitalis lanata EHRH. and Digitalis purpurea L. suspension cultures after electrofusion under microgravity conditions N91-19652
Plant protoplast development on Biokosmos 9 N91-19674
Electrofusion and regeneration of protoplasts from sunflower (Helianthus annuus L.) N91-19675

PROTOTYPES
Development of a vibration isolation prototype system for microgravity space experiments
[NASA-TM-103664] N91-19324

PROTOZOA
Microbiological assay using bioluminescent organism
[AD-D014651] N91-19249

PROVING
Formal proof of the AVM-1 microprocessor using the concept of generic interpreters
[NASA-CR-187491] N91-19756

PROXIMITY
Real-time sensor-based approach to the improvement of transitions of robot manipulator controls
[OUEL-1866/90] N91-19459

PSYCHOLOGICAL TESTS
Effects of high temperature and humidity on mental state and metabolism N91-19571

PUBLIC HEALTH
The dilemma of fossil fuel use and global climate change
[DE91-007859] N91-19533

PUBLIC RELATIONS
Airport apron research and development
[MBB-Z-0168-90-PUB] N91-19106

PULSARS
Search for the optical signatures of a pulsar in SN1987A
[MPE-PREPRINT-188] N91-19978

PULSE AMPLITUDE
Computer controlled MHD power consolidation and pulse generation system
[DE91-006793] N91-19347

PULSE DIFFRACTION
Elementary pulse diffraction problems and the generation of sound by a dipole moving across the edge of a half-plane
[LR-565] N91-19831

PULSE DURATION
Pulsed response of a traveling-wave tube
[NASA-TM-103672] N91-19348
Microsecond-pulse Nd-glass laser with monopulse duration control N91-19811
Coherent effects in generation of ultrashort light pulses by semiconductor injection laser N91-19820

PULSE GENERATORS
Computer controlled MHD power consolidation and pulse generation system
[DE91-006793] N91-19347
Generation of pulsed ion beams by an inductive storage pulsed power generator N91-19891

PULSE MODULATION
High pulse repetition frequency radar early warning receiver
[AD-D014655] N91-19328

PULSE RADAR
High pulse repetition frequency radar early warning receiver
[AD-D014655] N91-19328

PULSE RATE
High pulse repetition frequency radar early warning receiver
[AD-D014655] N91-19328

PULSED LASERS
High power, high frequency lasertron RF sources
[DE91-006007] N91-19414
Excimer laser surface processing for tribological applications in metals and ceramics
[DE91-002324] N91-19428
Investigation at two wavelengths of a modulated He-Xe rare gas laser
[AD-A229852] N91-19434
Theory of CW lidar aerosol backscatter measurements and development of a 2.1 microns solid-state pulsed laser radar for aerosol backscatter profiling
[NASA-CR-4347] N91-19498
Passive mode locking in optically pumped Al2O3:Ti(3+) laser N91-19803
Copper vapor as active medium for high-power oscillator-amplifier laser systems N91-19806
Microsecond-pulse Nd-glass laser with monopulse duration control N91-19811
Development of high current electron source using photoemission from metals with ultrashort laser pulses
[DE91-008438] N91-19850
UV Thomson scattering from x ray laser plasmas
[DE91-007347] N91-19895

PULSED RADIATION
Pulse-power characteristic of VIVA-1 (Versatile Inductive Voltage Adder) N91-19888
Reduction of low energy components in pulse ion beam N91-19889

PULSES
Reflections on some problems concerning the role of superfluid turbulence in the propagation of second-sound pulses in He 2
[MPIS-8/1990] N91-19827

PUPIL SIZE
Pupil size in parabolic flight N91-19693

PURIFICATION
The application of simulation model for the flow induced by air bubble plume in thermally stratified reservoirs
[DE91-003064] N91-19380

PYRAZINES
Studies of atmospheric molecules by multiphoton spectroscopy
[DE91-006738] N91-19554

Q

Q FACTORS
New experimental approach in quality factor and dose equivalent determination during a long term manned space mission N91-19679

Q SWITCHED LASERS
Microsecond-pulse Nd-glass laser with monopulse duration control N91-19811
Coherent effects in generation of ultrashort light pulses by semiconductor injection laser N91-19820

QUALIFICATIONS
The full-scale process and design changes for elimination of insulation edge separations and voids in tang flap area
[NASA-CR-184110] N91-19172

QUALITATIVE ANALYSIS
Remote detection of organics using Fourier transform infrared spectroscopy
[DE91-006045] N91-19253
The qualitative analysis of nonlinear parameterised systems. Part 2: A method for the global analysis of nonlinear systems
[RR-400-PT-2] N91-19754
The qualitative analysis of nonlinear parameterized systems. Part 1: Nonlinear systems representation and dynamical systems theory
[RR-408-PT-1] N91-19789
Stable hydrogen and carbon isotope ratios of extractable hydrocarbons in the Murchison meteorite N91-20006

QUALITY CONTROL
Space Shuttle: NASA should implement independent oversight of software development
[GAO/IMTEC-91-20] N91-19119
Sandia technology: Engineering and science applications
[DE91-006760] N91-19322
Problems at National Aeronautics and Space Administration
[S-HRG-101-1146] N91-19969
Hubble Space Telescope and the space shuttle problems
[S-HRG-101-1087] N91-19974

QUANTITATIVE ANALYSIS
Remote detection of organics using Fourier transform infrared spectroscopy
[DE91-006045] N91-19253

QUANTUM EFFICIENCY
GaAs solar cell photoresponse modeling using PC-1D V2.1 N91-19193

High-efficiency, radiation-resistant GaAs space cells N91-19194
Summary of the working group on transverse emissions from photocathodes
[DE91-008414] N91-19432
Photoemission studies using femtosecond pulses for high brightness electron beams
[DE91-008436] N91-19849
Development of high current electron source using photoemission from metals with ultrashort laser pulses
[DE91-008438] N91-19850

QUANTUM ELECTRODYNAMICS
Classical and quantum charge dynamics in small tunnel junctions
[ETN-91-98916] N91-19947

QUANTUM NUMBERS
He-like spectra through charge exchange processes in tokamak plasmas
[NIFS-69] N91-19894

QUANTUM OPTICS
Quantum optics reveals the nature of superconductivity
[TR-69] N91-19946

QUANTUM THEORY
Quantum fluctuations in laser with intracavity frequency doubling N91-19805
Symmetries on the space of (2,2) superstring vacua and automorphism groups of Calabi-Yau manifolds
[DE91-008218] N91-19951
How many times do we have in quantum gravity
[DE91-744973] N91-19991

QUARKS
Sixquarks in neutron stars
[DE91-615472] N91-19987

QUARTZ
Vibration and thermal vacuum qualification test results for a low-voltage tungsten-halogen light
[NASA-CR-187050] N91-19325

QUASARS
Origin of regularities in the redshift distributions of distant galaxies and quasars
[DE91-007889] N91-19986
Proceedings of the symposium Astrophysical Processes and Structures in the Universe
[PB91-123653] N91-19993

QUENCHING (ATOMIC PHYSICS)
Frontier orbital symmetry control of intermolecular electron transfer
[DE91-005699] N91-19834

QUENCHING (COOLING)
Studies of cold protection diodes
[DE91-008203] N91-19863

R

RABBITS
Gravitation receptor reaction in response to effect of acceleration N91-19569
Hindlimb suspension of rabbit for one week: Myofibrillar damage in the soleus may depend on long-lasting shortening and periodic contraction against no load N91-19647
Gravity dependence of pleural liquid turnover N91-19651

RACKS (FRAMES)
Wire-free arming system for an aircraft-delivered bomb
[AD-D014611] N91-19076

RADAR
Fiber optic feed
[AD-A229860] N91-19879

RADAR DATA
Radar-measured height profiles of Cn(2) and turbulence dissipation rate compared with radiosonde data during October 1989 at Denver
[PB91-125500] N91-19562

RADAR MAPS
Mars radar mapping: Strong depolarized echoes from the Elysium/Amazonis outflow channel complex N91-20001

RADAR MEASUREMENT
Theory of CW lidar aerosol backscatter measurements and development of a 2.1 microns solid-state pulsed laser radar for aerosol backscatter profiling
[NASA-CR-4347] N91-19498
Radar-measured height profiles of Cn(2) and turbulence dissipation rate compared with radiosonde data during October 1989 at Denver
[PB91-125500] N91-19562

RADAR RECEIVERS
High pulse repetition frequency radar early warning receiver
[AD-D014655] N91-19328

RADAR SCATTERING
Slope modulation of the radar backscatter by sea waves
[BCRS-88-05] N91-19327

RADAR TRACKING
BUBBLES: An automated decision support system for final approach controllers N91-19027
Preliminary results from an airdata enhancement algorithm with application to high-angle-of-attack flight
[NASA-TM-101737] N91-19095

RADIANCE
NOAA-9 SBUV/2 ozone sounding accuracy: Presentation summary N91-19519
A technique for directly comparing radiances from two satellites N91-19520
ICRCCM (intercomparison of radiation codes used in climate models). Phase 2: Verification and calibration of radiation codes in climate models
[DE91-007323] N91-19555

RADIANT FLUX DENSITY
Proposal for a conceptually new compact collecting optics for powerful light sources N91-19155

RADIATION ABSORPTION
Light guide fibers
[MBB-UA-1199-90-PUB] N91-19877

RADIATION DAMAGE
Radiation resistance of thin-film solar cells for space photovoltaic power
[NASA-TM-103715] N91-19176
InP/Ga0.47In0.53As monolithic, two-junction, three-terminal tandem solar cells N91-19191
Burst annealing of high temperature GaAs solar cells N91-19196
GaP betavoltaic cells as a power source N91-19211
Radiation damage studies on hybrid preamplifiers
[DE91-008411] N91-19359
Neutron radiation damage studies on silicon detectors
[DE91-008441] N91-19361
Defective embryogenesis of Arabidopsis induced by cosmic HZE-particles N91-19682
Arabidopsis thaliana (Heynh.) pollen: A new tool in heavy ions radiation N91-19685
Predictions of cell damage rates for Lifesat missions
[NASA-TM-102170] N91-19699
Potential health risks from postulated accidents involving the Pu-238 RTG (Radioisotope Thermoelectric Generator) on the Ulysses solar exploration mission
[DE91-007142] N91-19857

RADIATION DETECTORS
LDEF Experiment P0006 Linear Energy Transfer Spectrum Measurement (LETSME) quick look report
[NASA-CR-184115] N91-19223

RADIATION DISTRIBUTION
Cloud forcing: A modeling perspective
[DE91-007215] N91-19551
Semiconductor photodiodes as radiometric receivers in the field of soft radiation
[ETN-91-98925] N91-19856

RADIATION DOSAGE
New experimental approach in quality factor and dose equivalent determination during a long term manned space mission N91-19679
Genetic risk and physiological stress induced by heavy ions N91-19680
Principle and realization of the instrument used for the CIRCE experiment on board the Mir station N91-19684

RADIATION EFFECTS
High-efficiency, radiation-resistant GaAs space cells N91-19194
Effects of proton irradiation on the performance of InP/GaAs solar cells N91-19205
The Advanced Photovoltaic Solar Array (APSA) technology status and performance N91-19217
Strategy in space flight experiments N91-19220
Indium phosphide solar cells N91-19221
Effects of irradiation on crack-arrest toughness of two high-copper welds
[DE91-007189] N91-19270
Radiation-induced changes in electrical conductivity of a wide range of copper alloys
[DE91-007200] N91-19271
Low Earth orbital atomic oxygen and ultraviolet radiation effects on polymers
[NASA-TM-103711] N91-19294
Radiation damage studies on hybrid preamplifiers
[DE91-008411] N91-19359
Neutron radiation damage studies on silicon detectors
[DE91-008441] N91-19361
ICRCCM (intercomparison of radiation codes used in climate models). Phase 2: Verification and calibration of radiation codes in climate models
[DE91-007323] N91-19555
Fourth European Symposium on Life Sciences Research in Space
[ESA-SP-307] N91-19572
Arabidopsis thaliana (Heynh.) pollen: A new tool in heavy ions radiation N91-19685
Research in radiobiology: Work in progress in immunobiology of experimental host-tumor relationships
[DE91-007936] N91-19705
Rayleigh-Taylor instability in LIB ICF N91-19883

RADIATION HARDENING
High-efficiency, radiation-resistant GaAs space cells N91-19194
Radiation damage studies on hybrid preamplifiers
[DE91-008411] N91-19359
Monolithic radiation hard charge sensitive preamplifier using junction field effect transistors
[DE91-008437] N91-19360

RADIATION HAZARDS
Potential health risks from postulated accidents involving the Pu-238 RTG (Radioisotope Thermoelectric Generator) on the Ulysses solar exploration mission
[DE91-007142] N91-19857

RADIATION MEASUREMENT
LDEF Experiment P0006 Linear Energy Transfer Spectrum Measurement (LETSME) quick look report
[NASA-CR-184115] N91-19223
Principle and realization of the instrument used for the CIRCE experiment on board the Mir station N91-19684

RADIATION THERAPY
Research in radiobiology: Work in progress in immunobiology of experimental host-tumor relationships
[DE91-007936] N91-19705

RADIATION TOLERANCE
Radiation resistance of thin-film solar cells for space photovoltaic power
[NASA-TM-103715] N91-19176
Performance, size, mass, and cost estimates for projected 1kW EOL Si, InP, and GaAs arrays N91-19199
Effects of proton irradiation on the performance of InP/GaAs solar cells N91-19205
A comparative study of performance parameters of n(+)-p InP solar cells made by closed-ampoule sulfur diffusion into Cd- and Zn-doped p-type InP substrates N91-19209
Annealing characteristics of irradiated hydrogenated amorphous silicon solar cells N91-19214
Effect of dislocations on the open-circuit voltage, short-circuit current and efficiency of heteroepitaxial indium phosphide solar cells
[NASA-TM-103762] N91-19354
Studies of cold protection diodes
[DE91-008203] N91-19863

RADIATION TRANSPORT
Analysis of spherical geometry finite element transport solutions in the thick diffusion limit
[DE91-007598] N91-19780
Even- and odd-parity finite-element transport solutions in the thick diffusion limit
[DE91-007618] N91-19781
Discontinuous finite-element transport solutions in the thick diffusion limit in Cartesian geometry
[DE91-007620] N91-19782

RADIO ASTRONOMY
Quantum optics reveals the nature of superconductivity
[TR-69] N91-19946
A scientific program for infrared, submillimeter and radio astronomy from space: A report by the Management Operations Working Group
[NASA-TM-103333] N91-19979

RADIO FREQUENCIES
High pulse repetition frequency radar early warning receiver
[AD-D014655] N91-19328
Modeling a ferrite-tuned RF cavity
[DE91-008235] N91-19356
A pocket-size broadband electric field detection and storage device
[DE91-007710] N91-19406
High power, high frequency lasertron RF sources
[DE91-006007] N91-19414
New method for edge plasma control by RF ponderomotive force
[DE91-744823] N91-19911

RADIO RECEIVERS
Using a modified Hewlett Packard 8410 network analyzer as an automated farfield antenna range receiver
[NASA-TM-103700] N91-19349
Development of components and subsystems for low noise receivers at micro- and millimeter waves
[S-187] N91-19363

RADIO TELESCOPES
Mars radar mapping: Strong depolarized echoes from the Elysium/Amazonis outflow channel complex N91-20001

RADIOACTIVE DECAY
Effects of radiolytic tritium decay on the thermodynamic behavior of LaNi(4.25)Al(0.75) tritides
[DE91-007961] N91-19277
RADIOACTIVE ISOTOPES
Evaluation of a Photo-Electron Rejecting Alpha Liquid Scintillation (PERALS) spectrometer for the measurement of alpha-emitting radionuclides
[DE91-005652] N91-19399
Research in radiobiology: Work in progress in immunobiology of experimental host-tumor relationships
[DE91-007936] N91-19705
RADIOACTIVITY
Radioluminescent polymer lights
[DE91-005521] N91-19290
RADIOBIOLOGY
Research in radiobiology: Work in progress in immunobiology of experimental host-tumor relationships
[DE91-007936] N91-19705
RADIOIMMUNOASSAY
Human dermal fibroblast sensitivity to hypergravity
N91-19630
RADIOISOTOPE BATTERIES
Radioisotope thermal photovoltaic application of the GaSb solar cell N91-19210
GaP betavoltaic cells as a power source N91-19211
RADIOLYSIS
Effects of radiolytic tritium decay on the thermodynamic behavior of LaNi(4.25)Al(0.75) tritides
[DE91-007961] N91-19277
Research conducted at the Radiation Lab, Notre Dame Univ.
[DE91-007969] N91-19843
RADIOMETERS
Design, performance evaluation, and investigation of the theoretical capabilities of the NASA Millimeter-wave Imaging Radiometer (MIR)
[NASA-CR-187984] N91-19398
Semiconductor photodiodes as radiometric receivers in the field of soft radiation
[ETN-91-98925] N91-19856
RADIOSONDES
Radar-measured height profiles of Cn(2) and turbulence dissipation rate compared with radiosonde data during October 1989 at Denver
[PB91-125500] N91-19562
RAIL TRANSPORTATION
Safety of high speed magnetic levitation transportation systems. Preliminary safety review of the transrapid maglev system
[PB91-129684] N91-19326
RAMAN LASERS
Coherent effects in generation of ultrashort light pulses by semiconductor injection laser N91-19820
RAMAN SPECTRA
Breakup of femtosecond pulses during amplification in Er(3+)-doped single-mode optical fibers N91-19812
RAMJET ENGINES
Solid fuel combustion chamber
[LR-648] N91-19222
RAMPS (STRUCTURES)
Turbulent boundary layer separation over a rearward facing ramp and its control through mechanical excitation
[NASA-TM-103702] N91-19370
RANDOM ACCESS MEMORY
Enhanced crosstie random access memory element and process for the fabrication thereof
[AD-D014723] N91-19717
RANDOM NUMBERS
Correlations of pseudo-random numbers of multiplicative sequence
[DE91-615076] N91-19788
RANGEFINDING
Modeling selective availability of the NAVSTAR global positioning system N91-19030
RAPID TRANSIT SYSTEMS
Safety of high speed magnetic levitation transportation systems. Preliminary safety review of the transrapid maglev system
[PB91-129684] N91-19326
RARE EARTH ELEMENTS
Fluorescent lifetime measurements of rare Earth elements in gallium arsenide
[AD-A229865] N91-19265
Cosmic dust: Laboratory analyses of extremely small particles N91-20013
RARE GASES
Investigation at two wavelengths of a modulated He-Xe rare gas laser
[AD-A229852] N91-19434
Correlation of leak rates of various fluids with the leak rate of an inert gas in the same configuration
N91-20033
RATIONAL FUNCTIONS
Rational model identification using an extended least squares algorithm
[RR-388] N91-19753
RATIOS
Analysis of SBUV/2 measurements of solar UV irradiance variations N91-19526
RATS
Altered cartilage differentiation in tibial epiphyseal plates of Cosmos rats N91-19628
Effect of the centrifuge forces on pregnant rats
N91-19629
Blood pressure maturation curve in normotensive rats during growth in simulated microgravitational environment N91-19644
Contractile protein changes induced by hindlimb suspension in rat skeletal muscle N91-19646
Cosmos: 1989 immunology studies
[NASA-CR-188046] N91-19701
RAYLEIGH-BENARD CONVECTION
Filtering analysis of a direct numerical simulation of the turbulent Rayleigh-Benard problem
[NASA-CR-187488] N91-19366
REACTION KINETICS
Control of catalytic hydrotreating selectivity with ammonia
[DE91-005511] N91-19250
Direct conversion of methane to C2's
[DE91-005730] N91-19251
Methane to methanol conversion by direct partial oxidation
[DE91-007352] N91-19257
Studies of combustion kinetics and mechanisms
[DE91-007829] N91-19259
Comprehensive mechanisms for combustion chemistry: An experimental and numerical study with emphasis on applied sensitivity analysis
[DE91-008030] N91-19262
Mechanisms and controlling characteristics of the catalytic oxidation of methane
[DE91-008033] N91-19263
Research conducted at the Radiation Lab, Notre Dame Univ.
[DE91-007969] N91-19843
Thin film reactions on alloy semiconductor substrates
[DE91-007651] N91-19931
Mutual influence of doping and oxidation in highly doped silicon
[ETN-91-98924] N91-19948
Some limitations of detailed balance for inverse reaction calculations in the astrophysical P-process
[DE91-007258] N91-19983
REACTIVITY
Reactivity of pi-complexes of Ti, V, and Nb towards dithioacetic acid: Synthesis and structure of novel metal sulfur-containing complexes
[NASA-TM-103666] N91-19256
Synthesis and structures of metal chalcogenide precursors
[NASA-TM-103665] N91-19296
Aerosol formation in atmospheric mixtures
[PB91-129114] N91-19560
REACTOR DESIGN
Development of KrF lasers for inertial confinement fusion
[DE91-007349] N91-19419
Some neutronics and thermal-hydraulics codes for reactor analysis using personal computers
[DE91-006591] N91-19743
REACTOR MATERIALS
US-Japan workshops: Q-111, Development of Plasma Facing Components and Materials for Next Large Fusion Devices, and Q-112, Vacuum and First Wall Technology for Fusion Devices
[DE91-006879] N91-19896
REACTOR SAFETY
Lessons learned from the design and operation of steam generators for high temperature gas-cooled reactors
[DE91-006139] N91-19450
Petri nets and fault diagnosis in nuclear reactors
[RR-413] N91-19865
Introduction to fusion
[DE91-744831] N91-19912
REACTOR TECHNOLOGY
Lessons learned from the design and operation of steam generators for high temperature gas-cooled reactors
[DE91-006139] N91-19450
Symposium on Development of Intensed Pulsed Particle Beams and Its Applications
[NIFS-PROC-5] N91-19882
US-Japan workshops: Q-111, Development of Plasma Facing Components and Materials for Next Large Fusion Devices, and Q-112, Vacuum and First Wall Technology for Fusion Devices
[DE91-006879] N91-19896
REAL TIME OPERATION
Flight simulation for wind shear encounter
N91-19035
A simple dynamic engine model for use in a real-time aircraft simulation with thrust vectoring
[NASA-TM-4240] N91-19079
Visual navigation around curved obstacles
[OUEL-1861/90] N91-19458
Real-time sensor-based approach to the improvement of transitions of robot manipulator controls
[OUEL-1866/90] N91-19459
An on-line real-time system for fatigue crack growth monitoring
[DE91-007931] N91-19483
A new generation of real-time DOS technology for mission-oriented system integration and operation
N91-19725
Analyzing product test data in an INGRES database using SAS software
[DE91-008251] N91-19965
RECEIVERS
Ridge regression signal processing N91-19029
Semiconductor photodiodes as radiometric receivers in the field of soft radiation
[ETN-91-98925] N91-19856
RECOMBINATION REACTIONS
Optically-ionized plasma recombination x ray lasers
[DE91-007261] N91-19898
RECRYSTALLIZATION
Texture and microstructure development in Al-2 percent Mg during high-temperature deformation
[DE91-007355] N91-19480
RECTANGULAR WAVEGUIDES
Simulation of a standing-wave free-electron laser
[DE91-007330] N91-19418
RECYCLING
A ground based module for experimentations of cultivations and recycling in a closed environment
N91-19657
RED GIANT STARS
Proceedings of the symposium Astrophysical Processes and Structures in the Universe
[PB91-123653] N91-19993
RED SHIFT
Origin of regularities in the redshift distributions of distant galaxies and quasars
[DE91-007889] N91-19986
Observational relations in model universes dominated by domain-wall-like matter
[DE91-744969] N91-19988
REDUCED GRAVITY
COLD-SAT feasibility study safety analysis
[NASA-CR-187042] N91-19167
Microgravity strategic plan, 1988
[NASA-TM-103397] N91-19319
Free flow electrophoresis experiment TEPE 3 on Texus 24
[MBB-UO-0130-90-PUB] N91-19321
Integrated Cryogenic Experiment (ICE) microsphere investigation
[NASA-CR-177538] N91-19323
Development of a vibration isolation prototype system for microgravity space experiments
[NASA-TM-103664] N91-19324
A summary of existing and planned experiment hardware for low-gravity fluids research
[NASA-TM-103706] N91-19371
In-space experiment on thermoacoustic convection heat transfer phenomenon-experiment definition
[NASA-CR-187070] N91-19378
Liquid sloshing response in a spinning container due to pitching excitation
[LRT-WE-9-FB-11(1990)] N91-19388
Response of a differently axially excited viscous liquid layer in zero-gravity
[LRT-WE-9-FB-12(1990)] N91-19389
Response of a viscous liquid layer to pitch- and roll-excitation in zero-gravity environment
[LRT-WE-9-FB-13(1990)] N91-19390
Fourth European Symposium on Life Sciences Research in Space
[ESA-SP-307] N91-19572
Lung volumes, chest wall configuration, and pattern of breathing in microgravity N91-19574
Blood pressure regulation in parabolic flight
N91-19575
Ultrasound investigation of the cardiovascular system during the 25 days French-Soviet spaceflight (26 November - 21 December 1988) N91-19577
Ultrasound investigation of the cardiovascular system during the 25-days Soviet-French flight: Cardiac aspects
N91-19578
Vestibular function in altered states of gravity
N91-19579
Body proprioceptive references in weightlessness as studied by muscle tendon vibration N91-19581

Medex: A useful tool for counteracting orthostatic intolerance resulting from body fluid loss under microgravity N91-19585
Oxygen uptake during concentric and eccentric resistive exercise using a new gravity-independent ergometer N91-19587
Is physiological tremor (microvibration) influenced by microgravity N91-19595
Simulation expert system for physiological mechanisms of the space motion sickness N91-19596
Skeletal adaptation in altered gravity environments N91-19603
Tools for the preparation, performance and evaluation of life sciences experiments N91-19609
Effects of training with reduced perfusion pressure on performance and muscle fiber characteristics N91-19615
Gravity effects on cells N91-19618
Lymphocytes on sounding rockets N91-19620
Reduced lymphocyte activation in space: Role of cell-substratum interactions N91-19621
Developmental biology and microgravity N91-19622
Epidermal growth factor induced signal transduction in A431 cells is influenced by altered gravity conditions N91-19623
Fertilization of Xenopus eggs in space N91-19624
Microgravity and development of aquatic animals N91-19625
Preliminary study of a membrane bioreactor for cell culture in space N91-19627
Altered cartilage differentiation in tibial epiphyseal plates of Cosmos rats N91-19628
Cellular functions of Paramecium under different gravity conditions N91-19631
Growth rate of bacteria without and with antibiotic at different levels of gravity N91-19632
Microgravity, hypergravity, and aging: A unifying hypothesis N91-19633
An assay for bone cell differentiation in vitro as a tool for microgravity studies in space N91-19637
Unicellular algae in space. 1: Preparatory tests N91-19639
Unicellular algae in space. 2: Sounding-rocket experiment N91-19640
Unicellular algae in space. 3: Addendum N91-19641
Human and animal results on vestibular research in space: VERIS N91-19642
Bone adaptation to real and simulated microgravity N91-19643
Blood pressure maturation curve in normotensive rats during growth in simulated microgravitational environment N91-19644
Preliminary studies before defining a payload adapted to the primate model N91-19648
Review of EEG studies in non human primates exposed to microgravity N91-19649
Gravity dependence of pleural liquid turnover N91-19651
Regeneration and characterization of protoplast-derived cell lines from Digitalis lanata EHRH. and Digitalis purpurea L. suspension cultures after electrofusion under microgravity conditions N91-19652
A new approach to electrophoresis in space N91-19653
Free flow electrophoresis experiment TEPE 3 on TEXUS 24 N91-19654
Towards bioregenerative life support systems N91-19655
Cells in space: Sounding rocket facilities for cell biology and biotechnology in microgravity N91-19661
Protein purification in multicompartment electrolyzers for crystal growth of r-DNA products in microgravity N91-19665
Development of a miniature biology facility N91-19666
Graviperception in plants N91-19667
Gravitational effects on subcellular structures of plant cells N91-19669
Plant development in space: Observations on root formation and growth N91-19670
Plant growth under microgravity conditions: Experiments and problems N91-19671
Effect of gravity on the distribution of electron dense chromatin in the nucleus of root statocytes N91-19672
Graviorientation in photosynthetic flagellates N91-19673
Electrofusion and regeneration of protoplasts from sunflower (Helianthus annuus L.) N91-19675
The reference systems for tactile perception and for the orientation with respect to body N91-19691
Pupil size in parabolic flight N91-19693
Mental rotation of three-dimensional shapes in microgravity N91-19694
Potentials, message and challenges of life science research in space N91-19696
The 1989-1990 NASA space biology accomplishments [NASA-TM-4258] N91-19697
Cosmos: 1989 immunology studies [NASA-CR-188046] N91-19701
Experimental equipment for space biology [MBB-UO-0096-90-PUB] N91-19708
Responses of women to orthostatic and exercise stresses [NASA-TP-3043] N91-19711

REDUCTION (CHEMISTRY)
Plasma assisted NO(x) reduction in existing coal combustors [DE91-007380] N91-19536
Solid state, surface, and catalytic studies of oxides [DE91-007979] N91-19939
Experimental reduction of simulated lunar glass by carbon and hydrogen and implications for lunar base oxygen production N91-20009

REFLECTANCE
Radar-measured height profiles of Cn(2) and turbulence dissipation rate compared with radiosonde data during October 1989 at Denver [PB91-125500] N91-19562
The specification of glancing incidence mirrors in terms of system performance [DE91-007564] N91-19874

REFLECTED WAVES
Collision detection system [AD-D014645] N91-19072

REFLECTOR ANTENNAS
C-band antennas for regional communication systems [MBB-UK-0107-90-PUB] N91-19336
Measured performance of the half-scale accurate antenna reflector [NASA-CR-187047] N91-19350

REFLECTORS
Free vibration of hexagonal panels supported at discrete points [NASA-TM-102688] N91-19166

REFLEXES
Relation between perception of vertical axis rotation and vestibulo-ocular reflex symmetry [NASA-CR-187997] N91-19710
Carotid-cardiac baroreflex influence on forearm vascular resistance during low level LBNP N91-20030

REFRACTIVITY
Three-dimensional computed tomography from interferometric measurements within a narrow cone of views [NASA-TM-103257] N91-19404

REFRACTORY MATERIALS
NDE standards for high temperature materials [NASA-TM-103761] N91-19464
Application of MeV ions to the analysis and modification of high temperature superconducting materials [DE91-007317] N91-19927

REFRIGERANTS
Automatic control study of the icing research tunnel refrigeration system [NASA-TM-4257] N91-19115

REFRIGERATING
Automatic control study of the icing research tunnel refrigeration system [NASA-TM-4257] N91-19115
Loss analysis of the thermodynamic cycle of magnetic heat pumps [DE91-007669] N91-19950

REFUELING
Energy sciences supercomputing 1990 [DE91-007188] N91-19740

REGENERATION
Electrofusion and regeneration of protoplasts from sunflower (Helianthus annuus L.) N91-19675

REGENERATION (PHYSIOLOGY)
Towards bioregenerative life support systems N91-19655
A ground based module for experimentations of cultivations and recycling in a closed environment N91-19657

REGIONS
Initial estimate of NOAA-9 SBUV/2 total ozone drift: Based on comparison with re-calibrated TOMS measurements and pair justification of SBUV/2 N91-19523

REGRESSION ANALYSIS
Ridge regression signal processing N91-19029
Capattery double layer capacitor life performance [DE91-006639] N91-19344

REINFORCED PLASTICS
Investigation of ATP blades, part 3 [DE91-750104] N91-19105

REINFORCING FIBERS
An overview of self-consistent methods for fiber-reinforced composites [NASA-TM-103713] N91-19232
Effect of fiber reinforcements on thermo-oxidative stability and mechanical properties of polymer matrix composites [NASA-TM-103648] N91-19234

RELATIVISTIC ELECTRON BEAMS
A program of high power microwave source research and development from 8 GHz to 600 GHz [DE91-008320] N91-19358
Theory of the ion-channel laser [DE91-007643] N91-19423

RELATIVISTIC PARTICLES
Summary of discussions at the HIGH p (sub T) session [DE91-008196] N91-19848
Relativistic klystron research for future linear colliders [DE91-008063] N91-19862

RELATIVITY
How many times do we have in quantum gravity [DE91-744973] N91-19991

RELAXATION (MECHANICS)
Relaxed states with plasma flow [DE91-008199] N91-19909

RELIABILITY
Phase equilibrium modeling for high temperature metallization on GaAs solar cells N91-19192
Test analysis program evaluation: Item statistics as feedback to test developers [AD-A229851] N91-19713
Computers at risk: Safe computing in the information age [LC-90-22329] N91-19721
Hubble Space Telescope and the space shuttle problems [S-HRG-101-1087] N91-19974

RELIABILITY ANALYSIS
ETARA PC version 3.3 user's guide: Reliability, availability, maintainability simulation model [NASA-TM-103751] N91-19462
The challenge of standards for emerging NDT methods [DE91-007834] N91-19465
Software reliability through fault-avoidance and fault-tolerance [NASA-CR-187998] N91-19741

REMOTE CONTROL
Lag-stabilized force feedback damping [DE91-007572] N91-19481

REMOTE MANIPULATOR SYSTEM
Active damping application to the shuttle RMS [NASA-TM-102763] N91-19471

REMOTE SENSING
Remote detection of organics using Fourier transform infrared spectroscopy [DE91-006045] N91-19253
Solid earth science in the 1990s. Volume 1: Program plan [NASA-TM-4256-VOL-1] N91-19499
NO2 absorption cross-section in the 440 to 460 nm region at 298 and 220 K [NOTA-INTERNA-964] N91-19550

REPORTS
The 1989 JSC bibliography of scientific and technical papers [NASA-TM-102173] N91-19959

REPRODUCTION (BIOLOGY)
Plant production as part of a Controlled Ecological Life Support System (CELSS) N91-19656

REQUIREMENTS
Proposed draft military handbook presenting requirements for an Electronic Display System (EDS) for Interactive Electronic Technical Manuals (IETMs) [AD-A227471] N91-19342

RESEARCH
Measurement of eye movements in space-related research environments N91-19591
Potentials, message and challenges of life science research in space N91-19696

RESEARCH AND DEVELOPMENT
Dedication of National Institute for Aviation Research [NIAR-90-21] N91-19040
MBB's involvement in military helicopter programmes [MBB-UD-0588-90-PUB] N91-19091
Airport apron research and development [MBB-Z-0168-90-PUB] N91-19106
Space research for the sake of all [ETN-91-98807] N91-19113
Space station: The next logical step [NASA-TM-103398] N91-19123
Ceramic fabrication R and D [DE91-006537] N91-19298
Exploratory battery technology development and testing report for 1989 [DE91-006753] N91-19352
JPRS report: Science and technology. USSR: Life sciences [JPRS-ULS-91-001] N91-19567

JPRS report: Science and technology. USSR: Physics and mathematics
[JPRS-UPM-90-004] N91-19800
Materials sciences programs
[DE91-007601] N91-19953
Activities report of the Institute for Extraterrestrial Physics
[MPE-222] N91-19971
Research and technology, 1989
[NASA-TM-102264] N91-20039

RESEARCH FACILITIES
A summary of existing and planned experiment hardware for low-gravity fluids research
[NASA-TM-103706] N91-19371
Centrifuge Facility Conceptual System Study. Volume 1: Facility overview and habitats
[NASA-TM-102860] N91-19566
Biolab on Columbus: A facility for basic science and biotechnology N91-19658
Materials sciences programs
[DE91-007601] N91-19953
Research and technology, 1989
[NASA-TM-102264] N91-20039

RESEARCH PROJECTS
Exploratory battery technology development and testing report for 1989
[DE91-006753] N91-19352
Computation and graphics in mathematical research
[DE91-007333] N91-19776

RESIDUAL STRENGTH
Thermal shock of fiber reinforced ceramic matrix composites
[NASA-TM-103777] N91-19295

RESIDUAL STRESS
Computational simulation of hot composites structures
[NASA-TM-103681] N91-19230
Concurrent micromechanical tailoring and fabrication process optimization for metal-matrix composites
[NASA-TM-103670] N91-19237

RESISTOJET ENGINES
Enhancing space transportation: The NASA program to develop electric propulsion
[NASA-TM-4244] N91-19181

RESONANCE
Smoothness criteria for runway rehabilitation and overlays
[DOT/FAA/RD-90/23] N91-19102

RESONANCE CHARGE EXCHANGE
A modelling of unsteady air flow in the resonance charging system of high speed diesel engines
[ACTA-POLYTEC-SCAND-ME-97] N91-19454

RESONANCE SCATTERING
Experiments toward the development of new pulsed ion diodes N91-19885

RESONANCE TESTING
Dynamic behavior of pneumatic tyres
[BU-412] N91-19453

RESONANT FREQUENCIES
Free vibration of hexagonal panels supported at discrete points
[NASA-TM-102688] N91-19166
Modeling a ferrite-tuned RF cavity
[DE91-008235] N91-19356
Near resonant absorption by atoms in intense fluctuating fields
[DE91-007911] N91-19839

RESOURCE ALLOCATION
The temporal logic of the tower chief system N91-19026

RESPIRATORY PHYSIOLOGY
Gravity dependence of pleural liquid turnover N91-19651

RESPIRATORY SYSTEM
Lung volumes, chest wall configuration, and pattern of breathing in microgravity N91-19574

REVERBERATION CHAMBERS
Noise level reduction inside helicopter cabins
[MBB-UD-0578-90-PUB] N91-19828

REYNOLDS NUMBER
A finite Reynolds number approach for the prediction of boundary layer receptivity in localized regions
[NASA-TM-102781] N91-19061

RIBBONS
Recombination x ray laser experiments using exploding ribbon Al targets
[DE91-007146] N91-19429

RIBONUCLEIC ACIDS
Protein purification in multicompartment electrolyzers for crystal growth of r-DNA products in microgravity N91-19665
Characterization of a defective interfering RNA that contains a mosaic of a plant viral genome
[DE91-007897] N91-19702
Characterization of a defective interfering RNA that contains a mosaic of a plant viral genome
[DE91-007898] N91-19703

RIDING QUALITY
Smoothness criteria for runway rehabilitation and overlays
[DOT/FAA/RD-90/23] N91-19102

RIGID ROTORS
A flight-dynamic helicopter mathematical model with a single flap-lag-torsion main rotor
[NASA-TM-102267] N91-19041

RIGID STRUCTURES
Rigid mullitewhisker felt and method of preparation
[AD-D014648] N91-19225
A rigid body model and decoupled control architecture for two manipulators holding a complex object
[DE91-007827] N91-19444
Finite element analysis of geometrically non-linear problems using a corotational large rotation formulation
[SU-ATN-9001] N91-19470

RISK
Dual-purpose self-deliverable lunar surface PV electrical power system N91-19200
Potential health risks from postulated accidents involving the Pu-238 RTG (Radioisotope Thermoelectric Generator) on the Ulysses solar exploration mission
[DE91-007142] N91-19857

ROBOT ARMS
Stochastic satbility and performance robustness of linear multivariable systems N91-19038
A rigid body model and decoupled control architecture for two manipulators holding a complex object
[DE91-007827] N91-19444
Minimum-time trajectory control of a two-link flexible robotic manipulator
[DE91-001261] N91-19448
System description document for the Anthrobot-2: A dexterous robot hand
[NASA-TM-104535] N91-19449
Lag-stabilized force feedback damping
[DE91-007572] N91-19481
Some aspects of robotics calibration, design and control N91-20035

ROBOT CONTROL
Design and control of a fully omnidirectional and holonomic wheeled platform for robotic vehicles
[DE90-017746] N91-19445
A new wheel control system for the omnidirectional HERMIES-3 robot
[DE90-017764] N91-19446
DEMO 89: The initial experiment with the HERMIES-3 robot
[DE90-017765] N91-19447
Minimum-time trajectory control of a two-link flexible robotic manipulator
[DE91-001261] N91-19448
Real-time sensor-based approach to the improvement of transitions of robot manipulator controls
[OUEL-1866/90] N91-19459
Lag-stabilized force feedback damping
[DE91-007572] N91-19481
Some aspects of robotics calibration, design and control N91-20035
Robot tracking system improvements and visual calibration of orbiter position for radiator inspection N91-20037

ROBOT DYNAMICS
Minimum-time trajectory control of a two-link flexible robotic manipulator
[DE91-001261] N91-19448
System description document for the Anthrobot-2: A dexterous robot hand
[NASA-TM-104535] N91-19449
Real-time sensor-based approach to the improvement of transitions of robot manipulator controls
[OUEL-1866/90] N91-19459
Some aspects of robotics calibration, design and control N91-20035

ROBOT SENSORS
Visual navigation around curved obstacles
[OUEL-1861/90] N91-19458
Real-time sensor-based approach to the improvement of transitions of robot manipulator controls
[OUEL-1866/90] N91-19459

ROBOTICS
Sandia technology: Engineering and science applications
[DE91-006760] N91-19322
Design and control of a fully omnidirectional and holonomic wheeled platform for robotic vehicles
[DE90-017746] N91-19445
A new wheel control system for the omnidirectional HERMIES-3 robot
[DE90-017764] N91-19446
DEMO 89: The initial experiment with the HERMIES-3 robot
[DE90-017765] N91-19447
Practical path planning among movable obstacles
[DE91-000034] N91-19768
Research reports: 1990 NASA/ASEE Summer Faculty Fellowship Program
[NASA-CR-187638] N91-20022
Some aspects of robotics calibration, design and control N91-20035

ROBOTS
Design and control of a fully omnidirectional and holonomic wheeled platform for robotic vehicles
[DE90-017746] N91-19445
A new wheel control system for the omnidirectional HERMIES-3 robot
[DE90-017764] N91-19446
DEMO 89: The initial experiment with the HERMIES-3 robot
[DE90-017765] N91-19447
A haptic system for a multifingered hand
[DE90-017044] N91-19767
Navigation of a car-like mobile robot using a decomposition of the environment in convex cells
[DE91-000709] N91-19769

ROBUSTNESS (MATHEMATICS)
Investigation of air transportation technology at Princeton University, 1989-1990 N91-19033
Stochastic robustness: Towards a comprehensive robustness tool N91-19036
Stochastic satbility and performance robustness of linear multivariable systems N91-19038

ROCKET ENGINE DESIGN
Orbital transfer vehicle oxygen turbopump technology. Volume 1: Design, fabrication, and hydrostatic bearing testing
[NASA-CR-185175] N91-19174

ROCKET ENGINE NOISE
Rocket noise filtering system using digital filters N91-20031

ROCKET EXHAUST
Solar rocket plume/mirror interactions
[NASA-CR-185300] N91-19059

ROCKET LAUNCHING
Launching projectiles with hydrogen gas generated from titanium-water reactions
[AD-D014653] N91-19171
Rocket-triggered lightning strikes and forest fire ignition N91-20027

ROLL
Response of a viscous liquid layer to pitch- and roll-excitation in zero-gravity environment
[LRT-WE-9-FB-13(1990)] N91-19390

ROLLERS
Nonlinear analysis and redesign of the mixed-mode bending delamination test
[NASA-TM-102777] N91-19482

ROOTS
Electrofusion and regeneration of protoplasts from sunflower (Helianthus annuus L.) N91-19675

ROTARY WING AIRCRAFT
Introduction of the M-85 high-speed rotorcraft concept
[NASA-TM-102871] N91-19078
The selection of convertible engines with current gas generator technology for high speed rotorcraft
[NASA-TM-103774] N91-19097

ROTARY WINGS
Ongoing development of a computer jobstream to predict helicopter main rotor performance in icing conditions
[NASA-CR-187076] N91-19056
A novel potential/viscous flow coupling technique for computing helicopter flow fields
[NASA-CR-177568] N91-19060
A new methodology for free wake analysis using curved vortex elements
[NASA-CR-3958] N91-19067

ROTATING BODIES
Liquid sloshing response in a spinning container due to pitching excitation
[LRT-WE-9-FB-11(1990)] N91-19388
Finite element analysis of geometrically non-linear problems using a corotational large rotation formulation
[SU-ATN-9001] N91-19470

ROTATING GENERATORS
A non-linear method for the calculation of the power output of a rotating wind turbine
[BU-416] N91-19512

ROTATING LIQUIDS
Response of a solidly rotating amphora-type liquid column to axial excitation
[LRT-WE-9-FB-06(1990)] N91-19386

ROTATING SHAFTS
Monitoring techniques for the X-29A aircraft's high-speed rotating power takeoff shaft
[NASA-TM-101731] N91-19081
Vibration transmission through rolling element bearings in geared rotor systems
[NASA-CR-4334] N91-19435

ROTATION
Responses of Physarum polycephalum to varying light levels during fast clinostat rotation: A scientific preparation of an ESA biorack experiment during the IML-1 mission N91-19676
Mental rotation of three-dimensional shapes in microgravity N91-19694
Relation between perception of vertical axis rotation and vestibulo-ocular reflex symmetry [NASA-CR-187997] N91-19710
Ultrasonic investigations on superfluid He-3-A and He-3-B [ISBN-952-90-2241-7] N91-19830
ROTOR AERODYNAMICS
Modal analysis of UH-60A instrumented rotor blades [NASA-TM-4239] N91-19052
A new methodology for free wake analysis using curved vortex elements [NASA-CR-3958] N91-19067
Euler solutions to nonlinear acoustics of non-lifting hovering rotor blades [NASA-TM-103837] N91-19826
ROTOR BLADES
Modal analysis of UH-60A instrumented rotor blades [NASA-TM-4239] N91-19052
Development of a fatigue-life methodology for composite structures subjected to out-of-plane load components [NASA-TM-102885] N91-19241
ROTOR BLADES (TURBOMACHINERY)
Euler solutions to nonlinear acoustics of non-lifting hovering rotor blades [NASA-TM-103837] N91-19826
ROTORS
A novel potential/viscous flow coupling technique for computing helicopter flow fields [NASA-CR-177568] N91-19060
A new methodology for free wake analysis using curved vortex elements [NASA-CR-3958] N91-19067
Introduction of the M-85 high-speed rotorcraft concept [NASA-TM-102871] N91-19078
Vibration transmission through rolling element bearings in geared rotor systems [NASA-CR-4334] N91-19435
ROUTES
Synthesis and structures of metal chalcogenide precursors [NASA-TM-103665] N91-19296
The cost-constrained traveling salesman problem [DE91-004943] N91-19775
RUBIDIUM
The physics of laser polarized muonic atoms [DE91-008045] N91-19845
RUNNING
Effect of running and head down tilt bedrest on lymphocyte reactivity N91-19598
RUNWAY LIGHTS
Florida radioluminescent taxiway light development program [DE91-005650] N91-19104
RUNWAYS
The temporal logic of the tower chief system N91-19026
BUBBLES: An automated decision support system for final approach controllers N91-19027
Smoothness criteria for runway rehabilitation and overlays [DOT/FAA/RD-90/23] N91-19102

S

SACCADIC EYE MOVEMENTS
Gaze control and spatial memory in weightlessness N91-19692
SAFETY
Airport system technical aspects N91-19107
Safety of high speed magnetic levitation transportation systems. Preliminary safety review of the transrapid maglev system [PB91-129684] N91-19326
SAFETY FACTORS
Innovations in dynamic test restraint systems N91-19145
SAFETY MANAGEMENT
Space Shuttle: NASA should implement independent oversight of software development [GAO/IMTEC-91-20] N91-19119
SAMPLING
Ultrafine refractory particle formation in counterflow diffusion flames [DE91-007693] N91-19260
Characterization of devices, circuits, and high-temperature superconductor transmission lines by electro-optic testing [NASA-CR-187950] N91-19343
SANDWICH STRUCTURES
Reactivity of pi-complexes of Ti, V, and Nb towards dithioacetic acid: Synthesis and structure of novel metal sulfur-containing complexes [NASA-TM-103666] N91-19256
Piezoelectric sandwich polymer transducer [AD-D014650] N91-19341
A theoretical solution for the buckling of sandwich panels with laminated face plates using a computer algebra system [BU-407] N91-19486
SAPPHIRE
Passive mode locking in optically pumped Al2O3:Ti(3+) laser N91-19803
SAS
SIGNIF and GENFMT, SAS macros for computing and reporting significant digits [DE91-007702] N91-19795
SATELLITE ANTENNAS
C-band antennas for regional communication systems [MBB-UK-0107-90-PUB] N91-19336
SATELLITE COMMUNICATION
C-band antennas for regional communication systems [MBB-UK-0107-90-PUB] N91-19336
Pulsed response of a traveling-wave tube [NASA-TM-103672] N91-19348
SATELLITE DESIGN
SCD 02 thermal design N91-19129
SCD1 thermal design and test result analysis N91-19130
SATELLITE IMAGERY
NOAA-9 Solar Backscatter Ultraviolet (SBUV/2) Instrument and Derived Ozone Data: Review [NOAA-TR-NESDIS-53] N91-19514
Data status and availability N91-19515
SBUV/2 in-orbit performance N91-19517
NOAA-9 SBUV/2 ozone sounding accuracy: Presentation summary N91-19519
A technique for directly comparing radiances from two satellites N91-19520
SBUV/2 comparisons with ground-based and SBUV spacecraft data N91-19521
Ozone measurements from the NOAA-9 and the Nimbus-7 satellites: Implications of short and long term variabilities N91-19527
SATELLITE OBSERVATION
Calibration of long term satellite ozone data sets using the space shuttle N91-19524
High resolution infrared astronomy satellite observations of a selected spiral galaxy [NASA-CR-188019] N91-19975
SATELLITE-BORNE INSTRUMENTS
Superconducting instrumentation for critical He-4 measurements in space [DE91-007894] N91-19408
SCALARS
Examinations of inverse scattering problem for the scalar Helmholtz equation in the field of first order approximations for potentials with compact supports and safe real wave numbers [ETN-91-98949] N91-19339
SCALE MODELS
A simple dynamic engine model for use in a real-time aircraft simulation with thrust vectoring [NASA-TM-4240] N91-19079
SCALING LAWS
Tokamak ignition projections from dimensionally similar discharges [DE91-008195] N91-19908
SCANNERS
Assessment of tamper-revealing ceramic seals [DE91-007793] N91-19301
Nuclear-spectroscopy computerized tomography scanners [DE91-008447] N91-19466
SCATTERING
Quasi-molecular processes in dense plasmas [DE91-007388] N91-19899
SCATTERING COEFFICIENTS
Effects of soil and canopy characteristics on microwave backscattering of vegetation [NASA-CR-188022] N91-19497
SCATTERING CROSS SECTIONS
W(sub L)W(sub L) scattering at the SSC [DE91-008442] N91-19851
Cross section for production of excited hydrogen atoms following dissociative excitation of molecular hydrogen by electron impact [DE91-745035] N91-19852
SCHEDULES
BUBBLES: An automated decision support system for final approach controllers N91-19027
SCHOOLS
Test analysis program evaluation: Item statistics as feedback to test developers [AD-A229851] N91-19713
SCIENTIFIC SATELLITES
Predictions of cell damage rates for Lifesat missions [NASA-TM-102170] N91-19699
SCINTILLATION
Aperture-averaging factor for optical propagation through the turbulent atmosphere [PB91-129338] N91-19875
SCINTILLATION COUNTERS
Evaluation of a Photo-Electron Rejecting Alpha Liquid Scintillation (PERALS) spectrometer for the measurement of alpha-emitting radionuclides [DE91-005652] N91-19399
SCREWS
Graduated-load spring washer system for screws and threaded fasteners [AD-D014697] N91-19436
SEA LEVEL
Cosmic ray charged component variations at sea level [DE91-615480] N91-20021
SEA WATER
Microbiologically influenced corrosion in copper and nickel seawater piping systems [AD-A229874] N91-19287
Air/sea temperature probe [AD-D014674] N91-19397
Results of scoping tests for open-cycle OTEC (Ocean Thermal Energy Conversion) components operating with seawater [DE89-009514] N91-19501
SEALING
Assessment of tamper-revealing ceramic seals [DE91-007793] N91-19301
A test fixture for measuring high-temperature hypersonic-engine seal performance [NASA-TM-103658] N91-19442
SEALS (STOPPERS)
High temperature NASP engine seal development [NASA-TM-103716] N91-19441
SEISMIC WAVES
Lecture notes on nonlinear inversion and tomography [DE91-008238] N91-19558
Very low frequency seismo-acoustic scattering from a rough seafloor [AD-A227947] N91-19564
SEISMOLOGY
On the joint inversion of geophysical data for models of the coupled core-mantle system [NASA-TM-104536] N91-19557
SELECTION
Space operations: NASA is not archiving all potentially valuable data [GAO/IMTEC-91-3] N91-19955
SELENIUM COMPOUNDS
Synthesis and structures of metal chalcogenide precursors [NASA-TM-103665] N91-19296
SELF CONSISTENT FIELDS
Theoretical study of plasma focus diode N91-19887
SEMICONDUCTING FILMS
Activities report of the Istituto Elettrotecnico Nazionale Galileo Ferraris [ETN-91-98868] N91-19822
SEMICONDUCTOR DEVICES
Thermal/vacuum vs. thermal atmospheric testing of space flight electronic assemblies N91-19154
Semiconductor photodiodes as radiometric receivers in the field of soft radiation [ETN-91-98925] N91-19856
SEMICONDUCTOR DIODES
Unique Signal Override Plug (USOP) electromagnetic test report [DE91-004996] N91-19330
SEMICONDUCTOR JUNCTIONS
AlGaAs top solar cell for mechanical attachment in a multi-junction tandem concentrator solar cell stack N91-19187
Progress toward a 30 percent-efficient, monolithic, three-junction, two-terminal concentrator solar cell for space applications N91-19188
Progress in GaAs/CuInSe2 tandem junction solar cells N91-19190
InP/Ga0.47In0.53As monolithic, two-junction, three-terminal tandem solar cells N91-19191
SEMICONDUCTOR LASERS
Method for making holograms with coherent radiation from a stabilized laser diode that has been actively cooled [AD-D014673] N91-19396
Coherent effects in generation of ultrashort light pulses by semiconductor injection laser N91-19820
Compound semiconductors, strained layer epitaxy, and the information age [DE91-007735] N91-19932
SEMICONDUCTORS (MATERIALS)
Graded-bandgap AlGaAs solar cells for AlGaAs/Ge cascade cells N91-19186

Semiconductor structural damage attendant to contact formation in III-V solar cells N91-19203
Fluorescent lifetime measurements of rare Earth elements in gallium arsenide
[AD-A229865] N91-19265
Method of producing glass fiber with cores of a different material
[AD-D014664] N91-19288
Synthesis and structures of metal chalcogenide precursors
[NASA-TM-103665] N91-19296
Solid State Photovoltaic Research Branch
[DE91-002128] N91-19502
A photoemission investigation of compound semiconductor monodisperse clusters
[DE91-006707] N91-19921
Considerations relating to pulsed-beam modification of materials
[DE91-006771] N91-19922
Thin film reactions on alloy semiconductor substrates
[DE91-007651] N91-19931
Compound semiconductors, strained layer epitaxy, and the information age
[DE91-007735] N91-19932
Some roles for TEM in the development of new materials
[DE91-007742] N91-19933

SENSORS
Piezoelectric sandwich polymer transducer
[AD-D014650] N91-19341
The development of a rugged accelerometer
[DE91-007731] N91-19407

SENSORY PERCEPTION
Medical results of the fourth prime expedition on the orbital station Mir N91-19576
Does gravity play a role in the morphological development and function of the gravity sensory organ of vertebrates. DLR contribution to the D-2 project graviperception and neuronal plasticity, its technical realization and experimental execution N91-19635

SENTENCES
Improved syntactic disambiguation in the FASIT automatic indexing environment N91-19956

SEPARATED FLOW
The effect of body shape on the development of vortex asymmetry in the flow past slender bodies
[BU-413] N91-19068
Calculations of separated 3-D flows with a pressure-staggered Navier-Stokes equations solver
[NASA-CR-187065] N91-19367

SEPARATION
A new approach to electrophoresis in space N91-19653
Free flow electrophoresis experiment TEPE 3 on TEXUS 24 N91-19654

SEPARATORS
The full-scale process and design changes for elimination of insulation edge separations and voids in tang flap area
[NASA-CR-184110] N91-19172

SEQUENCING
Advanced sequencing technology
[DE91-008031] N91-19706

SERIES EXPANSION
Dynamics of collision processes
[DE91-007933] N91-19840

SEROTONIN
The biochemical and physiological variables in motion sickness followed modified neuroendocrine activity N91-19607

SERVICE LIFE
A 5-kW xenon ion thruster lifetest
[NASA-TM-103191] N91-19180

SERVICE MODULES
IAL SPACE: A test laboratory for the ISO cryogenic payload N91-19142

SET THEORY
Regular unitary dilation of commuting contractions and Markovian representations of Gaussian stationary processes on the set Z(2)
[TELECOM-90-D-009] N91-19798

SHAFTS (MACHINE ELEMENTS)
Life and dynamic capacity modeling for aircraft transmissions
[NASA-CR-4341] N91-19438

SHEATHS
Silver-sheathed multifilament wires
[DE91-008107] N91-19941

SHIELDING
Progressive feature of stepped leader on Japan sea coast in winter (basic data to establish shielding theory for lightning)
[DE91-742133] N91-19561

SHIP HULLS
Magneto-elastic behaviour of steels for naval applications
[MRL-TR-90-27] N91-19266

SHIPS
Liquid sloshing in cargo tanks. Liquid slosh loading in slack ship tanks: Forces on internal structure and pressures
[PB91-129262] N91-19383
Air/sea temperature probe
[AD-D014674] N91-19397

SHOCK LAYERS
Laws of heat transfer in three-dimensional viscous shock layer of stream flowing past blunt bodies at some angles of attack and glide N91-19801

SHOCK RESISTANCE
Thermal shock of fiber reinforced ceramic matrix composites
[NASA-TM-103777] N91-19295

SHOCK WAVES
Solution of one-dimensional problem in nonlinear theory of elasticity with structured shock wave N91-19809

SHORT CIRCUIT CURRENTS
Effect of dislocations on the open-circuit voltage, short-circuit current and efficiency of heteroepitaxial indium phosphide solar cells
[NASA-TM-103762] N91-19354

SHORT TAKEOFF AIRCRAFT
S87 close air support aircraft fatigue analysis
[ETN-91-98854] N91-19093

SHOT NOISE
Quantum fluctuations in laser with intracavity frequency doubling N91-19805

SIERRA NEVADA MOUNTAINS (CA)
Climatic water budgets, effective moisture, and elevation in the Southern Sierra Nevada, California, 1951-1980
[PB91-127878] N91-19500

SIGNAL ANALYSIS
Time-frequency domain analysis of vibration signals for machinery diagnostics. 1: Introduction to the Wigner-Ville distribution
[OUEL-1859/90] N91-19495

SIGNAL DETECTION
Wire-free arming system for an aircraft-delivered bomb
[AD-D014611] N91-19076

SIGNAL DETECTORS
Wire-free arming system for an aircraft-delivered bomb
[AD-D014611] N91-19076
High pulse repetition frequency radar early warning receiver
[AD-D014655] N91-19328

SIGNAL GENERATORS
Optical Fiber Backscatter Signature Generator (OFBSG)
[AD-D014668] N91-19870

SIGNAL MEASUREMENT
Using a modified Hewlett Packard 8410 network analyzer as an automated farfield antenna range receiver
[NASA-TM-103700] N91-19349

SIGNAL PROCESSING
Ridge regression signal processing N91-19029
The selection of window functions for the calculation of time domain averages on the vibration of the individual gears in an epicyclic gearbox
[OUEL-1818/90] N91-19457
Time-frequency domain analysis of vibration signals for machinery diagnostics. 1: Introduction to the Wigner-Ville distribution
[OUEL-1859/90] N91-19495

SIGNAL REFLECTION
Optical Fiber Backscatter Signature Generator (OFBSG)
[AD-D014668] N91-19870

SIGNAL TO NOISE RATIOS
Performance monitoring in nonlinear adaptive noise cancellation
[RR-409] N91-19362

SIGNAL TRANSMISSION
Epidermal growth factor induced signal transduction in A431 cells is influenced by altered gravity conditions N91-19623

SIGNATURES
Optical Fiber Backscatter Signature Generator (OFBSG)
[AD-D014668] N91-19870

SIGNS AND SYMPTOMS
Standardization of motion sickness induced by left-right and up-down reversing prisms N91-19611

SILICON
Progress toward the development of dual junction GaAs/Ge solar cells N91-19184
Neutron radiation damage studies on silicon detectors
[DE91-008441] N91-19361
A calorimeter design for high energy PP colliders
[NOTA-INTERNA-965] N91-19410
Limiting pulse signal in NbN-Si structure: Superconductor film on substrate N91-19815
Mutual influence of doping and oxidation in highly doped silicon
[ETN-91-98924] N91-19948

SILICON ALLOYS
Gas entrapment and evolution in aluminium alloys produced by powder metallurgy
[ETN-91-98918] N91-19285

SILICON CARBIDES
METCAN updates for high temperature composite behavior: Simulation/verification
[NASA-TM-103682] N91-19229
Thermal shock of fiber reinforced ceramic matrix composites
[NASA-TM-103777] N91-19295
Ceramic fabrication R and D
[DE91-006537] N91-19298

SILICON COMPOUNDS
In situ TEM studies of the growth of strained Si(1-x)Ge(x) by solid phase epitaxy
[DE91-007278] N91-19926

SILICON FILMS
Solid State Photovoltaic Research Branch
[DE91-002128] N91-19502

SILICON ISOTOPES
In situ TEM studies of the growth of strained Si(1-x)Ge(x) by solid phase epitaxy
[DE91-007278] N91-19926

SILICON NITRIDES
Atomic oxygen effects on boron nitride and silicon nitride: A comparison of ground based and space flight data N91-19146
Comparison of dynamic fatigue behavior between SiC whisker-reinforced composite and monolithic silicon nitrides
[NASA-TM-103707] N91-19293
Thermal shock of fiber reinforced ceramic matrix composites
[NASA-TM-103777] N91-19295

SILICON OXIDES
Thin film amorphous electrolytes: The Li2O-SiO2-P2O5 system
[DE91-007272] N91-19925

SILVER
Atomic oxygen effects on boron nitride and silicon nitride: A comparison of ground based and space flight data N91-19146

SIMULATION
Air traffic simulation with a view to system interpretation N91-19110
High power, high frequency lasertron RF sources
[DE91-006007] N91-19414
Simulation of a standing-wave free-electron laser
[DE91-007330] N91-19418
On the optimality of code options for a universal noiseless coder
[NASA-CR-187973] N91-19734
Energy sciences supercomputing 1990
[DE91-007188] N91-19740
Parallel processing for a 1-D time-dependent solution to impurity rate equations for fusion plasma simulations
[DE90-015857] N91-19759
Optically-ionized plasma recombination x ray lasers
[DE91-007261] N91-19898

SINE WAVES
Time-frequency domain analysis of vibration signals for machinery diagnostics. 1: Introduction to the Wigner-Ville distribution
[OUEL-1859/90] N91-19495

SINGLE CRYSTALS
Rigid mullitewhisker felt and method of preparation
[AD-D014648] N91-19225
Superconductivity of oxide film electrolytically deposited on surface of B(1-x)Sb(x) single crystal N91-19819
Diffuse x ray scattering YBa2Cu3O(6.95) monocrystal
[DE91-615182] N91-19943

SINTERING
Semiconductor structural damage attendant to contact formation in III-V solar cells N91-19203
The 70 percent tungsten heavy alloys: Processing and properties
[DE91-008259] N91-19282
Effects of atmosphere and heating rate during processing of a ceramic superconductor
[DE91-007761] N91-19299
Crystallization and properties of Sr-Ba aluminosilicate glass-ceramic matrices
[NASA-TM-103764] N91-19308
Part 1: The effect of lattice defects on the sintering of lithium fluoride; Part 2: The morphology of calcium oxide from calcium carbonate decomposition
[DE91-007743] N91-19934

SITE SELECTION
An expansion plan for the 60 Hz power distribution system at KSC: LC-39 substations load allocation plan N91-20028
SITES
Airport apron research and development [MBB-Z-0168-90-PUB] N91-19106
SKIN (ANATOMY)
Human dermal fibroblast sensitivity to hypergravity N91-19630
SLEEP DEPRIVATION
Review of EEG studies in non human primates exposed to microgravity N91-19649
SLENDER BODIES
The effect of body shape on the development of vortex asymmetry in the flow past slender bodies [BU-413] N91-19068
SMART STRUCTURES
I'm all 'light' Jack [MBB-UD-0576-90-PUB] N91-19101
SMOG
Regional Oxidant Model Multi-Processor (ROMMP) [PB91-131680] N91-19547
SOBOLEV SPACE
Approximation properties of wavelet transforms [ETN-91-98922] N91-19799
SODIUM
Sodium/metal chloride program conceptual design study [DE91-007216] N91-19353
SODIUM CHLORIDES
Physiology of body water and salt regulation. Part 1: Circadian rhythms of endocrine systems and urinary electrolyte excretion in humans N91-19592
Physiology of body water and salt regulation. Part 2: Volume and electrolyte homeostasis after an acute saline infusion N91-19593
SOFIA (AIRBORNE OBSERVATORY)
A scientific program for infrared, submillimeter and radio astronomy from space: A report by the Management Operations Working Group [NASA-TM-103333] N91-19979
SOFTWARE ENGINEERING
RICIS 1988 Symposium Proceedings. Presentation appendix [NASA-CR-188077] N91-19722
Software development environments: Status and trends N91-19723
The next generation N91-19724
Mission operations directorate: Facility and support systems division N91-19726
Empirical studies of software design: Implications for SSEs N91-19728
The role of software engineering in the space station program N91-19729
Lessons learned from an Ada conversion project N91-19730
Finding the object proceedings addendum [DE91-006724] N91-19738
Structured software design for an on-line laser-based particle size distribution instrument [DE91-007234] N91-19746
SOFTWARE TOOLS
RICIS 1988 Symposium Proceedings. Presentation appendix [NASA-CR-188077] N91-19722
Software development environments: Status and trends N91-19723
Tool and data interoperability in the SSE system N91-19727
Transferable Output ASCII Data (TOAD) gateway: Version 1.0 user's guide [NASA-CR-187489] N91-19737
Software reliability through fault-avoidance and fault-tolerance [NASA-CR-187998] N91-19741
Table of tables: A database design tool for SYBASE [DE91-007257] N91-19958
SOILS
Screening volatile organics by direct sampling ion trap and glow discharge mass spectrometry [DE91-007708] N91-19258
Effects of soil and canopy characteristics on microwave backscattering of vegetation [NASA-CR-188022] N91-19497
Climatic water budgets, effective moisture, and elevation in the Southern Sierra Nevada, California, 1951-1980 [PB91-127878] N91-19500
SOLAR ACTIVITY
The Rome neutron monitor data for four ground-level enhancements observed by the world-wide station network in 1990 [NOTA-INTERNA-967] N91-20019
SOLAR ARRAYS
Space Photovoltaic Research and Technology, 1989 [NASA-CP-3107] N91-19182
Progress toward the development of dual junction GaAs/Ge solar cells N91-19184
An approach for configuring space photovoltaic tandem arrays based on cell layer performance N91-19197
Review of thin film solar cell technology and applications for ultra-light spacecraft solar arrays N91-19198
Performance, size, mass, and cost estimates for projected 1kW EOL Si, InP, and GaAs arrays N91-19199
Feasibility of solar power for Mars N91-19201
Optimization and performance of Space Station Freedom solar cells N91-19215
Thermal cycle testing of Space Station Freedom solar array blanket coupons N91-19216
The Advanced Photovoltaic Solar Array (APSA) technology status and performance N91-19217
Mini-dome Fresnel lens photovoltaic concentrator development N91-19219
Strategy in space flight experiments N91-19220
SOLAR ATMOSPHERE
Neutron propagation from solar flare in the solar atmosphere [DE91-615465] N91-20016
SOLAR CELLS
The effect of the low Earth orbit environment on space solar cells [NASA-TM-103735] N91-19165
Radiation resistance of thin-film solar cells for space photovoltaic power [NASA-TM-103715] N91-19176
Solar electric propulsion for Mars transport vehicles [NASA-TM-103234] N91-19178
Space Photovoltaic Research and Technology, 1989 [NASA-CP-3107] N91-19182
Progress toward the development of dual junction GaAs/Ge solar cells N91-19184
Status of GaAs/Ge solar cells N91-19185
Graded-bandgap AlGaAs solar cells for AlGaAs/Ge cascade cells N91-19186
AlGaAs top solar cell for mechanical attachment in a multi-junction tandem concentrator solar cell stack N91-19187
Progress toward a 30 percent-efficient, monolithic, three-junction, two-terminal concentrator solar cell for space applications N91-19188
Tandem concentrator solar cells with 30 percent (AMO) power conversion efficiency N91-19189
Progress in GaAs/CuInSe2 tandem junction solar cells N91-19190
InP/Ga0.47In0.53As monolithic, two-junction, three-terminal tandem solar cells N91-19191
Phase equilibrium modeling for high temperature metallization on GaAs solar cells N91-19192
GaAs solar cell photoresponse modeling using PC-1D V2.1 N91-19193
High-efficiency, radiation-resistant GaAs space cells N91-19194
Thermal annealing of GaAs concentrator solar cells N91-19195
Burst annealing of high temperature GaAs solar cells N91-19196
An approach for configuring space photovoltaic tandem arrays based on cell layer performance N91-19197
Review of thin film solar cell technology and applications for ultra-light spacecraft solar arrays N91-19198
Performance, size, mass, and cost estimates for projected 1kW EOL Si, InP, and GaAs arrays N91-19199
Recent advances in the ITO/InP solar cell N91-19202
Semiconductor structural damage attendant to contact formation in III-V solar cells N91-19203
The effect of process conditions on the performance of epitaxial InP solar cells N91-19204
Effects of proton irradiation on the performance of InP/GaAs solar cells N91-19205
Key factors limiting the open circuit voltage of n(+)pp(+) indium phosphide solar cells N91-19206
Determination of series resistance of indium phosphide solar cells N91-19207
Investigation of anodic and chemical oxides grown on p-type InP with applications to surface passivation for n(+)-p solar cell fabrication N91-19208
A comparative study of performance parameters of n(+)-p InP solar cells made by closed-ampoule sulfur diffusion into Cd- and Zn-doped p-type InP substrates N91-19209
Radioisotope thermal photovoltaic application of the GaSb solar cell N91-19210
GaP betavoltaic cells as a power source N91-19211
Spaceflight performance of several types of silicon solar cells on the LIPS 3 satellite N91-19213
Annealing characteristics of irradiated hydrogenated amorphous silicon solar cells N91-19214
Optimization and performance of Space Station Freedom solar cells N91-19215
Indium phosphide solar cells N91-19221
Effect of dislocations on the open-circuit voltage, short-circuit current and efficiency of heteroepitaxial indium phosphide solar cells [NASA-TM-103762] N91-19354
Solid State Photovoltaic Research Branch [DE91-002128] N91-19502
SOLAR COLLECTORS
Solar rocket plume/mirror interactions [NASA-CR-185300] N91-19059
SOLAR CONSTANT
Solar thermal vacuum tests of Magellan spacecraft N91-19127
SCD 02 thermal design N91-19129
SOLAR CYCLES
Cosmic ray charged component variations at sea level [DE91-615480] N91-20021
SOLAR ELECTRIC PROPULSION
Solar electric propulsion for Mars transport vehicles [NASA-TM-103234] N91-19178
SOLAR ENERGY
Review of thin film solar cell technology and applications for ultra-light spacecraft solar arrays N91-19198
Laser Doppler velocimetry for continuous flow solar-pumped iodine laser system [NASA-TM-104029] N91-19415
Triton: A hot potato N91-20005
SOLAR ENERGY ABSORBERS
Space environmental effects on spacecraft thermal control coatings N91-19148
SOLAR ENERGY CONVERSION
Feasibility of solar power for Mars N91-19201
The design of future central receiver power plants based on lessons learned from the Solar One Pilot Plant [DE91-005224] N91-19510
SOLAR FLARES
Neutron propagation from solar flare in the solar atmosphere [DE91-615465] N91-20016
The Rome neutron monitor data for four ground-level enhancements observed by the world-wide station network in 1990 [NOTA-INTERNA-967] N91-20019
SOLAR GENERATORS
Productivity and photosynthesis of selected crop plants under orbital light conditions: An approach to solar powered CELSS N91-19662
SOLAR INSTRUMENTS
Data status and availability N91-19515
A technique for directly comparing radiances from two satellites N91-19520
Analysis of SBUV/2 measurements of solar UV irradiance variations N91-19526
SOLAR PHYSICS
Solar-geophysical data Number 554, October 1990. Part 2 (comprehensive reports): Data for April 1990 and miscellaneous. Explanation of data reports issued as Number 515 (supplement) July 1987 [PB91-124586] N91-20017
Solar-geophysical data Number 554, October 1990. Part 1 (prompt reports): Data for September, August 1990, and late data. Explanation of data reports issued as Number 515 (supplement) July 1987 [PB91-124594] N91-20018
SOLAR POSITION
SBUV/2 in-orbit performance N91-19517
NOAA-9 SBUV/2 ozone sounding accuracy: Presentation summary N91-19519
Initial estimate of NOAA-9 SBUV/2 total ozone drift: Based on comparison with re-calibrated TOMS measurements and pair justification of SBUV/2 N91-19523
SOLAR RADIATION
Proposal for a conceptually new compact collecting optics for powerful light sources N91-19155
A status report on the analysis of the NOAA-9 SBUV/2 sweep mode solar irradiance data N91-19518
Analysis of SBUV/2 measurements of solar UV irradiance variations N91-19526
SOLAR SIMULATORS
Solar thermal vacuum tests of Magellan spacecraft N91-19127
Proposal for a conceptually new compact collecting optics for powerful light sources N91-19155
SOLAR SPECTRA
An assessment of instrument performance for the NOAA-9 SBUV/2 N91-19516
SOLAR SYSTEM
Activities report of the Institute for Extraterrestrial Physics [MPE-222] N91-19971
Impact processes in the Solar System: New understandings through numerical modeling N91-19996

SOLAR THERMAL ELECTRIC POWER PLANTS
The design of future central receiver power plants based on lessons learned from the Solar One Pilot Plant
[DE91-005224] N91-19510
SOLID ELECTROLYTES
Theory of bulk and interface constant phase elements in electrode-electrolyte systems
[DE91-007181] N91-19255
Thermal-hydraulic model of a solid-oxide fuel cell
[DE91-006393] N91-19507
SOLID LUBRICANTS
Tribological properties of Ag/Ti films on Al2O3 ceramic substrates
[NASA-TM-103784] N91-19224
SOLID PHASES
In situ TEM studies of the growth of strained Si(1-x)Ge(x) by solid phase epitaxy
[DE91-007278] N91-19926
SOLID PROPELLANT COMBUSTION
Solid fuel combustion chamber
[LR-648] N91-19222
SOLID PROPELLANT ROCKET ENGINES
Detailed modal testing of a solid rocket motor using a portable test system N91-19144
The full-scale process and design changes for elimination of insulation edge separations and voids in tang flap area
[NASA-CR-184110] N91-19172
Study of the available finite element software packages at KSC N91-20029
SOLID PROPELLANTS
Detailed modal testing of a solid rocket motor using a portable test system N91-19144
SOLID SOLUTIONS
Theoretical investigation of phase stability in non-magnetic Fe-V substitutional alloys
[DE91-006711] N91-19268
SOLID STATE
Theory of CW lidar aerosol backscatter measurements and development of a 2.1 microns solid-state pulsed laser radar for aerosol backscatter profiling
[NASA-CR-4347] N91-19498
Solid state, surface, and catalytic studies of oxides
[DE91-007979] N91-19939
SOLID STATE DEVICES
Indium tin oxide for solid-state image sensors
[ETN-91-98932] N91-19949
SOLID STATE LASERS
Interferometry, streak photography, and stereo photography of laser-driven miniature flying plates
[DE91-007493] N91-19405
Theory of CW lidar aerosol backscatter measurements and development of a 2.1 microns solid-state pulsed laser radar for aerosol backscatter profiling
[NASA-CR-4347] N91-19498
Intracavity second-harmonic generation by laser with optical delay line and mode locking N91-19808
SOLIDIFICATION
Method of producing superconducting materials in bulk form
[AD-D014656] N91-19917
SOLIDS
The method of lines in analyzing solids containing cracks
[NASA-TM-103626] N91-19477
SOLITARY WAVES
Soliton Microwave Generator
[DE91-006277] N91-19335
Breakup of femtosecond pulses during amplification in Er(3+)-doped single-mode optical fibers N91-19812
SOUND FIELDS
J-85 jet engine noise measured in the ONERA S1 wind tunnel and extrapolated to far field
[NASA-TP-3053] N91-19823
SOUND GENERATORS
Elementary pulse diffraction problems and the generation of sound by a dipole moving across the edge of a half-plane
[LR-565] N91-19831
SOUND LOCALIZATION
A gradient microphone for locating sound targets
[MBB-Z-0341-90-PUB] N91-19829
SOUND PROPAGATION
Reflections on some problems concerning the role of superfluid turbulence in the propagation of second-sound pulses in He 2
[MPIS-8/1990] N91-19827
SOUND WAVES
Acoustic radiation from lifting airfoils in compressible subsonic flow
[NASA-TM-103650] N91-19053
Numerical and physical modelling of bubbly flow phenomena
[DE91-007461] N91-19377
Very low frequency seismo-acoustic scattering from a rough seafloor
[AD-A227947] N91-19564
Acoustic stabilization of laser beam wavefront in nonhomogeneous gaseous medium N91-19802
SOUNDING ROCKETS
Lymphocytes on sounding rockets N91-19620
Unicellular algae in space. 2: Sounding-rocket experiment N91-19640
Unicellular algae in space. 3: Addendum N91-19641
Cells in space: Sounding rocket facilities for cell biology and biotechnology in microgravity N91-19661
SOYBEANS
Carbon dioxide and water exchange of a soybean stand grown in the biomass production chamber N91-20026
SPACE BASES
Alternative strategies for the maintenance of geostationary space power plants
[ILR-MITT-249(1990)] N91-19170
SPACE CHARGE
Two-stage ion diode experiments on induction adder N91-19884
Theoretical study of plasma focus diode N91-19887
SPACE COMMERCIALIZATION
Key issues in space nuclear power
[NASA-TM-103656] N91-19179
Microgravity strategic plan, 1988
[NASA-TM-103397] N91-19319
Commercial Space Launch Act implementation
[GPO-27-944] N91-19968
SPACE DEBRIS
Hypervelocity impact physics
[NASA-CR-4343] N91-19164
Space debris: Orbital microparticulates impacting LDEF experiments favour a natural extraterrestrial origin N91-20008
SPACE ENVIRONMENT SIMULATION
Techniques for hot structures testing
[NASA-TM-101727] N91-19080
Sixteenth Space Simulation Conference Confirming Spaceworthiness Into the Next Millennium
[NASA-CP-3096] N91-19126
Solar thermal vacuum tests of Magellan spacecraft N91-19127
The test facility requirements for the thermal vacuum thermal balance test of the Cosmic Background Explorer Observatory N91-19128
SCD1 thermal design and test result analysis N91-19130
Thermal balance testing of the Anik-E spacecraft N91-19131
Flow fields of low pressure vent exhausts N91-19135
Optical testing cryogenic thermal vacuum facility N91-19137
Boeing infrared sensor (BIRS) calibration facility N91-19138
Infrared sensor test methodology and facilities N91-19139
Thermal control for the ground simulation of a space IR sensor system N91-19140
IAL SPACE: A test laboratory for the ISO cryogenic payload N91-19142
Non-linear generation of acoustic noise in the IAR spacecraft N91-19143
Advances in atomic oxygen simulation N91-19147
Space environmental effects on spacecraft thermal control coatings N91-19148
Space simulation test for thermal control materials N91-19149
Space simulation facilities providing a stable thermal vacuum facility N91-19150
The space simulation facilities at IAL SPACE N91-19151
Contamination control program for the Cosmic Background Explorer: An overview N91-19152
A unique approach to space thermal simulation N91-19153
Thermal/vacuum vs. thermal atmospheric testing of space flight electronic assemblies N91-19154
Proposal for a conceptually new compact collecting optics for powerful light sources N91-19155
Aeolian removal of dust types from photovoltaic surfaces on Mars N91-19156
Experimental determination of satellite bolted joints thermal resistance N91-19157
Simulation of Martian dust accumulation on surfaces N91-19160
Transfer orbit stage mechanisms thermal vacuum test N91-19161
Low Earth orbital atomic oxygen and ultraviolet radiation effects on polymers
[NASA-TM-103711] N91-19294
Neurological findings after 72 hours water immersion N91-19597
Skeletal adaptation in altered gravity environments N91-19603
Vertebral column length changes during simulated microgravity N91-19604
Determinants of spatial orientation in weightlessness N91-19605
Assessment of bone turnover in humans after space flight and hypokinesia N91-19608
Tools for the preparation, performance and evaluation of life sciences experiments N91-19609
Postural changes following sensory reinterpretation as an analog to spaceflight N91-19610
Standardization of motion sickness induced by left-right and up-down reversing prisms N91-19611
Vestibular tests on UK astronaut candidates for an Anglo/Russian space flight (Juno Mission) N91-19613
Head-down tilt test and space-related endocrine physiology N91-19614
Muscle function impairment following lower limb unloading in men N91-19616
Gravity effects on cells N91-19618
Experiment lymphocytes of Aragatz mission: Influence of the space flight on human T lymphocyte and monocyte functions N91-19619
SPACE EXPLORATION
Enhancing space transportation: The NASA program to develop electric propulsion
[NASA-TM-4244] N91-19181
Feasibility of solar power for Mars N91-19201
SPACE FLIGHT
Spaceflight performance of several types of silicon solar cells on the LIPS 3 satellite N91-19213
Strategy in space flight experiments N91-19220
Ultrasound investigation of the cardiovascular system during the 25 days French-Soviet spaceflight (26 November - 21 December 1988) N91-19577
Vertically moving visual stimuli and vertical vection: A tool against space motion sickness N91-19606
Assessment of bone turnover in humans after space flight and hypokinesia N91-19608
Human and animal results on vestibular research in space: VERIS N91-19642
Adaptive responses in monkeys during two week space flight N91-19645
Genetic risk and physiological stress induced by heavy ions N91-19680
Volume regulating hormones, fluid and electrolyte modifications during the Aragatz Mission (Mir station) N91-19689
SPACE FLIGHT STRESS
Effect of running and head down tilt bedrest on lymphocyte reactivity N91-19598
A new principle for dynamic fluid shift investigations in astronauts N91-19600
Skeletal adaptation in altered gravity environments N91-19603
Postural changes following sensory reinterpretation as an analog to spaceflight N91-19610
Experiment lymphocytes of Aragatz mission: Influence of the space flight on human T lymphocyte and monocyte functions N91-19619
Lymphocytes on sounding rockets N91-19620
Reduced lymphocyte activation in space: Role of cell-substratum interactions N91-19621
SPACE FLIGHT TRAINING
Central and peripheral cardiovascular responses to electrically induced and voluntary leg exercise N91-19687
SPACE INFRARED TELESCOPE FACILITY
A scientific program for infrared, submillimeter and radio astronomy from space: A report by the Management Operations Working Group
[NASA-TM-103333] N91-19979
SPACE LABORATORIES
Biolab on Columbus: A facility for basic science and biotechnology N91-19658
SPACE LOGISTICS
Plant production as part of a Controlled Ecological Life Support System (CELSS) N91-19656
SPACE MISSIONS
The OAST space power program N91-19183
A comparative study of performance parameters of n(+)-p InP solar cells made by closed-ampoule sulfur diffusion into Cd- and Zn-doped p-type InP substrates N91-19209
Developmental biology and microgravity N91-19622
SPACE NAVIGATION
Optimal observation directions for estimating a vector
[PREPRINT-1285] N91-19796
SPACE OBSERVATIONS (FROM EARTH)
Focusing infrared laser beams on targets in space without using adaptive optics
[DE91-007518] N91-19421
SPACE POWER REACTORS
Space reactor/Stirling cycle systems for high power lunar application
[NASA-TM-103698] N91-19112

SPACE PROCESSING
Microgravity strategic plan, 1988
[NASA-TM-103397] N91-19319
Response of a solidly rotating amphora-type liquid column to axial excitation
[LRT-WE-9-FB-06(1990)] N91-19386
Plant biotechnology in space: Facts and speculations N91-19664
Protein purification in multicompartment electrolyzers for crystal growth of r-DNA products in microgravity N91-19665

SPACE PROGRAMS
Space operations: NASA is not archiving all potentially valuable data
[GAO/IMTEC-91-3] N91-19955

SPACE SHUTTLE BOOSTERS
Study of the available finite element software packages at KSC N91-20029

SPACE SHUTTLE MAIN ENGINE
Ceramic composites for rocket engine turbines
[NASA-TM-103743] N91-19235
Probabilistic simulation of uncertainties in thermal structures
[NASA-TM-103680] N91-19472

SPACE SHUTTLE ORBITERS
Research reports: 1990 NASA/ASEE Summer Faculty Fellowship Program
[NASA-CR-187638] N91-20022
Robot tracking system improvements and visual calibration of orbiter position for radiator inspection N91-20037

SPACE SHUTTLE PAYLOADS
Calibration of long term satellite ozone data sets using the space shuttle N91-19524

SPACE SHUTTLES
Debris/ice/TPS assessment and photographic analysis for shuttle mission STS-35
[NASA-TM-103816] N91-19118
Active damping application to the shuttle RMS
[NASA-TM-102763] N91-19471
Atmospheric environment for space shuttle (STS-41) launch
[NASA-TM-103525] N91-19529
Hubble Space Telescope and the space shuttle problems
[S-HRG-101-1087] N91-19974
Low flow vortex shedding flowmeter for hypergolics/all media N91-20036

SPACE STATION PAYLOADS
The space simulation facilities at IAL SPACE N91-19151

SPACE STATIONS
Space station: The next logical step
[NASA-TM-103398] N91-19123
Multi-dimensional modeling of a thermal energy storage canister
[NASA-TM-103731] N91-19177
Optimization and performance of Space Station Freedom solar cells N91-19215
Thermal cycle testing of Space Station Freedom solar array blanket coupons N91-19216
ETARA PC version 3.3 user's guide: Reliability, availability, maintainability simulation model
[NASA-TM-103751] N91-19462
Centrifuge Facility Conceptual System Study. Volume 1: Facility overview and habitats
[NASA-TM-102860] N91-19566
The role of software engineering in the space station program N91-19729

SPACE TRANSPORTATION
Cycling space ship transportation device for continuous link between Earth and Mars
[ILR-MITT-247(1990)] N91-19121
Enhancing space transportation: The NASA program to develop electric propulsion
[NASA-TM-4244] N91-19181

SPACE TRANSPORTATION SYSTEM
Space station: The next logical step
[NASA-TM-103398] N91-19123
Electrochemical impedance spectroscopy of metal alloys in the space transportation system launch environment N91-20025

SPACE TRANSPORTATION SYSTEM FLIGHTS
Debris/ice/TPS assessment and photographic analysis for shuttle mission STS-35
[NASA-TM-103816] N91-19118
A multi-vehicle space carrier fleet cost model for a multi-mission scenario
[ILR-MITT-240(1990)] N91-19120
Atmospheric environment for space shuttle (STS-41) launch
[NASA-TM-103525] N91-19529

SPACEBORNE EXPERIMENTS
The effect of the low Earth orbit environment on space solar cells
[NASA-TM-103735] N91-19165
Strategy in space flight experiments N91-19220
Development of a vibration isolation prototype system for microgravity space experiments
[NASA-TM-103664] N91-19324
A summary of existing and planned experiment hardware for low-gravity fluids research
[NASA-TM-103706] N91-19371
In-space experiment on thermoacoustic convection heat transfer phenomenon-experiment definition
[NASA-CR-187070] N91-19378
NOAA-9 Solar Backscatter Ultraviolet (SBUV/2) Instrument and Derived Ozone Data: Review
[NOAA-TR-NESDIS-53] N91-19514
Fertilization of Xenopus eggs in space N91-19624
Microgravity and development of aquatic animals N91-19625
Unicellular algae in space. 1: Preparatory tests N91-19639
Preliminary studies before defining a payload adapted to the primate model N91-19648
A new approach to electrophoresis in space N91-19653
Free flow electrophoresis experiment TEPE 3 on TEXUS 24 N91-19654
Towards bioregenerative life support systems N91-19655
Cells in space: Sounding rocket facilities for cell biology and biotechnology in microgravity N91-19661
Development of a miniature biology facility N91-19666
Plant growth under microgravity conditions: Experiments and problems N91-19671
Cosmos: 1989 immunology studies
[NASA-CR-188046] N91-19701
Experimental equipment for space biology
[MBB-UO-0096-90-PUB] N91-19708
Space debris: Orbital microparticulates impacting LDEF experiments favour a natural extraterrestrial origin N91-20008

SPACEBORNE TELESCOPES
Thermal insulation of a cryogenic tank for a space telescope using a pretensioned suspension of Fiber Reinforced Composite (FRC)
[MBB-UD-0571-90-PUB] N91-19981

SPACECRAFT
A multi-vehicle space carrier fleet cost model for a multi-mission scenario
[ILR-MITT-240(1990)] N91-19120

SPACECRAFT CONFIGURATIONS
Multipurpose hardened spacecraft insulation N91-19136

SPACECRAFT CONSTRUCTION MATERIALS
An outgassing model of non-metallic materials for the ascent of a Titan 4 launch vehicle N91-19132
Advances in atomic oxygen simulation N91-19147
Space simulation test for thermal control materials N91-19149
Research on advanced NDE methods for aerospace structures
[AD-A226858] N91-19460

SPACECRAFT CONTAMINATION
Sixteenth Space Simulation Conference Confirming Spaceworthiness Into the Next Millennium
[NASA-CP-3096] N91-19126
Multipurpose hardened spacecraft insulation N91-19136
Contamination control program for the Cosmic Background Explorer: An overview N91-19152
A flight experiment to determine GPS photochemical contamination accumulation rates N91-19159

SPACECRAFT CONTROL
The 5th Annual NASA Spacecraft Control Laboratory Experiment (SCOLE) Workshop, part 2
[NASA-CP-10057-PT-2] N91-19122
Modal identification of a deployable space truss
[NASA-TM-102720] N91-19474

SPACECRAFT DESIGN
Space Vehicle Flight Mechanics
[AGARD-AR-294] N91-19124
Multipurpose hardened spacecraft insulation N91-19136

SPACECRAFT ENVIRONMENTS
Plant production as part of a Controlled Ecological Life Support System (CELSS) N91-19656

SPACECRAFT INSTRUMENTS
Low flow vortex shedding flowmeter for hypergolics/all media N91-20036

SPACECRAFT LAUNCHING
Innovations in dynamic test restraint systems N91-19145
Key issues in space nuclear power
[NASA-TM-103656] N91-19179
Atmospheric environment for space shuttle (STS-41) launch
[NASA-TM-103525] N91-19529
Electrochemical impedance spectroscopy of metal alloys in the space transportation system launch environment N91-20025

SPACECRAFT MAINTENANCE
Satellite servicing economic study
[NASA-CR-184112] N91-19162
Satellite servicing economic study
[NASA-CR-184113] N91-19163

SPACECRAFT PERFORMANCE
Active damping application to the shuttle RMS
[NASA-TM-102763] N91-19471

SPACECRAFT POWER SUPPLIES
Simulation of Martian dust accumulation on surfaces N91-19160
Radiation resistance of thin-film solar cells for space photovoltaic power
[NASA-TM-103715] N91-19176
Key issues in space nuclear power
[NASA-TM-103656] N91-19179
Space Photovoltaic Research and Technology, 1989
[NASA-CP-3107] N91-19182
The OAST space power program N91-19183
AlGaAs top solar cell for mechanical attachment in a multi-junction tandem concentrator solar cell stack N91-19187
Burst annealing of high temperature GaAs solar cells N91-19196
Review of thin film solar cell technology and applications for ultra-light spacecraft solar arrays N91-19198
Dual-purpose self-deliverable lunar surface PV electrical power system N91-19200
GaP betavoltaic cells as a power source N91-19211
Low cost space power generation N91-19212
Spaceflight performance of several types of silicon solar cells on the LIPS 3 satellite N91-19213
The Advanced Photovoltaic Solar Array (APSA) technology status and performance N91-19217
Integral bypass diodes in an amorphous silicon alloy photovoltaic module N91-19218
Conceptual study of on orbit production of cryogenic propellants by water electrolysis
[NASA-TM-103730] N91-19317
ETARA PC version 3.3 user's guide: Reliability, availability, maintainability simulation model
[NASA-TM-103751] N91-19462

SPACECRAFT PROPULSION
Advanced chemical propulsion at NASA Lewis: Metallized and high energy density propellants
[NASA-TM-103771] N91-19175

SPACECRAFT RADIATORS
Robot tracking system improvements and visual calibration of orbiter position for radiator inspection N91-20037

SPACECRAFT SHIELDING
Composite flexible insulation for thermal protection of space vehicles
[NASA-TM-103836] N91-19304

SPACECRAFT STRUCTURES
Control and mechanism interaction for ground-based testing of space structures N91-19125
Active damping application to the shuttle RMS
[NASA-TM-102763] N91-19471
Probabilistic simulation of uncertainties in thermal structures
[NASA-TM-103680] N91-19472

SPACECRAFT SURVIVABILITY
Infrared sensor test methodology and facilities N91-19139

SPACECRAFT TRACKING
Robot tracking system improvements and visual calibration of orbiter position for radiator inspection N91-20037

SPACING
BUBBLES: An automated decision support system for final approach controllers N91-19027
Quasi-molecular processes in dense plasmas
[DE91-007388] N91-19899

SPARK GAPS
Control of gap closure in applied-B diode N91-19893

SPATIAL DISTRIBUTION
Spatial and temporal variation in biomonitoring data
[DE91-007843] N91-19539
Optical diagnostics for low-temperature plasmas
[DE91-007896] N91-19907

SPATIAL RESOLUTION
Vertically moving visual stimuli and vertical vection: A tool against space motion sickness N91-19606

SPECIFICATIONS
Proposed draft military handbook presenting requirements for an Electronic Display System (EDS) for Interactive Electronic Technical Manuals (IETMs)
[AD-A227471] N91-19342
In-space experiment on thermoacoustic convection heat transfer phenomenon-experiment definition
[NASA-CR-187070] N91-19378

The specification of glancing incidence mirrors in terms of system performance
[DE91-007564] N91-19874

SPECTRAL SENSITIVITY
Semiconductor photodiodes as radiometric receivers in the field of soft radiation
[ETN-91-98925] N91-19856

SPECTRAL SIGNATURES
Search for the optical signatures of a pulsar in SN1987A
[MPE-PREPRINT-188] N91-19978

SPECTROMETERS
Evaluation of a Photo-Electron Rejecting Aipha Liquid Scintillation (PERALS) spectrometer for the measurement of alpha-emitting radionuclides
[DE91-005652] N91-19399

SPECTROSCOPIC ANALYSIS
Polymer characterization using the time-resolved phosphorescence of singlet oxygen as a spectroscopic probe
[DE91-001269] N91-19303

SPECTROSCOPY
Characterization of ion-implanted aluminum and iron by spectroscopic ellipsometry
[DE91-008371] N91-19283
Nuclear-spectroscopy computerized tomography scanners
[DE91-008447] N91-19466
Study of InGaAs based MODFET structures using variable angle spectroscopic ellipsometry
[NASA-TM-103792] N91-19935
Electrochemical impedance spectroscopy of metal alloys in the space transportation system launch environment N91-20025

SPECTRUM ANALYSIS
LDEF Experiment P0006 Linear Energy Transfer Spectrum Measurement (LETSME) quick look report
[NASA-CR-184115] N91-19223
Radar-measured height profiles of Cn(2) and turbulence dissipation rate compared with radiosonde data during October 1989 at Denver
[PB91-125500] N91-19562
Solar-geophysical data Number 554, October 1990. Part 1 (prompt reports): Data for September, August 1990, and late data. Explanation of data reports issued as Number 515 (supplement) July 1987
[PB91-124594] N91-20018

SPEECH RECOGNITION
Automatic speech recognition in air traffic control: A human factors perspective N91-19025

SPEED CONTROL
Some control problems with broad range variable speed for horizontal axis wind turbines
[FFA-TN-1990-37] N91-19513

SPEED REGULATORS
Some control problems with broad range variable speed for horizontal axis wind turbines
[FFA-TN-1990-37] N91-19513

SPIN EXCHANGE
The physics of laser polarized muonic atoms
[DE91-008045] N91-19845

SPIN-LATTICE RELAXATION
Effect of paramagnetic impurities on dynamics of magnetic fluxes in superconductors N91-19816

SPINE
Vertebral column length changes during simulated microgravity N91-19604

SPIRAL GALAXIES
High resolution infrared astronomy satellite observations of a selected spiral galaxy
[NASA-CR-188019] N91-19975
Proceedings of the symposium Astrophysical Processes and Structures in the Universe
[PB91-123653] N91-19993
Proceedings of 146th IAU Symposium on Dynamics of Galaxies and Molecular Cloud Distribution
[PB91-123661] N91-19994

SPLEEN
Cosmos: 1989 immunology studies
[NASA-CR-188046] N91-19701

SPRINGS (ELASTIC)
Graduated-load spring washer system for screws and threaded fasteners
[AD-D014697] N91-19436

SPUTTERING
Recent advances in the ITO/InP solar cell N91-19202
Heterogeneous magnetoresistant layer
[AD-D014665] N91-19289

STABILITY
Stochastic satbility and performance robustness of linear multivariable systems N91-19038
Progress in GaAs/CuInSe2 tandem junction solar cells N91-19190
Recent advances in the ITO/InP solar cell N91-19202
Theoretical investigation of phase stability in non-magnetic Fe-V substitutional alloys
[DE91-006711] N91-19268
Euler solutions to nonlinear acoustics of non-lifting hovering rotor blades
[NASA-TM-103837] N91-19826
The structure of nuclei far from beta stability
[DE91-008140] N91-19846

STABILITY TESTS
Control and mechanism interaction for ground-based testing of space structures N91-19125

STABILIZATION
Method for making holograms with coherent radiation from a stabilized laser diode that has been actively cooled
[AD-D014673] N91-19396

STANDARDIZATION
Proposed draft military handbook presenting requirements for an Electronic Display System (EDS) for Interactive Electronic Technical Manuals (IETMs)
[AD-A227471] N91-19342

STANDARDS
NDE standards for high temperature materials
[NASA-TM-103761] N91-19464
PHIGS PLUS for scientific graphics
[DE91-007615] N91-19747

STANDING WAVES
Simulation of a standing-wave free-electron laser
[DE91-007330] N91-19418
Phase stability of a standing-wave free-electron laser
[DE91-008068] N91-19427

STAR FORMATION
High resolution infrared astronomy satellite observations of a selected spiral galaxy
[NASA-CR-188019] N91-19975
Detection of an isotopic short submillimeter CO line: Column densities of warm gas in molecular clouds
[MPE-PREPRINT-178] N91-19976

STARBURST GALAXIES
Observations of CO isotopic emission and the far-infrared continuum of Centaurus A
[MPE-PREPRINT-183] N91-19977

STARK EFFECT
Measurements of stark-broadening in hot dense plasma
[DE91-008504] N91-19910

STARTING
Cool-down and frozen start-up behavior of a grooved water heat pipe
[NASA-CR-187053] N91-19376

STATE ESTIMATION
State estimation applications in aircraft flight-data analysis: A user's manual for SMACK
[NASA-RP-1252] N91-19082
A proposed Kalman filter algorithm for estimation of unmeasured output variables for an F100 turbofan engine
[NASA-TM-4234] N91-19099

STATE VECTORS
A proposed Kalman filter algorithm for estimation of unmeasured output variables for an F100 turbofan engine
[NASA-TM-4234] N91-19099
Quantum optics reveals the nature of superconductivity
[TR-69] N91-19946

STATIC STABILITY
The apparent strain stability and repeatability of a BCL3 resistance strain gage
[NASA-CR-187056] N91-19403

STATIC TESTS
Strength test of CFRP box beam model
[NAL-TR-1057] N91-19469

STATISTICAL ANALYSIS
Stochastic satbility and performance robustness of linear multivariable systems N91-19038
System identification for nonlinear control using neural networks N91-19039
Performance of underwater weldments
[PB91-129254] N91-19452
Statistical examination of climatological data relevant to global temperature variation
[DE91-007881] N91-19540
Overview of climate information needs for ecological effects models
[PB91-125898] N91-19549
C-statistic fitting routines: User's manual and reference guide
[NASA-CR-187992] N91-19736
Optimal observation directions for estimating a vector
[PREPRINT-1285] N91-19796
Some aspects of robotics calibration, design and control N91-20035

STATISTICAL CORRELATION
Responses of women to orthostatic and exercise stresses
[NASA-TP-3043] N91-19711

STATISTICAL DISTRIBUTIONS
Statistics of peaks in cosmological nonlinear density fields
[DE91-744972] N91-19990

STEADY FLOW
A numerical method for solving steady 2D and axisymmetrical viscoelastic flow problems with an application to inertia effects in contraction flows
[MEMT-11] N91-19394

STEAM
The magnetohydrodynamics coal-fired flow facility
[DE91-007672] N91-19906

STEELS
Magneto-elastic behaviour of steels for naval applications
[MRL-TR-90-27] N91-19266
Spatial and temporal relationships between localized microbial metabolic activity and electrochemical activity of steel
[DE91-008102] N91-19279

STELLAR ACTIVITY
Some limitations of detailed balance for inverse reaction calculations in the astrophysical P-process
[DE91-007258] N91-19983

STELLAR EVOLUTION
High energy physics and cosmology
[DE91-007369] N91-19859
Proceedings of the symposium Astrophysical Processes and Structures in the Universe
[PB91-123653] N91-19993

STELLARATORS
Review of recent stellarator results in the USA, the USSR, and Japan
[DE91-007798] N91-19901

STIFFNESS
Single-strain-gage force/stiffness buckling prediction techniques on a hat-stiffened panel
[NASA-TM-101733] N91-19077
Dynamic behavior of pneumatic tyres
[BU-412] N91-19453
Non-homogeneous bars under tension, pure bending, and temperature loads
[MBB-UD-0572-90-PUB] N91-19485

STIFFNESS MATRIX
Finite strip elements in thin plate buckling analysis
[LR-642] N91-19493

STIRLING CYCLE
Space reactor/Stirling cycle systems for high power lunar application
[NASA-TM-103698] N91-19112

STIRLING ENGINES
A 2-D oscillating flow analysis in Stirling engine heat exchangers
[NASA-TM-103781] N91-19375

STOCHASTIC PROCESSES
Stochastic robustness: Towards a comprehensive robustness tool N91-19036
Stochastic satbility and performance robustness of linear multivariable systems N91-19038
A stochastic performance model for the neutron diffusion nodal method on a multiuser parallel supercomputer
[DE90-017015] N91-19749
Orthogonal least squares parameter estimation algorithms for nonlinear stochastic systems
[RR-404] N91-19797

STORAGE RINGS (PARTICLE ACCELERATORS)
Computation of invariant tori in 2 (1/2) degrees of freedom
[DE91-007424] N91-19778
Longitudinal periodicity in superconducting dipole magnets
[DE91-008421] N91-19821
Electroweak interactions at LEP
[NOTA-INTERNA-962] N91-19853
Studies of cold protection diodes
[DE91-008203] N91-19863
A global fit to the Z(0) line shape
[NOTA-INTERNA-966] N91-19868

STORMS
Association of an auroral surge with plasma sheet recovery and the retreat of the substorm neutral line
[DE91-007351] N91-19552

STRAIN ENERGY METHODS
Development and applications of a multi-level strain energy method for detecting finite element modeling errors
[NASA-CR-187447] N91-19478

STRAIN GAGES
Single-strain-gage force/stiffness buckling prediction techniques on a hat-stiffened panel
[NASA-TM-101733] N91-19077

The apparent strain stability and repeatability of a BCL3 resistance strain gage
[NASA-CR-187056] N91-19403
STRAIN HARDENING
On the thermodynamics of stress rate in the evolution of back stress in viscoplasticity
[NASA-TM-103794] N91-19476
STRAIN MEASUREMENT
The application of neutron diffraction time-of-flight measurements to the study of strain in composites
[DE91-008106] N91-19242
STRAIN RATE
Application of high speed photography to the study of high strain rate materials testing
[OUEL-1852/90] N91-19411
STRATEGY
The impact of the new management strategy on senior operational commanders at group level within Royal Air Force Strike Command
[REPT-89SDM/MCHALE/03-MDA] N91-19954
STRATIFICATION
The application of simulation model for the flow induced by air bubble plume in thermally stratified reservoirs
[DE91-003064] N91-19380
STRATIGRAPHY
Lunar maria and related deposits: Preliminary Galileo imaging results N91-20000
STRATOSPHERE
An assessment of instrument performance for the NOAA-9 SBUV/2 N91-19516
A status report on the analysis of the NOAA-9 SBUV/2 sweep mode solar irradiance data N91-19518
Umkehr work N91-19522
Ozone measurements from the NOAA-9 and the Nimbus-7 satellites: Implications of short and long term variabilities N91-19527
Monitoring the response of the upper troposphere/lower stratosphere to a greenhouse gas scenario
[DE91-007976] N91-19541
STREAK PHOTOGRAPHY
Interferometry, streak photography, and stereo photography of laser-driven miniature flying plates
[DE91-007493] N91-19405
STREAMS
Spatial and temporal variation in biomonitoring data
[DE91-007843] N91-19539
STRESS ANALYSIS
New computer codes for the structural analysis of composite helicopter structures
[MBB-UD-0580-90-PUB] N91-19089
A knowledge based expert system for laminated composite strut design
[BU-410] N91-19247
On the thermodynamics of stress rate in the evolution of back stress in viscoplasticity
[NASA-TM-103794] N91-19476
The effect of elastic stress on Ostwald ripening phenomena
[DE91-008034] N91-19484
Dynamic applications of ABAQUS
[OUEL-1853/90] N91-19755
Study of the available finite element software packages at KSC N91-20029
STRESS CORROSION CRACKING
Stress corrosion cracking of Al-Li-Cu-Zr alloy 2090 in aqueous Cl(-) and mixed CO3(2-)/Cl(-) environments
[DE91-007064] N91-19269
STRESS DISTRIBUTION
The method of lines in analyzing solids containing cracks
[NASA-TM-103626] N91-19477
STRESS INTENSITY FACTORS
The correlation of transient crack growth under small-scale-creep conditions N91-19467
STRESS MEASUREMENT
Crack opening stress measurements of surface cracks in 7075-T6 Al alloy plate specimens through electron fractography
[LR-641] N91-19492
STRESS RELAXATION
Internal friction peaks due to interstitials in bcc alloys
[DE91-007411] N91-19272
STRESS WAVES
Dynamic applications of ABAQUS
[OUEL-1853/90] N91-19755
STRESS-STRAIN DIAGRAMS
METCAN updates for high temperature composite behavior: Simulation/verification
[NASA-TM-103682] N91-19229
STRESS-STRAIN RELATIONSHIPS
On the thermodynamics of stress rate in the evolution of back stress in viscoplasticity
[NASA-TM-103794] N91-19476
STRING THEORY
Symmetries on the space of (2,2) superstring vacua and automorphism groups of Calabi-Yau manifolds
[DE91-008218] N91-19951
STRINGERS
Design and testing of a circumferential and longitudinal joint of the A320 fuselage section 13/14 in GLARE
[LR-645] N91-19494
STROKE VOLUME
Ultrasound investigation of the cardiovascular system during the 25-days Soviet-French flight: Cardiac aspects N91-19578
STRUCTURAL ANALYSIS
New computer codes for the structural analysis of composite helicopter structures
[MBB-UD-0580-90-PUB] N91-19089
Comparative morphology of configurations with reduced part count derived from the octahedral-tetrahedral truss
[NASA-TM-102768] N91-19168
Computational simulation of hot composites structures
[NASA-TM-103681] N91-19230
A knowledge based expert system for laminated composite strut design
[BU-410] N91-19247
Structural reliability analysis of laminated CMC components
[NASA-TM-103685] N91-19292
Probabilistic simulation of uncertainties in thermal structures
[NASA-TM-103680] N91-19472
On the vectorization and parallelization of the shooting method using the convex C-240
[LR-639] N91-19491
STRUCTURAL BASINS
What were the effects of the formation of the Borealis basin, Mars N91-20014
STRUCTURAL DESIGN
Control and mechanism interaction for ground-based testing of space structures N91-19125
The full-scale process and design changes for elimination of insulation edge separations and voids in tang flap area
[NASA-CR-184110] N91-19172
Status of GaAs/Ge solar cells N91-19185
AlGaAs top solar cell for mechanical attachment in a multi-junction tandem concentrator solar cell stack N91-19187
Tandem concentrator solar cells with 30 percent (AMO) power conversion efficiency N91-19189
Thermal annealing of GaAs concentrator solar cells N91-19195
Dual-purpose self-deliverable lunar surface PV electrical power system N91-19200
Integral bypass diodes in an amorphous silicon alloy photovoltaic module N91-19218
Uncertainty reasoning applied to the assessment of composite material for structural design
[BU-405] N91-19244
Structural reliability analysis of laminated CMC components
[NASA-TM-103685] N91-19292
Monolithic radiation hard charge sensitive preamplifier using junction field effect transistors
[DE91-008437] N91-19360
Performance of underwater weldments
[PB91-129254] N91-19452
A theoretical solution for the buckling of sandwich panels with laminated face plates using a computer algebra system
[BU-407] N91-19486
Bolted joints in a laminated composite strut design expert system
[BU-415] N91-19488
STRUCTURAL FAILURE
Bolted joints in a laminated composite strut design expert system
[BU-415] N91-19488
Continuum damage mechanisms with an application to fatigue
[ISBN-90-9003688-1] N91-19490
STRUCTURAL MEMBERS
Liquid sloshing in cargo tanks. Liquid slosh loading in slack ship tanks: Forces on internal structure and pressures
[PB91-129262] N91-19383
STRUCTURAL PROPERTIES (GEOLOGY)
An evaluation of co-planar lineament analysis and some thoughts on using surface geological data to predict sub-surface geology
[DE90-009687] N91-19556
STRUCTURAL RELIABILITY
Structural reliability analysis of laminated CMC components
[NASA-TM-103685] N91-19292
STRUCTURAL STABILITY
Space simulation facilities providing a stable thermal vacuum facility N91-19150
Comparative morphology of configurations with reduced part count derived from the octahedral-tetrahedral truss
[NASA-TM-102768] N91-19168
STRUCTURAL STRAIN
Behavior of surface and corner cracks subjected to tensile and bending loads in Ti-6Al-4V alloy
[NASA-TM-102165] N91-19273
An evaluation of the fatigue crack growth and fracture toughness properties of beryllium-copper alloy CDA172
[NASA-TM-102166] N91-19274
STRUCTURAL VIBRATION
Thermoelastic vibration test techniques
[NASA-TM-101742] N91-19083
Modal identification of a deployable space truss
[NASA-TM-102720] N91-19474
STRUTS
Minimum weight optimization of composite laminated struts
[BU-409] N91-19246
A knowledge based expert system for laminated composite strut design
[BU-410] N91-19247
Bolted joints in a laminated composite strut design expert system
[BU-415] N91-19488
STUDENTS
Test analysis program evaluation: Item statistics as feedback to test developers
[AD-A229851] N91-19713
SUBMARINES
Magneto-elastic behaviour of steels for naval applications
[MRL-TR-90-27] N91-19266
SUBMERGING
Responses of Physarum polycephalum to varying light levels during fast clinostat rotation: A scientific preparation of an ESA biorack experiment during the IML-1 mission N91-19676
SUBMILLIMETER WAVES
Detection of an isotopic short submillimeter CO line: Column densities of warm gas in molecular clouds
[MPE-PREPRINT-178] N91-19976
A scientific program for infrared, submillimeter and radio astronomy from space: A report by the Management Operations Working Group
[NASA-TM-103333] N91-19979
SUBROUTINES
C-statistic fitting routines: User's manual and reference guide
[NASA-CR-187992] N91-19736
SUBSONIC FLOW
Acoustic radiation from lifting airfoils in compressible subsonic flow
[NASA-TM-103650] N91-19053
An experimental study of the turbulent boundary layer on a transport wing in subsonic and transonic flow
[NASA-TM-102206] N91-19062
Wind tunnel wall effects in a linear oscillating cascade
[NASA-TM-103690] N91-19098
J-85 jet engine noise measured in the ONERA S1 wind tunnel and extrapolated to far field
[NASA-TP-3053] N91-19823
SUBSONIC SPEED
Panel methods: An introduction
[NASA-TP-2995] N91-19058
SUBSONIC WIND TUNNELS
Automatic control study of the icing research tunnel refrigeration system
[NASA-TM-4257] N91-19115
SUBSTITUTES
Thermal properties of polyisocyanurate foam board insulation blown with CFC-11 substitutes
[DE90-016047] N91-19240
SUBSTRATES
Progress toward a 30 percent-efficient, monolithic, three-junction, two-terminal concentrator solar cell for space applications N91-19188
A comparative study of performance parameters of n(+)-p InP solar cells made by closed-ampoule sulfur diffusion into Cd- and Zn-doped p-type InP substrates N91-19209
Limiting pulse signal in NbN-Si structure: Superconductor film on substrate N91-19815
SULFATES
Performance characteristics of an MHD (Magnetohydrodynamic) pilot plant electrostatic precipitator
[DE91-007218] N91-19905
SULFUR
A comparative study of performance parameters of n(+)-p InP solar cells made by closed-ampoule sulfur diffusion into Cd- and Zn-doped p-type InP substrates N91-19209

SULFUR COMPOUNDS
Synthesis and structures of metal chalcogenide precursors
[NASA-TM-103665] N91-19296
SUN
SBUV/2 in-orbit performance N91-19517
Solar-geophysical data Number 554, October 1990. Part 2 (comprehensive reports): Data for April 1990 and miscellaneous. Explanation of data reports issued as Number 515 (supplement) July 1987
[PB91-124586] N91-20017
SUNFLOWERS
Electrofusion and regeneration of protoplasts from sunflower (Helianthus annuus L.) N91-19675
SUNLIGHT
Productivity and photosynthesis of selected crop plants under orbital light conditions: An approach to solar powered CELSS N91-19662
Mutation induction in dried yeast cells after irradiation with selected UVC- and UVB- wavelengths compared to simulated sunlight N91-19686
SUPERCHARGERS
A modelling of unsteady air flow in the resonance charging system of high speed diesel engines
[ACTA-POLYTEC-SCAND-ME-97] N91-19454
SUPERCOMPUTERS
Assessing the impact of large-scale computing on the size and complexity of first-principles electromagnetic models
[DE91-007491] N91-19333
Large-scale computing in the energy research programs
[DE91-007907] N91-19748
The PVM (Parallel Virtual Machine) system: Supercomputer level concurrent computation on a network of IBM RS/6000 power stations
[DE91-007844] N91-19757
SUPERCONDUCTING FILMS
Limiting pulse signal in NbN-Si structure: Superconductor film on substrate N91-19815
SUPERCONDUCTING MAGNETS
A variational approach to magneto-elastic buckling problems
[ETN-91-98929] N91-19338
Microtube strip heat exchanger
[DE91-005741] N91-19504
Longitudinal periodicity in superconducting dipole magnets
[DE91-008421] N91-19821
Studies of cold protection diodes
[DE91-008203] N91-19863
SUPERCONDUCTING SUPER COLLIDER
Neutron radiation damage studies on silicon detectors
[DE91-008441] N91-19361
Energy sciences supercomputing 1990
[DE91-007188] N91-19740
W(sub L)W(sub L) scattering at the SSC
[DE91-008442] N91-19851
Studies of cold protection diodes
[DE91-008203] N91-19863
Prototype document tracking and storage system for the Superconducting Super Collider Laboratory (SSCL)
[DE91-008204] N91-19963
SUPERCONDUCTIVITY
Superconducting instrumentation for critical He-4 measurements in space
[DE91-007894] N91-19408
Multiple energy computed tomography for neuroradiology with monochromatic x rays from the national synchrotron light source
[DE91-008108] N91-19712
Thermal conductivity of high-temperature superconductors in normal state N91-19818
Superconductivity of oxide film electrolytically deposited on surface of B(1-x)Sb(x) single crystal N91-19819
Magnetism and superconductivity in YBa2Cu3O(6+x) at 0.3 less than or equal to x less than or equal to 0.4
[DE91-615507] N91-19945
Quantum optics reveals the nature of superconductivity
[TR-69] N91-19946
SUPERCONDUCTORS
Effect of paramagnetic impurities on dynamics of magnetic fluxes in superconductors N91-19816
Method of producing superconducting materials in bulk form
[AD-D014656] N91-19917
Apparatus for determining microwave characteristics of superconductive materials using a resonant cavity and calibration waveguides
[AD-D014694] N91-19918
SUPERFLUIDITY
Superconducting instrumentation for critical He-4 measurements in space
[DE91-007894] N91-19408
Reflections on some problems concerning the role of superfluid turbulence in the propagation of second-sound pulses in He 2
[MPIS-8/1990] N91-19827
Ultrasonic investigations on superfluid He-3-A and He-3-B
[ISBN-952-90-2241-7] N91-19830
SUPERLATTICES
Application of MeV ions to the analysis and modification of high temperature superconducting materials
[DE91-007317] N91-19927
SUPERNOVA 1987A
Search for the optical signatures of a pulsar in SN1987A
[MPE-PREPRINT-188] N91-19978
SUPERNOVAE
Primordial nucleosynthesis: Beyond the standard model
[DE91-007264] N91-19984
Sixquarks in neutron stars
[DE91-615472] N91-19987
SUPERSATURATION
Vascular gas bubbles or decompression sickness: What is the proper endpoint for evaluating decompression procedures N91-19590
SUPERSONIC FLIGHT
Space Vehicle Flight Mechanics
[AGARD-AR-294] N91-19124
Solid fuel combustion chamber
[LR-648] N91-19222
SUPERSONIC FLOW
Development of a laser-induced heat flux technique for measurement of convective heat transfer coefficients in a supersonic flowfield
[NASA-TM-103778] N91-19063
Aerodynamic focusing of particles and heavy molecules
[DE91-006922] N91-19833
SUPERSONIC JET FLOW
Experimental investigation of a single flush-mounted hypermixing nozzle
[NASA-TM-103726] N91-19374
SUPERSONIC NOZZLES
Pitot measurements in the exhaust of a cluster of four small scale supersonic nozzles
[OUEL-1862/90] N91-19070
Experimental investigation of a single flush-mounted hypermixing nozzle
[NASA-TM-103726] N91-19374
SUPERSONIC SPEED
Experimental investigation of porous-floor effects on cavity flow fields at supersonic speeds
[NASA-TP-3032] N91-19042
Panel methods: An introduction
[NASA-TP-2995] N91-19058
SUPERSYMMETRY
Symmetries on the space of (2,2) superstring vacua and automorphism groups of Calabi-Yau manifolds
[DE91-008218] N91-19951
SUPPORT SYSTEMS
BUBBLES: An automated decision support system for final approach controllers N91-19027
SURFACE CRACKS
Behavior of surface and corner cracks subjected to tensile and bending loads in Ti-6Al-4V alloy
[NASA-TM-102165] N91-19273
The method of lines in analyzing solids containing cracks
[NASA-TM-103626] N91-19477
Crack opening stress measurements of surface cracks in 7075-T6 Al alloy plate specimens through electron fractography
[LR-641] N91-19492
SURFACE FINISHING
Excimer laser surface processing for tribological applications in metals and ceramics
[DE91-002324] N91-19428
SURFACE GEOMETRY
Local synthesis and tooth contact analysis of face-milled spiral bevel gears
[NASA-CR-4342] N91-19439
SURFACE LAYERS
Piezoelectric sandwich polymer transducer
[AD-D014650] N91-19341
SURFACE NAVIGATION
Cascading a systolic array and a feedforward neural network for navigation and obstacle avoidance using potential fields
[NASA-CR-177575] N91-19771
SURFACE PROPERTIES
Space environmental effects on spacecraft thermal control coatings N91-19148
Origin of residual surface resistance of ceramic high-temperature superconductors N91-19814
Atomic beam studies of the interaction of hydrogen with transition metal surfaces
[DE91-007938] N91-19841
The specification of glancing incidence mirrors in terms of system performance
[DE91-007556] N91-19873
The specification of glancing incidence mirrors in terms of system performance
[DE91-007564] N91-19874
Considerations relating to pulsed-beam modification of materials
[DE91-006771] N91-19922
Solid state, surface, and catalytic studies of oxides
[DE91-007979] N91-19939
SURFACE REACTIONS
Surface chemistry at semiconductor-electrolyte interfaces
[DE91-005915] N91-19920
Mutual influence of doping and oxidation in highly doped silicon
[ETN-91-98924] N91-19948
SURFACE ROUGHNESS
Smoothness criteria for runway rehabilitation and overlays
[DOT/FAA/RD-90/23] N91-19102
The characterization of interface roughness and other defects in multilayers by x ray scattering
[DE91-007558] N91-19929
SURFACE TEMPERATURE
In-space experiment on thermoacoustic convection heat transfer phenomenon-experiment definition
[NASA-CR-187070] N91-19378
SURFACE WATER
Throughfall and foliar extraction
[DE91-007184] N91-19535
SURVEILLANCE
Environmental surveillance data report for the first quarter of 1990
[DE91-008552] N91-19544
SUSPENDING (HANGING)
Muscle function impairment following lower limb unloading in men N91-19616
Contractile protein changes induced by hindlimb suspension in rat skeletal muscle N91-19646
Hindlimb suspension of rabbit for one week: Myofibrillar damage in the soleus may depend on long-lasting shortening and periodic contraction against no load N91-19647
SWEDEN
Some control problems with broad range variable speed for horizontal axis wind turbines
[FFA-TN-1990-37] N91-19513
SWIMMING
Effect of hyper-gravity on the swimming behavior of aquatic vertebrates N91-19626
Morphological, electronmicroscopical and biochemical aspects of hyper-gravity conditions during early ontogenetic development of Cichlid fish N91-19638
SWITCHING
Complete exchange on the iPSC-860
[NASA-CR-187498] N91-19715
Multiphase complete exchange on a circuit switched hypercube
[NASA-CR-187499] N91-19716
SWITCHING CIRCUITS
Computer controlled MHD power consolidation and pulse generation system
[DE91-006793] N91-19347
Development of a numerical computer code and circuit element models for simulation of firing systems
[DE91-007162] N91-19739
Limiting pulse signal in NbN-Si structure: Superconductor film on substrate N91-19815
Reduction of low energy components in pulse ion beam N91-19889
Generation of pulsed ion beams by an inductive storage pulsed power generator N91-19891
SWITCHING THEORY
Efficient connecting networks using directed links
[ETN-91-98855] N91-19762
SYMMETRY
Comparative morphology of configurations with reduced part count derived from the octahedral-tetrahedral truss
[NASA-TM-102768] N91-19168
Theoretical investigation of phase stability in non-magnetic Fe-V substitutional alloys
[DE91-006711] N91-19268
Relation between perception of vertical axis rotation and vestibulo-ocular reflex symmetry
[NASA-CR-187997] N91-19710
Phenomenological theory of phase transitions to nonhomogeneous noncommensurate phase with superconducting current N91-19817
W(sub L)W(sub L) scattering at the SSC
[DE91-008442] N91-19851

SYNCHROTRON RADIATION
The advanced light source: A new tool for research in atomic physics
[DE91-007739] N91-19861
SYNCHROTRONS
Phase stability of a standing-wave free-electron laser
[DE91-008068] N91-19427
Multiple energy computed tomography for neuroradiology with monochromatic x rays from the national synchrotron light source
[DE91-008108] N91-19712
SYNTAX
Improved syntactic disambiguation in the FASIT automatic indexing environment N91-19956
SYNTHESIS (CHEMISTRY)
Reactivity of pi-complexes of Ti, V, and Nb towards dithioacetic acid: Synthesis and structure of novel metal sulfur-containing complexes
[NASA-TM-103666] N91-19256
Late transition metal (mu)-oxo and (mu)-imido complexes
[DE91-005349] N91-19267
Synthesis and structures of metal chalcogenide precursors
[NASA-TM-103665] N91-19296
Effects of atmosphere and heating rate during processing of a ceramic superconductor
[DE91-007761] N91-19299
Aerosol formation in atmospheric mixtures
[PB91-129114] N91-19560
A photoemission investigation of compound semiconductor monodisperse clusters
[DE91-006707] N91-19921
SYNTHETIC FUELS
Alternative fuels for heavy duty engines: Status of fleet trials
[DE91-006799] N91-19315
Exhaust emissions from heavy duty vehicles
[DE91-006798] N91-19531
SYSTEM FAILURES
Integrated inertial/GPS N91-19032
Sodium/metal chloride program conceptual design study
[DE91-007216] N91-19353
SYSTEM IDENTIFICATION
Modeling selective availability of the NAVSTAR global positioning system N91-19030
System identification for nonlinear control using neural networks N91-19039
Modal identification of a deployable space truss
[NASA-TM-102720] N91-19474
Use of system identification techniques for improving airframe finite element models using test data
[NASA-CR-188041] N91-19750
SYSTEMS ANALYSIS
A multi-vehicle space carrier fleet cost model for a multi-mission scenario
[ILR-MITT-240(1990)] N91-19120
SYSTEMS ENGINEERING
Ridge regression signal processing N91-19029
System design for the Tiger helicopter
[MBB-UD-0581-90-PUB] N91-19090
Smoothness criteria for runway rehabilitation and overlays
[DOT/FAA/RD-90/23] N91-19102
Project Hitch Hiker: A feasibility study for a small telecommunication satellite
[LR-644] N91-19169
Army-NASA aircrew/aircraft integration program (A3I) software detailed design document, phase 3
[NASA-CR-177557] N91-19714
SYSTEMS INTEGRATION
A new generation of real-time DOS technology for mission-oriented system integration and operation N91-19725
Tool and data interoperability in the SSE system N91-19727
SYSTEMS SIMULATION
Computer Aided System Design and Simulation
[AGARD-AR-283] N91-19731
Fault detection using optimal control techniques
[RR-419] N91-19867
SYSTOLIC ARRAYS
Cascading a systolic array and a feedforward neural network for navigation and obstacle avoidance using potential fields
[NASA-CR-177575] N91-19771

T

TABLES (DATA)
Transferable Output ASCII Data (TOAD) gateway: Version 1.0 user's guide
[NASA-CR-187489] N91-19737
Table of tables: A database design tool for SYBASE
[DE91-007257] N91-19958
TACTILE SENSORS (ROBOTICS)
A haptic system for a multifingered hand
[DE90-017044] N91-19767
TAKEOFF
Feasibility of an onboard wake vortex avoidance system
[NASA-CR-187521] N91-19074
Monitoring techniques for the X-29A aircraft's high-speed rotating power takeoff shaft
[NASA-TM-101731] N91-19081
TARGET RECOGNITION
Method for determining astronomic azimuth
[AD-D014677] N91-19972
TARGETS
A gradient microphone for locating sound targets
[MBB-Z-0341-90-PUB] N91-19829
Method for determining astronomic azimuth
[AD-D014677] N91-19972
TASKS
Empirical studies of software design: Implications for SSEs N91-19728
TAXIING
Aircraft standstill, requirements for ground handling from the point of view of aircraft operation N91-19109
TAYLOR INSTABILITY
Rayleigh-Taylor instability in LIB ICF N91-19883
TECHNICAL WRITING
The 1989 JSC bibliography of scientific and technical papers
[NASA-TM-102173] N91-19959
TECHNOLOGIES
US technology policy: Executive Office of the President
[PB91-119677] N91-19970
TECHNOLOGY ASSESSMENT
Microgravity strategic plan, 1988
[NASA-TM-103397] N91-19319
Exploratory battery technology development and testing report for 1989
[DE91-006753] N91-19352
A summary of the status of biomass conversion technologies and opportunities for their use in developing countries
[DE91-006341] N91-19506
Technology modernization assessment flexible automation
[DE91-005620] N91-19751
TECHNOLOGY UTILIZATION
The application of aero gas turbine engine monitoring systems to military aircraft
[ETN-91-98852] N91-19096
Space research for the sake of all
[ETN-91-98807] N91-19113
Progress toward a 30 percent-efficient, monolithic, three-junction, two-terminal concentrator solar cell for space applications N91-19188
Review of thin film solar cell technology and applications for ultra-light spacecraft solar arrays N91-19198
Composite materials for space applications
[NASA-CR-187472] N91-19238
TECTONICS
Magellan: Preliminary description of Venus surface geologic units N91-20011
TELECOMMUNICATION
Project Hitch Hiker: A feasibility study for a small telecommunication satellite
[LR-644] N91-19169
TELEMETRY
Air/sea temperature probe
[AD-D014674] N91-19397
TELESCOPES
Focusing infrared laser beams on targets in space without using adaptive optics
[DE91-007518] N91-19421
A balloon-borne 102-cm telescope for far-infrared astronomy
[NASA-CR-187778] N91-19973
TELEVISION SYSTEMS
The provision of circuits to outside broadcast locations using spectrum within the UHF broadcasting bands
[BBC-RD-1990/12] N91-19329
TEMPERATURE CONTROL
The test facility requirements for the thermal vacuum thermal balance test of the Cosmic Background Explorer Observatory N91-19128
SCD 02 thermal design N91-19129
SCD1 thermal design and test result analysis N91-19130
Optical testing cryogenic thermal vacuum facility N91-19137
Thermal control for the ground simulation of a space IR sensor system N91-19140
Special requirements in the design of a sensor test and integration laboratory N91-19141
Space simulation test for thermal control materials N91-19149
TEMPERATURE DEPENDENCE
Thermal conductivity of high-temperature superconductors in normal state N91-19818
TEMPERATURE DISTRIBUTION
Thermal control for the ground simulation of a space IR sensor system N91-19140
Experimental determination of satellite bolted joints thermal resistance N91-19157
TEMPERATURE EFFECTS
Thermoelastic vibration test techniques
[NASA-TM-101742] N91-19083
The performance of multilayer insulation in a rapidly depressurizing environment N91-19133
Optical testing cryogenic thermal vacuum facility N91-19137
Special requirements in the design of a sensor test and integration laboratory N91-19141
Thermal/vacuum vs. thermal atmospheric testing of space flight electronic assemblies N91-19154
METCAN updates for high temperature composite behavior: Simulation/verification
[NASA-TM-103682] N91-19229
Computational simulation of hot composites structures
[NASA-TM-103681] N91-19230
Composite flexible insulation for thermal protection of space vehicles
[NASA-TM-103836] N91-19304
Capattery double layer capacitor life performance
[DE91-006639] N91-19344
The apparent strain stability and repeatability of a BCL3 resistance strain gage
[NASA-CR-187056] N91-19403
High temperature NASP engine seal development
[NASA-TM-103716] N91-19441
Effects of high temperature and humidity on mental state and metabolism N91-19571
Optically-ionized plasma recombination x ray lasers
[DE91-007261] N91-19898
Free energy simulation of grain boundary segregation the thermodynamics in Ni(3-x)Al(1+x)
[DE91-007473] N91-19928
Phase transitions and equation of state of CsI under high pressure and the development of a focusing system for x rays
[DE91-007646] N91-19930
Mutual influence of doping and oxidation in highly doped silicon
[ETN-91-98924] N91-19948
TEMPERATURE GRADIENTS
Special requirements in the design of a sensor test and integration laboratory N91-19141
The application of simulation model for the flow induced by air bubble plume in thermally stratified reservoirs
[DE91-003064] N91-19380
TEMPERATURE MEASUREMENT
In-space experiment on thermoacoustic convection heat transfer phenomenon-experiment definition
[NASA-CR-187070] N91-19378
TEMPERATURE MEASURING INSTRUMENTS
Air/sea temperature probe
[AD-D014674] N91-19397
TEMPERATURE PROBES
Air/sea temperature probe
[AD-D014674] N91-19397
TEMPERATURE PROFILES
Air/sea temperature probe
[AD-D014674] N91-19397
A flammability study of thin plastic film materials N91-20034
TEMPORAL DISTRIBUTION
Spatial and temporal variation in biomonitoring data
[DE91-007843] N91-19539
TEMPORAL RESOLUTION
Measurements with a 35 psec gate time microchannelplate camera
[DE91-006701] N91-19400
TENSILE PROPERTIES
High temperature tensile properties of nickel-base superalloys for intermediate heat exchangers of high temperature gas-cooled reactors
[DE91-744958] N91-19284
TENSILE STRENGTH
The 70 percent tungsten heavy alloys: Processing and properties
[DE91-008259] N91-19282
Thermal shock of fiber reinforced ceramic matrix composites
[NASA-TM-103777] N91-19295
TENSILE STRESS
Non-homogeneous bars under tension, pure bending, and temperature loads
[MBB-UD-0572-90-PUB] N91-19485

TENSILE TESTS
Bulging of fatigue cracks in a pressurized aircraft fuselage
[LR-647] N91-19094
Thermal shock of fiber reinforced ceramic matrix composites
[NASA-TM-103777] N91-19295
Bulging of fatigue cracks in a pressurized aircraft fuselage
[ETN-91-98927] N91-19489
TERMINOLOGY
NASA Thesaurus supplement: A four part cumulative supplement to the 1988 edition of the NASA Thesaurus (supplement 5)
[NASA-SP-7064-SUPPL-5] N91-19962
TERNARY ALLOYS
X ray determination of site occupation parameters in ordered ternaries Cu(Au(x)M(1-x))M = Ni,Pd
[DE91-007861] N91-19937
TEST CHAMBERS
A ground based module for experimentations of cultivations and recycling in a closed environment N91-19657
TEST EQUIPMENT
Characterization of devices, circuits, and high-temperature superconductor transmission lines by electro-optic testing
[NASA-CR-187950] N91-19343
TEST FACILITIES
Designing for explosive safety: The Explosive Components Facility at Sandia National Laboratories
[DE91-006432] N91-19103
The test facility requirements for the thermal vacuum thermal balance test of the Cosmic Background Explorer Observatory N91-19128
Optical testing cryogenic thermal vacuum facility N91-19137
Boeing infrared sensor (BIRS) calibration facility N91-19138
Infrared sensor test methodology and facilities N91-19139
Special requirements in the design of a sensor test and integration laboratory N91-19141
Non-linear generation of acoustic noise in the IAR spacecraft N91-19143
Detailed modal testing of a solid rocket motor using a portable test system N91-19144
Space simulation facilities providing a stable thermal vacuum facility N91-19150
Proposal for a conceptually new compact collecting optics for powerful light sources N91-19155
Results of scoping tests for open-cycle OTEC (Ocean Thermal Energy Conversion) components operating with seawater
[DE89-009514] N91-19501
Cells in space: Sounding rocket facilities for cell biology and biotechnology in microgravity N91-19661
Development of a miniature biology facility N91-19666
TETHERED SATELLITES
Magnetic cleanliness verification approach on tethered satellite N91-19158
TEXTILES
Load bearing connective damper
[AD-D014676] N91-19468
TEXTS
Improved syntactic disambiguation in the FASIT automatic indexing environment N91-19956
TEXTURES
Control of texture and defect structure for hot-filament-assisted CVD (Chemical Vapor Deposition) diamond Films
[DE91-008373] N91-19310
Texture and microstructure development in Al-2 percent Mg during high-temperature deformation
[DE91-007355] N91-19480
THALLIUM COMPOUNDS
Phase formation in the Tl-Ca-BaCu-O system
[DE91-008184] N91-19942
THEORETICAL PHYSICS
Computation and graphics in mathematical research
[DE91-007333] N91-19776
THERAPY
An introduction to biological dosimetry
[DE91-007125] N91-19698
THERMAL ANALYSIS
SCD1 thermal design and test result analysis N91-19130
Thermal balance testing of the Anik-E spacecraft N91-19131
The performance of multilayer insulation in a rapidly depressurizing environment N91-19133
Computational simulation of hot composites structures
[NASA-TM-103681] N91-19230
Probabilistic simulation of uncertainties in thermal structures
[NASA-TM-103680] N91-19472
THERMAL BUCKLING
Non-homogeneous bars under tension, pure bending, and temperature loads
[MBB-UD-0572-90-PUB] N91-19485
THERMAL CONDUCTIVITY
Superconducting instrumentation for critical He-4 measurements in space
[DE91-007894] N91-19408
Thermal conductivity of high-temperature superconductors in normal state N91-19818
Thermal insulation of a cryogenic tank for a space telescope using a pretensioned suspension of Fiber Reinforced Composite (FRC)
[MBB-UD-0571-90-PUB] N91-19981
THERMAL CONTROL COATINGS
Space environmental effects on spacecraft thermal control coatings N91-19148
THERMAL CYCLING TESTS
Thermal cycle testing of Space Station Freedom solar array blanket coupons N91-19216
Composite materials for space applications
[NASA-CR-187472] N91-19238
THERMAL ENERGY
Multi-dimensional modeling of a thermal energy storage canister
[NASA-TM-103731] N91-19177
The OAST space power program N91-19183
Thermal annealing of GaAs concentrator solar cells N91-19195
Finnigan ion trap mass spectrometer detection limits and thermal energy analyzer interface status report and present capabilities
[DE91-006220] N91-19254
Results of scoping tests for open-cycle OTEC (Ocean Thermal Energy Conversion) components operating with seawater
[DE89-009514] N91-19501
THERMAL ENVIRONMENTS
Techniques for hot structures testing
[NASA-TM-101727] N91-19080
THERMAL FATIGUE
Thermal/vacuum vs. thermal atmospheric testing of space flight electronic assemblies N91-19154
THERMAL INSTABILITY
Thermal instabilities in cooling flows: The evolution of nearly spherical perturbations
[MPE-PREPRINT-176] N91-19365
THERMAL INSULATION
Solar thermal vacuum tests of Magellan spacecraft N91-19127
The performance of multilayer insulation in a rapidly depressurizing environment N91-19133
Multipurpose hardened spacecraft insulation N91-19136
Thermal properties of polyisocyanurate foam board insulation blown with CFC-11 substitutes
[DE90-016047] N91-19240
Thermal insulation of a cryogenic tank for a space telescope using a pretensioned suspension of Fiber Reinforced Composite (FRC)
[MBB-UD-0571-90-PUB] N91-19981
THERMAL NEUTRONS
Exchange currents in low-energy nucleon capture by He3
[ETN-91-98917] N91-19855
THERMAL PROTECTION
Debris/ice/TPS assessment and photographic analysis for shuttle mission STS-35
[NASA-TM-103816] N91-19118
Composite flexible insulation for thermal protection of space vehicles
[NASA-TM-103836] N91-19304
Studies of cold protection diodes
[DE91-008203] N91-19863
THERMAL RADIATION
Analysis of spherical geometry finite element transport solutions in the thick diffusion limit
[DE91-007598] N91-19780
Even- and odd-parity finite-element transport solutions in the thick diffusion limit
[DE91-007618] N91-19781
THERMAL RESISTANCE
Experimental determination of satellite bolted joints thermal resistance N91-19157
THERMAL SHOCK
Thermal shock of fiber reinforced ceramic matrix composites
[NASA-TM-103777] N91-19295
THERMAL SIMULATION
Sixteenth Space Simulation Conference Confirming Spaceworthiness Into the Next Millennium
[NASA-CP-3096] N91-19126
A unique approach to space thermal simulation N91-19153
THERMAL STABILITY
Effect of fiber reinforcements on thermo-oxidative stability and mechanical properties of polymer matrix composites
[NASA-TM-103648] N91-19234
THERMAL STRESSES
Techniques for hot structures testing
[NASA-TM-101727] N91-19080
Special requirements in the design of a sensor test and integration laboratory N91-19141
Microtube strip heat exchanger
[DE91-005741] N91-19504
THERMAL VACUUM TESTS
Solar thermal vacuum tests of Magellan spacecraft N91-19127
The test facility requirements for the thermal vacuum thermal balance test of the Cosmic Background Explorer Observatory N91-19128
Thermal balance testing of the Anik-E spacecraft N91-19131
High vacuum facility for hydrazine thruster testing N91-19134
Optical testing cryogenic thermal vacuum facility N91-19137
Space simulation facilities providing a stable thermal vacuum facility N91-19150
The space simulation facilities at IAL SPACE N91-19151
A unique approach to space thermal simulation N91-19153
Thermal/vacuum vs. thermal atmospheric testing of space flight electronic assemblies N91-19154
Transfer orbit stage mechanisms thermal vacuum test N91-19161
Vibration and thermal vacuum qualification test results for a low-voltage tungsten-halogen light
[NASA-CR-187050] N91-19325
THERMODYNAMIC CYCLES
Loss analysis of the thermodynamic cycle of magnetic heat pumps
[DE91-007669] N91-19950
THERMODYNAMIC EFFICIENCY
Thermal-hydraulic model of a solid-oxide fuel cell
[DE91-006393] N91-19507
THERMODYNAMIC EQUILIBRIUM
Contributions to the Non Equilibrium Molecular Dynamics (NEMD) computer simulation for transport processes in simple fluids
[ETN-91-98921] N91-19393
Calculation of emission and absorption spectra of LTE plasma by the STA (Super Transition Array) method
[DE91-007617] N91-19900
THERMODYNAMIC PROPERTIES
Composite materials for space applications
[NASA-CR-187472] N91-19238
Ceramic Technology for Advanced Heat Engines project database
[DE91-007772] N91-19300
Atmospheric environment for space shuttle (STS-41) launch
[NASA-TM-103525] N91-19529
THERMODYNAMICS
Alkali metal corrosion of alumina: Thermodynamics, phase diagrams and testing
[ETN-91-98933] N91-19286
Application of thermal life prediction model to high-temperature aerospace alloys B1900+Hf and Haynes 188
[NASA-TM-4226] N91-19473
On the thermodynamics of stress rate in the evolution of back stress in viscoplasticity
[NASA-TM-103794] N91-19476
Free energy simulation of grain boundary segregation the thermodynamics in Ni(3-x)Al(1+x)
[DE91-007473] N91-19928
THERMOELASTICITY
Thermoelastic vibration test techniques
[NASA-TM-101742] N91-19083
THERMOELECTRIC GENERATORS
Radioisotope thermal photovoltaic application of the GaSb solar cell N91-19210
THERMOELECTRICITY
Potential health risks from postulated accidents involving the Pu-238 RTG (Radioisotope Thermoelectric Generator) on the Ulysses solar exploration mission
[DE91-007142] N91-19857
THERMOGRAVIMETRY
An outgassing model of non-metallic materials for the ascent of a Titan 4 launch vehicle N91-19132
THERMOHYDRAULICS
Thermal-hydraulic model of a solid-oxide fuel cell
[DE91-006393] N91-19507

Some neutronics and thermal-hydraulics codes for reactor analysis using personal computers
[DE91-006591] N91-19743
THERMONUCLEAR REACTIONS
Experimental study of external kink instabilities in the Columbia high beta tokamak
[DE91-008116] N91-19904
THERMOPHYSICAL PROPERTIES
Composite materials for space applications
[NASA-CR-187472] N91-19238
THESAURI
NASA Thesaurus supplement: A four part cumulative supplement to the 1988 edition of the NASA Thesaurus (supplement 5)
[NASA-SP-7064-SUPPL-5] N91-19962
THICKNESS
Spaceflight performance of several types of silicon solar cells on the LIPS 3 satellite N91-19213
THIN FILMS
Review of thin film solar cell technology and applications for ultra-light spacecraft solar arrays N91-19198
Tribological properties of Ag/Ti films on Al2O3 ceramic substrates
[NASA-TM-103784] N91-19224
XANES investigation of pH effects during cerium-sealing of anodized aluminum
[DE91-008101] N91-19302
Application of functional gradient materials in the aerospace industry
[MBB-Z-0320-90-PUB] N91-19311
Photoelectron diffraction of magnetic ultrathin films: Fe/Cu(001)
[DE91-007254] N91-19924
Thin film amorphous electrolytes: The Li2O-SiO2-P2O5 system
[DE91-007272] N91-19925
The characterization of interface roughness and other defects in multilayers by x ray scattering
[DE91-007558] N91-19929
Thin film reactions on alloy semiconductor substrates
[DE91-007651] N91-19931
Some roles for TEM in the development of new materials
[DE91-007742] N91-19933
Plasma, photon, and beam synthesis of diamond films and multilayered structures
[DE91-007934] N91-19938
A flammability study of thin plastic film materials N91-20034
THIN PLATES
Finite strip elements in thin plate buckling analysis
[LR-642] N91-19493
THOMAS-FERMI MODEL
Baroelectric effect in the present of gravitational forces
[DE91-615469] N91-19559
THOMSON SCATTERING
UV Thomson scattering from x ray laser plasmas
[DE91-007347] N91-19895
THREE DIMENSIONAL BODIES
Task reports on developing techniques for scattering by 3D composite structures and to generate new solutions in diffraction theory using higher order boundary conditions
[NASA-CR-188057] N91-19305
A finite element conjugate gradient FFT method for scattering N91-19306
A rigid body model and decoupled control architecture for two manipulators holding a complex object
[DE91-007827] N91-19444
THREE DIMENSIONAL BOUNDARY LAYER
The effect of small streamwise velocity distortion on the boundary layer flow over a thin flat plate with application to boundary layer stability theory
[NASA-TM-103668] N91-19372
Critical-layer nonlinearity in the resonance growth of three-dimensional waves in boundary layers
[NASA-TM-103639] N91-19373
THREE DIMENSIONAL FLOW
Summary of in-flight flow visualization obtained from the NASA high alpha research vehicle
[NASA-TM-101734] N91-19055
Three-component laser anemometer measurement systems
[NASA-TP-3080] N91-19057
Calculations of separated 3-D flows with a pressure-staggered Navier-Stokes equations solver
[NASA-CR-187065] N91-19367
Laws of heat transfer in three-dimensional viscous shock layer of stream flowing past blunt bodies at some angles of attack and glide N91-19801
THREE DIMENSIONAL MODELS
Regional Oxidant Model Multi-Processor (ROMMP)
[PB91-131680] N91-19547
Techniques for interactive 3-D scientific visualization
[DE91-007122] N91-19745
THROTTLING
Pneumatic launcher
[AD-D014658] N91-19116
THRUST DISTRIBUTION
A simple dynamic engine model for use in a real-time aircraft simulation with thrust vectoring
[NASA-TM-4240] N91-19079
THRUST VECTOR CONTROL
A simple dynamic engine model for use in a real-time aircraft simulation with thrust vectoring
[NASA-TM-4240] N91-19079
TIBIA
Altered cartilage differentiation in tibial epiphyseal plates of Cosmos rats N91-19628
TILT ROTOR AIRCRAFT
Propulsion system concept for the Eurofar tilt rotor aircraft
[MBB-UD-0573-90-PUB] N91-19084
The selection of convertible engines with current gas generator technology for high speed rotorcraft
[NASA-TM-103774] N91-19097
TIME
Topological models for space and time
[OUEL-1860/90] N91-19774
TIME DEPENDENCE
Time-dependent multimode simulation of gyrotron oscillators
[AD-A229861] N91-19413
TIME DIVISION MULTIPLE ACCESS
Pulsed response of a traveling-wave tube
[NASA-TM-103672] N91-19348
TIME FUNCTIONS
The selection of window functions for the calculation of time domain averages on the vibration of the individual gears in an epicyclic gearbox
[OUEL-1818/90] N91-19457
TIME MARCHING
Cascade flutter analysis with transient response aerodynamics
[NASA-TM-103746] N91-19475
TIME RESPONSE
Pulsed response of a traveling-wave tube
[NASA-TM-103672] N91-19348
Traveling time effects in a channel flow
[MPIS-10/1990] N91-19384
TIME SERIES ANALYSIS
Statistical examination of climatological data relevant to global temperature variation
[DE91-007881] N91-19540
TIME TEMPERATURE PARAMETER
A study on prediction of life due to creep behavior in CF/EPOXY and CF/PEEK laminates N91-19226
Hot isostatic pressing of high performance glass-ceramic to nickel- and iron-based metal components
[DE91-008130] N91-19281
TIN ALLOYS
Indium tin oxide for solid-state image sensors
[ETN-91-98932] N91-19949
TIN OXIDES
Recent advances in the ITO/InP solar cell N91-19202
Indium tin oxide for solid-state image sensors
[ETN-91-98932] N91-19949
TISSUES (BIOLOGY)
Plant biotechnology in space: Facts and speculations N91-19664
Plant development in space: Observations on root formation and growth N91-19670
TITAN LAUNCH VEHICLES
An outgassing model of non-metallic materials for the ascent of a Titan 4 launch vehicle N91-19132
TITANIUM
Passive mode locking in optically pumped Al2O3:Ti(3+) laser N91-19803
TITANIUM BORIDES
Low-density, high-strength intermetallic matrix composites by XD (trademark) synthesis
[NASA-TM-103724] N91-19233
TITANIUM CARBIDES
Instellar grains within interstellar grains N91-19998
TITANIUM COMPOUNDS
METCAN updates for high temperature composite behavior: Simulation/verification
[NASA-TM-103682] N91-19229
TITANIUM OXIDES
Surface chemistry at semiconductor-electrolyte interfaces
[DE91-005915] N91-19920
TITRATION
Low level vapor verification of monomethyl hydrazine N91-20032
TOKAMAK DEVICES
Energy sciences supercomputing 1990
[DE91-007188] N91-19740
Plasma boundary experiments on D3-D tokamak
[DE91-002429] N91-19881
He-like spectra through charge exchange processes in tokamak plasmas
[NIFS-69] N91-19894
US-Japan workshops: Q-111, Development of Plasma Facing Components and Materials for Next Large Fusion Devices, and Q-112, Vacuum and First Wall Technology for Fusion Devices
[DE91-006879] N91-19896
A method for determining poloidal coil configurations for tokamak devices
[DE91-007940] N91-19903
Experimental study of external kink instabilities in the Columbia high beta tokamak
[DE91-008116] N91-19904
Tokamak ignition projections from dimensionally similar discharges
[DE91-008195] N91-19908
Introduction to fusion
[DE91-744831] N91-19912
Effects of pressure profile and plasma shaping on the n=1 internal kink mode in JT-60/JT-60U pellet fuelled plasmas
[DE91-744965] N91-19914
TOLLMIEN-SCHLICHTING WAVES
A finite Reynolds number approach for the prediction of boundary layer receptivity in localized regions
[NASA-TM-102781] N91-19061
The effect of small streamwise velocity distortion on the boundary layer flow over a thin flat plate with application to boundary layer stability theory
[NASA-TM-103668] N91-19372
TOMOGRAPHY
Three-dimensional computed tomography from interferometric measurements within a narrow cone of views
[NASA-TM-103257] N91-19404
Lecture notes on nonlinear inversion and tomography
[DE91-008238] N91-19558
TOPOGRAPHY
An evaluation of co-planar lineament analysis and some thoughts on using surface geological data to predict sub-surface geology
[DE90-009687] N91-19556
TOPOLOGY
Efficient connecting networks using directed links
[ETN-91-98855] N91-19762
TOROIDAL DISCHARGE
Tokamak ignition projections from dimensionally similar discharges
[DE91-008195] N91-19908
TOROIDAL PLASMAS
A method for determining poloidal coil configurations for tokamak devices
[DE91-007940] N91-19903
Tokamak ignition projections from dimensionally similar discharges
[DE91-008195] N91-19908
TOROIDS
Energy sciences supercomputing 1990
[DE91-007188] N91-19740
TORSION
A flight-dynamic helicopter mathematical model with a single flap-lag-torsion main rotor
[NASA-TM-102267] N91-19041
Control and mechanism interaction for ground-based testing of space structures N91-19125
Load bearing connective damper
[AD-D014676] N91-19468
TORUSES
Invariant tori of the Poincare return map as solutions of functional difference equations
[DE91-007423] N91-19777
Computation of invariant tori in 2 (1/2) degrees of freedom
[DE91-007424] N91-19778
TOTAL OZONE MAPPING SPECTROMETER
Initial estimate of NOAA-9 SBUV/2 total ozone drift: Based on comparison with re-calibrated TOMS measurements and pair justification of SBUV/2 N91-19523
Ozone measurements from the NOAA-9 and the Nimbus-7 satellites: Implications of short and long term variabilities N91-19527
TOUCH
The reference systems for tactile perception and for the orientation with respect to body N91-19691
TOUGHNESS
Effects of irradiation on crack-arrest toughness of two high-copper welds
[DE91-007189] N91-19270
TOXIC HAZARDS
Low level vapor verification of monomethyl hydrazine N91-20032
TOXICITY
Spatial and temporal variation in biomonitoring data
[DE91-007843] N91-19539

An introduction to biological dosimetry
[DE91-007125] N91-19698

TOXINS AND ANTITOXINS
An introduction to biological dosimetry
[DE91-007125] N91-19698

TRACE ELEMENTS
Identification of flow and volume parameters in multizone systems using a single gas tracer technique
[DE91-006894] N91-19368
Evaluation of significant anthropogenic sources of radiatively important trace gases
[PB91-127753] N91-19545
Cosmic dust: Laboratory analyses of extremely small particles N91-20013

TRACKING (POSITION)
Simultaneous tracking of flagellates in real time by image analysis N91-19677

TRADEOFFS
Towards practical control design using neural computation
[NASA-TM-103785] N91-19766

TRAINING DEVICES
Weightlessness countermeasures and human physiology in space: A potential conflict N91-19695

TRAJECTORY CONTROL
Minimum-time trajectory control of a two-link flexible robotic manipulator
[DE91-001261] N91-19448
Visual navigation around curved obstacles
[OUEL-1861/90] N91-19458
Practical path planning among movable obstacles
[DE91-000034] N91-19768
Navigation of a car-like mobile robot using a decomposition of the environment in convex cells
[DE91-000709] N91-19769

TRAJECTORY PLANNING
Practical path planning among movable obstacles
[DE91-000034] N91-19768
Navigation of a car-like mobile robot using a decomposition of the environment in convex cells
[DE91-000709] N91-19769

TRANSDUCERS
Air/sea temperature probe
[AD-D014674] N91-19397
Rotating pressure measurement system using an on board calibration standard
[NASA-TM-103676] N91-19401

TRANSFORMATIONS (MATHEMATICS)
Simple object recognition by neural networks: Application of the Hough transform
[RR-410] N91-19761
Spectrum transformation for divergent iterations
[NASA-TM-103745] N91-19786
Approximation properties of wavelet transforms
[ETN-91-98922] N91-19799

TRANSISTOR AMPLIFIERS
Development of components and subsystems for low noise receivers at micro- and millimeter waves
[S-187] N91-19363

TRANSITION METALS
Late transition metal (mu)-oxo and (mu)-imido complexes
[DE91-005349] N91-19267
Chemical activation of molecules by metals: Experimental studies of electron distributions and bonding
[DE91-007695] N91-19275
Synthesis and structures of metal chalcogenide precursors
[NASA-TM-103665] N91-19296
Atomic beam studies of the interaction of hydrogen with transition metal surfaces
[DE91-007938] N91-19841

TRANSITION TEMPERATURE
The apparent strain stability and repeatability of a BCL3 resistance strain gage
[NASA-CR-187056] N91-19403
Thermal conductivity of high-temperature superconductors in normal state N91-19818

TRANSMISSION LINES
Coplanar waveguide EEsoF MICAD macros make circuit layout easy
[NASA-TM-103272] N91-19332
Reduction of low energy components in pulse ion beam N91-19889

TRANSMISSOMETERS
Data acquisition and analysis on the two-color laser transmissometer system
[DE91-007235] N91-19420

TRANSMITTANCE
Wire-free arming system for an aircraft-delivered bomb
[AD-D014611] N91-19076
Simulation of Martian dust accumulation on surfaces N91-19160

TRANSMITTERS
The provision of circuits to outside broadcast locations using spectrum within the UHF broadcasting bands
[BBC-RD-1990/12] N91-19329

TRANSONIC FLOW
An experimental study of the turbulent boundary layer on a transport wing in subsonic and transonic flow
[NASA-TM-102206] N91-19062
Result of ONERA standard model test in 2m x 2m transonic wind tunnel
[DE91-750115] N91-19066

TRANSONIC WIND TUNNELS
Result of ONERA standard model test in 2m x 2m transonic wind tunnel
[DE91-750115] N91-19066

TRANSPORT AIRCRAFT
Integrated inertial/GPS N91-19032

TRANSPORT PROPERTIES
Contributions to the Non Equilibrium Molecular Dynamics (NEMD) computer simulation for transport processes in simple fluids
[ETN-91-98921] N91-19393
Outer continental shelf environmental assessment program, volume 70
[PB91-129288] N91-19548
Tokamak ignition projections from dimensionally similar discharges
[DE91-008195] N91-19908

TRANSPORT THEORY
Plasma boundary experiments on D3-D tokamak
[DE91-002429] N91-19881

TRANSPORT VEHICLES
Solar electric propulsion for Mars transport vehicles
[NASA-TM-103234] N91-19178

TRAPPED PARTICLES
Review of recent stellarator results in the USA, the USSR, and Japan
[DE91-007798] N91-19901

TRAVELING SALESMAN PROBLEM
The cost-constrained traveling salesman problem
[DE91-004943] N91-19775

TRAVELING WAVE TUBES
Pulsed response of a traveling-wave tube
[NASA-TM-103672] N91-19348

TREMORS
Is physiological tremor (microvibration) influenced by microgravity N91-19595

TRENDS
Oxygen-enriched diesel engine performance: A comparison of analytical and experimental results
[DE91-006491] N91-19440
Umkehr work N91-19522
Calibration of long term satellite ozone data sets using the space shuttle N91-19524

TRIBOLOGY
Tribological properties of Ag/Ti films on Al2O3 ceramic substrates
[NASA-TM-103784] N91-19224
Excimer laser surface processing for tribological applications in metals and ceramics
[DE91-002324] N91-19428
Considerations relating to pulsed-beam modification of materials
[DE91-006771] N91-19922

TRITIUM
Florida radioluminescent taxiway light development program
[DE91-005650] N91-19104
Effects of radiolytic tritium decay on the thermodynamic behavior of LaNi(4.25)Al(0.75) tritides
[DE91-007961] N91-19277
Radioluminescent polymer lights
[DE91-005521] N91-19290
Investigation of condensed matter fusion
[DE91-007246] N91-19923

TROPOSPHERE
Monitoring the response of the upper troposphere/lower stratosphere to a greenhouse gas scenario
[DE91-007976] N91-19541

TRUCKS
Exhaust emissions from heavy duty vehicles
[DE91-006798] N91-19531

TRUSSES
Comparative morphology of configurations with reduced part count derived from the octahedral-tetrahedral truss
[NASA-TM-102768] N91-19168
Modal identification of a deployable space truss
[NASA-TM-102720] N91-19474

TUMORS
Genetic risk and physiological stress induced by heavy ions N91-19680

TUNABLE LASERS
Hole coupling resonator for free electron lasers
[DE91-007745] N91-19426
Passive mode locking in optically pumped Al2O3:Ti(3+) laser N91-19803

TUNGSTEN ALLOYS
The 70 percent tungsten heavy alloys: Processing and properties
[DE91-008259] N91-19282

TUNING
Modeling a ferrite-tuned RF cavity
[DE91-008235] N91-19356

TUNNEL DIODES
Classical and quantum charge dynamics in small tunnel junctions
[ETN-91-98916] N91-19947

TURBINE BLADES
Investigation of ATP blades, part 3
[DE91-750104] N91-19105
Heat transfer in rotating serpentine passages with trips normal to the flow
[NASA-TM-103758] N91-19443

TURBINE PUMPS
Orbital transfer vehicle oxygen turbopump technology. Volume 1: Design, fabrication, and hydrostatic bearing testing
[NASA-CR-185175] N91-19174
Ceramic composites for rocket engine turbines
[NASA-TM-103743] N91-19235

TURBOCOMPRESSORS
A modelling of unsteady air flow in the resonance charging system of high speed diesel engines
[ACTA-POLYTEC-SCAND-ME-97] N91-19454

TURBOFAN ENGINES
A simple dynamic engine model for use in a real-time aircraft simulation with thrust vectoring
[NASA-TM-4240] N91-19079
A proposed Kalman filter algorithm for estimation of unmeasured output variables for an F100 turbofan engine
[NASA-TM-4234] N91-19099

TURBOFANS
Improved visualization of flow field measurements
[NASA-TM-103679] N91-19044

TURBOGENERATORS
Elementary considerations on the gas dynamic design parameters of a MHD Faraday generator in relation to a gas turbine cycle
[LR-564] N91-19456

TURBOMACHINERY
Three-component laser anemometer measurement systems
[NASA-TP-3080] N91-19057
The effect of steady aerodynamic loading on the flutter stability of turbomachinery blading
[NASA-CR-187055] N91-19479

TURBOPROP AIRCRAFT
Unified aeroacoustics analysis for high speed turboprop aerodynamics and noise. Volume 1: Development of theory for blade loading, wakes, and noise
[NASA-CR-4329] N91-19049

TURBULENCE
State estimation applications in aircraft flight-data analysis: A user's manual for SMACK
[NASA-RP-1252] N91-19082
Filtering analysis of a direct numerical simulation of the turbulent Rayleigh-Benard problem
[NASA-CR-187488] N91-19366
Wavelets and turbulence on the sea surface
[AD-A229862] N91-19565
Reflections on some problems concerning the role of superfluid turbulence in the propagation of second-sound pulses in He 2
[MPIS-8/1990] N91-19827

TURBULENT BOUNDARY LAYER
An experimental study of the turbulent boundary layer on a transport wing in subsonic and transonic flow
[NASA-TM-102206] N91-19062
Turbulent boundary layer separation over a rearward facing ramp and its control through mechanical excitation
[NASA-TM-103702] N91-19370

TURBULENT FLOW
Multigrid solution of compressible turbulent flow on unstructured meshes using a two-equation model
[NASA-CR-187513] N91-19043
Basic research model of natural gas combustion in turbulent flow
[PB91-130260] N91-19264
Filtering analysis of a direct numerical simulation of the turbulent Rayleigh-Benard problem
[NASA-CR-187488] N91-19366
A 2-D oscillating flow analysis in Stirling engine heat exchangers
[NASA-TM-103781] N91-19375
Systems near the onset and in the well-developed regimes of turbulence
[DE91-008148] N91-19382

TURBULENT MIXING
Fluid mixing device having a conical inlet and a noncircular outlet
[AD-D014708] N91-19364
TWO DIMENSIONAL FLOW
Two-dimensional non-reacting jet-gas mixing in an MHD (magnetohydrodynamic) second stage combustor
[DE91-006015] N91-19252
A 2-D oscillating flow analysis in Stirling engine heat exchangers
[NASA-TM-103781] N91-19375
A numerical method for solving steady 2D and axisymmetrical viscoelastic flow problems with an application to inertia effects in contraction flows
[MEMT-11] N91-19394

U

U.S.S.R.
JPRS report: Science and technology. USSR: Life sciences
[JPRS-ULS-91-001] N91-19567
USSR Space Life Sciences Digest. Index to issues 26-29
[NASA-CR-3922(35)] N91-19700
JPRS report: Science and technology. USSR: Physics and mathematics
[JPRS-UPM-90-004] N91-19800
ULTRASHORT PULSED LASERS
Intracavity second-harmonic generation by laser with optical delay line and mode locking N91-19808
Breakup of femtosecond pulses during amplification in Er(3+)-doped single-mode optical fibers N91-19812
Coherent effects in generation of ultrashort light pulses by semiconductor injection laser N91-19820
ULTRASONIC FLAW DETECTION
Mechanical behavior of a ceramic matrix composite material
[NASA-CR-187072] N91-19461
ULTRASONIC RADIATION
Assessment of tamper-revealing ceramic seals
[DE91-007793] N91-19301
ULTRASONIC TESTS
Ultrasound investigation of the cardiovascular system during the 25 days French-Soviet spaceflight (26 November - 21 December 1988) N91-19577
ULTRASONICS
Research on advanced NDE methods for aerospace structures
[AD-A226858] N91-19460
Acoustic stabilization of laser beam wavefront in nonhomogeneous gaseous medium N91-19802
Ultrasonic investigations on superfluid He-3-A and He-3-B
[ISBN-952-90-2241-7] N91-19830
ULTRAVIOLET LASERS
Excimer laser surface processing for tribological applications in metals and ceramics
[DE91-002324] N91-19428
ULTRAVIOLET RADIATION
Low Earth orbital atomic oxygen and ultraviolet radiation effects on polymers
[NASA-TM-103711] N91-19294
A status report on the analysis of the NOAA-9 SBUV/2 sweep mode solar irradiance data N91-19518
Analysis of SBUV/2 measurements of solar UV irradiance variations N91-19526
Mutation induction in dried yeast cells after irradiation with selected UVC- and UVB- wavelengths compared to simulated sunlight N91-19686
The advanced light source: A new tool for research in atomic physics
[DE91-007739] N91-19861
UV Thomson scattering from x ray laser plasmas
[DE91-007347] N91-19895
ULTRAVIOLET SPECTROMETERS
NOAA-9 Solar Backscatter Ultraviolet (SBUV/2) Instrument and Derived Ozone Data: Review
[NOAA-TR-NESDIS-53] N91-19514
An assessment of instrument performance for the NOAA-9 SBUV/2 N91-19516
SBUV/2 in-orbit performance N91-19517
A status report on the analysis of the NOAA-9 SBUV/2 sweep mode solar irradiance data N91-19518
NOAA-9 SBUV/2 ozone sounding accuracy: Presentation summary N91-19519
A technique for directly comparing radiances from two satellites N91-19520
SBUV/2 comparisons with ground-based and SBUV spacecraft data N91-19521
Initial estimate of NOAA-9 SBUV/2 total ozone drift: Based on comparison with re-calibrated TOMS measurements and pair justification of SBUV/2 N91-19523
Analysis of SBUV/2 measurements of solar UV irradiance variations N91-19526
ULYSSES MISSION
Potential health risks from postulated accidents involving the Pu-238 RTG (Radioisotope Thermoelectric Generator) on the Ulysses solar exploration mission
[DE91-007142] N91-19857
UMKEHR EFFECT
Umkehr work N91-19522
Total ozone, ozonesonde, and Umkehr observations for satelliite ozone data validation N91-19525
UNITED STATES
World weather watch: Regional association 4: Hurricane operational plan, supplement 2
[WMO-524-SUPPL-2] N91-19563
UNIVERSE
High energy physics and cosmology
[DE91-007369] N91-19859
Observational relations in model universes dominated by domain-wall-like matter
[DE91-744969] N91-19988
Quasi-nonlinear theory of cosmological self-gravitating systems
[DE91-744971] N91-19989
Statistics of peaks in cosmological nonlinear density fields
[DE91-744972] N91-19990
How many times do we have in quantum gravity
[DE91-744973] N91-19991
Gravitational lens effect of wall-like objects and its cosmological implications
[DE91-744976] N91-19992
UNIVERSITY PROGRAM
Joint University Program for Air Transportation Research, 1989-1990
[NASA-CP-3095] N91-19024
Investigation of air transportation technology at Ohio University, 1989-1990 N91-19028
Dedication of National Institute for Aviation Research
[NIAR-90-21] N91-19040
Computation and graphics in mathematical research
[DE91-007333] N91-19776
Research reports: 1990 NASA/ASEE Summer Faculty Fellowship Program
[NASA-CR-187638] N91-20022
UNSTEADY AERODYNAMICS
Acoustic radiation from lifting airfoils in compressible subsonic flow
[NASA-TM-103650] N91-19053
Wind tunnel wall effects in a linear oscillating cascade
[NASA-TM-103690] N91-19098
The effect of steady aerodynamic loading on the flutter stability of turbomachinery blading
[NASA-CR-187055] N91-19479
UNSTEADY FLOW
Summary of in-flight flow visualization obtained from the NASA high alpha research vehicle
[NASA-TM-101734] N91-19055
Notes on the unsteady rectilinear motion of a perfect gas. 10: On the influence of gravity upon the expansion of an ideal gas with gamma = 3
[LR-640] N91-19395
A modelling of unsteady air flow in the resonance charging system of high speed diesel engines
[ACTA-POLYTEC-SCAND-ME-97] N91-19454
UPPER ATMOSPHERE
Space Vehicle Flight Mechanics
[AGARD-AR-294] N91-19124
UPPER STAGE ROCKET ENGINES
Advanced chemical propulsion at NASA Lewis: Metallized and high energy density propellants
[NASA-TM-103771] N91-19175
URANUS (PLANET)
Effects of a giant impact on Uranus N91-20012
URANUS SATELLITES
Effects of a giant impact on Uranus N91-20012
URINE
Physiology of body water and salt regulation. Part 1: Circadian rhythms of endocrine systems and urinary electrolyte excretion in humans N91-19592
Physiology of body water and salt regulation. Part 2: Volume and electrolyte homeostasis after an acute saline infusion N91-19593
Volume regulating hormones, fluid and electrolyte modifications during the Aragatz Mission (Mir station) N91-19689
USER MANUALS (COMPUTER PROGRAMS)
State estimation applications in aircraft flight-data analysis: A user's manual for SMACK
[NASA-RP-1252] N91-19082
ETARA PC version 3.3 user's guide: Reliability, availability, maintainability simulation model
[NASA-TM-103751] N91-19462
A valiant little terminal: A VLT user's manual
[DE91-007295] N91-19719
C-statistic fitting routines: User's manual and reference guide
[NASA-CR-187992] N91-19736
Anastasia: A solid model based 3D finite difference mesh generator
[DE91-007621] N91-19783
USER REQUIREMENTS
Mission operations directorate: Facility and support systems division N91-19726

V

VACUUM
Symmetries on the space of (2,2) superstring vacua and automorphism groups of Calabi-Yau manifolds
[DE91-008218] N91-19951
VACUUM CHAMBERS
Special requirements in the design of a sensor test and integration laboratory N91-19141
Experimental determination of satellite bolted joints thermal resistance N91-19157
US-Japan workshops: Q-111, Development of Plasma Facing Components and Materials for Next Large Fusion Devices, and Q-112, Vacuum and First Wall Technology for Fusion Devices
[DE91-006879] N91-19896
VACUUM PUMPS
Gas entrapment and evolution in aluminium alloys produced by powder metallurgy
[ETN-91-98918] N91-19285
VALENCE
Electronic charge density and bonding in alpha-boron: An experimental-theoretical comparison
[DE91-006629] N91-19936
VALVES
Pneumatic launcher
[AD-D014658] N91-19116
VANADIUM
Reactivity of pi-complexes of Ti, V, and Nb towards dithioacetic acid: Synthesis and structure of novel metal sulfur-containing complexes
[NASA-TM-103666] N91-19256
VANADIUM ALLOYS
Internal friction peaks due to interstitials in bcc alloys
[DE91-007411] N91-19272
VAPOR DEPOSITION
Control of texture and defect structure for hot-filament-assisted CVD (Chemical Vapor Deposition) diamond Films
[DE91-008373] N91-19310
VAPORS
Growth kinetics of physical vapor transport processes: Crystal growth of the optoelectronic material mercurous chloride
[NASA-TM-103788] N91-19320
Low level vapor verification of monomethyl hydrazine N91-20032
VARIATIONAL PRINCIPLES
Theoretical investigation of phase stability in non-magnetic Fe-V substitutional alloys
[DE91-006711] N91-19268
A variational approach to magneto-elastic buckling problems
[ETN-91-98929] N91-19338
VASOCONSTRICTION
Carotid-cardiac baroreflex influence on forearm vascular resistance during low level LBNP N91-20030
VECTOR ANALYSIS
Optimal observation directions for estimating a vector
[PREPRINT-1285] N91-19796
VECTOR PROCESSING (COMPUTERS)
On the vectorization and parallelization of the shooting method using the convex C-240
[LR-639] N91-19491
VEGETATION GROWTH
Effects of soil and canopy characteristics on microwave backscattering of vegetation
[NASA-CR-188022] N91-19497
Analysis of high frequency surface-induced concentration fluctuations
[DE91-007561] N91-19538
Plastids and gravity perception N91-19668
Plant development in space: Observations on root formation and growth N91-19670
Plant growth under microgravity conditions: Experiments and problems N91-19671
VELOCITY COUPLING
A novel potential/viscous flow coupling technique for computing helicopter flow fields
[NASA-CR-177568] N91-19060
VELOCITY DISTRIBUTION
A novel potential/viscous flow coupling technique for computing helicopter flow fields
[NASA-CR-177568] N91-19060

LOX/hydrogen coaxial injector atomization test program
[NASA-CR-187037] N91-19117
Calculations of separated 3-D flows with a pressure-staggered Navier-Stokes equations solver
[NASA-CR-187065] N91-19367
Development of a perturbation generator for vortex stability studies
[NASA-CR-188051] N91-19379
Laser Doppler velocimetry for continuous flow solar-pumped iodine laser system
[NASA-TM-104029] N91-19415

VELOCITY MODULATION
Calculation of pulsating liquid free jets
[MPIS-15/1990] N91-19385

VENTS
Experimental investigation of porous-floor effects on cavity flow fields at supersonic speeds
[NASA-TP-3032] N91-19042
Flow fields of low pressure vent exhausts N91-19135

VENUS SURFACE
Magellan: Preliminary description of Venus surface geologic units N91-20011

VERTEBRATES
Does gravity play a role in the morphological development and function of the gravity sensory organ of vertebrates. DLR contribution to the D-2 project graviperception and neuronal plasticity, its technical realization and experimental execution N91-19635

VERTICAL MOTION SIMULATORS
Vertically moving visual stimuli and vertical vection: A tool against space motion sickness N91-19606

VERTICAL ORIENTATION
Determinants of spatial orientation in weightlessness N91-19605

VERTICAL PERCEPTION
Determinants of spatial orientation in weightlessness N91-19605

VERY LARGE SCALE INTEGRATION
On the optimality of code options for a universal noiseless coder
[NASA-CR-187973] N91-19734

VERY LOW FREQUENCIES
Gamma ray astronomy
[NASA-CR-188031] N91-19980

VESTIBULAR NYSTAGMUS
Measurement of eye movements in space-related research environments N91-19591
Vestibular tests on UK astronaut candidates for an Anglo/Russian space flight (Juno Mission) N91-19613

VESTIBULAR TESTS
Vestibular function in altered states of gravity N91-19579
Ocular roll under changing z-axis acceleration and neck position N91-19580
Vestibular tests on UK astronaut candidates for an Anglo/Russian space flight (Juno Mission) N91-19613
Human and animal results on vestibular research in space: VERIS N91-19642
Relation between perception of vertical axis rotation and vestibulo-ocular reflex symmetry
[NASA-CR-187997] N91-19710

VIABILITY
Viability study of photovoltaic systems added to terrestrial electric vehicles
[DE91-007689] N91-19355

VIBRATION
Unified aeroacoustics analysis for high speed turboprop aerodynamics and noise. Volume 1: Development of theory for blade loading, wakes, and noise
[NASA-CR-4329] N91-19049
Monitoring techniques for the X-29A aircraft's high-speed rotating power takeoff shaft
[NASA-TM-101731] N91-19081
A study of carbon steel corrosion inhibition by phosphate ions and by an organic buffer using a scanning vibrating electrode
[DE91-008103] N91-19280
Development of a vibration isolation prototype system for microgravity space experiments
[NASA-TM-103664] N91-19324
Experimental studies on a nonlinear hydroelastic vibration of circular cylindrical tanks
[LRT-WE-9-FB-10(1990)] N91-19387
Vibration transmission through rolling element bearings in geared rotor systems
[NASA-CR-4334] N91-19435
The selection of window functions for the calculation of time domain averages on the vibration of the individual gears in an epicyclic gearbox
[OUEL-1818/90] N91-19457
Time-frequency domain analysis of vibration signals for machinery diagnostics. 1: Introduction to the Wigner-Ville distribution
[OUEL-1859/90] N91-19495
Is physiological tremor (microvibration) influenced by microgravity N91-19595

VIBRATION EFFECTS
Experimental studies on a nonlinear hydroelastic vibration of circular cylindrical tanks
[LRT-WE-9-FB-10(1990)] N91-19387

VIBRATION ISOLATORS
Space simulation facilities providing a stable thermal vacuum facility N91-19150
Development of a vibration isolation prototype system for microgravity space experiments
[NASA-TM-103664] N91-19324
Load bearing connective damper
[AD-D014676] N91-19468
Computational comparison of efficacies of aeolian vibration damping devices for multiconductor overhead power lines
[BU-411] N91-19487

VIBRATION MODE
Thermoelastic vibration test techniques
[NASA-TM-101742] N91-19083
Modal identification of a deployable space truss
[NASA-TM-102720] N91-19474

VIBRATION TESTS
Thermoelastic vibration test techniques
[NASA-TM-101742] N91-19083
Vibration and thermal vacuum qualification test results for a low-voltage tungsten-halogen light
[NASA-CR-187050] N91-19325
Liquid sloshing in cargo tanks. Liquid slosh loading in slack ship tanks: Forces on internal structure and pressures
[PB91-129262] N91-19383
Experimental studies on a nonlinear hydroelastic vibration of circular cylindrical tanks
[LRT-WE-9-FB-10(1990)] N91-19387

VIBRATORY LOADS
Introduction of the M-85 high-speed rotorcraft concept
[NASA-TM-102871] N91-19078

VIDEO EQUIPMENT
Measurement of eye movements in space-related research environments N91-19591
Computation and graphics in mathematical research
[DE91-007333] N91-19776

VIRULENCE
Research in radiobiology: Work in progress in immunobiology of experimental host-tumor relationships
[DE91-007936] N91-19705

VIRUSES
Characterization of a defective interfering RNA that contains a mosaic of a plant viral genome
[DE91-007897] N91-19702
Characterization of a defective interfering RNA that contains a mosaic of a plant viral genome
[DE91-007898] N91-19703

VISCOELASTIC DAMPING
Load bearing connective damper
[AD-D014676] N91-19468

VISCOELASTICITY
A numerical method for solving steady 2D and axisymmetrical viscoelastic flow problems with an application to inertia effects in contraction flows
[MEMT-11] N91-19394

VISCOPLASTICITY
Application of thermal life prediction model to high-temperature aerospace alloys B1900+Hf and Haynes 188
[NASA-TM-4226] N91-19473
On the thermodynamics of stress rate in the evolution of back stress in viscoplasticity
[NASA-TM-103794] N91-19476

VISCOUS FLOW
A novel potential/viscous flow coupling technique for computing helicopter flow fields
[NASA-CR-177568] N91-19060
Laws of heat transfer in three-dimensional viscous shock layer of stream flowing past blunt bodies at some angles of attack and glide N91-19801

VISCOUS FLUIDS
Response of a differently axially excited viscous liquid layer in zero-gravity
[LRT-WE-9-FB-12(1990)] N91-19389
Response of a viscous liquid layer to pitch- and roll-excitation in zero-gravity environment
[LRT-WE-9-FB-13(1990)] N91-19390

VISIBLE SPECTRUM
NO2 absorption cross-section in the 440 to 460 nm region at 298 and 220 K
[NOTA-INTERNA-964] N91-19550
He-Ne laser emitting five lines simultaneously N91-19813

VISION
Mental rotation of three-dimensional shapes in microgravity N91-19694

VISUAL AIDS
Real-time application of advanced three-dimensional graphic techniques for research aircraft simulation
[NASA-TM-101730] N91-19742

VISUAL PERCEPTION
Visual navigation around curved obstacles
[OUEL-1861/90] N91-19458
Relation between perception of vertical axis rotation and vestibulo-ocular reflex symmetry
[NASA-CR-187997] N91-19710

VISUAL STIMULI
Vertically moving visual stimuli and vertical vection: A tool against space motion sickness N91-19606

VLASOV EQUATIONS
Action principles for the Vlasov equation: Four old, one new
[DE91-008177] N91-19787

VOIDS
The full-scale process and design changes for elimination of insulation edge separations and voids in tang flap area
[NASA-CR-184110] N91-19172
Multi-dimensional modeling of a thermal energy storage canister
[NASA-TM-103731] N91-19177
Two reference time scales for studying the dynamic cavitation of liquid films
[NASA-TM-103673] N91-19369

VOLCANOLOGY
Magellan: Preliminary description of Venus surface geologic units N91-20011

VOLT-AMPERE CHARACTERISTICS
Superconductivity of oxide film electrolytically deposited on surface of B(1-x)Sb(x) single crystal N91-19819

VORTEX ALLEVIATION
Research on bluff-body vortex wakes
[AD-A229875] N91-19071

VORTEX AVOIDANCE
Feasibility of an onboard wake vortex avoidance system
[NASA-CR-187521] N91-19074

VORTEX FILAMENTS
A new methodology for free wake analysis using curved vortex elements
[NASA-CR-3958] N91-19067

VORTEX GENERATORS
Development of a perturbation generator for vortex stability studies
[NASA-CR-188051] N91-19379

VORTEX SHEDDING
Development of a perturbation generator for vortex stability studies
[NASA-CR-188051] N91-19379
Low flow vortex shedding flowmeter for hypergolics/all media N91-20036

VORTEX SHEETS
Research on bluff-body vortex wakes
[AD-A229875] N91-19071

VORTICES
Unified aeroacoustics analysis for high speed turboprop aerodynamics and noise. Volume 1: Development of theory for blade loading, wakes, and noise
[NASA-CR-4329] N91-19049
Summary of in-flight flow visualization obtained from the NASA high alpha research vehicle
[NASA-TM-101734] N91-19055
A new methodology for free wake analysis using curved vortex elements
[NASA-CR-3958] N91-19067
The effect of body shape on the development of vortex asymmetry in the flow past slender bodies
[BU-413] N91-19068
Research on bluff-body vortex wakes
[AD-A229875] N91-19071
Feasibility of an onboard wake vortex avoidance system
[NASA-CR-187521] N91-19074
Filtering analysis of a direct numerical simulation of the turbulent Rayleigh-Benard problem
[NASA-CR-187488] N91-19366
Development of a perturbation generator for vortex stability studies
[NASA-CR-188051] N91-19379
Systems near the onset and in the well-developed regimes of turbulence
[DE91-008148] N91-19382

VOYAGER 2 SPACECRAFT
Triton: A hot potato N91-20005

W

WAKEFULNESS
Review of EEG studies in non human primates exposed to microgravity N91-19649

WAKES
Research on bluff-body vortex wakes
[AD-A229875] N91-19071
Feasibility of an onboard wake vortex avoidance system
[NASA-CR-187521] N91-19074
WALLS
Large-scale aeroacoustic research feasibility and conceptual design of test-section inserts for the Ames 80- by 120-foot wind tunnel
[NASA-TP-3020] N91-19824
WARFARE
Sandia technology: Engineering and science applications
[DE91-006760] N91-19322
WARNING
World weather watch: Regional association 4: Hurricane operational plan, supplement 2
[WMO-524-SUPPL-2] N91-19563
WARNING SYSTEMS
The development of a rugged accelerometer
[DE91-007731] N91-19407
WASHERS (SPACERS)
Graduated-load spring washer system for screws and threaded fasteners
[AD-D014697] N91-19436
WATER
Screening volatile organics by direct sampling ion trap and glow discharge mass spectrometry
[DE91-007708] N91-19258
Conceptual study of on orbit production of cryogenic propellants by water electrolysis
[NASA-TM-103730] N91-19317
Climatic water budgets, effective moisture, and elevation in the Southern Sierra Nevada, California, 1951-1980
[PB91-127878] N91-19500
Physiology of body water and salt regulation. Part 1: Circadian rhythms of endocrine systems and urinary electrolyte excretion in humans N91-19592
Physiology of body water and salt regulation. Part 2: Volume and electrolyte homeostasis after an acute saline infusion N91-19593
A ground based module for experimentations of cultivations and recycling in a closed environment N91-19657
WATER BALANCE
Wavelets and turbulence on the sea surface
[AD-A229862] N91-19565
Carbon dioxide and water exchange of a soybean stand grown in the biomass production chamber N91-20026
WATER CURRENTS
Outer continental shelf environmental assessment program, volume 70
[PB91-129288] N91-19548
WATER FLOW
Wavelets and turbulence on the sea surface
[AD-A229862] N91-19565
WATER HEATING
DHE (Downhole Heat Exchangers)
[DE91-006620] N91-19509
WATER IMMERSION
Neurological findings after 72 hours water immersion N91-19597
Simulated absence of gravity impairs arterial baroreceptor control of heart rate in man N91-19599
Fluid shifts and regulation of plasma volume in humans during 12 hours of head-out water immersion N91-19602
Influence on natriuresis of prolonged (12 h) water immersion on central hemodynamics and endocrine elements in humans N91-19612
WATER POLLUTION
Spatial and temporal variation in biomonitoring data
[DE91-007843] N91-19539
WATER QUALITY
The application of simulation model for the flow induced by air bubble plume in thermally stratified reservoirs
[DE91-003064] N91-19380
Spatial and temporal variation in biomonitoring data
[DE91-007843] N91-19539
WATER SPLITTING
Conceptual study of on orbit production of cryogenic propellants by water electrolysis
[NASA-TM-103730] N91-19317
WATER TEMPERATURE
Cool-down and frozen start-up behavior of a grooved water heat pipe
[NASA-CR-187053] N91-19376
WATER TREATMENT
The application of simulation model for the flow induced by air bubble plume in thermally stratified reservoirs
[DE91-003064] N91-19380
WATER VAPOR
Design, performance evaluation, and investigation of the theoretical capabilities of the NASA Millimeter-wave Imaging Radiometer (MIR)
[NASA-CR-187984] N91-19398
WATER WAVES
Slope modulation of the radar backscatter by sea waves
[BCRS-88-05] N91-19327
WAVE AMPLIFICATION
Breakup of femtosecond pulses during amplification in Er(3+)-doped single-mode optical fibers N91-19812
WAVE DIFFRACTION
Characteristics of excimer laser with narrow emission line N91-19807
WAVE EQUATIONS
Elementary pulse diffraction problems and the generation of sound by a dipole moving across the edge of a half-plane
[LR-565] N91-19831
WAVE FRONTS
Acoustic stabilization of laser beam wavefront in nonhomogeneous gaseous medium N91-19802
WAVE FUNCTIONS
Examinations of inverse scattering problem for the scalar Helmholtz equation in the field of first order approximations for potentials with compact supports and safe real wave numbers
[ETN-91-98949] N91-19339
Approximation properties of wavelet transforms
[ETN-91-98922] N91-19799
Dynamics of collision processes
[DE91-007933] N91-19840
How many times do we have in quantum gravity
[DE91-744973] N91-19991
WAVE INTERACTION
Critical-layer nonlinearity in the resonance growth of three-dimensional waves in boundary layers
[NASA-TM-103639] N91-19373
WAVE PROPAGATION
Numerical and physical modelling of bubbly flow phenomena
[DE91-007461] N91-19377
Lecture notes on nonlinear inversion and tomography
[DE91-008238] N91-19558
Acoustic stabilization of laser beam wavefront in nonhomogeneous gaseous medium N91-19802
Solution of one-dimensional problem in nonlinear theory of elasticity with structured shock wave N91-19809
Gravitational lens effect of wall-like objects and its cosmological implications
[DE91-744976] N91-19992
WAVEGUIDES
Coplanar waveguide EEsoF MICAD macros make circuit layout easy
[NASA-TM-103272] N91-19332
Apparatus for determining microwave characteristics of superconductive materials using a resonant cavity and calibration waveguides
[AD-D014694] N91-19918
WAVELENGTH DIVISION MULTIPLEXING
Study of wavelength division multiplexing as a means of increasing the number of channels in multimode fiber optic communication links N91-20024
WEAK ENERGY INTERACTIONS
Electroweak interactions at LEP
[NOTA-INTERNA-962] N91-19853
WEAPONS
Designing for explosive safety: The Explosive Components Facility at Sandia National Laboratories
[DE91-006432] N91-19103
WEAPONS DEVELOPMENT
Sandia technology: Engineering and science applications
[DE91-006760] N91-19322
WEAR
Tribological properties of Ag/Ti films on Al2O3 ceramic substrates
[NASA-TM-103784] N91-19224
Considerations relating to pulsed-beam modification of materials
[DE91-006771] N91-19922
WEATHER FORECASTING
Rocket-triggered lightning strikes and forest fire ignition N91-20027
WEDGES
Large-scale aeroacoustic research feasibility and conceptual design of test-section inserts for the Ames 80- by 120-foot wind tunnel
[NASA-TP-3020] N91-19824
WEIGHT REDUCTION
Minimum weight optimization of composite laminated struts
[BU-409] N91-19246
Design and testing of a circumferential and longitudinal joint of the A320 fuselage section 13/14 in GLARE
[LR-645] N91-19494
WEIGHTING FUNCTIONS
The weighted-difference form of the nodal diffusion method in cylindrical geometry
[DE91-007849] N91-19784
WEIGHTLESSNESS
Control and mechanism interaction for ground-based testing of space structures N91-19125
Integrated Cryogenic Experiment (ICE) microsphere investigation
[NASA-CR-177538] N91-19323
Effects of short-lasting weightlessness on gas exchange during light exercise N91-19573
Ocular roll under changing z-axis acceleration and neck position N91-19580
Body proprioceptive references in weightlessness as studied by muscle tendon vibration N91-19581
Pedalling in space to simulate gravity: The twin-bike system N91-19583
Coordination of eye, head and arm movements in weightlessness N91-19588
Simulated absence of gravity impairs arterial baroreceptor control of heart rate in man N91-19599
A new principle for dynamic fluid shift investigations in astronauts N91-19600
Intra-individual variability V'O2 frequency responses in physically active subjects N91-19601
Determinants of spatial orientation in weightlessness N91-19605
Vertically moving visual stimuli and vertical vection: A tool against space motion sickness N91-19606
The biological and medical programme of the manned Aragatz mission on the Mir Space Station N91-19617
Microgravity, hypergravity, and aging: A unifying hypothesis N91-19633
Does gravity play a role in the morphological development and function of the gravity sensory organ of vertebrates. DLR contribution to the D-2 project graviperception and neuronal plasticity, its technical realization and experimental execution N91-19635
Adaptive responses in monkeys during two week space flight N91-19645
Volume regulating hormones, fluid and electrolyte modifications during the Aragatz Mission (Mir station) N91-19689
The reference systems for tactile perception and for the orientation with respect to body N91-19691
Gaze control and spatial memory in weightlessness N91-19692
Weightlessness countermeasures and human physiology in space: A potential conflict N91-19695
The 1989-1990 NASA space biology accomplishments
[NASA-TM-4258] N91-19697
WEIGHTLESSNESS SIMULATION
Isokinetic force velocity and electromyographic characteristic of knee and elbow extensor and flexor muscles in the 0-g environment N91-19584
Neurological findings after 72 hours water immersion N91-19597
Vertebral column length changes during simulated microgravity N91-19604
Postural changes following sensory reinterpretation as an analog to spaceflight N91-19610
Head-down tilt test and space-related endocrine physiology N91-19614
Muscle function impairment following lower limb unloading in men N91-19616
Blood pressure maturation curve in normotensive rats during growth in simulated microgravitational environment N91-19644
Contractile protein changes induced by hindlimb suspension in rat skeletal muscle N91-19646
Hindlimb suspension of rabbit for one week: Myofibrillar damage in the soleus may depend on long-lasting shortening and periodic contraction against no load N91-19647
Responses of Physarum polycephalum to varying light levels during fast clinostat rotation: A scientific preparation of an ESA biorack experiment during the IML-1 mission N91-19676
WELDED JOINTS
Effects of irradiation on crack-arrest toughness of two high-copper welds
[DE91-007189] N91-19270
Performance of underwater weldments
[PB91-129254] N91-19452
WEST GERMANY
Space research for the sake of all
[ETN-91-98807] N91-19113
WHEELS
Design and control of a fully omnidirectional and holonomic wheeled platform for robotic vehicles
[DE90-017746] N91-19445

A new wheel control system for the omnidirectional HERMIES-3 robot
[DE90-017764] N91-19446

WHISKER COMPOSITES
Comparison of dynamic fatigue behavior between SiC whisker-reinforced composite and monolithic silicon nitrides
[NASA-TM-103707] N91-19293

WHISKERS (CRYSTALS)
Rigid mullitewhisker felt and method of preparation
[AD-D014648] N91-19225

WHITE LIGHT HOLOGRAPHY
The challenge of standards for emerging NDT methods
[DE91-007834] N91-19465

WIDEBAND COMMUNICATION
Fiber optic feed
[AD-A229860] N91-19879

WIGGLER MAGNETS
Simulation of a standing-wave free-electron laser
[DE91-007330] N91-19418
Proceedings of the Workshop Prospects for a 1 Angstrom Free-Electron Laser
[DE91-007631] N91-19422
Summary of the working group on transverse emissions from photocathodes
[DE91-008414] N91-19432
Multiple energy computed tomography for neuroradiology with monochromatic x rays from the national synchrotron light source
[DE91-008108] N91-19712
Possibility of raising efficiency of free-electron laser in longitudinal magnetic field N91-19804

WIND SHEAR
Progress on intelligent guidance and control for wind shear encounter N91-19034
Flight simulation for wind shear encounter N91-19035

WIND TUNNEL APPARATUS
Large-scale aeroacoustic research feasibility and conceptual design of test-section inserts for the Ames 80- by 120-foot wind tunnel
[NASA-TP-3020] N91-19824

WIND TUNNEL CALIBRATION
Result of ONERA standard model test in 2m x 2m transonic wind tunnel
[DE91-750115] N91-19066

WIND TUNNEL MODELS
Experimental investigation of porous-floor effects on cavity flow fields at supersonic speeds
[NASA-TP-3032] N91-19042

WIND TUNNEL TESTS
F-18 high alpha research vehicle surface pressures: Initial in-flight results and correlation with flow visualization and wind-tunnel data
[NASA-TM-101724] N91-19051
Result of ONERA standard model test in 2m x 2m transonic wind tunnel
[DE91-750115] N91-19066
Wind tunnel wall effects in a linear oscillating cascade
[NASA-TM-103690] N91-19098
Experimental investigation of a single flush-mounted hypermixing nozzle
[NASA-TM-103726] N91-19374
J-85 jet engine noise measured in the ONERA S1 wind tunnel and extrapolated to far field
[NASA-TP-3053] N91-19823
Large-scale aeroacoustic research feasibility and conceptual design of test-section inserts for the Ames 80- by 120-foot wind tunnel
[NASA-TP-3020] N91-19824

WIND TUNNEL WALLS
Wind tunnel wall effects in a linear oscillating cascade
[NASA-TM-103690] N91-19098

WIND TURBINES
A non-linear method for the calculation of the power output of a rotating wind turbine
[BU-416] N91-19512

WIND VELOCITY
Aeolian removal of dust types from photovoltaic surfaces on Mars N91-19156
A non-linear method for the calculation of the power output of a rotating wind turbine
[BU-416] N91-19512

WINDOWS (INTERVALS)
The selection of window functions for the calculation of time domain averages on the vibration of the individual gears in an epicyclic gearbox
[OUEL-1818/90] N91-19457

WINDPOWER UTILIZATION
Some control problems with broad range variable speed for horizontal axis wind turbines
[FFA-TN-1990-37] N91-19513

WINDPOWERED GENERATORS
Some control problems with broad range variable speed for horizontal axis wind turbines
[FFA-TN-1990-37] N91-19513

WING PROFILES
An experimental study of the turbulent boundary layer on a transport wing in subsonic and transonic flow
[NASA-TM-102206] N91-19062

WING-FUSELAGE STORES
S87 close air support aircraft fatigue analysis
[ETN-91-98854] N91-19093

WINGS
An experimental study of a sting-mounted single-slot circulation control wing
[AD-A229867] N91-19111

WINTER
Progressive feature of stepped leader on Japan sea coast in winter (basic data to establish shielding theory for lightning)
[DE91-742133] N91-19561

WIRE
Wire-free arming system for an aircraft-delivered bomb
[AD-D014611] N91-19076
Air/sea temperature probe
[AD-D014674] N91-19397
Silver-sheathed multifilament wires
[DE91-008107] N91-19941

WORDS (LANGUAGE)
Improved syntactic disambiguation in the FASIT automatic indexing environment N91-19956

WORKING FLUIDS
Cool-down and frozen start-up behavior of a grooved water heat pipe
[NASA-CR-187053] N91-19376
The design of future central receiver power plants based on lessons learned from the Solar One Pilot Plant
[DE91-005224] N91-19510

WORKLOADS (PSYCHOPHYSIOLOGY)
Analysis of workload and load balancing issues in the NCAR community climate model
[DE91-008052] N91-19534

WORKSTATIONS
QUEST/Ada (query utility environment for software testing of Ada: The development of a program analysis environment for Ada, task 1, phase 3
[NASA-CR-187983] N91-19735

WORLD METEOROLOGICAL ORGANIZATION
World weather watch: Regional association 4: Hurricane operational plan, supplement 2
[WMO-524-SUPPL-2] N91-19563

X

X RAY ABSORPTION
X ray absorption spectroscopy of oxide films on metals
[DE91-008100] N91-19278

X RAY ANALYSIS
Proton induced x ray emission analysis N91-19832
X ray determination of site occupation parameters in ordered ternaries Cu(Au(x)M(1-x))M = Ni,Pd
[DE91-007861] N91-19937

X RAY LASERS
Soft x-ray laser gain prediction at high density for the nitrogen isoelectronic sequence
[DE91-007616] N91-19416
Recombination x ray laser experiments using exploding ribbon Al targets
[DE91-007146] N91-19429
Nickel-like x ray lasers
[DE91-008502] N91-19433
UV Thomson scattering from x ray laser plasmas
[DE91-007347] N91-19895
Optically-ionized plasma recombination x ray lasers
[DE91-007261] N91-19898

X RAY SCATTERING
The characterization of interface roughness and other defects in multilayers by x ray scattering
[DE91-007558] N91-19929
Diffuse x ray scattering YBa2Cu3O(6.95) monocrystal
[DE91-615182] N91-19943

X RAY SPECTRA
He-like spectra through charge exchange processes in tokamak plasmas
[NIFS-69] N91-19894

X RAYS
Multiple energy computed tomography for neuroradiology with monochromatic x rays from the national synchrotron light source
[DE91-008108] N91-19712
Proton induced x ray emission analysis N91-19832
The advanced light source: A new tool for research in atomic physics
[DE91-007739] N91-19861
Phase transitions and equation of state of CsI under high pressure and the development of a focusing system for x rays
[DE91-007646] N91-19930

X-29 AIRCRAFT
Monitoring techniques for the X-29A aircraft's high-speed rotating power takeoff shaft
[NASA-TM-101731] N91-19081
Real-time application of advanced three-dimensional graphic techniques for research aircraft simulation
[NASA-TM-101730] N91-19742

XENON
A 5-kW xenon ion thruster lifetest
[NASA-TM-103191] N91-19180

XENON CHLORIDE LASERS
Characteristics of excimer laser with narrow emission line N91-19807

Y

YEAST
Biological action of single accelerated heavy ions on individual yeast cells N91-19683
Mutation induction in dried yeast cells after irradiation with selected UVC- and UVB- wavelengths compared to simulated sunlight N91-19686

Z

ZENITH
SBUV/2 in-orbit performance N91-19517
NOAA-9 SBUV/2 ozone sounding accuracy: Presentation summary N91-19519
A technique for directly comparing radiances from two satellites N91-19520
Initial estimate of NOAA-9 SBUV/2 total ozone drift: Based on comparison with re-calibrated TOMS measurements and pair justification of SBUV/2 N91-19523

ZEOLITES
Chemical interactions in multimetal/zeolite catalysts
[DE91-007978] N91-19261

ZIRCONIUM ALLOYS
Stress corrosion cracking of Al-Li-Cu-Zr alloy 2090 in aqueous Cl(-) and mixed CO3(2-)/Cl(-) environments
[DE91-007064] N91-19269

ZIRCONIUM OXIDES
Assessment of tamper-revealing ceramic seals
[DE91-007793] N91-19301
High resolution microstructural and microchemical analysis of zirconia eutectic interfaces
[DE91-008032] N91-19940

ZONAL FLOW (METEOROLOGY)
Zonal statistics in (General Circulation Model) GCM/GCM/data intercomparisons
[DE91-006706] N91-19530

Typical Personal Author Index Listing

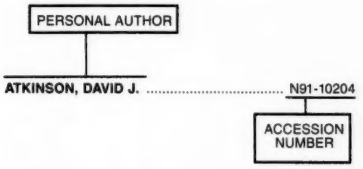

Listings in this index are arranged alphabetically by personal author. The accession number denotes the number by which the citation is identified.

A

AALTO, S. N91-19994
AARTMAN, LOUIS N91-19661
ABBOTT, KATHY HAMILTON N91-19073
ABDULAZIZ, S. N91-19214
ACHENBACH, F. N91-19678
ADAMS, M. L. N91-19780
N91-19781
N91-19782
ADDIS, F. W. N91-19193
AHMED, S. N91-19314
N91-19507
AHN, KYUNG H. N91-19375
AIHARA, Y. N91-19561
AKATOV, J. A. N91-19684
AKATOV, Y. A. N91-19679
AKHIL, A. A. N91-19352
AKIBA, T. N91-19884
AKIYAMA, HIDENORI N91-19891
ALAG, GURBUX S. N91-19099
ALAGHBAND, GITA N91-19732
ALBRECHT, R. N91-19584
ALBRITTON, D. L. N91-19535
ALCARAZ, A. N91-19254
ALEXANDER, S. W. N91-19178
ALEXANDER, Y. N91-19538
ALEXANDRE, C. N91-19643
N91-19690
ALFEYEV, V. N. N91-19819
ALI, MICHAEL S. N91-19449
ALIVISATOS, A. P. N91-19921
ALLEN, J. J. N91-19793
ALLEN, M. E. N91-19958
ALQUEZAR, RENE N91-19582
ALTEROVITZ, S. A. N91-19351
N91-19935
ALTURKI, F. A. N91-19362
AMARI, SACHIKO N91-19998
AMENDT, P. N91-19898
AMINOV, B. A. N91-19819
AMORUSO, ANTONELLA N91-19550
ANDERSON, K. R. N91-19271
ANDERSON, KENNETH D. N91-19397
ANDERSON, L. E. N91-19704
ANDERSON, LOREN A. N91-20022
ANDES, DAVID K. N91-19764
ANDRAS, MARIA T. N91-19256
N91-19296
ANDRE-DESHAYS, CLAUDIE N91-19581
N91-19692
ANDRE, MARCEL JEAN N91-19657
ANDRESEN, B. N91-19254
ANDREWS, ROBERT J. N91-19460
ANIKEYEV, B. V. N91-19811
ANKEN, R. N91-19638
ANSPAUGH, B. N91-19211
ANTON, G. N91-19649
ANTONSEN, T. M., JR. N91-19358
ANTONUTTO, GIULIOANDREA N91-19583
ANTROPOVA, I. N. N91-19619
ANZIL, A. P. N91-19647
AOKI, TAKAYUKI N91-19892
N91-19893
AOYAMA, T. N91-19888
APPELBAUM, JOSEPH N91-19201
ARBEILLE, PHILIPPE N91-19577
N91-19578
ARCHANGELSKY, V. V. N91-19679
ARENA, N. N91-19620
ARISAWA, TAKASHI N91-19913
ARNOLD, JACK H. N91-19200
ARVIDSON, R. N91-20011
ARYA, VINOD K. N91-19473
ASAKAWA, A. N91-19561
ASELAGE, T. L. N91-19243
N91-19942
ASH, ROBERT L. N91-19379
ASPHAUG, E. N91-19996
ASSANIS, D. N. N91-19440
ATASSI, HAFIZ M. N91-19053
ATENCIO, ADOLPH, JR. N91-19823
ATKOV, O. N91-19577
N91-19578
ATWELL, WILLIAM N91-19699
AUBERT, J. H. N91-19291
AUERNHEIMER, BRENT N91-20023
AUGUSTEIJN, T. N91-19978
AULL, J. E. N91-19720
AUREILLE, MARC N91-19648
AUSONI, S. N91-19646
AUWETER-KURTZ, M. N91-19173
AVERY, J. E. N91-19189
AVINASH, K. N91-19909
AYERS, JACK N91-19288
AZMY, Y. Y. N91-19749
N91-19784
AZUMI, MASAFUMI N91-19914

B

BABAEV, B. M. N91-19642
BABEL, H. W. N91-19148
BACA, W. E. N91-19344
BACH, RALPH E., JR. N91-19082
BACHL, NORBERT N91-19584
BACKHAUS, ROBERT N91-19656
BAEDER, J. D. N91-19826
BAEUERLE, A. N91-19638
BAEUMER, K. N91-19635
BAGGER, J. N91-19851
BAGGERUD, C. N91-19674
BAISCH, FRIEDHELM N91-19585
N91-19592
N91-19598
BAKER, J. T. N91-19711
BAKER, VICTOR R. N91-19997
BAKHLE, MILIND A. N91-19475
BALACHANDRAN, U. N91-19299
BALASHOV, N. S. N91-19808
BALCH, KRIS S. N91-19437
BALDIS, H. A. N91-19895
BALLINGER, C. T. N91-19794
BANDA, CAROLYN N91-19714
BANGERT, WOLFGANG N91-19585
BANGSBO, J. N91-19687
BANKS, DANIEL W. N91-19051
BANKS, S. P. N91-19761
BANSAL, NAROTTAM P. N91-19308
BAR-SHALON, A. N91-19900
BARBER, D. C. N91-19688
BAREISS, LYLE E. N91-19147
BARKER, THOMAS B. N91-19344
BARLOW, N. G. N91-20007
BARMIN, V. A. N91-19642
BARNES, C. W. N91-19908
BARNETT, A. M. N91-19187
BARNETT, JOHN W. N91-19181
BARNEY, RICHARD D. N91-19152
BARNI, S. N91-19620
BARON, R. N91-19584
BARRETT, JOAN N91-19526
BARROWS, R. D. N91-19132
BARSOV, S. G. N91-19945
BARTOSIK, L. G. N91-19148
BASARAN, O. A. N91-19779
BASILEVSKY, ALEXANDER T. N91-20011
BASTO, JOSE EDSON N91-19157
BATES, HARRY N91-20024
BATES, J. B. N91-19925
BATTS, G. W. N91-19529
BAUER, G. N91-19107
BAUER, HELMUT F. N91-19386
N91-19388
N91-19389
N91-19390
BAUM, KLAUS N91-19586
N91-19601
BAUMANN, THOMAS N91-19652
BAZYLEV, V. A. N91-19804
BEAN, ALAN J. N91-19164
BECHLER, B. N91-19598
N91-19620
N91-19634
BECKERMAN, M. N91-19447
BEHR, V. L. N91-19064
N91-19065
BEHRLE, R. N91-19663
BELAEVA, M. N91-19588
BELENOV, E. M. N91-19820
BELIEN, MARCEL J. N91-19169
BELJAJEVA, I. N91-19595
BELL, P. E. N91-19400
BELLANCA, S. N91-19141
BELOOZEROVA, I. N. N91-19642
BELTON, M. N91-20000
N91-20002
BENIEN, HANNELORE N91-19311
BENNETT, D. W. N91-19751
BENNETT, GARY L. N91-19181
N91-19183
BENOLKEN, MARTHA S. N91-19710
BENSON, ALAN J. N91-19613
BENTEN, MUHAMMAD S. N91-19732
BENTON, R. D. N91-19420
N91-19746
BENZ, W. N91-20012
BERENDSEN, W. N91-19624
BERG, HANS E. N91-19587
N91-19616
BERG, TIMOTHY M. N91-19763
BERGER, MEINHARD N91-19588
N91-19597
BERKOWITZ, BRIAN N91-19047
BERMAN, L. E. N91-19712
BERNARD, J. E. N91-19895
BERNARDI, G. N91-19647
BERNATOWICZ, THOMAS J. N91-19998
BERRONDO, M. N91-19923
BERRY, G. F. N91-19252
BERRYMAN, J. G. N91-19558
N91-19758
BERTHOZ, A. N91-19692
N91-19694
BERTNESS, K. A. N91-19188
N91-19194
BEYMER, MARK A. N91-20022
BHARATHAN, D. N91-19501
BHATTACHARYA, P. K. N91-19351
N91-19935
BIDWELL, COLIN S. N91-19046
BIDWELL, S. N91-19358
BIEDINGER, URSULA N91-19675
BIERMANN, ERICH N91-19948
BILANIN, ALAN J. N91-19074
BILLINGS, S. A. N91-19362
N91-19753
N91-19754
N91-19789
N91-19797
BINGEL, BRADFORD D. N91-19737
BINOT, P. N91-19627
BLAKE, A. N91-19458
BLANPAIN, R. N91-19142
BLATTNER, M. M. N91-19745
BLEIER, A. N91-19239
BLISS, DONALD B. N91-19050
N91-19067

BLOCK, INGRID N91-19676
BLUMENTHAL, PHILIP Z. N91-19401
BOGOMOLOV, V. V. N91-19576
BOKHARI, SHAHID H. N91-19715
N91-19716
BOLEF, L. N91-20000
BOLLINGER, L. N91-19857
BON, DAVID R. N91-19116
BONDARCHUK, YA. M. N91-19813
BONDE-PETERSEN, FLEMMING N91-19602
N91-19612
BONGERS, BERND N91-19981
BONN, R. H. N91-19330
BOONSTRA, JOHANNES N91-19623
BOOSKE, J. N91-19358
BOQUET, JEAN N91-19648
BORGIA, BRUNO N91-19410
N91-19853
BORK, U. N91-19682
BORODIN, A. I. N91-19801
BORREGO, J. M. N91-19204
BOUGHAROUAT, NORA N91-19589
BOUISSET, P. N91-19679
BOURCIER, R. J. N91-19922
BOURRIN, S. N91-19643
BOWER, M. N91-19215
BOWLES, KENNETH J. N91-19234
BOWLING, DONALD R. N91-19918
BOWMAN, H. D., II N91-19515
BOYD, D. R. N91-19751
BRAASCH, MICHAEL N91-19030
BRACK, ANDRE N91-19681
BRADY, M. N91-19458
BRAGHIN, MASSIMO N91-19158
BRAGINSKIY, A. YA. N91-19817
BRAITHWAITE, J. W. N91-19352
BRANDHORST, HENRY W. N91-19179
BRANDT, N. B. N91-19819
BRASCHE, L. J. H. N91-19272
BRASTED, DONALD K. N91-19165
BRECHIGNAC, FRANCOIS N91-19589
N91-19655
BREEDEN, T. N91-19835
BREITTMAYER, J. P. N91-19619
BREWE, DAVID E. N91-19369
BRIEGLEB, WOLFGANG N91-19631
N91-19635
N91-19636
N91-19676
N91-19678
BRILLHART, RALPH D. N91-19144
BRINKER, DAVID J. N91-19165
N91-19189
N91-19195
N91-19205
N91-19209
BRINKMANN, W. N91-19365
BRITTON, RANDALL K. N91-19056
BRODKIN, J. S. N91-19283
BROM, H. B. N91-19243
BROMEIS, B. N91-19635
BROOKS, N. N91-19881
BROTHERS, P. R. N91-19196
BROWN, B. C. N91-19958
BROWN, B. H. N91-19688
BROWN, DAVID B. N91-19735
BROWN, GERALD V. N91-19324
BROWN, JAY C. N91-19341
BROWN, R. C. N91-19483
BROWN, R. H. N91-20004
N91-20005
BROWN, S. A. N91-19233
BRUBAKK, ALF O. N91-19590
BRUIJS, WILLEM ELISABETH MARIA N91-19790
BRUMLEY, E. A. N91-19611
BRUNKER, SHANE A. N91-19434
BSCHORR, OSKAR N91-19829
BUCHANAN, M. V. N91-19258
BUCHHEIT, R. G. N91-19269
BUCK, O. N91-19272
BUCKMANN, P. S. N91-19174
BUFFUM, DANIEL H. N91-19098
BUKIN, A. D. N91-19788
BUMBA, W. N91-19584
BUNT, ALBERT-JAN N91-19169
BURD, H. J. N91-19791
BURENIN, A. A. N91-19809
BURGER, E. H. N91-19650
BURGESS, C. A. R. N91-19096
BURGESS, R. M. N91-19190
BURGIN, ROBERT EDWARD N91-19956
BURIAN, KARL M. N91-19662
BURLACSKOVA, N. N91-19597
BURLATSCHKOWA, N. N91-19595
BURNE, WILLIAM K. N91-19869
BURTON, D. E. N91-19381
BUSH, D. M. N91-19352
BUSS, R. J. N91-19907
BUTLER, C. M. N91-19331
BUTLER, P. L. N91-19447
BYERS, DAVID C. N91-19181
BYSTROV, V. V. N91-19577
N91-19578

C

CADIEUX, J. R. N91-19399
CAFFEY, T. W. H. N91-19334
CAHILL, P. A. N91-19872
CAIN, T. M. N91-19070
CALLE, LUZ N91-20025
CALVIN, W. M. N91-20004
CAMERON, A. G. W. N91-20012
CAMERON, M. N91-19977
CAMPBELL, J. N91-19141
CAMPBELL, K. D. N91-19251
N91-19313
N91-19318
CAMPIONE, M. N91-19646
CAPELLI, CARLO N91-19583
CARCAGNO, R. N91-19863
CARDOSO, HUMBERTO PONTES N91-19129
N91-19130
CARLSON, O. N. N91-19272
CARMEL, Y. N91-19358
CARPENTER, K. H. N91-19739
CARPENTER, WARREN A. N91-19137
CARR, M. N91-20000
N91-20002
CARTER, DANIEL N91-19665
CASALE, ELENA N91-19665
CASALNUOVO, S. A. N91-19407
CASTRUCCI, FILIPPO N91-19604
CATES, G. D. N91-19845
CAVICCHI, B. T. N91-19184
CEBECI, TUNCER N91-19047
CEBULA, R. P. N91-19518
CHABOCHE, J.-L. N91-19476
CHADHA, A. N91-19545
CHALMERS, ALAN G. N91-19391
CHAMIS, CHRISTOS C. N91-19229
N91-19230
N91-19236
N91-19237
N91-19472
CHANDRA, S. N91-19527
CHANG, CHAU-LYAN N91-19059
CHANG, R. P. H. N91-19938
CHANG, S. L. N91-19252
CHAPMAN, C. N91-20000
N91-20002
CHAPMAN, L. D. N91-19712
CHAPPARD, D. N91-19643
CHARAKHCHYAN, L. A. N91-20021
CHARAKHCHYAN, T. N. N91-20021
CHATTERJEE, A. N91-19306
CHAUVET, G. N91-19596
CHEN, D. N91-19094
N91-19489
CHEN, F. C. N91-19950
CHEN, G. L. N91-19950
CHEN, HSUN N91-19047
CHEN, PANG C. N91-19768
CHEN, S. R. N91-19480
CHEN, W. N91-19361
CHENG, XIANG SHENG N91-19773
CHERNENKOV, YU. P. N91-19943
CHERVENAK, ANN L. N91-19718
CHI, ZHIZANG N91-19027
CHIBA, MASAKATSU N91-19387
CHING, CHO ONG N91-19050
CHIU, ALEX N91-19714
CHIU, S. AMANDA N91-19304
CHLICK, G. N91-19649
CHOI, SUNG R. N91-19293
CHOJNACKI, E. N91-19414
CHOMET, SYLVIE N91-19915
CHONG, TECK HWA N91-19746
CHOO, YUNG K. N91-19054
CHOU, V. N91-19860
CHOUDHARI, MEELAN N91-19061
CHRETIEN, J. L. N91-19577
CHRISS, RANDALL M. N91-19063
CHRISTENSEN, NIELS JUEL N91-19593
N91-19612
CHRISTIAN, J. E. N91-19240
CHU, C. L. N91-19186
CHUANG, C. N91-19553
CHUNG, B.-C. N91-19188
CHUNG, M. N91-19184
CHUNG, M. A. N91-19192
CHURCH, E. L. N91-19873
N91-19874
CHURNSIDE, J. H. N91-19875
CHURSIN, A. D. N91-19806
CIPOLLA, R. N91-19458
CIULLA, M. N91-19644
CLANCY, TODD N91-20003
CLARK, NANCY H. N91-19344
CLARK, R. N. N91-20004
CLARKE, ANDREW H. N91-19591
CLAUSING, R. E. N91-19310
CLAYTON, ERIC N91-19832
CLEMENT, ANNE E. N91-19396
CLOUGH, R. L. N91-19303
COFFEY, H. E. N91-20017
N91-20018
COGOLI, AUGUSTO N91-19598
N91-19620
N91-19621
N91-19634
N91-19658
COGOLI, MARIANNE N91-19598
N91-19620
COHEN, G. C. N91-19756
COHEN, M. N91-19416
COLE, J. K. N91-19064
COLE, R. L. N91-19440
COLLINS, JEFFERY D. N91-19306
COLLINS, S. C. N91-19483
COLLINS, TIMOTHY J. N91-19168
COLPITTS, T. S. N91-19186
COLVIN, V. L. N91-19921
CONN, R. N91-19911
COOPERSTEIN, J. M. N91-19357
COPE, RANDALL D. N91-19072
COREY, KENNETH A. N91-20026
CORSETTI, THOMAS G. N91-19551
CORUZZI, P. N91-19599
CORWIN, W. R. N91-19270
COUCH, W. A. N91-19103
COULTER, K. N91-19958
COURAGE, WILHELMUS MARIA GERARDUS
N91-19248
COURVILLE, G. E. N91-19240
COUTTS, T. J. N91-19191
N91-19202
COVENTRY, D. H. N91-19546
COWLEY, S. J. N91-19372
COX, S. K. N91-19541
CRAIG, JAMES I. N91-19750
CRANE, ROGER M. N91-19468
CRAWFIS, R. A. N91-19747
CRAWFORD, R. R. N91-19368
CREWS, J. H., JR. N91-19482
CROCKER, D. S. N91-19378
CROLL, R. H. N91-19064
CRONIN, J. R. N91-20006
CROSS, ELDON R. N91-19200
CROSS, J. B. N91-19146
CROUTE, F. N91-19630
CSANADY, G. T. N91-19565
CUCCHIARO, A. N91-19142
N91-19151
CUCINOTTA, FRANCIS A. N91-19699
CULBERTSON, R. J. N91-19283
CULP, G. L. N91-19251
CULVER, G. N91-19509
CURTIS, H. B. N91-19178
N91-19195
CURTISS, HOWARD C., JR. N91-19074
CZIRR, J. B. N91-19923

D

DABLIES, MATTHIAS N91-19121
DAHM, W. J. A. N91-19264
DALE, B. C. N91-19322
DALEN, GOERAN N91-19513
DAMASKIN, B. B. N91-19819
DANEN, W. C. N91-19257
DANFORTH, RICHARD A. N91-19172
DANIEL, R. W. N91-19459
DARLINGTON, D. J. N91-19329
DARZI, KENT N91-19164
DASILVA, L. B. N91-19433
DAUGHERTY, W. L. N91-19483
DAUGHTRY, C. S. T. N91-19497
DAVENPORT, A. J. N91-19278
N91-19302
DAVID, KATJA N91-19656
N91-19659
DAVID, VALERIE N91-19572
DAVIES, M. N91-20000
N91-20002
DAVIS, DAVID O. N91-19374

DAVIS, J. M. N91-19541
DAVIS, JAMES BRADLEY N91-19118
DAVIS, STEVEN B. N91-19742
DAVISON, J. E. N91-19192
DAWBARN, RONALD N91-19139
DAWSON, S. N91-19851
DAY, A. C. N91-19210
DEANGELIS, V. MICHAEL N91-19080
DEBOO, J. C. N91-19908
DECKER, ARTHUR J. N91-19404
DECKER, D. L. N91-19923
DEECKE, L. N91-19606
DEERENBERG, E. N91-19491
DEFRANCISCIS, G. N91-19629
DEGRASSIE, J. S. N91-19335
DEGROOT, ROLF P. N91-19623
DEHEER, ERIK P. N91-19169
DEINO, A. L. N91-19999
DEJONG, H. A. A. N91-19579
N91-19693
DEJUAN, E. N91-19633
DELAAT, SIEGFRIED W. N91-19623
DELAMORA, JUAN FERNANDEZ N91-19833
DELAND, M. T. N91-19518
DELEANU, L. N91-19784
DELFRATE, JOHN H. N91-19055
DELLACORTE, CHRISTOPHER N91-19224
DELOOR, G. P. N91-19327
DELUISI, J. N91-19522
DEMCHUK, M. I. N91-19803
DEMETS, RENE N91-19639
N91-19640
N91-19641
DEMIDOVICH, A. A. N91-19803
DEMIRGIAN, J. C. N91-19253
DENHERTOG, JEROEN N91-19623
DEROOY, J. C. J. M. N91-19243
DESALVO, G. N91-19646
DESTLER, W. W. N91-19358
DEVANEY, D. M. N91-19738
DEVER, JOYCE A. N91-19294
DEWAART, DIRK N91-19169
DEWATERS, J. N91-19545
DEWILDE, J. P. N91-19222
DEWIT, JAAP N91-19641
DEXTER, R. J. N91-19452
DIANOV, YE. M. N91-19812
DIEGLE, R. B. N91-19352
DIEMOZ, M. N91-19868
DIJKSTRA, F. N91-19222
DILLARD, P. A. N91-19197
DILLON, M. P. N91-19303
DILMANIAN, F. A. N91-19712
DIMAURO, L. F. N91-19835
DINETTA, L. C. N91-19187
DIPIETRO, M. S. N91-19233
DIPRAMPERO, PIETRO E. N91-19573
N91-19583
DODD, A. N91-19092
DODGE, M. N91-19535
DOHOGNE, PATRICK W. N91-19137
DOMKEN, I. N91-19151
DONATO, MARC N91-19131
DONNELLY, M. N91-19347
DONNELLY, RICHARD F. N91-19526
DONZELLI, C. N91-19629
DOOSE, L. N91-20000
DORER, R. M. N91-19326
DORRIS, S. E. N91-19299
N91-19301
DOTSENKO, M. A. N91-19645
DOTY, F. D. N91-19504
DOXEY, D. D. N91-19610
DRACH, ROBERT S. N91-19551
DRAXIER, R. R. N91-19535
DRISS-ECOLE, DOMINIQUE N91-19672
DRUMMER, CHRISTIAN N91-19592
N91-19593
DRUMMOND, CHARLES H., III N91-19308
DRYER, F. L. N91-19262
DUCHEIN, M.-C. N91-19657
DUDLEY, G. A. N91-19616
DUDNEY, N. J. N91-19925
DUDOK, E. N91-19336
DUFFEL, LARRY E. N91-19723
DUFFY, STEPHEN F. N91-19292
DUFOUR, G. N91-19090
DUGGER, M. T. N91-19922
DUKE, J. N91-19634
DUKE, JOHN C., JR. N91-19461
DUKE, P. J. N91-19628
DUNCAN, R. V. N91-19408
DUNHAM, G. N91-19193
DUNNING, M. J. N91-19898
DURAJ, STAN A. N91-19256
N91-19296
DURANT, D. Q. N91-19153
DURNOVA, G. N91-19628
DURRANT-WHYTE, HUGH F. N91-19763
DUSEK, J. T. N91-19299
N91-19301
DUVAL, W. M. N91-19320
DUVOISIN, M. N91-19687

E

EATOUGH, M. O. N91-19942
ECKART, A. N91-19977
ECKEL, ANDREW J. N91-19235
N91-19295
ECKLES, WILLIAM E. N91-19296
EDELSTEIN, ALAN S. N91-19289
EDER, D. C. N91-19429
N91-19898
EFROMSON, RONALD A. N91-19133
EGAN, MARK P. N91-19072
EGOROV, A. D. N91-19576
EIDEL, WERNER N91-19386
EIDSON, T. M. N91-19366
EIKEN, O. N91-19615
EISBRECHER, HANS-DIETER N91-19087
EISENBERG, JOSEPH D. N91-19097
EISLER, G. R. N91-19448
ELANDS, P. J. M. N91-19222
ELBASSAM, NASIR N91-19659
ELLINGSON, R. G. N91-19555
ELPHINSTONE, R. N91-19552
EMELCHENKO, G. A. N91-19943
EMERY, K. A. N91-19191
EMIN, D. N91-19243
ENENKL, BERNHARD N91-19086
ENGEL, L. A. N91-19574
ENGLER, CHARLES, JR. N91-19449
ENRIGHT, G. D. N91-19895
EPSTEIN, S. N91-20006
ERDMANN, KLAUS N91-19121
ERICKSON, LARRY L. N91-19058
ESBJOERNSSON, M. N91-19615
ESSFELD, DIETER N91-19573
N91-19586
N91-19594
N91-19601
ESTENNE, M. N91-19574
ESTRADAHAEN, JOSE LUIS N91-19285
EVANS, ALAN G. N91-19972
EVANS, DAVID A. N91-19344
EVANS, K., JR. N91-19903
EVANS, N. D. N91-19926
EVANS, R. D. N91-19525
EWING, P. D. N91-19406

F

FAEHL, R. J. N91-19858
FANALE, F. N91-20000
FANG, T. N91-19872
FARWANA, VIDA N91-19736
FATEMI, NAVID S. N91-19203
N91-19209
FAULKNER, ALAN N91-19101
FAUPEL, MICHEL N91-19665
FAUR, MARIA N91-19208
N91-19209
FAUR, MIRCEA N91-19208
N91-19209
FAZIO, GIOVANNI G. N91-19973
FEDDEMA, J. T. N91-19448
FEDOTOV, V. K. N91-19945
FEHSENFELD, F. C. N91-19535
FELDMAN, U. N91-19416
FENNER, JAMES N91-20027
FENWICK, D. M. N91-19934
FERRIS, M. J. N91-19257
FERRUA, B. N91-19619
FIDDES, S. P. N91-19512
FIDDES, STEVEN P. N91-19391
FIELDS, D. J. N91-19433
FIELDS, ROGER A. N91-19080
FINOKHIN, V. I. N91-19816
FIOCCO, GIORGIO N91-19550
FIRSOV, V. V. N91-19808
FISCHER, AXEL N91-19084
FISCHER, E. N91-20002
FISCHER, EUGENE C. N91-19468
FISCHER, J. N91-19432
N91-19849
N91-19850
FISHER, DAVID F. N91-19051
N91-19055
FLAGAN, R. C. N91-19560
FLAISHER, H. N91-19218
FLECK, M. M. N91-19774
FLEETER, SANFORD N91-19098
FLIFLET, A. W. N91-19413
FLOOD, DENNIS J. N91-19200
N91-19354
FLORA, C. S. N91-19197
FLOYD, H. L. N91-19322
FOLDAGER, NIELS N91-19602
FOLKERTS, T. J. N91-19919
FOLLSTAEDT, D. M. N91-19922
FOMIN, N. V. N91-19814
FOMINA, GALINA N91-19577
N91-19578
FORMAN, ROYCE G. N91-19273
N91-19274
FOSTER, J. M. N91-19910
FOX, JEFFERY A. N91-19460
FRAAS, L. M. N91-19189
FRANCHOIS, P. N91-19525
FRANK, D. N. N91-19430
FRANKLIN, M. J. N91-19279
N91-19280
FRANZEN, W. N91-19283
FREED, ALAN D. N91-19232
N91-19476
FREEDMAN, ROBERT J. N91-19401
FREESE, J. M. N91-19352
FREHLICH, R. G. N91-19498
FRESE, JOHANNES N91-19088
FROCK, BRIAN G. N91-19460
FROECHTENIGT, JOSEPH F. N91-19147
FRY, A. R. N91-19433
FUJIMOTO, TAKASHI N91-19852
N91-19894
FULD, CHRISTOPHER J. N91-19145
FULKERSON, W. N91-19533
FULLER, JOSEPH J. N91-19342
FURUYAMA, Y. N91-19886
FUTCH, A. N91-19881

G

GABELLA, W. E. N91-19778
GADDIS, L. N91-20000
GAIER, JAMES R. N91-19156
N91-19160
N91-19231
GALE, R. P. N91-19190
GALLARDO, J. C. N91-19422
GALLASCH, EUGEN N91-19595
GALVIN, A. B. N91-19552
GAMBARDELLA, P. N91-19629
GAO, Y. N91-19299
GARCIA, I. A. N91-19405
GARDNER, D. G. N91-19983
GARDNER, M. A. N91-19983
GARG, SANJAY N91-19766
GARNER, F. A. N91-19271
GARRETT, R. F. N91-19712
GARVIN, J. B. N91-19999
GASIEWSKI, ALBIN J. N91-19398
GASSER, G. N91-19140
GASSET, G. N91-19632
GATSURA, YE. F. N91-19815
GAUBIN, YOLANDE N91-19630
GAUDEAU, CLAUDE N91-19596
GAUQUELIN, GUILLEMETTE N91-19689
GEAHEL, ISABELLE N91-19627
GEE, J. M. N91-19189
GEELEN, G. N91-19689
GEERLIGS, LAMBERT JOHAN N91-19947
GEIST, G. A. N91-19757
GENENS, L. N91-19508
GENERAZIO, EDWARD R. N91-19295
GENZEL, R. N91-19976
GERARDI, ANTHONY G. N91-19102
GERSTENBRAND, F. N91-19588
N91-19597
GESSERT, T. A. N91-19191
N91-19202
GESTELAND, R. F. N91-19706
GETALOV, A. L. N91-19945
GEVARTER, WILLIAM B. N91-19770
GHANDI, S. K. N91-19204
GHARIB, C. N91-19689
GIBAUD, A. N91-19929
GIBBEL, MARK N91-19154
GILBERT, MICHAEL G. N91-19471
GILBREATH, GAIL C. N91-19396
GILHODES, J. C. N91-19581
GILLAND, J. H. N91-19178
GILYARD, GLENN B. N91-19099
GINZBURG, S. L. N91-19944
GIVEON, A. N91-19951

GLASAUER, STEFAN N91-19605
GLASS, H. D. N91-19958
GLINERT, E. P. N91-19745
GLOSSON, R. N91-19958
GLOZMAN, VLADIMIR N91-19144
GMUENDER, FELIX K. N91-19598
N91-19621
N91-19674
GMUER, N. F. N91-19712
GOELZ, T. M. N91-19173
GOLD, S. H. N91-19413
GOLDBERG, L. N91-19879
GOLDBERG, LEW N91-19869
GOLDBERG, P. Y. N91-19544
GOLDMAN, LOUIS J. N91-19057
GOLDMAN, M. N91-19857
GOLDSTEIN, M. E. N91-19372
GOLDSTEIN, W. H. N91-19416
N91-19900
GOLDSTON, R. J. N91-19908
GOLIGHTLY, MICHAEL J. N91-19699
GOLLNICK, P. D. N91-19687
GOLOB, ALEX N91-19131
GORADIA, CHANDRA N91-19206
N91-19208
N91-19209
GORADIA, MANJU N91-19208
N91-19209
GORENFLO, NORBERT N91-19339
GORETTA, K. C. N91-19941
GOROBETS, YU. I. N91-19816
GOSSARD, E. E. N91-19562
GOUIFFES, C. N91-19978
GOULD, J. N91-19512
GOUTHIERE, L. N91-19596
GRABITZ, GEORG N91-19385
GRAF, U. U. N91-19976
GRAMOLL, KURT C. N91-19232
GRANATSTEIN, V. L. N91-19357
N91-19358
GRANDE, MAURIZIO N91-19158
GRANT, KENNETH J. N91-19434
GRASS, R. D. N91-19525
GRASSI, G. N91-19599
GRATCHEV, V. N91-19578
GRATCHOV, V. N91-19577
GRAVES, R. S. N91-19240
GRAY, H. L. N91-19540
GRAY, L. F. N91-19779
GRAZIANI, R. A. N91-19443
GREBOGI, C. N91-19792
GREELEY, R. N91-20000
GREEN, H. J. N91-19501
GREENBERG, R. N91-20000
GREVE, D. W. N91-19926
GRIFFIN, J. W. N91-19409
GRIGORIEV, A. I. N91-19576
N91-19607
N91-19689
GRIMALDA, JUSTUS N91-19160
GRISHANIN, D. V. N91-19607
GRITZNER, CHRISTIAN N91-19121
GRODSINSKY, CARLOS M. N91-19324
GROEBKE, HARALD H. N91-19946
GROSJEAN, D. N91-19560
GROSSKOPF, PAUL P. N91-19461
GROSSMAN, A. N91-19911
GROTCH, S. L. N91-19530
GROUNNER, M. N91-19194
GRUDININ, A. B. N91-19812
GRUNDY, DAVID N91-19688
GRUZALSKI, G. R. N91-19925
GU, X. U. N91-19523
GUCKERT, J. B. N91-19279
GUELL, ANTONIO N91-19689
GUENTHER, ROLF D. N91-19113
GUERIN, M. R. N91-19258
GUEST, J. E. N91-20011
GUEZENNEC, C. Y. N91-19646
GUFAN, YU. M. N91-19817
GULICK, VIRGINIA C. N91-19997
GUNGA, H.-C. N91-19604
GUNST, R. F. N91-19540
GUO, X. Q. N91-19924
GUPTA, MURLI M. N91-19786
GURFINKEL, VICTOR S. N91-19581
N91-19691
N91-19694
GURWELL, W. E. N91-19282
GUTIERREZ, F. N91-19978
GUTMAN, D. N91-19259
GUTMARK, EPHRAIM N91-19364
GUTOWSKI, W. J. N91-19532
GYEKENYESI, JOHN P. N91-19292
N91-19295
N91-19477

H

HACK, K. J. N91-19178
HAEDER, DONAT-P. N91-19631
N91-19673
N91-19677
HAEGGMARK, T. N91-19616
HAFF, K. W. N91-19104
HAFFNER, J. W. N91-19159
HAIDER, OTMAR N91-19981
HALES, J. M. N91-19535
HALFORD, GARY R. N91-19473
HALL, DANA N91-19729
HALL, R. C. N91-19964
HALLEY, TED H. N91-19412
HALSTEAD, THORA W. N91-19697
HAMADE, KAREN S. N91-19052
HAMLIN, N. A. N91-19383
HAMMETTER, W. F. N91-19942
HAMPP, R. N91-19652
HANAGUD, SATHYA V. N91-19750
HANAK, J. J. N91-19218
HANDROOS, HEIKKI N91-19392
HANFT, R. W. N91-19958
HANKS, R. N91-19400
HANNIG, K. N91-19321
N91-19654
HANNON, M. H. N91-19187
HANSEN, M. A. N91-19751
HANSEN, N. N91-19215
HANSEN, N. H. N91-19751
HANSON, D. B. N91-19049
HANSON, H. P. N91-19537
HARDGROVE, W. R. N91-19149
HARDIN, J. E. N91-19346
HARDING, D. J. N91-19958
HARDING, J. N91-19411
HARDY, ALVA C. N91-19699
HARELAND, W. A. N91-19907
HARGENS, A. N91-19687
HARGREAVES, T. N91-19357
HARM, D. L. N91-19610
HARMON, J. K. N91-20001
HARRIS, A. I. N91-19976
HARRIS, D. B. N91-19419
HARRIS, DAVID W. N91-19200
HARRIS, M. T. N91-19779
HARRISON, K. N91-19923
HARRISON, R. F. N91-19761
HARTL, E. N91-19876
HARTMANN, D. N91-19630
HASHEMI-KIA, MOSTAFA N91-19478
HASHIMOTO, Y. N91-19889
N91-19890
HASINGER, G. N91-19978
HATHAWAY, W. T. N91-19326
HAUGHT, DEBORAH A. N91-19225
HAYASHI, RYUICHI N91-19226
HAYDEN, W. R. N91-19174
HAYNES, B. R. N91-19754
N91-19789
HAZEL, G. N91-19357
HAZELTON, LYMAN R., JR. N91-19026
HAZEN, JOHN D. N91-19138
HEAD, J. N91-20002
HEAD, J. W., III N91-20011
HEALTH, DONALD F. N91-19516
HEATHERLY, L. N91-19310
HEER, M. N91-19592
N91-19593
HEIDELBERG, L. J. N91-19825
HEIMEL, H. N91-19600
HEINEMANN, N. C. N91-19552
HELMS, GRETCHEN N91-19714
HEMMERSBACH-KRAUSE, RUTH N91-19631
HENDERSON, SAMMY W. N91-19498
HENDREY, G. N91-19538
HENKENER, JULIE A. N91-19274
HENRIST, M. N91-19142
N91-19151
HENSHAW, W. F. N91-19917
HEPP, ALOYSIUS F. N91-19256
N91-19296
N91-20015
HERBELL, THOMAS P. N91-19235
N91-19295
HERMAN, R. G. N91-19263
HERZOG, K. J. N91-19785
HESS, R. A. N91-19406
HICKEY, JOHN R. N91-19165
HICKMAN, J. M. N91-19178
HICKS, B. B. N91-19535
HICKS, RAYMOND M. N91-19062
HIGGINBOTHAM, SCOTT A. N91-19118
HILBIG, R. N91-19626
HILL, D. N. N91-19881
HILL, MYRON E. N91-19371
HILLIS, S. L. N91-19451
HILLS, J. S. N91-19186
HILLS, R. E. N91-19976
HILLSDON, G. N91-19411
HILSENRATH, ERNEST N91-19524
HINGHOFER-SZALKAY, H. N91-19600
HINGST, WARREN R. N91-19063
N91-19374
HINKS, D. G. N91-19919
HIROOKA, Y. N91-19911
HISATSUNE, K. N91-19937
HITNEY, HERBERT V. N91-19397
HIVONEN, JUHA-PEKKA N91-19428
HJALMARSON, A. N91-19993
HO, BRYAN P. N91-19169
HO, F. N91-19185
HOARTY, D. J. N91-19910
HODGSON, J. W. N91-19451
HOEHN, ALEXANDER N91-19660
HOFFHEINS, B. S. N91-19406
HOFFLER, G. W. N91-19711
HOFFMAN, D. A. N91-19776
HOFFMAN, DAVID J. N91-19462
HOFFMANN, UWE N91-19573
N91-19586
N91-19594
N91-19601
HOFSTETTER, K. N91-19580
HOGAN, J. N91-19881
HOJO, MASAKI N91-19226
HOLGADO, M. C. N91-19633
HOLLAND, W. R. N91-19872
HOLT, J. K. N91-19905
HOMMA, H. N91-19929
HONECY, FRANK S. N91-19209
N91-19224
HONES, E. W. N91-19552
HONMA, T. N91-19884
HOOKER, R. J. N91-19453
HOOVER, M. D. N91-19857
HORIOKA, KAZUHIKO N91-19885
HORNE, W. E. N91-19196
N91-19210
HORNER, G. S. N91-19191
HORWEDEL, B. M. N91-19544
N91-19795
HORWEDEL, J. E. N91-19795
HOSOYA, AKIO N91-19991
HOUCK, T. L. N91-19862
HOULSBY, G. T. N91-19791
HOWARD, D. J. N91-19926
HOWELL, R. H. N91-19919
HOZUMI, Y. N91-19888
HSIEH, TEHMING N91-19714
HUBER, D. A. N91-19193
HUBER, HELMUT N91-19085
N91-19086
N91-19091
HUDSON, LARRY D. N91-19077
HUDSON, R. D. N91-19518
N91-19523
N91-19527
HUIJSER, RON N91-19661
HULSEN, MARTIN A. N91-19394
HUNG, CHENG-HUNG N91-19260
HUNT, J. T. N91-19430
HUNTER, MARK W. N91-19496
HUNTLEY, WILLIAM P. N91-19328
HUNZINGER, E. N91-19634
HURST, G. B. N91-19258
HURTL, HEIDEMARIE V. N91-19662
HUSSAINI, M. Y. N91-19366
HUTCHBY, J. A. N91-19186
HUTCHINS, NANCY N91-19959
HWANG, YONG K. N91-19768
HYATT, MARK J. N91-19308

I

IACONO, M. J. N91-19532
IBRAHIM, MOUNIR B. N91-19375
ICE, G. E. N91-19937
IGLESIAS, C. A. N91-19910
ILES, P. A. N91-19185
N91-19186
IMAM, M. S. N91-19917
IMASAKI, K. N91-19884
IMMERMANN, M. W. N91-19682
INDRAWIRAWAN, H. N91-19272
INGEBO, ROBERT D. N91-19402
ISAACS, H. S. N91-19278
N91-19280
N91-19302

ISAYEV, S. K. N91-19808
ISHCHENKO, A. A. N91-19803
ISKANDER, S. K. N91-19270
ISRAEL, I. N91-19692
IUCCI, N. N91-20019
IVANENKO, I. P. N91-20020
IVERS, T. H. N91-19904
IVERSEN, T.-H. N91-19674
IWAI, HIROSHI N91-19228
IZEN, STEVEN H. N91-19404

J

JACKSON, A. O. N91-19702
N91-19703
JACKSON, D. M. N91-19398
JACKSON, G. L. N91-19881
JACKSON, M. M. N91-19711
JAIN, RAJ K. N91-19207
N91-19354
JAKOB, RUEDIGER N91-19732
JALEL, N. A. N91-19772
N91-19864
N91-19865
N91-19866
N91-19867
JAMES, C. E. N91-19407
JAMES, PHILIP B. N91-20003
JANG, JONG HOON N91-19376
JANG, P. R. N91-19905
JANSEN, E. L. N91-19491
JARRETT, BOBBY R. N91-19100
JASPER, G. L. N91-19529
JAYNE, DOUGLAS N91-19208
JENKINS, PHILLIP N91-19208
JENSEN, E. DOUGLAS N91-19725
JENSEN, G. A. N91-19290
JENSEN, G. L. N91-19923
JERVIS, T. R. N91-19428
JEZOWSKI, A. N91-19818
JIANG, WEIHUA N91-19887
JIN, J.-M. N91-19306
JOHANSEN, LARS BO N91-19602
N91-19612
JOHANSSON, L. E. B. N91-19994
JOHENNING, BERND N91-19120
JOHNSON, B. V. N91-19443
JOHNSON, D. W. N91-19908
JOHNSON, P. M. N91-19554
JOHNSON, R. N91-19347
JOHNSON, R. L. N91-19711
JOHNSON, STEVEN A. N91-19079
JOHNSON, W. C. N91-19484
JOLLER, P. W. N91-19598
JONES, G. N. N91-19797
JONES, J. P. N91-19447
JONES, JOANNE M. N91-19287
JONES, S. E. N91-19923
JONES, T. V. N91-19070
JOOP, O. N91-19663
JORDAN, HARRY F. N91-19345
N91-19732
JORGENSEN, ERIC L. N91-19342
JUDKINS, R. R. N91-19533
JULIENNE, ALAIN N91-19823
JUNG-HEILIGER, HILDEGARD N91-19664
JUNK, P. N91-19635
JUREWICZ, AMY J. N91-20009

K

KACHANOV, B. O. N91-19810
KADAMBI, JAIKRISHNAN R. N91-19479
KAHN, RALPH N91-20003
KAIJSER, L. N91-19615
KAIPER, G. V. N91-19740
KALE, VISHWAS S. N91-19997
KALEV, A. V. N91-19559
KALLNE, E. N91-19894
KALU, ALEX N91-20028
KAMEGAI, MANABU N91-19602
KAMIHATA, S. N91-19886
KAMIKAWA, NEIL N91-19870
KANAO, S. N91-19561
KANN, R. P. N91-19670
KARAMAT, E. N91-19588
KARAVASSILEV, PLAMEN RAYTCHEV N91-19916
KAREMAKER, JOHN M. N91-19575
KARGEL, JEFFREY S. N91-19997
KARLSSON, JOAKIM N91-19025
KARPUR, PRASANNA N91-19460
KASUYA, KOICHI N91-19885
KATNIK, GREGORY N. N91-19118
KATO, T. N91-19894
KATSUKI, SUNAO N91-19891
KATZ, J. L. N91-19260
KATZ, ROBERT N91-19699
KAVAYA, MICHAEL J. N91-19498
KAWATA, SHIGEO N91-19883
KEANE, C. J. N91-19429
N91-19433
N91-19898
KEDWARD, KEITH T. N91-19241
KEEFER, K. D. N91-19942
KEHOE, MICHAEL W. N91-19083
KEHS, R. A. N91-19358
KEINIGS, R. K. N91-19858
KEITH, THEO G., JR. N91-19063
N91-19475
KELLER, TONY S. N91-19603
KELLY, M. D. N91-19281
KEMMOCHI, KIYOSHI N91-19226
KENDIG, M. W. N91-19302
KENNER, I. N91-19595
KENNY, SEAN P. N91-19471
KERKVLIET, S. N91-19624
KERLAU, J. N91-19684
KERSLAKE, THOMAS W. N91-19177
KEYES, B. L. P. N91-19300
KHAVRONIN, V. P. N91-19944
KHEMTHONG, S. N91-19215
KHRUSHCHEV, I. YU. N91-19812
KIEFER, JUERGEN N91-19683
N91-19686
N91-19696
KIEFFER, ARTHUR W. N91-19115
KIERSTEAD, J. A. N91-19359
KIESS, M. N91-19621
KILCHERT, L. N91-19109
KILKENNY, J. D. N91-19400
KILLOUGH, S. M. N91-19445
KILROY, KEVIN L. N91-19478
KIM, C. K. N91-19687
KIM, K. J. N91-19425
KIM, KWANG-JE N91-19426
KIM, N. P. N91-19190
KIM, S.-W. N91-19367
KINDER, S. J. N91-19762
KING, B. D. N91-19190
KING, T. V. V. N91-20004
KINGDON, J. N91-19589
KIRK, B. L. N91-19749
KIRK, H. N91-19432
KIRK, R. L. N91-20005
KIRSCH, K. A. N91-19604
KISSEL, GERHARD N91-19101
KITAMURA, A. N91-19886
KITSUNEZAKI, AKIO N91-19912
KLAMUT, J. N91-19818
KLAPISCH, M. N91-19416
KLIER, K. N91-19263
KLINE, PAUL N91-19032
KLINTWORTH, R. N91-19666
KLOECK, G. N91-19321
N91-19654
KLOEPPEL, VALENTIN N91-19086
N91-19087
KLOSTERMAN, EDWARD L. N91-19460
KOBANA, AKIRA N91-19913
KOCKS, U. F. N91-19480
KOEHLER, M. N91-19631
KOELLE, H. HERMANN N91-19120
KOENIG, EVA MARIA N91-19600
KOENIG, G. L. N91-19525
KOERTJE, J. H. N91-19638
KOIKE, A. N91-19066
KOIKE, F. N91-19894
KOKOVA, N. N91-19577
N91-19578
KOLAFA, J. J. N91-19611
KOLB, G. J. N91-19510
KOMATSU, GORO N91-19997
KOMATSU, Y. N91-19066
KOMHYR, W. D. N91-19525
KONDAUROV, M. N. N91-19752
KONECNY, R. N91-19414
KONSTANTINOVA, IRENA V. N91-19619
KOPTEV, V. P. N91-19945
KORDYUM, E. L. N91-19674
KORNILOVA, L. N. N91-19642
KORNIYENKO, L. S. N91-19808
KOROBKIN, D. V. N91-19812
KOROLKOV, V. I. N91-19645
KOROS, W. J. N91-19309
KORTING, P. A. O. G. N91-19222
KORTSCHOT, HENDRIKA W. N91-19579
N91-19693
KOSHIZAKI, NAOTO N91-19226
KOSLOVA, S. B. N91-19679
KOST, MICHAEL N91-19683
KOTOVSKAIA, A. N91-19617
KOURTIDES, DEMETRIUS A. N91-19304
KOWALSKI, M. N91-19321
N91-19654
KOZLOVA, S. B. N91-19684
KOZLOVSKAYA, I. B. N91-19576
N91-19588
N91-19597
N91-19642
KOZYREV, A. B. N91-19815
KRAMER, D. P. N91-19281
KRANER, H. W. N91-19359
N91-19361
KRANZ, A. R. N91-19680
N91-19682
N91-19685
KRASNER, HERB N91-19728
KRASNY, R. N91-19264
KRASOTKIN, A. F. N91-20021
KREIS, W. N91-19652
KRESS, ROBERT N91-19160
KREUZBERG, KARLHEINZ N91-19663
KRIKORIAN, ABRAHAM D. N91-19670
KRISHNAMURTHY, R. V. N91-20006
KRISTIANSEN, M. N91-19303
KROGERUS, O. N91-19316
KRUIJER, WIEBE N91-19623
KRUMPELT, M. N91-19314
KRUMREY, MICHAEL N91-19856
KRUSE, S. M. N91-19500
KRUT, D. D. N91-19184
KRUTYAKOV, V. V. N91-19811
KUBIAK, CLIFFORD P. N91-20015
KUCHKO, A. N. N91-19816
KUCHNIR, M. N91-19821
KUFELD, ROBERT M. N91-19052
KUHL, MARK R. N91-19029
KULKARNI, S. R. N91-19975
KUMAR, K. S. N91-19233
KUMAR, R. N91-19314
N91-19507
N91-19937
KUNATH, RICHARD R. N91-19349
KUNG, H. H. N91-19939
KUPPERMAN, D. S. N91-19242
N91-19301
KURATA, YUJI N91-19284
KURLAND, RICHARD M. N91-19217
KURTZ, H. L. N91-19173
KURYLA, M. S. N91-19188
N91-19194
KUYKENS, H. J. P. N91-19575
KUZHEVSKIJ, B. M. N91-20016
KUZMIN, L. A. N91-19945
KUZMIN, YU. V. N91-19987
KUZNETSOV, S. L. N91-19568
KUZNETSOV, V. P. N91-19819
KUZYK, M. G. N91-19872
KUZYUTA, E. I. N91-19571
KVARTSOV, N. V. N91-19808
KVETNANSKY, R. N91-19689
KYYNAERAEINEN, JUKKA N91-19830

L

LACAVA, F. N91-19854
LAFLIN, N. J. N91-19329
LAFONTAINE, B. N91-19895
LAGARDE, D. N91-19649
LAGUNA, G. N91-19783
LAI, MING-CHIA N91-19048
LALVANI, HARESH N91-19168
LAMBERT, KEVIN M. N91-19350
LAMPPA, D. L. N91-19942
LAN, E. H. N91-19146
LANAGAN, M. T. N91-19941
LANDEN, O. N91-19400
LANDHEIM, R. N91-20007
LANDIS, GEOFFREY A. N91-19176
N91-19198
N91-19201
N91-20015
LANGHORN, A. N91-19881
LAPCHINE, LYDIE N91-19632
LAPOTKO, D. O. N91-19802
LASSMANN, JENS N91-19121
LATHAM, P. E. N91-19358
LAUDIEN, ECKEHARD N91-19828
LAWRENCE, C. N91-19178
LAWTON, E. N91-19596
LAZARZ, N. M. N91-19712
LEE, CHUNG M. N91-19250
LEE, E. N91-19140
N91-19141
LEE, H.-J. N91-19229

LEE, J. N91-19621
N91-19634
LEE, JA H. N91-19415
LEE, R. C. N91-19413
LEE, R. W. N91-19910
LEE, STEVE N91-20003
LEE, WOODROW W. N91-19171
LEFORT, L. N91-19691
LEGASSE, R. R. N91-19297
LEGREE, PETER J. N91-19713
LEHMER, R. N91-19911
LEI, JIH-FEN N91-19403
LEIB, S. J. N91-19372
LEIKIND, B. N91-19881
LEITE, ROSANGELA M. G. N91-19130
LENZ, GUENTER N91-19683
LEONARD, ANTHONY N91-19071
LEONARD, J. A. N91-19322
LEONARD, R. K. N91-19525
LEPPENS, H. N91-19637
LESAR, R. N91-19928
LESLIE, P. K. N91-19297
LESTIENNE, F. N91-19691
LETOULLEC, C. N91-19596
LEUNG, W. N91-19911
LEVICK, Y. S. N91-19691
LEVINE, H. G. N91-19670
LEVITT, K. N91-19756
LEVUSH, B. N91-19358
LEVY, P. W. N91-19359
LEWIN, K. N91-19538
LEWIS, ROY S. N91-19998
LI, X. N91-19202
LI, Y. N91-19214
LI, YOUFU N91-19459
LI, ZHENG N91-19361
LICHIENBERGER, D. L. N91-19275
LICKLIDER, ROBERT A. N91-19764
LIENESCH, JAMES H. N91-19517
LILLEY, ROBERT W. N91-19028
LILLINGTON, D. R. N91-19184
LIM, TEIK CHIN N91-19435
LINDNER, J. S. N91-19905
LINDQVIST, M. N91-19993
LINK, H. F. N91-19501
LINKE-HOMMES, A. N91-19636
LINKOUS, R. L. N91-19240
LINNARSSON, DAD N91-19573
LINSE, DENNIS J. N91-19037
N91-19039
LIPFERT, F. W. N91-19538
N91-19542
LIPPMANN, S. N91-19881
LIPSCHITS, M. I. N91-19581
N91-19692
N91-19694
LITTLE, BRENDA J. N91-19287
LITVIN, FAYDOR L. N91-19439
LIU, CHING SHYONG N91-19467
LIU, S. H. N91-19255
LO, CHING F. N91-19765
LOAR, J. M. N91-19539
LOBACHIK, V. I. N91-19645
LOBAO, X. N91-19582
LOEFFLER, IRVIN J. N91-19045
LOGAN, C. M. N91-19466
LOGSDON, KIRK A. N91-19324
LOGVINOVA, G. YU. N91-19944
LOHMANN, ULRICH G. N91-19664
LONGO, E. N91-19868
LOOSE, WERNER N91-19393
LORENC, S. A. N91-19174
LOTT, S. E. N91-19352
LOTTES, S. A. N91-19252
LOU, W. R. N91-19358
LOUBATON, PHILIPPE N91-19798
LOWDERMILK, W. H. N91-19430
LOZOVAYA, V. V. N91-19674
LU, CHU-HO N91-20029
LU, SHIN-YEE N91-19758
LUBELL, M. S. N91-19950
LUCK, C. F. N91-19925
LUDWIG, DAVID N91-20030
LUE, J. W. N91-19950
LUHMANN, N. N91-19418
LUI, ANDREW N91-19714
LUSK, E. N91-19760
LUTTGES, MARVIN W. N91-19660
LUZYANIN, I. D. N91-19944
LYABIN, N. A. N91-19806
LYMAN, J. L. N91-19257
LYNCH, T. N91-19545
LYON, J. F. N91-19901

M

MAASS, H. N91-19598
MACAU, J. P. N91-19142
N91-19151
MACDONALD, RAINER N91-19878
MACGOWAN, B. J. N91-19429
N91-19433
MACHO, L. N91-19689
MACMILLAN, H. F. N91-19188
MAEDA, SADAO N91-19891
MAES, J. N91-19637
MAGDICH, L. N. N91-19808
MAGEDOV, V. N91-19649
MAGNANI, N. J. N91-19352
MAGOMEDOV, A. G. N91-19570
MAGRINI, FABIO N91-19644
MAHAJAN, APARAJIT J. N91-19475
MAHDAVI, M. A. N91-19881
MAJLRZAK, C. F. N91-19929
MAJUMDAR, S. N91-19242
MAKARENKO, A. YU. N91-19812
MAKHNOVSKIY, V. P. N91-19571
MALANEY, R. A. N91-19984
N91-19985
MANCIA, G. N91-19599
MANFREDI, P. F. N91-19360
MANG, VOLKER N91-19321
N91-19654
MANHEIMER, W. M. N91-19413
MANIE, S. N91-19619
MANKBADI, REDA R. N91-19373
MANTELLI, MARCIA BARBOSA HENRIQUES
N91-19130
N91-19157
MARCINIAK, T. J. N91-19440
MARCO, R. N91-19633
MARCOTTE, K. N91-19347
MARK, J. E. N91-19291
MARMAR, E. S. N91-19894
MAROSI, MIKLOS N91-19588
N91-19597
MARR, W. W. N91-19440
MARSOSUDIRO, P. N91-19545
MARTHY, HANS-JUERG N91-19625
MARTIN, LEONARD N91-20003
MARTIN, M. E. N91-19346
MARTIN, RICHARD W. N91-19460
MARTIN, W. R. N91-19254
N91-19794
MARTINELLI, L. N91-19043
MARTINEZ, D. R. N91-19793
MARTYNENKO, O. G. N91-19802
MARTZ, H. E. N91-19466
MARVIN, DEAN N91-19220
MASAI, K. N91-19894
MASE, G. T. N91-19236
MASON, LEE S. N91-19112
MASSA, R. N91-19647
MASSAGLIA, S. N91-19365
MASSIMINO, D. N91-19657
MASSIMINO, J. N91-19657
MASUGATA, KATSUMI N91-19887
N91-19888
MATHERNE, J. L. N91-19251
N91-19313
MATSAKIS, YOANI N91-19694
MATSUNASHI, S. N91-19380
MATTERN, DUANE N91-19766
MATTHEWS, D. L. N91-19429
N91-19433
N91-19895
MATTOUT, R. N91-19627
MATTY, JERE J. N91-19139
MAURITZEN, DAVID N91-20031
MAVRIPLIS, D. J. N91-19043
MAXON, S. N91-19433
MAY, BRIAN D. N91-19348
MAYDEW, M. C. N91-19322
MCALLISTER, DAVID F. N91-19741
MCARDLE, FRANK J. N91-19688
MCCLELLAND, R. W. N91-19190
MCCLUNG, R. W. N91-19465
MCCORD, R. A. N91-19961
MCDERMOTT, D. N91-19418
MCDONNELL, TONY N91-20008
MCELROY, D. L. N91-19240
MCFADDEN, P. D. N91-19457
N91-19495
MCGILL, G. E. N91-20011
MCGILL, R. N. N91-19451
MCHALE, J. N91-19954
MCHENRY, STEVEN T. N91-19167
MCINTYRE, D. C. N91-19922
MCIVOR, J. D. C. N91-19470
MCKAY, DAVID S. N91-20009
MCKEAN, M. E. N91-19860
MCKECHNIE, T. S. N91-19421
MCKINZIE, DANIEL J., JR. N91-19370
MCLAREN, ANNE N91-19622
MCNEELY, J. B. N91-19187
MCNEIL, MICHAEL B. N91-19287
MCPETERS, RICHARD D. N91-19520
N91-19523
N91-19527
MEAZZA, R. N91-19644
MEHRLE, WERNER N91-19652
MEHTA, NARINDER N91-20032
MEI, V. C. N91-19950
MEIER, THOMAS N91-19121
MELICHAR, T. N91-19588
MELIS, MATTHEW E. N91-19441
MELNICK, J. N91-19978
MELOSH, H. J. N91-19996
MENDELSOHN, M. L. N91-19698
MERKLE, CHARLES L. N91-19059
MERKLE, K. L. N91-19299
MERKYS, A. J. N91-19671
MERRILL, ALFRED H., JR. N91-19709
MERRILL, WALTER N91-19766
MERTZ, G. E. N91-19483
MESLAND, DICK A. M. N91-19618
MESSIDORO, PIERO N91-19158
METTU, SAMBI R. N91-19273
MEYER, MEINHARD N91-19311
MEYERS, T. P. N91-19535
MICHALAKES, J. G. N91-19534
MICHAUD, L. J. N91-19610
MICKELSEN, R. A. N91-19190
MIELKE, MICHAEL N91-19114
MIKHAYLOV, V. P. N91-19803
MIKHAYLOV, V. YU. N91-19808
MIKIRTYCHYANTS, S. M. N91-19945
MIKULSKI, BARBARA N91-19966
MILAM, LAURA J. N91-19128
MILES, JEFFREY HILTON N91-19044
MILHAUD, CLAUDE N91-19648
N91-19649
MILLER, A. C. N91-19263
MILLER, A. J. N91-19521
MILLER, DAVID P. N91-19054
MILLER, E. K. N91-19333
MILLER, JOHN R. N91-19344
MILLER, WARNER N91-19734
MIQUEL, JAIME N91-19633
MIRIN, A. A. N91-19740
MISEROCCHI, GIUSEPPE N91-19651
MISRA, MOHAN S. N91-19238
MITCHELL, T. J. N91-19785
MITRIKAS, V. G. N91-19679
MITTELSTAEDT, HORST N91-19605
MIX, G. N91-19659
MIYAHARA, A. N91-19896
MIYAKE, K. N91-19561
MIYAMOTO, S. N91-19884
MIYANAGA, Y. N91-19380
MOATTI, J. P. N91-19632
MOATTI, N. N91-19632
MOBELY, ROBERT L. N91-19551
MODDEMAN, W. E. N91-19281
MOES, TIMOTHY R. N91-19095
MOLTON, P. M. N91-19290
MOLZ, B. N91-19592
N91-19593
MONTANARI, S. N91-19999
MONTI, R. N91-19620
MONTOYA, N. I. N91-19405
MONTUFAR-SOLIS, DINA N91-19628
MOORE, H. J. N91-20011
MOORE, J. N91-19634
MOORE, M. R. N91-19406
MOORE, RICHARD K. N91-19340
MORAN, J. P. N91-19269
MORAN, MATTHEW E. N91-19317
MORCRETTE, JEAN-JACQUES N91-19551
MORE, H. N91-19614
MOREL, M. N91-19237
MORGAN, M. D. N91-19210
MOROSIN, B. N91-19936
MORRELL, FREDERICK R. N91-19024
MORRIS, H. E. N91-19334
MORRIS, M. D. N91-19785
MORRIS, RICHARD V. N91-20009
MORRIS, T. J. N91-19702
N91-19703
MORRISON, P. J. N91-19787
MORTON, S. K. N91-19244
N91-19245
N91-19247
MOSER, M. N91-19595
MOSLEY, W. C. N91-19277

MOSSAHEB, MASSUD N91-19584
MOULIN, H. R. N91-19712
MUELLER, CHRISTIAN N91-19606
MUELLER, E. N91-19365
MUELLER, J. N91-19598
MUELLER, OTFRIED N91-19634
MUELLER, R. N91-19876
MUIGG, ARMIN N91-19588
MULGUND, SANDEEP S. N91-19035
MURAOKA, ISSAMU N91-19130
MURCHIE, S. N91-20002
MURCRAY, D. N91-19555
MURPHREE, J. S. N91-19552
MURPHY, R. W. N91-19950
MURRAY, J. R. N91-19430
MURRAY, JERRY N91-19714
MURTHY, P. L. N. N91-19229
N91-19230
N91-19236
MYERS, S. M. N91-19922
MYLES, K. M. N91-19314

N

NAGASAWA, CHOHACHIRO N91-19226
NAGATANI, R. N91-19521
NAGY, J. N91-19538
NAJAFABADI, R. N91-19928
NAKAGAWA, ARTHUR N91-19870
NAKAI, S. N91-19884
NAKAJIMA, HAJIME N91-19284
NAKAJIMA, T. N91-19886
NAKAMURA, M. N91-19066
NAKAMURA, MASATO N91-19880
NALLASAMY, M. N91-19825
NANSTAD, R. K. N91-19270
NARAMOTO, HIROYA N91-19892
NARAYANAMURTI, V. N91-19932
NARRAWAY, J. N91-19624
NASTASI, M. N91-19428
NATHRATH, N. N91-19336
NEAL, CLIVE R. N91-20010
NEALY, JOHN E. N91-19699
NEARY, PATRICK F. N91-19134
NEDERBRAGT, ANNEKE N91-19641
NEGRINI, DANIELA N91-19651
NELSON, D. A. N91-19290
NELSON, R. C. N91-19857
NEMIROVSKII, S. K. N91-19827
NEUBERT, JUERGEN W. N91-19635
NEUMAN, JAMES C. N91-19127
NGUYEN, K. N91-19143
NGUYEN, VAN DAT N91-19679
N91-19684
NI, L. M. N91-19744
NICHIPORUK, I. A. N91-19607
NICHOLSON, H. N91-19772
N91-19864
N91-19865
N91-19866
N91-19867
NIESL, GEORGE N91-19828
NIEUWENHUIZEN, M. P. N91-19169
NIKOLAEV, R. K. N91-19945
NINANE, N. N91-19142
NITSCHKE, DIETER N91-19088
NIU, KEISHIRO N91-19892
N91-19893
NOBILE, A., JR. N91-19277
NOBLE, J. N91-19411
NOBUHARA, S. N91-19889
N91-19890
NOREM, J. N91-19414
NORRIS, E. B. N91-19452
NORSK, PETER N91-19592
N91-19593
N91-19602
N91-19612
NOSKOV, V. N91-19689
NOTENBOOM, RONALD P. N91-19493
NOTIS, M. R. N91-19940
NOUSEK, JOHN A. N91-19736
NOVAK, J. H. N91-19546
NOVARINI, A. N91-19599
NOVIKOV, V. E. N91-19608
NYGREN, A. N91-19615
NYMAN, L. A. N91-19993

O

OBRIEN, J. C. N91-19919
OEGELMAN, H. N91-19978
OGANOV, V. S. N91-19608
OGILBY, P. R. N91-19303
OGURA, KOICHI N91-19913
OHLSEN, H. N91-19616
OKHLOPKOV, V. P. N91-20021
OKHUYSEN, W. P. N91-19905
OLBERG, M. N91-19977
OLDENBORG, R. C. N91-19257
OLEARY, SCOTT T. N91-19161
OLOFSSON, H. N91-19993
N91-19994
OLSEN, K. B. N91-19409
OLSEN, L. C. N91-19193
OLSEN, LARRY E. N91-19824
OLSEN, RANDALL B. N91-19212
OLSON, D. A. N91-19931
OLSON, JACK R. N91-19397
OMALLEY, TERENCE F. N91-19371
OMATETE, O. O. N91-19239
OMIDI, N. N91-19860
ONEILL, MARK J. N91-19189
N91-19219
ONEILL, P. J. N91-19368
ONG, CHING CHO N91-19050
OOSTERVELD, WILHELMUS J. N91-19579
N91-19693
ORCUTT, JOHN A. N91-19564
OREG, J. N91-19900
ORLETSKI, DIRK N91-19441
ORMAN, J. L. N91-19960
N91-19965
ORR, E. N91-19413
ORZECHOWSKI, T. J. N91-19417
OSBORNE-LEE, A. E. N91-19544
OSTERHELD, A. L. N91-19433
OVCHARENKO, S. I. N91-19810
OVERSLUIZEN, T. N91-19712
OZEKI, TAKAHISA N91-19914
OZERNOY, L. M. N91-19986
OZKUL, M. H. N91-19291

P

PAAS, MICHEL HENDRIK JULIUS WILHELM N91-19490
PACIESAS, WILLIAM S. N91-19980
PADEKEN, DITTMAR N91-19609
PAINE, D. C. N91-19926
PAISLEY, D. L. N91-19405
PAIVA, MANUEL N91-19574
PAKUNOV, A. T. N91-19569
PALASZEWSKI, BRYAN A. N91-19175
PALKO, JOSEPH L. N91-19292
PALM, R. G. N91-19301
PALMER, E. P. N91-19923
PALMER, T. S. N91-19780
PALOSKI, WILLIAM H. N91-19610
PAMULAPATI, J. N91-19351
N91-19935
PANCHAL, C. B. N91-19501
N91-19508
PAPP, MARY L. N91-19460
PAPPA, RICHARD S. N91-19474
PARANG, M. N91-19378
PARATI, G. N91-19599
PARENT, M. G. N91-19879
PARKER, D. E. N91-19610
PARKER, G. N91-19478
PARKS, ROBERT N91-19871
PARMENTIER, N. N91-19679
PARROT, H. N91-19322
PARROT, L. N91-19322
PARSONS, B. K. N91-19501
PARSONS, J. M. N91-19501
PARTAIN, L. D. N91-19188
PASI, P. N91-19689
PATAT, F. N91-19577
N91-19578
PATRICK, D. L. N91-19424
PATTERSON, MICHAEL J. N91-19180
PAUL, D. R. N91-19309
PAULSON, S. E. N91-19560
PAULUS, RICHARD A. N91-19397
PAULUS, U. N91-19638
PAWLOWSKY, KARIN N91-19686
PAYSON, J. S. N91-19214
PEDERSEN, H. N91-19978
PEER, R. L. N91-19549
PELLETIER, MICHAEL E. N91-19111
PELTONEN, JUHANI K. N91-19363
PENNER, J. E. N91-19553
PEPPER, STEPHEN V. N91-19224
PERBAL, G. N91-19672
PERDIGAO, J. N91-19631
PEREZ-DAVIS, MARLA E. N91-19156
N91-19160
PERILLAT, P. N91-20001
PERKINS, F. W. N91-19908
PERLACK, R. D. N91-19506
PERRY, T. S. N91-19910
PESARAN, A. A. N91-19501
PESTOV, I. D. N91-19576
PETERKA, ROBERT J. N91-19710
PETERSON, D. T. N91-19272
PETRIY, O. A. N91-19819
PETROV, V. M. N91-19679
N91-19684
PETTERSON, B. J. N91-19481
PEYGIN, S. V. N91-19801
PHILLIP, T. N91-19746
PIANEZZI, B. N91-19630
PICCIOLO, J. J. N91-19299
PICCOT, S. D. N91-19545
PICKARD, P. S. N91-19431
PICKERT, M. N91-19682
N91-19685
PIERCE, T. E. N91-19546
PIETERS, C. N91-20002
PIETSCH, W. N91-19978
PIN, F. G. N91-19445
N91-19769
PIPPIA, P. N91-19620
PISZCZOR, MICHAEL F., JR. N91-19219
PIZZARELLO, S. N91-20006
PIZZUTI, G. P. N91-19629
PLAKHTIJ, V. P. N91-19943
PLANET, WALTER G. N91-19514
N91-19527
PLUMER, EDWARD S. N91-19771
PLUTCHAK, J. N91-20002
POEPPEL, R. B. N91-19299
N91-19941
POISEL, H. N91-19877
POLIAKOV, V. V. N91-19576
N91-19577
N91-19578
PONCHAK, GEORGE E. N91-19332
PONOMAREV, A. T. N91-19810
PONOMAREV, YA. G. N91-19819
POOL, F. S. N91-19211
POPOV, K. E. N91-19581
N91-19691
N91-19692
POPOVIC, M. N91-19356
PORRO, A. ROBERT N91-19063
N91-19374
PORTER, TIM N91-19730
PORTMAN, D. A. N91-19532
POTTER, GERALD L. N91-19551
POTTIER, J. M. N91-19577
N91-19578
POUGET, J. F. N91-19690
POWELL, M. R. N91-19544
PRIMM, R. T., III N91-19784
PRIVALOV, V. YE. N91-19813
PROKHOROV, A. M. N91-19812
N91-19817
PROVENZANO, V. N91-19917
PUTRA, ICHSAN S. N91-19492

Q

QUACKENBUSH, TODD R. N91-19050
N91-19067
QUONIAM, CYNTHIA N91-19581

R

RABAS, T. N91-19508
RACANELLI, M. N91-19926
RADEKA, V. N91-19359
N91-19360
RADER, D. J. N91-19922
RADOUSKY, H. B. N91-19919
RAHMANN, HINRICH N91-19626
N91-19638
RAINER, J. N91-19597
RAINEY, SAMUEL C. N91-19342
RAKHMANOV, A. S. N91-19608
RALPH, E. N91-19184
RAMIREZ, E. N91-19633
RANGARAJAN, G. N91-19427
RANSON, K. J. N91-19497
RAPOPORT, I. D. N91-20020
RAPP, HELMUT N91-19089
N91-19485
RAPTIS, A. C. N91-19301
RASMUSSEN, OLE N91-19674
RATHKOPF, J. A. N91-19794
RAVOGLI, ANTONELLA N91-19599
RAWAL, SURAJ P. N91-19238
RAY, LAURIE RYAN N91-19036

RE, F. N91-20019
READ, D. N91-19323
REED, E. K. N91-19331
REEDER, J. R. N91-19482
REEFMAN, D. N91-19243
REES, L. B. N91-19923
REGGIANI, P. N91-19644
REINACH, Y. N91-19604
REINHARD, E. N91-19652
REINL, WERNER N91-19085
REISER, M. N91-19580
REISTER, D. B. N91-19446
N91-19447
REITSTETTER, R. N91-19636
RENDER, M. E. J. N91-19093
RENK, THOMAS N91-19121
RENO, CHARLES J. N91-19054
RESCHKE, M. F. N91-19610
N91-19611
RESCIA, S. N91-19359
N91-19360
RHODES, PERCY H. N91-19653
RICE, J. E. N91-19894
RICE, ROBERT F. N91-19733
N91-19734
RICHOILLEY, G. N91-19632
RICHTER, PETER N91-19087
RICHWINE, DAVID M. N91-19051
RIEDER, ANDREAS N91-19799
RIEGER, D. N91-19276
RIESTER, J. E. N91-19379
RIGHETTI, PIER GIORGIO N91-19665
RIJKEN, PHILIP J. N91-19623
RIONDINO, G. N91-19614
RIPPEL, W. E. N91-19355
RISTOW, M. LADLE N91-19188
N91-19194
ROBERSON, G. P. N91-19466
ROBERTS, A. M. N91-19547
ROBERTSON, I. M. N91-19266
ROBERTSON, J. D. N91-19925
ROBINETT, R. D. N91-19481
ROCHELLE, R. W. N91-19406
RODI, W. L. N91-19558
ROECKER, LOTHAR N91-19592
N91-19593
ROETTGER, CHRISTIAN N91-19170
ROFER, C. K. N91-19257
ROLL, J. P. N91-19581
ROOS, FREDERICK W. N91-19062
ROSE, JAMES D. N91-19436
ROSEN, M. D. N91-19895
ROSENBLUTH, M. N. N91-19908
ROSHKO, ANATOL N91-19071
ROSS, DAN N91-19306
ROSSIKHIN, YU. A. N91-19809
ROSSITER, ROBERT J. N91-19434
ROTENBERG, V. N91-19649
ROTH, DON J. N91-19463
ROTHERMEL, H. N91-19977
RUDASHEVSKIY, YE. G. N91-19817
RUDDELL, MARK J. N91-19460
RUEGSEGGER, P. N91-19690
RUEL, CRISTIAN N91-19131
RUIZ, D. N91-19411
RUSSEL, A. P. G. N91-19976
RUSSELL, R. A. N91-19299
RUSSELL, T. N91-19536
RUSTAMOV, S. R. N91-19808
RUTH, R. D. N91-19778
RYAN, E. N91-19996
RYAN, LAURIE E. N91-19038
RYDBECK, G. N91-19977
N91-19994
RYNE, R. D. N91-19862
RYNNE, EDWARD F. N91-19341

S

SABIERS, R. L. N91-19174
SACHER, REINHARD A. N91-19662
SACHTLER, W. M. H. N91-19261
SACK, FRED D. N91-19668
SADANANDA, K. N91-19917
SAEED, M. N91-19835
SAENGER, G. N91-19155
SAITO, YASUHIRO N91-19885
SALEM, JONATHAN A. N91-19293
SALES, B. C. N91-19925
SALMON, N. J. N91-19487
SALMON, R. A. N91-19329
SALTIN, B. N91-19687
SALTSMAN, JAMES F. N91-19473
SAMOYLOVA, T. B. N91-19815
SANCESARIO, GIUSEPPE N91-19647
SANGANI, A. S. N91-19377
SANGHVI, M. K. N91-19533
SANTINI, C. N91-19978
SANYAL, M. K. N91-19929
SARAPH, G. N91-19357
SARAVANOS, D. A. N91-19237
SASAKI, MISAO N91-19989
SATIJA, S. K. N91-19929
SATO, M. N91-19889
N91-19890
SATO, TOSHIAKI N91-19883
SATTERFIELD, C. N. N91-19250
SAUNDERS, R. S. N91-20011
SAVAGE, MICHAEL N91-19438
SAWADA, H. N91-19066
SAWADA, KEIJI N91-19852
SCHABER, G. G. N91-20011
SCHADOW, KLAUS C. N91-19364
SCHAFFAR, LAURENCE N91-19619
SCHATZ, ALBRECHT N91-19635
N91-19636
SCHAUER, R. N91-19588
N91-19597
SCHAUS, J. E. N91-19440
SCHAUWER, J. N91-19708
SCHEIMAN, DAVID A. N91-19216
SCHENK, AXEL N91-19474
SCHENK, KARIN N91-19686
SCHERER, H. N91-19591
SCHIAFFINO, S. N91-19646
SCHIAVILLA, R. N91-19838
SCHICK, W. R. N91-19452
SCHIEMAN, DAVID A. N91-19216
SCHIJVE, J. N91-19492
SCHILLER, PETER N91-19589
SCHLACHTER, A. S. N91-19861
SCHLEIER, HOWARD N91-20033
SCHLESINGER, B. M. N91-19518
SCHLOSSBERGER, MATTHIAS N91-19592
N91-19593
SCHMIDT, D. W. N91-19827
SCHMIDT, GEORGE T. N91-19731
SCHMIED, J. N91-19600
SCHMITT N91-19108
SCHMITZ, L. N91-19911
SCHMITZ, P. N91-19675
SCHMITZ, PAUL C. N91-19112
SCHNABL, HEIDE N91-19675
SCHNEBERK, D. J. N91-19466
SCHNEIDER, D. A. N91-19297
SCHOENWALD, D. A. N91-19448
SCHOETERS, GREET E. R. N91-19637
SCHONBERG, WILLIAM P. N91-19164
SCHOUTEN, G. N91-19456
N91-19831
SCHRADE, H. O. N91-19173
SCHRANNER, RUDOLF N91-19090
SCHUBER, MARIANNE N91-19609
SCHULTZ, J. C. N91-19188
SCHULZ, THOMAS N91-19121
SCHUMACHER, J. N91-19110
SCHWARTZ, S. E. N91-19535
SCHWEE, LEONARD J. N91-19717
SCIALDONE, JOHN J. N91-19135
SCOFIELD, J. H. N91-19433
SCORSONE, L. V. N91-19138
SCOTT, JAMES R. N91-19053
SCOTT, MICHAEL A. N91-19471
SCOTT, S. D. N91-19908
SEABLOM, KIRK D. N91-19063
SECHI, G. N91-19620
SEE, MICHAEL J. N91-19726
SEGALMAN, D. J. N91-19448
SEIBT, DIETER N91-19609
SEIN, J. H. N91-19560
SEKAR, R. R. N91-19440
SEKIMOTO, Y. N91-19888
SEKULA-MOISE, P. A. N91-19935
SENYITKO, RICHARD G. N91-19401
SERDUKE, F. J. N91-19910
SEROV, I. N91-19619
SESSLER, A. M. N91-19418
N91-19427
SETTELS, J. J. N91-19575
SEVERNS, JAMES N91-19220
SEXTON, J. ANDREW N91-19325
SHANAZAROV, A. S. N91-19571
SHANKAR, RENUKA N91-19714
SHARP, PAUL R. N91-19267
SHARP, W. M. N91-19418
N91-19427
SHCHERBAKOV, G. V. N91-19945
SHEEN, S. H. N91-19301
SHELTON, R. N. N91-19919
SHERMAN, D. M. N91-20004
SHESTOPEROV, V. YA. N91-20020
SHI, D. N91-19941
SHIAO, MICHAEL N91-19472
SHIBATA, KIYOSHI N91-19888
SHIBATA, TAKEMASA N91-19913
SHIGETA, M. N91-19888
SHIKAMA, T. N91-19271
SHIMIYA, K. N91-19888
SHIMKAVEG, G. N91-19433
SHIMP, N. R. N91-19174
SHIN, JAIWON N91-19047
SHINDO, T. N91-19561
SHINN, JUDY N91-19699
SHIRAISHI, T. N91-19937
SHKADAREVICH, A. P. N91-19803
SHOJI, T. N91-19911
SHOTTON, CHUCK N91-19727
SHU, HAO-FENG N91-19420
SIDOROV, N. S. N91-19945
SIEG, R. E. N91-19351
SIEG, R. M. N91-19935
SIEGEL, D. I. N91-19543
SIEGRIST, M. N91-19679
N91-19684
SIEVERS, A. N91-19667
N91-19669
SIGGIA, E. D. N91-19382
SIGNORETTI, F. N91-20019
SILK, J. I. N91-19859
SILVER, J. N91-19213
SIMMONS, G. W. N91-19263
SIMPSON, A. N91-19487
SINDELAR, R. L. N91-19483
SINGER, K. D. N91-19872
SINGER, ROBERT N91-20003
SINGH, A. N91-19357
SINGH, J. P. N91-19242
SINGH, N. B. N91-19320
SINGH, RAJENDRA N91-19435
SINGHAL, S. N. N91-19230
SINHA, S. K. N91-19929
SIROTA, M. G. N91-19642
SKIDMORE, TRENT N91-19031
SKINNER, N. C. N91-19610
SKINNER, S. BALLOU N91-20034
SKOOG, AKE INGEMAR N91-19656
SLATKIN, D. N. N91-19712
SLATTERY, W. L. N91-20012
SLEEFE, G. E. N91-19407
SLENZKA, KLAUS N91-19626
N91-19638
SLIFER, LUTHER W., JR. N91-19199
SLINGO, JULIA M. N91-19551
SLUITER, M. N91-19268
SMIT, D. J. N91-19951
SMITH, A. C. N91-19556
SMITH, C. A. N91-19146
SMITH, C. C. N91-19910
SMITH, CHARLES F. N91-19918
SMITH, CLIFFORD E. N91-19048
SMITH, ROBERT A. N91-19364
SMITH, S. J. N91-19839
SMITH, S. R. N91-19192
SMITH, TODD E. N91-19479
SMITH, W. N91-19555
SNELL, C. M. N91-19858
SNYDER, H. TODD N91-19083
SNYDER, P. G. N91-19351
N91-19935
SNYDER, ROBERT S. N91-19653
N91-19665
SODA, JIRO N91-19991
SODERMAN, PAUL T. N91-19823
N91-19824
SOEDER, RONALD H. N91-19115
SOKKAPPA, P. R. N91-19775
SOKOLOV, A. N91-19588
N91-19597
SOLEIHAVOUP, J. P. N91-19630
SOLIMENE, RICCARDO N91-19629
SOLOMON, S. C. N91-20011
SOMMER, E. N91-19336
SOMMER, S. N91-19682
N91-19685
SOMMERLADE, B. N91-19384
SONNENFELD, GERALD N91-19621
N91-19701
SOPIN, A. I. N91-19803
SOUKANOV, J. N91-19689
SPAID, FRANK W. N91-19062
SPANGLER, ELSON B. N91-19102
SPARKS, C. J. N91-19937
SPECHT, E. D. N91-19310
N91-19937
SPEZIALI, V. N91-19360
SPRADLEY, I. N91-19323
SPRINGER, P. T. N91-19910

SPRUCK, J. N91-19776
SPURGASH, S. M. N91-19253
SRINIVASAN-RAO, T. N91-19432
N91-19849
N91-19850
SROLOVITZ, D. J. N91-19928
STADEAGER, CARSTEN N91-19592
N91-19593
N91-19602
N91-19612
STADERMANN, FRANK J. N91-20013
STAHL, D. B. N91-19405
STANBERY, B. J. N91-19190
STANSFIELD, S. A. N91-19767
STANTON, HORACE D. N91-19312
STARACE, A. F. N91-19840
STECHER, JOSEPH L., III N91-19126
STEFKO, GEORGE L. N91-19475
STEGEMANN, JUERGEN P. N91-19573
N91-19586
N91-19601
N91-19695
STEIMER, CARLOS H. N91-19136
STEIN, WILLIAM L. N91-19972
STEINETZ, BRUCE M. N91-19441
N91-19442
STEKETEE, J. A. N91-19395
STELLA, PAUL M. N91-19211
N91-19217
STENGEL, ROBERT F. N91-19033
N91-19038
N91-19039
STEPANTSOV, V. V. N91-19568
STERNBERG, AMIEL N91-19982
STERNE, P. A. N91-19919
STEVEN, G. P. N91-19470
STEVENS, A. N91-19359
STEVENS, B. N91-19834
STEVENS, M. M. N91-19544
STEWART, A. J. N91-19539
STEWART, I. B. N91-19486
STEWART, R. E. N91-19910
STIFFEY, ARTHUR V. N91-19249
STILWELL, P. D. N91-19879
STOFAN, ANDREW J. N91-19123
STOFAN, E. R. N91-20011
STONE, LYDIA RAZRAN N91-19700
STONER, G. E. N91-19269
STONER, K. J. N91-19483
STORM, E. N91-19430
STOTT, J. R. R. N91-19613
STRANGE, S. N91-19687
STRASH, DANIEL J. N91-19060
STRATILATOV, A. B. N91-19943
STRATTON, D. ALEXANDER N91-19034
STRAUCH, R. N91-19555
STRAUCH, R. G. N91-19562
STRAUSS, ALVIN M. N91-19603
STREET, CRAIG L. N91-19061
STREIT, G. E. N91-19257
STROGONOVA, L. N91-19578
STROLLO, FELICE N91-19592
N91-19593
N91-19614
STROLLO, G. N91-19614
STROM, ROBERT G. N91-19997
STROUB, ROBERT H. N91-19078
STUTZKI, J. N91-19976
SUBRAMANIAM, SHANKAR N91-19053
SUCHENTRUNK, RICHARD N91-19311
SUDAKOVA, M. V. N91-19819
SUDER, WILLIAM H., III N91-19436
SUGINOHARA, TATSUSHI N91-19990
SULLIVAN, J. A. N91-19419
SULZER, M. P. N91-20001
SUMICH, MARK N91-19241
SUMMA, J. MICHAEL N91-19060
SUN, D. C. N91-19369
SUN, XIAN-HE N91-19744
SUNDARAM, V. S. N91-19189
SUNDBERG, CARL J. N91-19573
N91-19615
SUNDERAM, V. S. N91-19757
SUNSHINE, J. N91-20002
SUTO, YASUSHI N91-19989
N91-19990
SUZUKI, K. N91-19066
SUZUKI, M. N91-19066
SVIRZHEVSKIJ, N. S. N91-20021
SWANICK, DAVID J. N91-19328
SWARTZ, C. K. N91-19178
N91-19205
SWAYZE, G. A. N91-20004
SWEENEY, F. J. N91-19447
SWENSON, RICHARD M. N91-19764
SWITENDICK, A. C. N91-19936
SYED, H. H. N91-19307
SYNNESTVEDT, ROBERT N91-19566

T

TABIBI, BAGHER M. N91-19415
TAEHTINEN, S. N91-19316
TAIRBEKOV, M. N91-19674
TAJIMA, T. N91-19897
TAKACS, P. Z. N91-19873
N91-19874
TAKAHASHI, MARC D. N91-19041
TAKAHATA, KIYOTO N91-19852
TAKAYANAGI, HIROSHI N91-19226
TALMY, INNA G. N91-19225
TALPALLIKAR, MILIND V. N91-19048
TANAKA, GRANT N91-19870
TANAKA, KENNETH L. N91-20014
TANNENBAUM, M. J. N91-19848
TANNER, R. L. N91-19535
TARDIFF, M. F. N91-19544
TATARCHENKO, V. A. N91-19943
TATRO, D. N91-19711
TAUBER, WOLFGANG N91-19981
TAWFIK, HAZEM N91-20035
TAYLOR, C. N. N91-19487
TAYLOR, J. B. N91-19909
TAYLOR, J. R. N91-19769
TAYLOR, LAWRENCE A. N91-20010
TAYLOR, LAWRENCE W., JR. N91-19122
TAYLOR, S. N91-19923
TAYLOR, S. L. N91-19523
TAYLOR, V. L. N91-19303
TAZIMA, NAOKI N91-19885
TEETER, BRENT A. N91-19076
TEIWES, WINFRIED N91-19591
TELLALIAN, MARTIN L. N91-19150
TERAMOTO, TAKAYUKI N91-19883
TERRY, JOHN D. N91-19349
TESCH, PER A. N91-19587
N91-19616
TESKE, MILTON E. N91-19067
N91-19074
TEST, MARK G. N91-19441
THEELEN, BAS J. N91-19169
THESLING, WILLIAM N91-19206
THINH, NGO N91-20036
THOMAS, R. S. N91-19406
THOMAS, RALPH D. N91-19209
THOMLINSON, W. C. N91-19712
THOMPSON, C. V. N91-19258
THOMPSON, RANDOLPH C. N91-19077
TIERNEY, M. N91-19140
TIMMONS, M. L. N91-19186
TISSOT, R. G. N91-19942
TIXADOR, R. N91-19632
TOBIN, J. G. N91-19921
N91-19924
TODT, OLIVER N91-19121
TOMBRELLO, T. A. N91-19927
TOMITA, KENJI N91-19988
N91-19992
TOMPKINS, J. A. N91-19104
TOMSON, ANNA N91-19639
N91-19640
N91-19641
TONG, S. Y. N91-19924
TONKAY, GREGORY N91-20037
TONTERI, H. N91-19316
TOPP, DANNY J. N91-19265
TOWNSEND, LAWRENCE W. N91-19699
TRAN, HUY K. N91-19304
TRAVIS, D. T. N91-19104
TREICHEL, R. N91-19663
TRENHOLME, J. B. N91-19430
TRIBBLE, A. C. N91-19159
TROITSKAYA, E. V. N91-20016
TROJNAR, J. N91-19818
TROMBLY-FREYTAG, K. N91-19958
TROMMER, G. N91-19877
TROTIGNON, J. P. N91-19227
TROUDET, TERRY N91-19766
TRUZHENNIKOV, A. N. N91-19645
TRYGGVASON, G. N91-19264
TSANG, T. N91-19432
N91-19849
N91-19850
TSURUDA, KOICHIRO N91-19880
TULUPOV, A. V. N91-19804
TURCHI, P. E. A. N91-19268
TURUNEN, RAIMO N91-19454
TYNAN, G. N91-19911

U

UBBELS, G. A. N91-19624
UEMURA, MASUJI N91-19228
ULEN, ESKIL N91-19513
UMEHARA, S. N91-19884
UNSEREN, M. A. N91-19444
UNTERHITZENBERGER, JOSEF N91-19084

V

V.D.HEUVEL, EDOUARD P. N91-19169
V.DIJK, MARK J. N91-19169
VALENCIA, G. N91-19851
VALENTINE, C. K. N91-19544
VALIYEV, K. A. N91-19807
VALORA, N. N91-19620
VANDENBRIEL, WIES N91-19639
N91-19640
VANDENENDE, HERMAN N91-19639
N91-19640
N91-19641
VANDERPLAETSE, F. N91-19637
VANDERPLOEG, J. M. N91-19611
VANDERPUTTEN, D. N91-19243
VANDEUSEN, S. B. N91-19942
VANFLEET, H. B. N91-19923
VANGRAAS, FRANK N91-19032
VANHOEK, JOHANNES ADRIANUS MARIA N91-19286
VANHOUTEN, MARINUS ALBERTUS N91-19337
VANLIESHOUT, PETER HENRICUS N91-19338
VANLOON, JACK J. W. A. N91-19650
VANLOON, S. L. N91-19132
VANMETER, A. R. N91-19546
VANWIMERSMAGREIDANUS, B. N91-19494
VARY, ALEX N91-19464
VASILEV, A. A. N91-19945
VASILYEV, P. P. N91-19820
VASINA, S. YA. N91-19819
VASSAUX, DIDIER N91-19617
VASSEUR, H. A. N91-19769
VEERASINGAM, R. N91-19759
VELDHUIJZEN, J. P. N91-19650
VELIKOV, L. V. N91-19807
VENIS, A. C. J. N91-19069
VENKATASUBRAMANIAN, R. N91-19186
VENTURINI, E. L. N91-19942
VERHAGEN, STEVEN P. N91-19169
VERHEY, TIMOTHY R. N91-19180
VERKLEIJ, ARIE J. N91-19623
VERRILLI, MICHAEL J. N91-19473
VERY, J. M. N91-19643
VICO, LAURENCE N91-19643
N91-19690
VILLENEUVE, D. M. N91-19895
VILLORESI, G. N91-20019
VINCENT, L. N91-19227
VINH, N. X. N91-19124
VIRSHUP, G. F. N91-19188
VISIC, NIKOLA N91-19332
VITERNA, LARRY A. N91-19462
VOGEL, KURT N91-19673
N91-19677
VOIGT, J. A. N91-19942
VOLAKIS, JOHN L. N91-19305
N91-19306
N91-19307
VOLKMANN, DIETER N91-19669
VOLKOV, G. S. N91-19807
VOLPE, MASSIMILIANO N91-19550
VONBAUMGARTEN, R. N91-19580
VONG, R. L. N91-19535
VOORHIES, COERTE V. N91-19557
VORACEK, DAVID F. N91-19081
VOROJTSOV, S. N91-19679
VOROTNIKOVA, I. E. N91-19619
VOUK, MLADEN A. N91-19741
VOZNYAK, R. M. N91-19813

W

WADDLE, D. B. N91-19506
WAGNER, J. H. N91-19443
WAGNER, M. K. N91-19924
WAGNER, PATRICIA A. N91-19287
WALBRIDGE, D. G. C. N91-19958
WALKER, D. W. N91-19902
WALKER, K. P. N91-19476
WALKER, KEVIN P. N91-19232
WALL, F. D. N91-19269
WALLIS, D. B. N91-19958
WALTERS, R. T. N91-19277
WALTZ, R. E. N91-19908

WAN, YI N91-19837
WANG, H. Y. N91-19928
WANG, S. C. N91-19560
WANG, W. N91-19495
WANG, W. C. N91-19532
WANLAAS, M. W. N91-19191
WANLASS, M. W. N91-19202
WARBERG, JERGEN N91-19593
WARBERG, JORGEN N91-19592
N91-19612
WARFIELD, D. N91-19213
WARNOCK, R. L. N91-19777
N91-19778
WARRELMANN, J. N91-19666
N91-19708
WARREN, A. N91-19140
WARREN, B. K. N91-19251
N91-19313
N91-19318
WATANABE, KAZUYA N91-19988
WATKINS, MARCUS A. N91-19181
WATSON, P. D. N91-19452
WEAGLEY, R. J. N91-19297
WEBBER, J. P. H. N91-19244
N91-19245
N91-19246
N91-19247
N91-19486
WEGMANN, HELMUT N91-19796
WEIJTENS, CHRISTIANUS HERMANUS L. N91-19949
WEINBERG, IRVING N91-19205
N91-19206
N91-19207
N91-19208
N91-19221
WEINSTEIN, AMANDA N91-19719
WEISS, HOWARD N91-19519
WEIZER, VICTOR G. N91-19203
WELLEMEYER, C. G. N91-19523
WELLER, JOSEPH F. N91-19869
WELLS, N. E. N91-19963
WELSH, D. C. N91-19562
WENDT, ROBERT G. N91-19238
WENISCH, ELISABETH N91-19665
WENTZ, WILLIAM H., JR. N91-19040
WERNER, J. C. N91-19481
WERTHEN, J. G. N91-19194
WERVELMAN, ROB N91-19855
WESSELING, K. H. N91-19575
WEST, B. H. N91-19451
WESTENSKOW, G. A. N91-19862
WESTLEY, M. S. N91-19143
WESTLEY, R. N91-19143
WESTMACOTT, K. H. N91-19933
WESTMORELAND, C. G. N91-19239
WESTON, NEIL J. N91-19750
WETZIG, JOACHIM N91-19580
WHATLEY, W. J. N91-19146
WHELAN, D. A. N91-19429
WHITAKER, JOHN F. N91-19343
WHITE, D. C. N91-19279
N91-19280
WHITING, M. A. N91-19738
WHITLEY, J. B. N91-19896
WHITLOW, JONATHAN E. N91-20038
WHITMORE, STEPHEN A. N91-19095
WHITTEN, D. G. N91-19836
WHITTENBERGER, J. D. N91-19233
WHITTUM, D. H. N91-19418
N91-19423
WIEST, G. N91-19606
WIJCHERS, T. N91-19222
WIKLIND, T. N91-19977
N91-19994
WILCOX, FLOYD J., JR. N91-19042
WILD, W. N91-19977
WILKS, S. C. N91-19898
WILLEMSEN, HARRY N91-19661
WILLIAMS, A. L. N91-19068
WILLIAMS, DEAN N. N91-19551
WILLIAMS, J. M. N91-19283
WILLIS, W. J. N91-19432
WILSON, B. G. N91-19910
WILSON, JOHN W. N91-19699
WILSON, KENNETH J. N91-19364
WILT, D. M. N91-19205
WIMBERLY, J. N91-19506
WINDLEY, P. N91-19756
WINNBERG, A. N91-19993
WINSKE, D. N91-19860
WIRINGA, R. B. N91-19842
WISCOMBE, W. J. N91-19555
WISE, M. B. N91-19258
WITCHER, DONALD H. N91-19764
WITTENBERG, H. N91-19222
WOHLHUTER, F. N91-19779
WOLF, D. A. N91-19544
WOLF, H. N91-19336
WOLKE, ANDREAS N91-19676
N91-19678
WOOD, J. L. N91-19847
WOOD, S. J. N91-19611
WOODRUFF, W. L. N91-19743
WOODWARD, RICHARD P. N91-19045
WOODWARD, W. A. N91-19540
WOODYARD, J. R. N91-19214
WOODYARD, JAMES R. N91-19176
WOOLLAM, J. A. N91-19351
N91-19935
WOROBEY, W. N91-19276
WU, C. M. L. N91-19246
N91-19247
N91-19488
WU, C. T. N91-19941
WU, K. CHAUNCEY N91-19166
WU, YAN N91-19930
WURTELE, J. S. N91-19418
N91-19427

X

XIA, YIREN N91-19755
XIE, MING N91-19426
XIE, Z. N91-19458
XU, D. N91-19299

Y

YAGER, DONALD R. N91-19102
YAGER, RONALD R. N91-19957
YAKUSHIN, S. B. N91-19642
YAMADA, KEN N91-19870
YAMAMOTO, M. N91-19884
YAMANAKA, C. N91-19884
YANG, B. N91-19835
YANG, LI-FARN N91-19125
YAO, H. D. N91-19351
N91-19935
YAO, S. C. N91-19536
YASUDA, Y. N91-19884
YATSUI, KIYOSHI N91-19882
N91-19887
N91-19888
YATSUZUKA, M. N91-19889
N91-19890
YE, HUANCHUN N91-19787
YEH, F. C. N91-19443
YEH, PEN-SHU N91-19733
N91-19734
YEH, Y. C. M. N91-19185
YETTER, R. A. N91-19262
YOO, SUNGYUL N91-19060
YORKE, J. A. N91-19792
YOST, JAMES M. N91-19167
YOUNG, A. C. N91-19239
YOUNG, J. O. N91-19547
YOUNG, P. E. N91-19895
YOUNGER, S. M. N91-19899
YOUNT, J. A. N91-19751
YU, H. S. N91-19791
YU, SHENG-TAO N91-19059
YUDKIN, HOWARD N91-19724
YUEN, G. U. N91-20006

Z

ZAKOU, A. N91-19884
ZALLER, M. N91-19117
ZANDBERGEN, B. T. C. N91-19222
ZANG, T. A. N91-19366
ZANGRANDO, F. N91-19501
ZANGRILLI, N. L. N91-20019
ZARNSTORFF, M. C. N91-19908
ZAROSLOV, D. YU. N91-19807
ZEIGLER, J. N91-19863
ZGANJAR, E. F. N91-19846
N91-19847
ZHANG, C. N91-19299
ZHANG, YI N91-19439
ZHAVORONKOV, N. I. N91-19803
ZHILIBA, A. I. N91-19805
ZHOU, WEIYU N91-19750
ZHU, Q. M. N91-19753
ZIEGLER, W. N91-19598
ZIGEL, M. N91-19819
ZIJP, JOHANNES PETRUS N91-19455
ZIMMERMANN, U. N91-19321
N91-19654
ZINNECKER, H. N91-19977
ZINNER, ERNST K. N91-19998
ZISSERMAN, A. N91-19458
ZSCHACK, P. N91-19937
ZUBOV, V. V. N91-19806
ZUHR, R. A. N91-19925
ZUNIGA, FANNY A. N91-19055
ZUREK, RICHARD N91-20003
ZWILLING, J. F. N91-19684

Typical Corporate Source Index Listing

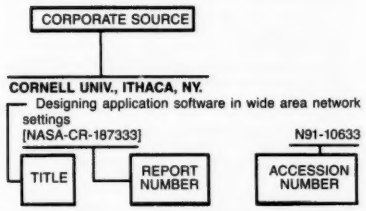

Listings in this index are arranged alphabetically by corporate source. The title of the document provides the user with a brief description of the subject matter. The report number helps to indicate the type of document cited (e.g., NASA report, translation, NASA contractor report). The accession number denotes the number by which the citation is identified. The titles are arranged under each corporate source in ascending accession number order.

A

AARHUS UNIV. (DENMARK).
Plant protoplast development on Biokosmos 9 N91-19674

ACADEMY OF SCIENCES OF THE LITHUANIAN SSR, VILNIUS.
Plant growth under microgravity conditions: Experiments and problems N91-19671

ACADEMY OF SCIENCES (USSR), GORKY.
Diffuse x ray scattering YBa2Cu3O(6.95) monocrystal [DE91-615182] N91-19943
Higher harmonics of magnetization in the critical state of ceramic high Tc superconductors [DE91-615506] N91-19944
Magnetism and superconductivity in YBa2Cu3O(6+x) at 0.3 less than or equal to x less than or equal to 0.4 [DE91-615507] N91-19945

ACADEMY OF SCIENCES (USSR), MOSCOW.
The reference systems for tactile perception and for the orientation with respect to body N91-19691

ACADEMY OF SCIENCES (USSR), NOVOSIBIRSK.
Software for the ODRENOK microcomputer. Program package for graphics editing [DE91-614980] N91-19752
Correlations of pseudo-random numbers of multiplicative sequence [DE91-615076] N91-19788

ADVISORY GROUP FOR AEROSPACE RESEARCH AND DEVELOPMENT, NEUILLY-SUR-SEINE (FRANCE).
Space Vehicle Flight Mechanics [AGARD-AR-294] N91-19124
Computer Aided System Design and Simulation [AGARD-AR-283] N91-19731

AERITALIA S.P.A., TURIN (ITALY).
Magnetic cleanliness verification approach on tethered satellite N91-19158

AERONAUTICAL RESEARCH INST. OF SWEDEN, STOCKHOLM.
Some control problems with broad range variable speed for horizontal axis wind turbines [FFA-TN-1990-37] N91-19513

AEROSPACE CORP., LOS ANGELES, CA.
Strategy in space flight experiments N91-19220

AGENCY OF INDUSTRIAL SCIENCE AND TECHNOLOGY, TSUKUBA (JAPAN).
A study on prediction of life due to creep behavior in CF/EPOXY and CF/PEEK laminates N91-19226

AGRICULTURAL RESEARCH SERVICE, BELTSVILLE, MD.
Effects of soil and canopy characteristics on microwave backscattering of vegetation [NASA-CR-188022] N91-19497

AIR FORCE INST. OF TECH., WRIGHT-PATTERSON AFB, OH.
An experimental study of a sting-mounted single-slot circulation control wing [AD-A229867] N91-19111
Fluorescent lifetime measurements of rare Earth elements in gallium arsenide [AD-A229865] N91-19265
Development of a piezoelectric polymer film pressure transducer for low frequency and dynamic pressure measurement [AD-A229848] N91-19412
Modeling and analysis of orthotropic plate with circular cutout and adhesive bonded patch [AD-A229866] N91-19496

AIRBUS INDUSTRIE, BLAGNAC (FRANCE).
Aircrafts, requirements for ground installations from the aircraft point of view N91-19108

AKRON UNIV., OH.
Life and dynamic capacity modeling for aircraft transmissions [NASA-CR-4341] N91-19438

ALABAMA UNIV., HUNTSVILLE.
Hypervelocity impact physics [NASA-CR-4343] N91-19164
Gamma ray astronomy [NASA-CR-188031] N91-19980

ALICANTE UNIV. (SPAIN).
Microgravity, hypergravity, and aging: A unifying hypothesis N91-19633

ALLIANCE TECHNOLOGIES CORP., CHAPEL HILL, NC.
Evaluation of significant anthropogenic sources of radiatively important trace gases [PB91-127753] N91-19545

AMERICAN PUBLIC POWER ASSOCIATION, WASHINGTON, DC.
COMPLEAT (community-oriented model for planning least-cost energy alternatives and technologies): A planning tool for publicly owned electric utilities [DE91-006955] N91-19511

AMES LAB., IA.
Internal friction peaks due to interstitials in bcc alloys [DE91-007411] N91-19272
A structured representation for parallel algorithm design on multicomputers [DE91-006674] N91-19744

AMSTERDAM UNIV. (NETHERLANDS).
Blood pressure regulation in parabolic flight N91-19575
Vestibular function in altered states of gravity N91-19579
Unicellular algae in space. 1: Preparatory tests N91-19639
Unicellular algae in space. 2: Sounding-rocket experiment N91-19640
Unicellular algae in space. 3: Addendum N91-19641
Pupil size in parabolic flight N91-19693

ANALEX CORP., FAIRVIEW PARK, OH.
COLD-SAT feasibility study safety analysis [NASA-CR-187042] N91-19167
Measured performance of the half-scale accurate antenna reflector [NASA-CR-187047] N91-19350

ANALYTICAL METHODS, INC., REDMOND, WA.
A novel potential/viscous flow coupling technique for computing helicopter flow fields [NASA-CR-177568] N91-19060

APPLIED SOLAR ENERGY CORP., CITY OF INDUSTRY, CA.
Status of GaAs/Ge solar cells N91-19185
Optimization and performance of Space Station Freedom solar cells N91-19215

ARGONNE NATIONAL LAB., IL.
The application of neutron diffraction time-of-flight measurements to the study of strain in composites [DE91-008106] N91-19242
Two-dimensional non-reacting jet-gas mixing in an MHD (magnetohydrodynamic) second stage combustor [DE91-006015] N91-19252
Remote detection of organics using Fourier transform infrared spectroscopy [DE91-006045] N91-19253
Effects of atmosphere and heating rate during processing of a ceramic superconductor [DE91-007761] N91-19299
Assessment of tamper-revealing ceramic seals [DE91-007793] N91-19301
Methanol reformers for fuel cell powered vehicles: Some design considerations [DE91-006465] N91-19314
High power, high frequency lasertron RF sources [DE91-006007] N91-19414
Oxygen-enriched diesel engine performance: A comparison of analytical and experimental results [DE91-006491] N91-19440
Thermal-hydraulic model of a solid-oxide fuel cell [DE91-006393] N91-19507
Design and cost of near-term OTEC (Ocean Thermal Energy Conversion) plants for the production of desalinated water and electric power [DE91-006406] N91-19508
Analysis of workload and load balancing issues in the NCAR community climate model [DE91-008052] N91-19534
Some neutronics and thermal-hydraulics codes for reactor analysis using personal computers [DE91-006591] N91-19743
Summer institute in parallel programming [DE91-007922] N91-19760
Variational Monte Carlo studies of electromagnetic structure of few-body nuclei [DE91-007756] N91-19838
Variational Monte Carlo calculations of nuclear ground states [DE91-007760] N91-19842
A method for determining poloidal coil configurations for tokamak devices [DE91-007940] N91-19903
Silver-sheathed multifilament wires [DE91-008107] N91-19941

ARIZONA STATE UNIV., TEMPE.
Lunar maria and related deposits: Preliminary Galileo imaging results N91-20000
Orientale and South Pole-Aitken basins on the Moon: Preliminary Galileo imaging results N91-20002

ARIZONA UNIV., TUCSON.
Chemical activation of molecules by metals: Experimental studies of electron distributions and bonding [DE91-007695] N91-19275
Hubble Space Telescope secondary mirror vertex radius/conic constant test [NASA-CR-187989] N91-19871
Impact processes in the Solar System: New understandings through numerical modeling N91-19996
Ancient oceans and Martian paleohydrology N91-19997
Orientale and South Pole-Aitken basins on the Moon: Preliminary Galileo imaging results N91-20002

ARMY AVIATION RESEARCH AND DEVELOPMENT COMMAND, MOFFETT FIELD, CA.
A flight-dynamic helicopter mathematical model with a single flap-lag-torsion main rotor [NASA-TM-102267] N91-19041
Euler solutions to nonlinear acoustics of non-lifting hovering rotor blades [NASA-TM-103837] N91-19826

ARMY RESEARCH INST. FOR THE BEHAVIORAL AND SOCIAL SCIENCES, ALEXANDRIA, VA.
Test analysis program evaluation: Item statistics as feedback to test developers [AD-A229851] N91-19713

ASTROPOWER, INC., NEWARK, DE.
AlGaAs top solar cell for mechanical attachment in a multi-junction tandem concentrator solar cell stack N91-19187

ATMOSPHERIC AND ENVIRONMENTAL RESEARCH, INC., CAMBRIDGE, MA.
Natural and anthropogenic climate change [DE91-007363] N91-19532

AUBURN UNIV., AL.
QUEST/Ada (query utility environment for software testing of Ada: The development of a program analysis environment for Ada, task 1, phase 3
[NASA-CR-187983] N91-19735
Rocket-triggered lightning strikes and forest fire ignition N91-20027

B

BELEIDSCOMMISSIE REMOTE SENSING, DELFT (NETHERLANDS).
Slope modulation of the radar backscatter by sea waves
[BCRS-88-05] N91-19327
BERN UNIV. (SWITZERLAND).
Increased mitogenic response in lymphocytes from chronically centrifuged mice N91-19634
BERTIN ET CIE., PLAISIR (FRANCE).
Preliminary study of a membrane bioreactor for cell culture in space N91-19627
Preliminary studies before defining a payload adapted to the primate model N91-19648
BETA POWER, INC., SALT LAKE CITY, UT.
Sodium/metal chloride program conceptual design study
[DE91-007216] N91-19353
BOEING AEROSPACE CO., SEATTLE, WA.
Boeing infrared sensor (BIRS) calibration facility N91-19138
Progress in GaAs/CuInSe2 tandem junction solar cells N91-19190
An approach for configuring space photovoltaic tandem arrays based on cell layer performance N91-19197
Radioisotope thermal photovoltaic application of the GaSb solar cell N91-19210
BOEING CO., SEATTLE, WA.
Burst annealing of high temperature GaAs solar cells N91-19196
BOEING MILITARY AIRPLANE DEVELOPMENT, SEATTLE, WA.
Formal proof of the AVM-1 microprocessor using the concept of generic interpreters
[NASA-CR-187491] N91-19756
BONN UNIV. (GERMANY, F.R.).
Graviperception in plants N91-19667
Gravitational effects on subcellular structures of plant cells N91-19669
BOSTON UNIV., MA.
Atomic beam studies of the interaction of hydrogen with transition metal surfaces
[DE91-007938] N91-19841
BRIGHAM YOUNG UNIV., PROVO, UT.
Investigation of condensed matter fusion
[DE91-007246] N91-19923
BRISTOL UNIV. (ENGLAND).
The effect of body shape on the development of vortex asymmetry in the flow past slender bodies
[BU-413] N91-19068
Uncertainty reasoning applied to the assessment of composite material for structural design
[BU-405] N91-19244
An expert system for laminated plate design using composite materials
[BU-406] N91-19245
Minimum weight optimization of composite laminated struts
[BU-409] N91-19246
A knowledge based expert system for laminated composite strut design
[BU-410] N91-19247
Parallel processing for panel methods
[BU-414] N91-19391
Dynamic behavior of pneumatic tyres
[BU-412] N91-19453
A theoretical solution for the buckling of sandwich panels with laminated face plates using a computer algebra system
[BU-407] N91-19486
Computational comparison of efficacies of aeolian vibration damping devices for multiconductor overhead power lines
[BU-411] N91-19487
Bolted joints in a laminated composite strut design expert system
[BU-415] N91-19488
A non-linear method for the calculation of the power output of a rotating wind turbine
[BU-416] N91-19512
BRITISH BROADCASTING CORP., KINGSWOOD (ENGLAND).
The provision of circuits to outside broadcast locations using spectrum within the UHF broadcasting bands
[BBC-RD-1990/12] N91-19329
BROOKHAVEN NATIONAL LAB., UPTON, NY.
X ray absorption spectroscopy of oxide films on metals
[DE91-008100] N91-19278
Spatial and temporal relationships between localized microbial metabolic activit/ and electrochemical activity of steel
[DE91-008102] N91-19279
A study of carbon steel corrosion inhibition by phosphate ions and by an organic buffer using a scanning vibrating electrode
[DE91-008103] N91-19280
XANES investigation of pH effects during cerium-sealing of anodized aluminum
[DE91-008101] N91-19302
Radiation damage studies on hybrid preamplifiers
[DE91-008411] N91-19359
Monolithic radiation hard charge sensitive preamplifier using junction field effect transistors
[DE91-008437] N91-19360
Neutron radiation damage studies on silicon detectors
[DE91-008441] N91-19361
Proceedings of the Workshop Prospects for a 1 Angstrom Free-Electron Laser
[DE91-007631] N91-19422
Summary of the working group on transverse emissions from photocathodes
[DE91-008414] N91-19432
Analysis of high frequency surface-induced concentration fluctuations
[DE91-007561] N91-19538
The NAPAP assessment of damages to materials from acid deposition
[DE91-008086] N91-19542
Multiple energy computed tomography for neuroradiology with monochromatic x rays from the national synchrotron light source
[DE91-008108] N91-19712
Intense field non-resonant multiphoton absorption of diatomic molecules
[DE91-006920] N91-19835
Summary of discussions at the HIGH p (sub T) session
[DE91-008196] N91-19848
Photoemission studies using femtosecond pulses for high brightness electron beams
[DE91-008436] N91-19849
Development of high current electron source using photoemission from metals with ultrashort laser pulses
[DE91-008438] N91-19850
W(sub L)W(sub L) scattering at the SSC
[DE91-008442] N91-19851
The specification of glancing incidence mirrors in terms of system performance
[DE91-007556] N91-19873
The specification of glancing incidence mirrors in terms of system performance
[DE91-007564] N91-19874
The characterization of interface roughness and other defects in multilayers by x ray scattering
[DE91-007558] N91-19929
BUNDESMINISTERIUM FUER FORSCHUNG UND TECHNOLOGIE, BONN (GERMANY, F.R.).
Space research for the sake of all
[ETN-91-98807] N91-19113

C

CALIFORNIA INST. OF TECH., PASADENA.
Research on bluff-body vortex wakes
[AD-A229875] N91-19071
High resolution infrared astronomy satellite observations of a selected spiral galaxy
[NASA-CR-188019] N91-19975
Stable hydrogen and carbon isotope ratios of extractable hydrocarbons in the Murchison meteorite N91-20006
CALIFORNIA STATE POLYTECHNIC UNIV., POMONA.
Detailed modal testing of a solid rocket motor using a portable test system N91-19144
CALIFORNIA STATE UNIV., FRESNO.
Formal specification of human-computer interfaces N91-20023
CALIFORNIA STATE UNIV., SACRAMENTO.
Low flow vortex shedding flowmeter for hypergolics/all media N91-20036
CALIFORNIA UNIV., BERKELEY.
Characterization of a defective interfering RNA that contains a mosaic of a plant viral genome
[DE91-007897] N91-19702
Characterization of a defective interfering RNA that contains a mosaic of a plant viral genome
[DE91-007898] N91-19703
Performance measurements of the first RAID prototype
[NASA-CR-187958] N91-19718
High energy physics and cosmology
[DE91-007369] N91-19859
CALIFORNIA UNIV., BERKELEY. LAWRENCE BERKELEY LAB.
Theory of the ion-channel laser
[DE91-007643] N91-19423
The evolution and limits of spectral bandwidth in free electron lasers
[DE91-007737] N91-19425
Hole coupling resonator for free electron lasers
[DE91-007745] N91-19426
The advanced light source: A new tool for research in atomic physics
[DE91-007739] N91-19861
Phase transitions and equation of state of CsI under high pressure and the development of a focusing system for x rays
[DE91-007646] N91-19930
Thin film reactions on alloy semiconductor substrates
[DE91-007651] N91-19931
Some roles for TEM in the development of new materials
[DE91-007742] N91-19933
Part 1: The effect of lattice defects on the sintering of lithium fluoride; Part 2: The morphology of calcium oxide from calcium carbonate decomposition
[DE91-007743] N91-19934
Symmetries on the space of (2,2) superstring vacua and automorphism groups of Calabi-Yau manifolds
[DE91-008218] N91-19951
CALIFORNIA UNIV., DAVIS.
Climatic water budgets, effective moisture, and elevation in the Southern Sierra Nevada, California, 1951-1980
[PB91-127878] N91-19500
Physiological genetics of denitrification: A route to conserving fixed nitrogen
[DE91-008157] N91-19707
Formal proof of the AVM-1 microprocessor using the concept of generic interpreters
[NASA-CR-187491] N91-19756
CALSPAN FIELD SERVICES, INC., ARNOLD AFS, TN.
Infrared sensor test methodology and facilities N91-19139
CARNEGIE-MELLON UNIV., PITTSBURGH, PA.
The effect of elastic stress on Ostwald ripening phenomena
[DE91-008034] N91-19484
Plasma assisted NO(x) reduction in existing coal combustors
[DE91-007380] N91-19536
Software development environments: Status and trends N91-19723
CATHOLIC UNIV. OF AMERICA, WASHINGTON, DC.
Studies of combustion kinetics and mechanisms
[DE91-007829] N91-19259
CBI NA-CON, OAK BROOK, IL.
Optical testing cryogenic thermal vacuum facility N91-19137
CELLER PFLANZEN- UND GEWEBELABOR G.M.B.H., CELLE (GERMANY, F.R.).
Plant biotechnology in space: Facts and speculations N91-19664
CENTRAL RESEARCH INST. OF ELECTRIC POWER INDUSTRY, CHIBA (JAPAN).
The application of simulation model for the flow induced by air bubble plume in thermally stratified reservoirs
[DE91-003064] N91-19380
CENTRAL RESEARCH INST. OF ELECTRIC POWER INDUSTRY, TOKYO (JAPAN).
Progressive feature of stepped leader on Japan sea coast in winter (basic data to establish shielding theory for lightning)
[DE91-742133] N91-19561
CENTRE D'ETUDE DE L'ENERGIE NUCLEAIRE, MOL (BELGIUM).
An assay for bone cell differentiation in vitro as a tool for microgravity studies in space N91-19637
CENTRE D'ETUDES ET DE RECHERCHES DE MEDECINE AEROSPATIALE, PARIS (FRANCE).
Preliminary studies before defining a payload adapted to the primate model N91-19648
CENTRE HOSPITALIER UNIV. PURPAN, TOULOUSE (FRANCE).
Human dermal fibroblast sensitivity to hypergravity N91-19630
CENTRE NATIONAL DE LA RECHERCHE SCIENTIFIQUE, ORLEANS (FRANCE).
Extraterrestrial organic molecules and the emergence of life on Earth N91-19681
CENTRE NATIONAL DE LA RECHERCHE SCIENTIFIQUE, PARIS (FRANCE).
Gaze control and spatial memory in weightlessness N91-19692
Mental rotation of three-dimensional shapes in microgravity N91-19694

CENTRE NATIONAL DE LA RECHERCHE SCIENTIFIQUE, TOURS (FRANCE).
Simulation expert system for physiological mechanisms of the space motion sickness N91-19596
CFD RESEARCH CORP., HUNTSVILLE, AL.
Rapid mix concepts for low emission combustors in gas turbine engines
[NASA-CR-185292] N91-19048
CHICAGO BRIDGE AND IRON CO., OAK BROOK, IL.
Space simulation facilities providing a stable thermal vacuum facility N91-19150
CHRONOS RESEARCH LABS., INC., SAN DIEGO, CA.
Low cost space power generation N91-19212
COHERENT TECHNOLOGIES, INC., BOULDER, CO.
Theory of CW lidar aerosol backscatter measurements and development of a 2.1 microns solid-state pulsed laser radar for aerosol backscatter profiling
[NASA-CR-4347] N91-19498
COLORADO STATE UNIV., FORT COLLINS.
Monitoring the response of the upper troposphere/lower stratosphere to a greenhouse gas scenario
[DE91-007976] N91-19541
COLORADO UNIV., BOULDER.
Thermohaline circulations and global climate change
[DE91-007458] N91-19537
Radar-measured height profiles of Cn(2) and turbulence dissipation rate compared with radiosonde data during October 1989 at Denver
[PB91-125500] N91-19562
Tuning the efficiencies of plant lighting systems: From primary energy to edible biomass: The LED as an alternative light source N91-19660
The FORCE: A highly portable parallel programming language
[NASA-CR-187928] N91-19732
Near resonant absorption by atoms in intense fluctuating fields
[DE91-007911] N91-19839
COLUMBIA UNIV., NEW YORK, NY.
Experimental study of external kink instabilities in the Columbia high beta tokamak
[DE91-008116] N91-19904
COMMISSARIAT A L'ENERGIE ATOMIQUE, CADARACHE (FRANCE).
A ground based module for experimentations of cultivations and recycling in a closed environment N91-19657
COMMISSARIAT A L'ENERGIE ATOMIQUE, FONTENAY-AUX-ROSES (FRANCE).
New experimental approach in quality factor and dose equivalent determination during a long term manned space mission N91-19679
COMMITTEE ON APPROPRIATIONS (U.S. SENATE).
Departments of Veterans Affairs and Housing and Urban Development, and Independent Agencies Appropriation Bill, 1991
[S-REPT-101-474] N91-19966
National Aeronautics and Space Administration N91-19967
Problems at National Aeronautics and Space Administration
[S-HRG-101-1146] N91-19969
COMMITTEE ON COMMERCE, SCIENCE, AND TRANSPORTATION (U.S. SENATE).
Global change: What you can do
[S-HRG-101-1160] N91-19528
Hubble Space Telescope and the space shuttle problems
[S-HRG-101-1087] N91-19974
COMMITTEE ON SCIENCE, SPACE AND TECHNOLOGY (U.S. HOUSE).
Commercial Space Launch Act implementation
[GPO-27-944] N91-19968
COMPUTER SCIENCES CORP., HAMPTON, VA.
Transferable Output ASCII Data (TOAD) gateway: Version 1.0 user's guide
[NASA-CR-187489] N91-19737
COMPUTER SCIENCES CORP., RESEARCH TRIANGLE PARK, NC.
Estimating lightning-generated NOx emissions for regional air pollution models
[PB91-131664] N91-19546
Regional Oxidant Model Multi-Processor (ROMMP)
[PB91-131680] N91-19547
CONCURRENT COMPUTER CORP., WESTFORD, MA.
A new generation of real-time DOS technology for mission-oriented system integration and operation N91-19725
CONTINUUM DYNAMICS, INC., PRINCETON, NJ.
Free wake analysis of hover performance using a new influence coefficient method
[NASA-CR-4309] N91-19050
A new methodology for free wake analysis using curved vortex elements
[NASA-CR-3958] N91-19067
Feasibility of an onboard wake vortex avoidance system
[NASA-CR-187521] N91-19074
COORDINATING RESEARCH COUNCIL, INC., ATLANTA, GA.
Aerosol formation in atmospheric mixtures
[PB91-129114] N91-19560
CORNELL UNIV., ITHACA, NY.
Systems near the onset and in the well-developed regimes of turbulence
[DE91-008148] N91-19382
Orientale and South Pole-Aitken basins on the Moon: Preliminary Galileo imaging results N91-20002
CRANFIELD INST. OF TECH., BEDFORD (ENGLAND).
TF89 design project airbrake and arrester hook design
[ETN-91-98853] N91-19092
S87 close air support aircraft fatigue analysis
[ETN-91-98854] N91-19093
The application of aero gas turbine engine monitoring systems to military aircraft
[ETN-91-98852] N91-19096

D

DANISH AEROSPACE MEDICAL CENTER OF RESEARCH, COPENHAGEN.
Fluid shifts and regulation of plasma volume in humans during 12 hours of head-out water immersion N91-19602
Influence on natriuresis of prolonged (12 h) water immersion on central hemodynamics and endocrine elements in humans N91-19612
DAYTON UNIV., OH.
Research on advanced NDE methods for aerospace structures
[AD-A226858] N91-19460
DEPARTMENT OF ENERGY, WASHINGTON, DC.
The National Energy Strategy: The role of geothermal technology development. Proceedings
[DE91-004623] N91-19503
Materials sciences programs
[DE91-007601] N91-19953
DEPARTMENT OF THE NAVY, WASHINGTON, DC.
Collision detection system
[AD-D014645] N91-19072
Wire-free arming system for an aircraft-delivered bomb
[AD-D014611] N91-19076
Alternate approach for obtaining dynamic range in monopulse guidance systems
[AD-D014644] N91-19100
Pneumatic launcher
[AD-D014658] N91-19116
Launching projectiles with hydrogen gas generated from titanium-water reactions
[AD-D014653] N91-19171
Rigid mullitewhisker felt and method of preparation
[AD-D014648] N91-19225
Microbiological assay using bioluminescent organism
[AD-D014651] N91-19249
Method of producing glass fiber with cores of a different material
[AD-D014664] N91-19288
Heterogeneous magnetoresistant layer
[AD-D014665] N91-19289
Extrudable PBX molding powder
[AD-D014667] N91-19312
High pulse repetition frequency radar early warning receiver
[AD-D014655] N91-19328
Piezoelectric sandwich polymer transducer
[AD-D014650] N91-19341
Fluid mixing device having a conical inlet and a noncircular outlet
[AD-D014708] N91-19364
Method for making holograms with coherent radiation from a stabilized laser diode that has been actively cooled
[AD-D014673] N91-19396
Air/sea temperature probe
[AD-D014674] N91-19397
Graduated-load spring washer system for screws and threaded fasteners
[AD-D014697] N91-19436
Solid state electronic emulator of a multiple track motor driven rotating magnetic memory
[AD-D014705] N91-19437
Load bearing connective damper
[AD-D014676] N91-19468
Enhanced crosstie random access memory element and process for the fabrication thereof
[AD-D014723] N91-19717
Artificial neural network implementation
[AD-D014663] N91-19764
A modulated high-power optical source specification
[AD-D014654] N91-19869
Optical Fiber Backscatter Signature Generator (OFBSG)
[AD-D014668] N91-19870
Method of producing superconducting materials in bulk form
[AD-D014656] N91-19917
Apparatus for determining microwave characteristics of superconductive materials using a resonant cavity and calibration waveguides
[AD-D014694] N91-19918
Method for determining astronomic azimuth
[AD-D014677] N91-19972
DEPARTMENT OF TRANSPORTATION, CAMBRIDGE, MA.
Safety of high speed magnetic levitation transportation systems. Preliminary safety review of the transrapid maglev system
[PB91-129684] N91-19326
DEUTSCHE AGENTUR FUER RAUMFAHRTANGELEGENHEITEN G.M.B.H., BONN (GERMANY, F.R.).
The slow-rotating centrifuge microscope (NIZEMI): A new research tool for terrestrial and space-related gravitational biology N91-19663
DEUTSCHE AIRBUS G.M.B.H., HAMBURG (GERMANY, F.R.).
Air traffic simulation with a view to system interpretation N91-19110
DEUTSCHE FORSCHUNGSANSTALT FUER LUFT- UND RAUMFAHRT, COLOGNE (GERMANY, F.R.).
Medex: A useful tool for counteracting orthostatic intolerence resulting from body fluid loss under microgravity N91-19585
Tools for the preparation, performance and evaluation of life sciences experiments N91-19609
Cellular functions of Paramecium under different gravity conditions N91-19631
Does gravity play a role in the morphological development and function of the gravity sensory organ of vertebrates. DLR contribution to the D-2 project graviperception and neuronal plasticity, its technical realization and experimental execution N91-19635
Gravity perception by non-specialized structures N91-19636
Responses of Physarum polycephalum to varying light levels during fast clinostat rotation: A scientific preparation of an ESA biorack experiment during the IML-1 mission N91-19676
Gravitaxis in Physarum polycephalum N91-19678
DEUTSCHE FORSCHUNGSANSTALT FUER LUFT- UND RAUMFAHRT, OBERPFAFFENHOFEN (GERMANY, F.R.).
Orientale and South Pole-Aitken basins on the Moon: Preliminary Galileo imaging results N91-20002
DEUTSCHE LUFTHANSA A.G., HAMBURG (GERMANY, F.R.).
Aircraft standstill, requirements for ground handling from the point of view of aircraft operation N91-19109
DEUTSCHE SPORTHOCHSCHULE, COLOGNE (GERMANY, F.R.).
Time courses of endurance performance parameters following 500 ml blood withdrawal N91-19586
Influence of various parameters on the V'O2 frequency response of the body. A theoretical study on the basis of a nonlinear model N91-19594
Intra-individual variability V'O2 frequency responses in physically active subjects N91-19601
Weightlessness countermeasures and human physiology in space: A potential conflict N91-19695
DORNIER SYSTEM G.M.B.H., FRIEDRICHSHAFEN (GERMANY, F.R.).
Plant production as part of a Controlled Ecological Life Support System (CELSS) N91-19656
DOTY SCIENTIFIC, INC., COLUMBIA, SC.
Microtube strip heat exchanger
[DE91-005741] N91-19504

E

ECOLE NATIONALE SUPERIEURE D'ARTS ET METIERS, PARIS (FRANCE).
Flexure fatigue tests for composites N91-19227
ECOLE NATIONALE SUPERIEURE DES TELECOMMUNICATIONS, PARIS (FRANCE).
Regular unitary dilation of commuting contractions and Markovian representations of Gaussian stationary processes on the set Z(2)
[TELECOM-90-D-009] N91-19798
EDGERTON, GERMESHAUSEN AND GRIER, INC., IDAHO FALLS, ID.
Laboratory testing of the Sonnenschein charger, Part number DTL 12040
[DE91-006543] N91-19346

Lessons learned from the design and operation of steam generators for high temperature gas-cooled reactors [DE91-006139] N91-19450

EG AND G MOUND APPLIED TECHNOLOGIES, MIAMISBURG, OH.

Hot isostatic pressing of high performance glass-ceramic to nickel- and iron-based metal components [DE91-008130] N91-19281

EIDGENOESSISCHE TECHNISCHE HOCHSCHULE, ZURICH (SWITZERLAND).

Effect of running and head down tilt bedrest on lymphocyte reactivity N91-19598

Lymphocytes on sounding rockets N91-19620

Reduced lymphocyte activation in space: Role of cell-substratum interactions N91-19621

Biolab on Columbus: A facility for basic science and biotechnology N91-19658

ELECTRONICS RESEARCH LAB., ADELAIDE (AUSTRALIA).

Investigation at two wavelengths of a modulated He-Xe rare gas laser [AD-A229852] N91-19434

EMORY UNIV., ATLANTA, GA.

Subcellular signal transduction systems in the cellular trauma of ischemia [AD-A229876] N91-19709

ERIL RESEARCH, INC., CORTE MADERA, CA.

LDEF Experiment P0006 Linear Energy Transfer Spectrum Measurement (LETSME) quick look report [NASA-CR-184115] N91-19223

ERLANGEN-NUREMBERG UNIV. (GERMANY, F.R.).

Graviorientation in photosynthetic flagellates N91-19673

Simultaneous tracking of flagellates in real time by image analysis N91-19677

ERNO RAUMFAHRTTECHNIK G.M.B.H. BREMEN (GERMANY, F.R.).

Development of a miniature biology facility N91-19666

ESSEX UNIV., COLCHESTER (ENGLAND).

Efficient connecting networks using directed links [ETN-91-98855] N91-19762

EUROPEAN SPACE AGENCY, PARIS (FRANCE).

Fourth European Symposium on Life Sciences Research in Space [ESA-SP-307] N91-19572

EUROPEAN SPACE AGENCY. EUROPEAN SPACE RESEARCH AND TECHNOLOGY CENTER, ESTEC, NOORDWIJK (NETHERLANDS).

Proposal for a conceptually new compact collecting optics for powerful light sources N91-19155

Life sciences in ESA TRP activity N91-19589

Gravity effects on cells N91-19618

Towards bioregenerative life support systems N91-19655

F

FERMI NATIONAL ACCELERATOR LAB., BATAVIA, IL.

Modeling a ferrite-tuned RF cavity [DE91-008235] N91-19356

Longitudinal periodicity in superconducting dipole magnets [DE91-008421] N91-19821

Table of tables: A database design tool for SYBASE [DE91-007257] N91-19958

FLORIDA INST. OF TECH., MELBOURNE.

Modeling of flow systems for implementation under KATE N91-20038

FOKKER B.V., AMSTERDAM (NETHERLANDS).

Cells in space: Sounding rocket facilities for cell biology and biotechnology in microgravity N91-19661

FORD AEROSPACE CORP., PALO ALTO, CA.

Satellite servicing economic study [NASA-CR-184112] N91-19162

Satellite servicing economic study [NASA-CR-184113] N91-19163

FREIE UNIV., BERLIN (GERMANY, F.R.).

Measurement of eye movements in space-related research environments N91-19591

Vertebral column length changes during simulated microgravity N91-19604

G

GENCORP AEROJET, SACRAMENTO, CA.

Orbital transfer vehicle oxygen turbopump technology. Volume 1: Design, fabrication, and hydrostatic bearing testing [NASA-CR-185175] N91-19174

GENERAL ACCOUNTING OFFICE, WASHINGTON, DC.

Space Shuttle: NASA should implement independent oversight of software development [GAO/IMTEC-91-20] N91-19119

Space operations: NASA is not archiving all potentially valuable data [GAO/IMTEC-91-3] N91-19955

GENERAL ATOMIC CO., SAN DIEGO, CA.

Soliton Microwave Generator [DE91-008277] N91-19335

Plasma boundary experiments on D3-D tokamak [DE91-002429] N91-19881

Tokamak ignition projections from dimensionally similar discharges [DE91-008195] N91-19908

GEOLOGICAL SURVEY, DENVER, CO.

Evidence for ammonium-bearing minerals in Ceres N91-20004

GEOLOGICAL SURVEY, FLAGSTAFF, AZ.

Orientale and South Pole-Aitken basins on the Moon: Preliminary Galileo imaging results N91-20002

Triton: A hot potato N91-20005

What were the effects of the formation of the Borealis basin, Mars N91-20014

GEORGE WASHINGTON UNIV., WASHINGTON, DC.

The 1989-1990 NASA space biology accomplishments [NASA-TM-4258] N91-19697

GEORGIA INST. OF TECH., ATLANTA.

Design, performance evaluation, and investigation of the theoretical capabilities of the NASA Millimeter-wave Imaging Radiometer (MIR) [NASA-CR-187984] N91-19398

Use of system identification techniques for improving airframe finite element models using test data [NASA-CR-188041] N91-19750

GIBBEL CORP., PALOS VERDES ESTATES, CA.

Thermal/vacuum vs. thermal atmospheric testing of space flight electronic assemblies N91-19154

GIESSEN UNIV. (GERMANY, F.R.).

Biological action of single accelerated heavy ions on individual yeast cells N91-19683

Mutation induction in dried yeast cells after irradiation with selected UVC- and UVB- wavelengths compared to simulated sunlight N91-19686

Potentials, message and challenges of life science research in space N91-19696

GOOD SAMARITAN HOSPITAL AND MEDICAL CENTER, PORTLAND, OR.

Relation between perception of vertical axis rotation and vestibulo-ocular reflex symmetry [NASA-CR-187997] N91-19710

GRAZ UNIV. (AUSTRIA).

Is physiological tremor (microvibration) influenced by microgravity N91-19595

A new principle for dynamic fluid shift investigations in astronauts N91-19600

GRUMMAN AEROSPACE CORP., BETHPAGE, NY.

Thermal control for the ground simulation of a space IR sensor system N91-19140

Special requirements in the design of a sensor test and integration laboratory N91-19141

H

HAMILTON STANDARD, WINDSOR LOCKS, CT.

Unified aeroacoustics analysis for high speed turboprop aerodynamics and noise. Volume 1: Development of theory for blade loading, wakes, and noise [NASA-CR-4329] N91-19049

HAWAII UNIV., HONOLULU.

Orientale and South Pole-Aitken basins on the Moon: Preliminary Galileo imaging results N91-20002

HELSINKI UNIV. OF TECHNOLOGY, ESPOO (FINLAND).

Development of components and subsystems for low noise receivers at micro- and millimeter waves [S-187] N91-19363

A modelling of unsteady air flow in the resonance charging system of high speed diesel engines [ACTA-POLYTEC-SCAND-ME-97] N91-19454

Ultrasonic investigations on superfluid He-3-A and He-3-B [ISBN-952-90-2241-7] N91-19830

HIMEJI INST. OF TECH. (JAPAN).

Reduction of low energy components in pulse ion beam N91-19889

Generation and focusing of carbon ion beam by the inverse pinch ion diode N91-19890

HIROSHIMA UNIV., TAKEHARA (JAPAN).

Observational relations in model universes dominated by domain-wall-like matter [DE91-744969] N91-19988

HOPITAL BRETONNEAU, TOURS (FRANCE).

Ultrasound investigation of the cardiovascular system during the 25 days French-Soviet spaceflight (26 November - 21 December 1988) N91-19577

HOUSTON UNIV., CLEAR LAKE, TX.

RICIS 1988 Symposium Proceedings. Presentation appendix [NASA-CR-188077] N91-19722

HUBRECHT LAB., UTRECHT (NETHERLANDS).

Epidermal growth factor induced signal transduction in A431 cells is influenced by altered gravity conditions N91-19623

Fertilization of Xenopus eggs in space N91-19624

I

ILLINOIS UNIV., CHICAGO.

Local synthesis and tooth contact analysis of face-milled spiral bevel gears [NASA-CR-4342] N91-19439

INDIANA UNIV.-PURDUE UNIV., FORT WAYNE.

Rocket noise filtering system using digital filters N91-20031

INNSBRUCK UNIV. (AUSTRIA).

Coordination of eye, head and arm movements in weightlessness N91-19588

Neurological findings after 72 hours water immersion N91-19597

INSTITUT FUER LANDWIRTSCHAFTLICHE BOTANIK, BONN (GERMANY, F.R.).

Electrofusion and regeneration of protoplasts from sunflower (Helianthus annuus L.) N91-19675

INSTITUT NATIONAL DE LA SANTE ET DE LA RECHERCHE MEDICALE, NICE (FRANCE).

Experiment lymphocytes of Aragatz mission: Influence of the space flight on human T lymphocyte and monocyte functions N91-19619

INSTITUT NATIONAL DE LA SANTE ET DE LA RECHERCHE MEDICALE, TOULOUSE (FRANCE).

Growth rate of bacteria without and with antibiotic at different levels of gravity N91-19632

INSTITUT NATIONAL DES SCIENCES APPLIQUEES, LYON (FRANCE).

A study of alkaline element interferences in analytical inductively coupled plasmas [ISAL-90-0069] N91-19915

INSTITUTE FOR COMPUTER APPLICATIONS IN SCIENCE AND ENGINEERING, HAMPTON, VA.

Multigrid solution of compressible turbulent flow on unstructured meshes using a two-equation model [NASA-CR-187513] N91-19043

Digital optical computers at the optoelectronic computing systems center [NASA-CR-187520] N91-19345

Filtering analysis of a direct numerical simulation of the turbulent Rayleigh-Benard problem [NASA-CR-187488] N91-19366

Complete exchange on the iPSC-860 [NASA-CR-187498] N91-19715

Multiphase complete exchange on a circuit switched hypercube [NASA-CR-187499] N91-19716

INSTITUTE FOR ENDOCRINOLOGICAL AND METABOLIC DISEASES, ROME (ITALY).

Head-down tilt test and space-related endocrine physiology N91-19614

INSTITUTE OF BIOMEDICAL PROBLEMS, MOSCOW (USSR).

Medical results of the fourth prime expedition on the orbital station Mir N91-19576

Ultrasound investigation of the cardiovascular system during the 25-days Soviet-French flight: Cardiac aspects N91-19578

Neurological findings after 72 hours water immersion N91-19597

The biochemical and physiological variables in motion sickness followed modified neuroendocrine activity N91-19607

Assessment of bone turnover in humans after space flight and hypokinesia N91-19608

The biological and medical programme of the manned Aragatz mission on the Mir Space Station N91-19617

Human and animal results on vestibular research in space: VERIS N91-19642

Adaptive responses in monkeys during two week space flight N91-19645

Principle and realization of the instrument used for the CIRCE experiment on board the Mir station N91-19684

INSTITUTE OF CROP SCIENCE AND PLANT BREEDING, BRUNSWICK (GERMANY, F.R.).

Physiological criteria and requirement of biomass production under controlled ecological life support systems N91-19659

INSTITUTO DE PESQUISAS ESPACIAIS, SAO JOSE DOS CAMPOS (BRAZIL).

SCD 02 thermal design N91-19129

SCD1 thermal design and test result analysis N91-19130

Experimental determination of satellite bolted joints thermal resistance N91-19157

INTERNATIONAL FUEL CELLS CORP., SOUTH WINDSOR, CT.
Molten carbonate fuel cell technology improvement
[DE91-005540] N91-19505
IONA COLL., NEW ROCHELLE, NY.
The development of structure for the representation and manipulation of sophisticated knowledge in intelligent systems
[AD-A229114] N91-19957
IOWA STATE UNIV. OF SCIENCE AND TECHNOLOGY, AMES.
Localization and electron-phonon interaction in disordered systems
[DE91-007654] N91-19837
ISTITUTO ELETTROTECNICO NAZIONALE (GALILEO FERRARIS), TURIN (ITLAY).
Activities report of the Istituto Elettrotecnico Nazionale Galileo Ferraris
[ETN-91-98868] N91-19822
ITALIAN SPACE AGENCY, ROME.
Blood pressure maturation curve in normotensive rats during growth in simulated microgravitational environment N91-19644

J

JAPAN ATOMIC ENERGY RESEARCH INST., TOKYO.
High temperature tensile properties of nickel-base superalloys for intermediate heat exchangers of high temperature gas-cooled reactors
[DE91-744958] N91-19284
Introduction to fusion
[DE91-744831] N91-19912
Electron temperature of Gd plasma produced by laser resonance ionization
[DE91-744833] N91-19913
Effects of pressure profile and plasma shaping on the n=1 internal kink mode in JT-60/JT-60U pellet fuelled plasmas
[DE91-744965] N91-19914
JAYCOR, VIENNA, VA.
Time-dependent multimode simulation of gyrotron oscillators
[AD-A229861] N91-19413
JET PROPULSION LAB., CALIFORNIA INST. OF TECH., PASADENA.
GaP betavoltaic cells as a power source N91-19211
Thermal cycle testing of Space Station Freedom solar array blanket coupons N91-19216
The Advanced Photovoltaic Solar Array (APSA) technology status and performance N91-19217
Viability study of photovoltaic systems added to terrestrial electric vehicles
[DE91-007689] N91-19355
Algorithms for a very high speed universal noiseless coding module
[NASA-CR-187974] N91-19733
On the optimality of code options for a universal noiseless coder
[NASA-CR-187973] N91-19734
Orientale and South Pole-Aitken basins on the Moon: Preliminary Galileo imaging results N91-20002
Magellan: Preliminary description of Venus surface geologic units N91-20011
JOHANN-WOLFGANG-GOETHE-UNIV., FRANKFURT AM MAIN (GERMANY, F.R.).
Genetic risk and physiological stress induced by heavy ions N91-19680
Defective embryogenesis of Arabidopsis induced by cosmic HZE-particles N91-19682
Arabidopsis thaliana (Heynh.) pollen: A new tool in heavy ions radiation N91-19685
JOHNS HOPKINS UNIV., BALTIMORE, MD.
Ultrafine refractory particle formation in counterflow diffusion flames
[DE91-007693] N91-19260
JOINT EUROPEAN TORUS PROJECT, ABINGDON (ENGLAND).
Plasma boundary experiments on D3-D tokamak
[DE91-002429] N91-19881
JOINT PUBLICATIONS RESEARCH SERVICE, ARLINGTON, VA.
JPRS report: Science and technology. USSR: Life sciences
[JPRS-ULS-91-001] N91-19567
Reactivity of exhausted human skeletal muscle fibers following prolonged antiorthostatic hypokinesia N91-19568
Gravitation receptor reaction in response to effect of acceleration N91-19569
Effects of hyperbaric oxygenation on central hemodynamics and oxygen consumption in severe physical trauma N91-19570
Effects of high temperature and humidity on mental state and metabolism N91-19571
JPRS report: Science and technology. USSR: Physics and mathematics
[JPRS-UPM-90-004] N91-19800
Laws of heat transfer in three-dimensional viscous shock layer of stream flowing past blunt bodies at some angles of attack and glide N91-19801
Acoustic stabilization of laser beam wavefront in nonhomogeneous gaseous medium N91-19802
Passive mode locking in optically pumped Al2O3:Ti(3+) laser N91-19803
Possibility of raising efficiency of free-electron laser in longitudinal magnetic field N91-19804
Quantum fluctuations in laser with intracavity frequency doubling N91-19805
Copper vapor as active medium for high-power oscillator-amplifier laser systems N91-19806
Characteristics of excimer laser with narrow emission line N91-19807
Intracavity second-harmonic generation by laser with optical delay line and mode locking N91-19808
Solution of one-dimensional problem in nonlinear theory of elasticity with structured shock wave N91-19809
Constructing mathematical model of adaptive anti-flutter system N91-19810
Microsecond-pulse Nd-glass laser with monopulse duration control N91-19811
Breakup of femtosecond pulses during amplification in Er(3+)-doped single-mode optical fibers N91-19812
He-Ne laser emitting five lines simultaneously N91-19813
Origin of residual surface resistance of ceramic high-temperature superconductors N91-19814
Limiting pulse signal in NbN-Si structure: Superconductor film on substrate N91-19815
Effect of paramagnetic impurities on dynamics of magnetic fluxes in superconductors N91-19816
Phenomenological theory of phase transitions to nonhomogeneous noncommensurate phase with superconducting current N91-19817
Thermal conductivity of high-temperature superconductors in normal state N91-19818
Superconductivity of oxide film electrolytically deposited on surface of B(1-x)Sb(x) single crystal N91-19819
Coherent effects in generation of ultrashort light pulses by semiconductor injection laser N91-19820

K

KANSAS UNIV. CENTER FOR RESEARCH, INC., LAWRENCE.
Radar backscatter from the sea controlled experiments
[AD-A229847] N91-19340
KAROLINSKA INST., STOCKHOLM (SWEDEN).
Effects of short-lasting weightlessness on gas exchange during light exercise N91-19573
Oxygen uptake during concentric and eccentric resistive exercise using a new gravity-independent ergometer N91-19587
Effects of training with reduced perfusion pressure on performance and muscle fiber characteristics N91-19615
Muscle function impairment following lower limb unloading in men N91-19616
KENT UNIV., CANTERBURY (ENGLAND).
Space debris: Orbital microparticulates impacting LDEF experiments favour a natural extraterrestrial origin N91-20008
KOBE UNIV. OF MERCANTILE MARINE (JAPAN).
Study on ablation of target material induced by pulsed ion beam bombardment N91-19886
KUMAMOTO UNIV. (JAPAN).
Generation of pulsed ion beams by an inductive storage pulsed power generator N91-19891
KYOTO UNIV., UJI (JAPAN).
Quasi-nonlinear theory of cosmological self-gravitating systems
[DE91-744971] N91-19989
Statistics of peaks in cosmological nonlinear density fields
[DE91-744972] N91-19990
How many times do we have in quantum gravity
[DE91-744973] N91-19991
Gravitational lens effect of wall-like objects and its cosmological implications
[DE91-744976] N91-19992

L

LABORATOIRE DE MEDECINE AEROSPATIALE, BRETIGNY-SUR-ORGE (FRANCE).
Review of EEG studies in non human primates exposed to microgravity N91-19649
LAWRENCE LIVERMORE NATIONAL LAB., CA.
Finnigan ion trap mass spectrometer detection limits and thermal energy analyzer interface status report and present capabilities
[DE91-006220] N91-19254
Theoretical investigation of phase stability in non-magnetic Fe-V substitutional alloys
[DE91-006711] N91-19268
Electromagnetic penetration through narrow slots in conducting surfaces and coupling to structures on the shadow side
[DE91-007155] N91-19331
Conservation of energy, momentum, and angular momentum in Lagrangian staggered-grid hydrodynamics
[DE91-008059] N91-19381
Measurements with a 35 psec gate time microchannelplate camera
[DE91-006701] N91-19400
Soft x-ray laser gain prediction at high density for the nitrogen isoelectronic sequence
[DE91-007616] N91-19416
Intense microwave generation using free-electron lasers
[DE91-007262] N91-19417
Simulation of a standing-wave free-electron laser
[DE91-007330] N91-19418
Phase stability of a standing-wave free-electron laser
[DE91-008068] N91-19427
Recombination x ray laser experiments using exploding ribbon Al targets
[DE91-007146] N91-19429
Upgrade of the LLNL Nova laser for inertial confinement fusion
[DE91-008060] N91-19430
Nickel-like x ray lasers
[DE91-008502] N91-19433
Nuclear-spectroscopy computerized tomography scanners
[DE91-008447] N91-19466
Zonal statistics in (General Circulation Model) GCM/GCM/data intercomparisons
[DE91-006706] N91-19530
Cloud forcing: A modeling perspective
[DE91-007215] N91-19551
The relationship between aerosol and drop size distributions in the marine atmosphere
[DE91-006514] N91-19553
Lecture notes on nonlinear inversion and tomography
[DE91-008238] N91-19558
An introduction to biological dosimetry
[DE91-007125] N91-19698
Development of a numerical computer code and circuit element models for simulation of firing systems
[DE91-007162] N91-19739
Energy sciences supercomputing 1990
[DE91-007188] N91-19740
Techniques for interactive 3-D scientific visualization
[DE91-007122] N91-19745
PHIGS PLUS for scientific graphics
[DE91-007615] N91-19747
Large-scale computing in the energy research programs
[DE91-007907] N91-19748
Convergence of linear programming using a Hopfield net
[DE91-007870] N91-19758
The cost-constrained traveling salesman problem
[DE91-004943] N91-19775
Analysis of spherical geometry finite element transport solutions in the thick diffusion limit
[DE91-007598] N91-19780
Even- and odd-parity finite-element transport solutions in the thick diffusion limit
[DE91-007618] N91-19781
Discontinuous finite-element transport solutions in the thick diffusion limit in Cartesian geometry
[DE91-007620] N91-19782
Anastasia: A solid model based 3D finite difference mesh generator
[DE91-007621] N91-19783
Response matrix Monte Carlo based on a general geometry local calculation for electron transport
[DE91-007638] N91-19794
Potential health risks from postulated accidents involving the Pu-238 RTG (Radioisotope Thermoelectric Generator) on the Ulysses solar exploration mission
[DE91-007142] N91-19857
Relativistic klystron research for future linear colliders
[DE91-008063] N91-19862
UV Thomson scattering from x ray laser plasmas
[DE91-007347] N91-19895
Optically-ionized plasma recombination x ray lasers
[DE91-007261] N91-19898
Calculation of emission and absorption spectra of LTE plasma by the STA (Super Transition Array) method
[DE91-007617] N91-19900

Measurements of stark-broadening in hot dense plasma
[DE91-008504] N91-19910
Positron lifetime studies of defect structures in Ba(1-x)K(x)BiO3
[DE91-007341] N91-19919
A photoemission investigation of compound semiconductor monodisperse clusters
[DE91-006707] N91-19921
Photoelectron diffraction of magnetic ultrathin films: Fe/Cu(001)
[DE91-007254] N91-19924
Application of MeV ions to the analysis and modification of high temperature superconducting materials
[DE91-007317] N91-19927
Some limitations of detailed balance for inverse reaction calculations in the astrophysical P-process
[DE91-007258] N91-19983
Primordial nucleosynthesis: Beyond the standard model
[DE91-007264] N91-19984
Two possible problems for standard big bang nucleosynthesis
[DE91-007342] N91-19985

LEHIGH UNIV., BETHLEHEM, PA.
Mechanisms and controlling characteristics of the catalytic oxidation of methane
[DE91-008033] N91-19263
High resolution microstructural and microchemical analysis of zirconia eutectic interfaces
[DE91-008032] N91-19940
Robot tracking system improvements and visual calibration of orbiter position for radiator inspection N91-20037

LIEGE UNIV. (BELGIUM).
IAL SPACE: A test laboratory for the ISO cryogenic payload N91-19142
The space simulation facilities at IAL SPACE N91-19151

LOCKHEED CORP., HOUSTON, TX.
Tool and data interoperability in the SSE system N91-19727

LOCKHEED ENGINEERING AND SCIENCES CO., WASHINGTON, DC.
USSR Space Life Sciences Digest. Index to issues 26-29
[NASA-CR-3922(35)] N91-19700

LOCKHEED MISSILES AND SPACE CO., AUSTIN, TX.
Empirical studies of software design: Implications for SSEs N91-19728

LOCKHEED MISSILES AND SPACE CO., PALO ALTO, CA.
Integrated Cryogenic Experiment (ICE) microsphere investigation
[NASA-CR-177538] N91-19323

LOS ALAMOS NATIONAL LAB., NM.
Atomic oxygen effects on boron nitride and silicon nitride: A comparison of ground based and space flight data N91-19146
Methane to methanol conversion by direct partial oxidation
[DE91-007352] N91-19257
Assessing the impact of large-scale computing on the size and complexity of first-principles electromagnetic models
[DE91-007491] N91-19333
Interferometry, streak photography, and stereo photography of laser-driven miniature flying plates
[DE91-007493] N91-19405
Development of KrF lasers for inertial confinement fusion
[DE91-007349] N91-19419
Excimer laser surface processing for tribological applications in metals and ceramics
[DE91-002324] N91-19428
Texture and microstructure development in Al-2 percent Mg during high-temperature deformation
[DE91-007355] N91-19480
Association of an auroral surge with plasma sheet recovery and the retreat of the substorm neutral line
[DE91-007351] N91-19552
Predicted Bremsstrahlung generation by energetic electron beams
[DE91-007164] N91-19858
Electromagnetic ion/ion cyclotron instability
[DE91-004841] N91-19860
Quasi-molecular processes in dense plasmas
[DE91-007388] N91-19899
Free energy simulation of grain boundary segregation the thermodynamics in Ni(3-x)Al(1+x)
[DE91-007473] N91-19928
Origin of regularities in the redshift distributions of distant galaxies and quasars
[DE91-007889] N91-19986
Effects of a giant impact on Uranus N91-20012

LOUISIANA STATE UNIV., BATON ROUGE.
The structure of nuclei far from beta stability
[DE91-008140] N91-19846
Electric monopole transitions and shape coexistence in nuclei
[DE91-008141] N91-19847

LOUISVILLE UNIV., KY.
Cosmos: 1989 immunology studies
[NASA-CR-188046] N91-19701

LUNAR AND PLANETARY INST., HOUSTON, TX.
Twenty-Second Lunar and Planetary Science Conference
[NASA-CR-187971] N91-19995

LYON-1 UNIV., VILLEURBANNE (FRANCE).
Volume regulating hormones, fluid and electrolyte modifications during the Aragatz Mission (Mir station) N91-19689

M

MAINZ UNIV. (GERMANY, F.R.).
Ocular roll under changing z-axis acceleration and neck position N91-19580

MARTIN MARIETTA AEROSPACE, DENVER, CO.
Solar thermal vacuum tests of Magellan spacecraft N91-19127
An outgassing model of non-metallic materials for the ascent of a Titan 4 launch vehicle N91-19132
Advances in atomic oxygen simulation N91-19147
Transfer orbit stage mechanisms thermal vacuum test N91-19161
Composite materials for space applications
[NASA-CR-187472] N91-19238

MARYLAND UNIV., COLLEGE PARK.
An energy recovery system for a quasi-optical gyrotron
[DE91-008317] N91-19357
A program of high power microwave source research and development from 8 GHz to 600 GHz
[DE91-008320] N91-19358
Time-dependent multimode simulation of gyrotron oscillators
[AD-A229861] N91-19413
ICRCCM (intercomparison of radiation codes used in climate models). Phase 2: Verification and calibration of radiation codes in climate models
[DE91-007323] N91-19555
The study of effects of small perturbations on chaotic systems
[DE91-007320] N91-19792

MASSACHUSETTS INST. OF TECH., CAMBRIDGE.
Automatic speech recognition in air traffic control: A human factors perspective N91-19025
The temporal logic of the tower chief system N91-19026
BUBBLES: An automated decision support system for final approach controllers N91-19027
Control of catalytic hydrotreating selectivity with ammonia
[DE91-005511] N91-19250

MASSACHUSETTS INST. OF TECH., LEXINGTON.
The performance of multilayer insulation in a rapidly depressurizing environment N91-19133

MASSACHUSETTS UNIV., AMHERST.
Computation and graphics in mathematical research
[DE91-007333] N91-19776
Carbon dioxide and water exchange of a soybean stand grown in the biomass production chamber N91-20026

MATERIALS RESEARCH LABS., ASCOT VALE (AUSTRALIA).
Magneto-elastic behaviour of steels for naval applications
[MRL-TR-90-27] N91-19266

MAX-PLANCK-INST. FUER PHYSIK UND ASTROPHYSIK, GARCHING (GERMANY, F.R.).
Thermal instabilities in cooling flows: The evolution of nearly spherical perturbations
[MPE-PREPRINT-176] N91-19365
An analytical study of neutral expansion, ionization, and charged particle acceleration in a neutral lithium release for the parallel electric field measurement
[MPE-PREPRINT-180] N91-19880
Activities report of the Institute for Extraterrestrial Physics
[MPE-222] N91-19971
Detection of an isotopic short submillimeter CO line: Column densities of warm gas in molecular clouds
[MPE-PREPRINT-178] N91-19976
Observations of CO isotopic emission and the far-infrared continuum of Centaurus A
[MPE-PREPRINT-183] N91-19977
Search for the optical signatures of a pulsar in SN1987A
[MPE-PREPRINT-188] N91-19978
Fluorescent HD emission from photodissociation regions
[MPE-PREPRINT-177] N91-19982

MAX-PLANCK-INST. FUER RADIOASTRONOMIE, BONN (GERMANY, F.R.).
Quantum optics reveals the nature of superconductivity
[TR-69] N91-19946

MAX-PLANCK-INST. FUER STROEMUNGSFORSCHUNG, GOETTINGEN (GERMANY, F.R.).
Traveling time effects in a channel flow
[MPIS-10/1990] N91-19384
Calculation of pulsating liquid free jets
[MPIS-15/1990] N91-19385
Reflections on some problems concerning the role of superfluid turbulence in the propagation of second-sound pulses in He 2
[MPIS-8/1990] N91-19827

MAX-PLANCK-INST. FUER VERHALTENSPHYSIOLOGIE, SEEWIESEN UBER STARNBERG (GERMANY, F.R.).
Determinants of spatial orientation in weightlessness N91-19605

MCDONNELL-DOUGLAS HELICOPTER CO., MESA, AZ.
Development and applications of a multi-level strain energy method for detecting finite element modeling errors
[NASA-CR-187447] N91-19478

MCDONNELL-DOUGLAS SPACE SYSTEMS CO., HUNTINGTON BEACH, CA.
Innovations in dynamic test restraint systems N91-19145
Space environmental effects on spacecraft thermal control coatings N91-19148
A unique approach to space thermal simulation N91-19153

MEMPHIS STATE UNIV., TN.
Study of the available finite element software packages at KSC N91-20029

MESSERSCHMITT-BOELKOW-BLOHM G.M.B.H., BREMEN (GERMANY, F.R.).
Free flow electrophoresis experiment TEPE 3 on Texus 24
[MBB-UO-0130-90-PUB] N91-19321
Free flow electrophoresis experiment TEPE 3 on TEXUS 24 N91-19654

MESSERSCHMITT-BOELKOW-BLOHM G.M.B.H., MUNICH (GERMANY, F.R.).
Propulsion system concept for the Eurofar tilt rotor aircraft
[MBB-UD-0573-90-PUB] N91-19084
BO 108 development status and prospects
[MBB-UD-0574-90-PUB] N91-19085
Development of bearingless tail rotors
[MBB-UD-0575-90-PUB] N91-19086
Design and first tests of individual blade control actuators
[MBB-UD-0577-90-PUB] N91-19087
Crashworthiness investigations in the preliminary design phase of the NH90
[MBB-UD-0579-90-PUB] N91-19088
New computer codes for the structural analysis of composite helicopter structures
[MBB-UD-0580-90-PUB] N91-19089
MBB's involvement in military helicopter programmes
[MBB-UD-0588-90-PUB] N91-19091
I'm all 'light' Jack
[MBB-UD-0576-90-PUB] N91-19101
Airport apron research and development
[MBB-Z-0168-90-PUB] N91-19106
Airport system technical aspects N91-19107
Noise level reduction inside helicopter cabins
[MBB-UD-0578-90-PUB] N91-19828
A gradient microphone for locating sound targets
[MBB-Z-0341-90-PUB] N91-19829
Fiber optic interferometric measuring method for the determination of a very small polarization coefficient
[MBB-UA-1185-90-PUB] N91-19876
Light guide fibers
[MBB-UA-1199-90-PUB] N91-19877

MESSERSCHMITT-BOELKOW-BLOHM G.M.B.H., OTTOBRUNN (GERMANY, F.R.).
System design for the Tiger helicopter
[MBB-UD-0581-90-PUB] N91-19090
Application of functional gradient materials in the aerospace industry
[MBB-Z-0320-90-PUB] N91-19311
C-band antennas for regional communication systems
[MBB-UK-0107-90-PUB] N91-19336
Non-homogeneous bars under tension, pure bending, and temperature loads
[MBB-UD-0572-90-PUB] N91-19485
Experimental equipment for space biology
[MBB-UO-0096-90-PUB] N91-19708

Thermal insulation of a cryogenic tank for a space telescope using a pretensioned suspension of Fiber Reinforced Composite (FRC)
[MBB-UD-0571-90-PUB] N91-19981

MICHIGAN UNIV., ANN ARBOR.
Basic research model of natural gas combustion in turbulent flow
[PB91-130260] N91-19264
Task reports on developing techniques for scattering by 3D composite structures and to generate new solutions in diffraction theory using higher order boundary conditions
[NASA-CR-188057] N91-19305
A finite element conjugate gradient FFT method for scattering N91-19306
Analytical solutions with Generalized Impedance Boundary Conditions (GIBC) N91-19307
Characterization of devices, circuits, and high-temperature superconductor transmission lines by electro-optic testing
[NASA-CR-187950] N91-19343

MIDWEST RESEARCH INST., GOLDEN, CO.
InP/Ga0.47In0.53As monolithic, two-junction, three-terminal tandem solar cells N91-19191
Recent advances in the ITO/InP solar cell N91-19202
Results of scoping tests for open-cycle OTEC (Ocean Thermal Energy Conversion) components operating with seawater
[DE89-009514] N91-19501
Solid State Photovoltaic Research Branch
[DE91-002128] N91-19502

MILAN UNIV. (ITALY).
Simulated absence of gravity impairs arterial baroreceptor control of heart rate in man N91-19599
Blood pressure maturation curve in normotensive rats during growth in simulated microgravitational environment N91-19644
Gravity dependence of pleural liquid turnover N91-19651

MISSISSIPPI STATE UNIV., MISSISSIPPI STATE.
Data acquisition and analysis on the two-color laser transmissometer system
[DE91-007235] N91-19420
Structured software design for an on-line laser-based particle size distribution instrument
[DE91-007234] N91-19746
Performance characteristics of an MHD (Magnetohydrodynamic) pilot plant electrostatic precipitator
[DE91-007218] N91-19905

MISSOURI UNIV., COLUMBIA.
Late transition metal (mu)-oxo and (mu)-imido complexes
[DE91-005349] N91-19267

MITECH, INC., WASHINGTON, DC.
The 1990-1991 aviation system capacity plan
[AD-A229863] N91-19075

MONTANA STATE UNIV., BOZEMAN.
Computer controlled MHD power consolidation and pulse generation system
[DE91-006793] N91-19347

MORGANTOWN TECHNOLOGY CENTER, WV.
An evaluation of co-planar lineament analysis and some thoughts on using surface geological data to predict sub-surface geology
[DE90-009687] N91-19556

MOSCOW STATE UNIV. (USSR).
Baroelectric effect in the present of gravitational forces
[DE91-615469] N91-19559
Sixquarks in neutron stars
[DE91-615472] N91-19987
Neutron propagation from solar flare in the solar atmosphere
[DE91-615465] N91-20016
Experimental data on study of cosmic ray particles in the E greater than or equal to 2 TeV energy range at the Cosmos-1713 satellite with the Sokol-2 device
[DE91-615479] N91-20020
Cosmic ray charged component variations at sea level
[DE91-615480] N91-20021

MSE, INC., BUTTE, MT.
Ceramic fabrication R and D
[DE91-006537] N91-19298

N

NAGAOKA TECHNOLOGICAL UNIV., NIIGATA (JAPAN).
Rayleigh-Taylor instability in LIB ICF N91-19883
Theoretical study of plasma focus diode N91-19887
Pulse-power characteristic of VIVA-1 (Versatile Inductive Voltage Adder) N91-19888

NAGOYA UNIV. (JAPAN).
New method for edge plasma control by RF ponderomotive force
[DE91-744823] N91-19911

NAPLES UNIV. (ITALY).
Effect of the centrifuge forces on pregnant rats N91-19629

NATIONAL ACADEMY OF SCIENCES - NATIONAL RESEARCH COUNCIL, WASHINGTON, DC.
Computers at risk: Safe computing in the information age
[LC-90-22329] N91-19721
Report of a workshop on Distributed Decision Making
[LC-89-64440] N91-19952

NATIONAL AERONAUTICS AND SPACE ADMINISTRATION, WASHINGTON, DC.
Space station: The next logical step
[NASA-TM-103398] N91-19123
Enhancing space transportation: The NASA program to develop electric propulsion
[NASA-TM-4244] N91-19181
The OAST space power program N91-19183
Microgravity strategic plan, 1988
[NASA-TM-103397] N91-19319
Solid earth science in the 1990s. Volume 1: Program plan
[NASA-TM-4256-VOL-1] N91-19499
The 1989-1990 NASA space biology accomplishments
[NASA-TM-4258] N91-19697
The role of software engineering in the space station program N91-19729
NASA Thesaurus supplement: A four part cumulative supplement to the 1988 edition of the NASA Thesaurus (supplement 5)
[NASA-SP-7064-SUPPL-5] N91-19962
A scientific program for infrared, submillimeter and radio astronomy from space: A report by the Management Operations Working Group
[NASA-TM-103333] N91-19979
Orientale and South Pole-Aitken basins on the Moon: Preliminary Galileo imaging results N91-20002

NATIONAL AERONAUTICS AND SPACE ADMINISTRATION. AMES RESEARCH CENTER, MOFFETT FIELD, CA.
Modal analysis of UH-60A instrumented rotor blades
[NASA-TM-4239] N91-19052
Panel methods: An introduction
[NASA-TP-2995] N91-19058
An experimental study of the turbulent boundary layer on a transport wing in subsonic and transonic flow
[NASA-TM-102206] N91-19062
Single-strain-gage force/stiffness buckling prediction techniques on a hat-stiffened panel
[NASA-TM-101733] N91-19077
Introduction of the M-85 high-speed rotorcraft concept
[NASA-TM-102871] N91-19078
State estimation applications in aircraft flight-data analysis: A user's manual for SMACK
[NASA-RP-1252] N91-19082
Development of a fatigue-life methodology for composite structures subjected to out-of-plane load components
[NASA-TM-102885] N91-19241
Composite flexible insulation for thermal protection of space vehicles
[NASA-TM-103836] N91-19304
Centrifuge Facility Conceptual System Study. Volume 1: Facility overview and habitats
[NASA-TM-102860] N91-19566
Simulating motivated cognition
[NASA-TM-102886] N91-19770
J-85 jet engine noise measured in the ONERA S1 wind tunnel and extrapolated to far field
[NASA-TP-3053] N91-19823
Large-scale aeroacoustic research feasibility and conceptual design of test-section inserts for the Ames 80- by 120-foot wind tunnel
[NASA-TP-3020] N91-19824
Research and technology, 1989
[NASA-TM-102264] N91-20039

NATIONAL AERONAUTICS AND SPACE ADMINISTRATION. GODDARD SPACE FLIGHT CENTER, GREENBELT, MD.
Sixteenth Space Simulation Conference Confirming Spaceworthiness Into the Next Millennium
[NASA-CP-3096] N91-19126
The test facility requirements for the thermal vacuum thermal balance test of the Cosmic Background Explorer Observatory N91-19128
Flow fields of low pressure vent exhausts N91-19135
Contamination control program for the Cosmic Background Explorer: An overview N91-19152
System description document for the Anthrobot-2: A dexterous robot hand
[NASA-TM-104535] N91-19449
A status report on the analysis of the NOAA-9 SBUV/2 sweep mode solar irradiance data N91-19518
A technique for directly comparing radiances from two satellites N91-19520
Initial estimate of NOAA-9 SBUV/2 total ozone drift: Based on comparison with re-calibrated TOMS measurements and pair justification of SBUV/2 N91-19523
Calibration of long term satellite ozone data sets using the space shuttle N91-19524
Ozone measurements from the NOAA-9 and the Nimbus-7 satellites: Implications of short and long term variabilities N91-19527
On the joint inversion of geophysical data for models of the coupled core-mantle system
[NASA-TM-104536] N91-19557
K/T age for the popigai impact event N91-19999

NATIONAL AERONAUTICS AND SPACE ADMINISTRATION. HUGH L. DRYDEN FLIGHT RESEARCH FACILITY, EDWARDS, CA.
F-18 high alpha research vehicle surface pressures: Initial in-flight results and correlation with flow visualization and wind-tunnel data
[NASA-TM-101724] N91-19051
Summary of in-flight flow visualization obtained from the NASA high alpha research vehicle
[NASA-TM-101734] N91-19055
A simple dynamic engine model for use in a real-time aircraft simulation with thrust vectoring
[NASA-TM-4240] N91-19079
Techniques for hot structures testing
[NASA-TM-101727] N91-19080
Monitoring techniques for the X-29A aircraft's high-speed rotating power takeoff shaft
[NASA-TM-101731] N91-19081
Thermoelastic vibration test techniques
[NASA-TM-101742] N91-19083
Preliminary results from an airdata enhancement algorithm with application to high-angle-of-attack flight
[NASA-TM-101737] N91-19095
A proposed Kalman filter algorithm for estimation of unmeasured output variables for an F100 turbofan engine
[NASA-TM-4234] N91-19099
Real-time application of advanced three-dimensional graphic techniques for research aircraft simulation
[NASA-TM-101730] N91-19742

NATIONAL AERONAUTICS AND SPACE ADMINISTRATION. JOHN F. KENNEDY SPACE CENTER, COCOA BEACH, FL.
Debris/ice/TPS assessment and photographic analysis for shuttle mission STS-35
[NASA-TM-103816] N91-19118
Central and peripheral cardiovascular responses to electrically induced and voluntary leg exercise N91-19687
Responses of women to orthostatic and exercise stresses
[NASA-TP-3043] N91-19711
Research reports: 1990 NASA/ASEE Summer Faculty Fellowship Program
[NASA-CR-187638] N91-20022

NATIONAL AERONAUTICS AND SPACE ADMINISTRATION. LYNDON B. JOHNSON SPACE CENTER, HOUSTON, TX.
Behavior of surface and corner cracks subjected to tensile and bending loads in Ti-6Al-4V alloy
[NASA-TM-102165] N91-19273
An evaluation of the fatigue crack growth and fracture toughness properties of beryllium-copper alloy CDA172
[NASA-TM-102166] N91-19274
Postural changes following sensory reinterpretation as an analog to spaceflight N91-19610
Standardization of motion sickness induced by left-right and up-down reversing prisms N91-19611
Predictions of cell damage rates for Lifesat missions
[NASA-TM-102170] N91-19699
Mission operations directorate: Facility and support systems division N91-19726
The 1989 JSC bibliography of scientific and technical papers
[NASA-TM-102173] N91-19959
Relative chronology of Martian volcanoes N91-20007
Experimental reduction of simulated lunar glass by carbon and hydrogen and implications for lunar base oxygen production N91-20009

NATIONAL AERONAUTICS AND SPACE ADMINISTRATION. LANGLEY RESEARCH CENTER, HAMPTON, VA.
Joint University Program for Air Transportation Research, 1989-1990
[NASA-CP-3095] N91-19024
Experimental investigation of porous-floor effects on cavity flow fields at supersonic speeds
[NASA-TP-3032] N91-19042
A finite Reynolds number approach for the prediction of boundary layer receptivity in localized regions
[NASA-TM-102781] N91-19061

Robust fault diagnosis of physical systems in operation
[NASA-TM-102767] N91-19073
The 5th Annual NASA Spacecraft Control Laboratory Experiment (SCOLE) Workshop, part 2
[NASA-CP-10057-PT-2] N91-19122
Free vibration of hexagonal panels supported at discrete points
[NASA-TM-102688] N91-19166
Comparative morphology of configurations with reduced part count derived from the octahedral-tetrahedral truss
[NASA-TM-102768] N91-19168
Laser Doppler velocimetry for continuous flow solar-pumped iodine laser system
[NASA-TM-104029] N91-19415
Active damping application to the shuttle RMS
[NASA-TM-102763] N91-19471
Modal identification of a deployable space truss
[NASA-TM-102720] N91-19474
Nonlinear analysis and redesign of the mixed-mode bending delamination test
[NASA-TM-102777] N91-19482

NATIONAL AERONAUTICS AND SPACE ADMINISTRATION. LEWIS RESEARCH CENTER, CLEVELAND, OH.

Improved visualization of flow field measurements
[NASA-TM-103679] N91-19044
Inflight source noise of an advanced full-scale single-rotation propeller
[NASA-TM-103687] N91-19045
Icing characteristics of a natural-laminar-flow, a medium-speed, and a swept, medium-speed airfoil
[NASA-TM-103693] N91-19046
Prediction of ice shapes and their effect on airfoil performance
[NASA-TM-103701] N91-19047
Acoustic radiation from lifting airfoils in compressible subsonic flow
[NASA-TM-103650] N91-19053
Implementation of control point form of algebraic grid-generation technique
[NASA-TM-103748] N91-19054
Three-component laser anemometer measurement systems
[NASA-TP-3080] N91-19057
Development of a laser-induced heat flux technique for measurement of convective heat transfer coefficients in a supersonic flowfield
[NASA-TM-103778] N91-19063
The selection of convertible engines with current gas generator technology for high speed rotorcraft
[NASA-TM-103774] N91-19097
Wind tunnel wall effects in a linear oscillating cascade
[NASA-TM-103690] N91-19098
Space reactor/Stirling cycle systems for high power lunar application
[NASA-TM-103698] N91-19112
Automatic control study of the icing research tunnel refrigeration system
[NASA-TM-4257] N91-19115
Aeolian removal of dust types from photovoltaic surfaces on Mars N91-19156
Simulation of Martian dust accumulation on surfaces N91-19160
The effect of the low Earth orbit environment on space solar cells
[NASA-TM-103735] N91-19165
Advanced chemical propulsion at NASA Lewis: Metallized and high energy density propellants
[NASA-TM-103771] N91-19175
Radiation resistance of thin-film solar cells for space photovoltaic power
[NASA-TM-103715] N91-19176
Multi-dimensional modeling of a thermal energy storage canister
[NASA-TM-103731] N91-19177
Solar electric propulsion for Mars transport vehicles
[NASA-TM-103234] N91-19178
Key issues in space nuclear power
[NASA-TM-103656] N91-19179
A 5-kW xenon ion thruster lifetest
[NASA-TM-103191] N91-19180
Space Photovoltaic Research and Technology, 1989
[NASA-CP-3107] N91-19182
Tandem concentrator solar cells with 30 percent (AMO) power conversion efficiency N91-19189
Thermal annealing of GaAs concentrator solar cells N91-19195
Review of thin film solar cell technology and applications for ultra-light spacecraft solar arrays N91-19198
Dual-purpose self-deliverable lunar surface PV electrical power system N91-19200
Feasibility of solar power for Mars N91-19201
Semiconductor structural damage attendant to contact formation in III-V solar cells N91-19203
Effects of proton irradiation on the performance of InP/GaAs solar cells N91-19205
Key factors limiting the open circuit voltage of n(+)pp(+) indium phosphide solar cells N91-19206
Determination of series resistance of indium phosphide solar cells N91-19207
Investigation of anodic and chemical oxides grown on p-type InP with applications to surface passivation for n(+)-p solar cell fabrication N91-19208
A comparative study of performance parameters of n(+)-p InP solar cells made by closed-ampoule sulfur diffusion into Cd- and Zn-doped p-type InP substrates N91-19209
Mini-dome Fresnel lens photovoltaic concentrator development N91-19219
Indium phosphide solar cells N91-19221
Tribological properties of Ag/Ti films on Al2O3 ceramic substrates
[NASA-TM-103784] N91-19224
METCAN updates for high temperature composite behavior: Simulation/verification
[NASA-TM-103682] N91-19229
Computational simulation of hot composites structures
[NASA-TM-103681] N91-19230
Prospects for using carbon-carbon composites for EMI shielding
[NASA-TM-103677] N91-19231
An overview of self-consistent methods for fiber-reinforced composites
[NASA-TM-103713] N91-19232
Low-density, high-strength intermetallic matrix composites by XD (trademark) synthesis
[NASA-TM-103724] N91-19233
Effect of fiber reinforcements on thermo-oxidative stability and mechanical properties of polymer matrix composites
[NASA-TM-103648] N91-19234
Ceramic composites for rocket engine turbines
[NASA-TM-103743] N91-19235
Probabilistic micromechanics and macromechanics of polymer matrix composites
[NASA-TM-103669] N91-19236
Concurrent micromechanical tailoring and fabrication process optimization for metal-matrix composites
[NASA-TM-103670] N91-19237
Reactivity of pi-complexes of Ti, V, and Nb towards dithioacetic acid: Synthesis and structure of novel metal sulfur-containing complexes
[NASA-TM-103666] N91-19256
Structural reliability analysis of laminated CMC components
[NASA-TM-103685] N91-19292
Comparison of dynamic fatigue behavior between SiC whisker-reinforced composite and monolithic silicon nitrides
[NASA-TM-103707] N91-19293
Low Earth orbital atomic oxygen and ultraviolet radiation effects on polymers
[NASA-TM-103711] N91-19294
Thermal shock of fiber reinforced ceramic matrix composites
[NASA-TM-103777] N91-19295
Synthesis and structures of metal chalcogenide precursors
[NASA-TM-103665] N91-19296
Crystallization and properties of Sr-Ba aluminosilicate glass-ceramic matrices
[NASA-TM-103764] N91-19308
Conceptual study of on orbit production of cryogenic propellants by water electrolysis
[NASA-TM-103730] N91-19317
Growth kinetics of physical vapor transport processes: Crystal growth of the optoelectronic material mercurous chloride
[NASA-TM-103788] N91-19320
Development of a vibration isolation prototype system for microgravity space experiments
[NASA-TM-103664] N91-19324
Coplanar waveguide EEsoF MICAD macros make circuit layout easy
[NASA-TM-103272] N91-19332
Pulsed response of a traveling-wave tube
[NASA-TM-103672] N91-19348
Using a modified Hewlett Packard 8410 network analyzer as an automated farfield antenna range receiver
[NASA-TM-103700] N91-19349
Ellipsometric study of InGaAs MODFET material
[NASA-TM-103286] N91-19351
Effect of dislocations on the open-circuit voltage, short-circuit current and efficiency of heteroepitaxial indium phosphide solar cells
[NASA-TM-103762] N91-19354
Two reference time scales for studying the dynamic cavitation of liquid films
[NASA-TM-103673] N91-19369
Turbulent boundary layer separation over a rearward facing ramp and its control through mechanical excitation
[NASA-TM-103702] N91-19370
A summary of existing and planned experiment hardware for low-gravity fluids research
[NASA-TM-103706] N91-19371
The effect of small streamwise velocity distortion on the boundary layer flow over a thin flat plate with application to boundary layer stability theory
[NASA-TM-103668] N91-19372
Critical-layer nonlinearity in the resonance growth of three-dimensional waves in boundary layers
[NASA-TM-103639] N91-19373
Experimental investigation of a single flush-mounted hypermixing nozzle
[NASA-TM-103726] N91-19374
A 2-D oscillating flow analysis in Stirling engine heat exchangers
[NASA-TM-103781] N91-19375
Rotating pressure measurement system using an on board calibration standard
[NASA-TM-103676] N91-19401
Cryogenic liquid-jet breakup in two-fluid atomizers
[NASA-TM-103734] N91-19402
Three-dimensional computed tomography from interferometric measurements within a narrow cone of views
[NASA-TM-103257] N91-19404
High temperature NASP engine seal development
[NASA-TM-103716] N91-19441
A test fixture for measuring high-temperature hypersonic-engine seal performance
[NASA-TM-103658] N91-19442
Heat transfer in rotating serpentine passages with trips normal to the flow
[NASA-TM-103758] N91-19443
ETARA PC version 3.3 user's guide: Reliability, availability, maintainability simulation model
[NASA-TM-103751] N91-19462
Property and microstructural nonuniformity in the yttrium-barium-copper-oxide superconductor determined from electrical, magnetic, and ultrasonic measurements
[NASA-TM-103732] N91-19463
NDE standards for high temperature materials
[NASA-TM-103761] N91-19464
Probabilistic simulation of uncertainties in thermal structures
[NASA-TM-103680] N91-19472
Application of thermal life prediction model to high-temperature aerospace alloys B1900+Hf and Haynes 188
[NASA-TM-4226] N91-19473
Cascade flutter analysis with transient response aerodynamics
[NASA-TM-103746] N91-19475
On the thermodynamics of stress rate in the evolution of back stress in viscoplasticity
[NASA-TM-103794] N91-19476
The method of lines in analyzing solids containing cracks
[NASA-TM-103626] N91-19477
Towards practical control design using neural computation
[NASA-TM-103785] N91-19766
Spectrum transformation for divergent iterations
[NASA-TM-103745] N91-19786
Unsteady blade pressure measurements for the SR-7A propeller at cruise conditions
[NASA-TM-103606] N91-19825
Study of InGaAs based MODFET structures using variable angle spectroscopic ellipsometry
[NASA-TM-103792] N91-19935
Chemical approaches to carbon dioxide utilization for manned Mars missions
[NASA-TM-103728] N91-20015

NATIONAL AERONAUTICS AND SPACE ADMINISTRATION. MARSHALL SPACE FLIGHT CENTER, HUNTSVILLE, AL.

Atmospheric environment for space shuttle (STS-41) launch
[NASA-TM-103525] N91-19529
A new approach to electrophoresis in space N91-19653
Protein purification in multicompartment electrolyzers for crystal growth of r-DNA products in microgravity N91-19665

NATIONAL AEROSPACE LAB., TOKYO (JAPAN).

Result of ONERA standard model test in 2m x 2m transonic wind tunnel
[DE91-750115] N91-19066
Investigation of ATP blades, part 3
[DE91-750104] N91-19105
Strength test of CFRP box beam model
[NAL-TR-1057] N91-19469

NATIONAL ASTRONOMY AND IONOSPHERE CENTER, ARECIBO, PUERTO RICO.
Mars radar mapping: Strong depolarized echoes from the Elysium/Amazonis outflow channel complex N91-20001
NATIONAL GEOPHYSICAL DATA CENTER, BOULDER, CO.
Solar-geophysical data Number 554, October 1990. Part 2 (comprehensive reports): Data for April 1990 and miscellaneous. Explanation of data reports issued as Number 515 (supplement) July 1987
[PB91-124586] N91-20017
Solar-geophysical data Number 554, October 1990. Part 1 (prompt reports): Data for September, August 1990, and late data. Explanation of data reports issued as Number 515 (supplement) July 1987
[PB91-124594] N91-20018
NATIONAL INST. FOR FUSION SCIENCE, NAGOYA (JAPAN).
Cross section for production of excited hydrogen atoms following dissociative excitation of molecular hydrogen by electron impact
[DE91-745035] N91-19852
Symposium on Development of Intensed Pulsed Particle Beams and Its Applications
[NIFS-PROC-5] N91-19882
He-like spectra through charge exchange processes in tokamak plasmas
[NIFS-69] N91-19894
NATIONAL OCEAN SERVICE, ANCHORAGE, AK.
Outer continental shelf environmental assessment program, volume 70
[PB91-129288] N91-19548
NATIONAL OCEANIC AND ATMOSPHERIC ADMINISTRATION, BOULDER, CO.
Total ozone, ozonesonde, and Umkehr observations for satellite ozone data validation N91-19525
Analysis of SBUV/2 measurements of solar UV irradiance variations N91-19526
Radar-measured height profiles of Cn(2) and turbulence dissipation rate compared with radiosonde data during October 1989 at Denver
[PB91-125500] N91-19562
Aperture-averaging factor for optical propagation through the turbulent atmosphere
[PB91-129338] N91-19875
NATIONAL OCEANIC AND ATMOSPHERIC ADMINISTRATION, WASHINGTON, DC.
NOAA-9 Solar Backscatter Ultraviolet (SBUV/2) Instrument and Derived Ozone Data: Review
[NOAA-TR-NESDIS-53] N91-19514
Data status and availability N91-19515
SBUV/2 in-orbit performance N91-19517
SBUV/2 comparisons with ground-based and SBUV spacecraft data N91-19521
Umkehr work N91-19522
NATIONAL RESEARCH COUNCIL OF CANADA, OTTAWA (ONTARIO).
Non-linear generation of acoustic noise in the IAR spacecraft N91-19143
NAVAL OCEANOGRAPHIC AND ATMOSPHERIC RESEARCH LAB., BAY SAINT LOUIS, MS.
Microbiologically influenced corrosion in copper and nickel seawater piping systems
[AD-A229874] N91-19287
NAVAL RESEARCH LAB., WASHINGTON, DC.
Time-dependent multimode simulation of gyrotron oscillators
[AD-A229861] N91-19413
Fiber optic feed
[AD-A229860] N91-19879
NAVAL SHIP RESEARCH AND DEVELOPMENT CENTER, BETHESDA, MD.
Proposed draft military handbook presenting requirements for an Electronic Display System (EDS) for Interactive Electronic Technical Manuals (IETMs)
[AD-A227471] N91-19342
NEBRASKA UNIV., LINCOLN.
Dynamics of collision processes
[DE91-007933] N91-19840
NEW SOUTH WALES UNIV., KENSINGTON (AUSTRALIA).
Proton induced x ray emission analysis N91-19832
NIHON UNIV., NARASHINO (JAPAN).
Flexural testing and evaluation methods of advanced composite materials N91-19228
NORTH CAROLINA STATE UNIV., RALEIGH.
Software reliability through fault-avoidance and fault-tolerance
[NASA-CR-187998] N91-19741
NORTH CAROLINA UNIV., CHAPEL HILL.
Improved syntactic disambiguation in the FASIT automatic indexing environment N91-19956
NORTH CAROLINA UNIV., GREENSBORO.
Carotid-cardiac baroreflex influence on forearm vascular resistance during low level LBNP N91-20030
NORTHWESTERN UNIV., EVANSTON, IL.
Chemical interactions in multimetal/zeolite catalysts
[DE91-007978] N91-19261
Plasma, photon, and beam synthesis of diamond films and multilayered structures
[DE91-007934] N91-19938
Solid state, surface, and catalytic studies of oxides
[DE91-007979] N91-19939
NORWALK STATE TECHNICAL COLL., CT.
Correlation of leak rates of various fluids with the leak rate of an inert gas in the same configuration N91-20033
NOTRE DAME UNIV., IN.
Research conducted at the Radiation Lab, Notre Dame Univ.
[DE91-007969] N91-19843
Wanted: Lunar detectives to unravel the mysteries of the Moon! Crime to be solved: Mass extinctions on the Moon by meteorite impact! N91-20010
NUEVAS TECNOLOGIAS ESPACIALES S.A., LLISSA D'AMUNT (SPAIN).
Design, implementation and evaluation of new fully automated algorithms for the extraction of cardiac parameters from 3D, 2D and M-mode echocardiograms N91-19582

O

OAK RIDGE NATIONAL LAB., TN.
Florida radioluminescent taxiway light development program
[DE91-005650] N91-19104
Gelcast zirconia-alumina composites
[DE91-007835] N91-19239
Thermal properties of polyisocyanurate foam board insulation blown with CFC-11 substitutes
[DE90-016047] N91-19240
Theory of bulk and interface constant phase elements in electrode-electrolyte systems
[DE91-007181] N91-19255
Screening volatile organics by direct sampling ion trap and glow discharge mass spectrometry
[DE91-007708] N91-19258
Effects of irradiation on crack-arrest toughness of two high-copper welds
[DE91-007189] N91-19270
Characterization of ion-implanted aluminum and iron by spectroscopic ellipsometry
[DE91-008371] N91-19283
Ceramic Technology for Advanced Heat Engines project database
[DE91-007772] N91-19300
Control of texture and defect structure for hot-filament-assisted CVD (Chemical Vapor Deposition) diamond Films
[DE91-008373] N91-19310
A pocket-size broadband electric field detection and storage device
[DE91-007710] N91-19406
A rigid body model and decoupled control architecture for two manipulators holding a complex object
[DE91-007827] N91-19444
Design and control of a fully omnidirectional and holonomic wheeled platform for robotic vehicles
[DE90-017746] N91-19445
A new wheel control system for the omnidirectional HERMIES-3 robot
[DE90-017764] N91-19446
DEMO 89: The initial experiment with the HERMIES-3 robot
[DE90-017765] N91-19447
Results from the third year of operation of the Federal methanol fleet at Argonne National Laboratory
[DE91-007822] N91-19451
The challenge of standards for emerging NDT methods
[DE91-007834] N91-19465
A summary of the status of biomass conversion technologies and opportunities for their use in developing countries
[DE91-006341] N91-19506
The dilemma of fossil fuel use and global climate change
[DE91-007859] N91-19533
Throughfall and foliar extraction
[DE91-007184] N91-19535
Spatial and temporal variation in biomonitoring data
[DE91-007843] N91-19539
Environmental surveillance data report for the first quarter of 1990
[DE91-008552] N91-19544
A stochastic performance model for the neutron diffusion nodal method on a multiuser parallel supercomputer
[DE90-017015] N91-19749
The PVM (Parallel Virtual Machine) system: Supercomputer level concurrent computation on a network of IBM RS/6000 power stations
[DE91-007844] N91-19757
Navigation of a car-like mobile robot using a decomposition of the environment in convex cells
[DE91-000709] N91-19769
Boundary integral equations and the Dirichlet problem
[DE91-004537] N91-19779
The weighted-difference form of the nodal diffusion method in cylindrical geometry
[DE91-007849] N91-19784
Bayesian approximation of solutions to linear ordinary differential equations
[DE91-007872] N91-19785
SIGNIF and GENFMT, SAS macros for computing and reporting significant digits
[DE91-007702] N91-19795
Review of recent stellarator results in the USA, the USSR, and Japan
[DE91-007798] N91-19901
Particle-in-cell plasma simulation codes on the connection machine
[DE91-007845] N91-19902
Thin film amorphous electrolytes: The Li2O-SiO2-P2O5 system
[DE91-007272] N91-19925
In situ TEM studies of the growth of strained Si(1-x)Ge(x) by solid phase epitaxy
[DE91-007278] N91-19926
X ray determination of site occupation parameters in ordered ternaries Cu(Au(x)M(1-x))M = Ni,Pd
[DE91-007861] N91-19937
Loss analysis of the thermodynamic cycle of magnetic heat pumps
[DE91-007669] N91-19950
Environmental Sciences Division computing and geographic information system facility user handbook
[DE91-007820] N91-19961
OFFICE OF SCIENCE AND TECHNOLOGY, WASHINGTON, DC.
US technology policy: Executive Office of the President
[PB91-119677] N91-19970
OHIO STATE UNIV., COLUMBUS.
Vibration transmission through rolling element bearings in geared rotor systems
[NASA-CR-4334] N91-19435
Plastids and gravity perception N91-19668
OHIO UNIV., ATHENS.
Investigation of air transportation technology at Ohio University, 1989-1990 N91-19028
Ridge regression signal processing N91-19029
Modeling selective availability of the NAVSTAR global positioning system N91-19030
Analyzing thought-related electroencephalographic data using nonlinear techniques N91-19031
Integrated inertial/GPS N91-19032
OLD DOMINION UNIV., NORFOLK, VA.
Control and mechanism interaction for ground-based testing of space structures N91-19125
Development of a perturbation generator for vortex stability studies
[NASA-CR-188051] N91-19379
Wavelets and turbulence on the sea surface
[AD-A229862] N91-19565
ONSALA SPACE OBSERVATORY (SWEDEN).
Proceedings of the symposium Astrophysical Processes and Structures in the Universe
[PB91-123653] N91-19993
Proceedings of 146th IAU Symposium on Dynamics of Galaxies and Molecular Cloud Distribution
[PB91-123661] N91-19994
OREGON INST. OF TECH., KLAMATH FALLS.
DHE (Downhole Heat Exchangers)
[DE91-006620] N91-19509
OSAKA UNIV. (JAPAN).
Two-stage ion diode experiments on induction adder N91-19884
OXFORD UNIV. (ENGLAND).
Pitot measurements in the exhaust of a cluster of four small scale supersonic nozzles
[OUEL-1862/90] N91-19070
Application of high speed photography to the study of high strain rate materials testing
[OUEL-1852/90] N91-19411
The selection of window functions for the calculation of time domain averages on the vibration of the individual gears in an epicyclic gearbox
[OUEL-1818/90] N91-19457
Visual navigation around curved obstacles
[OUEL-1861/90] N91-19458
Real-time sensor-based approach to the improvement of transitions of robot manipulator controls
[OUEL-1866/90] N91-19459

Time-frequency domain analysis of vibration signals for machinery diagnostics. 1: Introduction to the Wigner-Ville distribution
[OUEL-1859/90] N91-19495
Dynamic applications of ABAQUS
[OUEL-1853/90] N91-19755
Model distribution in decentralized multi-sensor data fusion
[OUEL-1868/90] N91-19763
Topological models for space and time
[OUEL-1860/90] N91-19774
A novel isoparametric finite element displacement formulation for axisymmetric analysis of nearly incompressible materials
[OUEL-1872/91] N91-19791

P

PACIFIC NORTHWEST LAB., RICHLAND, WA.
Radiation-induced changes in electrical conductivity of a wide range of copper alloys
[DE91-007200] N91-19271
The 70 percent tungsten heavy alloys: Processing and properties
[DE91-008259] N91-19282
Radioluminescent polymer lights
[DE91-005521] N91-19290
Identification of flow and volume parameters in multizone systems using a single gas tracer technique
[DE91-006894] N91-19368
A review of fiber optic and related technologies for environmental sensing applications
[DE91-007736] N91-19409
Biological effects of extremely low-frequency electromagnetic fields: In vivo studies
[DE91-007899] N91-19704
Finding the object proceedings addendum
[DE91-006724] N91-19738
Technology modernization assessment flexible automation
[DE91-005620] N91-19751
PADUA UNIV. (ITALY).
Contractile protein changes induced by hindlimb suspension in rat skeletal muscle N91-19646
PARIS VI UNIV., BANYULS-SUR-MER (FRANCE).
Microgravity and development of aquatic animals N91-19625
PARIS VI UNIV. (FRANCE).
Effect of gravity on the distribution of electron dense chromatin in the nucleus of root statocytes N91-19672
PENNSYLVANIA STATE UNIV., UNIVERSITY PARK.
C-statistic fitting routines: User's manual and reference guide
[NASA-CR-187992] N91-19736
Parallel processing for a 1-D time-dependent solution to impurity rate equations for fusion plasma simulations
[DE90-015857] N91-19759
Electron transfer, ionization, and excitation in atomic collisions
[DE91-008044] N91-19844
PENNSYLVANIA UNIV., PHILADELPHIA.
The correlation of transient crack growth under small-scale-creep conditions N91-19467
PRINCETON UNIV., NJ.
Investigation of air transportation technology at Princeton University, 1989-1990 N91-19033
Progress on intelligent guidance and control for wind shear encounter N91-19034
Flight simulation for wind shear encounter N91-19035
Stochastic robustness: Towards a comprehensive robustness tool N91-19036
Neural networks in nonlinear aircraft control N91-19037
Stochastic satbility and performance robustness of linear multivariable systems N91-19038
System identification for nonlinear control using neural networks N91-19039
Comprehensive mechanisms for combustion chemistry: An experimental and numerical study with emphasis on applied sensitivity analysis
[DE91-008030] N91-19262
The physics of laser polarized muonic atoms
[DE91-008045] N91-19845
Surface chemistry at semiconductor-electrolyte interfaces
[DE91-005915] N91-19920
PROVENCE UNIV., MARSEILLE (FRANCE).
Body proprioceptive references in weightlessness as studied by muscle tendon vibration N91-19581
PUERTO RICO UNIV., MAYAGUEZ.
Low level vapor verification of monomethyl hydrazine N91-20032

R

RADIAN CORP., RESEARCH TRIANGLE PARK, NC.
Overview of climate information needs for ecological effects models
[PB91-125898] N91-19549
RANDOLPH-MACON COLL., ASHLAND, VA.
Electrochemical impedance spectroscopy of metal alloys in the space transportation system launch environment N91-20025
RENSSELAER POLYTECHNIC INST., TROY, NY.
The effect of process conditions on the performance of epitaxial InP solar cells N91-19204
RESEARCH TRIANGLE INST., RESEARCH TRIANGLE PARK, NC.
Graded-bandgap AlGaAs solar cells for AlGaAs/Ge cascade cells N91-19186
Estimating lightning-generated NOx emissions for regional air pollution models
[PB91-131664] N91-19546
Regional Oxidant Model Multi-Processor (ROMMP)
[PB91-131680] N91-19547
ROCHESTER UNIV., NY.
Photoinduced electron transfer processes in homogeneous and microheterogeneous solutions
[DE91-007582] N91-19836
ROCKWELL INTERNATIONAL CORP., DOWNEY, CA.
A flight experiment to determine GPS photochemical contamination accumulation rates N91-19159
ROME UNIV. (ITALY).
A calorimeter design for high energy PP colliders
[NOTA-INTERNA-965] N91-19410
NO2 absorption cross-section in the 440 to 460 nm region at 298 and 220 K
[NOTA-INTERNA-964] N91-19550
Hindlimb suspension of rabbit for one week: Myofibrillar damage in the soleus may depend on long-lasting shortening and periodic contraction against no load N91-19647
Electroweak interactions at LEP
[NOTA-INTERNA-962] N91-19853
Punchthrough in hadronic showers: A parameterization of the total probability
[NOTA-INTERNA-968] N91-19854
A global fit to the Z(0) line shape
[NOTA-INTERNA-966] N91-19868
The Rome neutron monitor data for four ground-level enhancements observed by the world-wide station network in 1990
[NOTA-INTERNA-967] N91-20019
ROYAL AIR FORCE INST. OF AVIATION MEDICINE, FARNBOROUGH (ENGLAND).
Vestibular tests on UK astronaut candidates for an Anglo/Russian space flight (Juno Mission) N91-19613
ROYAL MILITARY COLL. OF SCIENCE, SHRIVENHAM (ENGLAND).
The impact of the new management strategy on senior operational commanders at group level within Royal Air Force Strike Command
[REPT-89SDM/MCHALE/03-MDA] N91-19954

S

SAINT-ETIENNE UNIV. (FRANCE).
Bone adaptation to real and simulated microgravity N91-19643
Aragatz Mission: Bone densitometric results obtained with the SCOOP miniscanner N91-19690
SANDIA NATIONAL LABS., ALBUQUERQUE, NM.
The development of a ram air decelerator for the recovery of artillery shells
[DE91-007732] N91-19064
The design and flight testing of a high-performance low-cost parachute system for a 1000 lb payload
[DE91-007733] N91-19065
Designing for explosive safety: The Explosive Components Facility at Sandia National Laboratories
[DE91-006432] N91-19103
Low temperature properties of boron carbides
[DE91-008172] N91-19243
Stress corrosion cracking of Al-Li-Cu-Zr alloy 2090 in aqueous Cl(-) and mixed CO3(2-)/Cl(-) environments
[DE91-007064] N91-19269
Application of non-cyanide gold for selective plating of microelectronic circuits
[DE91-007729] N91-19276
The mechanical behavior of microcellular foams
[DE91-006775] N91-19291
Phenomena affecting morphology of microporous poly(acrylonitrile) prepared via phase separation from solution
[DE91-004501] N91-19297
Polymer characterization using the time-resolved phosphorescence of singlet oxygen as a spectroscopic probe
[DE91-001269] N91-19303
Sandia technology: Engineering and science applications
[DE91-006760] N91-19322
Unique Signal Override Plug (USOP) electromagnetic test report
[DE91-004996] N91-19330
Measurement of electromagnetic fields over a small electrolytic tank
[DE91-007500] N91-19334
Capattery double layer capacitor life performance
[DE91-006639] N91-19344
Exploratory battery technology development and testing report for 1989
[DE91-006753] N91-19352
The development of a rugged accelerometer
[DE91-007731] N91-19407
Superconducting instrumentation for critical He-4 measurements in space
[DE91-007894] N91-19408
Focusing infrared laser beams on targets in space without using adaptive optics
[DE91-007518] N91-19421
Laser Tracker 2: Sandia National Laboratories' second generation laser tracking system
[DE91-007711] N91-19424
FALCON reactor-pumped laser description and program overview
[DE91-008185] N91-19431
Minimum-time trajectory control of a two-link flexible robotic manipulator
[DE91-001261] N91-19448
Lag-stabilized force feedback damping
[DE91-007572] N91-19481
The design of future central receiver power plants based on lessons learned from the Solar One Pilot Plant
[DE91-005224] N91-19510
A haptic system for a multifingered hand
[DE90-017044] N91-19767
Practical path planning among movable obstacles
[DE91-000034] N91-19768
Parameter estimation of structural dynamic models using Eigenvalue and Eigenvector information
[DE91-004379] N91-19793
Design considerations for multi component molecular-polymeric nonlinear optical materials
[DE91-006778] N91-19872
US-Japan workshops: Q-111, Development of Plasma Facing Components and Materials for Next Large Fusion Devices, and Q-112, Vacuum and First Wall Technology for Fusion Devices
[DE91-006879] N91-19896
Optical diagnostics for low-temperature plasmas
[DE91-007896] N91-19907
Considerations relating to pulsed-beam modification of materials
[DE91-006771] N91-19922
Compound semiconductors, strained layer epitaxy, and the information age
[DE91-007735] N91-19932
Electronic charge density and bonding in alpha-boron: An experimental-theoretical comparison
[DE91-006629] N91-19936
Phase formation in the Tl-Ca-BaCu-O system
[DE91-008184] N91-19942
Analyzing product test data in a relational database using SAS software
[DE91-007734] N91-19960
An architecture for accommodating referenceability among intelligent electronic documents
[DE91-008250] N91-19964
Analyzing product test data in an INGRES database using SAS software
[DE91-008251] N91-19965
SAVANNAH STATE COLL., GA.
An expansion plan for the 60 Hz power distribution system at KSC: LC-39 substations load allocation plan N91-20028
SCIENCE APPLICATIONS INTERNATIONAL CORP., MCLEAN, VA.
Lessons learned from an Ada conversion project N91-19730
SCRIPPS INSTITUTION OF OCEANOGRAPHY, LA JOLLA, CA.
Very low frequency seismo-acoustic scattering from a rough seafloor
[AD-A227947] N91-19564
SHEFFIELD UNIV. (ENGLAND).
Performance monitoring in nonlinear adaptive noise cancellation
[RR-409] N91-19362

Visualisation of fluid shifts within the body during a parabolic flight by measurements of electrical bio-impedance N91-19688
Rational model identification using an extended least squares algorithm
[RR-388] N91-19753
The qualitative analysis of nonlinear parameterised systems. Part 2: A method for the global analysis of nonlinear systems
[RR-400-PT-2] N91-19754
Simple object recognition by neural networks: Application of the Hough transform
[RR-410] N91-19761
The application of neural networks for fault diagnosis in nuclear reactors
[RR-411] N91-19772
The qualitative analysis of nonlinear parameterized systems. Part 1: Nonlinear systems representation and dynamical systems theory
[RR-408-PT-1] N91-19789
Orthogonal least squares parameter estimation algorithms for nonlinear stochastic systems
[RR-404] N91-19797
Expert systems for fault diagnosis in nuclear reactor control
[RR-412] N91-19864
Petri nets and fault diagnosis in nuclear reactors
[RR-413] N91-19865
The use of an object oriented technique for fault diagnosis in nuclear reactors
[RR-414] N91-19866
Fault detection using optimal control techniques
[RR-419] N91-19867

SMITHSONIAN ASTROPHYSICAL OBSERVATORY, CAMBRIDGE, MA.
A balloon-borne 102-cm telescope for far-infrared astronomy
[NASA-CR-187778] N91-19973

SOFTWARE PRODUCTIVITY CONSORTIUM, RESTON, VA.
The next generation N91-19724

SOLAREX CORP., ROCKVILLE, MD.
Performance, size, mass, and cost estimates for projected 1kW EOL Si, InP, and GaAs arrays N91-19199
Spaceflight performance of several types of silicon solar cells on the LIPS 3 satellite N91-19213

SOUTH CAROLINA UNIV., COLUMBIA.
A flammability study of thin plastic film materials N91-20034

SOUTHERN METHODIST UNIV., DALLAS, TX.
Statistical examination of climatological data relevant to global temperature variation
[DE91-007881] N91-19540

SOUTHWEST RESEARCH INST., SAN ANTONIO, TX.
Performance of underwater weldments
[PB91-129254] N91-19452

SOVONICS SOLAR SYSTEMS, TROY, MI.
Integral bypass diodes in an amorphous silicon alloy photovoltaic module N91-19218

SPAR AEROSPACE LTD., STE-ANNE-DE-BELLEVUE (QUEBEC).
Thermal balance testing of the Anik-E spacecraft N91-19131

SPECTROLAB, INC., SYLMAR, CA.
Progress toward the development of dual junction GaAs/Ge solar cells N91-19184

ST SYSTEMS CORP., LANHAM, MD.
An assessment of instrument performance for the NOAA-9 SBUV/2 N91-19516
NOAA-9 SBUV/2 ozone sounding accuracy: Presentation summary N91-19519

STANFORD LINEAR ACCELERATOR CENTER, CA.
A valiant little terminal: A VLT user's manual
[DE91-007295] N91-19719
Invariant tori of the Poincare return map as solutions of functional difference equations
[DE91-007423] N91-19777
Computation of invariant tori in 2 (1/2) degrees of freedom
[DE91-007424] N91-19778

STANFORD UNIV., CA.
Cascading a systolic array and a feedforward neural network for navigation and obstacle avoidance using potential fields
[NASA-CR-177575] N91-19771

STATE UNIV. OF NEW YORK, FARMINGDALE.
Some aspects of robotics calibration, design and control N91-20035

STATE UNIV. OF NEW YORK, STONY BROOK.
Studies of atmospheric molecules by multiphoton spectroscopy
[DE91-006738] N91-19554
Plant development in space: Observations on root formation and growth N91-19670

STERLING FEDERAL SYSTEMS, INC., PALO ALTO, CA.
Army-NASA aircrew/aircraft integration program (A3I) software detailed design document, phase 3
[NASA-CR-177557] N91-19714

STUTTGART UNIV. (GERMANY, F.R.).
High power arcjet
[NASA-CR-187986] N91-19173
Effect of hyper-gravity on the swimming behavior of aquatic vertebrates N91-19626
Morphological, electronmicroscopical and biochemical aspects of hyper-gravity conditions during early ontogenetic development of Cichlid fish N91-19638

SUPERCONDUCTING SUPER COLLIDER LAB., DALLAS, TX.
Studies of cold protection diodes
[DE91-008203] N91-19863
Prototype document tracking and storage system for the Superconducting Super Collider Laboratory (SSCL)
[DE91-008204] N91-19963

SURFACE DYNAMICS, INC., BLOOMFIELD HILLS, MI.
Smoothness criteria for runway rehabilitation and overlays
[DOT/FAA/RD-90/23] N91-19102

SVERDRUP TECHNOLOGY, INC., BROOK PARK, OH.
Ongoing development of a computer jobstream to predict helicopter main rotor performance in icing conditions
[NASA-CR-187076] N91-19056
Solar rocket plume/mirror interactions
[NASA-CR-185300] N91-19059
LOX/hydrogen coaxial injector atomization test program
[NASA-CR-187037] N91-19117
Vibration and thermal vacuum qualification test results for a low-voltage tungsten-halogen light
[NASA-CR-187050] N91-19325
Cool-down and frozen start-up behavior of a grooved water heat pipe
[NASA-CR-187053] N91-19376
The apparent strain stability and repeatability of a BCL3 resistance strain gage
[NASA-CR-187056] N91-19403
The effect of steady aerodynamic loading on the flutter stability of turbomachinery blading
[NASA-CR-187055] N91-19479

SYDNEY UNIV. (AUSTRALIA).
Finite element analysis of geometrically non-linear problems using a corotational large rotation formulation
[SU-ATN-9001] N91-19470

SYPHER-MUELLER INTERNATIONAL, INC., OTTAWA (ONTARIO).
Alternative fuels for heavy duty engines: Status of fleet trials
[DE91-006799] N91-19315
Exhaust emissions from heavy duty vehicles
[DE91-006798] N91-19531

SYRACUSE UNIV., NY.
Mechanisms controlling the production and transport of methane, carbon dioxide, and dissolved solutes within a large boreal peat basin
[DE91-008115] N91-19543

SYRACUSE UNIV. RESEARCH INST., NY.
Numerical and physical modelling of bubbly flow phenomena
[DE91-007461] N91-19377

T

TAMPERE UNIV. OF TECHNOLOGY (FINLAND).
Methods for combining a theoretical and an empirical approach in modelling pressure and flow control valves for CAE-programs for fluid power circuits
[ACTA-POLYTEC-SCAND-ME-96] N91-19392

TECHNICAL RESEARCH CENTRE OF FINLAND, ESPOO.
Hydrogen storage in metal hydrides
[DE91-746267] N91-19316

TECHNISCHE HOCHSCHULE, DARMSTADT (GERMANY, F.R.).
Optimal observation directions for estimating a vector
[PREPRINT-1285] N91-19796

TECHNISCHE UNIV., BERLIN (GERMANY, F.R.).
Project of a cost analysis model for the acquisition of a permanent lunar base
[ILR-MITT-245(1990)] N91-19114
A multi-vehicle space carrier fleet cost model for a multi-mission scenario
[ILR-MITT-240(1990)] N91-19120
Cycling space ship transportation device for continuous link between Earth and Mars
[ILR-MITT-247(1990)] N91-19121
Alternative strategies for the maintenance of geostationary space power plants
[ILR-MITT-249(1990)] N91-19170

TECHNISCHE UNIV., DELFT (NETHERLANDS).
The behaviour of flux-difference and flux-vector splitting methods in explicit schemes for hypersonic blunt body flow
[LR-643] N91-19069
Bulging of fatigue cracks in a pressurized aircraft fuselage
[LR-647] N91-19094
Project Hitch Hiker: A feasibility study for a small telecommunication satellite
[LR-644] N91-19169
Solid fuel combustion chamber
[LR-648] N91-19222
Gas entrapment and evolution in aluminium alloys produced by powder metallurgy
[ETN-91-98918] N91-19285
A numerical method for solving steady 2D and axisymmetrical viscoelastic flow problems with an application to inertia effects in contraction flows
[MEMT-11] N91-19394
Notes on the unsteady rectilinear motion of a perfect gas. 10: On the influence of gravity upon the expansion of an ideal gas with gamma = 3
[LR-640] N91-19395
Heat transport during gas tungsten arc welding
[ETN-91-98919] N91-19455
Elementary considerations on the gas dynamic design parameters of a MHD Faraday generator in relation to a gas turbine cycle
[LR-564] N91-19456
Bulging of fatigue cracks in a pressurized aircraft fuselage
[ETN-91-98927] N91-19489
On the vectorization and parallelization of the shooting method using the convex C-240
[LR-639] N91-19491
Crack opening stress measurements of surface cracks in 7075-T6 Al alloy plate specimens through electron fractography
[LR-641] N91-19492
Finite strip elements in thin plate buckling analysis
[LR-642] N91-19493
Design and testing of a circumferential and longitudinal joint of the A320 fuselage section 13/14 in GLARE
[LR-645] N91-19494
Design and implementation of an image understanding system: DADS
[ETN-91-98926] N91-19773
Elementary pulse diffraction problems and the generation of sound by a dipole moving across the edge of a half-plane
[LR-565] N91-19831
Exchange currents in low-energy nucleon capture by He3
[ETN-91-98917] N91-19855
Classical and quantum charge dynamics in small tunnel junctions
[ETN-91-98916] N91-19947

TECHNISCHE UNIV., EINDHOVEN (NETHERLANDS).
Constitutive models for composites based on numerical micromechanics
[ISBN-90-9003733-0] N91-19248
Alkali metal corrosion of alumina: Thermodynamics, phase diagrams and testing
[ETN-91-98933] N91-19286
Electromagnetic compatibility in high-voltage engineering
[ISBN-90-9002929-X] N91-19337
A variational approach to magneto-elastic buckling problems
[ETN-91-98929] N91-19338
Continuum damage mechanisms with an application to fatigue
[ISBN-90-9003688-1] N91-19490
Subcycling in transient finite element analysis
[ISBN-90-9003684-9] N91-19790
Examinations of inverse scattering problem for the scalar Helmholtz equation in the field of first order approximations for potentials with compact supports and safe real wave numbers
[ETN-91-98949] N91-19339
Contributions to the Non Equilibrium Molecular Dynamics (NEMD) computer simulation for transport processes in simple fluids
[ETN-91-98921] N91-19393
Approximation properties of wavelet transforms
[ETN-91-98922] N91-19799
Semiconductor photodiodes as radiometric receivers in the field of soft radiation
[ETN-91-98925] N91-19856
Nonlinear optic effects in liquid crystals
[ETN-91-98923] N91-19878
Mutual influence of doping and oxidation in highly doped silicon
[ETN-91-98924] N91-19948

Noble gas disk MHD generator performance with unstable nonequilibrium plasma
[ISBN-90-9003671-7] N91-19916
Indium tin oxide for solid-state image sensors
[ETN-91-98932] N91-19949

TECHNISCHE UNIV., MUNICH (GERMANY, F.R.).
Physiology of body water and salt regulation. Part 1: Circadian rhythms of endocrine systems and urinary electrolyte excretion in humans N91-19592
Physiology of body water and salt regulation. Part 2: Volume and electrolyte homeostasis after an acute saline infusion N91-19593

TECHNISCHE UNIV., VIENNA (AUSTRIA).
Isokinetic force velocity and electromyographic characteristic of knee and elbow extensor and flexor muscles in the 0-g environment N91-19584
Productivity and photosynthesis of selected crop plants under orbital light conditions: An approach to solar powered CELSS N91-19662

TENNESSEE UNIV., KNOXVILLE.
In-space experiment on thermoacoustic convection heat transfer phenomenon-experiment definition
[NASA-CR-187070] N91-19378

TENNESSEE UNIV., TULLAHOMA.
Engineering monitoring expert system's developer
[NASA-CR-187914] N91-19765

TENNESSEE UNIV. SPACE INST., TULLAHOMA.
The magnetohydrodynamics coal-fired flow facility
[DE91-007672] N91-19906

TEXAS UNIV., ARLINGTON.
Calculations of separated 3-D flows with a pressure-staggered Navier-Stokes equations solver
[NASA-CR-187065] N91-19367

TEXAS UNIV., AUSTIN.
Synthesis and analysis of novel polymers with potential for providing both high permselectivity and permeability in gas separation applications
[DE91-008283] N91-19309
Action principles for the Vlasov equation: Four old, one new
[DE91-008177] N91-19787
Summary of the International Dawson Symposium on The Physics of Plasmas
[DE91-006912] N91-19897
Relaxed states with plasma flow
[DE91-008199] N91-19909

TEXAS UNIV. HEALTH SCIENCE CENTER, HOUSTON.
Altered cartilage differentiation in tibial epiphyseal plates of Cosmos rats N91-19628

THIOKOL CORP., BRIGHAM CITY, UT.
The full-scale process and design changes for elimination of insulation edge separations and voids in tang flap area
[NASA-CR-184110] N91-19172

TOKYO INST. OF TECH., YOKAHAMA (JAPAN).
Experiments toward the development of new pulsed ion diodes N91-19885
Power plant by LIB fusion N91-19892
Control of gap closure in applied-B diode N91-19893

TOLEDO UNIV., OH.
Hubble Space Telescope observations of Mars N91-20003

TOWSON STATE UNIV., MD.
Study of wavelength division multiplexing as a means of increasing the number of channels in multimode fiber optic communication links N91-20024

TRONDHEIM UNIV. (NORWAY).
Vascular gas bubbles or decompression sickness: What is the proper endpoint for evaluating decompression procedures N91-19590

TRW DEFENSE AND SPACE SYSTEMS GROUP, REDONDO BEACH, CA.
High vacuum facility for hydrazine thruster testing N91-19134
Space simulation test for thermal control materials N91-19149

TRW SPACE TECHNOLOGY LABS., REDONDO BEACH, CA.
Multipurpose hardened spacecraft insulation N91-19136

TUEBINGEN UNIV. (GERMANY, F.R.).
Regeneration and characterization of protoplast-derived cell lines from Digitalis lanata EHRH. and Digitalis purpurea L. suspension cultures after electrofusion under microgravity conditions N91-19652

U

UDINE UNIV. (ITALY).
Pedalling in space to simulate gravity: The twin-bike system N91-19583

UNION CARBIDE CORP., SOUTH CHARLESTON, WV.
Direct conversion of methane to C2's
[DE91-005730] N91-19251
Direct conversion of methane to C2's and liquid fuels
[DE91-005729] N91-19313
Direct conversion of methane to C2's and liquid fuels
[DE91-007545] N91-19318

UNIVERSITAET DER BUNDESWEHR MUENCHEN, NEUBIBERG (GERMANY, F.R.).
Response of a solidly rotating amphora-type liquid column to axial excitation
[LRT-WE-9-FB-06(1990)] N91-19386
Experimental studies on a nonlinear hydroelastic vibration of circular cylindrical tanks
[LRT-WE-9-FB-10(1990)] N91-19387
Liquid sloshing response in a spinning container due to pitching excitation
[LRT-WE-9-FB-11(1990)] N91-19388
Response of a differently axially excited viscous liquid layer in zero-gravity
[LRT-WE-9-FB-12(1990)] N91-19389
Response of a viscous liquid layer to pitch- and roll-excitation in zero-gravity environment
[LRT-WE-9-FB-13(1990)] N91-19390

UNIVERSITY COLL., LONDON (ENGLAND).
Developmental biology and microgravity N91-19622

UNIVERSITY OF SOUTH FLORIDA, TAMPA.
Frontier orbital symmetry control of intermolecular electron transfer
[DE91-005699] N91-19834

UTAH UNIV., SALT LAKE CITY.
Research in radiobiology: Work in progress in immunobiology of experimental host-tumor relationships
[DE91-007936] N91-19705
Advanced sequencing technology
[DE91-008031] N91-19706

V

VANDERBILT UNIV., NASHVILLE, TN.
Skeletal adaptation in altered gravity environments N91-19603

VARIAN ASSOCIATES, PALO ALTO, CA.
Progress toward a 30 percent-efficient, monolithic, three-junction, two-terminal concentrator solar cell for space applications N91-19188
High-efficiency, radiation-resistant GaAs space cells N91-19194

VIRGINIA POLYTECHNIC INST. AND STATE UNIV., BLACKSBURG.
Mechanical behavior of a ceramic matrix composite material
[NASA-CR-187072] N91-19461

VRIJE UNIV., AMSTERDAM (NETHERLANDS).
Hypergravity and bone mineralization N91-19650

VRIJE UNIV., BRUSSELS (BELGIUM).
Lung volumes, chest wall configuration, and pattern of breathing in microgravity N91-19574

W

WASHINGTON STATE UNIV., PULLMAN.
GaAs solar cell photoresponse modeling using PC-1D V2.1 N91-19193

WASHINGTON UNIV., SAINT LOUIS, MO.
Instellar grains within interstellar grains N91-19998
Cosmic dust: Laboratory analyses of extremely small particles N91-20013

WAYNE STATE UNIV., DETROIT, MI.
Annealing characteristics of irradiated hydrogenated amorphous silicon solar cells N91-19214

WEBB INST. OF NAVAL ARCHITECTURE, GLEN COVE, NY.
Liquid sloshing in cargo tanks. Liquid slosh loading in slack ship tanks: Forces on internal structure and pressures
[PB91-129262] N91-19383

WESTINGHOUSE SAVANNAH RIVER CO., AIKEN, SC.
Effects of radiolytic tritium decay on the thermodynamic behavior of LaNi(4.25)Al(0.75) tritides
[DE91-007961] N91-19277
Evaluation of a Photo-Electron Rejecting Alpha Liquid Scintillation (PERALS) spectrometer for the measurement of alpha-emitting radionuclides
[DE91-005652] N91-19399
An on-line real-time system for fatigue crack growth monitoring
[DE91-007931] N91-19483
ARCHY (analysis and reverse engineering of code using hierarchy and Yourdon): A tool for FORTRAN code maintenance and development
[DE91-007241] N91-19720

WICHITA STATE UNIV., KS.
Dedication of National Institute for Aviation Research
[NIAR-90-21] N91-19040

WIEN UNIV. (AUSTRIA).
Vertically moving visual stimuli and vertical vection: A tool against space motion sickness N91-19606

WORLD METEOROLOGICAL ORGANIZATION, GENEVA (SWITZERLAND).
World weather watch: Regional association 4: Hurricane operational plan, supplement 2
[WMO-524-SUPPL-2] N91-19563

WRIGHT RESEARCH DEVELOPMENT CENTER, WRIGHT-PATTERSON AFB, OH.
Phase equilibrium modeling for high temperature metallization on GaAs solar cells N91-19192

Y

YALE UNIV., NEW HAVEN, CT.
Aerodynamic focusing of particles and heavy molecules
[DE91-006922] N91-19833

Typical Contract Number Index Listing

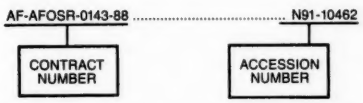

Listings in this index are arranged alphanumerically by contract number. Under each contract number the accession numbers denoting documents that have been produced as a result of research done under that contract are arranged in ascending order. The accession number denotes the number by which the citation is identified.

AF PROJ. 2304 ..... N91-19957
AF PROJ. 2418 ..... N91-19460
AF-AFOSR-0126-87 ..... N91-19957
AF-AFOSR-0182-89 ..... N91-19193
ASI-88-08 ..... N91-19647
BCRS-4544/AO-1.2 ..... N91-19327
BMFT-01-QV-87/2 ..... N91-19604
BMFT-01-QV-223-9 ..... N91-19580
BMFT-01-QV-8769 ..... N91-19652
BMFT-01-QV-8802 ..... N91-19591
BMFT-01-QV-85650 ..... N91-19680
N91-19682
BMFT-01-QV-87354 ..... N91-19586
N91-19594
N91-19601
CICYT-ESP-88-0351 ..... N91-19633
CNES-88/1305 ..... N91-19672
CNES-89/1263 ..... N91-19619
CNES-500193 ..... N91-19581
CNES-500243 ..... N91-19581
DA PROJ. 1L1-61102-AH-45 ..... N91-19369
DA PROJ. 1L1-62211-A-47-A N91-19438
N91-19439
DAAL03-89-K-0092 ..... N91-19038
N91-19039
DANISH-SB-1112-14/89 ..... N91-19612
DE-AC02-76CH-00016 ..... N91-19278
N91-19279
N91-19280
N91-19302
N91-19359
N91-19360
N91-19361
N91-19422
N91-19432
N91-19538
N91-19542
N91-19712
N91-19835
N91-19848
N91-19849
N91-19850
N91-19851
N91-19873
N91-19874
N91-19929
DE-AC02-76CH-03000 ..... N91-19356
N91-19821
N91-19958
DE-AC02-76CH-03073 ..... N91-19908
DE-AC02-76ER-00038 ..... N91-19843
DE-AC02-79ET-10815 ..... N91-19906
DE-AC02-80ET-15601 ..... N91-19420
N91-19746
N91-19905
DE-AC02-83CH-10093 ..... N91-19202
N91-19501
N91-19502
DE-AC02-83ER-13044 ..... N91-19382
DE-AC02-89CH-10406 ..... N91-19353
DE-AC02-89ER-40486 ..... N91-19863
N91-19963
DE-AC03-76DP-00789 ..... N91-19881
DE-AC03-76SF-00098 ..... N91-19416
N91-19418
N91-19423
N91-19425
N91-19426
N91-19427
N91-19861
N91-19930
N91-19931
N91-19933
N91-19934
N91-19951
DE-AC03-76SF-00515 ..... N91-19719
N91-19777
N91-19778
DE-AC03-84OR-21400 ..... N91-19881
DE-AC03-87SF-17119 ..... N91-19335
DE-AC03-89ER-51114 ..... N91-19881
DE-AC03-89ER-53277 ..... N91-19908
DE-AC04-76DP-00789 ..... N91-19064
N91-19065
N91-19103
N91-19243
N91-19269
N91-19276
N91-19291
N91-19297
N91-19303
N91-19322
N91-19330
N91-19334
N91-19344
N91-19352
N91-19407
N91-19408
N91-19421
N91-19424
N91-19431
N91-19448
N91-19481
N91-19510
N91-19767
N91-19768
N91-19793
N91-19872
N91-19896
N91-19907
N91-19922
N91-19932
N91-19936
N91-19942
N91-19960
N91-19964
N91-19965
DE-AC04-88DP-43495 ..... N91-19281
DE-AC05-76OR-00033 ..... N91-19847
N91-19926
DE-AC05-84OR-21400 ..... N91-19104
N91-19239
N91-19240
N91-19255
N91-19258
N91-19270
N91-19279
N91-19280
N91-19283
N91-19300
N91-19310
N91-19406
N91-19444
N91-19445
N91-19446
N91-19447
N91-19451
N91-19465
N91-19506
N91-19533
N91-19535
N91-19539
N91-19544
N91-19749
N91-19757
N91-19769
N91-19779
N91-19784
N91-19785
N91-19795
N91-19847
N91-19901
N91-19902
N91-19925
N91-19926
N91-19937
N91-19950
N91-19961
DE-AC06-76RL-01830 ..... N91-19271
N91-19282
N91-19290
N91-19368
N91-19409
N91-19704
N91-19738
N91-19751
DE-AC07-76ID-01570 ..... N91-19346
N91-19450
DE-AC07-88ID-12735 ..... N91-19298
DE-AC09-89SR-18035 ..... N91-19277
N91-19399
N91-19483
N91-19720
DE-AC21-87MC-23270 ..... N91-19505
DE-AC22-87PC-79680 ..... N91-19347
DE-AC22-87PC-79817 ..... N91-19251
N91-19313
N91-19318
DE-AI01-85CE-89008 ..... N91-19355
DE-FG01-87CE-27462 ..... N91-19511
DE-FG01-90CE-15440 ..... N91-19504
DE-FG02-84ER-45150 ..... N91-19940
DE-FG02-84ER-45166 ..... N91-19484
DE-FG02-85ER-13421 ..... N91-19839
DE-FG02-85ER-13438 ..... N91-19920
DE-FG02-85ER-45222 ..... N91-19841
DE-FG02-86ER-13501 ..... N91-19275
DE-FG02-86ER-13503 ..... N91-19262
DE-FG02-86ER-13504 ..... N91-19836
DE-FG02-86ER-13549 ..... N91-19844
DE-FG02-86ER-13580 ..... N91-19263
DE-FG02-86ER-13590 ..... N91-19554
DE-FG02-86ER-25015 ..... N91-19776
DE-FG02-86ER-53222 ..... N91-19904
DE-FG02-86ER-60422 ..... N91-19532
DE-FG02-87ER-13654 ..... N91-19261
DE-FG02-87ER-13725 ..... N91-19939
DE-FG02-87ER-13750 ..... N91-19833
DE-FG02-87ER-45314 ..... N91-19938
DE-FG02-87ER-53252 ..... N91-19759
DE-FG02-88ER-13880 ..... N91-19267
DE-FG02-88ER-13955 ..... N91-19840
DE-FG02-88ER-45356 ..... N91-19260
DE-FG02-88ER-60700 ..... N91-19706
DE-FG02-89ER-60836 ..... N91-19705
DE-FG02-90ER-12105 ..... N91-19923
DE-FG02-90ER-14136 ..... N91-19377
DE-FG02-90ER-40557 ..... N91-19845
DE-FG02-90ER-60970 ..... N91-19541
DE-FG02-90ER-61013 ..... N91-19543
DE-FG02-90ER-61019 ..... N91-19537
DE-FG03-84ER-40161 ..... N91-19859
DE-FG03-85ER-13356 ..... N91-19707
DE-FG03-88ER-13908 ..... N91-19702
N91-19703
DE-FG03-89ER-51121 ..... N91-19881
DE-FG05-80ET-53088 ..... N91-19787
N91-19897
N91-19909
DE-FG05-84ER-40159 ..... N91-19846
N91-19847
DE-FG05-86ER-13507 ..... N91-19309
DE-FG05-87ER-25036 ..... N91-19792
DE-FG05-87ER-40330 ..... N91-19847
DE-FG05-87ER-52147 ..... N91-19357
N91-19358
DE-FG05-88ER-13975 ..... N91-19834

DE-FG05-89ER-14015 ..... N91-19259
DE-FG05-89ER-45384 ..... N91-19302
DE-FG05-90ER-60971 ..... N91-19555
DE-FG05-90ER-61015 ..... N91-19540
DE-FG07-90ID-13040 ..... N91-19509
DE-FG22-88PC-88932 ..... N91-19536
DE-FG22-89PC-89775 ..... N91-19250
DE-GI01-87CE-50182 ..... N91-19315
N91-19531
DRET-89-237 ..... N91-19689
DTCG23-82-C-20016 ..... N91-19383
DTCG23-82-C-20017 ..... N91-19452
DTFA01-86-C-00035 ..... N91-19102
DTFA01-89-Y-01047 ..... N91-19075
DTRS-57-85-C-000123 ..... N91-19074
EPA-68-01-7365 ..... N91-19546
EPA-68-02-4274 ..... N91-19545
EPA-68-02-4288 ..... N91-19549
EPA-68-02-4396 ..... N91-19545
EPA-68-09-0173 ..... N91-19545
ESA-7320/87/NL/PP N91-19582
F04611-84-C-0026 ..... N91-19059
F33615-86-C-5016 ..... N91-19460
F33615-87-C-2804 ..... N91-19186
F33615-88-C-2845 ..... N91-19188
F33615-88-C-5415 ..... N91-19185
F33615-89-C-2900 ..... N91-19184
GRI-5088-260-1692 ..... N91-19264
MDA903-88-C-0031 ..... N91-19952
MDA903-89-K-0074 ..... N91-19952
NAGW-17 ..... N91-19973
NAGW-799 ..... N91-19497
NAGW-1529 ..... N91-19670
NAGW-1736 ..... N91-19173
NAG1-530 ..... N91-19379
NAG1-640 ..... N91-19732
NAG1-983 ..... N91-19741
NAG1-1007 ..... N91-19750
NAG1-1091 ..... N91-19415
NAG2-541 ..... N91-19305
NAG2-591 ..... N91-19718
NAG2-596 ..... N91-19765
NAG2-614 ..... N91-19701
NAG3-55 ..... N91-19438
NAG3-172 ..... N91-19461
NAG3-604 ..... N91-19204
NAG3-773 ..... N91-19435
NAG3-832 ..... N91-19404
NAG3-833 ..... N91-19176
NAG3-964 ..... N91-19439
NAG3-1137 ..... N91-19475
NAG5-1164 ..... N91-19975
NAG5-1211 ..... N91-19736
NAG5-1332 ..... N91-19398
NAG8-863 ..... N91-19871
NAG9-117 ..... N91-19710
NAG9-181 ..... N91-19621
NASA ORDER C-3000-K N91-19202
NASA ORDER C-99066-G N91-19375
N91-19786
NASW-4292 ..... N91-19700
NASW-4324 ..... N91-19697
NAS1-11395 ..... N91-19670
NAS1-17498 ..... N91-19478
NAS1-17742 ..... N91-19074
NAS1-18230 ..... N91-19238
NAS1-18240 ..... N91-19061
NAS1-18586 ..... N91-19756
NAS1-18605 ..... N91-19043
N91-19345
N91-19366
N91-19715
N91-19716
NAS1-19038 ..... N91-19737
NAS2-11295 ..... N91-19067
NAS2-11555 ..... N91-19714
NAS2-12148 ..... N91-19050
NAS2-12897 ..... N91-19323
NAS2-12962 ..... N91-19060
NAS3-23691 ..... N91-19443
NAS3-23720 ..... N91-19049
NAS3-23772 ..... N91-19174
NAS3-24105 ..... N91-19825
NAS3-25266 ..... N91-19056
N91-19059
N91-19117
N91-19176
N91-19216
N91-19325
N91-19376
N91-19403
N91-19479
N91-20015
NAS3-25274 ..... N91-19320
NAS3-25359 ..... N91-19378
NAS3-25515 ..... N91-19167
NAS3-25570 ..... N91-19187
NAS3-25776 ..... N91-19350
NAS3-25787 ..... N91-19233
NAS3-25834 ..... N91-19048
NAS8-30490 ..... N91-19172
NAS8-36955 ..... N91-19164
N91-19980
NAS8-37580 ..... N91-19498
NAS8-38142 ..... N91-19162
N91-19163
NAS8-38188 ..... N91-19223
NAS9-14880 ..... N91-19711
NAS10-11624 ..... N91-19711
NCC3-130 ..... N91-19343
NCC3-153 ..... N91-19054
NCC3-162 ..... N91-19296
NCC3-180 ..... N91-19367
NCC8-14 ..... N91-19735
NCC9-16 ..... N91-19722
NGL-22-009-640 ..... N91-19026
NGL-31-001-252 ..... N91-19038
N91-19039
NGT-50642 ..... N91-19771
NGT-60002 ..... N91-20022
N91-20023
N91-20024
N91-20025
N91-20026
N91-20027
N91-20028
N91-20029
N91-20030
N91-20031
N91-20032
N91-20033
N91-20034
N91-20035
N91-20036
N91-20037
N91-20038
NSF CDR-86-22236 ..... N91-19345
N00014-85-6-0093 ..... N91-19952
N00014-86-K-0204 ..... N91-19732
N00014-88-K-0101 ..... N91-19565
N00014-89-J-1017 ..... N91-19564
N00014-89-J-1027 ..... N91-19709
N00014-89-J-1731 ..... N91-19721
N00014-89-J-3022 ..... N91-19340
N00014-90-J-1589 ..... N91-19071
SERC-GK/F24177 ..... N91-19797
SERC-GR/F2417-7 ..... N91-19753
SNRF-3-338-0-86 ..... N91-19620
SNSF-3-338-0-86 ..... N91-19634
SNSF-3-382-0-86 ..... N91-19598
SRON-MG020-1988 ..... N91-19575
STEV-506-266-4 ..... N91-19513
W-31-109-ENG-38 ..... N91-19242
N91-19252
N91-19253
N91-19299
N91-19301
N91-19314
N91-19414
N91-19440
N91-19507
N91-19508
N91-19534
N91-19743
N91-19760
N91-19838
N91-19842
N91-19903
N91-19919
N91-19941
W-7405-ENG-36 ..... N91-19257
N91-19333
N91-19405
N91-19419
N91-19428
N91-19480
N91-19552
N91-19858
N91-19860
N91-19899
N91-19928
N91-19986
W-7405-ENG-48 ..... N91-19254
N91-19268
N91-19331
N91-19381
N91-19400
N91-19416
N91-19417
N91-19418
N91-19427
N91-19429
N91-19430
N91-19433
N91-19466
N91-19530
N91-19551
N91-19553
N91-19558
N91-19698
N91-19739
N91-19740
N91-19745
N91-19747
N91-19748
N91-19758
N91-19775
N91-19780
N91-19781
N91-19782
N91-19783
N91-19794
N91-19857
N91-19862
N91-19881
N91-19895
N91-19898
N91-19900
N91-19910
N91-19919
N91-19921
N91-19924
N91-19927
N91-19983
N91-19984
N91-19985
W-7405-ENG-82 ..... N91-19272
N91-19744
N91-19837
186-30-21 ..... N91-19566
199-26-11-24-6A N91-19687
244-10-00 ..... N91-19323
307-50-62-11 ..... N91-19824
307-50-81 ..... N91-19823
307-51-00 ..... N91-19256
N91-19296
326-31-15 ..... N91-19178
474-12-10 ..... N91-19462
474-52-10 ..... N91-19177
505-01-01 ..... N91-19234
505-02-22 ..... N91-19373
505-59-30-03 ..... N91-19737
505-59-50-01 ..... N91-19061
505-60-21 ..... N91-19051
N91-19058
505-61-00 ..... N91-19714
505-61-21 ..... N91-19062
505-61-51 ..... N91-19041
N91-19050
N91-19052
N91-19060
N91-19067
N91-19826
505-61-71-01 ..... N91-19042
505-62-3B N91-19115
505-62-4D N91-19049
N91-19825
505-62-01 ..... N91-19403
N91-19404
505-62-21 ..... N91-19044
N91-19054
N91-19059
N91-19370
N91-19375
N91-19786
505-62-31 ..... N91-19372
N91-19374
505-62-52 ..... N91-19053
N91-19063
N91-19367
N91-19402
N91-19443
505-62-84 ..... N91-19401
505-63-1A N91-19224
505-63-1B N91-19292
N91-19441
N91-19442
N91-19473
505-63-1M N91-19293
505-63-5A N91-19369
505-63-5B N91-19475
N91-19477
505-63-01-05 ..... N91-19482
505-63-31 ..... N91-19077
N91-19080
505-63-36 ..... N91-19438
N91-19439
505-63-36-01 ..... N91-19478

505-63-51 ..... N91-19435
505-63-52 ..... N91-19476
505-64-13 ..... N91-19073
505-66-01-02 ..... N91-19024
505-66-31 ..... N91-19083
505-66-41 ..... N91-19082
505-66-41-41 ..... N91-19756
505-68-10 ..... N91-19046
N91-19047
505-68-11 ..... N91-19056
505-68-27 ..... N91-19742
505-68-30-10 ..... N91-19074
505-68-71 ..... N91-19055
505-69-51 ..... N91-19097
505-90-01 ..... N91-19461
505-90-21-01 ..... N91-19366
505-90-52-01 ..... N91-19043
N91-19345
N91-19715
N91-19716
506-41-11 ..... N91-19165
N91-19176
N91-19182
N91-19354
N91-20015
506-41-41 ..... N91-19231
506-41-41-01 ..... N91-19415
506-42-00 ..... N91-19117
N91-19175
506-42-31 ..... N91-19180
506-43-11 ..... N91-19294
N91-19463
506-43-21-04 ..... N91-19238
506-43-41-02 ..... N91-19166
N91-19168
506-44-2B N91-19332
506-44-21 ..... N91-19351
N91-19935
506-46-11-01 ..... N91-19122
506-48-4A N91-19378
506-48-00 ..... N91-19167
N91-19317
510-01-0A N91-19230
N91-19236
N91-19237
510-01-01 ..... N91-19232
N91-19233
N91-19308
510-01-50 ..... N91-19464
510-10-50 ..... N91-19229
532-06-21 ..... N91-19078
532-09-91 ..... N91-19241
533-02-01 ..... N91-19079
N91-19095
533-02-21 ..... N91-19099
533-02-51 ..... N91-19081
535-03-01 ..... N91-19045
535-03-10 ..... N91-19475
535-05-01 ..... N91-19098
537-02-11 ..... N91-19048
553-13-00 ..... N91-19472
582-01-11 ..... N91-19235
N91-19766
590-12-11 ..... N91-19770
590-13-11 ..... N91-19112
N91-19179
590-13-51 ..... N91-19376
590-14-61-01 ..... N91-19471
N91-19474
590-21-11 ..... N91-19295
590-21-31 ..... N91-19479
591-41-11 ..... N91-19174
592-01-11 ..... N91-19304
650-60-20 ..... N91-19349
N91-19350
674-21-05 ..... N91-19320
679-40-00 ..... N91-19348
694-03-0A N91-19371
694-03-03 ..... N91-19324
694-03-06 ..... N91-19325

Typical Report Number Index Listing

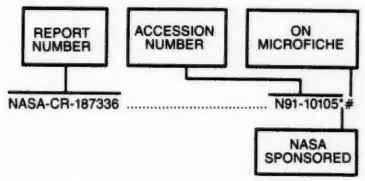

Listings in this index are arranged alphanumerically by report number. The accession number denotes the number by which the citation is identified. An asterisk (*) indicates that the item is a NASA report. A pound sign (#) indicates that the item is available on microfiche.

A-88007 ..... N91-19824* #
A-88203 ..... N91-19082* #
A-89194 ..... N91-19062* #
A-89265 ..... N91-19823* #
A-89266 ..... N91-19058* #
A-90030 ..... N91-20039* #
A-90037 ..... N91-19041* #
A-90091 ..... N91-19050* #
A-90197 ..... N91-19714* #
A-90252 ..... N91-19052* #
A-90268-VOL-1 ..... N91-19566* #
A-90283 ..... N91-19060* #
A-90307 ..... N91-19078* #
A-91014 ..... N91-19241* #
A-91015 ..... N91-19770* #
A-91062 ..... N91-19304* #
A-91063 ..... N91-19826* #
A-91066 ..... N91-19771* #

ACTA-POLYTEC-SCAND-ME-96 ..... N91-19392 #
ACTA-POLYTEC-SCAND-ME-97 ..... N91-19454 #

AD-A226858 ..... N91-19460 #
AD-A227471 ..... N91-19342 #
AD-A227947 ..... N91-19564 #
AD-A229114 ..... N91-19957 #
AD-A229847 ..... N91-19340 #
AD-A229848 ..... N91-19412 #
AD-A229851 ..... N91-19713 #
AD-A229852 ..... N91-19434 #
AD-A229860 ..... N91-19879 #
AD-A229861 ..... N91-19413 #
AD-A229862 ..... N91-19565 #
AD-A229863 ..... N91-19075 #
AD-A229865 ..... N91-19265 #
AD-A229866 ..... N91-19496 #
AD-A229867 ..... N91-19111 #
AD-A229874 ..... N91-19287 #
AD-A229875 ..... N91-19071 #
AD-A229876 ..... N91-19709 #

AD-D014611 ..... N91-19076
AD-D014644 ..... N91-19100
AD-D014645 ..... N91-19072
AD-D014648 ..... N91-19225
AD-D014650 ..... N91-19341
AD-D014651 ..... N91-19249
AD-D014653 ..... N91-19171 #
AD-D014654 ..... N91-19869 #
AD-D014655 ..... N91-19328 #
AD-D014656 ..... N91-19917 #
AD-D014658 ..... N91-19116 #
AD-D014663 ..... N91-19764 #
AD-D014664 ..... N91-19288 #
AD-D014665 ..... N91-19289 #
AD-D014667 ..... N91-19312
AD-D014668 ..... N91-19870
AD-D014673 ..... N91-19396
AD-D014674 ..... N91-19397
AD-D014676 ..... N91-19468
AD-D014677 ..... N91-19972
AD-D014694 ..... N91-19918
AD-D014697 ..... N91-19436
AD-D014705 ..... N91-19437
AD-D014708 ..... N91-19364
AD-D014723 ..... N91-19717

AEROJET-2459-54-2-VOL-1 ..... N91-19174* #

AFIT/GAE/ENY/90D-09 ..... N91-19412 #
AFIT/GAE/ENY/90D-11 ..... N91-19496 #
AFIT/GAE/ENY/90D-18 ..... N91-19111 #

AFIT/GEP/ENP/90D-9 ..... N91-19265 #

AFOSR-90-1112TR ..... N91-19957 #

AGARD-AR-283 ..... N91-19731 #
AGARD-AR-294 ..... N91-19124 #

AIAA-90-2166 ..... N91-19079* #
AIAA-90-2543 ..... N91-19180* #
AIAA-90-3018 ..... N91-19051* #
AIAA-90-3911 ..... N91-19053* #
AIAA-90-4022 ..... N91-19825* #
AIAA-90-5240 ..... N91-19374* #
AIAA-91-0253 ..... N91-19370* #
AIAA-91-0264 ..... N91-19047* #
AIAA-91-0273 ..... N91-19044* #
AIAA-91-0447 ..... N91-19046* #
AIAA-91-0594 ..... N91-19045* #
AIAA-91-0777 ..... N91-19371* #

ANL-HEP-CP-90-53 ..... N91-19414 #

ANL/ACTV-90/5 ..... N91-19301 #

ANL/FPP/TM-156 ..... N91-19903 #

ANL/MCS-TM-144 ..... N91-19534 #
ANL/MCS-TM-147 ..... N91-19760 #

ARI-RN-91-03 ..... N91-19713 #

AVSCOM-TR-90-C-019 ..... N91-19435* #
AVSCOM-TR-90-C-027 ..... N91-19438* #
AVSCOM-TR-90-C-028 ..... N91-19439* #
AVSCOM-TR-90-C-030 ..... N91-19369* #

BBC-RD-1990/12 ..... N91-19329

BCRS-88-05 ..... N91-19327 #

BNL-44673 ..... N91-19360 #
BNL-44894 ..... N91-19538 #
BNL-45381 ..... N91-19361 #
BNL-45469 ..... N91-19849 #
BNL-45481 ..... N91-19850 #
BNL-45482 ..... N91-19432 #
BNL-45579 ..... N91-19873 #
BNL-45579-REV ..... N91-19874 #
BNL-45623 ..... N91-19359 #
BNL-45645 ..... N91-19542 #
BNL-45651 ..... N91-19279 #
BNL-45653 ..... N91-19835 #
BNL-45672 ..... N91-19278 #
BNL-45674 ..... N91-19302 #
BNL-45676 ..... N91-19280 #
BNL-45696 ..... N91-19848 #
BNL-45732 ..... N91-19929 #
BNL-45750 ..... N91-19712 #
BNL-45782 ..... N91-19651 #
BNL-52273 ..... N91-19422 #

BU-405 ..... N91-19244 #
BU-406 ..... N91-19245 #
BU-407 ..... N91-19486 #
BU-409 ..... N91-19246 #
BU-410 ..... N91-19247 #
BU-411 ..... N91-19487 #
BU-412 ..... N91-19453 #
BU-413 ..... N91-19068 #
BU-414 ..... N91-19391 #
BU-415 ..... N91-19488 #
BU-416 ..... N91-19512 #

CDI-84-6 ..... N91-19067* #
CDI-87-02 ..... N91-19074* #

CESAR-91/01 ..... N91-19444 #

CONF-900348-21 ..... N91-19863 #
CONF-900450-13 ..... N91-19847 #
CONF-900505-9 ..... N91-19881 #
CONF-900563-18 ..... N91-19399 #
CONF-900603-58 ..... N91-19414 #
CONF-900623-25 ..... N91-19270 #
CONF-900688-1 ..... N91-19929 #
CONF-900731-4 ..... N91-19310 #
CONF-900756-57 ..... N91-19400 #
CONF-900834-1 ..... N91-19873 #
CONF-900870-6 ..... N91-19936 #
CONF-900870-8 ..... N91-19243 #
CONF-900923-9 ..... N91-19861 #
CONF-900993-2 ..... N91-19712 #
CONF-901025-40 ..... N91-19908 #
CONF-901035-17 ..... N91-19921 #
CONF-901038-1 ..... N91-19440 #
CONF-901047-1 ..... N91-19932 #
CONF-901057-28 ..... N91-19983 #
CONF-901073-14 ..... N91-19278 #
CONF-901073-15 ..... N91-19302 #
CONF-901105-84 ..... N91-19268 #
CONF-901105-85 ..... N91-19291 #
CONF-901105-86 ..... N91-19925 #
CONF-901105-87 ..... N91-19924 #
CONF-901105-88 ..... N91-19926 #
CONF-901105-89 ..... N91-19919 #
CONF-901105-90 ..... N91-19928 #
CONF-901105-94 ..... N91-19907 #
CONF-901105-95 ..... N91-19937 #
CONF-901105-96 ..... N91-19283 #
CONF-901106-3 ..... N91-19314 #
CONF-901125-10 ..... N91-19942 #
CONF-901141-1 ..... N91-19985 #
CONF-901155-5 ..... N91-19507 #
CONF-901155-6 ..... N91-19260 #
CONF-901194-9 ..... N91-19508 #
CONF-901240-1 ..... N91-19542 #
CONF-901248-1 ..... N91-19357 #
CONF-901259-2 ..... N91-19553 #
CONF-901263-2 ..... N91-19419 #
CONF-901263-7 ..... N91-19433 #
CONF-901269-1 ..... N91-19506 #
CONF-901278-1-VUGRAPHS ..... N91-19431 #
CONF-910108-4 ..... N91-19538 #
CONF-910116-19 ..... N91-19857 #
CONF-910123-2 ..... N91-19421 #
CONF-910123-7 ..... N91-19898 #
CONF-910123-9 ..... N91-19427 #
CONF-910123-10 ..... N91-19430 #
CONF-910123-12 ..... N91-19862 #
CONF-910127-4 ..... N91-19368 #
CONF-910162-2 ..... N91-19239 #
CONF-910162-3 ..... N91-19281 #
CONF-910170-2 ..... N91-19408 #
CONF-910172-2 ..... N91-19409 #
CONF-910184-1 ..... N91-19704 #
CONF-910202-3 ..... N91-19282 #
CONF-910207-2 ..... N91-19902 #
CONF-910212-1 ..... N91-19299 #
CONF-910212-2 ..... N91-19941 #
CONF-910252-2 ..... N91-19481 #
CONF-910276-2-VUGRAPHS ..... N91-19964 #
CONF-910276-3-VUGRAPHS ..... N91-19965 #
CONF-910278-1 ..... N91-19258 #
CONF-910279-1 ..... N91-19276 #
CONF-910279-2-VUGRAPHS ..... N91-19407 #
CONF-910280-1 ..... N91-19960 #
CONF-910280-2 ..... N91-19795 #
CONF-910281-1 ..... N91-19758 #
CONF-910328-2 ..... N91-19269 #
CONF-910328-3 ..... N91-19279 #
CONF-910374-1 ..... N91-19272 #
CONF-910399-1 ..... N91-19466 #
CONF-910402-1 ..... N91-19297 #
CONF-910402-4 ..... N91-19257 #

CONF-910402-7 N91-19533 #
CONF-910402-8 N91-19905 #
CONF-910414-1 N91-19759 #
CONF-910414-3 N91-19749 #
CONF-910414-14 N91-19780 #
CONF-910414-17 N91-19782 #
CONF-910414-18 N91-19781 #
CONF-910414-19 N91-19794 #
CONF-910414-21 N91-19784 #
CONF-910427-1 N91-19899 #
CONF-910446-2 N91-19240 #
CONF-910450-2 N91-19424 #
CONF-910451-1 N91-19767 #
CONF-910451-4 N91-19445 #
CONF-910451-5 N91-19447 #
CONF-910451-6 N91-19446 #
CONF-910451-7 N91-19768 #
CONF-910451-9 N91-19769 #
CONF-910451-10 N91-19448 #
CONF-910473-1 N91-19303 #
CONF-910478-1 N91-19428 #
CONF-910494-1 N91-19793 #
CONF-910498-1 N91-19779 #
CONF-9002156-2 N91-19253 #
CONF-9002167-1 N91-19535 #
CONF-9002169 N91-19896 #
CONF-9004131 N91-19503 #
CONF-9004232 N91-19422 #
CONF-9004232-4 N91-19432 #
CONF-9004232-5 N91-19850 #
CONF-9005316-1 N91-19951 #
CONF-9006105-13 N91-19252 #
CONF-9006212-5 N91-19984 #
CONF-9006242-3 N91-19849 #
CONF-9006267-23 N91-19851 #
CONF-9006314-1 N91-19842 #
CONF-9007111-15 N91-19358 #
CONF-9007198-2 N91-19838 #
CONF-9008185-1 N91-19872 #
CONF-9008186-1 N91-19255 #
CONF-9009108-2 N91-19743 #
CONF-9009109-1 N91-19552 #
CONF-9009118-2 N91-19417 #
CONF-9009123-64 N91-19418 #
CONF-9009141-12 N91-19277 #
CONF-9009166-17 N91-19425 #
CONF-9009166-18 N91-19426 #
CONF-9009201-11 N91-19290 #
CONF-9009241-2-REV N91-19874 #
CONF-9009248-5 N91-19405 #
CONF-9009266-7 N91-19895 #
CONF-9009266-10-REV-1 N91-19429 #
CONF-9009337-SUMM N91-19897 #
CONF-9009344-SUMM N91-19760 #
CONF-9010135-1 N91-19933 #
CONF-9010138-1 N91-19280 #
CONF-9010151-8 N91-19483 #
CONF-9010212-33 N91-19963 #
CONF-9010212-34 N91-19359 #
CONF-9010212-35 N91-19361 #
CONF-9010220-26 N91-19360 #
CONF-9010232-2 N91-19333 #
CONF-9010249-3-REV-1 N91-19698 #
CONF-9010256-6 N91-19720 #
CONF-9010270-2 N91-19777 #
CONF-9010270-3 N91-19778 #
CONF-9010277-2 N91-19530 #
CONF-9010298-2 N91-19416 #
CONF-9010298-5 N91-19910 #
CONF-9010298-7 N91-19900 #
CONF-9010307-1 N91-19738 #
CONF-9010317-1 N91-19480 #
CONF-9010320-1 N91-19848 #
CONF-9011149-11 N91-19381 #
CONF-9011175-1 N91-19922 #
CONF-9011179-1 N91-19551 #
CONF-9011180-1 N91-19539 #
CONF-9103102-4 N91-19344 #
CONF-9103130-1 N91-19242 #
CONF-9104109-1 N91-19860 #
CONF-9104111-1 N91-19465 #
CONF-9104123-1 N91-19510 #
CONF-9104158-1 N91-19744 #
CONF-9104161-3 N91-19406 #
CONF-9104164-1 N91-19835 #
CONF-9104166-2 N91-19757 #
CONF-9104168-1 N91-19745 #
CONF-9104171-1 N91-19065 #
CONF-9104171-2 N91-19064 #
CONF-9104173-1 N91-19747 #

CRIE-T-89048 N91-19561 #

CRIE-U-88029 N91-19380 #

CRINC-RSL-TR-4191-13 N91-19340 #

CSDG-89-2 N91-19732* #

DE89-009514 N91-19501 #
DE90-009687 N91-19556 #
DE90-015857 N91-19759 #
DE90-016047 N91-19240 #
DE90-017015 N91-19749 #
DE90-017044 N91-19767 #
DE90-017746 N91-19445 #
DE90-017764 N91-19446 #
DE90-017765 N91-19447 #
DE91-000034 N91-19768 #
DE91-000709 N91-19769 #
DE91-001261 N91-19448 #
DE91-001269 N91-19303 #
DE91-002128 N91-19502 #
DE91-002324 N91-19428 #
DE91-002429 N91-19881 #
DE91-003064 N91-19380 #
DE91-004379 N91-19793 #
DE91-004501 N91-19297 #
DE91-004537 N91-19779 #
DE91-004623 N91-19503 #
DE91-004841 N91-19860 #
DE91-004943 N91-19775 #
DE91-004996 N91-19330 #
DE91-005224 N91-19510 #
DE91-005349 N91-19267 #
DE91-005511 N91-19250 #
DE91-005521 N91-19290 #
DE91-005540 N91-19505 #
DE91-005620 N91-19751 #
DE91-005650 N91-19104 #
DE91-005652 N91-19399 #
DE91-005699 N91-19834 #
DE91-005729 N91-19313 #
DE91-005730 N91-19251 #
DE91-005741 N91-19504 #
DE91-005915 N91-19920 - #
DE91-006007 N91-19414 #
DE91-006015 N91-19252 #
DE91-006045 N91-19253 #
DE91-006139 N91-19450 #
DE91-006220 N91-19254 #
DE91-006341 N91-19506 #
DE91-006393 N91-19507 #
DE91-006406 N91-19508 #
DE91-006432 N91-19103 #
DE91-006465 N91-19314 #
DE91-006491 N91-19440 #
DE91-006514 N91-19553 #
DE91-006537 N91-19298 #
DE91-006543 N91-19346 #
DE91-006591 N91-19743 #
DE91-006620 N91-19509 #
DE91-006629 N91-19936 #
DE91-006639 N91-19344 #
DE91-006674 N91-19744 #
DE91-006701 N91-19400 #
DE91-006706 N91-19530 #
DE91-006707 N91-19921 #
DE91-006711 N91-19268 #
DE91-006724 N91-19738 #
DE91-006738 N91-19554 #
DE91-006753 N91-19352 #
DE91-006760 N91-19322 #
DE91-006771 N91-19922 #
DE91-006775 N91-19291 #
DE91-006778 N91-19872 #
DE91-006793 N91-19347 #
DE91-006798 N91-19531 #
DE91-006799 N91-19315 #
DE91-006879 N91-19896 #
DE91-006894 N91-19368 #
DE91-006912 N91-19897 #
DE91-006920 N91-19835 #
DE91-006922 N91-19833 #
DE91-006955 N91-19511 #
DE91-007064 N91-19269 #
DE91-007122 N91-19745 #
DE91-007125 N91-19698 #
DE91-007142 N91-19857 #
DE91-007146 N91-19429 #
DE91-007155 N91-19331 #
DE91-007162 N91-19739 #
DE91-007164 N91-19858 #
DE91-007181 N91-19255 #
DE91-007184 N91-19535 #
DE91-007188 N91-19740 #
DE91-007189 N91-19270 #
DE91-007200 N91-19271 #
DE91-007215 N91-19551 #
DE91-007216 N91-19353 #
DE91-007218 N91-19905 #
DE91-007234 N91-19746 #
DE91-007235 N91-19420 #

DE91-007241 N91-19720 #
DE91-007246 N91-19923 #
DE91-007254 N91-19924 #
DE91-007257 N91-19958 #
DE91-007258 N91-19983 #
DE91-007261 N91-19898 #
DE91-007262 N91-19417 #
DE91-007264 N91-19984 #
DE91-007272 N91-19925 #
DE91-007278 N91-19926 #
DE91-007295 N91-19719 #
DE91-007317 N91-19927 #
DE91-007320 N91-19792 #
DE91-007323 N91-19555 #
DE91-007330 N91-19418 #
DE91-007333 N91-19776 #
DE91-007341 N91-19919 #
DE91-007342 N91-19985 #
DE91-007347 N91-19895 #
DE91-007349 N91-19419 #
DE91-007351 N91-19552 #
DE91-007352 N91-19257 #
DE91-007355 N91-19480 #
DE91-007363 N91-19532 #
DE91-007369 N91-19859 #
DE91-007380 N91-19536 #
DE91-007388 N91-19899 #
DE91-007411 N91-19272 #
DE91-007423 N91-19777 #
DE91-007424 N91-19778 #
DE91-007458 N91-19537 #
DE91-007461 N91-19377 #
DE91-007473 N91-19928 #
DE91-007491 N91-19333 #
DE91-007493 N91-19405 #
DE91-007500 N91-19334 #
DE91-007518 N91-19421 #
DE91-007545 N91-19318 #
DE91-007556 N91-19873 #
DE91-007558 N91-19929 #
DE91-007561 N91-19538 #
DE91-007564 N91-19874 #
DE91-007572 N91-19481 #
DE91-007582 N91-19836 #
DE91-007598 N91-19780 #
DE91-007601 N91-19953 #
DE91-007615 N91-19747 #
DE91-007616 N91-19416 #
DE91-007617 N91-19900 #
DE91-007618 N91-19781 #
DE91-007620 N91-19782 #
DE91-007621 N91-19783 #
DE91-007631 N91-19422 #
DE91-007638 N91-19794 #
DE91-007643 N91-19423 #
DE91-007646 N91-19930 #
DE91-007651 N91-19931 #
DE91-007654 N91-19837 #
DE91-007669 N91-19950 #
DE91-007672 N91-19906 #
DE91-007689 N91-19355 #
DE91-007693 N91-19260 #
DE91-007695 N91-19275 #
DE91-007702 N91-19795 #
DE91-007708 N91-19258 #
DE91-007710 N91-19406 #
DE91-007711 N91-19424 #
DE91-007729 N91-19276 #
DE91-007731 N91-19407 #
DE91-007732 N91-19064 #
DE91-007733 N91-19065 #
DE91-007734 N91-19960 #
DE91-007735 N91-19932 #
DE91-007736 N91-19409 #
DE91-007737 N91-19425 #
DE91-007739 N91-19861 #
DE91-007742 N91-19933 #
DE91-007743 N91-19934 #
DE91-007745 N91-19426 #
DE91-007756 N91-19838 #
DE91-007760 N91-19842 #
DE91-007761 N91-19299 #
DE91-007772 N91-19300 #
DE91-007793 N91-19301 #
DE91-007798 N91-19901 #
DE91-007820 N91-19961 #
DE91-007822 N91-19451 #
DE91-007827 N91-19444 #
DE91-007829 N91-19259 #
DE91-007834 N91-19465 #
DE91-007835 N91-19239 #
DE91-007843 N91-19539 #
DE91-007844 N91-19757 #
DE91-007845 N91-19902 #
DE91-007849 N91-19784 #
DE91-007859 N91-19533 #

DE91-007861 ..... N91-19937 #
DE91-007870 ..... N91-19758 #
DE91-007872 ..... N91-19785 #
DE91-007881 ..... N91-19540 #
DE91-007889 ..... N91-19986 #
DE91-007894 ..... N91-19408 #
DE91-007896 ..... N91-19907 #
DE91-007897 ..... N91-19702 #
DE91-007898 ..... N91-19703 #
DE91-007899 ..... N91-19704 #
DE91-007907 ..... N91-19748 #
DE91-007911 ..... N91-19839 #
DE91-007922 ..... N91-19760 #
DE91-007931 ..... N91-19483 #
DE91-007933 ..... N91-19840 #
DE91-007934 ..... N91-19938 #
DE91-007936 ..... N91-19705 #
DE91-007938 ..... N91-19841 #
DE91-007940 ..... N91-19903 #
DE91-007961 ..... N91-19277 #
DE91-007969 ..... N91-19843 #
DE91-007976 ..... N91-19541 #
DE91-007978 ..... N91-19261 #
DE91-007979 ..... N91-19939 #
DE91-008030 ..... N91-19262 #
DE91-008031 ..... N91-19706 #
DE91-008032 ..... N91-19940 #
DE91-008033 ..... N91-19263 #
DE91-008034 ..... N91-19484 #
DE91-008044 ..... N91-19844 #
DE91-008045 ..... N91-19845 #
DE91-008052 ..... N91-19534 #
DE91-008059 ..... N91-19381 #
DE91-008060 ..... N91-19430 #
DE91-008063 ..... N91-19862 #
DE91-008068 ..... N91-19427 #
DE91-008086 ..... N91-19542 #
DE91-008100 ..... N91-19278 #
DE91-008101 ..... N91-19302 #
DE91-008102 ..... N91-19279 #
DE91-008103 ..... N91-19280 #
DE91-008106 ..... N91-19242 #
DE91-008107 ..... N91-19941 #
DE91-008108 ..... N91-19712 #
DE91-008115 ..... N91-19543 #
DE91-008116 ..... N91-19904 #
DE91-008130 ..... N91-19281 #
DE91-008140 ..... N91-19846 #
DE91-008141 ..... N91-19847 #
DE91-008148 ..... N91-19382 #
DE91-008157 ..... N91-19707 #
DE91-008172 ..... N91-19243 #
DE91-008177 ..... N91-19787 #
DE91-008184 ..... N91-19942 #
DE91-008185 ..... N91-19431 #
DE91-008195 ..... N91-19908 #
DE91-008196 ..... N91-19848 #
DE91-008199 ..... N91-19909 #
DE91-008203 ..... N91-19863 #
DE91-008204 ..... N91-19963 #
DE91-008218 ..... N91-19951 #
DE91-008235 ..... N91-19356 #
DE91-008238 ..... N91-19558 #
DE91-008250 ..... N91-19964 #
DE91-008251 ..... N91-19965 #
DE91-008259 ..... N91-19282 #
DE91-008277 ..... N91-19335 #
DE91-008283 ..... N91-19309 #
DE91-008317 ..... N91-19357 #
DE91-008320 ..... N91-19358 #
DE91-008371 ..... N91-19283 #
DE91-008373 ..... N91-19310 #
DE91-008411 ..... N91-19359 #
DE91-008414 ..... N91-19432 #
DE91-008421 ..... N91-19821 #
DE91-008436 ..... N91-19849 #
DE91-008437 ..... N91-19360 #
DE91-008438 ..... N91-19850 #
DE91-008441 ..... N91-19361 #
DE91-008442 ..... N91-19851 #
DE91-008447 ..... N91-19466 #
DE91-008502 ..... N91-19433 #
DE91-008504 ..... N91-19910 #
DE91-008552 ..... N91-19544 #
DE91-614980 ..... N91-19752 #
DE91-615076 ..... N91-19788 #
DE91-615182 ..... N91-19943 #
DE91-615465 ..... N91-20016 #
DE91-615469 ..... N91-19559 #
DE91-615472 ..... N91-19987 #
DE91-615479 ..... N91-20020 #
DE91-615480 ..... N91-20021 #
DE91-615506 ..... N91-19944 #
DE91-615507 ..... N91-19945 #
DE91-742133 ..... N91-19561 #
DE91-744823 ..... N91-19911 #
DE91-744831 ..... N91-19912 #
DE91-744833 ..... N91-19913 #
DE91-744958 ..... N91-19284 #
DE91-744965 ..... N91-19914 #
DE91-744969 ..... N91-19988 #
DE91-744971 ..... N91-19989 #
DE91-744972 ..... N91-19990 #
DE91-744973 ..... N91-19991 #
DE91-744976 ..... N91-19992 #
DE91-745035 ..... N91-19852 #
DE91-746267 ..... N91-19316 #
DE91-750104 ..... N91-19105 #
DE91-750115 ..... N91-19066 #

DODA-AR-006-434 ..... N91-19434 #

DOE/CE-15440/T1 ..... N91-19504 #
DOE/CE-27462/T1 ..... N91-19511 #
DOE/CE-50182/T1 ..... N91-19531 #
DOE/CE-50182/T2 ..... N91-19315 #

DOE/CH-10406/T2 ..... N91-19353 #

DOE/ER-0483P ..... N91-19953 #
DOE/ER-00038/3345 ..... N91-19843 #
DOE/ER-12105/1 ..... N91-19923 #
DOE/ER-13044/8 ..... N91-19382 #
DOE/ER-13356/T2 ..... N91-19707 #
DOE/ER-13421/9 ..... N91-19839 #
DOE/ER-13438/1 ..... N91-19920 #
DOE/ER-13501/2 ..... N91-19275 #
DOE/ER-13503/4 ..... N91-19262 #
DOE/ER-13504/5 ..... N91-19836 #
DOE/ER-13507/6 ..... N91-19309 #
DOE/ER-13549/5 ..... N91-19844 #
DOE/ER-13580/1 ..... N91-19263 #
DOE/ER-13590/9 ..... N91-19554 #
DOE/ER-13654/7 ..... N91-19261 #
DOE/ER-13725/4 ..... N91-19939 #
DOE/ER-13750/2 ..... N91-19833 #
DOE/ER-13880/3 ..... N91-19267 #
DOE/ER-13908/2 ..... N91-19702 #
DOE/ER-13908/3 ..... N91-19703 #
DOE/ER-13955/11 ..... N91-19840 #
DOE/ER-13975/2 ..... N91-19834 #
DOE/ER-14015/2 ..... N91-19259 #
DOE/ER-14136/1 ..... N91-19377 #
DOE/ER-25015/30 ..... N91-19776 #
DOE/ER-25036/4 ..... N91-19792 #
DOE/ER-40159/166 ..... N91-19847 #
DOE/ER-40159/174 ..... N91-19846 #
DOE/ER-40161/T5 ..... N91-19859 #
DOE/ER-40557/1 ..... N91-19845 #
DOE/ER-45150/6 ..... N91-19940 #
DOE/ER-45166/3 ..... N91-19484 #
DOE/ER-45222/5 ..... N91-19841 #
DOE/ER-45314/3 ..... N91-19938 #
DOE/ER-53222/105 ..... N91-19904 #
DOE/ER-53252/22 ..... N91-19759 #
DOE/ER-60422/6 ..... N91-19532 #
DOE/ER-60700/3 ..... N91-19706 #
DOE/ER-60836/2 ..... N91-19705 #
DOE/ER-60970/1 ..... N91-19541 #
DOE/ER-60971/1-PHASE-2 ..... N91-19555 #
DOE/ER-61013/T1 ..... N91-19543 #
DOE/ER-61015/1 ..... N91-19540 #
DOE/ER-61019/1 ..... N91-19537 #

DOE/ET-10815/154 ..... N91-19906 #
DOE/ET-15601/T52 ..... N91-19746 #
DOE/ET-15601/T53 ..... N91-19420 #
DOE/ET-53088/435 ..... N91-19787 #
DOE/ET-53088/469 ..... N91-19897 #
DOE/ET-53088/472 ..... N91-19909 #

DOE/ID-12735/T13 ..... N91-19298 #
DOE/ID-13040/1 ..... N91-19509 #

DOE/MC-23270/2923 ..... N91-19505 #

DOE/METC-90/4102 ..... N91-19556 #

DOE/PC-79680/T4 ..... N91-19347 #
DOE/PC-79817/4 ..... N91-19318 #
DOE/PC-79817/5 ..... N91-19251 #
DOE/PC-79817/6 ..... N91-19313 #
DOE/PC-88932/T3 ..... N91-19536 #
DOE/PC-89775/2 ..... N91-19250 #

DOT-VNTSC-FRA-90-3 ..... N91-19326 #

DOT/FAA/RD-90/23 ..... N91-19102 #

DOT/FRA/ORD-90/09 ..... N91-19326 #

DTRC-90/025 ..... N91-19342 #
E-5000 ..... N91-19373* #
E-5511 ..... N91-19473* #
E-5526 ..... N91-19057* #
E-5579 ..... N91-19180* #
E-5588 ..... N91-19115* #
E-5654 ..... N91-19178* #
E-5688 ..... N91-19404* #
E-5705 ..... N91-19351* #
E-5714 ..... N91-19332* #
E-5716 ..... N91-19435* #
E-5728 ..... N91-19182* #
E-5754 ..... N91-19825* #
E-5759-1 ..... N91-19372* #
E-5774 ..... N91-19059* #
E-5780 ..... N91-19442* #
E-5794 ..... N91-19477* #
E-5824 ..... N91-19438* #
E-5830 ..... N91-19053* #
E-5834 ..... N91-19234* #
E-5842 ..... N91-19463* #
E-5847 ..... N91-19179* #
E-5849 ..... N91-19117* #
E-5854 ..... N91-19402* #
E-5860 ..... N91-19370* #
E-5865 ..... N91-19439* #
E-5871 ..... N91-19324* #
E-5872 ..... N91-19296* #
E-5873 ..... N91-19256* #
E-5876 ..... N91-19236* #
E-5877 ..... N91-19237* #
E-5884 ..... N91-19348* #
E-5885 ..... N91-19369* #
E-5886 ..... N91-19350* #
E-5890 ..... N91-19325* #
E-5892 ..... N91-19401* #
E-5893 ..... N91-19231* #
E-5896 ..... N91-19044* #
E-5897 ..... N91-19472* #
E-5898 ..... N91-19230* #
E-5899 ..... N91-19229* #
E-5903 ..... N91-19292* #
E-5906 ..... N91-19045* #
E-5909 ..... N91-19098* #
E-5912 ..... N91-19046* #
E-5920 ..... N91-19112* #
E-5922 ..... N91-19349* #
E-5923 ..... N91-19376* #
E-5924 ..... N91-19047* #
E-5929 ..... N91-19479* #
E-5931 ..... N91-19371* #
E-5932 ..... N91-19293* #
E-5940 ..... N91-19403* #
E-5943 ..... N91-19294* #
E-5946 ..... N91-19232* #
E-5948 ..... N91-19176* #
E-5949 ..... N91-19441* #
E-5955 ..... N91-19233* #
E-5960 ..... N91-19374* #
E-5962 ..... N91-20015* #
E-5964 ..... N91-19317* #
E-5966 ..... N91-19177* #
E-5973 ..... N91-19165* #
E-5986 ..... N91-19235* #
E-5988 ..... N91-19367* #
E-5989 ..... N91-19786* #
E-5991 ..... N91-19475* #
E-5997 ..... N91-19054* #
E-6003 ..... N91-19462* #
E-6006 ..... N91-19295* #
E-6015 ..... N91-19443* #
E-6021-VOL-1 ..... N91-19049* #
E-6023 ..... N91-19464* #
E-6024 ..... N91-19354* #
E-6026 ..... N91-19056* #
E-6027 ..... N91-19308* #
E-6034 ..... N91-19175* #
E-6041 ..... N91-19097* #
E-6049 ..... N91-19063* #
E-6055 ..... N91-19375* #
E-6060 ..... N91-19224* #
E-6061 ..... N91-19766* #
E-6065 ..... N91-19320* #
E-6069 ..... N91-19935* #
E-6071 ..... N91-19476* #

EGG-EP-9015 ..... N91-19346 #

EGG-NPR-9334 ..... N91-19450 #

EPA/600/D-90/173 ..... N91-19547 #
EPA/600/D-90/177 ..... N91-19546 #
EPA/600/3-90/089 ..... N91-19549 #
EPA/600/8-90/079 ..... N91-19545 #

ERL-0508-RN ..... N91-19434 #
ERL-290666-3 ..... N91-19347 #

ESA-SP-307 ..... N91-19572 #

ETN-88-93455 ..... N91-19327 #
ETN-91-98600 ..... N91-19365
ETN-91-98601 ..... N91-19982
ETN-91-98602 ..... N91-19976
ETN-91-98604 ..... N91-19880
ETN-91-98607 ..... N91-19977
ETN-91-98612 ..... N91-19978
ETN-91-98803 ..... N91-19572 #
ETN-91-98806 ..... N91-19971 #
ETN-91-98807 ..... N91-19113 #
ETN-91-98808 ..... N91-19796 #
ETN-91-98809 ..... N91-19946 #
ETN-91-98810 ..... N91-19827 #
ETN-91-98811 ..... N91-19384 #
ETN-91-98812 ..... N91-19385 #
ETN-91-98813 ..... N91-19386 #
ETN-91-98814 ..... N91-19387 #
ETN-91-98815 ..... N91-19388 #
ETN-91-98816 ..... N91-19389 #
ETN-91-98817 ..... N91-19390 #
ETN-91-98818 ..... N91-19876 #
ETN-91-98820 ..... N91-19877 #
ETN-91-98821 ..... N91-19981 #
ETN-91-98822 ..... N91-19485 #
ETN-91-98823 ..... N91-19084 #
ETN-91-98824 ..... N91-19085 #
ETN-91-98825 ..... N91-19086 #
ETN-91-98826 ..... N91-19101 #
ETN-91-98827 ..... N91-19087 #
ETN-91-98828 ..... N91-19828 #
ETN-91-98829 ..... N91-19088 #
ETN-91-98830 ..... N91-19089 #
ETN-91-98831 ..... N91-19090 #
ETN-91-98832 ..... N91-19091 #
ETN-91-98833 ..... N91-19708 #
ETN-91-98834 ..... N91-19321 #
ETN-91-98835 ..... N91-19336 #
ETN-91-98836 ..... N91-19106 #
ETN-91-98837 ..... N91-19311 #
ETN-91-98838 ..... N91-19829 #
ETN-91-98839 ..... N91-19753 #
ETN-91-98840 ..... N91-19754 #
ETN-91-98841 ..... N91-19797 #
ETN-91-98842 ..... N91-19789 #
ETN-91-98843 ..... N91-19362 #
ETN-91-98844 ..... N91-19761 #
ETN-91-98845 ..... N91-19772 #
ETN-91-98846 ..... N91-19864 #
ETN-91-98847 ..... N91-19865 #
ETN-91-98848 ..... N91-19866 #
ETN-91-98851 ..... N91-19867 #
ETN-91-98852 ..... N91-19096 #
ETN-91-98853 ..... N91-19092 #
ETN-91-98854 ..... N91-19093 #
ETN-91-98855 ..... N91-19762 #
ETN-91-98856 ..... N91-19954 #
ETN-91-98857 ..... N91-19244 #
ETN-91-98858 ..... N91-19245 #
ETN-91-98859 ..... N91-19486 #
ETN-91-98860 ..... N91-19246 #
ETN-91-98861 ..... N91-19247 #
ETN-91-98862 ..... N91-19487 #
ETN-91-98863 ..... N91-19453 #
ETN-91-98864 ..... N91-19068 #
ETN-91-98865 ..... N91-19391 #
ETN-91-98866 ..... N91-19488 #
ETN-91-98867 ..... N91-19512 #
ETN-91-98868 ..... N91-19822 #
ETN-91-98883 ..... N91-19853 #
ETN-91-98884 ..... N91-19550 #
ETN-91-98885 ..... N91-19410 #
ETN-91-98886 ..... N91-19868 #
ETN-91-98887 ..... N91-20019 #
ETN-91-98888 ..... N91-19854 #
ETN-91-98894 ..... N91-19915 #
ETN-91-98895 ..... N91-19798 #
ETN-91-98906 ..... N91-19513 #
ETN-91-98911 ..... N91-19563 #
ETN-91-98912 ..... N91-19830 #
ETN-91-98913 ..... N91-19363 #
ETN-91-98914 ..... N91-19392 #
ETN-91-98915 ..... N91-19454 #
ETN-91-98916 ..... N91-19947 #
ETN-91-98917 ..... N91-19855 #
ETN-91-98918 ..... N91-19285 #
ETN-91-98919 ..... N91-19455 #
ETN-91-98920 ..... N91-19120 #
ETN-91-98921 ..... N91-19393 #
ETN-91-98922 ..... N91-19799 #
ETN-91-98923 ..... N91-19878 #
ETN-91-98924 ..... N91-19948 #
ETN-91-98925 ..... N91-19856 #
ETN-91-98926 ..... N91-19773 #
ETN-91-98927 ..... N91-19489 #
ETN-91-98928 ..... N91-19337 #
ETN-91-98929 ..... N91-19338 #
ETN-91-98930 ..... N91-19490 #
ETN-91-98931 ..... N91-19916 #
ETN-91-98932 ..... N91-19949 #
ETN-91-98933 ..... N91-19286 #
ETN-91-98934 ..... N91-19790 #
ETN-91-98935 ..... N91-19248 #
ETN-91-98936 ..... N91-19222 #
ETN-91-98937 ..... N91-19394 #
ETN-91-98938 ..... N91-19456 #
ETN-91-98939 ..... N91-19831 #
ETN-91-98940 ..... N91-19491 #
ETN-91-98941 ..... N91-19395 #
ETN-91-98942 ..... N91-19492 #
ETN-91-98943 ..... N91-19493 #
ETN-91-98944 ..... N91-19069 #
ETN-91-98945 ..... N91-19169 #
ETN-91-98946 ..... N91-19494 #
ETN-91-98947 ..... N91-19094 #
ETN-91-98949 ..... N91-19339 #
ETN-91-98950 ..... N91-19114 #
ETN-91-98951 ..... N91-19121 #
ETN-91-98952 ..... N91-19170 #
ETN-91-98953 ..... N91-19457 #
ETN-91-98955 ..... N91-19411 #
ETN-91-98956 ..... N91-19755 #
ETN-91-98957 ..... N91-19495 #
ETN-91-98958 ..... N91-19774 #
ETN-91-98959 ..... N91-19458 #
ETN-91-98960 ..... N91-19070 #
ETN-91-98962 ..... N91-19459 #
ETN-91-98963 ..... N91-19763 #
ETN-91-98964 ..... N91-19791 #

FCR-11191 ..... N91-19505 #

FEL-1987-102 ..... N91-19327 #

FFA-TN-1990-37 ..... N91-19513 #

FNAL-TM-1707 ..... N91-19958 #
FNAL-TM-1710 ..... N91-19356 #
FNAL-TM-1712 ..... N91-19821 #

GA-A-20130 ..... N91-19881 #
GA-A-20267 ..... N91-19908 #

GA-C-19942-REV-1 ..... N91-19335 #

GAO/IMTEC-91-3 ..... N91-19955 #
GAO/IMTEC-91-20 ..... N91-19119 #

GPO-27-944 ..... N91-19968 #
GPO-34-529 ..... N91-19966 #
GPO-36-688 ..... N91-19974 #
GPO-36-778 ..... N91-19969 #
GPO-38-022 ..... N91-19528 #

GRI-90/0262 ..... N91-19264 #

H-1633 ..... N91-19051* #
H-1639 ..... N91-19099* #
H-1642 ..... N91-19742* #
H-1643 ..... N91-19079* #
H-1660 ..... N91-19077* #
H-1664 ..... N91-19080* #
H-1680 ..... N91-19081* #
H-1686 ..... N91-19055* #
H-1691 ..... N91-19095* #
H-1707 ..... N91-19083* #

IAEA-CN-53/D-4-7 ..... N91-19908 #

ICASE-IR-15 ..... N91-19366* #

ICASE-91-4 ..... N91-19715* #
ICASE-91-5 ..... N91-19716* #
ICASE-91-11 ..... N91-19043* #
ICASE-91-18 ..... N91-19345* #

ICOMP-90-25 ..... N91-19372* #
ICOMP-91-02 ..... N91-19786* #
ICOMP-91-04 ..... N91-19375* #

IFSR-435 ..... N91-19787 #
IFSR-469 ..... N91-19897 #
IFSR-472 ..... N91-19909 #

ILR-MITT-240(1990) ..... N91-19120 #
ILR-MITT-245(1990) ..... N91-19114 #
ILR-MITT-247(1990) ..... N91-19121 #
ILR-MITT-249(1990) ..... N91-19170 #

IRS-91-P3 ..... N91-19173* #

IS-M-657 ..... N91-19744 #
IS-M-662 ..... N91-19272 #

IS-T-1459 ..... N91-19837 #

ISAL-90-0069 ..... N91-19915 #

ISBN-90-370-0044-4 ..... N91-19394 #
ISBN-90-9002929-X ..... N91-19337 #
ISBN-90-9003671-7 ..... N91-19916 #
ISBN-90-9003684-9 ..... N91-19790 #
ISBN-90-9003688-1 ..... N91-19490 #
ISBN-90-9003733-0 ..... N91-19248 #
ISBN-92-835-0570-0 ..... N91-19124 #
ISBN-92-835-0596-6 ..... N91-19731 #
ISBN-92-9092-070-X ..... N91-19572 #
ISBN-951-22-0382-0 ..... N91-19363 #
ISBN-951-666-315X ..... N91-19392 #
ISBN-951-666-320-6 ..... N91-19454 #
ISBN-952-90-2241-7 ..... N91-19830 #
ISBN-0309-04199-6 ..... N91-19952 #
ISBN-0309-04388-3 ..... N91-19721 #

ISSN-0001-687X ..... N91-19392 #
ISSN-0001-687X ..... N91-19454 #
ISSN-0178-7101 ..... N91-19971 #
ISSN-0355-5712 ..... N91-19363 #
ISSN-0389-4010 ..... N91-19469 #
ISSN-0436-1199 ..... N91-19384 #
ISSN-0436-1199 ..... N91-19385 #
ISSN-0436-1199 ..... N91-19827 #
ISSN-0751-1345 ..... N91-19798 #
ISSN-0915-633X ..... N91-19894 #
ISSN-0915-6348 ..... N91-19882 #
ISSN-0931-9757 ..... N91-19106 #

IYAF-89-77 ..... N91-19752 #
IYAF-89-86 ..... N91-19788 #

JAERI-M-90-150 ..... N91-19912 #
JAERI-M-90-157 ..... N91-19284 #
JAERI-M-90-162 ..... N91-19913 #
JAERI-M-90-170 ..... N91-19914 #

JPL-D-7824 ..... N91-19355 #

JPL-PUBL-91-1 ..... N91-19733* #
JPL-PUBL-91-2 ..... N91-19734* #

JPRS-ULS-91-001 ..... N91-19567 #

JPRS-UPM-90-004 ..... N91-19800 #

L-16711 ..... N91-19042* #
L-16848 ..... N91-19024* #

LA-UR-90-3455 ..... N91-19428 #
LA-UR-90-3859 ..... N91-19860 #
LA-UR-91-7 ..... N91-19419 #
LA-UR-91-16 ..... N91-19552 #
LA-UR-91-19 ..... N91-19257 #
LA-UR-91-92 ..... N91-19480 #
LA-UR-91-124 ..... N91-19899 #
LA-UR-91-276 ..... N91-19928 #
LA-UR-91-373 ..... N91-19333 #
LA-UR-91-397 ..... N91-19405 #

LA-11742-MS ..... N91-19858 #
LA-12017-MS ..... N91-19986 #

LBL-28303 ..... N91-19934 #
LBL-29470 ..... N91-19951 #
LBL-29589 ..... N91-19933 #
LBL-29644 ..... N91-19861 #
LBL-29720 ..... N91-19423 #
LBL-29724 ..... N91-19425 #
LBL-29837 ..... N91-19931 #
LBL-29844 ..... N91-19930 #
LBL-29956 ..... N91-19426 #

LC-89-64440 ..... N91-19952 #
LC-90-22329 ..... N91-19721 #

LIYF-1451 ..... N91-19943 #
LIYF-1524 ..... N91-19944 #
LIYF-1552 ..... N91-19945 #

LMSC-F279204 ..... N91-19323* #

LPI-CONTRIB-758 ..... N91-19995* #

LR-564 ..... N91-19456 #
LR-565 ..... N91-19831 #
LR-639 ..... N91-19491 #
LR-640 ..... N91-19395 #
LR-641 ..... N91-19492 #

LR-642 ..... N91-19493 #
LR-643 ..... N91-19069 #
LR-644 ..... N91-19169 #
LR-645 ..... N91-19494 #
LR-647 ..... N91-19094 #
LR-648 ..... N91-19222 #

LRT-WE-9-FB-06(1990) ..... N91-19386 #
LRT-WE-9-FB-10(1990) ..... N91-19387 #
LRT-WE-9-FB-11(1990) ..... N91-19388 #
LRT-WE-9-FB-12(1990) ..... N91-19389 #
LRT-WE-9-FB-13(1990) ..... N91-19390 #

MBB-UA-1185-90-PUB ..... N91-19876 #
MBB-UA-1199-90-PUB ..... N91-19877 #

MBB-UD-0571-90-PUB ..... N91-19981 #
MBB-UD-0572-90-PUB ..... N91-19485 #
MBB-UD-0573-90-PUB ..... N91-19084 #
MBB-UD-0574-90-PUB ..... N91-19085 #
MBB-UD-0575-90-PUB ..... N91-19086 #
MBB-UD-0576-90-PUB ..... N91-19101 #
MBB-UD-0577-90-PUB ..... N91-19087 #
MBB-UD-0578-90-PUB ..... N91-19828 #
MBB-UD-0579-90-PUB ..... N91-19088 #
MBB-UD-0580-90-PUB ..... N91-19089 #
MBB-UD-0581-90-PUB ..... N91-19090 #
MBB-UD-0588-90-PUB ..... N91-19091 #

MBB-UK-0107-90-PUB ..... N91-19336 #

MBB-UO-0096-90-PUB ..... N91-19708 #
MBB-UO-0130-90-PUB ..... N91-19321 #

MBB-Z-0168-90-PUB ..... N91-19106 #
MBB-Z-0320-90-PUB ..... N91-19311 #
MBB-Z-0341-90-PUB ..... N91-19829 #

MCR-90-502 ..... N91-19238* #

MEMT-11 ..... N91-19394 #

MPE-PREPRINT-176 ..... N91-19365
MPE-PREPRINT-177 ..... N91-19982
MPE-PREPRINT-178 ..... N91-19976
MPE-PREPRINT-180 ..... N91-19880
MPE-PREPRINT-183 ..... N91-19977
MPE-PREPRINT-188 ..... N91-19978

MPE-222 ..... N91-19971 #

MPIS-8/1990 ..... N91-19827 #
MPIS-10/1990 ..... N91-19384 #
MPIS-15/1990 ..... N91-19385 #

MRL-TR-90-27 ..... N91-19266 #

NAL-TM-616 ..... N91-19066 #
NAL-TM-618 ..... N91-19105 #

NAL-TR-1057 ..... N91-19469 #

NAS 1.15:4226 ..... N91-19473* #
NAS 1.15:4234 ..... N91-19099* #
NAS 1.15:4239 ..... N91-19052* #
NAS 1.15:4240 ..... N91-19079* #
NAS 1.15:4244 ..... N91-19181* #
NAS 1.15:4256-VOL-1 ..... N91-19499* #
NAS 1.15:4257 ..... N91-19115* #
NAS 1.15:4258 ..... N91-19697* #
NAS 1.15:101724 ..... N91-19051* #
NAS 1.15:101727 ..... N91-19080* #
NAS 1.15:101730 ..... N91-19742* #
NAS 1.15:101731 ..... N91-19081* #
NAS 1.15:101733 ..... N91-19077* #
NAS 1.15:101734 ..... N91-19055* #
NAS 1.15:101737 ..... N91-19095* #
NAS 1.15:101742 ..... N91-19083* #
NAS 1.15:102165 ..... N91-19273* #
NAS 1.15:102166 ..... N91-19274* #
NAS 1.15:102170 ..... N91-19699* #
NAS 1.15:102173 ..... N91-19959* #
NAS 1.15:102206 ..... N91-19062* #
NAS 1.15:102264 ..... N91-20039* #
NAS 1.15:102267 ..... N91-19041* #
NAS 1.15:102688 ..... N91-19166* #
NAS 1.15:102720 ..... N91-19474* #
NAS 1.15:102763 ..... N91-19471* #
NAS 1.15:102767 ..... N91-19073* #
NAS 1.15:102768 ..... N91-19168* #
NAS 1.15:102777 ..... N91-19482* #
NAS 1.15:102781 ..... N91-19061* #
NAS 1.15:102860 ..... N91-19566* #
NAS 1.15:102871 ..... N91-19078* #
NAS 1.15:102885 ..... N91-19241* #
NAS 1.15:102886 ..... N91-19770* #
NAS 1.15:103191 ..... N91-19180* #
NAS 1.15:103234 ..... N91-19178* #
NAS 1.15:103257 ..... N91-19404* #
NAS 1.15:103272 ..... N91-19332* #
NAS 1.15:103286 ..... N91-19351* #
NAS 1.15:103333 ..... N91-19979* #
NAS 1.15:103397 ..... N91-19319* #
NAS 1.15:103398 ..... N91-19123* #
NAS 1.15:103525 ..... N91-19529* #
NAS 1.15:103606 ..... N91-19825* #
NAS 1.15:103626 ..... N91-19477* #
NAS 1.15:103639 ..... N91-19373* #
NAS 1.15:103648 ..... N91-19234* #
NAS 1.15:103650 ..... N91-19053* #
NAS 1.15:103656 ..... N91-19179* #
NAS 1.15:103658 ..... N91-19442* #
NAS 1.15:103664 ..... N91-19324* #
NAS 1.15:103665 ..... N91-19296* #
NAS 1.15:103666 ..... N91-19256* #
NAS 1.15:103668 ..... N91-19372* #
NAS 1.15:103669 ..... N91-19236* #
NAS 1.15:103670 ..... N91-19237* #
NAS 1.15:103672 ..... N91-19348* #
NAS 1.15:103673 ..... N91-19369* #
NAS 1.15:103676 ..... N91-19401* #
NAS 1.15:103677 ..... N91-19231* #
NAS 1.15:103679 ..... N91-19044* #
NAS 1.15:103680 ..... N91-19472* #
NAS 1.15:103681 ..... N91-19230* #
NAS 1.15:103682 ..... N91-19229* #
NAS 1.15:103685 ..... N91-19292* #
NAS 1.15:103687 ..... N91-19045* #
NAS 1.15:103690 ..... N91-19098* #
NAS 1.15:103693 ..... N91-19046* #
NAS 1.15:103698 ..... N91-19112* #
NAS 1.15:103700 ..... N91-19349* #
NAS 1.15:103701 ..... N91-19047* #
NAS 1.15:103702 ..... N91-19370* #
NAS 1.15:103706 ..... N91-19371* #
NAS 1.15:103707 ..... N91-19293* #
NAS 1.15:103711 ..... N91-19294* #
NAS 1.15:103713 ..... N91-19232* #
NAS 1.15:103715 ..... N91-19176* #
NAS 1.15:103716 ..... N91-19441* #
NAS 1.15:103724 ..... N91-19233* #
NAS 1.15:103726 ..... N91-19374* #
NAS 1.15:103728 ..... N91-20015* #
NAS 1.15:103730 ..... N91-19317* #
NAS 1.15:103731 ..... N91-19177* #
NAS 1.15:103732 ..... N91-19463* #
NAS 1.15:103734 ..... N91-19402* #
NAS 1.15:103735 ..... N91-19165* #
NAS 1.15:103743 ..... N91-19235* #
NAS 1.15:103745 ..... N91-19786* #
NAS 1.15:103746 ..... N91-19475* #
NAS 1.15:103748 ..... N91-19054* #
NAS 1.15:103751 ..... N91-19462* #
NAS 1.15:103758 ..... N91-19443* #
NAS 1.15:103761 ..... N91-19464* #
NAS 1.15:103762 ..... N91-19354* #
NAS 1.15:103764 ..... N91-19308* #
NAS 1.15:103771 ..... N91-19175* #
NAS 1.15:103774 ..... N91-19097* #
NAS 1.15:103777 ..... N91-19295* #
NAS 1.15:103778 ..... N91-19063* #
NAS 1.15:103781 ..... N91-19375* #
NAS 1.15:103784 ..... N91-19224* #
NAS 1.15:103785 ..... N91-19766* #
NAS 1.15:103788 ..... N91-19320* #
NAS 1.15:103792 ..... N91-19935* #
NAS 1.15:103794 ..... N91-19476* #
NAS 1.15:103816 ..... N91-19118* #
NAS 1.15:103836 ..... N91-19304* #
NAS 1.15:103837 ..... N91-19826* #
NAS 1.15:104029 ..... N91-19415* #
NAS 1.15:104535 ..... N91-19449* #
NAS 1.15:104536 ..... N91-19557* #
NAS 1.21:7064-SUPPL-5 ..... N91-19962* #
NAS 1.26:3922(35) ..... N91-19700* #
NAS 1.26:3958 ..... N91-19067* #
NAS 1.26:4309 ..... N91-19050* #
NAS 1.26:4329 ..... N91-19049* #
NAS 1.26:4334 ..... N91-19435* #
NAS 1.26:4341 ..... N91-19438* #
NAS 1.26:4342 ..... N91-19439* #
NAS 1.26:4343 ..... N91-19164* #
NAS 1.26:4347 ..... N91-19498* #
NAS 1.26:177538 ..... N91-19323* #
NAS 1.26:177557 ..... N91-19714* #
NAS 1.26:177568 ..... N91-19060* #
NAS 1.26:177575 ..... N91-19771* #
NAS 1.26:184110 ..... N91-19172* #
NAS 1.26:184112 ..... N91-19162* #
NAS 1.26:184113 ..... N91-19163* #
NAS 1.26:184115 ..... N91-19223* #
NAS 1.26:185175 ..... N91-19174* #
NAS 1.26:185292 ..... N91-19048* #
NAS 1.26:185300 ..... N91-19059* #
NAS 1.26:187037 ..... N91-19117* #
NAS 1.26:187042 ..... N91-19167* #
NAS 1.26:187047 ..... N91-19350* #
NAS 1.26:187050 ..... N91-19325* #
NAS 1.26:187053 ..... N91-19376* #
NAS 1.26:187055 ..... N91-19479* #
NAS 1.26:187056 ..... N91-19403* #
NAS 1.26:187065 ..... N91-19367* #
NAS 1.26:187070 ..... N91-19378* #
NAS 1.26:187072 ..... N91-19461* #
NAS 1.26:187076 ..... N91-19056* #
NAS 1.26:187447 ..... N91-19478* #
NAS 1.26:187472 ..... N91-19238* #
NAS 1.26:187488 ..... N91-19366* #
NAS 1.26:187489 ..... N91-19737* #
NAS 1.26:187491 ..... N91-19756* #
NAS 1.26:187498 ..... N91-19715* #
NAS 1.26:187499 ..... N91-19716* #
NAS 1.26:187513 ..... N91-19043* #
NAS 1.26:187520 ..... N91-19345* #
NAS 1.26:187521 ..... N91-19074* #
NAS 1.26:187638 ..... N91-20022* #
NAS 1.26:187778 ..... N91-19973* #
NAS 1.26:187914 ..... N91-19765* #
NAS 1.26:187928 ..... N91-19732* #
NAS 1.26:187950 ..... N91-19343* #
NAS 1.26:187958 ..... N91-19718* #
NAS 1.26:187971 ..... N91-19995* #
NAS 1.26:187973 ..... N91-19734* #
NAS 1.26:187974 ..... N91-19733* #
NAS 1.26:187983 ..... N91-19735* #
NAS 1.26:187984 ..... N91-19398* #
NAS 1.26:187986 ..... N91-19173* #
NAS 1.26:187989 ..... N91-19871* #
NAS 1.26:187992 ..... N91-19736* #
NAS 1.26:187997 ..... N91-19710* #
NAS 1.26:187998 ..... N91-19741* #
NAS 1.26:188019 ..... N91-19975* #
NAS 1.26:188022 ..... N91-19497* #
NAS 1.26:188031 ..... N91-19980* #
NAS 1.26:188041 ..... N91-19750* #
NAS 1.26:188046 ..... N91-19701* #
NAS 1.26:188051 ..... N91-19379* #
NAS 1.26:188057 ..... N91-19305* #
NAS 1.26:188077 ..... N91-19722* #
NAS 1.55:3095 ..... N91-19024* #
NAS 1.55:3096 ..... N91-19126* #
NAS 1.55:3107 ..... N91-19182* #
NAS 1.55:10057-PT-2 ..... N91-19122* #
NAS 1.60:2995 ..... N91-19058* #
NAS 1.60:3020 ..... N91-19824* #
NAS 1.60:3032 ..... N91-19042* #
NAS 1.60:3043 ..... N91-19711* #
NAS 1.60:3053 ..... N91-19823* #
NAS 1.60:3080 ..... N91-19057* #
NAS 1.61:1252 ..... N91-19082* #

NASA-CP-3095 ..... N91-19024* #
NASA-CP-3096 ..... N91-19126* #
NASA-CP-3107 ..... N91-19182* #
NASA-CP-10057-PT-2 ..... N91-19122* #

NASA-CR-3922(35) ..... N91-19700* #
NASA-CR-3958 ..... N91-19067* #
NASA-CR-4309 ..... N91-19050* #
NASA-CR-4329 ..... N91-19049* #
NASA-CR-4334 ..... N91-19435* #
NASA-CR-4341 ..... N91-19438* #
NASA-CR-4342 ..... N91-19439* #
NASA-CR-4343 ..... N91-19164* #
NASA-CR-4347 ..... N91-19498* #
NASA-CR-177538 ..... N91-19323* #
NASA-CR-177557 ..... N91-19714* #
NASA-CR-177568 ..... N91-19060* #
NASA-CR-177575 ..... N91-19771* #
NASA-CR-184110 ..... N91-19172* #
NASA-CR-184112 ..... N91-19162* #
NASA-CR-184113 ..... N91-19163* #
NASA-CR-184115 ..... N91-19223* #
NASA-CR-185175 ..... N91-19174* #
NASA-CR-185292 ..... N91-19048* #
NASA-CR-185300 ..... N91-19059* #
NASA-CR-187037 ..... N91-19117* #
NASA-CR-187042 ..... N91-19167* #
NASA-CR-187047 ..... N91-19350* #
NASA-CR-187050 ..... N91-19325* #
NASA-CR-187053 ..... N91-19376* #
NASA-CR-187055 ..... N91-19479* #
NASA-CR-187056 ..... N91-19403* #
NASA-CR-187065 ..... N91-19367* #
NASA-CR-187070 ..... N91-19378* #
NASA-CR-187072 ..... N91-19461* #
NASA-CR-187076 ..... N91-19056* #
NASA-CR-187447 ..... N91-19478* #

NASA-CR-187472 ..... N91-19238* #
NASA-CR-187488 ..... N91-19366* #
NASA-CR-187489 ..... N91-19737* #
NASA-CR-187491 ..... N91-19756* #
NASA-CR-187498 ..... N91-19715* #
NASA-CR-187499 ..... N91-19716* #
NASA-CR-187513 ..... N91-19043* #
NASA-CR-187520 ..... N91-19345* #
NASA-CR-187521 ..... N91-19074* #
NASA-CR-187638 ..... N91-20022* #
NASA-CR-187778 ..... N91-19973* #
NASA-CR-187914 ..... N91-19765* #
NASA-CR-187928 ..... N91-19732* #
NASA-CR-187950 ..... N91-19343* #
NASA-CR-187958 ..... N91-19718* #
NASA-CR-187971 ..... N91-19995* #
NASA-CR-187973 ..... N91-19734* #
NASA-CR-187974 ..... N91-19733* #
NASA-CR-187983 ..... N91-19735* #
NASA-CR-187984 ..... N91-19398* #
NASA-CR-187986 ..... N91-19173* #
NASA-CR-187989 ..... N91-19871* #
NASA-CR-187992 ..... N91-19736* #
NASA-CR-187997 ..... N91-19710* #
NASA-CR-187998 ..... N91-19741* #
NASA-CR-188019 ..... N91-19975* #
NASA-CR-188022 ..... N91-19497* #
NASA-CR-188031 ..... N91-19980* #
NASA-CR-188041 ..... N91-19750* #
NASA-CR-188046 ..... N91-19701* #
NASA-CR-188051 ..... N91-19379* #
NASA-CR-188057 ..... N91-19305* #
NASA-CR-188077 ..... N91-19722* #

NASA-RP-1252 ..... N91-19082* #

NASA-SP-7064-SUPPL-5 ..... N91-19962* #

NASA-TM-4226 ..... N91-19473* #
NASA-TM-4234 ..... N91-19099* #
NASA-TM-4239 ..... N91-19052* #
NASA-TM-4240 ..... N91-19079* #
NASA-TM-4244 ..... N91-19181* #
NASA-TM-4256-VOL-1 ..... N91-19499* #
NASA-TM-4257 ..... N91-19115* #
NASA-TM-4258 ..... N91-19697* #
NASA-TM-101724 ..... N91-19051* #
NASA-TM-101727 ..... N91-19080* #
NASA-TM-101730 ..... N91-19742* #
NASA-TM-101731 ..... N91-19081* #
NASA-TM-101733 ..... N91-19077* #
NASA-TM-101734 ..... N91-19055* #
NASA-TM-101737 ..... N91-19095* #
NASA-TM-101742 ..... N91-19083* #
NASA-TM-102165 ..... N91-19273* #
NASA-TM-102166 ..... N91-19274* #
NASA-TM-102170 ..... N91-19699* #
NASA-TM-102173 ..... N91-19959* #
NASA-TM-102206 ..... N91-19062* #
NASA-TM-102264 ..... N91-20039* #
NASA-TM-102267 ..... N91-19041* #
NASA-TM-102688 ..... N91-19166* #
NASA-TM-102720 ..... N91-19474* #
NASA-TM-102763 ..... N91-19471* #
NASA-TM-102767 ..... N91-19073* #
NASA-TM-102768 ..... N91-19168* #
NASA-TM-102777 ..... N91-19482* #
NASA-TM-102781 ..... N91-19061* #
NASA-TM-102860 ..... N91-19566* #
NASA-TM-102871 ..... N91-19078* #
NASA-TM-102885 ..... N91-19241* #
NASA-TM-102886 ..... N91-19770* #
NASA-TM-103191 ..... N91-19180* #
NASA-TM-103234 ..... N91-19178* #
NASA-TM-103257 ..... N91-19404* #
NASA-TM-103272 ..... N91-19332* #
NASA-TM-103286 ..... N91-19351* #
NASA-TM-103333 ..... N91-19979* #
NASA-TM-103397 ..... N91-19319* #
NASA-TM-103398 ..... N91-19123* #
NASA-TM-103525 ..... N91-19529* #
NASA-TM-103606 ..... N91-19825* #
NASA-TM-103626 ..... N91-19477* #
NASA-TM-103639 ..... N91-19373* #
NASA-TM-103648 ..... N91-19234* #
NASA-TM-103650 ..... N91-19053* #
NASA-TM-103656 ..... N91-19179* #
NASA-TM-103658 ..... N91-19442* #
NASA-TM-103664 ..... N91-19324* #
NASA-TM-103665 ..... N91-19296* #
NASA-TM-103666 ..... N91-19256* #
NASA-TM-103668 ..... N91-19372* #
NASA-TM-103669 ..... N91-19236* #
NASA-TM-103670 ..... N91-19237* #
NASA-TM-103672 ..... N91-19348* #
NASA-TM-103673 ..... N91-19369* #
NASA-TM-103676 ..... N91-19401* #
NASA-TM-103677 ..... N91-19231* #
NASA-TM-103679 ..... N91-19044* #
NASA-TM-103680 ..... N91-19472* #
NASA-TM-103681 ..... N91-19230* #
NASA-TM-103682 ..... N91-19229* #
NASA-TM-103685 ..... N91-19292* #
NASA-TM-103687 ..... N91-19045* #
NASA-TM-103690 ..... N91-19098* #
NASA-TM-103693 ..... N91-19046* #
NASA-TM-103698 ..... N91-19112* #
NASA-TM-103700 ..... N91-19349* #
NASA-TM-103701 ..... N91-19047* #
NASA-TM-103702 ..... N91-19370* #
NASA-TM-103706 ..... N91-19371* #
NASA-TM-103707 ..... N91-19293* #
NASA-TM-103711 ..... N91-19294* #
NASA-TM-103713 ..... N91-19232* #
NASA-TM-103715 ..... N91-19176* #
NASA-TM-103716 ..... N91-19441* #
NASA-TM-103724 ..... N91-19233* #
NASA-TM-103726 ..... N91-19374* #
NASA-TM-103728 ..... N91-20015* #
NASA-TM-103730 ..... N91-19317* #
NASA-TM-103731 ..... N91-19177* #
NASA-TM-103732 ..... N91-19463* #
NASA-TM-103734 ..... N91-19402* #
NASA-TM-103735 ..... N91-19165* #
NASA-TM-103743 ..... N91-19235* #
NASA-TM-103745 ..... N91-19786* #
NASA-TM-103746 ..... N91-19475* #
NASA-TM-103748 ..... N91-19054* #
NASA-TM-103751 ..... N91-19462* #
NASA-TM-103758 ..... N91-19443* #
NASA-TM-103761 ..... N91-19464* #
NASA-TM-103762 ..... N91-19354* #
NASA-TM-103764 ..... N91-19308* #
NASA-TM-103771 ..... N91-19175* #
NASA-TM-103774 ..... N91-19097* #
NASA-TM-103777 ..... N91-19295* #
NASA-TM-103778 ..... N91-19063* #
NASA-TM-103781 ..... N91-19375* #
NASA-TM-103784 ..... N91-19224* #
NASA-TM-103785 ..... N91-19766* #
NASA-TM-103788 ..... N91-19320* #
NASA-TM-103792 ..... N91-19935* #
NASA-TM-103794 ..... N91-19476* #
NASA-TM-103816 ..... N91-19118* #
NASA-TM-103836 ..... N91-19304* #
NASA-TM-103837 ..... N91-19826* #
NASA-TM-104029 ..... N91-19415* #
NASA-TM-104535 ..... N91-19449* #
NASA-TM-104536 ..... N91-19557* #

NASA-TP-2995 ..... N91-19058* #
NASA-TP-3020 ..... N91-19824* #
NASA-TP-3032 ..... N91-19042* #
NASA-TP-3043 ..... N91-19711* #
NASA-TP-3053 ..... N91-19823* #
NASA-TP-3080 ..... N91-19057* #

NDRL-3345 ..... N91-19843 #

NIAR-90-21 ..... N91-19040 #

NIFS-DATA-4 ..... N91-19852 #

NIFS-PROC-5 ..... N91-19882 #

NIFS-69 ..... N91-19894 #

NIIYAF-MGU-89-16/93 ..... N91-19987 #
NIIYAF-MGU-89-23/100 ..... N91-19559 #
NIIYAF-MGU-89-28/105 ..... N91-20016 #
NIIYAF-MGU-89-29/106 ..... N91-20020 #
NIIYAF-MGU-89-65/142 ..... N91-20021 #

NOAA-TM-ERL-WPL-188 ..... N91-19875 #

NOAA-TR-ERL-442-WPL-63 ..... N91-19562 #

NOAA-TR-NESDIS-53 ..... N91-19514 #

NOARL-PR-90-055-333 ..... N91-19287 #

NOTA-INTERNA-962 ..... N91-19853 #
NOTA-INTERNA-964 ..... N91-19550 #
NOTA-INTERNA-965 ..... N91-19410 #
NOTA-INTERNA-966 ..... N91-19868 #
NOTA-INTERNA-967 ..... N91-20019 #
NOTA-INTERNA-968 ..... N91-19854 #

NRL-MR-6741 ..... N91-19879 #
NRL-MR-6746 ..... N91-19413 #

OCS/MMS-90/0084 ..... N91-19548 #

ORNL/M-1154 ..... N91-19544 #
ORNL/M-1286 ..... N91-19300 #

ORNL/TM-11608 ..... N91-19950 #
ORNL/TM-11620 ..... N91-19901 #
ORNL/TM-11633 ..... N91-19104 #
ORNL/TM-11688 ..... N91-19785 #
ORNL/TM-11711 ..... N91-19961 #
ORNL/TM-11736 ..... N91-19451 #
ORNL/TM-11752 ..... N91-19444 #

OTN-027673 ..... N91-19106 #

OUEL-1818/90 ..... N91-19457 #
OUEL-1852/90 ..... N91-19411 #
OUEL-1853/90 ..... N91-19755 #
OUEL-1859/90 ..... N91-19495 #
OUEL-1860/90 ..... N91-19774 #
OUEL-1861/90 ..... N91-19458 #
OUEL-1862/90 ..... N91-19070 #
OUEL-1866/90 ..... N91-19459 #
OUEL-1868/90 ..... N91-19763 #
OUEL-1872/91 ..... N91-19791 #

PB91-119677 ..... N91-19970 #
PB91-123653 ..... N91-19993 #
PB91-123661 ..... N91-19994 #
PB91-124586 ..... N91-20017 #
PB91-124594 ..... N91-20018 #
PB91-125500 ..... N91-19562 #
PB91-125898 ..... N91-19549 #
PB91-127753 ..... N91-19545 #
PB91-127878 ..... N91-19500 #
PB91-129114 ..... N91-19560 #
PB91-129254 ..... N91-19452 #
PB91-129262 ..... N91-19383 #
PB91-129288 ..... N91-19548 #
PB91-129338 ..... N91-19875 #
PB91-129684 ..... N91-19326 #
PB91-130260 ..... N91-19264 #
PB91-131664 ..... N91-19546 #
PB91-131680 ..... N91-19547 #

PML-1990-C139 ..... N91-19222 #

PNL-SA-18612 ..... N91-19290 #
PNL-SA-18944 ..... N91-19368 #
PNL-SA-18945 ..... N91-19738 #
PNL-SA-19017 ..... N91-19704 #
PNL-SA-19021 ..... N91-19409 #
PNL-SA-19062 ..... N91-19271 #
PNL-SA-19071 ..... N91-19282 #

PNL-7329 ..... N91-19751 #

PREPRINT-1285 ..... N91-19796 #

PSC-9 ..... N91-19911 #

PUBL-911032 ..... N91-19172* #

REPT-89SDM/MCHALE/03-MDA ..... N91-19954 #
REPT-90B00146 ..... N91-19126* #
REPT-91B00072 ..... N91-19557* #
REPT-91E01238 ..... N91-19449* #

RR-388 ..... N91-19753 #
RR-400-PT-2 ..... N91-19754 #
RR-404 ..... N91-19797 #
RR-408-PT-1 ..... N91-19789 #
RR-409 ..... N91-19362 #
RR-410 ..... N91-19761 #
RR-411 ..... N91-19772 #
RR-412 ..... N91-19864 #
RR-413 ..... N91-19865 #
RR-414 ..... N91-19866 #
RR-419 ..... N91-19867 #

RRK-90-11 ..... N91-19988 #

S-HRG-101-1087 ..... N91-19974 #
S-HRG-101-1146 ..... N91-19969 #
S-HRG-101-1160 ..... N91-19528 #

S-REPT-101-474 ..... N91-19966 #

S-187 ..... N91-19363 #
S-611 ..... N91-19273* #
S-612 ..... N91-19274* #
S-616 ..... N91-19699* #
S-621 ..... N91-19959* #

SAND-89-3107 ..... N91-19330 #
SAND-90-0805 ..... N91-19334 #
SAND-90-1195 ..... N91-19352 #
SAND-90-1478C ..... N91-19896 #

SAND-90-1609C ..... N91-19421 #
SAND-90-1754C ..... N91-19907 #
SAND-90-2001C ..... N91-19767 #
SAND-90-2025C ..... N91-19793 #
SAND-90-2113C ..... N91-19065 #
SAND-90-2220C ..... N91-19064 #
SAND-90-2246C ..... N91-19344 #
SAND-90-2341 ..... N91-19322 #
SAND-90-2383C ..... N91-19768 #
SAND-90-2460 ..... N91-19103 #
SAND-90-2472C ..... N91-19448 #
SAND-90-2548C ..... N91-19269 #
SAND-90-2646C ..... N91-19303 #
SAND-90-2754C ..... N91-19942 #
SAND-90-2929C ..... N91-19297 #
SAND-90-3113C ..... N91-19424 #
SAND-90-3142C ..... N91-19510 #
SAND-90-3233C ..... N91-19922 #
SAND-90-3269C ..... N91-19936 #
SAND-91-0038C ..... N91-19408 #
SAND-91-0125C ..... N91-19291 #
SAND-91-0139C ..... N91-19872 #
SAND-91-0194C ..... N91-19481 #
SAND-91-0259C ..... N91-19431 #
SAND-91-0312C ..... N91-19960 #
SAND-91-0342C ..... N91-19276 #
SAND-91-0348C ..... N91-19407 #
SAND-91-0362C ..... N91-19932 #
SAND-91-0414C ..... N91-19964 #
SAND-91-0431C ..... N91-19965 #
SAND-91-0460C ..... N91-19243 #

SERI/TP-212-3675 ..... N91-19502 #
SERI/TP-253-3561 ..... N91-19501 #

SFCC-PUBL-61 ..... N91-19222 #

SGD-554-PT-1 ..... N91-20018 #
SGD-554-PT-2 ..... N91-20017 #

SM-114/91 ..... N91-19791 #

SSC-335 ..... N91-19452 #
SSC-336 ..... N91-19383 #

SSCL-270 ..... N91-19863 #
SSCL-338 ..... N91-19963 #

SU-ATN-9001 ..... N91-19470 #

SU-SLAC-PUB-5412 ..... N91-19777 #
SU-SLAC-PUB-5414 ..... N91-19778 #

SU-SLAC-370-REV ..... N91-19719 #

TELECOM-90-D-009 ..... N91-19798 #

TR-41 ..... N91-19500 #
TR-69 ..... N91-19946 #
TR-062188-3273F2 ..... N91-19331 #

TWR-50143-2 ..... N91-19172* #

UCB-PTH-90/37 ..... N91-19951 #

UCB/CSD-90/574 ..... N91-19718* #

UCRL-CR-105373 ..... N91-19927 #
UCRL-CR-105603 ..... N91-19739 #
UCRL-CR-105773 ..... N91-19331 #

UCRL-ID-105197 ..... N91-19254 #

UCRL-JC-103724 ..... N91-19921 #
UCRL-JC-103725 ..... N91-19924 #
UCRL-JC-103826 ..... N91-19418 #
UCRL-JC-104161 ..... N91-19433 #
UCRL-JC-104407-REV-1 ..... N91-19429 #
UCRL-JC-104435 ..... N91-19430 #
UCRL-JC-104593 ..... N91-19268 #
UCRL-JC-104612 ..... N91-19400 #
UCRL-JC-104640 ..... N91-19417 #
UCRL-JC-104716 ..... N91-19983 #
UCRL-JC-104787 ..... N91-19782 #
UCRL-JC-104788 ..... N91-19781 #
UCRL-JC-104789 ..... N91-19780 #
UCRL-JC-104810-REV-1 ..... N91-19698 #
UCRL-JC-105008 ..... N91-19553 #
UCRL-JC-105139 ..... N91-19466 #
UCRL-JC-105205 ..... N91-19910 #
UCRL-JC-105255 ..... N91-19758 #
UCRL-JC-105536 ..... N91-19551 #
UCRL-JC-105569 ..... N91-19427 #
UCRL-JC-105626 ..... N91-19794 #
UCRL-JC-105691 ..... N91-19745 #
UCRL-JC-105745 ..... N91-19530 #
UCRL-JC-105779 ..... N91-19857 #
UCRL-JC-105797 ..... N91-19747 #
UCRL-JC-105876 ..... N91-19919 #
UCRL-JC-105905 ..... N91-19895 #
UCRL-JC-105926 ..... N91-19381 #
UCRL-JC-105957 ..... N91-19900 #
UCRL-JC-105959 ..... N91-19416 #
UCRL-JC-105970 ..... N91-19985 #
UCRL-JC-105971 ..... N91-19984 #
UCRL-JC-106216 ..... N91-19862 #
UCRL-JC-106272 ..... N91-19898 #

UCRL-LR-105145 ..... N91-19775 #
UCRL-LR-105358 ..... N91-19558 #
UCRL-LR-106412 ..... N91-19748 #

UCRL-MA-105580 ..... N91-19783 #

UCRL-53916 ..... N91-19740 #

UDR-TR-89-81 ..... N91-19460 #

UMICH-025921-19-T ..... N91-19305* #

US-PATENT-APPL-SN-135969 ..... N91-19249
US-PATENT-APPL-SN-143492 ..... N91-19396
US-PATENT-APPL-SN-180751 ..... N91-19364
US-PATENT-APPL-SN-229517 ..... N91-19225
US-PATENT-APPL-SN-241873 ..... N91-19341
US-PATENT-APPL-SN-263455 ..... N91-19764 #
US-PATENT-APPL-SN-274587 ..... N91-19468
US-PATENT-APPL-SN-341598 ..... N91-19076
US-PATENT-APPL-SN-348740 ..... N91-19397
US-PATENT-APPL-SN-350172 ..... N91-19870
US-PATENT-APPL-SN-374127 ..... N91-19072
US-PATENT-APPL-SN-376278 ..... N91-19972
US-PATENT-APPL-SN-389233 ..... N91-19918
US-PATENT-APPL-SN-417616 ..... N91-19328 #
US-PATENT-APPL-SN-489313 ..... N91-19917 #
US-PATENT-APPL-SN-505617 ..... N91-19717
US-PATENT-APPL-SN-531416 ..... N91-19869 #
US-PATENT-APPL-SN-560703 ..... N91-19288 #
US-PATENT-APPL-SN-564892 ..... N91-19171 #
US-PATENT-APPL-SN-565781 ..... N91-19289 #
US-PATENT-APPL-SN-596188 ..... N91-19312
US-PATENT-APPL-SN-633361 ..... N91-19116 #
US-PATENT-APPL-SN-723262 ..... N91-19100
US-PATENT-APPL-SN-751350 ..... N91-19437

US-PATENT-CLASS-89-1.55 ..... N91-19076
US-PATENT-CLASS-124-75 ..... N91-19116 #
US-PATENT-CLASS-149-19.91 ..... N91-19312
US-PATENT-CLASS-239-590 ..... N91-19364
US-PATENT-CLASS-324-636 ..... N91-19918
US-PATENT-CLASS-342-29 ..... N91-19072
US-PATENT-CLASS-342-357 ..... N91-19972
US-PATENT-CLASS-350-320 ..... N91-19396
US-PATENT-CLASS-356-73.1 ..... N91-19870
US-PATENT-CLASS-364-807 ..... N91-19764 #
US-PATENT-CLASS-364-900 ..... N91-19437
US-PATENT-CLASS-365-87 ..... N91-19717
US-PATENT-CLASS-374-136 ..... N91-19397
US-PATENT-CLASS-411-12 ..... N91-19436
US-PATENT-CLASS-428 ..... N91-19468
US-PATENT-CLASS-435-32 ..... N91-19249
US-PATENT-CLASS-501-128 ..... N91-19225

US-PATENT-4,936,187 ..... N91-19076
US-PATENT-4,948,766 ..... N91-19225
US-PATENT-4,950,076 ..... N91-19100
US-PATENT-4,950,594 ..... N91-19249
US-PATENT-4,950,936 ..... N91-19341
US-PATENT-4,951,056 ..... N91-19072
US-PATENT-4,951,239 ..... N91-19764 #
US-PATENT-4,951,644 ..... N91-19116 #
US-PATENT-4,952,057 ..... N91-19870
US-PATENT-4,952,255 ..... N91-19312
US-PATENT-4,953,951 ..... N91-19396
US-PATENT-4,953,986 ..... N91-19397
US-PATENT-4,954,377 ..... N91-19468
US-PATENT-4,954,833 ..... N91-19972
US-PATENT-4,957,242 ..... N91-19364
US-PATENT-4,958,315 ..... N91-19437
US-PATENT-4,958,970 ..... N91-19436
US-PATENT-4,959,614 ..... N91-19918
US-PATENT-4,962,477 ..... N91-19717

USAAVSCOM-TM-90-A-004 ..... N91-19041* #
USAAVSCOM-TM-90-A-007 ..... N91-19826* #

VTT-TUTK-677 ..... N91-19316 #

WMO-524-SUPPL-2 ..... N91-19563 #

WRDC-TR-89-4134 ..... N91-19460 #

WSRC-MS-90-16 ..... N91-19277 #
WSRC-MS-90-37 ..... N91-19483 #
WSRC-MS-90-150 ..... N91-19720 #

WSRC-RP-89-1383 ..... N91-19399 #

YITP/U-90-13 ..... N91-19989 #
YITP/U-90-14 ..... N91-19990 #
YITP/U-90-15 ..... N91-19991 #
YITP/U-90-18 ..... N91-19992 #

Appendix

NASA SCIENTIFIC AND TECHNICAL INFORMATION PROGRAM PRODUCTS AND SERVICES

The NASA Scientific and Technical Information (STI) Program provides for the collection and announcement of aerospace-related reports and literature obtained worldwide through agreements and exchanges. The result of the collection is the comprehensive NASA STI Database that covers aeronautics, space, and supporting disciplines.

The STI Database, documents generated or obtained by NASA, and products and services derived from or supporting the database are made available to the NASA research community and to the public. Descriptions and sources of these items are presented in the following pages.

Scientific and Technical Aerospace Reports (*STAR*) is an abstract journal, listing citations with abstracts for aerospace-related reports obtained from worldwide sources. *STAR* is issued on the 8th and 23rd of each month and announces current documents that have been entered into the NASA STI Database during the previous two weeks. The reports are of the following types:

- NASA, NASA contractor, and NASA grantee reports;
- Reports issued by other U.S. Government agencies, domestic and foreign institutions, universities, and private firms;
- Translations in report form;
- NASA-owned patents and patent applications;
- Other U.S. Government agency and foreign patents and patent applications;
- Domestic and foreign dissertations and theses.

Journal, book, and conference literature, journal translations, and certain foreign dissertations having the same subject scope as *STAR* are announced in a companion journal, *International Aerospace Abstracts* (*IAA*). *IAA* is issued on the 1st and 15th of each month and is available from the American Institute of Aeronautics and Astronautics, Technical Information Service, 555 West 57th Street, 12th Floor, New York, NY 10019.

ELIGIBILITY AND REGISTRATION FOR NASA STI PRODUCTS AND SERVICES

Organizations of the type listed below that have registered with NASA can receive products and services.

- NASA offices and installations, contractors, subcontractors, grantees, and consultants;
- Other U.S. Government agencies and their contractors;
- Libraries in the United States that have arrangements with NASA to maintain collections of NASA documents for public reference;
- Other organizations in the United States having a need for NASA documents in work related to aeronautics and space research;
- Organizations abroad that have established reciprocal documents exchange arrangements with NASA.

Only the central service points or central points of document acquisition and control within qualified organizations are eligible to register for NASA STI products and services. Domestic organizations that may be eligible to receive various classes of NASA publications and services should address their requests for registration or further information to:

NASA Center for AeroSpace Information
ATTN: Registration Services
P.O. Box 8757
BWI Airport, MD 21240
301-621-0153

Organizations abroad should direct requests to:

National Aeronautics and Space Administration
Director, Scientific and Technical Information Program
Code NTT
Washington, DC 20546
USA
703-271-5640

SUBJECT SCOPE

The subject scope of *STAR* and *IAA* includes all aspects of aeronautics and space research and development, supporting basic and applied research, and applications. Aerospace aspects of Earth resources, energy development, conservation, oceanography, environmental protection, urban transportation, and other topics of high national priority are also covered.

HOW TO USE *STAR* SUBJECT CATEGORIES

Abstracts in *STAR* are categorized by 10 major subject divisions that are divided further into 76 specific subject categories. The subject divisions and categories are listed in the Table of Contents together with a note for each that defines its scope and provides any cross-references. For example:

16 SPACE TRANSPORTATION
Includes passenger and cargo space transportation, e.g., shuttle operations; and space rescue techniques. For related information see also *03 Air Transportation and Safety* and *18 Spacecraft Design, Testing and Performance.* For space suits see *54 Man/System Technology and Life Support.*

CROSS-REFERENCES

Individual *STAR* abstracts are not ordinarily cross-referenced, except for certain conference reports or book translations that have had separate abstracts written for their component papers or chapters. Citations and abstracts of the components follow immediately after those of the parent document. When the subject content of a component differs sufficiently from the general content of the parent, a cross-reference citation also is printed at the end of the category to which it normally would have been assigned if it were independent.

DOCUMENTS ON MICROFICHE

Documents available on microfiche are designated by a pound sign (#) following the accession number.

LIMITED REPRODUCIBILITY

A note of limited reproducibility appears in the citation, if there are factors affecting the reproducibility of more than 20% of the document. These factors include faint or broken type, color photographs, black and white photographs, foldouts, dot matrix print, or some other factor that limits the reproducibility of the document. This notation also appears on the microfiche header with the specific factor checked off on a list visible in the second frame.

COLOR COPIES

An increasing number of NASA scientific and technical reports are being produced with color graphs, charts, illustrations, and photographs. An indication that a document has color pages follows the source and pricing (SAP) information in the *STAR* citation.

Registered users of the NASA Scientific and Technical Information Program will receive ordered documents with color at no additional cost, as long as stock copies of the document are available. Otherwise, an additional fee of $2.00 per color page will be charged. The NASA Center for AeroSpace Information staff will contact registered users to determine individual user's needs.

NASA PATENTS AND PATENT APPLICATIONS

Patents and patent applications owned by NASA are announced in *STAR* under appropriate subject categories and are referenced in the *STAR* indexes. In the Report/Accession Number Index, patents are indexed by the NASA Case Number, and the U.S. Patent Class. Patent applications are indexed by the NASA Case Number and the U.S. Patent Application Serial Number.

Printed copies of patents (which are not microfiched) are available for purchase from the U.S. Patent and Trademark Office.

NASA patent application specifications are sold in both paper copy and microfiche by the National Technical Information Service (NTIS). The US-Patent-Appl-SN-number should be used in ordering either paper copy or microfiche from NTIS.

When ordering patents, the U.S. Patent Number should be used, and payment must be remitted in advance, by money order or check payable to the Commissioner of Patents and Trademarks. Prepaid purchase coupons for ordering are also available from the U.S. Patent and Trademark Office.

The patents and patent applications announced in *STAR* are owned by NASA and are available for royalty-free licensing. Requests for licensing terms and further information should be addressed to:

National Aeronautics and Space Administration
Associate General Counsel for Intellectual Property
Code GP
Washington, DC 20546

SOURCES FOR DOCUMENTS

One or more sources from which a document announced in *STAR* is available to the public is given in each citation. The most commonly indicated sources and their acronyms or abbreviations are listed on page A-6. If the publication is available from a source other than those listed, the publisher and address will be displayed on the availability line or in combination with the corporate source line.

Avail: NTIS. Sold by the National Technical Information Service. Prices for hard copy (HC) and microfiche (MF) are indicated by a price code following the letters HC or MF in the *STAR* citation. Current values for the price codes are given in the tables on page A-7.

Initially distributed microfiche under the NTIS SRIM (Selected Research in Microfiche) is available at greatly reduced unit prices. For this service and for information concerning subscription to NASA printed reports, consult the NTIS Subscription Section, Springfield, VA 22161.

NOTE ON ORDERING DOCUMENTS: When ordering NASA publications (those followed by the * symbol), use the N accession number. NASA patent applications (only the specifications are offered) should be ordered by the US-Patent-Appl-SN number. Non-NASA publications (no asterisk) should be ordered by the AD, PB, or other *report number* shown on the last line of the citation, not by the N accession number. It is also advisable to cite the title and other bibliographic identification.

Avail: SOD (or GPO). Sold by the Superintendent of Documents, U.S. Government Printing Office, in hard copy. The current price and order number are given following the availability line. (NTIS will fill microfiche requests, as indicated above, for those documents identified by a # symbol.)

Avail: BLL (formerly NLL): British Library Lending Division, Boston Spa, Wetherby, Yorkshire, England. Photocopies available from this organization at the price shown. (If none is given, address inquiry to the BLL.)

Avail: DOE Depository Libraries. Organizations in U.S. cities and abroad that maintain collections of Department of Energy reports, usually in microfiche form, are listed in *Energy Research Abstracts.* Services available from the DOE and its depositories are described in a booklet, *DOE Technical Information Center - Its Functions and Services* (TID-4660), which may be obtained without charge from the DOE Technical Information Center.

Avail: ESDU. Pricing information on specific data, computer programs, and details on Engineering Sciences Data Unit (ESDU) topic categories can be obtained from ESDU International Ltd. Requesters in North America should use the Virginia address while all other requesters should use the London address, both of which are on page A-6.

Avail: Fachinformationszentrum, Karlsruhe. Sold by the Fachinformationszentrum Energie, Physik, Mathematik GMBH, Eggenstein Leopoldshafen, Federal Republic of Germany, at the price shown in deutschmarks (DM).

Avail: HMSO. Publications of Her Majesty's Stationery Office are sold in the U.S. by Pendragon House, Inc. (PHI), Redwood City, CA. The U.S. price (including a service and mailing charge) is given, or a conversion table may be obtained from PHI.

Avail: NASA Public Document Rooms. Documents so indicated may be examined at or purchased from the National Aeronautics and Space Administration, Public Documents Room (Room 126), 600 Independence Ave., S.W., Washington, DC 20546, or public document rooms located at NASA installations, and the NASA Pasadena Office at the Jet Propulsion Laboratory.

Avail: Univ. Microfilms. Documents so indicated are dissertations selected from *Dissertation Abstracts* and are sold by University Microfilms as xerographic copy (HC) and microfilm. All requests should cite the author and the Order Number as they appear in the citation.

Avail: US Patent and Trademark Office. Sold by Commissioner of Patents and Trademarks, U.S. Patent and Trademark Office, at the standard price of $1.50 each, postage free. (See discussion of NASA patents and patent applications below.)

Avail: (US Sales Only). These foreign documents are available to users within the United States from the National Technical Information Service (NTIS). They are available to users outside the United States through the International Nuclear Information Service (INIS) representative in their country, or by applying directly to the issuing organization.

Avail: USGS. Originals of many reports from the U.S. Geological Survey, which may contain color illustrations, or otherwise may not have the quality of illustrations preserved in the microfiche or facsimile reproduction, may be examined by the public at the libraries of the USGS field offices whose addresses are listed on page A-6. The libraries may be queried concerning the availability of specific documents and the possible utilization of local copying services, such as color reproduction.

Avail: Issuing Activity, or Corporate Author, or no indication of availability. Inquiries as to the availability of these documents should be addressed to the organization shown in the citation as the corporate author of the document.

FEDERAL DEPOSITORY LIBRARIES: To provide the general public with greater access to U.S. Government publications, Congress established the Federal Depository Library Program under the Government Printing Office (GPO), with 51 regional depositories responsible for permanent retention of material, inter-library loan, and reference services. (These libraries are not sales outlets.) At least one copy of nearly every NASA and NASA-sponsored publication, either in printed or microfiche format, is received and retained by the 51 regional depositories. A list of the regional GPO libraries, appears on page A-8. A local library can contact a regional depository library to help locate specific reports, or direct contact may be made by an individual.

PUBLIC COLLECTION OF NASA DOCUMENTS

An extensive collection of NASA and NASA-sponsored publications is maintianed by the British Library Lending Divison, Boston Spa, Wetherby, Yorkshire, England, for public access. The British Library Lending Division also has available many of the non-NASA publications cited in *STAR*.

European requesters may purchase facsimile copy or microfiche of NASA and NASA-sponsored documents, those identified by both the symbols # and * from ESA—Information Retrieval Service, European Space Agency, 8-10 rue Mario-Nikis, 75738 Paris CEDEX 15, France.

SUBMITTING DOCUMENTS

All users of this abstract service are urged to forward reports to be considered for announcement in *STAR*. This will aid NASA in its efforts to provide the fullest possible coverage of all scientific and technical publications that might support aeronautics and space research and development. If you have prepared relevant reports (other than those you will transmit to NASA, DOD, or DOE through the usual contract- or grant-reporting channels), please send them for consideration to the NASA Center for AeroSpace Information, P.O. Box 8757, BWI Airport, MD 21240.

Reprints of journal articles, book chapters, and conference papers are also welcome. These will be considered for announcement in *STAR*'s companion journal, *IAA*.

You may specify a particular source to be included in a report announcement if you wish; otherwise the report will be placed on a public sale at the National Technical Information Service. Copyrighted publications will be announced but not distributed or sold.

PURCHASE OF *STAR*

STAR is publicly available on annual subscription from the Superintendent of Documents, U.S. Government Printing Office, Washington, DC 20402.

STAR is available to registered users on annual subscription from the NASA Center for AeroSpace Information, ATTN: Registration Services, P.O. Box 8757, BWI Airport, MD 21240.

Microfiche of the abstract sections of *STAR* are available, on annual subscription only, from NTIS as PB91-911300, Attn: Subscriptions, 5285 Port Royal Road, Springfield, VA 22161. Annual subscription rates are $85.00 North America; $170.00 foreign. Abstract sections for previous years retroactive to 1964 are available at the current rates.

ADDRESSES OF ORGANIZATIONS

American Institute of Aeronautics and Astronautics
Technical Information Service
555 West 57th Street, 12th Floor
New York, New York 10019

British Library Lending Division,
Boston Spa, Wetherby, Yorkshire,
England

Commissioner of Patents and Trademarks
U.S. Patent and Trademark Office
Washington, DC 20231

Department of Energy
Technical Information Center
P.O. Box 62
Oak Ridge, Tennessee 37830

European Space Agency-Information Retrieval Service
ESRIN
Via Galileo Galilei
00044 Frascati (Rome) Italy

Engineering Sciences Data Unit International
P.O. Box 1633
Manassas, Virginia 22110

Engineering Sciences Data Unit International, Ltd.
251-259 Regent Street
London, W1R 7AD, England

Fachinformationszentrum Energie, Physik, Mathematik
GMBH
7514 Eggenstein Leopoldshafen
Federal Republic of Germany

Her Majesty's Stationery Office
P.O. Box 569, S.E. 1
London, England

NASA Center for AeroSpace Information
P.O. Box 8757
BWI Airport, Maryland 21240

National Aeronautics and Space Administration
Scientific and Technical Information Program (NTT)
Washington, DC 20546

National Technical Information Service
5285 Port Royal Road
Springfield, Virginia 22161

Pendragon House, Inc.
899 Broadway Avenue
Redwood City, California 94063

Superintendent of Documents
U.S. Government Printing Office
Washington, DC 20402

University Microfilms
A Xerox Company
300 North Zeeb Road
Ann Arbor, Michigan 48106

University Microfilms, Ltd.
Tylers Green
London, England

U.S. Geological Survey Library National Center
MS 950
12201 Sunrise Valley Drive
Reston, Virginia 22092

U.S. Geological Survey Library
2255 North Gemini Drive
Flagstaff, Arizona 86001

U.S. Geological Survey
345 Middlefield Road
Menlo Park, California 94025

U.S. Geological Survey Library
Box 25046
Denver Federal Center, MS914
Denver, Colorado 80225

NTIS PRICE SCHEDULES

(Effective January 1, 1991)

Schedule A
STANDARD PRICE DOCUMENTS AND MICROFICHE**

PRICE CODE	NORTH AMERICAN PRICE	FOREIGN PRICE
A01	$ 8.00	$ 16.00
A02	11.00	22.00
A03	15.00	30.00
A04-A05	17.00	34.00
A06-A09	23.00	46.00
A10-A13	31.00	62.00
A14-A17	39.00	78.00
A18-A21	45.00	90.00
A22-A25	53.00	106.00
A99	*	*
N01	60.00	120.00
N02	59.00	118.00
N03	20.00	40.00

Schedule E
EXCEPTION PRICE DOCUMENTS AND MICROFICHE**

PRICE CODE	NORTH AMERICAN PRICE	FOREIGN PRICE
E01	$10.00	$ 20.00
E02	12.00	24.00
E03	14.00	28.00
E04	16.50	33.00
E05	18.50	37.00
E06	21.50	43.00
E07	24.00	48.00
E08	27.00	54.00
E09	29.50	59.00
E10	32.50	65.00
E11	35.00	70.00
E12	38.50	77.00
E13	41.00	82.00
E14	45.00	90.00
E15	48.50	97.00
E16	53.00	106.00
E17	57.50	115.00
E18	62.00	124.00
E19	69.00	138.00
E20	80.00	160.00
E99	*	*

* Contact NTIS for price quote.

** Effective January 1, 1991, the microfiche copy of any new document entering the NTIS collection will be priced the same as the paper copy of the document.

IMPORTANT NOTICE

NTIS Shipping and Handling Charges

U.S., Canada, Mexico — ADD $3.00 per TOTAL ORDER

All Other Countries — ADD $4.00 per TOTAL ORDER

Exceptions — Does NOT apply to:

ORDERS REQUESTING NTIS RUSH HANDLING
ORDERS FOR SUBSCRIPTION OR STANDING ORDER PRODUCTS *ONLY*

NOTE: Each additional delivery address on an order requires a separate shipping and handling charge.

FEDERAL REGIONAL DEPOSITORY LIBRARIES

ALABAMA

AUBURN UNIV. AT MONTGOMERY LIBRARY
Documents Department
Montgomery, AL 36193
(205) 279-9110 ext.253

UNIV. OF ALABAMA LIBRARY
Reference Department/Documents
Box S
Tuscaloosa, AL 35486
(205) 348-6046

ARIZONA

DEPT. OF LIBRARY, ARCHIVES, AND PUBLIC RECORDS
Third Floor State Capitol
1700 West Washington
Phoenix, AZ 85007
(602) 255-4121

ARKANSAS

ARKANSAS STATE LIBRARY
Documents Service Section
One Capitol Mall
Little Rock, AR 72201
(501) 371-2090

CALIFORNIA

CALIFORNIA STATE LIBRARY
Govt. Publications Section
914 Capitol Mall
Sacramento, CA 95814
(916) 322-4572

COLORADO

UNIV. OF COLORADO
Norlin Library
Government Publications Division
Campus Box 184
Boulder, CO 80309
(303) 492-8834

DENVER PUBLIC LIBRARY
Govt. Pub. Department
1357 Broadway
Denver, CO 80203
(303) 571-2346

CONNECTICUT

CONNECTICUT STATE LIBRARY
231 Capitol Avenue
Hartford, CT 06106
(203) 566-4971

FLORIDA

UNIV. OF FLORIDA LIBRARIES
Documents Department
Library West
Gainesville, FL 32611
(904) 392-0367

GEORGIA

UNIV. OF GEORGIA LIBRARIES
Government Documents Dept.
Athens, GA 30602
(404) 542-8949

HAWAII

UNIV. OF HAWAII
Hamilton Library
Government Documents Collection
2550 The Mall
Honolulu, HI 96822
(808) 948-8230

IDAHO

UNIV. OF IDAHO LIBRARY
Documents Section
Moscow, ID 83843
(208) 885-6344

ILLINOIS

ILLINOIS STATE LIBRARY
Federal Documents
Centennial Building
Springfield, IL 62756
(217) 782-5012

INDIANA

INDIANA STATE LIBRARY
Serials Section
140 North Senate Avenue
Indianapolis, IN 46204
(317) 232-3686

IOWA

UNIV. OF IOWA LIBRARIES
Government Publications Dept.
Iowa City, IA 52242
(319) 335-5926

KANSAS

UNIVERSITY OF KANSAS
Spencer Research Library
Government Documents
Lawrence, KS 66045
(913) 864-4662

KENTUCKY

UNIV. OF KENTUCKY LIBRARIES
Government Publications/Maps Dept.
Lexington, KY 40506
(606) 257-8400

LOUISIANA

LOUISIANA STATE UNIVERSITY
Middleton Library
Government Documents Dept.
Baton Rouge, LA 70803
(504) 388-2570

LOUISIANA TECHNICAL UNIV.
Prescott Memorial Library
Government Documents Dept.
Ruston, LA 71272
(318) 257-4962

MAINE

UNIVERSITY OF MAINE
Raymond H. Fogler Library
Govt. Documents & Microforms Dept.
Orono, ME 04469
(207) 581-1680

MARYLAND

UNIVERSITY OF MARYLAND
McKeldin Library
Documents/Maps Room
College Park, MD 20742
(301) 454-3034

MASSACHUSETTS

BOSTON PUBLIC LIBRARY
Government Documents Dept.
666 Boylston Street
Boston, MA 02117
(617) 536-5400 ext.226

MICHIGAN

DETROIT PUBLIC LIBRARY
5201 Woodward Avenue
Detroit, MI 48202
(313) 833-1409

LIBRARY OF MICHIGAN
Government Documents
P.O. Box 30007
735 E. Michigan Avenue
Lansing, MI 48909
(517) 373-1593

MINNESOTA

UNIVERSITY OF MINNESOTA
Wilson Library
Government Publications
309 Nineteenth Avenue South
Minneapolis, MN 55455
(612) 373-7813

MISSISSIPPI

UNIV. OF MISSISSIPPI LIB.
Government Documents Dept.
106 Old Gym Bldg.
University, MS 38677
(601) 232-5857

MISSOURI

University of Missouri at Columbia Library
Government Documents
Columbia, MO 65201
(314) 882-6733

MONTANA

UNIV. OF MONTANA
Mansfield Library
Documents Division
Missoula, MT 59812
(406) 243-6700

NEBRASKA

UNIVERSITY OF NEBRASKA - LINCOLN
Love Memorial Library
Documents Department
Lincoln, NE 68588
(402) 472-2562

NEVADA

UNIV. OF NEVADA-RENO LIB.
Govt. Pub. Department
Reno, NV 89557
(702) 784-6579

NEW JERSEY

NEWARK PUBLIC LIBRARY
U.S. Documents Division
5 Washington Street
P.O. Box 630
Newark, NJ 07101
(201) 733-7812

NEW MEXICO

UNIVERSITY OF NEW MEXICO
General Library
Government Publications/Maps Dept.
Albuquerque, NM 87131
(505) 277-5441

NEW MEXICO STATE LIBRARY
325 Don Gaspar Avenue
Santa Fe, NM 87501
(505) 827-3826

NEW YORK

NEW YORK STATE LIBRARY
Documents Sect. Cultural Educ. Ctr.
Empire State Plaza
Albany, NY 12230
(518) 474-5563

NORTH CAROLINA

UNIVERSITY OF NORTH CAROLINA AT CHAPEL HILL
Davis Library 080A
BA/SS Department Documents
Chapel Hill, NC 27514
(919) 962-1151

NORTH DAKOTA

NORTH DAKOTA STATE UNIVERSITY LIBRARY
Government Documents Dept.
Fargo, ND 58105
(701) 237-8352
In cooperation with Univ. of North Dakota, Chester Fritz Library
Grand Forks

OHIO

STATE LIBRARY OF OHIO
Documents Section
65 South Front Street
Columbus, OH 43266
(614) 644-7051

OKLAHOMA

OKLAHOMA DEPT. OF LIBRARIES
Government Documents
200 NE 18th Street
Oklahoma City, OK 73105
(405) 521-2502, ext. 252

OKLAHOMA STATE UNIV. LIB.
Documents Department
Stillwater, OK 74078
(405) 624-0489

OREGON

PORTLAND STATE UNIV.
Millar Library
934 SW Harrison - P.O. Box 1151
Portland, OR 97207
(503) 229-3673

PENNSYLVANIA

STATE LIBRARY OF PENN.
Government Publications Section
Box 1601
Walnut St. & Commonwealth Ave.
Harrisburg, PA 17105
(717) 787-3752

SOUTH CAROLINA

CLEMSON UNIV. COOPER LIB.
Documents Department
Clemson, SC 29634
(803) 656-5174
In cooperation with Univ. of South Carolina, Thomas Cooper Library, Columbia

TEXAS

TEXAS STATE LIBRARY
Public Services Department
P.O. Box 12927 - 1201 Brazos
Austin, TX 78711
(512) 463-5455

TEXAS TECH. UNIV. LIBRARY
Documents Department
Lubbock, TX 79409
(806) 742-2268

UTAH

UTAH STATE UNIVERSITY
Merrill Library & Learning Resources Center, UMC-30
Documents Department
Logan, UT 84322
(801) 750-2682

VIRGINIA

UNIVERSITY OF VIRGINIA
Alderman Library
Government Documents
Charlottesville, VA 22903
(804) 924-3133

WASHINGTON

WASHINGTON STATE LIBRARY
Document Section
Olympia, WA 98504
(206) 753-4027

WEST VIRGINIA

WEST VIRGINIA UNIV. LIB.
Government Documents Section
P.O. Box 6069
Morgantown, WV 26506
(304) 293-3640

WISCONSIN

ST. HIST SOC. OF WISCONSIN LIB.
Government Pub. Section
816 State Street
Madison, WI 53706
(608) 262-2781
In cooperation with Univ. of Wisconsin-Madison, Memorial Library

MILWAUKEE PUBLIC LIBRARY
Documents Division
814 West Wisconsin Avenue
Milwaukee, WI 53233
(414) 278-3065

WYOMING

WYOMING STATE LIBRARY
Supreme Court & Library Bldg.
Cheyenne, WY 82002
(307) 777-5919

National Aeronautics and
Space Administration
Code NTT
Washington, D.C.
20546
Official Business
Penalty for Private Use, $300

SPECIAL FOURTH-CLASS RATE
POSTAGE & FEES PAID
NASA
PERMIT No. G27

POSTMASTER: If Undeliverable (Section 158
Postal Manual) Do Not Return